James M. Provenzale ♦ Rendon C. Nelson ♦ Emily N. Vinson

# DUKE RADIOLOGY Case Review

SECOND EDITION

Imaging, Differential Diagnosis, and Discussion

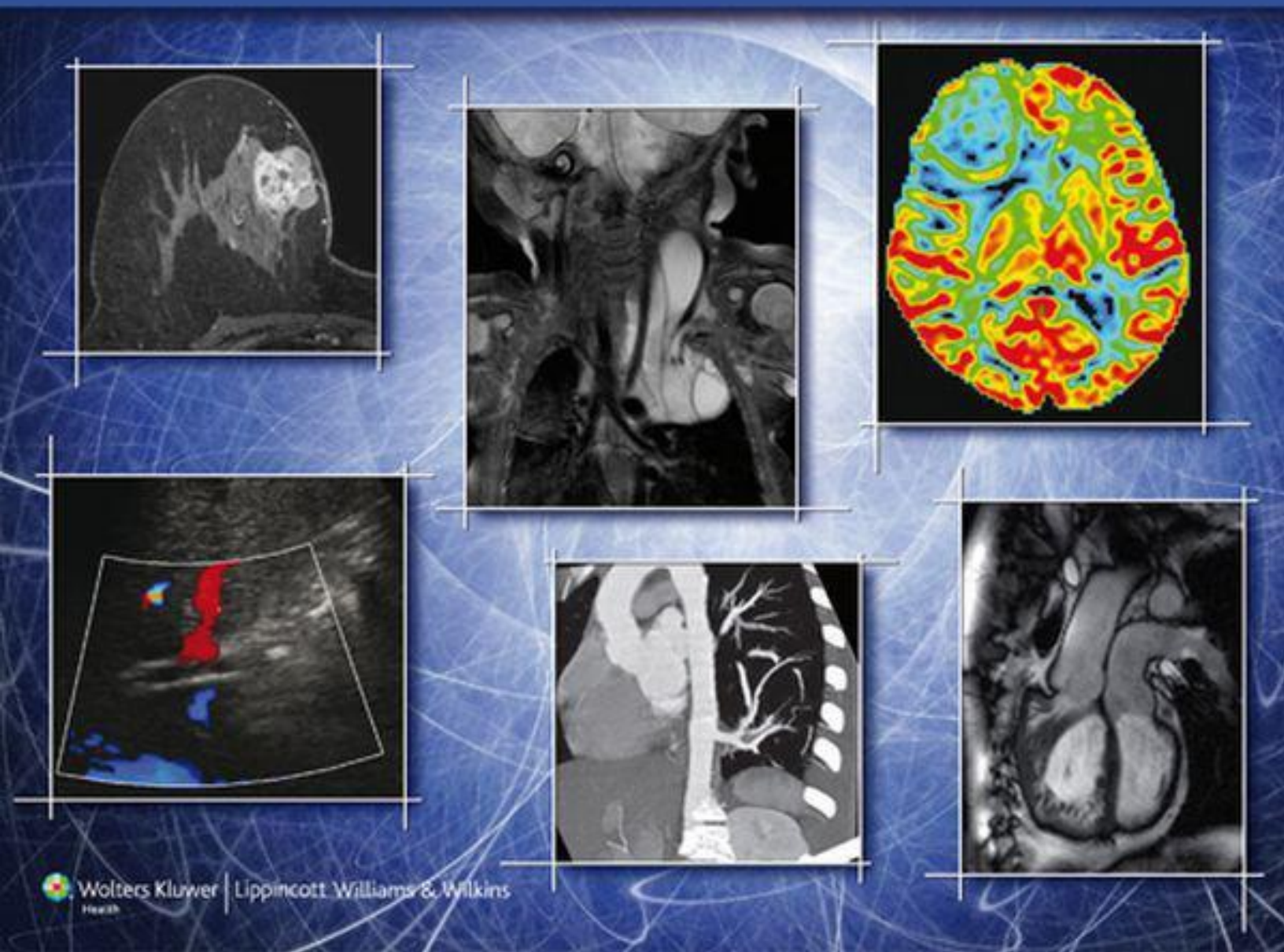

Wolters Kluwer | Lippincott Williams & Wilkins

James M. Provenzale ♦ Rendon C. Nelson ♦ Emily N. Vinson

# DUKE RADIOLOGY Case Review

SECOND EDITION

Imaging, Differential Diagnosis, and Discussion

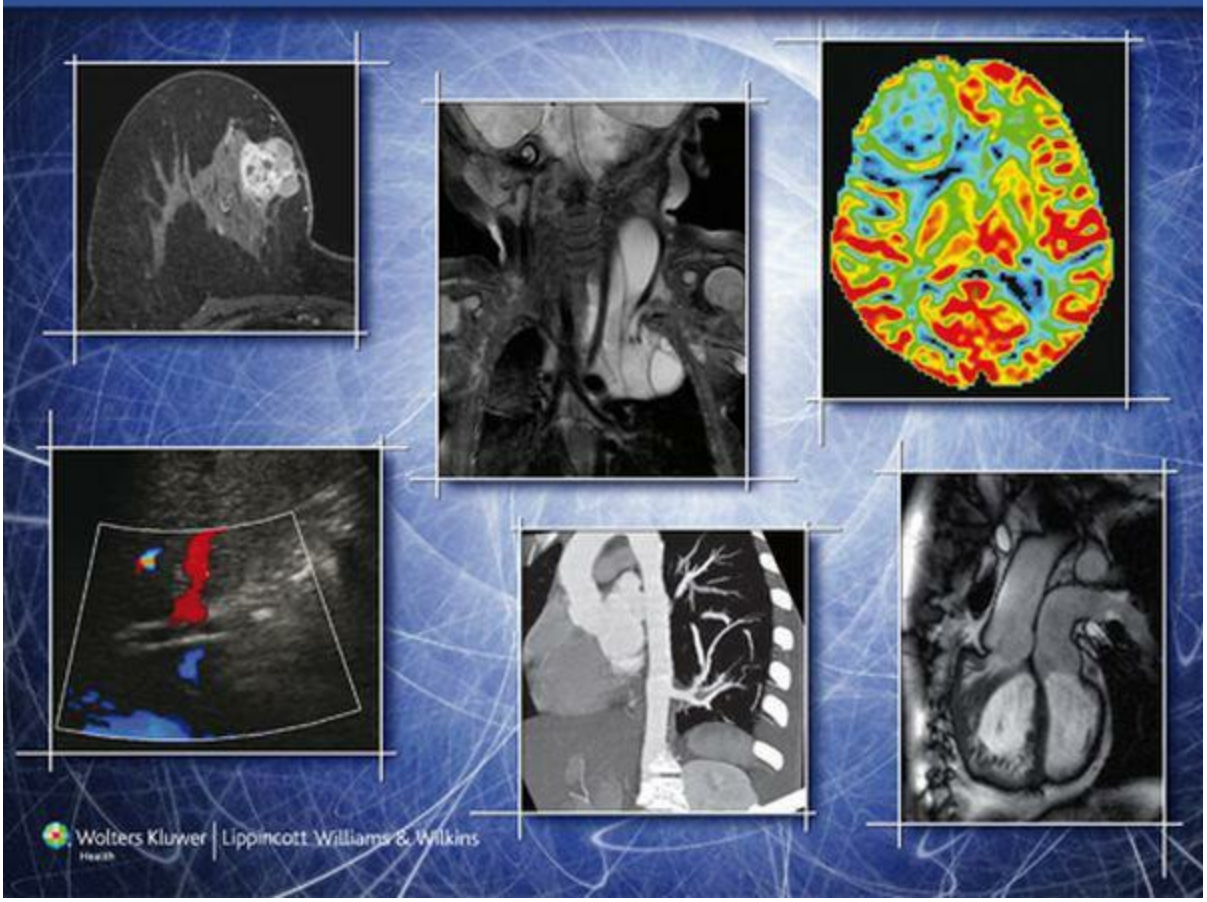

Wolters Kluwer | Lippincott Williams & Wilkins

2nd EDITION

# Duke Radiology Case Review

*Imaging, Differential Diagnosis, and Discussion*

## EDITORS


**JAMES M. PROVENZALE, M. D., FACR**

Professor of Radiology
Duke University Medical Center
Durham, North Carolina and
Professor of Radiology Oncology and Biomedical Engineering
Emory University School of Medicine
Atlanta, GA

**RENDON C. NELSON, M. D., FACR**

Reed and Martha Rice Professor of Radiology
Division of Abdominal Imaging
Duke University Medical Center
Durham, North Carolina

**EMILY N. VINSON, M. D.**

Assistant Professor of Radiology
Division of Musculoskeletal Radiology
Duke University Medical Center
Durham, North Carolina


Wolters Kluwer | Lippincott Williams & Wilkins
Health

Philadelphia • Baltimore • New York • London
Buenos Aires • Hong Kong • Sydney • Tokyo

Executive Editor: Charles W. Mitchell
Product Manager: Ryan Shaw
Vendor Manager: Alicia Jackson
Senior Manufacturing Manager: Benjamin Rivera
Senior Marketing Manager: Angela Panetta
Creative Director: Doug Smock
Production Service: SPi Global


**Two Commerce Square**
**2001 Market Street**
**Philadelphia, PA 19103 USA**
**LWW.com**



Printed in China

---

**Library of Congress Cataloging-in-Publication Data**
Duke radiology case review : imaging, differential diagnosis, and discussion / [edited by] James
M. Provenzale, Rendon C. Nelson. — 2nd ed.
p. ; cm.
Radiology case review
Includes bibliographical references and index.
ISBN 978-0-7817-7860-2 (alk. paper)
I. Provenzale, James M. II. Nelson, Rendon C. III. Duke University. Medical Center. Dept. of Radiology. IV. Title: Radiology case review.
[DNLM: 1. Radiology—methods—Case Reports. 2. Diagnosis, Differential —Case Reports. WN 100]
LC classification not assigned
616.07’57—dc23

2011034423



To purchase additional copies of this book, call our customer service department at (800) 638-3030 or fax orders to (301) 223-2320. International customers should call (301) 223-2300.

Visit Lippincott Williams & Wilkins on the Internet: at LWW.com. Lippincott Williams & Wilkins customer service representatives are available from 8:30 am to 6 pm, EST.

10 9 8 7 6 5 4 3 2 1

*To Dawn, Kate, and Elizabeth, for their support and patience during the writing of this book.*
—JMP

*To my son Curran, for his support and encouragement.*
—RCN

*To my husband, Stephen, and our children, Allison and Matthew, who make my life complete.*
—ENV

# CONTRIBUTORS

**TIMOTHY J. AMRHEIN, M.D.**
Radiology Fellow
Duke University Medical Center
Durham, North Carolina

**GEORGE S. BISSET III, M.D.**
*At time of contribution* Duke Department of Radiology
*Presently* Chief of Pediatric Radiology
Texas Children's Hospital
Houston, Texas

**SALVADOR BORGES-NETO, M.D.**
Professor of Radiology and Internal Medicine
Duke University Medical Center
Durham, North Carolina

**JAMES D. BOWIE, M.D.**
Formerly of the Department of Radiology
Duke University Medical Center
Durham, North Carolina

**ADAM CHARLES BRITHWAITE, M.D.**
Assistant Consulting Professor
Duke Raleigh Hospital
Raleigh, North Carolina

**JOSHUA A. BRYANT, M.D.**
*At time of contribution* Duke Department of Radiology
*Presently* Colorado Imaging Associates
Denver, Colorado

**D. LAWRENCE BURK, M.D.**
Formerly of the Department of Radiology
Duke University Medical Center
Durham, North Carolina

**CAROLINE W.T. CARRICO, M.D.**
Assistant Professor of Radiology and Pediatrics

Duke University Medical Center
Durham, North Carolina

**BARBARA A. CARROLL, M.D.**
Formerly of the Department of Radiology
Duke University Medical Center
Durham, North Carolina

**BENNETT B. CHIN, M.D.**
Associate Professor of Radiology
Duke University Medical Center
Durham, North Carolina

**JARED D. CHRISTENSEN, M.D.**
Assistant Professor of Radiology
Duke University Medical Center
Durham, North Carolina

**R. EDWARD COLEMAN, M.D.**
Professor of Radiology
Director, Division of Nuclear Medicine
Duke University Medical Center
Durham, North Carolina

**JOSEPH B. CORNETT, M.D.**
*At time of contribution* Duke Department of Radiology
*Presently* Wake Radiology Consultants
Raleigh, North Carolina

**R. LEE COTHRAN JR, M.D.**
Assistant Professor of Radiology
Duke University Medical Center
Durham, North Carolina

**CHARLES B. DONOVAN, M.D.**
*At time of contribution* Duke Department of Radiology
*Presently* Consulting Radiologists
Minneapolis, Minnesota

**SCOTT M. DUNCAN, M.D.**
*At time of contribution* Duke Department of Radiology

*Presently* Priority Radiology
New Albany, Indiana

**THOMAS SCOTT DZIEDZIC, M.D.**
*At time of contribution* Duke Department of Radiology
*Presently* Washington Hospital Center
Washington, D.C.

**BJORN ENGSTROM, M.D.**
Radiology Resident
Duke University Medical Center
Durham, North Carolina

**DAVID S. ENTERLINE, M.D.**
Associate Professor of Radiology
Director, Division of NeuroRadiology
Duke University Medical Center
Durham, North Carolina

**ANTHONY M. FOTI, M.D.**
*At time of contribution* Duke Department of Radiology
*Presently* Windsong Radiology
Williamsville, New York

**M. GENA FREDERICK, M.D.**
Formerly of the Department of Radiology
Duke University Medical Center
Durham, North Carolina

**KELLY S. FREED, M.D.**
*At time of contribution* Duke Department of Radiology
*Presently* Chief, Section of Genitourinary Radiology
Medical Imaging of Lehigh Valley
Allentown, Pennsylvania

**DONALD FRUSH, M.D.**
Professor of Radiology and Pediatrics
Director, Division of Pediatric Imaging
Duke University Medical Center
Durham, North Carolina

**ROSALIE J. HAGGE, M.D.**
*At time of contribution* Duke Department of Radiology
*Presently* Associate Clinical Professor
UC Davis Health System
Sacramento, California

**MICHAEL W. HANSON, M.D.**
Professor of Radiology and Assistant Professor of Medicine
Duke University Medical Center
Durham, North Carolina

**MELISSA A. HAYES, M.D.**
Radiology Fellow
Duke University Medical Center
Durham, North Carolina

**CLARE M. HAYSTEAD, M.D.**
Medical Instructor in Radiology
Duke University Medical Center
Durham, North Carolina

**E. RALPH HEINZ, M.D.**
Formerly of the Department of Radiology
Duke University Medical Center
Durham, North Carolina

**BARBARA S. HERTZBERG, M.D.**
Professor of Radiology and Associate Professor in Obstetrics and Gynecology
Duke University Medical Center
Durham, North Carolina

**LAURA E. HEYNEMAN, M.D.**
*At time of contribution* Associate Professor of Radiology
Duke University Medical Center
Durham, North Carolina
*Presently* Associate Professor of Radiology
University of North Carolina Hospitals
Chapel Hill, North Carolina

**JENNY K. HOANG, M.B.B.S.**
Assistant Professor of Radiology and Radiation Oncology

Duke University Medical Center
Durham, North Carolina

**PHIL B. HOANG, M.D.**
*At time of contribution* Duke Department of Radiology
*Presently* Southeast Louisiana Veterans Health Care System
New Orleans, Louisiana

**CAROLINE L. HOLLINGSWORTH, M.D., M.P.H.**
Assistant Professor of Radiology and Pediatrics
Duke University Medical Center
Durham, North Carolina

**DAVID M. HOUGH, M.B., CH.B.**
*At time of contribution* Duke Department of Radiology
*Presently* Assistant Professor of Radiology
Mayo Clinic
Rochester, Minnesota

**KURT HUSUM, M.D.**
*At time of contribution* Duke Department of Radiology
*Presently* Colorado Imaging Associates
Denver, Colorado

**MARY T. KEOGAN, M.D.**
*At time of contribution* Duke Department of Radiology
*Presently* St. James Hospital
Dublin, Ireland

**MICHAEL L. KERNER, M.D.**
*At time of contribution* Duke Department of Radiology
*Presently* Burlington Imaging
Burlington, North Carolina

**CHARLES Y. KIM, M.D.**
Assistant Professor of Radiology
Duke University Medical Center
Durham, North Carolina

**MARK A. KLIEWER, M.D., M.H.SC.**
*At time of contribution* Duke Department of Radiology

*Presently* Professor of Radiology
University of Wisconsin
Madison, Wisconsin

**TAMRA M. KNUTSON, M.D.**
*At time of contribution* Duke Department of Radiology
*Presently* Radiology Associates of the Fox Valley, S.C.
Neenah, Wisconsin

**PHYLLIS J. KORNGUTH, M.D., PH.D., FACR**
*At time of contribution* Duke Department of Radiology
*Presently* Professor of Radiology
Boston University School of Medicine
Boston, Massachusetts

**DAVID K. KRUG, M.D.**
*At time of contribution* Duke Department of Radiology
*Presently* Sibley Memorial Hospital
Johns Hopkins Medicine
Washington, District of Columbia

**JEREMY A.L. LAWRANCE, M.B., CH.B. (UCT), M.R.C.P. (UK)**
*At time of contribution* Duke Department of Radiology
*Presently* Divisional Director of Clinical Support Services
Christie Hospital
Manchester, United Kingdom

**RICHARD A. LEDER, M.D.**
Associate Professor of Radiology and Clinical Associate of Surgery
Duke University Medical Center
Durham, North Carolina

**VINCENT H.S. LOW, M.D.**
Formerly of the Department of Radiology
Duke University Medical Center
Durham, North Carolina

**DANIELE MARIN, M.D.**
Radiology Fellow
Duke University Medical Center
Durham, North Carolina

**SALUTARIO J. MARTINEZ, M.D.**
Professor of Radiology
Duke University Medical Center
Durham, North Carolina

**CHARLES M. MAXFIELD, M.D.**
Associate Professor of Radiology and Pediatrics
Duke University Medical Center
Durham, North Carolina

**VINCENT G. MCDERMOTT, M.B., B.CH.**
*At time of contribution* Duke Department of Radiology
*Presently* Bon Secours Hospital
Cork, Ireland

**MICHAEL J. MILLER JR., M.D.**
Assistant Professor of Radiology
Duke University Medical Center
Durham, North Carolina

**RENDON C. NELSON, M.D., FACR**
Reed and Martha Rice Distinguished Professor of Radiology
Duke University Medical Center
Durham, North Carolina

**GLENN E. NEWMAN, M.D. (POSTHUMOUS)**
Formerly of the Department of Radiology
Duke University Medical Center
Durham, North Carolina

**SARA M. O'HARA, M.D.**
*At time of contribution* Duke Department of Radiology
*Presently* Associate Professor of Radiology and Pediatrics
University of Cincinnati College of Medicine
Cincinnati, Ohio

**KAVITA M. PATEL, M.D.**
*At time of contribution* Duke Department of Radiology
*Presently* Hackensack University Medical Center
Hackensack, New Jersey

**ERIK K. PAULSON, M.D.**
Professor of Radiology
Vice Chairman of Radiology
Director, Division of Abdominal Imaging
Duke University Medical Center
Durham, North Carolina

**CYNTHIA S. PAYNE, M.D.**
*At time of contribution* Duke Department of Radiology
*Presently* Raleigh Radiology
Raleigh, North Carolina

**NICOLE PROSCIA, M.D.**
*At time of contribution* Duke Department of Radiology
*Presently* Washington Hospital Center
Washington, D.C.

**JAMES M. PROVENZALE, M.D., FACR**
Professor of Radiology
Duke University Medical Center
Durham, North Carolina *and*
Professor of Radiology, Oncology, and Biomedical Engineering
Emory University School of Medicine
Atlanta, Georgia

**ROBERT R. REIMAN, JR., M.D.**
Assistant Professor of Radiology
Duke University Medical Center
Durham, North Carolina

**CHRISTOPHER J. ROTH, M.D.**
Assistant Professor of Radiology
Duke University Medical Center
Durham, North Carolina

**JEFFREY T. SEABOURN, M.D.**
*At time of contribution* Duke Department of Radiology
*Presently* Intermountain Medical Imaging
Boise, Idaho

**DOUGLAS H. SHEAFOR, M.D.**

*At time of contribution* Duke Department of Radiology
*Presently* Charlotte Radiology
Charlotte, North Carolina

**TONY P. SMITH, M.D.**
Professor of Radiology
Director, Division of Vascular and Interventional Radiology
Duke University Medical Center
Durham, North Carolina

**MARY SCOTT SOO, M.D., FACR**
Associate Professor of Radiology
Duke University Medical Center
Durham, North Carolina

**CHARLES E. SPRITZER, M.D.**
Professor of Radiology
Duke University Medical Center
Durham, North Carolina

**DANIEL J. STACKHOUSE, M.D.**
*At time of contribution* Duke Department of Radiology
*Presently* Charlotte Radiology
Charlotte, North Carolina

**JOHN A. STAHL, M.D.**
*At time of contribution* Duke Department of Radiology
*Presently* Greensboro Imaging
Greensboro, North Carolina

**PAUL V. SUHOCKI, M.D.**
Associate Professor of Radiology
Duke University Medical Center
Durham, North Carolina

**ROBERT TIEN, M.D., M.P.H.**
Formerly of the Department of Radiology
Duke University Medical Center
Durham, North Carolina

**GLEN A. TOOMAYAN, M.D.**

*At time of contribution* Duke Department of Radiology
*Presently* Pinehurst Radiology Associates
Pinehurst, North Carolina

**ROBERT M. VANDEMARK, M.D.**
*At time of contribution* Duke Department of Radiology
*Presently* Orlando VA Medical Center
Orlando, Florida

**EMILY N. VINSON, M.D.**
Assistant Professor of Radiology
Duke University Medical Center
Durham, North Carolina

**RUTH WALSH, M.D.**
Associate Professor of Radiology
Duke University Medical Center
Durham, North Carolina

**LACEY WASHINGTON, M.D.**
Associate Professor of Radiology
Duke University Medical Center
Durham, North Carolina

**DANIELLE L. WELLMAN, M.D.**
*At time of contribution* Duke Department of Radiology
*Presently* Wake Radiology Consultants
Raleigh, North Carolina

**BETH E. WHITESIDE, M.D.**
*At time of contribution* Duke Department of Radiology
*Presently* Assistant Professor of Radiology
Albany Medical College
Albany, New York

**ROBERT H. WILKINSON JR., M.D.**
Formerly of the Department of Radiology
Duke University Medical Center
Durham, North Carolina

**MARGARET E. WILLIFORD, M.D.**

Assistant Professor of Radiology
Duke University Medical Center
Durham, North Carolina

**FERNANDO M. ZALDUONDO, M.D.**
*At time of contribution* Duke Department of Radiology
*Presently* San Patricio MRI & CT Center
San Juan, Puerto Rico

# PREFACE

Since the publication of the first edition of this book in 1998, a number of important changes in radiology have transpired. Some previously existing techniques have found new applications in various organ systems. For example, in 1998, magnetic resonance (MR) imaging of the breast was predominantly a research tool rather than a clinical application. However, breast MR imaging is now a common means of evaluating cancer and other disorders of the breast. Similarly, in 1998, MR imaging of the cardiovascular system was relatively underutilized; its use has substantially increased since then. Finally, use of multidetector-row computed tomography was in its nascent stages at the time of preparation of the first edition of this book. Subsequently, this imaging technique has assumed great importance in many areas of radiology. With these examples in mind, we have revised this book and now publish a second edition that is intended to take recent advances in imaging into account. The second edition contains many new cases but also often incorporates new images for cases that are retained from the first edition. We hope that readers will find these changes to their liking and that the cases herein prove instructive and challenging.

Although imaging techniques have changed, the need for radiologists (and radiologists-in-training) to recognize characteristic imaging findings, develop an appropriate differential diagnosis, and reach the correct diagnosis has not changed. The present edition again emphasizes the process of deduction of the correct diagnosis based on correct understanding of the clinical features and interpretation of the imaging findings. We have again restricted the selection of cases to entities that radiologists encounter with some frequency in clinical practice or disease processes that are important diagnostic considerations.

One further change from the first edition of this book is worth noting. Emily Vinson, MD, a musculoskeletal radiologist at our institution, has joined as coeditor. Many of the important changes in the second edition are examples of Dr. Vinson's substantial contributions.

*Rendon C. Nelson, M.D., FACR*
*Emily N. Vinson, M.D.*
*James M. Provenzale, M.D., FACR*

## ACKNOWLEDGMENTS

We acknowledge the substantial efforts of Duke Radiology faculty, residents, and fellows; without their contributions, this book could not have been published.

*Rendon C. Nelson, M.D., FACR*
*Emily N. Vinson, M.D.*
*James M. Provenzale, M.D., FACR*

# CONTENTS

**JAMES M. PROVENZALE ■ Chapter Editor**

Fernando M. Zalduondo, E. Ralph Heinz, David S. Enterline, Joseph B. Cornett, Charles B. Donovan, Robert Tien

## 7 Vascular Radiology

**CHARLES Y. KIM ■ Chapter Editor**

Glenn E. Newman (posthumous), Tony P. Smith, Daniel J. Stackhouse, Paul V. Suhocki, Cynthia S. Payne, Kurt Husum, Joshua A. Bryant, Melissa A. Hayes, Bjorn Engstrom, Glen A. Toomayan, Timothy J. Amrhein, Scott Duncan

## 8 Pediatric Radiology

**DONALD P. FRUSH ■ Chapter Editor**

Caroline L. Hollingsworth, Sara M. O'Hara, Caroline Carrico, Charles Maxfield, George S. Bisset III, Ana M. Gaca

## 9 Ultrasound

**CLARE HAYSTEAD ■ Chapter Editor**

Clare M. Haystead, James D. Bowie, Mark A. Kliewer, Barbara S. Hertzberg, Tamra M. Knutson, Barbara A. Carroll

## 10 Nuclear Medicine

**R. EDWARD COLEMAN ■ Chapter Editor**

R. Edward Coleman, Salvadore Borges-Neto, Robert H. Wilkinson, Jr., Sara M. O'Hara, Michael W. Hanson, Robert R. Reiman, Jr., Rosalie J. Hagge, Bennett B. Chin

## 11 Cardiac Imaging

**LAURA E. HEYNEMAN ■ Chapter Editor**

Glen A. Toomayan, Nicole Proscia, Phil B. Hoang, Joshua A. Bryant, Christopher J. Roth, Melissa Hayes, Danielle L. Wellman

# Chapter ONE

# Chest Radiology

**LAURA E. HEYNEMAN** ▪ CHAPTER EDITOR

Lacey Washington

Jared D. Christensen

Jenny K. Hoang

Tamra M. Knutson

Phil B. Hoang

# CASE 1

**LACEY WASHINGTON**

### HISTORY

A 26-year-old woman with malaise and night sweats.

A

■**FIGURE 1-1A** Posteroanterior chest radiograph shows lateralization of the AP reflection, convexity in the AP window, widening of the right paratracheal stripe, and convexity of the azygoesophageal recess. These findings indicate prevascular (anterior mediastinal), AP window, right paratracheal, and subcarinal lymphadenopathy.

B

■**FIGURE 1-1B** Left lateral chest radiograph confirms increased soft tissue density in the anterior mediastinum and subcarinal regions.

C

**FIGURE 1-1C** Contrast-enhanced chest CT (mediastinal window) reveals a conglomerate, lobular anterior mediastinal mass with minimal enhancement.

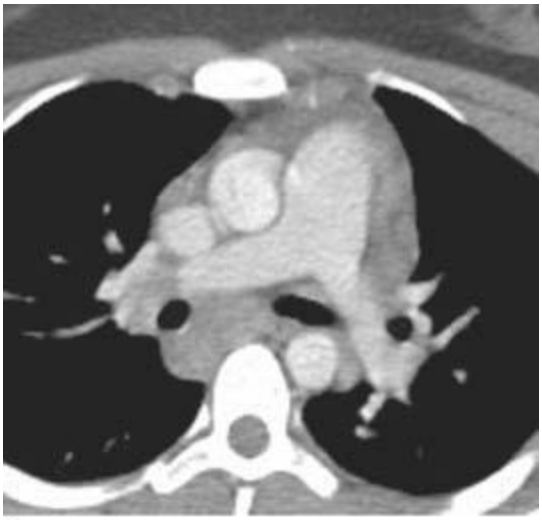

D

**FIGURE 1-1D** Contrast-enhanced chest CT (mediastinal window) also reveals enlarged subcarinal and right hilar lymph nodes.

## DIFFERENTIAL DIAGNOSIS

**Lymphoma:** This is the most likely diagnosis given the age of the patient and associated paratracheal and subcarinal lymphadenopathy.

**Thymoma:** This is less likely because these lesions usually occur in older patients, are typically more focal and unilateral, and are not associated with right paratra-cheal or subcarinal lymphadenopathy.

**Germ cell tumor:** A primary germ cell tumor of the mediastinum cannot be definitively excluded on the basis of age or radiologic appearance. However, in an

adult female patient, teratoma would be the more common germ cell tumor, and there are no features such as calcification or fat within the mass to suggest a teratoma. Malignant germ cell tumors, which are more likely to present as homogeneous soft tissue masses, are much more common in male than female patients.

- **Metastatic disease:** The mediastinum is a common site of metastatic disease from testicular germ cell tumors, renal cell carcinoma, and melanoma. However, the middle mediastinum is often preferentially involved with sparing of the anterior mediastinum, making this a less likely possibility.

## DIAGNOSIS

**Hodgkin's lymphoma**

## KEY FACTS

### Clinical

- At least 50% of patients with Hodgkin's lymphoma have intrathoracic lymph node disease.
- At least 90% of those with intrathoracic disease have an anterior mediastinal mass. Paratracheal lymph nodes are the second most commonly involved area.
- Pleural disease is unusual at presentation.

### Radiologic

- Hodgkin's lymphoma typically manifests as a lobulated anterior mediastinal mass that most likely represents matted lymph nodes. Associated mediastinal lymph-adenopathy is common and is a *key* differentiating feature from thymoma and germ cell tumor.
- Intratumoral calcification is rare in patients with untreated lymphoma.
- Unlike non-Hodgkin's lymphoma, Hodgkin's lymphoma tends to involve contiguous areas, and lung parenchy-mal involvement in the absence of hilar or mediastinal adenopathy is rare before therapy.

## SUGGESTED READING

Ansell SM, Armitage JO. Management of Hodgkin lymphoma. Mayo Clin Proc 2006;81:419–426.

Bae YA, Lee KS. Cross-sectional evaluation of thoracic lymphoma. Radiol Clin North Am 2008;46:253–264.

# CASE 2

**LACEY**

**WASHINGTON**

## HISTORY

Asymptomatic 45-year-old woman who had a preoperative chest radiograph obtained prior to cholecystectomy.

A

■**FIGURE 1-2A** Posteroanterior chest radiograph. There is a right-sided, smoothly marginated mediastinal mass.

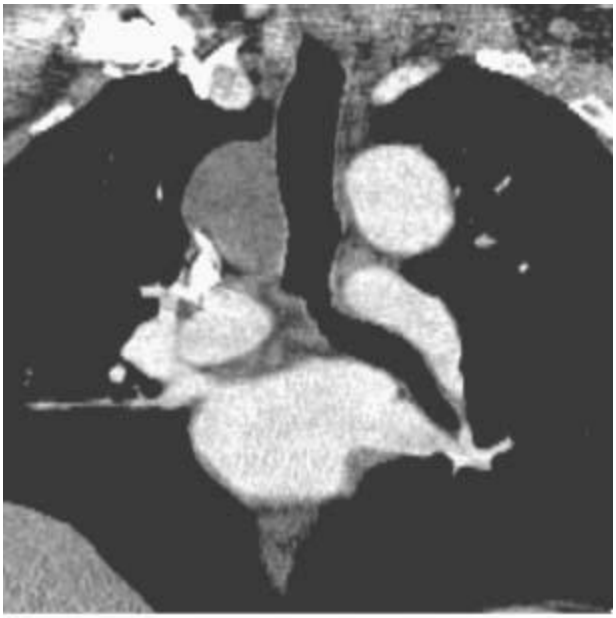

B

**FIGURE 1-2B** Coronal reformatted image from contrast-enhanced chest CT (mediastinal window) reveals a homogeneous, low-attenuation mass in the right paratracheal region.

## DIFFERENTIAL DIAGNOSIS

**Bronchogenic cyst:** This is the most likely diagnosis given the location and predominantly cystic appearance.

**Lymphadenopathy:** Low-attenuation paratracheal ade-nopathy can result from central necrosis due to tumor or infection (mycobacterial, fungal). In the setting of tumor, necrotic nodes are most commonly associated with squamous cell primaries. Necrotic nodes are typically more heterogeneous than is the mass in the current case, and may have an enhancing rim.

## DIAGNOSIS

**Bronchogenic cyst**

## KEY FACTS

### Clinical

- Bronchogenic cysts, also known as *foregut malformations*, are congenital anomalies caused by abnormal budding of the tracheobronchial tree.
- In order to definitively establish bronchogenic origin of a cyst, cartilage should be demonstrated in the wall. In the absence of cartilage in the walls, bronchogenic cysts within the lungs cannot be definitively distinguished from healed abscess cavities, and

in the mediastinum, they cannot be definitively distinguished from cysts of esophageal derivation.

- Bronchogenic cysts are filled with variable amounts of mucus, protein, and cellular debris.
- A stalk or pedicle commonly attaches the cyst to a mediastinal structure.
- Bronchogenic cysts may be associated with other congenital anomalies of lung development such as sequestration, lobar emphysema, and diaphragmatic hernia.
- Bronchogenic cysts are usually asymptomatic but can enlarge and produce symptoms, such as pain, dyspnea, stridor, cough, and respiratory infection, by compression of adjacent mediastinal structures.
- Rare complications include infection, hemorrhage, and carcinoma arising within the cyst.

## Radiologic

- Bronchogenic cysts most commonly occur in the sub-carinal and right paratracheal regions.
- They usually manifest as smooth, well-marginated mediastinal masses on radiographs and CT.
- They are typically homogeneous on CT. Approximately, half are of water attenuation and half are of soft tissue attenuation due to intracystic hemorrhage or protein-aceous debris.
- Bronchogenic cysts that are not of water attenuation may still be characterized as cystic with unenhanced CT if layering milk of calcium is present or on contrast-enhanced CT if they are homogeneous with no central enhancement and a thin wall.
- Approximately, two-thirds of bronchogenic cysts can be characterized as cystic with CT, based on attenuation, enhancement characteristics, or layering milk of calcium.
- On MRI, they are usually of high signal intensity on T2-weighted images. Signal intensity on T1-weighted images is variable depending on the presence of hemorrhage or protein (high signal intensity).
- Air-fluid levels are rare and are usually due to infection or instrumentation.

# SUGGESTED READING

Cioffi U, Bonavina L, De Simone M, et al. Presentation and surgical management of bronchogenic and esophageal duplication cysts in adults. Chest 1998;113:1492–1496.

Fraser RS, Colman N, Muller NL, Pare PD. Fraser and Pare's Diagnosis of Diseases of the Chest (4th ed). Philadelphia, PA: WB Saunders Co., 1999.

McAdams HP, Kirejczyk WM, Rosado-de-Christenson ML, Matsumoto S. Bronchogenic cyst: imaging features with clinical and histopathologic correlation. Radiology 2000;217:441-446.

# CASE 3

**LACEY**
**WASHINGTON**

## HISTORY

A 33-year-old woman with mild upper back pain.

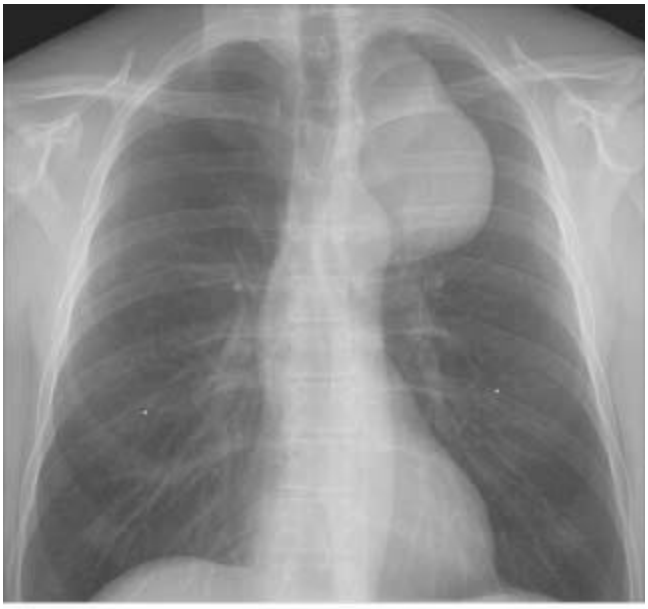

A

■**FIGURE 1-3A** Posteroanterior chest radiograph with nipple markers. There is a left-sided, smooth, sharply marginated mass in the superior mediastinum. Note that the well-defined borders of the mass extend above the clavicles, indicating that it is in the posterior mediastinum (“cervicothoracic sign”).

B

■**FIGURE 1-3B** Left lateral chest radiograph confirms the posterior location of the mass.

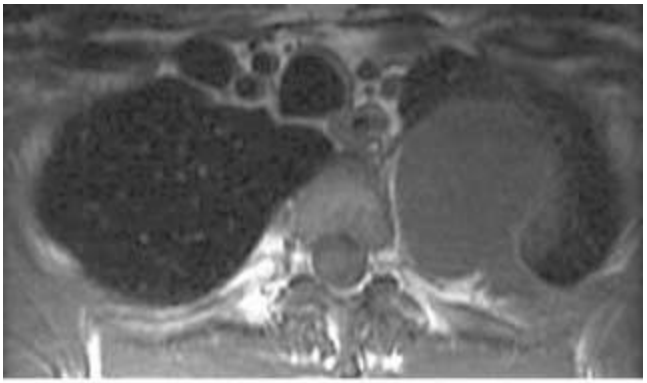

C

■**FIGURE 1-3C** Tl-weighted axial MR image without intravenous contrast administration reveals a homogeneous, low signal intensity left paraspinal mass with a preserved fat plane between the mass and the adjacent rib.

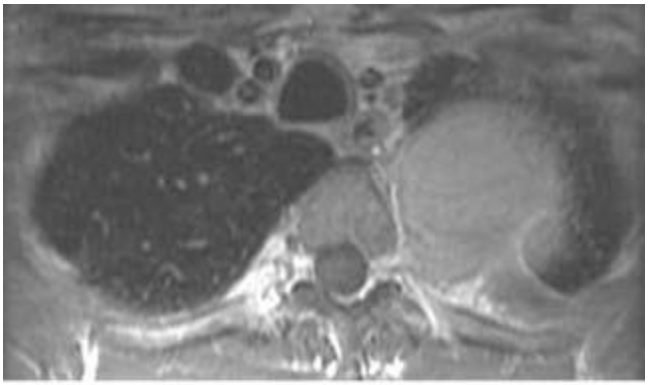

D

**FIGURE 1-3D** Tl-weighted axial MR image after intravenous contrast administration reveals diffuse homogeneous enhancement of the left paraspinal mass. There is suggestion of minimal extension of the mass into the left neural foramen.

## DIFFERENTIAL DIAGNOSIS

**Neurogenic tumor:** A neurogenic tumor is the most common cause of a posterior mediastinal or paraverte-bral mass. The slight extension of the mass into the left neural foramen would favor this diagnosis.

**Neuroenteric cyst:** These are most commonly associated with vertebral body anomalies such as butterfly vertebrae. On the MR images, the diffuse central enhancement indicates that this mass is solid. Therefore, a neuroenteric cyst is not a viable differential consideration.

**Paraspinal abscess:** This is unlikely in a minimally symptomatic patient without radiologic evidence of vertebral body destruction or disk space narrowing. Additionally, the MR images demonstrate that the mass is solid.

**Extramedullary hematopoiesis:** This usually manifests with bilateral, lobulated paraspinal masses in a patient with severe anemia. The adjacent ribs are often expanded with coarsened trabecula. The absence of these findings and the absence of a history of anemia would make extramedullary hematopoiesis an unlikely diagnosis.

**Lymphoma:** Isolated paraspinal disease is an uncommon manifestation of thoracic lymphoma. Patients much more commonly present with additional lymph-adenopathy in the anterior and middle mediastinum.

**Metastatic disease:** Isolated metastatic disease to the pleura or mediastinum is less likely than a neurogenic tumor given minimal symptoms and no history of a primary malignancy.

**Solitary fibrous tumor of pleura:** This is a rare pleu-ral tumor that can manifest as a paraspinal mass and mimic neurogenic tumors. These tumors are often pedunculated, and as a result may shift with differences in patient positioning. The rarity of solitary

fibrous tumors of the pleura and the fact that the mass appears to extend slightly into the left neural foramen makes a solitary fibrous tumor of the pleura an unlikely diagnosis.

## DIAGNOSIS

**Neurogenic tumor; in this case, a schwannoma**

## KEY FACTS

### Clinical

- There are three groups of neurogenic tumors of varying malignant potential: peripheral nerve sheath tumors (schwannomas, neurofibromas, malignant nerve sheath tumors), sympathetic ganglia tumors (neuroblastomas, ganglioneuroblastomas, ganglioneuromas), and, the least common group, tumors of the parasympathetic ganglia or paragangliomas.
- The most common neurogenic tumors in adults are nerve sheath tumors (schwannomas and neurofibromas), while sympathetic ganglia tumors are more common in children.
- Schwannomas and neurofibromas are the most common neurogenic tumors of the posterior mediastinum.
- Patients with schwannomas or neurofibromas can be asymptomatic or present with back pain.
- Most neurofibromas and schwannomas are solitary and are not associated with neurofibromatosis. However, multiple neurofibromas are usually associated with neurofibromatosis type 1.
- Malignant degeneration (malignant nerve sheath tumor) is rare and is most commonly seen in the setting of neurofibromatosis.

### Radiologic

- The peripheral nerve tumors (schwannomas and neu-rofibromas) manifest as round, paravertebral masses that usually span two vertebral bodies or less. They may invade the neural canal. Rib erosion is common, particularly in neurofibromas.
- The tumors of the sympathetic ganglia manifest as elongated paraspinal masses, spanning multiple vertebral levels. Intratumoral calcification is common in these tumors.
- On CT, the peripheral nerve tumors manifest as homogeneous, round soft tissue masses that tend to enhance homogeneously. On MR, signal characteristics of the tumors are nonspecific. Most commonly, the masses demonstrate homogeneous signal that is isointense to skeletal muscle on T1-weighted imaging, and mildly heterogeneous high signal on T2-weighted imaging. There tends to be only slight contrast enhancement after intravenous gadolinium administration.

- In large nerves, schwannomas may be differentiated from neurofibromas by the fact that schwannomas tend to be eccentric to the involved nerve. In contrast, the affected nerve in neurofibromas tends to be centrally located or obliterated.
- The "target sign" has been described for both schwannomas and neurofibromas, and is more common in neurofibromas. This refers to the appearance on T2W imaging in which there is low signal intensity centrally and higher signal intensity peripherally. This corresponds to the histologic finding of central fibrous elements and peripheral myxomatous components. However, the absence of the "target sign" does not preclude the diagnosis of a peripheral nerve sheath tumor.
- The multiplanar capability and high contrast resolution of MRI may be helpful in demonstrating intracanalicu-lar extension of neurogenic tumors.

## SUGGESTED READING

Camilla RW, Sameer K, Graham JM, Sisa G. A diagnostic approach to mediastinal abnormalities. Radiographics 2007;27:657–671.

Forsythe A, Volpe J, Muller R. Posterior mediastinal ganglioneuroma. Radiographics 2004;24:594-597.

Tanaka O, Kiryu T, Hirose Y, et al. Neurogenic tumors of the mediastinum and chest wall: MR imaging appearance. J Thorac Imaging 2005;20:316-320.

# CASE 4

**LACEY**
**WASHINGTON**

### HISTORY

A 61-year-old man presents with progressive shortness of breath. A CXR was performed, followed by thoracentesis and contrast-enhanced CT of the chest.

A

**FIGURE 1-4A** Posteroanterior chest radiograph. There is a lobulated soft tissue mass surrounding the right hemithorax with mild mass effect on the trachea. Several poorly defined opacities project over the lateral left hemithorax.

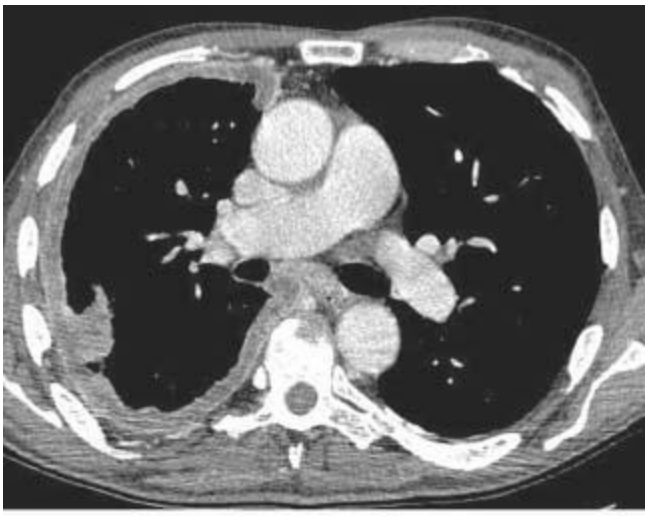

B

**FIGURE 1-4B** Contrast-enhanced chest CT (mediastinal window) demonstrates enhancing nodular pleural soft tissue encasing the right lung. There is also a component of loculated right pleural effusion. There is suggestion of subcarinal lymphadenopathy. Several calcified pleural plaques are seen in the left hemithorax.

C

**FIGURE 1-4C** Coronal reformat of contrast-enhanced CT (mediastinal window) confirms the circumferential right pleural nodularity, pleural enhancement, and loculated right pleural effusion. There is extension of the right pleural soft tissue into the right superolateral chest wall. A calcified right diaphragmatic pleural plaque and a calcified pleural plaque within the lateral left hemithorax are also present.

## DIFFERENTIAL DIAGNOSIS

- **Malignant pleural mesothelioma (MPM):** This is the most likely diagnosis given the age of the patient, the radiologic appearance of the pleura, and the evidence of prior asbestos exposure (pleural plaques).
- **Pleural metastatic disease:** Metastatic disease is the most common malignancy of the pleura. However, the appearance of circumferential pleural thickening, in some areas >1 cm in thickness, and a tumor rind with mediastinal pleural involvement is more suggestive of mesothelioma than metastases, particularly in a patient with bilateral pleural calcifications.
- **Loculated empyema:** This patient had no signs or symptoms of empyema. The degree of pleural thickening argues for a neoplastic process, making empyema a less likely possibility.

## DIAGNOSIS

**Malignant pleural mesothelioma (MPM)**

## KEY FACTS

### Clinical

- Mesothelioma is rare. Its incidence has peaked in the United States but continues to rise in Europe due to continued asbestos use in the 1970s.
- There is a high association with prior asbestos exposure, but no exposure history is found in up to 20% of cases. There is a long latency period, with the tumor occurring up to 50 years following asbestos exposure.
- Patients may present with increasing dyspnea or chest pain, commonly in the sixth to seventh decade of life, and mesothelioma should be considered in any patient who presents with chest pain and either a history of asbestos exposure or unilateral radiographic pleural abnormalities.
- There are three histologic subtypes—epithelial, sarcomatous, and mixed—and while overall prognosis is poor, the epithelial subtype is associated with a somewhat better prognosis.
- There is no relationship with smoking.
- Extrapleural pneumonectomy may be considered in which the lung and all the parietal pleura, pericardium, and diaphragm are removed.

### Radiologic

- At CT, circumferential pleural thickening, nodular pleural thickening, mediastinal pleural involvement, and possibly pleural thickening >1 cm are suggestive of pleural malignancy with a fairly high positive predictive value; the absence of these findings, however, does not exclude pleural malignancy.
- Rind-like pleural involvement, mediastinal pleural involvement, and pleural thickness >1 cm favor meso-thelioma over metastatic pleural disease.
- Pleural fluid is usually seen at the time of presentation.
- Contralateral pleural plaques from prior asbestos exposure may be identified.
- Local invasion of the chest wall, mediastinum, or diaphragm is common. Chest wall involvement is commonly seen at the site of previous interventions including biopsy and drain sites.
- If surgical resection is being considered, CT imaging should be extended to the level of the third lumbar vertebra with reformatted sagittal and coronal images to better assess for chest wall and intra-abdominal extension.
- Lymphadenopathy occurs with more extensive tumor and in the later stages of disease.
- Contralateral lung or brain metastases are unusual features.

## SUGGESTED READING

Benamore RE, O'Doherty MJ, Entwisle JJ. Use of imaging in the management of malignant pleural mesothelioma. Clin Radiol 2005;60: 1237–1247.

Gottschall EB. Occupational and environmental thoracic malignancies. J Thorac Imaging 2002;17:189-197.

Metintas M, Ucgun I, Elbek O, et al. Computed tomography features in malignant pleural mesothelioma and other commonly seen pleural diseases. Eur J Radiol 2002;41:1-9.

Seely JM, Nguyen ET, Churg AM, Muller NL. Malignant pleural mesothe-lioma: computed tomography and correlation with histology. Eur J Radiol 2009;70:485-491.

# CASE 5

**LAURA E. HEYNEMAN**

## HISTORY

An otherwise healthy 25-year-old woman with a history of recurrent left lower lobe pneumonias who presents with fever, cough, and chest pain.

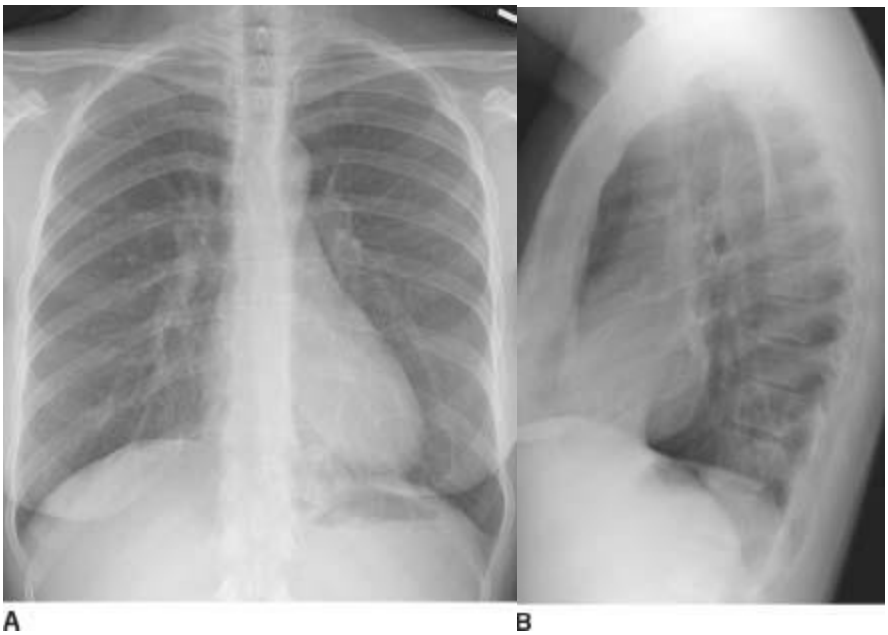


■**FIGURES 1-5A and 1-5B** Posteroanterior and lateral chest radiographs reveal minimal opacity in the medial posterior left lung base; the opacity is best seen on the lateral view ("positive spine sign").

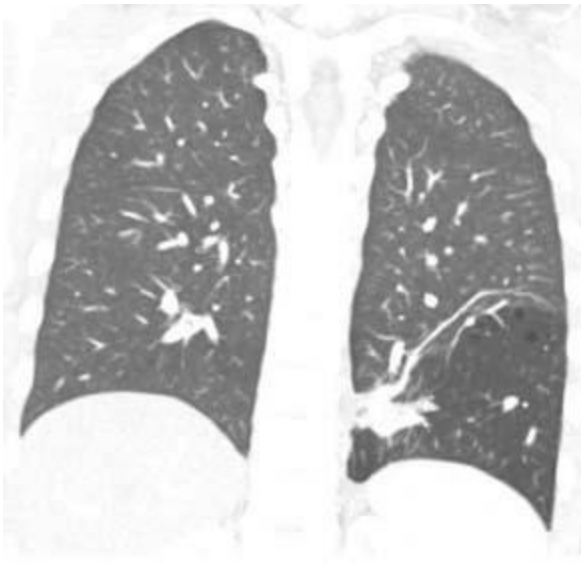

C

**FIGURE 1-5C** Coronal reformat from contrast-enhanced chest CT (lung window) reveals hyperinflation and hyperlucency within the left lower lobe. There are tiny focal air cysts. Additionally, there is a tubular, branching opacity that extends from midline and likely represents the opacity seen on the radiographs. On other images, this tubular opacity connects to the abdominal aorta.

D

**FIGURE 1-5D** Oblique sagittal maximum intensity projection image from contrast-enhanced spiral CT (mediastinal window) demonstrates an anomalous vessel arising from the distal thoracic aorta. This vessel supplies the hyperlucent segment in the left lower lobe.

## DIFFERENTIAL DIAGNOSIS

**Intralobar sequestration (ILS):** This is the most likely diagnosis given the history of

recurrent pneumonia, the hyperlucency of the left lower lobe, and the radiologic demonstration of a systemic vascular supply to the left lower lobe.

- **Postobstructive pneumonia:** This is a consideration when a patient has recurrent infections in the same distribution. An endobronchial lesion from an aspirated foreign body or an indolent neoplasm such as a hamar-toma or carcinoid tumor is a consideration in a young individual.
- **Recurrent aspiration:** While aspiration may recur in the dependent lung, this is unlikely in an otherwise healthy young woman in whom there are no risk factors for aspiration.
- **Congenital cystic adenomatoid malformation (CCAM):** Although the location and appearance of the lesion is consistent with this diagnosis, CCAM is very rarely diagnosed in adults.

# DIAGNOSIS

**Intralobar sequestration (ILS)**

# KEY FACTS

## Clinical

- A sequestration is defined as a malformation of pulmonary tissue characterized by lack of communication with the tracheobronchial tree as well as systemic arterial supply. There are two types of sequestration: ILS and extralobar sequestration (ELS).
- Both types of sequestration lack a normal connection to the tracheobronchial tree. ELS is contained within its own pleura and has systemic venous drainage into the right atrium. In contrast, ILS has normal pulmonary venous drainage and is not enveloped in its own pleura.
- ILS is much more common than ELS, and accounts for 75% of bronchopulmonary sequestrations.
- ILS may be an acquired abnormality due to recurrent infections with secondary bronchial obstruction and recruitment of systemic arteries.
- ILS usually occurs in the posterior or medial basilar segments of the lower lobes, left greater than right (3 to 2).
- ILS typically manifests in young patients with signs and symptoms of recurrent pneumonia.
- ELS is often associated with other congenital anomalies and is usually diagnosed within the first 6 months of life.

## Radiologic

- On radiographs, ILS commonly manifests as focal parenchymal consolidation. Cystic changes and air-fluid levels are also common.
- Other, less common, manifestations include a focal mass or a hyperlucent segment.
- By CT, MRI, or ultrasound, ILS usually manifests as a unilocular or multilocular cystic mass. Solid masses are sometimes seen.
- The systemic arterial supply to both ILS and ELS usually arises from the abdominal or thoracic aorta but may originate from lumbar arteries or the celiac axis. Venous drainage of ILS is usually via an inferior pulmonary vein.
- Diagnosis of ILS is made by radiologic demonstration of systemic vascular supply. This can be accomplished with angiography, contrast-enhanced CT (ideally performed as a CT angiogram), or MRI.

## SUGGESTED READING

Berrocal T, Madrid C, Novo S, et al. Congenital anomalies of the tracheobronchial tree, lung, and mediastinum: embryology, radiology, and pathology. Radiographics 2004;24:e17.

Bolca N, Topal U, Bayram S. Bronchopulmonary sequestration: radiologic flndings. Eur J Radiol 2004;52:185-191.

Lee EY, Boiselle PM, Cleveland RH. Multidetector CT evaluation of congenital lung anomalies. Radiology 2008;247:632-648.

# CASE 6

**LAURA E. HEYNEMAN**

### HISTORY

A 35-year-old male with no past medical history, who presents with cough and hemoptysis.

A

■**FIGURE 1-6A** Frontal scout image from CT scan reveals a homogeneous opacity with sharply demarcated lateral border within the medial inferior right hemithorax. The right hilum is small and inferiorly displaced, and there is mediastinal shift to the right. Additionally, the right heart border is obscured and there is apparent elevation of the right hemidiaphragm. The findings are consistent with combined right lower lobe and middle lobe collapse.

B

■**FIGURE 1-6B** Axial image from a noncontrasted CT (mediastinal window) reveals a right hilar mass that contains a punctate calcification. The mass obliterates the bronchus interme-dius, with only a tiny focus of air remaining within the bronchus.

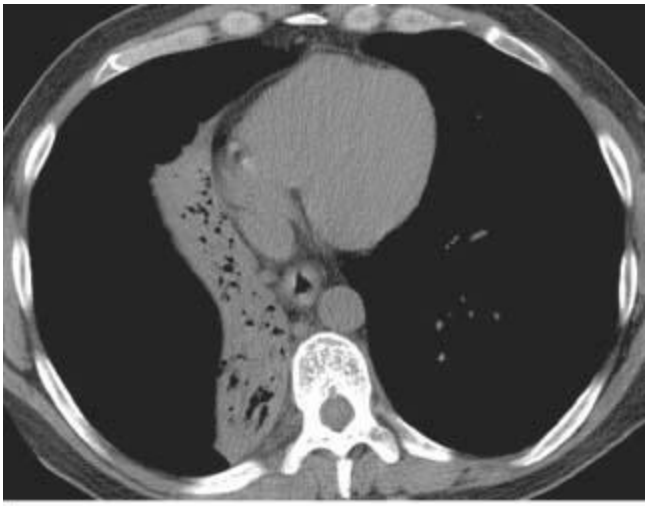

C

**FIGURE 1-6C** Axial image from the noncontrasted CT (mediastinal window) confirms the right middle and lower lobe collapse due to the more proximal bronchial obstruction.

## DIFFERENTIAL DIAGNOSIS

- **Bronchial carcinoid tumor:** This is the best single diagnosis given the radiologic appearance and the age of the patient.
- **Lung cancer:** Although lung cancer cannot be excluded, it is less likely in a patient of this age.
- **Lymphoma:** Bronchial obstruction is a relatively uncommon manifestation of lymphoma, and a hilar mass without lymphadenopathy elsewhere in the mediastinum would also be an unusual presentation.
- **Adenoid cystic carcinoma:** This tumor is also a possible diagnosis; however, these tumors are much less common than carcinoid tumors. They occur in the trachea and bronchi with equal frequency but, because tracheal tumors are generally less common than bronchial tumors, adenoid cystic carcinomas represent a larger percentage of tracheal tumors than of bronchial tumors.
- **Mucoepidermoid cancer:** This tumor is also a differential consideration, but is extremely rare.
- **Endobronchial metastasis:** Endobronchial metasta-ses from a lung, breast, renal, melanoma, or colonic primary can occur, but are unlikely in a young patient without a known history of a primary malignancy.

## DIAGNOSIS

**Bronchial carcinoid tumor**

## KEY FACTS

### Clinical

- Eighty-five percent of carcinoid tumors occur within the central bronchi (central carcinoid); 15% arise distal to segmental bronchi (peripheral carcinoid).
- Peripheral tumors manifest as asymptomatic pulmonary nodules.
- Central tumors manifest with symptoms of bronchial obstruction such as hemoptysis, chest pain, or recurrent pneumonia.
- Bronchial carcinoid tumors are only rarely associated with paraneoplastic syndromes such as Cushing's syndrome, carcinoid syndrome, or acromegaly. Only 2% of patients with bronchopulmonary carcinoid have Cush-ing's syndrome from ectopic adrenocorticotropic hormone (ACTH) production.
- Carcinoids are histologically divided into two types: typical (75% to 90%) and atypical (10% to 25%). Prognosis depends on the histologic subtype as well as on nodal status and tumor size.

The prognosis for typical carcinoid tumors is excellent even with hilar or ipsilateral mediastinal lymph node metastases. The prognosis for atypical carcinoid tumors is less favorable.

### Radiologic

- Peripheral tumors manifest as solitary, well-circumscribed pulmonary nodules.
- Central lesions manifest as hilar masses with or without obstructive atelectasis or pneumonia. Other potential manifestations of central obstruction include air trapping and mucoid impaction.
- In some cases, a small endobronchial component is associated with a larger exobronchial component. This is termed the "tip-of-the-iceberg" sign.
- Calcifications, which may be eccentric, punctate, or coarse, are seen by CT in up to 26% of cases. Diffuse calcification may be seen and simulate broncholithiasis.
- Carcinoids are characteristically highly vascular, and enhance intensely when intravenous contrast is administered. However, the absence of intense enhancement does not preclude the diagnosis of carcinoid, and the degree of contrast enhancement cannot be used to differentiate bronchial carcinoid from bronchogenic carcinoma.
- On T2-weighted MR images, bronchial carcinoid tumors have a very high signal intensity.
- In the few patients who have symptoms of ectopic ACTH production, octreotide scintigraphy is positive. The octreotide scans are particularly helpful when the tumors are small (<1 cm) and relatively inconspicuous on cross-sectional imaging.
- Radiologic manifestations of typical and atypical carci-noids are similar. Atypical

carcinoids tend to be larger, more peripheral, and more necrotic than the typical variant, but this is quite variable.

## SUGGESTED READING

Bertino EM, Confer PD, Colonna JE, et al. Pulmonary neuroendocrine tumors: a review article. Cancer 2009;115:4434–4441.

Chong S, Lee KS, Chung MJ, et al. Neuroendocrine tumors of the lung: clinical, pathologic, and imaging findings. Radiographics 2006;26:41–57.

Scarsbrook AF, Ganeshan A, Statham J, et al. Anatomic and functional imaging of metastatic carcinoid tumors. Radiographics 2007;27:455-477.

# CASE 7

**LAURA E. HEYNEMAN**

### HISTORY

A 35-year-old woman with a long history of sinus disease presents with sudden onset of cough, fever, and hemoptysis.

A

**FIGURE 1-7A** Posteroanterior chest radiograph. There are bilateral, mid lung cavitary nodules with an air-fluid level noted within a right perihilar nodule. A nodular opacity over the right anterior first rib may represent an additional subtle pulmonary nodule.

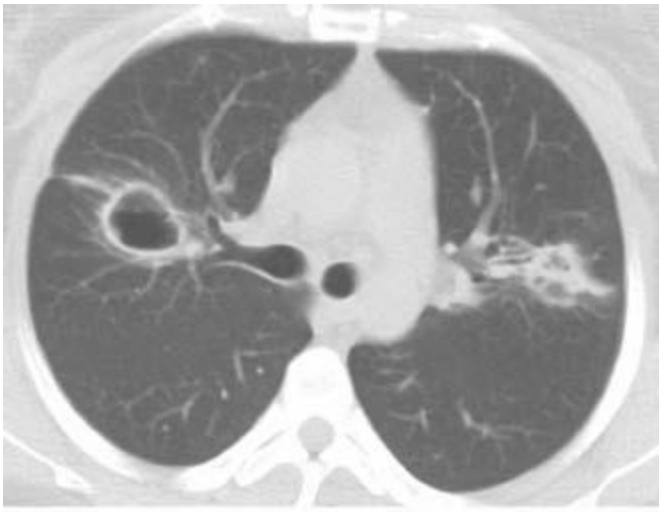

B

**FIGURE 1-7B** Chest CT (lung window) performed 2 weeks later reveals a thin-walled cavity within the right upper lobe with an adjacent linear focus that may represent subsegmental atelectasis. There is a nodular opacity within the left upper lobe with suggestion of central lucency.

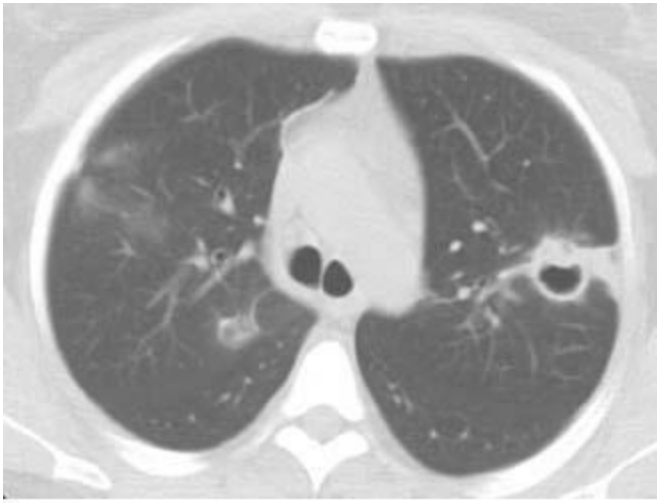

C

**FIGURE 1-7C** Image from the same chest CT (lung window) confirms the cavitation within the left upper lobe nodule. The nodule has an eccentric focus of soft tissue anteriorly, and there is a small amount of consolidation peripheral to the nodule. Additionally, there are scattered foci of ground glass within the right upper lobe, some of which are somewhat nodular in configuration. The patient has undergone right upper lobe wedge resection, with a suture line noted in the medial right upper lobe.

## DIFFERENTIAL DIAGNOSIS

**Vasculitis:** Potential vasculitic etiologies include Wegen-er's granulomatosis and,

much less likely, cavitary rheumatoid nodules. Since rheumatoid nodules tend to be a late manifestation of the disease, and the nodules tend to wax-and-wane with the course of subcutaneous nodules, the absence of a known history of rheumatoid arthritis would make this diagnosis unlikely. However, the given history of chronic sinus disease makes Wegener's granulomatosis a very likely diagnosis.

- **Infection:** Given that the patient is febrile, an atypical infection must be considered. Infectious differential considerations for cavitary nodules include fungi such as angioinvasive aspergillosis or coccidiomycosis, nocardia, anaerobes and gram-negative bacteria, and septic emboli. The absence of a travel history or an immunocompromised status would make opportunistic infections and fungal infections less likely. Furthermore, the given history of chronic sinus disease would not be pertinent for a diagnosis of an acute infection.
- **Neoplasm:** Potential neoplastic etiologies for cavitary nodules include synchronous primary lung cancers (squamous cell carcinoma), metastatic disease, or less likely, cavitary parenchymal lymphoma (Hodgkin's disease). Tumors that cavitate after metastasizing to the lung include squamous cell carcinoma of the head and neck, squamous cell carcinoma of the cervix, and metastatic sarcoma. However, the absence of a known primary malignancy would make the diagnosis of metastases unlikely. Furthermore, the presence of fever and the acute onset of the patient's symptoms would be unusual in the setting of malignancy.

## DIAGNOSIS

**Wegener's granulomatosis**

## KEY FACTS

### Clinical

- Wegener's granulomatosis is a multisystem granuloma-tous vasculitis.
- Major sites of involvement include the sinonasal cavity, lungs, and kidneys.
- Elevated c-ANCA (antineutrophil cytoplasm antibody) titers are sensitive and specific for active Wegener's granulomatosis.
- Wegener's granulomatosis has a good prognosis with aggressive medical management.

### Radiologic

- Patients typically present with multiple pulmonary nodules or masses, but the nodules may be solitary. One-third to one-half of nodules cavitate, particularly, when the nodules are >2 cm in diameter. The cavity walls may be thin and smooth or thick and nodular.

- An air-fluid level may be present within a Wegener's cavity, although the presence of an air-fluid level does raise the possibility of superimposed infection. Similarly, new pulmonary opacities in a patient being treated for known Wegener's granulomatosis suggest opportunistic infection, either fungal or *Pneumocystis jiovecii* pneumonia (PCP).
- The disease can also manifest as focal or diffuse paren-chymal consolidation. Diffuse pulmonary hemorrhage is the presenting manifestation in up to 10% of cases.
- Involvement of the trachea and bronchi occurs as a late complication in 15% to 25% of patients and can result in lobar atelectasis and bronchial stenoses.
- Pleural effusions are uncommon and adenopathy is rare.

## SUGGESTED READING

Allen SD, Harvey CJ. Imaging of Wegener's granulomatosis. Br J Radiol 2007;80:757–765.

Ananthakrishnan L, Sharma N, Kanne J. Wegener's granulomatosis in the chest: high-resolution CT findings. Am J Roentgenol 2009;192:676-682.

# CASE 8

**LAURA E. HEYNEMAN**

### HISTORY

A 25-year-old man with progressive dyspnea.

A

**FIGURE 1-8A** Posteroanterior chest radiograph shows bilateral 3- to 5-mm nodular and reticular opacities within the upper lobes. The lung volumes are normal. There is no lymphadenopathy or pleural abnormality.

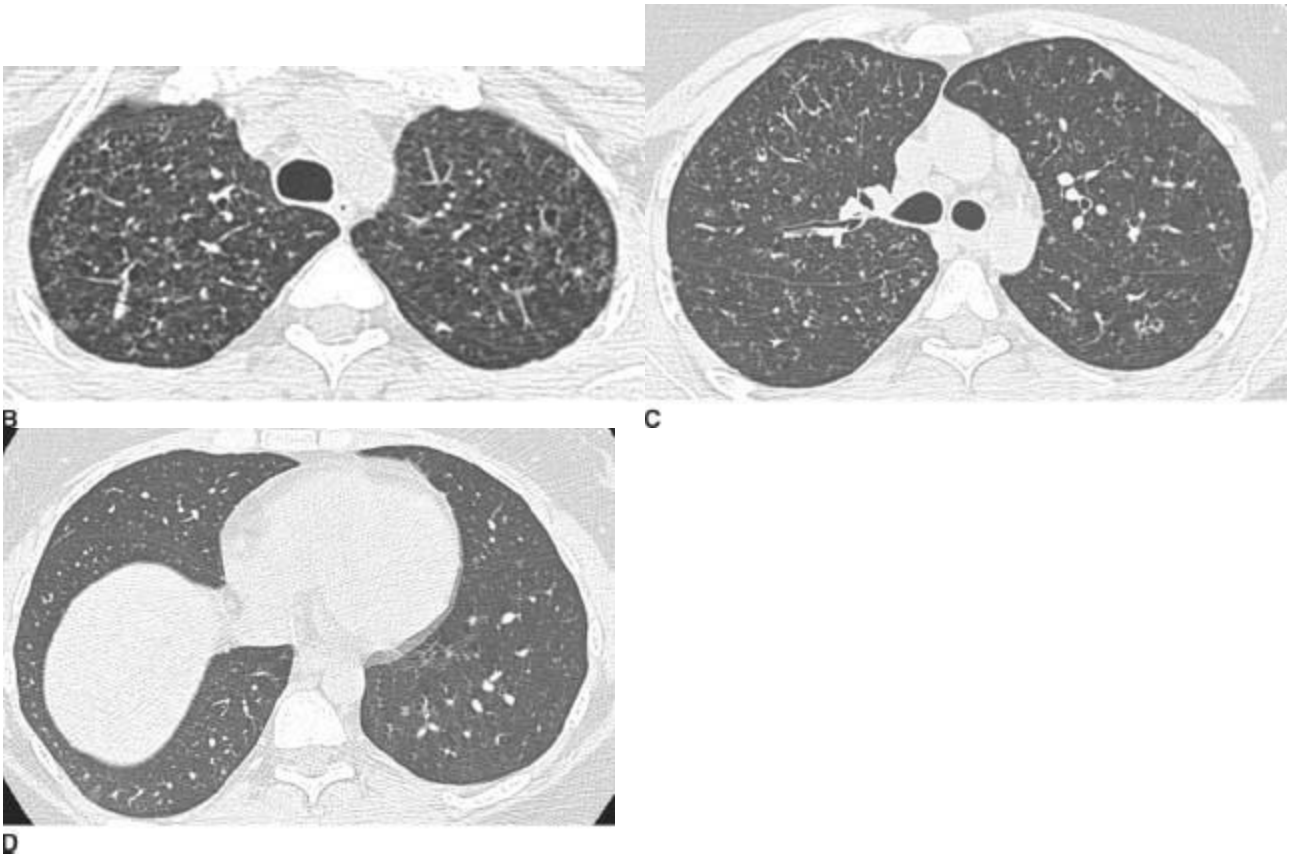


**FIGURES 1-8B**, **1-8C, and 1-8D** HRCT images (lung window) show multiple upper lobe air cysts and scattered small nodules (**B** and **C**). A few of the nodules demonstrate central lucencies. The process spares the lung bases and costophrenic angles (**D**).

## DIFFERENTIAL DIAGNOSIS

- Chest radiograph: Differential diagnosis based on the radiograph, includes sarcoidosis, pulmonary histiocytosis X (PHX), infection such as tuberculosis (TB) or disseminated fungal infection, pneumoconiosis (silicosis or coal worker's pneumoconiosis), and hypersensitivity pneumonitis (HP).
- High-resolution CT (HRCT)—nodules: Differential diagnosis for centrilobular (CL) nodules on HRCT includes sarcoidosis, PHX, HP, pneumoconiosis, TB, and various forms of bronchiolitis.
- HRCT—air cysts: Differential diagnosis for air cysts or ring lucencies on HRCT includes lymphangioleiomyo-matosis, PHX, *Pneumocystis jirovecii* pneumonia (PCP), bronchiectasis, and "honeycomb" lung (idiopathic pulmonary fibrosis [IPF]). Additionally, small nodules with central cavitation ("cheerio sign") may be seen with bronchioloalveolar cell carcinoma (BAC).
- The combination of upper lobe predominant nodules and ring lucencies on HRCT

makes PHX the most likely diagnosis.

## DIAGNOSIS

**Pulmonary histiocytosis X**

## KEY FACTS

### Clinical

- Also known as Langerhans cell histiocytosis or eosino-philic granuloma of lung.
- Patients are typically young to middle aged, with a higher incidence in men.
- Patients typically present with cough and dyspnea. Twenty percent present with a spontaneous pneumothorax.
- Almost all patients (at least 90%) with PHX are cigarette smokers.

### Radiologic

- Typical radiographic manifestations include nodular or reticulonodular opacities in the mid- and upper-lung zones. Lung volumes are typically normal or increased. Adenopathy and pleural effusion are uncommon. A pneumothorax may be evident.
- Early PHX manifests on HRCT as 3- to 5-mm nodules that are predominantly CL in distribution. The nodules may develop central cavitation, and eventually evolve into thick- and thin-walled air cysts. The cysts may coalesce into unusual shapes. Both cysts and nodules are more common in the mid- to upper-lung zones, and typically spare the costophrenic angles.
- The combination of air cysts and 3- to 5-mm nodules is highly suggestive of the diagnosis.

## SUGGESTED READING

Attili AK, Kazerooni EA, Gross BH, et al. Smoking related interstitial lung disease: radiologic-clinical-pathologic correlation. radiographics 2008;28:1383–1398.

Leatherwood DL, Heitkamp DE, Emerson RE. Best cases from the AFIP: Pulmonary Langerhans cell histiocytosis. Radiographics 2007;27:265-268.

# CASE 9

**LAURA E. HEYNEMAN**

## HISTORY

A 65-year-old man with progressive dyspnea and dry cough.

A

**FIGURE 1-9A** Posteroanterior chest radiograph. There are bilateral irregular linear opacities with low lung volumes. There is no evidence of adenopathy and there are no pleural abnormalities.

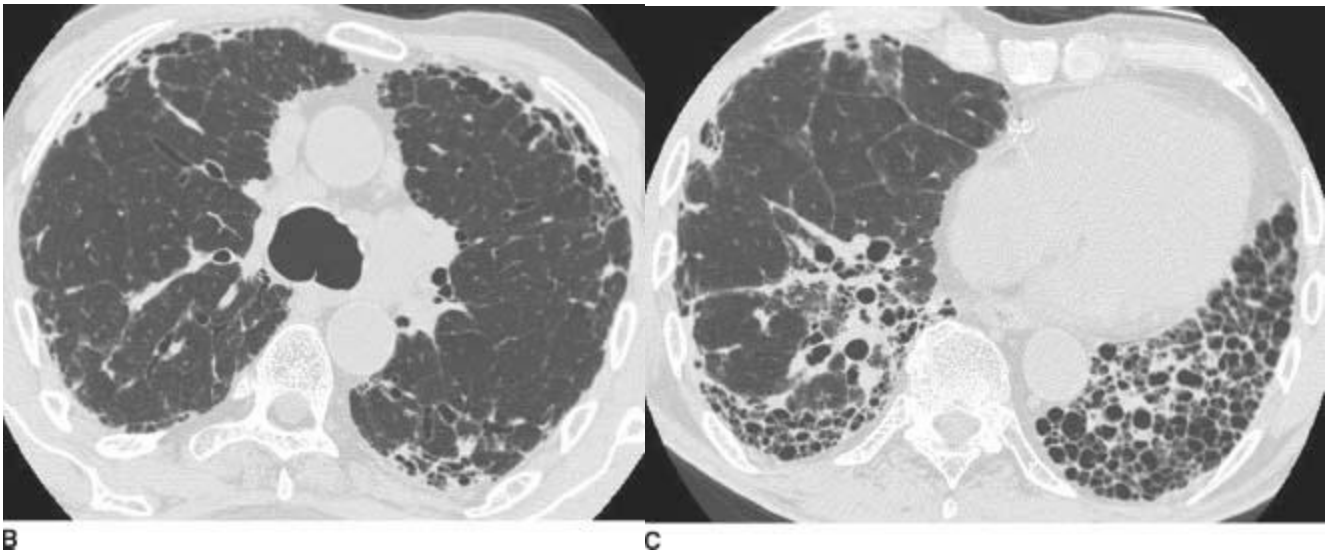

B C

**FIGURE 1-9B and 1-9C** HRCT images of the chest (lung window) shows irregular linear opacities, traction bronchiectasis, and honeycomb cyst formation. The findings are subpleural in distribution and most severe in the lung bases.

## DIFFERENTIAL DIAGNOSIS

**Usual interstitial pneumonia (UIP):** This is the most likely diagnosis because of the

pattern of subpleural irregular linear opacities, traction bronchiectasis, and honeycombing that is most marked in the lung bases.

- **Nonspecific interstitial pneumonia (NSIP):** NSIP is the second most common type of fibrosis, and is even more strongly associated with collagen vascular diseases than UIP. Honeycomb change is not a characteristic finding in NSIP. Therefore, while the irregular reticu-lar opacities and low lung volumes seen in this patient are indicative of fibrosis and would be seen in NSIP, the presence of honeycombing would make NSIP a much less likely diagnosis.
- **Chronic hypersensitivity pneumonitis (CHP):** CHP may result in a fibrosis that is very difficult to distinguish from UIP. Both entities may cause honeycomb cyst formation. However, CHP tends to cause fibrosis that is upper lobe predominant. Additionally, small centrilobu-lar nodules are often seen in CHP, and are not typically present in UIP.
- **Sarcoidosis:** The fibrosis associated with pulmonary sarcoid tends to have a perihilar and upper lobe predominance, particularly affecting the posterior aspects of the upper lobes. Therefore, the lower lobe predominance of the abnormalities seen in this case would not be characteristic of sarcoidosis. Additional radiologic clues that would suggest sarcoid would include lymph-adenopathy, upper lobe perilymphatic nodules, and progressive massive fibrosis.

# DIAGNOSIS

**Usual interstitial pneumonia (UIP)**

# KEY FACTS

## Clinical

- UIP typically manifests in middle-aged to elderly adults with progressive dyspnea and dry cough.
- UIP is a pathologic diagnosis and is caused by multiple entities such as asbestos exposure (“asbestosis”) and collagen vascular disease. However, in the majority of patients, there is no known cause; when there is no known etiology of the UIP, the patient is said to have idiopathic pulmonary fibrosis (IPF).
- UIP is more common in smokers and former smokers.
- UIP is a progressive, fatal illness with a median survival of 4 years.
- Corticosteroid and cytotoxic therapy is of limited benefit. Lung transplantation is a viable option in appropriate candidates.

## Radiologic

- Typical chest radiographic manifestations of UIP include low lung volumes and irregular linear opacities, which are more severe in the lung bases. There may be cystic lucencies due to honeycombing; this finding is often more conspicuous on the lateral view.
- Pleural effusions are rare.
- On HRCT, UIP manifests with irregular linear opacities (intralobular lines and irregular septal thickening), traction bronchiectasis, bronchiolectasis, and honeycomb cyst formation. When this pattern of findings is seen in a subpleural, basilar distribution, the HRCT is considered diagnostic of UIP.
- Ground glass opacities may be seen on HRCT, but are less extensive than the reticular, linear opacities.
- Lymphadenopathy is seen in 70% of patients, although the lymph node enlargement is usually mild (<1.5 cm in short axis).
- A search for the etiology of the UIP should be made on both radiographs and CT. For example, esophageal dilation or resorption of the distal clavicles raises the possibility of an underlying collagen vascular disorder. The presence of pleural plaques in the setting of UIP suggests a diagnosis of asbestosis.
- Complications of UIP that may be seen on the radiograph include pneumomediastinum or pneumothorax; these are caused by rupture of a distal alveolus in the context of stiff, noncompliant lung. Other complications that may be radiographically apparent include mycetoma formation within honeycomb cysts and lung cancer.

## SUGGESTED READING

Mueller-Mang C, Grosse C, Schmid K, et al. What every radiologist should know about idiopathic interstitial pneumonias. Radiographics 2007;27:595–615.

Silva CI, Muller NL. Idiopathic interstitial pneumonias. J Thorac Imaging 2009;24:260–273.

# CASE 10

**LAURA E. HEYNEMAN**

### HISTORY

A 58-year-old previously healthy woman with progressive dyspnea, cough, and low-grade fever over the past 6 weeks.

A

■**FIGURE 1-10A** Posteroanterior chest radiograph reveals bilateral peripheral homogeneous opacities within the lower lobes (right greater than left) and right upper lobe.

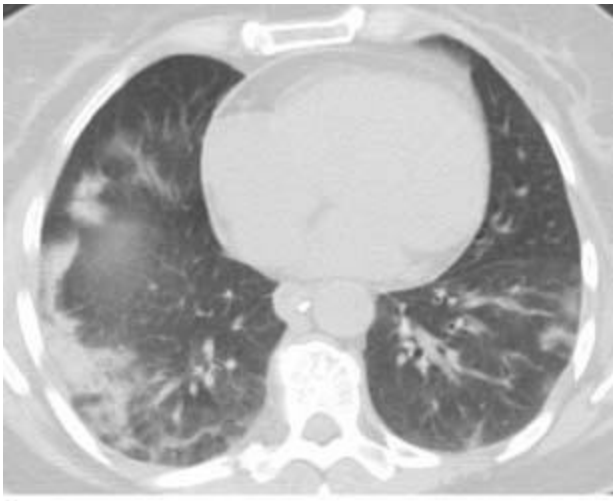

B

■**FIGURE 1-10B** Chest CT (lung window) shows bilateral, right greater than left, subpleural lower lobe consolidation with air bronchograms. There is no pleural effusion. Incidental note is made of a calcified paraesophageal lymph node.

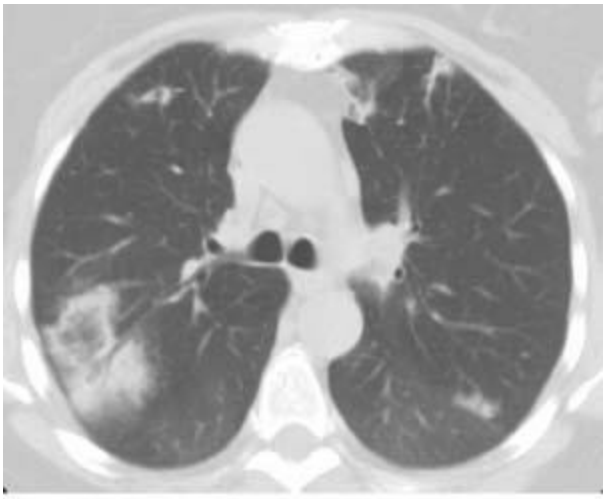

C

**FIGURE 1-10C** Chest CT (lung window) shows a focus of nodular ground glass opacity within the right lower lobe; this ground glass opacity is surrounded by a rim of consolidation (the "reversed halo" sign). Additional small foci of ground glass opacity and consolidation are present bilaterally. The anterior left upper lobe foci are subpleural in distribution.

## DIFFERENTIAL DIAGNOSIS

**Cryptogenic organizing pneumonia (COP):** This is the most likely diagnosis, given the patient's symptoms as well as the CT findings of peripheral consolidation and the "reversed halo" sign.

**Atypical pneumonia:** Atypical infections such as TB and invasive fungal infections may cause multifocal consolidation and have been described as resulting in the "reversed halo" sign on CT. However, in this case, the clinical history would make these infections much less likely.

**Eosinophilic pneumonia:** Although chronic eosino-philic pneumonia should be considered in the differential for subpleural consolidation, it usually manifests with peripheral, upper lobe consolidation that parallels the chest wall. Furthermore, to date, eosinophilic pneumonia has not been described as a cause of the "reversed halo" sign.

**Wegener's granulomatosis:** A vasculitis can cause constitutional symptoms, pulmonary nodules, and the "reversed halo" sign on CT. Pulmonary hemorrhage from Wegener's granulomatosis may result in multifo-cal consolidation with air bronchograms. However, the absence of hemoptysis or epistaxis in this case would make a diagnosis of Wegener's granulomatosis unlikely.

**Alveolar sarcoidosis:** While this is a differential consideration for chronic air space opacities and has been described as a cause of the "reversed halo" sign, the age of the patient, the clinical signs and symptoms, and the lack of adenopathy argue against

sarcoidosis.

- **Multifocal bronchioalveolar carcinoma (BAC):** Bron-chioloalveolar cell carcinoma may result in chronic, multifocal ground glass, nodules, and consolidation, and the regions of consolidation may demonstrate air bron-chograms. However, BAC has not yet been described as resulting in the "reversed halo" sign. Additionally, the clinical history would favor COP over BAC.
- **Pulmonary lymphoma:** Again, although the presence of consolidation and nodules may be consistent with lymphoma, the clinical history and the presence of the "reversed halo" sign makes COP more likely.

## DIAGNOSIS

**Cryptogenic organizing pneumonia (COP)**

## KEY FACTS

### Clinical

- Organizing pneumonia is caused by a loose plug of connective tissue within distal small airways with resultant chronic inflammation of the adjacent lung parenchyma. Histologically, this is known as bronchiolitis obliterans organizing pneumonia (BOOP). Fifty percent of cases of BOOP are idiopathic; the remainder are associated with collagen vascular disease, drug toxicity, toxic fume exposure, infection, radiation therapy, or recurrent aspiration.
- Idiopathic BOOP is known as COP. It manifests as a sub-acute illness with cough, dyspnea, and low-grade fever.
- Restrictive abnormalities on pulmonary function testing are common.
- COP responds well to steroids and has a good prognosis.

### Radiologic

- COP manifests with multifocal air space consolidation. These are typically peripheral and subpleural in distribution but may also be bronchocentric.
- Less common manifestations include small nodules or irregular linear opacities.
- The "reversed halo" or "atoll" sign on CT is a focal rounded area of ground glass surrounded by a complete or near-complete ring of consolidation. It was originally described as a rare but specific finding in COP, but subsequently has been described in a variety of other conditions such as sarcoidosis, TB, zygomyco-sis, and paracoccidioidomycosis.
- Ground glass is seen in approximately 60% of patients, and is usually associated with regions of consolidation.

- Bronchiectasis and bronchial wall thickening are common in the regions of consolidation.
- Pleural effusions are seen in approximately 20% of cases.

## SUGGESTED READING

Johkoh T. Imaging of idiopathic interstitial pneumonias. Clin Chest Med 2008;29:133–147.

Silva CIS, Muller NL. Idiopathic interstitial pneumonias. J Thorac Imaging 2009;24:260–273.

# CASE 11

**LAURA E. HEYNEMAN**

## HISTORY

A 40-year-old woman with progressive dyspnea.

A

**FIGURE 1-11A** Posteroanterior chest radiograph. There is marked hyperinflation with hyperlucency and attenuated vessels within the lower lungs bilaterally. Bands of subsegmental atelectasis are present in the bilateral infrahilar regions.

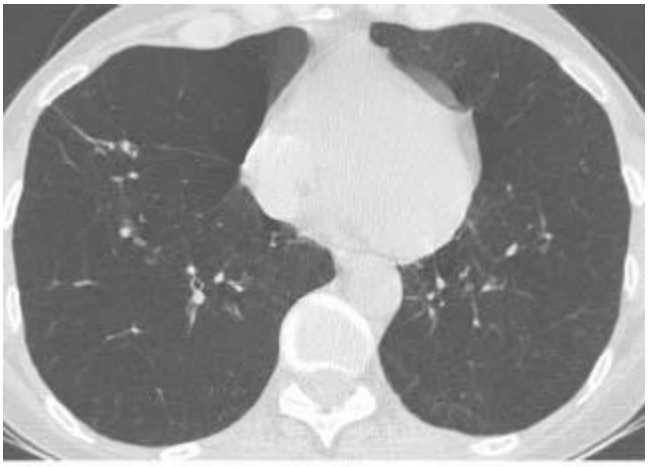

B

**FIGURE 1-11B** HRCT image through the lower lungs reveals uniform destruction of the pulmonary lobules, with widespread areas of decreased lung attenuation. A few regions of hyperlucency are outlined by interlobular septa.

## DIFFERENTIAL DIAGNOSIS

**Panlobular (PL) emphysema secondary to alpha-1-antitrypsin disease (A1AD):** This is the best diagnosis given the radiographic findings of increased lung volumes and attenuation of vessels that is most marked in the lung bases, combined with the HRCT findings of diffuse basilar hyperluency with small associated vessels. There are no discrete walls surrounding the hyperlucencies to suggest the presence of discrete air cysts. PL emphysema is often associated with A1AD.

**Centrilobular (CL) emphysema:** This is not the best diagnosis since CL emphysema tends to affect the upper lobes preferentially, and on HRCT, CL emphysema initially manifests as focal (2 to 10 mm) lucen-cies surrounding a spared core lobular artery. In the images provided, the lucencies are not centered around a centrilobular vessel; rather the lung simply appears diffusely lucent.

**Pulmonary histiocytosis X (PHX):** This is unlikely because the air "cysts" of PHX have well-defined walls that displace normal vessels, and are usually located predominantly in the upper lobes with sparing of the lower lungs and costophrenic angles.

**Lymphangiolieomyomatosis (LAM):** This is unlikely because the air "cysts" of LAM have thin well-defined walls that displace normal vessels. There is no zonal predominance of the cysts in LAM.

## DIAGNOSIS

**Panlobular emphysema due to alpha-1-antitrypsin deficiency**

## KEY FACTS

### Clinical

- Alpha-1-antiprotease (A1A) inhibits proteolytic enzymes such as trypsin, elastase, and collagenase that can cause emphysema. Patients with low levels of A1A are at risk for early onset of emphysema, and the risk is increased in smokers.
- A1A deficiency (A1AD) is an autosomal recessive disease. Homozygotes have 10% to 15% of the normal A1A levels, and heterozygotes have 60%.
- Almost all homozygotes develop early-onset emphysema (age 35 to 50 years). Smokers present 10 years earlier. Heterozygotes can develop emphysema in the presence of other risk factors.
- Histologically, in A1AD, the emphysema is PL in type, and the findings are most marked in the lower lungs. PL (also known as panacinar) emphysema is characterized by uniform dilation of the airspaces from the terminal bronchiole to the alveoli. Therefore, the entirety of the secondary pulmonary lobule is affected rather than simply the CL region (as seen in CL emphysema).
- There is an association between A1AD and cirrhosis.
- Cigarette smoking usually results in CL emphysema, but it can also cause PL emphysema, even without an underlying A1A deficiency. Another rare cause of PL emphysema is intravenous Ritalin abuse.

### Radiologic

- Radiographic evidence of PL emphysema is seen in up to 80% of homozygous A1AD patients.
- Because the entire secondary pulmonary lobule is affected by PL emphysema, on HRCT images of PL emphysema, the lungs look uniformly hyperlucent. The lungs may appear to have simply "vanished." Occasionally, the regions of hyperlucency may be outlined by thin polygonal interlobular septa. The vessels in the regions of emphysema are small and often the airways are diminutive.
- PL emphysema is distinguished from cystic lung diseases (such as LAM or PHX) by the absence of definable walls surrounding the hyperlucencies. The lucencies in patients with true cystic lung disease demonstrate perceptible walls. Additionally, in patients with cystic lung disease, the pulmonary vessels are displaced by the air cysts. The vessels in the regions of PL emphysema are small but course normally through the lucencies.
- In A1AD, the lower lungs are affected in 98% of cases and are the only site of disease in 24%.

- Bullae are less common in PL emphysema than in CL emphysema.

## SUGGESTED READING

Litmanovich D, Boiselle PM, Bakier AA. CT of pulmonary emphysema—current status, challenges, and future directions. Eur Radiol 2009;19: 537–551.

Pipavath SNJ, Schmidt RA, Takasugi JE, Godwin JD. Chronic obstructive pulmonary disease: radiology-pathology correlation. J Thorac Imaging 2009;24:171–180.

# CASE 12

**LAURA E. HEYNEMAN**

## HISTORY

A 23-year-old woman with chronic sinusitis and recurrent respiratory infection.

A

**FIGURE 1-12A** Posteroanterior chest radiograph. The cardiac apex, aortic arch, and gastric bubble are all right-sided, consistent with situs inversus totalis. Within the lungs, there are bilateral reticular and small nodular opacities that are most marked within the lower lobes. Additionally, there is suggestion of mild bronchial wall thickening and "tram tracking" within the lower lungs.

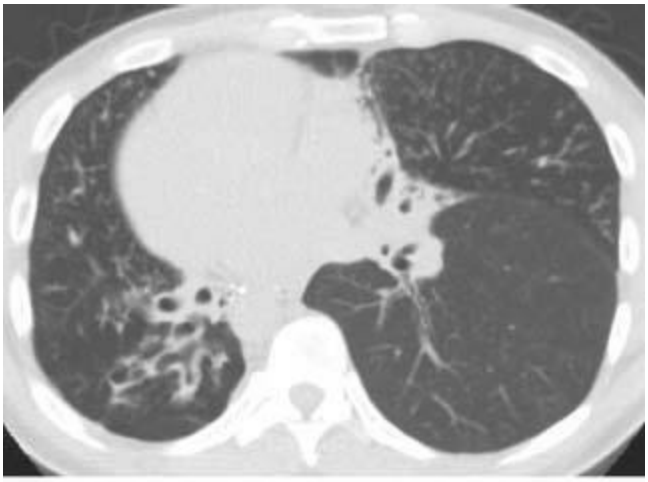

B

**FIGURE 1-12B** Chest CT (lung window) of the lower lungs reveals dextrocardia as well as multifocal cylindrical and varicoid bronchiectasis. There are multiple foci of "tree in bud" centrilobular nodules from mucoid impaction within the dilated small airways. There is consolidation, bronchiectasis, and volume loss within the left middle lobe.

## DIFFERENTIAL DIAGNOSIS

**Primary ciliary dyskinesia (PCD):** The clinical history and radiologic findings of basilar bronchiectasis, mucoid impaction, and situs inversus totalis make this the most likely diagnosis. The presence of situs inversus totalis in a patient with PCD is suggestive of Karta-gener's syndrome.

**Cystic fibrosis (CF)**: While CF is a strong differential consideration for the cause of bronchiectasis in a young patient, it tends to involve the upper lobes to a greater extent than the lower lobes. Additionally, there is no association between CF and situs inversus totalis. Therefore, this diagnosis is unlikely.

**Allergic bronchopulmonary aspergillosis (ABPA)**: ABPA typically manifests with cylindrical or saccular central (not peripheral) bronchiectasis, often associated with large foci of central mucoid impaction. Also, ABPA preferentially involves the upper lobe bronchi. There is no association between ABPA and situs inver-sus totalis, making this diagnosis unlikely.

**Postinfectious bronchiectasis**: Repeated bouts of pneumonia from an immunodeficiency may result in bronchiectasis, and the bronchiectasis may be most prominent in the bases. Similarly, prior childhood viral pneumonia (adenovirus, measles), repeated aspiration, or prior necrotizing pneumonias can also result in basilar bronchiectasis. However, sequela of prior infection or repeated infections from an immunodeficiency is not the most likely diagnosis in this case given the presence of

situs inversus totalis.

# DIAGNOSIS

**Primary ciliary dyskinesia (Kartagener's syndrome)**

# KEY FACTS

## Clinical

Symptoms of bronchiectasis include chronic cough, excess sputum production, and recurrent pulmonary infection.

- Hemoptysis occurs in 50% of patients with bronchiecta-sis, usually due to bronchial artery hypertrophy.
- Aggressive medical therapy has largely obviated the need for surgical resection of lobes affected by bron-chiectasis.
- PCD is a genetic disease that results from a genetic defect in the dynein arms of the cilia. This causes abnormal ciliary structure and function, and results in bronchiectasis, chronic sinusitis, chronic ear infections, and infertility.
- Fifty percent of patients with PCD have situs inversus. Kartagener's syndrome is composed of the triad of situs inversus, bronchiectasis, and chronic sinusitis.

## Radiologic

- Radiographic findings of bronchiectasis include parallel lines (tram tracks), ring shadows, and mucus plugs.
- On a radiograph, the walls of the dilated bronchi may appear as reticular opacities. Foci of mucoid impaction within regions of saccular bronchiectasis may appear nodular. Therefore, bronchiectasis can result in both reticular and nodular opacities, and can be considered in the differential for both radiographic patterns.
- CT, especially HRCT, is more sensitive than chest radiography in the detection of bronchiectasis.
- CT findings of bronchiectasis include bronchial wall thickening and the signet ring sign, in which the bronchus is larger than the adjacent pulmonary artery. Other CT signs include lack of tapering of the bronchus and visualization of a bronchus (bronchiole) within 1 cm of costal pleura or abutting mediastinal pleura.
- The distribution of the bronchiectasis can suggest an etiology. Central bronchiectasis suggests ABPA. Upper lobe bronchiectasis suggests mycobacterial infection or cystic fibrosis. Basilar disease suggests postinfection bronchiectasis, immune deficiencies, or PCD.

## SUGGESTED READING

Javidan-Nejad C, Bhalla S. Bronchiectasis. Radiol Clin North Am 2009;47: 289–306.

O'Donnell AE. Bronchiectasis. Chest 2008;134:815–823.

# CASE 13

**LAURA E. HEYNEMAN**

## HISTORY

An asymptomatic 65-year-old woman with a remote history of coronary artery bypass grafting presents to her cardiologist for an annual evaluation.

A B

■**FIGURES 1-13A and 1-13B** Posteroanterior **(A)** and lateral **(B)** chest radiographs reveal a round nodular opacity within the left lower lobe. The nodule projects as a well-defined nodular opacity over the left heart on the frontal view, and as a more ill-defined opacity within the posterior lower lobe on the lateral. There is subtle evidence of volume loss within the left lower lobe and blunting of the posterior left costophrenic angle.

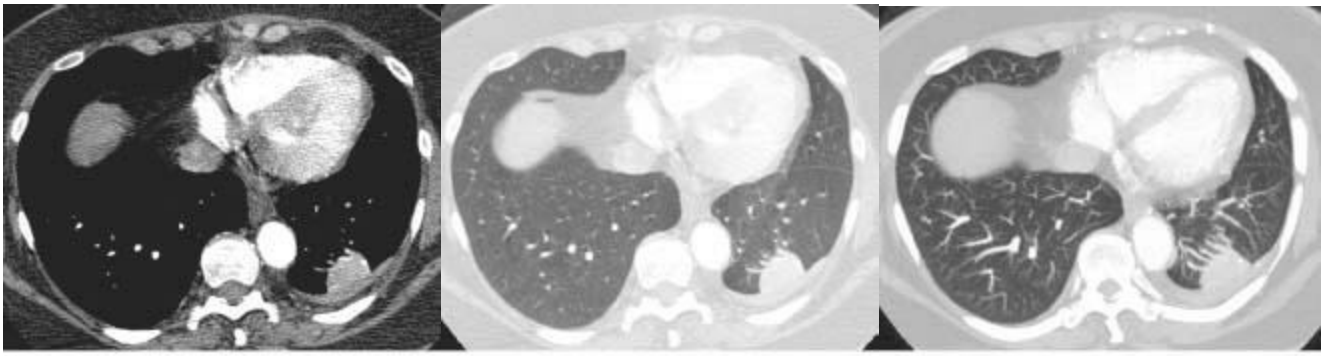


**FIGURE 1-13C, 1-13D and 1-13E** Axial CT images (soft tissue window, **C;** and lung window, **D)** and maximum intensity projection (MIP) image (lung window, **E)** from a contrast-enhanced CT reveals a focus of pleural thickening within the posterior left pleural space. A rounded soft tissue focus of mass-like consolidation abuts the pleural thickening. Several bronchovascular bundles are identified swirling into the mass-like consolidation. Incidental note is also made of a punctate calcification within the lateral aspect of the mass. The lung window images **(D** and **E)** accentuate the convergence of the brochovascular bundles into the mass-like focus of consolidation (the "comet tail" sign).

## DIFFERENTIAL DIAGNOSIS

**Round atelectasis:** This is the favored diagnosis due to the fact that the mass abuts abnormal pleura, there is evidence of associated volume loss, and the broncho-vascular bundles within the adjacent lung converge on the mass with a swirled appearance.

**Bronchogenic carcinoma:** Lung cancer must be considered whenever there is a pulmonary parenchymal mass. However, round atelectasis is favored over bron-chogenic carcinoma given that all of the CT findings characteristic of round atelectasis are present.

**Pulmonary infarct:** Infarcts may cause peripheral, sub-pleural consolidation. However, infarcts tend to be wedge-shaped rather than round. While occluded arteries may course into a region of infarction, the vessels adjacent to an infarct should not exhibit a swirled appearance. Furthermore, the clinical history, particularly the fact that the patient is asymptomatic, would make a diagnosis of pulmonary infarction very unlikely.

**Organizing pneumonia:** Organizing pneumonia may result in peripheral consolidation. It is often multifo-cal, and may demonstrate the "reversed halo" or "atoll" sign on CT, whereby the consolidation surrounds a central focus of ground glass. Organizing pneumonia does not result in atelectasis and generally does not distort the adjacent parenchyma so that there is no convergence of the adjacent bronchovascular bundles onto the mass. Therefore, the presence of atelectasis and the "comet tail" sign in this

case makes organizing pneumonia an unlikely diagnosis.

# DIAGNOSIS

**Round atelectasis**

# KEY FACTS

## Clinical

- Round atelectasis is a mass-like form of chronic atelec-tasis that occurs adjacent to a region of chronic pleural thickening.
- Patients are usually asymptomatic, with a mass discovered incidentally on a radiograph or CT.
- The cause of round atelectasis is unclear. The original theory suggests that round atelectasis results from a pleural effusion that compresses the adjacent lung parenchyma. The atelectatic lung is then fixed in place by a pleural fibrinous exudate. As the pleural effusion resolves, the atelectatic lung folds in on itself and is engulfed by the re-expanding adjacent normal lung.
- The second theory regarding the etiology of round atelectasis suggests that the primary culprit is pleural fibrosis, without an initial pleural effusion that causes passive atelectasis. The pleural fibrosis adheres to the lung; as it contracts, the lung collapses on itself.
- Round atelectasis is most commonly associated with the benign pleural abnormalities caused by prior asbestos exposure. However, any chronic pleural thickening may result in round atelectasis, and round atelectasis has been reported in association with a multitude of pleural processes including chronic empyemas, hemothorax, and uremic pleuritis. Round atelectasis can also be associated with mesothelioma.

## Radiologic

- The most common radiographic finding of round atel-ectasis is a peripheral nodular or mass-like opacity. The pleural abnormality adjacent to the mass may or may not be radiographically apparent. There may be evidence of volume loss such as hilar or fissural displacement.
- The pleural abnormality is often more conspicuous on CT than on the radiograph.
- On CT, there are four findings that are characteristic of round atelectasis. These findings include a rounded shape to the mass; the mass abuts a pleural abnormality; there must be evidence of atelectasis (usually manifested by fissural displacement); and the broncho-vascular bundles of the normal adjacent lung must converge toward the mass in a swirling pattern (the “comet tail” or “parachute cord” sign).

- If all four CT findings of round atelectasis are not present, the mass must be considered indeterminate for malignancy and further follow-up or workup is required.
- In situations where not all four CT findings are present, FDG-PET imaging can be considered for further characterization. Round atelectasis is either not metabolically active or only mildly hypermetabolic on FDG-PET scans.
- Over time, round atelectasis may remain stable in size or increase in size. It rarely resolves.
- Percutaneous biopsy is rarely required but has been performed to exclude malignancy in situations where the mass increases in size and is mildly hypermetabolic on FDG-PET imaging.

## SUGGESTED READING

Roach HD, Davies GJ, Attanoos R, et al. Asbestos: when the dust settles. An imaging review of asbestos-related disease. Radiographics 2002;22:S167–S184.

Yi E, Aubry MC. Pulmonary pseudoneoplasms. Arch Pathol Lab Med 2010;134:417–426.

# CASE 14

**LAURA E. HEYNEMAN**

### HISTORY

A 12-year-old boy on steroids for rheumatoid arthritis presents with weight loss, fever, malaise, and nonproductive cough.

A

■**FIGURE 1-14A** Posteroanterior chest radiograph. There are bilateral and diffuse 1- to 3-mm pulmonary nodules; the nodules are slightly more numerous in the lower lungs. There is a calcified nodule overlying the right anterior second rib as well as a calcified lymph node in the right tracheobronchial angle. The calcifications suggest previous exposure to a granulomatous infection such as tuberculosis. There is no lymphadenopathy, consolidation, cavitation, or pleural effusion.

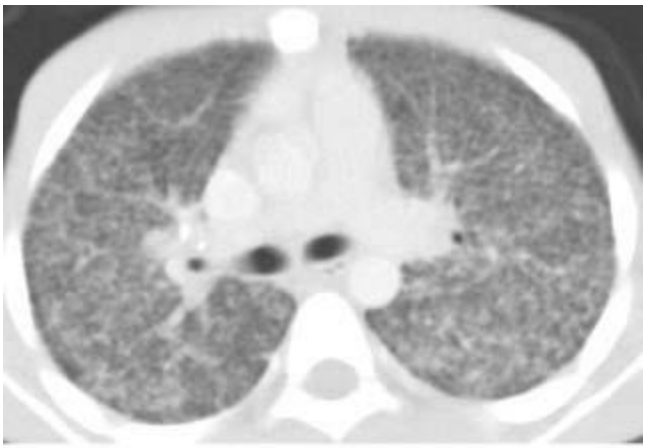

B

■**FIGURE 1-14B** Contrast-enhanced chest CT (lung window) confirms the radiographic finding of innumerable 1- to 3-mm pulmonary nodules. There are two calcified right hilar lymph nodes.

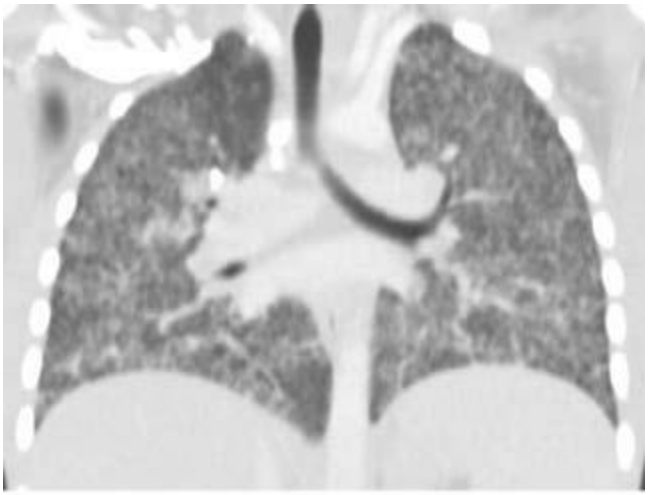

C

**FIGURE 1-14C** Coronal reformat from contrast-enhanced chest CT (lung window) demonstrates the symmetric, diffuse distribution of the pulmonary nodules. There are calcified mediastinal lymph nodes and a calcified nodule in the right suprahilar region. Incidental note is made of contrast within the right subclavian vein.

## DIFFERENTIAL DIAGNOSIS

- **Disseminated (miliary) tuberculosis (TB):** The clinical and radiologic findings are most consistent with this diagnosis.
- **Disseminated fungal infection:** The radiologic findings are also consistent with disseminated histoplasmosis, coccidioidomycosis, blastomycosis, or cryptococcosis. Disseminated fungal infection most commonly occurs in immunocompromised patients but is less common than miliary TB, and is not considered a public health risk.
- **Sarcoidosis:** The absence of significant intrathoracic adenopathy makes this a less likely diagnosis.
- **Metastatic disease:** Metastatic nodules are usually more variable in size. Furthermore, the patient history makes this diagnosis very unlikely. Primary malignancies that can present with miliary nodules include thyroid, breast, and pancreatic carcinoma as well as melanoma.
- **Silicosis:** While silicosis and coal worker's pneumo-coniosis can cause miliary nodules, the nodules are usually upper lobe predominant. Furthermore, the patient's age and history makes the diagnosis of silico-sis extremely unlikely.
- **Hypersensitivity pneumonitis (HP):** The radiographs of patients with subacute HP are most often normal or demonstrate subtle ground glass opacities. However, miliary nodules can be a manifestation of HP. The nodules may be slightly more prominent within the upper lungs. Furthermore, this patient's age and clinical history makes this very unlikely.

# DIAGNOSIS
**Miliary tuberculosis**

# KEY FACTS
## Clinical
- Miliary TB is due to systemic hematogenous extension of the mycobacterial infection. This hematogenous dissemination occurs in 2% to 6% of patients with primary TB, but may also occur in the setting of postprimary infection.
- Miliary TB is more frequent in young children (<2 years), the elderly, and immunocompromised patients.
- Miliary dissemination usually occurs within 6 months of the primary infection.
- Given its systemic dissemination, miliary TB often involves multiple organ systems.
- In two-thirds of the patients with miliary TB, the sputum is negative for acid fast bacilli. Diagnosis may require transbronchial or open lung biopsy, or biopsy of a different involved organ.

## Radiologic
- As the nodules may not be radiographically visible until 6 weeks after dissemination, the radiograph is often normal at the onset of symptoms.
- Once a radiographic abnormality develops, miliary TB manifests with diffuse 1- to 3-mm nodules. The nodules may have a slight predominance in the lower lobes given the hematogenous route of dissemination.
- When associated with primary TB infection, the mili-ary dissemination usually occurs within 6 months of the primary infection.
- When associated with postprimary TB infection, the miliary nodules may be seen in conjunction with cavi-tary consolidation or may be the only manifestation of the disease.
- In 15% of patients, the distribution is asymmetric.
- On high-resolution CT, the nodules usually have a random distribution. Therefore, nodules are seen in both CL and perilymphatic locations.
- Intrathoracic adenopathy is seen in 95% of children but only 12% of adults.
- Associated consolidation is seen in 42% of children and 12% of adults.
- Response to appropriate antituberculous therapy is typically rapid, with radiographic resolution within 4 to 6 weeks. Resolution of the miliary nodules is complete; they do not calcify, unlike the Ghon foci of primary TB.

## SUGGESTED READING

Andronikou S, Vanhoenacker FM, De Backer AI. Advances in imaging chest tuberculosis: blurring of differences between children and adults. Clin Chest Med 2009;30:717–744, viii.

Jeong YJ, Lee KS. Pulmonary tuberculosis: up-to-date imaging and management. Am J Roentgenol 2008;191:834–844.

# CASE 15

**LAURA E. HEYNEMAN**

## HISTORY

A 45-year-old homeless woman presents with fever, weight loss, and productive cough

A

■**FIGURE 1-15A** Posteroanterior chest radiograph. There is extensive bilateral apical consolidation with multiple foci of cavita-tion. There is bronchiectasis within the right upper lobe. Ill-defined heterogeneous opacity is present within the left mid lung.

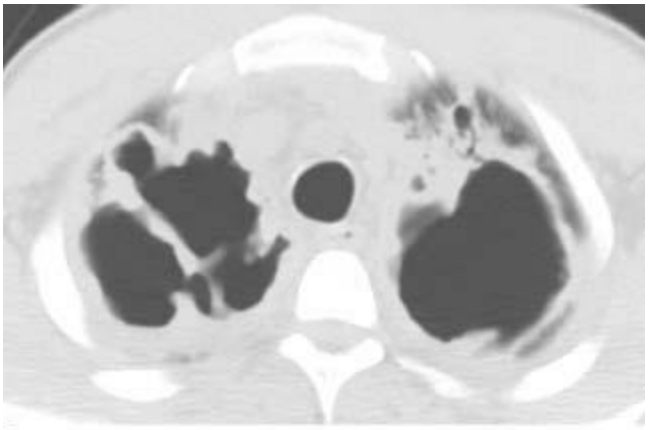

B

**FIGURE 1-15B** Chest CT (lung window) through the apices shows bilateral thick-walled cavities. There is adjacent consolidation with additional cavitation or bronchiectasis within the left apex.

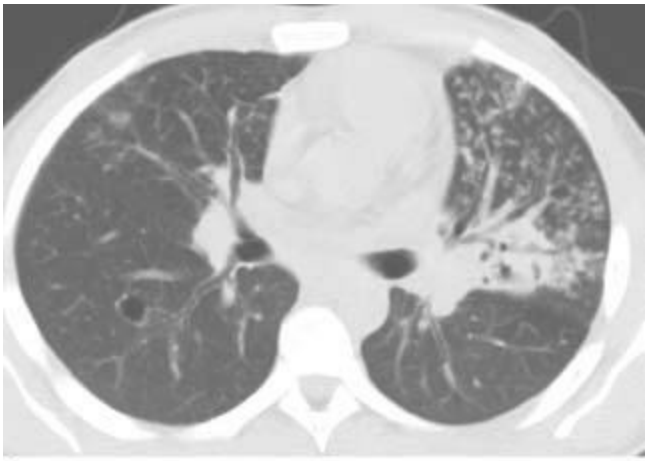

C

**FIGURE 1-15C** CT (lung window) through the mid portion of the lungs. There are multiple branching centrilobular nodules in the lingula, consistent with a "tree-in-bud" pattern. The lingula also demonstrates consolidation with ucencies suggestive of cavitation or bronchiectasis. There is a small cluster of nodules in the right middle lobe, and a small cavity within the superior segment of the right lower lobe.

## DIFFERENTIAL DIAGNOSIS

**Pneumonia, particularly from postprimary TB**: Postprimary TB is the diagnosis of exclusion given the cavitary consolidation within the apices as well as the airway disseminated nodules suggestive of endobron-chial spread of infection. While cavitary consolidation can result from other necrotizing bacterial infections such as *Staphylococcus aureus, Klebsiella, Pseudomo-nas*, and *Proteus* species, the public health concerns associated with *Mycobacterium tuberculosis* require that the patient be isolated until infection by TB is excluded.

- **Aspiration:** If partially digested food particles are aspirated rather than infectious material, the result is usually bilateral, multilobar, poorly defined consolidation that resolves without treatment in approximately 48 hours. However, if anaerobic bacteria or gram-negative rods are aspirated, the result may be a necro-tizing pneumonia that appears as cavitary consolidation on the radiograph. Either type of aspiration may cause "tree in bud" nodules on CT; this finding is simply suggestive of an airway disseminated process that is filling the small airways. Aspiration, generally, involves the portions of lung that are dependent when the aspiration occurs. When a patient is upright, aspiration generally affects the lung bases, but when the patient is supine, the superior segment of the lower lobe and the apical and posterior segments of the upper lobe are most frequently involved. Of note, these are the same segments that are most frequently affected by postprimary TB. Multiple sputum cultures may be required to distinguish aspiration pneumonia from postprimary TB.
- **Wegener's granulomatosis:** Pulmonary consolidation occurs in approximately 30% of patients with Wegen-er's granulomatosis and may be scattered and heterogeneous, or homogeneous and lobar. However, discrete pulmonary nodules that may cavitate are the most common radiographic abnormality. Patients with Wegener's granulomatosis usually present with hemoptysis as well as upper respiratory involvement (i.e., sinusitis), and therefore this diagnosis would not be favored.
- **Pulmonary malignancy:** Patients with a central, obstructing endobronchial neoplasm may develop a postobstructive pneumonia that can cavitate. Frequently, there may be associated volume loss, and CT would demonstrate the central endobronchial lesion. Invasive mucinous adenocarcinoma (formerly called bronchioloalveolar cell carcinoma, or BAC) may present as lobar consolidation, but cavitation is an infrequent finding in that entity.

# DIAGNOSIS

**Postprimary TB (drug-resistant strain)**

# KEY FACTS

## Clinical

- Postprimary TB usually occurs due to reactivation of dormant bacilli, although some cases may be due to reinfection of a previously sensitized host.
- The highest incidence of postprimary TB is in patients >65 years of age.
- Reactivation most commonly occurs in the apical/posterior segments of the upper lobes and superior segments of the lower lobes.
- Because of host hypersensitivity acquired from primary infection, progressive disease

with caseous necrosis occurs and can rapidly destroy the lung.

- Most patients have a delayed cutaneous response to the intradermal injection of purified protein derivative (PPD).
- Patients suspected of having postprimary TB must be isolated until two or three sputum samples are negative for acid fast bacilli. However, only 40% of patients with postprimary TB have sputum that is positive for acid-fast bacilli, and the growth of the bacterium in culture may take 2 weeks.
- Novel methods for more rapid diagnosis of TB in sputum or bronchoalveolar lavage samples have been developed, including nucleic acid amplification tests.
- The development of multidrug resistant strains of *M. tuberculosis* is a major worldwide public health concern due to the ineffectiveness of existing chemotherapeutic agents and a resultant high mortality rate.

## Radiologic

- The earliest radiographic findings of postprimary TB are heterogeneous, poorly marginated opacities in the apical or posterior segments of the upper lobes, or in the superior segments of the lower lobes.

- The initial opacities usually evolve into more well-defined reticular and nodular opacities.
- The infection may occasionally progress to lobar or complete lung consolidation.
- Cavitation is common (40% to 87%) and typically occurs within areas of consolidation. Air-fluid levels may be present within the cavities.
- A complication of cavitation is endobronchial spread of infection into distal small airways throughout the lung.
- On HRCT, endobronchial dissemination is most often manifest by branching, Centrilobular “tree-in-bud” nodules.
- The presence of cavitation and “tree-in-bud” nodules is suggestive of active, communicable disease.
- Miliary TB occurs less commonly in postprimary than in primary TB, and the classic radiographic findings are diffuse, small (1 to 3 mm), well-defined nodules.
- In approximately 5% of patients, postprimary TB manifests as a solitary pulmonary nodule, a tuberculoma. These may mimic lung cancer; furthermore, because tuberculomas contain active inflammation, they may be hypermetabolic on FDG-PET scans.
- Pleural effusions occur in approximately 15% to 20% of patients, and are usually unilateral. Rarely, a pleu-ral effusion may be the only manifestation of postpri-mary TB.
- In immunocompetent adults, postprimary TB rarely results in hilar or mediastinal lymphadenopathy. Lymphadenopathy in an adult with reactivation TB is more common in the setting of immunosuppression, particularly in patients who are HIV positive with a CD4 count of <200 cells/uL.
- The radiologic findings of drug-resistant *M. tuberculosis* infection are similar to those of drug-sensitive infection, although the presence of multiple cavities and extensive bronchiectasis (which is suggestive of chro-nicity) is more common in the resistant strains. This is exemplified by the findings in this patient in whom there are multiple cavities and regions of severe bron-chiectasis; this patient was infected with a strain of *M. tuberculosis* that was resistant to multiple traditional chemotherapeutic agents.
- Healing from postprimary TB may be associated with scarring, cicatricial atelectasis, traction bronchiectasis, residual nodules, and parenchymal calcification. The cavities may either resolve or remain stable in size.

## SUGGESTED READING

Jeong YJ, Lee KS. Pulmonary tuberculosis: up-to-date imaging and management. Am J Roentgenol 2008;191:834–844.

Tan CH, Kontoyiannis DP, Viswanathan C, Iyer RB. Tuberculosis: a benign imposter. Am J Roentgenol 2010;194:555–561.

# CASE 16

**LAURA E. HEYNEMAN**

## HISTORY

A 45-year-old woman with cough, chronic weight loss, and no history of fever.

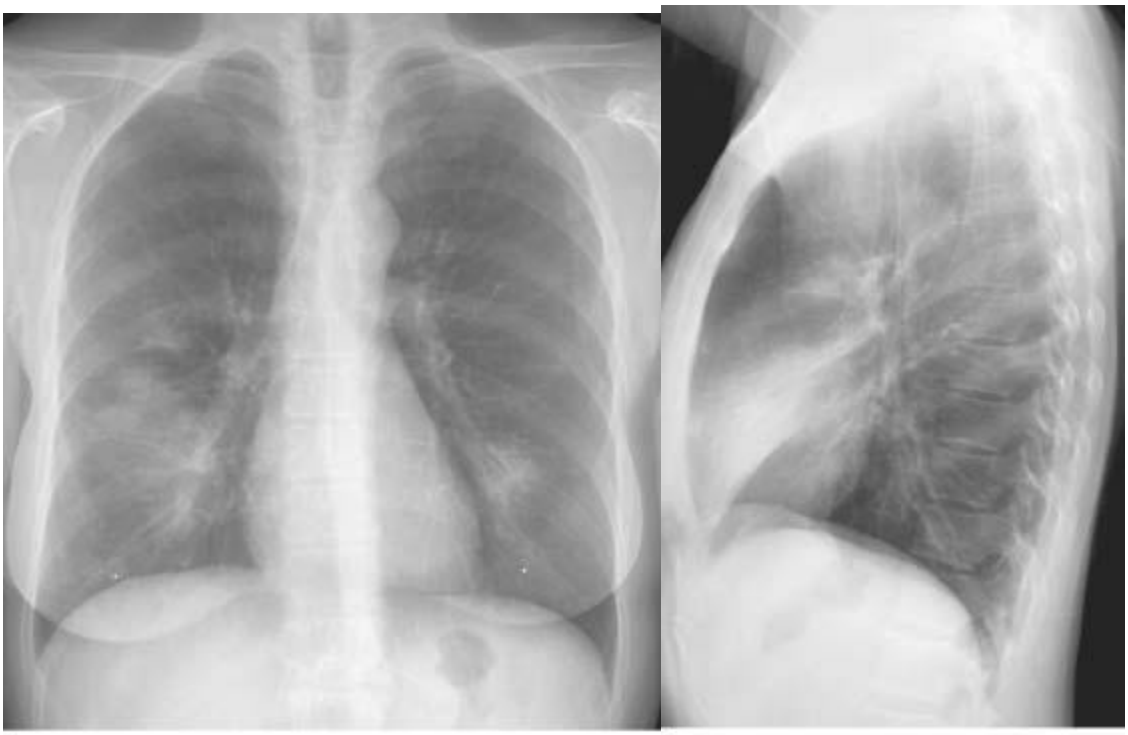


■**FIGURES 1-16A and 1-16B** Posteroanterior and lateral chest radiographs. There is homogeneous consolidation in the right middle lobe and, to a lesser extent, the lingula. No hilar or mediastinal adenopathy is present. Incidental note is made of nipple markers on the frontal radiograph.

C

**FIGURE 1-16C** Chest CT (lung window) through the lower lungs, obtained several weeks after the radiograph. There is homogeneous consolidation without cavitation throughout the majority of the right middle lobe and portions of the lingula. Air bronchograms are present within the right middle lobe consolidation.

## DIFFERENTIAL DIAGNOSIS

**If the findings are acute and/or resolve on follow-up imaging**:

**Pneumonia:** Lobar consolidation is usually caused by bacterial infection. Organisms include *Streptococcus pneumoniae, Staphylococcus aureus, Legionella pneu-mophila*, gram-negative bacteria, and *M. tuberculosis*. A bacterial infection is unlikely with a history of chronic weight loss and no fever, although TB or fungal infections (e.g., blastomycosis) can have subacute presentations. As TB or fungal infections such as blastomycosis can cause consolidation that does not resolve with standard antibiotic therapy, they should be differential considerations in this patient.

**Aspiration pneumonia:** Aspiration of gram-negative or anaerobic bacteria may cause lobar consolidation. Aspiration most commonly causes scattered, poorly defined consolidation or "tree-in-bud" centrilobular nodules in the dependent segments of lung. Involvement of the anterior portions of the lungs as in this patient would make this diagnosis less likely.

**If the findings are chronic and/or do not resolve on follow-up imaging**:

**Invasive mucinous adenocarcinoma [formally known as mucinous bronchioloalveolar cell carcinoma (BAC)]:** The clinical presentation and homogeneous consolidation with air bronchograms could be due to invasive mucinous adenocarcinoma. Since in this case the consolidative opacities failed to resolve on follow-up imaging, this is a strong diagnostic possibility in this patient. A histologic diagnosis, such as from lung biopsy, is necessary to confirm this diagnosis.

**Primary lymphoma of lung:** This rare non-Hodgkin's lymphoma is usually low grade,

and patients are often asymptomatic. Consolidation with air bronchograms and poorly defined margins is the most common presentation; therefore, based on the images provided, this is a diagnostic possibility in this patient. Mass-like and reticulonodular opacities are less frequent imaging appearances of this rare disease.

- **Alveolar sarcoid:** While sarcoid may cause chronic consolidation with air bronchograms, the consolidation is most often nodular in configuration. Large foci of consolidation that occupy the majority of a lobe would be unusual.
- **Exogenous lipoid pneumonia:** The aspiration of lipid containing material can result in chronic consolidation. On CT, the consolidation often contains foci of fat attenuation. However, the inflammation that results as a result of the aspiration can obscure the fat droplets; therefore, lipoid pneumonia does not always demonstrate fat attenuation on CT. As with other forms of aspiration noted above, the anterior location of the consolidation as seen in this patient would be unusual.

## DIAGNOSIS (ON BIOPSY, AFTER CONSOLIDATION FAILED TO RESOLVE)

**Invasive mucinous adenocarcinoma**

## KEY FACTS

### Clinical

- Invasive mucinous adenocarcinoma is a subtype of ade-nocarcinoma that contains tumor cells that: have a goblet morphology; contain abundant cytoplasmic mucin; and demonstrate "lepidic" growth, which means that the cells line the alveoli without distorting the underlying lung architecture.
- The 2011 classification of lung adenocarcinoma replaced the term "bronchioloalveolar cell carcinoma," or BAC, with several different subtypes of adenocarcinoma.
- Invasive mucinous adenocarcinoma was previously known as "mucinous BAC." This form of adenocarci-noma demonstrates lepidic growth but is usually multifo-cal and may involve one or more entire lobes of the lung.
- The 2011 classification of lung adenocarcinoma replaced the term "nonmucinous BAC" with three different terms. A solitary, focal adenocarcinoma that demonstrates lepidic growth but does not invade the vessels, lymphatics, or pleura is now referred to as "adenocar-cinoma in situ" (AIS). A solitary, focal adenocarcinoma that demonstrates primarily lepidic growth but shows minimal (< 5 mm) invasion of stroma is termed "minimally invasive adenocarcinoma" (MIA). A solitary, focal adenocarcinoma that demonstrates primarily lepidic growth but shows > 5 mm stromal invasion is referred to as "lepidic predominant adenocarcinoma" (LPA).

- Clinical features that distinguish invasive mucinous ade-nocarcinoma from other lung cancers are (1) younger age at presentation, (2) higher incidence in women compared to other forms of lung cancer, (3) copious watery sputum (bronchorrhea), and (4) higher incidence in nonsmokers.
- AIS, MIA, and LPA have an indolent course, with a very high 5-year survival rate. Invasive mucinous adenocar-cinoma, however, behaves more aggressively, and the 5-year survival rate is much lower.

### Radiologic

- AIS and MIA present as solitary pulmonary nodules that are purely ground glass in attenuation. These pure ground glass nodules may remain stable over long periods of time or may grow very slowly. Comparison with remote prior studies or follow- up for extended periods of time is warranted to exclude indolent growth.
- LPA presents as a solitary pulmonary nodule that is primarily ground glass in attenuation.
- When nodules that were previously purely ground glass in attenuation acquire a soft tissue component, the change is worrisome for development of invasion.
- Invasive mucinous adenocarcinoma most often presents as consolidation with air bronchograms, and radiologically may resemble pneumonia.
- In patients with chronic consolidation that is concerning for invasive mucinous adenocarcinoma, a search for findings that would suggest metastatic disease (such as adenopa-thy, pleural effusions, or adrenal masses) is warranted.

## SUGGESTED READING

Travis WD, Brambilla E, Noguchi M et al. International Association for the Study of Lung Cancer/American Thoracic Society/European Respiratory Society international multidisciplinary classification of lung adenocarcinoma. *J Thorac Oncol* 2011;6:244–85.

Patsios D, Roberts HC, Paul NS, et al. Pictorial review of the many faces of bronchioloalveolar cell carcinoma. *Br J Radiol* 2007;80:1015–1023.

# CASE 17

**LACEY**
**WASHINGTON**

### HISTORY

Asymptomatic 71-year-old man undergoes a routine annual chest radiograph.

A

■**FIGURE 1-17A** Posteroanterior chest radiograph. There is a well- circumscribed 1.5-cm nodule in the right costophrenic angle.

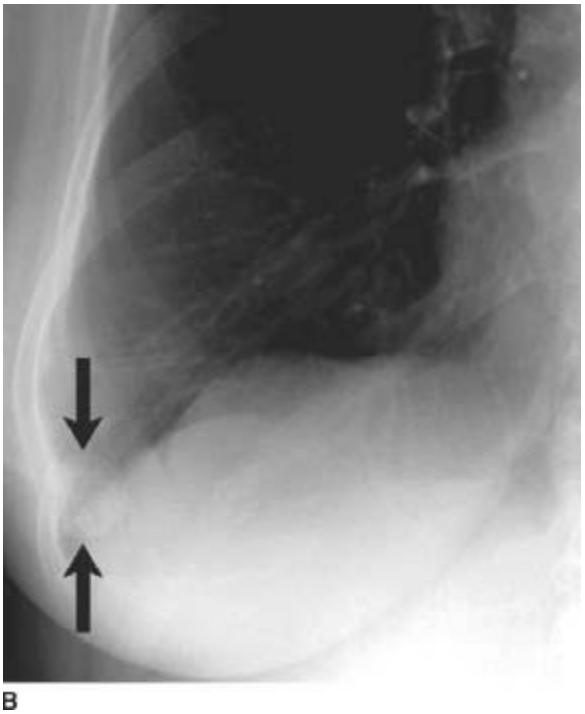

B

■**FIGURE 1-17B** Magnification of the right costophrenic angle better displays the well-circumscribed nodule (*black arrows*).

C

**FIGURE 1-17C** Noncontrast chest CT (mediastinal window). There is a right lower lobe well-circumscribed nodule that contains foci of fat attenuation (areas of density measuring – 41 HU).

## DIFFERENTIAL DIAGNOSIS

**Hamartoma:** This is the best diagnosis because of the presence of fat within the nodule as evident on CT.

**Exogenous lipoid pneumonia:** This is a differential consideration given the internal fat density on CT. However, aspiration of lipoid material (such as mineral oil) usually results in an ill-defined focus of consolidation rather than the smoothly marginated nodule, as seen in this patient.

**Tuberculoma:** Round noncalcified solitary nodules are an uncommon manifestation of parenchymal TB. They are usually encountered in asymptomatic adults. The majority (75%) occur in the upper lobes, as opposed to the lung base as seen in this patient. Additionally, tuberculomas do not contain fat density, as does the nodule in this patient.

**Malignancy:** A primary bronchogenic carcinoma or a single, isolated metastatic nodule would be differential considerations for the nodule seen on the CXR. However, metastases or primary bronchogenic carcinoma should not contain central fat density. Unless the patient has a history of a liposarcoma, the presence of internal fat density on CT excludes the diagnosis of malignancy.

**Arteriovenous malformation:** These are single in about two-thirds of cases, and may be included in the differential for a solitary pulmonary nodule. Feeding and draining vessels, which must be identified to make the diagnosis, may be difficult to visualize on

plain radiographs. While this would be a possible diagnosis based on the radiograph, the absence of a feeding artery and draining vein on CT and the presence of central fat density exclude this as a possibility.

## DIAGNOSIS

**Hamartoma**

## KEY FACTS

### Clinical

- A hamartoma is a developmental malformation of disorganized tissues that normally constitute the organ in which the tumor occurs.
- In the lung, these lesions are better regarded as benign neoplasms than as developmental malformations.
- Peak incidence is in the sixth decade, and they are uncommon in patients <30 years of age.
- Although they are uncommon pulmonary tumors, they are nevertheless the most common benign tumors of the lung.
- They occur more commonly in males, with a male to female ratio between 2:1 and 3:1.
- Pulmonary hamartomas are usually solitary, although multiple pulmonary hamartomas can occur rarely.
- Multiple hamartoma syndrome (Cowden's disease) is a rare autosomal dominant dermatosis, which is characterized by multiple mucocutaneous lesions and gastrointestinal hamartomatous polyps; hamartomas of the lung occur only rarely in this disease.

### Radiologic

- Hamartomas characteristically are well-defined solitary nodules that are usually <4 cm in diameter.
- The majority are located peripherally (90%), although occasionally they may arise in the central bronchi.
- Calcification is less commonly seen on radiographs than at pathology; the rate of calcification is variable in different series, from 5% to 50%. A popcorn pattern of calcification is considered diagnostic of hamartoma.
- The presence of fat attenuation (with or without calcification) within the mass is best demonstrated on CT, and is also a diagnostic feature. Fat may be identified by CT density in the range of -40 to -120 HU.

- Fat is not present in approximately one-third of hamartomas.
- In patients with hamartomas without diagnostic imaging features, FDG-PET scan may be helpful. Ham-artomas generally do not demonstrate significant hypermetabolism, although mild FDG activity has been described. Occasionally, when there is mild FDG activity within the nodule, a percutaneous biopsy may need to be performed in order to obviate surgical biopsy.
- In the small percentage of centrally occurring hamarto-mas, atelectasis and obstructive pneumonia may occur.

## SUGGESTED READING

Goldin JG, Brown MS, Petkovska I. Computer-aided diagnosis in lung nodule assessment. J Thorac Imaging 2008;23:97–104.

Jeong YJ, Yi CA, Lee KS. Solitary pulmonary nodules: detection, characterization, and guidance for further diagnostic workup and treatment. Am J Roentgenol 2007;188:57–68.

Truong MT, Sabloff BS, Ko JP. Multidetector CT of solitary pulmonary nodules. Radiol Clin North Am 2010;48:141-55.

# CASE 18

**LACEY**
**WASHINGTON**

### HISTORY

A 52-year-old previously healthy man presenting with a cerebral stroke.

A

**FIGURE 1-18A** Posteroanterior chest radiograph. There is an approximately 1.5-cm noncalcified nodule that projects in the left perihilar region. Two vessels appear to extend from the hilum into the nodule.

B

**FIGURE 1-18B** Oblique axial MIP image from chest CT (lung window). Well-defined, lobulated lingular nodule with enlarged feeding artery and draining vein.

## DIFFERENTIAL DIAGNOSIS

**Arteriovenous malformation (AVM):** The well-defined, lobulated contour, medial

location, and identification of feeding and draining vessels are characteristic for this diagnosis.

- **Non-small cell carcinoma:** The age of the patient and the presence of a solitary pulmonary nodule would be concerning for primary bronchogenic carcinoma. However, the presence of enlarged vessels coursing to and from the nodule would exclude the diagnosis.
- **Metastatic lung disease:** The absence of a history of primary extrathoracic malignancy would make this diagnosis less likely, although solitary metastases can occur. A so-called feeding vessel sign consisting of an artery directly entering a nodule is actually seen in only a minority of metastases, and would not explain enlargement of the artery. The findings are therefore not characteristic of metastasis.
- **Hamartoma:** The presence of enlarged vessels also excludes this diagnosis. The diagnosis can be made definitively on CT when fat, sometimes with coarse "popcorn" calcification, is seen in a nodule.

# DIAGNOSIS

**Arteriovenous malformation (AVM)**

# KEY FACTS

## Clinical

- Ten percent of cases are identified in infancy or childhood, although the vast majority are not recognized until the third and fourth decades of life.
- They are twice as frequent in women as in men.
- The AVM acts as a right-to-left shunt from the pulmonary artery to the pulmonary vein. A small shunt will not result in clinical symptoms, but if the amount of right-to-left shunting is >20% of the cardiac output, the patient may become cyanotic and develop clubbing and polycythemia.
- Patients with pulmonary AVMs are often asymptomatic. However, the most common presenting symptom is dyspnea on exertion.
- Patients may also present with neurologic complications including transient ischemic attacks, strokes, and cerebral abscesses due to paradoxical emboli across the AVM. Other presenting symptoms include hemoptysis and hemothorax.
- The most common clinical sign of a pulmonary AVM is a pulmonary bruit. The bruit may increase during inspiration and the Muller maneuver (forced inspiration through a closed glottis after full expiration) due to increased pulmonary blood flow. The bruit typically decreases during Valsalva maneuver, which decreases pulmonary blood flow.
- Because most pulmonary AVMs are located at the lung bases, preferential flow

through the low-resistance AVM circulation will increase when patients are upright. This may result in orthostatic hypoxemia (orthodeoxia).

- 60% to 90% of congenital pulmonary AVMs are associated with Osler-Weber-Rendu disease (hereditary hem-orrhagic telangiectasia). This is an autosomal dominant disorder that manifests clinically in adult life. Many of these patients have arteriovenous communications elsewhere, including the skin, mucous membranes, and other organs.
- Patients with hereditary hemorrhagic telangiectasia should be screened for pulmonary AVMs, since the absence of dyspnea and the presence of normal resting oxygen saturation do not exclude clinically significant AVMs.

### Radiologic

- The typical finding is a round, lobulated, well-defined nodule or mass, most often in the medial third of the lung and more commonly in the lower than the middle or upper lobes.
- About 33% of cases will have multiple pulmonary AVMs.
- Pulmonary AVMs range in size from less than one centimeter up to several centimeters in diameter.
- The feeding artery and draining vein are often enlarged and may be identifiable on the CXR. Chest radiography is highly specific but not sensitive for pulmonary AVMs.
- Helical CT is the imaging procedure of choice in diagnosing pulmonary AVMs, but pulmonary angiography is also routinely performed to delineate the anatomy of the feeding and draining vessels, and to allow access for embolization.
- The 3D reconstructions using helical CT data sets allow assessment of the architecture of the malformations.
- Embolization is now the preferred treatment for this condition and is performed with coils or Amplatzer plugs. Embolization is reserved for AVMs with a feeding artery that is ≥3 mm in diameter.

## SUGGESTED READING

Begbie ME, Wallace GMF, Shovlin CL. Hereditary haemorrhagic telangi-ectasia (Osler-Weber-Rendu syndrome): a view from the twenty-first century. Postgrad Med J 2003;79:18–24.

Do KH, Goo JM, Im JG, et al. Systemic arterial supply to the lungs in adults: spiral CT findings. Radiographics 2001:21;387–402.

Erasmus JJ, Connolly JE, McAdams HP, Roggli VL. Solitary pulmonary nodules: Part I. Morphologic evaluation for differentiation of benign and malignant lesions. Radiographics 2000;20:43-58.

Khurshid I, Downie GH. Pulmonary arteriovenous malformation. Postgrad Med J 2002;78:191-197.

# CASE 19

**LAURA E. HEYNEMAN**

## HISTORY

A 60-year-old construction worker presents with progressive dyspnea.


A

■**FIGURE 1-19A** Posteroanterior chest radiograph. There are bilateral suprahilar masses, the lateral borders of which parallel the chest wall. Additionally, there are multiple bilateral pulmonary nodules with upper lobe and perihilar predominance. Several of the nodules are quite dense for size and are likely calcified.

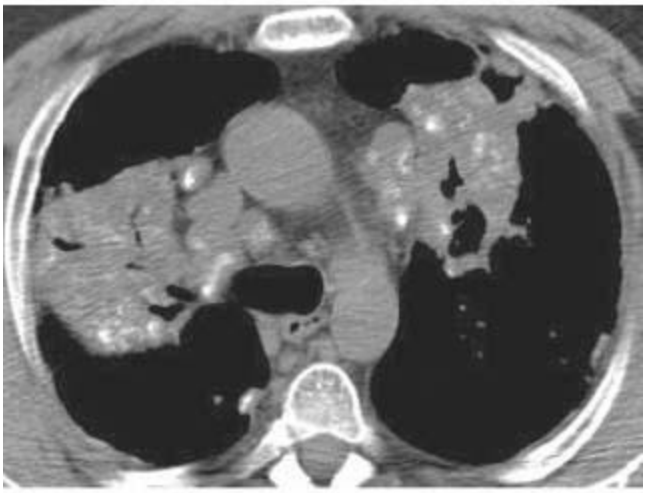

B

**FIGURE 1-19B** Axial image from noncontrasted CT (medi-astinal window) demonstrates bilateral upper lobe foci of mass-like consolidation. Multiple calcifications are present within the conglomerate suprahilar masses. Additionally, subpleural partially calcified nodules ("pseudoplaques") are present. There is also partially calcified precarinal and prevascular lymphadenopathy.

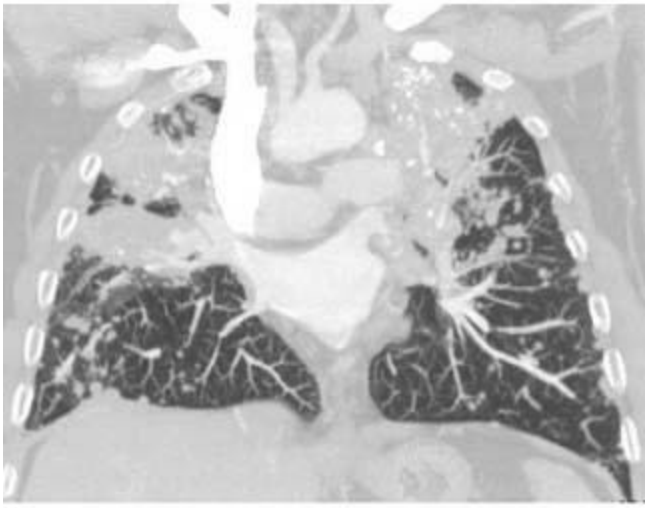

C

**FIGURE 1-19C** Coronal reformat MIP image (lung window) from a contrast-enhanced CT in a different patient with the same diagnosis reveals upper lobe conglomerate masses which contain foci of calcification. At the periphery of the masses, there are several small discrete pulmonary nodules. Small, discrete nodules are also present within the lower lobes bilaterally.

## DIFFERENTIAL DIAGNOSIS

**Silicosis:** This is the best diagnosis given the calcified mediastinal lymph nodes, the calcified pulmonary nodules, and the perihilar conglomerate masses. Coal worker's pneumoconiosis is indistinguishable radio-graphically from silicosis and should be included in the differential diagnosis.

**Sarcoidosis:** Perihilar conglomerate masses and calcified mediastinal lymph nodes can also be seen in sarcoidosis. However, calcification of the pulmonary nodules is much less common in sarcoidosis than in sili-cosis. Furthermore, this patient's clinical history makes silicosis the more likely diagnosis.

**Tuberculosis (TB)/histoplasmosis:** Calcified pulmonary nodules and conglomerate masses can result from pulmonary infection by TB or histoplasmosis. However, findings in TB or histoplasmosis tend to be unilateral or asymmetric; the bilateral symmetry, along with the clinical history, makes silicosis the more likely diagnosis in this case.

**Lymphoma:** Treated lymphoma can result in calcification of hilar or mediastinal

lymph nodes, but calcification of pulmonary nodules is unusual. Therefore, the parenchymal findings and clinical history make silicosis more likely.

## DIAGNOSIS

**Complicated silicosis with progressive massive fibrosis**

## KEY FACTS

### Clinical

- Silicosis is a chronic, nodular, and fibrotic disease caused by long-term exposure to silica.
- Typical occupational histories include construction, hard-rock mining, foundry work, and sandblasting.
- Radiographic abnormalities usually only occur after prolonged exposure, of 10 to 20 years, although an accelerated variant of the disease may occur after shorter exposures to higher concentrations of dust. Chronic and accelerated forms of the disease are histologically identical.
- A histologically distinct phenomenon, acute silicopro-teinosis, occurs after heavy exposure and can occur over a period of several months. Its clinical and radio-graphic course resembles alveolar proteinosis.
- Silicosis impairs pulmonary macrophage function and thereby increases the risk of mycobacterial infection, including TB.

### Radiologic

- Simple silicosis is characterized by multiple 1- to 10-mm nodules that predominate in the upper lobes; 20% of nodules calcify.
- Complicated silicosis is characterized by coalescence of the nodules into conglomerate opacities >1 cm in diameter. These masses, which represent areas of progressive massive fibrosis, are typically bilaterally symmetric and migrate toward the hila with time. With convergence toward the hila, paracicatricial emphysema frequently develops between the masses and the pleura.
- CT is superior to radiographs in the detection of early silicosis and in identifying other conditions that cause dyspnea, such as emphysema. It can also be helpful in the recognition of superimposed TB or lung cancer.
- On HRCT, simple silicotic nodules present as centri-lobular nodules with upper lobe predominance. Coalescence of nodules in the subpleural region may result in an appearance similar to that of pleural plaques (“pseudoplaques”).
- Mediastinal and hilar lymphadenopathy is common, and calcifications within the

lymph nodes are frequently seen. The calcifications may be central, diffuse, or peripheral ("egg shell").

- The conglomerate masses may cavitate due to ischemic necrosis. Development of TB in these cavities (silicotu-berculosis) may also occur. Other signs of TB in patients with silicosis include pleural thickening, pleural effusions, and rapid progression of consolidation.
- Caplan's syndrome (cavitary rheumatoid nodules in patients with coal worker's pneumoconiosis) can closely resemble complicated silicosis.

## SUGGESTED READING

Chong S, Lee KS, Chung MJ, et al. Pneumoconiosis: comparison of imaging and pathologic findings. Radiographics 2006;26:59–77.

Leung CC, Yew WW, Law WS, et al. Smoking and tuberculosis among silicotic patients. Eur Respir J 2007;29:745-750.

Sirajuddin A, Kanne JP. Occupational lung disease. J Thorac Imaging 2009;24:310–320.

# CASE 20

**LAURA E. HEYNEMAN**

### HISTORY

A 25-year-old HIV negative woman with a history of intravenous drug abuse presents with rigors, high fever, dyspnea, and a nonproductive cough.

A

**FIGURE 1-20A** Anteroposterior chest radiograph shows multiple bilateral nodular opacities, with confluence of the opacities within the right apex. A few of the nodules contain central lucencies suggestive of cavitation. An endotracheal tube, a nasogastric tube, and a right internal jugular central venous catheter are in place.

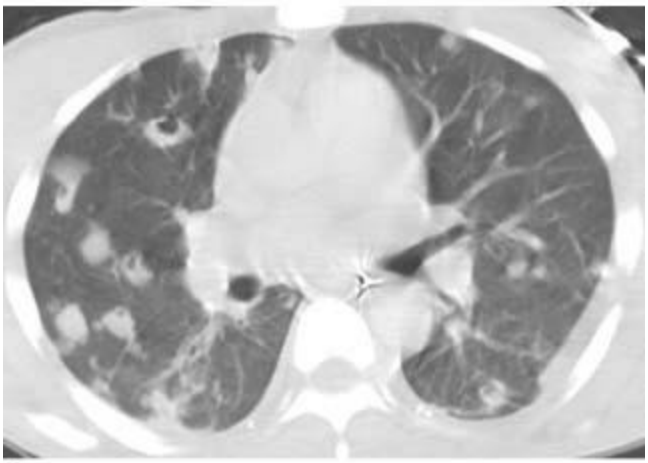

B

**FIGURE 1-20B** Chest CT (lung window) confirms the presence of cavitation within several of the multiple bilateral nodules. The nodules are primarily well-defined, although a nodule in the right lower lobe has borders that are partially obscured by adjacent ground glass and consolidation. Note is made of small bilateral pleural effusions. A nasogastric tube is present within the esophagus.

## DIFFERENTIAL DIAGNOSIS

**Septic emboli:** This is the most likely diagnosis given the multiple cavitary nodules

and the patient's history of intravenous drug abuse.

- **Fungal pneumonia:** Fungal infections such as angio-invasive aspergillosis may result in cavitary nodules. However, angioinvasive aspergillosis generally affects patients who are immunocompromised, particularly patients with leukemia. Therefore, the absence of immunosuppression in this patient makes the diagnosis unlikely. Coccidiomyocosis may cause thin-walled cav-itary nodules in an immunocompetent patient, but is a fungus that is endemic to the southwestern United States. Unless the patient had a history of recent travel to the southwest, this diagnosis would be unlikely.
- **Aspiration:** Anaerobes or gram-negative bacteria that are aspirated in patients with periodontal disease can result in pulmonary abscesses that present as cavitary nodules containing air-fluid levels. Abscesses are usually solitary. While more than one abscess can occur, the large number of nodules seen in this patient would be highly unusual.
- **Collagen vascular disease:** Diseases such as rheumatoid arthritis and Wegener's granulomatosis can result in waxing and waning thin-walled cavitary nodules. Pulmonary nodules are generally a late manifestation of rheumatoid arthritis; therefore, the absence of a history of rheumatoid arthritis would make the diagnosis unlikely. Patients with Wegener's granulomatosis usually have symptoms of upper respiratory tract involvement (such as sinusitis) and may develop hemoptysis. The presence of a high fever and chills would be highly unusual symptoms for this disorder.
- **Metastatic disease:** Multiple cavities can result from metastatic disease to the lung, particularly from squa-mous cell carcinoma primary tumors. The high fever and pleuritic chest pain would be atypical symptoms from metastatic disease.
- **Trauma:** Pulmonary contusion often occurs in the lung periphery, and lung cysts or cavitation can also occur after thoracic trauma in the form of posttraumatic pneumatoceles. However, the number of lesions seen in this case (as well as the history) makes this diagnosis less likely.

## DIAGNOSIS

**Septic emboli**

## KEY FACTS

### Clinical

- Septic pulmonary emboli usually result from tricuspid valve endocarditis due to intravenous drug abuse, head and neck infections with pharyngeal or internal jugular vein phlebitis, or phlebitis from an indwelling catheter or an infected arteriovenous fistula.
- Symptoms include high fever, cough, dyspnea, chest pain, and occasional hemoptysis.

- Typical organisms include *Staphylococcus aureus* and anaerobes.
- Antibiotic therapy is usually successful, although clinical improvement can take several weeks.

### Radiologic

- Septic emboli manifest as poorly defined nodules (usually 1 to 2 cm in diameter), most often in the lung periphery. They are usually more numerous in cases of tricuspid valve endocarditis than from other sources.
- Cavitation within the nodules occurs after several days and is seen in approximately 50% of nodules. The walls are moderately thick and irregular.
- The peripheral nodules may rupture into the pleural space and result in a bronchopleural fistula.
- Pleural effusion(s) are not uncommon. Empyemas may occur as a result of direct seeding of the pleural space or from hematogenous spread of infection.
- CT is generally not indicated but, as in other situations, can reveal a greater extent of involvement than radiographs.
- On CT, the nodules may be well-defined or ill-defined, and the cavitation may be more evident than on the radiographs. Associated consolidation and ground glass, reflecting both inflammation and extension of infection, is common.

## SUGGESTED READING

Colen TW, Gunn M, Cook E, et al. Radiologic manifestations of extra-cardiac complications of infective endocarditis. Eur Radiol 2008;18:2433–2445.

Hagan IG, Burney K. Radiology of recreational drug abuse. Radiographics 2007;27:919–940.

# CASE 21

**LAURA E. HEYNEMAN**

### HISTORY

A 55-year-old previously healthy woman with a persistent cough after an upper respiratory tract infection.

A

**FIGURE 1-21A** Posteroanterior chest radiograph reveals a small right hemithorax with mediastinal shift to the right. The heart is shifted into the right hemithorax and it is difficult to ascertain whether the apex is pointed toward the right or the left. The right lung is small and hyperlucent. The right pulmonary artery is poorly visualized. Several vessels in the right perihilar region appear tortuous and disorganized. There is a large abnormal vessel that originates from the right midlung and courses toward the medial right hemidiaphragm. The right lateral costophrenic angle is blunted.

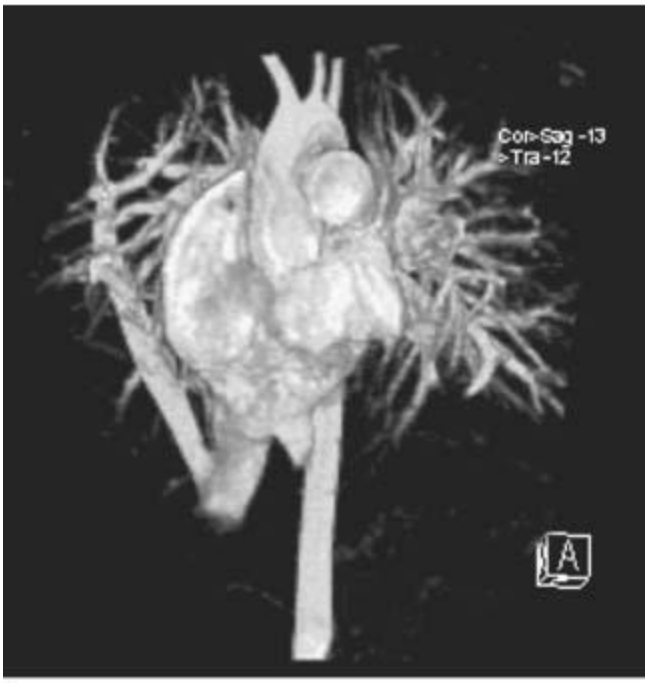


B

**FIGURE 1-21B** Volume-rendered image from an MR angiogram reveals a large vessel which courses inferomedially from the right mid lung and drains into the inferior vena cava.

## DIFFERENTIAL DIAGNOSIS

**Scimitar (venolobar) syndrome:** This is the most likely diagnosis given the small right hilum, the small right hemithorax, the mediastinal shift to the right, and the presence of an abnormal vessel in the right lung that courses toward the right hemidiaphragm.

**Congenital hypoplasia of the right pulmonary artery:** The radiographic findings of a small right hilum and small right hemithorax are consistent with congenital hypoplasia of the right pulmonary artery. However, a diagnosis of right pulmonary artery hypoplasia by itself does not account for the abnormal vessel coursing toward the right hemidiaphragm.

**Right lower lobe collapse:** Lobar collapse can cause the ipsilateral hilum to appear small, and can result in significant volume loss that manifests as mediastinal shift. However, the collapsed lobe should cause a well-defined, triangular opacity that abuts the mediastinum. The absence of such an opacity in this case excludes the diagnosis of lobar collapse.

**Swyer-James syndrome:** Swyer-James syndrome (postinfectious bronchiolitis obliterans) is a consideration in the context of a small hilum. In patients in whom bronchiolitis obliterans affects the majority of one lung, there is such severe small

airways disease within the lung that blood is diverted away from the diseased lung and toward the normal lung. This differential blood flow may cause the hilum of the affected lung to appear small in relation to the hilum of the other—normal lung. However, because of severe air trapping in the diseased lung, the affected lung in patients with Swyer-James syndrome is usually hyperinflated. The presence of a small ipsilateral hemithorax in this patient would argue against a diagnosis of Swyer-James syndrome. Furthermore, there is no reason why a patient with Swyer-James syndrome would have an abnormal vessel coursing toward the hemidiaphragm.

## DIAGNOSIS

**Scimitar (venolobar) syndrome**

## KEY FACTS

### Clinical

- Scimitar syndrome is also known as hypogenetic lung syndrome or venolobar syndrome.
- It is a combined vascular and lung anomaly that involves the right lung almost exclusively.
- The vascular anomalies that comprise scimitar syndrome are both venous and arterial.
- The venous anomaly is partial anomalous pulmonary venous return (PAPVR); the anomalous vein (or veins) drain either the entire right lung or a portion of the right lung.
- The arterial anomaly is a hypoplastic right pulmonary artery.
- Since the embryologic development of the lung is determined by in uterine pulmonary blood flow, the presence of a hypoplastic right pulmonary artery causes the right lung to be small. This in turn results in a small right hemithorax and mediastinal shift to the right. The mediastinal shift results in dextroposition of the heart; the heart is located within the right hemithorax but the cardiac apex remains pointed toward the left.
- Other congenital abnormalities associated with scimitar syndrome include sinus venosus type atrial septal defect (ASD), seen in 25% of patients; systemic arterial supply to the right lung; bilateral left-sided isomer-ism (bilateral bilobed lungs with hyparterial bronchi); accessory right hemidiaphragm; bronchiectasis; tra-cheal diverticula; and “horseshoe” lung (lungs fused by an isthmus of lung tissue that crosses the posterior mediastinum).
- The PAPVR results in an extracardiac left-to-right shunt. If the shunt is large enough, which usually is due to the presence of an associated sinus venosus ASD, the increased flow through the right heart may eventually cause pulmonary artery hypertension. Patients with scimitar syndrome who present in childhood tend to have large left-to-

right shunts, whereas patients who present in adulthood usually have a small degree of shunting and are often asymptomatic. These adult patients are often diagnosed after a CXR is obtained for reasons either unrelated to scimitar syndrome or related to associated abnormalities such as bronchiectasis.

## Radiologic

- The diagnosis of venolobar syndrome may be made on the radiograph. The classic radiographic findings include a small right hilum and a small right hemi-thorax, with dextroposition of the heart as a result of rightward mediastinal shift. Additionally, radiographs show a curved vessel that courses inferiorly toward the right hemidiaphragm instead of coursing to the right hilum; this vessel tends to broaden as it curves downward and thus resembles a Turkish sword, also known as a scimitar.
- When there is severe hypoplasia of the pulmonary artery, the lung may appear hyperlucent. Systemic collaterals may be seen in the perihilar region as small, serpiginous, disorganized vessels.
- The accessory right hemidiaphragm that can be associated with scimitar syndrome may manifest as blunting of the costophrenic angle or a retrosternal opacity on the lateral view.
- CT or MRI can further delineate the vascular anomalies. With cross-sectional imaging, the small right pulmonary artery can be visualized, the course of the anomalous right pulmonary veins may be traced (and therefore the determination made as to whether the anomalous drainage affects the whole right lung or just a portion of the right lung), and the site of drainage of the anomalous veins can be determined.
- CT may also show associated pulmonary abnormalities such as left isomerism and bronchiectasis.
- CT or MR angiogram may demonstrate systemic arteries serving the right lung. Large arteries feeding the right lower lobe may arise directly off of the aorta or off of the inferior phrenic artery.
- Cross-sectional imaging may also identify the presence of a sinus venosus ASD. Phase contrast imaging MRI can quantify the degree of left-to-right shunting from both the PAPVR as well as from an associated sinus venosus ASD.

# SUGGESTED READING

Ahamed MF, Al Hameed F. Hypogenetic lung syndrome in an adolescent: imaging findings with short review. Ann Thorac Med 2008;3:60–63.

Martinez-Jimenez S, Heyneman LE, McAdams HP, et al. Nonsurgical extra-cardiac vascular shunts in the thorax: clinical and imaging characteristics. Radiographics 2010;30:e41.

Zylak CJ, Eyler WR, Spizarny DL, Stone CH. Developmental lung anomalies in the adult: radiologic-pathologic correlation. Radiographics 2002;22:S25–S43.

# CASE 22

**LAURA E. HEYNEMAN**

## HISTORY

A 45-year-old previously healthy woman presents with a 2-month history of progressive shortness of breath, cough, and unintentional weight loss.

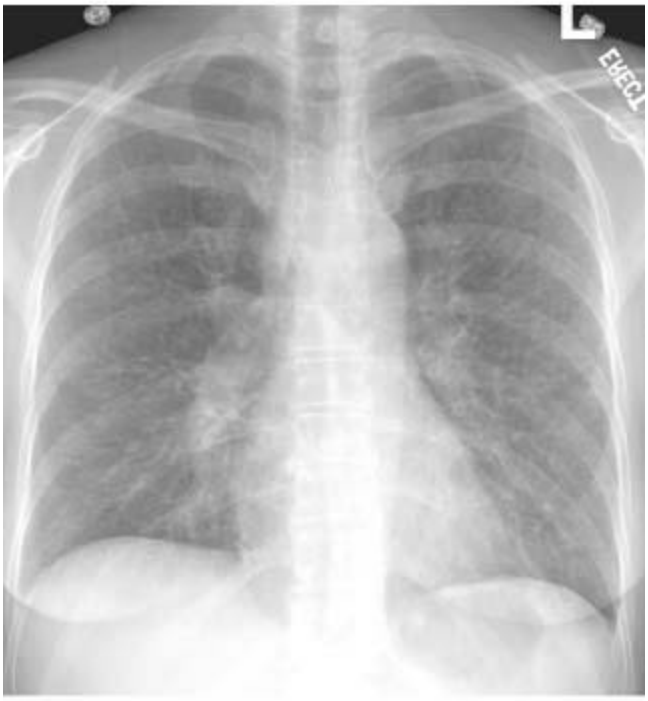

A

■**FIGURE 1-22A** Anteroposterior chest radiograph shows bilateral reticular opacities with septal lines noted in the lower lungs bilaterally. There is also right hilar and right paratracheal lymphadenopathy.

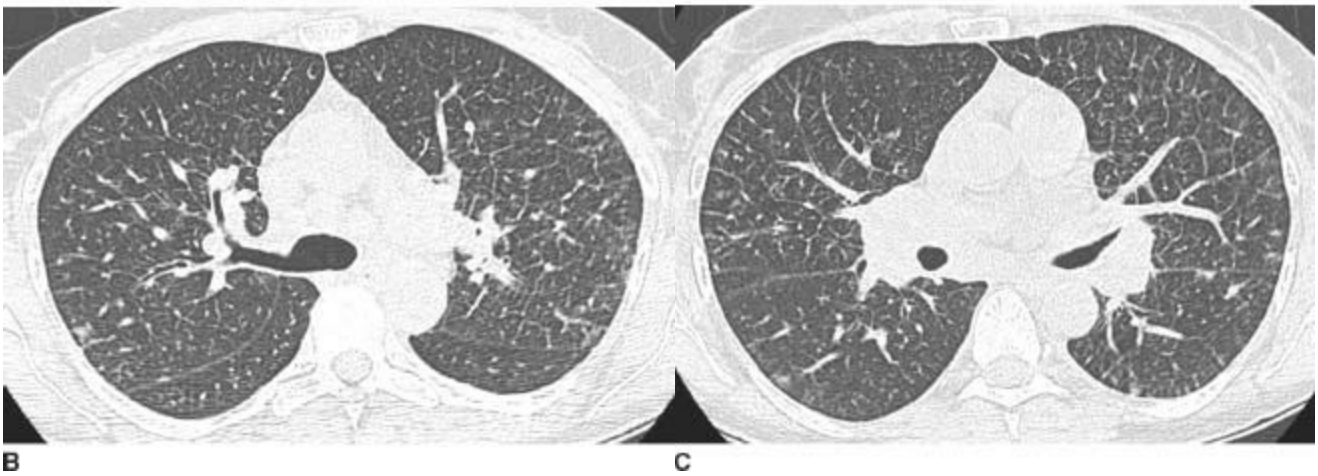


**FIGURES 1-22B and 1-22C** HRCT images (lung window) show striking interlobular septal thickening, which is beaded in several locations. Additionally, there is right hilar and mediastinal lymphadenopathy as well as scattered small bilateral pulmonary nodules.

## DIFFERENTIAL DIAGNOSIS

**Lymphangitic carcinomatosis:** This is the favored diagnosis, given the clinical history suggestive of a persistent process and the radiologic findings of reticular opacities with beaded interlobular septal thickening, scattered small pulmonary nodules, and lymphadenopathy.

**Pulmonary edema:** Interstitial pulmonary edema may result in reticular opacities and interlobular septal thickening. However, on HRCT, the septal thickening of pulmonary edema should be smooth, unlike the nodular, beaded appearance of many of the interlobular septa in the images provided. Additionally, pulmonary edema would not explain the small, scattered pulmonary nodules. Furthermore, while patients in congestive heart failure may demonstrate lymphadenopathy on CT, the lymph nodes tend to be only mildly enlarged, and are usually not asymmetric as seen in this patient.

**Atypical (viral) pneumonia:** Atypical infections, primarily viral infections, may cause reticular opacities and may occasionally result in small pulmonary nodules. However, septal thickening does not tend to be a predominant finding and, when present, tends to be smooth rather than nodular. Furthermore, other than in infectious mononucleosis and measles, lymphade-nopathy is a relatively rare finding in immunocompetent adults with viral pneumonias. Finally, the patient's clinical history of weight loss over 2 months is not suggestive of a viral infection.

**Leukemia:** Leukemia may infiltrate the pulmonary lymphatics and cause beaded interlobular septal thickening as is seen in this patient. Leukemic infiltration of the lungs usually occurs when patients are in blast crisis. Furthermore, leukemic infiltrates rarely

result in pulmonary symptoms. Therefore, the absence of a history of blast crisis and the presence of a chronic cough makes this diagnosis unlikely.

- **Pulmonary amyloid:** Amyloid may involve the pulmonary interstitium, and result in both beaded interlobu-lar septal thickening and nodules. However, this is a very rare entity, and would not be favored over the much more common diagnosis of lymphangitic carcino-matosis. Furthermore, while patients with amyloid can present with weight loss and cough, it is more common for patients to present with multiorgan system involvement; patients often have concomitant renal, cardiac, and/or neural dysfunction as a result of amyloid deposition within those organs.

# DIAGNOSIS

**Lymphangitic carcinomatosis**

# KEY FACTS

## Clinical

- Lymphangitic carcinomatosis occurs when a malignancy invades the pulmonary lymphatics, which lie within the interlobular septa and along the central bronchovascular bundles. The routes by which malignant cells reach the pulmonary lymphatics are multiple: some tumors spread hematogenously into small pulmonary arteri-oles, and subsequently invade the nearby pulmonary lymphatics; other tumors appear to extend in a retrograde fashion from the hilar lymph nodes into the pulmonary interstitium. Primary lung cancers may directly invade the local pulmonary lymphatic system.
- Tumors of the lung, breast, stomach, colon, pancreas, and prostate are the most common types of malignancy that cause lymphangitic carcinomatosis. The cell type involved in most cases is adenocarcinoma.
- Patients usually present with increasing shortness of breath and a dry cough. They may be symptomatic before any radiographic abnormality is detected.
- The diagnosis of lymphangitic carcinomatosis carries with it a poor prognosis, but a long-term survival with the disease has been reported.

## Radiologic

- Lymphangitic carcinomatosis manifests radiographi-cally as reticular or reticulonodular opacities. Septal lines (Kerley B lines) are usually a prominent finding.
- There is often fissural thickening from subpleural edema resulting from lymphatic obstruction.
- The process may be unilateral or bilateral. Unilateral lymphangitic carcinomatosis is

most frequently seen in the setting of a primary lung cancer that has directly invaded the adjacent lymphatics.

- On CT, particularly HRCT, the most striking finding is thickening of the interlobular septa, leading to linear and polygonal opacities. The septal thickening is usually nodular and beaded, but may be smooth.
- On HRCT, thickening of the bronchovascular bundles is also present. The peribronchovascular thickening may be smooth or nodular.
- The presence of nodular septal thickening is a feature that distinguishes lymphangitic carcinomatosis from pulmonary edema; in pulmonary edema, the septal thickening is always smooth. However, since septal thickening from lymphangitic tumor may also be smooth, the presence of smooth interlobular septal thickening is not helpful in distinguishing edema from lymphangitis. It is only when the interlobular septal thickening is nodular or beaded that the distinction may be made.
- The peribronchovascular nodularity in lymphangitic carcinomatosis may mimic sarcoidosis. However, inter-lobular septal thickening is generally not a predominant finding in sarcoidosis, whereas it is a key feature of lymphangitic tumor.
- The portions of lung involved by lymphangitic carcino-matosis are often hypermetabolic on FDG-PET imaging.

## SUGGESTED READING

Castaner E, Gallardo X, Pallardo Y, et al. Diseases affecting the peribron-chovascular interstitium: CT findings and pathologic correlation. Curr Probl Diagn Radiol 2005;24:63–75.

Collins J. CT signs and patterns of lung disease. Radiol Clin North Am 2001;39:1115–1135.

# CASE 23

**LAURA E. HEYNEMAN**

### HISTORY

A 32-year-old man who is on high-dose corticosteroids for treatment of a brain tumor presents with low-grade fever and progressive shortness of breath over 1 week.

A

■**FIGURE 1-23A** Posteroanterior chest radiograph obtained when patient first presented shows perihilar reticular opacities bilaterally, with slight confluence in the left mid-lung. There is no evidence of lymphadenopathy, and there are no pleural abnormalities.

B

■**FIGURE 1-23B** High-resolution CT image (lung window) obtained on the same day reveals multifocal ground glass which is slightly more confluent on the left. There are small foci of consolidation within the left lung. Very mild interlobular septal thickening is present within the left lower lobe. There is no pleural effusion or pneumothorax.

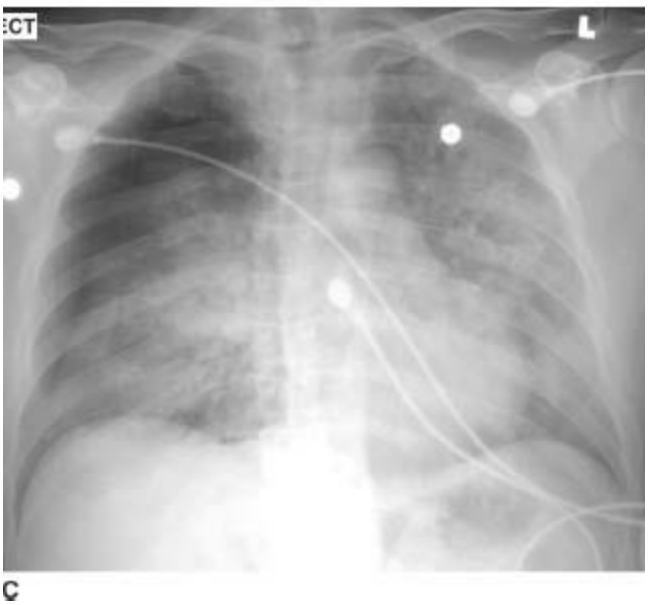


C

**FIGURE 1-23C** Posteroanterior chest radiograph obtained 5 days later shows a new moderate-sized right pneumothorax. There has been an interval increase in the opacities to more extensive airspace consolidation, although a slight perihilar distribution of the abnormalities is maintained.

## DIFFERENTIAL DIAGNOSIS

***Pneumocystis jirovecii* pneumonia (PCP):** Given the patient's immunocompromised status, his low-grade fever, and his presentation with increasing dyspnea over 1 week, this is the favored diagnosis. The progression of the lung abnormalities from perihilar reticulation to more extensive bilateral opacification is common in untreated pneumocystis pneumonia. Furthermore, pneumothorax is a common complication of PCP.

**Noncardiogenic edema:** Permeability edema due to a variety of causes including sepsis and drug toxicity may have a virtually identical radiographic appearance, and may result in reticular opacities that progress to diffuse parenchymal opacification. Furthermore, if the permeability edema develops into adult respiratory distress syndrome (ARDS), the lung becomes noncom-pliant and pneumothorax may develop. However, most causes of permeability edema result in a very acute presentation rather than dyspnea that progresses over 1 week, as was seen in this patient. Acute interstitial pneumonia (AIP), which is a rare entity and which essentially represents idiopathic ARDS, can present over a longer period of time than other forms of ARDS and is a consideration in this patient. However, the clinical history would strongly favor PCP; there is no association between brain tumors, corticosteroid use, and AIP.

**Collagen vascular diseases:** Wegener's granulomatosis and systemic lupus erythematosus may cause diffuse alveolar hemorrhage (DAH), which in turn may result

in extensive multifocal ground glass, as seen in this patient. However, the initial radiograph demonstrating reticular opacities would be atypical for hemorrhage. Furthermore, patients with DAH generally present with hemoptysis rather than fever and shortness of breath.

## DIAGNOSIS

***Pneumocystis jioveci* pneumonia (PCP)**

## KEY FACTS

### Clinical

- The organism originally thought to be responsible for pneumocystis pneumonia in humans was *Pneumocystis carinii*. However, phenotypic differences were discovered between the organism that infects humans and the organism that infects other mammals, and in 2001 the name *Pneumocystis jirovecii* was chosen to designate the species that infects humans. The acronym "PCP" has remained in use, formed from Pneumo Cystis Pneumonia.
- *Pneumocystis*, initially considered a trypanosome, was then reclassified as a protozoan; it is now phylogeneti-cally considered to be a fungus.
- In the United States, clinically identifiable disease manifests in severely immunocompromised patients. Patients considered to be at high risk for *Pneumocystis* infection include patients who are positive for the human immunodeficiency virus (HIV) with a CD4 count of <200 cells/uL; non-HIV immunocompromised patients with hematologic malignancies or solid tumors (particularly patients with brain tumors treated with high-dose corticosteroids); patients who have undergone solid organ or bone marrow transplantation; patients on high-dose corticosteroid therapy; and patients with primary immunodeficiencies.
- Symptoms are generally nonspecific, including fever, dyspnea, and nonproductive cough. Symptoms in HIV-infected individuals often present with a more subacute course, with symptoms progressing over 3 to 4 weeks rather than the progression of symptoms over approximately 1 week in other immunosuppressed individuals.
- The diagnosis is made by observing organisms on induced sputum, bronchoalveolar lavage, or lung biopsy specimens.
- Prophylaxis with trimethoprim-sulfamethoxasole (TMP-SMX) therapy has been effective in decreasing the number of patients presenting with *Pneumocystis* pneumonia. Dapsone or aerosolized pentamadine are considered less effective as prophylaxis, and are generally used when side effects from TMP-SMX cannot be tolerated.
- Treatment is generally with TMP-SMX or pentamidine. Dapsone, or clindamycin-primaquine have also been used. The use of steroids in treatment is controversial.

- Response to therapy is generally excellent. Clinical improvement is typically seen within several days. Nevertheless, some patients will proceed to respiratory failure, requiring stringent therapeutic supportive measures.

## Radiologic

- PCP typically manifests with diffuse, bilateral, fine to medium reticulonodular opacities. These reticular opacities are often perihilar in distribution. If untreated, the reticular opacities may progress to diffuse ground glass, which is often granular in appearance.
- At the time of initial presentation with symptoms, the radiograph may be normal.
- Unusual appearances include focal homogeneous opacities and larger (1 to 2 cm) nodules, with or without cavitation. Pleural effusions and lymphadenopathy are extremely rare.
- Pneumatoceles are seen in approximately 10% of patients with PCP, and may take months to resolve. Fluid levels within pneumatoceles are extremely rare and should suggest superinfection.
- Spontaneous pneumothorax occurs in 5% to 6% of patients with PCP, and the presence of pneumatoceles increases the risk of pneumothorax formation.
- On CT, particularly HRCT, multifocal ground glass is the most common finding. The ground glass may be geographic in distribution. Other CT findings may include consolidation, cysts, and a "crazy paving" pattern of interlobular septal thickening superimposed on regions of ground glass opacity.
- HRCT may be helpful in demonstrating ground glass abnormalities in patients with a normal radiograph. Additionally, CT may be used by bronchoscopists as a "roadmap" to determine which segments to target for bronchoalveolar lavage.
- With appropriate therapy, the abnormalities (other than the pneumatoceles) may resolve in as quickly as 10 days. Occasionally, residual fibrosis is observed.
- Due to the fact that patients with PCP are immunocom-promised, they may be infected with more than one organism. Imaging may be helpful in suggesting the presence of multiple infectious agents. For example, if PCP is suspected in a patient with multifocal ground glass, the presence of a pleural effusion should initiate a search for an additional organism, since pleural effusions are extremely rare in the setting of PCP. Diagnosis usually requires bronchoscopy with bronchoalveolar lavage.

## SUGGESTED READING

Catherinot E, Lanternier F, Bougnoux ME, et al. *Pneumocystis jirovecii* pneumonia. Infect Dis Clin North Am 2010;24:107–138.

Chong S, Lee KS, Yi CA, et al. Pulmonary fungal infection: imaging findings in immunocompromised and

immunocompetent patients. Eur J Radiol 2006;59:371–383.

# CASE 24

**JARED D.
CHRISTENSEN**

## HISTORY

A 44-year-old female smoker with slowly progressive dyspnea and cough.


A

**FIGURE 1-24A** Posteroanterior chest radiograph. Diffuse bilateral heterogenous mixed alveolar and interstitial reticular opacities with relative apical sparing. The heart is of normal size. There are no pleural effusions.

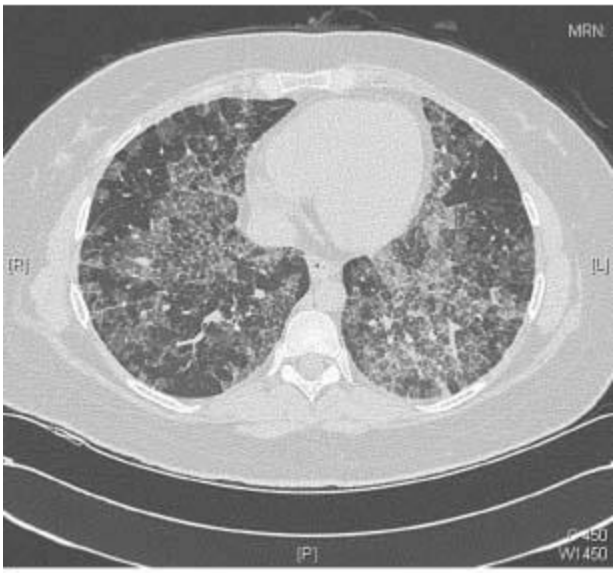

B

**FIGURE 1-24B** Representative axial high-resolution chest CT image (lung window). Bilateral geographic ground glass opacities with smooth interlobular septal thickening extending to the pleural surface are present. No appreciable pulmonary nodules or consolidation.

## DIFFERENTIAL DIAGNOSIS

**Pulmonary alveolar proteinosis:** Pulmonary alveolar proteinosis (PAP) manifests radiographically as central and symmetric alveolar opacities, often sparing the lung apices and costophrenic sulci. CT features thickening of the interlobular septa with a background of ground glass opacities, a pattern referred to as "crazy paving." Pulmonary fibrosis occurs in advanced disease. Given the clinical history and radiologic features, this is the most likely diagnosis.

**Pulmonary edema:** Pulmonary edema may be caused by increased pulmonary venous pressure (hydrostatic) or capillary permeability (nonhydrostatic). Common hydrostatic etiologies include left-sided heart failure, volume overload, or renal failure. Diffuse alveolar opacities represent the most advanced form of hydrostatic pulmonary edema. A common manifestation of nonhydrostatic edema is ARDS, which represents the most severe form of diffuse lung injury (DLI), characterized by diffuse alveolar damage, resulting in increased capillary permeability. The onset of dyspnea related to edema may be sudden, unlike the presented case, and in the setting of hydrostatic edema, the clinical symptoms may fluctuate.

**Hypersensitivity pneumonitis (HP):** CL nodules with ground glass opacities with basilar sparing are characteristic of this disorder. The lung apices are routinely involved. The presented case does not exhibit pulmonary nodules, and demonstrates relative sparing of the apices, making this a less likely option.

- **Pulmonary hemorrhage:** DAH results in ground glass opacities, which may progress to areas of confluent consolidation. Etiologies are diverse and include Wegener's granulomatosis, anti-glomerular basement membrane (anti-GBM) syndrome, vasculitides, and connective tissue disorders, such as systemic lupus erythematosis (SLE). The onset is typically more sudden than in the presented case, making this diagnosis less likely.
- ***Pneumocystis jirovecii* pneumonia (PCP):** The alveolar opacities associated with PCP are classically perihi-lar in distribution, but can be diffuse with progressive disease and during the course of steroid treatment. *Pneumocystis jirovecii* is one of several infections that may present as diffuse alveolar opacities, particularly in immunocompromised patients; other pathogens include cytomegalovirus (CMV) and herpes simplex virus (HSV).
- **Invasive mucinous adenocarcinoma (formerly bronchioloalveolar cell carcinoma, or BAC):** This malignancy most often presents as a focal, subpleural consolidation with areas of ground glass opacities. When the lung is diffusely involved, ground glass opacities are a predominant feature, but rarely occur without associated multifocal consolidation. The lack of consolidation despite diffuse lung involvement in the presented case makes this a less likely diagnosis.

## DIAGNOSIS

**Pulmonary alveolar proteinosis**

## KEY FACTS

### Clinical

- Patients with PAP accumulate abnormal amounts of surfactant within the alveoli, which subsequently interferes with capillary oxygen diffusion. Patients therefore often present with profound hypoxia, which may be chronic and slowly progressive.
- Primary causes include idiopathic (accounting for 90% of all cases) and hereditary forms of the disease. Secondary PAP is associated with lymphoproliferative disorders and occupational exposure to silica, aluminum, and titanium dusts. There is a high association with smoking (>70%).
- Patients with PAP are at risk for superimposed infection with atypical pathogens, particularly *Nocardia*, but also including *Aspergillus, Cryptococcus neoformans, Candida, pneumocystis jirovecii*, and both tuberculous and nontuberculous mycobacteria.
- The primary treatment for PAP focuses on removing excess surfactant from the alveoli via whole lung lavage. Posttreatment radiographs may demonstrate increased alveolar

opacities due to retained fluid and should not be confused with disease progression.

- Approximately a third of patients have spontaneous remission, a third have persistent disease requiring whole lung lavage, and a third progress to pulmonary fibrosis despite therapy.

### Radiologic

- Findings on chest radiography are highly variable and correlate to disease burden. The classic presentation is bilateral central and symmetric opacities with sparing of the apices and costophrenic angles. However, radiographs may be normal, demonstrate multifocal opacities, or exhibit diffuse alveolar opacities, as in the case presented.
- Pleural effusions and cardiomegaly are typically absent.
- The characteristic CT features of PAP are diffuse ground glass opacities with smooth interlobular sep-tal thickening—an appearance referred to as "crazy-paving." The crazy-paving pattern is seen in a broad variety of diffuse lung diseases, but has the highest prevalence in PAP.
- PAP often spares the lung apices and costophrenic sulci. Subpleural sparing is seen in up to 50%.
- Imaging findings in conjunction with appropriate clinical presentation are suggestive; however, bronchoalve-olar lavage or biopsy is required for definitive diagnosis.

## SUGGESTED READING


Frazier AA, Franks TJ, Cooke EO, et al. From the archives of the AFIP:

Pulmonary alveolar proteinosis. Radiographics 2008;28:883–899.

Holbert JM, Costello P, Li W, et al. CT features of pulmonary alveolar proteinosis. Am J Roentgenol 2001;176:1287–1294.

Lee CH. The crazy-paving sign. Radiology 2007;243:905–906.

Miller WT Jr, Shah RM. Isolated diffuse ground-glass opacity in thoracic CT: causes and clinical presentations. Am J Roentgenol 2005;184:613–622.

Trapnell BC, Whitsett JA, Nakata K. Pulmonary alveolar proteinosis. New Engl J Med 2003;349:2527-2539.


# CASE 25


**JENNY K. HOANG**


### HISTORY

A 37-year-old woman presents with worsening dyspnea with minimal exertion.

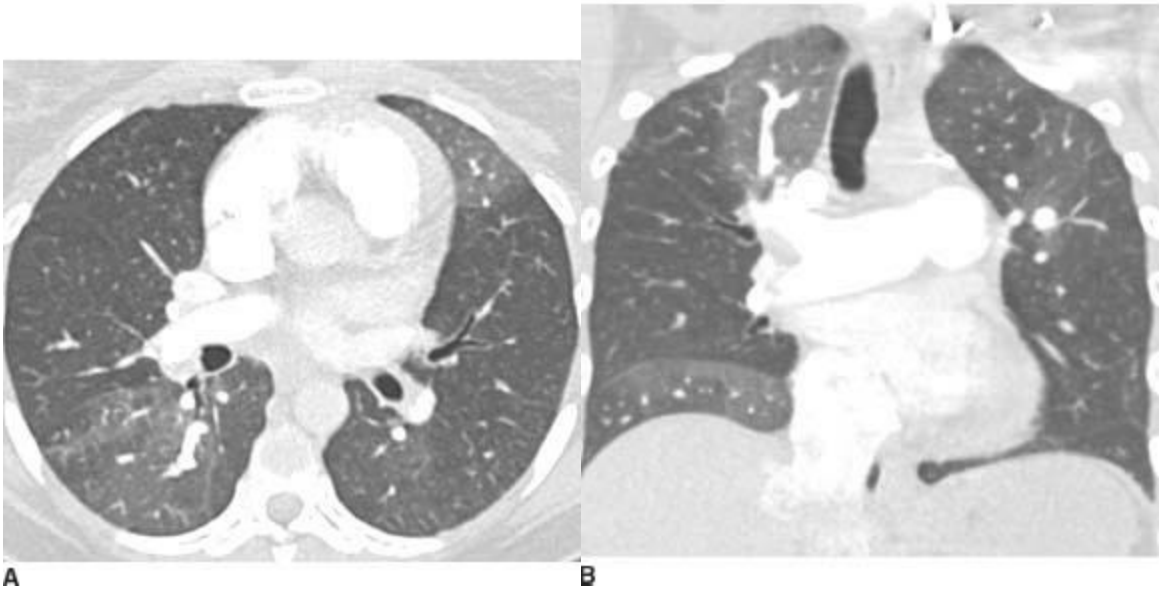


■**FIGURES 1-25A and 1-25B** Axial **(A)** and coronal reformatted **(B)** images (lung window) from a contrast-enhanced CT scan showing mosaic perfusion, with smaller arteries in areas of low attenuation and larger pulmonary arteries within areas of high attenuation. The main pulmonary artery is also enlarged.


■**FIGURE 1-25C** Axial image from a CT pulmonary angio-gram (mediastinal window) showing bilateral intraluminal webs. There is also a mural thrombus with obtuse margins with the vessel wall in the right interlobar artery. The findings are consistent with chronic PE.

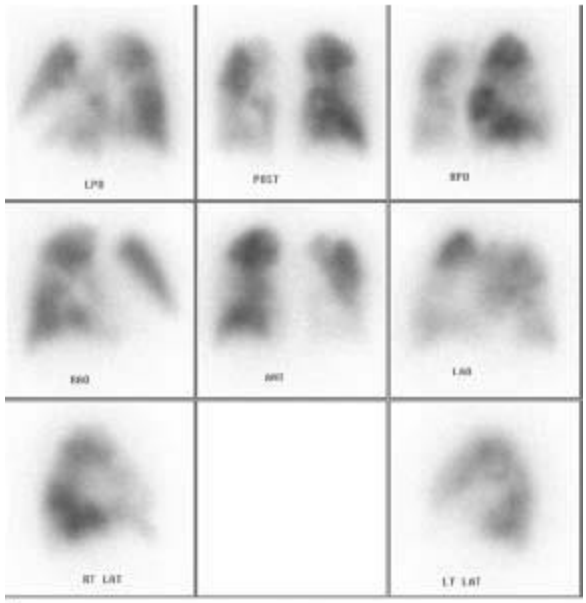


D

**FIGURE 1-25D** Perfusion scan from a lung scintigra-phy study demonstrates multiple perfusion defects which were not matched (ventilation not shown) in keeping with pulmonary embolism.

## DIFFERENTIAL DIAGNOSIS

**Mosaic perfusion pattern secondary to chronic thromboembolic disease:** Mosaic perfusion, the presence of webs and mural thrombus in the pulmonary arteries and enlarged central pulmonary arteries are consistent with chronic thromboembolic disease with pulmonary arterial hypertension.

**Mosaic perfusion pattern secondary to small airways disease:** Asthma and bronchiolitis obliterans can cause mosaic perfusion. No expiratory images have been performed to assess for air trapping, which should distinguish small airways disease from thromboembolic disease.

**Hypersensitivity pneumonitis (HP):** Mosaic attenuation is a major finding in HP. However, the pattern of mosaic attenuation in HP is usually more heterogenous with smaller lobular sized areas of air trapping, and multiple different levels of attenuation secondary to both small airways and infiltrative lung disease (the so-called head-cheese pattern).

**Infiltrative lung disease:** Heterogenous lung attenuation from multifocal ground glass opacities from infection, sarcoidosis, pulmonary edema, organizing pneumonia or idiopathic interstitial pneumonitis are not associated with differences in vessel caliber.

## DIAGNOSIS

**Mosaic perfusion pattern secondary to chronic thrombo-embolic disease**

## KEY FACTS

### Clinical

- Only a small proportion of patients with treated acute pulmonary embolism fail to resolve resulting in chronic pulmonary embolism (CPE). Of the CPE group, only 0.01% have chronic thromboembolic pulmonary hypertension (CTEPH).
- Without surgical treatment, there is 90% 3-year mortality due to progressive increased pulmonary vascular resistance resulting in pulmonary hypertension and right heart failure.
- The primary treatment for CTEPH is surgical pulmonary thromboendarterectomy. Unsuitable patients with substantial peripheral CPE can be considered for lung or heart-lung transplant.

### Radiologic

- Mosaic attenuation is a pattern of sharply demarcated patchy high and low pulmonary parenchymal attenuation areas seen on HRCT.
- The term "mosaic perfusion" applies to the mosaic attenuation pattern caused by regional reduced lung perfusion secondary to airway disease (hypoxic vaso-constriction) or pulmonary vascular disease (vascular occlusion).
- In mosaic perfusion, the pulmonary arteries are reduced in size in the lucent lung regions, thus allowing mosaic perfusion to be distinguished from ground glass opacities.
- Small airways disease can be differentiated from small vessel disease by performing end-expiratory imaging, which shows accentuated decreased attenuation consistent with air trapping.
- The direct signs of CPE are mural thrombus with obtuse margins with the vessel wall, intimal irregularities, webs, and abrupt vessel narrowing. Indirect signs, in addition to mosaic perfusion, are enlargement of the main pulmonary artery and enlarged bronchial arteries.

## SUGGESTED READING

Hoeper MM, Mayer E, Simonneau G, Rubin LJ. Chronic thromboembolic pulmonary hypertension. Circulation 2006;113:2011–2020.

Wittram C, Kalra MK, Maher MM, Greenfield A, McLoud TC, Shepard JA. Acute and chronic pulmonary emboli: angiography-CT correlation. Am J Roentgenol 2006;186:S421–S429.

Worthy SA, Muller NL, Hartman TE, et al. Mosaic attenuation pattern on thin-section CT scans of the lung: differentiation among infiltrative lung, airway, and vascular diseases as a cause. Radiology 1997;205:465–470.

# CASE 26

**TAMRA M.**
**KNUTSON**

## HISTORY

A 38-year-old female, nonsmoker with a 1-year history of worsening dyspnea, cough, and wheezing.

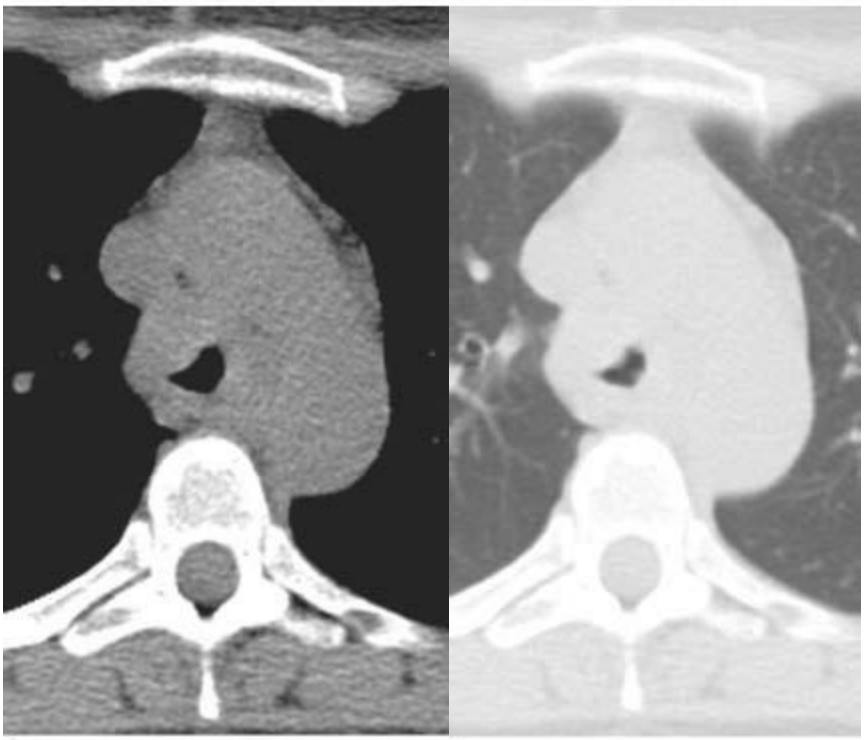


■**FIGURES 1-26A and 1-26B** Axial noncontrast CT images through the distal trachea demonstrate an annular soft tissue mass encasing the trachea with polypoid intraluminal extension.

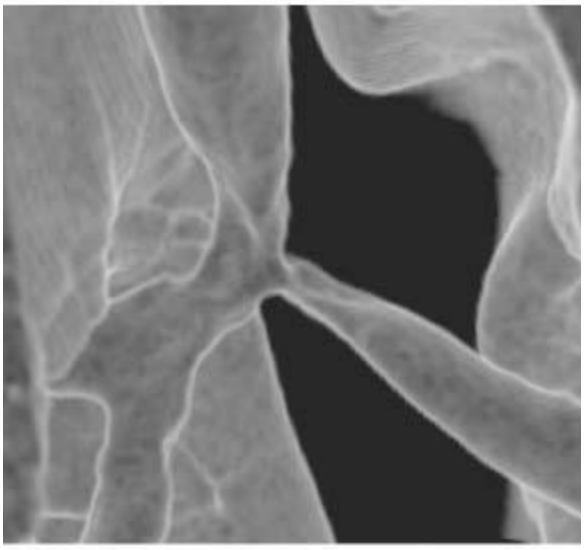

C

**FIGURE 1-26C** 3D volume-rendered image, viewed from anterior perspective, reveals circumferential narrowing of the carina and mainstem bronchi.

## DIFFERENTIAL DIAGNOSIS

- **Adenoid cystic carcinoma:** Given the fact that the patient is young and a nonsmoker, and the fact that the mass involves the distal trachea, this is the favored diagnosis.
- **Squamous cell carcinoma:** While squamous cell carcinoma is the most common primary tracheal neoplasm and could have this radiographic appearance, it classically presents in an older patient population and in the setting of tobacco abuse. Additionally, it more commonly involves the upper third of the trachea.
- **Mucoepidermoid carcinoma:** Mucoepidermoid carcinoma is a rare minor salivary gland tumor of the airway that more commonly involves the bronchi than the trachea.
- **Metastatic disease:** Metastatic disease is much less frequent than primary tracheal neoplasms, especially in the absence of a known primary malignancy. The most common primary neoplasms to metastasize to the trachea are renal cell carcinoma, melanoma, and breast and colon adenocarcinoma.
- **Stricture:** While benign strictures from intubation, trauma, and foreign body aspiration are a common cause of airway narrowing, a benign stricture fails to account for the soft tissue mass.

## DIAGNOSIS

**Adenoid cystic carcinoma**

## KEY FACTS

## Clinical

- The majority of tracheal neoplasms are malignant (>90%) and present as dyspnea, wheezing, and coughing. Patients may be initially misdiagnosed with adult onset asthma.
- Adenoid cystic carcinoma is the second most common primary tracheal neoplasm after squamous cell carcinoma, accounting for approximately 33% of tracheal neoplasms.
- Adenoid cystic carcinoma originates in the minor salivary glands of the trachea and bronchi, located in the posterolateral wall. Survival depends on the chance for complete resection.
- Adenoid cystic carcinoma is more common in a younger patient population than squamous cell carcinoma, demonstrating a peak incidence in the fifth decade of life.
- In contrast to squamous cell carcinoma, there is no association between adenoid cystic carcinoma and tobacco usage.

## Radiologic

- Tracheal neoplasms are often occult on radiographs and are best evaluated on CT.
- Adenoid cystic carcinoma characteristically occurs in the posterolateral wall of the distal two-thirds of the trachea and mainstem bronchi. Involvement of the peripheral airways is rare.
- Adenoid cystic carcinoma can present as an intralumi-nal soft tissue mass, annular wall thickening, or mass encasing the airway. Extratracheal tumor extension and involvement of >180 degrees of the airway circumference is a typical feature.
- Adenoid cystic carcinoma has a propensity for submu-cosal and perineural spread in the longitudinal plane and the extent of the disease is easily underestimated by CT.
- When approaching airway lesions, it is helpful to distinguish focal lesions from diffuse/multifocal lesions. Focal lesions include neoplasms, infection, and strictures related to aspirated foreign bodies and previous trauma including intubation. Diffuse diseases include infection, sarcoidosis, Wegener's granulomatosis, relapsing poly-chondritis, amyloidosis, papillomatosis, and tracheo-pathia osteoplastica.

# SUGGESTED READING

Kim TS, Lee KS, Han J, et al. Sialadenoid tumors of the respiratory tract: radiologic—pathologic correlation. Am J Roentgenol 2001;177:1145–1150.

Kwak SH, Lee KS, Chung MJ, et al. Adenoid cystic carcinoma of the airways: helical CT and histopathologic correlation. Am J Roentgenol 2004;183:277–281.

Marom EM, Goodman PC, McAdams HP. Focal abnormalities of the trachea and main bronchi. Am J Roentgenol 2001;176:707–711.

Marom EM, Goodman PC, McAdams HP. Diffuse abnormalities of the trachea and main bronchi. Am J Roentgenol 2001;176:713–717.

# CASE 27

**PHIL B. HOANG**

## HISTORY

A 29-year-old African American man complains of a 3-month history of progressive dyspnea on exertion and nonproductive cough.


■**FIGURES 1-27A and 1-27B** Posteroanterior **(A)** and lateral **(B)** chest radiographs demonstrate bilateral hilar enlargement with reticulonodular opacities in the right mid- and upper-lung zones. There are no pleural effusions or areas of consolidation.

C

**FIGURE 1-27C** High-resolution chest CT axial image (lung window) demonstrates small, well defined peribroncho-vascular and subpleural nodules. There is also fine nodularity involving the right major fissure (confirming subpleural nodules). Enlarged right hilar lymph nodes are noted in this image.

## DIFFERENTIAL DIAGNOSIS

**Sarcoidosis:** Bilateral, symmetric adenopathy is characteristic of sarcoidosis. The mirconodular lung disease with small (2 to 4 mm), well-defined nodules in an upper lobe, peribronchovascular and subpleural distribution is also characteristic. Based on the clinical history and radiographic features, this is the most likely diagnosis.

**Silicosis:** Similar to sarcoidosis, nodular involvement in silicosis typically involves the upper lung zones; however, nodules are centrilobular and subpleural but spare the central bronchovascular bundles and fissures. Nodules will calcify in 20% of cases. Hilar enlargement may also be seen with this process.

**Miliary spread of infection/tumor:** In this process, nodules are randomly distributed throughout all lung zones and are of similar size; indicative of hematog-enous dissemination of disease. Nodal enlargement in the setting of infection (tuberculosis, fungal) is often unilateral or asymmetric. Nodal enlargement due to malignant etiologies (lymphoma, nodal metastases) is also often unilateral or asymmetric, and often affects the superior mediastinal region.

**Lymphangitic spread of tumor:** This process is characterized by peribronchovascular, interstitial, and fis-sural thickening with small nodules, mainly involving the lower lung zones; involvement is usually focal, unilateral, and asymmetric, which are distinguishing features from sarcoid and interstitial edema. Again, nodal enlargement due to malignant etiologies is often unilateral or asymmetric.

# DIAGNOSIS

**Sarcoidosis (Stage II)**

# KEY FACTS

## Clinical

- Inflammatory, multiorgan disease of unknown etiology characterized pathologically by noncaseating granulomas.
- In the United States, African Americans are affected four times more than Caucasians; age distribution is bimodal, with 25- to 35-year-olds affected in 70% to 90% of cases, and a second peak occurring in the 5th and 6th decades.
- Most patients are asymptomatic (60% to 80%); however, pulmonary radiologic manifestations are present in up to 90%.
- 10% to 30% of patients will progress to chronic lung disease and functional impairment, mainly from complications stemming from pulmonary fibrosis and hypertension. The remaining patients will undergo spontaneous remission or long-term symptomatic improvement.

## Radiologic

- Chest radiograph stages
    - Stage 0: Normal chest radiograph
    - Stage 1: Hilar and mediastinal adenopathy *without* parenchymal lung disease
    - Stage 2: Hilar and mediastinal adenopathy *with* parenchymal lung disease other than fibrosis
    - Stage 3: Parenchymal lung disease other than fibro-sis without adenopathy
    - Stage 4: Endstage fibrosis
- Bilateral, symmetric hilar (90%) and right paratracheal adenopathy (60%) is the classic pattern and is referred to as the *1-2-3 sign* on radiographs.
- Lung disease is characterized by interlobular septal thickening and small nodules in a mid- to upper-lung and perilymphatic distribution (involving broncho-vascular bundles and subpleural lung); *fine nodular fissural thickening is fairly specific for sarcoid*.
- Confluence of interstitial granulomas can appear as large, ill-defined areas of consolidation (“alveolar sarcoid”); the *galaxy sign* refers to small satellite nodules along the periphery of these areas of consolidation.
- Endstage lung disease is characterized by upper lobe pulmonary fibrosis, honeycombing, cyst formation, and traction bronchiectasis.

## KEY FACTS

### Clinical

- Inflammatory, multiorgan disease of unknown etiology characterized pathologically by noncaseating granulo-mas.
- In the United States, African Americans are affected four times more than Caucasians; age distribution is bimodal, with 25- to 35-year-olds affected in 70% to 90% of cases, and a second peak occurring in the 5th and 6th decades.

## SUGGESTED READING

Fraser RS, Colman N, Muller NL, Pare PD. Fraser and Pare's Diagnosis of Diseases of the Chest (4th ed). Philadelphia, PA: WB Saunders Co., 1999.

Prabhakar HB, Rabinowitz CB, Gibbons FK, et al. Imaging features of sarcoidosis on MDCT, FDG PET and PET/CT. Am J Roentgenol 2008;190:S1–S6.

Traill ZC, Maskell GF, Gleeson FV. High-resolution CT findings of pulmonary sarcoidosis. Am J Roentgenol 1997;168:1557-1560.

Webb WR, Higgins CB. Thoracic Imaging: Pulmonary and Cardiovascular Radiology. Philadelphia, PA: Lippincott Williams & Wilkins, 2004.

# CASE 28

**JENNY K. HOANG**

## HISTORY

A 62 year-old man presenting with shortness of breath.

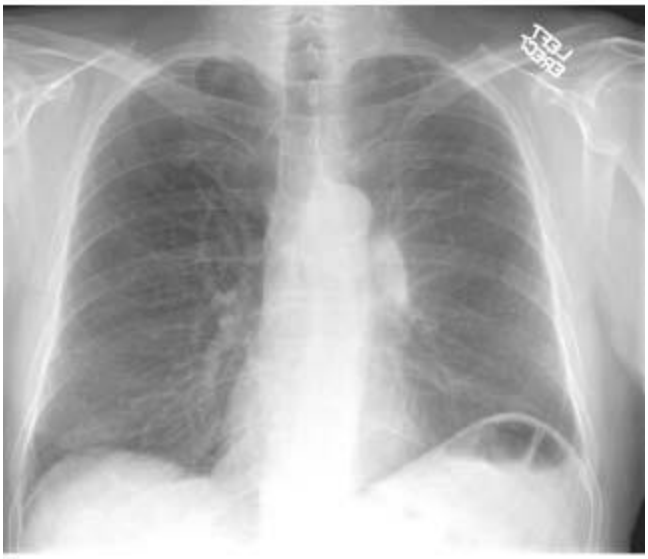

A

■**FIGURE 1-28A** Posteroanterior chest radiograph shows left upper lobe collapse with reduced left hemithorax volume, left perihi-lar hazy opacity and superior retraction of the left hilum.

B

■**FIGURE 1-28B** Lateral chest radiograph shows left upper lobe collapse with anterior displacement of the major fissure and retrosternal opacity.

C

**FIGURE 1-28C** Chest CT (lung window) at the level of the left main bronchus birfurcation confirms left upper lobe collapse. There is occlusion of the left upper lobe bronchus due to a centrally located endobronchial carcinoma.

## DIFFERENTIAL DIAGNOSIS

**Left upper lobe collapse:** A hazy opacity over the left hemithorax is accompanied by volume loss (elevation of the left hemidiaphragm) and silhouette sign of the left heart border. The retrosternal opacity in the lateral view corresponds to the collapsed left upper lobe. When lobar collapse is a possibility, consideration should be given to potential causes of obstruction.

Left pleural effusion: A layering pleural effusion can cause a hazy opacity of the hemithorax on supine chest radiograph. However, the posteroanterior radiograph was taken in the erect position and the lateral film shows no pleural fluid. Furthermore, the silhouette sign along the left heart border and mediastinum indicates that the abnormality is located anteriorly within the left hemithorax, whereas a layering left pleural effusion on a supine view would be located posteriorly.

Asymmetric soft tissues: Asymmetry of soft tissues as in Poland syndrome or mastectomy can cause diffuse asymmetry of opacity between the two hemithoraces. However, one would not expect associated volume loss or a silhouette sign.

## DIAGNOSIS

**Left upper lobe collapse due to obstructing endobronchial carcinoma**

## KEY FACTS

## Clinical

- In adults, bronchogenic carcinoma should be considered first as a cause for lobar collapse.
- In children, foreign body aspiration and mucous plugging are more common.
- The causes of atelectasis are:
    - Obstructive: An obstructed bronchus results in resorption of gases from the alveoli, which are not replenished. Obstructive causes can be subclassified by etiology as endobronchial, bronchial wall, and extraluminal.
    - Relaxation (or passive): Collapse is due to elastic recoil of the lung from changes in intrapleural pressure (pleural air or fluid) or an adjacent space-occupying lesion.
    - Cicatrizing: Collapse is due to decreased lung compliance in abnormally stiff fibrotic lungs. Volume loss is always seen in the setting of fibrosis, but the word "atelectasis" is relatively infrequently used in this context.
    - Adhesive: Collapse arises from a deficiency of surfactant causing an increase in alveolar surface tension.

## Radiologic

- Findings of left upper lobe collapse on a posteroante-rior chest radiograph are (1) reduced left lung volume, (2) veil-like opacity in the left hilar region with silhouetting of the left heart border, and (3) the luftsichel sign.
- The luftsichel sign (German for sickle of air) is due to expansion of the superior segment of the left lower lobe insinuating itself between the collapsed upper lobe and the mediastinum. It appears as a para-aortic crescent of hyperlucency with sharp margins that can extend from the apex of the left hemithorax to the left superior pulmonary vein, outlining the medial aspect and sometimes the upper aspect of the opaque collapsed left upper lobe. It is a helpful sign of left upper lobe collapse when it is seen, but, as in this case, it is not always present.
- Secondary findings of left upper lobe collapse on a posteroanterior chest radiograph are deviation of the trachea to the left and a small left juxtaphrenic peak
- The lateral radiograph shows a retrosternal elongated opacity of the collapsed left upper lobe extending from the apex to the diaphragm. The collapsed left upper lobe is sharply bordered posteriorly by the major fissure that becomes orientated in a plane almost parallel to the anterior chest wall.

## SUGGESTED READING

Blankenbaker DG. The luftsichel sign. Radiology 1998;208:319–320.

Fraser RS, Colman N, Muller NL, Pare PD. Fraser and Pare's Diagnosis of Diseases of the Chest (4th ed). Philadelphia, PA: WB Saunders Co., 1999.

Proto AV, Tocino I. Radiographic manifestations of lobar collapse. Semin Roentgenol 1980;15:117–173.

# CASE 29

**JENNY K. HOANG**

## HISTORY

A 72-year-old man presents with shortness of breath and fever. There is no recent history of surgery or an invasive procedure.

A

■**FIGURE 1-29A** Posteroanterior chest radiograph shows a peripherally located large air-fluid collection in the left hemithorax which has an oblong shape (longer longitudinally than axially) and marked medial compression of the left lung parenchyma.

B

**FIGURE 1-29B** Intravenous contrast enhanced chest CT (mediastinal window) through the lower lung shows a large peripheral left hemithorax collection with appearances of an empyema. The collection is oblong shaped with obtuse margins with the pleura, smooth inner margins and the split pleura sign. The presence of an air-fluid level in absence of an invasive procedure is worrisome for a bronchopleural fistula. An additional smaller left pleural collection is noted posteriorly.

C

**FIGURE 1-29C** Chest CT (lung window) through the lower lung shows that the surrounding lung parenchyma is displaced by the pleural collections. A left lower lobe bronchus runs posterior to the empyema rather than into or toward it.

## DIFFERENTIAL DIAGNOSIS

**Empyema complicated by bronchopleural fistula:** The shape of the fluid collection in this case (oblong) and the obtuse margins the collection has with the pleura favor a pleural collection such as an empyema. The presence of air in a pleural collection, in the absence of intervention, is worrisome for a bronchopleural fistula.

- **Hydropneumothorax:** Although the radiographic findings could represent a hydropneumothorax following surgery or thoracentesis, the CT appearances of thickened enhancing pleura, clinical history of fever, and absence of recent intervention make this diagnosis less likely.
- **Lung abscess:** Lung abscesses can be peripheral in location with air-fluid levels and thick walls, but the oblong shape and smooth inner margins of the collection argue against the diagnosis of an abscess.

## DIAGNOSIS

**Empyema complicated by bronchopleural fistula**

## KEY FACTS

### Clinical

- The presence of air in a pleural fluid collection is most commonly iatrogenic in origin, secondary to thoracot-omy, thoracentesis, or tube drainage. In the absence of previous intervention, a bronchopleural fistula must be considered; this is usually accompanied by infection. Infection with gas-producing organisms may be considered, but unlike abdominal infections, pleural infections rarely are accompanied by gas production.
- Pleural effusions associated with pneumonia can be simple parapneumonic effusions, complicated para-pneumonic effusions, or empyemas. Differentiation is made pathologically on pleural fluid analysis.
- Organisms responsible for empyema are most commonly gram-negative bacteria, *Staphylococcus aureus, Streptococcus pneumonia* and *M. tuberculosis*.
- The differentiation between empyema and lung abscess is crucial to management. Empyemas require tube drainage of the pleural space, while lung abscess requires antibiotic therapy. Tube drainage of a lung abscess is contraindicated because of the risk of development of secondary empyemas and parenchymal spread of the abscess.

### Radiologic

- In the setting of infection, when differential considerations include abscess or empyema, fluid collections that are longer in one dimension than the other (oblong shaped) and have obtuse margins with the pleura are more likely to represent empyema.
- Empyemas have smooth inner margins and displace adjacent lung away from the collection.
- In contrast to empyemas, lung abscesses form spherical cavitary lesions, which have acute margins with the pleura, irregular inner margins, and circumferentially destroy lung parenchyma rather than displacing it. Lung destruction is seen as surrounding

consolidated lung with airways traveling into the abscess.

- The split pleura sign is a CT finding of thickened and enhancing visceral and parietal pleura separated by pleural fluid. This finding is observed in empyema, but in other clinical settings can also be seen with pleural malignancy or inflammatory pleural disease.
- Multidetector CT with multiplanar reconstructions can be useful in guiding surgery by identifying and localizing the peripheral bronchopleural fistula.

## SUGGESTED READING

Kuhlman JE. Complex disease of the pleural space: the 10 questions most frequently asked of the radiologist—new approaches to their answers with CT and MR imaging. Radiographics 1997;17:1043–1050.

Kuhlman JE, Singha NK. Complex disease of the pleural space: radio-graphic and CT evaluation. Radiographics 1997;17:63–79.

Ricci ZJ, Haramati LB, Rosenbaum AT, Liebling MS. Role of computed tomography in guiding the management of peripheral bronchopleural fistula. J Thorac Imaging 2002;17:214–218.

# Chapter TWO

# Breast Imaging

**MARY SCOTT SOO** ▪ CHAPTER EDITOR

Margaret E. Williford

Ruth Walsh

Phyllis J. Kornguth

Danielle L. Wellman

Adam Charles Braithwaite

Beth Whiteside

# CASE 1

**MARGARET E. WILLIFORD**

**AND**

**MARY SCOTT SOO**

**HISTORY**

Screening mammogram in a 44-year-old woman.

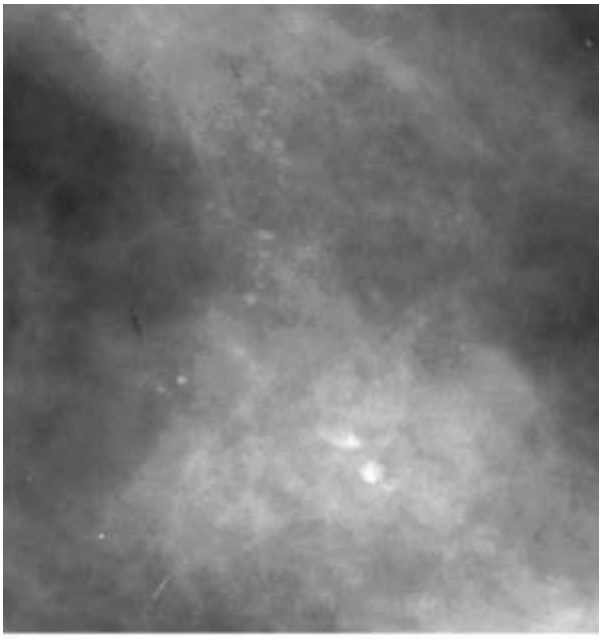

A

■**FIGURE 2-1A** Photographically enlarged, magnified craniocaudal mammogram of the right breast demonstrates heterogeneously dense fibroglandular tissue. Multiple vague, round, and indistinct calcifications are present. No calcifications were identified in other regions of the breast.

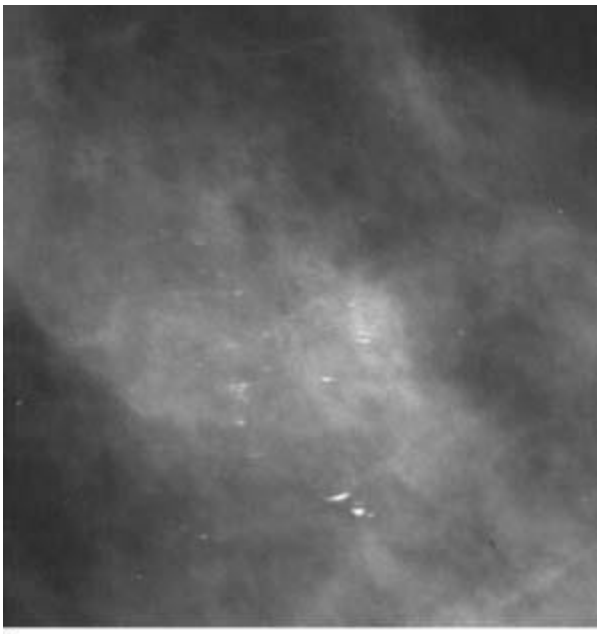

B

■**FIGURE 2-1B** Photographically enlarged, magnified true lateral mammogram of the right breast in the same region seen in Figure 2-1A. The calcifications are denser and assume a teacup or meniscus appearance as they layer ependently.

## DIFFERENTIAL DIAGNOSIS

- **Milk of calcium:** This is the best diagnosis because milk of calcium has different appearances depending on the mammographic projection obtained. The calcifications are often smudge-like or indistinct on the craniocaudal views but have a teacup or meniscus appearance on horizontal beam, 90-degree lateral radiographs.
- **Fat necrosis:** The calcifications associated with fat necrosis often vary in density and shape and can be indistinguishable from carcinoma. Many of the calcifications evolve over time to a more coarse configuration, or may have an eggshell appearance, as seen in oil cysts. However, the appearance of fat necrosis does not usually vary on the different projections, making this an unlikely diagnosis in this case.
- **Carcinoma:** Calcifications associated with carcinoma are often pleomorphic, varying in shape and density. However, the appearance of calcifications associated with carcinoma does not change on the different mammographic projections, making carcinoma a poor choice in this case.

**After assessing the imaging findings and considering the differential diagnosis, the final assessment is BI-RADS Category 2, benign. Recommend annual screening mammography.**

## DIAGNOSIS

**Milk of calcium**

## KEY FACTS

### Clinical

- Milk of calcium represents calcified debris that is sedi-mented in the dependent portions of microcysts or cystically dilated acini of cystic lobular hyperplasia.
- Benign milk of calcium calcifications are seen in 4% to 6% of women undergoing mammography.
- Milk of calcium is usually seen in multiple areas of the breast and is usually bilateral. It can be a diagnostic problem when it appears as a unilateral focus. It is important to recognize milk of calcium so that an inappropriate biopsy is not recommended.
- Milk of calcium calcifications are benign and do not require a biopsy, but carcinomas can occur adjacent to such microcystic calcifications. Therefore, each group of calcifications must be inspected carefully.

### Radiologic

- The shape of milk of calcium calcifications has been described as meniscus, crescent, teacup, or semilunar. The meniscus or crescent shape is best seen on an erect 90-degree lateral projection since the x-ray beam is horizontal and therefore tangential to the fluid calcium interface in the microcyst.
- On the 90-degree lateral view, the linear, curvilinear, or meniscus-shaped calcifications will be oriented parallel to one another along the horizontal axis. The upper border of the calcification may be less distinct than the lower border where the sedimented calcified debris is sharply bounded by the wall of the microcyst.
- The characteristic meniscus or crescent shape is not as well seen on the 45-degree mediolateral oblique view.
- On the craniocaudal projection, the calcifications are seen en face since the x-ray beam is vertical and therefore perpendicular to the fluid calcium interface in the microcyst.
- On the craniocaudal projection, the calcifications are round or ovoid smudges. They can be so faint that they are invisible.
- The dramatic difference in the appearance of the calcifications on the craniocaudal, mediolateral, and 90-degree lateral projections is a characteristic feature of benign milk of calcium.
- When milk of calcium calcifications are suspected, magnification views in the 90-degree lateral projection and craniocaudal projection should be performed.

## SUGGESTED READING

Hamer MJ, Cooper AG, Pile-Spellman ER. Milk of calcium in breast microcysts: manifestation as a solitary focal disease. Am J Roentgenol 1988;150:789.

Linden SS, Sickles EA. Sedimented calcium in benign breast cysts. Am J Roentgenol 1989;152:957.

Moy L, Slanetz PJ, Yeh ED, et al. The pendent view: an additional projection to confirm the diagnosis of milk of calcium. Am J Roentgenol 2001;177:173–175.

Sickles EA, Abele JS. Milk of calcium within tiny benign breast cysts. Radiology 1981;141:655.

D'Orsi CJ, Mendelson EB, Ikeda DM, et al. Breast Imaging Reporting and Data System: ACR BI-RADS - Breast Imaging Atlas. Reston, VA: American College of Radiology, 2003.

# CASE 2

**RUTH WALSH**

**AND**

**MARY SCOTT SOO**

**HISTORY**

A 45-year-old asymptomatic woman presenting for a screening mammogram. A breast ultrasound was subsequently performed.

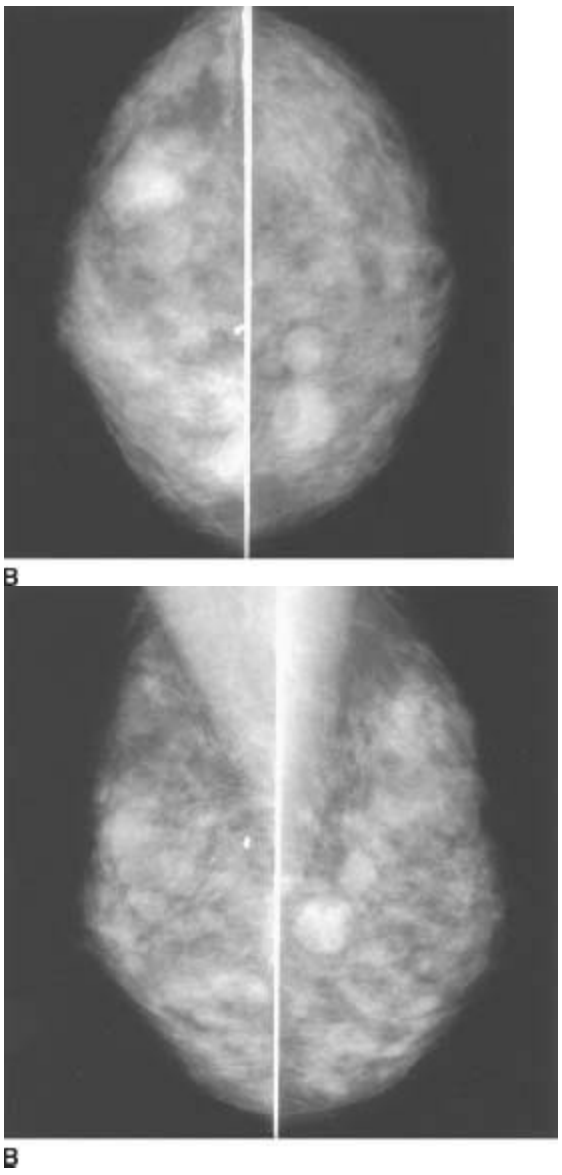


**FIGURES 2-2A and 2-2B** Craniocaudal **(A)** and mediolateral oblique **(B)** mammograms of both breasts show heterogeneously dense fibroglandular tissue. Multiple, bilateral, and predominantly well-circumscribed oval and round masses are present.

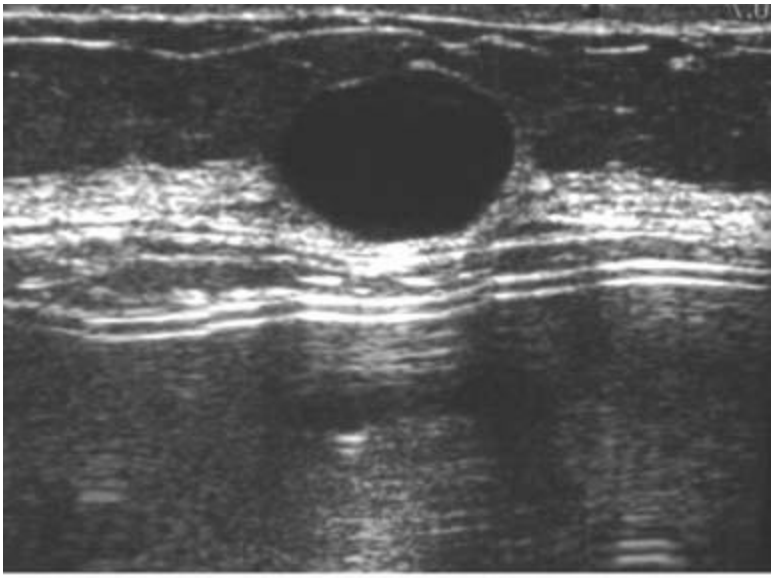

C

**FIGURE 2-2C** Longitudinal sonographic image of the medial left breast, 10:00 position. Sonography of one of the masses shows an anechoic, well-circumscribed oval mass with posterior acoustic enhancement. This appearance was typical of the remainder of the masses.

## DIFFERENTIAL DIAGNOSIS

**Cysts:** As seen in this case, cysts are anechoic, well-circumscribed masses that have posterior acoustic enhancement. Cysts are the most commonly encountered breast masses, which cannot be differentiated from other circumscribed masses at mammography unless they contain milk of calcium. Sonography can be used to differentiate cysts from solid breast masses accurately.

**Fibroadenomas:** Fibroadenomas can be multiple or bilateral in 15% of cases and are the most common palpable breast masses in adolescents and young women. Although noncalcified fibroadenomas cannot be differentiated at mammography from other circumscribed masses, fibroadenomas appear solid at sonography, unlike the lesions in this case. Large, coarse, popcornlike calcifications are pathognomonic mammographic findings of degenerating fibroadenomas.

**Metastases:** The sonographic appearance of metastases is that of a solid mass, differing from the lesions seen in this case. Metastatic disease to the breast from an extramammary primary malignancy is rare (0.5% to 1.3% of breast malignancies) and most often has the mammographic appearance of single or multiple circumscribed masses. A clinical history of extramammary malignancy should be present to suspect this diagnosis.

**Papillomas:** Papillomas are less common masses seen at mammography. They are usually <1 cm in size and are typically located in the subareolar region. At sonog-raphy,

papillomas are often solid, lobulated masses, making this diagnosis unlikely in the case illustrated. A papilloma can also present as a complex mass at sonography (intracystic or intraductal papilloma), for which biopsy is indicated to exclude a malignant lesion.

- **Lymph nodes:** Intramammary lymph nodes are typically <1 cm in size, often demonstrate a fatty hilus at mammography, and are usually located in the upper outer quadrants of the breasts. At sonography, lymph nodes are usually hypoechoic with an echogenic fatty hilus. All these features make this an unlikely diagnosis in this case.

**After assessing the imaging findings and considering the differential diagnosis, the final assessment is BI-RADS Category 2, benign. Recommend annual screening mammography**.

## DIAGNOSIS

**Bilateral simple cysts confirmed by ultrasound**

## KEY FACTS

### Clinical

- Cysts can be seen in all age groups but are more common in women 30 to 50 years of age.
- Cysts arise in the terminal duct lobular units. They can be grossly visible at mammography or seen only microscopically.
- Autopsy studies report grossly visible cysts in 20% to 50% of women.
- Cysts cannot be differentiated reliably from solid palpable masses on physical examination. Therefore, sonog-raphy or needle aspiration is necessary to confirm the diagnosis.

### Radiologic

- Cysts are typically round, oval, or lobular in shape and often multiple and bilateral.
- Cyst margins are usually well-defined on mammography if not obscured by adjacent fibroglandular tissue. Occasionally, the margins can be indistinct.
- Because cysts cannot be differentiated from other circumscribed masses at mammography, sonography is performed to establish the diagnosis.
- Strict sonographic criteria for a simple cyst include anechoic round or oval appearance, smooth, well-circumscribed margins, and posterior acoustic enhancement.
- When multiple, bilateral, round or oval well-circumscribed masses are present on a baseline screening mammogram, sonography can be performed to determine if the masses are cystic or solid. A 12-month follow-up mammogram is usually recommended

for these cystic or solid masses if there are no suspicious features, dominant mass, or history of an extramammary malignancy.

## SUGGESTED READING

Adler DD. Mammographic evaluation of masses. In DB Kopans (ed). Syllabus: A Categorical Course in Breast Imaging. Oak Brook, IL: RSNA,1995:107-116.

Bohman LG, Bassett LW, Gold RH, Volt R. Breast metastases from extramammary malignancies. Radiology 1982;144:309-312.

Jackson VP. Circumscribed microlobulated noncalcified mass. In BA Siegel (ed). Breast Disease Test and Syllabus (2nd Series). Reston, VA: American College of Radiology, 1993:89-99.

Kopans DB (ed). Breast Imaging. Philadelphia, PA: Lippincott, 1989.

Soo MS, Ghate SV, Baker JA, et al. Streaming detection for evaluation of indeterminate sonographic breast masses: a pilot study. Am J Roentgenol 2006;186:1335-1341.

Weinstein SP, Conant EF, Sehgal C. Technical advances in breast ultrasound imaging. Semin Ultrasound CT MR 2006;27:273-283.

# CASE 3

**RUTH WALSH**

**AND**

**MARY SCOTT SOO**

## HISTORY

A 43-year-old woman with a palpable lump in the upper outer quadrant of the right breast presents for diagnostic mammography. There is no past surgical history.

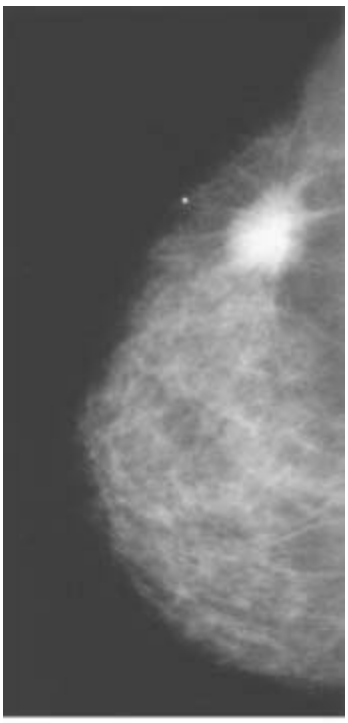

A

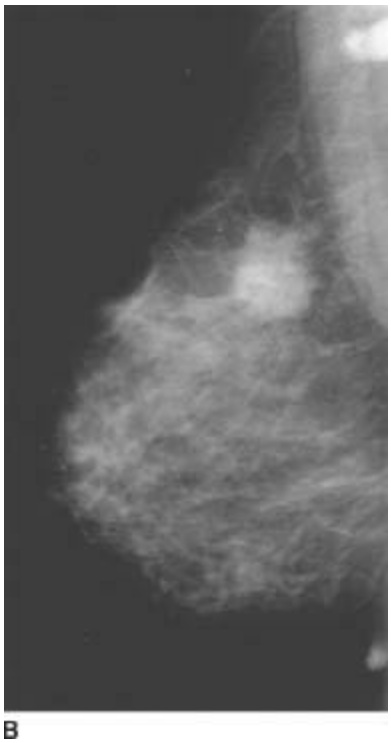

B

■**FIGURES 2-3A and 2-3B** Exaggerated lateral craniocaudal view of the right breast with cutaneous BB marking the palpable lump **(A),** and mediolateral oblique view of the right breast **(B)** show heterogeneously dense fibroglandular tissue. A 3-cm irregular mass with spiculated margins is present in the upper outer quadrant of the right breast. Several faint punctate microcalcifications are present within the mass. A rounded, dense 1.5-cm lymph node is present in the right axilla.

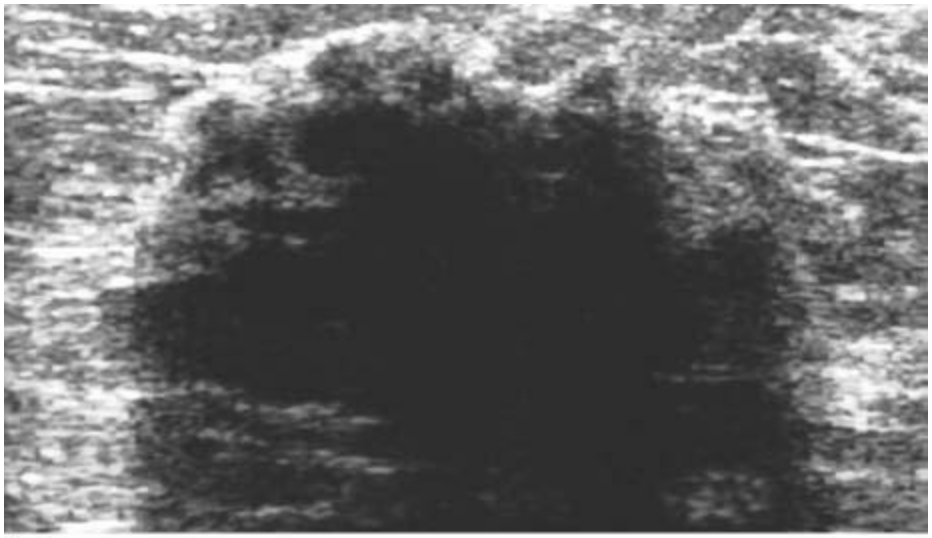

C

**FIGURE 2-3C** Ultrasound of the right breast mass demonstrates an irregular, hypoechoic, microlobulated mass with posterior acoustic shadowing.

## DIFFERENTIAL DIAGNOSIS

**Carcinoma:** A mass with spiculated margins is almost pathognomonic of malignancy. The abnormal axillary lymph node is suggestive of metastatic disease. These features make carcinoma the most likely diagnosis. Although a few rare benign processes can present as spiculated lesions, biopsy is indicated to exclude malignancy.

**Posttraumatic scarring and fat necrosis:** There is no history of prior trauma or breast surgery, making this diagnosis unlikely. A postoperative scar can appear as an area of architectural distortion or a spiculated mass that should either decrease in size and density or remain stable over time. Any increase in size should prompt biopsy. To confirm the diagnosis of a surgical scar, the site of the spiculated lesion must match the location of the patient's cutaneous scar and the location of the biopsied lesion on preoperative or needle localization mammograms.

**Radial scar/complex sclerosing lesion:** Radial scars are regions of architectural distortion that typically have long, thin spicules radiating outward from a radiolucent center. However, occasionally they can appear dense centrally and contain microcalcifications. The large central mass in this case makes the diagnosis of radial scar unlikely. The term *radial scar* is used when the lesion measures <1 cm and *complex sclerosing lesion* is used when the lesion measures >1 cm. These benign proliferative lesions of unknown etiology are usually nonpalpable and cannot be differentiated reliably from carcinoma without biopsy.

**Abscess:** Because there is no history of pain, swelling, or erythema, this is an unlikely diagnosis. Abscesses tend to occur in the subareolar region and often are associated with mammographic changes of mastitis, such as diffuse skin thickening and increased

trabecular density.

- **Granular cell tumor:** These benign tumors have a spic-ulated appearance at mammography but are very rare, making this diagnosis less likely. Biopsy is indicated to differentiate these lesions from carcinoma.
- **Extraabdominal desmoid tumor:** These are locally invasive tumors that do not metastasize. Their mam-mographic appearance mimics that of an invasive breast cancer, requiring biopsy for diagnosis. These, too, are rare, making the diagnosis unlikely in the case illustrated.

**After assessing the imaging findings and considering the differential diagnosis, the final assessment is BI-RADS Category 5, highly suggestive of malignancy. Biopsy and other appropriate clinical action should be taken.**

## DIAGNOSIS

**Infiltrating ductal carcinoma with metastatic carcinoma to axillary lymph nodes**

## KEY FACTS

### Clinical

- Breast cancer is the most common malignancy in American women, excluding skin cancers. After lung cancer, it is the second leading cause of cancer death among women.
- According to current estimates, breast cancer will be diagnosed in approximately one in eight women in their lifetime.
- Invasive ductal carcinoma, not otherwise specified, comprises 65% to 80% of invasive breast cancers. The second most common type is invasive lobular carcinoma, accounting for 3% to 14% of cases. Other, less common specific forms of ductal carcinoma include medullary, mucinous, papillary, and tubular carcinoma.

### Radiologic

- A spiculated mass, characterized by lines radiating outward from a central mass, is the most common mam-mographic appearance for invasive ductal carcinoma.
- Spiculated margins usually signify invasion.
- Spiculated projections result from (1) a desmoplastic response (connective tissue proliferation) that distorts the adjacent tissue, (2) tumor infiltrating into the surrounding tissue, or (3) both conditions.
- A spectrum of mammographic appearances can be seen with invasive ductal carcinoma, including (1) masses with either spiculated, microlobulated, indistinct, and circumscribed margins; (2) architectural distortion; and (3) focal asymmetric or developing densities.

- Ultrasound often shows an irregular, hypoechoic, shadowing mass that can have ill-defined, microlobulated, or spiculated margins.

## SUGGESTED READING

Adler DD. Mammographic evaluation of masses. In DB Kopans (ed). Syllabus: A Categorical Course in Breast Imaging. Oak Brook, IL: RSNA, 1995:107–116.

De Paredes ES. Atlas of Film-Screen Mammography. Baltimore, MD: Williams & Wilkins, 1992.

Feig SA. Breast masses: mammographic and sonographic evaluation. Radiol Clin North Am 1992;30:67–92.

Smith RA. The epidemiology of breast cancer. In DB Kopans (ed). Syllabus: A Categorical Course in Breast Imaging. Oak Brook, IL: RSNA, 1995:7–20.

Yang WT, Hennessy B, Broglio K, et al. Imaging differences in metaplastic and invasive ductal carcinomas of the breast. Am J Roentgenol 2007;189:1288–1293.

# CASE 4

**MARGARET E.**

**WILLIFORD AND**

**MARY SCOTT SOO**

## HISTORY

Annual diagnostic mammogram in a 70-year-old woman, status post right lumpectomy in the upper central breast and radiation therapy for treatment of carcinoma.

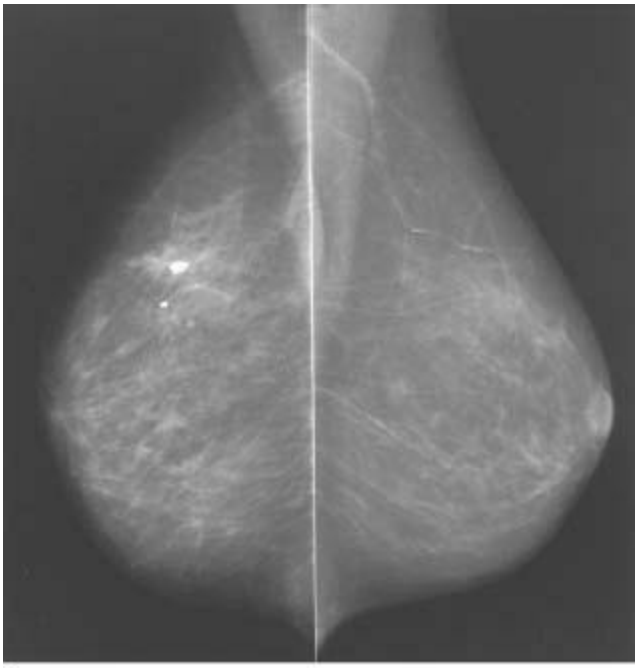

A

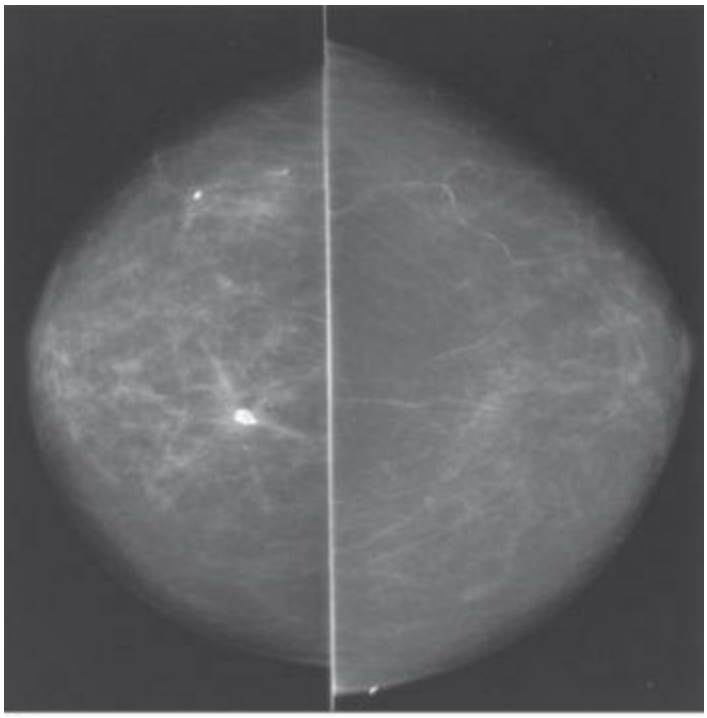

B

**FIGURES 2-4A and 2-4B** Mediolateral oblique **(A)** and craniocaudal **(B)** mammograms of right and left breasts show scattered fibroglandular tissue bilaterally. Right breast shows focal asymmetry and focal distortion with coarse benign dystrophic calcification in the superior medial quadrant.

## DIFFERENTIAL DIAGNOSIS

**Postoperative and postradiation changes of right breast:** This is the best diagnosis, given the history and correlation of architectural distortion and coarse dystrophic

calcification to the site of lumpectomy.

- **Edema:** This diagnosis is less likely because edema is commonly bilateral, with no associated mass or focal distortion. Correlation with physical exam is helpful.
- **Inflammatory carcinoma:** Inflammatory carcinoma has prominent, diffuse asymmetric density and skin thickening. In its pure form, there is no focal mass or distortion, but in many cases, there is a focal mass-like density. Clinical presentation and physical exam are important correlates, which demonstrate an erythema-tous, nontender breast with peau d'orange appearance of the skin. This diagnosis is considered less likely due to the history of radiation therapy. Inflammatory carcinoma also would not be expected to be associated with dystrophic calcifications.
- **Mastitis:** Mastitis presents with a clinical history of tenderness and fever, not present in this case. Physical exam reveals cutaneous inflammatory changes and tenderness. Focal mass is usually not present unless there is an abscess. Biopsy is indicated if there is incomplete resolution with antibiotic therapy.

**After assessing the imaging findings and considering the differential diagnosis, the final assessment is BI-RADS Category 2, benign. Recommend annual mammography**.

## DIAGNOSIS

**Postoperative and postradiation changes following lumpectomy and radiation therapy**

## KEY FACTS

### Clinical

- Lumpectomy creates focal distortion of normal breast parenchyma at the site of the tumor. Radiation causes fibrosis throughout the breast and can enhance the distortion created by the surgical excision.
- Skin thickening and asymmetry in breast size may be evident on clinical exam.

### Radiologic

- Diagnosis of postoperative distortion can be confirmed by correlating posttherapy films with preoperative films showing the site of the tumor and needle localization done before the surgical excision. Scar markers can also be placed on the skin at the site of surgical scar, aiding in correlating the distortion with the surgical site.
- Postoperative distortion and asymmetric increased density due to surgery and radiation are most prominent on the first posttherapy mammogram done 6 to 12 months

after therapy.

- Distortion and asymmetric density gradually stabilize or resolve over time, usually 2.5 to 3.0 years following therapy.
- Benign, dystrophic calcifications are a commonly associated finding, particularly at the lumpectomy site. Radiation and surgery can also cause benign fat necrosis calcifications.
- Recurrent tumor can occur at the site of the primary tumor; therefore, magnification views of the lumpec-tomy site are routinely performed during annual diagnostic mammography. Increased mass, distortion, or malignant-appearing calcifications are signs that may indicate recurrence. These findings should prompt biopsy.

## SUGGESTED READING

Dershaw DD. Evaluation of the breast undergoing lumpectomy and radiation therapy. Radiol Clin North Am 1995;33:1147–1160.

Mendelson EB. Evaluation of the post-operative breast. Radiol Clin North Am 1992;30:107–138.

Preda L, Villa G, Rizzo S, et al. Magnetic resonance mammography in the evaluation of recurrence at the prior lumpectomy site after conservative surgery and radiotherapy. Breast Cancer Res 2006;8:R53.

# CASE 5

**MARY SCOTT SOO**

### HISTORY

Diagnostic mammogram in a 33-year-old woman with pain in her left breast. Sixteen years ago she underwent breast augmentation with silicone implants; the right implant was ruptured and replaced 3 years before the mammogram shown in Figure 2-5A. One year prior to the mammogram shown in Figure 2-5B, she underwent explantation of both implants.

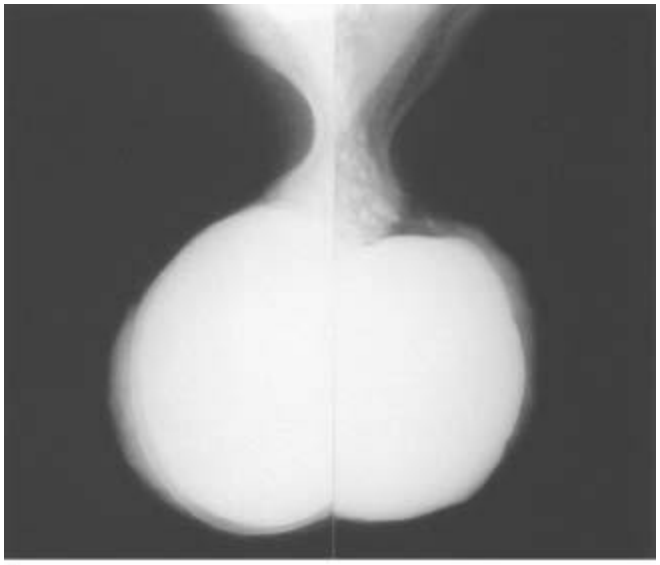

A

■**FIGURE 2-5A** Mediolateral oblique mammograms of both breasts. Bilateral subglandular implants are present. On the left, the contour of the single-lumen silicone implant is lobulated, and multiple high-density nodules are seen in the left axilla. On the right, a double-lumen implant is present with the outer saline lumen intact.

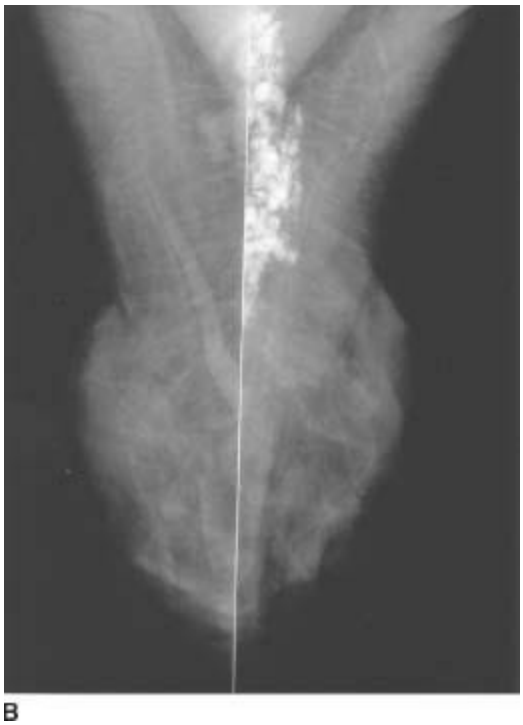

B

■**FIGURE 2-5B** Repeat mediolateral oblique mammograms of both breasts 1 year after explantation of the prostheses. The prostheses have been removed. There are persistent high-density nodules within the left axilla. No mammographic abnormality is seen within either breast.

## DIFFERENTIAL DIAGNOSIS

- **Ruptured silicone implant with free silicone extravasation into the left axilla:** This is the best diagnosis because the high-density nodules in the axilla are equal in density to the silicone prosthesis, resulting from migration of free silicone away from the ruptured prosthesis. The lobulated contour of the prosthesis is not specific for implant rupture if seen as an isolated finding but should raise the question of rupture and prompt further evaluation.
- **Breast carcinoma metastatic to axillary lymph nodes:** This diagnosis is unlikely because the density of the nodules in the axilla is equal to silicone, higher even than expected for nodes involved with metastatic disease. In addition, there are no breast lesions that are suspicious for carcinoma.
- **Sarcoidosis:** Axillary lymph nodes can be seen at mammography in patients with sarcoidosis. However, the process is usually bilateral, and nodes are usually enlarged. Abnormal lymph nodes associated with sar-coidosis are denser than normal fatty-replaced lymph nodes but do not have density as high as silicone, making this an unlikely diagnosis in this case.

**After assessing the imaging findings and considering the differential diagnosis, the final assessment is BI-RADS Category 2, Benign. Further evaluation of free silicone in the left axilla should be based on clinical examination**.

## DIAGNOSIS

**Ruptured silicone prosthesis on the left, with residual free silicone seen 1 year later**

## KEY FACTS

### Clinical

- Rupture of prostheses (intracapsular or extracapsular) is considered a major complication of prosthesis placement, which necessitates surgical explantation of the ruptured implant.
- Intracapsular rupture occurs when the gel escaping from a ruptured implant is contained within the surrounding fibrous capsule.
- Extracapsular rupture occurs when free silicone from a ruptured implant extends outside of the fibrous capsule. This free silicone is difficult to remove completely at surgery and can stimulate a granulomatous reaction within the breast.
- Silicone granulomas can cause a palpable mass, which is difficult to differentiate from carcinoma.

### Radiologic

- When extracapsular free silicone is present, the diagnosis of rupture can often be made mammographically because the density of the free silicone within the breast tissue is higher than that of other structures.
- The presence of extracapsular silicone is often diagnostic of implant rupture. However, sometimes prior films are needed to document the source of the rupture. For instance, in a patient in whom a previously ruptured implant has been replaced, prior films would be needed to determine which implant was the source of the extracapsular silicone.
- Ruptures that occur posteriorly or ruptures in which only a small amount of silicone escapes into the breast parenchyma may not be detected mammographically because they are either not included on the image or the dense prosthesis obscures visualization of the free silicone. In these situations, other imaging studies, such as MRI or sonography, are necessary to make the diagnosis.
- Mammography cannot detect intracapsular rupture reliably. MRI has the highest sensitivity and specificity for diagnosing intracapsular rupture.

## SUGGESTED READING


Berg WA, Caskey CI, Hamper UM, et al. Diagnosing breast implant rupture with MR imaging, US, and mammography. Radiographics 1993;13:1323–1336.

Berg WA, Caskey CI, Hamper UM, et al. Single- and double-lumen silicone breast implant integrity: prospective evaluation of MR and US criteria. Radiology 1995;197:45–52.

Caskey CI, Berg WA, Hamper UM, et al. Imaging spectrum of extracapsu-lar silicone: correlation of US, MR imaging, mammographic, and histo-pathologic findings. Radiographics 1999;19 Spec No:S39–S51.

Destouet JM, Monsees BS, Oser RF, et al. Screening mammography in 350 women with breast implants: prevalence and findings of implant complications. Am J Roentgenol 1992;159:973–987.

Everson LI, Parantainen H, Detlie T, et al. Diagnosis of breast implant rupture: imaging findings and relative efficacies of imaging techniques. Am J Roentgenol 1994;163:57–60.

Gorczyca DP, Gorczyca SM, Gorczyca KL. The diagnosis of silicone breast implant rupture. Plast Reconstr Surg 2007;120:49S–61S.

Gorczyca DP, Sinha S, Ahn CY, et al. Silicone breast implants in vivo: MR imaging. Radiology 1992;185:407–410.


# CASE 6


**RUTH WALSH**

**AND**

**MARY SCOTT SOO**

**HISTORY**

Diagnostic mammogram in a 52-year-old female, status post left mastectomy for breast cancer and right subcutaneous mastectomy with implant reconstruction.

A

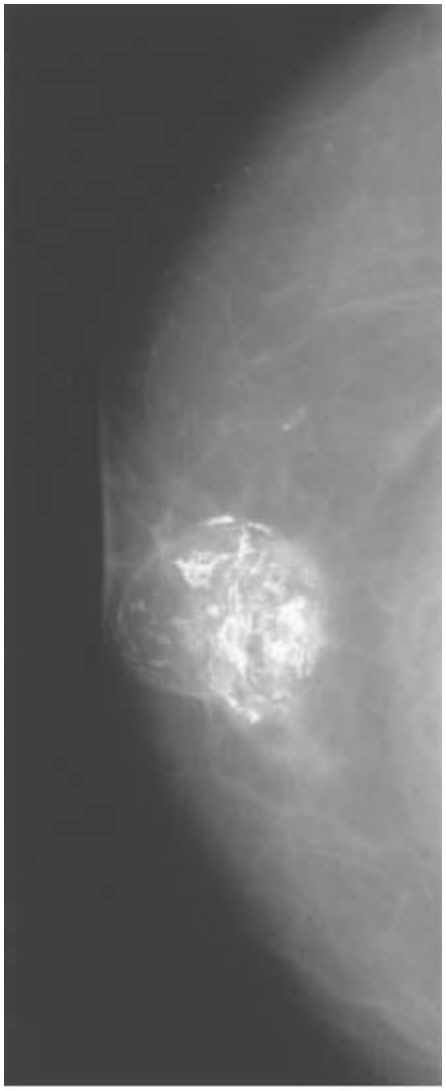

B

**FIGURES 2-6A and 2-6B** Routine mediolateral oblique **(A)** and craniocaudal **(B)** "implant exclusion"or "push-back"mammograms of the right breast. Minimal residual fibroglandular tissue remains in the breast status post subcutaneous mastectomy. A 3-cm radiolucent mass with associated rim-like and dystrophic calcifications is present in the subareolar region. A submuscular silicone implant is partially visualized on the mediolateral oblique view.

## DIFFERENTIAL DIAGNOSIS

**Fat necrosis:** Low-density (fatty) masses in the breast are almost always benign. A low-density mass associated with dystrophic (bizarre, irregular, and plaquelike) calcifications, as is seen in this case, is most consistent with fat necrosis. Dystrophic calcifications can be seen with fat necrosis secondary to trauma, surgery, or radiation therapy.

**Carcinoma:** Malignant calcifications are usually <0.5 mm in size, ranging from minute

up to 3 mm. Many of the calcifications in the case illustrated are >2 to 3 mm in size and have benign rim and plaque-like shapes, making carcinoma an unlikely diagnosis.

- **Fibroadenoma:** Although fibroadenomas can contain large, bizarre, irregular calcifications, as seen in this case, involuting fibroadenomas typically contain coarse or "popcorn-like"calcifications. The mass in this case is not consistent with a fibroadenoma because it has low density, as opposed to fibroadenomas, which are water-density masses.
- **Secondary hyperparathyroidism with metastatic calcifications:** Patients with hypercalcemia can develop coarse amorphous calcifications within the breast. However, this is rare, and calcifications would not be expected to be rim-like or associated with a radiolucent mass, making this diagnosis unlikely.

**After assessing the imaging findings and considering the differential diagnosis, the final assessment is BI-RADS Category 2, benign. Recommend annual screening mammography for the right breast**.

## DIAGNOSIS

**Fat necrosis secondary to prior subcutaneous mastectomy surgery**

## KEY FACTS

### Clinical

- Fat necrosis is an inflammatory response that is usually due to trauma or surgery but can be idiopathic.
- Fat necrosis can be difficult to distinguish from carcinoma on both physical examination and mam-mography.
- Clinically, fat necrosis can present as a hard painless mass that is ill-defined and poorly mobile. Skin thickening or retraction may also be identified, increasing the clinical suspicion of carcinoma.
- In some cases, the traumatic event leading to fat necrosis is forgotten or unknown.

### Radiologic

- At mammography, fat necrosis has a wide spectrum of appearances, ranging from well-defined oil cysts to spiculated masses that simulate carcinoma.
- Calcifications are commonly associated with fat necrosis. When calcifications first appear, they can be small and pleomorphic, mimicking malignant calcifications. However, they usually evolve into larger, coarse, plaque-like calcifications that have a more benign appearance.

- Early dystrophic calcifications can be difficult to distinguish from malignancy. If calcifications cannot be assessed as benign following magnification mammography, then core biopsy may be warranted to exclude malignancy.

## SUGGESTED READING

De Paredes ES. Atlas of Film-Screen Mammography. Baltimore, MD: Williams & Wilkins, 1992.

Feig SA. Mammographic evaluation of calcifications. In DB Kopans, EB Mendelson (eds), Syllabus: A Categorical Course in Breast Imaging. Oak Brook, IL: RSNA, 1995.

Mendelson EB. Evaluation of the post operative breast. Radiol Clin North Am 1992;30:107–138.

Morrow M. Breast trauma, hematoma, and fat necrosis. In JR Harris, S Hellman, IC Henderson, DW Kinne (eds). Breast Disease. Philadelphia, PA: Lippincott, 1991.

Tan PH, Lai LM, Carrington EV, et al. Fat necrosis of the breast—a review. Breast 2006;15:313–318.

# CASE 7

**PHYLLIS J. KORNGUTH**

**AND**

**MARY SCOTT SOO**

## HISTORY

Screening mammogram in a 36-year-old woman. The family history is significant for a sister with premenopausal breast carcinoma. The patient's prior mammogram was normal.

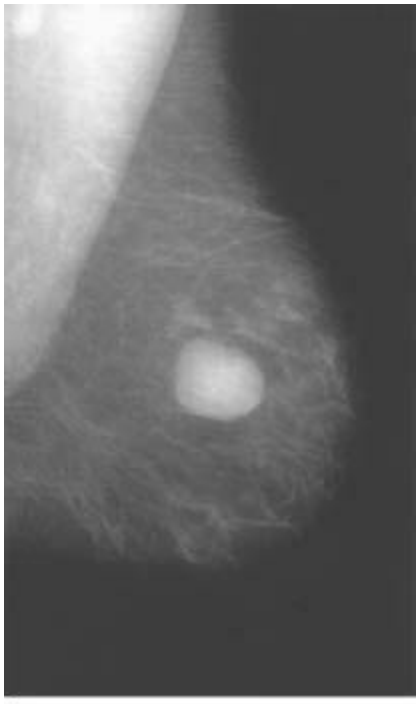

A

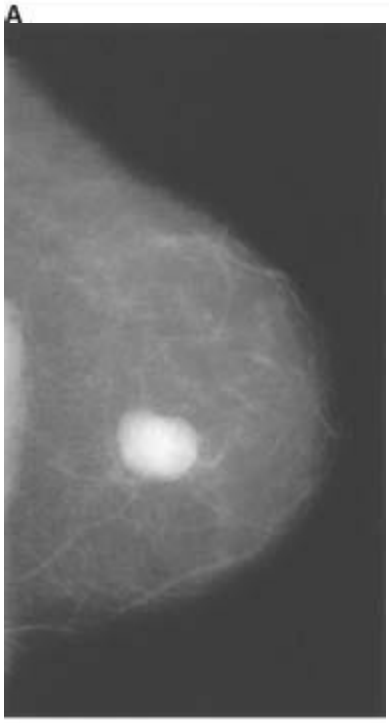

B

■**FIGURES 2-7A and 2-7B** Mediolateral oblique **(A)** and craniocaudal **(B)** mammograms of the left breast show a large, well-circumscribed, solitary noncalcified mass located centrally in a predominantly fatty-replaced breast. The mass was new compared to the prior exam.


C

**FIGURE 2-7C** Sonogram of the mass seen in Figures 2-7A and 2-7B shows a well-defined, solid hypoechoic mass with no posterior acoustic enhancement or shadowing.

## DIFFERENTIAL DIAGNOSIS

**Fibroadenoma:** The mammographic and sonographic features of this lesion, as well as the young age of the patient, are typical of a fibroadenoma.

**Carcinoma:** Some well-defined carcinomas (medullary, mucinous, papillary) can have these mammographic and sonographic features. However, these tumors are uncommon tumors, making this diagnosis less likely.

**Phyllodes tumor:** At mammography, phyllodes tumors are well-circumscribed, often large masses indistinguishable from fibroadenomas or other tumors. The sonographic appearance of a phyllodes tumor can be identical to the lesion in the case illustrated. However, many phyllodes tumors contain cystic spaces, producing a more heterogeneous sonographic appearance.

**Cyst:** The mammographic features of a cyst can be identical to the appearance of the mass in this case. However, the sonogram reveals a solid mass, not a simple cyst.

**After assessing the imaging findings and considering the differential diagnosis, the final assessment is BI-RADS Category 4-A. Low suspicion for malignancy. Biopsy should be considered**.

## DIAGNOSIS

**Fibroadenoma**

## KEY FACTS

### Clinical

- Fibroadenomas are common benign breast lesions that occur in premenopausal and perimenopausal age groups.
- On physical examination, the mass is usually firm, well-defined, and mobile.
- Growth of fibroadenomas is stimulated by hormonal influence.
- Fibroadenomas can be multiple and bilateral. Multiplicity and bilaterality are more common in black women.

### Radiologic

- Biopsy is the standard of care for management of any new mammographic mass that is solid on ultrasound.
- In the case illustrated, the mass had benign features by mammographic and sonographic criteria, including oval shape and circumscribed margins; however, biopsy is the standard of care because the mass was new. The BI-RADS Category 4-A reflects the fact that the lesion has a low suspicion for malignancy, given the high likelihood that it was a fibroadenoma.
- Ultrasound-guided core biopsy is frequently performed to make the diagnosis because it is less invasive and less expensive than open surgical biopsy, yet it allows for surgical planning if a malignancy is diagnosed.
- If a noncalcified, well-circumscribed, benign-appearing solid mass is identified on a *baseline* screening mammogram (i.e., the mass is not palpable and there is no evidence that the mass is new), then 6-month follow-up mammography (BI-RADS Category 3, probably benign finding) would be an acceptable final assessment category and follow-up recommendation.

## SUGGESTED READING


Liberman L, Bonaccio E, Hamele-Bena D, et al. Benign and malignant phyllodes tumors: mammographic and sonographic findings. Radiology 1996;198:122–124.

Sickles EA. Nonpalpable, circumscribed, noncalcified solid breast masses: likelihood of malignancy based on lesion size and age of patient. Radiology 1994;192:439–442.

Skaane P, Engedal K. Analysis of sonographic features in the differentiation of fibroadneoma and invasive ductal carcinoma. Am J Roentgenol 1998;170:109–114.

Sklair-Levy M, Sella T, Alweiss T, et al. Incidence and management of complex fibroadneomas. Am J Roentgenol 2008;190:214–218.

Smith BL. Fibroadenomas. In JR Harris, S Hellman, IC Henderson, DW Kinne (eds). Breast Diseases. Philadelphia, PA: Lippincott, 1991:34–37.

# CASE 8

**MARGARET E. WILLIFORD**

**AND**

**MARY SCOTT SOO**

## HISTORY

**Screening mammogram in a 49-year-old premenopausal woman. She had no palpable abnormality or history of surgery.**

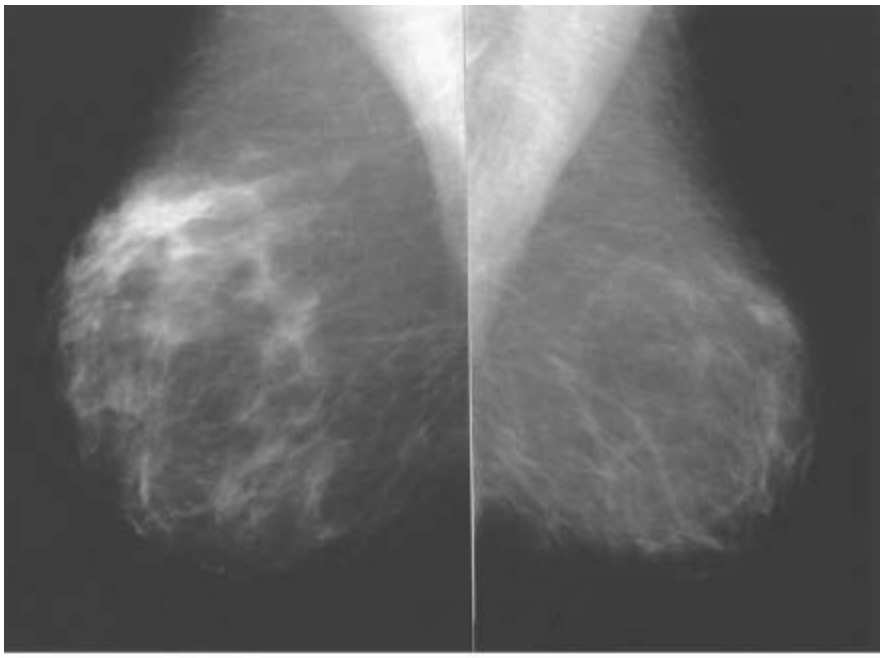

A

■**FIGURE 2-8A** There is scattered fibroglandular tissue in the left breast and heterogeneously dense tissue in the right breast. Mediolateral oblique mammograms of right and left breasts show global asymmetry in the lateral right breast.

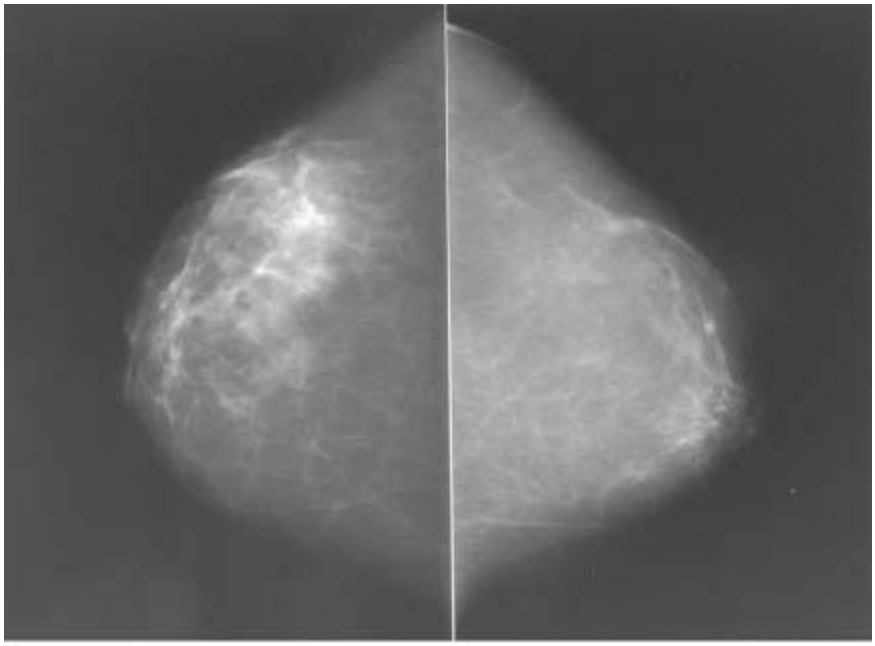

B

**FIGURE 2-8B** Craniocaudal mammograms of right and left breasts show global asymmetry in the outer right breast.

## DIFFERENTIAL DIAGNOSIS

- **Global asymmetry of fibroglandular tissue:** This is the best diagnosis because the asymmetry is dispersed throughout the lateral right breast and has the appearance of normal parenchyma with no underlying suspicious characteristics. No corresponding palpable mass was identified to raise the suspicion for other processes.
- **Postoperative change with removal of breast tissue from the contralateral breast:** This diagnosis is unlikely because there is no history of prior breast surgery.
- **Carcinoma:** Although carcinoma may rarely present as global asymmetry, there is no associated palpable mass or associated suspicious mammographic feature to suggest malignancy.
- **Focal asymmetry:** This diagnosis is unlikely because the asymmetry involves a large area of the breast.

**After assessing the imaging findings and considering the differential diagnosis, the final assessment is BI-RADS Category 3, probably benign. A 6-month interval follow-up is suggested**.

## DIAGNOSIS

**Global asymmetry of breast tissue**

## KEY FACTS

### Clinical

- At least 3% of women have asymmetric breast tissue that appears as an increased volume or asymmetry relative to the contralateral breast. This is most commonly seen in the upper outer quadrants. It reflects normal asymmetric development or variable response to hormonal stimulation.
- The area of asymmetry should be evaluated with a careful physical breast examination. If there is a palpable abnormality or palpable asymmetry, biopsy should be recommended.
- A clinical history of prior breast surgery is important. For instance, asymmetry can be due to removal of tissue during biopsy of the contralateral breast.

### Radiologic

- Asymmetries are areas of glandular density that are differentiated from masses in that they lack convex borders or evidence of a 3D mass. Two types of asymmetries are defined in the *Breast Imaging Reporting and Data System*, 4th edition: "global"asymmetries and "focal"asymmetries.
- Global asymmetry involves a larger area of the breast (at least one quadrant) compared to focal asymmetry and is only rarely a secondary sign of malignancy. Global asymmetry represents a normal variant if the glandular structures and fat are normally dispersed in the area with no mass, distortion, or microcalcifications, and no corresponding palpable abnormality.
- Additional mammographic views, including magnification compression images, are necessary to evaluate the global asymmetry for underlying mass, architectural distortion, or subtle microcalcifications.
- Comparison with prior films should be performed to assess stability of the asymmetry, or if no prior films are available, a 6-month mammographic follow-up is recommended to document the stability of the pattern.
- Focal asymmetry involves a smaller area of breast and is of more concern at mammography. Magnification compression images and sometimes ultrasound are necessary to exclude an underlying mass in an area of focal asymmetry.

## SUGGESTED READING

American College of Radiology (ACR). ACR BI-RADS—mammography. In ACR Breast Imaging Reporting and Data System, Breast Imaging Atlas. Reston, VA: American College of Radiology, 2003;253–254.

Kopans DB (ed). Breast Imaging. Philadelphia, PA: Lippincott, 1989.

Kopans DB, Swann CA, White CA, et al. Asymmetric breast tissue. Radiology 1989;171:639–643.

Sickles, EA. The spectrum of breast asymmetries: imaging features, work-up and management. Radiol Clin North Am 2007;45:765–771.

# CASE 9

**RUTH WALSH**
**AND**

**MARY SCOTT SOO**

## HISTORY

A 43-year-old asymptomatic woman presenting for a screening mammogram.

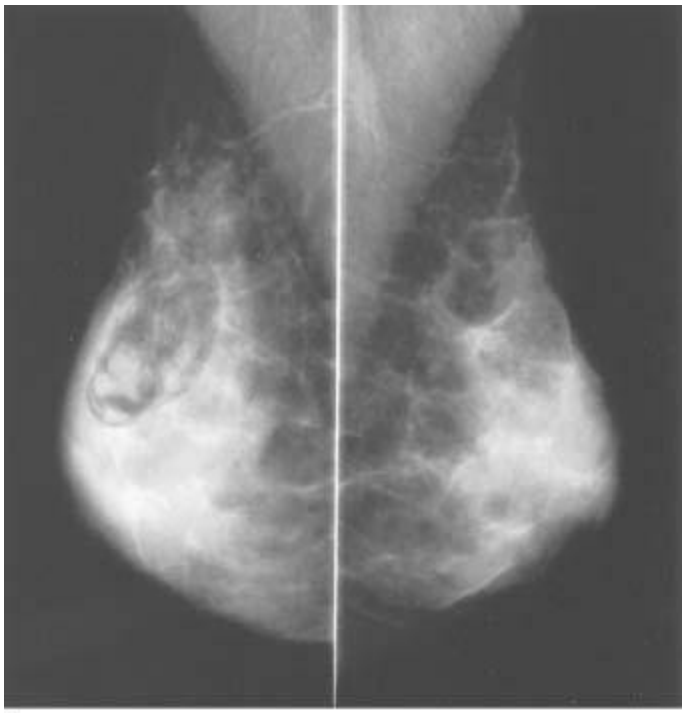

A

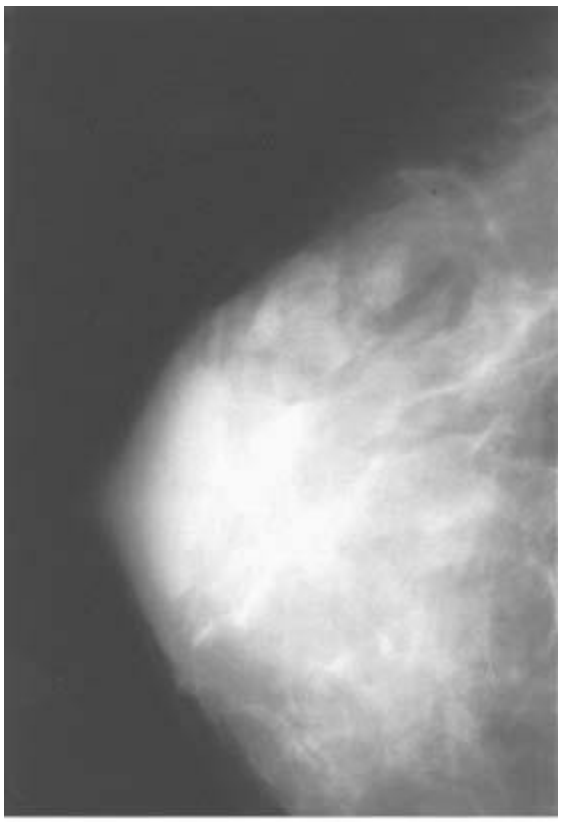

B

**FIGURES 2-9A and 2-9B** Mediolateral oblique mammograms of both breasts **(A)** and craniocaudal mammogram of the right breast **(B)** show extremely dense fibroglandular tissue. There is a circumscribed 3- x 2-cm mass present in the upper outer quadrant of the right breast. This mass contains both radiolucent regions and regions that are isodense to parenchyma.

## DIFFERENTIAL DIAGNOSIS

**Hamartoma (fibroadenolipoma):** The encapsulated, well-circumscribed mass with internal fat and fibroglandular tissue in disorganized array seen in the upper lateral right breast is typical of a hamartoma. These findings make hamartoma the best diagnosis.

**Intramammary lymph node:** Normal intramammary lymph nodes are typically round, oval, or lobulated isodense masses that measure <1 cm in size and usually contain a central fatty hilum. The size of the lesion presented here and the haphazardly arranged fatty and soft tissue components make the lymph node an unlikely diagnosis.

**Galactocele:** Galactoceles are milk-containing cysts that appear as a radiolucent or mixed-density circumscribed mass that can have a mottled appearance, mimicking a hamartoma. A fat-fluid level can be seen on a horizontal beam radiograph, which is not present in this case. This diagnosis is also unlikely in the present case because there is no history of current or recent lactation.

**Lipoma:** Lipomas are circumscribed, fat-containing masses that are radiolucent on

mammograms. However, in addition to radiolucent regions, the lesion presented here has regions that are isodense with breast parenchyma. This finding would not be found in a pure lipoma and makes this diagnosis unlikely.

- **Oil cyst:** Oil cysts would also be a consideration in a lesion that was predominantly radiolucent. Again, the mixed density arranged in a haphazard pattern argues against this diagnosis in the case illustrated.

**After assessing the imaging findings and considering the differential diagnosis, the final assessment is BI-RADS Category 2, benign. Recommend annual screening mammography**.

## DIAGNOSIS

**Hamartoma**

## KEY FACTS

### Clinical

- Hamartomas are uncommon, benign breast tumors containing ducts, lobules, adipose tissue, and fibrous tissue in varying proportions. Smooth muscle can also be present.
- Hamartomas can be discovered incidentally on screening mammography or present clinically as a painless breast lump or enlarging breast.
- When palpable, hamartomas are usually firm, smooth, and mobile.
- Hamartomas usually grow slowly but can reach a large size, producing marked asymmetry of the breast. In these cases, surgical excision may be performed.

### Radiologic

- The characteristic mammographic appearance of a hamartoma is a circumscribed oval or round mass composed of mixed radiolucent and radiodense areas. This classic appearance is pathognomonic for a hamartoma, obviating the need for surgical excision.
- Not all hamartomas have a classic mammographic appearance. The mass can vary from relatively radiolucent to very dense, depending on the proportions of fibrous and fatty tissue. Sometimes the mass can be uniformly dense with obscured margins. In these cases, the appearance is nonspecific, and biopsy may be required for diagnosis.
- The mass displaces adjacent fibroglandular tissue, often leaving a thin intervening radiolucent zone. It usually has a well-defined margin and can appear encapsulated.
- If small or in a dense breast, hamartomas can be inapparent at mammography.

## SUGGESTED READING

Dean D, Trus T, D'souza TJ, et al. Hamartoma of the breast, an underrecognized breast lesion. Am J Clin Pathol

1995;103:685–689.

Georgian-Smith D, Kricun B, McKee G, et al. The mammary hamartoma: appreciation of additional imaging characteristics. J Ultrasound Med 2004;23:1267–1273.

Helvie MA, Adler DD, Rebner M, Oberman HA. Breast hamartomas: variable mammographic appearance. Radiology 1989;170:417–421.

Kopans DB (ed). Breast Imaging. Philadelphia, PA: Lippincott, 1989.

McGuire LI, Cohn D. Hamartoma of the breast. Aust N Z J Surg 1991;61: 713–716.

Murat A, Ozdemir H, Yildirim H, et al. Hamartoma of the breast. Australas Radiol 2007;51:B37–B39.

# CASE 10

## MARY SCOTT SOO

## HISTORY

Screening mammogram in a 36-year-old asymptomatic woman with no past surgical history. She has no palpable breast masses.

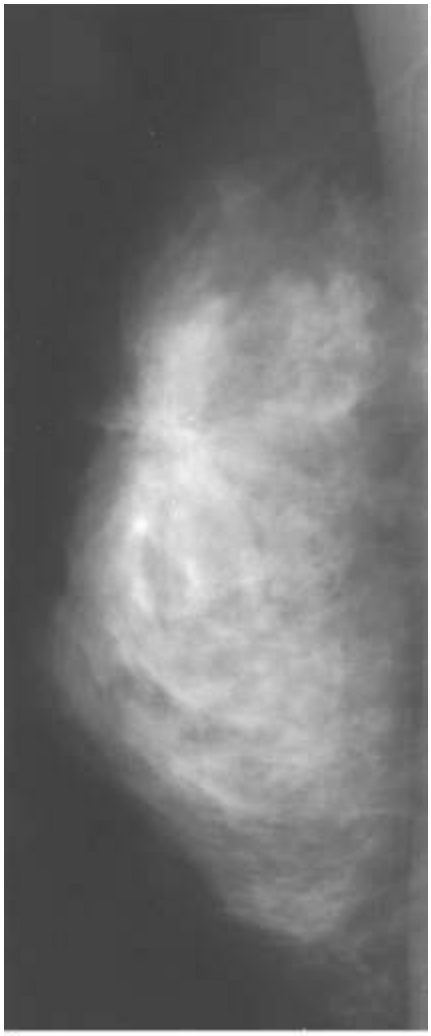

A

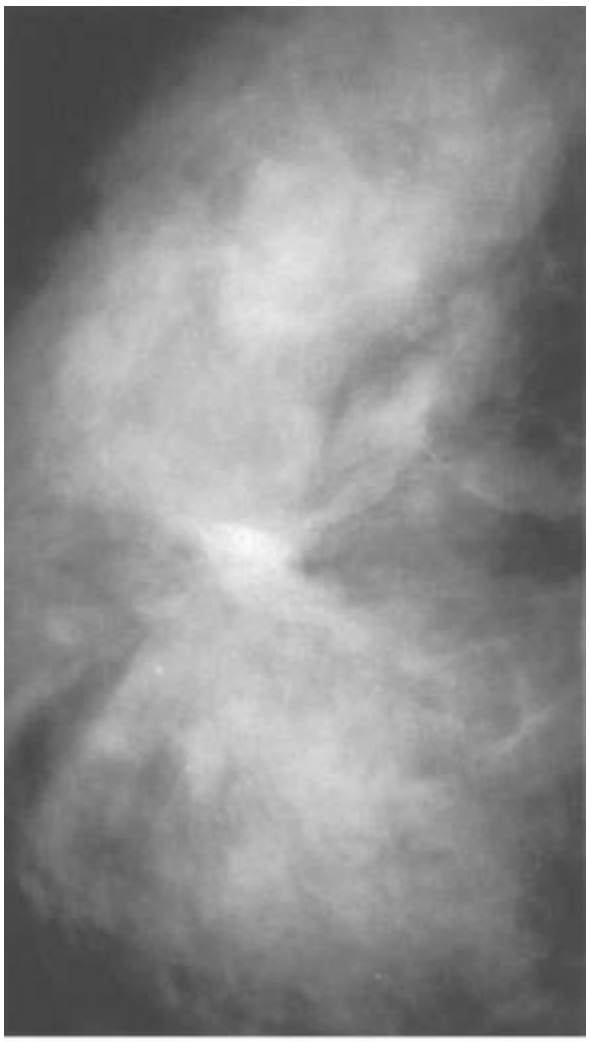

B

**FIGURES 2-10A and 2-10B** True lateral **(A)** and craniocaudal **(B)** mammograms of the right breast demonstrate extremely dense fibroglandular tissue. A 3-cm area of architectural distortion is present in the upper central right breast. Numerous calcifications are associated with the distortion.

## DIFFERENTIAL DIAGNOSIS

**Infiltrating ductal carcinoma:** The mammographic finding of a large area of architectural distortion associated with pleomorphic microcalcifications is consistent with infiltrating carcinoma and is an indication for biopsy. However, the absence of a palpable mass in this large area of architectural distortion raises the possibility of another diagnosis.

**Complex sclerosing lesion/radial scar:** Because this lesion is not palpable, a complex sclerosing lesion is a diagnostic consideration. A complex sclerosing lesion often appears at mammography as an area of architectural distortion or a spiculated mass with a lucent center. However, any area of architectural distortion that does not correspond

to a surgical scar must be biopsied to exclude malignancy.

- **Postsurgical scar:** Surgical scars often appear as an area of architectural distortion that may appear somewhat mass-like in one view but elongated in another view. Although the mammographic appearance of a surgical scar can be similar to the findings in this case, this diagnosis is not possible because there is no history of surgical biopsy.

**After assessing the imaging findings and considering the differential diagnosis, the final assessment is BI-RADS Category 4 C, suspicious for malignancy. Biopsy should be considered**.

## DIAGNOSIS

**Complex sclerosing lesion**

## KEY FACTS

### Clinical

- The term *complex sclerosing lesion* refers to a lesion that measures >10 mm. Similar lesions measuring <10 mm are termed *radial scar, infiltrating epitheliosis, elastosis*, or *indurative mastopathy*.
- Complex sclerosing lesions are not usually palpable. They are most often detected at mammography.
- Histologically, complex sclerosing lesions are characterized by a central area of elastosis surrounded by a disorganized array of tubules. They can also contain papillomas, apocrine change, and sclerosing adeno-sis. Some cases may be associated with atypical ductal hyperplasia or carcinoma, and should be completely sampled histologically to exclude these coexistent lesions.
- Excisional biopsy is necessary to differentiate complex sclerosing lesions from malignant lesions because histologically they can be difficult to differentiate from tubular carcinoma on limited core biopsy samples. Therefore, although many surgeons request core biopsy of these lesions to aid in surgical planning, the patient should be informed that surgical excision will ultimately be necessary, regardless of the core biopsy outcome, given the fact that complex sclerosing lesions must be excised.

### Radiologic

- Complex sclerosing lesions often present as focal areas of architectural distortion or a spiculated mass with central density.
- Associated microcalcifications have been reported in 14% to 40% of cases.
- Central lucency can be evident, but this does not differentiate this lesion from malignant lesions reliably.

- The length of spiculations cannot differentiate these lesions from malignant lesions reliably.

## SUGGESTED READING

Alleva DO, Smetherman DH, Farr GH Jr, Cederbom GJ. Radial scar of the breast: radiologic pathologic correlation in 22 cases. Radiographics 1999;19 Spec No:S27–S35.

Ciatto S, Morrone D, Catarzi S, et al. Radial scars of the breast: review of 38 consecutive mammographic diagnoses. Radiology 1993;187: 57–760.

Douglas-Jones AG, Denson JL, Cox AC, et al. Radial scar lesions of the breast diagnosed by needle core biopsy: analysis of cases containing occult malignancy. J Clin Pathol 2007;60:295–298.

Franquet T, DeMiguel C, Cozcolleula R, Donoso L. Spiculated lesions of the breast: mammographic-pathologic correlation. Radiographics 1993;13:841–852.

Mendelson EB. Evaluation of the post-operative breast. Radiol Clin North Am 1992;30:107–138.

Orel SC, Evers K, Yeh I-T, Troupin RH. Radial scar with microcalcifications: radiologic pathologic correlation. Radiology 1992;183:479–482.

# CASE 11

### MARY SCOTT SOO

### HISTORY

An asmymptomatic 45-year-old woman presenting for screening mammography. There is no past surgical history.

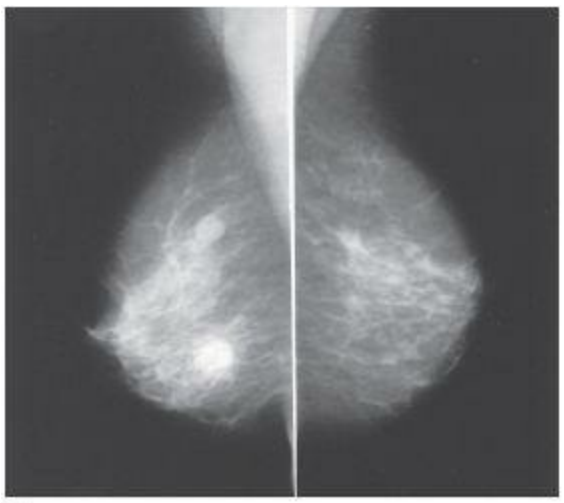

A

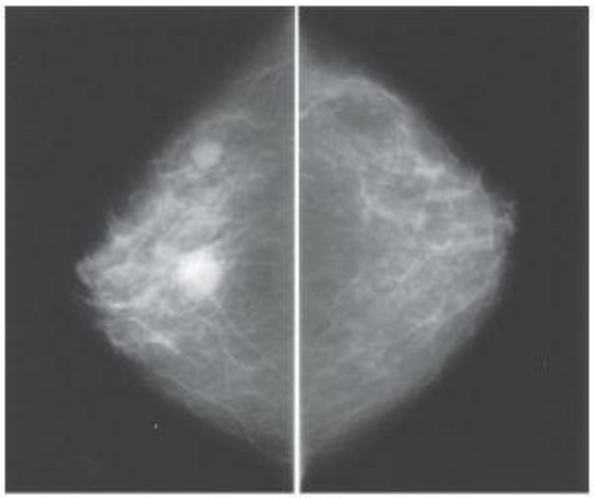

B

■**FIGURES 2-11A and 2-11B** Mediolateral oblique **(A)** and craniocaudal **(B)** mammograms of the left breast show extremely dense fibroglandular tissue. In the upper inner quadrant of the breast, there is a cluster of microcalcifications, which maintains a similar appearance in both projections.

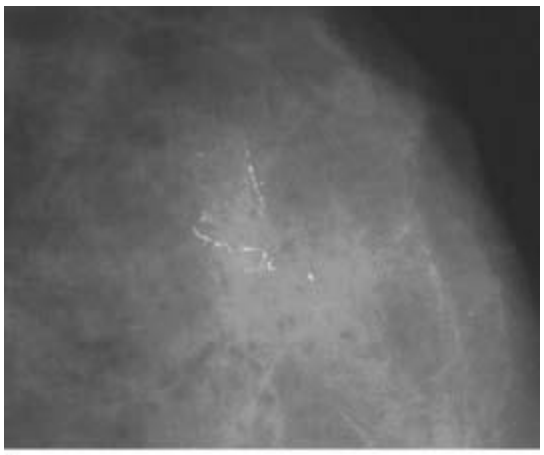

C

■**FIGURE 2-11C** Mediolateral magnification mammogram of the left breast microcalcifications. The magnification view demonstrates fine, linear and punctate calcifications, in a linear distribution. A large number of calcifications are present in a small area.

## DIFFERENTIAL DIAGNOSIS

■**Sclerosing adenosis:** Sclerosing adenosis is a benign lobular proliferation that results in enlargement and distortion of the lobules. Sclerosing adenosis can have many mammographic appearances. However, the associated calcifications are usually seen diffusely throughout the breast, characterized by uniformly dense and round or amorphous intralobular calcifications, unlike the calcifications in this case. Sclerosing

adenosis sometimes forms an isolated cluster of calcifications that may require biopsy to differentiate them from malignant lesions.

- **Ductal carcinoma in situ (DCIS) with comedo necrosis:** This is the best diagnosis because the calcifications in this case are predominantly linear and punctate, in a linear distribution, which is typical of comedo necrosis associated with ductal carcinoma in situ.
- **Plasma cell mastitis:** In plasma cell mastitis, calcific deposits occur in areas of extruded cellular debris surrounding inflamed ducts. Unlike the pleomorphic calcifications in this case, secretory calcifications associated with plasma cell mastitis are usually large (>0.5 mm) and rod shaped, with uniform density, making this diagnosis unlikely.
- **Dystrophic calcifications from fat necrosis following surgery and radiation therapy or trauma:** Calcifications associated with fat necrosis can sometimes mimic malignant calcifications. When they first appear, they can vary in size and density and have irregular, pleomorphic shapes. These calcifications are often clustered, being localized to the site of traumatic insult. Dystrophic calcifications usually evolve over time to coarser, plaque-like forms that have a more benign appearance. In the case illustrated, the calcifications are in a linear pattern and there is no history of surgery, making fat necrosis an unlikely diagnosis.

**After assessing the imaging findings and considering the differential diagnosis, the final assessment is BI-RADS Category 5, highly suggestive of malignancy. Appropriate action should be taken**.

## DIAGNOSIS

**DCIS with comedo necrosis**

## KEY FACTS

### Clinical

- DCIS with comedo necrosis is one of several forms of DCIS, characterized histologically by central necrosis within the involved ducts. Calcification of the necrotic tissue is common. Tumor cells often demonstrate nuclear pleomorphism, and mitotic cells are frequently seen.
- DCIS with comedo necrosis can be present alone or associated with invasive ductal carcinoma.
- DCIS with comedo necrosis has a higher recurrence rate than low-grade forms of DCIS.

## Radiologic

- Microcalcifications are described as clustered or grouped if there are five or more microcalcifications localized to a 1-$cm^3$ area.
- For morphologically suspicious appearing clustered microcalcifications, histologic sampling is necessary to make the diagnosis. However, the specificity of this finding is low, as carcinoma may be identified in only 10% to 35% of cases with this mammographic appearance. Stereotactic core biopsy of calcifications is commonly performed and can reliably diagnose these lesions.
- DCIS with comedo necrosis most commonly presents mammographically as clustered microcalcifications. Spot compression magnification images in craniocaudal and medial lateral projections are required to fully evaluate questionable clustered calcifications.
- Calcifications associated with comedo necrosis in ductal carcinoma are often pleomorphic in appearance, demonstrating calcific particles that vary in size, shape, and density. Other appearances include fine linear or branching calcifications due to necrotic debris within the central portion of the ducts, and less commonly, amorphous calcifications.
- Ultrasound of clustered microcalcifications seen at mammography associated with DCIS can sometimes reveal echogenic foci (calcifications) within a hypoechoic dilated duct-like structure or mass. Ultrasound-guided biopsy of the hypoechoic mass or duct with calcifications is possible in these cases, and may even reduce sampling error and underestimation of disease by localizing the more suspicious mass-like component of these lesions.

## SUGGESTED READING

Feig SA. Ductal carcinoma in situ. Implications for screening mammography. Radiol Clin North Am 2000;38:653–668.

Page DL, Anderson TJ, Rogers LW. Carcinoma in situ. In DL Page, TJ Anderson (eds). Diagnostic Histopathology of the Breast. New York, NY: Churchill Livingstone, 1987:157–192.

Shin HJ, Kim HH, Kim SM, et al. Screening-detected and symptomatic ductal carcinoma in situ: differences in the sonographic and pathologic. Am J Roentgenol 2008;190:516–525.

Soo MS, Baker JA, Rosen EL. Sonographic detection and sonographically guided biopsy of breast microcalcifications. Am J Roentgenol 2003;180:941–948.

Stomper PC, Margolin FR. Ductal carcinoma in situ: the mammographer's perspective. Am J Roentgenol 1994;162:585–591.

# CASE 12

**RUTH WALSH**

**AND**

**MARY SCOTT SOO**

## HISTORY

Diagnostic mammogram in a 58-year-old woman with a palpable lump in the right central breast and a clinical history of melanoma. There were no prior mammograms for comparison.

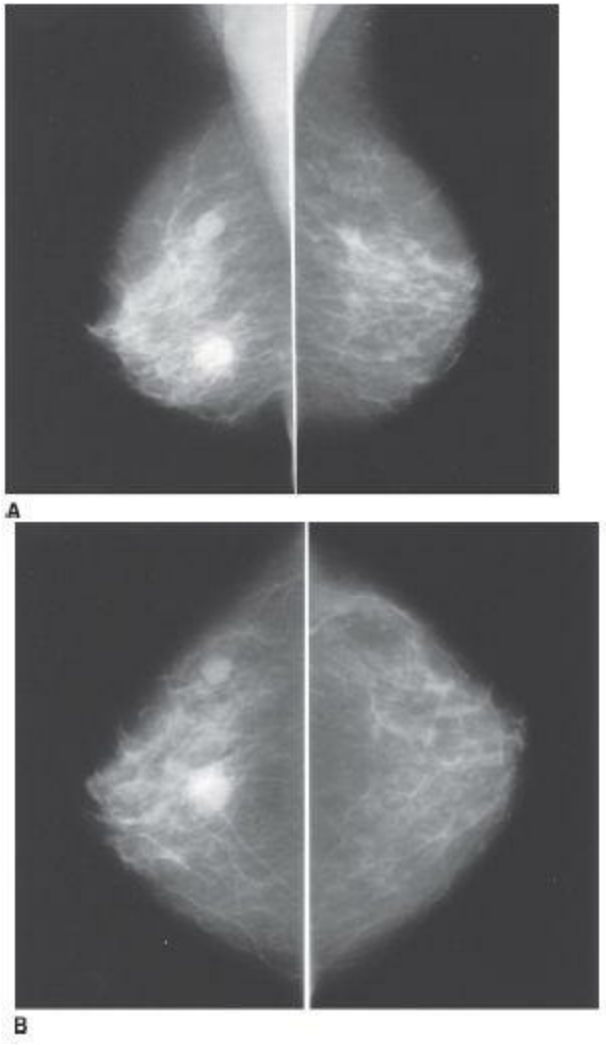


■**FIGURES 2-12A and 2-12B** Mediolateral oblique **(A)** and craniocaudal **(B)** mammograms of both breasts show heterogeneously dense fibroglandular tissue. Two round masses are present in the right breast. The smaller mass in the 10:00 position is well-circumscribed, measuring 10 mm; the larger mass in the central breast is partly obscured.

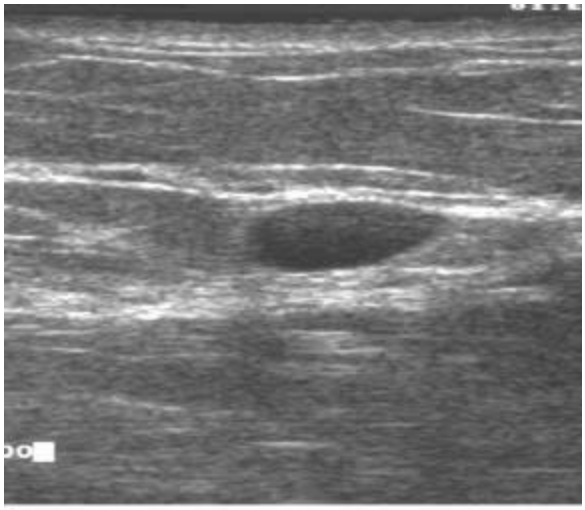

C

**FIGURE 2-12C** Ultrasound shows a circumscribed solid mass with normal sound transmission.

## DIFFERENTIAL DIAGNOSIS

**Cysts:** Cysts are a common cause of palpable masses, and present as well-circumscribed breast masses that are often multiple and bilateral and can fluctuate in size or resolve over time. This diagnosis would be a good consideration in this case, based on the mam-mogram alone. However, these lesions proved solid at sonography, making this an incorrect diagnosis.

**Fibroadenomas:** Fibroadenomas are also common breast masses in premenopausal and perimenopausal patients that cannot be differentiated from cysts or other solid circumscribed masses by mammography unless they contain characteristic coarse, “popcornlike" calcifications. Fibroadenomas are often oval or lobulated in shape and tend to be oriented toward the nipple. This diagnosis would be considered in this case but cannot be confirmed without biopsy. The history of melanoma and age of the patient prompt consideration of other etiologies as well.

**Metastases:** Metastases to the breast are usually well-circumscribed round masses that cannot be differentiated from cysts or fibroadenomas by mammography alone. Knowledge of a history of an extramammary malignancy is necessary for the diagnosis of metastases to be considered, and biopsy is necessary to confirm the diagnosis.

**Lymph nodes:** The masses in this case are not consistent with benign intramammary lymph nodes because benign lymph nodes are typically oval or reniform in shape and have a fatty hilar notch or lucent center. Intramammary nodes tend to be <1 cm in size. Enlarged reactive or metastatic nodes could have this appearance.

**Multifocal or multicentric breast cancer:** Multifocal breast cancer usually presents at mammography as multiple, ill-defined, or spiculated masses or multiple clusters of

microcalcifications, making this diagnosis unlikely in this case. However, primary breast cancers rarely present as multiple, unilateral, well-circumscribed masses (e.g., an invasive papillary carcinoma with satellite nodules).

**After assessing the imaging findings and clinical history, and considering the differential diagnosis, the final assessment is BI-RADS Category 4, suspicious for malignancy. Biopsy should be considered**.

## DIAGNOSIS

**Metastatic melanoma of the right breast**

## KEY FACTS

### Clinical

- Melanoma is the eighth most prevalent malignancy in the United States, with approximately 32,000 new cases each year.
- The most common sites for metastases from melanoma are skin, subcutaneous tissue, lymph nodes, lungs, bone, central nervous system, and liver.
- Although the breast is an unusual site for melanoma metastases, melanoma is the most common source of metastases to the breast. Lymphoma and lung carcinoma are also common causes of metastases to the breast.
- When metastases to the breast are considered in a patient with appropriate history and physical examination, mammograms are necessary to exclude primary breast carcinoma, support the clinical suspicion of metastases, and monitor any therapeutic response following treatment.

### Radiologic

- Metastatic disease to the breast from an extramammary malignancy can present as a solitary circumscribed mass, multiple circumscribed masses, or much less commonly as diffuse involvement of skin and parenchyma. Associated microcalcifications are very rarely identified.
- Sonography should be used to differentiate cystic from solid masses. If simple cysts are identified, routine follow-up is recommended.
- If sonography shows multiple bilateral nonpalpable circumscribed solid masses corresponding to round masses on a baseline mammogram, and there is no history of extramammary malignancy, short-term mammographic follow-up would be recommended (every 6 months for 1 year, then every 12 months). In patients with a history of extramammary malignancy, nonpalpable solid masses should be compared with prior films to determine stability, and if stability cannot be established, biopsy

should be performed. In patients with or without a history of extramammary malignancy, any new or palpable solid masses corresponding to round masses at mammography should undergo biopsy. In this case, biopsy was recommended because of the new palpable mass, and the suspicion for metastases was raised because of the history of melanoma.

## SUGGESTED READING

Bartella L, Kaye J, Perry NM, et al. Metastases to the breast revisited: radiological-histopathological correlation. Clin Radiol 2003;58:524–531.

Feig SA. Breast masses: mammographic and sonographic evaluation. Radiol Clin North Am 1992;30:67–92.

Paulus DD, Libshitz HI. Metastases to the breast. Radiol Clin North Am 1982;20:561–568.

Runkle GP, Zaloznik AJ. Malignant melanoma. Am Fam Physician 1994;49:91–98.

Soo MS, Williford ME, Walsh R, et al. Papillary carcinoma of the breast: imaging findings. Am J Roentgenol 1995;164:321–326.

# CASE 13

**MARGARET E. WILLIFORD**

**AND**

**MARY SCOTT SOO**

## HISTORY

A 73-year-old asymptomatic woman presenting for a screening mammogram who had begun hormone replacement therapy 1 year previously. She had no family history of breast cancer.

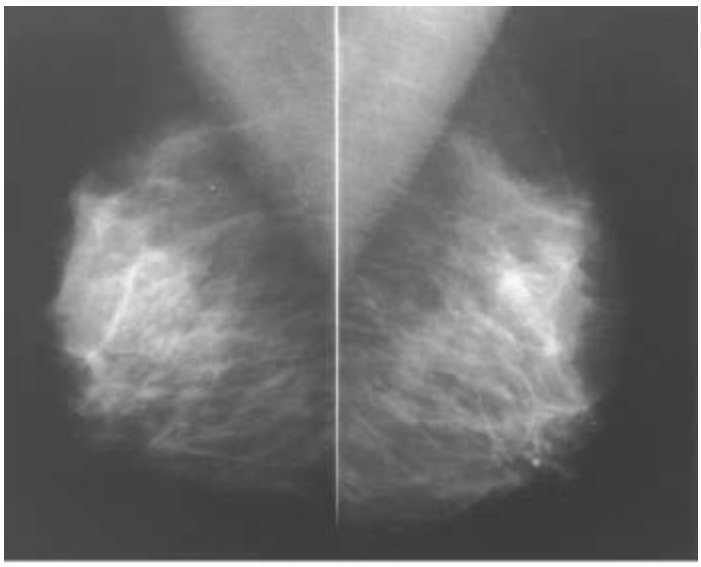

A

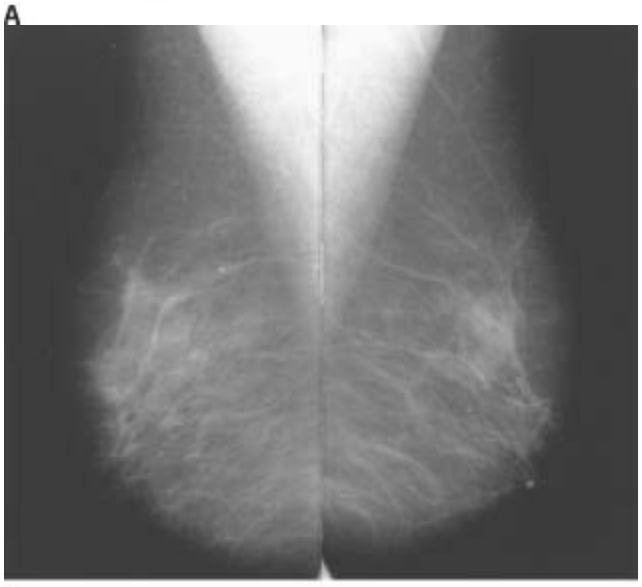

B

**FIGURES 2-13A and 2-13B** Mediolateral oblique mammograms of right and left breasts **(A)** reveal heterogeneously dense fibroglandular tissue, and mediolateral oblique mammograms of right and left breasts from 18 months earlier **(B)** reveal scattered fibroglandular tissue. Diffuse bilateral increased parenchymal density is present relative to the prior mammogram **(B)**.

## DIFFERENTIAL DIAGNOSIS

**Glandular stimulation from hormone replacement therapy:** This is the best diagnosis because the increase in breast parenchymal density has occurred diffusely and bilaterally, without other associated suspicious features. The clinical history is also consistent with this diagnosis.

**Edema:** This diagnosis is less likely because the change predominantly involves the breast parenchyma, without skin or trabecular thickening, which is commonly associated

with edema.

- **Mastitis:** This diagnosis is unlikely because the change is bilateral. Mastitis can present as a segmental area of increased density and can be associated with abscess. The clinical history is also inconsistent with mastitis, as the patient was asymptomatic.
- **Carcinoma:** Although locally advanced breast carcinoma can present as a diffuse increase in density, the bilateral change makes this very unlikely. Other features such as skin and trabecular thickening often seen with inflammatory carcinoma are not present, and the breasts do not appear smaller and contracted compared with the prior study.

**After assessing the imaging findings and considering the differential diagnosis, the final assessment is BI-RADS Category 2, benign. Recommend annual screening mammography**.

## DIAGNOSIS

**Glandular stimulation from hormone replacement therapy**

## KEY FACTS

### Clinical

- Hormone replacement therapy has been relatively common among menopausal and postmenopausal women due to the beneficial result of decreasing menopausal symptoms and osteoporosis.
- Estrogen promotes growth of ducts and stimulates surrounding connective tissue. Progesterone promotes growth of lobuloalveolar structures and differentiation of ductal cells.
- Treatment with estrogen promotes enlargement of cysts and fibroadenomas. Treatment with a combination of estrogen and progesterone is associated with diffuse increase in fibroglandular tissue.
- A number of studies have evaluated the risk of breast cancer for women on hormone replacement therapy. The results are conflicting, but there appears to be some increase in risk based on the duration of use.

### Radiologic

- Effects of hormone replacement therapy that can be apparent on mammograms include symmetric or asymmetric increase in breast density, increase in size of fibroadenomas, and development or increase in size of cysts.
- Mammographic changes develop in 24% of postmenopausal women undergoing hormone replacement therapy.

- Mammographic changes are more common in women treated with the combination of estrogen and progesterone than in women treated with estrogen alone.
- Asymmetric or focal increase in breast density is more problematic. It may be interpreted as a developing focal asymmetry. Further evaluation may include breast ultrasound, physical correlation, mammographic follow-up with or without cessation of hormones, or even biopsy to exclude malignancy.

## SUGGESTED READING

Berkowitz JE, Gatewood OMB, Goldblum LE, Gayler BM. Hormonal replacement therapy: mammographic manifestations. Radiology 1990;174:199–201.

Cyrlak D, Wang CH. Mammographic changes in postmenopausal women undergoing hormonal replacement therapy. Am J Roentgenol 1993;161:1177–1183.

Laya MB, Gallagher JC, Schreiman JS, et al. Effect of postmenopausal hormonal replacement therapy on mammographic density and parenchymal pattern. Radiology 1995;196:433–437.

Marugg RC, van der Mooren JM, Hendriks JH, et al. Mammographic changes in postmenopausal women on hormonal replacement therapy. Eur Radiol 1997;7:749–755.

Stamper DC, Von Voorhis BJ, Ravnikar VA, Meyer JE. Mammographic changes associated with post-menopausal hormone replacement therapy: a longitudinal study. Radiology 1990;174:487–490.

# CASE 14

**PHYLLIS J. KORNGUTH**

**AND**

**MARY SCOTT SOO**

### HISTORY

Screening mammogram in a 73-year-old female. Family history is significant for a sister with postmenopausal breast carcinoma. There is no past surgical history or history of hormone replacement therapy.

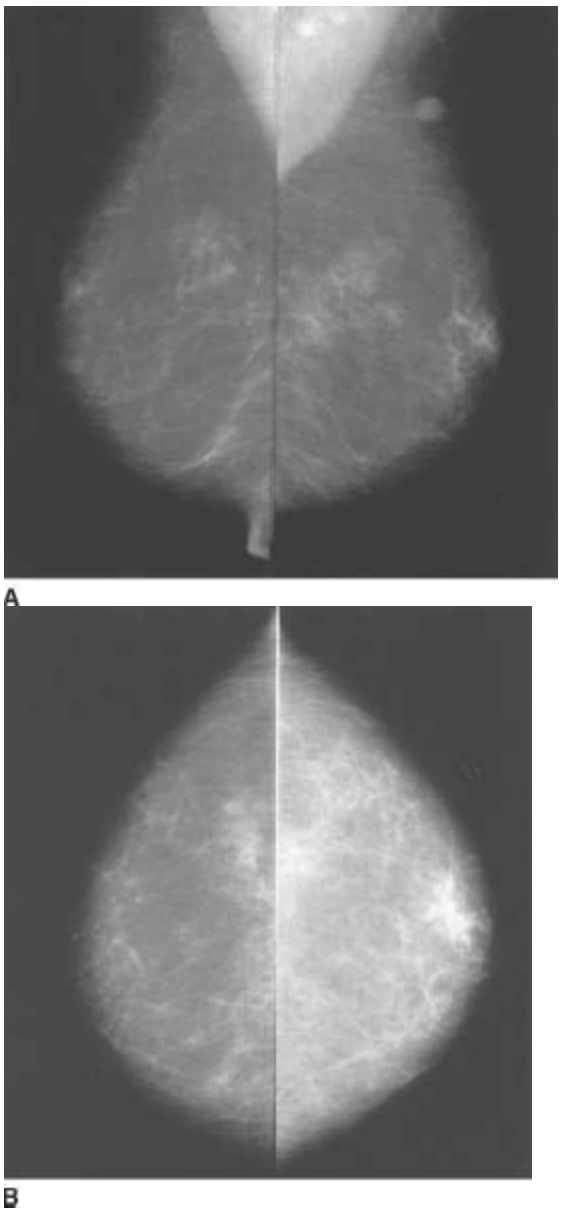


■**FIGURES 2-14A and 2-14B** Mediolateral oblique **(A)** and craniocaudal **(B)** mammograms of both breasts demonstrate scattered fibroglandular tissue. Figures show a focal asymmetry in the retroareloar region of the left breast and a 10-mm, well-circumscribed, solitary mass in the upper outer quadrant of the left breast.

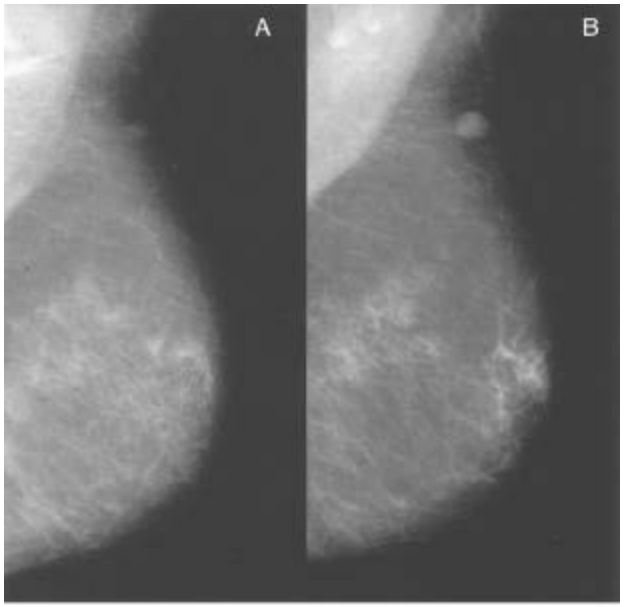


C

**FIGURE 2-14C** Mediolateral oblique mammogram of the left breast 1 year ago **(A)** and mediolateral oblique left mammogram from the current study **(B).** The focal asymmetry is new compared to the prior study. The mass previously represented an intramammary lymph node and has enlarged compared to the prior exam.

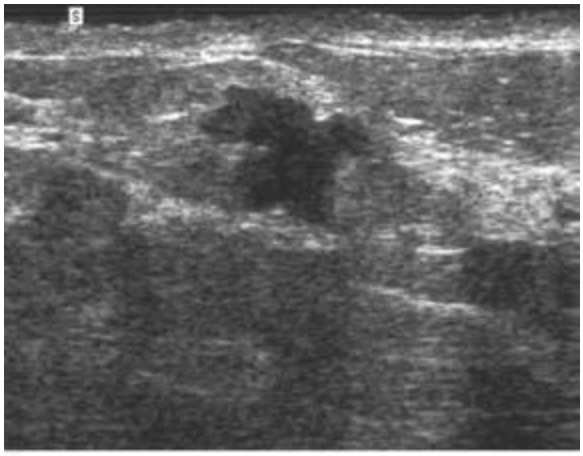


D

**FIGURE 2-14D** Ultrasound of the left breast in the subareolar region of developing focal asymmetry reveals an irregular, hypoechoic, microlobulated mass.

## DIFFERENTIAL DIAGNOSIS

**Invasive ductal carcinoma with metastatic disease to an intramammary lymph node:** A developing focal asymmetry within the breast must be viewed with suspicion because this is one mammographic presentation of breast carcinoma. The associated enlargement and increased density of the intramammary lymph node increases the suspicion for carcinoma with metastatic disease. Ultrasound of the region of focal

asymmetry in this case confirms a highly suspicious, irregular, microlobulated hypoechoic mass, making this the best diagnosis.

- **Mastitis with abscess and reactive lymph node:** Mastitis with underlying abscess can be seen at mammography as a localized focal asymmetry, and intramammary lymph nodes can enlarge as a result of infections of the breast. However, mastitis usually presents with skin and trabecular thickening, not present in this case, and the patient was asymptomatic and had no physical signs of infection. Although an abscess in a region of mastitis can be seen as a rounded or irregular ill-defined mass at ultrasound, the mass in this case is microlobulated and highly suggestive of malignancy. Abscesses at ultrasound also usually present with surrounding edema and skin thickening, which was not present in this case. Considering all of the above, the diagnosis of mastitis with abscess is unlikely.
- **Focal glandular stimulation from hormone replacement therapy:** This process could cause a developing focal asymmetry within the breast, with enlargement of masses corresponding to cyst formation. However, the patient in the case illustrated has no history of hormone replacement therapy, and the mass seen in this case was previously shown to represent an intramammary lymph node.
- **Normal asymmetric breast parenchyma:** The mammographic appearance of the focal asymmetry in this case could be consistent with asymmetric glandular tissue. However, glandular tissue would not be expected to increase over time without hormonal stimulation, and the enlargement of the intramammary lymph node could not be explained with this diagnosis.

**After assessing the mammographic and sonographic findings and considering the differential diagnosis, the final assessment is BI-RADS Category 5, highly suggestive of malignancy. Biopsy and other appropriate clinical action should be taken**.

## DIAGNOSIS

**Invasive ductal carcinoma with 1/34 positive lymph nodes**

## KEY FACTS

### Clinical

- Invasive ductal carcinoma can be metastatic to intramammary lymph nodes.
- Intramammary lymph nodes with metastatic involvement are often palpable, located in the upper outer quadrant of the breast. Careful physical examination in this breast proved this node to be palpable.

## Radiologic

- When a new focal asymmetry is identified on the mammogram, additional magnification compression images and targeted ultrasound with physical examination are necessary to evaluate for an underlying mass.
- When intramammary lymph nodes enlarge over time, the breast must be inspected carefully for evidence of primary breast carcinoma. Considerations in the differential diagnosis of enlarged intramammary nodes include metastatic disease from breast primary, metastatic disease from extramammary malignancies, reactive change from inflammatory processes, and HIV or autoimmune diseases. If no corresponding clinical history is provided to confirm a benign etiology for nodal enlargement in the setting of a negative mammogram, then biopsy of the lymph node should be considered. In this case, a focal asymmetry had developed on the mammogram, and subsequent ultrasound revealed the breast primary.

## SUGGESTED READING

Gunhan-Bilgen I, Memis A, Ustun EE. Metastatic intramammary lymph nodes: mammographic and ultrasonographic features. Eur J Radiol 2001;40:24–29.

Kopans DB, Meyer JE. Benign lymph nodes associated with dermatitis presenting as breast masses. Radiology 1980;137:15-19.

Leung JW, Sickles EA. Developing asymmetry identified on mammography: Correlation with imaging outcome and pathologic findings. Am J Roentgenol 2007;188:667-675.

Lindfors KK, Kopans DB, McCarthy KA, et al. Breast metastasis to intramammary lymph nodes. Am J Roentgenol 1986;146:133-136.

Sickles EA. The spectrum of breast asymmetries: imaging features, work-up, management. Radiol Clin North Am 2007;45:765-771.

Svane G, Franzen S. Radiologic appearance of nonpalpable intramammary lymph nodes. Acta Radiol 1993;34:577-580.

# CASE 15

**PHYLLIS J. KORNGUTH**

**AND**

**MARY SCOTT SOO**

## HISTORY

Diagnostic mammogram in a 70-year-old woman who presented with a painless,

swollen erythematous right breast. There was no significant past medical history.

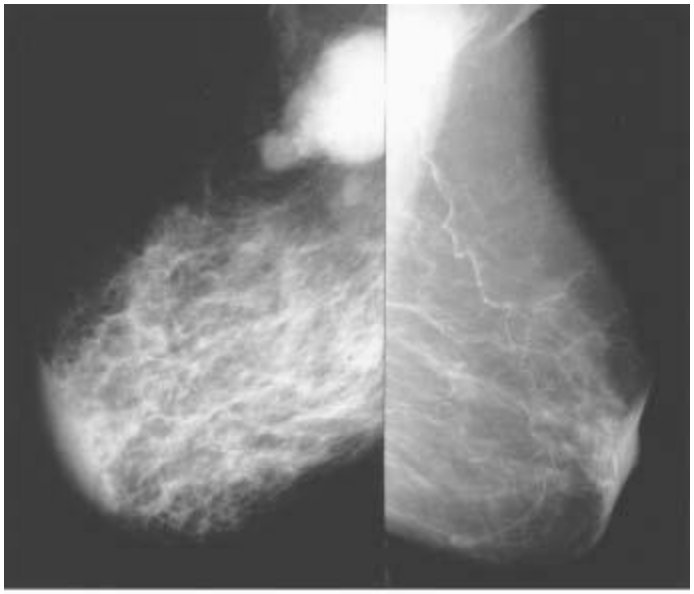


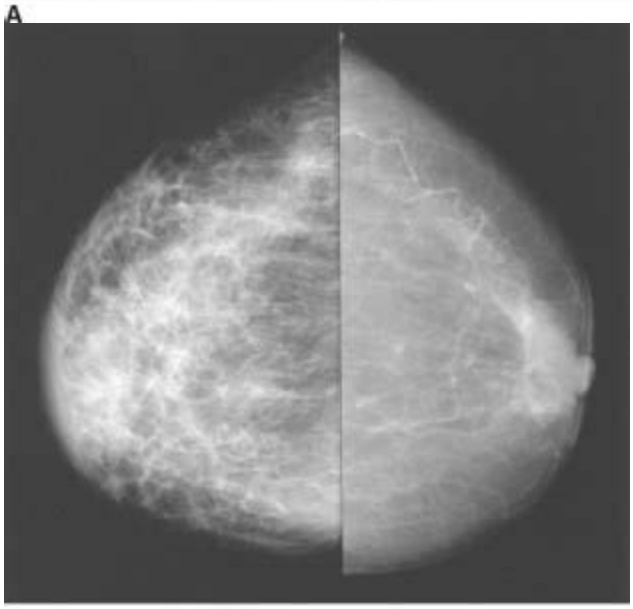


**FIGURES 2-15A and 2-15B** Mediolateral oblique **(A)** and craniocaudal **(B)** mammograms of both breasts show scattered fibroglandular tissue on the left. There is diffuse increased density throughout the right breast, with marked thickening of the skin and trabeculae. A large lobulated mass is seen in the right axilla.

## DIFFERENTIAL DIAGNOSIS

**Inflammatory breast carcinoma:** The clinical presentation of a painless, swollen, erythematous breast and the mammographic findings of thickening of the skin and trabeculae in association with a mass make this the most likely diagnosis.

- **Axillary mass obstructing the lymphatics:** The mam-mographic findings of the large axillary mass and tra-becular and skin thickening make this a possible choice. However, this diagnosis is uncommon and would be ruled out based on the physical examination because obstructed lymphatics would not result in an inflamed, erythematous appearance of the breast.
- **Radiation therapy:** Radiation therapy often results in skin and trabecular thickening. However, there was no history of radiation therapy in this case.
- **Mastitis:** Mammographic changes of skin and trabecu-lar thickening are often seen in cases of mastitis, and the large axillary mass could represent reactive lymph node(s) due to infection. In cases of mastitis, however, skin and trabecular thickening are usually localized to one segment or region, not spread diffusely throughout the breast. Furthermore, the clinical history of "painless"swelling of the breast is not consistent with mastitis.
- **Congestive heart failure (CHF):** CHF can result in unilateral skin and trabecular thickening in the dependent breast if the patient lies on one side. However, the mass in the right axilla makes this diagnosis unlikely.

**After assessing the imaging findings and considering the differential diagnosis, the final assessment is BI-RADS Category 5, highly suggestive of malignancy. Appropriate action should be taken**.

# DIAGNOSIS

**Inflammatory breast carcinoma**

# KEY FACTS

## Clinical

- Inflammatory breast carcinoma is a diffuse carcinoma involving all portions of the breast, including the dermal lymphatics.
- On physical examination, the patient has a painless, red, hot, swollen breast with a p' eau d'orange appearance of the skin.
- Antibiotics (used if mastitis is considered in the differential diagnosis) can result in clinical regression of symptoms of inflammatory carcinoma. Biopsy is often necessary to make the diagnosis.
- The diagnosis can be made by a punch biopsy of the skin to determine the presence of carcinoma in the dermal lymphatics, or by core biopsy of any suspicious mass identified within the breast or axilla.

## Radiologic

- The involved breast is asymmetrically dense compared to the contralateral breast.
- Thickening of the skin and trabeculae are typically present throughout the involved breast.
- An underlying dominant mass may or may not be present.

## SUGGESTED READING

Chow CK. Imaging in inflammatory breast carcinoma. Breast Dis 2005–2006;22:45–54.

Kopans DB. Pathologic, mammographic, and sonographic correlation. In DB Kopans (ed). Breast Imaging. Philadelphia, PA: Lippincott, 1989:299–301.

Rosen, PP. The pathology of invasive breast carcinoma. In JR Harris, S Hellman, IC Henderson, DW Kinne (eds). Breast Diseases. Philadelphia, PA: Lippincott, 1991:278–279.

# CASE 16

**MARGARET E. WILLIFORD**

**AND**

**MARY SCOTT SOO**

### HISTORY

Diagnostic mammogram in a 60-year-old woman who is status post lumpectomy for invasive ductal carcinoma in the inferior medial portion of the right breast.

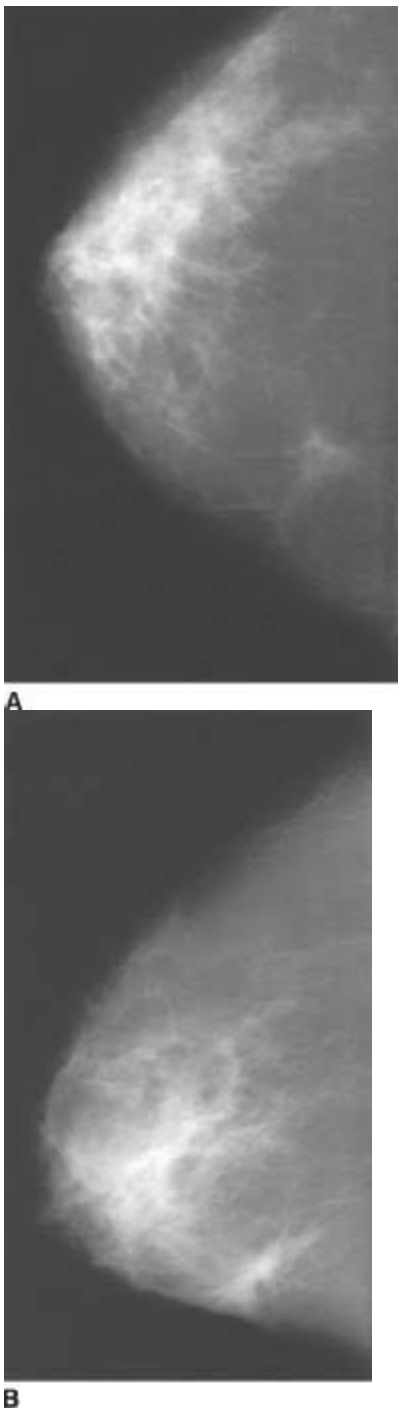


■**FIGURES 2-16A and 2-16B** Craniocaudal **(A)** and mediolateral oblique **(B)** mammograms of the right breast show heterogeneously dense fibroglandular tissue. A spiculated mass is present in the medial and inferior portions of the breast. Comparison to prior mammograms (not shown) demonstrated no change in this mass.

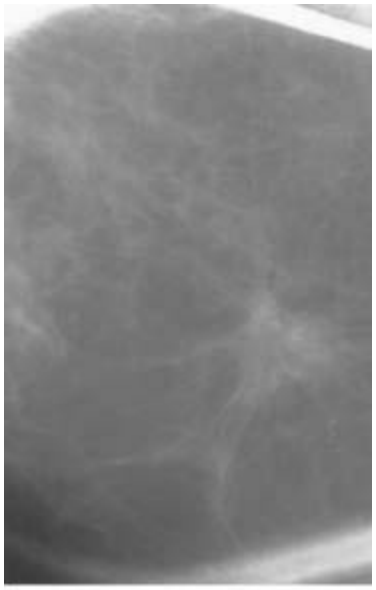

C

**FIGURE 2-16C** Craniocaudal spot magnification compression image. The lesion with long spicules is present without a central mass or density. The central portion of the lesion is lucent.

## DIFFERENTIAL DIAGNOSIS

**Invasive ductal carcinoma:** Although invasive carcinoma often presents as a spiculated mass or an area of architectural distortion, the lesion in the case illustrated corresponds to the site of prior biopsy, making carcinoma a less likely diagnosis. While central lucency can be seen in certain carcinomas, this finding is typical of an excisional biopsy scar. For confirmation, the use of biopsy scar markers and correlation with prior mammograms and wire localization films from the time of excisional biopsy is necessary.

**Postsurgical or posttraumatic scar:** A postsurgical scar often appears as an area of architectural distortion or a spiculated mass that tends to decrease in size over time. The site of the spiculated lesion must match the location of the patient's cutaneous scar and the location of the biopsied lesion on preoperative or needle localization mammograms. The lesion in the case illustrated corresponds to the site of prior biopsy, making this a likely diagnosis.

**Radial scar:** Radial scars typically appear as lesions with long, thin spicules radiating outward from a radio-lucent center. The lesion in the case illustrated has some of the mammographic features of a radial scar. However, a radial scar would not be expected to occur at a site of prior biopsy, making this diagnosis less likely.

**Granular cell tumor:** These benign tumors have a spiculated appearance at mammography but are very rare and would not be expected to occur at biopsy sites, making this diagnosis unlikely.

- **Extraabdominal desmoid tumor:** These are locally invasive tumors that do not metastasize. Their mam-mographic appearance mimics that of an invasive breast cancer, requiring biopsy for diagnosis. These lesions are rare, and the location at a site of prior biopsy would be unlikely, unless a desmoid tumor was initially excised at that site.

**After assessing the imaging findings and considering the differential diagnosis, the final assessment is BI-RADS Category 2, benign. Recommend annual diagnostic mammography**.

## DIANOSIS

**Postsurgical scar, status postlumpectomy for invasive**

## KEY FACTS

### Clinical

- Fibrosis and fat necrosis at a surgical site (or site of trauma) can cause a spiculated mass or architectural distortion simulating the appearance of tumor.
- On palpation, scars feel like an area of thickening, whereas carcinomas feel more discrete and larger than an associated abnormality seen on mammogram.
- History of surgery at the site of the mammographic abnormality is helpful. The cutaneous surgical scar may not always correlate with the parenchymal scar since the surgeon may make the skin incision at some distance from the lesion to be removed.

### Radiologic

- Postsurgical or posttraumatic scars frequently present as a spiculated mass or area of architectural distortion on mammogram, which is often identical to the appearance of carcinoma.
- Scars do not have a central mass or density after initial postoperative seroma has resolved; central lucency is commonly seen within the scar.
- The preoperative and needle localization mammo-grams and specimen radiograph can be used to confirm that the suspected scar correlates with the surgical site.
- If prior mammograms are not available but the lesion is strongly suspected to be a scar, based on appearance and correlation with the cutaneous scar, close-interval mammographic follow-up can be performed.
- A scar should decrease in size, density, and distortion or remain stable during follow-up.
- Any increase in size or density of a suspected scar warrants biopsy.
- On a long-term follow-up, benign postsurgical scars generally do not enhance with

contrast at MRI scanning. If new enhancement is seen in a postsurgical scar at MRI scanning, recurrent tumor should be considered and biopsy suggested.

## SUGGESTED READING

Peters ME. The benign post surgical breast. In ME Peters (ed), Handbook of Breast Imaging. New York, NY: Churchill Livingstone, 1989.

Preda L, Villa G, Rizzo S, et al. Magnetic resonance mammography in the evaluation of recurrence at the prior lumpectomy site after conservative surgery and radiotherapy. Breast Cancer Res 2006;8:R53.

Sickles FA, Herzog KA. Intrammary scar tissue: A mimic of the mam-mographic appearance of carcinoma. Am J Roentgenol 1980;135: 349–352.

Stigers KB, King JG, Dowey DD, Stelling CB. Abnormalities of the breast caused by biopsy: spectrum of mammographic findings. Am J Roentgenol 1991;156:287–291.

# CASE 17

**MARY SCOTT SOO**

### HISTORY

Diagnostic mammogram in a 62-year-old woman with pain in her left breast. She had a right-sided modified radical mastectomy for carcinoma and a left-sided subcutaneous mastectomy, with breast reconstruction bilaterally using double lumen silicone and saline prostheses. Subsequent sonogram and MRI of the left breast were performed.

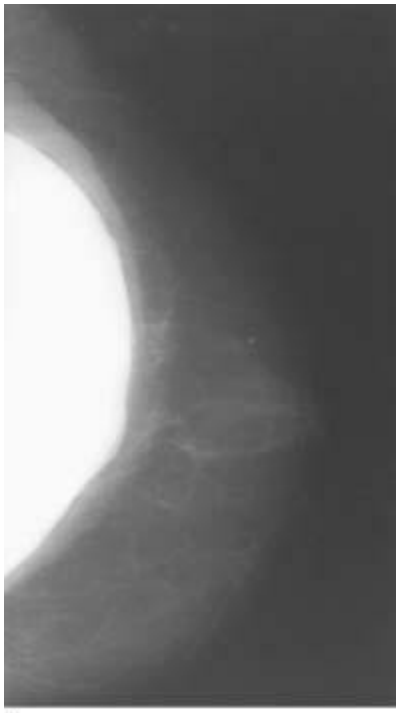

A

■**FIGURE 2-17A** Craniocaudal mammogram of the left breast shows predominantly fatty tissue. Mild contour irregularity of the anterior margin of the subpectoral silicone implant is seen. No outer saline lumen is identified. No abnormalities are seen within the breast tissue.

B

■**FIGURE 2-17B** Sonogram of a breast prosthesis in another patient with the same diagnosis. Multiple, parallel echogenic lines are present within the silicone implant

("stepladder"sign).

C

**FIGURE 2-17C** Sagittal T2-weighted, fast spin-echo water suppression MRI of the left breast. A hyperintense silicone prosthesis is present, surrounded by a hypointense fibrous capsule. Curvilinear hypointense lines ("linguine"sign) are present within the silicone, and the valve of this double-lumen implant is displaced anteriorly from its normal position along the posterior aspect of the fibrous capsule. No saline remains in the collapsed outer lumen.

## DIFFERENTIAL DIAGNOSIS

**Intracapsular implant rupture:** This is the best diagnosis because MRI demonstrates numerous curvilinear hypointense lines within the hyperintense sili-cone gel, corresponding to the ruptured and collapsed shell of the prosthesis ("linguine"sign). No silicone is seen outside of the fibrous capsule.

**Extracapsular implant rupture:** The mild contour abnormality of the implant on the mammogram is a nonspecific finding, but in conjunction with the clinical symptoms, raised the question of implant rupture, prompting further investigation using MRI. Neither the mammogram nor MRI shows signs of free silicone within the breast parenchyma, making extracapsular rupture unlikely. The breast parenchyma should be studied carefully on all MRI images obtained to search for free silicone, particularly when intracapsular implant rupture is identified.

**Intact implant with radial folds:** Radial folds are infoldings of the intact silicone shell, generally seen on MRI as straight, hypointense, double thickness lines, originating at the fibrous capsule and ending blindly in the silicone gel. Occasionally, they appear angular or curvilinear. The lines seen centrally in the case illustrated do not correspond to radial folds, making this diagnosis unlikely.

**Breast carcinoma:** Localized breast pain is only very infrequently associated with

breast carcinoma. However, on any breast imaging examination (whether the study is indicated for screening or for prosthesis evaluation), the breast parenchyma must be evaluated carefully for signs of occult carcinoma. Large silicone implants are identified by both modalities in this case, which can obscure lesions at mammography. Carcinoma is unlikely in this case because no mass or other paren-chymal abnormality is identified on the mammogram. If MRI scanning is performed to evaluate for breast carcinoma, then precontrast and postcontrast T1-weighted dynamic scanning must be performed to evaluate for suspicious enhancing lesions. T2-weighted MRI images as in this case are not sensitive for cancer detection.

**After assessing the imaging findings and considering the differential diagnosis, the final assessment is BI-RADS Category 2, benign. Recommend annual screening mammography**.

## DIAGNOSIS

**Intracapsular rupture of the silicone breast prosthesis**

## KEY FACTS

### Clinical

- Implantable silicone prostheses have been in use since 1962 for breast augmentation or breast reconstruction following subcutaneous or modified radical mastectomy.
- Silicone, saline, or doublelumen silicone and saline implants have been used most commonly and can be placed in subglandular or submuscular positions.
- Early complications of silicone prostheses include hemorrhage or infection in the postoperative period. Sonography is useful for detecting these periprosthetic fluid collections. CT and MRI are less frequently used for this purpose.
- Late complications of breast prostheses include capsular contracture, rupture, migration of silicone, and rarely, extrusion of the implant.
- Silicone implants were initially implicated in causing autoimmune diseases, prompting the Food and Drug Administration to limit their use. Subsequent studies have not confirmed an association between silicone and autoimmune diseases, and they now can be implanted in specific cases.
- Most of the late complications of silicone prostheses are best evaluated by physical examination. However, imaging studies are often necessary to detect implant rupture.

### Radiologic

- *Mammography:* Mammograms have high specificity in evaluating implant integrity, but sensitivity is low because intracapsular rupture is frequently not detected by

mammography.

- Reliable signs of extracapsular implant rupture at mammography include free silicone within the breast parenchyma, irregular or large smooth protrusions of the silicone implant, and streaming of silicone away from the body of the implant.
- *Sonography:* Sonographic findings of implant rupture include the "snowstorm"sign (an echodense column located at the site of extracapsular silicone that obscures underlying structures), the "stepladder"sign (echogenic parallel lines resembling a stepladder within the implant, corresponding to the collapsed silicone shell) of intracapsular rupture, and the presence of anechoic nodules with echogenic back wall and echogenic reverberation, corresponding to free silicone globules in the breast parenchyma.
- *MRI:* Intracapsular rupture (ruptured implant with silicone contained within the surrounding fibrous capsule) is best detected by MRI, where the "linguine"sign corresponds to the collapsed silicone shell. Extracapsular silicone (gel extravasation into the breast tissue) can also be detected by MRI as parenchymal masses that have signal intensities paralleling those of the implant on T2-weighted fast spinecho images (with and without water suppression) and on T1-weighted images. These sequences allow differentiation between silicone and other breast masses.

## SUGGESTED READING


Caskey CI, Berg WA, Hamper UM, et al. Imaging spectrum of extracapsular silicone: correlation of US, MR imaging, mammographic, and histopathologic findings. Radiographics 1999;19:S39–S51.

DeBruhl ND, Gorczyca DP, Ahn CY, et al. Silicone breast implants: US evaluation. Radiology 1993;189:95–98.

Everson LI, Parantainen H, Detlie T, et al. Diagnosis of breast implant rupture: imaging findings and relative efficacies of imaging techniques. Am J Roentgenol 1994;163:57–60.

Gorczyca DP, Sinha S, Ahn CY, et al. Silicone breast implants in vivo: MR imaging. Radiology 1992;185:407–410.

Harris KM, Ganott MA, Shestak KC, et al. Silicone implant rupture: detection with US. Radiology 1993;187:761–768.

Piccoli CW. Imaging of the patient with silicone gel breast implants. Magn Reson Imaging Clin N Am 2001;9:393–408.


# CASE 18


**DANIELLE L. WELLMAN**


## HISTORY

A 48-year-old woman with a new abnormality in the medial right breast on a screening mammogram presents for diagnostic evaluation.

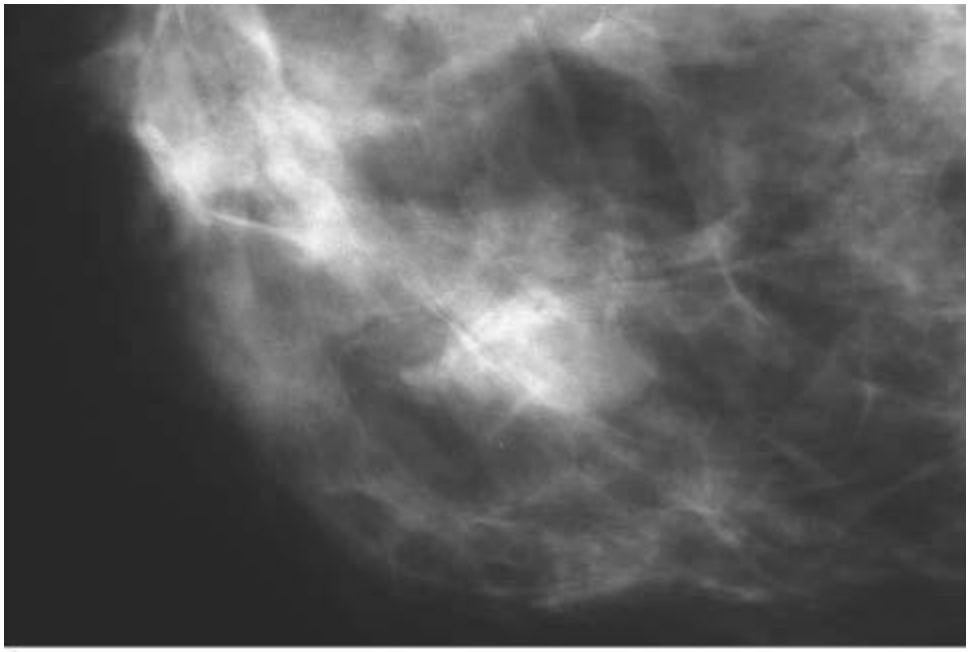

A

■**FIGURE 2-18A** Mediolateral oblique spot compression mammogram of the inferior right breast demonstrates heterogeneously dense breast tissue with an oval, partly obscured, non-calcified mass.

B

■**FIGURE 2-18B** Sonography of right breast demonstrates a lobulated, hypoechoic mass corresponding to the mammographic abnormality. There is no posterior acoustic enhancement.

## DIFFERENTIAL DIAGNOSIS

- **Fibroadenoma:** These lesions are very common benign fibroepithelial tumors with mixed epithelial and stromal components. A fibroadenoma would be high on the differential list given the oval obscured mass at mammography and parallel oriented, oval, solid mass with possible septation at sonography. Degenerating fibroadenomas often contain coarse or popcorn calcifications, which are not present in this case.
- **Invasive ductal carcinoma:** Invasive ductal carcinoma often presents as an ill-defined or spiculated irregular mass at mammography that appears irregularly shaped with indistinct, angular, microlobulated, or spiculated margins at sonography. The imaging appearance in this case is that of an obscured mass at mammography, and a hypoechoic mass without circumscribed margins at sonography, making invasive ductal carcinoma a reasonable consideration in this case.
- **Pseudoangiomatous stromal hyperplasia (PASH):** Although an unusual lesion, PASH often presents as a noncalcified mass or developing focal asymmetry at mammography and can be seen as a solid mass at sonography.
- **Phyllodes tumor:** Although phyllodes tumors are rare, these lesions can have a similar appearance to fibroadenomas, and should be considered the differential for oval or rounded solid breast masses. At ultrasound, phyllodes tumors can have mixed echogenicity due to multiple small cystic areas within the mass.
- **Fibroadenolipoma:** The presence of fat in these lesions at mammography makes this diagnosis unlikely.
- **Focal fibrosis:** The incidence of focal fibrosis ranges from 2% to 8%. Focal fibrosis can present as well-circumscribed masses or developing focal asymmetries on mammograms, and at ultrasound can be either mass-like, vague hypoechoic shadowing regions, or hyperechoic. Focal fibrosis is also known as fibrous mastopathy, seen in patients with type I diabetes mellitus.
- **Asymmetric glandular parenchyma:** This is unlikely because asymmetric glandular parenchyma does not have well-defined borders. A focal circumscribed mass would not be seen on ultrasound as in this case.

**After assessing the imaging findings and considering the differential diagnosis, the final assessment is BI-RADS Category 4, suspicious for malignancy. Biopsy should be considered**.

## DIAGNOSIS

**Nodular PASH**

## KEY FACTS

## Clinical

- PASH is a benign proliferation of mammary stroma/ myofibroblasts creating a complex pattern of slit like pseudovascular spaces seen on histopathology.
- PASH is a common incidental microscopic finding on breast biopsy (reported up to 23% incidence). Nodular PASH, or the tumoral form, as in this case, is much less common.
- PASH is benign and not associated with other malignancies or increased risk of malignancy. Wide local excision is usually curative if indicated either by significant interval growth, symptoms, or atypical features on imaging. In some cases, PASH can recur after resection. PASH can be initially confused with low-grade angiosarcoma or hamartoma histologically but is unrelated.
- PASH lesions are often progesterone receptor antibody positive and most commonly occur in premenopausal females or in postmenopausal patients on hormone replacement therapy. There have been reports of males with PASH, nearly always associated with gynecomastia.
- FNA can be inconclusive and can mimic phyllodes or mucinous carcinoma. Core biopsy is usually diagnostic.

## Radiologic

- Mammographically, PASH most often presents as a circumscribed or obscured mass that can be quite large (1 to 10 cm). PASH also can present as a focal developing asymmetry at mammography.
- On ultrasound, these masses are most often circumscribed hypoechoic oval or round masses with heterogeneous internal echoes. These lesions may have a thin hyperechoic rim.
- The reported MR appearance is isointense to background breast tissue on T1 and heterogeneous on T2. The enhancement characteristics of PASH lesions can range from focal areas of enhancement within the mass to irregular heterogeneous enhancement throughout the mass. These lesions reportedly usually demonstrate a benign-type slow persistent enhancement curve.
- The diagnosis of PASH can be made by core biopsy. Once a diagnosis of nodular PASH is made, the lesions are generally followed at mammography. However, resection should be considered if there are imaging characteristics that are worrisome for malignancy, if there is significant interval growth over time, or if the patient is symptomatic from the mass.

## SUGGESTED READING

Cohen MA, Morris EA, Rosen PP, et al. Pseudoangiomatous stromal hyperplasia: mammographic, sonographic, and

clinical patterns. Radiology 1996;198:117–120.

Cylak D, Carpenter PM. Breast imaging case of the day: pseudoangiomatous stromal hyperplasia. Radiographics 1999;19:1086–1088.

Kirkpatrick UJ, Burrows C, Loughran CF. Imaging appearances of pseudoangiomatous hyperplasia of mammary stroma. Clin Radiol 2000; 55:576–578.

Okashi K, Ogawa H, Suwa H, et al. A case of nodular pseudoangiomatous stromal hyperplasia (PASH). Breast Cancer 2006;13:349–53.

Polger MR, Denison CM, Lester S, et al. Pseudoangiomatous stromal hyperplasia: mammographic and sonographic appearances. Am J Roentgenol 1996;166:349–352.

# CASE 19

**ADAM CHARLES BRAITHWAITE**

**AND**

**MARY SCOTT SOO**

## HISTORY

A 48-year-old female with spontaneous bloody left nipple discharge.

A

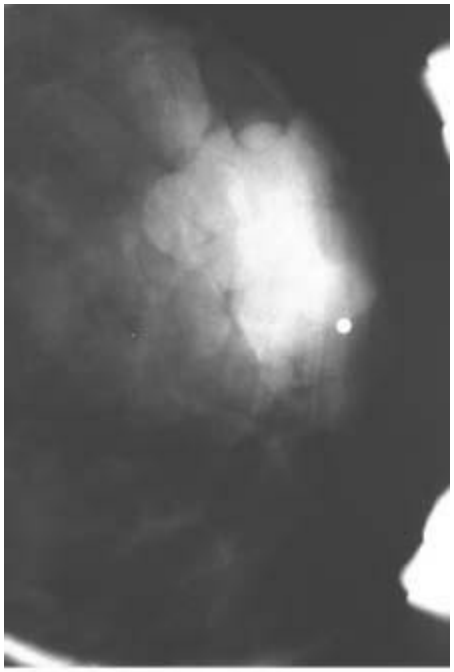

B

■**FIGURES 2-19A and 2-19B** Craniocaudal **(A)** and spot magnification **(B)** mammograms of the left breast show heterogeneously dense fibroglandular tissue, with a large, lobulated mass located in the subareolar region.

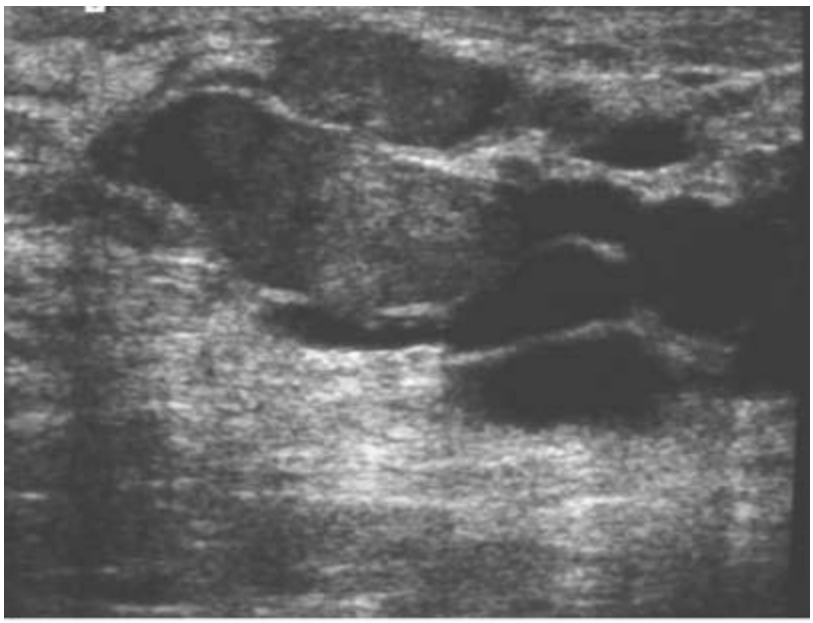

C

■**FIGURE 2-19C** Sonogram of the mass seen in Figures 2-19A and 2-19B shows numerous enlarged subareolar ducts with a mixed echogenicity solid mass filling at least two of the ducts.

## DIFFERENTIAL DIAGNOSIS

- **Intraductal papilloma:** The mammographic and sonographic features of this lesion, as well as the history or bloody nipple discharge, are typical of a benign intraductal papilloma.
- **Benign duct ectasia:** The presence of a mass within the dilated duct excludes this diagnosis.
- **Intraductal carcinoma:** Papillary and other intraductal carcinomas can have mammographic and sonographic features of an intraductal mass. These tumors are far less common than benign papillomas, making this diagnosis less likely. However, core needle biopsy is recommended to exclude malignancy. Due to the bloody nipple discharge, surgical excision is warranted as well.

**After assessing the imaging findings and considering the differential diagnosis, the final assessment is BI-RADS Category 4-B, intermediate suspicion for malignancy. Biopsy should be considered**.

# DIAGNOSIS

**Intraductal papilloma**

# KEY FACTS

## Clinical

- An intraductal papilloma is the most common intraductal mass, frequently developing in the major ducts and lactiferous sinuses of the subareolar breast.
- Intraductal papillomas often present with *spontaneous* bloody, clear, or serous nipple discharge.
- Most solitary intraductal papillomas occur in perimenopausal and postmenopausal women and have no increased risk of subsequent cancer.
- Management of benign papillomas diagnosed at core biopsy is controversial. If atypical papillomas or papillary carcinoma in situ is identified during core biopsy of an intraductal or intracystic mass, then surgical excision is required. If a benign papilloma is identified at core biopsy, then some authors recommend surgical excision because of the possibility of underestimation of disease, whereas others suggest short-term follow-up.

## Radiologic

- Most solitary papillomas are located in the central or subareolar breast, and often present as round, well-circumscribed masses that may contain amorphous or heterogeneous calcifications.
- Multiple papillomas are usually more peripherally located, asymptomatic lesions

found at mammography, presenting as masses or clusters of calcifications without a mass.

- The ultrasound appearance of a papilloma is often a complex intracystic or intraductal mass that may be highly vascular. Occasionally, a papilloma may present as a mass without an apparent intraductal or intracystic location.
- Ductography often reveals an intraductal filling defect.
- Enhancing subareolar mass or nonmass-like linear or ductal enhancement may be seen at MRI.

## SUGGESTED READING

El-Amin LC, Ghate SV, Bentley RC, Baker JA. Is surgical excision of core biopsy proven benign papillomas of the breast necessary?[abstract]. In: 2007 Radiological Society of North America Scientific Assembly and Annual Meeting; 2007 Nov 25–30; Chicago, II.

Liberman L, Tornos C, Huzjan R, et al. Is surgical excision warranted after benign, concordant diagnosis of papilloma at percutaneous breast biopsy? Am J Roentgenol 2006;186:1328–1334.

Mercado CL, Bena DH, Oken SM, et al. Papillary lesions of the breast at percutaneous core needle biopsy. Radiology 2006;238:801–808.

Renshaw AA, Derhagopian RP, Tizol-Blanco DM, et al. Papillomas and atypical papillomas in breast core needle biopsy specimens: risk of carcinoma in subsequent excision. Am J Clin Pathol 2004;122:217–221.

Sydnor MK, Wilson JD, Hijaz TA, et al. Underestimation of the presence of breast carcinoma in papillary lesions initially diagnosed at core needle biopsy. Radiology 2007;242:58–62.

Valdes EK, Feldman SM, Boolbol SK. Papillary lesions: a review of the literature. Ann Surg Oncol 2007;14:1009–1013.

# CASE 20

### MARY SCOTT SOO

### HISTORY

Staging breast MRI in a 45-year-old female with a recent excisional biopsy diagnosis of invasive ductal carcinoma involving a palpable abnormality in the posterior superior lateral aspect of the left breast.

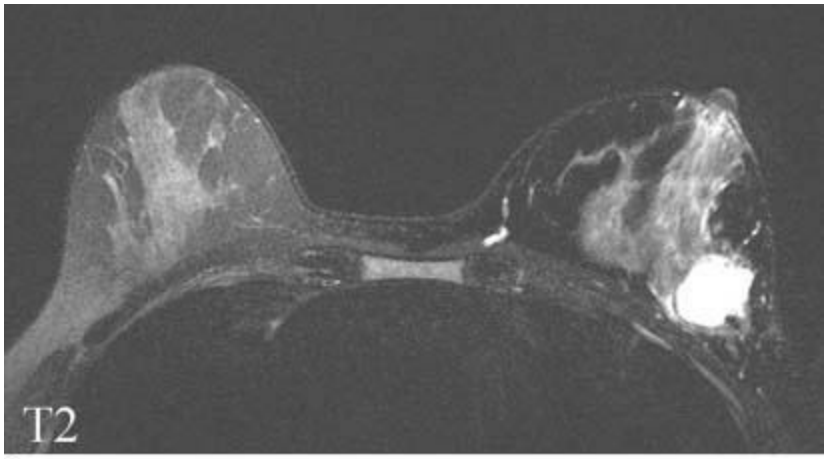


A

■**FIGURE 2-20A** Axial T2-weighted image of both breasts at the level of recently excised mass in the posterior lateral left breast. There is a rounded high signal mass in the posterior lateral left breast, corresponding to the site of recent surgery.

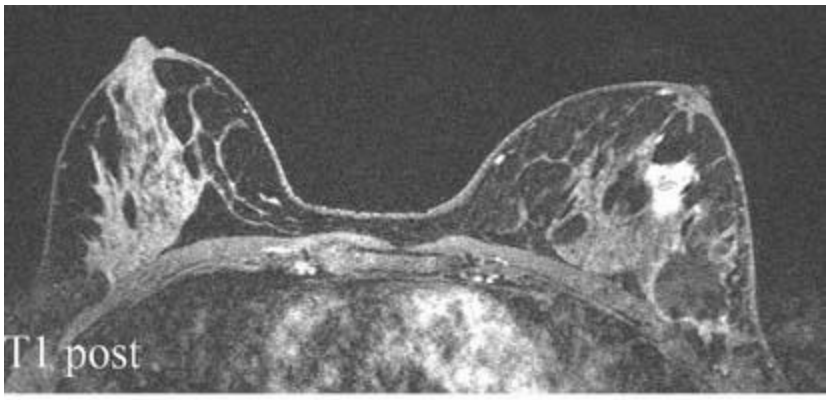


B

■**FIGURE 2-20B** Dynamic post-contrast axial Tl-weighted fat suppressed image of both breasts at the level seen in Figure 2-20A. There is irregular clumped high signal enhancement seen along the margin of the mass in the posterior lateral left breast at the site of recent surgery. There is a second large, irregular, rapidly enhancing mass seen anterior to the first mass, which was not identified on the T2 weighted image and demonstrated washout kinetics on subsequent images (not shown). No high signal was seen in these areas on pre-contrast images (not shown). No abnormal enhancement is seen in the right breast.

## DIFFERENTIAL DIAGNOSIS

■**Multiple cysts in the left breast:** Simple cysts at MRI tend to be round or oval high signal masses on T2-weighted images. On T1-weighted images, they are isointense to breast tissue, and show no significant contrast enhancement. Although the high signal mass on T2-weighted images in the posterior left breast does represent a fluid

collection, this corresponds to the site of recent surgery, and has irregular enhancement of the walls of the cavity, which is not seen in simple cysts. The second lesion located more anteriorly in the breast is irregular in shape, is low in signal on T2-weighted images, and enhances with contrast on T1-weighted images making the diagnosis of benign simple cysts very unlikely.

- **Multifocal invasive ductal carcinoma with positive surgical margins at the postoperative cavity:** This is the best diagnosis given the irregular enhancement of the walls of the surgical biopsy cavity, and the second, more anteriorly located large, irregular enhancing mass that demonstrated washout kinetics.
- **Positive surgical margins at the initial postbiopsy cavity with multifocal DCIS:** While this diagnosis is possible, DCIS usually presents as non-mass-like linear or clumped enhancement at MRI, unlike the large irregular enhancing mass seen anterior to the surgical biopsy cavity, in this case. This enhancing mass is more typical of invasive ductal carcinoma.
- **Invasive ductal carcinoma with breast cyst:** This is not the best diagnosis because, although there is a fluid filled mass in the posterior lateral left breast, this represents a seroma at the site of recent surgical excisional biopsy. There is irregular and clumped enhancement of the walls of this biopsy cavity, which would not be identified around a benign breast cyst.

**After assessing the MRI findings and considering the differential diagnosis, the final assessment is BI-RADS Category 5, highly suggestive of malignancy. Biopsy and other appropriate clinical action should be taken**.

## DIAGNOSIS

**Multifocal invasive ductal carcinoma with positive surgical margins at the postoperative cavity**

## KEY FACTS

### Clinical

- Many small invasive and in situ carcinomas of the breast are treated with breast conservation therapy (e.g., lumpectomy). The use of needle core biopsy to make an initial diagnosis (which did not occur in this case) can reduce the number of surgical procedures required for diagnosis and treatment of breast carcinoma.
- The use of breast MRI to evaluate for positive margins and multifocal (two or more cancers in one quadrant) or multicentric (two or more cancers within more than one quadrant) disease can also help to more accurately stage the disease and in some cases will alter the surgical management.

- The incidence of local-regional recurrence after breast conservation therapy ranges from 5% to 22% for Stage 0-II disease. The risk of local recurrence increases with positive margins, high grade DCIS, absence of radiation therapy following surgery, and young age.

### Radiologic

- MRI is frequently used for staging the breast in patients with newly diagnosed breast carcinoma, and is particularly useful for determining the extent of disease, where the sensitivity of mammography is limited due to the presence of fibroglandular tissue.
- In patients with newly diagnosed carcinoma, MRI depicts otherwise unsuspected malignant areas in 6% to 34% of ipsilateral breasts, and 3% to 24% of contralateral breasts.
- MRI is most likely to find additional malignant foci in women with family history of breast cancer and in women diagnosed with invasive lobular carcinoma.
- The disadvantages of breast MRI for staging relate to the high cost of MRI scanning and false positive studies, which result in additional biopsies and follow-up scans.
- If MRI is used for staging of newly diagnosed breast carcinoma, it is necessary to have MRI-guided biopsy capability, to sample lesions detected by MRI alone.

## SUGGESTED READING

Fischer U, Kopka L, Grabbe E. Breast carcinoma: effect of preoperative contrastenhanced MR imaging on the therapeutic approach. Radiology 1999;213:881–888.

Hollingsworth AB, Stough RG, O'Dell CA, Brekke CE. Breast magnetic resonance imaging for preoperative locoregional staging. Am J Surg 2008;196:389–397.

Lee JM, Orel SG, Czerniecki BJ, et al. MRI before reexcision surgery in patients with breast cancer. Am J Roentgenol 2004;182:473–480.

Liberman L. Breast MR imaging in assessing extent of disease. Magn Reson Imaging Cli N Am 2006;14:339–349.

Mumtaz H, Hall-Craggs MA, Davidson T, et al. Staging of symptomatic primary breast cancer with MR imaging. Am J Roentgenol 1997;169:417–424.

# CASE 21

**ADAM CHARLES**

**BRAITHWAITE**
**AND**

**MARY SCOTT SOO**

## HISTORY

A 42-year-old female presenting with a heavy, painless, erythematous right breast. She is afebrile and has no significant past medical or surgical history.

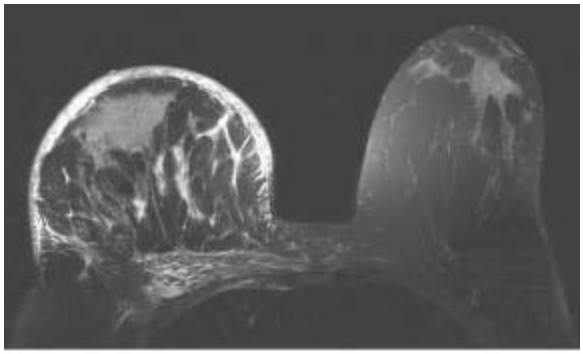

A

■**FIGURE 2-21A** Axial unenhanced T2-weighted MR image through both breasts shows asymmetry in breast size, with the right much thicker than the left. There is marked skin thickening with high signal edema of the skin and underlying trabeculae. There is an irregular mass in the anterior breast, isointense to breast parenchyma.

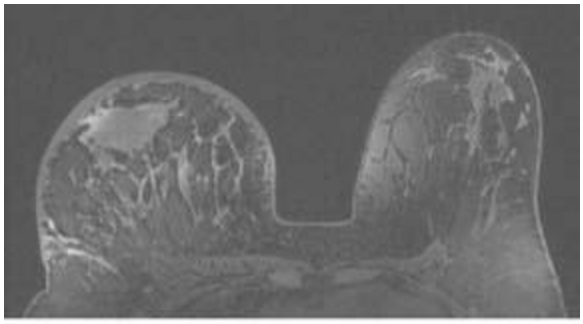

B

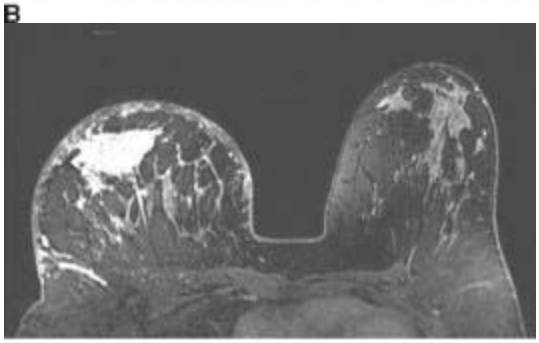

C

■**FIGURES 2-21B and 2-21C** Bilateral precontrast **(B)** and dynamic postcontrast **(C)** axial Tl-weighted fat suppressed MR images at the level of 2-21A again show asymmetry in breast size and marked skin and trabecular thickening. The postcontrast image **(C)** shows patchy enhancement of the skin and marked enhancement of the irregular mass in the anterior right breast.

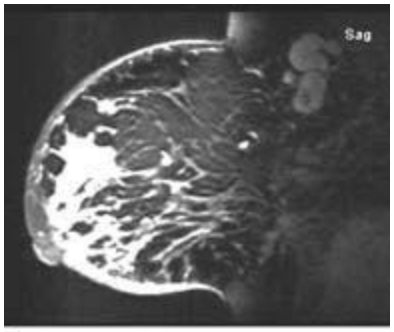


D

**FIGURE 2-21D** Dynamic fat suppressed postcontrast sagittal T1-weighted MR images of the right breast shows marked enhancement of the mass anteriorly, patchy enhancement of the skin, diffuse non-mass-like enhancement throughout the breast, and enlarged right axillary lymph nodes.

## DIFFERENTIAL DIAGNOSIS

- **Inflammatory breast carcinoma:** In the clinical setting of a painless, erythematous breast, the MRI findings of diffuse skin thickening and enhancement, an irregular enhancing mass, diffuse non-mass-like enhancement throughout the involved breast, and axillary lymphadenopathy are typical of inflammatory carcinoma.
- **Mastitis:** Bacterial infection may present with many similar MR imaging findings as are seen in this case, although an irregularly shaped, fairly homogeneously enhancing mass is unlikely with mastitis. Also, the typical clinical presentation for mastitis includes fever and marked tenderness.
- **Lymphedema/prior radiation:** Although diffuse edema and skin thickening throughout the breast may be caused by lymphedema or radiation therapy, the presence of an irregular enhancing mass, skin enhancement and non-mass-like enhancement throughout the breast would be unlikely in these situations. Likewise, the patient does not have a history of axillary surgery or radiation therapy to the breast; therefore, lymphedema would not be a consideration.
- **Lymphoma:** Lymphomatous involvement of the breast may have similar imaging findings to those seen in this case, although this would be an uncommon presentation.
- **Congestive heart failure (CHF)/renal failure/superior vena cava (SVC) obstruction:** Although cases of CHF, renal failure, or SVC obstruction can demonstrate a similar pattern of edema as is seen in this case, the findings are most often bilateral, unless the patient is chronically in a decubitus position. An irregular mass, lymph-adenopathy, and skin and non-mass-like enhancement would not be present with these diagnoses.

**After assessing the MR imaging findings and considering the differential diagnosis, the final assessment is BI-RADS Category 5, highly suggestive of malignancy. Biopsy and other appropriate action should be taken**.

## DIAGNOSIS

**Inflammatory breast carcinoma**

## KEY FACTS

### Clinical

- Inflammatory carcinoma is rare, comprising 1% to 4% of all breast cancers.
- Invasive ductal carcinoma is most common subtype.
- Inflammatory carcinoma often presents as rapid breast enlargement with heaviness, erythema, and skin warmth and thickening (peau d'orange). Lymphadenopathy is often present (58%).
- Findings are caused by tumor invasion and emboli into dermal lymphatics.
- Primary differential consideration is mastitis. However, mastitis is often painful and the patient usually has a fever.
- A course of antibiotics is often the first course of treatment. If the symptoms do not resolve by the completion of the course of antibiotics, a skin punch biopsy is necessary to evaluate for tumor invasion in the dermal lymphatics.

### Radiologic

- The diagnosis of inflammatory breast carcinoma is usually made with mammograms, clinical history, and skin punch biopsy.
- Mammographic findings include global asymmetry of the involved breast with skin and trabecular thickening. An underlying mass is common, but may be absent.
- Ultrasound may be useful to target underlying focal mass for biopsy.
- MRI is also useful for detecting underlying masses if mammograms and ultrasound are inconclusive and for evaluating axillary adenopathy and extent of disease.
- MRI findings include diffuse edema, skin thickening with enhancement, diffuse non-mass-like enhancement, and possibly focal enhancing masses and lymphadenopathy.

## SUGGESTED READING

Belli P, Costantini M, Romani M, et al. Role of magnetic resonance imaging in inflammatory carcinoma of the breast. Rays 2002;27:299–305.

Dershaw DD, Moore MP, Liberman L, Deutch BM. Inflammatory breast carcinoma: mammographic findings. Radiology 1994;190:831–834.

Gunhan-Bilgen I, Ustun EE, Memis A. Inflammatory breast carcinoma:mammographic, ultrasonographic, clinical, and pathologic findings in 142 cases. Radiology 2002;223:829–838.

Kushwaha AC, Whitman GJ, Stelling CB, et al. Primary inflammatory carcinoma of the breast: Retrospective review of mammographic findings. Am J Roentgenol 2000;174(2):535–538.

Lee KW, Chung SY, Yang I, et al. Inflammatory breast cancer: imaging findings. Clin Imaging 2005;29:22–25.

# CASE 22

**BETH WHITESIDE**

**AND**

**MARY SCOTT SOO**

## HISTORY

A high-risk screening MRI in a 58-year-old woman with past surgical history of lumpectomy for invasive ductal carcinoma in the right breast medially.

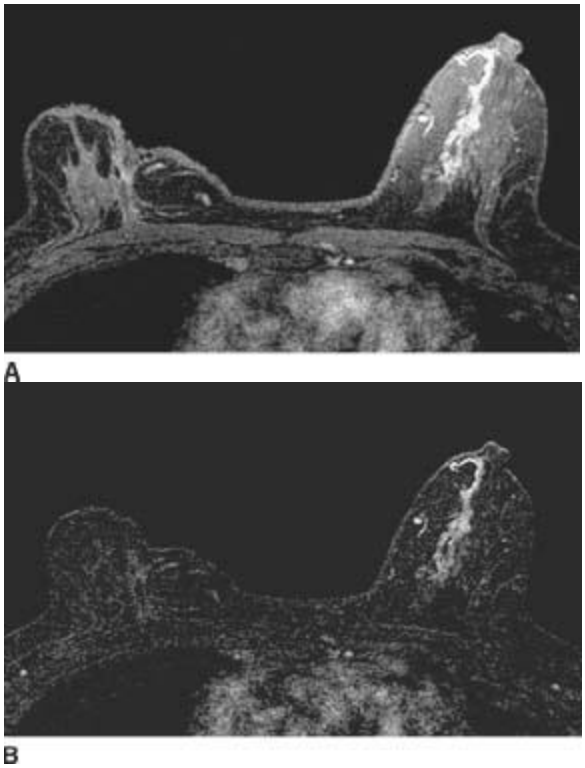


■**FIGURES 2-22A and 2-22B** Dynamic contrastenhanced fat-suppressed second pass axial Tl-weighted MRI images without subtraction **(A)** and with subtraction **(B)** at the

same level through both breasts show clumped enhancement in a linear distribution extending from the nipple posteriorly in the left breast. A plateau kinetics enhancement pattern was demonstrated in this area over the entire series of enhanced Tl-weighted MRI images (images from some series not shown). In the right breast, there is deformity with skin retraction and skin thickening at the postsurgical lumpectomy site in the medial breast. There is no significant enhancement at the lumpectomy site or throughout the remainder of either breast.

C

**FIGURE 2-22C** Sagittally reconstructed subtraction Tl-weighted MRI image of the left breast at the level of abnormality seen in Figures 2-22A and 2-22B. Clumped enhancement in a linear distribution is seen extending posteriorly from the nipple.

## DIFFERENTIAL DIAGNOSIS

- **Ductal carcinoma in situ (DCIS):** Clumped enhancement in a segmental or linear distribution as seen in the left breast makes this the most likely diagnosis.
- **Benign breast disease, such as fibrocystic disease, multiple papillomas, focal mastitis of the left breast:** The appearance of these benign conditions on MRI may overlap with the appearance of DCIS. Biopsy is necessary for diagnosis.
- **Atypical hyperplasia or other high-risk lesions:** The appearance of high-risk lesions overlaps with the appearance of DCIS and therefore biopsy is necessary for diagnosis.
- **Invasive carcinoma:** Invasive carcinomas commonly present as a mass with rapid enhancement and subsequent washout kinetics, making this a less likely diagnosis.

**After assessing the imaging findings and considering the differential diagnosis, the**

**final assessment is BI-RADS Category 4-B, intermediate suspicion for malignancy. Biopsy should be considered**.

## DIAGNOSIS

**DCIS of the left breast**

## KEY FACTS

### Clinical

- DCIS is ductal carcinoma confined to the milk duct.
- DCIS is often asymptomatic, but may present with bloody nipple discharge, or rarely as a palpable mass.
- DCIS is a precursor that may develop into invasive breast cancer.
- DCIS is commonly treated with local excision and radiation.

### Radiologic

- Mammography has been the gold standard for diagnosing DCIS, highly sensitive for detecting microcalcifications corresponding to areas of DCIS. Microcalcifications are not visible on MRI.
- MRI sensitivity for DCIS has been reported to be between 40% and 100%.
- MRI enhancement depends on the capillary permeability and vessel density. DCIS tumor vascularity may be less permeable than invasive disease and may, therefore, not have the rapid enhancement and washout characteristics, often seen with invasive disease.
- High spatial resolution should increase sensitivity of MRI for DCIS as the pattern and distribution of enhancement is more important than the enhancement kinetics.
- Enhancement patterns at MRI that are suspicious for DCIS:
    - *Segmental enhancement:* Triangular-shaped non-mass enhancement extending toward the nipple
    - *Ductal enhancement:* A single line or several branching lines of enhancement pointing toward the nipple
    - *Clumped regional enhancement:* Non-mass-like, clumped enhancement, in a regional distribution
- Findings suspicious for DCIS at MRI must be correlated with mammography. If no corresponding microcalcifications are seen on the mammogram, then MRI guided core needle biopsy will be necessary. If corresponding microcalcifications are seen, biopsy may be obtained with stereotactic guidance.

## SUGGESTED READING

Burstein HJ, Polyak K, Wong JS, et al. Ductal carcinoma in situ of the breast. N Engl J Med 2004;350:1430–1441.

Kuhl CK, Schrading S, Bieling HB, et al. MRI for diagnosis of pure ductal carcinoma in situ: a prospective observational study. Lancet 2007;370:485–492.

Morakkabati-Spitz N, Leutner C, Schild H, et al. Diagnostic usefulness of segmental and linear enhancement in dynamic breast MRI. Eur Radiol 2005;15:2010–2017.

# CASE 23

**MARY SCOTT SOO**

## HISTORY

Diagnostic MRI in a 56-year-old female with abnormalities seen on recent mammography and ultrasound, with subsequent core biopsy of a palpable abnormality. Multiple palpable masses are present in the right breast.

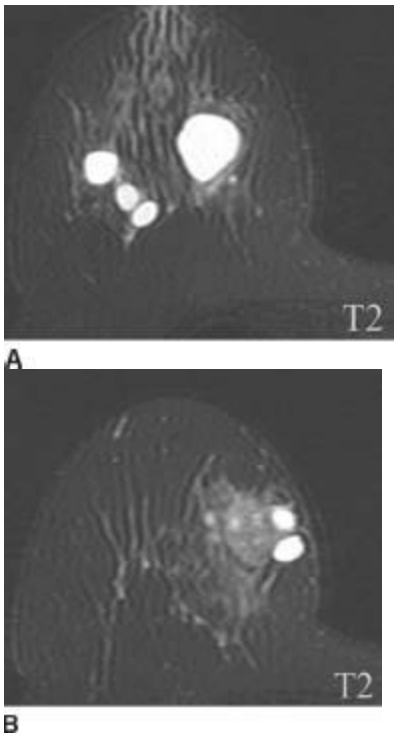


■**FIGURES 2-23A and 2-23B** T2-weighted axial MRI of the central **(A)** and superior **(B)** right breast show oval hyperintense circumscribed masses in both breasts, best seen in the central right breast **(A)** and a heterogeneous complex cystic mass in the superior right breast **(B).** The lesion in **B** shows peripheral dominant cysts and smaller central

cystic components.

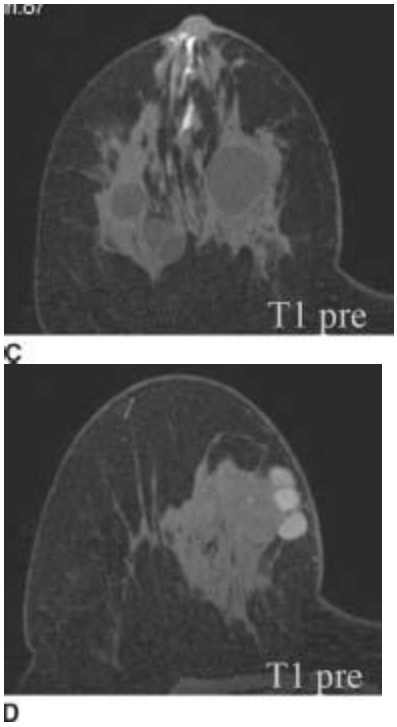


■**FIGURES 2-23C and 2-23D** Precontrast Tl-weighted axial images of the right breast at the levels seen in Figures 2-23A and 2-23B, respectively, show low signal within the circumscribed masses centrally **(C),** and high signal within the peripheral cystic components of the complex mass in the superior breast **(D).** High signal is seen within subareolar ducts from a prior core biopsy.

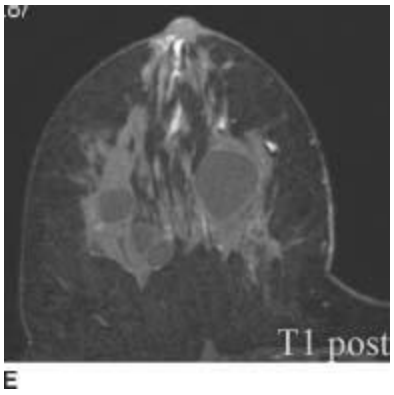

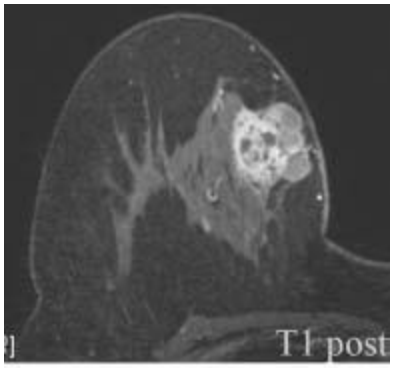


F

**FIGURES 2-23E and 2-23F** Postcontrast dynamic Tl-weighted axial images of the right breast at the levels seen in 2-23C and 2-23D, respectively, show no enhancement of the oval masses in the central breast **(E).** In the superior breast **(F),** there is rapid enhancement of the complex mass with additional hypointense necrotic cystic components revealed within the central portion of the heterogeneous enhancing mass.

## DIFFERENTIAL DIAGNOSIS

**Papillary carcinoma in situ:** Papillary carcinoma in situ can present as a large complex mass with easily seen cystic and solid components at MRI. While papillary carcinoma is a possibility for this case, papillary carcinoma in situ presenting as a large mass usually demonstrates enhancing, elongated, frond-like projections that extend into the cystic components of the mass, correlating with the morphologic make-up of this lesion. No frond-like projections are seen in this case, making it slightly less likely.

**Fibroadenoma:** Large fibroadenomas, which more tend to occur in younger, premenopausal patients and even in very young women in their teens, can present at MRI as large enhancing masses. Hypervascular fibro-adenomas can demonstrate rapid enhancement and a washout pattern. However, it is very unusual for fibro-adenomas to have large cystic components, as were seen in this case. Due to the cystic components and the age of the patient, this diagnosis is unlikely.

**Phyllodes tumor:** Phyllodes tumors are rare fibro-epithelial tumors that are characterized by increased cellularity of the stroma, compared to fibroadenomas. Their classification ranges from benign to malignant, depending on their degree of cellularity and number of mitoses per high-powered field, and about 25% will metastasize. They present as large, well-circumscribed, oval or lobular masses that occasionally have cystic components. At MRI, they demonstrate large lobular masses with smooth margins and rapid increase in signal intensity on dynamic contrast-enhanced imaging, and may have cystic components. Given the findings in this case, a phyllodes tumor could be a reasonable diagnosis.

**Invasive metaplastic carcinoma presenting as a complex mass in the right breast,**

**with numerous benign simple cysts seen in the remainder of the breast:** Although metaplastic carcionomas are uncommon tumors, this is a good diagnosis because the lesion in the medial right breast is a large lobulated and partly circumscribed heterogeneously and rapidly enhancing complex mass, with internal and peripheral cystic components. The masses seen in the remainder of the breast are high in signal intensity on the T2-weighted images, and demonstrate no contrast enhancement on dynamic enhanced images.

- **Papilloma:** Papillomas are the most common complex cystic mass occurring in womens' breasts, and are the most common cause of bloody nipple discharge. However, large benign solitary papillomas are usually located in subareolar dilated ducts. They are often intraductal or intracystic masses, rather than presenting as a solid enhancing mass with cystic components. For these reasons, papilloma is an unlikely diagnosis in this case.

**After assessing the findings and considering the differential diagnosis, the final assessment is BI-RADS Category 5, highly suggestive of malignancy. Biopsy and other appropriate clinical action should be taken**.

## DIAGNOSIS

**Invasive metaplastic carcinoma medially within the breast, and benign cysts elsewhere**

## KEY FACTS

### Clinical

- Metaplastic carcinomas of the breast are a heterogeneous group of neoplasms with mixed epithelial and mesenchymal differentiation, and account for <5% of breast carcinomas. Variants include matrix-producing carcinoma, spindle cell carcinoma, squamous cell carcinoma, carcinosarcoma, and metaplastic carcinoma with osteoclastic giant cells.
- Metaplastic carcinomas tend to present at younger ages than ductal carcinomas. They tend to be large at presentation and have a worse overall survival compared to invasive ductal carcinoma. Although they have a low incidence of regional lymph node involvement at diagnosis, they have a greater tendency for early hematogenous spread.

### Radiologic

- Compared to invasive ductal carcinoma, metaplastic carcinomas tend to show more benign imaging features, such as round, oval, or lobular shapes with circumscribed margins at mammography, and calcifications are less frequently noted.

- At sonography, metaplastic carcinomas tend to have circumscribed or indistinct margins with posterior acoustic enhancement. They often appear as complex masses and are highly vascular on Doppler imaging. Irregularly shaped masses with angular margins and posterior acoustic shadowing are uncommon in metaplastic carcinomas.
- At MRI, metaplastic carcinomas are round or lobular masses and have a variable T2 appearance, with homogeneous, mottled, or isointense patterns. Enhancement kinetics on T1-weighted dynamic imaging varies among tumors, and can be progressive, plateau, or washout patterns.
- Simple cysts at MRI present as circumscribed round or oval masses with high T2 signal intensity. On T1-weighted dynamic imaging, simple cysts have thin walls and do not show any significant enhancement with contrast administration.

## SUGGESTED READING

Goel NB, Knight TE, Pandey S, et al. Fibrous lesions of the breast: imaging-pathologic correlation. Radiographics 2005;25:1547–1559.

Velasco M, Santamaria G, Ganau S, et al. MRI of metaplastic carcinoma of the breast. Am J Roentgenol 2005;184:1274–1278.

Yang WT, Hennessy B, Broglio K et al. Imaging differences in metaplastic and invasive ductal carcinomas of the breast. Am J Roentgenol 2007;189:1288–1293.

Yabuuchi H, Soeda H, Matsuo Y, et al. Phyllodes tumor of the breast: correlation with MR findings and histologic grade. Radiology 2006;241:702–709.

# CASE 24

**BETH WHITESIDE**
**AND**

**MARY SCOTT SOO**

### HISTORY

A 56-year-old male patient with tender, palpable, left breast mass. No history of trauma was reported.

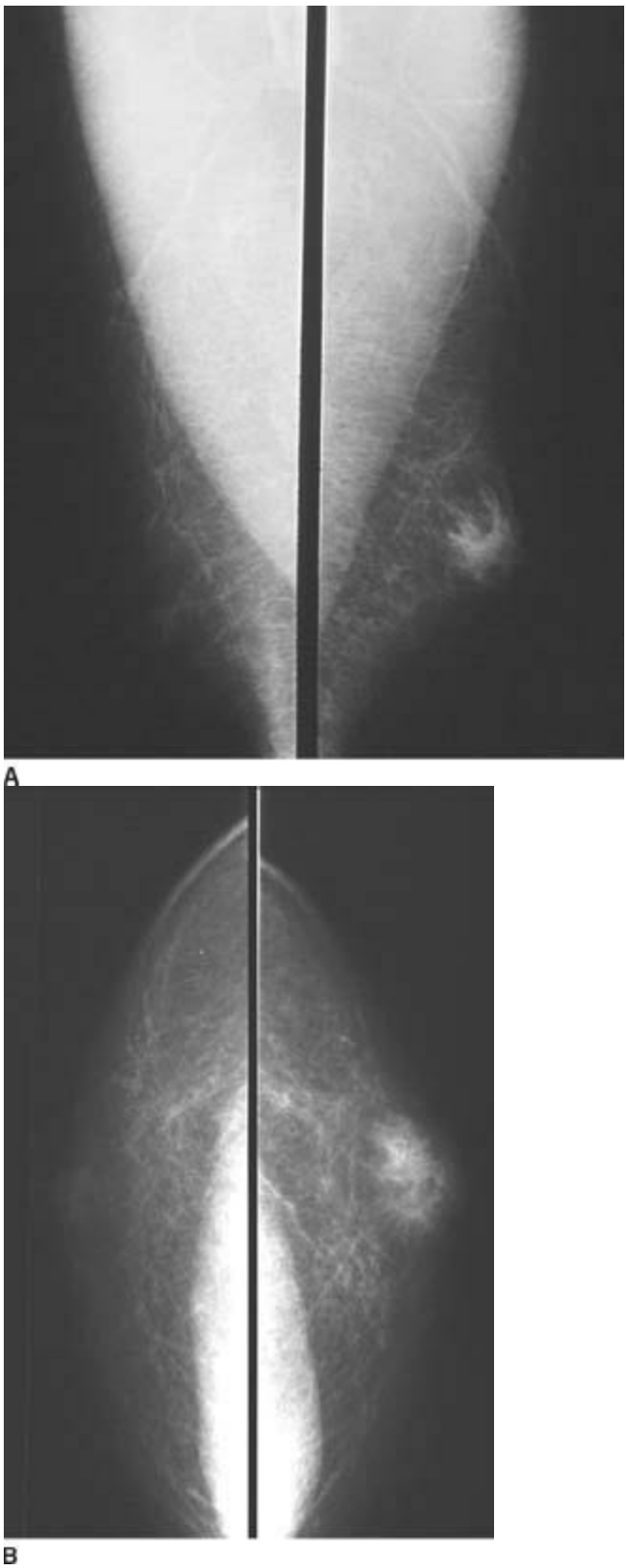


■**FIGURES 2-24A and 2-24B** Mediolateral oblique **(A)** and craniocaudal **(B)** mammograms of the both breasts show prominent pectoralis muscles. There is scattered fibroglandular tissue located in the subareolar regions, much greater on the left than the right. On the left, this region corresponded to the palpable tender abnormality.

## DIFFERENTIAL DIAGNOSIS

- **Gynecomastia:** This is the typical mammographic appearance of gynecomastia and is the best diagnosis.
- **Breast cancer:** <1% of breast cancer occurs in males. Male breast cancer has a similar appearance to female breast cancer and often presents as a high-density irregular mass. This case shows no suspicious mass or microcalcifications, making breast cancer an unlikely diagnosis.
- **Lipoma:** In the retroareolar region of the left breast, glandular tissue is seen. There is not a fat-containing encapsulated mass to suggest a lipoma.
- **Sebaceous cyst:** These are typically round, well-circumscribed masses found in the skin. Inspection of the skin commonly reveals a prominent dilated pore. There is no mammographic mass to suggest a sebaceous cyst, making this an unlikely diagnosis.
- **Hematoma:** Hematomas present as ill-defined oval masses or asymmetries. Clinical history is important in making this diagnosis. There was no history of trauma in this case making hematoma unlikely.

**After assessing the imaging findings and considering the differential diagnosis, the final assessment is BI-RADS 2; benign. Clinical follow-up is recommended**.

## DIAGNOSIS

**Gynecomastia**

## KEY FACTS

### Clinical

- Gynecomasatia is a common male condition that has been reported to be present on physical exam in greater that half of the male population over 44 years of age.
- The peak ages for gynecomastia are neonatal, pubertal, and in the elderly.
- Gynecomastia represents a proliferation of ductal and stromal elements (not lobules).
- Gynecomastia is caused by a hormonal change in estrogen/testosterone balance, with etiologies that increase estrogen or decrease testosterone levels.
- Etiologies for gynecomastia include medications, liver disease, endocrine/thyroid disorders, marijuana use, and testicular tumors.
- A bilateral diagnostic mammogram should be ordered for diagnostic evaluation.
- The typical presentation for gynecomastia is a tender, retroareolar mass that is soft and mobile.

## Radiologic

- Gynecomastia is often bilateral and may be unilateral or asymmetric (72%), and has the appearance of glandular tissue at mammography.
- Ultrasound is performed if typical gynecomastia is not seen, if there is concern that gynecomastia is obscuring an underlying lesion, or to evaluate a suspicious mammographic abnormality.
- Clinical follow-up is recommended to search for reversible causes of gynecomastia and to ensure no worsening signs on physical exam.

# SUGGESTED READING

Applebaum AH, Evans GF, Levy KR, et al. Mammographic appearances of male breast disease. Radiographics 1999;19:559–568.

Chantra PK, So GJ, Wollman JS, et al. Mammography of the male breast. Am J Roentgenol 1995;164:853.

Chen LC, Chantra PK, Larsen LH, et al. Imaging characteristics of malignant lesions of the male breast. Radiographics 2006;26:993–1006.

# Chapter THREE

# Gastrointestinal Imaging

**RENDON C. NELSON** ▪ CHAPTER EDITOR

Vincent H.S. Low

David M. Hough

Erik K. Paulson

Jeffrey T. Seabourn

Kelly S. Freed

Michael L. Kerner

Mary T. Keogan

Daniele Marin

Paul V. Suhocki

# CASE 1

**VINCENT H.S. LOW**

### HISTORY

A 28-year-old man presents with odynophagia.

A

■**FIGURE 3-1A** Barium swallow: Mucosal relief view of the mid to distal esophagus. There is a large (3 cm), shallow ulcer, sometimes given the term“giant”ulcer, in the mid to distal esophagus. The floor of the ulcer appears clean and smooth. There is no evidence of a mass, mucosal irregularity, infiltration, or rigidity.

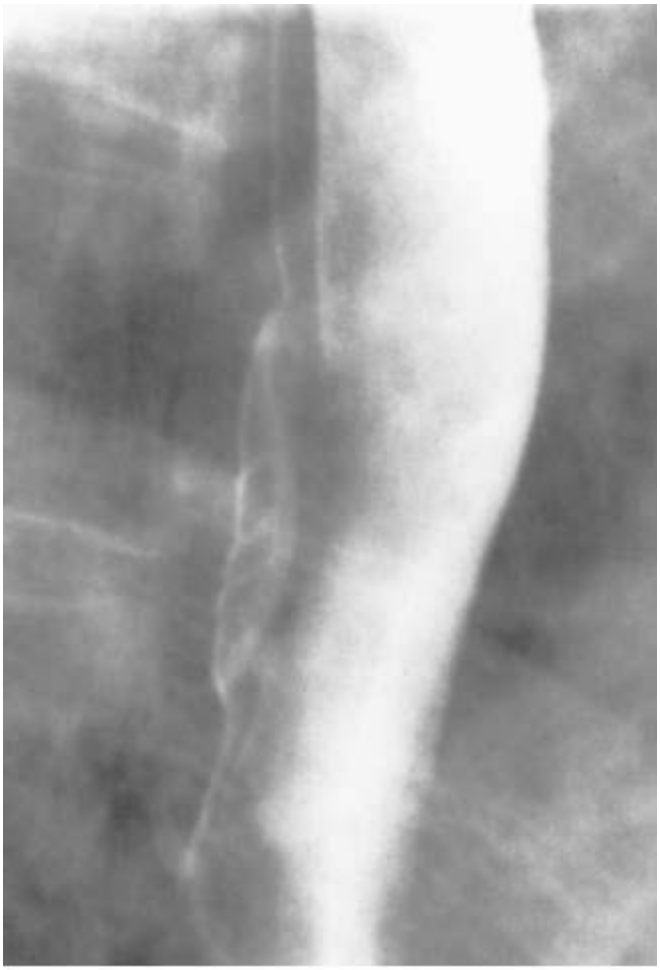

B

**FIGURE 3-1B** Barium swallow: Detail distended view of the lesion at the junction of the mid to distal esophagus. The ulcer has a well-defined lucent rim, suggesting that it is benign.

## DIFFERENTIAL DIAGNOSIS

- **Gastroesophageal reflux disease:** This is the most common cause of esophageal ulceration, and such a large proximal ulcer raises the possibility of Barrett's change.
- **Infectious esophagitis:** Cytomegalovirus (CMV) should be suspected in the immunocompromised patient. The fact that this is a young patient makes this condition more likely. The human immunodeficiency virus (HIV) itself can also result in giant esophageal ulcers.
- **Medication-induced esophagitis:** A history of recent ingestion of certain medications (particularly tetracycline antibiotics) would be relevant.
- **Radiation esophagitis:** Close anatomic relationship of the area of ulceration to the portal of radiation therapy would be relevant.

# DIAGNOSIS
**CMV esophagitis**

# KEY FACTS
## Clinical
- CMV is a member of the herpes virus group. It causes opportunistic esophagitis in patients with acquired immunodeficiency syndrome (AIDS) and only rarely in other immunocompromised patients.
- Patients usually present with odynophagia, which may be severe. On endoscopy, ulcerative esophagitis is seen with lesions that may be shallow or deep. It is impossible to differentiate this disorder from other viral esophagitides, including involvement by the HIV itself.
- Diagnosis is made from endoscopic brushings or biopsy specimens from the base of ulcers, by microscopic detection of characteristic intranuclear inclusion bodies in endothelial cells or fibroblasts, or by positive viral cultures. Histologic findings are required to differentiate CMV from herpetic esophagitis. HIV ulcers may respond to the administration of steroids, but CMV esophagitis requires antiviral agents such as ganciclovir.

## Radiologic
- CMV esophagitis may appear as discrete, small, superficial ulcers similar to those of herpes. Occasionally, a nonspecific esophagitis with nodular thickened folds only is seen, which may simulate reflux esophagitis.
- Giant, flat, single, or multiple ulcers, often with a thin radiolucent rim of edematous mucosa, are very suggestive of CMV esophagitis. These ulcers may be several centimeters in length and appear ovoid because of the limited diameter of the esophagus.
- HIV ulcers may have an identical radiologic appearance, requiring endoscopy and biopsy for culture and histologic examination to make a definitive diagnosis before appropriate treatment can commence.
- *Candida* esophagitis is characterized by longitudinally orientated, small, plaque-like filling defects. Severe disease appears as extensive, confluent, large plaques, giving the mucosa a“shaggy”pattern. These patterns are not typical for CMV, allowing radiologic differentiation.

# SUGGESTED READING
Balthazar EJ, Megibow AJ, Hulnick D, et al. Cytomegalovirus esophagitis in AIDS: radiographic features in 16

patients. AJR Am J Roentgenol 1987;149:919–923.

Sor S, Levine MS, Kowalski TE, et al. Giant ulcers of the esophagus in patients with human immunodeficiency virus: clinical, radiographic and pathologic findings. Radiology 1995;194:447–451.

Yee J, Wall SD. Infectious esophagitis. Radiol Clin North Amer 1994;32: 1135–1145.

# CASE 2

**DAVID M. HOUGH**

## HISTORY

A 55-year-old man presents with dysphagia.

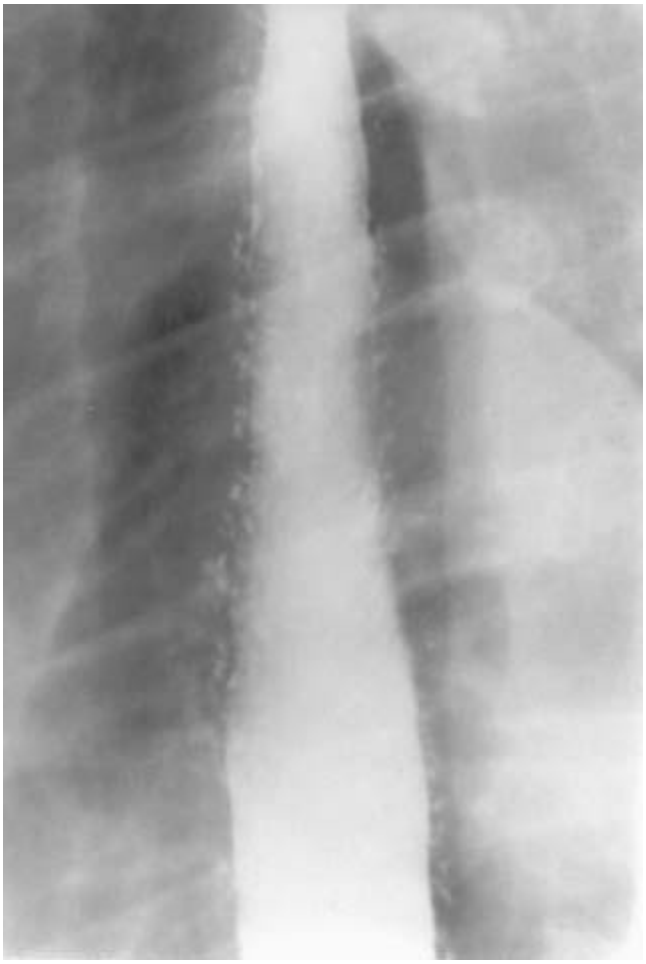

**FIGURE 3-2** Barium swallow: Spot film of the upper esophagus in single contrast. There are multiple, small, flask-shaped outpouchings from the esophageal lumen. Where visible, the neck of these outpouchings is very narrow.

## DIFFERENTIAL DIAGNOSIS

- **Intramural pseudodiverticulosis:** The finding of multiple flask-shaped collections of barium, oriented almost perpendicular to the long axis of the esophagus, is characteristic of this condition. Not all of the pseudodi-verticula show a clear communication with the esopha-geal lumen.
- **Esophagitis:** Features may include fold thickening, mucosal nodularity, an irregular mucosal contour, and focal erosions or ulcers. Ulcers can usually be seen to clearly communicate with the esophageal lumen, whereas in this case, some of the barium collections do not communicate. There are no plaque-like filling defects, as may be seen with *Candida* and other causes of esophagitis.
- **True esophageal diverticula:** True diverticula are larger and less numerous than pseudodiverticula.

## DIAGNOSIS

**Esophageal intramural pseudodiverticula**

## KEY FACTS

### Clinical

- Esophageal intramural pseudodiverticula is caused by dilated excretory ducts of the deep esophageal mucous glands, due to chronic inflammation. It is usually a sequela of chronic reflux esophagitis. Secondary infection with *Candida* is a common associated finding, but it is not considered a causal factor.
- Esophageal intramural pseudodiverticula most commonly occurs in elderly patients, with a slight male predominance. In as many as 90% of cases, there is an associated stricture. The most common presenting symptom is dysphagia, due to the associated stricture, and management is directed at treating the stricture.
- Esophageal intramural pseudodiverticula occurs in approximately 0.1% of patients undergoing barium esophagography, with an increased prevalence in patients with esophageal cancer (4.5%).

### Radiologic

- Single-contrast barium examination with low-density barium, which more readily enters the gland ducts, is more sensitive than a double-contrast technique with high-density barium for detecting intramural pseudodi-verticula. Endoscopy is relatively insensitive because it is difficult to visualize the tiny duct orifices.

- The characteristic appearance is that of numerous small (1 to 4 mm), flask-shaped outpouchings from the esophagus. The tiny necks may not fill completely, resulting in an apparent lack of communication with the esophageal lumen.
- Distribution is more often segmental than diffuse. Pseu-dodiverticula may occur at, above, or below the level of a stricture.
- Strictures associated with intramural pseudodiver-ticula should be evaluated carefully for evidence of malignancy.

## SUGGESTED READING

Canon CL, Levine MS, Cherukuri R, et al. Intramural tracking: a feature of esophageal intramural pseudodiverticulosis. AJR Am J Roentgenol 2000;175:371–374.

Levine MS, Moolten DN, Herlinger H, et al. Esophageal intramural pseudo-diverticulosis: a re-evaluation. AJR Am J Roentgenol 1986;147:1165–1170.

Luedtke P, Levine MS, Rubesin SE, et al. Radiologic diagnosis of benign esophageal strictures: a pattern approach. Radiographics 2003;23:897–909.

Plavsic BN, Chen MYM, Gelfand DW, et al. Intramural pseudodiverticulosis of the esophagus detected on barium esophagograms: increased prevalence in patients with esophageal carcinoma. AJR Am J Roentgenol 1995;165:1381–1385.

# CASE 3

**ERIK K. PAULSON**

## HISTORY

A 57-year-old man presents with a long history of heartburn and gradual onset of dysphagia.

A

■**FIGURE 3-3A** Barium swallow, single-contrast view. There is a smooth stricture in the mid esophagus with a small ulcer crater filled with barium.

B

**FIGURE 3-3B** Barium swallow, double-contrast view, shows smooth mucosa within the stricture.

## DIFFERENTIAL DIAGNOSIS

**Peptic stricture:** Peptic strictures are nearly always located in the distal esophagus, making this diagnosis unlikely. There is, however, an overlap in the appearance of peptic strictures and Barrett's esophagus.

**Caustic ingestion:** A caustic stricture could have this appearance. In this scenario, clinical history would be the key to the diagnosis.

**Mediastinal radiation:** While radiation strictures may be long and smooth, as in this case, clinical history and port-limited changes should be apparent in the mediastinum and pulmonary parenchyma. With radiation strictures, there is often displacement of both walls of the esophagus.

**Barrett's esophagus:** This is the most likely diagnosis given the ulcer, the length of the stricture, and the mid-esophageal location.

**Esophageal carcinoma:** It is uncommon for esophageal carcinoma to present with a smooth stricture.

# DIAGNOSIS

**Barrett's esophagus with a stricture and ulcer**

# KEY FACTS

## Clinical

- Barrett's esophagus represents columnar metaplasia of the squamous mucosa of the esophagus, associated with gastroesophageal reflux and esophagitis.
- Barrett's is a premalignant condition, placing the patient at risk for esophageal carcinoma. Prevalence of adeno-carcinoma in this population is approximately 15%.
- Of patients with Barrett's esophagus, 20% to 40% are asymptomatic.
- Approximately 10% of patients with chronic reflux esophagitis also have Barrett's esophagus.

## Radiologic

- The classic findings of Barrett's esophagus include a high esophageal stricture with or without an associated ulcer. However, the classic findings are relatively uncommon. Patients with Barrett's esophagus may have an unremarkable esophagram or may have a stricture in the distal esophagus, giving the appearance of a peptic stricture.
- As in this case, the stricture may be long and smooth or web-like.
- On double-contrast esophagography, a reticular pattern may be present in the region of the columnar metaplasia that may resemble the area gastricae pattern found in the stomach.
- Radiographic findings are neither sensitive nor specific for this condition. Therefore, endoscopy and biopsy are the procedures of choice to diagnose and follow these patients.

# SUGGESTED READING


Levine MS. Gastroesophageal reflux disease. In RM Gore, MS Levine, I Laufer (eds), Textbook of Gastrointestinal Radiology. Philadelphia, PA: Saunders, 1994;360–384.

Levine MS, Caroline DF, Thompson JJ, et al. Adenocarcinoma of the esophagus: relationship to Barrett mucosa. Radiology 1984;150:305–309.

Levine MS, Kressel HY, Caroline DF, et al. Barrett's esophagus: reticular pattern of the mucosa. Radiology 1983;147:663–667.

Levine MS, Herman JB, Furth EE. Barrett's esophagus and esophageal adenocarcinoma: the scope of the problem. Abdom Imaging 1995;20: 291–298.

Yamamoto AJ, Levine MS, Katzka DA, et al. Short-segment Barrett's esophagus: findings on double-contrast esophagography in 20 patients. AJR Am J Roentgenol 2001;176:1173–1178.

# CASE 4

**JEFFREY T.**

**SEABOURN**

## HISTORY

A 22-year-old woman presents with a several-month history of dysphagia and a 25-pound weight loss.

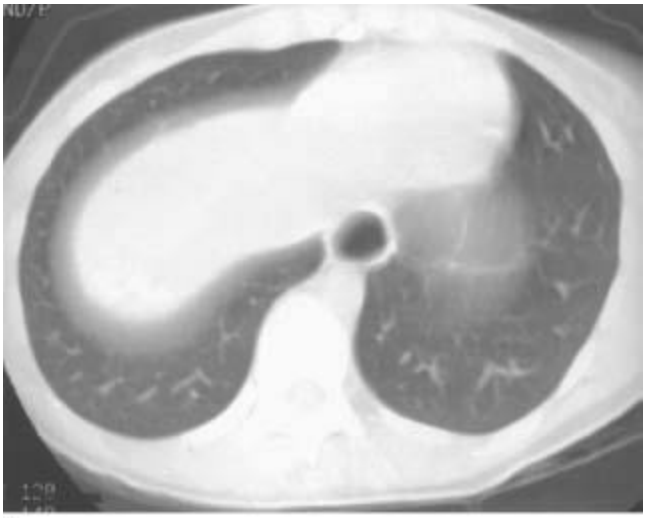

A

■**FIGURE 3-4A** Chest CT (lung window) at the level of the gastroesophageal junction. There is marked dilatation of the distal esophagus with an air-fluid level. Neither mural thickening nor a mass at the gastroesophageal junction is present. The lung bases are normal.

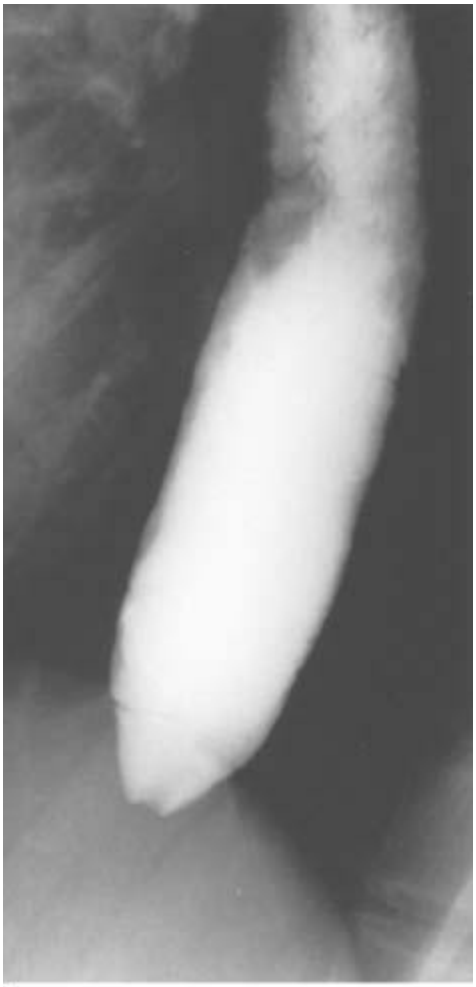

B

**FIGURE 3-4B** Barium swallow, single-contrast view. The esophagus is dilated, with smoothly marginated tapering at the gas-troesophageal junction. Mucous and debris remain in the proximal esophagus. Primary peristaltic activity was absent fluoroscopically.

## DIFFERENTIAL DIAGNOSIS

- **Peptic stricture:** Although peptic strictures typically cause narrowing of the distal esophagus, they are usually smoothly marginated and relatively fixed.
- **Primary achalasia:** Lack of primary peristaltic activity with smooth tapering at the gastroesophageal (GE) junction and intermittent opening of the lower esopha-geal sphincter (LES) argue for a primary motor disorder of the esophagus. The age of the patient and lack of an obstructing or infiltrating mass favors primary achalasia.
- **Secondary achalasia due to an intrinsic or extrinsic neoplasm:** The age of the patient, duration of symptoms, and lack of a mass on imaging studies rules this entity out.
- **Complicated scleroderma:** Narrowing of the distal esophagus in complicated

scleroderma is the result of a patulous LES with free GE reflux, eventually causing a peptic stricture. The chest CT usually reveals normal lung bases.

- **Chagas disease:** This protozoal infection, which involves the myenteric plexus, results in a motor disorder of the esophagus similar to achalasia.

## DIAGNOSIS

**Primary achalasia**

## KEY FACTS

### Clinical

- Achalasia is a primary motility disorder of the esophagus characterized by aperistalsis in the distal two-thirds of the esophagus and failure of the LES to relax.
- The etiology is unknown, but it is thought to be neurogenic in origin. Pathologic specimens reveal a decrease in the number of ganglion cells in Auerbach's myenteric plexus.
- Primary achalasia results in a slowly progressive dysphagia with both solids and liquids that may develop over many months or years. The patient may be able to modify dietary needs with smaller, frequent meals and, as a result, present without weight loss despite severe dysphagia.
- Odynophagia and chest pain are much less common symptoms.
- Regurgitation may lead to choking and coughing and even to aspiration and pneumonitis.

### Radiologic

- Fluoroscopic examination of esophageal motility will identify characteristic absence of the primary peristaltic wave in the distal two-thirds of the esophagus.
- The esophagus eventually dilates, with distal tapering (bird-beak or rat-tail appearance) at the GE junction.
- An important cause of this radiologic appearance is pseudoachalasia due to malignancy. This typically occurs in an older age group (>50 years) with a shorter duration (<6 months) of dysphagia. This is most commonly due to a carcinoma of the gastric cardia or fun-dus with invasion of the distal esophagus. This may also be due to actual infiltration of the myenteric plexus or to high-grade obstruction at the GE junction.

## SUGGESTED READING

Kahrilas PJ, Kishk SM, Helm JF, et al. Comparison of pseudoachalasia and achalasia. Am J Med 1987;82:439–446.

Laufer I. Motor disorders of the esophagus. In MS Levine (ed), Radiology of the Esophagus. Philadelphia, PA: Saunders, 1989;229–246.

Liang CY, Lin MS. Images in clinical medicine. Achalasia. N Engl J Med 2009;360:801.

Pohl D, Tutuian R. Achalasia: an overview of diagnosis and treatment. J Gastrointestin Liver Dis 2007;16:297–303.

# CASE 5

**DAVID M. HOUGH**

## HISTORY

A 34-year-old man presents with crampy abdominal pain and diarrhea.

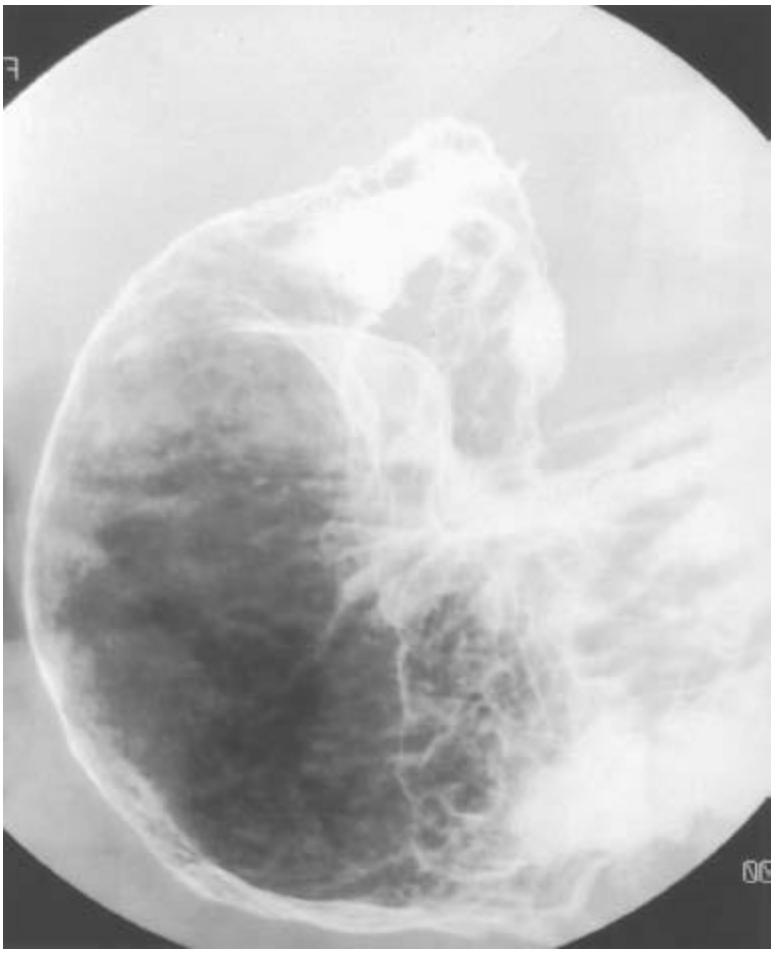

**FIGURE 3-5** Double-contrast upper gastrointestinal series: spot film of the distal stomach and proximal duodenum. There is narrowing of the gastric antrum with multiple punctate collections of barium and surrounding halos of edema (aph-thous lesions). The duodenal bulb is not distended, and there are ulcerations in the bulb and second portion

of the duodenum.

## DIFFERENTIAL DIAGNOSIS

- **Erosive gastritis:** Varioliform (meaning“resembling smallpox") erosions may result from ingestion of alcohol, aspirin and nonsteroidal anti-inflammatory drugs. Other causes include ischemia, stress, and trauma. Duodenal involvement would be unusual.
- **Infectious gastritis:** *Helicobacter pylori* is an important cause of antral gastritis. Features include fold thickening, ulceration, and sometimes antral narrowing. There may also be duodenal ulceration. CMV infection occurs in AIDS and other immunocompromised patients. Nonspecific findings also include fold thickening, erosions or ulcers, and antral narrowing. *Pneumocystis carinii* pneumonia, herpes virus, toxoplasmosis, and crypto-sporidiosis may also have similar findings.
- **Granulomatous disease:** Gastroduodenal Crohn’s disease typically has antral aphthous lesions, duodenal ulcers, and tapering of the antrum and pylorus, resulting in a“ram’s horn”configuration. Sarcoidosis, tuberculosis (TB), and syphilis may have similar features, with antral ulcers progressing to fibrosis and scarring.
- **Zollinger-Ellison syndrome (ZES):** Although the presence of postbulbar ulcers suggests ZES, there should also be gastric fold thickening and an increase in intra-luminal secretions and fluid.
- **Eosinophilic gastritis:** Although eosinophilic gastritis typically involves the gastric antrum and proximal small bowel, nodular fold thickening is a more common feature. Gastric erosions are atypical, and duodenal ulcers are rare.
- **Scirrhous carcinoma:** This entity typically causes a smooth, funnel-shaped narrowing of the antrum. Irregular fold thickening and ulceration may also occur. It is unlikely to cross the pylorus.

## DIAGNOSIS

**Gastroduodenal Crohn’s disease**

## KEY FACTS

### Clinical

- Gastroduodenal Crohn’s is almost always associated with concomitant ileocecal disease but rarely may occur before the development of more distal disease.
- Although it may be asymptomatic in the early stages, pain, nausea, vomiting, and weight loss are common in advanced stages. Gastric outlet obstruction may even occur.

## Radiologic

- Gastric Crohn's disease typically involves the antrum and sometimes the body. Fundal involvement is uncommon. Duodenal disease usually occurs in association with antral involvement, but isolated duodenal disease is possible.
- Aphthous lesions may appear as punctate or slit-like collections of barium with a lucent halo, indistinguishable from varioliform ulcers of erosive gastritis. Larger ulcers, mucosal effacement, or cobblestoning may also occur.
- Fibrosis may result in a funnel-shaped or"ram's horn"antrum. A pseudo-Billroth I sign is due to scarring of the antrum and duodenum with obliteration of the pylorus.
- Duodenal ulcers may be single or multiple. Duodenal strictures are usually postbulbar, smoothly tapering, and may be multiple. Skip lesions may occur.
- Asymmetric or eccentric scarring in the duodenum may result in pseudodiverticula.

## SUGGESTED READING


Farman J, Faegenburg D, Dallemand S, et al. Crohn's disease of the stomach: the"rams-horn"sign. AJR Am J Roentgenol 1975;123:242–251.

Levine M. Crohn's disease of the upper gastrointestinal tract. Radiol Clin North Am 1987;25:79–91.

Nelson SW. Some interesting and unusual manifestations of Crohn's disease of the stomach, duodenum and small intestine. AJR Am J Roentgenol 1969;107:86–101.

Hizawa K, Iida M, Kohrogi N, et al. Crohn disease: early recognition and progress of aphthous lesions. Radiology 1994;190:451–454.

Gore RM, Ghahremani GG. Crohn's disease of the upper gastrointestinal tract. Crit Rev Diagn Imaging 1986;25:305–331.


# CASE 6


### VINCENT H.S. LOW


### HISTORY

A 40-year-old man presents with dyspepsia. He is taking nonsteroidal anti-inflammatory agents for arthritis.

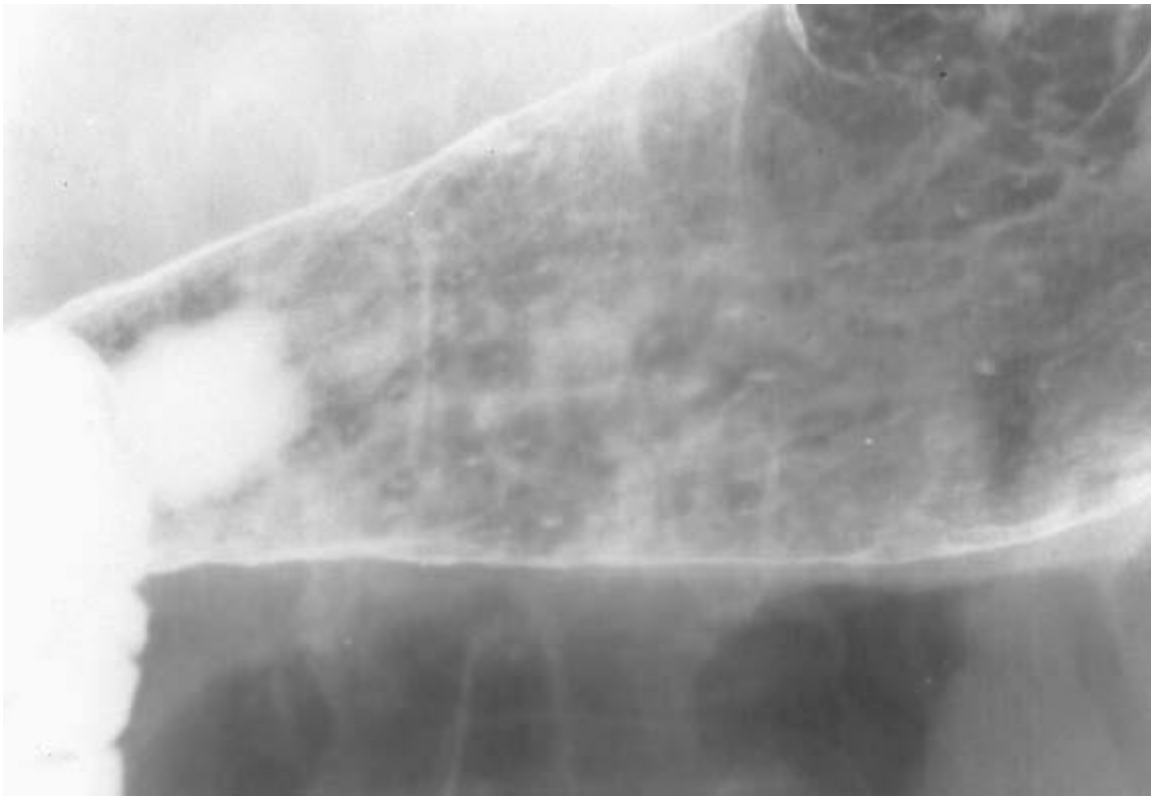

**FIGURE 3-6** Double-contrast upper examination: view of distal body and antrum of the stomach. Numerous dense specks are seen along the gastric antrum, predominantly toward the greater curvature. Some of these appear longitudinally oriented, and most demonstrate a lucent surrounding halo, representing edema.

## DIFFERENTIAL DIAGNOSIS

- **Erosive gastritis:** This is the most likely diagnosis given the history and linear distribution of lesions along the rugal folds.
- **Crohn's disease:** Gastric involvement usually occurs in the presence of advanced disease elsewhere, particularly the terminal ileum.
- **Viral infection:** This type of gastritis usually occurs in patients with immunodeficiency.
- **Ulcerated submucosal masses:** With these masses, the central ulcer, as well as the surrounding mass, tends to be larger than in this case.
- **Barium precipitates:** These artifacts do not have a radiolucent halo and will move when the patient is repositioned, either by the effect of gravity or the flowing pool of liquid barium.

## DIAGNOSIS

**Erosive gastritis**

## KEY FACTS

### Clinical

- These erosions are superficial epithelial defects that do not extend beyond the muscularis mucosa.
- Drugs are an identifiable cause of erosive gastritis, including aspirin, nonsteroidal anti-inflammatory drugs, steroids, and alcohol.
- In half the cases, no cause is identified. These cases are probably a manifestation of peptic disease.
- Other causes of gastric erosions include Crohn's disease, viral infection, and iatrogenic trauma (gastric catheters and endoscopic therapy).

### Radiologic

- Erosions appear as very shallow collections of barium. These are always small and may have a variety of shapes, including round, polygonal, linear, and punctate.
- There is associated nodular thickening of the rugal folds, and the erosions are aligned along the crest of these folds. On barium studies, the abnormal folds are often more easily visualized than the erosions themselves, and they may persist after the erosions have healed.
- Because the lesions are shallow, the changes are subtle. Disease on the more dependent posterior wall is visualized more readily by manipulating a thin film of barium into the region to opacify the erosions and the spaces between the folds. Disease on the anterior wall is visualized best in the prone position using compression.

## SUGGESTED READING

Catalano D, Pagliari U. Gastroduodenal erosions: radiological findings. Gastrointest Radiol 1982;7:235–240.

Laufer I, Hamilton J, Mullens JE. Demonstration of superficial gastric erosions by double contrast radiography. Gastroenterology 1975;68:387–391.

Levine MS. Erosive gastritis and gastric ulcers. Radiol Clin North Am 1994;32:1203–1214.

Momoshima S, Imai Y, Sugino Y, et al. Radiologic findings of linear gastric erosions. AJR Am J Roentgenol 1986;147:701–703.

# CASE 7

**VINCENT H.S.**
**LOW**

**HISTORY**

A 50-year-old woman presents with epigastric pain for several months.

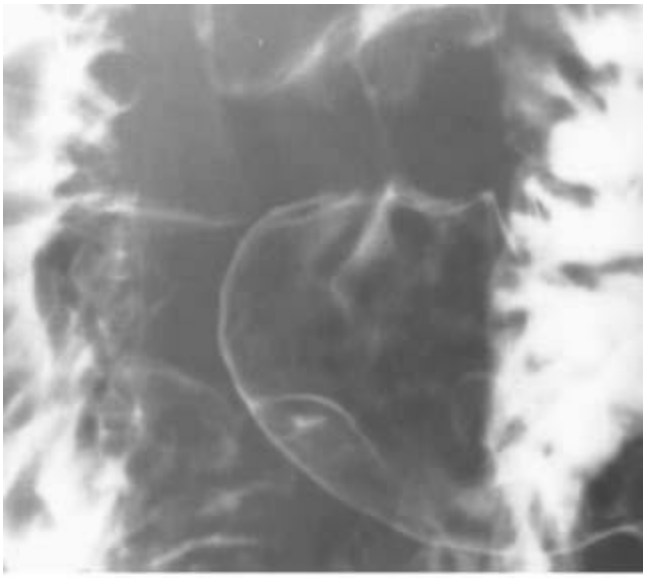

A

■**FIGURE 3-7A** Double-contrast upper gastrointestinal barium examination: view of the distal gastric antrum in the left posterior oblique position. There is elevation of the mucosa measuring 2.5 cm in diameter along the greater curvature, just proximal to the pylorus. A central small collection of barium is seen within this lesion. The margins of the lesion appear smooth.

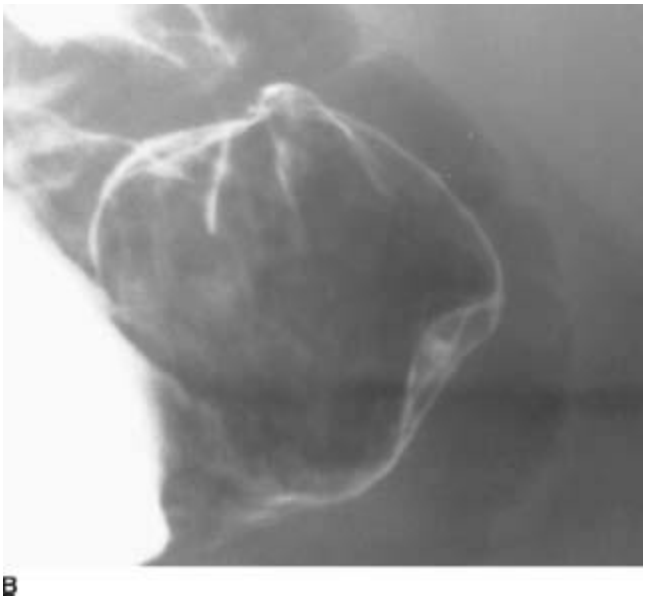

B

■**FIGURE 3-7B** Right posterior oblique position view of the distal gastric antrum. Rotation of the patient into the right posterior oblique position brings the lesion into

profile, further demonstrating the smooth outline of the lesion and the central (5-mm deep) niche of barium.

## DIFFERENTIAL DIAGNOSIS

- **Gastric ulcer:** An ulcer would have a central niche of barium and a surrounding mound of edema. However, such mounds usually have peripheral indistinct or fading borders, in contrast to the sharp outline of this lesion.
- **Leiomyoma:** This uncommon benign tumor could have this appearance, as would other benign mesenchymal tumors.
- **Ectopic pancreatic rest:** This is the most likely diagnosis by virtue of its benign submucosal appearance with central umbilication, as well as its typical location in the distal antrum along the greater curvature.
- **Bull's-eye"metastases:** These can appear with metastatic melanoma, lymphoma, or Kaposi's sarcoma. However, they are almost always multiple and occur in the context of disseminated disease elsewhere.

## DIAGNOSIS

**Ectopic pancreatic rest**

## KEY FACTS

### Clinical

- Ectopic pancreas occurs due to an anomaly in embryo-logic development, where a fragment of migrating pancreatic precursor becomes implanted in the intestinal wall. Histologically, all normal pancreatic elements are present but show a disorganized arrangement.
- The majority of pancreatic rests occur in the stomach (80%). They are also found in the duodenum and proximal jejunum. They have also been reported in the gallbladder, bile ducts, liver, spleen, appendix, Meckel's diverticulum, omentum, mesentery, and mediastinum.
- These lesions are usually asymptomatic and discovery of such should not be accepted as the cause of a patient's symptoms.
- Rarely, enzyme production results in epigastric pain and intestinal bleeding. These lesions have also been reported to cause gastric outlet obstruction due to their strategic position near the pylorus.

### Radiologic

- The lesion appears as a smooth, broad-based, solitary, submucosal mass.
- The most common location is along the distal greater curvature of the stomach, several centimeters from the pylorus.
- The central umbilication or dimple is thought to represent the orifice of the duct in this rest. It usually measures 1 to 5 mm in diameter and 5 to 10 mm in depth. Rarely, a rudimentary ductal system may fill with contrast material.

## SUGGESTED READING

Kim JY, Lee JM, Kim KW, et al. Ectopic pancreas: CT findings with emphasis on differentiation from small gastrointestinal stromal tumor and leiomyoma. Radiology 2009;252:92–100.

Levine MS. Benign tumors of the stomach and duodenum. In RM Gore, MS Levine, I Laufer (eds), Textbook of Gastrointestinal Radiology. Philadelphia, PA: Saunders, 1994:649–651.

Rubesin SE, Furth EE, Birnbaum BA, et al. Ectopic pancreas complicated by pancreatitis and pseudocyst formation mimicking jejunal diverticulitis. Br J Radiol 1997;70:311–313.

Thoeni RF, Gedgaudas RK. Ectopic pancreas: usual and unusual features. Gastrointest Radiol 1980;5:37–42.

# CASE 8

**JEFFREY T.**
**SEABOURN**

### HISTORY

A 44-year-old woman with stage IV breast carcinoma is status post bone marrow transplant and high-dose chemotherapy.

A

**FIGURE 3-8A** CT of the upper abdomen at the level of the celiac axis following intravenous contrast material. The wall of the stomach is diffusely thickened. Enlarged lymph nodes are also noted along the gastrohepatic ligament. There is an incidental cyst in the left hepatic lobe.

B

**FIGURE 3-8B** CT of the upper abdomen at a lower level reveals diffuse thickening of the gastric antrum.

## DIFFERENTIAL DIAGNOSIS

**Diffusely infiltrating (scirrhous) adenocarcinoma of the stomach:** The appearance

of diffuse gastric wall thickening in a poorly distensible stomach is radio-graphically indistinguishable from diffusely infiltrating metastatic disease.

- **Diffusely infiltrating metastatic disease:** Given the patient's clinical history, this is the most likely diagnosis.
- **Lymphoma:** Diffuse gastric involvement with lym-phoma may give this appearance. While there are enlarged lymph nodes along the gastrohepatic ligament in this patient, there is no retroperitoneal lymphadenopathy. The spleen is normal in size. When there is gastric involvement of lymphoma, it may cross the pylorus to involve the duodenum. The duodenum is normal in this patient.
- **Infectious/inflammatory gastritis:** Crohn's disease, chronic gastric ulcer disease with spasm, eosinophilic gastritis, sarcoidosis, TB, and brucellosis are other causes of gastric wall thickening and luminal narrowing. These more typically involve the gastric antrum.
- **Physical/chemical gastritis:** Corrosive gastritis, post-radiation injury, and hepatic arterial chemotherapy infusion are other less common causes of this appearance.

## DIAGNOSIS

**Diffusely infiltrating metastatic breast carcinoma to the stomach (linitis plastica appearance)**

## KEY FACTS

### Clinical

- Metastatic disease to the stomach is not uncommon. The most common organs of origin include malignant melanoma, breast, lung, colon, prostate, leukemia, and secondary lymphoma.
- The pattern of gastric involvement is variable. Solitary mass: 50%; multiple nodules: 30%; and linitis plastica (diffusely infiltrating): 20%. The diffusely infiltrating variety is most commonly seen in breast carcinoma.
- Patients often present with early satiety, nausea, and vomiting. This patient could not tolerate oral contrast material due to severe nausea and vomiting.

### Radiologic

- The differential diagnosis for diffuse gastric wall thickening with a poorly distensible lumen is fairly extensive. Malignant causes head the list and are most commonly due to the diffusely infiltrating variety of adenocarcinoma of the stomach, metastatic disease, or non-Hodgkin's lymphoma.
- Other causes of this radiographic appearance include inflammation secondary to

chronic gastritis, Crohn's disease giving a pseudo-Billroth I appearance, eosino-philic gastritis, and sarcoidosis.

- Infectious etiologies include TB and brucellosis. TB may be radiographically indistinguishable from Crohn's disease as a cause of antral narrowing.
- Physical/chemical causes are most commonly due to corrosive gastritis and radiation therapy.

## SUGGESTED READING


Eisenberg RL. Gastrointestinal Radiology: a Pattern Approach (2nd ed). Philadelphia, PA: Lippincott, 1990;205–222.

Elliott LA, Hall GD, Perren TJ, Spencer JA. Metastatic breast carcinoma involving the gastric antrum and duodenum: computed tomography appearances. Br J Radiol 1995;68:970–972.

Jaffe M. Metastatic involvement of the stomach secondary to breast carcinoma. AJR Am J Roentgenol 1975;123:512–521.

Karadeniz-Bilgili MY, Hyslop B, Pamuklar E, et al. MRI findings of gastric metastases from breast carcinoma. Magn Reson Imaging 2005;23:115–118.

Levine MS, Kong V, Rubesin SE, et al. Scirrhous carcinoma of the stomach: radiologic and endoscopic diagnosis. Radiology 1990;175:151–154.

Levine MS, Megibow AJ. Stomach and duodenum: carcinoma. In RM Gore, MS Levine, I Laufer (eds), Textbook of Gastrointestinal Radiology (vol.1). Philadelphia, PA: Saunders, 1994;660–683.

Winston CB, Hadar O, Teitcher JB, et al. Metastatic lobular carcinoma of the breast: patterns of spread in the chest, abdomen, and pelvis on CT. AJR Am J Roentgenol 2000;175:795–800.


# CASE 9


### DAVID M. HOUGH


### HISTORY

A 38-year-old woman presents with nausea, vomiting, abdominal pain, and weight loss. Her serum amylase and lipase levels were elevated.

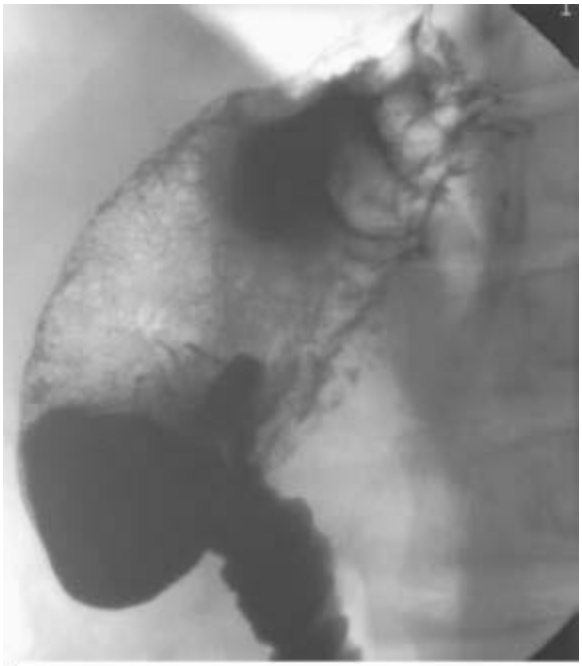

A

**FIGURE 3-9A** Double-contrast upper gastrointestinal barium examination: spot film of the stomach and duodenum. There is lobulated fold thickening in the gastric fundus.

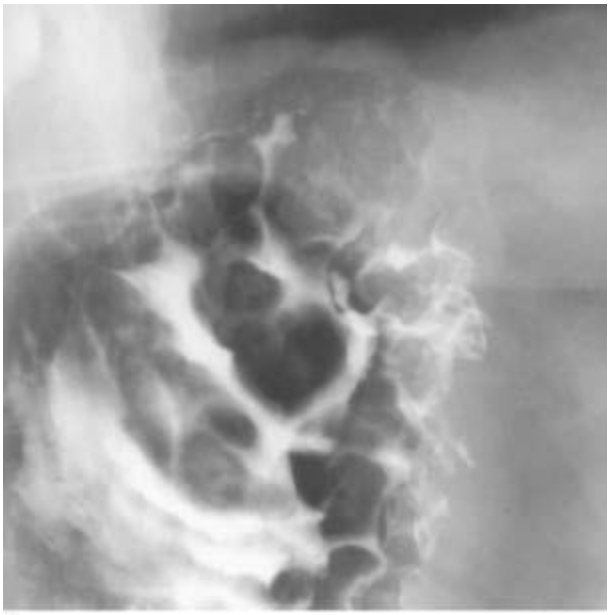

B

**FIGURE 3-9B** Spot film of the gastric fundus from the same examination. Gastric fold thickening is again seen, although the mucosa appears intact. The esophagus (not shown) was normal in appearance.

## DIFFERENTIAL DIAGNOSIS

**Hypertrophic gastritis:** This is a condition characterized by glandular hyperplasia and

increased acid secretion, with thickened folds predominantly in the fundus and body of the stomach. The majority of cases have an associated peptic ulcer. The focal nature of fold thickening in this case makes the diagnosis unlikely.

- **Ménétriers disease:** The gastric folds are usually more thickened than in hypertrophic gastritis, and there is relative sparing of the antrum. There may be mass-like fold thickening, although the abnormality is unlikely to be as focal as in this case. The folds in Menetriers disease also tend to follow the distribution of normal rugae, and there are increased secretions.
- **Lymphoma:** Gastric lymphoma may cause irregular or lobulated fold thickening due to submucosal infiltration or multiple submucosal masses. Submucosal infiltration by carcinoma may also cause this appearance.
- **Varices:** Gastric varices typically appear as multiple, smooth, lobulated, filling defects that tend to change in size and shape on fluoroscopy. The serpentine appearance of the folds in this case favors this diagnosis.

## DIAGNOSIS

**Isolated gastric varices**

## KEY FACTS

### Clinical

- Gastric varices are less likely to bleed than esophageal varices. However, they may present with low-grade bleeding or massive hematemesis.
- Gastric varices are usually associated with esopha-geal varices and are secondary to cirrhosis with portal hypertension.
- Isolated gastric varices may be caused by splenic vein thrombosis, resulting in shunting of blood from the spleen through the short gastric veins to the fundus, where they anastomose with branches of the coronary vein and esophageal plexus. With normal portal venous pressure, the blood can drain via the coronary vein into the portal vein without producing esophageal varices.

### Radiologic

- Gastric varices are characteristically multiple, lobulated, serpentine masses, but they may produce a single polypoid mass in the fundus.
- Gastric varices may be obscured on barium studies by the normal overlying gastric rugae. Gastric varices are seen radiographically in <50% of patients with uphill esophageal varices.
- It is important to examine the distal esophagus in patients with gastric varices in order

to identify esopha-geal varices.

- A double-contrast barium technique is considered more reliable than a single-contrast technique for identification of varices.
- The isolated gastric varices in this patient were due to splenic vein occlusion secondary to pancreatitis. Because portal hypertension is much more common than splenic vein occlusion, most patients with isolated gastric varices are found to have portal hypertension as the underlying cause.

## SUGGESTED READING

Evans JA, Delany F. Gastric varices. Radiology 1953;60:46–51.

Levine MS, Kieu K, Rubesin SE, et al. Isolated gastric varices: splenic vein obstruction or portal hypertension? Gastrointest Radiol 1990;15:188–192.

Kim SH, Kim YJ, Lee JM, et al. Esophageal varices in patients with cirrhosis: multidetector CT esophagography-comparison with endoscopy. Radiology 2007;242:759–768.

Kim YJ, Raman SS, Yu NC, et al. Esophageal varices in cirrhotic patients: evaluation with liver CT. AJR Am J Roentgenol 2007;188:139–144.

Muhletaler C, Gerlock J, Goncharenko V, et al. Gastric varices secondary to splenic vein occlusion: radiographic diagnosis and clinical significance. Radiology 1979;132:593–598.

# CASE 10

### VINCENT H.S.

### LOW

### HISTORY

A 33-year-old man presents with dyspepsia. He has had many hospital admissions since childhood for recurrent pulmonary infections.

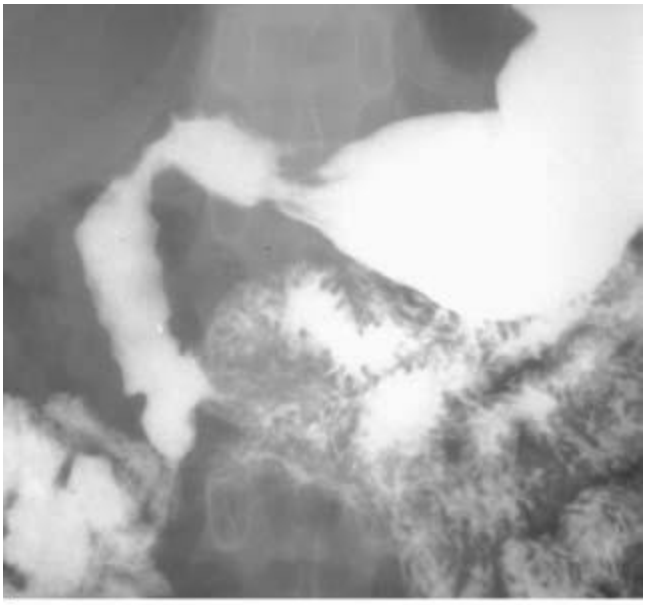

A

■**FIGURE 3-10A** Full-column, single-contrast upper gastrointestinal barium examination: view of the duodenum. There are nodular indentations in the duodenal walls.

B

■**FIGURE 3-10B** Double-contrast upper gastrointestinal barium examination: view of the duodenum. The duodenal folds appear flattened, smudged, and poorly defined.

C

**FIGURE 3-10C** Frontal chest radiograph. There is fibrosis and bronchiectasis with a predominant upper lobe distribution.

D

**FIGURE 3-10D** Contrast-enhanced CT of the upper abdomen. The pancreatic parenchyma has been replaced completely by fat.

## DIFFERENTIAL DIAGNOSIS

**Peptic duodenitis:** This is a common condition that may coexist with other pathologic conditions that cause pulmonary abnormalities. Alternatively, the duodenitis may have been caused by steroids or other medications used to treat the lung condition. They do not explain the pancreatic findings.

**Cystic fibrosis:** This is the most likely diagnosis as it would explain both the

pulmonary, duodenal, and pancreatic findings. The patient's age, however, is rather advanced for this condition.

- **Scleroderma:** Intestinal fibrosis from scleroderma may produce this duodenal pattern and may also be associated with pulmonary fibrosis.
- **Tuberculosis (TB):** TB would explain the upper lobe fibrotic changes. Duodenal involvement, however, is rare and usually results in strictures and fistulae.
- **Pancreatitis and other periduodenal inflammatory processes:** These conditions may cause the nonspecific duodenal changes as well as pancreatic atrophy but do not adequately explain the pulmonary abnormalities.

## DIAGNOSIS

**Cystic fibrosis**

## KEY FACTS

### Clinical

- Cystic fibrosis occurs in 1 in 2,000 births, predominantly in whites. Clinical and radiologic manifestations occur due to viscous secretions.
- The diagnosis is usually made clinically in infancy, but in about 2% of patients, symptoms may not manifest until after 18 years of age. Older patients typically present with hepatobiliary or gastrointestinal tract symptoms.
- With improvements in pulmonary care, increasing numbers of cystic fibrosis patients are surviving into adulthood.
- A majority (85%) of patients will have malabsorption due to impaired exocrine pancreatic secretions. These secretions are viscous, low in bicarbonates, and low in enzymes.

### Radiologic

- Duodenal changes are seen in 60% to 80% of patients and consist of fold thickening, mucosal nodularity, fold flattening, luminal dilatation, smudging, and poor definition of the mucosal fold pattern. These changes are usually confined to the first and second portions of the duodenum and occur without ulcerations.
- In the small bowel, blobs of mucous result in a network pattern of curved lines, predominantly involving the distal small bowel.
- Intestinal obstruction and impaction can occur during and after childhood.
- Pancreatic calcification may be evident on plain radiographs. Profound fatty replacement of the pancreas is often seen on CT or MR. Beaded dilatation of the main

pancreatic duct may also be seen as can intrapancre-atic cysts, likely representing markedly dilated side branches.

## SUGGESTED READING

Nijs EL, Callahan MJ. Congenital and developmental pancreatic anomalies: ultrasound, computed tomography, and magnetic resonance imaging features. Semin Ultrasound CT MR 2007;28:395–401.

Phelan MS, Fine DR, Zentler-Munro L, et al. Radiographic abnormalities of the duodenum in cystic fibrosis. Clin Radiol 1983;34:573–577.

Robertson MB, Choe KA, Joseph PM. Review of the abdominal manifestations of cystic fibrosis in the adult patient. Radiographics 2006;26:679–690.

Saavedra MT, Lynch DA. Emerging roles for CT imaging in cystic fibrosis. Radiology 2009;252:327–329.

Taussig LM, Saldino RM, di Sant'Agnese PA. Radiographic abnormalities of the duodenum and small bowel in cystic fibrosis of the pancreas (mucoviscidosis). Pediatr Radiol 1973;106:369–376.

# CASE 11

**KELLY S. FREED**

## HISTORY

A 35-year-old man presents with a 6-month history of diarrhea.

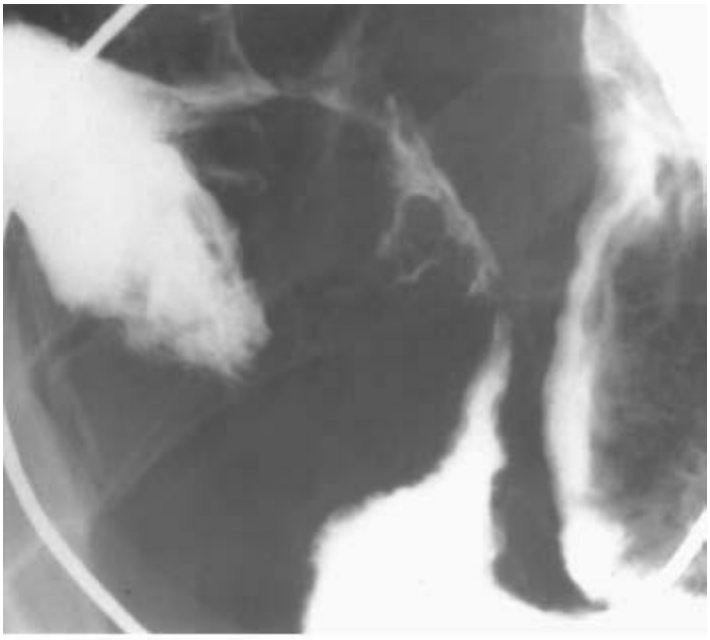

A

■**FIGURE 3-11A** Small-bowel follow-through barium examination: spot film of the terminal ileum. The terminal ileum demonstrates luminal narrowing, known as the"string

sign."There is also involvement of an adjacent loop of ileum. The intervening section of small bowel, which is relatively dilated, is less involved by the disease process. Linear ulceration is seen along the mesenteric border of the terminal ileum. At least two fistulae are seen along the antimesenteric border.

**FIGURE 3-11B** CT scan of the pelvis following intravenous and oral contrast material. The terminal ileum and cecum demonstrate bowel wall thickening with inflammatory change in the adjacent mesenteric fat.

## DIFFERENTIAL DIAGNOSIS

- **Crohn's disease:** Involvement of the distal and terminal ileum, discontinuous segments of disease, as well as stricture and/or fistulae formation are characteristic of Crohn's disease. The CT appearance is also typical, with the marked mural thickening and inflammatory change in the mesenteric fat.
- **Ulcerative colitis:** Ulcerative colitis can involve the terminal ileum by backwash ileitis, but the discontinuous involvement makes this diagnosis less likely. Additionally, the fistula formation and inflammatory change in the adjacent mesenteric fat are unusual.
- **Ischemia:** The distribution of disease makes a vascular etiology lower in the differential diagnosis. An ischemic insult to bowel more commonly involves the left than the right colon, and small bowel involvement is less common.
- **Neoplasms:** Adenocarcinoma more commonly involves the distal duodenum and proximal jejunum. Lymphoma usually presents as polypoid masses or large ulcerative/ excavating lesions.
- **Infection:** TB is rare in developed countries. Features that suggest TB rather than Crohn's disease include greater involvement of the cecum than the terminal ileum and

the fact that ulcers tend to be larger with TB. *Yersinia* ileitis may also have an appearance similar to Crohn's disease, but the disease is self-limited and the radiographic changes would return to normal in time.

- **Other perienteric inflammatory conditions:** Appendicitis or endometriosis are included in the differential diagnosis. The involvement of a loop of distal ileum in addition to the cecum and terminal ileum makes appendicitis less likely. Endometriosis may cause serosal abnormalities on the bowel, but not the strictures and fistulas seen in this patient. Additionally, endometriosis more commonly affects the sigmoid and transverse mesocolon.

## DIAGNOSIS

**Crohn's disease**

## KEY FACTS

### Clinical

- Crohn's disease is an inflammatory bowel disease of unknown etiology. There is a family history in approximately 40% of cases. The overall incidence is approximately 5 in 100,000. The age of onset is usually in adolescence or young adulthood.
- Early Crohn's disease is a mucosal disorder characterized by aphthous lesions, which can be detected by a double contrast barium examination or endoscopy. The disease progresses to the submucosa and eventually becomes transmural. Any portion of the gastrointestinal tract can be involved, although the terminal ileum is the most common site of disease. Extraintestinal involvement includes uveitis, arthritis, and erythema nodosum. The treatment includes medical suppression of the inflammatory reaction and surgical resection. The disease commonly recurs following surgical resection, often at the anastomotic site.

### Radiologic

- The radiologic diagnosis is typically made by a contrast examination such as an upper gastrointestinal examination, small-bowel follow-through (SBFT), enterocly-sis, or barium enema. The earliest changes of Crohn's disease are aphthous lesions, which appear as a central fleck of barium surrounded by a translucent halo. These initial changes occur in the mucosal lymphoid tissue. The appearance is nonspecific and can be seen in other inflammatory diseases.
- With progression of disease, mural thickening occurs, often >1 cm. The bowel wall thickening in Crohn's disease is usually greater than that seen in ulcerative colitis. Asymmetric or discontinuous involvement of the gastrointestinal tract is characteristic,

as opposed to the continuous involvement by ulcerative colitis. A typical nodular, cobblestone appearance is seen consisting of longitudinally oriented ulcerations.

- The terminal ileum is the most common site of involvement. Techniques to delineate the terminal ileum include enteroclysis, peroral pneumocolon, and a prone-angled compression view on SBFT. Strictures, fistulae, and abscess formation are more commonly seen in Crohn's disease than in ulcerative colitis.
- CT demonstrates the extraluminal extent of disease. The most common CT finding in Crohn's disease is bowel wall thickening. Another common finding is inflammatory change in the adjacent mesenteric fat. This mes-enteric change is seen in Crohn's disease rather than ulcerative colitis as the former is a transmural process and the latter is limited to the mucosa. Fibrofatty proliferation of the mesentery and enlarged mesenteric lymph nodes are also seen in Crohn's disease. CT is also helpful in the diagnosis of abscess formation.

## SUGGESTED READING


Helper DJ. Medical management of Crohn's disease: a guide for radiologists. Eur J Radiol 2009;69:371–374.

Hizawa K, Iida M, Kohrogi N, et al. Crohn's disease: early recognition and progress of aphthous lesions. Radiology 1994;190:451–454.

Huprich JE, Rosen MP, Fidler JL, et al. ACR appropriateness criteria(R) on Crohn's disease. J Am Coll Radiol 2010;7:94–102.

Nanakawa S, Takahashi M, Takagi K, Takano M. The role of computed tomography in management of patients with Crohn's disease. Clin Imaging 1993;17:193–198.

Siddiki HA, Fidler JL, Fletcher JG, et al. Prospective comparison of state-of-the-art MR enterography and CT enterography in small-bowel Crohn's disease. AJR Am J Roentgenol 2009;193:113–121.

Yue NC, Jones B. Crohn's disease: prone-angled compression view in radiographic evaluation. Radiology 1993;187:577–580.


# CASE12


### VINCENT H.S. LOW


### HISTORY

A 61-year-old woman has frequent and severe episodes of abdominal pain and distention.

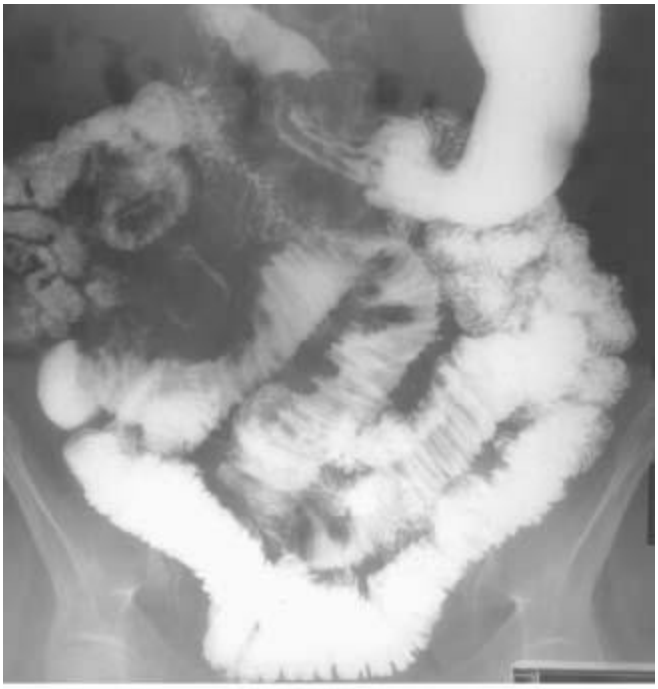

A

■**FIGURE 3-12A** Barium small-bowel follow-through: 60-minute frontal overview. There is a large area of mass effect in the right mid abdomen, displacing loops of bowel. Caliber change is seen, with dilatation of proximal small bowel. Abnormal separation of loops of small bowel is present in the lower abdomen. There is spiculation of the margins of small bowel loops adjacent to these areas of separation and mass effect.

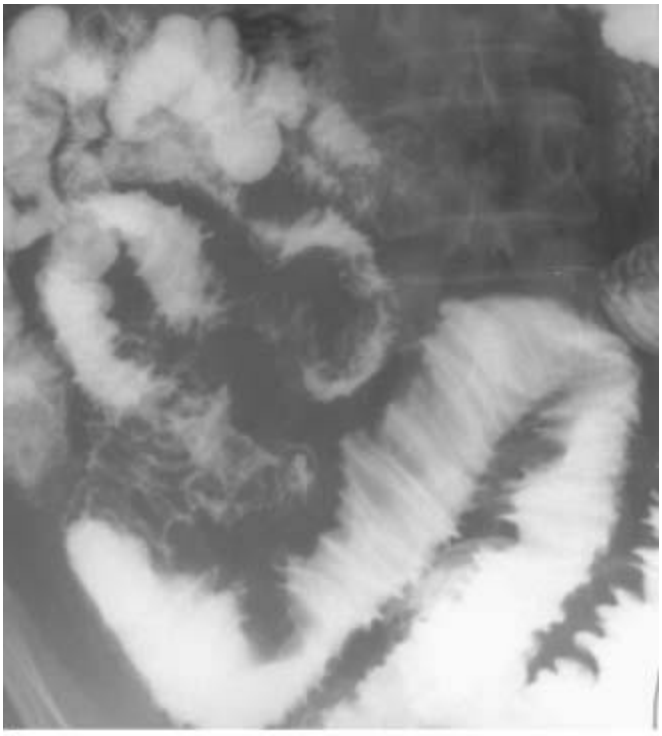

B

**FIGURE 3-12B** Barium small-bowel follow-through: spot view of the right lower quadrant. The mucosal folds are thickened, smooth in some areas and nodular in others. No specific intraluminal mass is seen.

## DIFFERENTIAL DIAGNOSIS

- **Mesenteric metastatic disease:** Marked desmoplastic reaction may be seen with certain metastatic tumors, such as scirrhous gastrointestinal tract cancers and breast cancer.
- **Carcinoid tumor:** This would explain the region of mass effect, which may be due to the tumor itself together with surrounding fibrosis. Similarly, small-bowel loop separation represents mesenteric infiltration, and the spiculation is due to the tumor's desmoplastic response. Note that the mesenteric mass is a metastasis not the primary tumor.
- **Endometriosis:** This entity can give eccentric mesen-teric implants but is unlikely, as the patient is post-menopausal.
- **Crohn's disease:** This disorder could provide an explanation for the inflammatory mass and mesenteric inflammation. However, the lack of fistula formation and terminal ileal disease makes this diagnosis unlikely.
- **Hemorrhage:** Mesenteric and intramural hemorrhage may occur with bleeding disorders or anticoagulant therapy but the patient has not history of these conditions.

## DIAGNOSIS

**Carcinoid tumor**

## KEY FACTS

### Clinical

- Carcinoid tumors account for one-fourth of small-bowel tumors, and the ileum is the most common site.
- Carcinoids arise from enterochromaffin cells and are slow growing, but essentially all are potentially malignant. The jejunum may remain asymptomatic for many years. Later, symptoms suggestive of a small-bowel lesion may occur, such as intermittent obstruction, diarrhea, and blood loss.
- The tumor produces active hormones such as 5-hydroxytryptamine, histamine, and serotonin. These result in the carcinoid syndrome (cutaneous flushing, diarrhea, and bronchospasm) only when there are metastases to the liver.

## Radiologic

- Early tumors (<2 cm in diameter) are usually found in the distal or terminal ileum as nonspecific smooth, round mucosal, or submucosal masses.
- When the tumor invades through the muscularis, serotonin is released, resulting in an intense desmoplastic reaction. This produces fibrosis with tethering, angulation, and spiculation of adjacent loops of bowel. This phenomenon may be well in excess of the extent of the tumor mass itself. Actual extension of tumor beyond the bowel will be seen as a soft tissue mass displacing and surrounding adjacent bowel loops. The tumor will also spread through the mesentery.
- On CT, a carcinoid tumor is seen as a mesenteric mass with soft tissue strands extending through the mesentery toward adjacent bowel loops. Liver metastases are usually well-defined and hypervascular. They tend to be isoattenuating to hypoattenuating precontrast, hyper-attenuating in the hepatic arterial dominant phase, and hypoattenuating to isoattenuating in the portal venous dominant phase.

## SUGGESTED READING

Balthazar EJ. Carcinoid tumors of the elementary tract: radiographic diagnosis. Gastrointest Radiol 1978;3:47–56.

Herlinger H, Maglinte DDT. Tumors of the small intestine. In H Herlinger, DDT Maglinte (eds), Clinical Radiology of the Small Intestine. Philadelphia, PA: Saunders, 1989;406–409.

Pinchot SN, Holen K, Sippel RS, Chen H. Carcinoid tumors. Oncologist 2008;13:1255–1269.

Wong M, Kong A, Constantine S, et al. Radiopathological review of small bowel carcinoid tumours. J Med Imaging Radiat Oncol 2009;53:1–12.

# CASE 13

### MICHAEL L.

### KERNER

### HISTORY

A 49-year-old woman presents with crampy abdominal pain, steatorrhea, and weight loss.

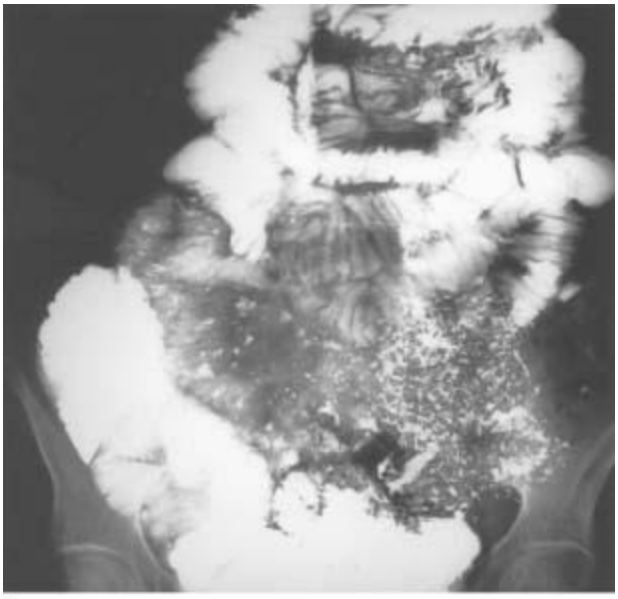

A

**FIGURE 3-13A** Barium small-bowel follow-through examination: 2 hours frontal overview. There is diffuse small-bowel dilatation, flocculation of the barium column, and reversal of the small-bowel fold pattern (jejunization of the ileum).

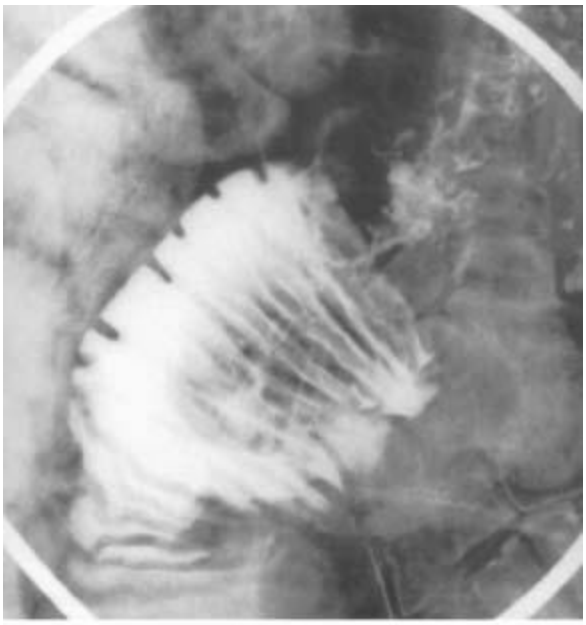

B

**FIGURE 3-13B** Barium small-bowel follow-through examination: spot film of an ileal loop. There is an intussuscept-ing mass in the right-lower quadrant that was transient.

## DIFFERENTIAL DIAGNOSIS

**Sprue, tropical or nontropical (celiac disease):** The hallmark of sprue is small-bowel dilatation with segmentation, flocculation, fragmentation of the barium column. Other

signs on a small bowel follow through include jejunization of ileal loops, transient nonobstructive intussusceptions, and the“moulage sign”(50%).

- **Lymphoma of small bowel:** Lymphoma does not have signs of hypersecretion or jejunization of the ileum but can present as a diffuse small-bowel disease with nodular fold thickening. Lymphoma can also be associated with intussusceptions.
- **Crohn’s disease:** This disorder typically involves the terminal ileum, typically involving the jejunum and Ileum in 15% and 55% of cases, respectively. Findings on a small bowel follow through include luminal narrowing, skip areas, and transmural disease with fistula formation. Crohn’s is not associated with intussusceptions.

# DIAGNOSIS

**Nontropical sprue (celiac disease)**

# KEY FACTS

## Clinical

- Sprue is manifested by diarrhea and steatorrhea, as well as fatigue, weight loss, anemia, neuropathy, stomatitis, osteomalacia, and depression.
- Nontropical sprue responds to a gluten-free diet, and tropical sprue responds to antibiotics.
- The diagnosis is made by a mucosal biopsy of the duodenal or jejunal showing total or subtotal villous atrophy and a clinical and histologic response to a gluten-free diet or antibiotic regimen.

## Radiologic

- The classic radiographic findings in patients with sprue are small-bowel dilatation, segmentation and flocculation of the barium column, hypersecretion, and the“moulage sign."
- Jejunization of the ileum is the result of atrophy of mucosal folds in the jejunum associated with an adaptive response in the ileum due to increase functional surface area.
- Intussusceptions are seen on small-bowel series in approximately 20% of celiac patients. Intussusceptions can be transient and asymptomatic and are diagnosed when there is a localized filling defect with a“coiled-spring”appearance. These intussusceptions typically involve a short segment of bowel and do not have proximal dilatation.

# SUGGESTED READING

Buckley O, Brien JO, Ward E, et al. The imaging of coeliac disease and its complications. Eur J Radiol 2008;65:483–490.

Cohen MD, Lintott DJ. Transient small bowel intussusception in adult celiac disease. Clin Radiol 1978;29:529–534.

Eisenberg RL. Gastrointestinal Radiology. Philadelphia, PA: Lippincott, 1983;448–451.

Rubesin SE, Herlinger H, Saul SH, et al. Adult celiac disease and its complications. Radiographics 1989;9:1045–1065.

Soyer P, Boudiaf M, Dray X, et al. CT enteroclysis features of uncomplicated celiac disease: retrospective analysis of 44 patients. Radiology 2009;253:416–424.

# CASE 14

**VINCENT H.S. LOW**

## HISTORY

A 57-year-old woman presents with sudden onset of watery diarrhea, fever, and abdominal tenderness.


A

■**FIGURE 3-14A** Supine abdominal radiograph. Nodular haustral fold thickening is seen in the transverse colon. There is also small-bowel dilatation indicating ileus.

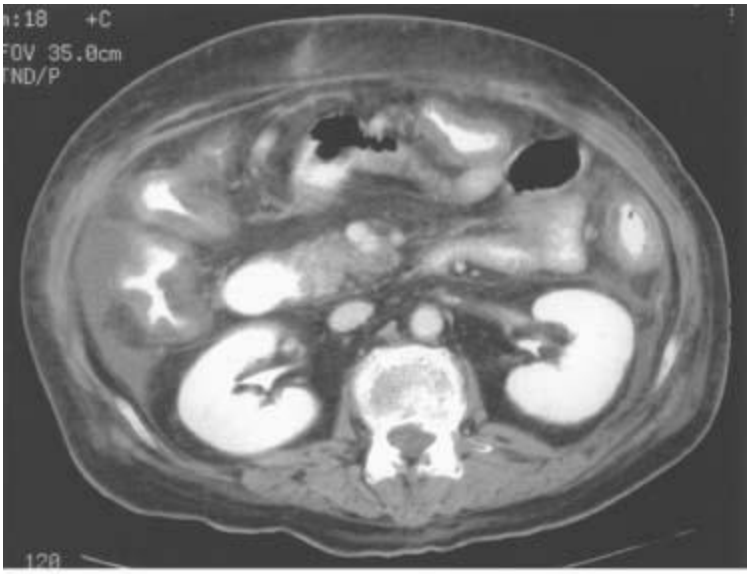


**FIGURE 3-14B** CT scan of the midabdomen following intravenous and oral contrast material. There is extensive nodular thickening of the wall of the colon. Ascites is present in the paracolic gutters.

## DIFFERENTIAL DIAGNOSIS

**Pseudomembranous colitis:** This is the best diagnosis because of widespread thumbprinting in the colon, as well as ascites, and small bowel ileus.

**Infectious colitis:** Colitis with thumbprinting can be seen with bacterial infections, including *Salmonella* and *Escherichia coli,* and parasitic infections, including *Anisakis* and *Amoebae.*

**Ischemic colitis:** The distribution is atypical for ischemia since the watershed region between the superior mesenteric artery and inferior mesenteric artery is located toward the splenic flexure. However, ischemia due to a vasculitis may not follow such vascular territories.

**Intramural hemorrhage:** A history of trauma, bleeding disorder, or anticoagulant therapy would be contributory.

**Inflammatory bowel disease:** This is unlikely because Crohn's disease is usually segmental, and ulcerative colitis of this severity would tend to show toxic dilatation as well.

**Lymphoma:** This is unlikely because there is usually a large cavitary mass, most often localized to the right colon. Diffuse changes may be seen in advanced disseminated lymphoma, although lymphadenopathy would be expected.

## DIAGNOSIS

**Pseudomembranous colitis**

# KEY FACTS

## Clinical

- Pseudomembranous colitis occurs due to toxins (A and B) liberated by *Clostridium difficile,* a gram-positive organism in patients with recent exposure to either antibiotics (most commonly clindamycin, ampicillin, or cephalosporins, but almost all antibiotics have been implicated) or chemotherapy (usually methotrexate or fluorouracil). Onset is usually within 2 days to 2 weeks after introduction of the treatment but may be as late as 8 weeks.
- The clinical illness ranges from mild diarrhea to fulminant colitis with toxic megacolon and death. Fever, leukocytosis, and abdominal pain may also occur.
- Characteristic pseudomembranes may be seen endoscopically. However, the distal colon may appear normal in up to 50% of patients. Visible pseudomembranes may not have developed early in the course of the disease, and colitis may be limited to the right colon and remain undetected unless full colonoscopy is performed.
- The diagnosis is established by detection of the specific toxins in the stool, but this takes 2 days to complete.
- Specific treatment is comprised of oral vancomycin or metronidazole.

## Radiologic

- The plain abdominal radiograph is normal in >60% of patients with pseudomembranous colitis. When abnormal, thumbprinting due to mucosal edema is visible in over half the cases. Other manifestations include colonic or small bowel ileus and ascites.
- Abdominal CT is more sensitive to the detection of colonic or other manifestations of the disease, but up to 40% of patients have normal scans. CT has the advantage of visualizing the colonic wall directly without having to rely on the presence of luminal gas to render the mucosal surface radiographically visible. Additional signs include pericolonic stranding and ascites.

# SUGGESTED READING

Boland GW, Lee MJ, Cats A, Mueller PR. Pseudomembranous colitis: diagnostic sensitivity of the abdominal plain radiograph. Clin Radiol 1994;49:473–475.

Boland GW, Lee MJ, Cats A, et al. Antibiotic-induced diarrhea: specificity of abdominal CT for the diagnosis of *Clostridium difficile* disease. Radiology 1994;191:103–106.

Fishman EK, Kavaru M, Jones B, et al. Pseudomembranous colitis: CT evaluation of 26 cases. Radiology 1991;180:57–60.

Glick SN. Other inflammatory conditions. In RM Gore, MS Levine, I Laufer (eds), Textbook of Gastrointestinal Radiology. Philadelphia, PA: Saun-ders, 1994;1156–1157.

Kawamoto S, Horton KM, Fishman EK. Pseudomembranous colitis: spectrum of imaging findings with clinical and pathologic correlation. Radiographics 1999;19:887–897.

Thoeni RF, Cello JP. CT imaging of colitis. Radiology 2006;240:623–638.

# CASE 15

**JEFFREY T. SEABOURN**

## HISTORY

A 56-year-old woman has fevers, left-lower quadrant tenderness, and an elevated white blood cell count.


A

■**FIGURE 3-15A** CT of the pelvis following rectal contrast material administration. There is mild soft tissue stranding in the fat surrounding the sigmoid colon, with fluid and focal thickening at the root of the sigmoid mesocolon. There is also a long segment of irregular luminal narrowing secondary to circumferential wall thickening.

B

**FIGURE 3-15B** Barium enema 3 weeks later: spot view of the sigmoid colon. The sigmoid colon is narrowed and markedly distorted. An intramural track of barium extends inferiorly from the center of this diseased segment. Numerous diverticula are seen in the descending colon.

## DIFFERENTIAL DIAGNOSIS

- **Diverticulitis:** The CT findings and clinical history make this the most likely diagnosis. The lack of extensive diverticular changes should not discourage one from making this diagnosis.
- **Perforated colon cancer:** Circumferential tumor infiltration can be difficult to distinguish from diverticulitis. A longer segment of colonic involvement argues against colon cancer. The saw-tooth appearance of the lumen also favors diverticulitis.
- **Crohn's disease:** Mural thickening and pericolic inflammatory changes may also be seen in Crohn's disease. Crohn's disease, however, typically has eccentric mural thickening as well as skip areas of involvement in the colon and/or small bowel.
- **Radiation colitis:** There is no clinical history to support this diagnosis. Radiation therapy to the pelvis would likely involve the rectum as well.
- **Ischemic colitis:** Isolated ischemia of the sigmoid colon would be unusual.

## DIAGNOSIS

**Sigmoid diverticulitis**

## KEY FACTS

## Clinical

- Classic clinical features are left-lower quadrant pain, tenderness, fever, and leukocytosis. Of patients with diverticulosis, 15% to 30% will develop diverticulitis.
- Clinical management includes antibiotics for mild disease and surgery for more severe cases. Percutaneous abscess drainage and antibiotics can obviate surgery in some patients and help convert colonic surgery into a single- rather than a two-stage procedure in other patients.
- Complications of diverticulitis include perforation, obstruction (exacerbated by muscular hypertrophy), pericolonic abscess formation, and the development of a colovesicle fistula. Most inflammatory complications are secondary to a ruptured diverticulum and occur in a pericolonic location.
- The sigmoid colon is involved in 95%, and the cecum in 5% of cases.

## Radiologic

- A contrast enema (CE) depicts the bowel lumen, spasm, and muscle hypertrophy, but the pericolonic inflammatory changes can only be inferred indirectly. A CE underestimates the degree of pericolonic inflammatory changes that are the hallmark of diverticulitis. However, CE is often valuable in differentiating diverticulitis from colon cancer.
- The CT hallmark of diverticulitis is the presence of inflammatory changes in the pericolonic fat. Induration and thickening of the root of the sigmoid mesocolon is not pathognomonic but highly suggestive of sigmoid diverticulitis.
- On CT, associated diverticuli are seen in 84%, thickened colonic wall in 79%, and pericolonic fluid collections/ abscess in approximately 35% of cases.
- CT is not able to distinguish colon cancer from diver-ticulitis in approximately 10% of cases.
- CT should be the primary method of radiologic diagnosis as well as the method for evaluation and staging of complicated diverticulitis.

# SUGGESTED READING


Baker ME. Imaging and interventional techniques in acute left-sided diverticulitis. J Gastrointest Surg 2008;12:1314–1317.

Birnbaum BA, Balthazar EJ. CT of appendicitis and diverticulitis. Radiol Clin North Am 1994;32:885–898.

Johnson CD, Baker ME, Rice RP, et al. Diagnosis of acute colonic diver-ticulitis: comparison of barium enema and CT. AJR Am J Roentgenol 1987;148:541–546.

Lohrmann C, Ghanem N, Pache G, et al. CT in acute perforated sigmoid diverticulitis. Eur J Radiol 2005;56:78–83.

Neff CC, vanSonnenberg E. CT of diverticulitis: diagnosis and treatment.

Radiol Clin North Am 1989;27:743–752. Pohlman T. Diverticulitis. Gastroenterol Clin North Am 1988;17:357–358.

# CASE 16

**ERIK K. PAULSON**

## HISTORY

A 63-year-old woman with a palpable right-upper quadrant mass.

A

■**FIGURE 3-16A** Dynamic contrast-enhanced CT scan of the upper abdomen during the hepatic arterial dominant phase. There is a large mass in the posterior segment of the right hepatic lobe with peripheral globular,“cloud-like”enhancement.

B

**FIGURE 3-16B** Dynamic contrast-enhanced CT scan of the upper abdomen during the portal venous dominant phase. The peripheral nodules have increased in size and the degree of enhancement exceeds the blood pool (i.e., the aorta). The interior of the mass remains unenhanced and there is a small central scar.

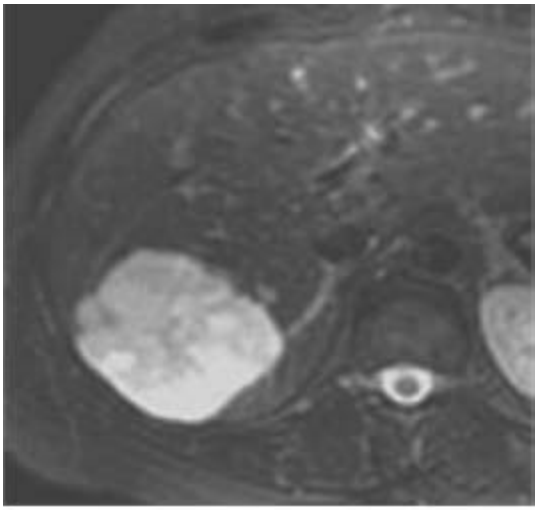

C

**FIGURE 3-16C** T2-weighted MRI of the upper abdomen shows a well-circumscribed, somewhat lobulated mass with uniform, homogenous, high-signal intensity. The small central scar is mildly hypointense.

## DIFFERENTIAL DIAGNOSIS

**Hypervascular metastases:** Metastases to the liver from an islet cell tumor of the

pancreas, thyroid carcinoma, breast carcinoma, and carcinoid tumors may be hypervascular. Because hypervascular metastases may enhance in a fashion similar to normal liver parenchyma, they may be difficult to detect during the portal venous dominant phase of enhancement. However, the peripheral globular enhancement in this case would be atypical for any hypervascular metastases. Further, while metastases are typically of high signal intensity compared to liver on T2-weighted MRI, they are not usually this“bright."

- **Focal nodular hyperplasia:** These tumors are hamarto-mas and have imaging characteristics similar to hepatic parenchyma. On dynamic contrast-enhanced CT during the hepatic arterial dominant phase, these tumors typically have early intense uniform enhancement, not present in this case. In about half of the cases, there may be a central scar that may be of low attenuation on a dynamic contrast-enhanced CT. On T2-weighted MRI, these lesions may be slightly hyperintense but often are quite subtle, with signal characteristics similar to those of normal liver (so called“stealth”lesion).
- **Hepatocellular carcinoma:** These tumors are often heterogenous“ugly”masses that may invade the portal and/or hepatic veins. While they are often hypervas-cular, they usually have areas of central enhancement due to prominent central feeding arteries; they lack the peripheral globular enhancement shown in this lesion. Patients with hepatocellular carcinoma have underlying cirrhosis in about 70% of cases, which is not present here.
- **Metastatic colon cancer:** Occasionally, colon cancer may present as a solitary mass in the liver. However, colon carcinoma metastases are not hypervascular, very rarely have delayed contrast enhancement, and are of lower signal intensity on T2-weighted MRI than shown in this case.
- **Cavernous hemangioma:** This is the most likely diagnosis, given the very high signal intensity on T2-weighted MRI and peripheral nodular enhancement pattern with centripetal“fill-in."

## DIAGNOSIS

**Cavernous hemangioma of the liver**

## KEY FACTS

### Clinical

- Second to cysts, hemangiomas are the most common benign tumor of the liver, with a reported incidence ranging from 1% to 10%. There is a female predominance of 4 to 1.
- Pathologically, the tumor represents numerous endo-thelial-lined, blood-filled spaces. Larger hemangiomas (≤20cm) are nearly always heterogenous, with central areas of fibrosis, necrosis, and cyst formation. Calcifications are uncommon.

- Hemangiomas are one of the few tumors that can be confidently diagnosed using noninvasive imaging techniques, including ultrasound, dynamic contrast-enhanced CT, MRI, or $Tc^{99m}$-tagged red blood cell scin-tigraphy. Biopsy is rarely indicated unless the lesion has atypical features.

## Radiologic

- On ultrasound, hemangiomas are well circumscribed and are uniformly hyperechoic relative to the liver parenchyma. They may demonstrate enhanced through-transmission but do not have a halo. With color Doppler ultrasound, they usually do not have central blood flow.
- On precontrast CT, hemangiomas are usually of uniform low attenuation with well-circumscribed, lobulated borders. On dynamic contrast-enhanced CT, heman-giomas nearly always demonstrate globular enhancement about the periphery. Over time (<30 minutes) the tumors“fill-in”in a centripetal fashion. Large tumors may have central areas of necrosis, fibrosis, or scarring that may not entirely“fill-in”with contrast material.
- On T1-weighted MRI, the lesions are well-circumscribed and of low signal intensity compared to the hepatic parenchyma. On a dynamic contrast-enhanced MRI with a gadolinium-chelate, hemangiomas demonstrate enhancement, identical to that described for dynamic CT. On T2-weighted MRI, hemangiomas typically have a very high signal intensity, similar to that of a hepatic cyst or fluid in the gallbladder or spinal canal, leading some to call hemangiomas“light bulb”lesions. Because of this characteristic appearance, MRI has proven useful in distinguishing hemangiomas from other hepatic tumors.
- On $Tc^{99m}$-labeled red blood cell scintigraphy, hemangio-mas will appear as a defect in the early phases of the scan that will“fill-in”on delayed scans. SPECT imaging improves the accuracy in detecting and characterizing small hemangiomas.

# SUGGESTED READING

Bioulac-Sage P, Laumonier H, Laurent C, et al. Benign and malignant vascular tumors of the liver in adults. Semin Liver Dis 2008;28:302–314.

Nelson RC, Chezmar JL. Diagnostic approach to hepatic hemangiomas. Radiology 1990;176:11–13.

Quinn SF, Benjamin GG. Hepatic cavernous hemangiomas: simple diagnostic sign with dynamic bolus CT. Radiology 1992;182:545–548.

Ros PR. Benign liver tumors. In RM Gore, MS Levine, I Laufer (eds), Textbook of Gastrointestinal Radiology. Philadelphia, PA: Saunders, 1994;1861–1898.

Silva AC, Evans JM, McCullough AE, et al. MR imaging of hypervas-cular liver masses: a review of current techniques. Radiographics 2009;29:385–402.

# CASE 17

**DAVID M. HOUGH**

## HISTORY

A 30-year-old woman presents with right-upper quadrant pain and intermittent jaundice.

A

■**FIGURE 3-17A** Contrast-enhanced CT scan of the liver. There is a low-attenuation cystic structure located medial to the gallbladder. Adjacent scans showed the structure to extend from the porta hepatis to the pancreatic head. The wall is smooth and well defined, and the contents are of water attenuation. There is no dilatation of the intrahepatic bile ducts.

B

**FIGURE 3-17B** Percutaneous transhepatic cholangiogram shows a large tubular contrast-filled structure communicating with the gallbladder and cystic duct.

## DIFFERENTIAL DIAGNOSIS

**Loculated biloma:** A biloma would be unlikely in the absence of a history of recent trauma or biliary surgery, and would not have a well-defined tubular appearance on cholangiography.

**Enteric duplication cyst:** These cysts can be of water attenuation on CT but would be unlikely to follow the line of the common bile duct and would not communicate with the biliary tree on cholangiography.

**Hepatic cyst:** The extrahepatic location of this structure on CT and communication with the biliary tree on cholangiography excludes this diagnosis.

**Choledochal cyst:** This is the most likely diagnosis since on CT the cystic structure is in the expected location of the extrahepatic biliary tree, and on cholangiography the cyst is confirmed to be in continuity with the biliary tree.

**Pancreatic pseudocyst:** A pseudocyst could have this appearance on CT, but the cholangiogram excludes this diagnosis.

**Biliary cystadenoma:** A cystadenoma would be unlikely because of the extrahepatic location. Biliary cyst adenomas are usually intrahepatic, of low attenuation, and may have internal septa and a thick, irregular wall. Furthermore, they do not communicate

with the biliary tree.

# DIAGNOSIS

**Choledochal cyst**

# KEY FACTS

## Clinical

- Choledochal cysts are an uncommon cause of biliary obstruction and are characterized as cystic dilatation of the extrahepatic or intrahepatic biliary tree, or both.
- They are three times more common in females than males. Although they may present at any age, they are typically discovered in children and young adults, with 60% presenting before the age of 10 years.
- The classic clinical triad of pain, jaundice, and an abdominal mass occurs in only 30% of patients.
- The etiology is unknown, but they are thought to be related to an anomalous insertion of the common bile duct (CBD) into the pancreatic duct proximal to the ampulla, resulting in chronic reflux of pancreatic enzymes into the biliary tree. They are associated with other biliary anomalies, including a double CBD, double gallbladder, absent gallbladder, atresia of bile ducts, sclerosing cholangitis, congenital hepatic fibrosis, and annular pancreas.
- Complications include cholangitis, biliary cirrhosis, portal hypertension, calculi, and cyst rupture. They are associated with an increased risk of carcinoma of the bile duct.

## Radiologic

- The diagnosis can be made with CT and ultrasound, if direct communication between the cyst and the biliary tree can be shown. Appearances depend on the extent of involvement and degree of dilatation. Scans may show mild dilatation of the extrahepatic biliary tree, or a large water attenuation mass in the porta hepatis.
- Cholangiography, either via endoscopic retrograde cholangiopancreatography (ERCP) or magnetic resonance cholangiopancreatography (MRCP), may be necessary to demonstrate communication with the biliary tree. Percutaneous transhepatic cholangiography (PTC) allows detailed imaging of the intrahepatic ductal anatomy in addition to imaging the cyst. ERCP provides detailed information about the distal portion of the CBD and about the often anomalous junction with the pancreatic duct. MRCP can also provide detailed information about the biliary tree in a noninvasive fashion and without intravenous contrast material. The use of gadolinium-based contrast agents that are excreted by the hepatocytes into the bile ducts, namely gadobenate

dimeglumine (Multihance) and gadoxetate disodium (Eovist), can also demonstrate communication with the biliary tree.

- $Tc^{99m}$-hepatobiliary scanning shows late filling of the cyst with delayed clearance, and effectively excludes all other possibilities from the differential diagnosis.
- Choledochal Cyst Type I: the most common type (89% to 90%), characterized by cystic or fusiform dilatation of the CBD
- Choledochal Cyst Type II (2%): diverticulum from the CBD
- Choledochal Cyst Type III (1% to 5%): choledochocele; characterized by dilatation of the intraduodenal portion of the CBD
- Choledochal Cyst Type IV: multiple cysts of the extrahe-patic and intrahepatic bile ducts
- Choledochal Cyst Type V: Caroli's disease; multiple intrahepatic duct cysts

## SUGGESTED READING


Brancatelli G, Federle MP, Vilgrain V, et al. Fibropolycystic liver disease: CT and MR imaging findings. Radiographics 2005;25:659–670.

Crittenden SL, McKinley MJ. Choledochal cyst: clinical features and classification. Am J Gastroenterol 1985;80:643–647.

Mortele KJ, Rocha TC, Streeter JL, Taylor AJ. Multimodality imaging of pancreatic and biliary congenital anomalies. Radiographics 2006;26:715–731.

Savedar SJ, Benenati JF, Venbrux AC, et al. Choledochal cysts: classification and cholangiographic appearance. AJR Am J Roentgenol 1991;156:327–331.

Todani T, Watanabe Y, Narusue M. Congenital bile duct cyst. Am J Surg 1977;134:263–269.


# CASE 18


**VINCENT H.S.**
**LOW**


### HISTORY

A 65-year-old man with jaundice and anorexia.

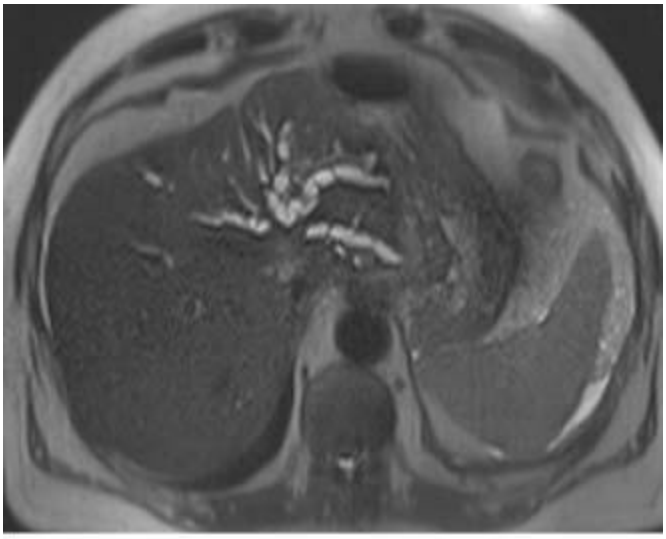

A

■**FIGURE 3-18A** Axial T2-weighted HASTE MR image demonstrates moderately severe intrahepatic biliary ductal dilatation involving the left and to a lesser extent the right intrahepatic ducts. The ductal obstruction appears to be at the level of the biliary hilum where there is a small, subtle hyperintense mass. Furthermore, there is mild atrophy of the left hepatic lobe.

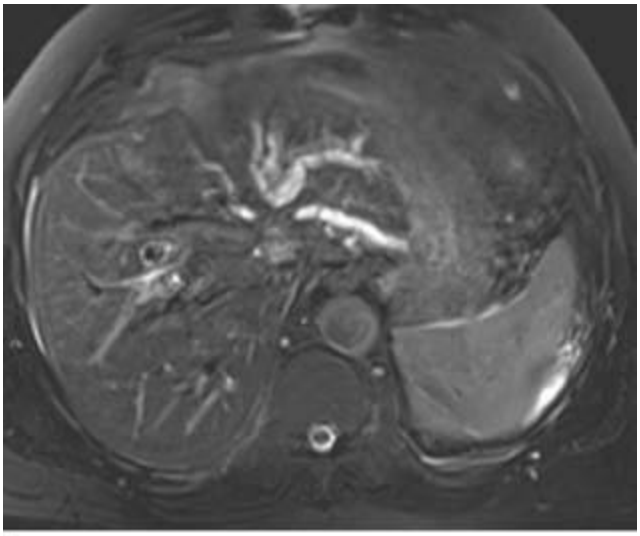

B

■**FIGURE 3-18B** Axial T2-weighted and fat-suppressed MR image further delineates the small, hyperintense mass at the confluence of the right and left intrahepatic bile ducts.

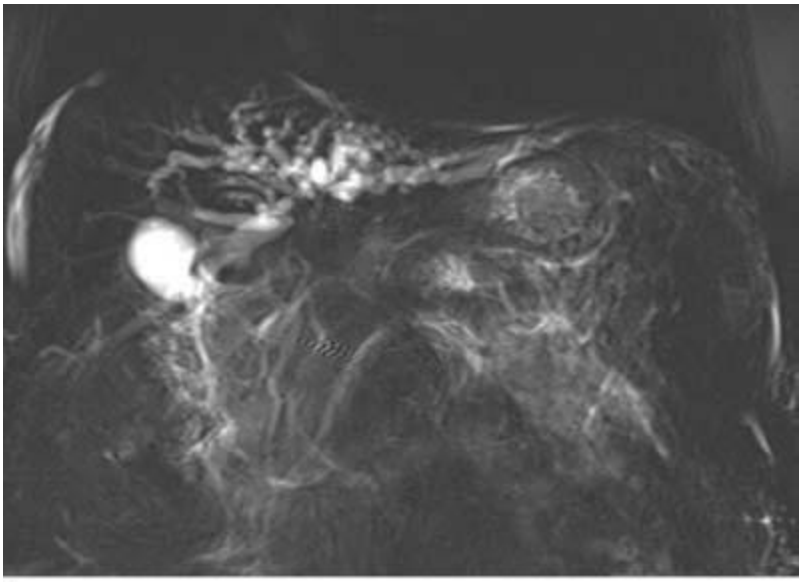

C

**FIGURE 3-18C** Coronal T2-weighted thick slab projection MRCP image again shows the moderately severe intrahepatic biliary ductal dilatation predominantly involving the left hepatic lobe and to a lesser extent the right hepatic lobe. The obstruction is at the level of the biliary hilum. The distal common bile duct is faintly visualized but is not dilated.

## DIFFERENTIAL DIAGNOSIS

- **Cholangiocarcinoma:** Hilar type (Klatskin tumor). This is the most likely diagnosis to explain all the signs and symptoms observed in this case.
- **Primary sclerosing cholangitis (PSC):** PSC can result in tight biliary strictures that will extend over a long segment. However, the absence of ectasia or stricturing elsewhere in the biliary tree makes this diagnosis less likely.
- **Hepatic or hilar tumor:** Bile ducts may be compressed by adjacent primary hepatic tumors or by metastases to either hilar lymph nodes or to the liver itself. The absence of multiple masses in the liver and of hilar lymphadenopathy on the MR scan makes this diagnosis less likely.
- **Traumatic biliary stricture:** A relevant history of biliary trauma, including violent injury, iatrogenic (surgical) misadventure, or a deliberate biliary diversion procedure would be required to consider this possibility.

## DIAGNOSIS

**Hilar cholangiocarcinoma (Klatskin tumor)**

## KEY FACTS

## Clinical

- Clinical presentations include jaundice, anorexia, weight loss, vague abdominal discomfort, and abnormal liver function tests.
- Risk factors include sclerosing cholangitis, choledochal cysts, congenital hepatic fibrosis, *Clonorchis sinensis* infection, and thorotrast exposure.
- Most cholangiocarcinomas are found at the hepatic duct confluence, as in this case. Distal extrahepatic and intrahepatic types are less commonly seen.
- Morphologically, the hilar type is usually a scirrhous infiltrating tumor causing a stricture. The intrahepatic type appears as a nonspecific, ill-defined mass lesion with contrast enhancement and areas of necrosis. The distal extrahepatic type is usually small and appears as a short stricture or a small polypoid mass.

## Radiologic

- The hilar type of cholangiocarcinoma is usually scirrhous in nature. The resulting tumor is infiltrative and usually poorly defined. There is associated marked biliary dilatation above the obstruction and, eventually, hepatic atrophy of the segments involved.
- Ultrasonography is most useful to identify dilated ducts, as well as segmental or lobar atrophy seen as crowded dilated bile ducts. The tumor mass is normally not seen, but if it is, it usually appears echogenic.
- CT is most sensitive in detecting the offending mass, which will appear less dense than the normal liver on precontrast scans. Following intravenous contrast material administration, a variable enhancement pattern is seen. About a third of tumors demonstrate delayed washout of contrast material (hyperenhance-ment) several minutes after the injection, a finding associated with desmoplasia. CT is very sensitive to the detection of associated lobar atrophy.
- MRI with MRCP is useful for depicting the mass, whether intrahepatic, hilar or, as well as the degree and pattern of bile duct dilatation, if any. The tumors tend be slightly hypointense on T1-weighted images precontrast and slightly hyperintense on T2-weighted images. Lobar atrophy may be apparent. Postcon-trast, cholangiocarcinomas are hypoenhancing during the hepatic arterial and portal venous phases and may demonstrate delayed washout during the equilibrium phase.
- Imaging is used to assess extension of tumor, most commonly to the liver parenchyma and the hepatoduodenal ligament. Lymphadenopathy may be recognized; but is often underestimated due to the presence of tumor extension to normal-sized nodes. Vascular invasion is relatively unusual.
- Cholangiography is required to evaluate the extent of the tumor. The severity of the obstruction often requires opacification of ducts both from above and below, and

requires correlation with cross-sectional imaging to ensure that all obstructed segments are opacified.

## SUGGESTED READING

Asayama Y, Tajima T, Okamoto D, et al. Imaging of cholangiolocellular carcinoma of the liver. Eur J Radiol 2010;75:e120–e125.

Klatskin G. Adenocarcinoma of the hepatic ducts at its bifurcation within the porta hepatis. Am J Med 1965;38:241–246.

Masselli G, Gualdi G. Hilar cholangiocarcinoma: MRI/MRCP in staging and treatment planning. Abdom Imaging 2008;33:444–451.

Motosugi U, Ichikawa T, Nakajima H, et al. Cholangiolocellular carcinoma of the liver: imaging findings. J Comput Assist Tomogr 2009;33:682–688.

Ward EM, Stephens DH. Neoplasms of the gall bladder and biliary tract. In RM Gore, MS Levine, I Laufer (eds), Textbook of Gastrointestinal Radiology. Philadelphia, PA: Saunders, 1994;1718–1723.

# CASE 19

**MARY T. KEOGAN**

## HISTORY

A 67-year-old woman presents with abdominal pain and weight loss.

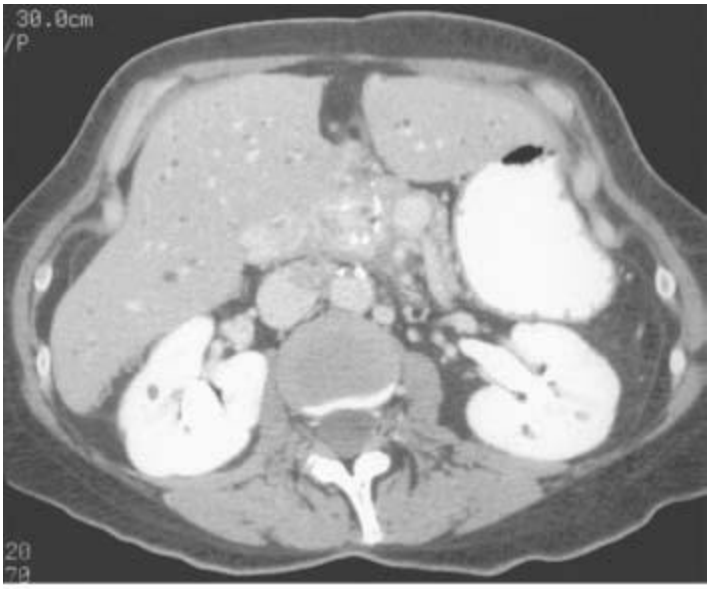


A

■**FIGURE 3-19A** Dynamic contrast-enhanced CT of the upper abdomen. There is a mass with scattered calcifications in the head of the pancreas and mild intrahepatic

ductal dilatation.

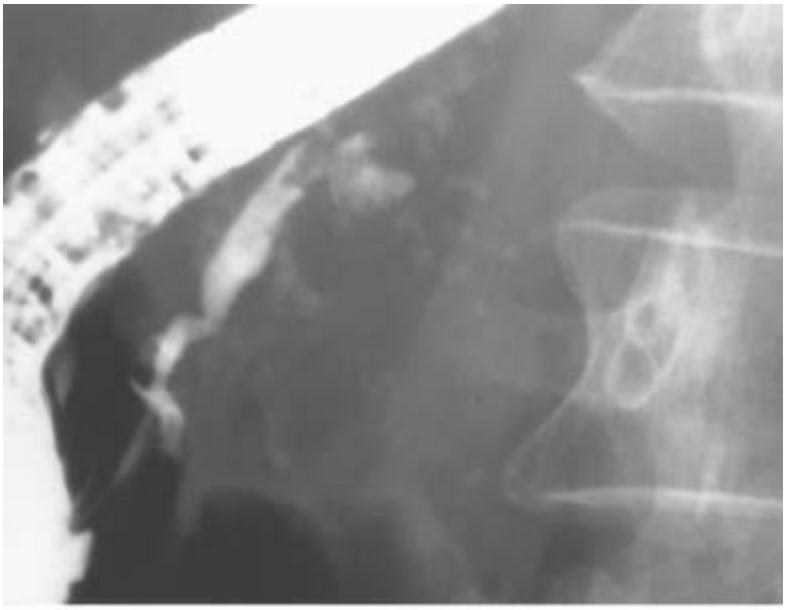

B

**FIGURE 3-19B** Endoscopic retrograde cholangiopancreatography showing a pancreatogram. Calcifications are noted in the region of the pancreatic head. The pancreatogram shows irregularity and intraluminal filling defects in the main pancreatic duct.

## DIFFERENTIAL DIAGNOSIS

- **Pancreatic carcinoma:** This diagnosis is unlikely in view of the calcifications, which are rarely seen in pancreatic adenocarcinoma.
- **Cystic pancreatic neoplasm:** A microcystic adenoma of the pancreas may contain calcification, but small cysts, typically <2 cm in diameter, would also be visible.
- **Pancreatic islet cell tumor:** These tumors may calcify but typically show marked enhancement postcontrast due to hypervascularity.
- **Chronic pancreatitis:** Pancreatitis often manifests as diffuse glandular enlargement, although it may present as a focal mass. Parenchymal and/or intraductal calcifications may or may not be present.

## DIAGNOSIS

**Chronic calcific pancreatitis**

## KEY FACTS

## Clinical

- Symptoms at presentation are usually nonspecific, although patients may have either weight loss, upper abdominal pain, or both.
- A history of long-term alcohol abuse is often present.
- Most patients have had a prior episode of acute pancreatitis; with each episode, there is progressive pancreatic parenchymal destruction.

## Radiologic

- ERCP is the most sensitive test for early disease, as duct strictures, side branch enlargement, and intraluminal filling defects may be seen before CT and ultrasound changes occur.
- Intraluminal filling defects in the pancreatic ducts on ERCP usually represent mucin collections, which may be detected before they calcify and thus before they are apparent on CT.
- Either CT or ultrasound may show a heterogenous gland due to the presence of fat and fibrosis. Encapsulated fluid collections or pseudocysts may also be present. The gland size is variable and may be involved either diffusely or focally. The gland may be normal in size, small (atrophy of the gland), or large (recent exacerbation of pancreatitis).
- CT may also show a focal mass with or without dilatation of the pancreatic and/or bile ducts.
- Calcifications are present in only 50% of cases; therefore, a noncalcified mass can still represent chronic pancreatitis.

## SUGGESTED READING

Balci NC, Smith A, Momtahen AJ, et al. MRI and S-MRCP findings in patients with suspected chronic pancreatitis: correlation with endo-scopic pancreatic function testing (ePFT). J Magn Reson Imaging 2010;31:601–606.

Ferrucci JT, Wittenberg J, Mack EB, et al. Computed body tomography in chronic pancreatitis. Radiology 1979;130:175–182.

Luetmer PH, Stephens DH, Ward EM. Chronic pancreatitis: reassessment with current CT. Radiology 1989;171:353–357.

Yamada Y, Mori H, Matsumoto S, et al. Pancreatic adenocarcinoma versus chronic pancreatitis: differentiation with triple-phase helical CT. Abdom Imaging 2010 35:163–171.

# CASE 20

**DANIELE MARIN**

**HISTORY**

A 12-year old girl presents with a 1-week history of abdominal pain and nausea.

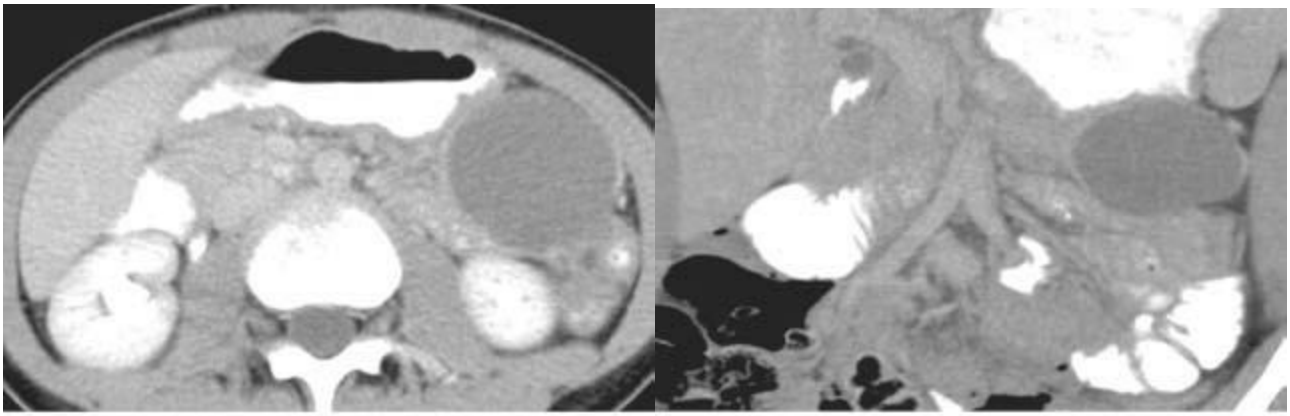

A B

**FIGURES 3-20A and 3-20B** Axial **(A)** and coronal **(B)** contrast-enhanced CT images demonstrate a large, well-defined, cystic mass (mean attenuation, +6 Hounsfield units) in the pancreatic tail. The mass demonstrates expansile growth and is surrounded by a relatively thick wall.

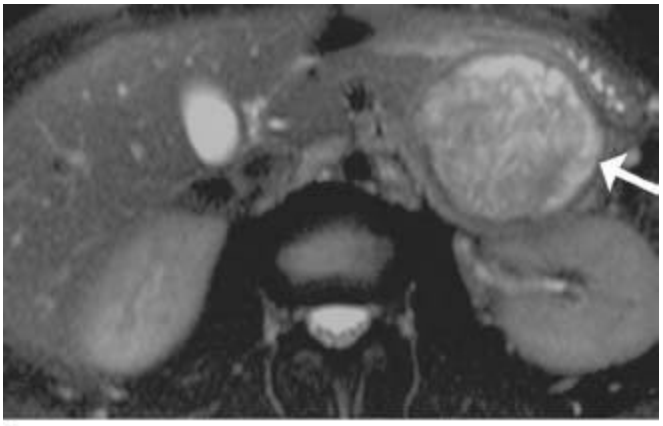

C

■**FIGURE 3-20C** Axial T2-weighted MR image shows the mixed solid and cystic components of the lesion.

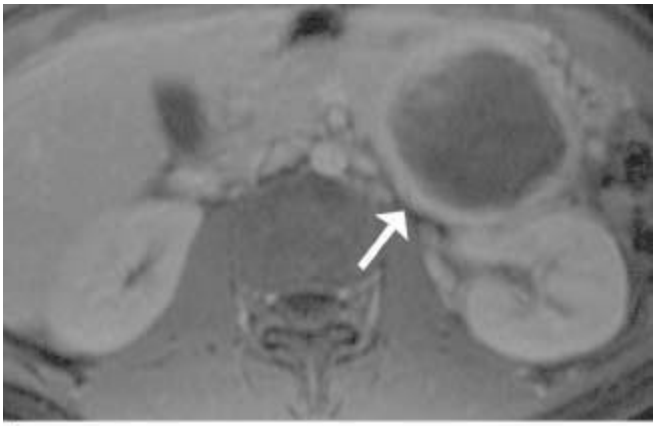

D

**FIGURE 3-20D** Axial Tl-weighted MR image postgadolini-um demonstrates the thick wall of the cyst ***(arrow)*** and nonenhance-ment of the cyst contents.

## DIFFERENTIAL DIAGNOSIS

**Pancreatic pseudocyst:** Pseudocysts are the most common cystic lesion of the pancreas (85% to 90% of all cystic lesions). A pseudocyst manifests as a round or oval fluid collection surrounded by a thin, faintly perceptible, fibrous wall showing subtle enhancement after contrast material administration. A history of acute or chronic pancreatitis, pancreatic trauma, or pancreatic surgery is pivotal for a diagnosis.

**Serous cystadenoma:** Serous cystadenoma occur in older patients and generally manifest as a round, well-defined, cystic lesion in the pancreatic head or uncinate process. Most serous cystadenomas have a honeycomb appearance due to numerous cysts varying in size from 0.2 to 2.0 cm. A characteristic central stellate scar with calcification may sometimes be observed.

**Mucinous cystic neoplasm:** Although mucinous cystic neoplasms may have a nonspecific appearance, manifesting as a thin- or thick-walled unilocular or multi-locular cystic lesion of the pancreas, subtle imaging findings may sometimes provide a clue to the diagnosis, including the evidence of solid papillary excrescences protruding from the cystic wall into the lumen or peripheral calcification in 10% to 25%.

**Solid Pseudopapillary Epithelial Neoplasm (SPEN):** A SPEN manifests as a large, well-defined, cystic mass surrounded by a thick enhancing capsule. Although larger lesions demonstrate expansile growth and may exert a compressive effect on adjacent organs as well as the main pancreatic duct, communication of the lesion with the pancreatic ductal system is never observed.

## DIAGNOSIS

**Solid Pseudopapillary Epithelial Neoplasm (SPEN)**

## KEY FACTS

### Clinical

- SPEN account for 1% to 2% of all pancreatic cystic neoplasms.
- SPEN is typically found in young women with a predilection for Asian and black patients.
- Most patients present with nonspecific signs and symptoms including nausea, vomiting, and abdominal pain or fullness.
- SPEN generally manifests as a large, well-circumscribed, slow-growing mass.
- At the cut surface, SPEN demonstrates a heterogeneous appearance, including areas of cystic degeneration, hemorrhage, or solid texture. Most tumors are surrounded by well-defined thick fibrous capsule. In a small percentage of cases (-15%), SPEN may undergo malignant degeneration. For this reason, this tumor is currently regarded as a low-grade malignant epithelial neoplasm with low metastatic rate and high overall survival.
- Surgical excision is commonly recommended to rule out or prevent malignant degeneration.

### Radiologic

- SPEN demonstrates variable echotexture at US, including anechoic areas consistent with cystic degeneration and hypo-, iso-, and hyperechoic areas corresponding to a solid component or lesion hemorrhage.
- At contrast-enhanced CT, SPEN manifests as a complex lesion with a mixed solid and cystic internal texture and a thick, well-defined, enhancing capsule.
- On T2-weighted MR images, SPEN demonstrates a signal intensity comparable to that of other cystic structure (e.g., gallbladder) due to the predominantly cystic nature of the tumor. Internal areas of signal void may be occasionally seen and are consistent with areas of hemorrhage or calcifications.
- Regions of high signal intensity on T1-weighted images correspond to areas of necrosis or hemorrhage within the tumor.

## SUGGESTED READING

Lee JH, Yu JS, Kim H, et al. Solid pseudopapillary carcinoma of the pancreas: differentiation from benign solid pseudopapillary tumour using CT and MRI. Clin Radiol 2008;63:1006–1014.

Sidden CR, Mortele KJ. Cystic tumors of the pancreas: ultrasound, computed tomography, and magnetic resonance imaging features. Semin Ultrasound CT MR 2007;28:339–356.

Yang F, Jin C, Long J, et al. Solid pseudopapillary tumor of the pancreas: a case series of 26 consecutive patients. Am J Surg 2009;198:210–215.

# CASE 21

**MARY T. KEOGAN**

## HISTORY

A 61-year-old woman has weight loss and a history of peptic ulcer disease.


A

■**FIGURE 3-21A** Ultrasound of the upper abdomen in the transverse plane. A hypoechoic mass is seen in the body of the pancreas anterior to the portal venous confluence.


**FIGURE 3-21B** Contrast-enhanced CT of the upper abdomen during the pancreatic parenchymal phase. There is a hyperenhancing mass in the pancreatic body. There is atrophy of the pancreatic tail and dilatation of the main pancreatic duct.

## DIFFERENTIAL DIAGNOSIS

- **Pancreatic islet cell tumor, nonfunctioning:** These tumors do not secrete hormones and are clinically silent. Hence, they are often of larger size at presentation than functioning tumors. They may calcify.
- **Pancreatic islet cell tumor, functioning:** Gastrinoma is a likely diagnosis in view of the history of peptic ulcer disease. Insulinomas are the most common functioning tumor but are usually small and not associated with peptic ulcers. Calcifications are rare in functioning tumors.
- **Pancreatic hypervascular metastasis (e.g., renal):** This diagnosis is unlikely since pancreatic metastases are usually not isolated and there is no history of a renal cell carcinoma.

## DIAGNOSIS

**Gastrinoma**

## KEY FACTS

**Clinical**

- These tumors present early with symptoms of gastric hypersecretion, the so called Zollinger-Ellison Syndrome (ZES).
- Peptic ulcers are often resistant to medical management and present in atypical locations—for example, the postbulbar region. The most common location continues to be the duodenal bulb.
- They are associated with multiple endocrine neoplasm (MEN) syndrome, type 1, which consists of tumors of the parathyroid glands, pancreatic islet cells, and the pituitary gland.

### Radiologic

- Islet cell tumors are very vascular and, when large enough, are seen on CT as an enhancing pancreatic mass.
- Up to 50% of gastrinomas have metastasized to the liver at the time of presentation (typically hyperenhanc-ing metastases); hence, CT is important for staging. By comparison, only 10% of insulinomas will have metas-tases at the time of presentation.
- Barium studies often show associated peptic ulcers, which may be multiple and/or postbulbar.
- Gastrinomas causing ZES usually originate in the head of the pancreas or the duodenum.

## SUGGESTED READING

Chung EM, Travis MD, Conran RM. Pancreatic tumors in children: radiologic-pathologic correlation. Radiographics 2006;26:1211–1238.

Frucht H, Doppman JL, Norton JA, et al. Gastrinomas: comparison of MR imaging with CT, angiography and ultrasound. Radiology 1989;171:713–717.

Pfannenberg AC, Burkart C, Krober SM, et al. Dual-phase multidetector thin-section CT in detecting duodenal gastrinoma. Abdom Imaging 2005;30:543–547.

Semelka RC, Ascher SM. MR Imaging of the pancreas. Radiology 1993;188:593–602.

Wank SA, Doppman JL, Miller DL, et al. Prospective study of the ability of computed axial tomography to localize gastrinomas in patients with Zollinger-Ellison syndrome. Gastroenterology 1987;92:905–912.

# CASE 22

**MARY T. KEOGAN**

### HISTORY

A 55-year-old woman presents with progressive back pain and rapid weight loss.

A B

**FIGURES 3-22A and 3-22B** Contrast-enhanced CT of the pancreas during the pancreatic phase **(A)** and venous phase **(B).** There is a low-attenuation mass in the head of the pancreas with dilatation of the pancreatic duct and associated atrophy of the gland. Note the absence of pancreatic calcifications.

C

■**FIGURE 3-22C** Volume-rendered projection image from the pancreatic phase CT dataset reveals conventional arterial anatomy. There is no obvious narrowing or irregularity of the peripancreatic arteries to suggest tumor encasement. (See color insert)

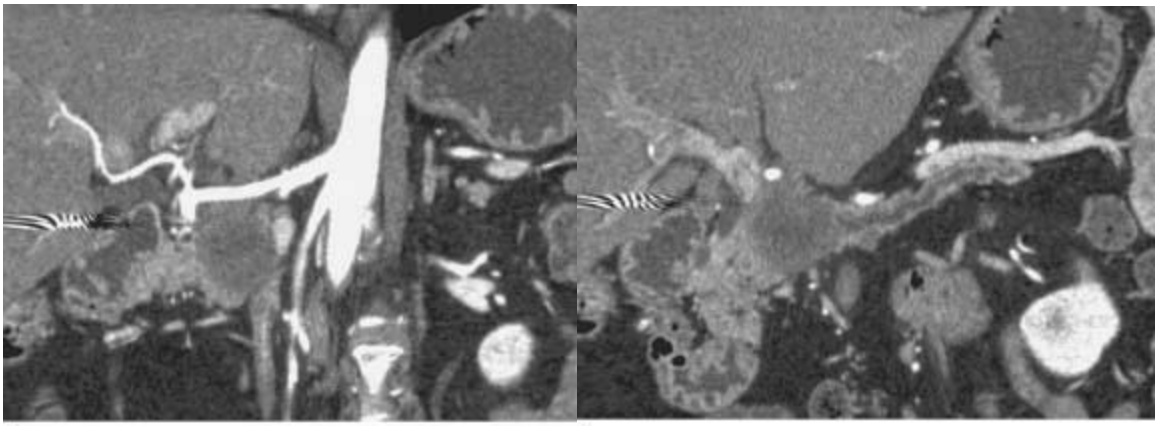


**FIGURES 3-22D and 3-22E** Curved planar reformations through the common hepatic artery **(D)** and the main pancreatic duct **(E).** The hypoenhancing tumor in the pancreatic head in Figure 3-22D is noted to abut the caudal aspect of the common hepatic artery. Since this degree of tumor encasement involves <50% or <180 degrees of the lumen, the patient is considered to be resectable for palliation. Note the abrupt cutoff of the dilated main pancreatic duct by the tumor in the head and the parenchymal atrophy of the tail in Figure 3-22E.

## DIFFERENTIAL DIAGNOSIS

**Pancreatic adenocarcinoma:** This patient has the classic appearance of a pancreatic adenocarcinoma: a hypoenhancing mass in the pancreatic head associated with obstruction of the pancreatic duct and atrophy of the body and tail of the pancreas.

**Chronic pancreatitis:** There may be a focal mass in patients with chronic pancreatitis that is indistinguishable from pancreatic carcinoma, particularly in the absence of calcifications. Only 50% of patients with chronic pancreatitis demonstrate calcifications (referred to as chronic calcific pancreatitis). A biopsy is often required to make this distinction, typically via endoscopic ultrasound.

**Pancreatic lymphoma:** Lymphoma rarely arises in the pancreas. Involvement of peripancreatic lymph nodes is more typical. Associated abdominal lymphadenopa-thy would also be expected.

**Pancreatic metastases:** Malignancy of the lung, breast, kidneys, or gastrointestinal tract may spread hematog-enously to the pancreas. This diagnosis should be considered if there is a history of a primary malignancy.

## DIAGNOSIS

**Pancreatic adenocarcinoma**

# KEY FACTS

## Clinical

- Pancreatic carcinoma presents late in the course of the disease, usually with liver and nodal metastases. Less than 30% are resectable for either cure or palliation at initial presentation.
- Pancreatic carcinoma is more common in males and African Americans.
- There is an association between pancreatic carcinoma and smoking as well as familial pancreatitis. There is no association, however, with alcohol use.

## Radiologic

- Typically, a focal mass is present, 75% to 90% of which are located in the pancreatic head. The tumors, located in the pancreatic body and tail, tend to be larger at presentation and may have invaded adjacent structures. On contrast-enhanced CT, 85% to 90% of the tumors are hypoenhanc-ing, although they may be isoenhancing in 10% to 15%. In this case, indirect signs of a mass include focal enlargement of the gland, a contour abnormality, or a dilated pancreatic and/or common bile duct with an abrupt cut-off.
- The pancreatic duct may be dilated and the pancreatic parenchyma atrophic.
- Local tumor extension is present in 90% of patients—that is, either into the duodenum, the celiac/axis or porta hepatis lymph nodes, or both. Vascular encasement (hepatic artery, splenic artery, and/or superior mesenteric artery) indicates an incurable tumor. Arteries that have <50% or 180 degrees encasement may be resectable for palliation.
- CT is 95% accurate in determining unresectability, but it is only 50% accurate in determining resectability as small liver metastases and peritoneal implants may not be detected.

# SUGGESTED READING


Delbeke D, Martin WH. PET and PET/CT for pancreatic malignancies. Surg Oncol Clin N Am 2010;19:235–254.

DelMaschio A, Vanzulli A, Sironi S, et al. Pancreatic cancer versus chronic pancreatitis: diagnosis with CA 19-9 assessment, US, CT, and CT-guided fine-needle biopsy. Radiology 1991;178:95–99.

Deshmukh SD, Willmann JK, Jeffrey RB. Pathways of extrapancreatic perineural invasion by pancreatic adenocarcinoma: evaluation with 3D volume-rendered MDCT imaging. AJR Am J Roentgenol 2010;194: 668–674.

Ozkan E, Balachandran A, Bhosale PR, et al. Pictorial essay: multimodality imaging of metastases from pancreatic ductal adenocarcinoma. Clin Imaging 2010;34:277–287.

Perez-Johnston R, Lenhart DK, Sahani DV. CT angiography of the hepatic and pancreatic circulation. Radiol Clin North Am 2010;48:311–330, viii.

Zeiss J, Coombs RJ, Bielke D. CT presentation and staging accuracy of pancreatic adenocarcinoma. J Pancreatol 1990;7:49–53.

# CASE 23

**VINCENT H.S. LOW**

## HISTORY

A 30-year-old man with a history of endocarditis presents with a fever and abdominal pain.

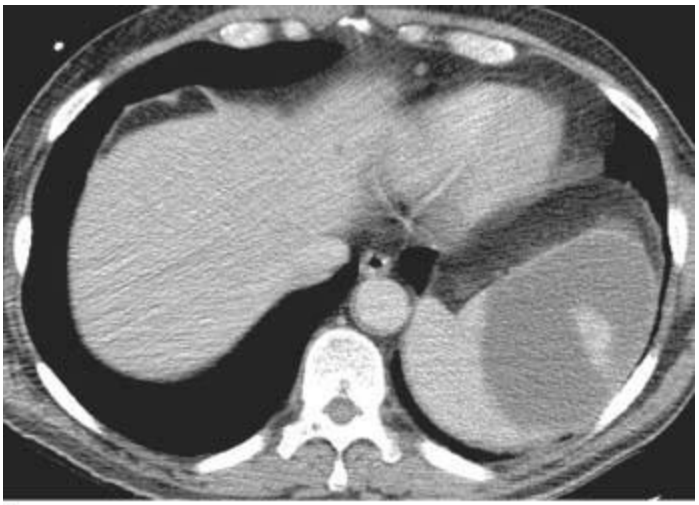

A

■**FIGURE 3-23A** Contrast-enhanced CT of the upper abdomen. The spleen is enlarged, and there is a large, well-defined area of hypoenhancement in the lateral aspect.

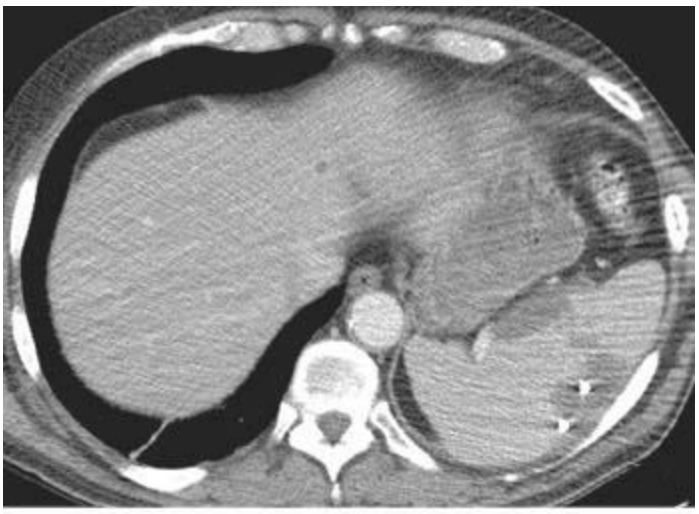

B

■**FIGURE 3-23B** Contrast-enhanced CT of the upper abdomen 2 weeks later. A pigtail catheter was placed into the abscess percutaneously using CT guidance and an

intercostal approach. Approximately 350 mL of purulent fluid was aspirated. Follow-up CT reveals the tip of the catheter and a significant reduction in the size of the abscess. Note the small residual fluid collection in the splenic hilum.

## DIFFERENTIAL DIAGNOSIS

- **Pyogenic abscess:** In the immunocompetent patient, an abscess is usually due to aerobic organisms, including *Salmonella,* which develop in the setting of underlying splenic damage.
- **Opportunistic infection:** In the immunocompromised patient, unusual organisms including fungi, *Mycobacte-rium tuberculosis, Mycobacterium avium-intracellulare* (MAI), and *Pneumocystis carinii* may infect the liver and spleen. The lesions usually appear as multiple microabscesses.
- **Lymphoma:** Diffuse histiocytic or immunoblastic types of lymphoma are seen occasionally as ill-defined, low-attenuation splenic masses on CT.
- **Hematoma:** This should be considered in the context of trauma or a coagulopathy, either due to an underlying disease state or as a result of therapy.
- **Metastases:** Apart from malignant melanoma, macroscopic metastases to the spleen are very unusual. In the immunocompromised patient, disseminated Kaposi's sarcoma may occur, although there is usually evidence of disseminated disease elsewhere.
- **Cysts:** The majority of cysts in the liver (70% to 85%) are posttraumatic (i.e. old hemorrhagic cysts). Simple cysts (with an endothelial lining) are relatively uncommon and appear as round, well-defined, water attenuation lesions. They may, however, be complicated by infection or hemorrhage giving them an atypical appearance. In the setting of pancreatitis, pseudocysts may on occasion dissect into the spleen via the hilum. Hydatid cysts *(Echinococcus* infection) should be considered in patients exposed to areas where this condition is endemic.

## DIAGNOSIS

**Splenic abscess**

## KEY FACTS

### Clinical

- Splenic abscesses are uncommon, but their frequency has grown because of an increasing number of immu-nocompromised patients. Specific diseases at risk for splenic abscess include sickle cell anemia, childhood granulomatous disease, and diabetes mellitus.

- The spleen may be infected by several routes, including hematogenous infection (e.g., bacterial endocarditis), contiguous infection (e.g., infected pancreatitis), infection of splenic infarcts or trauma, and immunodeficiency states. One-fifth of splenic abscesses have no apparent underlying source.
- The mortality rate for splenic abscess has historically been very high—up to 70%—but with earlier diagnosis by imaging, improved antibiotic therapy, image-guided diagnostic aspiration for identification of organisms, and/or percutaneous catheter drainage, the mortality has been reduced to <10%.
- Over half of splenic abscesses are infected by aerobic organisms, especially gram-positive cocci. Fungi are found in about one-fourth of splenic abscesses.
- The classic clinical picture of a splenic abscess consists of fever, chills, left-upper quadrant pain and tenderness, and splenomegaly. However, the majority of patients do not present with this classic picture early in the disease process, and signs localizing to the left-upper quadrant are often absent.
- Complications of an abscess, such as rupture, sub-phrenic abscess, and peritonitis, will occur if the diagnosis is delayed, and these are associated with a high mortality rate.

## Radiologic

- CT is the optimum diagnostic modality for the diagnosis of splenic infection, with a reported sensitivity of up to 96%. Not only will this technique localize a splenic abscess but it will also provide anatomic and diagnostic information about the perisplenic area, be useful for showing evidence of adjacent disease, and will help plan for surgical or radiologic intervention.
- A bacterial abscess appears as a low-attenuation mass lesion with an ill-defined, thick, and irregular rim. There may be slight peripheral enhancement. Occasionally, the abscess contains gas. There may be internal septa and/or fluid-debris levels.
- Fungal infections essentially occur only in immuno-compromised patients. The lesions are usually small, typically <2 cm in diameter and may be <5 mm. The very small lesions may be difficult to detect on imaging. When seen on CT, they appear as nonenhancing, low-attenuation lesions. Occasionally, they may demonstrate a“bull’s-eye”appearance on ultrasound or CT. TB commonly involves the spleen in a miliary form. However, the lesions are usually small, <60;1 cm in size, and difficult to visualize on imaging. The macronodular form of the disease (tuberculoma) is a rare manifestation, appearing as large, single or multiple, ill-defined low-attenuation masses.
- In the patient with AIDS, the spleen may be infected by *M. avium-intracellulare* or *P. carinii* organisms. The individual infected foci are usually tiny, resulting only in splenomegaly on imaging. Over time, the lesions may calcify.

- Image-guided intervention is an ideal method of sampling these lesions for identification of the organism(s). Percutaneous abscess drainage is a reasonable option to surgical resection, and on occasion is completely curative.

## SUGGESTED READING

Elsayes KM, Narra VR, Mukundan G, et al. MR imaging of the spleen: Spectrum of abnormalities. Radiographics 2005;25:967–982.

Freeman JL, Jafri SZ, Roberts JL, et al. CT of congenital and acquired abnormalities of the spleen. Radiographics 1993;13:597–610.

Kamaya A, Weinstein S, Desser TS. Multiple lesions of the spleen: differential diagnosis of cystic and solid lesions. Semin Ultrasound CT MR 2006;27:389–403.

Kawashima A, Fishman EK. Benign splenic lesions. In RM Gore, ES Levine, I Laufer (eds), Textbook of Gastrointestinal Radiology. Philadelphia, PA: Saunders, 1994;2251–2258.

# CASE 24

**RENDON C.**
**NELSON**

## HISTORY

A 48-year-old man with fever and generalized abdominal pain.


A

**FIGURE 3-24A** Dynamic contrast-enhanced CT of the upper abdomen. There is an L-shaped hypoattenuating mass in the right portal vein.

B

**FIGURE 3-24B** Dynamic contrast-enhanced CT during the hepatic arterial phase obtained 6 weeks later. There is no significant enhancement in the region of the portal venous mass.

C

**FIGURE 3-24C** Dynamic contrast-enhanced CT during the portal venous phase obtained 6 weeks later. The previously noted hypoattenuating mass in the right portal vein has been replaced by a nest of collateral veins, so called cavernous transformation.

## DIFFERENTIAL DIAGNOSIS

**Hepatic metastasis:** Metastases can diminish in size or disappear after chemotherapy, although the shape of the mass favors a lesion in the right portal vein. Furthermore, malignant portal vein thrombosis is more commonly associated with hepatocellular carcinoma than with metastases.

**Hepatocellular carcinoma (HCC):** HCC is often associated with either portal vein or hepatic vein thrombosis. The thrombus may be bland or malignant. Furthermore,

malignant thrombosis can even occur with a tumor that is remote from a major vein. This diagnosis, however, is unlikely since the mass diminished on the 6-week follow-up examination.

- **Traumatic laceration of the liver:** Lacerations can have an unusual, somewhat angular shape, although they usually extend to the capsular surface of the liver and are associated with perihepatic or subcapsular hemorrhage.
- **Portal vein thrombosis (PVT) with cavernous transformation:** This is the most likely diagnosis since there is a mass in the lumen of the portal vein that is replaced by a nest of collateral veins within a relatively short period of time (several weeks).
- **Hepatic infarction:** Infarcts present as wedge-shaped, hypoattenuating parenchymal defects that originate from the central portion of the liver and extend to the capsular surface. In time, bubbles may develop, and later they become more rounded and cystic in nature.

## DIAGNOSIS

**PVT with cavernous transformation**

## KEY FACTS

### Clinical

- Pediatrics: Idiopathic PVT is the principal cause of portal hypertension. Patients present with variceal hemorrhage without elevation of liver enzymes. They often have splenomegaly, but ascites is uncommon. Other causes include neonatal septicemia, omphalitis, or umbilical vein catheterization.
- Adults: Causes of PVT include cirrhosis (due to either slow flow, intimal hyperplasia, or both), inflammatory and neoplastic pancreatic diseases, inflammatory processes involving the gastrointestinal tract (pyothrombo-phlebitis is rare), pregnancy, and oral contraceptives.
- PVT is characterized as being extrahepatic and/or intrahepatic. In extrahepatic PVT, peribiliary venous collaterals enlarge and reconstitute the intrahepatic portal branches if patent (cavernous transformation).

### Radiologic

- Portal venous thrombi that partially occlude the lumen may propagate proximally and/or distally, progress to complete occlusion, or diminish/resolve following anticoagulant therapy.
- Portal venous thrombi that totally occlude the lumen tend to be replaced by a nest of small collaterals, and this process occurs over a period weeks to months. The thrombus

itself tends to shrink in size and is often difficult to identify. Occasionally, the thrombus calcifies. Cavernous transformation is best demonstrated by a contrast-enhanced CT or MRI. Although ultrasound is helpful at times, particularly using color Doppler, it tends to underestimate collateral formation.

- PVT can be either bland or malignant in the presence of hepatic malignancy, especially hepatocellular carcinoma. Thrombosis can develop even if the tumor is remote to the portal vein. Malignant thrombosis is suspected when enhancement is demonstrated post-contrast, particularly when it occurs in the hepatic arterial phase. The presence of arterial signal within the thrombus on Doppler ultrasound is also diagnostic. At times, a percutaneous biopsy is required to make this differentiation.
- PVT often develops in patients with an inflammatory process along the venous system draining the abdominal viscera. Therefore, it is prudent to look also for the presence of enteritis, inflammatory bowel disease, diverticulitis, appendicitis, or an abscess.

## SUGGESTED READING


Burkart DJ, Johnson CD, Morton MJ, Ehman RL. Phase-contrast cine MR-angiography in chronic liver disease. Radiology 1993;187:407–412.

Dodd GD III, Carr BI. Percutaneous biopsy of portal vein thrombosis: new staging technique for hepatocellular carcinoma. AJR Am J Roentgenol 1993;161:229–233.

Marn CS, Francis IR. CT or portal venous occlusion. AJR Am J Roentgenol 1992;159:717–726.

Ponziani FR, Zocco MA, Campanale C, et al. Portal vein thrombosis: insight into physiopathology, diagnosis, and treatment. World J Gastroenterol 2010;16:143–155.

Pozniak MA, Baus KM. Hepatofugal arterial signal in the main portal vein: an indicator of intravascular tumor spread. Radiology 1991;180:663–666.

Zhang LJ, Yang GF, Jiang B, et al. Cavernous transformation of portal vein: 16-slice CT portography and correlation with surgical procedure of orthotopic liver transplantation. Abdom Imaging 2008;33:529–535.


# CASE 25


**RENDON C.**
**NELSON**


### HISTORY

A 42-year-old woman presents with vague abdominal pain.

A

■**FIGURE 3-25A** CT of the upper abdomen during the portal venous phase. There is a large is attenuating, faintly perceptible mass predominantly located in the left hepatic lobe. The large central scar is hypoattenuating.

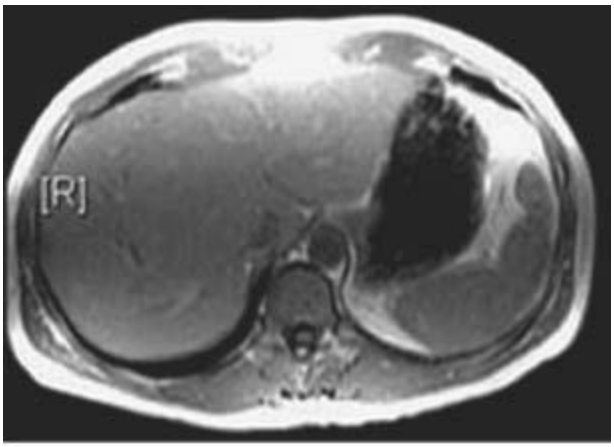


B

■**FIGURE 3-25B** T1-weighted MRI of the liver acquired when the water and fat protons are in-phase. The mass is isoin-tense to the surrounding hepatic parenchyma. The central scar is not well seen.

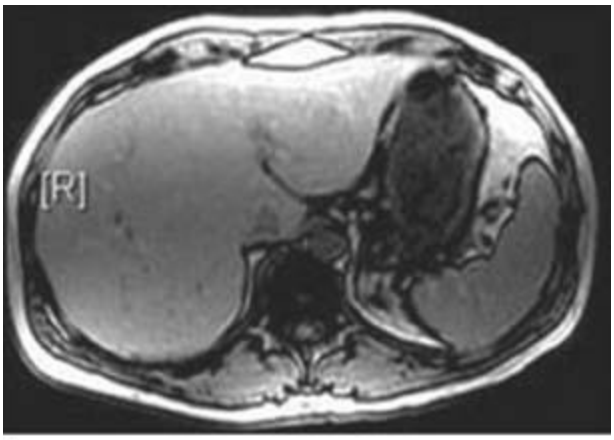


C

**FIGURE 3-25C** T1-weighted MRI of the liver acquired when the water and fat protons are out-of-phase. There is no change in the signal intensity pattern of the mass indicating that there is no internal fat.

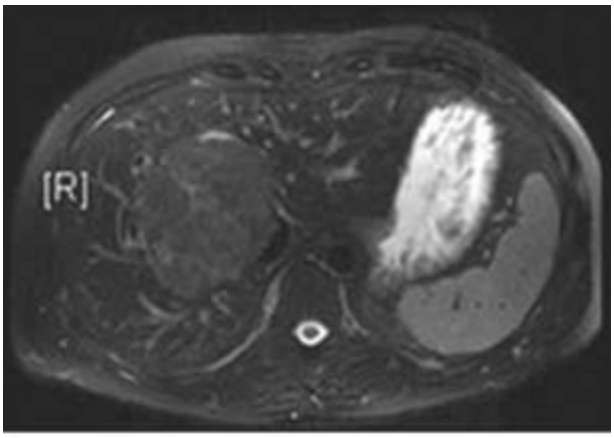


D

**FIGURE 3-25D** T2-weighted MRI of the liver. The mass demonstrates a subtle increase in signal intensity compared to the surrounding hepatic parenchyma. The central scar has a slightly higher signal intensity pattern.

## DIFFERENTIAL DIAGNOSIS

**Hepatocellular carcinoma (HCC):** Some well-differentiated hepatomas may have these attenuation, intensity and enhancement characteristics, but when as large as this particular lesion, they are usually heterogenous.

**Hepatocellular adenoma:** In the absence of internal hemorrhage, internal fat, or a capsule, these rare and benign tumors may have an identical appearance. A history of oral contraceptive use might suggest favoring an adenoma over focal nodular hyperplasia.

**Hypervascular metastasis:** Many of these metastatic deposits will be visualized only in the hepatic arterial phase, although when they are this large, they are usually hypoattenuating precontrast as well as hypoat-tenuating in the portal venous phase.

**Cavernous hemangioma:** This mass has *no* enhancement features of a hemangioma. The peripheral nodular or cotton-wool enhancement pattern characteristic for these benign lesions is not present.

**Focal nodular hyperplasia (FNH):** This is the most likely diagnosis since the mass has the classic precon-trast and postcontrast imaging features of FNH, particularly when the lesions are this large.

**Regenerating nodule:** These masses are predominantly supplied by the portal vein, similar to normal parenchyma, and do not enhance significantly in the hepatic arterial

phase.

■**FIGURE 3-25E** Contrast-enhanced T1-weighted MRI of the liver during the hepatic arterial phase. The mass demonstrates vivid homogenous enhancement with the exception of the central scar.

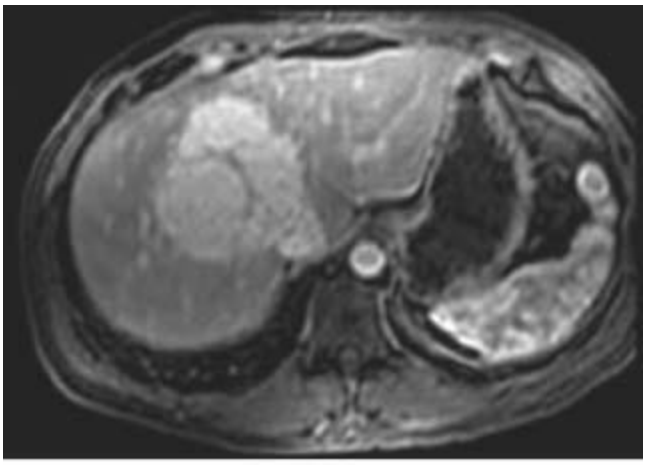

E

■**FIGURE 3-25F** Contrast-enhanced Tl-weighted MRI of the liver during the portal venous phase. The mass demonstrates persistent homogenous enhancement slightly higher than the surrounding hepatic parenchyma. Note that the central scar has filled in with contrast material.

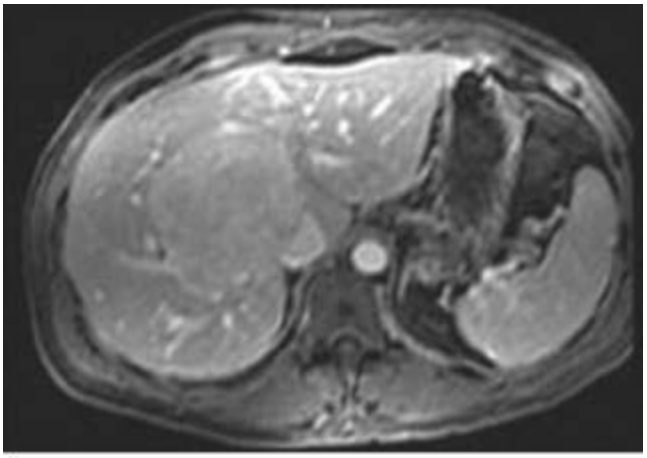

F

## DIAGNOSIS

**Focal nodular hyperplasia**

## KEY FACTS

### Clinical

- FHN is much more common in woman (85%); they typically present in the third to fifth

decade of life.

- They are usually asymptomatic and therefore detected incidentally. Only 10% are symptomatic, presenting with an abdominal mass or pain.
- FNH are *not* associated with oral contraceptives, although there is evidence that oral contraceptives increase the otherwise low propensity for intratumoral hemorrhage.
- The alpha-fetoprotein level is normal.
- FNH are benign tumors that do not degenerate into well-differentiated hepatocellular carcinomas.

## Radiologic

- Histologically, FNH are composed of hepatocytes, bile ducts, and Kuppfer cells to a variable degree (there is a much higher population of Kuppfer cells compared to adenomas), laid along fibrous strands that coalesce centrally to form a scar. These features determine the imaging findings.
- Although most FNH are solitary, 20% are multiple.
- Classically, they are isoattenuating precontrast, hyper-attenuating during the hepatic arterial phase, and iso-attenuating during the portal venous phase.
- A central hypoattenuating scar is present about 50% of the time, but this finding is not specific for FNH as it can also be seen in hepatic adenomas and hepato-cellular carcinomas, especially fibrolamellar types. On MRI, the scar tends to be of high signal intensity on T2-weighted images in FNH and of low signal intensity in HCC, although this signal intensity pattern is not reliable.

# SUGGESTED READING


Kim T, Hori M, Onishi H. Liver masses with central or eccentric scar. Semin Ultrasound CT MR 2009;30:418–425.

Klatskin G. Hepatic tumors: possible relationship to the use of oral contraceptives. Gastroenterology 1977;73:386–394.

Lee MJ, Saini S, Hamm B, et al. Focal nodular hyperplasia of the liver: MR findings in 35 proven cases. AJR Am J Roentgenol 1991;156:317–320.

Marin D, Brancatelli G, Federle MP, et al. Focal nodular hyperplasia: typical and atypical MRI findings with emphasis on the use of contrast media. Clin Radiol 2008;63:577–585.

Park CH, Kim SM, Intenzo CM, et al. Focal nodular hyperplasia of the liver: diagnosis by dynamic and SPECT scintigraphy. Clin Nucl Med 1993;18:701–703.

Procacci C, Fugazzola C, Cinquino M, et al. Contribution of CT to characterization of focal nodular hyperplasia of the liver. Gastrointest Radiol 1992;17:63–73.

Shamsi K, De Shepper A, Degryse H, et al. Focal nodular hyperplasia of the liver: radiologic findings. Abdom Imaging 1993;18:32–38.

van den Bos IC, Hussain SM, de Man RA, Zondervan PE, Ijzermans JN, Krestin GP. Primary hepatocellular lesions: imaging findings on state-of-the-art magnetic resonance imaging, with pathologic correlation. Curr Probl Diagn Radiol 2008;37:104–114.

# CASE 26

**PAUL V. SUHOCKI**

## HISTORY

A 62-year-old man has a long-standing history of postprandial abdominal bloating. Laboratory values include a normal bilirubin level and slight elevation of alkaline phosphatase, serum glutamic-oxaloacetic transaminase (SGOT), and serum glutamic-pyruvic transaminase (SGPT).

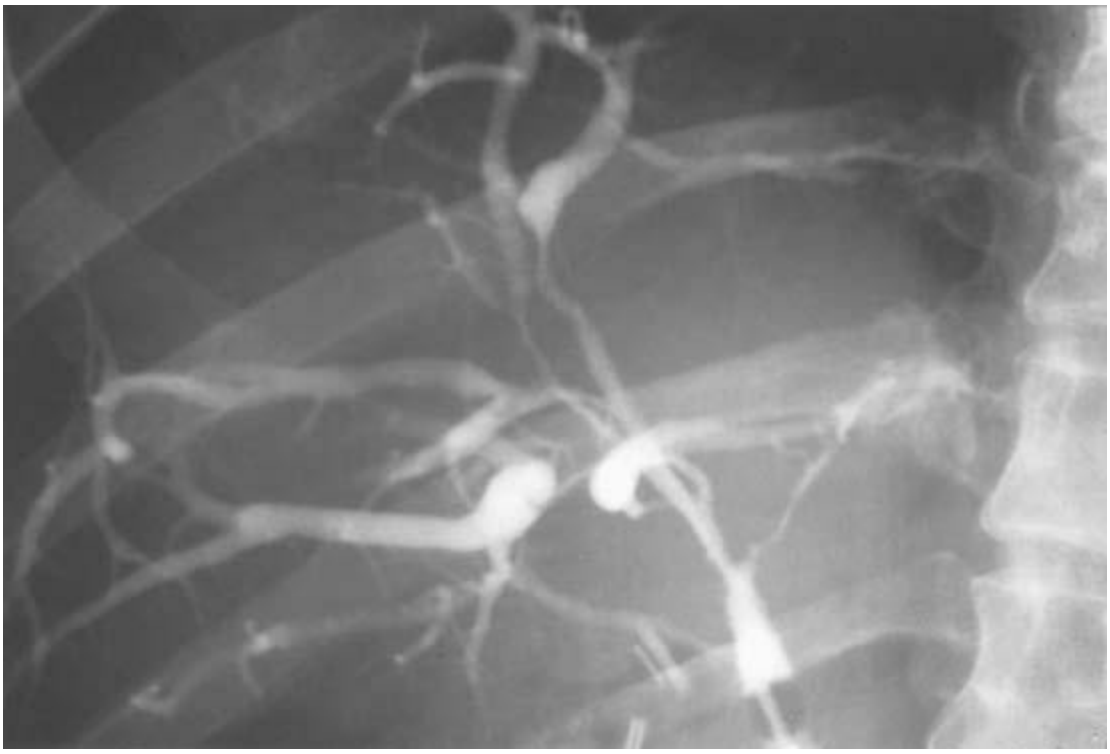

**FIGURE 3-26** Balloon occlusion cholangiogram of the intrahepatic ducts during endoscopic retrograde cholangio-gram. There are multiple sites of narrowing and dilatation, involving both the right and left intrahepatic bile ducts in a diffuse multifocal fashion. No intraluminal filling defects are appreciated.

## DIFFERENTIAL DIAGNOSIS

**Bile duct carcinoma:** Bile duct carcinomas typically have the appearance of a short biliary stricture and proximal biliary obstruction. In the case illustrated here, the

intrahepatic biliary system is diffusely involved. Bile duct carcinoma can rarely involve the majority of the biliary system in a diffuse fashion. It should be remembered that bile duct carcinoma can occur secondary to underlying primary sclerosing cholangitis, another cause of biliary duct narrowing.

- **Primary sclerosing cholangitis (PSC):** The appearance of multifocal strictures involving the biliary tree in a diffuse multifocal fashion is typical of PSC. This is the most likely diagnosis.
- **Secondary sclerosing cholangitis (SSC):** This process has a radiologic appearance that simulates that of PSC. The clinical history is important in distinguishing the two entities. Secondary sclerosing cholangitis is associated with a history of recurrent biliary infections from calculus disease, a surgical stricture, or a choledocho-enterostomy; all features that are absent in the case presented.

## DIAGNOSIS

**Primary sclerosing cholangitis**

## KEY FACTS

### Clinical

- PSC is a rare, chronic hepatobiliary disease of unknown cause. It is characterized by patchy, progressive fibrosis of either the intrahepatic bile ducts, the extrahepatic bile ducts, or both.
- PSC is seen primarily in males, with a male-to-female ratio of 3 to 1. It typically occurs in the third to fifth decades.
- PSC is associated with inflammatory bowel disease. Sixty percent of patients have ulcerative colitis. On the other hand, between 1% and 4% of patients with chronic ulcerative colitis develop PSC. Five percent of patients with PSC have Crohn's disease.
- The HLA-B8 antigen is present in 60% to 80% of patients with PSC.
- PSC seems to originate in the intrahepatic ducts and progresses to involve the extrahepatic ducts. Extrahe-patic ductal involvement eventually occurs in >90% of patients. Some studies indicate that intrahepatic ducts are almost always included (often to a greater degree than extrahepatic ducts).
- No histologic feature is pathognomonic for PSC. Typically, concentric layers of connective tissue surround the ducts, with a sparse, mixed inflammatory infiltrate.
- PSC can progress to biliary cirrhosis or cholangiocarcinoma(s).
- The diagnosis is based on clinical features (recurrent right-upper quadrant pain and symptoms of chronic cholestasis, including jaundice and pruritus) and the appearance at

cholangiography. The clinical and histologic findings overlap with those of primary biliary cirrhosis. However, the latter entity typically affects middle-aged women, does not involve the extrahepatic ducts, and is associated with high titers of antimitochondrial antibodies.

### Radiologic

- The appearance of PSC at cholangiography is that of multifocal strictures that are diffusely distributed, usually involving both the intrahepatic and extrahepatic bile ducts.
- On occasion, the disease is confined to the intrahepatic bile ducts alone or the extrahepatic ducts alone.
- The strictures are usually short and annular, and located between normal or slightly dilated segments.

## SUGGESTED READING

Clement AR. The interpretation of the direct cholangiogram. In RN Berk, AR Clemett (eds), Radiology of the Gallbladder and Bile Ducts. Philadelphia, PA: Saunders, 1977;285–330.

Hyslop WB, Kierans AS, Leonardou P, et al. Overlap syndrome of autoimmune chronic liver diseases: MRI findings. J Magn Reson Imaging 2010;31:383–389.

Meyers WC, Jones RS. Primary sclerosing cholangitis. In WC Meyers, RS Jones (eds), Textbook of Liver and Biliary Surgery. Philadelphia, PA: Lippincott, 1990;351–358.

# CASE 27

**RENDON C.**
**NELSON**

### HISTORY

A 32-year old asymptomatic woman undergoing multiphasic CT for an incidentally discovered hepatic lesion at ultrasonography.

A

■**FIGURE 3-27A** CT scan of the upper abdomen during the unenhanced state. There is an oval homogenous soft tissue mass projecting of the lesser curvature of the stomach. The mass does not contain calcifications.

B

■**FIGURE 3-27B** CT scan of the upper abdomen during the portal venous phase. The soft tissue mass demonstrates subtle and uniform enhancement. There is incidental note of a hemangioma in the right hepatic lobe.

## DIFFERENTIAL DIAGNOSIS

■**Gastric adenocarcinoma:** Although gastric adenocarci-noma may extend beyond the

wall of the stomach and infiltrate adjacent organs, unlike in this case, the bulk of tumor growth occurs within the wall of the stomach with subsequent protrusion into the lumen of the vis-cus, which may become substantially narrowed.

- **Gastrointestinal stromal tumor (GIST):** This is the most likely diagnosis given the well-defined margins of the tumor and its predominantly exophytic growth from the body of the stomach. Since the mass is relatively small in size, the frequently observed intralesional areas of heterogenous attenuation secondary to hemorrhage and necrosis, are not present in this case.
- **Leiomyoma/leiomyosacrcoma:** Either benign or malignant leiomyomas can demonstrate imaging findings that overlap with GISTs, such as tumor location, growth pattern, and enhancement pattern. For these reasons, the differential diagnosis can be challenging based on imaging solely, thus requiring histologic confirmation with immunohistochemical analysis (see below).
- **Gastrointestinal schwannoma:** Although schwannomas can be generally differentiated from GISTs on the basis of their homogenous and usually low attenuation on both precontrast and postcontrast CT, imaging findings may overlap for smaller lesions, as in this case. Definitive diagnosis of schwannoma requires demonstration of expression of S-100 protein and GFAP (glial fibrillary acidic protein) at immunohistochemical analysis.
- **Gastric mucosa-associated lymphoid tissue (MALT) lymphoma:** Unlike in this case, gastric lymphoma manifests as either a single or multiple thickened areas generally confined within the gastric wall, and are associated with mucosal ulcer in 50% of cases.
- **Enlarged celiac axis lymph node:** Although an enlarged lymph node of the celiac axis may virtually show a similar nonspecific appearance, it is an unlikely diagnosis in this case based on the broad-based contact of the lesion with the gastric wall along with a negative clinical history for malignancy.

## DIAGNOSIS

**Gastrointestinal stromal tumor of the stomach**

## KEY FACTS

### Clinical

- GISTs are the most common mesenchymal neoplasms of the gastrointestinal tract.
- GISTs generally occur in adult patients, with no gender predilection and have been associated with several genetic disorders, such as neurofibromatosis type 1 (NF1), Carney triad, which also includes extra-adrenal paragangliomas and pulmonary

chondromas, and *KIT* germ line mutations.

- Expression of KIT (CD117), a tyrosine kinase growth factor receptor, currently represents the best defining feature of GISTs as well as the molecular target of recently developed pharmacologic agents.
- Although GISTs can occur anywhere along the gastrointestinal tract from the esophagus to the anus, the stomach is the most common location for these tumors, which represent 2% to 3% of all gastric neoplasms.
- At the time of diagnosis, GISTs usually manifests as large masses (mean maximum diameter, 10 cm; range 4 to 25 cm), although smaller lesions are expected to be identified more frequently in asymptomatic patients undergoing imaging studies for unrelated reasons.
- The most common presenting sign is gastrointestinal bleeding secondary to lesion ulceration.

## Radiologic

- GISTs may be occasionally seen at a plain film radiograph of the abdomen due to a nonspecific soft tissue mass indenting or displacing the gastric gas shadow.
- In barium studies of the stomach, GISTs typically show similar imaging findings of submucosal masses (e.g., leiomyoma and leiomyosarcoma), including well-defined, smooth margins, which forms obtuse angles with the gastric wall when viewed in profile.
- Although all GISTs originally arise from the gastric wall, in a consistent number of cases the bulk of the tumor growth is outward, away from the stomach lumen, in an extragastric location.
- At contrast-enhanced CT, most tumors show peripheral enhancement of viable tissue with a central hypoat-tenuating region, which correspond to areas of tumor necrosis and/or hemorrhage. Occasionally, massive tumor necrosis may give the lesion a cystic appearance.
- Ancillary signs of malignant degeneration include: (a) distant metastases, particularly to the liver, (b) adjacent organ invasion, and (c) peritoneal spread. Metastatic lymph nodes are an uncommon finding in patients with GISTs, even in advanced stages.

# SUGGESTED READING

Ghanem N, Altehoefer C, Furtwangler A, et al. Computed tomography in gastrointestinal stromal tumors. Eur Radiol 2003;13:1669–1678.

Kim HC, Lee JM, Kim KW, et al. Gastrointestinal stromal tumors of the stomach: CT findings and prediction of malignancy. AJR Am J Roentgenol 2004;183:893–898.

Levy AD, Remotti HE, Thompson WM, et al. Gastrointestinal stromal tumors: Radiologic features with pathologic

correlation. Radiographics 2003;23:283–304.

# CASE 28

**RENDON C.**
**NELSON**

## HISTORY

A 28-years old man presents to the Emergency Department with acute onset of abdominal pain.

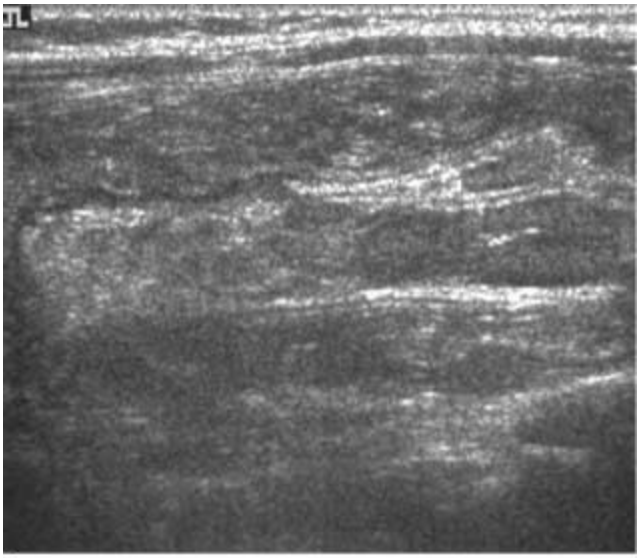


**FIGURE 3-28A** Gray-scale ultrasound of the left upper quadrant in the transverse plane. There is a hypoechoic sausage-like tubular structure within a thick-walled hypoechoic mass.

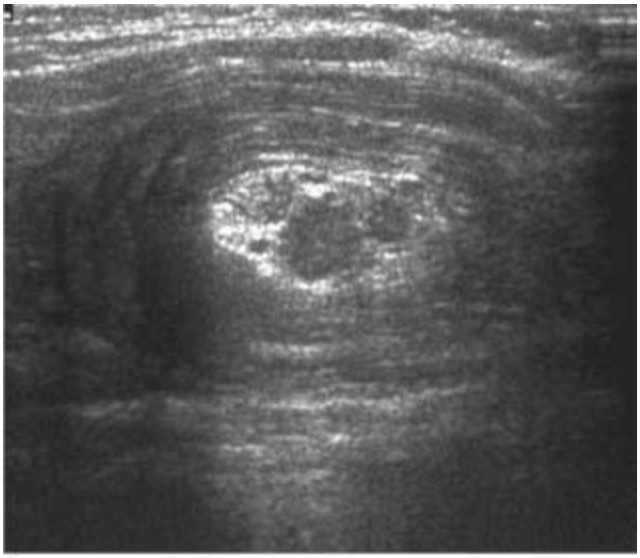

B

■**FIGURE 3-28B** Gray-scale ultrasound of the left upper quadrant in the longitudinal plane. The hypoechoic tubular structure is now viewed in cross-section demonstrating rings of alternating echogenicity.

C

■**FIGURE 3-28C** Contrast-enhanced CT of the upper abdomen. There is a tubular structure in the left upper quadrant at the level of the Ligament of Trietz that has a wind-sock appearing intraluminal filling defect.

D

**FIGURE 3-28D** Contrast-enhanced CT of the upper abdomen. The tubular structure is now viewed in cross-section demonstrating a ring within the lumen of the proximal jejunum.

## DIFFERENTIAL DIAGNOSIS

- **Small-bowel intussusception:** This is the most likely diagnosis given the"pseudokidney"appearance at US as well as the finding of an intussusceptum, with an accompanying complex of mesenteric fat and blood vessels, surrounded by the thick-walled intussus-cipiens at contrast-enhanced CT. Note the"sausage"or"target"appearance of the intussusception on CT images either parallel or perpendicular to its longitudinal axis, respectively.
- **Paraduodenal internal hernia:** Unlike in this case, paraduodenal internal hernia manifests as a cluster of dilated small-bowel loops lying between the pancreatic body and/or tail and the stomach. There is usually mass effect causing displacement of the posterior wall of the stomach, duodenojejunal flexure, and transverse colon.
- **Volvulus:** Unlike in this case, volvulus typically manifests as a soft tissue mass with an internal architecture of swirling strands of soft tissue and fat attenuation (the so-called whirl sign), which correspond to tightly twisted mesentery along the axis of rotation of the afferent and efferent bowel loops.

## DIAGNOSIS

**Small-bowel intussusception caused by a hamartomatous polyp in a patient with Peutz-Jeghers syndrome**

## KEY FACTS

## Clinical

- Peutz-Jeghers syndrome is characterized by mucocu-taneous pigmentation and hamartomas of the gastrointestinal system.
- Inheritance of the syndrome is autosomal dominant with incomplete penetrance, with some cases arising from spontaneous mutations
- Gastrointestinal hamartomatous polyps are most commonly found in the small bowel, although they can occur anywhere from the stomach to the rectum.
- Patients with Peutz-Jeghers syndrome often present with a history of intermittent abdominal pain due to small-bowel intussusception caused by the polyps. Some intussusceptions spontaneously reduce, while others lead to development of small-bowel obstruction.
- Patients with Peutz-Jeghers syndrome are at increased risk of developing gastrointestinal adenocarcinomas.

## Radiologic

- An intussusception is composed of two parts the intus-suscipiens, or receiving loop, and the intussusceptum, or donor loop, which include an entering limb and a returning limb with attached mesenteric fat interposed between them.
- Although several imaging signs have been described on plain abdominal radiographs, this modality generally provides limited information in the investigation of patients with intussusception.
- At US, an intussusception may have a“doughnut”or“pseudokidney”appearance on images obtained transversely or longitudinally to the long axis, with the hypoechoic outer area corresponding to the edema-tous bowel wall of the intussuscipiens and the hyper-echoic central area representing mesenteric fat that is dragged with the intussusceptum.
- On CT images, an intussusception appears as a complex soft tissue mass composed of a central intussusceptum and outer intussuscipiens with interposed mesenteric fat, which may contain crowded and engorged mesen-teric vessels. Depending on the orientation of the bowel loops respect to the imaging plane, the intussusception may show either a“target”(transverse) or a“sausage”(longitudinal) appearance.

# SUGGESTED READING

Kim YH, Blake MA, Harisinghani MG, et al. Adult intestinal intussusception: CT appearances and identification of a causative lead point. Radiographics 2006;26:733–744.

Rufener SL, Koujok K, McKenna BJ, Walsh M. Small bowel intussusception secondary to Peutz-Jeghers polyp. Radiographics 2008;28:284–288.

Warshauer DM, Lee JK. Adult intussusception detected at CT or MR imaging: clinical-imaging correlation. Radiology

1999;212:853–860.

# CASE 29

**RENDON C.**
**NELSON**

## HISTORY

A 65-year old man presents with a long history of diabetes mellitus and recurrent abdominal pain.


A

■**FIGURE 3-29A** Contrast-enhanced CT during the pancreatic phase demonstrates an oval cystic mass in the region of the pancreatic neck. The upstream portion of the main pancreatic duct is dilated.

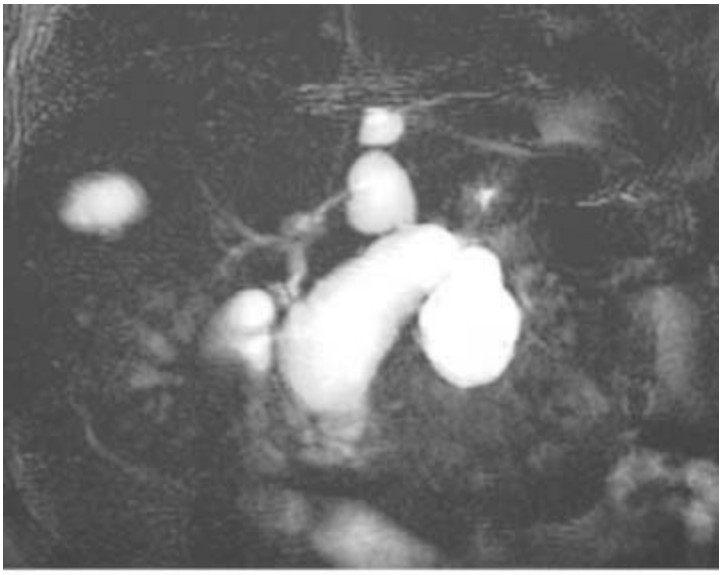

B

**FIGURE 3-29B** Thick slab projection MRCP in the coronal plane also demonstrates the oval cystic mass in the pancreatic head and neck as well as two additional cystic masses projecting off the pancreatic neck and tail.

C

**FIGURE 3-29C** Endoscopic retrograde pancreatogram reveals communication of the main pancreatic with the oval mass in the neck, large intraluminal filling defects and upstream dilatation of the duct.

## DIFFERENTIAL DIAGNOSIS

**Chronic pancreatitis:** Although this condition may demonstrate a similar appearance on advanced stages, irregularities or beading of both main and branch pancreatic ducts are generally more prominent and are frequently associated with either pancreatic

calcification and/or intraluminal stones. In addition, unlike in this case, the clinical history often documents existence of well-defined predisposing factors, such as alcohol consumption, hyperlipidemia, or hyperparathyroidism.

- **Secondary ductal dilatation:** This finding is generally associated with ductal adenocarcinoma of the pancreas. Typical imaging findings include a narrow transition point and frequent coexistence of biliary dilatation (the so-called double duct sign).
- **Intraductal papillary mucinous neoplasm (IPMN):** This is the most likely diagnosis given the markedly distended and fluid-filled main pancreatic duct with a bulging papilla into the duodenal lumen.
- **Pseudocyst:** Pseudocysts are the most common cystic lesions of the pancreas (about 85% to 90% of all cystic lesions). Pseudocysts can occur anywhere in the pancreas and classically manifest as either a round or oval fluid collection with a thin, barely perceptible wall or a thick wall that shows contrast enhancement.
- **Serous pancreatic cystadenoma:** Unlike this case, serous pancreatic cystadenoma typically manifests as a round, well-defined cystic lesion in the head of the pancreas. As a rule, a cystadenoma does not communicate with the pancreatic duct. A central fibrous scar with peripherally radiating septa may also be seen giving the lesion a honeycombing appearance.
- **Mucinous pancreatic cystadenoma:** Mucinous pancreatic cystadenoma typically manifests as a well-defined, round, or oval large cystic mass at the tail of the pancreas. Like the serous type, a mucinous cystadenoma, does not communicate with the main pancreatic duct. An inspissated, peripheral fibrous capsule with amorphous calcification can also be seen.

## DIAGNOSIS

**Main pancreatic duct IPMN**

## KEY FACTS

### Clinical

- IPMN account for 21% to 33% of all pancreatic cystic neoplasms.
- IPMN arises from the epithelial lining of the main pancreatic duct and/or the branch pancreatic ducts and is associated characteristically with secretion of abundant amount of thick mucin, which results in ductal dilatation and obstruction.
- Histologic appearance can range from hyperplasia to papillary adenoma and then carcinoma, with different histo-logic grades frequently coexisting within the same lesion.
- Compared with ductal adenocarcinoma of the pancreas, IPMN is almost invariably

associated with a better prognosis, and most lesions can be resected even if malignant.

- Due to long lasting, progressive dilatation of the main pancreatic duct, most lesions manifest with abdominal pain and mild elevation of pancreatic laboratory test, thus mimicking chronic pancreatitis. Diabetes can occasionally occur and has been associated with an increased risk of malignant degeneration.

## Radiologic

- According to the site of involvement, IPMNs are classified as either affecting the main pancreatic duct (20%), the branch pancreatic duct (52%), or both (28%).
- Main pancreatic duct IPMN, as in this case, manifests as a diffuse, moderate to marked dilatation of the duct lumen, which is associated with atrophy of the pancreatic parenchyma. In some cases (-22%), a mucin-distended papilla may be seen protruding into the duodenal lumen.
- Branch pancreatic duct IPMN manifests as either single or multilocular septated cystic lesions, more commonly arising in the head or uncinate process of the pancreas. Channel-like communication with the main pancreatic duct is a requisite for diagnosis and it can be demonstrated at either multidetector-row CT (MDCT) with curved multiplanar reformations or MR cholangiopan-creatography.

## SUGGESTED READING

1. Koito K, Namieno T, Ichimura T, et. al. Mucin-producing pancreatic tumors: comparison of MR cholangiopancreatography with endoscopic retrograde cholangiopancreatography. Radiology 1998;208(1):231–237.

2. Takeshita K, Kutomi K, Takada K, et. al. Differential diagnosis of benign or malignant intraductal papillary mucinous neoplasm of the pancreas by multidetector row helical computed tomography: evaluation of predictive factors by logistic regression analysis. J Comput Assist Tomogr. 2008;32(2):191–197.

3. Grogan JR, Saeian K, Taylor AJ, Quiroz F, Demeure MJ, Komorowski RA. Making sense of mucin-producing pancreatic tumors. Am J Roentgenol. 2001;176(4):921–929.

4. Irie H, Honda H, Aibe H, et. al. MR cholangiopancreatographic differentiation of benign and malignant intraductal mucin-producing tumors of the pancreas. Am J Roentgenol. 2000;174(5):1403–1408.

# CASE 30

**RENDON C.**
**NELSON**

### HISTORY

A 63-year old woman with recent onset of left-lower quadrant pain. She denies nausea or vomiting.

A

**FIGURE 3-30A** Contrast enhanced CT of the mid abdomen in the axial plane demonstrates numerous dilated loops of small bowel with air-contrast levels. In the region of the left paracolic gutter there is a round fat-containing mass that has a whirled appearance.

B

**FIGURE 3-30B** Contrast-enhanced CT of the upper abdomen in the coronal plane demonstrates a tear-drop shaped fat-containing mass in the region of the left paracolic gutter.

## DIFFERENTIAL DIAGNOSIS

**A primary tumor of the colon or a metastasis to the greater omentum:** Unlike in

this case, patients with either a primary colonic tumor or a metastasis to the omentum typically present with a painless abdominal mass and vague symptoms.

- **Acute epiploic appendagitis:** Although acute appendagi-tis can have a similar appearance, these lesions are generally smaller than 5 cm in maximum diameter (typical diameter range, 1.5 to 3.5 cm).
- **Omental infarction:** This is the most likely diagnosis given the large size of this heterogeneously attenuating fatty mass and its characteristic shape and location in the adipose tissue adjacent to the colon.
- **Diverticulitis:** By causing mild to severe inflammatory stranding of the paracolic fat, acute diverticulitis can simulate an extracolic mass. However, CT findings of multiple diverticula as well as other ancillary signs of acute inflammation, such as intraabdominal fluid and engorged mesenteric vessels (the so-called centipede sign), usually favour diverticulitis.

## DIAGNOSIS

**Segmental infarction of the greater omentum**

## KEY FACTS

### Clinical

- Omental infarction is a rare cause of acute abdomen in adults, although in about 15% of cases infarction may also affect pediatric patients. Risk factors include obesity and prior surgery.
- Although in a limited number of cases infarction may result from omental torsion, most cases occur without a clearly defined etiologic factor. In most of these idiopathic forms, venous insufficiency or thrombosis of the omental veins have been suggested as a possible causes of infarction.
- Clinical signs and symptoms are typically nonspecific and include abdominal pain, fever, and small-bowel obstruction. When right-sided, omental infarction may mimic either acute appendicitis or gallbladder disease.
- The key role of imaging is to firmly establish a diagnosis, thus avoiding unnecessary aggressive management of the lesion by either surgery or antibiotic therapy.
- Spontaneous resolution of the symptoms, typically within 2 weeks, is the rule.

### Radiologic

- At CT examination, the infarcted omentum appears as a large, cake-like, high-attenuation fatty mass centered in the omentum.

- The mass may or may not be immediately adjacent to the colon, depending on the anatomic location of the infarcted omentum.
- Reactive bowel wall thickening may occur, but the inflammatory process in the omentum usually is disproportionately more severe.

## SUGGESTED READING

Pereira JM, Sirlin CB, Pinto PS, et al. Disproportionate fat stranding: A helpful CT sign in patients with acute abdominal pain. Radiographics 2004;24:703–715.

Pickhardt PJ, Bhalla S. Unusual nonneoplastic peritoneal and subperitoneal conditions: CT findings. Radiographics 2005;25:719–730.

Singh AK, Gervais DA, Hahn PF, et al. Acute epiploic appendagitis and its mimics. Radiographics 2005;25:1521–1534.

# CASE 31

**DANIELE MARIN**

### HISTORY

A 42-year-old man presents with chronic right-lower quadrant pain.

**FIGURE 3-31** Axial CT image of the pelvis with IV contrast material demonstrates a tubular thick-walled fluid collection associated with inflammatory stranding in the

surrounding fat. There is a fleck of high attenuation material in the center of the collections suggesting an enterolith.

## DIFFERENTIAL DIAGNOSIS

- **Acute appendicitis:** This is a reasonable diagnosis in the appropriate clinical setting unless a normal appendix is identified. The diameter of this tubular structure is larger than is typically seen with appendicitis but this does not exclude the diagnosis.
- **Meckel diverticulitis:** This is the most likely diagnosis given the evidence of a large blind-ending fluid-filled pouch that communicates with the terminal ileum. At contrast-enhanced CT, ancillary findings of acute inflammation include a markedly thickened wall, which demonstrates vivid enhancement, as well as irregular stranding of the adjacent mesentery.
- **Crohn's disease:** Crohn's disease can be confidently excluded in this case by differentiating the inflamed diverticulum from the normal terminal ileum. In addition, common ancillary findings of Crohn's disease, such as mesenteric fibrofatty proliferation, fistula formation, and colonic involvement, are absent.

## DIAGNOSIS

**Meckel diverticulitis**

## KEY FACTS

### Clinical

- Meckel diverticulum is the most common congenital anomaly of the gastrointestinal tract (2% to 3% of the general population), which results from improper closure and resorption of the omphalomesenteric duct on the antimesenteric border of the distal ileum usually within 40 to 100 cm of the ileocecal valve.
- Although a Meckel diverticulum is generally asymptomatic and is discovered incidentally during a radiologic evaluation or surgical procedure performed for unrelated medical reasons, it has been estimated that in about 25% of cases patients may develop signs and symptoms secondary to diverticular complication, such as hemorrhage, intestinal obstruction, and acute diverticulitis. Occasionally, a Meckel diverticulum may be entrapped in an inguinal hernia (the so-called Littre hernia).
- Acute Meckel diverticulitis may result from either obstruction or narrowing of the mouth of the diverticu-lum. This is most commonly caused by an enterolith or a fecolith, although it can also be caused by peptic ulceration of ileal mucosa due to the presence of ectopic gastric mucosa within the diverticulum (-50% of cases).
- Since signs and symptoms are typically nonspecific (i.e., abdominal pain, fever, and

suspicion of small bowel obstruction), a Meckel diverticulum cannot be clinically differentiated from other intraabdominal inflammatory processes, such as acute appendicitis, inflammatory bowel disease, or other causes of small-bowel obstruction.

## Radiologic

- At CT, an uncomplicated Meckel diverticulum is difficult to distinguish from normal small bowel. A blind-ending fluid or gas-filled structure in continuity with the small bowel is the most important clues for a positive diagnosis.
- CT can clearly depict the complication associated with a Meckel diverticulum, such as intussusception, diverticulitis, small-bowel obstruction, and enterolith formation.
- Due to better depiction of well-distended small-bowel loops, CT enterography promises to further increase the sensitivity of CT to the diagnosis of a Meckel diverticulum.
- Scintigraphy with $^{99m}$Tc-Na-pertechnetate may demonstrate heterotopic gastric mucosa within the diverticu-lum although the overall sensitivity is only 60%. This is of paramount significance, however, because it can result in serious complications such as bleeding and inflammation.

## SUGGESTED READING

Bennett GL, Birnbaum BA, Balthazar EJ. CT of Meckel's diverticulitis in 11 patients. AJR Am J Roentgenol 2004;182:625–629.

Elsayes KM, Menias CO, Harvin HJ, Francis IR. Imaging manifestations of Meckel's diverticulum. AJR Am J Roentgenol 2007;189:81–88.

Levy AD, Hobbs CM. From the archives of the AFIP. Meckel diverticulum: Radiologic features with pathologic correlation. Radiographics 2004;24:565–587.

# Chapter FOUR

# Genitourinary Imaging

**RICHARD A. LEDER** ▪ CHAPTER EDITOR

Kelly S. Freed

Mary T. Keogan

Anthony M. Foti

Jeremy A.L. Lawrance

Richard A. Leder

M. Gena Frederick

Daniele Marin

Vincent G. McDermott

Douglas H. Sheafor

John A. Stahl

Erik K. Paulson

# CASE 1

**KELLY S.FREED**

### HISTORY

**Patient A: A 31-year-old woman who had been in a motor vehicle accident presents with gross hematuria. Patient B: A 21-year-old woman who also had been in a motor vehicle accident presents with microscopic hematuria.**

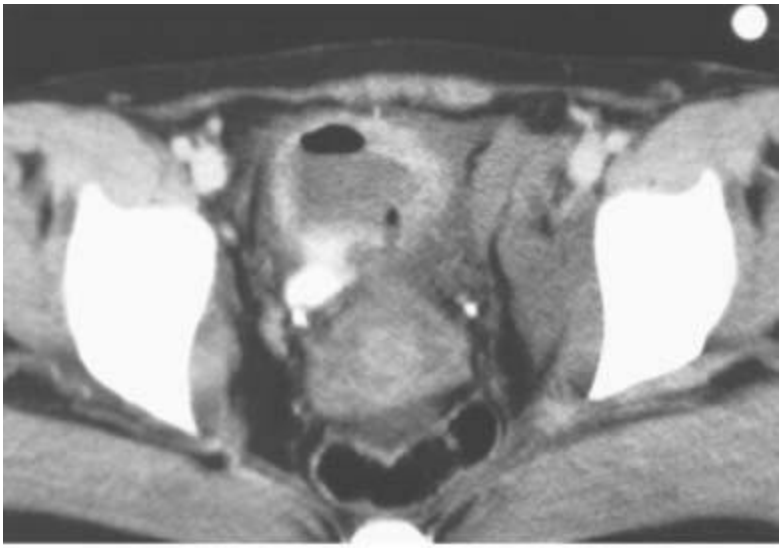

A

■**FIGURE 4-1A** Patient A: Contrast-enhanced CT through the bladder. Extravasation of contrast material is seen from the right lateral aspect of the urinary bladder. The bladder is not well distended, and it is difficult to determine if the rupture is intraperitoneal or extraperitoneal. A CT cystogram or conventional cystogram could be performed to clarify this issue.

B

■**FIGURE 4-1B** Patient A: Anteroposterior plain film of the abdomen performed following the contrast-enhanced CT scan. Contrast material is seen superior to the bladder, tracking up along the right paracolic gutter and adjacent to the liver.

C

**FIGURE 4-1C** Patient B: Spot film from a conventional cystogram via a Foley catheter. There is a fracture of the left inferior pubic ramus. Contrast material is extravasating into the left inguinal region.

## DIFFERENTIAL DIAGNOSIS

- The differential diagnosis for both patients includes **intraperitoneal bladder rupture, extraperitoneal bladder rupture, or a combination of the two**.
- In Patient A, **intraperitoneal rupture** is diagnosed because the contrast outlines the right paracolic gutter and liver.
- In Patient B, **extraperitoneal rupture** is diagnosed because the contrast material does not flow into the peritoneal cavity but extends into the proximal thigh via the left inguinal region. There is an associated fracture of the inferior pubic ramus.

## DIAGNOSIS

**Patient A: Intraperitoneal bladder rupture Patient B: Extraperitoneal bladder rupture**

## KEY FACTS

### Clinical

- Bladder rupture can be seen following blunt or penetrating trauma and may be extraperitoneal, intraperitoneal, or both.

- Extraperitoneal bladder rupture is more common, composing approximately 80% of cases, and is frequently associated with pelvic fractures. The rupture usually occurs at the base of the bladder. Intraperitoneal bladder rupture occurs at the dome of the bladder when the bladder is distended. Pelvic fractures are seen less commonly in intraperitoneal bladder rupture than in extraperitoneal bladder rupture.
- Intraperitoneal rupture is more common in children than adults.
- Physical findings of bladder rupture include hematuria and the inability to urinate. Significant hematuria (> 50 red blood cells/high-power field) is a sensitive indicator of bladder trauma.
- Intraperitoneal bladder rupture requires surgery with bladder closure, whereas extraperitoneal bladder rupture can be managed with catheter drainage, antibiotics, and clinical follow-up.

## Radiologic

- Radiologic diagnosis includes conventional cystography and CT of the abdomen and pelvis, including CT cystography.
- In extraperitoneal rupture, there are often associated fractures of the pubic rami or anterior pelvic ring. The extravasated contrast material can track down into the proximal thigh or scrotum. The extravasated contrast material may be ill-defined and feathery or contained.
- With intraperitoneal rupture, the contrast material flows freely into the peritoneum and may outline bowel loops or the paracolic gutters.
- CT of the abdomen and pelvis performed with the bladder only mildly or moderately distended is not as sensitive as conventional cystography for bladder injury. However, recent articles have demonstrated that CT cystography is comparably sensitive to conventional cystography. The bladder must be well distended on the CT study, either from instillation of contrast material through a Foley catheter or by using delayed images. Postdrainage CT images should also be obtained.

# SUGGESTED READING


Bodner DR, Selzman AA, Spirnak JP. Evaluation and treatment of bladder rupture. Semin Urol 1995;13:62–65.

Chan DP, Abujudeh HH, Cushing GL Jr, Novelline RA. CT cystography with multiplanar reformation for suspected bladder rupture: Experience in 234 cases. AJR Am J Roentgenol 2006;187:1296–302.

Horstman WG, McClennan BL, Heiken JP. Comparison of computed tomography and conventional cystography for detection of traumatic bladder rupture. Urol Radiol 1991;12:188–193.

Morey AF, Iverson AJ, Swan A, et al. Bladder rupture after blunt trauma: guidelines for diagnostic imaging. J Trauma 2001;51:683–686.

Rehm CG, Mure AJ, O'Malley KF, Ross SE. Blunt traumatic bladder rupture: The role of retrograde cystogram. Ann Emerg Med 1991;20:845–847.

# CASE 2

**MARY T. KEOGAN**

## HISTORY

A 56-year-old woman presents with a low-grade fever.

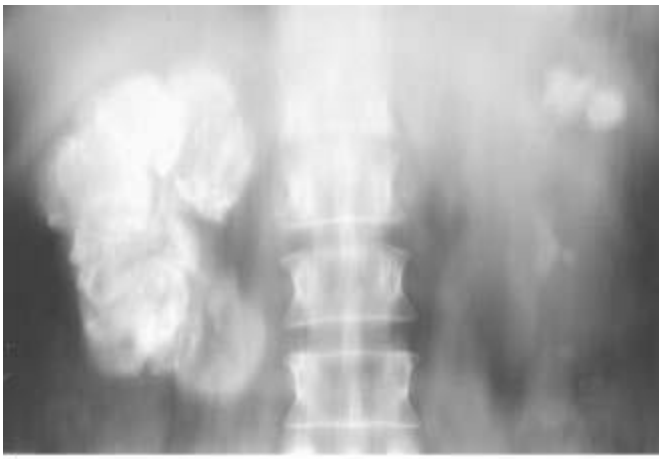

A

■**FIGURE 4-2A** Noncontrast linear coronal tomogram of the renal area. Extensive calcifications are noted in the right kidney. Calcifications are also noted in the upper and lower pole calyces of the left kidney.

B

■**FIGURE 4-2B** Five-minute anteroposterior view of the kidneys during an intravenous urogram. There is no excretion of contrast material from the right kidney. Calcifications are noted in the right proximal ureter. The left upper pole calyces are dilated, and there

is no filling of the left lower pole calyces.

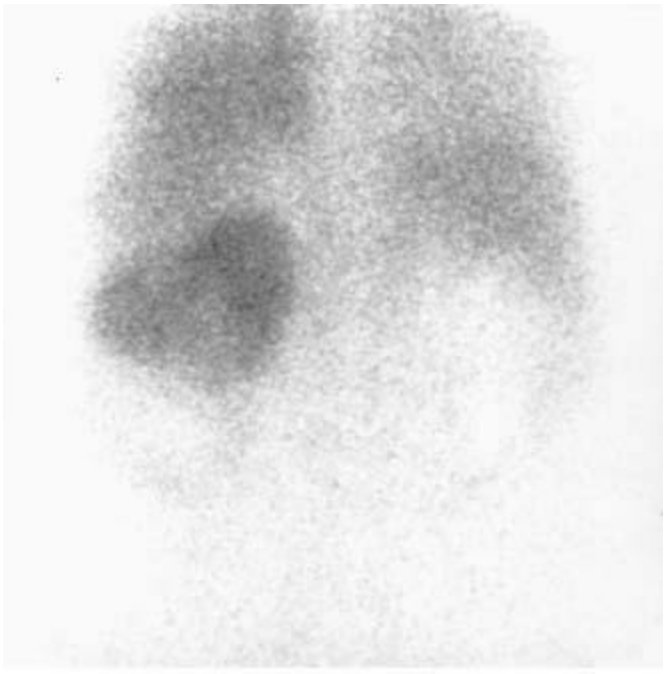

C

■**FIGURE 4-2C** $Tc^{99m}$-diethylenetriamine penta-acetic acid scan of the renal area in the posteroanterior projection. There is marked reduction of activity in the left lower pole, with a faint rim of cortical activity. No right renal activity is seen.

D

■**FIGURE 4-2D** Noncontrast CT of the lower abdomen. There are dense calcifications in the right kidney and ureter. Low-attenuation areas are noted in the left lower pole consistent with a dilated collecting system.

## DIFFERENTIAL DIAGNOSIS

- **Renal tuberculosis (TB):** This is the best diagnosis due to extensive replacement of the nonfunctioning right kidney by calcification, the so called putty kidney. Calcifications in the ureter are also typical. Pyonephrosis is present in the lower pole of the left kidney.
- **Xantogranulomatosis pyelonephritis (XGP):** This inflammatory process is usually related to a chronic urinary obstruction and a staghorn calculus. Calcification in the ureter is atypical.
- **Schistosomiasis:** This infection characteristically affects the distal ureters, causing dilation and/or stenosis. The proximal ureters and ureteropelvic junctions are rarely involved. Schistosomiasis typically causes bladder calcification, but renal calcifications are uncommon.

## DIAGNOSIS

**TB with right autonephrectomy and left lower pole pyonephrosis**

## KEY FACTS

### Clinical

- Renal TB results from hematogenous spread of TB bacilli to the kidneys. Ureteral involvement is secondary to bacilluria from the kidneys.
- Although both kidneys are usually involved, the disease process is typically more severe in one kidney.
- Patients are typically >40 years and present with hematuria, frequency, dysuria, or suprapubic pain.
- About 10% of patients may be asymptomatic and have sterile urine.

### Radiologic

- Radiographic findings depend on the extent of the disease process but are present in the majority of cases of renal TB.
- Papillary necrosis is common and may be extensive. Necrosis in renal granulomas may lead to the formation of communicating cavities.
- Parenchymal calcifications are present in 50% of patients. They may be amorphous in association with granulomatous masses, or dense in healed tuberculomas. Renal calculi develop in 20% of patients.
- Parenchymal scarring occurs in 20% of patients, either localized or involving the entire kidney. There are also associated calcifications and underlying calyceal

abnormalities.

- Calyceal abnormalities are common, with multiple irregular strictures of the infundibula and subsequent hydrocalycosis.
- Renal function is impaired in 50% of patients. Antegrade or retrograde pyelography is often required for evaluation.
- Advanced disease eventually results in a nonfunctioning kidney (autonephrectomy or "putty" kidney). These cases are associated with extensive calcifications.
- Failure of contrast material excretion often signifies the presence of tuberculous pyonephrosis due to stricture formation.
- Abnormalities of the ureters occur in 50% of cases of renal TB due to ulceration, with fibrosis, stricture, and calcification. Alternating segments of dilation and stricture produce a characteristic beaded appearance. Shortening of the ureter may also occur, producing a "pipestem" appearance.
- Other sites of urinary tract involvement include the prostate, epididymis, scrotum, and bladder, producing calcification with abscess formation and fistulous tracts.

## SUGGESTED READING

Renal inflammatory disease. In NR Dunnick, RW McCallum, CM Sandler (eds), Textbook of Uroradiology. Baltimore: Williams & Wilkins, 1991;135–157.

The ureter. In NR Dunnick, RW McCallum, CM Sandler (eds), Textbook of Uroradiology. Baltimore: Williams & Wilkins, 1991;287–319.

Craig WD, Wagner BJ, Travis MD. Pyelonephritis: Radiologic-pathologic review. Radiographics 2008;28:255–277.

Elkin M. Urogenital tuberculosis. In HM Pollock, H Elkin (eds), Clinical Urography. Philadelphia: Saunders, 1990;1020–1052.

Paterson A. Urinary tract infection: An update on imaging strategies. Eur Radiol 2004;14(Suppl 4):L89–L100.

# CASE 3

**ANTHONY M. FOTI**

## HISTORY

A 50-year-old man has back pain and an elevated serum creatinine.

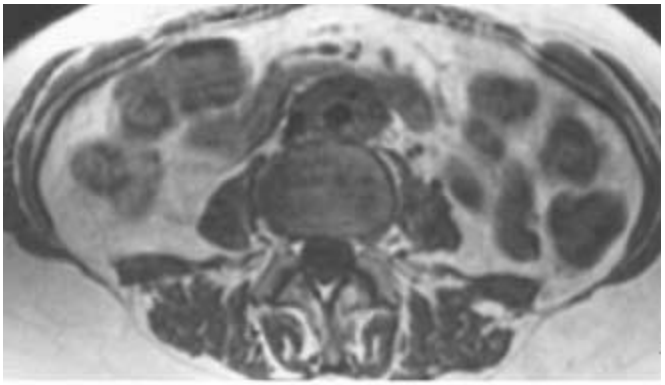

A

■**FIGURE 4-3A** Axial T1-weighted MRI of the abdomen. There is a well-circumscribed mantle of soft tissue surrounding the aorta and abutting the IVC. The mass does not displace the aorta anteriorly away from the spine and is isointense to muscle.

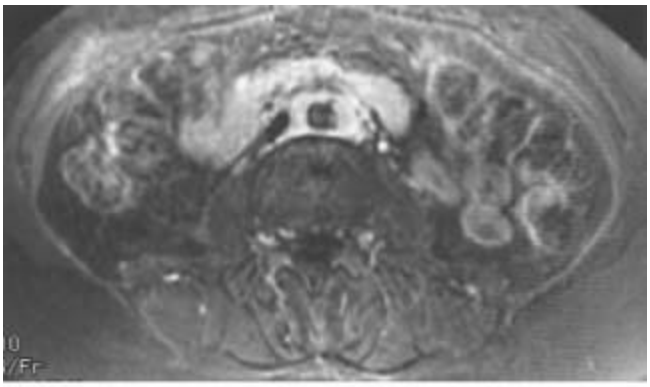

B

■**FIGURE 4-3B** Axial fat-suppressed T2-weighted MRI of the abdomen. The mantle of soft tissue is mildly hyperintense and relatively homogenous.

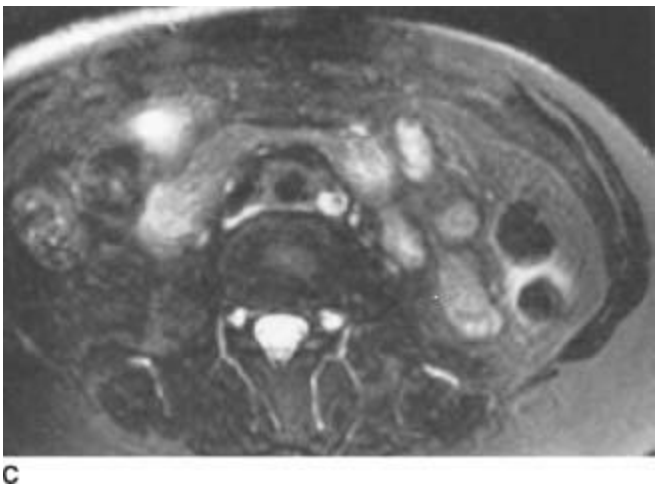

C

■**FIGURE 4-3C** Axial contrast-enhanced T1-weighted MRI following the intravenous administration of a gadolinium-chelate. There is uniform enhancement of the soft tissue mass.

## DIFFERENTIAL DIAGNOSIS

- **Malignant retroperitoneal fibrosis (RPF):** Imaging cannot differentiate malignant from nonmalignant RPF reliably; however, malignant RPF tends to be more heterogeneous on T2-weighted MR images.
- **Malignant lymphadenopathy and lymphoma:** These entities tend to displace the aorta anteriorly, away from the spine.
- **Idiopathic RPF:** The periaortic distribution and signal characteristics are classic for this entity.

## DIAGNOSIS

**Idiopathic (nonmalignant) RPF**

## KEY FACTS

### Clinical

- RPF is a rare disorder in which a fibrotic plaque encases the aorta and extends laterally to engulf the inferior vena cava (IVC) and ureters. It usually begins near the aortic bifurcation and extends cephalad to the renal hila. Occasionally, it may extend cranially into the mediastinum or anteriorly into the mesentery.
- 70% of patients are 30 to 60 years of age at the time of diagnosis.
- Symptoms are nonspecific and include dull back pain, fatigue, and weight loss. Laboratory values include elevated serum creatinine levels and erythrocyte sedimentation rates.
- Two-thirds of cases are idiopathic (Ormond's disease). The presumed mechanism is autoimmune, likely a response to leakage of ceroid, an insoluble lipid, from atherosclerotic plaques into periaortic tissue. Twelve percent of cases are secondary to methysergide administration; beta blockers, hydralazine, methyldopa, and bromocriptine have also been implicated. Other causes include malignancy, hemorrhage, and aneurysms (so-called perianeurysmal fibrosis).
- Malignant RPF is an intense desmoplastic response to retroperitoneal metastases from a variety of primary malignancies (breast, lung, thyroid, gastrointestinal tract, genitourinary tract, and Hodgkin's lymphoma). There are only scattered malignant cells, and thus deep surgical biopsy is required to differentiate nonmalignant from malignant RPF.
- Histologically, perianeurysmal fibrosis (also referred to as an inflammatory aneurysm) is identical to RPF. The only difference is the caliber of the aorta.

- RPF usually results in ureteral dilatation by impairing peristalsis, rather than directly invading the ureter.
- RPF may obstruct the IVC and, rarely, the portal vein or common bile duct.
- Treatment consists of a combination of surgery to release the ureters (ureterolysis) and steroids.
- RPF has a similar histology and is associated with other systemic sclerosing diseases, including sclerosing cholangitis, orbital pseudotumor, mediastinal fibrosis, and Riedel's thyroiditis. There is also an association with other immune-mediated connective tissue disorders such as ankylosing spondylitis, Wegener's granulomatosis, systemic lupus erythematosus, Raynaud's disease, polyarteritis nodosa, and systemic vasculitis. RPF is associated with the major histocompatibility complex HLA-B27.

## Radiologic

- On intravenous urography there is hydronephrosis with medial deviation of the middle third of the ureters, which then taper near the L4 to L5 level. This is in contradistinction to most cases of lymphoma and other causes of lymphadenopathy, which are not associated with a desmoplastic response and thus cause lateral deviation of the ureters due to mass effect.
- On CT, a homogeneous mantle of soft tissue envelopes, but usually does not displace —the aorta. It extends laterally to involve the IVC and ureters, but usually does not extend >1 cm lateral to the ureters. It may obstruct the gonadal vessels. The margins are usually sharply circumscribed and not nodular. However, it may be ill-defined, although the margin characteristics cannot be used to distinguish nonmalignant from malignant RPF reliably. Precontrast, it is isoattenuating with the psoas muscles. Postcontrast, the soft tissue mass enhances uniformly, although enhancement diminishes with the chronicity of the disease.
- On ultrasound, a homogeneous hypoechoic perivascular mantle is characteristic.
- With MRI, the soft tissue mass is relatively homogeneous on all imaging sequences. It is isointense to psoas muscle on Tl-weighted images. The signal intensity on T2-weighted images and the enhancement on Tl-weighted images post-gadolinium-chelate administration vary with the stage. Early in the disease, the cellular nature of the infiltrate results in high signal intensity on T2-weighted images and discernible contrast enhancement. Late in the disease, the signal intensity on T2-weighted images and contrast enhancement decreases, reflecting the fibrotic process. Heterogeneous high signal intensity on T2-weighted images suggests malignancy, while uniformly low signal suggests late-stage benign disease.

## SUGGESTED READING

Amis ES Jr. Retroperitoneal fibrosis. AJR Am J Roentgenol 1991;157: 321-329.

Arrive L, Hricak H, Tavares NJ, Miller TR. Malignant versus nonmalignant retroperitoneal fibrosis: differentiation with MR imaging. Radiology 1989;172:139–143.

Brooks AP, Reznek RH, Webb JA. Aortic displacement on computed tomography of idiopathic retroperitoneal fibrosis. Clin Radiol 1989;40:51–52.

Brun B, Laursen K, Sorensen IN, et al. CT in retroperitoneal fibrosis. AJR Am J Roentgenol 1981;137:535–538.

Cronin CG, Lohan DG, Blake MA, et al. Retroperitoneal fibrosis: a review of clinical features and imaging findings. AJR Am J Roentgenol 2008;191:423–431.

Degesys GE, Dunnick NR, Silverman PM, et al. Retroperitoneal fibrosis: use of CT in distinguishing among possible causes. AJR Am J Roentgenol 1986;146:57–60.

Kottra JJ, Dunnick NR. Retroperitoneal fibrosis. Radiol Clin North Am 1996;34:1259–1275.

# CASE 4

**JEREMY A.L. LAWRANCE**

## HISTORY

A 67-year-old woman who was previously healthy presents with a 6-week history of epigastric pain.

A

■**FIGURE 4-4A** Axial T2-weighted MRI of the upper abdomen. There is a 5-cm left-upper quadrant mass. It is of relatively high signal intensity and heterogeneous in nature. In addition, a highsignal intensity mass is noted in the IVC.

B

■**FIGURE 4-4B** Coronal T2-weighted MRI of the upper abdomen. The mass is superior to and clearly separate from the left kidney.

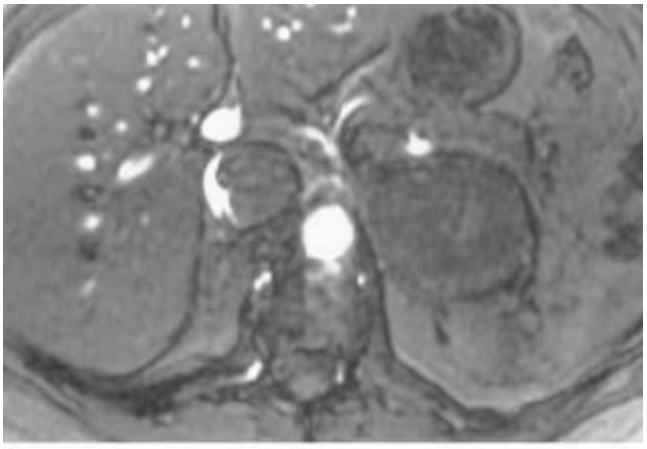

C

■**FIGURE 4-4C** Axial T1-weighted gradient echo MRI of the upper abdomen shows a crescent of flow around the IVC filling defect.

## DIFFERENTIAL DIAGNOSIS

- **Renal cell carcinoma:** The mass is separate from the kidney; therefore, this diagnosis is excluded.
- **Pheochromocytoma:** These tumors usually demonstrate very high signal on T2-weighted MR images. They are usually > 3 cm and are frequently necrotic and hemorrhagic. The IVC invasion, however, is not a feature of pheochromocytomas.
- **Adrenal metastasis:** Tumors > 5 cm are more likely malignant. Furthermore, metastases are usually of higher signal intensity than adenomas. Apart from an adrenal metastasis in a patient with renal cell carcinoma, IVC invasion by an adrenal metastasis would be uncommon. The kidneys show no evidence of tumor in this case.
- **Adrenal adenoma:** This diagnosis is extremely unlikely unless IVC thrombosis is coincidental.
- **Adrenal carcinoma:** Although these tumors typically are larger at presentation, direct IVC invasion makes this the most likely diagnosis.

## DIAGNOSIS

**Adrenal carcinoma with inferior vena cava invasion**

## KEY FACTS

### Clinical

- Adrenal carcinomas are rare malignant tumors with an annual incidence of 0.5 to 2.0 cases per million per year.
- The average age in one large study was 47 years.
- There is a slight female preponderance.
- In a series of 156 cases, 53% had a functional endocrine syndrome. Cushing's syndrome is the most common, with virilization, hypertension, and feminization occurring less frequently.
- Up to 5% of cases are bilateral.

### Radiologic

- Adrenal carcinomas tend to be large at presentation, usually > 5 cm in diameter. Functional tumors tend to be smaller at presention than nonfunctioning tumors. The range of sizes in one study was 3 to 30 cm, with a mean diameter of 12 cm.
- The problem with small adrenal carcinomas is that it is often impossible to differentiate benign from malignant tumors. Tumors > 5 cm are more likely malignant, while evidence of local invasion into adjacent organs or distant metastases are features

of malignant tumors.

- In recent studies, metastases from adrenal carcinoma were present in 22%, while older studies reported higher incidences of metastases. The most common sites are liver, lymph nodes, bone, and lungs.
- Areas of necrosis, hemorrhage, and calcification are common. The latter is best detected by CT and found in approximately 30% of cases.
- By MRI, adrenal carcinoma shows low signal intensity on T1-weighted images and signal intensity greater than liver on T2-weighted images. Pheochromocytomas tend to have very high signal intensity on T2-weighted images and can be difficult to distinguish from adrenal carcinomas with MRI. Detection and delineation of vascular invasion, as well as multiplanar capability, make MRI a useful diagnostic tool in cases of adrenal carcinoma.

## SUGGESTED READING

Dunnick NR. Adrenal carcinoma. Radiol Clin North Am 1994;32:99–108.

Icard P, Chapuis Y, Andreassian B, et al. Adrenocortical carcinoma in surgically treated patients: a retrospective study on 156 cases. French Assoc Endocrine Surg 1992;112:972–980.

Johnson PT, Horton KM, Fishman EK. Adrenal mass imaging with multi-detector CT: pathologic conditions, pearls, and pitfalls. Radiographics 2009;29:1333–1351.

Slattery JM, Blake MA, Kalra MK, et al. Adrenocortical carcinoma: Contrast washout characteristics on CT. AJR Am J Roentgenol 2006;187:W21-W24.

Zografos GC, Driscoll DL, Karakousis CP, Humen RP. Adrenal adenocarcinoma: a review of 53 cases. Surg Oncol 1994;55:160–164.

# CASE 5

**RICHARD A.**
**LEDER**

## HISTORY

A 46-year-old man presents with urinary frequency.

A

■**FIGURE 4-5A** Anteroposterior supine 10-minute film of the bladder from an intravenous urogram demonstrates an oval to round filling defect along the left side of the bladder with no evidence of ureteral obstruction on that side.

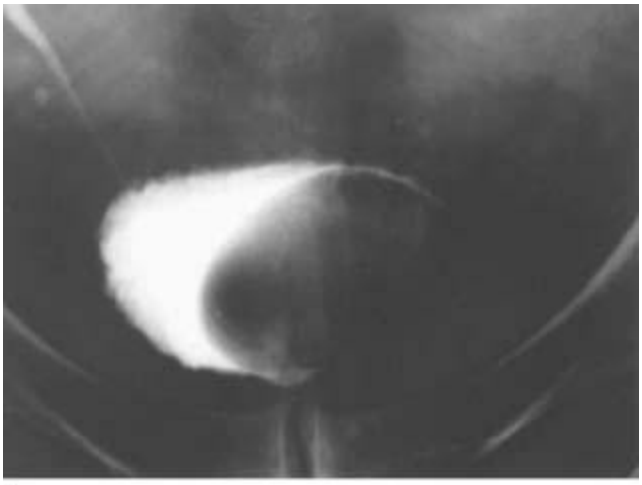

B

■**FIGURE 4-5B** Anteroposterior postvoid film from the same intravenous urogram shows a smooth filling defect involving the left lateral wall of the bladder.

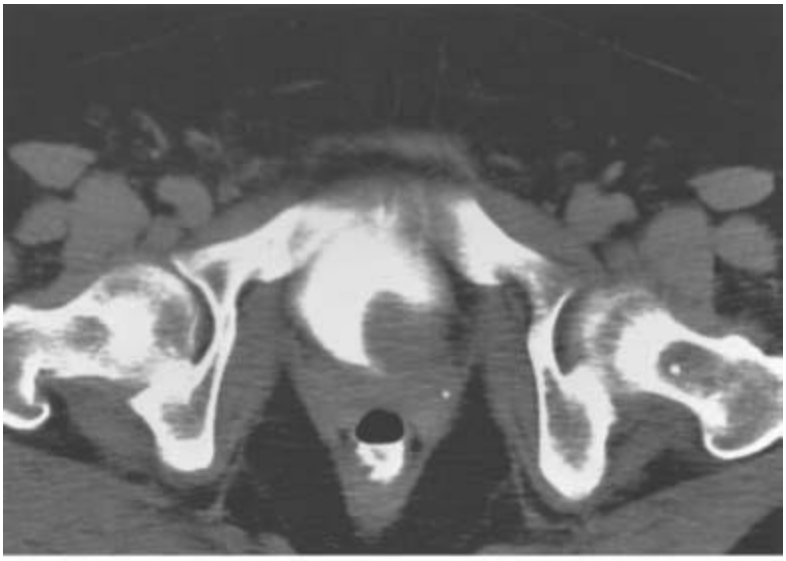

C

**FIGURE 4-5C** Contrast-enhanced CT through the urinary bladder shows a smooth, round filling defect in the left posterolateral wall of the bladder. The filling defect is of soft tissue attenuation.

## DIFFERENTIAL DIAGNOSIS

**Transitional cell carcinoma (TCC):** TCC must be included in the differential diagnosis of this lesion, but some features mitigate against this as the most likely diagnosis. Large intravesical transitional cell tumors are frequently of the papillary variety. They have a stippled surface and are unlikely to appear as smooth, as in this case. The location will dictate whether a large lesion of this size will obstruct the ureter. In this case, no ureteral obstruction was present.

**Hematoma or fungus ball:** There are a multitude of nonfixed filling defects that can occur within the bladder. It is useful in cases where hematomas or fungus balls are being considered to image the patient using ultrasound to document that these are not fixed to the bladder wall. While ultrasound was not performed in this patient, it is essential to document whether filling defects within the bladder are likely to be mobile or fixed.

**Bladder calculus:** Almost all urinary calculi are hyper-attenuating on CT (> +100 Hounsfield units [HU]). This filling defect measured soft tissue attenuation.

**Cystitis:** *Bullous cystitis* can appear as a bladder wall lesion. *Cystitis glandularis* is a proliferative lesion in which glandular elements of the bladder mucosa occur in the submucosa. Many patients have infections and associated *cystitis cystica.* These masses are typically villous. Submucosal fluid-filled cysts describe cystitis cystica, which can cause filling defects within the bladder. Chronic infection is postulated as the chief etiologic factor.

- **Bladder leiomyoma:** Smooth muscle tumors of the bladder wall may have this appearance and should be considered in the differential diagnosis of a smooth bladder wall filling defect.

## DIAGNOSIS

**Leiomyoma of the bladder**

## KEY FACTS

### Clinical

- Leiomyomas may occur in any site in the genitourinary tract. These lesions occur in all age groups and affect both sexes equally.
- Lesions may be endovesical (63%), intramural (7%), or extravesical (30%).
- The cause of these tumors is unknown.
- The tumor is usually asymptomatic and may be detected incidentally on physical examination or cystoscopy.
- The endovesical form may present with irritative urinary symptoms, gross hematuria, or obstructive symptoms.
- Small endovesical lesions can be managed with transurethral resection and fulguration. Larger endovesical, intramural, or extravesical tumors are best treated with segmental resection.
- The prognosis of this tumor is excellent. No malignant degeneration has been reported.

### Radiologic

- Intravenous urography or cystography usually reveals a smooth filling defect within the bladder.
- CT is useful to determine consistency (attenuation), size, location, and possible adjacent organ involvement.
- The endovesical form can be sessile or pedunculated on cystoscopy and is usually covered with normal bladder mucosa.

## SUGGESTED READING

Fasih N, Prasad Shanbhogue AK, Macdonald DB, et al. Leiomyomas beyond the uterus: unusual locations, rare manifestations. Radiographics 2008;28:1931–1948.

Illescas FF, Baker ME, Weinerth JL. Bladder leiomyoma: Advantages of sonography over computed tomography. Urol Radiol 1986;8:216–218.

Knoll LD, Segura JW, Scheithauer BW. Leiomyoma of the bladder. J Urol 1986;136:906–908.

Wong-You-Cheong JJ, Woodward PJ, Manning MA, Sesterhenn IA. From the Archives of the AFIP: neoplasms of

the urinary bladder: Radiologic-pathologic correlation. Radiographics 2006;26:553–580.

# CASE 6

**M. GENA**
**FREDERICK**

## HISTORY

A 63-year-old woman has microscopic hematuria.

A

■**FIGURE 4-6A** Anteroposterior supine 5-minute film of the urinary bladder from an intravenous urogram. There is bilateral columnation of both ureters to the level of the ureterovesical junction, with a rounded distal configuration.

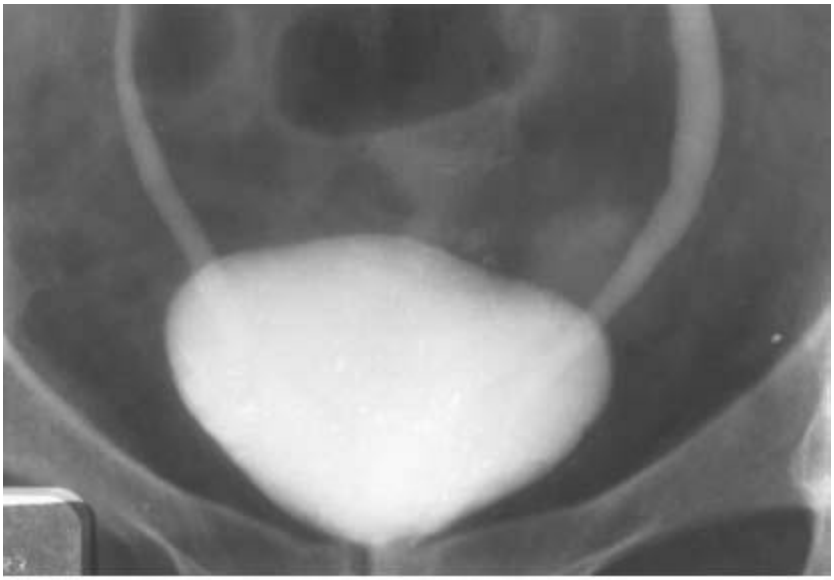

B

**FIGURE 4-6B** Anterosuperior supine 15-minute film of the urinary bladder from an intravenous urogram. Within the bladder, there is a "cobra head" appearance bilaterally. Note the lucent outline of the bulbous ureteral termination.

## DIFFERENTIAL DIAGNOSIS

**Pseudoureterocele:** This appearance is caused by a TCC of the bladder or a stone obstructing the ureter. It is unlikely because of the lack of a filling defect or mass, as well as the bilaterality of the defects. Other less common causes of the "pseudoureterocele" appearance include cervical carcinoma invading the ureterovesical orifice, radiation cystitis, or edema of the ureterovesical junction from recent stone passage. However, these are unlikely in this case because the former are identified by asymmetry of the distal lumen and irregularity of the wall and generally do not have intravesicular protrusion. However, they are capable of distending the distal ureter and thus mimicking an orthotopic ureterocele.

**Bilateral simple ureteroceles:** This is the most likely diagnosis given the lack of a bladder mass or irregularity, the intravesicular protrusion, the absence of upper tract dilatation, and the bilaterality.

## DIAGNOSIS

**Bilateral simple ureteroceles**

## KEY FACTS

### Clinical

- An orthotopic ureterocele forms in a ureter with a normal insertion into the trigone, as

opposed to an ectopic ureterocele.

- Orthotopic ureteroceles usually occur in single collecting systems, as opposed to ectopic ureteroceles, which occur in duplicated collecting systems.
- Orthotopic ureteroceles are usually unilateral, asymptomatic, and incidental. However, a calculus may lodge or form in the ureterocele.
- A ureterocele is a congenital deformity.
- A ureterocele consists of a prolapse of the distal ureter into the bladder with associated dilation of the distal ureter.
- The wall of the ureterocele is composed of a thin layer of muscle between the outer surface of the bladder uroepithelium and the inner surface of the ureteral uroepithelium.

### Radiologic

- The typical radiographic appearance is the so-called cobra head deformity, which is formed by the projection of the minimally dilated distal ureter into the lumen of the bladder, with opacified urine surrounding the ureterocele.
- The thin line of radiolucency represents the wall of the ureterocele.

## SUGGESTED READING

Berrocal T, López-Pereira P, Arjonilla A, Gutiérrez J. Anomalies of the distal ureter, bladder, and urethra in children: embryologic, radiologic, and pathologic features. Radiographics 2002;22:1139–1164.

Davidson AJ, Hartman DS. Radiology of the Kidney and Urinary Tract (2nd ed). Philadelphia: Saunders, 1994;520-523.

Mitty HA, Schapira HE. Ureterocele and pseudoureterocele: cobra versus cancer. J Urol 1977;117:557–561.

# CASE 7

**M. GENA**
**FREDERICK**

**AND**

**DANIELE MARIN**

### HISTORY

A 54-year-old man presents with abdominal pain.

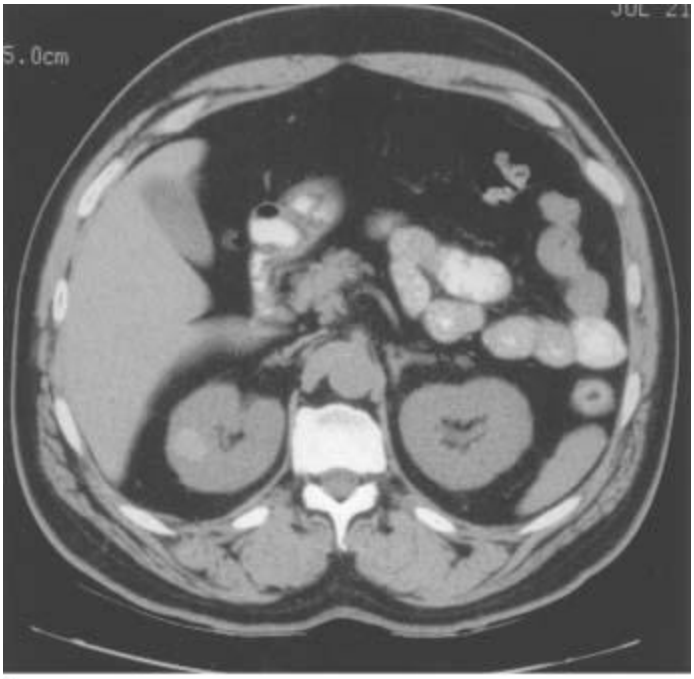


A

■**FIGURE 4-7A** Noncontrast CT of the abdomen demonstrates a small, well-defined lesion in the lateral portion of the right kidney with increased attenuation (+59 Hounsfield units [HU]) compared to the adjacent renal tissue.

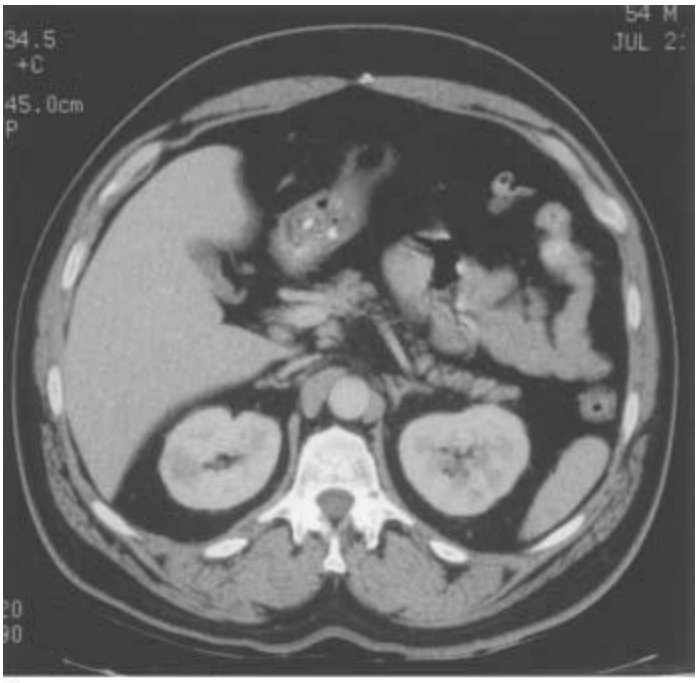


B

■**FIGURE 4-7B** On corresponding contrast-enhanced CT image, the lesion demonstrates lack of contrast enhancement (attenuation increase compared to the noncontrast scan = +1 HU).

## DIFFERENTIAL DIAGNOSIS

- **Hemorrhagic renal cell carcinoma (RCC):** This diagnosis is unlikely because the entire lesion is of uniform increased attenuation on the noncontrast study.
- **Hemorrhagic angiomyolipoma:** This diagnosis is unlikely due to the absence of macroscopic fat on the noncontrast CT.
- **Hemorrhagic renal cyst:** This is the most likely diagnosis due to the small size, uniform appearance, and lack of enhancement of this renal lesion.

## DIAGNOSIS

**Hemorrhagic renal cyst**

## KEY FACTS

### Clinical

- Renal cysts account for approximately 60% of all renal masses.
- Renal cysts increase in frequency with age (approximately 50% of cases occur past the age of 50).
- Most renal cysts are asymptomatic, whether hemorrhagic or not.
- Hemorrhagic cysts are frequently seen in patients with autosomal dominant polycystic kidney disease and acquired renal cystic disease.

### Radiologic

- Noncontrast CT is necessary to evaluate the attenuation of the lesion before contrast material administration.
- Cysts that are "hyperdense" exhibit attenuation values between +50 and +80 HU. The high attenuation is due to a high content of protein, blood breakdown products, or iodine. To be considered a benign hyperdense cyst, the lesion must be sharply marginated, homogeneous, and nonenhancing (< 10 HU increase postcontrast).
- Because of the thickness of the wall and the internal structure of the lesion, these cysts cannot be evaluated reliably with ultrasound, and only 50% of hyper-attenuating lesions demonstrate typical sonographic cyst criteria. CT is necessary to assess or rule out lesion enhancement.

## SUGGESTED READING

Israel GM, Bosniak MA. How I do it: evaluating renal masses. Radiology 2005;236:441–450.

Israel GM, Bosniak MA. Pitfalls in renal mass evaluation and how to avoid them. Radiographics 2008;28:1325–1338.

Bosniak MA. The small (≤ 3.0 cm) renal parenchymal tumor: detection, diagnosis, and controversies. Radiology 1991;179:307–317.

# CASE 8

**RICHARD A.
LEDER**

**AND**

**DANIELE MARIN**

## HISTORY

A 33-year-old man has a history of urinary tract infections.

A

**FIGURE 4-8A** Anteroposterior film of the kidneys, ureters, and bladder from an intravenous urogram shows two collecting systems on the left side of the abdomen. On this film, only the distal left ureter is seen

B

■**FIGURE 4-8B** Anteroposterior coned view of the pelvis from the intravenous urogram shows normal insertion into the bladder trigone of both the left and right ureters.

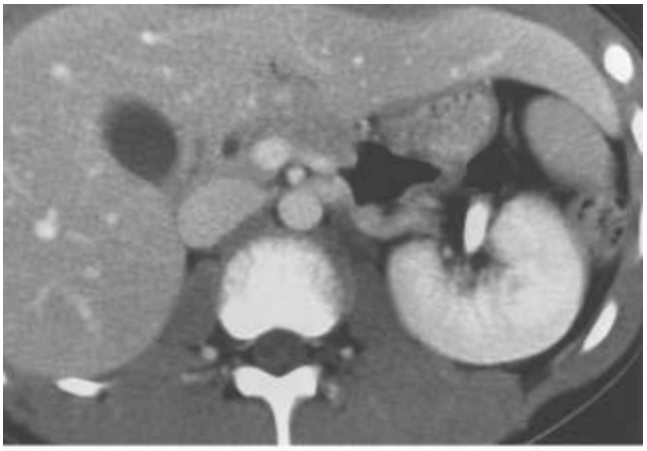

C

■**FIGURE 4-8C** Contrast-enhanced CT of the midabdomen shows enhancement of the left kidney, with absence of renal tissue in the right renal fossa.

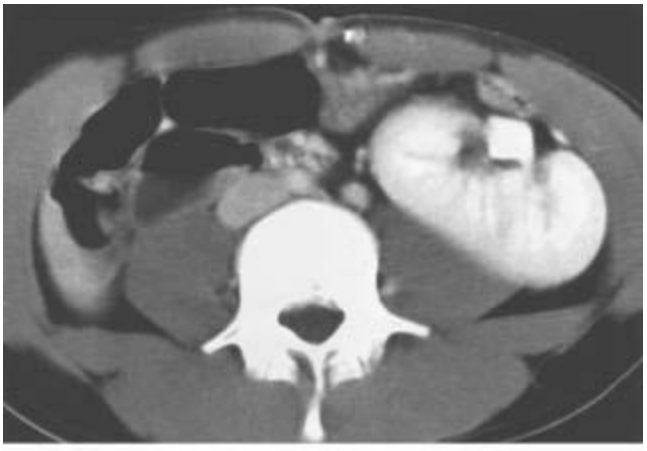

D

■**FIGURE 4-8D** Contrast-enhanced CT of the lower abdomen. The right kidney is

present in the left lower quadrant.

## DIFFERENTIAL DIAGNOSIS

- **Retroperitoneal mass with displacement of the kidney:** This diagnosis is unlikely due to the absence of an obvious abdominal mass.
- **Renal duplication with agenesis of the contralateral kidney:** Although renal duplication may cause enlargement of the kidney and could account for the presence of two left ureters, this diagnosis can be ruled out with a careful inspection of the course of both ureters, which demonstrates crossing of one ureter into the opposite side of the pelvis and normal insertion in the bladder trigone.
- **Crossed renal ectopia:** This is the most likely diagnosis, given the position of the kidneys and the insertion of the ureters.

## DIAGNOSIS

**Crossed renal ectopia**

## KEY FACTS

### Clinical

- There are four types of crossed renal ectopia: (i) crossed renal ectopia with fusion, (ii) crossed renal ectopia without fusion, (iii) solitary crossed renal ectopia, where monolateral renal agenesis is associated with ureteral insertion on the opposite side of the solitary kidney, and (iv) bilateral crossed renal ectopia, where both kidneys are crossed to the opposite side of the abdomen with their ureters inserting into the contralateral ureterovesicle junction.
- The most common varieties are fused and unfused ectopia; crossed fused ectopia occurs in 85% to 90% of cases.
- Crossed renal ectopia is seen more commonly in males than females.
- The most common scenario is the left kidney crossing to the right side of the abdomen.
- There are associated urinary tract abnormalities, including obstruction, stones, infection, vesicoureteral reflux, primary megaureter, hypospadius, cryptorchi-dism, urethral valves, and multicystic dysplastic kidney.
- There are associated abnormalities of other organ systems, including skeletal anomalies, unilateral ovarian and fallopian tube agenesis, and cardiac and gastrointestinal anomalies.
- Theories of occurrence include faulty development of the ureteral bud with crossing of the midline to contact the contralateral metanephric blastema, obstruction of renal ascent

by blood vessels, and local environmental factors involving surrounding tissues and organs.

### Radiologic

- The most common form of crossed renal ectopia is a crossed fused ectopia. Radiographically, this can be diagnosed on either ultrasound, CT, or intravenous urography when renal tissue lies on the opposite side of the abdomen from its ureteral insertion, and renal tissue from the crossed kidney fuses with the kidney native to that side of the abdomen. Helical CT, particularly using coronal reformation, or MRI may be useful in distinguishing fused from unfused ectopia.
- CT is also useful for excluding secondary causes of renal displacement, such as large retroperitoneal masses.
- Patients with this abnormality are usually asymptomatic, although they may present with a palpable abdominal mass or a history of repeated urinary tract infections.

## SUGGESTED READING

Gay SB, Armistead JP, Weber ME, Williamson BR. Left infrarenal region: anatomic variants, pathologic conditions, and diagnostic pitfalls. Radiographics 1991;11:549–570.

Silva JM, Jafri SZH, Cacciarelli AA, et al. Abnormalities of the kidney: embryogenesis and radiologic appearance. Appl Radiol 1995;24:19–24.

# CASE 9

**RICHARD A. LEDER**

**AND**

**DANIELE MARIN**

### HISTORY

A 60-year-old man presents with a palpable right-sided abdominal mass, flank pain, and hematuria.


A

■**FIGURE 4-9A** Transabdominal ultrasound of the right kidney in the longitudinal plane shows a solid, hyperechoic, partially exophytic mass at the lower pole.

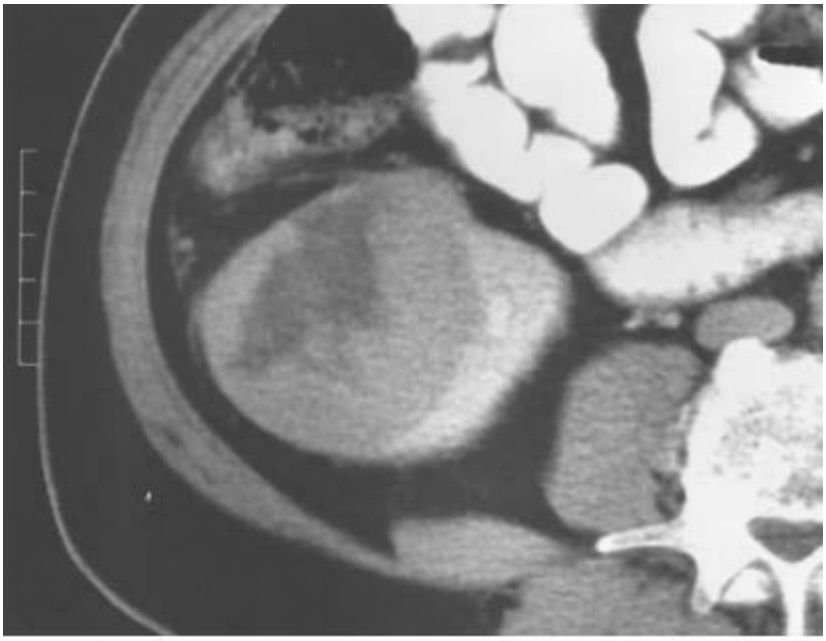

B

■**FIGURE 4-9B** Contrast-enhanced CT shows a large, solid mass in the right kidney. Within the central and lateral portion of the mass, there is a broad area of decreased attenuation, corresponding to areas of cystic tumor necrosis.

## DIFFERENTIAL DIAGNOSIS

■**Renal cell carcinoma (RCC):** The imaging features in this case reveal the presence of a solid, enhancing right renal mass with features that are consistent with RCC. The

broad area of low attenuation within the mass could represent internal hemorrhage or necrosis.

- **Oncocytoma:** There are no imaging features that confidently allow for the diagnosis of a benign oncocytoma. However, this diagnosis belongs in the differential diagnosis of a solitary renal mass in a patient who has no evidence of metastatic disease (no retroperitoneal lymphadenopathy and no osseous, hepatic, or pulmonary parenchymal metastases).
- **Renal metastasis:** Metastatic disease to the kidney is uncommon and would be only included in the differential diagnosis of patients with a known primary malignancy, most commonly lung, breast, or colon cancer. No such history existed in this patient.
- **Angiomyolipoma:** The diagnosis of angiomyolipoma is made when fat is detected within a renal mass. It is possible that given sufficient hemorrhage within an angiomyolipoma, no fat may be detected. No fat was detected within this mass, and there was no evidence of subcapsular or perinephric hemorrhage.
- **Lymphoma:** This patient has no history of non-Hodg-kin's lymphoma. Furthermore, no retroperitoneal lymphadenopathy is present, although lymphomatous masses may exist within the kidneys in the absence of lymphadenopathy.

## DIAGNOSIS

**Renal oncocytoma**

## KEY FACTS

### Clinical

- An "oncocyte" is a transformed epithelial cell with an enlarged, homogeneous, dense cytoplasm filled with acidophilic granules.
- Microscopically, a renal oncocytoma is characterized by eosinophilic epithelial cells with protuberant mitochondria within the cytoplasm.
- A renal oncocytoma has a distal tubular or collecting duct origin.
- On gross examination, lesions are well circumscribed, often encapsulated, without necrosis or hemorrhage. A central stellate scar may be present.
- The right kidney is affected as often as the left kidney. Cases of bilateral synchronous tumors have been reported.
- The tumor size ranges from 0.1 to 26.0 cm.
- The age at diagnosis ranges from 26 to 94 years.
- There is a 1.63 to 1.0 male-to-female ratio.
- Less than one-third of patients will present with the classic triad of renal cell tumors,

including flank pain, hematuria, with a palpable abdominal mass.

- Rarely, renal oncocytomas may demonstrate a malignant growth pattern with distant metastatic disease.

## Radiologic

- Ultrasound shows a homogeneous, isoechoic to hyperechoic, well-marginated mass. These are indistinguishable from RCC.
- Although rarely performed, angiography may demonstrate a "spoke-wheel" appearance due to the characteristic vascular architecture of the tumor. Other common but less specific angiographic findings include a dense parenchymal blush and no contrast media puddling, arteriovenous shunting, or renal vein invasion as commonly seen in RCC.
- On CT, oncocytomas demonstrate well-defined and smooth margins, with or without a central stellate scar. Lesions demonstrate intense and homogeneous enhancement after dynamic administration of contrast material.
- Only 67% of large oncocytomas (> 3 cm) and 82% smaller tumors (< 3 cm) demonstrate typical imaging findings at CT (i.e., homogeneous attenuation throughout the tumor, a central, sharply marginated stellate area of low attenuation). In the remaining cases (33% and 18%, respectively), CT in unable to differentiate oncocytomas from RCC.
- On MRI, oncocytomas show homogenous, low signal intensity on T1-weighted images and high signal intensity on T2-weighted images. The presence of a capsule or a central stellate scar and the absence of either internal hemorrhage or necrosis also favor this diagnosis.

## SUGGESTED READING

Davidson AJ, Hayes WS, Hartman DS, et al. Renal oncocytoma and carcinoma: failure of differentiation with CT. Radiology 1993;186:693–696.

Hélénon O, Merran S, Paraf F, et al. Unusual fat-containing tumors of the kidney: a diagnostic dilemma. Radiographics 1997;17:129–144.

Velasquez G, Glass TA, D'Souza VJ, Formanek AG. Multiple oncocytomas and renal carcinoma. AJR Am J Roentgenol 1984;142:123–124.

# CASE 10

**RICHARD A.**
**LEDER**

**AND**

**DANIELE MARIN**

## HISTORY

A 48-year-old man was referred for CT after seeing his ophthalmologist.

A

■**FIGURE 4-10A** Noncontrast CT of the abdomen shows enlargement of both the head and tail of the pancreas, although it is difficult to determine whether there are solid or cystic lesions present. There is marked deformity of the right kidney, with a hydrocalyx containing a small calculus in the upper pole, exophytic renal masses, and a solid mass medially.

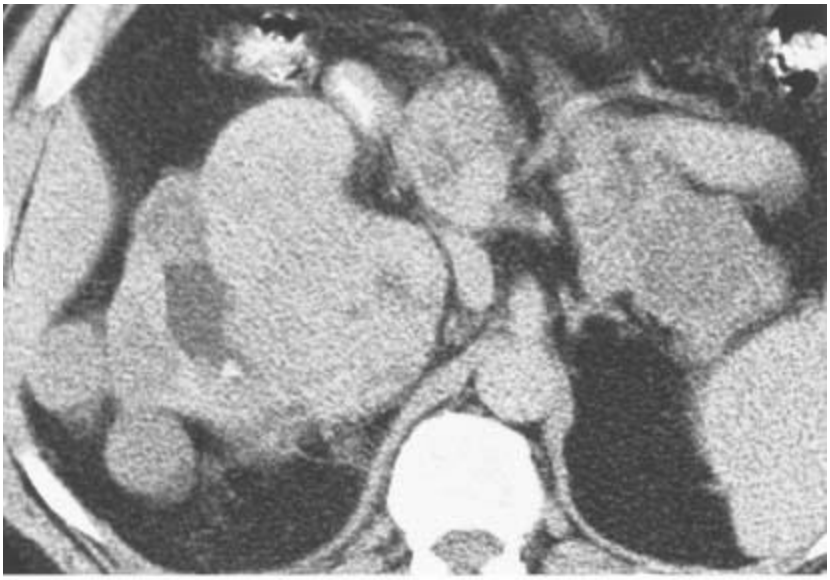

B

**FIGURE 4-10B** Corresponding contrast-enhanced CT demonstrates multiple low-attenuation lesions in the pancreatic head and tail and an enhancing solid mass in the medial aspect of the right kidney. Additional exophytic masses are also noted in the right kidney.

## DIFFERENTIAL DIAGNOSIS

**Multiple RCCs in a patient with von Hippel-Lindau (VHL) disease:** The constellation of bilateral renal enlargement with multiple solid and cystic lesions in combination with solid and cystic pancreatic lesions is virtually diagnostic of VHL. The patient was seeing the ophthalmologist because of a retinal angioma.

## DIAGNOSIS

**VHL disease with multiple RCCs**

## KEY FACTS

### Clinical

- VHL is characterized by retinal angiomas, central nervous system hemangioblastomas, cystic and solid tumors of the pancreas, pheochromocytomas, renal cysts, and RCCs.
- Inheritance follows an autosomal dominant pattern. Common clues leading to a clinical suspicion of VHL include a family history of VHL, pheochromocytoma or RCC, an epididymal cystadenoma, bilateral multifocal RCC, bilateral multifocal renal cysts, bilateral pheochromocytomas, an RCC in a patient < 30 years of age, pancreatic cysts, multiple hemangioblastomas of the central nervous system, and retinal angiomas.
- Early symptoms are usually caused by cerebellar and retinal tumors.

- Renal involvement is characterized by multiple bilateral cysts and RCCs. The mean age of presentation of RCC is approximately 39 years; this is 20 years earlier than the mean age for sporadic RCC. RCC in VHL has a slight male predominance.

## Radiologic

- RCC has been reported in 28% to 45% of patients with VHL. Other common renal lesions in these patients include renal cysts (59% of patients) and renal adenomas (14%).
- Renal involvement is characterized by multiple bilateral cysts and RCCs.
- Renal involvement in VHL is multicentric and bilateral in up to 75% of patients.
- Renal cysts in VHL may present a simple or complex appearance due to the presence of solid papillary projections into cystic lumina. Small nodules of tumor may be found in the walls of cysts. Cysts may grow, typically at a rate of 0.5 cm/year; other cysts involute over time, leaving small scars on the renal surface. Extensive cystic disease in VHL can mimic autosomal dominant polycystic kidney disease.
- RCCs in patients with VHL grow at the rate of 0.2 to 2.2 cm/year, which is faster than that of patients with sporadic RCC.
- CT is more sensitive for small lesions (< 2 cm). Thin section, contrast-enhanced CT is mandatory for the evaluation of renal lesions in patients with VHL. Yearly radiographic imaging with either ultrasound, CT, or MR imaging is recommended to survey for renal lesions.
- Small renal lesions can be managed noninvasively. Nephron sparing surgery tend to be performed for lesions larger than 2 to 3 cm in size. After surgery is performed, close imaging follow-up is recommended. Approximately 7% to 18% of all patients with VHL have pheochromocytomas. Pheochromocytomas when associated with VHL are often multiple and frequently occur at extra-adrenal sites; approximately 50% to 80% are bilateral.
- Pancreatic lesions also occur in the setting of VHL, including pancreatic cysts, serous microcystic adenomas, and adenocarcinomas. Cysts are present throughout the pancreas and have no predilection for a particular site. Lesions range from several millimeters in size to > 10 cm.
- A serous cystadenoma is a grape-like cluster of multiple microscopic and macroscopic cysts separated by thickened walls of stroma. There may be a central nidus, which may be calcified or scar-like.
- Cysts and cystadenomas of the pancreas are benign in patients with VHL and need not be removed.
- Additional lesions present in a patient with VHL include papillary cystadenomas of

the epididymis (10% to 26% of men with VHL). Epididymal cystadenomas can be unilateral or bilateral and are often found in the globus major. Lesions range in size from 1 to 5 cm but are typically 2 to 3 cm.

## SUGGESTED READING

Choyke PL, Glenn GM, Walther MM, et al. The natural history of renal lesions in von Hippel-Lindau disease: a serial CT study in 28 patients. AJR Am J Roentgenol 1992;159:1229–1234.

Sheth S, Scatarige JC, Horton KM, et al. Current concepts in the diagnosis and management of renal cell carcinoma: role of multidetector CT and three-dimensional CT. Radiographics 2001;21:S237-S254.

Suh M, Coakley FV, Qayyum A, et al. Distinction of renal cell carcinomas from high-attenuation renal cysts at portal venous phase contrast-enhanced CT. Radiology 2003;228:330–334.

# CASE 11

**KELLY S.**
**FREED**

**AND**

**DANIELE MARIN**

### HISTORY

A 41-year-old man involved in a motor vehicle accident presents with microscopic hematuria.

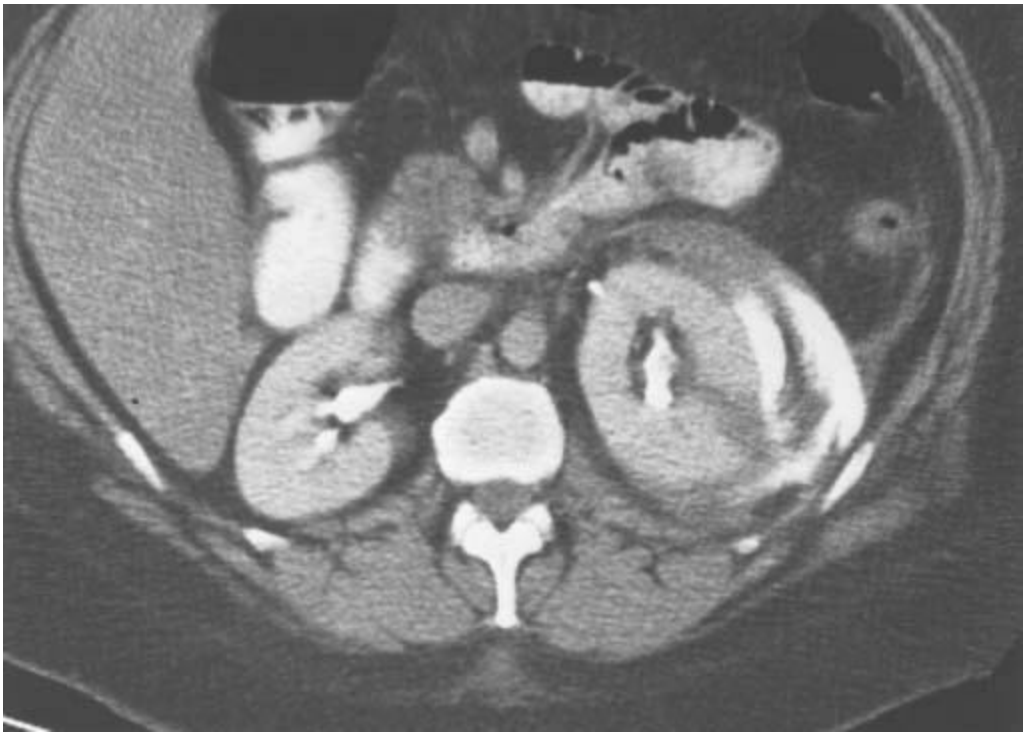

**FIGURE 4-11** Contrast-enhanced CT at the level of the kidneys. A linear defect is noted in the lateral aspect of the lower pole of the left renal parenchyma. There is disruption of the renal capsule, with blood and extravasated contrast material in the left perinephric space.

## DIFFERENTIAL DIAGNOSIS

- **Renal contusion:** A renal contusion can be diagnosed as a hypoperfused area on postcontrast CT. There may be subtle changes in the perinephric fat and subcutaneous tissues to indicate a traumatic injury.
- **Renal laceration:** A renal laceration appears as a linear defect in the nephrogram on the CT evaluation. Lacerations may be either minor or major. A minor laceration does not extend to the level of the collecting system, whereas a major laceration involves the collecting system. A minor laceration will most often be accompanied by a perinephric hematoma; a major laceration is accompanied by both hematoma and urinoma.
- **Renal fracture:** A renal fracture is diagnosed when there is cleavage of the kidney into two separate portions. These injuries often occur along planes that spare renal vasculature; therefore, enhancement is seen in both portions of the fractured kidney.
- **Subcapsular hematoma:** A subcapsular hematoma is identified as a fluid collection contained within the renal capsule. This is easily diagnosed on noncontrast CT as a high-density fluid collection.
- **Renovascular injury:** Renovascular injuries are identified by nonenhancement of the kidney. Absence of the nephrogram is referred to as a *negative CT nephrogram.* Loss of

the pyelogram postcontrast is called a *negative CT pyelogram.* Arterial renal vascular injuries may be secondary to thrombosis or laceration; thrombosis is more common. Given appropriate imaging, cut-off may be seen in the renal artery after a bolus of contrast material, the so-called renal artery cutoff sign. Renal vein injuries tend to be lacerations as opposed to thrombotic in nature. In these cases, large retroperitoneal hematomas can occur without significant renal parenchymal injury.

## DIAGNOSIS

**enal laceration with perinephric hematoma/Airinoma**

## KEY FACTS

### Clinical

- Hematuria may be found in patients with injury to the genitourinary system, as well as in patients with intraabdominal injury not related to the genitourinary system. The degree of hematuria does not reflect the severity of the injury. Furthermore, patients may have severe injury to the genitourinary system, including a renal pedicle injury, without the presence of hematuria.
- Traumatic injury to the kidney may cause a renal laceration or fracture, a contusion, a subcapsular hematoma, or a renovascular injury. Although many renal injuries, such as contusions or minor lacerations, are managed conservatively, surgery is generally indicated in patients with a shattered kidney or a renovascular injury.

### Radiologic

- A contrast-enhanced CT of the abdomen and pelvis is the single best imaging modality to evaluate the nature and extent of renal injury in the trauma setting. However, if renal vascular injury is suspected and the CT is negative or equivocal, angiography may be required.
- Renal contusion is manifest as a focal area of renal parenchyma that does not enhance to the degree of normal renal parenchyma, without evidence of laceration or fracture.
- A renal laceration is a focal parenchymal tear, demonstrated as an area of decreased attenuation within the renal parenchyma, as in this case. The tear often extends to involve the collecting system, resulting in extravasation of blood and urine into the perinephric space. In the early phase of contrast media excretion, the perinephric fluid may be of relatively low attenuation. Delayed images, however, are very helpful in confirming extravasation, because there will be progressive opacification of this fluid.
- A renal fracture implies cleavage or transection of the kidney into two poles, with extravasation of blood and urine.

- A shattered kidney denotes multiple fractures or fragments.
- On CT, a subcapsular hematoma is seen as a high-attenuation fluid collection in the perinephric region, often lenticular in shape, that may cause mass effect or flattening of the renal cortex.
- A renal vascular injury may be identified by extravasation of venous or arterial contrast material, or as focal or global areas of nonenhancement of renal parenchyma.

## SUGGESTED READING

Alonso RC, Nacenta SB, Martinez PD, et al. Kidney in danger: CT findings of blunt and penetrating renal trauma. RadioGraphics 2009;29:2033–2053.

Kawashima A, Sandler CM, Corl FM, et al. Imaging of renal trauma: a comprehensive review. Radiographics 2001;21:557–574.

Smith JK, Kenney PJ. Imaging of renal trauma. Radiol Clin North Am 2003;41:1019–1035.

# CASE 12

**RICHARD A. LEDER**

**AND**

**DANIELE MARIN**

## HISTORY

A 52-year-old Asian woman presents with left flank pain.

A

■**FIGURE 4-12A** Contrast-enhanced CT of the upper portion of the kidneys shows a water attenuation lesion (+10 Hounsfield units) in the left upper pole. The wall of this lesion is thick and enhances medially.

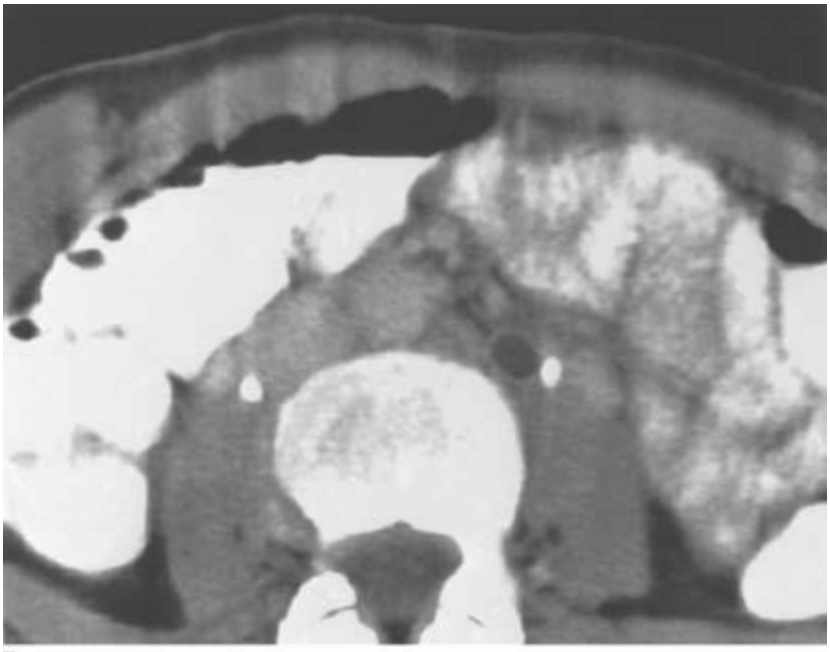

B

■**FIGURE 4-12B** Contrast-enhanced CT through the proximal ureters shows contrast enhancement of ureters bilaterally, with a water attenuation circular structure adjacent and medial to the proximal left ureter. On more cranial CT sections (not shown), this structure demonstrates direct communication with the cystic renal lesion of the left upper pole.

## DIFFERENTIAL DIAGNOSIS

- **Complicated renal cyst of the left upper pole:** The water attenuation of the lesion may be suggestive for a simple cyst; however, the perceptible wall excludes the diagnosis of a simple cyst. A cyst that is infected or hemorrhagic could have this appearance.
- **Cystic RCC:** Some RCCs are cystic or may mimic cystic renal lesions due to extensive necrosis or hemorrhage.
- **Renal abscess:** An infection within the kidney that has liquefied could have this appearance. It is helpful in these cases to correlate imaging findings with urinalysis and characteristic clinical signs of infection, such as fever, leukocytosis, and flank pain.
- **Ureteral duplication with obstruction of the upper pole moiety:** This diagnosis can be made due to the presence of the fluid attenuation tubular structure adjacent to the left ureter. This tubular structure may be confused with a thrombosed gonadal vein, and therefore its path must be followed. If this tubular structure enters the left renal vein, a thrombosed gonadal vein can be diagnosed. If this tubular structure is in continuity with the cystic upper pole mass, the diagnosis of an obstruction duplicated system can be made with confidence. This will subsequently be confirmed by cystoscopy, with the identification of two ureteral orifices on this side.

## DIAGNOSIS

**Complete ureteral duplication with obstruction of the upper pole collecting system**

## KEY FACTS

### Clinical

- Patient with obstruction of the upper pole moiety may present with nonspecific abdominal pain; this is the most common complaint leading to clinical evaluation.
- Alternatively, patients may present with lower urinary tract signs and symptoms related to the ectopic insertion of the duplicated ureter—for example, incontinence.
- Other clinical presentations in these patients are related to the obstruction of the upper pole moiety, which predisposes to both calculus disease and urinary infection.

### Radiologic

- Duplication anomalies of the kidney are relatively common. In patients with a completely duplicated excretory system, both ureters may insert orthotopically; in most cases, however, the ureter arising from the upper pole moiety inserts ectopically either intravesically or extravesically. Patients most often present with symptoms related to obstruction of the upper pole moiety or reflux into the lower pole moiety.
- Imaging is useful for documenting the presence of complete duplication and whether

the upper pole is obstructed. CT is useful for evaluating the amount of residual parenchyma in the upper pole. Cystography is frequently used to document reflux. Ultrasound can image the obstructed upper pole but usually cannot image the entire ureter.

## SUGGESTED READING

Cramer BC, Twomey BP, Katz D. CT findings in obstructed upper moieties of duplex kidneys. J Comput Assist Tomogr 1983;7:251–253.

Cronan JJ, Amis ES, Zeman RK, Dorfman GS. Obstruction of the upper-pole moiety in renal duplication in adults: CT evaluation. Radiology 1986;161:17–21.

Fernbach SK, Feinstein KA, Spencer K, Lindstrom CA. Ureteral duplication and its complications. Radiographics 1997;17:109–127.

# CASE 13

**VINCENT G. MCDERMOTT**

**AND**

**DANIELE MARIN**

## HISTORY

A 48-year-old woman is referred for renal ultrasound following a urinary tract infection.

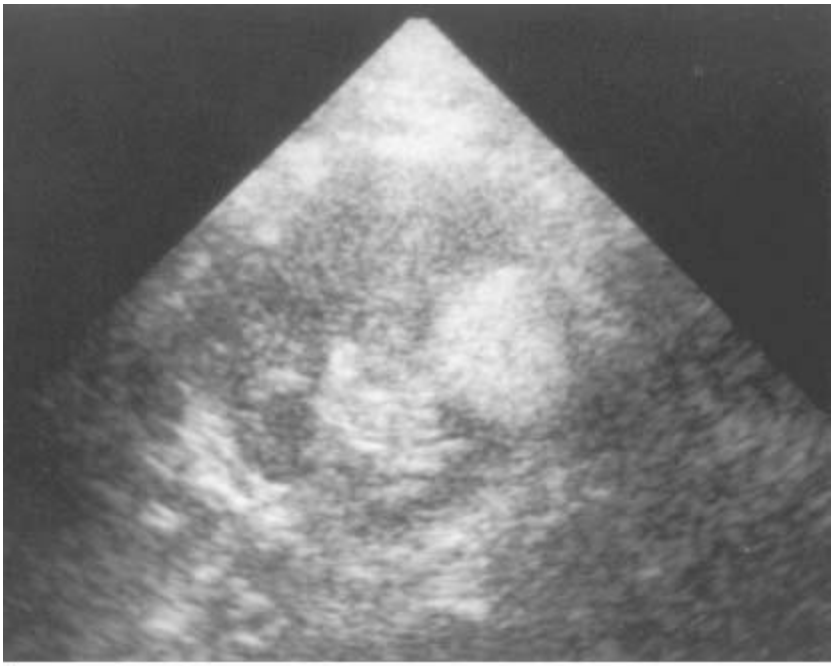

A

■**FIGURE 4-13A** Ultrasound of the left kidney in the transverse plane demonstrate a 2.5-cm, well-demarcated, hyperechoic lesion in the posterior mid cortex.

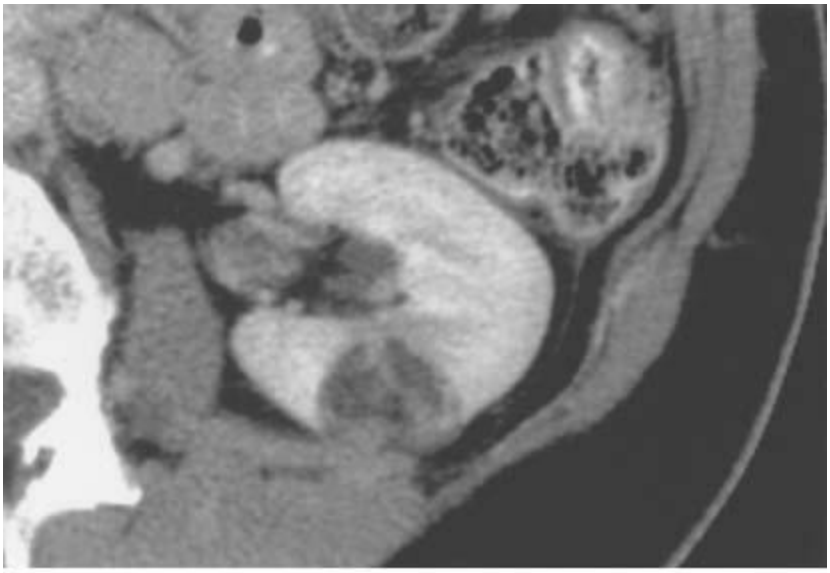

B

■**FIGURE 4-13B** On corresponding contrast-enhanced CT, this lesion shows a complex appearance with coexistence of both solid enhancing and fat-attenuating (-18 HU) areas.

## DIFFERENTIAL DIAGNOSIS

■**RCC:** Approximately 30% of small RCCs are markedly hyperechoic at ultrasound. Hyperechoic areas may correspond to fat-attenuating foci at CT. This finding may be related to lipid-producing necrosis in the tumor, entrapment of the perinephric fat from

large exophytic tumors or, rarely, osseous metaplasia.

- **Lipoma:** A lipoma is a rare benign tumor of the kidney composed of adipose tissue.
- **Liposarcoma:** A renal liposarcoma is usually located peripherally, beneath the renal capsule. The tumor is large and bulky and extends into the perirenal space.
- **Fat-containing renal oncocytoma:** Fat may be seen within large oncocytomas due to entrapment of perinephric or sinus fat.
- **Adrenal myelolipoma:** Multiplanar imaging with either CT or MR should help in the differential diagnosis between a fat-containing adrenal mass and a fat-containing renal mass.
- **Renal angiomyolipoma (AML):** This is the most likely diagnosis for a fat-containing renal mass.

# DIAGNOSIS

**Renal AML**

# KEY FACTS

## Clinical

- AMLs are benign hamartomas composed of fat, smooth muscle, and blood vessels.
- Around 80% of AMLs are solitary; they occur sporadically, and they are most common in women 40 to 60 years of age.
- Twenty percent are multiple and bilateral, usually in association with tuberous sclerosis.
- These tumors are usually an incidental finding.
- Hemorrhage may occur when lesions are large, producing hematuria, flank pain and, in severe cases, hypovolemic shock.
- Treatment of AMLs includes embolization or resection and is indicated for lesions > 4 cm in diameter due to the high potential risk of spontaneous hemorrhage.

## Radiologic

- Plain films may reveal subtle lucencies due to fat content; however, this finding is seen in < 10% of cases. Calcifications are seldom seen and, if present, may also suggest a RCC.
- Intravenous urography reveals a nonspecific mass, which is frequently exophytic.
- Ultrasound demonstrates a well-demarcated, highly echogenic renal mass, although echo-poor areas may be seen due to internal necrosis or hemorrhage, particularly in larger tumors.

- On CT, either with or without contrast material, the presence of fat (< -10 HU) is diagnostic of AML. In the minority of cases, however, the fat component may be negligible and cannot be seen at imaging.
- With angiography, 95% of the tumors are hypervascular, with dilated arteries. Angiography, however, is rarely performed unless embolization is recommended.
- On MRI, there is variable high signal intensity on T1-weighted images and intermediate signal intensity on T2-weighted images depending on the fat content. Fat suppressing sequences may increase the sensitivity for fat detection within the lesion.

## SUGGESTED READING

Halpenny D, Snow A, McNeill G, Torreggiani WC. The radiological diagnosis and treatment of renal angiomyolipoma-current status. Clin Radiol 2010;65:99–108.

Jinzaki M, Tanimoto A, Narimatsu Y, et al. Angiomyolipoma: imaging findings in lesions with minimal fat. Radiology 1997;205:497–502.

Lemaitre L, Claudon M, Dubrulle F, Mazeman E. Imaging of angiomyolipomas. Semin Ultrasound CT MR 1997;18:100–114.

Obuz F, Karabay N, Secil M, et al. Various radiological appearances of angiomyolipomas in the same kidney. Eur Radiol 2000;10:897–899.

# CASE 14

**RICHARD A. LEDER**

**AND**

**DANIELE MARIN**

## HISTORY

A 60-year-old man has a palpable abdominal mass on the left.


A

■**FIGURE 4-14A** Noncontrast CT of the abdomen shows a large cystic lesion in the left kidney with a peripheral solid nodule.

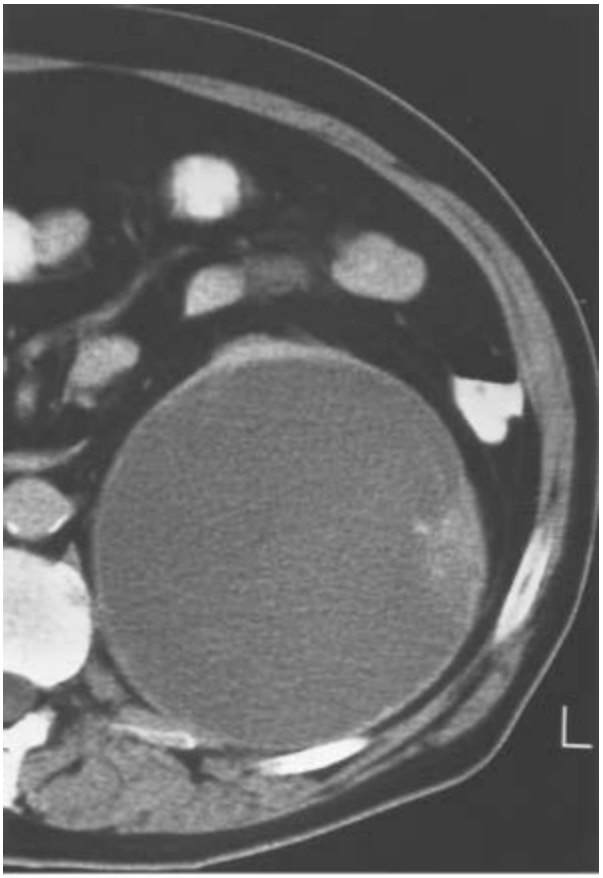


B

**FIGURE 4-14B** Corresponding contrast-enhanced CT image demonstrates contrast enhancement (> 10 HU increase in attenuation compared to the noncontrast scan) of both the solid nodule and the thickened cystic wall.

## DIFFERENTIAL DIAGNOSIS

- **Renal abscess:** This diagnosis is unlikely due to absence of associated clinical signs of infection, such as fever, leukocytosis, and pyuria. Although renal abscesses may present with a thickened, enhancing wall, this lesions are commonly accompanied by inflammatory findings in the perinephric fat, which cannot be seen in this case.
- **Hemorrhagic cyst:** Over time the attenuation within a hemorrhagic renal cyst may decrease, causing an old hemorrhagic cyst to have a more cystic appearance. The eccentric, lateral wall prominence that enhances, however, prevents one from calling this lesion a hemorrhagic cyst.
- **Cystic RCC:** This is the most likely diagnosis for a cystic renal mass with an enhancing mural nodule.

## DIAGNOSIS

**Cystic RCC (Bosniak type 4 lesion)**

## KEY FACTS

### Clinical

- Patients with RCC may present with the classic triad of pain, mass, and hematuria.
- Other symptoms include fatigue, malaise, anorexia, weight loss, fever, and anemia.
- Men are most commonly afflicted, with a male-to-female ratio of 2:1.
- Patients are typically in the sixth to seventh decade.

### Radiologic

- A Bosniak type 4 cyst is one that clearly has malignant features as well as large cystic components. Lesions in this category show irregular margins and one or more solid enhancing components and should be treated surgically.
- Cysts are sometimes complicated by the presence of calcifications, septations, abnormal attenuation, wall thickening, or nodularity. A solid nodule within a cyst lumen that enhances is a feature that indicates the presence of a malignancy with high reliability. Vascularity within the nodule combined with nodular thickening of a cyst wall is also a clear indication of malignancy.
- This lesion should not be classified as a Bosniak type 3 lesion. Type 3 cysts exhibit some of the features of malignant lesions and radiographically cannot be distinguished from malignancy. Resection is necessary to distinguish a benign from a malignant lesion.
- A multilocular cystic nephroma is a benign Bosniak type 3 lesion, while a multicystic RCC is a malignant Bosniak type 3 lesion. These two tumors may be indistinguishable radiographically.

## SUGGESTED READING

Bosniak MA. The small (<3.0 cm) renal parenchymal tumor: detection, diagnosis, and controversies. Radiology 1991;179:307–317.

Israel GM, Bosniak MA. How I do it: evaluating renal masses. Radiology 2005:236:441–450.

Israel GM, Bosniak MA. Pitfalls in renal mass evaluation and how to avoid them. Radiographics 2008;28:1325–1338.

# CASE 15

**RICHARD A.**
**LEDER**

**AND**

**DANIELEMARIN**

**HISTORY**

**A 62-year-old man has a history of chronic urinary tract infections.**

**FIGURE 4-15** Anteroposterior view from a left retrograde pyelogram. Multiple small filling defects are present in the left ureter.

## DIFFERENTIAL DIAGNOSIS

**Blood clots:** Blood clots can cause multiple ureteral filling defects. One would expect that the patient would have an accompanying history of hematuria. Additional history may be helpful and could include known bleeding disorders or trauma.

- **Multiple ureteral stones:** Stones can cause multiple filling defects, although typically, due to their calcium content, stones are most often radiopaque. This limits their detectability on contrasted examinations. The fixed nature of the filling defects, as seen in this patient, would make this an unlikely possibility.
- **Multiple ureteral transitional cell carcinomas (TCCs):** While TCC has a propensity to be multifocal, this would represent an extremely rare manifestation of urothelial carcinoma. Correlation should be made with findings of urine cytology to establish whether malignant cells are present.
- **Ureteritis cystica:** This is one of several causes of multiple ureteral filling defects. Ureteritis cystica is often seen in the setting of chronic urinary tract infections.

## DIAGNOSIS

**Ureteritis cystica**

## KEY FACTS

### Clinical

- Ureteritis cystica is associated with chronic mucosal irritation secondary to inflammation.
- These lesions are secondary to degeneration and cavitation of metaplastic surface urethelium or submucosal Brunn's cell nests.
- Patients may be asymptomatic or have hematuria and symptoms of a urinary tract infection.
- These lesions are not premalignant.
- The lesions may be unilateral or bilateral.
- Females are affected slightly more with ureteritis cystica than males.
- Patients are typically 50 to 60 years old.

### Radiologic

- Lesions are typically 2 to 3 mm in size, although they can range from 1 mm to 2 cm in size.
- Lesions are multiple, smooth, well-rounded or oval filling defects with sharp borders.
- Lesions are said to predominate in the proximal ureter but may be seen throughout the ureter, in the renal pelvis (pyelitis cystica), or in the bladder (cystitis cystica).

## SUGGESTED READING

Frederick MG, Kakani L, Dyer RB. Ureteritis cystica and pseudodiverticulosis in ureteral stumps. Appl Radiol

1995;24:32–33.

Loitman BS, Chiat H. Ureteritis cystica and pyelitis cystica. Radiology 1957;68:345–351.

# CASE 16

**RICHARD A. LEDER**

**AND**

**DANIELE MARIN**

## HISTORY

A 76-year-old man has benign prostatic hypertrophy and bladder outlet obstruction.

A

■**FIGURE 4-16A** Anteroposterior compression view from an intravenous urogram shows multiple small left ureteral outpouchings.

B

**FIGURE 4-16B** Oblique compression view from an intravenous urogram confirms the presence of multiple proximal left ureteral outpouchings.

## DIFFERENTIAL DIAGNOSIS

- **True ureteral diverticula:** True diverticula are typically large, saccular, round or oval, and usually solitary. True diverticula fill slowly with contrast material during an intravenous urogram. Depending on their location, they may be confused with a hydroureter, a bladder diverticulum, or a large ureterocele.
- **Ureteritis cystica:** It is important to recognize that in ureteritis cystica, there are filling defects within the ureteral lumen. This case demonstrates ureteral out-pouchings as opposed to mural filling defects.
- **Ureteral pseudodiverticulosis:** The small ureteral out-pouchings present in this patient are characteristic of ureteral pseudodiverticulosis.

## DIAGNOSIS

**Ureteral pseudodiverticulosis**

## KEY FACTS

### Clinical

- Ureteral pseudodiverticulosis is a pathologic disease associated with urinary tract infections, obstruction, and stones.
- Patients may present with hematuria or symptoms of a urinary tract infection.
- Pathologically, these lesions are outpouchings of proliferated hyperplastic transitional epithelium extending into loose subepithelial connective tissue.
- The lesions do not extend through the muscularis propria; therefore, they are not true diverticula.
- Fifty percent of patients have epithelial cells with signs of atypia on urine cytology. A similar percentage of patients can progress to a TCC (most common site is the bladder).

### Radiologic

- The outpouchings are small, typically measuring 2 to 4 mm in diameter.
- The outpouching are nearly always multiple, numbering three to eight lesions per ureter.
- The findings are bilateral in 70% of cases.
- The abnormalities predominate in the proximal and mid ureter (85% of cases).
- Retrograde or antegrade urography is better than intravenous urography, which is positive in only 60% of cases.

## SUGGESTED READING

Wasserman NF. Pseudodiverticulosis: unusual appearance for metastases to the ureter. Abdom Imag 1994;19:376–378.

Wasserman NF, Pointe SL, Posalaky IP. Ureteral pseudodiverticulosis. Radiology 1985;155:561–566.

Wasserman NF, Zhang G, Posalaky IP, Reddy PK. Ureteral pseudodiverticula: frequent association with uroepithelial malignancy. AJR Am J Roentgenol 1991;157:69–72.

# CASE 17

**RICHARD A. LEDER**

**AND**

**DANIELE MARIN**

## HISTORY

A 22-year-old man presents with weight loss.

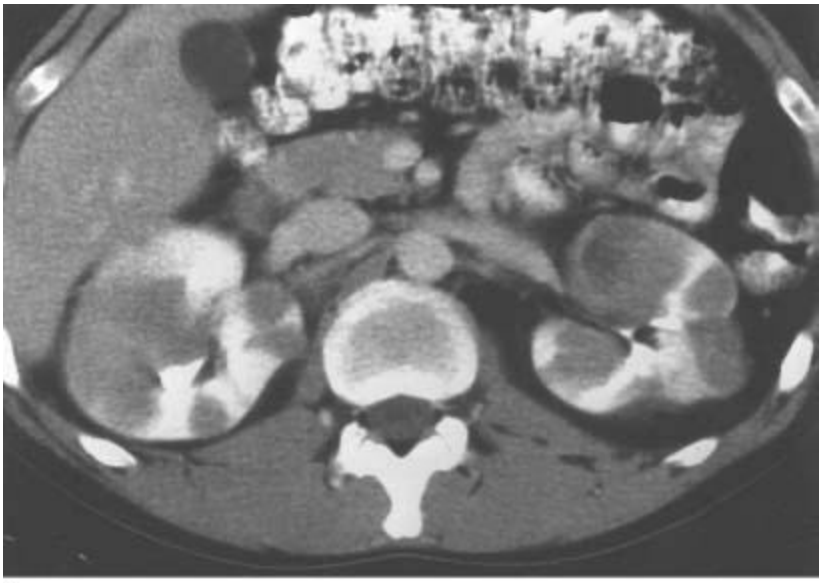

A

■**FIGURE 4-17A** Contrast-enhanced CT of the abdomen demonstrates bilateral enlargement of the kidneys with multiple, hypoattenuating, soft tissue masses (+35 Hounsfield units [HU]).


B

■**FIGURE 4-17B** Transabdominal ultrasound of the right kidney in the longitudinal plane shows a large, hypoechoic, solid mass in the upper pole.

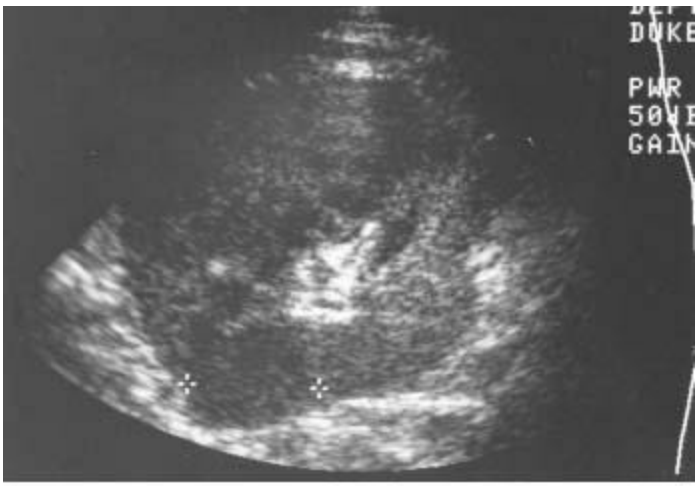


C

**FIGURE 4-17C** Transabdominal ultrasound of the lower pole of the left kidney in the transverse plane shows a hypoechoic but solid mass in the lower pole. Other images of the left kidney revealed additional mass lesions.

## DIFFERENTIAL DIAGNOSIS

- **Renal metastases:** Renal metastases may occur in patients with a primary tumor typically of the lung, breast, colon, or skin (melanoma). Renal metastases are usually discovered at autopsy rather than radio-graphically. To make a diagnosis of renal metastases, careful inspection should be made for potential additional sites of metastatic disease (lung, liver, adrenals, lymph nodes) as well as determination of appropriate clinical history.
- **Multifocal RCC:** While RCC can be multifocal, particularly in patients with VHL disease, this would be an uncommon appearance and presentation for this renal malignancy.
- **Lymphoma:** The most common presentation of renal lymphoma is that of bilateral renal masses. This can occur with or without accompanying retroperitoneal lymphadenopathy.
- **Hemorrhagic renal cysts:** Patients with autosomal-dominant polycystic kidney disease often experience hemorrhage into renal cysts. Clinical history as well as noncontrast imaging should permit the radiologist to determine whether the lesions are solid and enhancing or hemorrhagic.

## DIAGNOSIS

**Renal lymphoma**

## KEY FACTS

## Clinical

- Genitourinary lymphoma is most commonly of the non-Hodgkin's variety.
- Lymphoma involves the genitourinary tract in 10% to 50% of cases.
- Of patients with non-Hodgkin's lymphoma, 10% to 20% either present with or eventually suffer from genitourinary-related symptoms.
- Sites of involvement in the genitourinary tract in descending order of frequency include the kidneys, testes, bladder, and prostate.
- Symptomatically, patients may have vague abdominal pain, weight loss, fever, night sweats, anemia, and hematuria. Additional manifestations may include lymphadenopathy, hepatosplenomegaly, and a palpable abdominal mass.

## Radiologic

- The most common presentation of renal lymphoma on CT is bilateral soft tissue masses (61%). This can often occur without accompanying retroperitoneal lymph-adenopathy.
- The second most common presentation of renal lymphoma is that of invasion from retroperitoneal or perinephric masses.
- A third presentation is that of a single, bulky renal mass.
- The least common presentation is isolated lymphomatous disease in the perirenal space.
- Intravenous urography may show enlargement of one or both kidneys, a localized expanding mass, or masses with calyceal distortion.
- On ultrasound, lymphomatous masses are typically anechoic without posterior acoustical enhancement or hypoechoic.
- MRI may be used in patients in whom iodinated contrast material cannot be given. The multifocal nature of the disease process is usually readily apparent, particularly following the intravenous administration of a gadolinium-chelate.

## SUGGESTED READING

Sheth S, Ali S, Fishman E. Imaging of renal lymphoma: Patterns of disease with pathologic correlation. Radiographics 2006;26:1151–1168.

Urban BA, Fishman EK. Renal lymphoma: CT patterns with emphasis on helical CT. Radiographics 2000;20:197–212.

# CASE 18

**RICHARD A.**
**LEDER**

**AND**

**DANIELE MARIN**

## HISTORY

A 15-year-old boy has a history of urinary tract infections.

A

■**FIGURE 4-18A** Contrast-enhanced CT of the kidneys. There is similar enhancement of both kidneys, in combination with pelvicaliectasis on the right.

B

■**FIGURE 4-18B** Contrast-enhanced CT through the pelvis. There is a contrast/urine level within the dilated distal right ureter. The distal left ureter is normal in caliber.

C

**FIGURE 4-18C** Anteroposterior supine postvoid film from an intravenous urogram shows a markedly dilated, sausage-shaped distal ureter with "rat tail" narrowing at the ureterovesicle junction. The ureter is also dilated proximally, and there is mild pelvicaliectasis.

## DIFFERENTIAL DIAGNOSIS

**Right renal "obstruction" secondary to a distal right ureteral calculus:** While a stone with secondary edema could explain the narrowing of the distal ureter, the CT clearly shows that there was no delay in enhancement on the right side, and the "pelvicaliectasis" is more likely on the basis of congenital megacalyces. Clinically, the patient did not have renal colic, nor did he have hematuria.

**Distal right ureteral stricture:** While a stricture could cause narrowing of the distal ureter, the appearance of the proximal ureter and kidney suggests that there is no obstruction of the distal ureter.

**Primary megaureter:** The fusiform dilatation of the distal ureter above a narrowed segment is classic for primary megaureter. The associated megacalyces on the right also support this diagnosis.

## DIAGNOSIS

**Primary megaureter**

## KEY FACTS

### Clinical

- Primary megaureter has also been called *megaloureter, primary megaloureter, aperistaltic megaureter*, or *achalasia* of the ureter.
- In this condition, ureteral dilation occurs above a short, adynamic, extravesicle distal ureteral segment.
- The abnormal segment of distal ureter may have increased collagen between the muscle fibers at this level or a deficiency in longitudinal muscle.
- In adults, the lesion is 2.5 times more frequent on the left. In children, it is four times more frequent in boys, and bilateral involvement is almost exclusively a male disease. In all age groups, 20% of cases are bilateral.
- Surgery is considered in patients with infection, stones, persistent symptoms, or significant hydronephrosis. Mild cases may be followed radiographically.

### Radiologic

- This abnormal distal ureteral segment is approximately 1.5 cm long and does not transmit a peristaltic wave when examined fluoroscopically.
- There is a high association with other abnormalities of the genitourinary system. ureteropelvic junction obstruction may be found in 25% of cases. Contralateral reflux has been reported in 6% to 8% of cases, contralateral renal agenesis in 4% to 15%, contralateral ureteral duplication in 4% to 6%, a calyceal diverticulum in 4%, and contralateral ureterocele in 3%.
- Megacalyces, ipsilateral cryptorchidism, and ectopic ureteroceles have also occurred in association with this condition.

## SUGGESTED READING

Berrocal T, Lopez-Pereira P, Arjonilla A, Gutierrez J. Anomalies of the distal ureter, bladder, and urethra in children: embryologic, radiologic, and pathologic features. Radiographics 2002;22:1139–1164.

McLaughlin AP, Pfister RC, Leadbetter WF, et al. The pathophysiology of primary megaloureter. J Urol 1973;109:805–811.

Mellins HZ. Cystic dilatations of the upper urinary tract: a radiologist's developmental model. Radiology 1984;153:291–301.

# CASE 19

**DOUGLAS H. SHEAFOR**

**AND**

**DANIELE MARIN**

## HISTORY

A 32-year-old diabetic woman presents with dysuria.

A

**FIGURE 4-19A** Anteroposterior supine radiograph of the pelvis. Curvilinear and small rounded lucencies outline the expected location of the urinary bladder wall.

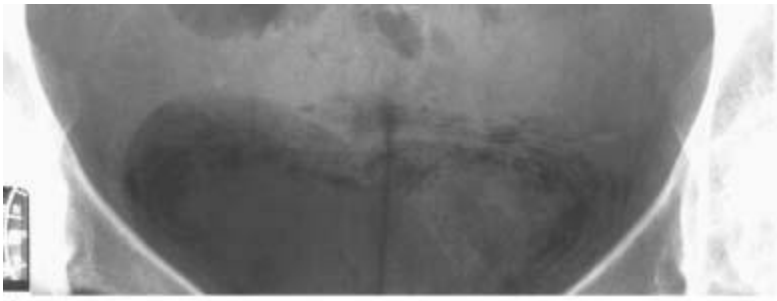

B

**FIGURE 4-19B** Anteroposterior coned down radiograph of the bladder dome. There are central lucencies within the bladder, with suggestive findings of bladder wall thickening.

## DIFFERENTIAL DIAGNOSIS

- **Enterovesicle fistula:** This is most commonly caused by diverticulitis, inflammatory bowel disease, or colorectal carcinoma. While intraluminal gas is characteristic, submucosal gas collections are uncommon.
- **Penetrating trauma:** In a patient with a history of knife or gunshot injury, a small amount of pelvic gas is possible, but it should not create such a large collection.
- **Instrumentation:** Intraluminal gas may be seen following cystoscopy, cystography, or Foley catheter placement. Again, linear submucosal gas would not be expected.
- **Pneumatosis intestinalis:** Gas within the wall of small or large bowel can have a linear appearance; however, the size and location of this abnormality strongly suggest bladder pathology.
- **Emphysematous cystitis:** This diagnosis is most likely in a diabetic patient with gas in the expected position of the bladder lumen and wall.

## DIAGNOSIS

**Emphysematous cystitis (cystitis emphysematosa)**

## KEY FACTS

### Clinical

- This is an uncommon inflammatory condition of the urinary bladder, usually with a transient and benign course.
- Gas localizes in the bladder submucosa, and often within the bladder lumen.
- E. coli is the most common causative organism, with glycosuria, stasis, neurogenic bladder, and chronic urinary tract infection as predisposing factors.
- The female-to-male ratio is 2 to 1.

- Symptoms include frequency, dysuria, and, occasionally, pneumaturia.
- Treatment consists of antibiotics, control of diabetes, and relief of obstruction, if present.

### Radiologic

- The plain radiograph is often diagnostic.
- Gas within the submucosa may be linear or have a cobblestone appearance.
- CT is rarely indicated but elegantly demonstrates gas within the lumen and within a thickened bladder wall.
- Ultrasound also depicts a thickened bladder wall and irregular echogenic foci with acoustic shadowing.

## SUGGESTED READING

Grayson DE, Abbott RM, Levy AD, Sherman PM. Emphysematous infections of the abdomen and pelvis: a pictorial review. Radiographics 2002;22:543–561.

Grupper M, Kravtsov A, Potasman I. Emphysematous cystitis: illustrative case report and review of the literature. Medicine 2007;86:47–53.

Thomas AA, Lane BR, Thomas AZ, et al. Emphysematous cystitis: a review of 135 cases. BJU Int 2007;100:17–20.

# CASE 20

**RICHARD A. LEDER**

**AND**

**DANIELE MARIN**

### HISTORY

A 72-year-old woman presents with hematuria.

A

■**FIGURE 4-20A** Anteroposterior postvoid film of the distal left ureter and bladder from an intravenous urogram shows a small “cobra head” deformity of the distal left ureter. There is also columnation on this side.

B

**FIGURE 4-20B** Anteroposterior film of the distal left ureter and bladder obtained before the postvoid film shows nodular thickening of the bladder wall just medial to the "cobra head" deformity in the distal left ureter.

## DIFFERENTIAL DIAGNOSIS

**Pseudoureterocele:** The eccentric halo just medial to the distal left ureterocele indicates there is a left pseudoureterocele.

**Ureterocele:** The postvoid film shows no evidence of a periureteral abnormality. The mucosa adjacent to the left ureterocele is not optimally imaged on the postvoid film and precludes the diagnosis of a pseudoureterocele. Given the patient's history of hematuria and what would otherwise appear to be a negative study, cystos-copy would follow, revealing bladder pathology adjacent to the distal left ureter.

## DIAGNOSIS

**Left-sided pseudoureterocele secondary to a TCC of the bladder**

## KEY FACTS

### Clinical

- Ureteroceles are due to a defect in the muscular layer of the ureter, often with a defect in the bladder wall itself.
- There are two types of ureteroceles: intravesicle and ectopic.
- Intravesicle ureteroceles may be unilateral or bilateral, and they are more often seen in females than in males. A "cobra head" defect is seen in the bladder, with a thin lucent line or halo around the lumen.
- Ectopic ureteroceles insert medially and caudally to the site of the normal ureteral orifice, often extending into the bladder neck or urethra.
- Pseudoureteroceles are secondary to edema from a ureteral stone, bullous edema of the bladder, or neoplastic disease. Neoplasms that can cause this appearance include TCC of the bladder or invasion of the bladder by squamous cell carcinoma of the cervix. Radiation cystitis can also lead to the appearance of a pseudoureterocele.

### Radiologic

- The cobra head deformity with a thin lucent halo is the typical finding in a ureterocele. Deformity or thickening of the surrounding halo is a worrisome finding. Further workup should include cystoscopy.
- Pseudoureteroceles are distinguished by asymmetry of the dilated ureteral lumen, moderate to severe obstruction of the upper tract, and evidence that this is an acquired abnormality.

## SUGGESTED READING

Thornbury JR, Silver TM, Vinson RK. Ureteroceles vs. pseudoureteroceles in adults. Radiology 1977;122:81–84.

# CASE 21

**JOHN A.
STAHL**

**AND**

**DANIELE MARIN**

### HISTORY

A 60-year-old man presents with left flank pain.

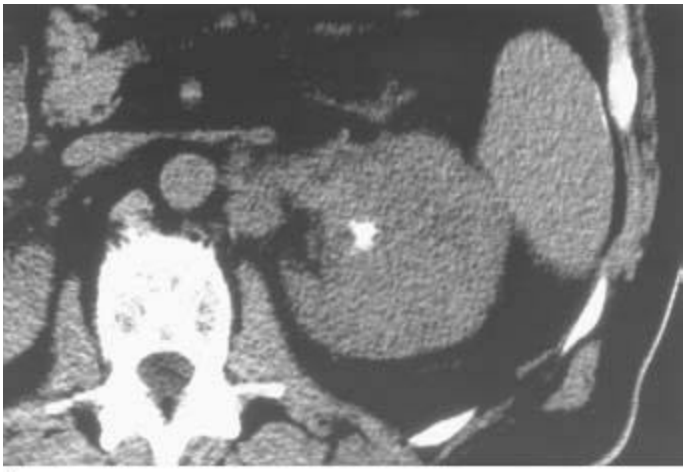

A

■**FIGURE 4-21A** Noncontrast CT of the left kidney. There is a large, low attenuation mass with calcifications located centrally within the left kidney.

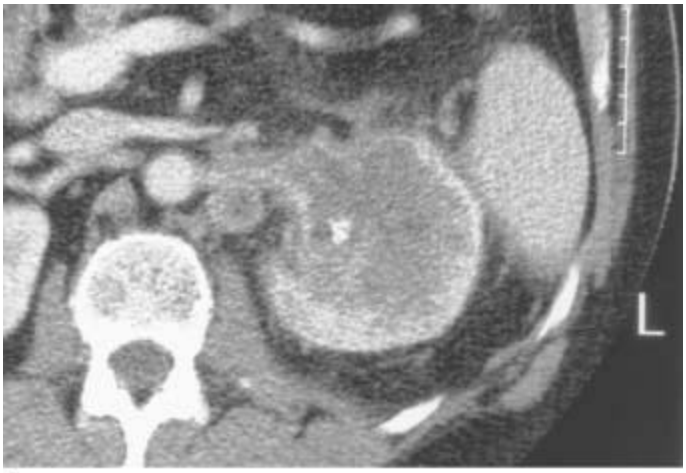


B

■**FIGURE 4-21B** Contrast-enhanced CT of the left kidney. The mass is seen to infiltrate both the hilum and parenchyma on the left. Tumor is also noted to extend beyond the renal capsule anteriorly, although it remains within Gerota's fascia. The left renal vein is spared.

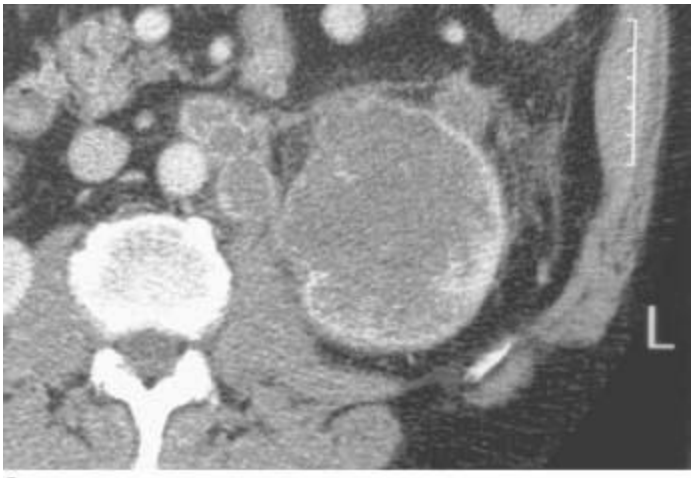


C

**FIGURE 4-21C** Contrast-enhanced CT of the left kidney at a more caudal level. Retroperitoneal lymphadenopathy, which has similar enhancement properties to the renal mass, is also seen in the left paraortic region.

## DIFFERENTIAL DIAGNOSIS

- **RCC:** Although RCC can occasionally manifest as a central renal mass with an infiltrative growth pattern, most lesions tend to be hypervascular on contrast enhanced CT.
- **TCC:** TCC originates from the urothelium of the pelvicaliceal system. There are many manifestations of TCC, one of which is an infiltrative renal mass. Regional lymphadenopathy and vascular invasion are seen less commonly than in patients with RCC.
- **Lymphoma:** A solitary infiltrative renal mass is one of the presentations of renal lymphoma. More common presentations include multifocal renal masses and infiltration from bulky retroperitoneal lymphadenopathy.
- **Metastasis:** A renal metastasis can cause a mass with this appearance, and the presence of retroperitoneal lymphadenopathy does not exclude the possibility of a renal metastasis. It is useful to investigate for a history or the presence of common primary neoplasms in patients with this CT appearance, particularly of the lung, colon, and breast.

## DIAGNOSIS

**Transitional cell carcinoma**

## KEY FACTS

### Clinical

- Peak incidence of TCC is in the seventh decade.
- TCC occurs most often in men, with a male-to-female ratio of 2 to 1.
- Presenting symptoms include hematuria, flank pain, and either or both dysuria and an abdominal mass.
- The upper urinary tract is the site of 10-15% of TCCs. TCC comprises < 10% of malignant renal tumors.
- Renal parenchymal invasion by TCC results in a poor prognosis.
- Risk factors for TCC of the upper tract include highgrade bladder TCC, analgesic abuse, cigarette smoking, cyclophosphamide therapy, radiation exposure, aniline dye professional exposure, and chronic inflammation (pyelitis cystica/glandularis).
- TCC may contain coarse punctate calcific deposits in < 10% of cases.

## Radiologic

- The radiologic manifestations of TCC are varied.
- On intravenous urography, TCC may appear as a discrete filling defect within the renal collecting system, a filling defect within a distended calyx, caliceal obliteration, caliceal amputation, hydronephrosis with renal enlargement, or reduced function without renal enlargement.
- The surface of a pelvicaliceal filling defect may be smooth, irregular, or stippled (the "stipple-sign"). An oncocalyx occurs when transitional cell tumor distends a calyx.
- A phantom calyx occurs when tumor obstructs a caliceal infundibulum.
- CT manifestations of TCC mimic their appearance on intravenous urography. Patterns of disease include caliceal or renal pelvis filling defect, pelvicaliceal irregularity, infundibular stenosis, caliceal cutoff, caliceal expansion, and focal or global nonvisualization.
- Differentiation of TCC from RCC is aided by the more modest enhancement of a transitional cell lesion as opposed to the typical hypervascular, nonnecrotic, and noncystic RCC.
- Transitional cell tumors are typically centrally located, with either or both centrifugal expansion and invasion of the kidney.
- There are unusual forms of TCC on CT, including the hydronephrotic form where an enhancing soft tissue mass may be seen at the apex of a dilated renal pelvis indicative of tumor-causing ureteropelvic junction obstruction. Nodular thickening of the wall of the renal pelvis may also occur.

## SUGGESTED READING

Browne RF, Meehan CP, Colville J, et al. Transitional cell carcinoma of the upper urinary tract: spectrum of imaging

findings. Radiographics 2005;25:1609–1627.

Leder RA, Dunnick NR. Transitional cell carcinoma of the pelvicalices and ureter. AJR Am J Roentgenol 1990;155:713–722.

Vikram R, Sandler CM, Ng CS. Imaging and staging of transitional cell carcinoma: Part 2, upper urinary tract. Am J Roentgenol 2009;192:1488–1493.

# CASE 22

**RICHARD A. LEDER**

**AND**

**DANIELE MARIN**

## HISTORY

A middle-aged woman has a several-month history of chronic flank pain and a palpable flank mass.

A

■**FIGURE 4-22A** Anteroposterior postvoid film of the kidneys from an intravenous urogram. There is a large staghorn calculus in the right kidney. Enhancement of the right kidney is not demonstrated, nor is there excretion into the collecting system or ureter. The left kidney is normal.

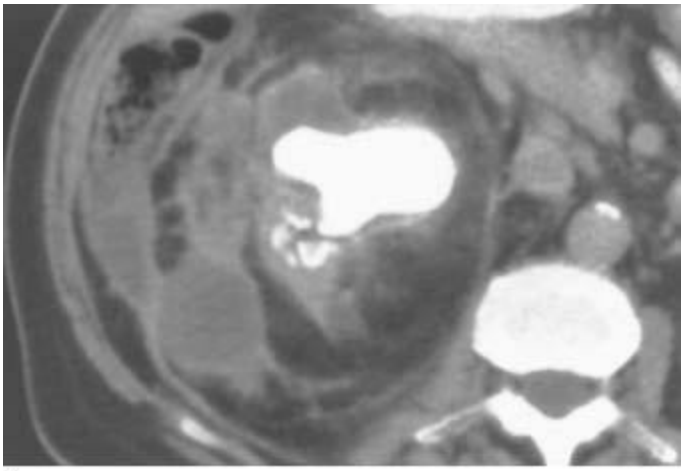

B

**FIGURE 4-22B** Noncontrast CT through the mid-right kidney. There is a dense staghorn calculus in the renal pelvis. There is a small amount of low-attenuation material surrounding this staghorn calculus, as well as low-attenuation fluid collections in the perirenal space.

C

**FIGURE 4-22C** Contrast-enhanced CT through the upper pole of the right kidney. There is a staghorn calculus in the right upper pole calyx with fluid replacement of the kidney extending into Morrison's pouch. Rim enhancement is present secondary to inflammatory tissue.

## DIFFERENTIAL DIAGNOSIS

- **Pyonephrosis secondary to an obstructing calculus:** While this may have been a possibility at an earlier stage, one can no longer discern dilated calyces, and the kidney appears destroyed by a process more extensive than one would expect for pyonephrosis.
- **Xanthogranulomatous pyelonephritis (XGP):** A poorly or nonfunctioning kidney with

an associated staghorn calculus makes this the most likely diagnosis, although definitive diagnosis requires pathologic confirmation.

- **Chronic pyelonephritis secondary to calculus disease:** Since XGP is a pathologic diagnosis, the possibility exists that this is a nongranulomatous response of the kidney to chronic obstruction. The spread of disease into the perirenal space, however, makes XGP a more likely diagnosis.
- **Replacement lipomatosis of the kidney (RLK):** This can be differentiated from XGP by its fibrofatty proliferation. The attenuation of the tissue replacing the kidney in this case is near that of water and is not characteristic of fat; therefore, RLK is unlikely.

## DIAGNOSIS

**Xanthogranulomatous pyelonephritis**

## KEY FACTS

### Clinical

- XGP is a chronic granulomatous inflammation of the kidney. The parenchyma is replaced by xanthoma cells, which are lipidladen macrophages.
- The etiology of XGP is unknown, though it may be caused by chronic urinary tract obstruction with superimposed recurrent infection. Diabetes mellitus and primary hyperparathyroidism may be associated with XGP in some cases.
- Fever, dysuria, and flank pain in a middle-aged woman is the classic presentation. Approximately 70% of patients are women. Tenderness in the renal area and a palpable abdominal or flank mass is found in approximately 50% of cases.
- Multiorganism urinary tract infections are characteristic. While *Proteus* is common, *E. coli, Klebsiella, Pseudomonas*, and *Enterobacter* may also be cultured. More than 80% of patients have pyuria and proteinuria. Laboratory studies show elevated erythrocyte sedimentation rate, anemia, and leukocytosis.
- Reversible hepatic dysfunction has been reported in association with XGP.
- A staghorn calculus is often found. An acalculous variety of XGP has been reported.
- Both diffuse and focal (tumefactive) varieties exist. The diffuse form is more common, occurring in 85% of cases.
- Involvement of the perirenal spaces, psoas muscles, small bowel, diaphragm, lung, or soft tissues of the flank may occur.

### Radiologic

- The plain radiograph typically demonstrates enlargement of the infected kidney with

evidence of a staghorn calculus. Extension into the perirenal space or pararenal space is suggested by indistinct outlines of the kidney or psoas muscle.

- The intravenous urogram shows nonfunction or faint opacification of the kidney.
- On ultrasound, the kidney is typically enlarged, with multiple fluid collections representing dilated calyces and areas of parenchymal destruction. Irregular masses, either anechoic or hypoechoic, with low-level internal echoes and varying degrees of through-transmission are frequently seen. Acoustical shadowing of the central staghorn calculus may be obscured by peripelvic fibrosis. Hypoechoic fluid in the perirenal space is secondary to extension of disease.
- On CT, the kidney is enlarged diffusely and the renal parenchyma is replaced by low-attenuation masses. These masses measure between -20 and +10 HU, depending on lipid content. True fat density is not seen in XGP. Rim enhancement of well-vascularized granulation tissue may occur. Central calcification is seen frequently, as well as calyceal calculi or small areas of calcification in the adjacent parenchyma. The renal pelvis is contracted. Gerota's fascia may be thickened. Low-attenuation masses may be present in the pararenal and perirenal spaces. Less common CT findings include acalculous XGP, a small contracted kidney with parenchymal destruction, and massive pelvic dilation mimicking obstructive hydronephrosis. Focal (tumefactive) XGP can mimic an RCC. Enhancement is demonstrated on postcontrast CT. Typically, a calculus is seen at the apex of the focal mass.
- Approximately 70% of patients have either staghorn calculi or multiple calyceal stones.
- XGP can extend to involve the perirenal and pararenal spaces or ipsilateral psoas muscle. Rarely XGP can involve the diaphragm, the paraspinal muscles, and the skin.

## SUGGESTED READING

Craig WD, Wagner BJ, Travis MD. Pyelonephritis: Radiologic-pathologic review. Radiographics 2008;28:255–276.

Goldman SM, Hartman DS, Fishman EK, et al. CT of xanthogranulomatous pyelonephritis: radiologic-pathologic correlation. Am J Roentgenol 1984;141:963–969.

Hayes WS, Hartman DS, Sesterbenn IA. Xanthogranulomatous pyelonephritis. Radiographics 1991;11:485–498.

Kenney PJ. Imaging of chronic renal infections. AJR Am J Roentgenol 1990;155:485–494.

# CASE 23

**ERIK K. PAULSON**

**AND**

**DANIELE MARIN**

## HISTORY

A 39-year-old man presents with right flank pain.

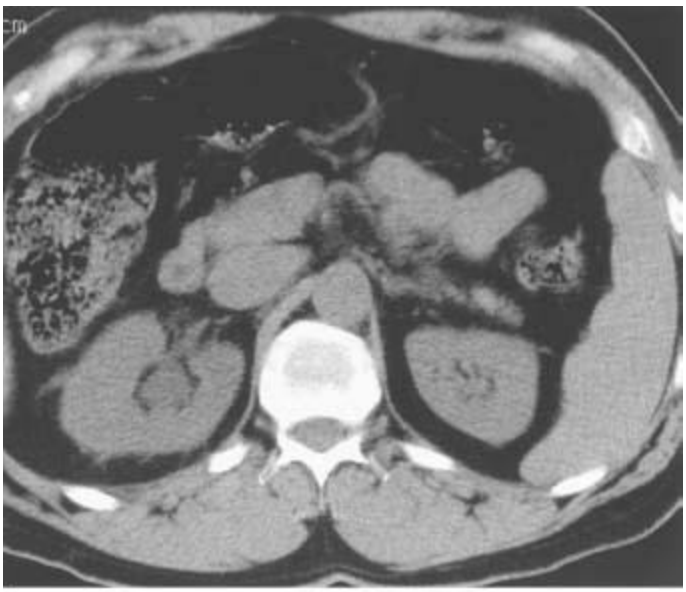

A

■**FIGURE 4-23A** Noncontrast CT of the upper pole of the kidneys. There is right nephromegaly, stranding of the perinephric fat, and pelvicaliectasis. The left kidney is normal.

B

**FIGURE 4-23B** Noncontrast CT of the lower pole of the kidneys. There is dilation of the right proximal ureter. The left ureter is normal. There is stranding of the perinephric and periureteric fat.

C

**FIGURE 4-23C** Noncontrast CT at the level of the ureters. A 3- to 4-mm calcification is identified in the right midureter.

## DIFFERENTIAL DIAGNOSIS

**Pyelonephritis:** Patients with this common condition present with flank pain, fever, nausea, and vomiting. Imaging studies, including intravenous urography, ultrasound, and CT, are usually normal, although on contrast-enhanced CT, parenchymal striations may be seen. While acute pyelonephritis may cause nephromegaly and stranding of the perinephric fat, the ureteral dilation and ureteral calculus argue against this being the primary diagnostic choice.

**Renal lymphoma:** Lymphoma involves the kidneys either by hematogeneous spread or by direct extension of hilar adenopathy. On CT, renal lymphoma may present as multiple masses, a solitary mass, or a renal hilar/ retroperitoneal mass directly invading the kidney.

**Ureteral obstruction due to a calculus:** The unilateral nephromegaly, perinephric fluid, pelvicaliureterectasis, and ureteral calcification all indicate an obstruction caused by a ureteral calculus.

## DIAGNOSIS

**Acute ureteral obstruction caused by a calculus**

## KEY FACTS

### Clinical

- The most common cause of ureteral obstruction is a calculus lodged in the ureter.
- Common sites of obstruction include the ureteropelvic junction, sites of blood vessels crossing the ureter, the pelvic brim, and the ureterovesical junction.
- Most small stones < 5 mm in diameter will pass spontaneously.
- Calcium oxylate and calcium oxylate mixed with phosphate are the most common stones.
- Uric acid stones are associated with acidic urine, uricosuric drugs, and hyperuricemia. These stones are often radiolucent on plain radiographs but are always hyper-attenuating on CT.

### Radiologic

- Intravenous urography is the traditional method to confirm a suspected ureteral obstruction in a patient with renal colic. Classic findings include delayed parenchymal enhancement, delayed excretion, and collecting system dilation to the level of the calculus.
- CT has been shown to be accurate in the workup of patients with renal colic. These studies are best performed using a helical technique without intravenous or oral contrast material. Classic findings include nephromegaly, perinephric stranding, and collecting system dilation that extends to the level of the calculus.
- Advantages of helical CT over intravenous urography include elimination of the need for intravenous contrast material, the occasional demonstration of nonurinary causes of flank pain, and a shorter examination time.
- Disadvantages of helical CT include difficulty in differentiating vascular calcifications and phleboliths from ureteral stones, inaccurate demonstration of stone size, particularly along the cranial-caudal axis of stones, and lack of "functional" information in regard to the degree of obstruction.

## SUGGESTED READING

Dunnick NR, McCallum RW, Sandler CM (eds). Nephrocalcinosis and nephrolithiasis. In Textbook of Uroradiology. Baltimore: Williams & Wilkins, 1991;189–214.

Smith RC, Rosenfield AT, Choe KA, et al. Acute flank pain: comparison of non-contrast-enhanced CT and intravenous urography. Radiology 1995;194:789–794.

Sommer FG, Jeffrey RB Jr, Rubin GD, et al. Detection of ureteral calculi in patients with suspected renal colic: value of reformatted noncontrast helical CT. AJR Am J Roentgenol 1995;165:509–513.

# CASE 24

**KELLY S. FREED**

**AND**

**DANIELE MARIN**

## HISTORY

A 75-year-old asymptomatic woman with a history of colon cancer.

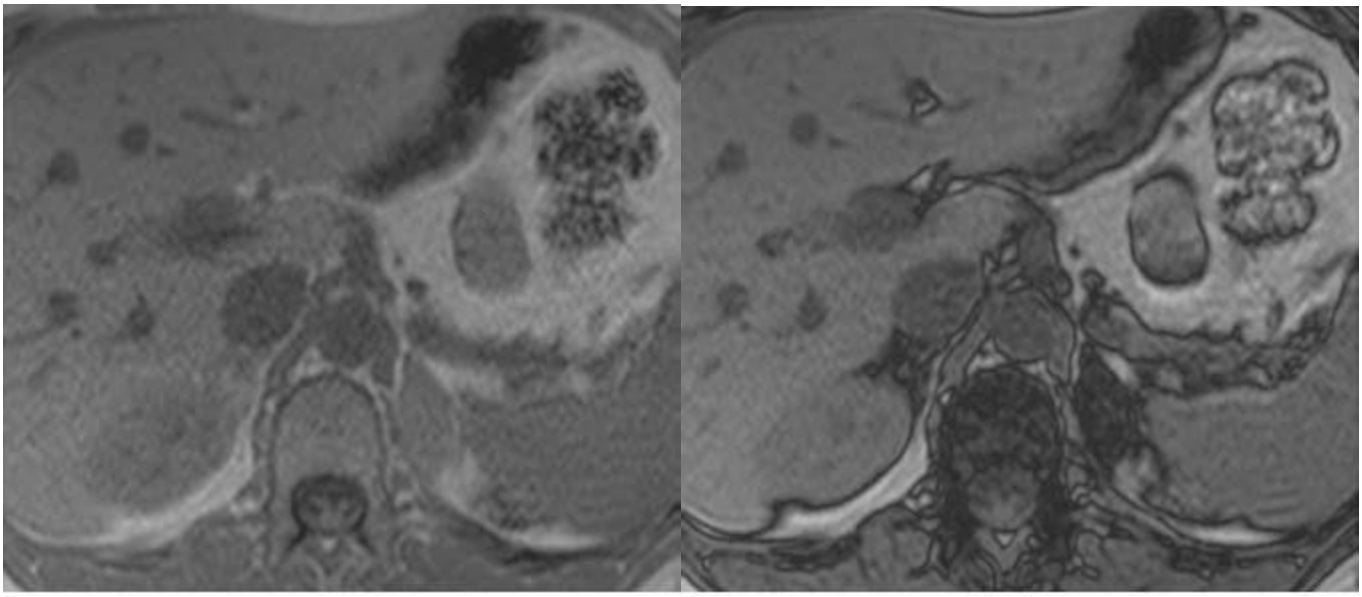

A B

**FIGURE 4-24A** and **4-24B A**: Transverse in-phase Tl-weighted MR image of the upper abdomen demonstrates a well-defined, 2-cm, left adrenal mass with a relative signal intensity of 240 arbitrary units (au). **B:** Corresponding transverse opposed-phase Tl-weighted MR image shows marked signal drop of the lesion, with a relative signal intensity of 170 au.

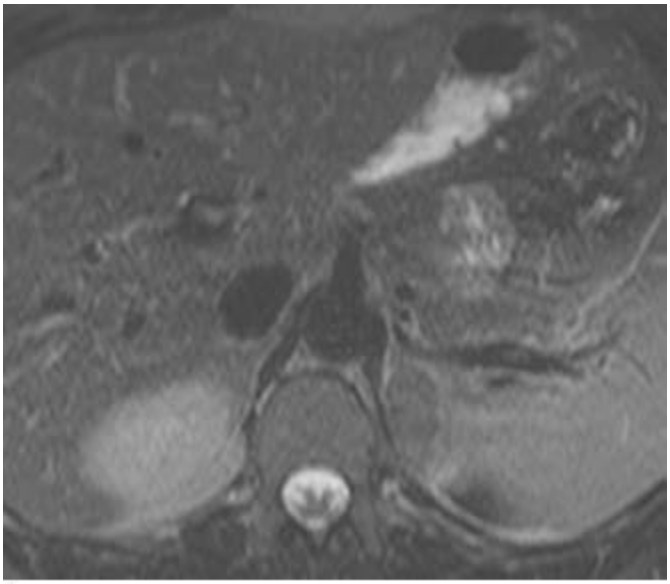

C

**FIGURE 4-24C** On the transverse T2-weighted MR image, the lesion demonstrates a signal intensity similar to the liver parenchyma.

## DIFFERENTIAL DIAGNOSIS

- **Metastasis:** This diagnosis is unlikely because the mass has a high lipid content, as demonstrated by the loss of signal intensity on the opposed-phase image.
- **Pheochromocytoma:** Generally, this tumor shows no signal drop on opposed-phase images, due to a lack of intracellular fat, and demonstrates a higher signal intensity on T2-weighted images (the so-called light bulb sign).
- **Nonhyperfunctioning adenoma:** This is the most likely diagnosis, given the size and loss of signal intensity on the opposed-phase image, even though the patient has a known history of malignancy.

## DIAGNOSIS

**Nonhyperfunctioning adenoma**

## KEY FACTS

### Clinical

- Adrenocortical adenomas may be nonhyperfunctioning or hyperfunctioning. The incidence of nonhyperfunctioning adenomas in the general population is 1% to 3%.
- Hyperfunctioning adenomas may produce symptoms due to the secretion of active hormones, such as cortisol (Cushing's syndrome), aldosterone (Conn's syndrome) or, more infrequently, androgens (virilization syndrome).

### Radiologic

- On CT, a precontrast attenuation value < 0 Hounsfield units (HU) signifies a benign condition; a precontrast attenuation value +1-10 HU signifies that the adenoma is likely benign and may warrant follow-up based on the clinical setting.
- Opposed-phase MRI is the most accurate imaging modality for the diagnosis of adrenal adenomas. These lesions classically demonstrate marked signal loss on opposed-phase images due to the presence of abundant amounts of intracelullar fat.
- Because malignant adrenal tumors, such as adrenocortical carcinoma, may occasionally contain increased amounts of intracellular fat, intense follow-up or biopsy is recommended for adrenal masses > 5 cm in diameter, with heterogeneous contrast enhancement, or that increase in size during imaging follow-up.
- Imaging studies cannot differentiate hyperfunctioning from nonhyperfunctioning adenomas.

## SUGGESTED READING

Boland GW, Blake MA, Hahn PF, Mayo-Smith WW. Incidental adrenal lesions: Principles, techniques, and algorithms for imaging characterization. Radiology 2008;249:756–775.

Mayo-Smith WW, Boland GW, Noto RB, et al. State-of-the-art adrenal imaging. RadioGraphics 2001;21:995–1012.

# CASE 25

**DANIELE MARIN**

### HISTORY

A 63-year-old man with acute pancreatitis develops acute renal failure complicated by septic shock.

**FIGURE 4-25** Transverse, contrast-enhanced CT during the corticomedullary phase demonstrates a hypoattenuating, circumferential avascular zone within the renal cortex of both kidneys. Note preserved enhancement of the medulla and a thin rim of the outer, subcapsular cortex. Note also the small amount of perihepatic fluid.

## DIFFERENTIAL DIAGNOSIS

**Acute cortical necrosis:** This is the most likely diagnosis based on the imaging findings, corroborated by the patient's history of septic shock secondary to acute pancreatitis.

**Vasculitis:** Although patients with renal involvement secondary to vasculitis, such as in the case of polyarteritis nodosa or systemic lupus erythematosus, may show multiple hypoattenuating areas due to parenchymal infarction, these findings are generally patchy in their distribution. Additionally, clinical symptoms at presentation, including renin-mediated hypertension, and occasionally, intrarenal, subcapsular, or perinephric hematoma, are generally associated with a better prognosis compared to that of acute cortical necrosis.

## DIAGNOSIS

**Acute cortical necrosis**

## KEY FACTS

### Clinical

- A rare form of acute renal failure (2% of all cases of acute renal failure in adults) that

results from ischemic necrosis of the renal cortex, with sparing of the renal medulla, and a thin rim (approximately 1 to 2 mm) of the subcapsular cortex. It is likely secondary to vasospasm of the small vessels, toxic damage to the glomerular capillary endothelium followed by primary intravascular thrombosis.

- Cortical necrosis can result from any condition that produces acute, prolonged shock, such as complications from pregnancy, dehydration, transfusion reaction, hemolytic uremic syndrome, or a venomous snake bite.
- Acute cortical necrosis is usually extensive and generally associated with a poor chance of recovery (mortality rate can exceed 50%) if not promptly treated.

### Radiologic

- The radiographic findings are generally nonspecific and vary with the extent and stage of the disease. In the early phase, the kidneys are diffusely enlarged and poorly visualized.
- Contrast-enhanced CT and MR imaging during the corticomedullary phase demonstrates a characteristic enhancement of the medulla and a thin rim of the outer cortex but no enhancement of the remaining cortex. The rim of subcapsular cortical enhancement is a result of collateral flow from the capsular vessels.
- Although the kidneys are typically enlarged during the acute phase, they reduce progressively in size over subsequent months, and a single thin rim of calcification or "tramline" calcification can form in the renal cortex.
- As a general rule, there are no perinephric manifestations.

## SUGGESTED READING

Badiola-Varela CM. Acute renal cortical necrosis: contrast-enhanced CT and pathologic correlation. Urol Radiol 1992;14:159–160.

Kawashima A, Sandler CM, Ernst RD, et al. CT evaluation of renovascular disease. Radiographics 2000;20:1321–1340.

Mertens PR, Duque-Reina D, Ittel TH, et al. Contrast-enhanced computed tomography for demonstration of bilateral renal cortical necrosis. Clin Invest 1994;72:499–501.

# CASE 26

**DANIELE MARIN**

### HISTORY

A 54-year-old woman with a 2-month history of frequent micturition and recent onset of

hematuria.

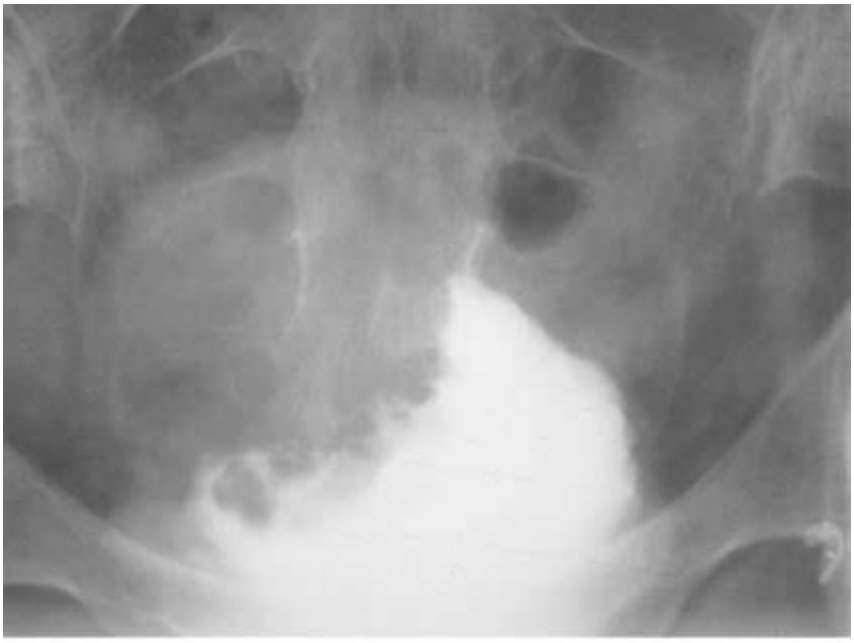

A

■**FIGURE 4-26A** Anteroposterior coned view of the pelvis from an intravenous urogram demonstrates a large, irregular, broad-base filling defect in the superolateral urinary bladder.

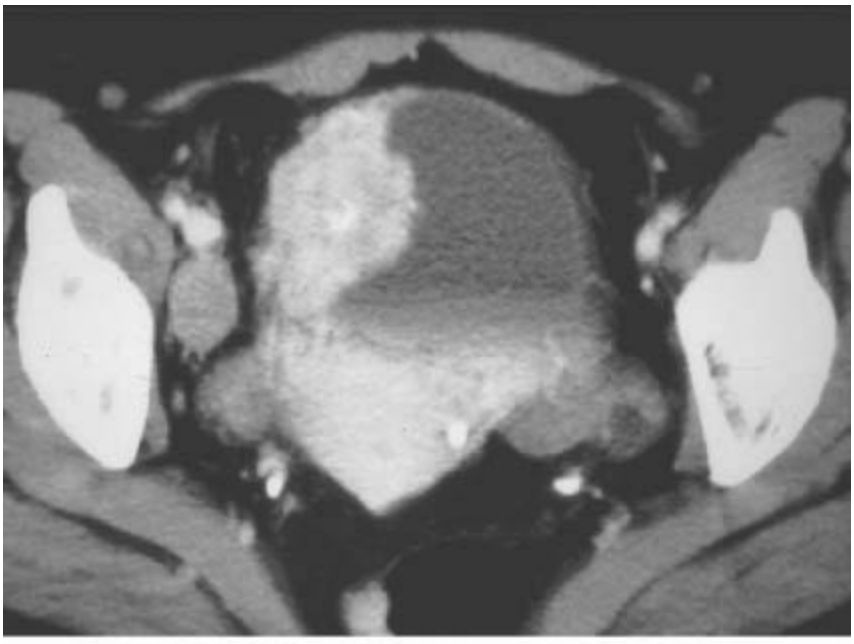

B

■**FIGURE 4-26B** Transverse, contrast-enhanced CT during the venous phase demonstrates a large, expansile, lobulated, and vividly enhancing mass that protrudes into the lumen of the urinary bladder from the anterolateral bladder wall.

## DIFFERENTIAL DIAGNOSIS

- **Urothelial (TCC) carcinoma:** Although most urothelial carcinomas are located at the bladder base (80% of cases at initial diagnosis), these tumors are by far the most common malignant tumor of the urinary bladder and manifest with the same imaging findings as the present case.
- **Urinary bladder pheochromocytoma:** Although pheochromocytomas of the urinary bladder are extremely rare, demonstration of vivid enhancement of the tumor on contrast-enhanced CT is highly suggestive of this diagnosis.
- **Squamous cell carcinoma:** Although squamous cell carcinoma can manifest as solitary, focal masses, most lesions demonstrate diffuse thickening of the bladder wall. Additionally, this tumor is almost invariably associated with well-defined risk factors, such as chronic irritation from indwelling catheters, bladder calculi, or chronic infection (e.g., schistosomiasis).
- **Carcinoid:** Unlike this case, carcinoids typically manifest as small (mean diameter, 6 mm), well-defined, round or polypoid masses frequently located in the bladder neck or near the bladder trigone.

## DIAGNOSIS

**Urinary bladder pheochromocytoma**

## KEY FACTS

### Clinical

- Although > 90% of pheochromocytomas are located within the adrenal glands, extra-adrenal pheochromocytomas (also known as paragangliomas) may occur anywhere from the base of the brain to the urinary bladder.
- Urinary bladder pheochromocytomas account for 0.1% of all bladder tumors and 1% of all pheochromocytomas.
- Urinary bladder pheochromocytomas can occur within a wide age range (from 10 to 78 years), with a predilection for females.
- In approximately 10% of patients, pheochromocytomas are hereditary, frequently as a part of a clinical syndrome such as multiple endocrine neoplasia II and III and various neuroectodermal disorders (e.g., neurofibromatosis or VHL syndrome).
- Due to potentially life-threatening hypertension or cardiac arrhythmias secondary to excessive catecholamine secretion, pheochromocytomas warrant a prompt diagnosis.
- A characteristic clinical syndrome that occurs in approximately 50% of patients with

urinary bladder pheochromocytomas is the so-called micturition attack secondary to catecholamine release by the tumor. Hematuria is common.

- Treatment consists of local excision following pharma-cologic prophylaxis with adrenergic blockade.

## Radiologic

- With recent advances of modern cross-sectional imaging techniques, pheochromocytomas are frequently identified at imaging, even in completely asymptomatic patients with silent pheochromocytomas.
- With contrast-enhanced CT and MR imaging, most urinary bladder pheochromocytomas manifest as a solitary, solid, homogeneous, lobulated, well-margin-ated mass that protrudes from the bladder wall into its lumen. Larger tumors may show a heterogeneous appearance due to cystic areas secondary to tumor necrosis or hemorrhage.
- Vivid tumor enhancement with either contrast-enhanced CT or MR imaging during the arterial phase represents the hallmark of urinary bladder pheochro-mocytomas.
- Ring calcification around the circumference of the mass, although uncommonly seen, is highly suggestive of a urinary bladder pheochromocytoma.
- Similar to most pheochromocytomas, urinary bladder pheochromocytomas demonstrate avid uptake of iodine 131 ($^{131}$I) metaiodobenzylguanidine (MIBG) at MIBG scintigraphy.

## SUGGESTED READING

Crecelius SA, Bellah R. Pheochromocytoma of the bladder in an adolescent: sonographic and MR imaging findings. AJR Am J Roentgenol 1995;165:101–103.

Doran F, Varinli S, Bayazit Y, et al. Pheochromocytoma of the urinary bladder. APMIS 2002;110:733–736.

Wong-You-Cheong JJ, Woodward PJ, Manning MA, Sesterhenn IA. From the Archives of the AFIP: neoplasms of the urinary bladder: radiologic-pathologic correlation. Radiographics 2006;26:553–580.

# CASE 27

**DANIELE MARIN**

### HISTORY

Patient A: A 13-year-old girl with a 4-month history of right flank pain. Patient B: A 22-year-old man with known sickle cell trait who presented with a 3-weeks history of fever, malaise, and weight loss.

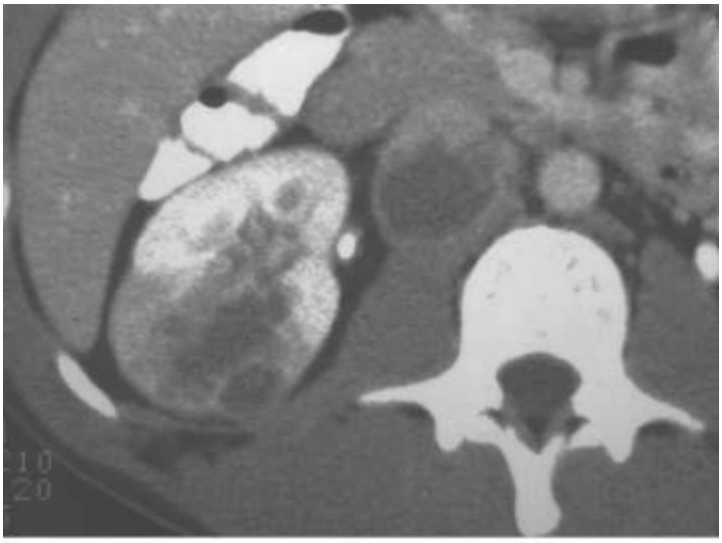

A

**FIGURE 4-27A** Patient A: Transverse, contrast-enhanced CT during the excretory phase demonstrates a large, heterogeneous, infiltrative renal mass in the right kidney that extends from the renal pelvis to the renal cortex without deforming the reniform contour. Note a large, hypoattenuating, metastatic lymph node in the retroperiteum/retrocaval space.

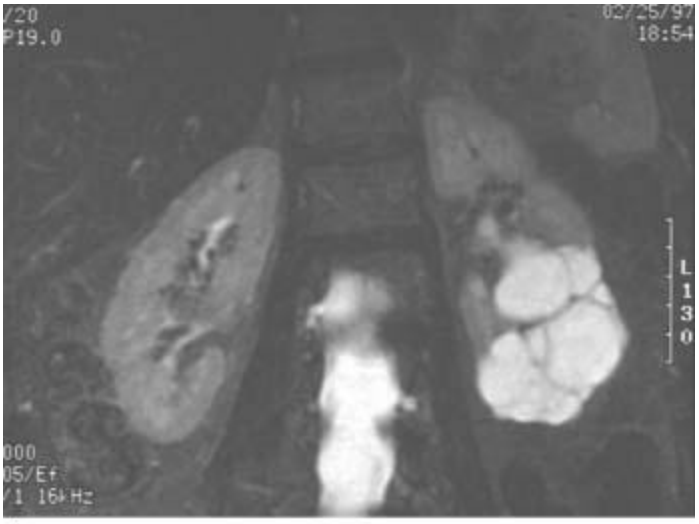

B

**FIGURE 4-27B** Patient B: Coronal **(left)** T2-welghted MR image and **(right)** gadolinium-enhanced T1-welghted MR image during the excretory phase demonstrate a large, multilocular cystic mass in the lower pole of the left kidney. The post contrast-enhanced MR image **(right)** demonstrates lack of communication between the lesion and the renal excretory system.

## DIFFERENTIAL DIAGNOSIS

- **Multilocular cystic RCC:** Although a multiseptated cystic variant of RCC may present the same imaging appearance, this neoplasm tends to occur in older patients (mean age, 51 years) and is generally associated with an excellent prognosis after surgery.
- **Renal medullary carcinoma:** This is the most likely diagnosis due to the central location of the tumor, the infiltrative growth pattern, and the association with a sickle cell trait in one of the two patients.
- **Acute pyelonephritis:** Although a severe form of acute pyelonephritis may demonstrate a similar appearance, this diagnosis can be excluded based on the absence of clinical signs and symptoms of infection in both patients, including fever, pyuria with leukocyte casts, and a positive urine culture.
- **Wilms tumor:** Unlike the two cases presented, most Wilms tumors present with a large abdominal mass that frequently extends across the midline and down into the pelvis.
- **Collecting duct carcinoma:** Although collecting duct carcinomas may demonstrate a similar appearance, most of these lesions occur in older patients (mean age, 60 years) without sickle cell trait.

## DIAGNOSIS

**Renal medullary carcinoma**

## KEY FACTS

### Clinical

- Extremely rare malignant renal neoplasm (< 1% of malignant renal tumors) occurring almost exclusively in young patients (mean age, 22 years, age range, 10 to 40 years) with sickle cell trait.
- In patients younger than 24 years, renal medullary carcinoma demonstrates a predilection for males with a male-to-female ratio of 2:1.
- Renal medullary carcinoma is hypothesized to arise from caliceal epithelia in or near the renal papilla. For undetermined reasons, this tumor has a predilection for the right kidney (approximately 80% of patients).
- The most common presenting symptoms include hematuria, flank or abdominal pain, and a palpable mass.
- Renal medullary carcinoma is generally associated with an extremely poor prognosis, with early metastatic dissemination to distant organs. Mean survival after the diagnosis is generally 3 months (range, 1 to 7 months).

## Radiologic

- Tumor extension into the renal sinus can cause distortion of the renal collecting system on intravenous urography.
- On contrast-enhanced CT and MR imaging, most tumors show an infiltrative growth pattern from the renal medulla toward both the renal cortex laterally and the renal pelvis and sinus medially. The tumor typically causes overall expansion of the kidney while maintaining the reniform contour. Medullary origin can be difficult to appreciate with large tumors.
- Typically, renal medullary carcinoma demonstrate a heterogeneous appearance at CT and MR imaging either before or after contrast administration, likely due to the coexistence of areas of necrosis and hemorrhage within the lesion. These hemorrhagic foci, although not specific, manifest as areas of signal void on T2-weighted, gradient-recalled MR images with longer echo times, due to susceptibility effect caused by by-products of hemorrhage.
- Owing to its central location, renal medullary carcinoma is often associated with caliectasis without pelviectasis.
- At the time of diagnosis, most tumors present at an advanced stage with infiltration of adjacent organs and vascular structures, such as the renal vein and IVC, adrenal gland, liver, and perinephric or retroperitoneal soft tissue. Frequently, metastatic dissemination to local and nonregional lymph nodes, and to distant target organs, including the liver and lungs, are also present.

## SUGGESTED READING

Davidson AJ, Choyke PL, Hartman DS, Davis CJ Jr. Renal medullary carcinoma associated with sickle cell trait: radiologic findings. Radiology 1995;195:83–85.

Dyer R, DiSantis DJ, McClennan BL. Simplified imaging approach for evaluation of the solid renal mass in adults. Radiology 2008;247:331–343.

Prasad SR, Humphrey PA, Menias CO, et al. Neoplasms of the renal medulla: Radiologicpathologic correlation. Radiographics 2005;25:369–380.

Prasad SR, Humphrey PA, Catena JR, et al. Common and uncommon histologic subtypes of renal cell carcinoma: imaging spectrum with pathologic correlation. Radiographics 2006;26:1795–1806.

# CASE 28

**DANIELE MARIN**

### HISTORY

A 45-year-old man presents with a left flank mass and gross hematuria.

**FIGURE 4-28** Transverse, contrast-enhanced CT during the excretory phase demonstrates a large, expansile mass in the left kidney that extends toward both the renal sinus and cortex, causing a focal bulging of the renal contour. Note multiple hypoattenuating, metastatic lymph nodes in the retroperitoneum.

## DIFFERENTIAL DIAGNOSIS

**Clear cell RCC:** Since demonstration of a large, expansile renal mass, which extends toward both the renal sinus and the renal cortex, is a common finding for most malignant renal neoplasms, RCC cannot be readily excluded in this case.

**Renal medullary carcinoma:** Unlike the present case, renal medullary carcinoma shows an infiltrative growth pattern that gradually expands the kidney while maintaining the reniform contour. Additionally, renal medullary carcinoma almost invariably occurs in younger patients with sickle cell trait.

**Collecting duct carcinoma (Bellini duct carcinoma):** Though relatively nonspecific, the lesion's central location, partial replacement of the renal sinus fat, and protrusion into the renal pelvis may be suggestive of a collecting duct carcinoma. A lesion's

exophytic component beyond the expected renal contour is also a common finding (approximately 60%) of this rare renal tumor.

- **Urothelial carcinoma:** Urothelial tumors of the renal pelvis, namely invasive TCC and squamous cell carcinoma, may also manifest as a centrally located mass with extension into the renal pelvis. However, urothelial tumors more often demonstrate an infiltrative growth pattern and poorly defined tumor margins.
- **Renal lymphoma:** Although renal lymphoma may present as a solitary renal parenchymal mass associated with adenopathy, renal involvement is more often multifocal and commonly bilateral. Additionally, renal involvement by lymphoma is typically asymptomatic.

# DIAGNOSIS

**Collecting duct carcinoma (Bellini duct carcinoma)**

# KEY FACTS

## Clinical

- Extremely rare malignant renal neoplasm (< 1% of malignant renal tumors).
- Typically, collecting duct carcinoma occurs in middle-aged patients (mean age, 55 years; age range, 13 to 83 years) with a predilection for males (male-to-female ratio 2:1).
- Immunocytochemistry studies demonstrated an origin of this tumor from epithelial cells of the collecting ducts of Bellini in the renal medulla.
- The most common presenting signs and symptoms include hematuria, flank or abdominal pain, and a palpable mass. Since the same findings can be observed for most malignant renal neoplasms, the final diagnosis relies on both suggestive imaging findings and histopathologic analysis.
- Most collecting duct carcinomas are biologically aggressive neoplasms: one-third of patients have meta-static disease at presentation, and less than one-third of patients survive more than two years after diagnosis.

## Radiologic

- Tumor extension into the renal sinus can manifest as distortion of the renal collecting system at conventional radiograph from excretory urography.
- At contrast-enhanced CT and MR imaging, collecting duct carcinomas manifest as a centrally located lesion with either an infiltrative or expansile growth pattern from the renal medulla toward both the renal cortex and the renal pelvis and sinus. Medullary origin can be difficult to appreciate with large tumors.

- Most tumors have a heterogeneous appearance at CT and MR imaging either before or after contrast administration, likely due to the coexistence of areas of necrosis and hemorrhage within the lesion. These hemorrhagic foci, although not specific, manifest as areas of signal void on T2-weighted, gradient-recalled MR images with longer echo times, due to susceptibility effect caused by by-products of the hemorrhage.
- Calcification is seen in approximately 25% of patients.
- At the time of diagnosis, most tumors frequently infiltrate adjacent organs and vascular structures, such as the renal vein and IVC, adrenal gland, liver, and perinephric or retroperitoneal soft tissues. Additionally, these findings are associated with metastatic dissemination to local and nonregional lymph nodes, and to distant target organs, including the liver and lungs.

## SUGGESTED READING

Dyer R, DiSantis DJ, McClennan BL. Simplified imaging approach for evaluation of the solid renal mass in adults. Radiology 2008;247:331–343.

Pickhardt PJ, Siegel CL, McLarney JK. Collecting duct carcinoma of the kidney: are imaging findings suggestive of the diagnosis? AJR Am J Roentgenol 2001;176:627–633.

Prasad SR, Humphrey PA, Catena JR, et al. Common and uncommon histologic subtypes of renal cell carcinoma: imaging spectrum with pathologic correlation. Radiographics 2006;26:1795–1806.

Prasad SR, Humphrey PA, Menias CO, et al. Neoplasms of the renal medulla: radiologicpathologic correlation. Radiographics 2005;25:369–380.

# CASE 29

**DANIELE MARIN**

### HISTORY

A 52-year-old female presents with flank pain and recurrent urinary tract infections.

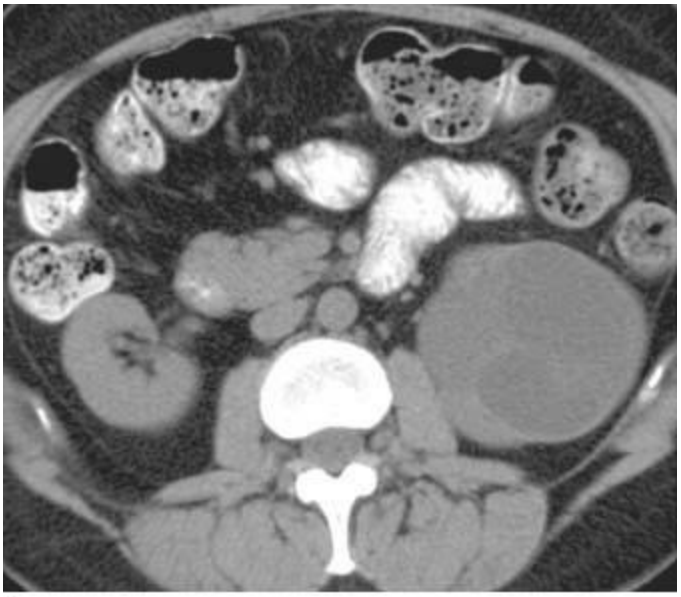

A

■**FIGURE 4-29A** Transverse, noncontrast CT demonstrates a large, well-defined, cystic mass (mean attenuation, +5 Hounsfield units) arising from the left kidney, with a peripheral capsule and multiple thin septations. The mass shows expansile growth extending into the renal pelvis. Residual normal renal parenchyma is seen.

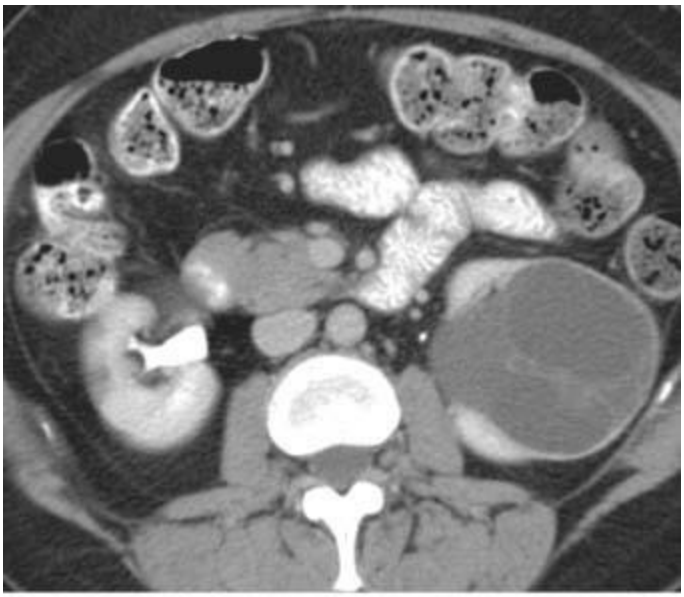

B

■**FIGURE 4-29B** Corresponding contrast-enhanced CT during the excretory phase shows mild contrast enhancement of the capsule and internal septations.

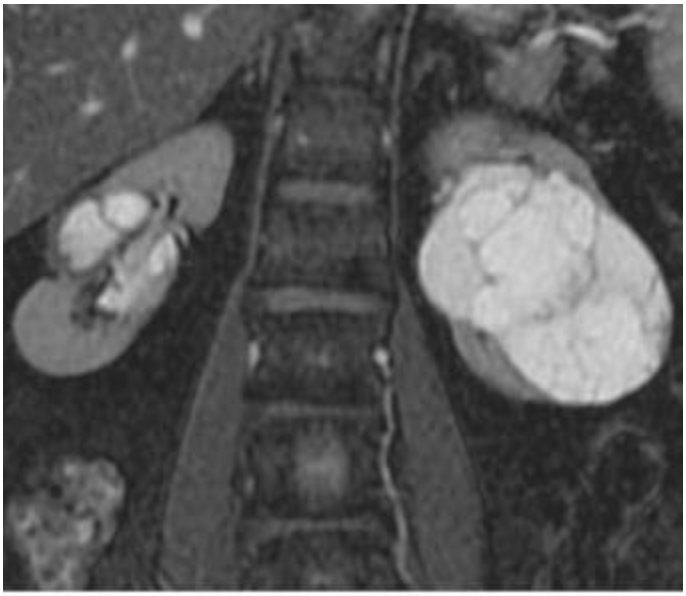

C

**FIGURE 4-29C** Coronal, fat-suppressed, T2-weighted MR imaging confirms the cystic nature and multiloculated appearance of the lesion.

## DIFFERENTIAL DIAGNOSIS

- **Cystic RCC:** Although cystic RCC may manifest as a multiloculated, cystic renal mass, this diagnosis is unlikely in the absence of an apparent solid component.
- **Multiloculated cystic nephroma (MCN):** The presence of a multicystic renal mass with no solid or nodular elements and lack of direct communication with the collecting duct system is suggestive of a multiloculated cystic nephroma.
- **Multicystic dysplastic kidney:** Multicystic dysplastic kidney is a congenital anomaly that typically involves the entire kidney. Association with other congenital anomalies of the collecting excretory ducts (e.g., absent or atretic collecting system or ectopic ureterocele) is common. The latter anomalies may be diagnosed with a delayed or absent excretion of contrast material by the diseased kidney on contrast-enhanced CT during the excretory phase.
- **Calyceal diverticulum:** Due to the absence of an obvious communication between the cystic renal lesion and the collecting duct system, a calyceal diverticulum is unlikely.

## DIAGNOSIS

**Multiloculated cystic nephroma**

## KEY FACTS

### Clinical

- Rare, nonhereditary benign renal neoplasm that is purely cystic, is lined by an epithelium and has fibrous septa that contain mature tubules.
- MCN has a bimodal age and sex distribution and tends to occur in children (mostly boys) between 3 months and 4 years of age and in adults (mostly women) between 40 and 60 years of age.
- MCN is usually solitary, but bilateral tumors have been described.
- In children, it most frequently manifests as a painless abdominal mass. Adults are more likely to present with abdominal pain or hematuria.
- At gross inspection, MCN is a well-circumscribed mass with a thick fibrous capsule that contains multiple, fluid-filled, noncommunicating loculi separated by thin translucent septa (the so-called honeycombed appearance).
- At microscopic examination, the septa are lined by flattened or cuboidal epithelia, with areas of eosinophilic cuboidal cells protruding into the lumen producing a hobnail or teardrop appearance.
- Because neither the clinical nor the imaging features of multicystic renal tumors can predict the histologic characteristics, surgery—either nephrectomy or neph-ron-sparing surgery—is required for both diagnosis and treatment.

## Radiologic

- Large masses may be evident on radiographs and calcifications, although uncommonly (5%), may be seen.
- US is often the initial modality used to evaluate abdominal masses, particularly with pediatric patients. At US, MCN typically appears as a multicystic renal mass with no solid or nodular elements. Associated urinary tract obstruction may be evident. The loculi can range in size from a few millimeters to 4 cm in diameter.
- At CT, MCN typically appears as a well-circumscribed, encapsulated multicystic mass with variably enhancing septa and no excretion of contrast material into the loculi.
- The contents of the cyst may have similar or slightly higher attenuation than that of water, and if the cystic spaces are very small, the closely packed septa can mimic a solid mass.
- MCN demonstrates very characteristic imaging findings at MR imaging. Lesions manifest as a multicystic mass with a capsule and septa that are hypointense regardless of pulse sequence, presumably because of the predominant fibrous tissue in these structures.
- Contents of the cyst are hyperintense on T2-weighted images; their signal intensity varies on T1-weighted images, possibly because of old hemorrhage or high protein content. The septa have also been shown to enhance on MR images following

intravenous administration of gadolinium agents.

- Although renal scintigraphy has been described in the workup of MCN, it presently has no diagnostic role.

## SUGGESTED READING

Agrons GA, Wagner BJ, Davidson AJ, Suarez ES. Multilocular cystic renal tumor in children: radiologic-pathologic correlation. Radiographics 1995;15:653–669.

Kettritz U, Semelka RC, Siegelman ES, et al. Multilocular cystic nephroma: MR imaging appearance with current techniques, including gadolinium enhancement. J Magn Reson Imaging 1996;6:145–148.

Madewell JE, Goldman SM, Davis CJ Jr, et al. Multilocular cystic nephroma: a radiographic-pathologic correlation of 58 patients. Radiology 1983;146:309–321.

Sacher P, Willi UV, Niggli F, Stallmach T. Cystic nephroma: a rare benign renal tumor. Pediatr Surg Int 1998;13:197–199.

# Chapter FIVE

# Musculoskeletal Imaging

**EMILY N. VINSON** ■ CHAPTER EDITOR

Charles E. Spritzer

Robert M. Vandemark

R. Lee Cothran, Jr.

Salutario J. Martinez

D. Lawrence Burk

Thomas Dziedzic

Glen A. Toomayan

David K. Krug

Kavita M. Patel

# CASE 1

**EMILY N. VINSON**

### HISTORY

A 40-year-old woman with diffuse bone pain and a chronic disease.

A

■**FIGURE 5-1A** Anteroposterior radiograph of lumbar spine and pelvis. There is increased density of the bones. There is a partially calcified renal transplant overlying the right hemipelvis. Small lucent lesions are seen in the bilateral ilia and proximal left femur. There are erosive changes and subchondral sclerosis of the bilateral sacroiliac joints, with ill-defined cortical margins, consistent with subchondral bone resorption.

B

**FIGURE 5-1B** Lateral radiograph of lumbar spine. Bandlike areas of sclerosis are noted to involve the vertebral body marrow adjacent to the superior and inferior endplates. Erosive changes are present at the discovertebral junctions of multiple vertebral body endplates, consistent with subchondral bone resorption.

## DIFFERENTIAL DIAGNOSIS

**Osteopetrosis:** Diffuse sclerosis results in a bone-within-bone appearance or a sandwich vertebra appearance. Anterior vascular notches may be seen in the vertebral bodies, but subchondral bone resorption and lytic lesions do not occur, making this an unlikely diagnosis.

**Systemic mastocytosis:** Osteosclerosis may be diffuse or patchy and multifocal. Multiple lytic lesions can also occur, which are usually surrounded by a halo of sclerosis. Subchondral bone resorption is not a typical characteristic of this disease.

**Renal osteodystrophy and secondary hyperparathyroidism:** Osteosclerosis manifests as a "rugger-jersey spine" appearance. Subperiosteal, subchondral, and subligamentous bone resorption simulating erosions, and lytic brown tumors are additional features. The presence of a partially calcified renal transplant confirms that this patient has chronic renal disease. This is the most likely diagnosis.

- **Myelofibrosis:** A diffuse increase in bone density is most commonly seen, but small areas of relative radio-lucency or lytic lesions can also be present. Subchondral bone resorption is not characteristic of this disease process, and this disease does not usually manifest as a "rugger-jersey spine."

# DIAGNOSIS

**Renal osteodystrophy and secondary hyperparathyroidism**

# KEY FACTS

## Clinical

- Musculoskeletal manifestations of chronic renal insufficiency are increasingly common due to prolonged survival with hemodialysis.
- Symptomatic bone disease may consist of pain, tenderness, swelling, and deformity.
- The two main mechanisms of renal osteodystrophy (also called uremic osteopathy) are secondary hyperparathyroidism and vitamin D deficiency.
- Secondary hyperparathyroidism in patients with chronic renal disease is caused by a combination of hypocalcemia (due to elevated serum phosphate levels, skeletal resistance to calcium mobilization by parathyroid hormone, and decreased intestinal absorption of calcium caused by decreased vitamin D levels) and decreased renal degradation of parathyroid hormone.
- As renal cell mass decreases in moderate and advanced renal disease, so does the body's ability to synthesize the physiologically active form of vitamin D. In addition, elevated serum phosphate levels inhibit vitamin D production. This leads to skeletal changes of osteomalacia, rickets, or both.

## Radiologic

- Radiographic abnormalities in renal osteodystrophy reflect both hyperparathyroidism and vitamin D deficiency, and include bone resorption, brown tumors, bone sclerosis, osteomalacia, osteoporosis, and soft tissue and vascular calcifications.
- Bone resorption is typically subperiosteal, subchondral, and subligamentous in distribution. Characteristic sites of subperiosteal resorption include the radial margins of the middle phalanges of the hands and the medial margins of the proximal tibiae. Characteristic sites of subchondral resorption include the sacroiliac joints, pubic symphysis, and acromioclavicular joints.
- Osteosclerosis and soft tissue and vascular calcifications are more common in patients with secondary hyperparathyroidism due to renal disease compared to patients with

primary hyperparathyroidism.

- Osteosclerosis in these patients usually involves the axial skeleton, but may also involve long bones, pelvis, clavicles, and the bones of the face. In the spine, the bone subjacent to the cartilaginous endplate is usually preferentially involved, leading to the characteristic “rugger-jersey spine” appearance. Small subchondral resorptive changes may be seen at the discovertebral junctions.
- Brown tumors or osteoclastomas are well-defined lytic lesions that may heal with sclerosis after treatment of the hyperparathyroidism.
- The skeletal changes associated with renal osteodys-trophy can be halted or reversed by early detection and careful management of vitamin D, parathyroid hormone, and mineral levels.

## SUGGESTED READING

Murphey MD, Sartoris DJ, Quale JL, et al. Musculoskeletal manifestations of chronic renal insufficiency. Radiographics 1993;13:357–379.

Resnick D. Diagnosis of Bone and Joint Disorders (3rd ed). Philadelphia, PA: W.B. Saunders Company, 1995:1902–1905, 2036–2061.

Slatopolsky E. The role of calcium, phosphorus and vitamin D metabolism in the development of secondary hyperparathyroidism. Nephrol Dial Transplant 1998;13(Suppl 3):3–8.

Sundaram M. Founders lecture 2007: metabolic bone disease: what has changed in 30 years? Skeletal Radiol 2009;38:841–853.

# CASE 2

**EMILY N.**
**VINSON**

### HISTORY

A 33-year-old man with 2 months of worsening left hip pain and tenderness.

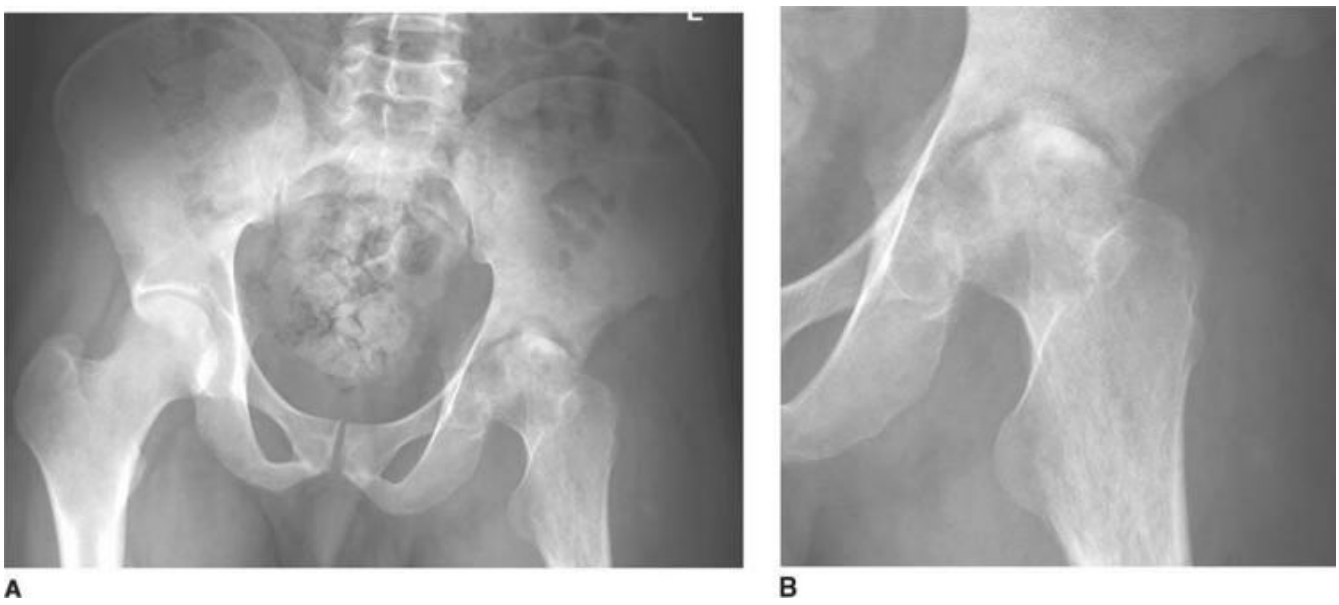


**FIGURES 5-2A and 5-2B (A)** Anteroposterior radiograph of the pelvis with **(B)** magnification of the left hip. The right hip is normal in appearance. There is joint space narrowing of the left hip, along with indistinctness of the articular cortex of the left acetabulum and left femoral head. The supraacetabular line is not visualized on the left, a striking difference compared with the normal right hip. There is juxta-articular osteopenia with ill-defined periarticular lucencies and erosive changes.

## DIFFERENTIAL DIAGNOSIS

**Septic joint:** The presence of joint space narrowing, erosions, and juxta-articular osteopenia in the setting of a painful joint are very worrisome for a septic joint. While patients usually present within 2 weeks of symptom onset, the presentation may be delayed in the setting of low-virulence and mycobacterial organisms. Based on the clinical presentation and radiographic findings, this is the most likely diagnosis, and must be excluded prior to entertaining other possible diagnoses. When septic joint is a possible diagnosis, urgent arthro-centesis (joint aspiration) is indicated.

**Rheumatoid arthritis:** The appearance of the left hip, with juxta-articular osteopenia, erosive changes, joint space narrowing, and the absence of bone formation such as osteophytosis are features suggestive of rheumatoid arthritis. However, rheumatoid arthritis is typically bilateral and symmetrical in distribution; in this case, the right hip is asymptomatic and normal in radiographic appearance, and therefore this is not the most likely diagnosis.

**Psoriatic arthritis:** It is unusual for the hip to be affected with psoriatic arthritis, and when it is, findings are often bilateral. In contrast to the current case, there is usually maintenance of juxta-articular bone mineralizaion and there are often peri articular bony proliferative changes. For these reasons, this is not the most likely diagnosis.

- **Avascular necrosis (AVN) of the femoral head:** AVN of the femoral head can cause areas of lucency and sclerosis in the femoral head, as are seen in this case. However, juxta-articular osteopenia and loss of visualization of the articular cortex are not features. Though joint space narrowing can occur due to secondary degenerative changes caused by AVN, it would be accompanied by osteophytosis and subchondral sclerosis, which are absent in this case. For these reasons, this is not the correct diagnosis.
- **Calcium pyrophosphate deposition disease (CPPD):** CPPD is a common cause of monoarticular arthritis in adult patients and an acute episode can be accompanied by a fever; however, CPPD usually affects patients over the age of 40 years. CPPD usually has an appearance similar to osteoarthritis; in the hip osteophytosis and subchondral sclerosis would be expected, and are absent in this case. In addition, there is no evidence of chondro-calcinosis of the visualized cartilaginous structures such as the pubic symphysis fibrocartilage in this case.

## DIAGNOSIS

**Septic joint. In this particular case, the organism isolated on culture of synovial fluid was *Mycobacterium tuberculosis***

## KEY FACTS

### Clinical

- An adult patient presenting with an acutely painful joint is a common medical emergency with many possible diagnoses, the most serious of which is a septic joint.
- The most common presentation is that of a hot, swollen, tender joint with reduced range of motion. Patients usually present within 2 weeks of symptom onset, but presentation may be delayed in the setting of low-virulence organisms, fungal organisms, mycobacterial organisms, or infections of prosthetic joints. Fever is present in only about 60% of patients at the time of presentation.
- Risk factors include underlying joint pathology (such as due to rheumatoid arthritis or osteoarthritis), age >80 years, immunocompromised status, prior intra-articular steroid injection, history of intravenous drug abuse, alcoholism, diabetes mellitus, the presence of cutaneous ulcers, recent joint surgery, and the presence of a joint prosthesis. However, these risk factors are only helpful when present; the absence of risk factors does not substantially reduce the likelihood of septic joint.
- The most commonly involved joints are the knee, hip, ankle, wrist, shoulder, and elbow. Polyarticular involvement is rare but does occur.

- The most common organisms isolated from patients with septic arthritis are staphylococci and streptococci. Infection is introduced into the joint by either hematogenous spread (which is the most common route), direct inoculation due to penetrating trauma or iatrogenic procedure, or direct spread from an adjacent infection such as cellulitis or osteomyelitis.
- While adjunctive tests such as erythrocyte sedimentation rate, C-reactive protein, and white blood cell count are helpful in assessing a patient's likelihood of having a septic joint and in monitoring a patient's progress if septic joint is diagnosed, no clinical, laboratory, or radiographic findings are sufficiently sensitive and specific to exclude a septic joint.
- When septic joint is a possibility, urgent arthrocentesis is indicated. However, Gram stain and culture of synovial fluid, obtained prior to antibiotic administration, identify the causative organism in only approximately 67% of cases of septic joint; thus, even a negative culture does not exclude a septic joint, though it does make the diagnosis less likely. An elevated synovial fluid white cell count increases the likelihood of septic arthritis, but is also not sufficiently reliable to confirm or exclude infection.
- Blood cultures should also be drawn if septic joint is suspected, and in some patients positive blood cultures will provide organism identification even when synovial fluid cultures are negative.
- Treatment includes appropriate antibiotic coverage, removal of purulent material from the joint space, and supportive measures.
- Delayed or inadequate treatment for septic joint can lead to permanent joint damage and functional disability due to rapid, irreversible cartilage destruction. Even in the setting of prompt and appropriate treatment, sepsis and/or permanent joint damage may occur. In addition, there is significant mortality, with fatality rates estimated at 7% to 15% despite the use of antibiotics.

## Radiologic

- Imaging techniques cannot accurately distinguish infective from noninfective inflammatory arthritis. In addition, radiographs of the affected joint may be normal, especially early in the course of infection. Urgent arthrocentesis is indicated if septic joint is clinically suspected, even in the absence of radiographic findings.
- When radiographs are abnormal, findings that may be seen include soft tissue swelling, joint effusion (which is particularly visible on radiographs of the elbow, knee, and ankle), uniform joint space narrowing due to cartilage destruction, juxta-articular osteopenia, and erosions. MR findings that may be seen in the setting of septic joint include joint effusion, surrounding soft tissue edema, diffuse joint space narrowing, cartilage loss, adjacent bone marrow edema, and erosions.

- MR imaging can be useful in delineating the extent of infection, identifying coexistent osteomyelitis, and identifying the extension of infected material into the periarticular soft tissues. However, MR imaging is not sufficiently sensitive or specific in diagnosing septic arthritis to be diagnostically useful. Therefore, arthrocentesis should not be delayed for the sake of advanced imaging.
- For most joints, arthrocentesis is performed under the guidance of fluoroscopy. For some joints, such as the sternoclavicular or sacroiliac joints, CT guidance is often favored. Pediatric hip aspirations are commonly performed utilizing ultrasound guidance.
- Arthrography (the instillation of contrast material) during arthrocentesis is necessary to confirm the intra-articular location of the needle. In addition, arthrography may reveal the presence of sinus tracts.
- Needle approaches during arthrocentesis should avoid overlying skin ulcers, areas of inflammation/ cellulitis, skin lesions such as psoriasis, and visualized sinus tracts if possible to avoid inoculating a sterile joint during the procedure. If cross-sectional imaging is available for review prior to the procedure, overlying fluid collections/ abscesses should be noted and aspirated separately, and not traversed by the needle on the way into the joint.
- Synovial fluid is commonly sent to the laboratory for cell count and differential, Gram stain, and aerobic and anaerobic cultures. Other stains and cultures, including fungal and acid-fast bacillus (AFB), are sent when atypical organisms are suspected. The fluid may also be examined for the presence of crystals if gout or CPPD are diagnostic possibilities.
- If the aspirate contains pus, as much as possible should be removed at the time of arthrocentesis.
- If no or insufficient fluid is retrieved during arthrocentesis (a “dry tap”), the needle should be repositioned several times; arthrography should be performed to confirm intra-articular position of the needle and to look for the presence of a sinus tract which may have a decompressing effect on the joint, making retrieval of fluid difficult. In the setting of a dry tap, some practitioners routinely perform joint washings with nonbacteriostatic sterile saline and send that material for culture, though the added diagnostic utility of this practice is unknown.

## SUGGESTED READING

Lin HM, Learch TJ, White EA, Gottsegen CJ. Emergency joint aspiration: a guide for radiologists on call. Radiographics 2009;29:1139–1158.

Margaretten ME, Kohlwes J, Moore D, Bent S. Does this adult patient have septic arthritis? JAMA 2007;297:1478–1488.

Mathews CJ, Kingsley G, Field M, et al. Management of septic arthritis: a systematic review. Ann Rheum Dis

2007;66:440–445.

Mathews CJ, Weston VC, Jones A, et al. Bacterial septic arthritis in adults. Lancet 2010;375:846–855.

# CASE 3

**CHARLES E. SPRITZER**

## HISTORY

A 39-year-old man with pain, tenderness, and mass-like swelling of the medial aspect of the left knee.

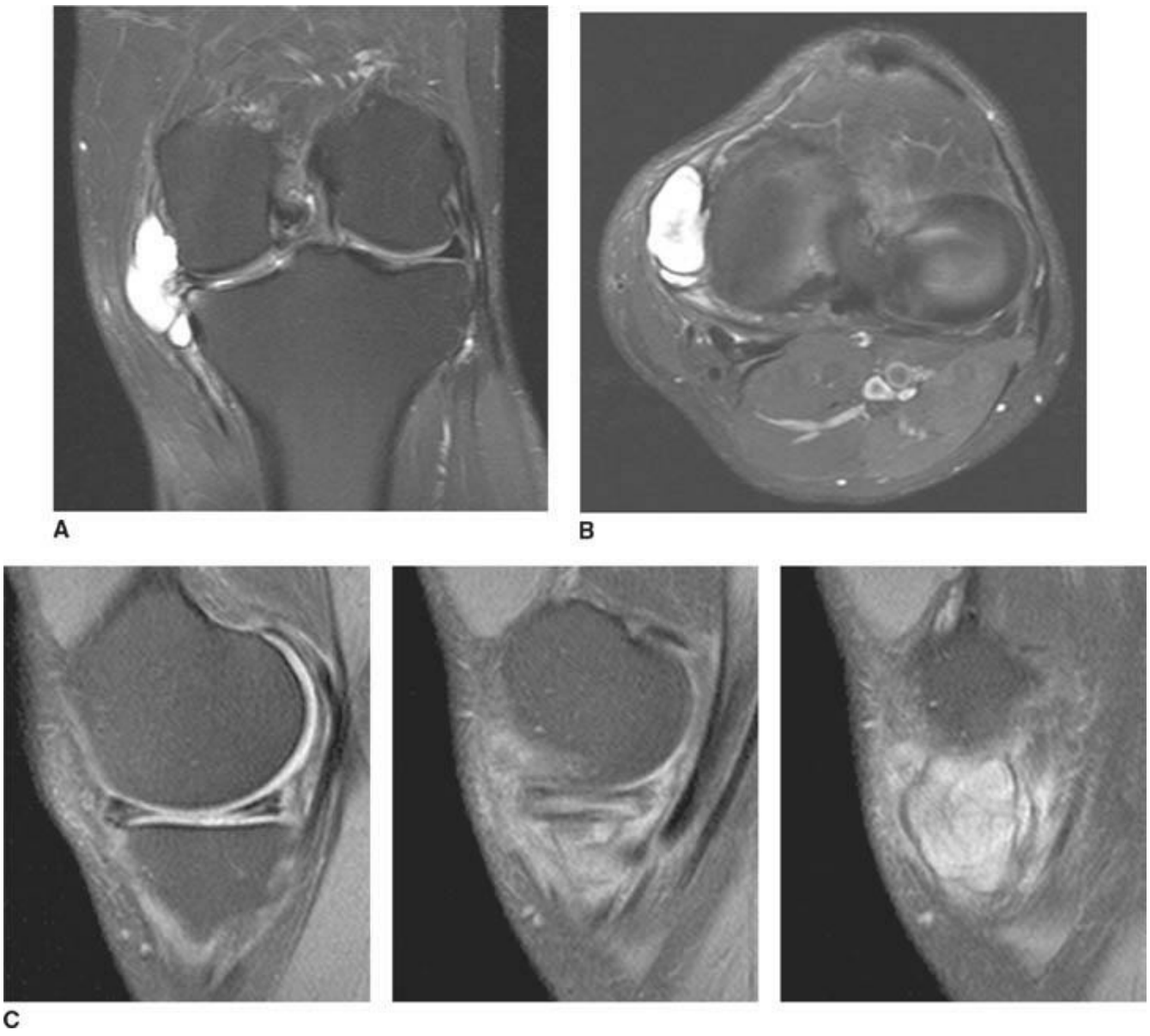


**FIGURES 5-3A, 5-3B and 5-3C (A)** Coronal and **(B)** axial fat suppressed fast spin echo T2-weighted MR images of the knee. **(C)** Sagittal fat suppressed proton density-weighted MR images of the medial knee. A loculated fluid signal intensity collection is seen adjacent to the medial joint line on T2-weighted images **(A** and **B).** There is diffuse intermediate intensity signal abnormality within the substance of the periphery of the medial meniscus body **(C),** and this intrameniscal signal abnormality appears to extend directly into the adjacent fluid signal intensity collection in the parameniscal soft tissues **(A** and **C).** There is signal abnormality within the medial meniscus which extends to the articular surface of the medial meniscus **(A** and **C),** with oblique undersurface and horizontal components.

## DIFFERENTIAL DIAGNOSIS

- **Popliteal cyst:** These cysts tend to be located more posteriorly and not as medially as in this case. The neck of a popliteal cyst protrudes through the space between the medial head of the gastrocnemius and the semimembranosus muscles, not through the medial aspect of the joint as in this case.
- **Parameniscal cyst and tear of the medial meniscus:** There is signal abnormality in the medial meniscus which extends to the articular surface, diagnostic of a menis-cal tear. A cystic structure emanating from an abnormal appearing meniscus, which in this case is the torn medial meniscus, is diagnostic of a parameniscal cyst.
- **Ganglion cyst or synovial cyst:** Because it is difficult to tell based on imaging features whether or not a synovial lining is truly present, the terms "ganglion cyst" and "synovial cyst" are sometimes used interchangeably in imaging. While the signal intensity of the loculated collection is consistent with a fluid-filled/jellylike viscous substance, and while this collection is technically a "ganglion" in the most general sense, the fact that this collection emanates from the medial meniscus distinguishes this entity from a simple "ganglion." This distinction is important in the management of these lesions, which differs from that of simple ganglia as the underlying meniscal abnormality must be addressed.
- **Pes anserinus bursitis:** Fluid and/or edema are often seen in association with inflammation of the pes anserine, namely, the distal semitendinosis, sartorius, and gracilis tendons. Thus, fluid collections due to pes bur-sitis are medial in location, like the current case, but are typically inferior to the joint line, and therefore this is not the correct diagnosis.
- **Medial collateral ligament bursitis:** A fluid-filled medial or tibial collateral ligament bursa is located medially, at the level of the joint line, and deep to the medial collateral ligament, features that make this a possible diagnosis in this case. However, in this case the fluid is seen to emanate from a region of signal abnormality in the medial meniscus, and therefore this is not the correct diagnosis.

## DIAGNOSIS

**Parameniscal cyst and tear of the medial meniscus**

## KEY FACTS

### Clinical

- Classically, these lesions have been referred to as "meniscal cysts." With the advent of advanced imaging has come the recognition that meniscal cysts may exist within the confines of the meniscus (some refer to this as an "intrameniscal cyst") with or without

extension into the parameniscal soft tissues. Now, some describe the parameniscal cystic component of these lesions as a "parameniscal cyst" or as a "meniscal cyst with a parameniscal component." Some continue to use the more general term "meniscal cyst" to refer to the entire spectrum of cystic lesions of the meniscus.

- Meniscal cysts contain jelly-like mucinous or synovial fluid. They may occur laterally or medially, and most but not all meniscal cysts are seen in association with a meniscal tear extending to the articular surface of the meniscus.
- The pathogenesis and treatment of meniscal cysts is somewhat controversial. Possible etiologies include traumatic and degenerative.
- Some advocate a "one-way valve" mechanism, whereby synovial fluid is absorbed via a meniscal tear into the substance of the meniscus, where it collects and may subsequently spread into the parameniscal soft tissues. Others favor that these cysts—particularly when no meniscal tear is evident—form from a myxoid degenerative process within the substance of the meniscus, which may enlarge the meniscus ("intrameniscal cyst") and which may subsequently be expressed into the adjacent soft tissues, forming a parameniscal component or "parameniscal cyst."
- For most ganglion cysts, excision of the lesion is sufficient. However, if a parameniscal cyst is excised in a similar fashion, it will typically recur. As such, the diagnosis of a meniscal cyst in this situation requires treatment of the underlying meniscal abnormality to prevent recurrence.
- In the past, treatment of meniscal cysts often consisted of open arthrotomy and complete meniscectomy. Increased appreciation of the importance of the conservation of meniscal tissue has led to the arthroscopic treatment of meniscal cysts with either open excision of any parameniscal cystic component and arthroscopic assessment of the meniscus involved, or a entirely arthroscopic procedure with arthroscopic decompression of the cyst prior to addressing the meniscus itself. In either case, a careful arthroscopic assessment of the meniscus involved is warranted to inspect for and address any meniscal tear to the articular surface that may be present.

## Radiologic

- MR imaging of the knee is useful in distinguishing meniscal cysts from other cystic lesions around the knee, such as bursae, which may extend adjacent to and even abut the outer edge of the meniscus; a true meniscal cyst has a clear, identifiable connection of the parameniscal cystic component to the adjacent meniscus, and the demonstration of abnormal signal intensity within the adjacent meniscus itself. This is particularly important medially, where several bursae are located in the soft tissues adjacent to the medial meniscus, and can sometimes mimic parameniscal cysts.
- On MR imaging, an intrameniscal cyst demonstrates abnormal signal intensity, usually

of intermediate signal intensity, within the substance of the meniscus with associated bulging, convex borders. The convex contour of the meniscus may not be evident in cases with associated meniscal tears and/or parameniscal cystic components due to decompression of the meniscus itself.

- When a parameniscal cystic component is present, it is almost always of fluid signal intensity on T2-weighted MR images, and usually manifests as a loculated fluid collection extending from the joint line.
- MR imaging is useful in determining whether or not an associated meniscal tear is present, which is an important consideration in planning treatment. Meniscus sensitive sequences, such as proton density or Tl-weighted MR imaging, are utilized to inspect for associated tears. These tears often have a horizontal component as well as an oblique component to the articular surface.

## SUGGESTED READING


Anderson JJ, Connor GF, Helms CA. New observations on meniscal cysts. Skeletal Radiol 2010;39:1187–1191.

Campbell SE, Sanders TG, Morrison WB. MR imaging of meniscal cysts: incidence, location, and clinical significance. Am J Roentgenol 2001;177:409–413.

De Maeseneer M, Shahabpour M, Vanderdood K, et al. MR imaging of meniscal cysts: evaluation of location and extension using a three-layer approach. Eur J Radiol 2001;39:117–124.

Sarimo J, Rainio P, Rantanen J, Orava S. Comparison of two procedures for meniscal cysts: a report of 35 patients with a mean follow-up of 33 months. Am J Sports Med 2002;30:704–707.

Tschirch FTC, Schmid MR, Pfirrmann CWA, et al. Prevalence and size of meniscal cysts, ganglionic cysts, synovial cysts of the popliteal space, fluid-filled bursae, and other fluid collections in asymptomatic knees on MR imaging. Am J Roentgenol 2003;180:1431–1436.


# CASE 4


**ROBERT M. VANDEMARK AND R. LEE COTHRAN. JR.**


### HISTORY

Patient A: A 35-year-old man who fell from a ladder onto an outstretched hand and now complains of shoulder pain. Patient B: A 45-year-old woman who complains of severe shoulder pain following a grand mal seizure.

A

■**FIGURE 5-4A** Anteroposterior internal rotation radiograph of the shoulder in patient A. There is widening of the joint space.

B

■**FIGURE 5-4B** Anteroposterior external rotation radiograph of the shoulder in patient A. This view also shows identical joint space widening, which indicates lack of any motion at the glenohu-meral joint.

C

■**FIGURE 5-4C** Anteroposterior radiograph of the shoulder in patient B. There is widening of the joint space and an oblique sclerotic band through the articular segment of the humerus.

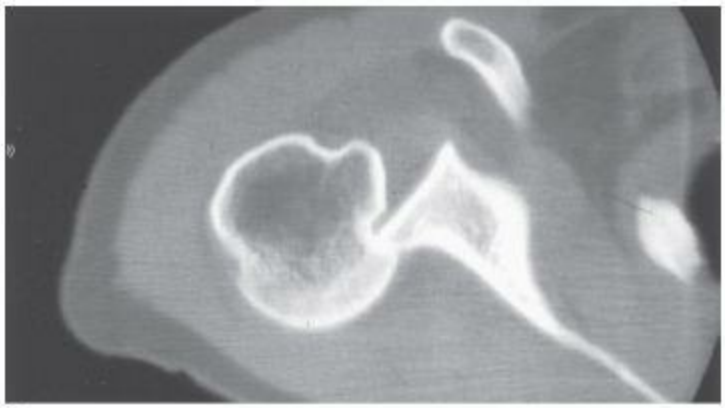

D

■**FIGURE 5-4D** Axial CT of the glenohumeral joint in patient B. There is an impaction fracture produced by collision of the posterior glenoid rim on the humeral head.

## DIFFERENTIAL DIAGNOSIS

■**Anterior dislocation of the shoulder:** Anterior shoulder dislocations

characteristically cause anteroinferior displacement of the humeral head relative to the gle-noid. This position of the humeral head is never seen in patients with posterior dislocation. In addition, anterior dislocation leads to total obscuration of the normal glenohumeral joint space due to overlap of the humeral head and the glenoid. This is not the correct diagnosis based on the imaging appearance.

- **Posterior dislocation of the shoulder:** Posterior dislocations are rare but are characteristic in patients with seizures, electrical injury, and, occasionally, blunt injury to the anterior aspect of the shoulder. In virtually all cases of posterior dislocation, the humeral head and glenoid remain in the same transverse plane, unlike anterior dislocation, where the humeral head displaces inferomedially. Some posterior dislocations give the appearance of a widened glenohumeral joint space, caused by "perching" of the humeral head on the posterior glenoid. As a result, the distance between the humeral head and the anterior glenoid is widened, which gives the false impression of a widened joint space. This feature is never seen in anterior dislocation. This is the correct diagnosis.
- **Pseudodislocation of the shoulder:** This term applies to a clinical presentation in which physical findings suggest an abnormal position of the humeral head consistent with a shoulder dislocation. Subsequent radiographs fail to show a dislocation but do demonstrate inferior subluxation of the humeral head relative to the glenoid. Pseudodislocation can be seen in the setting of brachial plexus injury, chronic shoulder joint instability, hemarthrosis, and, occasionally, pyarthrosis. The current cases do not demonstrate inferior subluxation of the humeral head, and instead demonstrate a posterior position of the humeral head relative to the gle-noid; therefore, this is not the correct diagnosis.

## DIAGNOSIS

**Posterior dislocation of the shoulder**

## KEY FACTS

### Clinical

- Less than 3% of all shoulder dislocations are posterior.
- The characteristic setting for this injury is in a patient after a seizure.

### Radiologic

- "Fixed" internal rotation should immediately raise the possibility of posterior dislocation of the shoulder.

- A “positive” rim sign is present when the distance between the anterior glenoid rim and the humerus is >6 mm.
- Posterior dislocation remains a challenging diagnosis when the axillary or “Y” views are unavailable. Such would be the case on portable chest radiographs obtained for patients with blunt trauma, electrical injury, or seizure disorders. Under these circumstances, it is important to recognize the clues of posterior dislocation on an anteroposterior view alone. The radiologist must recognize fixed internal rotation, widening of the joint space (rim sign), and loss of the overlap appearance (half moon) of the normal shoulder joint as characteristic findings of posterior dislocation on a frontal film.
- A posttraumatic dent in the humeral head (trough sign) is a helpful sign but is not always present. Posterior dislocations can also be seen in conjunction with comminuted fracture-dislocations of the proximal humerus. In any event, the reader should keep in mind that posterior dislocations when missed can easily escape clinical detection and become chronic dislocations. It is not unusual for patients with chronic posterior dislocation to remain undiagnosed for months at a time. The radiologist must always have a high index for a “missed” posterior dislocation when reviewing outpatient radiographs in patients with chronic shoulder pain.
- A clinical history of any or all of the following symptoms—a frozen shoulder, limited range of motion, and old trauma—should motivate the radiologist to obtain a dislocation view (axillary view preferred) to exclude the possibility of a chronic posterior dislocation.

## SUGGESTED READING

Helms CA. Fundamentals of Skeletal Radiology (3rd ed). Philadelphia, PA: Elsevier Saunders, 2005:97–101.

Resnick D. Diagnosis of Bone and Joint Disorders (4th ed). Philadelphia, PA: Saunders, 2002:2784–2796.

Rogers LF, Lenchik L. The shoulder and humeral shaft. In LF Rogers (ed), Radiology of Skeletal Trauma. Philadelphia, PA: Saunders, 2002: 662–669.

# CASE 5

**EMILY N.**
**VINSON**

### HISTORY

A 57-year-old man who has had pain in his hands for over 25 years. On physical examination, there are patches of red, scaly skin behind his ears, on the left frontal

portion of his scalp, and on his left elbow. In addition, several of his fingernails appear thickened and discolored.


■**FIGURES 5-5A and 5-5B** Anteroposterior radiographs of the left **(A)** and right **(B)** hands demonstrate severe erosive changes involving the DIP joints bilaterally, with "pencil-in-cup" deformities. Bone mineralization is preserved, and the MCP joints are relatively spared.


■**FIGURE 5-5C** Anteroposterior radiograph of the right foot toes. There is joint space

loss of the great toe IP joint with periarticular erosions and new bone formation. There are similar changes at the second, third, and fourth DIP joints. There is erosion and sclerosis of the distal tuft of the great toe.

## DIFFERENTIAL DIAGNOSIS

- **Rheumatoid arthritis (RA):** RA has a predilection for bilateral symmetric involvement of the hands, as is seen in this case. However, RA tends to involve the more proximal joints of the hand and wrist such as the carpus, ulnar styloid, MCP joints, and PIP joints, whereas in this case involvement of the DIP joints predominates. The IP joint of the great toe can be involved in RA, but the more classic site for erosive change in the foot due to RA is the head of the fifth metatarsal, which does not appear involved in this case. There is no evidence of juxta-articular or generalized osteoporosis in this case, a common feature of RA. Perhaps most importantly, this case demonstrates bone proliferation, which should be absent in RA. For these reasons, this is not the correct diagnosis.
- **Psoriatic arthritis:** The severe erosive changes affecting the DIP joints of the hands with "pencil-in-cup" appearance and sparing of the MCP joints is most consistent with psoriatic arthritis. Other findings that support this diagnosis are proliferative erosive changes of the great toe IP joint, an "ivory phalanx" of the great toe distal phalanx, and maintenance of normal bone mineralization. The provided clinical history of skin lesions and nail involvement is also characteristic of this disorder.
- **Reiter's disease/reactive arthritis:** Reactive arthritis has an identical radiologic appearance to psoriatic arthritis, including ill-defined erosions and bone proliferation. However, reactive arthritis has a slightly different distribution, with hand involvement very uncommon. In addition, the patient's clinical history makes this diagnosis unlikely; reactive arthritis usually presents in males between the ages of 15 and 35 years and is often associated with urethritis and conjunctivitis rather than skin lesions. For these reasons, this is not the correct diagnosis.

## DIAGNOSIS

**Psoriatic arthritis**

## KEY FACTS

### Clinical

- Psoriatic arthritis is a chronic inflammatory arthritis associated with the skin disorder psoriasis, and is estimated to occur in up to 30% of patients with psoriasis.

- In the past, psoriatic arthritis was considered a “rheumatoid variant.” Psoriatic arthritis was recognized as an entity distinct from RA in the 1940s, following the discovery of the rheumatoid factor. Patients with pso-riatic arthritis are usually seronegative (meaning no rheumatoid factor is detected in their serum).
- Psoriatic arthritis is considered one of the spondyloar-thropathies due to the presence of spondylitis in up to 40% of patients and an association with HLA-B27 antigen.
- The skin manifestations of psoriasis usually precede the development of psoriatic arthritis by an average of 10 years. Less commonly, seen in 15% to 20% of patients, the arthritis will manifest earlier than evidence of psoriasis skin lesions.
- Nail lesions are very common in patients with psoriatic arthritis (occurring in about 87%).
- Up to 20% of patients with psoriatic arthritis will experience a very destructive, disabling form of arthritis.
- Mild psoriatic arthritis may be managed with non-steroidal anti-inflammatory drugs. Newer treatment options for moderate to severe disease include disease-modifying antirheumatic drugs and biologic agents such as tumor necrosis factor-alpha inhibitors.

## Radiologic

- Psoriatic arthritis is an inflammatory arthritis characterized by uniform joint space narrowing, erosions, bone proliferation, periostitis, and enthesitis.
- Radiographic findings in psoriatic arthritis may be bilateral or unilateral, symmetric or asymmetric.
- The most common site of involvement is the hands, and there are several different patterns of hand involvement: DIP and PIP joint involvement with sparing of the MCP joints and carpus; involvement of all joints of one to three fingers, with sparing of the other fingers; and diffuse involvement with a distribution similar to RA, differing from RA in that there are usually bone prolif-erative changes and DIP involvement present.
- There is often soft tissue swelling affecting an entire digit in the hand or foot, known as the “sausage digit.”
- Erosions start at the margins of the joint and progress to involve the central portion. Erosions may become so destructive that the joint appears widened. The ends of phalangeal bones may become pointed, with saucer-ization of the articulating bone, causing the “pencil-in-cup” appearance. Acro-osteolysis may occur. The characteristic erosive changes seen in psoriatic arthritis help distinguish it from another of the seronegative spondyloarthropathies, ankylosing spondylitis.
- Even in the setting of severe erosive disease, normal bone mineralization is usually maintained. Other radiographic features that help distinguish psoriatic arthritis from RA

are the presence of bone proliferation and a distribution that is often asymmetric.

- Bone proliferation occurs adjacent to erosions (and is often initially irregular and ill-defined in appearance), along the diaphysis (periostitis), across joints (ankylo-sis, particularly common at the interphalangeal joints), and at tendinous and ligamentous insertion sites (enthesitis).
- Findings in the foot are similar to those in the hand. Destruction of the great toe IP joint is more common in psoriatic arthritis than with any other arthritis.
- An "ivory phalanx" may be seen in psoriatic arthritis, due to sclerosis and/or bone proliferation affecting a distal phalanx in the foot (most commonly, the great toe distal phalanx).
- Other appendicular joints may be affected, including the knee, ankle, and shoulder. Involvement of the hip joint is uncommon, although enthesitis affecting the greater trochanter is common.
- Up to half of patients with psoriatic arthritis will have involvement of the synovial portion of the SI joints, which is usually asymmetric but can be symmetric, characterized by erosive and bulky proliferative changes. Anky-losis can occur. Ossification of the ligamentous portion of the SI joints may also occur.
- In the spine, large, bulky, often asymmetric paraverte-bral ossifications are characteristic. Except in the cervical spine, the facet joints are usually spared.

## SUGGESTED READING

Brower AC, Flemming DJ. Arthritis in Black and White (2nd ed). Philadelphia, PA: W.B. Saunders Company, 1997.

Gladman DD, Antoni C, Mease P, et al. Psoriatic arthritis: epidemiology, clinical features, course, and outcome. Ann Rheum Dis 2005;64(Suppl Il):ii14–ii17.

Jacobson JA, Girish G, Jiang Y, Resnick D. Radiographic evaluation of arthritis: inflammatory conditions. Radiology 2008;248:378–389.

Spira D, Kotter I, Henes J, et al. MRl findings in psoriatic arthritis of the hands. Am J Roentgenol 2010;195:1187–1193.

# CASE 6

**ROBERT M. VANDEMARK AND R. LEE COTHRAN, Jr.**

## HISTORY

A 21-year-old man who was a restrained passenger in a head-on collision with another vehicle.

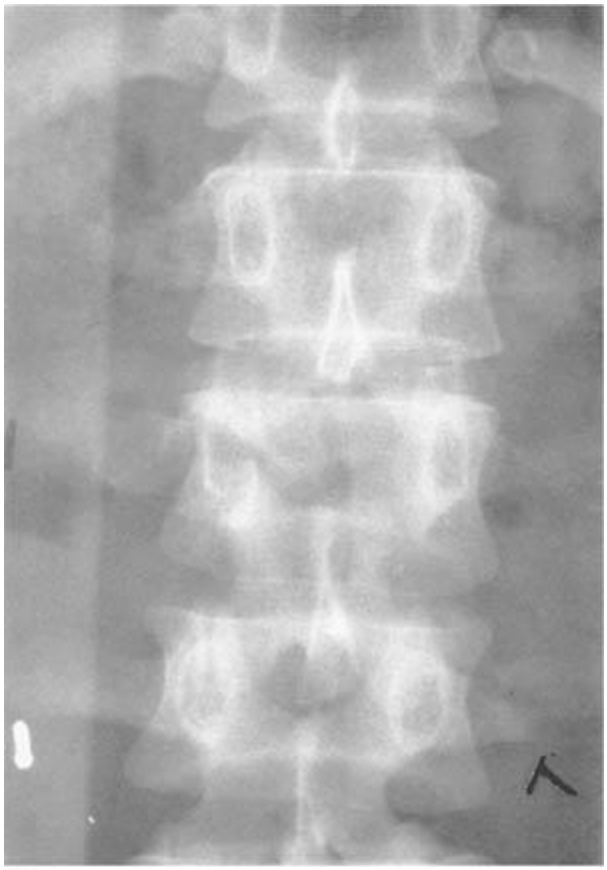

A

■**FIGURE 5-6A** Anteroposterior radiograph of the lumbar spine. There is a subtle horizontal lucency through the right pedicle of L2. In addition, there is distraction of the spinous processes of L1 and L2, resulting in a relative lucency of the L2 vertebral body.

B

■**FIGURE 5-6B** Lateral radiograph of the lumbar spine. There is only a minor compression fracture of the body of L2.

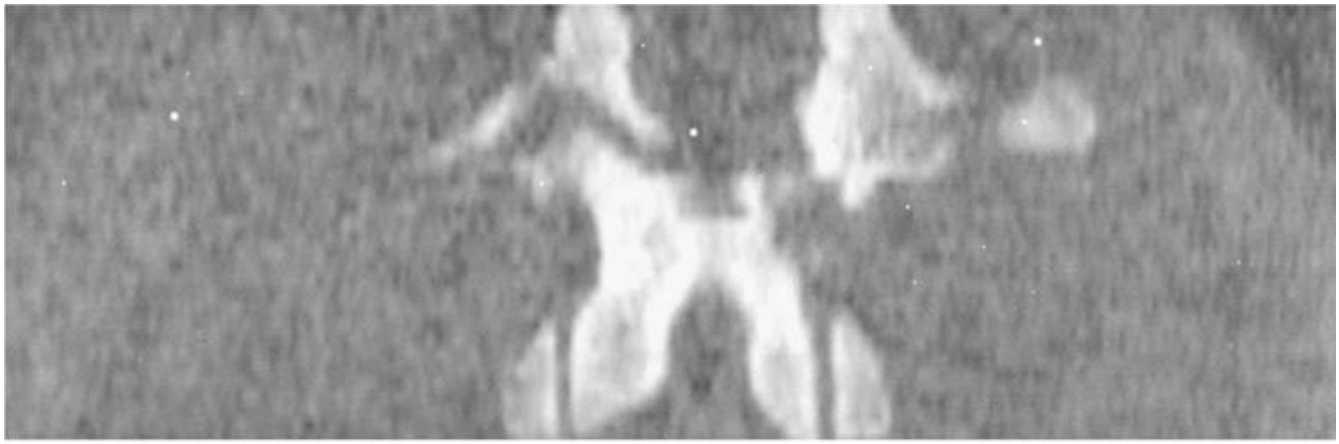

C

■**FIGURE 5-6C** Axial CT scan of the lumbar spine reformatted in the coronal plane. There is a horizontally oriented fracture of the posterior elements.

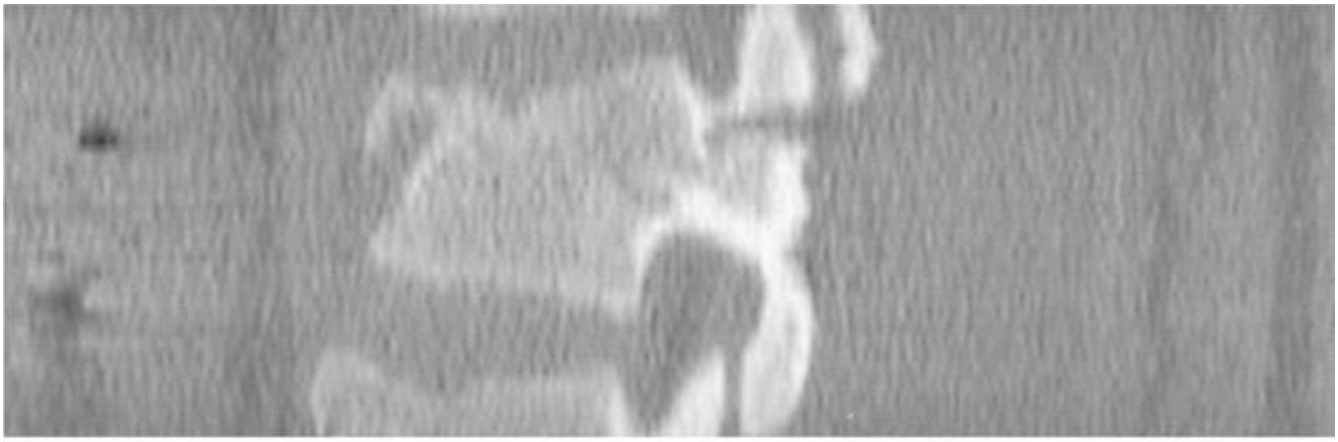

D

**FIGURE 5-6D** Axial CT scan of the lumbar spine reformatted in the sagittal plane shows both the anterior and posterior components of the fracture.

## DIFFERENTIAL DIAGNOSIS

**Simple compression fracture:** Minor compression fractures of the vertebral column are common but do not usually disrupt the middle or posterior columns of stability. Usually the degree of compression is <25% of the vertebral body height, and there is no evidence of ret-ropulsion or extension of the fracture into the posterior elements. Given the posterior element involvement in this case, this is not the correct diagnosis.

**Burst fracture:** Burst fractures are caused by an axial load on the vertebral column as would occur during a fall from a significant height. CT examination would demonstrate radial dispersion of the vertebral body fragments with retropulsion into the spinal canal. The longitudinal distraction of the fractured posterior elements in this case is not consistent with a burst-type fracture; therefore, this is not the correct diagnosis.

**Chance fracture:** The Chance fracture is produced by a flexion-distraction mechanism. Fracture lines are typically seen extending into the posterior elements of the vertebrae on a lateral view. Characteristically, subtle bilateral pedicle fractures can be seen on the AP radiograph and should be sought. Chance fractures sometimes produce only minimal anterior compression and can be confused with simple compression fractures when the pedicle and posterior element extension of the fracture are not appreciated. Based on the images provided, this is the correct diagnosis.

## DIAGNOSIS

**Chance fracture**

## KEY FACTS

## Clinical

- Chance fractures are flexion-distraction injuries of the spine most commonly located in the thoracolumbar region and characterized by a transversely oriented facture with separation of the posterior elements in the longitudinal plane. These are unstable fractures with disruption of the middle and posterior columns, and often also involve extension into the anterior column.
- They are associated with seatbehVlapbelt restraint.
- There is a high association with intra-abdominal injuries.
- Despite the substantial posterior element injury seen in Chance fractures, neurologic deficits are less common than with other serious thoracolumbar spine injuries such as burst fractures or fracture-dislocations of the spine.

## Radiologic

- Though unstable injuries, Chance fractures usually occur in the absence of neurologic compromise and can be very subtle radiographically.
- Chance fractures can be difficult to diagnose when undue emphasis is placed on the lateral view of the spine. The degree of vertebral compression may be slight, giving the false impression of a simple compression fracture. Regardless of the site of trauma, it is imperative to give equal time to the inspection of the AP view and lateral radiographs in spine trauma. This is particularly true for Chance fractures in which the posterior element component is often quite impressive on the AP view while unappreciated on the lateral view.
- Vertical separation of the spinous processes in the setting of a Chance fracture can often be detected on the AP radiograph, as the involved vertebral body may appear relatively lucent when the spinous processes are displaced such that they are no longer superimposed on the vertebral body (the “empty vertebral body sign”).
- Simple compression fractures of the spine are common, and although they produce severe back pain, they do not cause neurologic injury. Simple compression fractures with <25% loss in vertical body height can be treated conservatively; additional imaging is not needed.
- Compression fractures >25% can be deceptive on radiographs, and CT can be helpful in excluding retropulsion of fragments, a finding that is commonly underestimated from radiograph analysis.
- The fracture line in a Chance fracture often lies within the plane of an axial CT; therefore, sagittal and/or coronal reformatted images often provide better visualization of the fracture morphology.
- Burst fractures, regardless of their location in the spine, imply an axial load with

radial dispersion of fracture fragments. An increase in the interpediculate distance on the frontal radiograph is a key finding. This further emphasizes the importance of inspecting the posterior elements on the anteroposterior radiograph in spinal trauma. CT and sometimes MRI are used in the evaluation of burst injuries due to the high propensity for spinal canal compromise.

- It is not uncommon for Chance fractures to be accompanied by a burst fracture component; this finding can have significance in the management of these fractures due to the presence of osseous retropulsion related to the burst component.

## SUGGESTED READING

Bernstein MP, Mirvis SE, Shanmuganathan K. Chance-type fractures of the thoracolumbar spine: Imaging analysis in 53 patients. Am J Roentgenol 2006;187:859–868.

Berquist TH. Imaging of Orthopedic Trauma. New York, NY: Raven, 1992:169–194.

Harris JH, Harris WH, Novelline RA. The Radiology of Emergency Medicine. Baltimore, MD: Williams & Wilkins, 1993:247–280.

Rogers LF, Daffner RH. The thoracic and lumbar spine. Radiology of Skeletal Trauma (3rd ed). New York: Churchill Livingstone, 2002:521–525.

# CASE 7

**EMILY N.**
**VINSON**

### HISTORY

A 13-year-old boy with a 1-month history of progressive left shoulder pain and swelling.

A

■**FIGURE 5-7A** Anteroposterior radiograph of the left shoulder. There is an aggressive-appearing, predominantly sclerotic lesion in the proximal left humeral metaphysis, with cloud-like areas of increased density in the interosseous portion of the lesion, as well as vague increased density in the extraosseous soft tissues just medial to the lesion. There is associated aggressive-appearing periostitis along the lateral cortical margin and a Codman's triangle at the inferomedial aspect of the lesion. The cortex is indistinct at the superomedial aspect of the lesion.

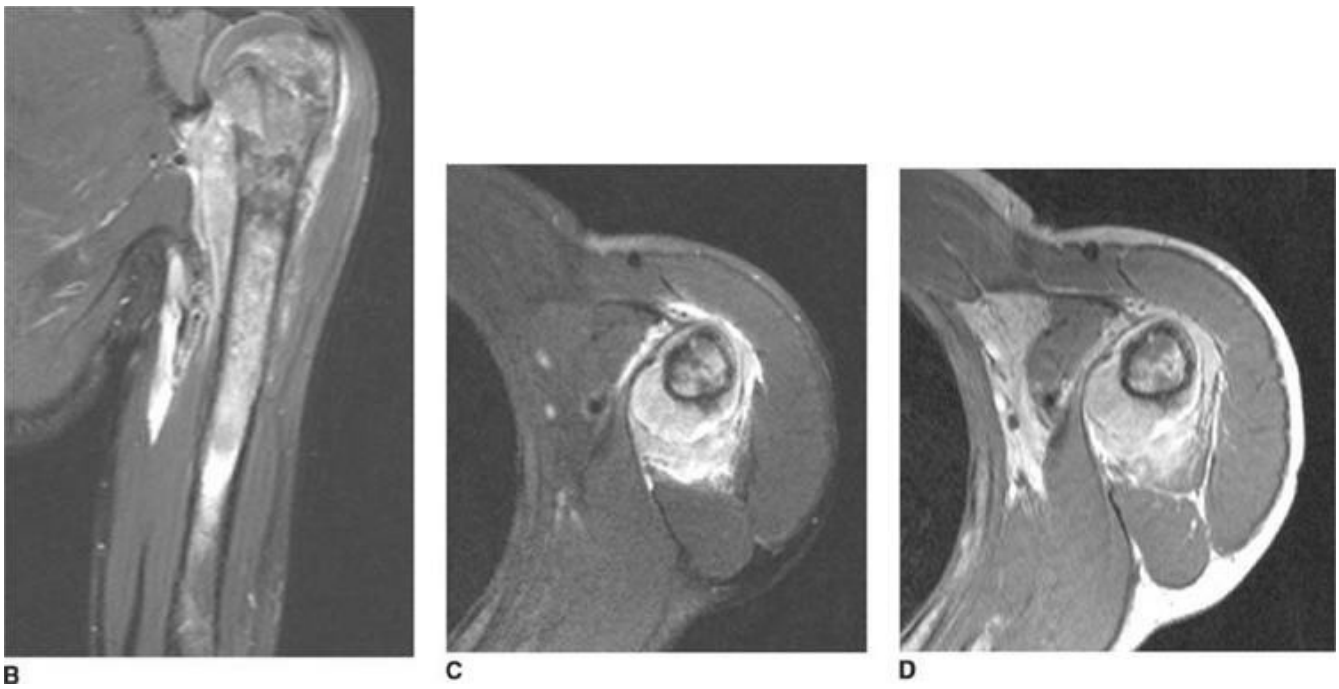


**FIGURES 5-7B, 5-7C, and 5-7D** Fat-suppressed FSE T2-weighted images in the coronal **(B)** and axial **(C)** planes, and postcontrast axial Tl-weighted image **(D).** The lesion is of heterogeneous signal intensity on the T2-weighted images, with areas of low signal intensity corresponding to areas of mineralization. There is violation of the humeral cortex at the superomedial aspect of the mass with an associated soft tissue mass. There is edema in the soft tissues surrounding the lesion.

## DIFFERENTIAL DIAGNOSIS

**Ewing's sarcoma:** Though Ewing's sarcoma is primarily thought of as having a permeative, lytic appearance, this tumor can elicit reactive new bone formation, resulting in a patchy sclerosis throughout the lesion, similar to what is seen in this case. This tumor is most commonly seen in the pelvis or in the metadiaphysis of a long bone, but can occur in the metaphysis of a long bone. Therefore, while not the most likely diagnosis, Ewing's sarcoma should remain on the list of possible diagnoses in this case.

**Conventional osteosarcoma:** The lesion has an aggressive appearance, with patchy areas of cloudlike increased density, aggressive periostitis, cortical destruction, and a soft tissue mass. These are features of conventional osteosarcoma. The location of the lesion in the metaphysis of a long bone and the patient's age are also typical for osteosarcoma. Therefore, this is the most likely diagnosis.

**Osteomyelitis:** Osteomyelitis can have a very aggressive appearance, and may manifest as a mixed lytic and sclerotic lesion due to bone resorption and reactive new bone formation, respectively. Aggressive periostitis can be present on radiographs, and a soft tissue mass may also be seen. However, the areas of increased density on the

radiograph and the low signal intensity areas on the MR images in this case are most suggestive of oste-oid material, which would not be expected in infection. This makes osteomyelitis less likely.

# DIAGNOSIS

**Conventional osteosarcoma**

# KEY FACTS

## Clinical

- Osteosarcoma is a malignant neoplasm of bone in which the tumor cells produce osteoid matrix, and is the most common primary malignant bone tumor in children. Most patients are between the ages of 10 and 20 years at the time of diagnosis, with the vast majority under the age of 30 years. Osteosarcomas rarely occur in older patients, usually in the setting of malignant degeneration of Paget's disease or at a site of prior external beam radiation therapy.
- "Conventional" osteosarcoma is the term used for the high-grade intramedullary type of osteosarcoma that occurs in the metaphysis of a long bone in children and adolescents, and is the most common type. This discussion refers to conventional osteosarcoma.
- The most common sites of involvement are the distal femur, proximal tibia, and proximal humerus. Most of the tumors are intramedullary, and in a long bone the metaphysis is by far the most common location (90% to 95%). However, any portion of any bone can be involved.
- Pathologic fractures are seen in 15% to 20% of cases, either at the time of presentation or during therapy.
- About 20% of children will have detectable metastatic disease at the time of initial diagnosis, most commonly involving the lungs as the result of hematogenous spread. Other common sites of metastatic disease include the skeleton and regional and distal lymph nodes.
- Patients are usually treated with neoadjuvant courses of chemotherapy to treat potential micrometastatic disease prior to definitive resection of the tumor. Neo-adjuvent chemotherapy also often leads to maturation/ ossification of any associated soft tissue mass, allowing for an easier resection.
- The advent of effective preoperative chemotherapy has markedly improved the prognosis of patients with osteosarcoma. The 5-year survival rate is 60% to 80%.
- Histologic response to preoperative chemotherapy is the strongest prognostic factor.

## Radiologic

- Conventional osteosarcoma usually has a very destructive and aggressive appearance on radiographs. It may be a lytic, blastic, or mixed lytic and blastic bone lesion. The initial characterization of these tumors is usually best performed with radiography.
- The tumors are typically large, with indistinct margins, cortical destruction, aggressive periosteal reaction (such as sunburst and Codman's triangle), and a soft tissue mass. Permeative lytic areas represent bone destruction, and cloud-like areas of increased density represent the malignant osteoid matrix produced by the tumor cells. This osteoid matrix may be visible within both the intraosseous and extraosseous portions of the tumor.
- MR imaging does not play a major role in the initial characterization of the lesion beyond what is provided by the radiographic assessment, but plays a major role in local staging and pre-operative planning. The fact that limb-sparing resection techniques are now favored over amputation has necessitated highly accurate local staging to depict intramedullary and extramedullary disease extent prior to surgery.
- MR imaging allows preoperative assessment of the longitudinal intramedullary extent of the neoplasm and detects epiphyseal involvement and skip metastases. The intramedullary extent of the tumor determines the resection margins. Spin echo T1-weighted sequences along the long-axis of the bone are considered the most accurate at determining the longitudinal intraosseous extent of macroscopic tumor.
- Skip metastases are estimated to occur in anywhere from 1% to 25% of cases of conventional osteosarcoma.
- By MR imaging, epiphyseal extension of osteosar-coma across an open physis is detected in up to 80% of metaphyseal osteosarcomas.
- MR imaging also depicts the extramedullary extent of the tumor, including the size and location of any soft tissue mass and its relationship to the neurovascular bundle and compartments of the extremity, and the presence or absence of joint involvement. These features help determine whether or not limb-salvage resection will be feasible and what type of surgery will be performed.
- To stage distant disease, patients also undergo radio-nuclide bone scintigraphy to evaluate for distant osseous metastatic disease and CT of the chest to evaluate for distant soft tissue metastatic disease, which is most common in the lungs.

## SUGGESTED READING

Wootton-Gorges SL. MR imaging of primary bone tumors and tumor-like conditions in children. Radiol Clin N Am 2009;47:957–975.

Unni KK. Osteosarcoma of bone. J Orthop Sci 1998;3:287–294.

Saifuddin A. The accuracy of imaging in the local staging of appendicular osteosarcoma. Skeletal Radiol 2002;31:191–201.

Brisse H, Ollivier L, Edeline V, et al. Imaging of malignant tumours of the long bones in children: monitoring response to neoadjuvant chemotherapy and preoperative assessment. Pediatr Radiol 2004;34:595–605.

Suresh S, Saifuddin A. Radiological appearances of appendicular osteosar-coma: a comprehensive pictorial review. Clin Radiol 2007;62:314–323.

Murphey MD, Robbin MR, McRae GA, et al. The many faces of osteosarcoma. Radiographics 1997;17:1205–1231.

# CASE 8

**SALUTARIO J.**
**MARTINEZ**
**AND**
**R. LEE**
**COTHRAN, Jr.**

## HISTORY

A 16-year-old boy with persistent left ankle pain following hardware removal.


A

■**FIGURE 5-8A** Anteroposterior radiograph of the left ankle. There is a lucent expansile lesion of the medial talus, with a thin sclerotic margin. Evidence of prior hardware in the distal tibial and fibula is incidentally noted.

B

C

**FIGURES 5-8B and 5-8C** Coronal and sagittal reformatted images from a CT scan of the left ankle. There is a well-circumscribed, mildly expansile lesion of the medial left talus with a thin sclerotic margin and containing calcified chondroid matrix. There is mild sclerosis in the adjacent marrow.

D

**FIGURE 5-8D** Sagittal fat-suppressed FSE T2-weighted MRI of the left ankle. There is a well-circumscribed lesion of the medial talus of predominantly low signal intensity containing a few foci of increased signal intensity. The adjacent marrow and soft tissues demonstrate diffuse increased signal intensity related to edema.

## DIFFERENTIAL DIAGNOSIS

- **Brodie's abscess:** This would be a possibility based on the initial radiograph. However, the presence of a predominately low signal intensity lesion on the MRI makes this much less likely.
- **Eosinophilic granuloma:** Although variable in appearance, these lesions are most often metaphyseal and multifocal with less marrow edema and muscle edema than the current case demonstrates.
- **Aneurysmal bone cyst (ABC):** The mildly expansile radiographic appearance favors

this diagnosis. However, this diagnosis would not account for the solid, low signal intensity component apparent on the MR images.

- **Chondroblastoma:** This tumor may involve the talus, and can have an aneurysmal component with edema of adjacent muscle and marrow. The radiographic and MRI features and the patient's age are most consistent with a chondroblastoma.
- **Giant cell tumor (GCT):** The location of this mass is reasonable for a GCT. However, the presence of a sclerotic margin on the radiograph, the presence of internal matrix, and the patient's young age make this diagnosis unlikely.

## DIAGNOSIS

**Chondroblastoma of the medial talus**

## KEY FACTS

### Clinical

- Chondroblastoma is a benign cartilaginous tumor comprising <1% of all primary bone tumors.
- Its incidence is intermediate among other benign cartilaginous tumors; it is more common than chon-dromyxoid fibroma but rarer than enchondroma or osteochondroma.
- The second decade of life is the most common age of presentation (70%). About 90% of chondroblastomas present between the ages of 5 and 25 years. The male-to-female ratio has been variably reported at ranges from 1.4:1 to 2.4:1.
- Symptoms are nonspecific and include pain referred to the joint adjacent to the lesion.
- Curettage and bone grafting is the treatment of choice. However, case reports have been published suggesting radiofrequency ablation of chondroblastomas as an alternative, less invasive treatment in select cases.
- Local recurrence can occur following surgery. However, malignant transformation is rare.

### Radiologic

- Chondroblastoma is a geographic lucent lesion with thin sclerotic margins arising eccentrically in an epiph-ysis or apophysis, with or without extension into the metaphysis.
- The most common sites of involvement include the epiphyses of the distal femur, proximal tibia, proximal humerus, and apophysis of the greater trochanter.
- Detectable punctate calcified chondroid matrix is found in about 50% of patients.

- Up to 60% of patients have benign-appearing perios-teal reaction away from the lesion, often in the adjacent metadiaphysis in the case of epiphyseal lesions.
- On MRI, chondroblastomas have a lobulated margin. The signal intensity characteristics are distinct from those of hyaline cartilage (i.e., enchondroma). Chondro-blastomas appear homogeneously isointense to muscle on T1-weighted images and have variable signal intensity on T2-weighted images, often with some intermediate to low signal intensity. There frequently is increased T2 signal within the surrounding marrow and soft tissues. In the case of an epiphyseal lesion, there may also be a joint effusion in the adjacent joint. In 10% to 20% of chondroblastomas there may be an associated "secondary" ABC characterized by scattered foci of high signal intensity on T2-weighted images, potentially with fluid levels, along with expansion of the bone.

## SUGGESTED READING

Dahlin DC, Ivins JC. Benign chondroblastoma: a study of 125 cases. Cancer 1972;30:401–413.

Erickson JK, Rosenthal DI, Zaleske DJ, et al. Primary treatment of chondroblastoma with percutaneous radiofrequency heat ablation: report of three cases. Radiology 2001;221:463–468.

Petsas T, Megas P, Papathanassiou Z. Radiofrequency ablation of two femoral head chondroblastomas. Eur J Radiol 2007;63:63–67.

Resnick D. Diagnosis of Bone and Joint Disorders (4th ed). Philadelphia, PA: Saunders, 2002:3850–3866.

Weatherall, PT, Maale GE, Mendelsohn DB, et al. Chondroblastoma: classic and confusing appearance at MR imaging. Radiology 1994;190: 467–474.

# CASE 9

**CHARLES E.
SPRITZER**

## HISTORY

A 28-year-old man with an acute injury to the knee incurred when standing from a crouched position.

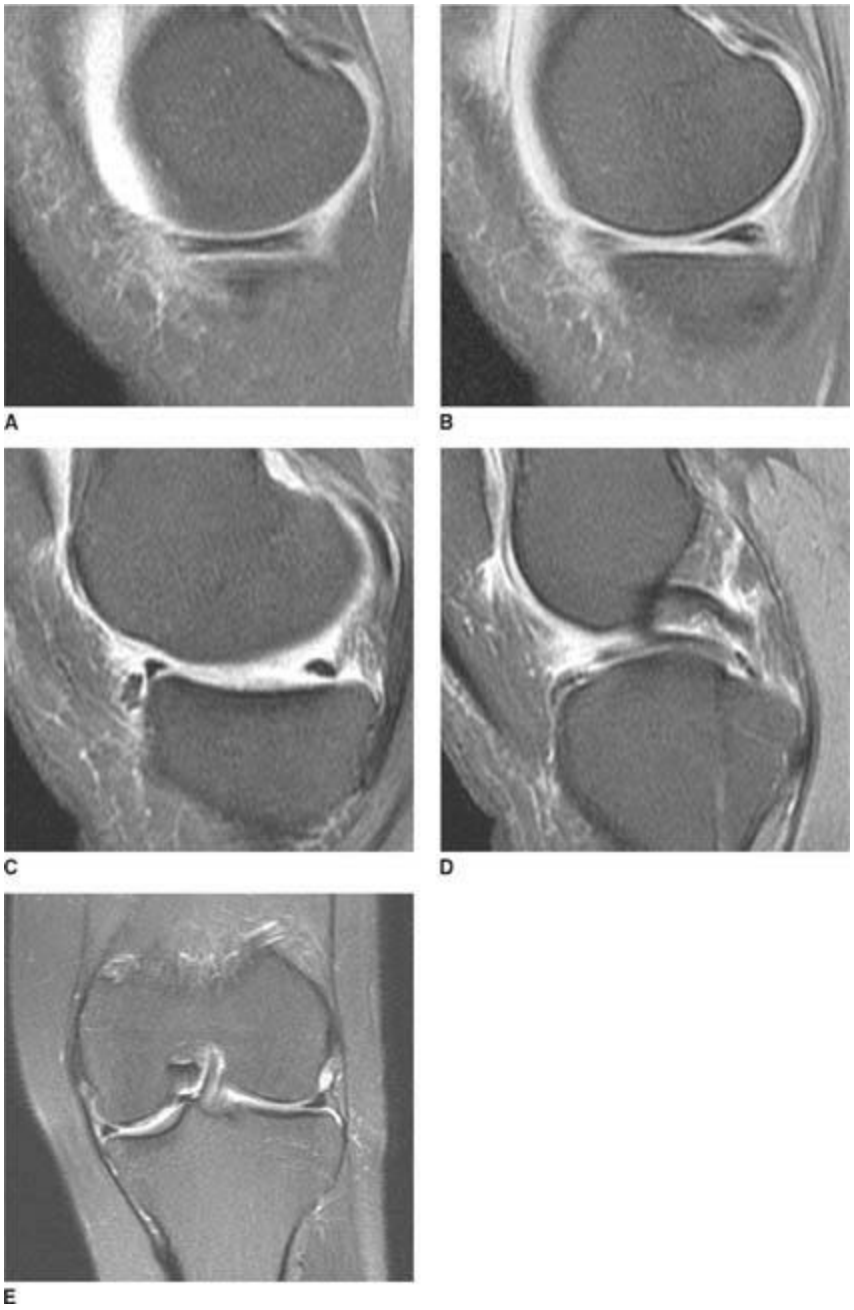


■**FIGURES 5-9A-5-9E** Sagittal fat suppressed proton density MR images through the medial compartment of the knee (A through D). There is deficiency of the body of the medial meniscus, evidenced by the lack of two full body segments **(A** and **B),** known as the "absent bow tie sign." A "double-anterior horn sign" is seen **(C),** with the true anterior horn located just anterior to a portion of the displaced meniscal tissue. A "double-PCL sign" is seen in the intercondylar notch, due to displaced meniscal tissue lying just beneath and anterior to the PCL **(D).** Coronal fat suppressed FSE T2-weighted MR image of the knee **(E).** The body of the medial meniscus appears truncated. There is also a low signal intensity meniscal fragment seen displaced from the body of the meniscus within the intercondylar notch, lying next to the ACL and just beneath the PCL **(E)**.

## DIFFERENTIAL DIAGNOSIS

- **Prior arthroscopic meniscectomy:** While deficiency of the meniscus is often seen following partial menis-cectomy, meniscal material in the intercondylar notch following an arthroscopy would not be expected. Furthermore, the patient has no history of arthroscopic surgery.
- **Bucket-handle meniscal tear with displaced fragment:** The body of the medial meniscus is truncated and is in direct continuity with displaced meniscal material in the intercondylar notch. This is the best diagnosis.
- **Loose osteochondral fragment:** The linear appearance of the loose fragment is more in keeping with a menis-cal fragment than osteochondral bodies, which are typically round or oval in shape. In addition, no osteo-chondral donor site is seen on the available images.

## DIAGNOSIS

**Bucket-handle tear of the medial meniscus, with a displaced fragment of meniscal tissue**

## KEY FACTS

### Clinical

- A bucket-handle tear consists of a vertical or longitudinal tear extending around a portion of the circumference of the meniscus, usually starting in the posterior horn and extending longitudinally through the body, with variable extension into the anterior horn. The tear is typically located in the periphery of the meniscus and creates an inner fragment of meniscal tissue (the “handle”) that has a tendency to displace away from the remainder of the meniscus (the “bucket”), often displacing into the intercondylar notch.
- This type of tear can occur in either the medial or lateral meniscus. Occasionally, concurrent bucket-handle tears of both the medial and lateral menisci may exist.
- This type of meniscal injury may be associated with rotation of either the femur or the tibia. Clinical history is usually a simple twisting injury or an injury sustained during crouching. Some patients have no known injury.
- Occasionally, bucket-handle meniscal tears are seen in association with anterior cruciate ligament (ACL) tears.
- Patients often present clinically with a locked knee or with an inability to fully extend the knee. Others present with a history of a locked knee at the time of the initial injury

that has subsequently become unlocked. Some patients have no history of locking.

## Radiologic

- A thinned and somewhat truncated appearance to the body of the meniscus extending into the posterior horn is characteristic. There may be foreshortening of the posterior horn without a history of prior arthroscopy. Visualization of a displaced fragment of meniscal tissue is key in making the diagnosis of a bucket-handle tear on MR imaging. Careful examination of the intercondy-lar notch typically reveals the torn and displaced inner component of the meniscus. This is often seen beneath the ACL or posterior cruciate ligament (PCL) (as in this case, Figures 5-12D and 5-12E).
- Other imaging findings described in patients with bucket-handle tears of the meniscus include the *absent bow tie sign,* the *double-anterior horn* sign, and the *double-PCL* sign.
- The absent bow tie sign occurs because of the deficiency of the meniscal body caused by displacement of the torn inner margin of the meniscus. Normally on sagittal images, assuming a slice thickness of 4 to 5 mm, the meniscal body will be visible on two consecutive images, and resembles a bow tie. Seeing no body segment or only one body segment suggests either prior partial meniscectomy, a small meniscus, a radial tear of the meniscal body, severe degenerative arthritis, or a bucket-handle tear (Figures 5-12A and 5-12B). Therefore, the presence of this sign prompts a careful search for other evidence of a bucket-handle tear, such as a displaced fragment of meniscal tissue.
- The double-anterior horn sign describes the fact that the displaced meniscal tissue is often located next to the normal anterior horn in the horizontal plane. On sagittal images, there is the appearance of two anterior horns, one immediately anterior to the other. In this situation, the more anterior of the two apparent anterior horns is the true anterior horn, and the more posterior is the displaced meniscal tissue (Figure 5-12C).
- The double-PCL sign describes a displaced maniscal fragment located anterior and parallel to the under-surface of the PCL on sagittal images (Figure 5-12D). In the setting of an intact ACL, only a medial meniscal bucket-handle tear can produce a double-PCL sign. In the setting of an acute or chronic ACL tear, either a medial or lateral meniscus bucket-handle tear can produce this sign.
- Tears may also be present within the displaced handle.

# SUGGESTED READING

Aydingoz U, Firat AK, Atay OA, Doral MN. MR imaging of meniscal bucket-handle tears: a review of signs and their relation to arthroscopic classification. Eur Radiol 2003;13:618–625.

Dorsay TA, Helms CA. Bucket-handle meniscal tears of the knee: sensitivity and specificity of MRI signs. Skeletal Radiol 2003;32:266–272.

Helms CA, Laorr A, Cannon WD Jr. The absent bow tie sign in bucket-handle tears of the menisci in the knee. Am J

Roentgenol 1998;170:57–61.

Shakespeare DT, Rigby HS. The bucket-handle tear of the meniscus: a clinical and arthrographic study. J Bone Joint Surg (Br) 1983;65-B:383–387.

# CASE 10

**CHARLES E. SPRITZER**

## HISTORY

A 65-year-old man with 6 months of shoulder pain.

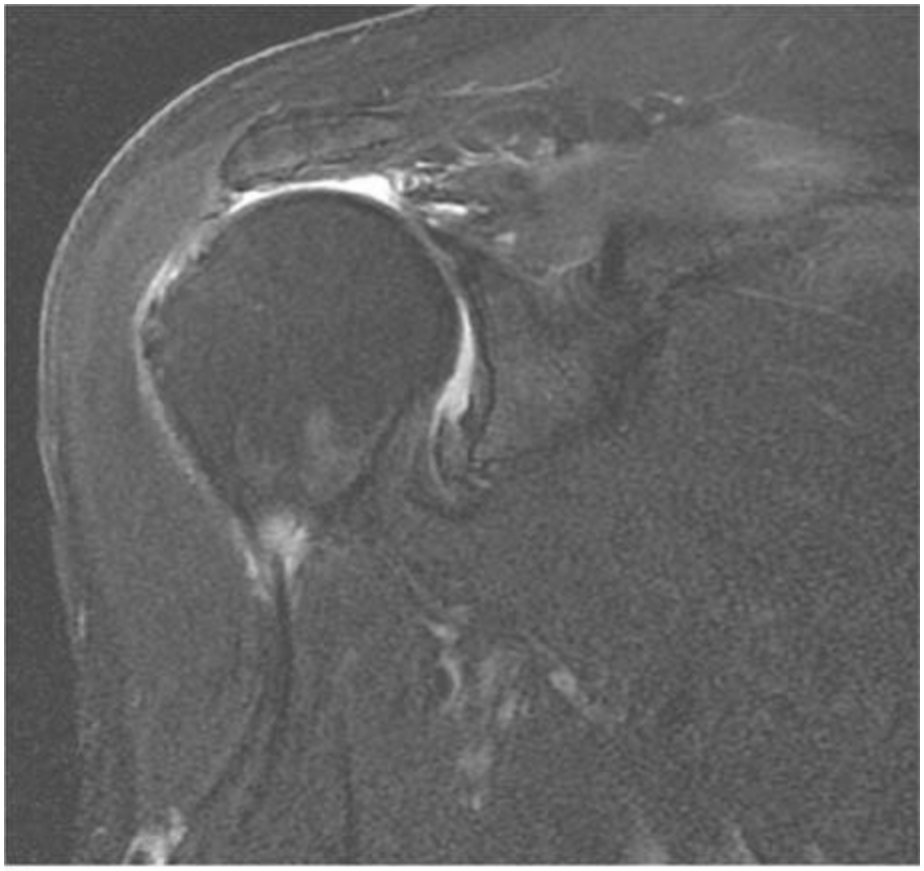

A

■**FIGURE 5-10A** Oblique coronal fat-suppressed FSE T2-weighted MR image of the shoulder. There is fluid signal intensity in the expected region of the supraspinatus tendon, with abrupt termination of the tendon several centimeters medial to its expected insertion site on the humeral head. There is mild T2-signal abnormality noted in the supraspinatus muscle belly, consistent with edema.

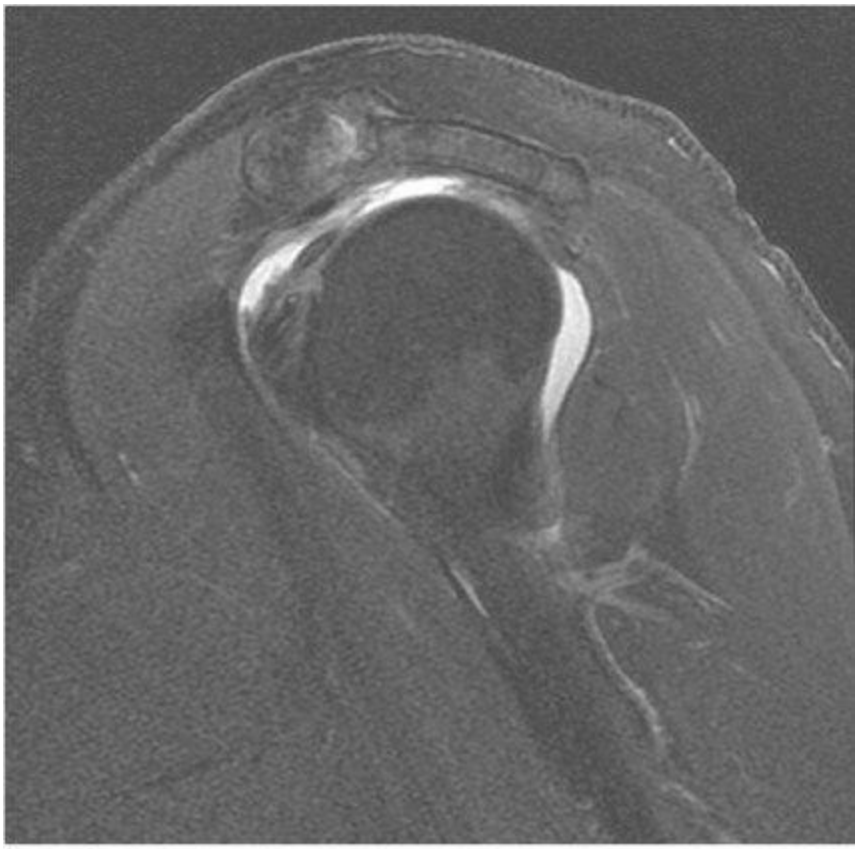

B

■**FIGURE 5-10B** Oblique sagittal fat-suppressed FSE T2-weighted MR image demonstrates nonvisualization of the supraspinatus and infraspinatus tendons and fluid extending from the joint space into the subacromial-subdeltoid bursa.

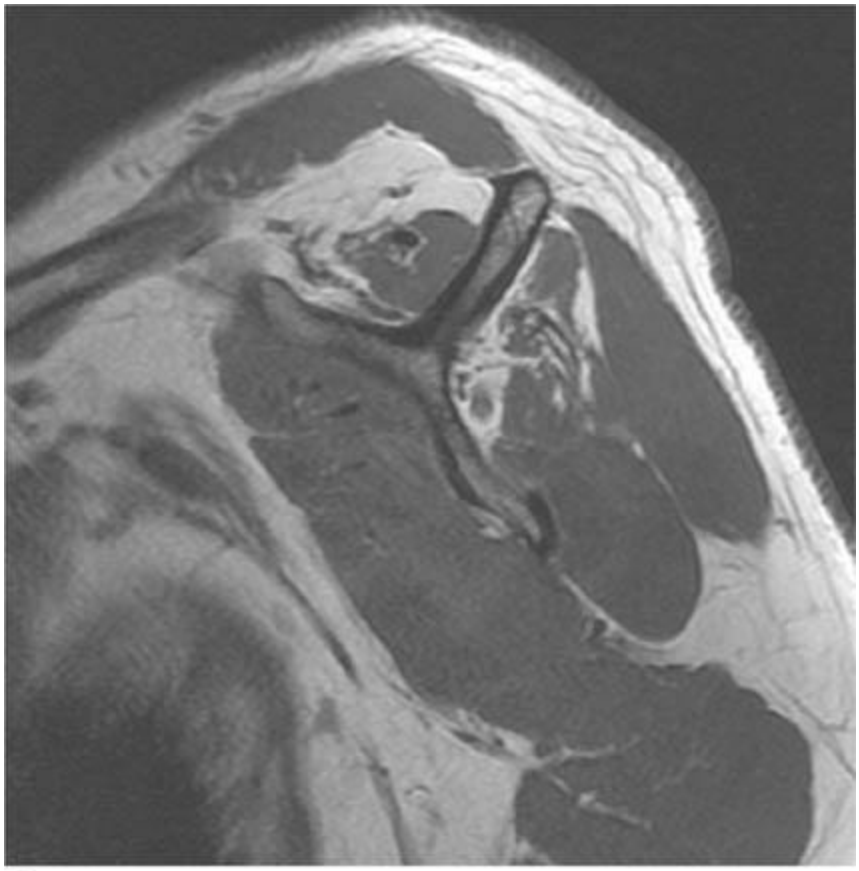

C

**FIGURE 5-10C** Oblique sagittal Tl-weighted MR image of the shoulder, at the level of the rotator cuff muscle bellies. The supraspinatus and infraspinatus muscle bellies are small; while some of this is likely due to retraction, there is also likely a component of size atrophy. In addition, there is mild fatty infiltration of the infraspinatus muscle belly.

## DIFFERENTIAL DIAGNOSIS

**Full thickness tear of the rotator cuff tendon:** The findings are consistent with this diagnosis. There is abrupt termination of the low signal intensity supraspi-natus tendon at the level of the glenoid, with high signal intensity equaling that of fluid in the expected position of the tendon. This is associated with some retraction of the muscle and tendon. In addition, fluid is seen in the subacromial/subdeltoid bursa.

**Partial tear of the rotator cuff tendon:** In the case shown, a full thickness rather than a partial thickness tear is present, as evidenced by high signal intensity traversing the entire thickness of the supraspinatus tendon. The abrupt cut-off of the low signal intensity in the normal tendon and the presence of retraction imply a full thickness, not partial thickness, tear.

**Tendinosis:** While tendinosis may show slightly increased signal intensity on T2-weighted images, it should not be equal to the signal intensity of fluid and usually does

not involve the entire tendon width.

- **Bursitis:** Bursitis could produce fluid in the subacro-mion-subdeltoid bursa, but the fluid would not be expected to communicate with the glenohumeral space in the presence of an intact rotator cuff tendon.

# DIAGNOSIS

**Full thickness tear of the rotator cuff tendon**

# KEY FACTS

## Clinical

- The rotator cuff functions as a shoulder abductor and rotator, as well as a dynamic stabilizer of the glenohu-meral joint. Clinically, rotator cuff tears may be associated with loss of shoulder strength and stability.
- The pathogenesis and natural history of rotator cuff tears have not been fully elucidated. Codman believed that a combination of tendinitis and trauma occurring in a degenerated tendon leads to rotator cuff tears ("intrinsic" theory). Neer believed in the importance of impingement of the cuff beneath the coracoacro-mial arch ("extrinsic" theory), and that impingement and rotator cuff tears represent a continuum from less severe to most severe injury. Most authors now believe that the pathogenesis of cuff tears involves two main mechanisms: subacromial impingement and intrinsic degeneration of the tendon, perhaps due to repeated trauma and hypovascularity. Rotator cuff tears can also be seen following acute trauma.
- Asymptomatic rotator cuff tears are not uncommon, especially in elderly individuals.
- Rotator cuff tears may be treated conservatively or surgically. Indications for surgical management of rotator cuff disease are unclear, in part because the natural history of this disease process is poorly understood. Treatment decisions are based on a number of factors, including the patient's symptoms and the chronicity of the injury.

## Radiologic

- MRI, MR arthrography, and ultrasound are very sensitive and specific in the diagnosis of full thickness rotator cuff tears. MR arthrography detects partial thickness rotator cuff tears with greater accuracy than either MRI or ultrasound. Both MRI and MR arthrography have the advantage of allowing the evaluation of other structures in the shoulder, such as the labrum and cartilage, which are potential contributors to shoulder pain.
- Full thickness rotator cuff tears extend from the articular surface of the cuff tendon to

the bursal surface. Partial thickness tears usually involve either the articular surface or the bursal surface. Interstitial tears are partial thickness tears that occur within the substance of the cuff tendon and do not involve either surface. The majority of rotator cuff tears originate in the supraspi-natus tendon.

- On MRI, a full thickness tear is diagnosed when there is discontinuity of the cuff fibers and fluid signal extends from the articular surface of the cuff into the subacro-mial/subdeltoid bursa. Secondary signs include tendon retraction, fluid in the subacromial/subdeltoid bursa, and muscle atrophy. Full thickness tears are usually classified according to size.
- MR imaging of the shoulder in the setting of rotator cuff tear can provide useful information to the orthopedic surgeon including tear dimensions, degree of tendon retraction, presence of muscle atrophy and/or fatty infiltration, and depth of partial thickness tears.

## SUGGESTED READING

De Jesus JO, Parker L, Frangos AJ, Nazarian LN. Accuracy of MRI, MR arthrography, and ultrasound in the diagnosis of rotator cuff tears: a meta-analysis. Am J Roentgenol 2009;192:1701–1707.

Dunn WR, Schackman BR, Walsh C, et al. Variation in orthopaedic surgeons' perceptions about the indications for rotator cuff surgery. J Bone Joint Surg Am 2005;87:1978–1984.

Ko JY, Huang CC, Chen WJ, et al. Pathogenesis of partial tear of the rotator cuff: a clinical and pathologic study. J Shoulder Elbow Surg 2006;15:271–278.

Morag Y, Jacobson JA, Miller B, et al. MR imaging of rotator cuff injury: what the clinician needs to know. Radiographics 2006;26:1045–1065.

Opsha O, Malik A, Baltazar R, et al. MRI of the rotator cuff and internal derangement. Eur J Radiol 2008;68:36–56.

# CASE 11

**CHARLES E. SPRITZER**

## HISTORY

A 55-year-old woman with a history of bilateral hip pain.


A

■**FIGURE 5-11A** Anteroposterior radiograph of the bilateral hips. There are no abnormalities noted.

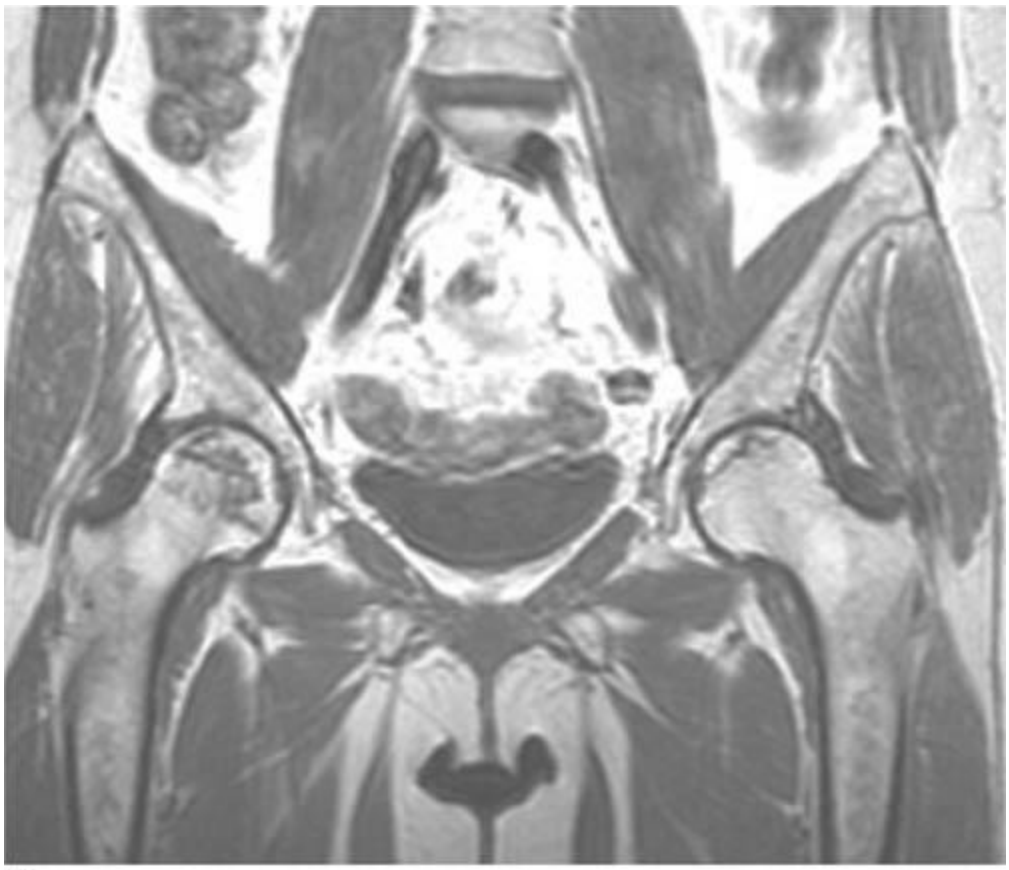

B

■**FIGURE 5-11B** Coronal Tl-weighted MRI of the hips. Serpiginous bands of decreased signal intensity, surrounding a fatty center, are seen in both femoral heads.

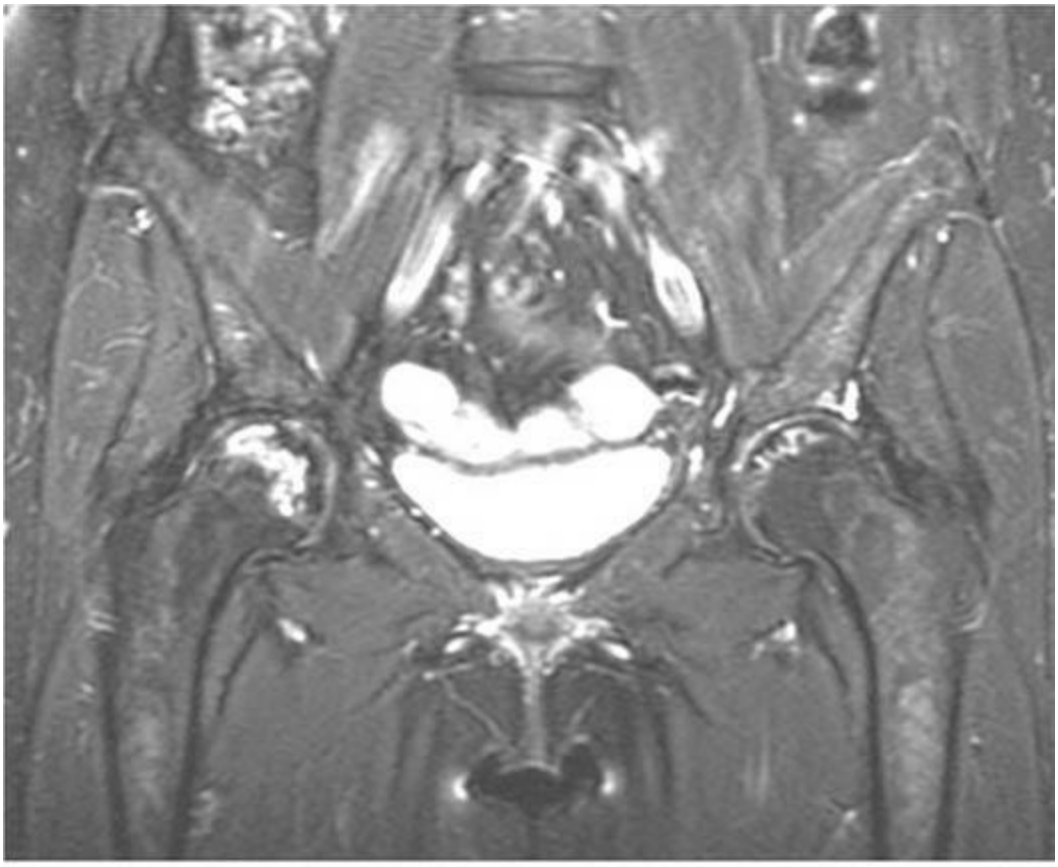

C

**FIGURES 5-11C** Coronal fat suppressed fast spin echoT2-weighted MRI of the bilateral hips. Serpiginous bands of increased signal intensity are seen in both femoral heads.

## DIFFERENTIAL DIAGNOSIS

**Osteoarthritis:** While subcortical cysts associated with osteoarthritis may have areas of high signal intensity on T2-weighted images, the absence of findings on the radiograph and lack of significant changes on the ace-tabular side of the joint argue against this diagnosis.

**Osteochondral injury:** The bilaterality of this process would be atypical for an osteochondral injury. The osseous abnormalities also appear farther away from the articular surface than would be expected. Osteo-chondral injuries would be expected to be associated with secondary degenerative changes, given the size of the abnormality in each femoral head.

**Inflammatory arthritides:** This diagnosis is unlikely given preservation of the joint space on the radiograph and the constellation of findings on MRI, including the relative lack of acetabular involvement.

**Avascular necrosis (AVN):** Preservation of the articular surface, the serpiginous

nature of the signal abnormality involving the superior aspects of the femoral heads, and the bilaterality of the process are all consistent with this diagnosis.

## DIAGNOSIS

**AVN of the bilateral femoral heads**

## KEY FACTS

### Clinical

- AVN is a consequence of vascular injury resulting in bone death.
- Patients, who are usually young adults in the third or fourth decade of life, may experience an insidious onset of vague, aching pain around the hip joint. There are no specific signs or symptoms.
- The causes of AVN are numerous, including drugs such as corticosteroids, protease inhibitors, and ethanol; sickle cell disease; prior trauma such as hip dislocation or femoral neck fracture; marrow replacement processes such as Gaucher's disease; radiation- or lupus-induced vasculitis; and embolic etiologies including emboli secondary to trauma and Caisson disease. Other etiologies, in which the pathophysiology is less well understood, include idiopathic disease (in which there is no clearly identifiable etiology or risk factor), Legg-Perthes disease, chronic renal disease, inflammatory bowel disease, and pancreatitis. Some patients may also have a genetic predisposition to AVN.
- Treatment is based on the stage of the lesion, the presence of symptoms, patient age, activity level, and life expectancy. There are numerous staging systems that in general take into account the size of the area of necrosis, the presence or absence of collapse of the articular surface, the degree of depression of the femoral head contour, and the presence or absence of ace-tabular involvement with osteoarthritis.
- Early diagnosis (i.e., before plain radiographs demonstrate collapse and subchondral lucency) is associated with less morbidity, as joint-salvaging treatment options may be available. When collapse of the articular surface is present, there is a high probability that the patient will eventually require a total hip replacement.
- Operative treatment options include core decompression (for early stage disease), vascularized bone grafting, rotational osteotomy, limited resurfacing arthroplasty, and total joint arthroplasty.

### Radiologic

- Radiographs may be normal, or may demonstrate a sclerotic rim surrounding an

osteopenic area, representing bone remodeling at the junction of necrotic and viable bone. A crescentic subchondral lucency, the "crescent sign," results from a subchondral fracture. Advanced disease is characterized by flattening of the superior articular surface of the femoral head, with or without secondary osteoarthritis.

- MRI has been shown to be more sensitive than both radionuclide imaging and CT for the detection of early AVN. This is important since early intervention in these patients is associated with a better prognosis.
- Abnormalities typically occur in the weight-bearing region of the femoral head. The process is bilateral in 40% of cases.
- A well-demarcated serpiginous band of low signal abnormality, which is dark on Tl-weighted images and bright on fat-suppressed T2-weighted images, is seen and is thought to represent the vascular and repair tissue at the periphery of the necrosis.
- About half of patients with femoral head AVN have hip joint effusions on MRI, regardless of the presence of articular surface collapse. Some patients also have bone marrow edema adjacent to the serpiginous sub-chondral signal abnormality, which often correlates with the presence of pain.

## SUGGESTED READING

Malizos KN, Karantanas AH, Varitimidis SE, et al. Osteonecrosis of the femoral head: etiology, imaging, and treatment. Eur J Radiol 2007;63: 16–28.

Mont MA, Jones LC, Hungerford DS. Nontraumatic osteonecrosis of the femoral head: ten years later. J Bone Joint Surg Am 2006;88-A:1117–1132.

Scheiber C, Meyer ME, Dumitresco B, et al. The pitfalls of planar three-phase bone scintigraphy in nontraumatic hip avascular osteonecrosis. Clin Nuc Med 1999;24:488–494.

# CASE 12

**CHARLES E.**
**SPRITZER**

### HISTORY

A 32-year-old man who twisted and injured his knee while playing basketball.

A

■**FIGURE 5-12A** Sagittal fat suppressed FSE T2-welghted MR image of the knee. High signal Intensity regions, consistent with bone contusions, of the lateral femoral condyle and posterior lateral tibial plateau are noted.

B

**FIGURE 5-12B** Sagittal fat suppressed FSE T2-welghted MR image of the knee. High signal Intensity within the ACL, with discontinuity of ACL fibers, consistent with ACL tear. A joint effusion is also noted.

## DIFFERENTIAL DIAGNOSIS

**Osteochondral injury of the lateral femoral condyle:** This diagnosis is unlikely as the overlying cartilage appears grossly intact. In addition, the pattern of edema is more in keeping with an acute injury rather than a more chronic insult. Finally, this diagnosis does not explain all of the observed abnormalities.

**Acute tear of the ACL:** There is discontinuity of the ACL with associated edema. Other findings in keeping with an acute injury include the bone contusions on both the lateral femoral condyle and the posterior lateral tibial plateau. In addition, the presence of a joint effusion suggests an acute injury.

**Chronic tear of the ACL:** Discontinuity of the ACL can be seen with a chronic ACL tear, also termed ACL deficiency. The presence of bone marrow contusions and joint effusion, as well as the appearance of the ACL with increased signal intensity in the intercondylar notch, confirm that in this case the injury is acute rather than chronic.

**Sprain of the ACL:** While there is certainly either or both edema and hemorrhage

within the ACL, the discontinuity of the ACL fibers proves that in this case the injury is more than a simple sprain. In addition, the presence of pivot-shift bone marrow contusions in an adult is highly suggestive of an acute ACL tear.

## DIAGNOSIS

**Acute tear of the ACL**

## KEY FACTS

### Clinical

- Most ACL tears occur without direct physical contact. The classic mechanism of injury in the noncontact setting is external rotation of a minimally flexed femur on a fixed tibia, such as may occur during a landing or during a sudden deceleration prior to a change of direction. When contact is the cause of injury, the mechanism is usually a direct blow to the lateral aspect of the knee, resulting in a valgus type injury.
- In addition to nonspecific pain and swelling, the patient often remembers a "popping" sensation—or even an audible "popping" sound—during the traumatic insult.
- A positive anterior drawer or Lachman's sign may be present. In patients with acute pain and/or muscle spasms, these physical examination signs may be difficult to elicit.
- Patients who have persistent instability during normal activities and patients who wish to resume activities involving cutting and pivoting are often managed surgically. The surgical approach involves reconstruction of the ACL with a tendon graft passed through tunnels in the femur and tibia. The tunnels are positioned to approximate the normal attachment sites of the native ACL.
- An ACL tear increases the risk of premature osteoar-thritis. The presence of meniscal tears or chondral injuries in association with an ACL tear further increases this risk.

### Radiologic

- The overall accuracy of MRI in determining the presence of ACL injury is approximately 95%.
- The normal ACL has low signal intensity on all pulse sequences and runs parallel to the roof of the inter-condylar notch. Primary signs of ACL tear on MRI include discontinuity of the ACL fibers, abnormally increased signal intensity within and around the ACL on T2-weighted images, and abnormal orientation of the ACL (i.e., not parallel to the roof of the intercondy-lar notch).
- Secondary signs of ACL tear on MRI, which may be useful in the setting of inconclusive primary signs, include hyperbuckled posterior cruciate ligament, anterior

tibial translation, uncovering of the posterior horn lateral meniscus, and bone contusions on the lateral femoral condyle and posterior lateral tibial plateau.

- Osseous injuries are typically associated with acute tears of the ACL. A bone contusion of the posterior lateral tibial plateau, with or without a corresponding contusion on the lateral femoral condyle, is a very frequent finding in acute ACL tears, and when present in an adult is highly suggestive of an acute ACL tear.
- Meniscal tears are commonly seen in association with acute and chronic ACL tears, and the presence of an ACL tear should prompt close inspection of the menisci on MRI. Common locations of meniscal tears in ACL-deficient knees include the posterior horn lateral meniscus and the periphery of the posterior horn medial meniscus.

## SUGGESTED READING


Brandser EA, Riley MA, Berbaum KS, et al. MR imaging of anterior cruciate ligament injury: independent value of primary and secondary signs. Am J Roentgenol 1996;167:121–126.

De Smet AA, Graf BK. Meniscal tears missed on MR imaging: relationship to meniscal tear patterns and anterior cruciate ligament tears. Am J Roentgenol 1994;162:905–911.

Robertson PL, Schweitzer ME, Bartolozzi AR, Ugoni A. Anterior cruciate ligament tears: evaluation of multiple signs with MR imaging. Radiology 1994;193:829–834.

Smith JP 3rd, Barrett GR. Medial and lateral meniscal tear patterns in anterior cruciate ligament-deficient knees. A prospective analysis of 575 tears. Am J Sports Med 2001;29:415–419.

Spindler KP, Wright RW. Clinical practice. Anterior cruciate ligament tear. New Engl J Med 2008;359:2135–2142.


# CASE 13


**CHARLES E. SPRITZER**


## HISTORY

A healthy 22-year-old female with intermittent left ankle pain and swelling for 2 years. On physical exam, there is palpable fullness at the anteromedial aspect of the ankle.

A

■**FIGURE 5-13A** Lateral radiograph of the left ankle. Prominent soft tissue anterior to the ankle joint, with no evidence of soft tissue calcification.

B

C

■**FIGURES 5-13B and 5-13C** Sagittal Tl-weighted **(B)** and fat-suppressed T2-

weighted **(C)** MRI images of the left ankle. There is a mass at the anterior aspect of the ankle joint, with small erosive changes on the dorsal aspect of the talus. The mass is low to intermediate in signal intensity on both pulse sequences, and contains focal areas of very low signal intensity, consistent with hemosiderin deposition.

## DIFFERENTIAL DIAGNOSIS

- **Synovial chondromatosis:** This is an intraarticular process that can produce bony erosions, as is seen in this case. In over half of cases of synovial chondro-matosis, there is some degree of mineralization of the hyaline cartilage nodules, though the absence of calcification on the radiograph does not exclude this diagnosis. However, in synovial chondromatosis there is a typically high signal intensity on the T2-weighted images due to hyperplasia of the synovium and/or the presence of unmineralized cartilage. If calcification is present, multiple hypointense nodules are also seen. While possible, this is not the best diagnosis in this case given the appearance on the T2-weighted images.
- **Pigmented villonodular synovitis (PVNS):** This is an intraarticular process that can produce bony erosions and that typically produces a nodular pattern with areas of hemorrhage and hemosiderin deposition on MR imaging, manifest as low signal intensity on T1-and T2-weighted images, as is seen in this case. This is a process that does not calcify. Based on the imaging features, this is the best diagnosis for this case.
- **Synovial hemangioma:** This rare entity is included in the differential diagnosis of intraarticular masses, but would be expected to be of higher signal intensity on the T2-weighted images; also, these lesions may demonstrate phleboliths on the plain film, or adjacent heman-giomas and/or large feeding and draining vessels on the MRI, none of which were present in this case. Based on the imaging appearance, this is not a likely diagnosis.
- **Gout:** The presence of erosions and a soft tissue mass make gout a consideration. The soft tissue tophi associated with gout usually have intermediate signal intensity on T1-weighted images and intermediate to low signal intensity on T2-weighted images, similar to the case shown. However, hemosiderin deposition would not be a typical feature. Primary gout is a disease of older patients than the patient in this case. While a possibility, this is not the best diagnosis based on patient history and imaging findings.
- **Amyloid arthropathy:** This disease is caused by the deposition of amyloid in and around joints, usually seen in patients on chronic hemodialysis (due to elevated levels of beta-2-microglobulin) or patients with plasma cell dyscrasia (due to elevated monoclonal immuno-globulin light chain fragments). The most frequently affected sites are the spine, hips, shoulders, wrists, and knees, and changes are often bilateral. This entity may have similar imaging features as the case shown here, with a juxta-articular soft tissue mass with low to intermediate signal intensity on all pulse sequences and the

presence of erosions; however, amyloid lesions do not have hemosiderin deposition, and the clinical history in this case virtually excludes this diagnosis.

## DIAGNOSIS

**Pigmented villonodular synovitis**

## KEY FACTS

### Clinical

- PVNS is an uncommon, benign proliferative disorder of the synovium of unknown etiology. It is not felt to represent a neoplastic condition, but whether it is an inflammatory or hyperplastic process due to an unknown stimulus, or the consequence of repeated trauma and hemorrhage, is controversial.
- PVNS is almost always a monoarticular process. The knee is the most frequently affected joint. While usually present in a diffuse form in the joint, PVNS can less commonly present as a smaller focal nodular mass within a joint.
- The typical presentation of PVNS is pain, joint swelling, and decreased range of motion, with an insidious onset of symptoms. PVNS is most commonly seen in young adults, with peak presentation between the third and fourth decades of life.
- When fluid is aspirated from the joint, it is usually sero-sanguineous, although it may be yellow or chocolate brown in 30% of cases.
- Treatment of diffuse PVNS consists of complete syno-vectomy, with relatively high rates of local recurrence (reported rates of up to 46%). Open synovectomy generally has a lower rate of recurrence, but a higher rate of postoperative stiffness, than arthroscopic synovectomy.

### Radiologic

- On radiographs, a joint effusion is typically seen. The effusion may be of increased density due to hemosid-erin deposition. Visible calcifications are not seen with this disorder, and the joint space is usually preserved until late in the disease process.
- Bony erosions and/or cysts with sclerotic margins are visualized in up to 50% of patients, although these are less frequently seen in joints that are naturally capacious such as the knee.
- On noncontrast CT, those portions of the synovial membrane containing hemosiderin often are found to have high attenuation characteristics.
- On MRI, there is diffuse or multinodular synovial thickening, with areas of hemosiderin deposition. The hemo-siderin results in the characteristically seen low

signal intensity on both T1- and T2-weighted images, due to magnetic susceptibility effect. This low signal intensity is more pronounced on gradient echo acquisitions and at high field strengths. The lesions typically enhance.

- When there are erosions or lytic lesions present in the periarticular bones, the signal intensity within the bone lesions is variable, and may indicate the presence of fluid, synovium, and/or hemosiderin.
- There is a limited differential diagnosis for intraarticular processes, with the majority either synovial proliferative processes (including inflammatory arthritis, infection, synovial chondromatosis, PVNS) or deposition diseases (such as gout or amyloid arthropathy); less common intraarticular entities to be considered include infectious granulomatous diseases (e.g., tuberculous arthritis) and vascular malformations (e.g., synovial hemangioma).

## SUGGESTED READING

Llauger J, Palmer J, Roson N, et al. Pigmented villonodular synovitis and giant cell tumors of the tendon sheath: radiologic and pathologic features. Am J Roentgenol 1999;172:1087–1091.

Myers BW, Masi AT. Pigmented villonodular synovitis and tenosynovitis: a clinical epidemiologic study of 166 cases and literature review. Medicine 1980;59:223–238.

Sheldon PJ, Forrester DM, Learch TJ. Imaging of intraarticular masses. Radiographics 2005;25:105–119.

Tyler WK, Vidal AF, Williams, RJ, Healey JH. Pigmented villonodular synovitis. J Am Acad Orthop Surg 2006;14:376–385.

# CASE 14

**EMILY N.**
**VINSON**

### HISTORY

A 12-year-old girl with 3 months of persistent shin pain, onset while trying out for volleyball team. The pain occasionally awakens her at night.

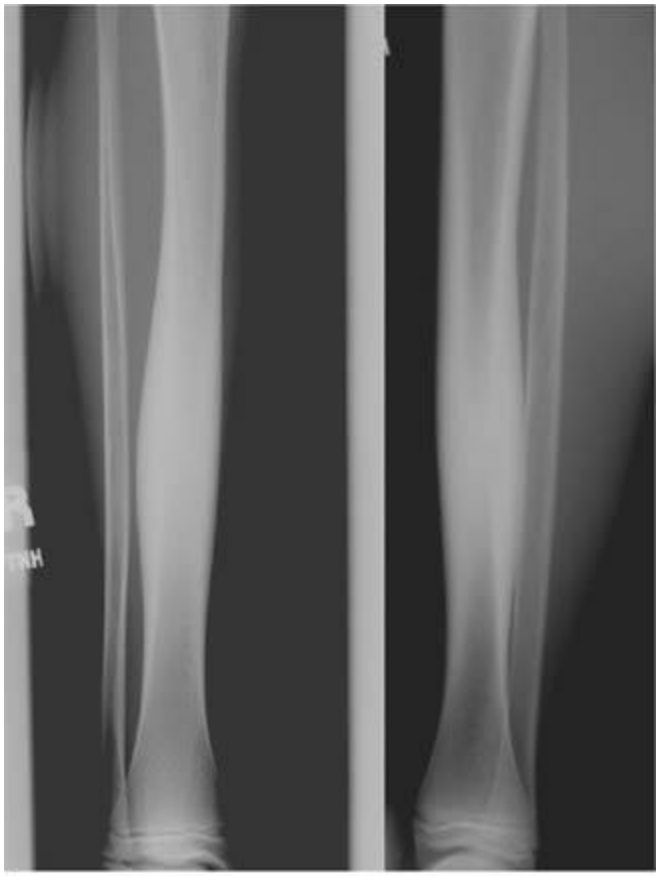

A

■**FIGURE 5-14A** Anteroposterior and lateral radiographs of the right tibia and fibula. There is thick, benign-appearing periosteal reaction in the mid tibial diaphysis, without an obvious underlying lesion.

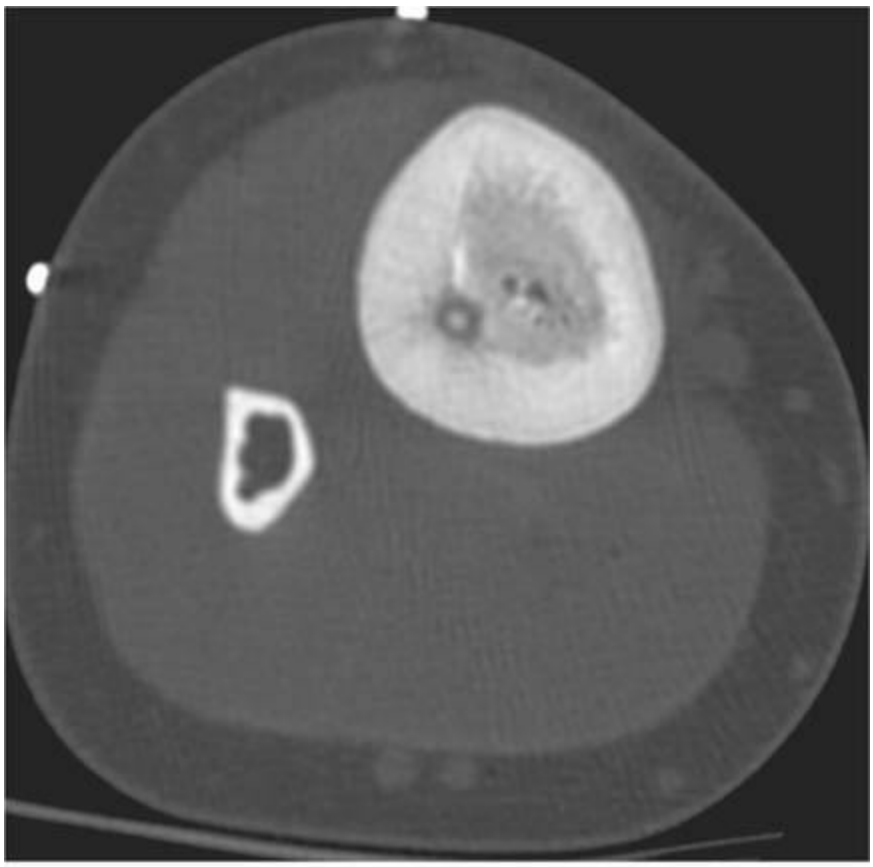

B

■**FIGURE 5-14B** Axial CT image of the right lower leg. A small, well-circumscribed, round lucent lesion with central mineralization is present at the posterolateral cortical-medullary junction of the tibia. There is marked thickening of the regional cortical bone and sclerosis of the regional medullary bone.

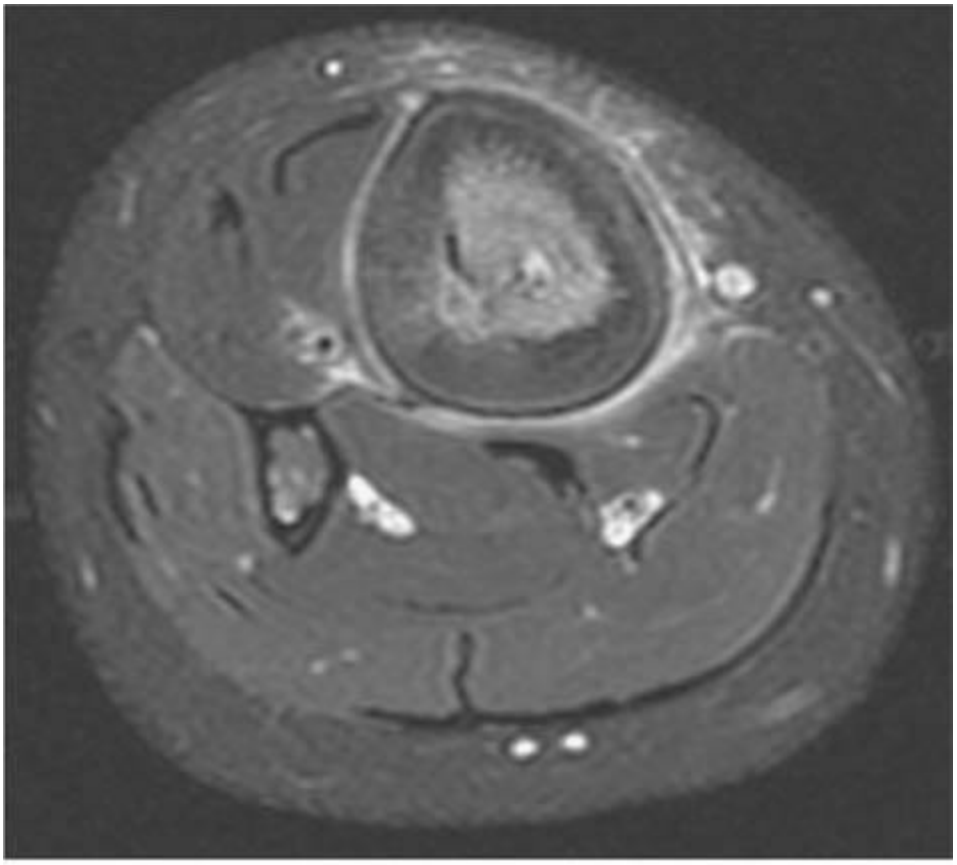

C

■**FIGURE 5-14C** Axial fat-suppressed T2-weighted image of the right lower leg. The small lesion is seen posterolaterally, and there is marked edema in the adjacent bone and soft tissues.

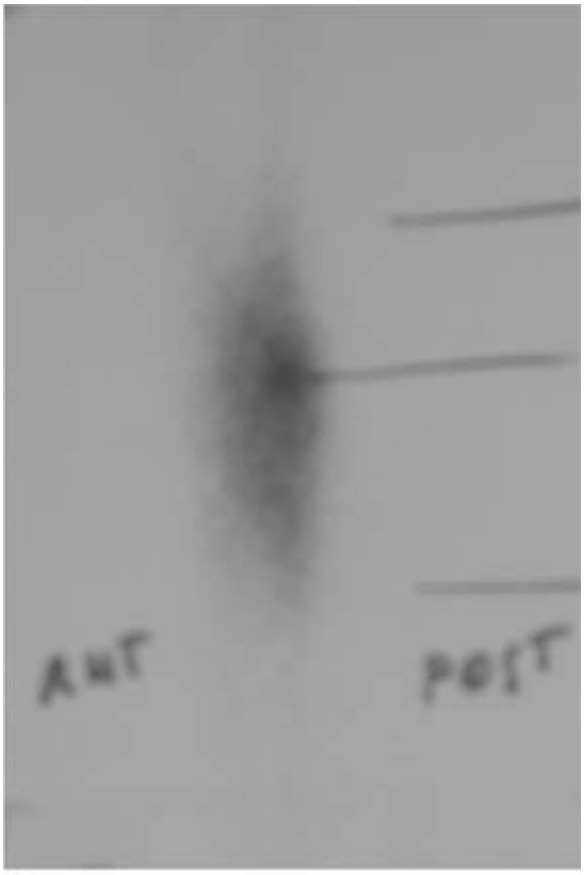


D

**FIGURE 5-14D** Delayed image from a regional bone scan in a different patient with the same entity. There is increased activity in the tibial diaphysis, with a superimposed smaller focus of very increased activity (the "double density" sign).

## DIFFERENTIAL DIAGNOSIS

**Stress fracture:** The plain film finding of periosteal reaction without a visible fracture line suggests the possibility of a stress-related injury. Bone marrow edema may be much more extensive than the size of the cortical abnormality. The visualization of a lesion on the CT and MR images excludes this diagnosis.

**Osteomyelitis:** Bone marrow involvement and perios-teal reaction could represent evidence of infection. The lucent lesion with central mineralization seen on the CT scan could represent an intraosseous abscess with a sequestrum. However, the presence of the "double density" sign on radionuclide imaging does not support this diagnosis. If the small lucency seen on the CT scan represented an intraosseous abscess, an area of decreased, rather than increased, radionuclide uptake corresponding with the lucency would be expected.

**Osteoid osteoma:** The CT image reveals a lucent lesion with a central calcification surrounded by cortical thickening and benign periosteal reaction, which would be

consistent with an osteoid osteoma with a calcifying nidus. The MR images reveal marked associated edema. The radionuclide study demonstrates the "double density" sign, with a focus of very increased activity corresponding to the vascular nidus, surrounded by a zone of increased activity related to the reactive sclerosis. This is the most likely diagnosis based on the imaging findings and given the patient's history.

## DIAGNOSIS

**Osteoid osteoma**

## KEY FACTS

### Clinical

- Osteoid osteoma is a benign osteoblastic neoplasm characterized by a central vascular nidus composed of osteoid and woven bone, usually surrounded by a peripheral zone of dense, reactive sclerotic bone.
- The clinical hallmark of osteoid osteoma is pain, which is usually worse at night and often relieved by nonste-roidal anti-inflammatory drugs.
- Patients with these lesions are usually young, most commonly between the ages of 10 and 20 years; this process is uncommon in patients younger than 5 years or older than 40 years.
- Lesions may occur in any bone, although there is a predilection for the lower extremities (the femur, tibia, and bones of the foot are the most commonly affected).
- Lesions are most often cortical (frequently occurring in the diaphysis or metaphysis in long bones), but can also be medullary or subperiosteal, which produce less reactive sclerosis than the cortical lesions. When medullary lesions occur close to the joint space they may be associated with a reactive synovitis.
- Periarticular lesions may present with premature arthritis due to chronic reactive synovitis.

### Radiologic

- The nidus lesion itself is usually <1.5 cm in size; surrounding sclerosis can sometimes give the lesion the appearance of being larger.
- The reactive periostitis around the nidus may be solid or laminated, and may be so dense that the lucent nidus is not demonstrated on plain radiographs.
- On CT scans, the nidus of a cortical or medullary oste-oid osteoma is a well-defined lucent lesion, and about half of the time will contain punctuate, amorphous, ringlike, or dense mineralization. There is surrounding reactive change, which may range from mild

sclerosis to extensive, dense periosteal thickening.

- The nidus is often more conspicuous on CT imaging compared with MR imaging. Adjacent soft tissue and bone marrow changes are more conspicuous on MR imaging.
- The nidus is usually low to intermediate in signal intensity on T1-weighted images, may be low or high in signal intensity on T2-weighted images, and is typically surrounded by bone marrow and soft tissue edema and inflammation.
- Osteoid osteoma avidly accumulates bone-seeking radiopharmaceuticals. The nidus accumulates more of the radiopharmaceutical than the surrounding reactive bone, leading to the "double density" sign. This helps differentiate osteoid osteoma from a small intraosseous abscess, which would share many of the imaging features of osteoid osteoma, but which would be expected to have a central focus of decreased radiopharmaceuti-cal accumulation.
- Complete surgical excision of the nidus is curative. However, surgical treatment can be difficult because the entire nidus must be resected to prevent recurrence, and this may necessitate a prolonged period of non-weight bearing and restricted activity. CT-guided percutaneous radiofrequency thermocoagulation is a minimally invasive procedure associated with high rates of clinical success and minimal morbidity.

## SUGGESTED READING

Assoun J, Richardi G, Railhac J-J, et al. Osteoid osteoma: MR imaging versus CT. Radiology 1994;191:217–223.

Helms CA. Osteoid osteoma. The double density sign. Clin Orthop Rel Res 1987;222:167–173.

Kransdorf MJ, Stull MA, Gilkey FW, Moser RP Jr. From the archives of the AFIP: Osteoid osteoma. Radiographics 1991;11:671–696.

Rosenthal DI, Hornicek FJ, Torriani M, et al. Osteoid osteoma: percutaneous treatment with radiofrequency energy. Radiology 2003;229:171–175.

# CASE 15

**ROBERT M. VANDEMARK AND EMILY N. VINSON**

### HISTORY

A 49-year-old man who fell from a ladder onto his outstretched left hand.

A

■**FIGURE 5-15A** Posteroanterior radiograph of the left wrist. There is disruption of the normal proximal carpal arc (i.e., disruption of a line drawn along the proximal surfaces of the scaphoid, lunate, and triquetrum) and a displaced scaphoid waist fracture.

B

**FIGURE 5-15B** Lateral radiograph of the left wrist. The lunate and proximal scaphoid fracture fragment remain aligned with the radius, while all other carpal bones are dislocated dorsally.

## DIFFERENTIAL DIAGNOSIS

**Isolated lunate dislocation:** This injury can be excluded by noting the position of the lunate, which is in contact with the distal radius. With isolated lunate dislocation, the capitate aligns with the radius, while the lunate is usually dislocated into the palmar aspect of the wrist.

**Dorsal perilunate dislocation:** This diagnosis would be correct if no other carpal fractures were identified. In the illustrated case, the presence of a scaphoid fracture (or other carpal fracture) indicates a more severe fracture-dislocation.

**Trans-scaphoid dorsal perilunate fracture-dislocation:** This injury is distinguished from dorsal perilunate dislocation by the presence of a displaced fracture through the scaphoid waist. Typically, the proximal scaphoid fragment remains in anatomic position, adjacent to the lunate, while the distal fragment travels dorsally with the remainder of the carpus.

# DIAGNOSIS

**Trans-scaphoid dorsal perilunate fracture-dislocation**

# KEY FACTS

## Clinical

- Wrist dislocations are usually high energy injuries. The typical mechanism of injury is acute hyperextension of the wrist, such as a fall onto an outstretched hand, with the forearm pronated and the wrist in ulnar deviation and extension.
- The trans-scaphoid dorsal perilunate fracture-dislocation is considered the most common wrist dislocation.
- Perilunate dislocations, perilunate fracture-dislocations, and lunate dislocations are diagnosed late in up to 25% of cases.
- This type of injury usually requires open reduction, fracture fixation, and ligamentous repair.

## Radiologic

- Fundamentally, the detection of carpal dislocations relies on recognizing the abnormal relationships of the carpal bones on properly positioned radiographs. When patients are badly injured, positioning can be difficult, with obliquity and various degrees of flexion and extension leading to distortion and misdiagnosis. If the distal radius and ulna are properly positioned on posteroan-terior and lateral views, disorganization of the carpal landmarks usually will be apparent. Obscuration or overlap of the normal carpal arcs is diagnostic of intra-carpal derangement and is the sine qua non of carpal fracture-dislocations.
- It is important to assess the scaphoid for a fracture when confronted with an apparent case of carpal dislocation. Associated fractures are sometimes more apparent on postreduction radiographs.
- Long-term consequences of these injuries may include chronic carpal instability, posttraumatic arthritis, median nerve dysfunction, and osteonecrosis when associated with a scaphoid fracture.

# SUGGESTED READING


Berquist TH. Imaging of Orthopedic Trauma. New York, NY: Raven, 1992:827–831.

Gilula LA, Yin Y. Imaging of the Wrist and Hand. Philadelphia, PA: Saunders, 1996;303–309.

Murray PM. Dislocations of the wrist: carpal instability complex. J Am Soc Surg Hand 2003;3:88–99.

Rogers LF. Radiology of Skeletal Trauma (3rd ed). New York, NY: Churchill Livingstone, 2002:849–855.

# CASE 16

**EMILY N.**
**VINSON**

## HISTORY

A 38-year-old man who sustained a left ankle injury when he landed awkwardly on a diving board. On exam, he had a palpable defect consistent with an Achilles tendon tear (not shown), and was also exquisitely tender over the lateral malleolus.

A

■**FIGURE 5-16A** Magnified internal oblique radiograph of distal fibula. There Is a thin silver of bone adjacent to the posterolateral aspect of the distal fibula, consistent with a "fleck sign," or a small avulsion fracture at the attachment of the superior peroneal retinaculum (SPR).

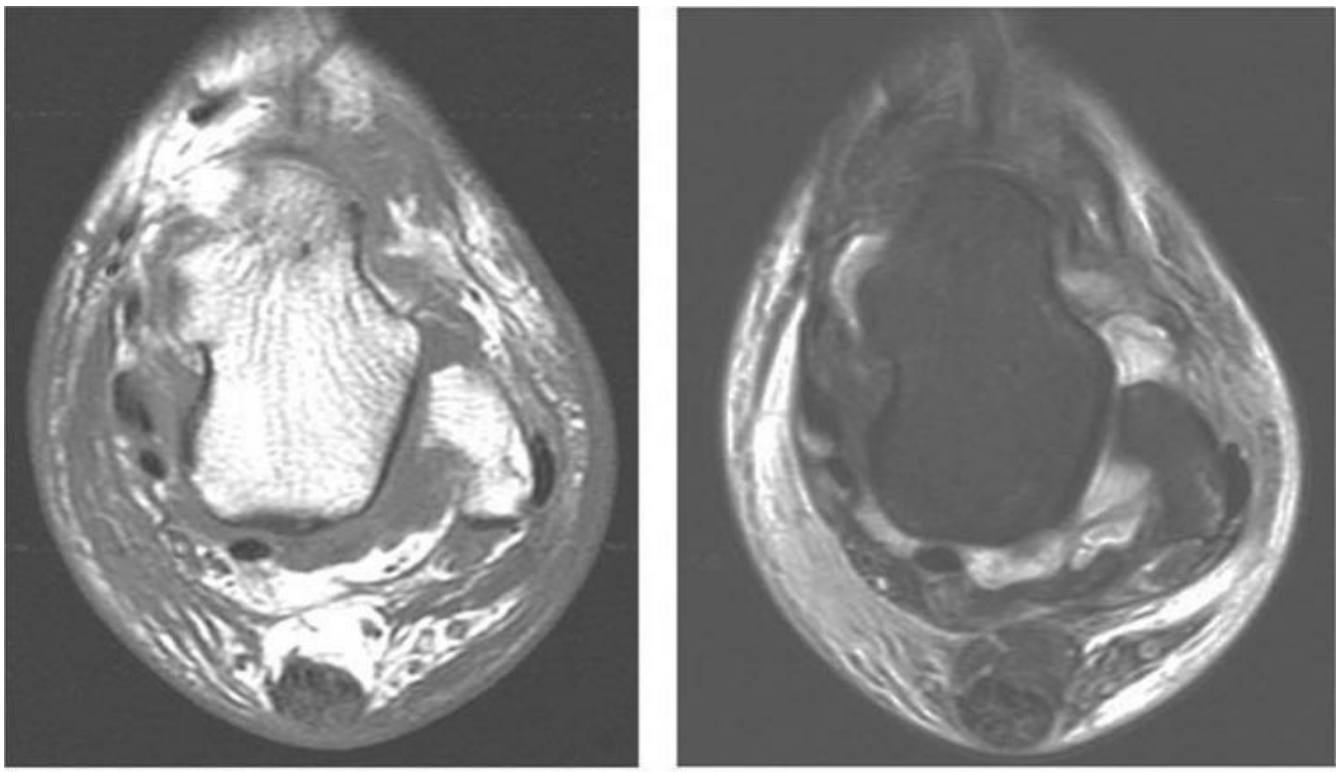


**FIGURES 5-16B and 5-16C** Axial Tl-weighted **(B)** and fat suppressed fast spin echo T2-weighted **(C)** images of the ankle at the level of the distal fibula. There is dislocation of the peroneal tendons anteriorly, lateral to the distal fibula. The SPR is avulsed from the posterolateral margin of the distal fibula, with associated mild bone marrow edema. There is an ankle joint effusion and diffuse subcutaneous edema. The Achilles tendon is expanded and contains signal abnormality.

## DIFFERENTIAL DIAGNOSIS

**Isolated lateral ligament injury:** There is an apparent tear of the anterior talofibular ligament in this case, and this could account for lateral pain and tenderness, soft tissue swelling, and ankle joint effusion. However, this diagnosis alone does not account for the avulsion fracture of the lateral margin of the distal fibula or for the abnormal position of the peroneal tendons on the MR images.

**Superior peroneal retinaculum (SPR) injury with peroneal tendon dislocation:** The characteristic appearance of the avulsion fracture on the internal oblique radiograph is pathognomonic for this diagnosis, and the axial MR images confirm the dislocated position of the peroneal tendons. This is the correct diagnosis.

## DIAGNOSIS

**SPR injury with peroneal tendon dislocation**

## KEY FACTS

### Clinical

- The retromalleolar groove is the fibroosseous tunnel through which the peroneus longus and peroneus bre-vis tendons travel posterior to the lateral malleolus. At this level, the tendons are stabilized by the SPR and the calcaneofibular ligament.
- The SPR is a fibrous band of tissue extending from the inferior lateral malleolus to the posterolateral calca-neus, and is the primary restraint to lateral subluxation and dislocation of the peroneal tendons. Disruption of the SPR allows the peroneal tendons to dislocate anteriorly over the lateral malleolus.
- An injury to the SPR may be sustained with sudden dor-siflexion of the ankle with simultaneous contraction of the peroneal muscles, causing stripping or tearing of the SPR from its distal fibular attachment. In this patient, the sudden dorsiflexion also resulted in an Achilles tendon tear (not fully visible on the images shown).
- Clinically, acute injuries to the SPR can be mistaken for an isolated ankle sprain as patients present with swelling, ecchymosis, pain, and tenderness over the lateral malleolus, thus delaying the diagnosis.
- SPR injuries are associated with peroneal tendon dislocations, peroneal tendon tears, and lateral ankle ligament injuries.
- Flattening or convexity of the normally concave surface of the posterior distal fibula predisposes to peroneal tendon dislocations and tears.
- Acutely, some patients are treated nonoperatively with immobilization; however, results may be disappointing due to a high rate of recurrence. Operative treatment, which may consist of reconstruction of the SPR and/or fibular osteotomy and deepening of the fibular groove, has been advocated in athletic individuals and in chronic cases of peroneal subluxation or dislocation.

### Radiologic

- A characteristic avulsion fracture consisting of small linear cortical fragment adjacent and parallel to the lateral margin of the distal fibula indicates an SPR injury and peroneal tendon dislocation. However, this finding, termed the “fleck sign,” is rarely encountered. When present, the “fleck sign” is best seen on internal oblique or anteroposterior ankle radiographs.
- MR imaging of the ankle is very useful in detecting SPR injuries and peroneal tendon dislocations. The SPR is best seen on axial images. Associated peroneal tendon tears and lateral ankle ligament injuries are also readily evaluated.
- While the SPR may be difficult to visualize on CT images in the setting of an acute

ankle injury, dislocation of the peroneal tendons can be readily appreciated on soft tissue windows, and is an important finding in the setting of ankle trauma.

- SPR injuries are graded as one of four types, according to Oden's classification system. In type I injuries, the SPR and the fibular periosteum onto which it inserts are elevated, creating a pouch at the lateral aspect of the distal fibula into which the peroneal tendons can dislocate; this is the most common type of injury. In type II injuries, the SPR avulses from its fibular attachment without an associated avulsion fracture; type III injuries denote an SPR avulsion from the fibula with a small avulsion fracture fragment, as was seen in this case. The avulsed bone fragment may be very small and difficult to visualize on MR imaging. Type IV injuries involve disruption of the posterior aspect of the SPR, and are the least common type of injury.

## SUGGESTED READING


Heckman DS, Reddy S, Pedowitz D, et al. Operative treatment for peroneal tendon disorders. J Bone Joint Surg Am 2008;90:404–418.

Ho RT, Smith D, Escobedo E. Peroneal tendon dislocation: CT diagnosis and clinical importance. Am J Roentgenol 2001;177:1193.

Rogers LF, Wilson AJ. The ankle. In: LF Rogers (ed), Radiology of Skeletal Trauma (3rd ed). New York, NY: Churchill Livingstone, 2002;1246.

Rosenberg ZS, Bencardino J, Astion D, et al. MRI features of chronic injuries to the superior peroneal retinaculum. Am J Roentgenol 2003;181:1551–1557.

Wang X-T, Rosenberg ZS, Mechlin MB, Schweitzer ME. Normal variants and diseases of the peroneal tendons and superior peroneal retinaculum: MR imaging features. Radiographics 2005;25:587–602.


# CASE 17


**EMILY N.**
**VINSON**


### HISTORY

A 29-year-old woman with a 20-year history of periarticular pain around multiple joints.


A

**FIGURE 5-17A** Anteroposterior radiograph of the pelvis. There is bilateral coxa valga, as well as a widened appearance of the bilateral femoral necks and left superior pubic rami.


B

■**FIGURES 5-17B** Anteroposterior **(B)** radiograph of the right knee demonstrates undertubulation of the distal femoral metaphysis (Erlenmeyer flask deformity) as well as multiple osseous excrescences.


C

**FIGURES 5-17C** Anteroposterior radiograph of the left wrist demonstrates ulnar shortening and undertubulation of the distal radial metaphysis, and a mild bowing deformity of the distal radius.

## DIFFERENTIAL DIAGNOSIS

**Hereditary multiple exostoses (HME):** The findings in this patient, including multiple osseous exostoses, undertubulation of multiple bones, bilateral coxa valga, bowing of the radius, and a shortened ulna, are characteristic of HME.

**Enchondromatosis:** Patients with enchondromatosis may have undertubulated bones causing the Erlenmeyer flask deformity as well as shortened ulna and bowing of the radius. However, this case does not have evidence of lucent lesions containing calcified matrix, which are characteristic of enchondromatosis. In addition, exostoses are not a feature of enchondromatosis. For these reasons, this is not the correct diagnosis.

**Gaucher's disease:** Gaucher's disease is a lysosomal storage disorder that results in bony changes including the Erlenmeyer flask deformity due to bone marrow infiltration by Gaucher cells as well as growth disturbances and bone deformities. Exostoses are not a feature of Gaucher's disease, and therefore this is not the correct diagnosis.

# DIAGNOSIS

**Hereditary multiple exostoses (HME)**

# KEY FACTS

## Clinical

- HME—also known as diaphyseal aclasis or osteochondromatosis—is characterized by multiple osteochon-dromas and the undertubulation of bones.
- Osteochondromas, also called exostoses, are cartilage-capped bone outgrowths which may be pedunculated (narrow stalk of attachment to the underlying bone) or sessile (broad attachment to the underlying bone). They are usually found near the ends of rapidly growing long bones, but are also seen in flat bones such as the scapulae, ribs, and pelvis.
- There is an autosomal dominant inheritance pattern. There is controversy as to whether the disease represents a developmental dysplasia or a familial neoplastic syndrome.
- HME is variable in severity and extent between individuals, even within the same family.
- Most patients with HME are diagnosed at a young age, usually before age 12 years, due to the multiplicity of lesions and the deformity caused by the lesions. Patients with few and small lesions may remain asymptomatic.
- Patients with HME may experience the same potential complications as patients with a solitary osteochondroma, but there is an increased prevalence of complications in HME due to the increased number of lesions.
- Complications include pain, cosmetic deformities (which are the most common clinical presentation), pressure erosions on adjacent bones, vascular compromise (including compression and pseudoaneurysm formation), neurologic compromise due to central or peripheral compression, reactive bursa formation overlying lesions, and malignant transformation.
- Common deformities include ulnar shortening, radial bowing, dislocation of the radial head, valgus deformities of the hip, knee, and ankle, limb length discrepancies, and short stature.
- Osteochondromas enlarge from growth at the cartilage cap, similar to growth at a physis, and thus enlarge while the physes are open; osteochondromas should not grow after skeletal maturity is reached.
- Malignant transformation, characterized by the development of chondrosarcoma in the cartilage cap, is a rare complication, occurring in <1% of solitary osteochondromas and

estimated to occur in 3% to 5% of patients with HME. The lesions are most commonly low-grade with good overall prognosis, though dedif-ferentiated lesions also occur.

- Growth of an osteochondroma in a skeletally mature patient or the development of pain in a previously asymptomatic osteochondroma are clinical features worrisome for malignant transformation. Malignant transformation is uncommon prior to age 20 in the setting of HME, and typically occurs even later in life in cases of solitary osteochondroma.
- Malignant transformation is more common in proximal lesions (pelvis, shoulders, and hips) than peripheral lesions.
- Overlying bursae may clinically mimic malignant transformation, as they may enlarge and may cause new or worsening pain.

## Radiologic

- Radiographs demonstrate osteochondromas, undertu-bulation of long bones, and other characteristic deformities including ulnar shortening and radial bowing. Findings are variable depending on the severity of disease.
- Imaging features of osteochondromas in HME are identical to those of solitary osteochondromas, whether sessile or pedunculated: the key radiologic feature is continuity of the cortex and of the medullary space between the osteochondroma and the underlying native bone.
- A classic finding in HME is undertubulation of the distal femur with a widened metaphysis (Erlenmeyer flask deformity).
- The hyaline cartilage cap of osteochondromas may contain variable amounts of chondroid matrix.
- The thickness of the cartilage cap is in large part dependent on the degree of skeletal maturity; the cap tends to be thicker in children and adolescents, and thinner to absent in adults.
- The cartilage cap thickness can be measured with ultrasound, CT, or MR imaging. CT and MR imaging also depict the continuity of the medullary space of the osteochondroma with the underlying native bone. MR imaging can depict any effects the osteochondroma may have on surrounding structures.
- Imaging is important in distinguishing a large overlying bursa from a thickened cartilage cap; however, this distinction may be difficult due to the high water content and variable mineralization of the cartilage cap, and due to mineralization occasionally occurring within an overlying bursa due to intrabursal fragments of cartilage.
- Radiographic features suggestive of malignant transformation include growth of a previously stable osteo-chondroma in a skeletally mature patient; erosion or destruction of the adjacent native bone; focal regions of radiolucency in the interior portion of a

lesion; large soft tissue mass containing irregular areas of calcification; cartilage cap >1.5 cm thick in a skeletally mature patient (skeletally immature patients commonly have cartilage caps up to 3 cm in thickness in benign lesions).

## SUGGESTED READING

Murphey MD, Choi JJ, Kransdorf MJ, et al. From the archives of the AFIP. Imaging of osteochondroma: Variants and complications with radio-logic-pathologic correlation. Radiographics 2000;20:1407–1434.

Porter DE, Simpson AHRW. The neoplastic pathogenesis of solitary and multiple osteochondromas. J Pathol 1999;188:119–125.

Schmale GA, Conrad EU 3rd, Raskind WH. The natural history of hereditary multiple exostoses. J Bone Joint Surg Am 1994;76:986–992.

Stieber JR, Dormans JP. Manifestations of hereditary multiple exostoses. J Am Acad Orthop Surg 2005;13:110–120.

# CASE 18

**D. LAWRENCE BURK AND EMILY N. VINSON**

### HISTORY

A 12-year-old boy with a painless palpable mass along the lateral aspect of the left knee.

A

■**FIGURE 5-18A** Anteroposterior radiograph of the left knee. A well-circumscribed, expansile lytic lesion is seen in the metaphysis of the proximal left fibula. The lesion has a narrow zone of transition.

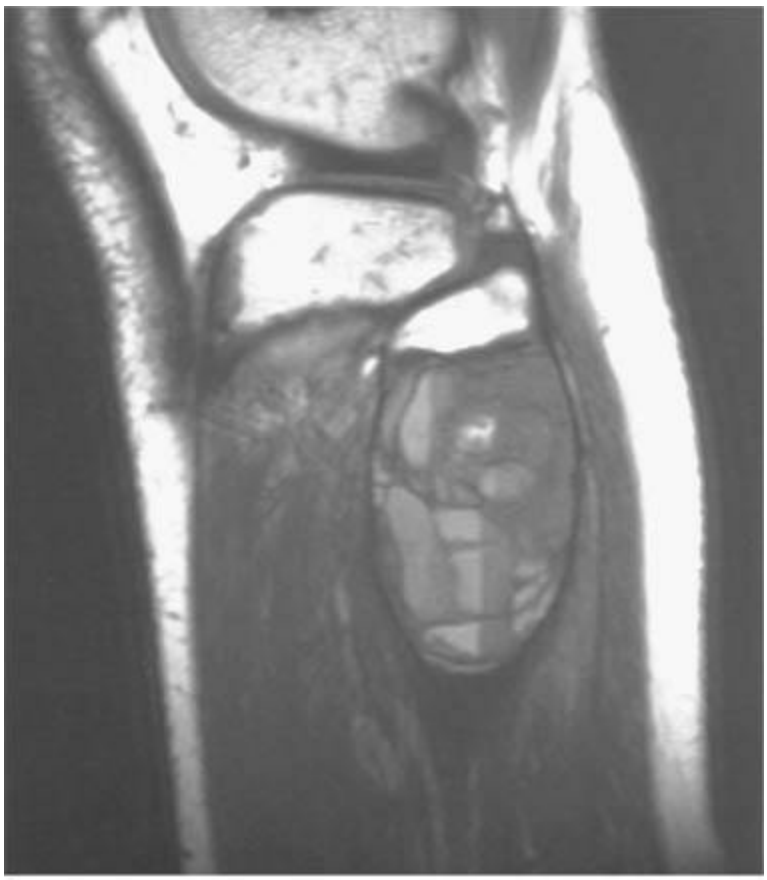

B

**FIGURE 5-18B** Sagittal Tl-weighted MR image of the left knee. Many fluid-fluid levels are seen in multiple small compartments within the expansile fibular lesion. A layer of high signal intensity fluid is noted along the ventral, nondependent aspects of each compartment, with lower signal intensity fluid noted dorsally.

## DIFFERENTIAL DIAGNOSIS

**Telangiectatic osteosarcoma:** This predominantly lytic lesion may demonstrate hemorrhage and fluid-fluid levels. However, these lesions usually have more destructive and aggressive features than the case shown here, with a wide zone of transition and geographic bone destruction on radiographs. In addition, on MR imaging there is often an associated soft tissue mass and/ or nodularity along the septa or peripheral rim of the lesion, representing foci of sarcomatous cells. Therefore, based on the radiographic and MRI appearances, this is not the best diagnosis.

**Simple bone cyst:** Fluid-fluid levels may be seen in bone cysts, particularly when a pathologic fracture has occurred. These lesions, which are almost always asymptomatic in the absence of a pathologic fracture, do not usually expand the cortex to a significant degree or have as many septations as the current case, making this an unlikely diagnosis.

**Aneurysmal bone cyst (ABC):** These expansile lesions are characterized by multiple

compartments containing internal fluid-fluid levels on cross-sectional imaging. On T1-weighted MRI, extracellular methemoglobin (high signal intensity) in the supernatant contrasts with intracellular methemoglobin (low signal intensity) within intact, dependent red blood cells. This is the best diagnosis based on the age of the patient and the imaging appearance.

- **Fibrous dysplasia with cystic degeneration:** With these lesions, cyst formation may occur with expansion of the cortex and fluid-fluid levels. A ground-glass appearance is often noted in the noncystic portions of the lesion, which is not present in this case, making this less likely.

## DIAGNOSIS

**Aneurysmal bone cyst**

## KEY FACTS

### Clinical

- ABCs are uncommon, rapidly growing, benign bone lesions.
- ABCs may be divided into either primary lesions or secondary lesions occurring in the setting of a preexisting lesion (which is most commonly GCT of bone, osteoblastoma, angioma, or chondroblastoma); it is estimated that a preexisting lesion is identified in up to one-third of cases.
- Primary ABCs occur in pediatric patients and young adults; the vast majority are seen in patients 20 years old and younger.
- While any bone can be involved, the most common locations are the metadiaphyseal region of long bones, the pelvis, and the spine.
- These lesions are expansile and contain multiple thin-walled, cystic, blood-filled cavities.
- Most patients present with pain and/or swelling. In some cases, an enlarging palpable mass may be painless, as in this patient. It is also not uncommon for these lesions to present with a pathologic fracture.
- The pathogenesis of ABCs is controversial. Some believe the lesions to be the result of venous obstruction and/or arteriovenous fistula formation; others postulate that alterations in local hemodynamics leads to the development of a dilated vascular bed. Recent genomic data suggests primary ABCs may be benign neoplasms.
- Treatment of these lesions is usually surgical curettage with bone grafting, with local recurrence rates ranging from 10% to 20%.

## Radiologic

- As with most bone lesions, the imaging evaluation of an ABC should begin with radiographs and correlation with clinical history, including patient age. The typical radiographic appearance of a primary ABC is an expansile lytic lesion, sometimes with internal septa-tions, surrounded by a thin shell of bone. Margins are usually well-defined and may be sclerotic. Associated lamellated periosteal reaction is common.
- In long bones, the lesion is usually eccentric and metaphyseal, although central lesions and epiphyseal lesions do occur. Cortical and subperiosteal lesions also occur.
- In some cases, the cortex is so thin in regions of expansion that it is not visible on radiographs. Even with cross-sectional imaging, the cortex may not be visible over a portion of the expanded lesion; in these cases, the margin of the mass still appears smooth as it is contained by intact periosteum.
- MR imaging readily shows the lobulated contours and internal septations of these lesions; multiple small compartments are usually seen with fluid-fluid levels, the result of a layered hematocrit effect within each compartment due to previous hemorrhage.
- Fluid-fluid levels can also be seen with CT, but after positioning, a short waiting period before scanning is needed to allow layering to occur and the fluid-fluid level to be shown.

## SUGGESTED READING

Helms CA. Fundamentals of Skeletal Radiology (3rd ed.). Philadelphia, PA: Elsevier Saunders, 2005.

Keenan S, Bui-Mansfield LT. Musculoskeletal lesions with fluid-fluid level: a pictorial essay. J Comput Assist Tomogr 2006;30:517–524.

Kransdorf MJ, Sweet DE. Aneurysmal bone cyst: concept, controversy, clinical presentation, and imaging. Am J Roentgenol 1995;164:573–580.

Mendenhall WM, Zlotecki RA, Gibbs CP, et al. Aneurysmal bone cyst. Am J Clin Oncol 2006;29:311–315.

# CASE 19

**EMILY N.**
**VINSON**

### HISTORY

A 44-year-old right hand dominant woman with acute onset of right hand pain, swelling, and tenderness, localized to the long finger metacarpophalangeal joint. Her erythrocyte sedimentation rate is mildly elevated. She has no history of prior trauma and no significant past medical history.


**FIGURE 5-19** Anteroposterior radiograph of the right hand demonstrates well-defined, homogeneous calcific density in the soft tissues adjacent to the ulnar aspect of the long finger metacarpophalangeal joint. There is no significant joint space narrowing. There are no visible erosive changes.

## DIFFERENTIAL DIAGNOSIS

- Gout: Gouty tophy typically do occur in a periarticular location and often present with acute severe pain and swelling. Characteristic bony erosive changes may be seen, which are not present in this case. In addition, calcification is usually not visible within a tophus on radiographs in the absence of a history of abnormal calcium metabolism, such as may be seen in patients with renal failure. Therefore, this is not the correct diagnosis.
- Pyogenic arthritis: While this is a possibility based on the patient's presentation and clinical findings, calcifications are not seen in acute pyogenic infection. Therefore, this is not the correct diagnosis.
- Acute calcific periarthritis (ACP): This is the most likely diagnosis, given the acute

clinical presentation and the presence of periarticular calcification localized to the site of symptoms.

- Heterotopic ossification due to prior trauma: While this could be seen in a periarticular location, the calcification in this case is very homogeneous and lacks visible cortical and trabecular bone. This appearance and the lack of a history of trauma make this an unlikely diagnosis.

## DIAGNOSIS

**Acute calcific periarthritis**

## KEY FACTS

### Clinical

- ACP is a form of hydroxyapatite deposition disease which manifests clinically as acute periarticular inflammation and severe pain. The pain is usually localized to a specific point of extreme tenderness. Swelling and erythema at the site of pain are often present.
- The erythrocyte sedimentation rate may be normal or mildly elevated. White blood cell count, serum phosphorus, serum chemistry, and uric acid are typically normal.
- The most common site affected by ACP is the shoulder, where it is often called "calcific tendinitis" or "calcific bursitis." Involvement of the hand and wrist is less common. While in general ACP affects males and females over a broad age range, ACP of the hand is more common in premenopausal and perimenopausal women.
- Most cases of ACP are unifocal and self-limited in nature, with resolution of symptoms and disappearance of periarticular calcifications several weeks after symptom onset.

### Radiologic

- The pathognomonic finding in ACP is radiographic evidence of calcification at the site of pain.
- The calcific deposits localize to periarticular soft tissues such as the joint capsule, tendons, and collateral ligaments.
- The amount of calcification present does not correlate with severity of symptoms; the area of calcification may be very small and difficult to diagnosis without awareness of the specific site of pain.
- Overtime, the calcification usually fragments and becomes less distinct, before disappearing within a few weeks of symptom onset. The disappearance of the

calcification coincides with resolution of clinical symptoms.

## SUGGESTED READING

Chung CB, Gentili A, Chew FS. Calcific tendinosis and periarthritis: classic magnetic resonance imaging appearance and associated findings. J Comput Assist Tomogr 2004;28:390–396.

Doumas C, Vazirani RM, Clifford PD, Owens P. Acute calcific periarthritis of the hand and wrist: a series and review of the literature. Emerg Radiol 2007;14:199–203.

Hayes CW, Conway WF. Calcium hydroxyapatite deposition disease. Radiographics 1990;10:1031–1048.

# CASE 20

**EMILY N. VINSON**

### HISTORY

A 53-year-old woman presents with vague back pain.

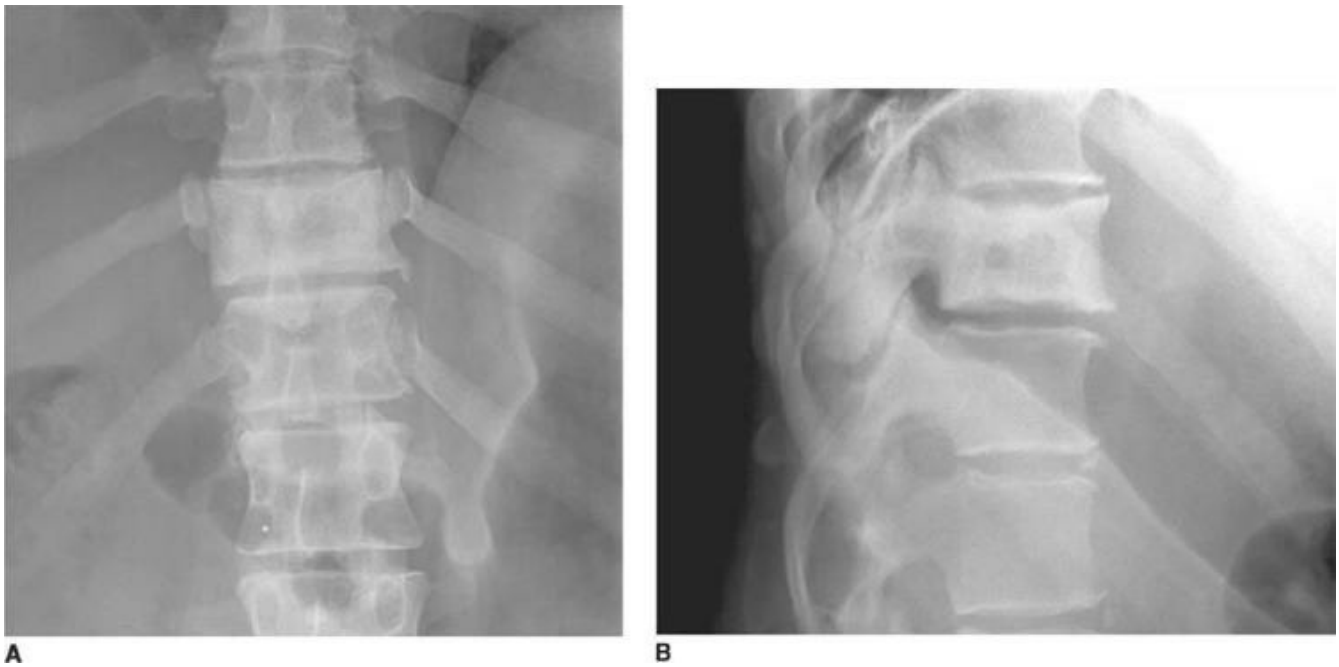


■**FIGURES 5-20A and 5-20B** Anteroposterior **(A)** and lateral **(B)** radiographs of the thoracolumbar junction. The T11 vertebral body is of diffusely increased density, particularly in its periphery. This appearance is known as the "ivory vertebra" sign. In addition, the vertebral body and posterior elements of T11 are enlarged compared with the adjacent vertebrae.

## DIFFERENTIAL DIAGNOSIS

- **Metastatic disease:** Osteoblastic metastasis is a common cause of vertebral body sclerosis due to the replacement of vertebral body spongiosa with a dense and amorphous bony mass that may become confluent and involve the entire vertebral body. While multiple levels are often involved, it is not uncommon to have a single level of involvement. However, metastatic disease does not result in enlargement of the involved bone, and therefore this is not the correct diagnosis.
- **Lymphoma:** While lymphoma commonly involves the skeleton, and is capable of causing an osteoblastic response resulting in diffuse sclerosis and causing an "ivory vertebra" appearance, destructive lytic lesions are more common. In addition, lymphoma does not cause enlargement of a bone, and therefore this is not the correct diagnosis.
- **Paget's disease of bone:** The sclerotic vertebrae in this case is enlarged in both height and width compared with the adjacent vertebrae, which is pathognomonic of Paget's disease. In addition, the periphery of the vertebral body is denser than the central portion, which is also characteristic of Paget's disease of bone.

## DIAGNOSIS

**Paget's disease of bone, involving T11**

## KEY FACTS

### Clinical

- Paget's disease of bone, also known as osteitis deformans, is a common chronic bone disorder characterized by excessive and abnormal remodeling of bone.
- Paget's disease becomes more prevalent with increasing age. It is estimated to affect 3% to 4% of the population over the age of 40 years and 10% to 11% of the population over the age of 80 years.
- The cause of Paget's disease remains unknown, though a viral origin is suspected. Genetic susceptibility may also play a role. There are likely also environmental determinants of disease, as in the past few decades there has been a trend towards disease presentation later in life and in a milder form, leading some to predict that Paget's disease will become increasingly more rare with time.
- Frequent sites of involvement include the skull, spine, pelvis, and proximal long bones. Polyostostic disease is more common than monostotic disease.

- There are three phases of disease, which actually exist in a continuum. In the lytic (active) phase, osteoclasts predominate. In the mixed (active) phase, osteoblastic activity begins superimposed on osteoclastic activity. In the blastic (late or inactive) phase, osteoblastic activity gradually declines. In polyostotic disease, different sites of involvement may be in different phases of disease simultaneously.
- During the lytic phase of disease, there are increased serum and urine hydroxyproline levels. During the mixed and blastic phases, there is elevated serum alkaline phosphatase, reflecting an increased rate of bone formation.
- Up to 20% of patients with Paget's disease of bone are initially asymptomatic. Patients may experience localized pain and tenderness, bony overgrowth, kyphosis, bowing deformities of long bones, and neurologic symptoms due to mechanical compression of cranial nerves caused by bony enlargement of foramina, and by spinal stenosis caused by canal encroachment.
- Complications of Paget's disease include osseous weakening, resulting in bowing of bones and pathologic fractures; secondary osteoarthritis; neurologic abnormalities; benign and malignant GCTs, particularly involving the skull and facial bones; superimposed met-astatic disease, myeloma, lymphoma, or leukemia; and sarcomatous degeneration, which is estimated to occur in about 1% of patients with longstanding disease.
- Patients with bone pain are often treated with bisphos-phonates to reduce bone turnover.

## Radiologic

- The radiographic appearances of Paget's disease of bone are a reflection of the pathologic changes occurring during each phase of the disease process: the lytic phase is manifest by sharply well-defined areas of osteolysis, particularly in the skull (osteoporosis circumscripta) and in the long bones, where the lucency typically progresses from one end of the bone toward the other ("blade-of-grass" appearance); during the mixed phase there is coarse tra-becular and cortical thickening and often enlargement of bone; and during the blastic phase areas of sclerosis may develop and bony enlargement is common.
- In the pelvis, cortical thickening of the iliopectineal and ilioishial lines is a common finding, is often asymmetric, and is often associated with bony enlargement.
- Paget's disease involving a vertebral body can give an "ivory vertebra" appearance or, more commonly, a "picture frame" appearance due to the sclerosis being most marked at the periphery of the vertebral body. The increased size of the involved vertebral body in Paget's disease allows differentiation from other causes of the "ivory vertebra" appearance.

- The disorganized trabecular thickening that occurs in Paget's disease is better seen on CT than on radiographs, and can also be appreciated on MR imaging. Cortical thickening is usually evident on radiographs and cross-sectional imaging. Bone enlargement, however, is often more easily appreciated on radiographs.
- Bone enlargement is pathognomonic of Paget's disease, and when present allows confident differentiation from other causes of bone sclerosis.
- On MR imaging, the marrow interspersed between areas of trabecular thickening most commonly has fatty signal intensity reflecting prominent yellow marrow. During the lytic and early mixed active phases, however, there may be diffuse heterogeneity of marrow signal intensity, with some foci of preserved fatty marrow, reflecting fibrovascular marrow replacement occurring during these more active phases of disease. During the late blastic inactive phase, there may be diffuse low signal intensity reflecting sclerosis.
- Bone scintigraphy typically demonstrates increased uptake of radionuclide during all three phases of Pag-et's disease, though may be near normal during late phase quiescent disease; in general, the degree of bone scan abnormality correlates with the presence of symptomatic disease.
- Sarcomatous transformation may manifest on radiographs as a new area of lucency in a region of previously stable disease, and is readily demonstrated on CT and MR images as mass-like marrow replacement and cortical destruction, usually with an associated soft tissue mass. Because these secondary malignancies are highly anaplastic and aggressively and rapidly destroy bone, periosteal reaction is often not present.
- The presence of lytic or blastic lesions in areas of the skeleton not affected by Paget's disease suggests superimposed metastatic disease rather than sarcomatous transformation. It is speculated that increased blood flow to pagetic bone may make it more susceptible to hematogenously-spread metastatic disease.

## SUGGESTED READING

Bastin S, Bird H, Gamble G, Cundy T. Paget's disease of bone - becoming a rarity? Rheumatology 2009;48:1232–1235.

Graham TS. The ivory vertebra sign. Radiology 2005;235:614–615.

Ralston SH, Langston AL, Reid IR. Pathogenesis and management of Paget's disease of bone. Lancet 2008;372:155–163.

Smith SE, Murphey MD, Motamedi K, et al. From the archives of the AFIP: radiologic spectrum of Paget disease of bone and its complications with pathologic correlation. Radiographics 2002;22:1191–1216.

# CASE 21

**EMILY N.**

**VINSON**

## HISTORY

A 23-year-old woman with aching right knee pain for the past 6 weeks.


■**FIGURES 5-21A and 5-21B** Anteroposterior **(A)** and lateral **(B)** radiographs of the right knee. There is a lobulated, dense, exophytic mass along the posterior surface of the distal right femur.

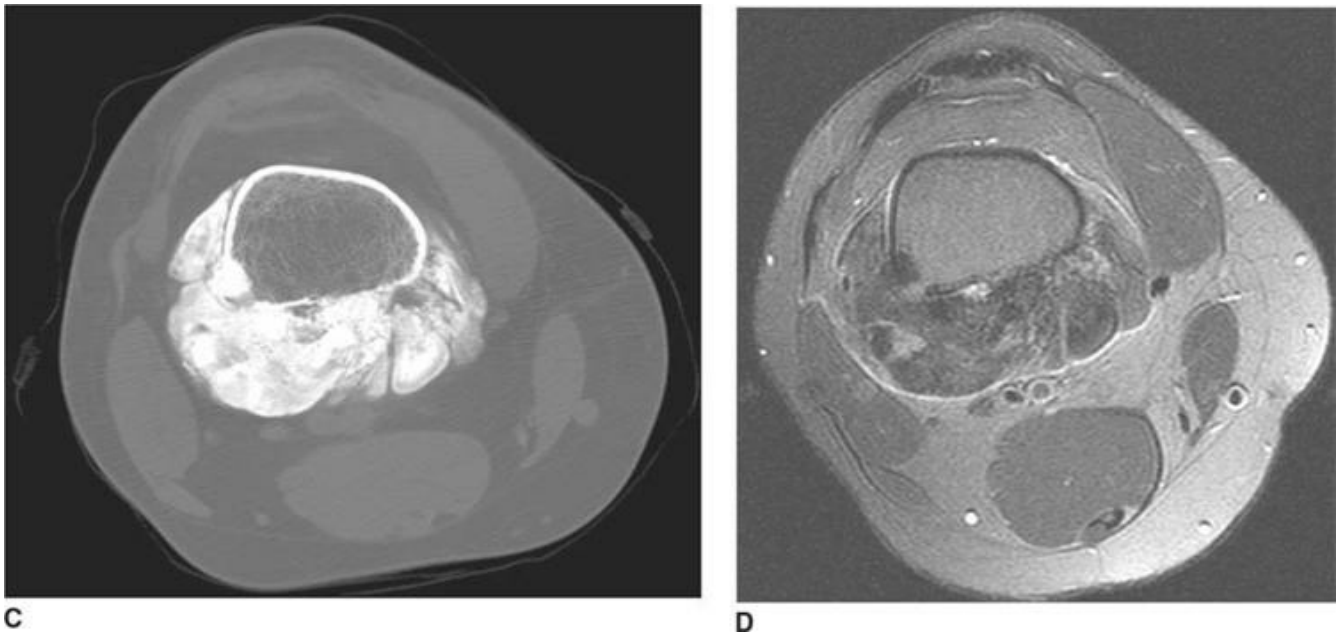


**FIGURES 5-21C and 5-21D** Axial CT **(C)** and fat-suppressed FSE T2-weighted MR **(D)** images just above the level of the right knee demonstrate density equal to that of cortical bone throughout the mass **(C),** which is relatively hypoin-tense on MR imaging **(D).** There is very little involvement of the posterior femoral marrow.

## DIFFERENTIAL DIAGNOSIS

**Myositis ossificans:** This is a common, benign, ossified soft tissue mass, and can occasionally be very close to the surface of a bone. However, the ossification in myositis ossifications forms first at the periphery of the mass and progresses toward the center of the mass, with the resultant imaging appearance of a mass that is densest peripherally and more lucent centrally. That is not the appearance of the current case, which is dense throughout. Therefore, this is not the correct diagnosis.

**Osteochondroma:** Osteochondroma is a common benign bone lesion and is characterized by an exophytic appearance, as is seen in this case. However, the key imaging feature of an osteochondroma is continuity of the native bone cortex and medullary space with that of the exo-phytic lesion, a feature absent in this case. In addition, there is often undertubulation of the adjacent metaphy-sis in a long bone osteochondroma, which is also absent in this case. For these reasons, osteochondroma can be excluded as a possibility.

**Parosteal osteosarcoma:** A lobulated, exophytic, dense mass along the surface of the bone, with homogeneous high attenuation on CT imaging and lack of a soft tissue mass on MR imaging, is typical of a low-grade parosteal osteosarcoma. The posterior aspect of the distal femur is the most common location for this mass to occur. This is the best diagnosis.

# DIAGNOSIS
**Parosteal osteosarcoma**

# KEY FACTS

## Clinical

- There are three main types of surface or juxtacorti-cal osteosarcomas: parosteal osteosarcoma, periosteal osteosarcoma, and high-grade surface osteosarcoma.
- Parosteal osteosarcoma is the most common of the jux-tacortical osteosarcoma types, accounting for about 5% of all osteosarcomas.
- These tumors tend to occur at the metaphyses of long bones. The most common location is the posterior aspect of the distal femoral metaphysis. These tumors are most common during second through fourth decades of life, a slightly older age range than conventional osteosarcoma.
- Low-grade parosteal osteosarcoma carries a better prognosis (5-year survival rate 86% to 91%) than conventional osteosarcoma (5-year survival rate 53% to 61%).
- Parosteal osteosarcoma may dedifferentiate into a higher grade tumor, usually conventional osteosarcoma. Paros-teal osteosarcoma with areas of higher grade tumor has a worse prognosis than those that are low grade throughout.
- While "parosteal" osteosarcoma sounds similar to "periosteal" osteosarcoma, which is another of the jux-tacortical osteosarcoma types, they are very dissimilar in origin, imaging appearance, and prognosis. Paros-teal osteosarcoma originates from the outer fibrous layer of the periosteum and is typically a low-grade malignancy. In contradistinction, periosteal osteosar-coma arises from the inner layer of the periosteum, and is typically an intermediate-grade neoplasm, with survival rates better than those of conventional osteosarcoma but worse than those of parosteal osteosaroma. As described below, these two entities also differ in radiologic appearance.
- Patients with low-grade parosteal osteosarcoma are usually treated surgically with wide local resection. Higher-grade tumors may be treated with neoadjuvant chemotherapy and subsequent attempted resection with limb salvage techniques.

## Radiologic

- On radiographs, parosteal osteosarcoma typically appears as a lobulated, dense, exophytic mass along the surface of a bone.
- There is occasionally a cleavage plane between the mass and the bone due to the presence of periosteum between the cortex of the underlying bone and the mass. On

cross-sectional imaging, the tumor is most commonly homogeneously dense and images much like the cortex of the adjacent bone; the next most common appearance is amorphous and irregular increased density.

- There may be cortical thickening of the adjacent bone. As the tumor grows, it tends to encircle the host bone. Aggressive periostitis is usually not present.
- On CT or MR imaging, involvement of the medullary space of the underlying bone is variably present and does not necessary correlate with histologic grade.
- Due to the dense mineralization within the tumor, the mass is usually very low in signal intensity on both T1- and T2-weighted images. The presence of areas of increased signal intensity on T2-weighted images corresponding to regions of unmineralized soft tissue suggests that portions of the tumor are of higher grade.
- Increasing areas of lucency within the mass or the presence of a large soft tissue mass also suggest dedifferentiation into a high-grade tumor.
- Multiplanar MR imaging is an important part of presurgical planning prior to resection of a parosteal osteosarcoma as it depicts intramedullary extension, which must be excised completely. In addition, areas of higher-grade tumor can be detected and treatment modified accordingly.
- Parosteal osteosarcoma and periosteal osteosarcoma should never be mentioned in the same radiology differential diagnosis as they have very dissimilar imaging appearances. Periosteal osteosarcomas are usually diaphyseal and have a chondroid matrix. On imaging they are characterized by the presence of a high signal intensity juxta-cortical mass on T2-weighted images, a hypodense mass on CT imaging (reflecting the predominantly cartilaginous make-up), associated cortical erosion, and periosteal reaction within the soft tissue mass oriented perpendicular to the cortex of the underlying bone and extending to the outer margin of the tumor. Parosteal osteosarcomas are typically metaphyseal and composed of dense osteoid matrix, with a notable lack of periosteal reaction.

## SUGGESTED READING

Jelinek JS, Murphey MD, Kransdorf MJ, et al. Parosteal osteosarcoma: value of MR imaging and CT in the prediction of histologic grade. Radiology 1996;201:837–842.

Lindell MM Jr, Shirkhoda A, Raymond AK, et al. Parosteal osteosarcoma: radiologic-pathologic correlation with emphasis on CT. Am J Roentgenol 1987;148:323–328.

Logan PM, Mitchell MJ, Munk PL. Imaging of variant osteosarcomas with an emphysis on CT and MR imaging. Am J Roentgenol 1998;171:1531–1537.

Yarmish G, Klein MJ, Landa J, et al. Imaging characteristics of primary osteogenic sarcoma: nonconventional subtypes. Radiographics 2010;30:1653–1672.

# CASE 22

**EMILY N. VINSON**

## HISTORY

A 49-year-old woman with a history of Raynaud's phenomenon and episodic digital ischemia, as well as mild diffuse arthralgias and joint stiffness. She is a nonsmoker.

A

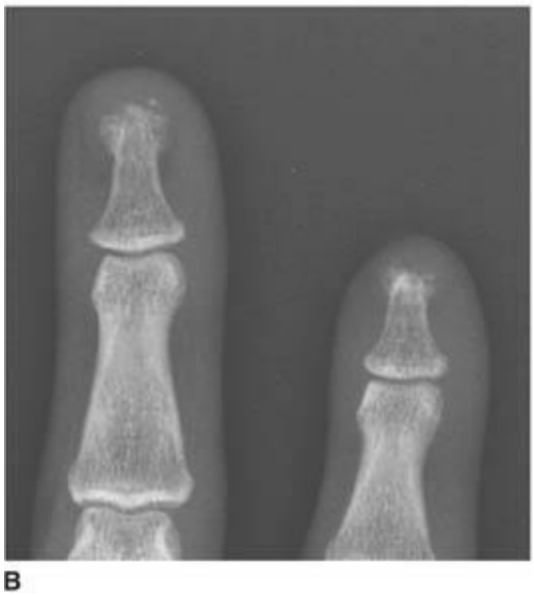

B

C

■**FIGURES 5-22A, 5-22B, and 5-22C** Anteroposterior **(A),** magnified **(B),** and lateral **(C)** radiographs of the left hand demonstrate acroosteolysis involving the distal tufts of the index and long finger distal phalanges, as well as several soft tissue calcifications in the thumb, index finger, and long finger. There is no significant joint space narrowing,

articular or periarticular erosive changes, vascular calcification, or evidence of subperiosteal bone resorption.

## DIFFERENTIAL DIAGNOSIS

- **Hyperparathyroidism:** Resorption of the distal phalan-gal tuft may be seen in hyperparathyroidism. However, the most characteristic feature of hyperparathyroidism in the hands is subperiosteal bone resorption, usually along the radial aspects of the middle phalanges, a feature which is absent in this case. In addition, the patient's clinical history of Raynaud's phenomenon does not suggest hyperparathyroidism.
- **Systemic sclerosis (SSc) (scleroderma):** This is the best diagnosis given the presence of acro-osteolysis and subcutaneous calcinosis. The clinical history of Raynaud's phenomenon further supports this diagnosis.
- **Thromboangiitis obliterans (Buerger's disease):** Patients with Buerger's disease commonly experience digital vascular complaints, including Raynaud's phenomenon. However, there is virtually always a history of current or recent cigarette smoking, which is lacking in this case, and there are often overt gangrenous changes in the soft tissues of the fingertips. Subcutaneous calcinosis is not a feature of this vasculitis. In addition, arthralgias are not a typical clinical feature. For these reasons, this is not the correct diagnosis.
- **Psoriasis:** Acroosteolysis can be seen in patients with psoriatic arthritis. However, there is usually evidence of an erosive arthropathy, particularly at the DIP joint of the affected finger. The overlying nailbed is also usually abnormal, and there is associated soft tissue swelling of the affected digit. None of these features are present in this case. In addition, the clinical history of Raynaud's phenomenon does not suggest psoriasis.

## DIAGNOSIS

**Systemic sclerosis (scleroderma)**

## KEY FACTS

### Clinical

- SSc, also known as scleroderma, is a multisystem connective tissue disorder characterized by the deposition of collagen and other extracellular matrix constituents in the skin and target internal organs. The skin is the most commonly affected organ system, and there is typically hardening and scarring of the skin. The lungs, heart, gastrointestinal tract, musculoskeletal system, and peripheral circulation are also often affected.

- Tissue damage in patients with SSc is the result of vas-culopathy, inflammation, and fibrosis.
- While SSc is associated with increased morbidity and mortality, there is considerable variability in disease course between patients depending on the distribution and extent of organ system involvement. Pulmonary arterial hypertension is a major cause of morbidity and mortality, as is renal crisis due to uncontrolled hypertension.
- The disease is clinically classified as diffuse SSc, limited SSc, or scleroderma overlap syndrome. CREST syndrome is a form of limited SSc, and consists of calcinosis, Raynaud's phenomenon, esophageal dysfunction, sclerodactyly, and telangiectasia. Several hallmark autoantibodies, including anticentromere antibody (ACA), have been shown to have clinical and prognostic significance in patients with SSc.
- Articular involvement occurs across all clinical and serological subsets of the disease, and is a major determinant of disability. In particular, involvement of the joints and soft tissues of the hands is a major source of symptoms and disability in SSc patients.
- Raynaud's phenomenon occurs in up to 98% of patients with SSc, and may precede other symptoms by up to 20 years.
- There is no cure for SSc; patient-specific treatments are instituted for control of symptoms.

## Radiologic

- Radiology plays an important role in the diagnosis and management of SSc and in defining the distribution and extent of visceral involvement.
- Joint involvement is very common, and is estimated to affect anywhere from 46% to 97% of patients. The most common locations for arthralgias are the hands and feet.
- The major features of hand involvement in patients with SSc include arthritis, articular erosions, joint space narrowing, acroosteolysis, flexion contractures, and subcutaneous calcinosis. Of these, acroosteolysis (most commonly affecting the distal aspect of the tuft), and calcinosis are thought to be the most characteristic findings in SSc.
- Several patterns of hand involvement in SSc have been described. The most frequent pattern, called the periarticular pattern, consists of acroosteolysis and calcinosis, with or without the presence of flexion contractures. An inflammatory pattern, consisting of periarticular osteoporosis, joint space narrowing, and erosions, with or without flexion contractures, is also common. Whether erosive changes are a manifestation of SSc or of an overlapping RA is still a matter of debate.
- Calcinosis is frequently localized to the hands, and is more common in limited SSc. Calcinosis typically occurs at sites of chronic stress, is more common in the dominant

hand, and is seen more frequently in patients with erosive lesions.

- Vascular injury may play a role in the development of acroosteolysis and calcinosis, as these features appear to be associated with the presence of digital and systemic vascular complications.

## SUGGESTED READING

Avouac J, Guerini H, Wipff J, et al. Radiological hand involvement in systemic sclerosis. Ann Rheum Dis 2006;65:1088–1092.

Erre GL, Marongiu A, Fenu P, et al. The "sclerodermic hand": a radiological and clinical study. Joint Bone Spine 2008;75:426–431.

La Montagna G, Sodano A, Capurro V, et al. The arthropathy of systemic sclerosis: a 12 month prospective clinical and imaging study. Skeletal Radiol 2005;34:35–41.

Madani G, Katz RD, Haddock JA, et al. The role of radiology in the management of systemic sclerosis. Clin Radiol 2008;63:959–967.

# CASE 23

**EMILY N. VINSON**

### HISTORY

A 57-year-old man with a several year history of bilateral foot pain and irregular soft tissue swelling.


**FIGURES 5-23A and 5-23B** Anteroposterior radiograph of the left foot **(A)** and oblique radiograph of the right foot **(B).** There are multiple well-defined erosions with sclerotic margins, some of which have overhanging edges. These are most obvious about the left foot first metatarsophalangeal joint, the right foot first interphalangeal joint, and involving multiple tarsometatarsal joints bilaterally. There is focal soft tissue swelling at the right first interphalangeal joint.

## DIFFERENTIAL DIAGNOSIS

**Rheumatoid arthritis (RA):** RA is manifest by joint space narrowing, juxta-articular osteopenia, and marginal erosions, with a lack of proliferative changes. In the feet, erosive changes at the lateral aspect of the fifth metatarsal head are characteristic, and are not a prominent feature in this case. In addition, the sclerosis at the margins of the erosions and the overhanging edges of several erosions in this case are not features of RA. This is not the correct diagnosis.

**Psoriasis:** Psoriasis is an inflammatory arthritis that may affect the feet in an asymmetric distribution and may have associated soft tissue swelling, as is seen in this case. The interphalangeal joint of the great toe is a target joint for psoriasis, and is involved in this case. However, the erosions associated with psoriasis have proliferative or “fuzzy” margins, not well-defined sclerotic margins, and there is usually

associated new bone formation and periostitis around erosions. For these reasons, this is not the correct diagnosis.

- **Gout:** The presence of well-defined erosions with sclerotic margins and overhanging edges is characteristic of gout. This is the best diagnosis.

## DIAGNOSIS

**Gout**

## KEY FACTS

### Clinical

- Gout is the oldest recognized arthropathy, with written evidence of the disease's existence dating back to Hip-pocratic writings.
- Gout results from the deposition of monosodium urate crystals in and around articular joints; the precipitation of crystals leads to an inflammatory response which causes the clinical symptoms. Thus, most patients with gouty arthropathy have longstanding hyperuricemia. However, many patients with longstanding hyperurice-mia never develop clinical gout.
- Primary or idiopathic gout is due to inborn errors of purine metabolism or decreased renal secretion of urate, resulting in hyperuricemia. Secondary gout is that associated with a disease that causes increased production of uric acid (such as inherited enzyme defects or diseases with high cellular turnover such as myeloproliferative disorders) or decreased excretion of uric acid (such as in renal failure); certain medications such as diuretics and cytotoxic chemotherapy can also cause secondary gout. Secondary gout does not usually result in visible changes on radiographs.
- Gout affects 1% to 2% of adults in developed countries, and is increasing in prevalence. The disease is much more common in men than in women, and incidence increases with age. In general, primary gout is uncommon in men prior to age 30 years and is uncommon in women prior to menopause (serum uric acid levels increase in post menopausal women as estrogen levels decrease).
- Patients with gout typically experience many years of asymptomatic hyperuricemia, followed by intermittent attacks of acute gout with intervening asymptomatic periods; some patients will go on to develop chronic tophaceous gout.
- The first episode of acute gout typically occurs in the first metatarsophalangeal joint, a clinical entity known as *podagra.* Acute attacks may be unprovoked, or can be provoked by such inciting events as dehydration, trauma, dietary indiscretions, and infection. The joint involved with acute gout is typically red, hot, tender, and

excruciatingly painful.

- Tophaceous gout occurs in some patients with longstanding disease, and is characterized by the formation of tophi in the periarticular soft tissues including bursae, ligaments, and tendons. Tophi within tendons and ligaments predispose to rupture. Tophi consist of urate crystals, protein matrix, inflammatory cells, and foreign body giant cells.
- Serum uric acid concentrations alone cannot confirm or exclude gout, and may be within the normal range during an acute gout flare. The disease is diagnosed definitely by the demonstration of monosodium urate crystals in aspirated synovial fluid or in material aspirated from a tophus. Negatively birefringent crystals are seen under polarized microscopy.
- With appropriate dietary restrictions and medical therapy, primary gout is a curable disease.
- Primary gout is associated with many other conditions including hypertension, diabetes mellitus, metabolic syndrome, renal disease, and cardiovascular disease. The most common form of renal disease is the development of uric acid kidney stones, which occurs in 10% to 40% of patients.

## Radiologic

- Radiographs are usually normal during acute flares of gout, or may show only nonspecific soft tissue swelling, and thus are not useful in the diagnosis of acute or recent gout. Radiographic changes may not be visible for up to 10 years or more following the initial gout flare, and then only if treatment has not been instituted and maintained.
- In the setting of chronic disease, radiographs may show changes of osteoarthritis and/or changes of chronic tophaceous gout. Characteristic radiographic findings of tophaceous gout include well-marginated eccentric erosions with overhanging edges. The erosions may have a “punched-out” appearance due to thin sclerotic margins, and may be intraarticular, paraarticular, or extraarticu-lar in location. The overhanging edge is due to a thin margin of bone partially covering the expanding tophus.
- There is often associated soft tissue swelling due to the presence of tophi, and pressure erosions may be seen in bones adjacent to tophi. Joint space narrowing and periarticular osteopenia are typically not seen until very late in the disease process.
- In patients with polyarticular involvement, the distribution of disease is random and asymmetric. The distal extremities are most commonly involved.
- Tophi are typically dense (mean attenuation of 160 to 170 Hounsfield units on CT imaging) and may appear cloud-like. Radiographically-visible calcification is uncommon in tophi, except in the setting of abnormal calcium metabolism, such as in

patients with coexistent renal failure.

- Gout has a variable appearance on MRI. An acutely inflamed joint may show a joint effusion and subchon-dral edema. Gouty tophi may be seen on MR imaging as periarticular masses, typically low in signal intensity on T1-weighted images and low to intermediate signal intensity on T2-weighted images; a single tophus may be difficult to differentiate from a neoplastic mass if the history of gout is not known.
- Gout can mimic a septic joint both clinically and by imaging.

## SUGGESTED READING

Gentili A. Advanced imaging of gout. Semin Musculoskelet Radiol 2003;7:165–174.

Jacobson JA, Girish G, Jiang Y, Sabb BJ. Radiographic evaluation of arthritis: degenerative joint disease and variations. Radiology 2008;248: 737–747.

Monu JUV, Pope TL Jr. Gout: a clinical and radiologic review. Radiol Clin N Am 2004;42:169–184.

Richette P, Bardin T. Gout. Lancet 2010;375:318–328.

# CASE 24

**EMILY N. VINSON**

### HISTORY

A 56-year-old man with low back pain. Additional studies, including serum and urine electrophoresis and radiographic skeletal survey, were normal. Bone scintigraphy demonstrated decreased radionuclide uptake in the region of the lesion.

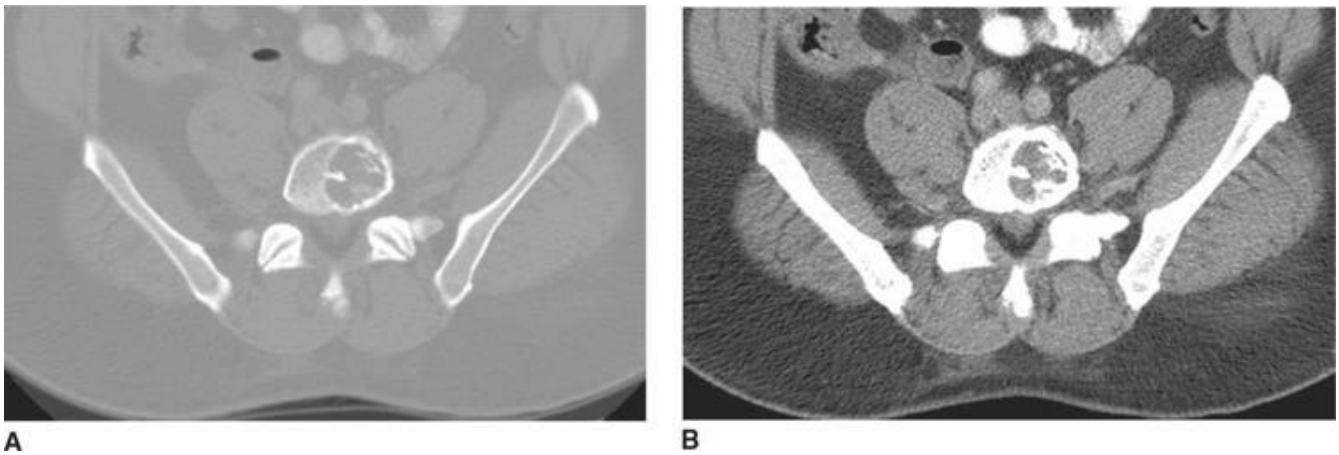


**FIGURES 5-24A and 5-24B** Axial CT images through the lower lumbar spine in bone **(A)** and soft tissue **(B)** window settings demonstrate a lytic lesion in the left aspect of

the L5 vertebral body, with a thin sclerotic border and with a thickened trabecula oriented radially in the periphery of the lesion.

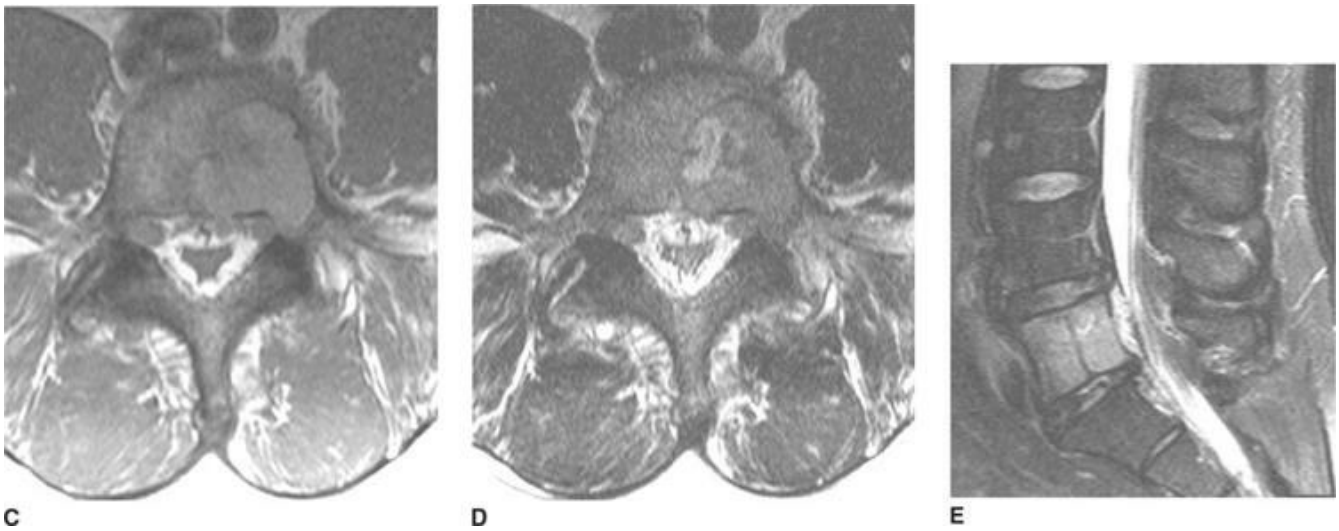


**FIGURES 5-24C, 5-24E, and 5-24E** Axial Tl-weighted **(C),** axial fast spin echo T2-weighted **(D),** and sagittal fat-suppressed fast spin echo T2-weighted **(E)** MR images of the lumbar spine. The lesion is intermediate in signal intensity on Tl-weighted image and hyperintense on fat-suppressed T2-weighted image.

## DIFFERENTIAL DIAGNOSIS

**Metastatic disease:** A lytic lesion in a patient over the age of 40 years could represent metastatic disease; this is true whether the lesion has an aggressive or nonaggressive appearance. Most (but not all) metastases, however, demonstrate increased uptake on bone scintigraphy. In addition, while solitary metastases do occur, metastases are usually multiple at the time of discovery. So while metastasis remains a diagnostic possibility, these features decrease its likelihood.

**Solitary plasmacytoma of bone:** Myeloma can present as solitary or multiple lytic lesions of bone, and is typically seen in patients over the age of 35 years. Lesions may have an aggressive or nonaggressive appearance. A patient with a plasma cell neoplasm presenting consisting of a single lytic lesion and without laboratory evidence of multiple myeloma is said to have a solitary plasmacytoma; this diagnosis is usually confirmed by biopsy of the lesion due to the nonspecific imaging appearance. However, one fairly specific imaging feature for plasmacytoma is the presence of thickened trabeculae at the periphery of the lesion with a radial orientation, as is seen in this case. This is the most likely diagnosis.

**Giant cell tumor (GCT):** While rare, GCTs do occur in the spine, most commonly involving the sacral segments. On MR imaging there are often cystic spaces within the

mass, a feature lacking in this case. These tumors usually demonstrate increased uptake on radionuclide bone scans. Also, this lesion is more common in younger adults. For these reasons, GCT is a less likely diagnosis in this case.

- **Monostotic fibrous dysplasia:** Although the CT and MR appearances are compatible with this diagnosis, fibrous dysplasia typically demonstrates increased uptake of radiotracer on a bone scintigraphy, making this an unlikely diagnosis in this case.

## DIAGNOSIS

**Solitary plasmacytoma of bone**

## KEY FACTS

### Clinical

- The monoclonal gammopathies are a group of disorders associated with a monoclonal proliferation of plasma cells, and include, among other entities, monoclonal gammopathy of undetermined significance (MGUS), asymptomatic ("smoldering") myeloma, symptomatic multiple myeloma, and solitary plasmacytoma of bone.
- Plasmacytoma of bone is defined as a single region of bone destruction due to monoclonal plasma cells.
- Solitary plasmacytoma is uncommon, accounting for approximately 3% to 5% of patients with a plasma cell neoplasm. The diagnosis is based on biopsy of the lesion with the presence of monoclonal plasma cells on histo-pathology, and on the absence of additional lesions on bone survey (and MRI of spine and pelvis, if performed).
- In patients with solitary plasmacytoma, laboratory analysis typically reveals no significant monoclonal protein in serum or urine, and nonselective bone marrow aspirate is normal (<10% plasma cells).
- Patients with a diagnosis of solitary plasmacytoma should have no organ or tissue impairment—including anemia, hypercalcemia, or renal insufficiency—related to the plasmacytoma.
- On average, patients with solitary plasmacytoma present at an earlier age (median age 55 years) than those presenting with symptomatic multiple myeloma (median age 65 years).
- Common clinical presentations include pain at the site of the skeletal lesion, pathologic fracture, cord compression, or palpable mass.
- The axial skeleton is the most common site of involvement, with the thoracic vertebrae more commonly involved than cervical or lumbar. Involvement of the pelvis and shoulder girdle is not rare; involvement of the distal appendicular skeleton is rare.

- Almost half of patients with solitary plasmacytoma will progress to overt multiple myeloma. This progression usually occurs within 3 to 4 years of diagnosis, but may occur as much as 15 years later. Patients with lesions >5 cm in size are at increased risk of progression.
- Treatment consists of radiotherapy to the solitary lesion.
- The clinical prognosis is much better than in multiple myeloma, even in those patients who eventually develop multiple lesions.

## Radiologic

- The radiographic skeletal survey remains the initial imaging tool in the evaluation of patients with suspected plasma cell neoplasm. However, whole body MR imaging has a higher sensitivity for lesion detection, and is now recommended in the setting of MGUS or solitary plasmacytoma with a normal radiographic skeletal survey to search for additional lesions and to better assess the extent of the local disease. Some patients diagnosed with solitary plasmacytoma by standard radiographic criteria may be understaged if MRI of the spine is not performed due to the underdetection of small lesions by skeletal survey.
- Plasmacytomas are variable in appearance, and can be included in the differential of virtually any lytic lesion in a patient 35 years of age or older.
- Technetium bone scintigraphy is not useful in the evaluation of the monoclonal gammopathies, as the disease process in multiple myeloma inhibits osteoblastic activity and therefore many lesions will not demonstrate radionuclide uptake.
- Plasmacytoma is typically isointense to skeletal muscle on T1-weighted images and hyperintense to skeletal muscle on T2-weighted images, making it often indistinguishable from other marrow-replacing processes, such as metastatic disease. Therefore, a biopsy with histo-pathological analysis is often required for diagnosis.
- Occasionally, a plasmacytoma will have a “mini brain” appearance on CT or MR imaging, due to the presence of thickened trabeculae in the periphery of the lesion arranged in a radial pattern, resembling a cross-section of the sulci of the brain. Thickened trabeculae can also be seen in other processes, such as hemangioma; however, the peripheral radial orientation of the trabeculae suggests the diagnosis of plasmacytoma. This appearance has been described in both axial and appendicular plasmacytoma.

## SUGGESTED READING

Delorme S, Baur-Melnyk A. Imaging in multiple myeloma. Eur J Radiol 2009;70:401–408.

Dimopoulos M, Terpos E, Comenzo RL, et al. International myeloma working group consensus statement and guidelines regarding the current role of imaging techniques in the diagnosis and monitoring of multiple myeloma. Leukemia 2009;23:1545–1556.

Hanrahan CJ, Christensen CR, Crim JR. Current concepts in the evaluation of multiple myeloma with MR imaging and FDG PET/CT. Radiographics 2010;30:127–142.

International Myeloma Working Group. Criteria for the classification of monoclonal gammopathies, multiple myeloma and related disorders: a report of the International Myeloma Working Group. Br J Haematol 2003;121:749–757.

Major NM, Helms CA, Richardson WJ. The "mini brain": plasmacytoma in a vertebral body on MR imaging. Am J Roentgenol 2000;175:261–263.

Subhas N, Bauer TW, Joyce MJ, Sundaram M. The "mini brain" appearance of plasmacytoma in the appendicular skeleton. Skeletal Radiol 2008;37:771–774.

# CASE 25

**THOMAS DZIEDZIC**

## HISTORY

A 41-year-old male experienced an acute onset of left shoulder pain, severe enough to wake him at night, 2 weeks following a surgical procedure. On initial exam he demonstrated normal strength and normal sensation. Over the course of the next several months, the patient began having weakness of the left shoulder with gradual improvement in pain.

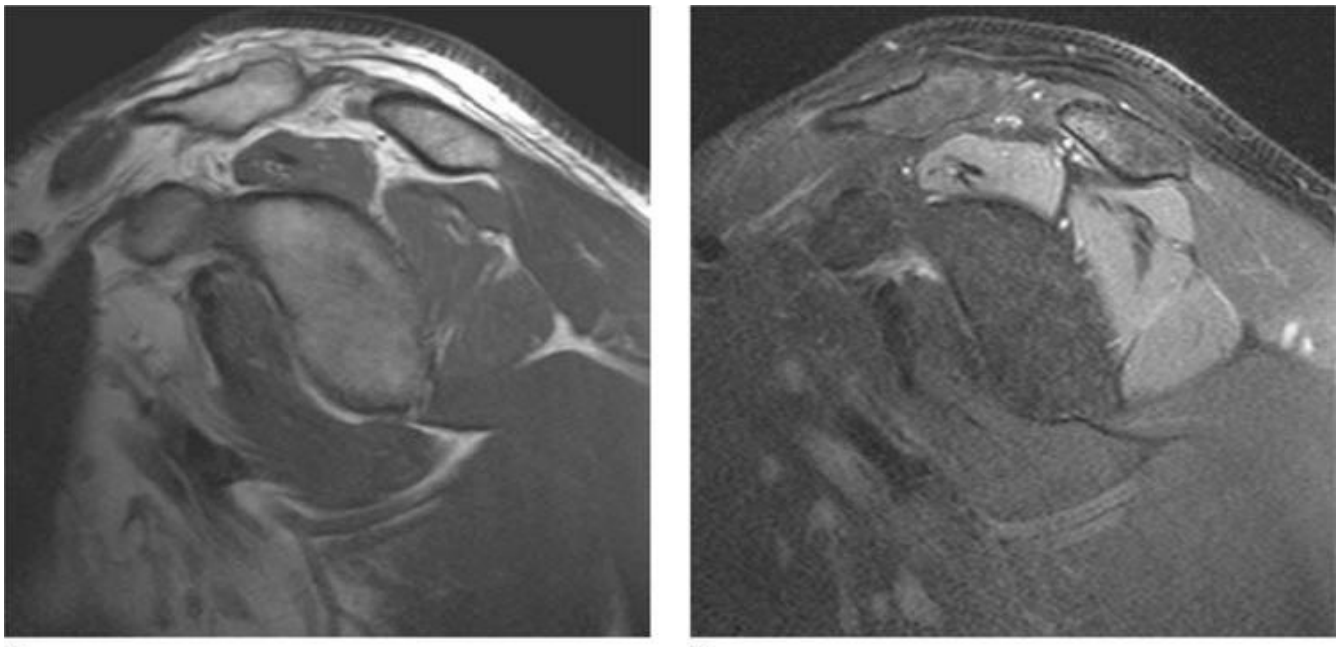


■**FIGURES 5-25A and 5-25B** Sagittal oblique Tl-weighted **(A)** and fat-suppressed T2-weighted **(B)** images. There is diffuse increased signal intensity throughout the supraspinatus, infraspinatus, and teres minor muscle bellies on the T2-weighted image.

The Tl-weighted image demonstrates no evidence of atrophy or fatty infiltration of the muscles.

## DIFFERENTIAL DIAGNOSIS

- **Peripheral nerve compression:** Compression of the suprascapular nerve, such as by a paralabral cyst or other mass in the suprascapular notch, could cause neurogenic edema within the supraspinatus and infra-spinatus muscles, but should not cause edema in the teres minor, which is innervated by the axillary nerve. Additionally, no compressing lesions were identified on the shoulder MRI of this patient. Clinically, the symptoms associated with nerve compression are usually more insidious in onset than experienced by the patient in this case.
- **Cervical radiculopathy:** Patients with cervical radicu-lopathy can have abnormal muscle signal in a pattern similar to this patient. However, the clinical features are often different, with the pain aggravated by neck extension. In addition, a sensory deficit is usually present, which was not seen in this patient.
- **Parsonage-Turner syndrome:** This disorder typically presents with severe shoulder girdle pain, followed by progressive weakness. The supraspinatus, infraspina-tus, and teres minor muscles are commonly affected. Based on the imaging findings and clinical history, this is the best diagnosis.
- **Rotator cuff tear:** Patients with rotator cuff tears can present with sudden onset of pain, and on imaging may demonstrate edema within one or more of the muscle bellies around the shoulder. Usually, there will be a history of trauma associated with the injury. The patient in this case had no history of trauma, and imaging revealed the rotator cuff to be intact.
- **Brachial plexus injury:** a traumatic nerve injury could have a similar appearance on imaging, however the clinical history given in this case excludes this possibility.

## DIAGNOSIS

**Parsonage-Turner syndrome**

## KEY FACTS

### Clinical

- Also called acute brachial neuritis.
- Classic clinical history is the sudden onset of nontraumatic intense pain in the shoulder girdle lasting several weeks. Strength is initially normal, followed by the onset of

progressive muscle weakness coinciding with the resolution of pain, typically occurring in approximately 4 weeks.

- Wide age range of affected patients but most commonly affects patients in the fourth through seventh decades. Reported male to female ratio of 2:1 or higher.
- Diagnosis made with combination of history and physical exam, electromyographic (EMG) studies, and MRI. EMG and nerve conduction studies demonstrate muscle denervation in the brachial plexus distribution.
- Etiology unknown, but thought to be immune system mediated with inflammation against the nerve and subsequent muscle denervation. Parsonage-Turner syndrome (PTS) has been reported following viral infection, vaccination, surgery, and childbirth. There is no known relation to trauma, hand dominance, or excessive overhead activity.
- PTS is self-limited, so treatment is palliative with analgesics for pain and physical therapy once weakness develops. Strength gradually returns, but weakness can last several years. Symptoms can recur in a small number of patients, and bilateral involvement may occur in up to one-third of patients.

## Radiologic

- Role of MRI is to exclude more common pathologies, such as rotator cuff tendon abnormalities, as a cause of the shoulder pain and weakness.
- Muscles in more than one nerve distribution may be involved, but most commonly involves the supraspi-natus and infraspinatus muscles. Many muscles have been reported to be involved, including the deltoid, teres minor, subscapularis, latissimus dorsi, and ser-ratus anterior.
- Denervation leads to the signal changes within the muscles on MRI. With early imaging in the acute or subacute phase (as early as 2 weeks) there is reversible, diffuse, homogeneous increased T2 signal intensity in the affected muscles due to edema. Typically, all of the muscles is a given nerve distribution will be affected.
- In the chronic phase, MR imaging may also demonstrate atrophy of the muscle (gross muscle volume loss) and/or fatty infiltration, as demonstrated by linear increased intramuscular signal intensity on Tl-weighted images. Fatty infiltration is nonreversible.

# SUGGESTED READING

Gaskin CM, Helms CA. Parsonage-Turner syndrome: MR imaging findings and clinical information of 27 patients. Radiology 2006;240:501–507.

McCarty EC, Tsairis P, Warren RF. Brachial neuritis. Clin Orthop Rel Res 1999;368:37–43.

Misamore GW, Lehman DE. Parsonage-Turner syndrome (acute brachial neuritis). J Bone Joint Surg Am 1996;78:1405–1408.

Sallomi D, Janzen DL, Munk PL, et al. Muscle denervation patterns in upper limb nerve injuries: MR imaging findings and anatomic basis. Am J Roentgenol 1998;171:779–784.

Scalf RE, Wenger DE, Frick MA, et al. MRI findings of 26 patients with Parsonage-Turner syndrome. Am J Roentgenol 2007;189:W39–W44.

# CASE 26

**R. LEE COTHRAN, Jr.**

## HISTORY

A 31-year-old-male with several years of hip pain. Now with increasing hip pain and locking.

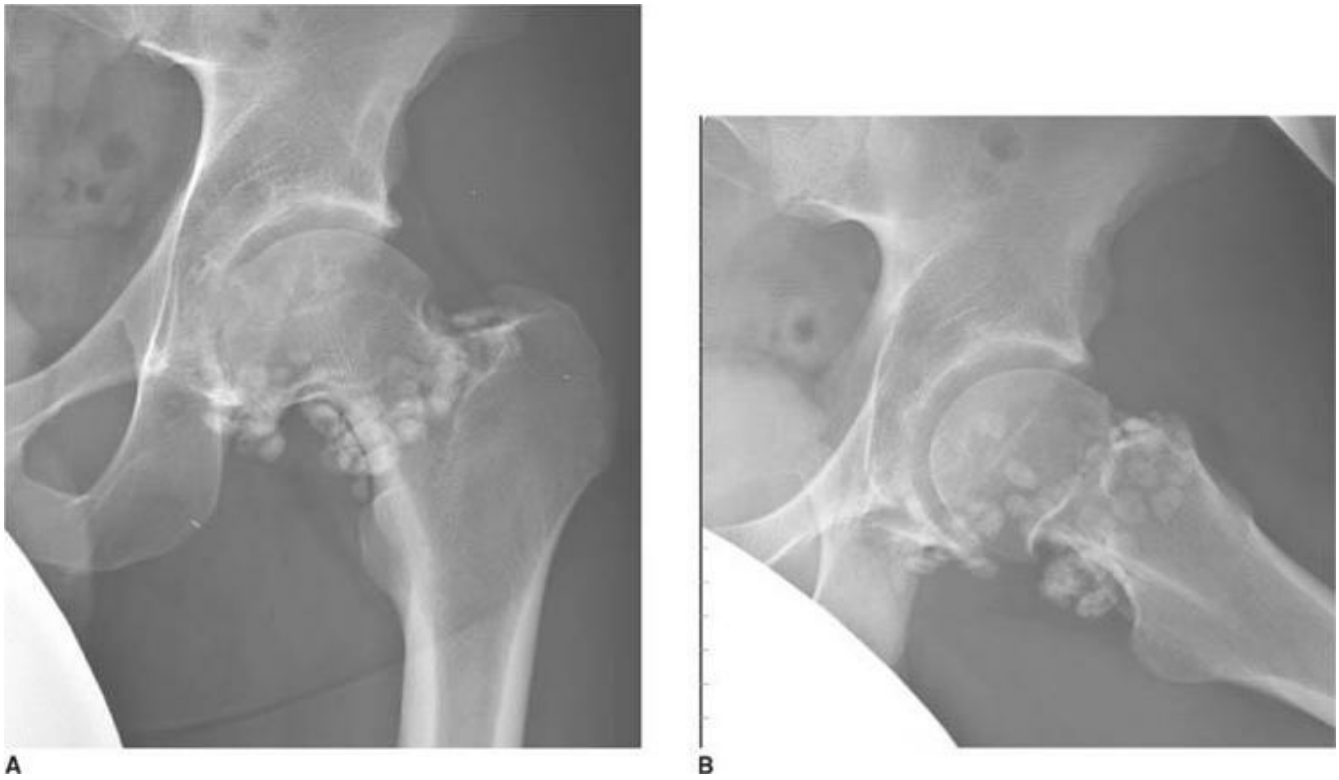


**FIGURES 5-26A and 5-26B (A)** Anteroposterior view of left hip. **(B)** Frog-leg lateral view of left hip. Multiple extraosseous, ovoid, calcified densities in left hip are of uniform size. The number of bodies is out of proportion to degree of joint space loss. Note erosion of femoral neck with "apple core" appearance on AP view **(A)**.

## DIFFERENTIAL DIAGNOSIS

**Loose bodies (secondary synovial chondromatosis):** The bodies present within the joint are typically fewer in number than in primary synovial (osteochondromatosis.

When multiple, they are more often variable in size and degree of mineralization than in this case.

- **Primary synovial chondromatosis:** Given the multiplicity of the bodies and their uniform size, this is the better diagnosis in this case.

## DIAGNOSIS

**Primary synovial chondromatosis with ossification**

## KEY FACTS

### Clinical

- Benign neoplastic process resulting in hyaline cartilage nodule formation in the subsynovial tissue.
- Clinical symptoms on presentation include pain, swelling and restricted range of motion of the affected joint.
- On exam there may be tenderness, crepitus and locking in addition to swelling and palpable masses or nodules.
- Symptoms may be present for several years prior to diagnosis.
- Typically occurs in joints, usually monoarticular, with the hip and knee being most common, but may rarely occur in tendon sheaths (tenosynovial chondromatosis) or bursae (bursal chondromatosis).
- Treatment for primary synovial chondromatosis is surgical synovectomy and removal of bodies.

### Radiologic

- Multiple calcifications are present in the majority (70% to 95%) of cases, typically distributed throughout the joint. These calcifications may exhibit a “ring and arc” pattern. Progression to true ossification may also occur with peripheral cortical bone and central trabecular bone. Nonmineralized disease may also occur.
- The nodules or lobules are typically numerous and similar in size to each other, although they may occasionally coalesce into a single larger body. Joint space is usually preserved, although chronic or recurrent disease may result in secondary degenerative changes.
- Extrinsic osseous erosion may be present on both sides of the joint.
- CT will reveal multiple nodular areas of low attenuation in nonmineralized synovial chondromatosis. If mineralized disease is present, then high attenuation areas of

calcification will be present in the nodules. If ossified disease is present, then cortical and trabecular bone may be defined in the nodules.

- MR imaging will reveal multiple nodular areas of similar size. The signal characteristics will be dependent upon the presence or absence of mineralization and ossification.
- Hypercellularity and atypia may be present and may histologically mimic a malignant neoplasm (Grade 1 to 2 chondrosarcoma). Therefore, it is important that the histology be correlated with the imaging characteristics (particularly intra-articular, bursal or tenosynovial location) to avoid misdiagnosis.

## SUGGESTED READING

Murphey MD, Vidal JA, Fanburg-Smith JC, Gajewski DA. Imaging of synovial chondromatosis with radiologic-pathologic correlation. Radiographics 2007;27:1465–1488.

Resnick D. Diagnosis of Bone and Joint Disorders (4th ed). Philadelphia, PA: Saunders, 2002:4204–4207.

# CASE 27

**GLEN A. TOOMAYAN**

### HISTORY

A 28-year-old man with progressive shoulder pain and weakness.

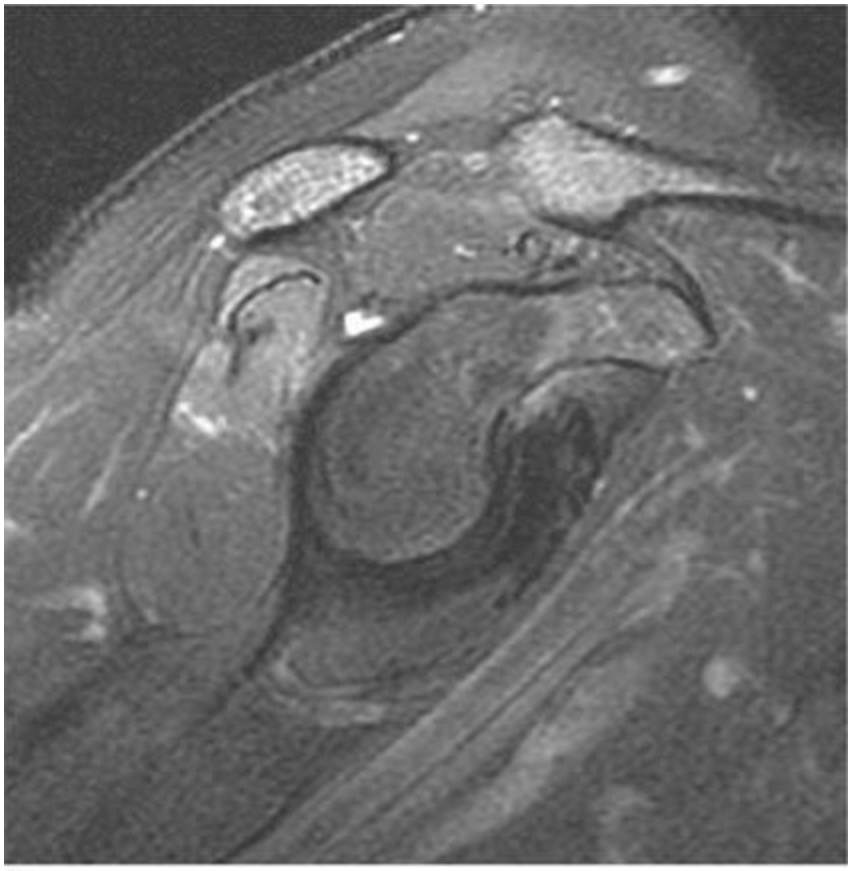

A

**FIGURE 5-27A** Oblique sagittal fat-suppressed T2-weighted image at the level of the glenoid fossa demonstrates abnormal hyperintensity throughout the infraspinatus muscle belly, indicative of edema. The remainder of the rotator cuff muscles are normal. A small hyperintense lesion is seen within the soft tissues adjacent to the posterosuperior rim of the glenoid.

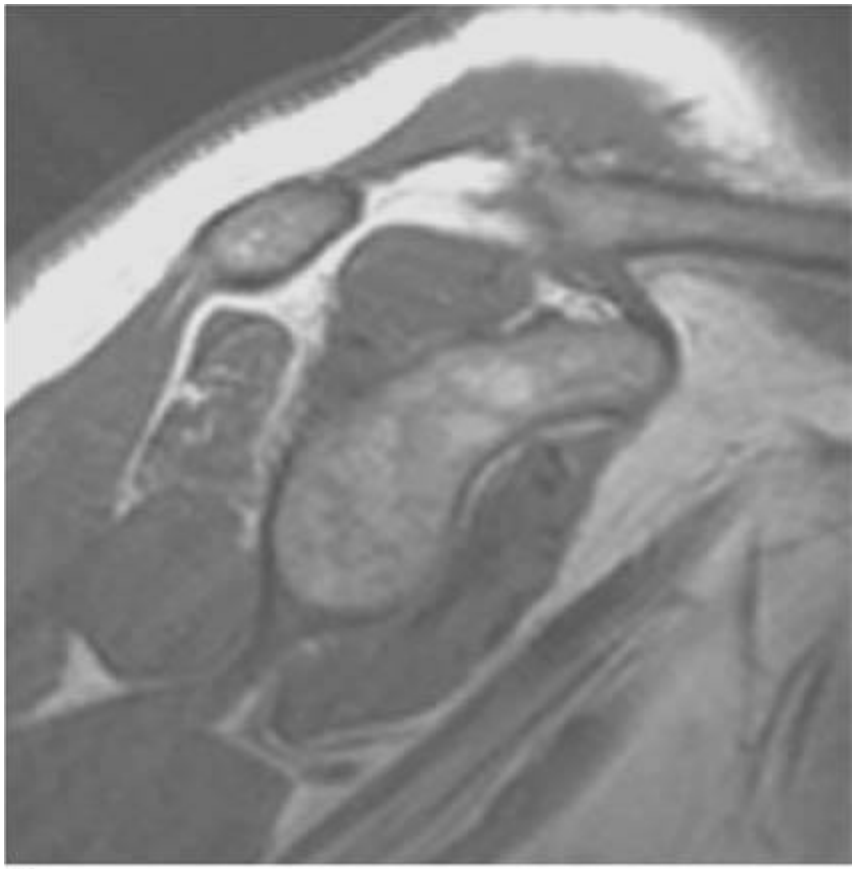

B

■**FIGURE 5-27B** Oblique sagittal T1-welghted image at the level of the glenoid fossa demonstrates atrophy and mild fatty infiltration of the infraspinatus muscle belly. The remainder of the rotator cuff muscles are normal in size and signal intensity.

C

**FIGURE 5-27C** Axial fat-suppressed T2-weighted image demonstrates a lobular hyperintense mass occupying the spinoglenoid notch, with a small neck extending to the posterior superior glenoid rim, consistent with a paralabral cyst. Again noted is edema in the infraspinatus muscle belly.

## DIFFERENTIAL DIAGNOSIS

- **Spinoglenoid notch paralabral cyst with suprascapular nerve compression:** There is atrophy and edema of the infraspinatus muscle without atrophy of the supraspina-tus muscle, suggesting suprascapular nerve compression at the spinoglenoid notch. The lobular T2 hyperintense mass occupying the spinoglenoid notch appears to extend from the posterior superior labrum, indicating the presence of a labral tear and confirming the mass to be a paralabral cyst. This is the correct diagnosis.
- **Spinoglenoid notch venous varix:** If the mass had a more tubular configuration, a dilated venous structure could be considered and intravenous contrast could be administered to exclude a non-thrombosed dilated vein.
- **Spinoglenoid notch lipoma:** The mass is hyperintense on fat saturated T2-weighted imaging, indicating that it is not fat containing.
- **Spinoglenoid notch metastasis or primary tumor:** The lobular T2 hyperintense mass

abuts the posterior glenoid, indicating the presence of a labral tear. Further inspection of the labrum usually demonstrates the labral tear, confirming the mass to be a paralabral cyst. If the mass did not abut the labrum, intravenous contrast could be administered to exclude a rare solid mass in this location.

## DIAGNOSIS

**Spinoglenoid notch paralabral cyst causing suprascapular neuropathy**

## KEY FACTS

### Clinical

- Suprascapular neuropathy is an uncommon clinical condition presenting with chronic pain, progressive weakness, and late development of atrophy of the infra-spinatus and possibly the supraspinatus muscles.
- The diagnosis is difficult to make clinically and may be misdiagnosed as rotator cuff or labral pathology.
- The suprascapular nerve arises from upper trunk of the brachial plexus and provides primarily motor innervation to the supraspinatus and infraspinatus muscles. The nerve passes through the suprascapular notch and into the supraspinatus fossa to innervate the supraspinatus muscle. The nerve then continues inferi-orly through the spinoglenoid notch along the posterior scapula to terminate in the infraspinatus fossa, where it innervates the infraspinatus muscle.
- The nerve may be entrapped within the suprascapu-lar notch or spinoglenoid notch by various etiologies, including a congenitally small notch, tight ligament overlying the notch, bony spur, venous varix, cyst, or rarely a mass such as a lipoma, hematoma, metastatic disease, or primary tumor.
- A paralabral cyst is the most common cause of supra-scapular neuropathy, almost always occurring in the setting of an adjacent glenoid labral tear.
- If nerve entrapment occurs in the suprascapular notch (before innervating the supraspinatus), the neuropathy affects both the supraspinatus and infraspinatus musculature. If the entrapment occurs beyond the supra-scapular notch (i.e., within the spinoglenoid notch as in this case), the neuropathy only affects the infraspinatus musculature.
- Treatment options include conservative treatment, percutaneous cyst aspiration, or surgery to excise the cyst and/or repair the torn labrum.

### Radiologic

- The diagnosis of suprascapular neuropathy can be made with MRI or electromyography. MRI offers the advantages of excluding other causes of shoulder pain such as rotator cuff tears and characterizing the cause of entrapment.
- Atrophy of only the infraspinatus muscle suggests suprascapular neuropathy occurring at the level of the spinoglenoid notch. Atrophy of both the infraspinatus and supraspinatus muscles suggests nerve compression at the level of the suprascapular notch. Hyperintensity within the muscles on T2-weighted images, consistent with neurogenic edema, is a variable finding.
- Paralabral cysts are lobular structures abutting the glenoid labrum which are hyperintense on T2-weighted imaging and hypointense on Tl-weighted imaging. These cysts occur in the setting of glenoid labral tears. Close inspection of the labrum usually reveals the tear.
- Paralabral cysts often extend into the suprascapular notch, spinoglenoid notch, or both, where they may cause suprascapular nerve compression.
- If a mass with these imaging characteristics does not abut the labrum, intravenous gadolinium may be administered to evaluate for the presence of a solid mass. A solid mass demonstrates central enhancement and requires further evaluation.

## SUGGESTED READING

Carroll KW, Helms CA, Otte MT, et al. Enlarged spinoglenoid notch veins causing suprascapular nerve compression. Skeletal Radiol 2003;32: 72–77.

Fritz RC, Helms CA, Steinbach LS, Genant HK. Suprascapular nerve entrapment: evaluation with MR imaging. Radiology 1992;182:437–444.

Hazrati Y, Miller S, Moore S, et al. Suprascapular nerve entrapment secondary to a lipoma. Clin Orthop Relat Res 2003;411:124–128.

Piatt BE, Hawkins RJ, Fritz RC, el al. Clinical evaluation and treatment of spinoglenoid notch ganglion cysts. J Shoulder Elbow Surg 2002;11: 600–604.

Tirman PF, Feller JF, Janzen DL, et al. Association of glenoid labral cysts with labral tears and glenohumeral instability: radiologic findings and clinical significance. Radiology 1994;190:653–658.

# CASE 28

**GLEN A. TOOMAYAN**

### HISTORY

A 27-year-old woman with 2-year history of enlarging nontender left lower leg mass.

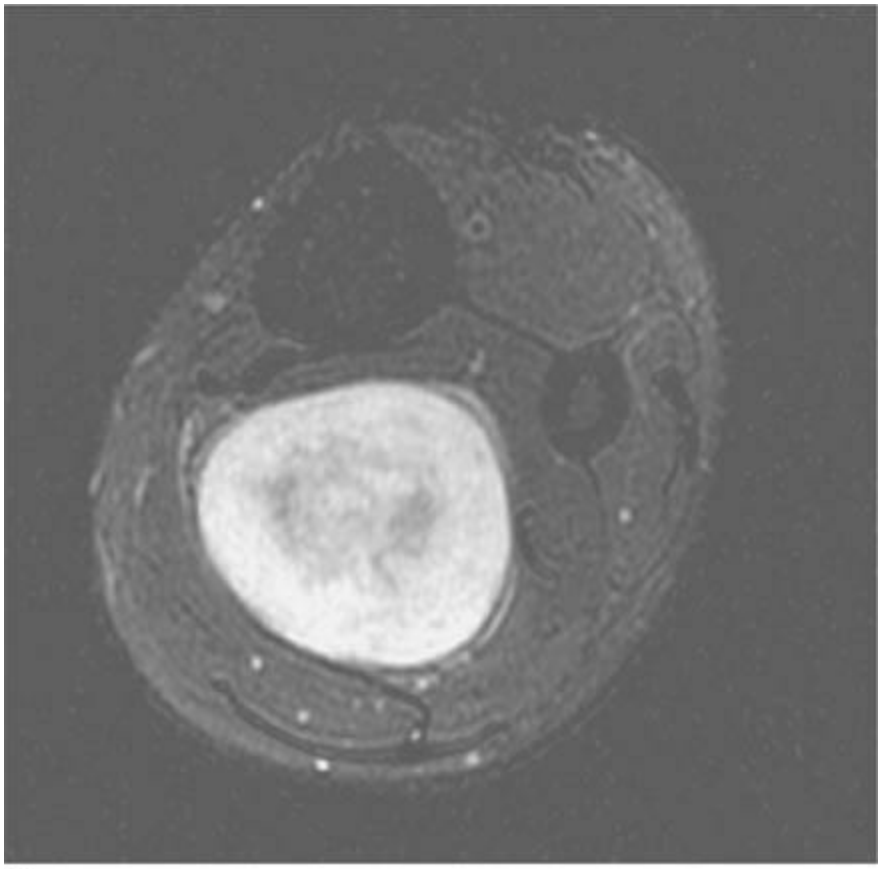

A

■**FIGURE 5-28A** Axial fat-suppressed T2-weighted image through the lower leg demonstrates a large, well-defined, rounded mass arising within the posterior soft tissues of the calf. The mass is hyperintense with areas of hypointensity centrally.

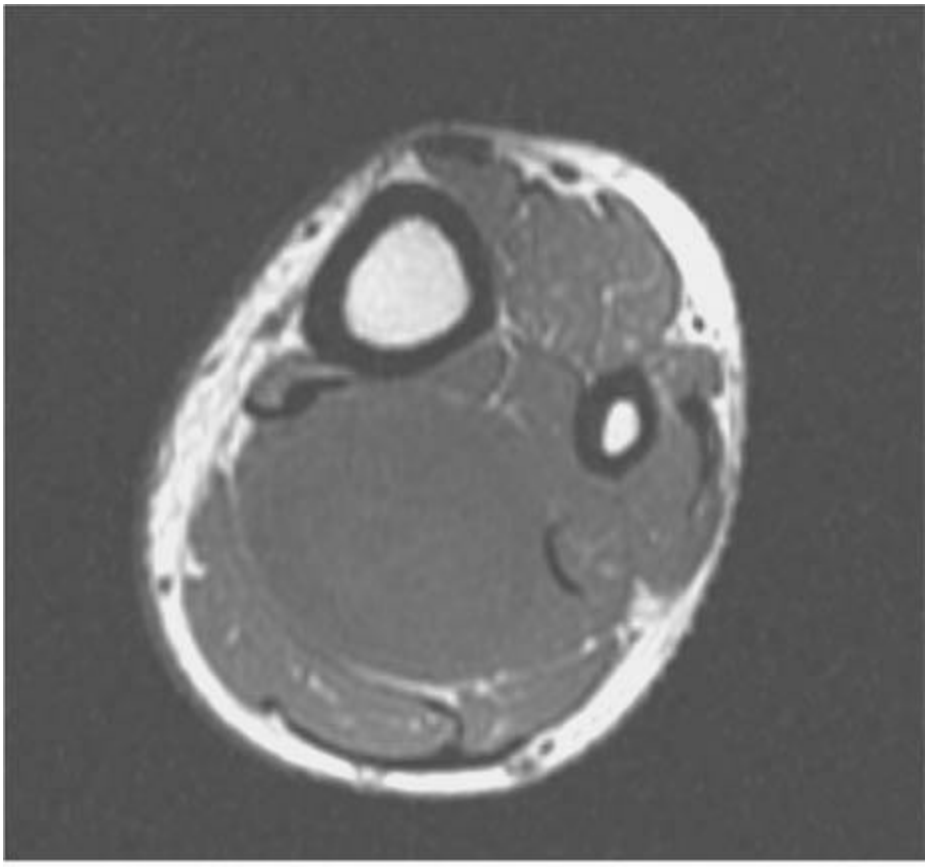

B

■**FIGURE 5-28B** Axial T1-weighted Image at the same location as in (A) demonstrates the mass to be homogeneously hypoin-tense. The mass arises in an intermuscular location between the soleus and gastrocnemius musculature.

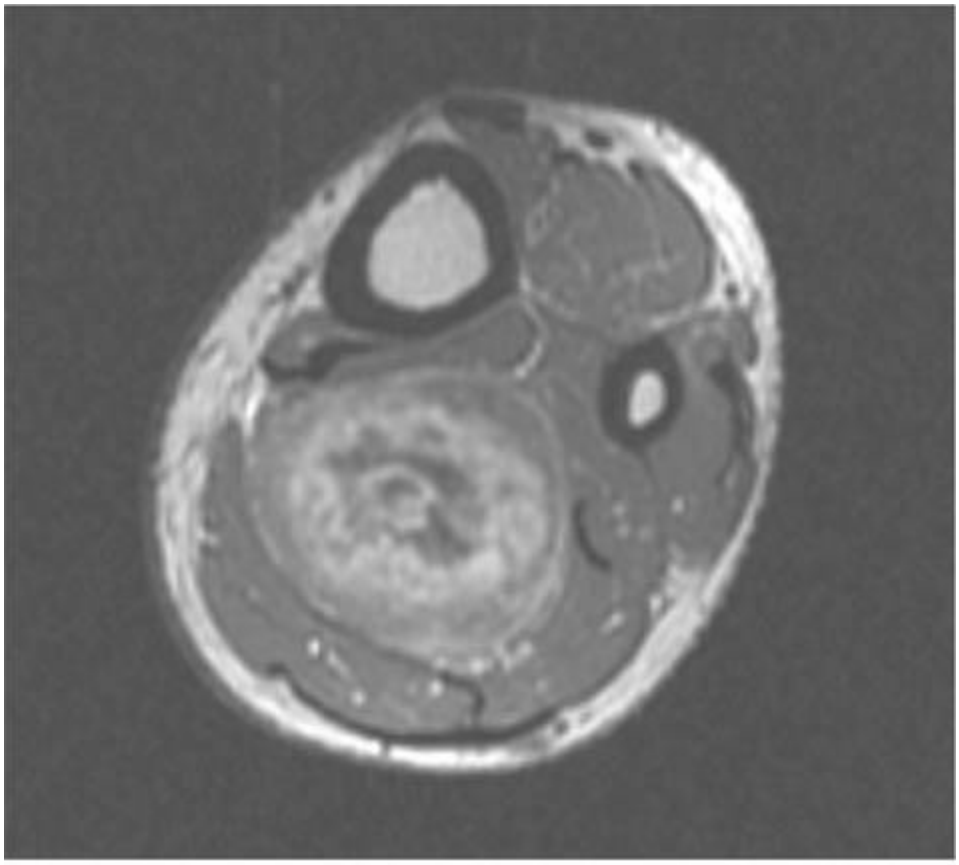

C

■**FIGURE 5-28C** Axial T1-weighted image after the intravenous administration of gadolinium demonstrates heterogeneous enhancement of this mass with areas of relative hypoenhancement centrally.

D

**FIGURE 5-28D** Sagittal fat-suppressed T2-weighted image demonstrates the fusiform shape of this mass. A peripheral nerve is seen leading into the superior aspect of the mass and away from the inferior aspect of the mass.

## DIFFERENTIAL DIAGNOSIS

**Peripheral nerve sheath tumor:** The mass is well defined and demonstrates hyperintensity on T2-weighted images with heterogeneous hypointensity centrally, referred to as the "target sign." The mass is fusiform in shape and is located between muscle layers. A peripheral nerve is seen leading into and away from this mass. These are all features that are typical of benign peripheral nerve sheath tumors.

**Hematoma:** While hematomas can mimic other soft tissue masses, the relatively diffuse enhancement as well as the shape and location of this mass exclude this possibility. In this particular case, the history would also exclude this diagnosis.

**Soft tissue sarcoma:** While this diagnosis cannot be entirely excluded, it is unlikely in this case given the constellation of imaging findings described above that are characteristic of a nerve sheath tumor. There are many cases of enhancing soft tissue masses that cannot be reliably characterized as benign lesions. In these cases, soft tissue sarcomas would need to be included in the differential diagnosis. This patient was

referred to an orthopaedic oncologic surgeon who performed a core needle biopsy to confirm the diagnosis of a benign schwannoma.

## DIAGNOSIS

**Peripheral nerve sheath tumor, in this case a schwannoma**

## KEY FACTS

### Clinical

- Benign peripheral nerve sheath tumors are characterized as schwannomas and neurofibromas, both of which arise from the Schwann cell within peripheral nerves.
- Schwannomas are distinguished from neurofibromas histologically by alternating Antoni A and B regions and the presence of large quantities of S-100 protein by immunohistochemical analysis.
- Benign peripheral nerve sheath tumors usually present as painless, slow growing masses.
- Neurofibromas most frequently affect patients between the ages of 20 and 30.
- Most neurofibromas are solitary. Only 10% of neurofibromas occur in patients with neurofibromatosis type 1 (NF-1). Multiple neurofibromas can be seen in patients with NF-1.
- Peripheral neurofibromas typically arise from small peripheral nerves in the skin and subcutaneous tissues although they can also arise from deeper peripheral nerves.
- Neurofibromas may be localized, diffuse, or plexiform. Plexiform neurofibromas involve a long nerve segment and its branches and are pathognomonic for NF-1.
- Schwannomas are slightly less common than neurofi-bromas and occur most frequently in patients between 20 and 50 years of age.
- Most schwannomas are solitary and are not associated with NF-1.
- Schwannomas most commonly occur in the head and neck and along major nerve trunks.
- Treatment of benign peripheral nerve sheath tumors is usually surgical resection. Schwannomas are generally separable from the nerve after incising the epineurium, allowing nerve function to be spared. Neurofibro-mas are usually inseparable from the nerve, meaning tumors arising from deep nerves are often partially resected or debulked to preserve nerve function.
- Malignant nerve sheath tumors account for 5% to 10% of all soft tissue sarcomas. While 25% to 75% of malignant tumors arise in patients with NF-1, only 5% to 13% of

patients with NF-1 develop malignant peripheral nerve sheath tumors.

- Malignant tumors usually present as rapidly enlarging, painful masses.

## Radiologic

- Schwannomas and neurofibromas are indistinguishable by imaging.
- Deep peripheral nerve sheath tumors grow in fusiform fashion along the long axis of the nerve. The fusiform shape is the most reliable indicator of a peripheral nerve sheath tumor.
- These masses classically taper at either end and the nerve from which the tumor arises may be seen to enter and exit the mass.
- Nerve sheath tumors demonstrate nonspecific hypoin-tense signal intensity on T1-weighted images and hyperintense signal intensity on T2-weighted images, and usually demonstrate heterogeneous enhancement after the intravenous administration of gadolinium.
- The mass may demonstrate a central region of lower signal intensity on T2-weighted images known as the "target sign." This results from greater fluid content within myxoid tissue at the periphery of the mass. The central hypointense component corresponds to collag-enous or fibrous tissue.
- The "fascicular sign" may be seen on T2-weighted imaging as multiple small circular structures within the mass with surrounding hyperintensity. This is attributed to nerve fascicles within the mass.
- The "split fat sign" is a rim of hyperintense tissue on T1-weighted images surrounding the tumor. This is seen when a nerve sheath tumor arises in an intermuscular location and is surrounded by intermuscular fat.
- Muscle atrophy is a variable finding that may be seen in a muscle supplied by the affected nerve.
- Schwannomas are more likely to be located eccentrically along the course of a nerve while neurofibromas are more likely to be situated centrally.
- Schwannomas are more likely to demonstrate cystic components than neurofibromas.
- Malignant peripheral nerve sheath tumors may appear similar to benign peripheral nerve sheath tumors by imaging. Imaging findings that may suggest malignancy include large size (>5 cm) and poorly defined margins with infiltration of surrounding structures.

# SUGGESTED READING

Furniss D, Swan MC, Morritt DG, et al. A 10-year review of benign and malignant peripheral nerve sheath tumors in a single center: clinical and radiographic features can help to differentiate benign from malignant lesions. Plast Reconstr Surg 2008;121:529–533.

Lin J, Martel W. Cross-sectional imaging of peripheral nerve sheath tumors: characteristic signs on CT, MR imaging, and sonography. Am J Roentgenol 2001;176:75–82.

Murphey MD, Smith WS, Smith SE, et al. From the archives of the AFIP. Imaging of musculoskeletal neurogenic tumors: radiologic-pathologic correlation. Radiographics 1999;19:1253–1280.

Pilavaki M, Chourmouzi D, Kiziridou A, et al. Imaging of peripheral nerve sheath tumors with pathologic correlation: pictorial review. Eur J Radiol 2004;52:229–239.

# CASE 29

**DAVID K. KRUG**

## HISTORY

A 16-year-old female who injured her knee while playing softball.

A

■**FIGURE 5-29A** Sagittal fat suppressed FSE T2-weighted MRI of the knee. High signal intensity in the lateral femoral condyle consistent with bone contusion.

B

■**FIGURE 5-29B** Sagittal fat suppressed FSE T2-weighted MRI of the knee. High signal intensity in the inferomedial patella consistent with bone contusion. Joint effusion with fluid-fluid level consistent with hemarthrosis. Osteochondral fragment is seen in the anterior intercondylar notch.

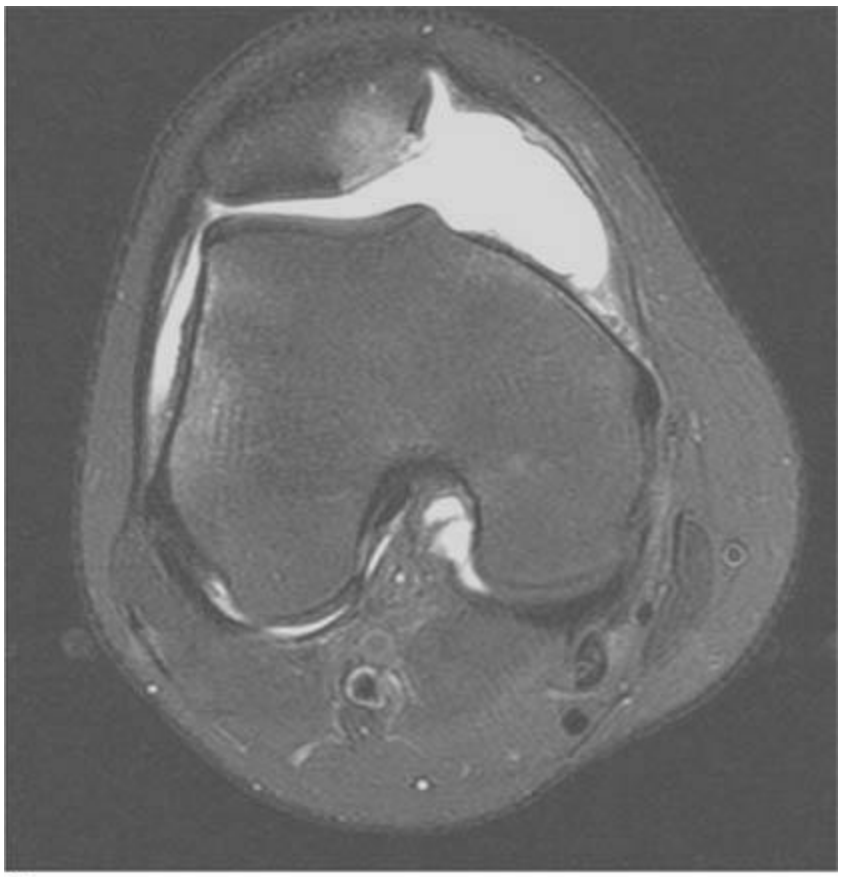

C

**FIGURE 5-29C** Axial fat suppressed FSE T2-weighted MRI of the knee. High signal intensity in the inferomedial patella and anterolat-eral aspect of the lateral femoral condyle consistent with "kissing" bone contusions. There is associated chondral injury of the medial patellar facet.

## DIFFERENTIAL DIAGNOSIS

- **Transient patellar dislocation (TPD):** This diagnosis is favored given the constellation of findings including bone contusions of the anterolateral lateral femoral condyle and inferomedial patella, medial patellar chon-dral injury, loose body and hemarthrosis.
- **Acute tear of the anterior cruciate ligament (ACL):** Contusions in the lateral femoral condyle are often seen with acute ACL tears. The classic pivot shift contusion in acute ACL injury involves the lateral femoral condyle and posterior lateral tibial plateau. Contusion of the medial patella is not associated with this injury.
- **Direct trauma:** Direct blow to the lateral knee, such as seen in clipping injury in football players, can result in bone contusions about the knee most commonly in the lateral femoral condyle. This diagnosis would not account for the patellar contusion or osteochondral defect, and is therefore not the best diagnosis.

# DIAGNOSIS

**Transient patellar dislocation**

# KEY FACTS

## Clinical

- Classic mechanism of TPD is internal rotation of the femur on a fixed tibia while the knee is flexed. Contraction of the quadriceps results in net lateral force on the patella and dislocation. Direct blow to the medial knee may also result in lateral patellar dislocation.
- Comprises 9% to 16% of all acute knee trauma in young athletes with hemarthrosis. Dislocation is usually transient with spontaneous relocation, and most patients do not realize this type of injury has occurred.
- It is estimated that 50% to 75% of all patellar dislocations are incorrectly diagnosed at initial clinical evaluation. MRI can accurately diagnose suspected or occult patellar dislocation, and is useful for evaluation of the extent of associated soft tissue injuries and intra-articular abnormalities.
- Surgical management may be indicated for significant osteochondral defects, loose bodies, or associated meniscal or ligamentous injuries.

## Radiologic

- Mechanism of injury results in a characteristic pattern of bone marrow contusions involving the lateral femoral condyle, which is seen in up to 100% of patients on MRI, and the inferomedial patella.
- Injury to the medial retinacular complex is invariably present, and is commonly seen on MRI.
- Joint effusion or hemarthrosis is almost always present in the acute setting, and is often large.
- Close evaluation of the cartilage is extremely important, as chondral injuries of the patellofemoral joint and of the anterior aspect of the lateral femoral condyle are common in these patients, and in some cases indicate surgical management. Osteochondral loose bodies are seen in up to one third of patients.
- Other MRI findings may include lateral patellar tilt or subluxation, injury to Hoffa's infrapatellar fat pad, and shallow femoral trochlea.

## SUGGESTED READING

Elias DA, White LM, Fithian DC. Acute lateral patellar dislocation at MR imaging: Injury patterns of medial patellar soft-tissue restraints and osteochondral injuries of the inferomedial patella. Radiology 2002;225:736–743.

Kirsch MD, Fitzgerald MD, Friedman H, Rogers LF. Transient lateral patellar dislocation: Diagnosis with MR imaging. Am J Roentgenol 1993;161:109–113.

Pope TL Jr. MR imaging of patellar dislocation and relocation. Semin Ultrasound CT MR 2001;22:371–382.

Rogers LF. Radiology of Skeletal Trauma (3rd ed). Philadelphia, PA: Churchill Livingstone, 2002;1169–1173.

Spritzer CE, Courneya DL, Burk DL, et al. Medial retinacular complex injury in acute patellar dislocation: MR findings and surgical implications. Am J Roentgenol 1997;168:117–122.

Virolainen H, Visuri T, Kuusela T. Acute dislocation of the patella: MR findings. Radiology 1993;1989:243–246.

# CASE 30

### KAVITA M. PATEL

### HISTORY

A 19-year-old female college student with 4 months of wrist pain.

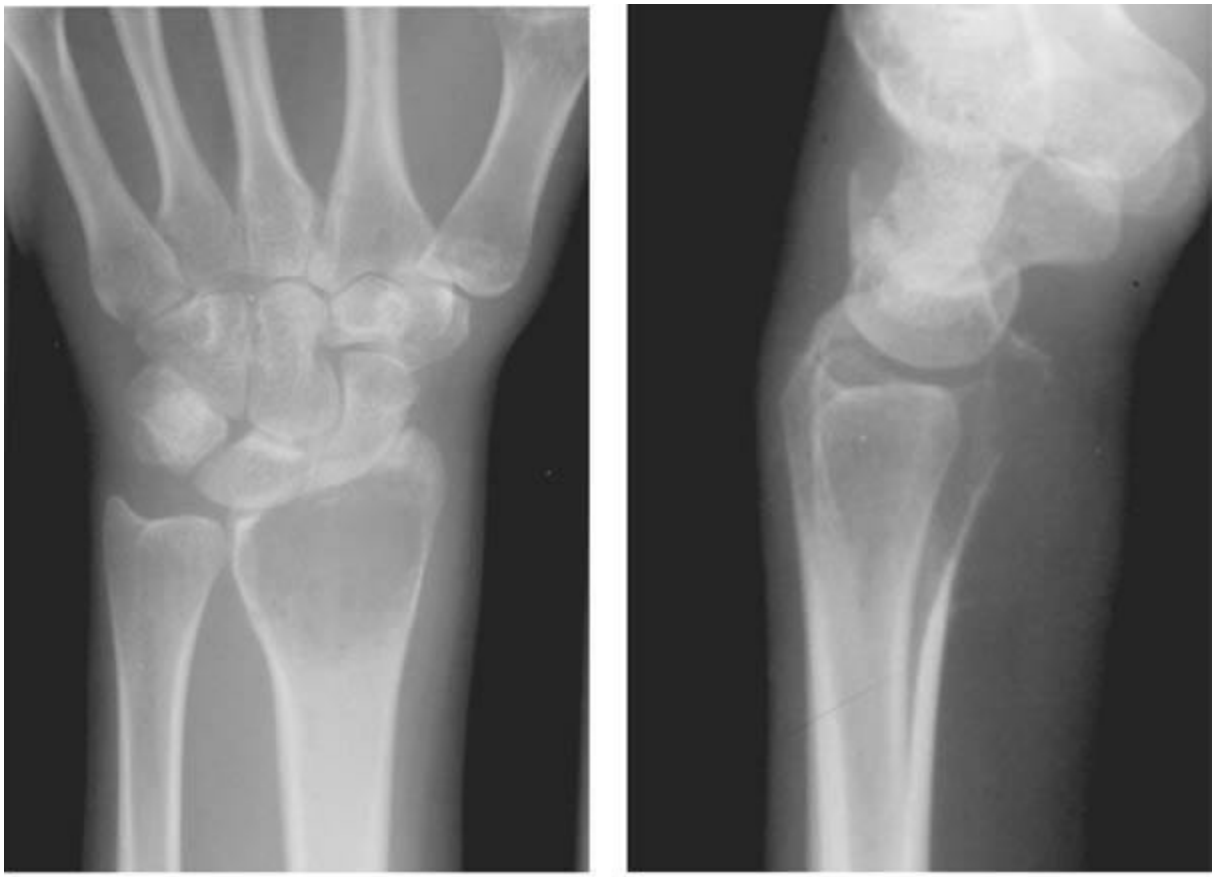

A B

■**FIGURES 5-30A and 5-30B** AP **(A)** and lateral **(B)** radiographs demonstrate a large, somewhat expansile lucent lesion centered in the distal radial epiphysis, with a narrow zone of transition, which extends to the distal radius subchondral bone. The lesion does not have a sclerotic margin and there is no evidence of internal matrix.

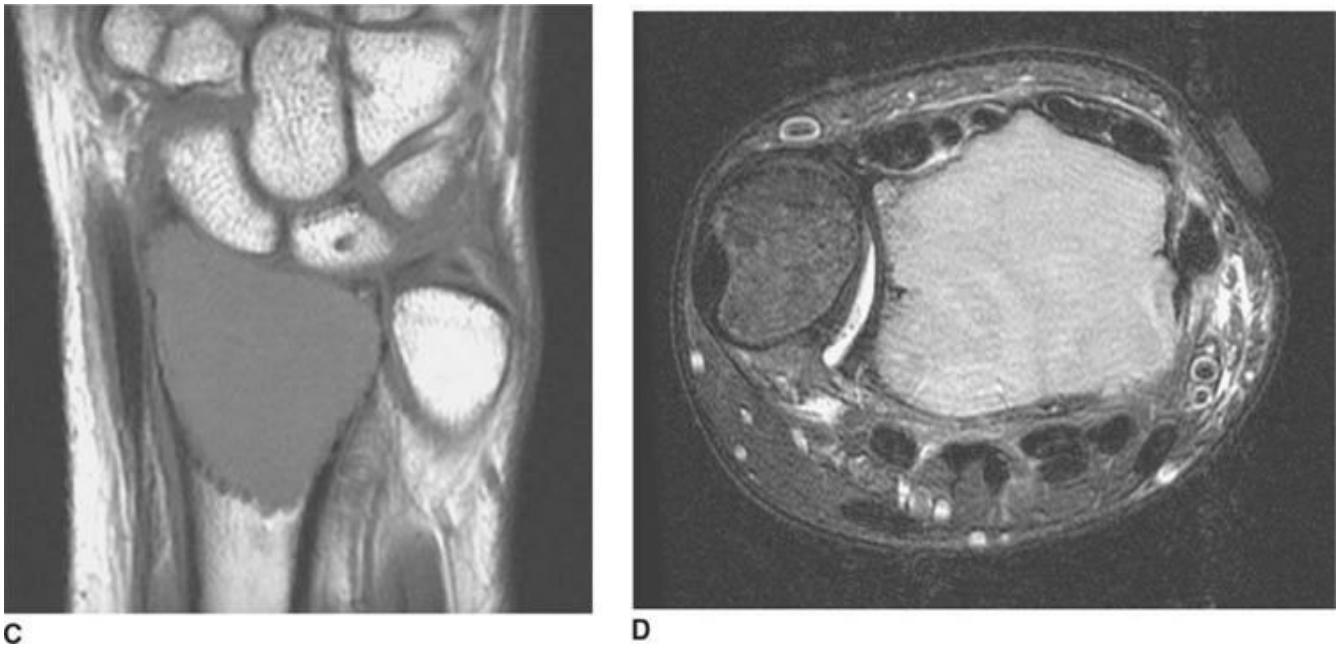

C D

**FIGURES 5-30C and 5-30D** Coronal Tl-weighted **(C)** and axial fat-suppressed FSE T2-weighted **(D)** images demonstrate a solid lesion of decreased signal intensity on the Tl-weighted image and increased signal intensity on the T2-weighted image, which is a nonspecific appearance. The axial image demonstrates the expansile nature of the mass along the volar aspect of the radius.

## DIFFERENTIAL DIAGNOSIS

**Giant cell tumor (GCT) of bone:** This is the best diagnosis given the location of the lytic lesion in the meta-epiphysis of a long bone, extending into the subchondral bone. The lesion meets the criteria for a GCT of a long bone, given lack of sclerotic margin, lack of internal matrix, and occurring in a patient with closed physes.

**Aneurysmal Bone Cyst (ABC):** This is a possible diagnosis as ABCs can occur in the epiphysis of long bones (though they do not have to), and the lesion in this case is mildly expansile and occurring in a patient <30 years old, which are features typical of ABCs. However, ABCs usually have fluid-fluid levels demonstrated on MR imaging, which is not seen in this case.

**Intra-osseous ganglion or large subchondral cyst:** On plain x-ray, intra-osseous ganglion is a well-circumscribed lucent lesion with a sclerotic rim, most frequently seen in the medial malleolus of the tibia, carpal bones, femoral head or acetabulum. It is thought to be due to osseous penetration of a soft tissue ganglion or perhaps proliferation of synovial rests. These lesions are usually not painful, unless associated with inflammatory or degenerative arthritis, which is not evident in this case. Also, these lesions are usually cystic, rather than solid, on MRI.

**Chondroblastoma:** Chondroblastoma is an epiphyseal lytic lesion with a narrow zone of transition usually seen in skeletally immature individuals. Chondroblastoma typically demonstrates a peripheral rim of sclerosis and can contain chondroid matrix. Chondroblastoma often elicits thick metaphyseal periostitis, remote from the epiphyseal location of the lesion, which is not seen in this case.

**Metastasis/Myeloma:** Metastatic or myelomatous lesions are the most common cause for a lytic lesion in individuals over 50, and these lesions can occur in the epiphysis. The patient's young age in this case makes this a very unlikely diagnosis.

## DIAGNOSIS

**Giant cell tumor (GCT) of bone**

## KEY FACTS

## Clinical

- GCT of bone is a relatively common benign bone neoplasm which almost always occurs in skeletally mature patients, most commonly presenting in the third or fourth decade. Patients usually present with pain. Sometimes localized swelling, decreased range of motion or a pathologic fracture is present.
- Women are affected slightly more commonly than men, although malignant GCT is more common in men (3:1).
- Approximately 10% of GCTs are "malignant." Determination of malignancy is made either by histology or by the presence of pulmonary metastases, as even benign GCTs may demonstrate "aggressive" features (such as cortical disruption and soft tissue mass) at imaging. A rare subtype, "benign metastasizing GCT," presents with pulmonary metastases that are histologically identical to benign GCT. The majority of malignant GCTs are due to irradiation of a previously documented GCT.
- Multifocal GCTs of bone are rare. There is a rare, possibly familial, association of multiple GCTs with Paget's disease.
- Definitive treatment consists of intralesional surgical resection. Marginal resections are associated with a higher recurrence rate (40% to 60%) than newer techniques utilizing extended surgical margins and bone grafting or methylmethacrylate packing of the defect (<25% recurrence rate).

## Radiologic

- The characteristic radiographic appearance of GCT of bone is an eccentric lytic lesion in the meta-epiphysis of a long bone, although large lesions often appear more central. The lesion extends into the subchondral bone, causing the appearance of extension to the articular surface. There is usually a narrow zone of transition, and surrounding sclerosis is extremely rare. As these tumors occur in skeletally mature patients, the physes are closed. CT improves detection of cortical penetration, which is seen in up to one half of cases, and subtle pathologic fractures. MRI improves detection and delineation of any associated soft tissue mass.
- The most common sites for these tumors are the long tubular bones about the knee (50% to 65%), distal radius (10%), sacrum, and proximal humerus. GCTs occurring in flat bones (such as the pelvis), the calca-neus, apophyses, and other growth centers, such as the patella, do not always follow the same rules as those in long bones do; that is, the classic imaging findings of long bone metaepiphyseal GCTs are not always present.
- MRI of GCT demonstrates a well-defined solid lesion, often with cystic components, with a variably present low-intensity peripheral pseudo-capsule. Solid components are typically low to intermediate intensity on T1 and T2-weighted images. MRI best

demonstrates soft tissue extension and solid elements, with secondary aneurysmal components manifested by fluid-fluid levels. Secondary ABC components occur in approximately 14% of these lesions.

- Biopsy of suspected GCT should be directed toward the solid components and away from the cystic components. Contrast enhanced MRI aids in differentiation of solid from cystic components, with solid components enhancing diffusely and cystic components demonstrating a thin peripheral rim of enhancement.
- Patients undergo routine clinical and radiographic surveillance following resection of GCT due to the risk of recurrence. Bony recurrence presents radiographically as increasing areas of osteolysis about the surgical site. Soft tissue recurrence presents as increasing/new soft tissue calcifications or an enlarging soft tissue mass with a shell of peripheral calcification.

## SUGGESTED READING

Helms CA. Fundamentals of Skeletal Radiology (3rd ed). Philadelphia, PA: Elsevier Saunders, 2005:13–15.

Murphey MD, Nomikos GC, Flemming DJ, et al. From the archives of the AFIP. Imaging of giant cell tumor and giant cell reparative granuloma of bone: radiologic-pathologic correlation. Radiographics 2001;21:1283–1309.

Resnick D, Kransdorf MJ. Imaging of Bone and Joint Disorders (3rd ed). Philadelphia, PA: Elsevier, 2005:1164–1167.

# Chapter SIX

# Neuroradiology

JAMES M. PROVENZALE ▪ CHAPTER EDITOR

Fernando M. Zalduondo

E. Ralph Heinz

David S. Enterline

Joseph B. Cornett

Charles B. Donovan

Robert Tien

# CASE 1

**JAMES M. PROVENZALE**

**HISTORY**

A 21-year-old man with a sudden onset of the worst headache of his life.

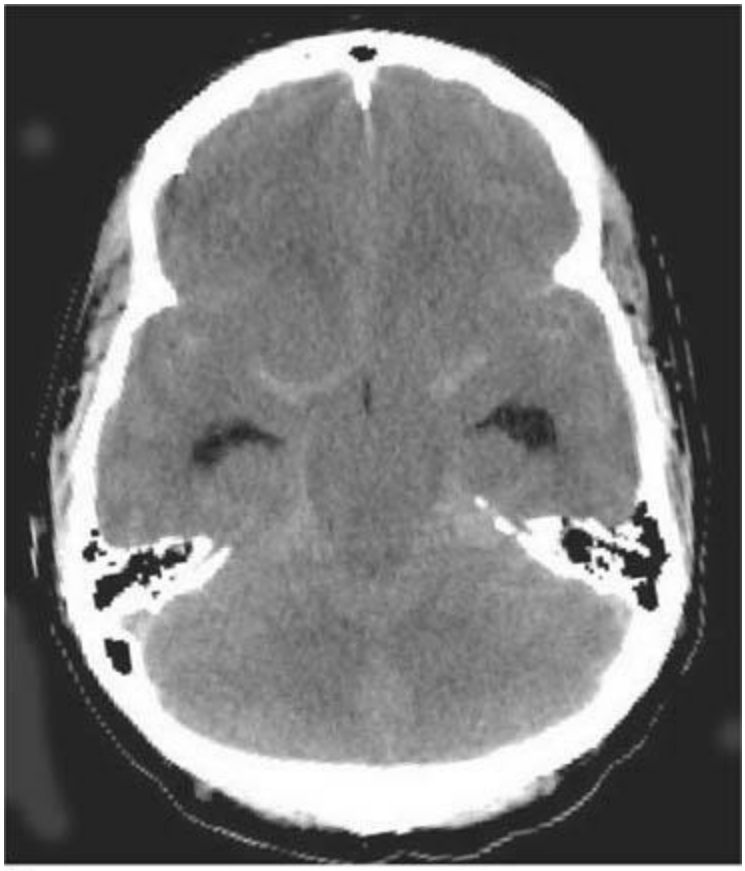

A

■**FIGURE 6-1A** Unenhanced axial CT image shows marked narrowing of the basal cisterns, hydrocephalus, and a hyperdense appearance of the subarachnoid space.

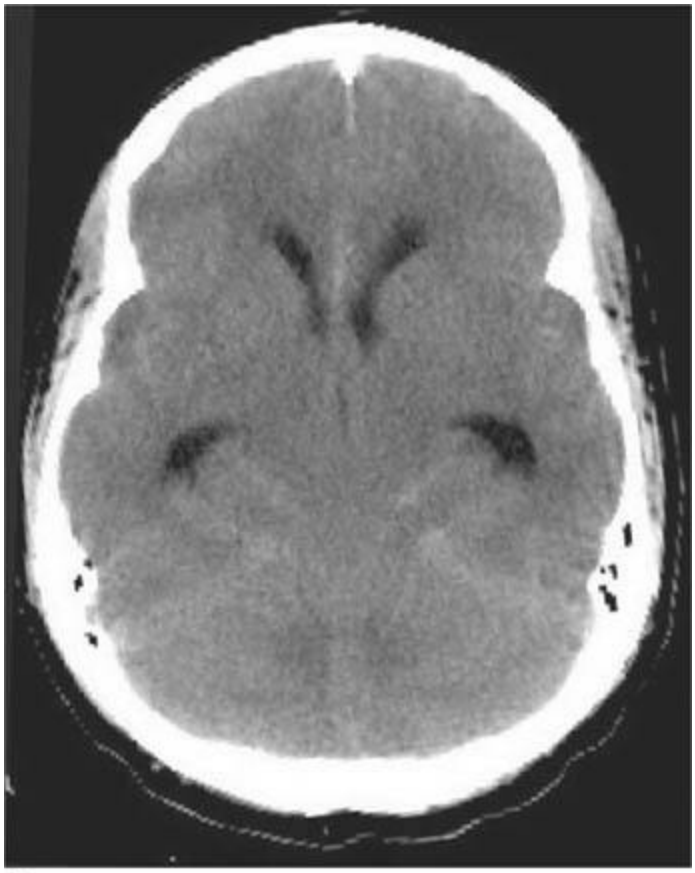

B

■**FIGURE 6-1B** Unenhanced axial CT image in the same patient as Figure 6-1A shows a rounded density in the cephalad portion of the third ventricle bordering the posteromedial aspect of the frontal horns of the lateral ventricles that is isodense with brain tissue. Figures 6-2A and 6-2B are from a different patient with the same diagnosis.

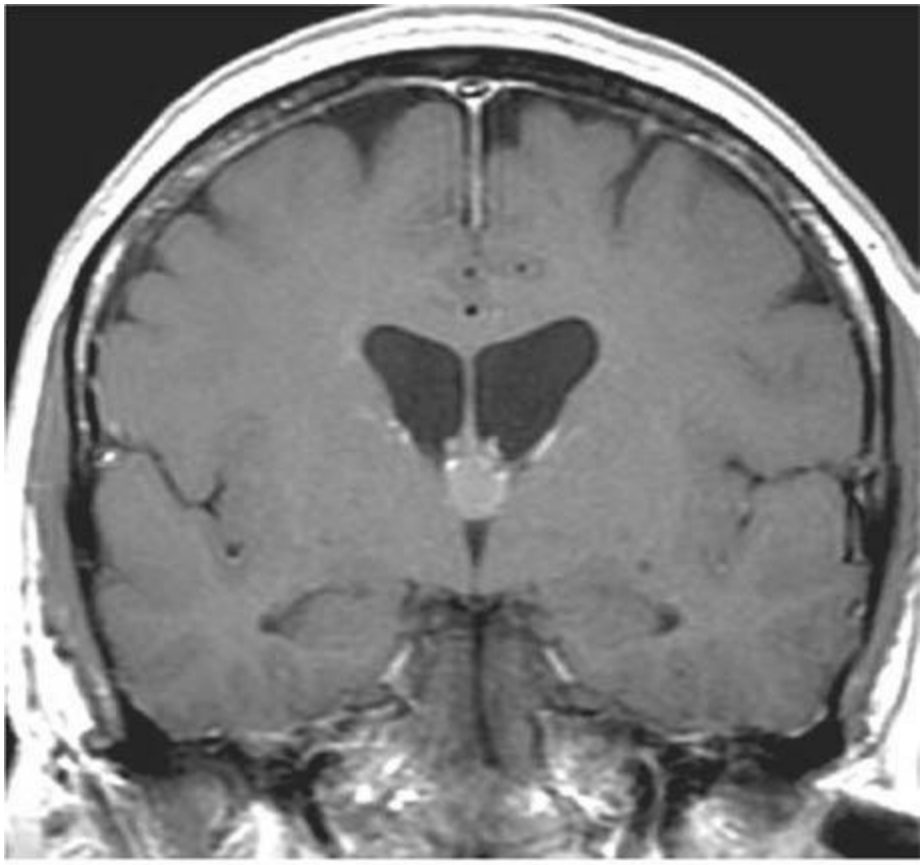

C

■**FIGURE 6-1C** Contrast-enhanced coronal T1-weighted image shows a rounded mass that abuts the fornix and is hyperintense relative to CSF. When compared to unenhanced T1-weighted images (not shown), the lesion did not contrast-enhance.

D

**FIGURE 6-1D** Sagittal T2-weighted image shows an oval mass in the roof of the third ventricle that is relatively isointense to gray matter. The mass is located just cephalad and anterior to the (darker) massa intermedia located in the center of the third ventricle.

## DIFFERENTIAL DIAGNOSIS

**Ruptured cerebral aneurysm:** This diagnosis might be considered because of the oval lesion associated with hyperdensity of the subarachnoid spaces (Figures 6-1A and 6-1B), suggesting subarachnoid hemorrhage (SAH). However, Figures 6-2A and 6-2B are not typical for an aneurysm because the lesion lacks the typical appearance of a "flow void" and has a very unusual location for an aneurysm. In fact, the patient shown in Figure 6-1 does not have SAH but instead has compression of small vessels in the subarachnoid space (due to raised intra-cranial pressure associated with the hydrocephalus) mimicking SAH, a phenomenon termed "pseudo-SAH."

**Arachnoid cyst:** This diagnosis might be considered because the lesions shown are oval extraaxial lesions. However, arachnoid cysts are isodense with cerebro-spinal fluid (CSF) on CT and isointense with CSF on MRI, unlike the lesions shown, making this an incorrect diagnosis.

**Neurocysticercosis:** Neurocysticercosis lesions can occur within brain ventricles and

may present as a solitary lesion. However, such lesions typically have a region that is similar in appearance to CSF, not seen in this case. Nonetheless, cysticercosis remains as a diagnostic consideration.

- **Dermoid cyst:** This diagnosis might be considered because the lesions shown are located in the midline, typical of dermoid tumors. However, dermoid cysts are typically hypodense on CT relative to CSF due to their fat content, making this an unlikely diagnosis.
- **Colloid cyst:** This lesion is commonly slightly isodense or hyperdense on unenhanced CT, hyperintense to CSF on unenhanced T1-weighted MR images, and hypoin-tense on T2-weighted images. In addition, it causes obstructive hydrocephalus (as shown in this case) that may be intermittent. This diagnosis is a likely one.

## DIAGNOSIS

**Colloid cyst**

## KEY FACTS

### Clinical

- A number of entities must be considered when a patient presents with the complaint of "worst headache of my life." The differential diagnosis includes aneurysm, arterial dissection, dural sinus thrombosis (DST), spontaneous intracranial hypertension, intracranial hemorrhage, pituitary apoplexy, and colloid cyst of the third ventricle.
- Colloid cysts are benign masses that account for <1% of intracranial neoplasms.
- Colloid cysts are almost always located in the anterosu-perior portion of the third ventricle. Rarely, they can be found in other locations, such as the lateral ventricle, fourth ventricle, and brainstem.
- These lesions are usually discovered in adolescence or young adulthood. The typical presentation is that of severe headaches of short duration. The headache, which is due to intermittent obstructive hydrocephalus at the level of the foramina of Monro, is often positional (e.g., worsened by leaning forward) and can be relieved by lying down (which is unusual for headache due to intracranial tumors).
- Performance of lumbar puncture in the setting of the acute hydrocephalus caused by a colloid cyst is contra-indicated because of the possibility of cerebellar tonsil-lar herniation.
- These lesions are thin-walled, well-circumscribed, round structures with various degrees of attachment to the roof of the third ventricle.
- The exact cells of origin of colloid cysts are not well established. Some authors have

suggested that colloid cysts are derived from neuroepithelium (which is the category of cells from which ependyma and cho-roid plexus develop). According to this way of thinking, the lesions are derived from the paraphysis, a stalked protuberance of extraventricular choroid plexus that is derived from the neuroepithelial lining of the roof of the diencephalon. However, other authors have found structural elements very similar to respiratory epithelium, suggesting an endodermal (rather than a neuro-epithelial) origin.

- Contents of colloid cysts include mucinous substances (including secretory products, such as fat and cholesterol crystals), hemorrhagic products, and variable types of ions, such as calcium, magnesium, and sodium.
- Currently, microsurgical techniques and endoscopic surgery are preferred by many surgeons for treatment of these lesions, rather than conventional craniotomy.

## Radiologic

- On CT, colloid cysts are typically homogeneous and hyperdense relative to CSF due to their mucinous contents. Following administration of contrast material, a small amount of enhancement of the cyst capsule can occasionally be present. However, dense enhancement is not a feature of these lesions.
- Lesions can be difficult to identify on either CT or MR when the cyst is very small or when the cyst contents are not conspicuous against the background appearance of adjacent CSF.
- Variable degrees of obstructive hydrocephalus can be seen. Because the lesion is located in the anterior portion of the third ventricle, only the lateral ventricles would be expected to be enlarged.
- Calcification is rare and considered a finding that makes the diagnosis of colloid cyst less likely.
- MRI can be used for localizing the lesion to the anterior third ventricle rather than adjacent sites such as the hypothalamus, optic tract, or suprasellar cistern.
- On MRI, the cyst will almost always be seen to differ in signal intensity from CSF on one or more pulse sequences. The cysts are often hyperintense relative to CSF on T1-weighted sequences due to the mucinous contents and, possibly, presence of cholesterol crystals.
- Often, colloid cysts are hypointense to CSF on T2-weighted images, which some authors have considered to be due to paramagnetic properties of ions contained within the cyst fluid. Such lesions are difficult to identify on fluid attenuated inversion recovery (FLAIR) images against the background of hypointense CSF.
- Because in some cases colloid cysts are relatively isointense with CSF on all MR pulse sequences, the lesions occasionally are more evident on CT than on MR imaging.

- Occasionally, CSF flow artifacts in the anterior third ventricle can simulate the appearance of a colloid cyst. Careful evaluation of this region on all pulse sequences can help one avoid this pitfall.

## SUGGESTED READING

Given CA, II, Burdette JH, Elster AD, Williams DW, III. Pseudo-subarach-noid hemorrhage: a potential imaging pitfall associated with diffuse cerebral edema. AJNR Am J Neuroradiol 2003;24:254–256.

Cakirer S, Karaarslan E, Arslan A. Spontaneously T1-hyperintense lesions of the brain on MRI: a pictorial review. Curr Probl Diagn Radiol 2003;32:194–217.

Grondin RT, Hader W, MacRae ME, Hamilton MG. Endoscopic versus microsurgical resection of third ventricle colloid cysts. Can J Neurol Sci 2007;34:197–207.

Spears RC. Colloid cyst headache. Curr Pain Headache Rep 2004;8: 297–300.

Armao D, Castillo M, Chen H, Kwock, L. Colloid cyst of the third ventricle: Imaging-pathologic correlation. AJNR Am J Neuroradiol 2000;21:1470–1477.

Osborn AG, Preece MT. Intracranial cysts: radiologic-pathologic correlation and imaging approach. Radiology 2006;239:650–664.

Gupta A, Nadimpalli SP, Cavallino RP. Intraventricular neurocysticercosis mimicking colloid cyst. J Neurosurg 2002;97:208–210.

# CASE 2

**JAMES M. PROVENZALE AND FERNANDO M. ZALDUONDO**

### HISTORY

A 26-year-old woman with acquired immunodeficiency syndrome (AIDS), headache, and confusion.

A

■**FIGURE 6-2A** Axial contrast-enhanced CT image shows an unenhancing hypodense lesion in the white matter of the posterior right temporal and occipital lobes.

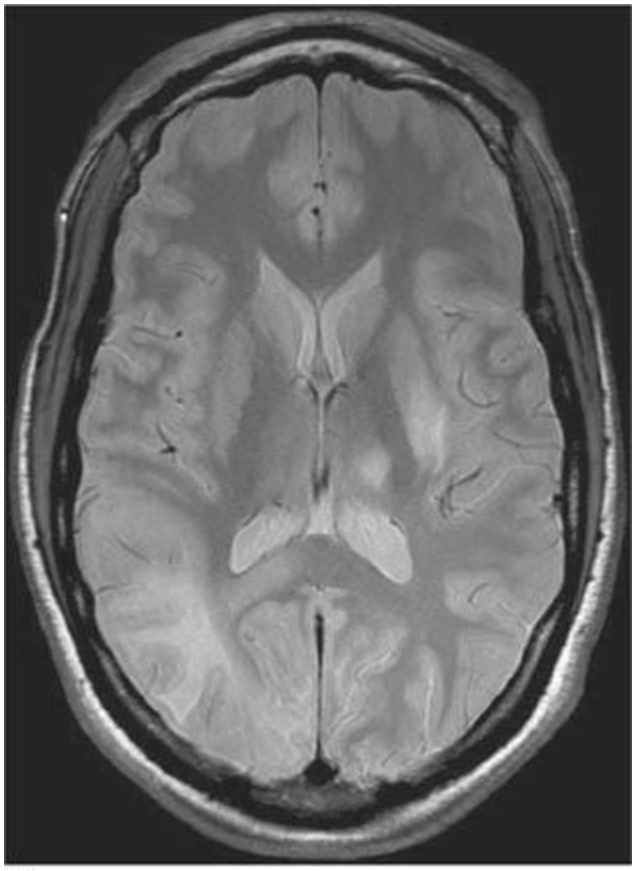

B

■**FIGURE 6-2B** Axial proton density-weighted MR image shows the right hemisphere lesion is hyperintense on this pulse sequence. Additional abnormalities are present in the left thalamus, basal ganglia and external capsule. No mass effect is present.

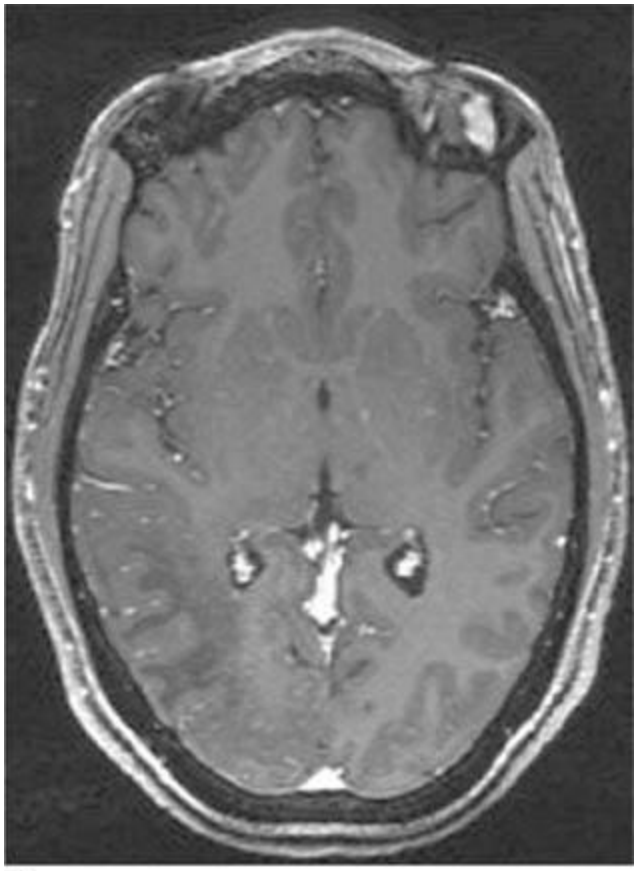

C

■**FIGURE 6-2C** Axial contrast-enhanced T1-weighted image shows the right hemisphere lesion is hypointense and does not contrast-enhance. The left basal ganglia lesion minimally contrast-enhances and the left thalamic lesion does not contrast-enhance.

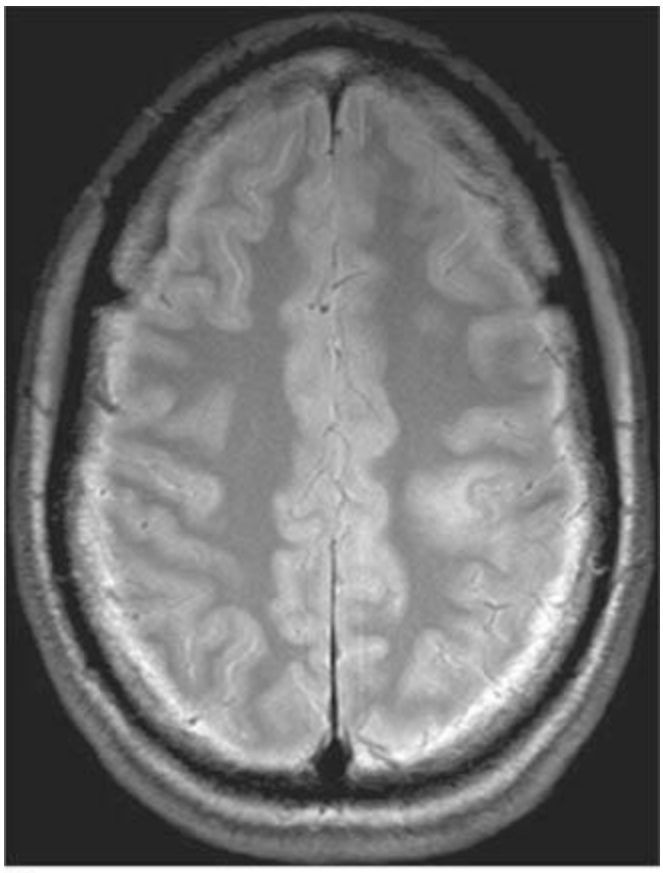

D

**FIGURE 6-2D** Axial proton density-weighted MR image shows a hyperintense lesion in the posterior left frontal lobe. On contrast-enhanced imaging (not shown), the lesion did not contrast-enhance.

## DIFFERENTIAL DIAGNOSIS

**Toxoplasmosis:** This diagnosis might be considered because it is common in AIDS patients. Although lesions can occur anywhere in the brain, a more central location (in the periventricular regions) is typical. Furthermore, lesions generally contrast-enhance and have edema and mass effect, making this an unlikely diagnosis.

**Lymphoma:** Primary B cell central nervous system (CNS) lymphoma is also relatively common in AIDS patients. However, in the immunocompromised patient, ring-enhancement is typical and frequently accompanied by edema and mass effect. These features make lymphoma an unlikely diagnosis.

**Cryptococcosis:** Cryptococcal infection is common in AIDS patients and can have a number of radiologic appearances: meningeal enhancement (due to meningitis), nonenhancing (or rim-enhancing) masses typically occurring in the basal ganglia (so-called gelatinous pseudocysts), ring-enhancing parenchymal masses (cryptococcomas), and intraventricular masses. Unen-hancing lesions lacking mass effect would be

distinctly unusual.

- **Infarction:** Infarcts commonly occur in the periphery of the brain, usually in the setting of embolic infarction. However, the extent of these lesions—that is, abrupt termination at the gray-white junction with sparing of the cortex (as opposed to involvement of both gray matter and white matter)—would be very unusual for infarction. This is an unlikely diagnosis.
- **Progressive multifocal leukoencephalopathy (PML):** The typical appearance of PML is that of one or more nonenhancing white matter lesions lacking mass effect in an immunocompromised host. This is the correct diagnosis.

## DIAGNOSIS

**Progressive multifocal leukoencephalopathy**

## KEY FACTS

### Clinical

- PML is due to an infection caused by the human papo-vavirus (also known as the JC virus, the initials of the patient in whom it was first described). Asymptomatic infection likely occurs early in life in many individuals but remains latent until reactivated by acquisition of an immunodeficient state.
- The JC virus can be detected by polymerase chain reaction testing of the CSF.
- This infection occurs primarily in immunocompromised patients. It occurs in 1% to 4% of adult AIDS patients but is extremely rare in children. Organ transplant recipients are another non-AIDS group at increased risk of acquiring the infection.
- Symptoms include visual deficits and cranial nerve palsy, focal neurologic deficits such as motor weakness and sensory loss, and nonfocal neurologic symptoms—for example, encephalopathy or headache.
- Prognosis is generally very poor with a mean survival of only a few months after diagnosis. However, recently, administration of highly active antiretroviral therapy has shown some promise of relatively longer survival in AIDS-related PML.

### Radiologic

- On CT, lesions are typically seen as unenhancing, hypodense white matter lesions lacking mass effect. MRI is superior to CT in displaying the number and size of lesions.
- On T2-weighted and FLAIR images, lesions are hyper-intense; they are hypointense on T1-weighted images. With disease progression, lesions become more hypoin-tense on

T1-weighted images: particularly, aggressive infection may be indicated by markedly low signal intensity.

- Lesions are frequently bilateral but distributed in an asymmetric manner between the hemispheres. The posterior centrum semiovale is the most common location.
- White matter lesions in PML have been reported to start subcortically before extending into the deep white matter; this feature is considered by some as a feature distinguishing PML from HIV encephalitis.
- External capsule and posterior fossa involvement is less common but can occur even in the absence of centrum semiovale lesions.
- The absence of mass effect and contrast-enhancement is a characteristic feature. Faint peripheral enhancement can rarely be seen. Nonetheless, the lack of contrast-enhancement and mass effect is a useful finding in distinguishing PML from other AIDS-related lesions.
- Cavitary changes can be seen as a late manifestation of PML.
- On diffusion-weighted images, hyperintense signal consistent with restricted diffusion can be seen in acute lesions. Some lesions have both restricted diffusion at the periphery (possibly representing acute demyelin-ation) and elevated diffusion centrally.

## SUGGESTED READING

Hurley RA, Ernst T, Khalili K, et al. Identification of HIV-associated progressive multifocal leukoencephalopathy: magnetic resonance imaging and spectroscopy. J Neuropsychiatry Clin Neurosci 2003;15:1–6.

Thurnher M, Donovan Post J, Rieger A, et al. Initial and follow-up MR imaging findings in AIDS-related progressive multifocal leukoencephalopathy treated with highly active antiretroviral therapy. AJNR 2001; 22:977–984.

Bergui M, Bradac GB, Oguz KK, et al. Progressive multifocal leukoenceph-alopathy: diffusion-weighted imaging and pathological correlations. Neuroradiology 2004;46:22–25.

Donovan Post MJD, Yiannoutsos C, Simpson D, et al. Progressive multifocal leukoencephalopathy in AIDS: are there any MR findings useful to patient management and predictive of patient survival? AJNR Am J Neuroradiol 1999;20:1896–1906.

# CASE 3

**JAMES M. PROVENZALE**

### HISTORY

A 16-year-old boy with lethargy, confusion, and increasing thirst and urination.

A

■**FIGURE 6-3A** Unenhanced axial CT image shows an inhomogeneous mass projected over the back of the midbrain. The lesion is actually within the pineal recess.

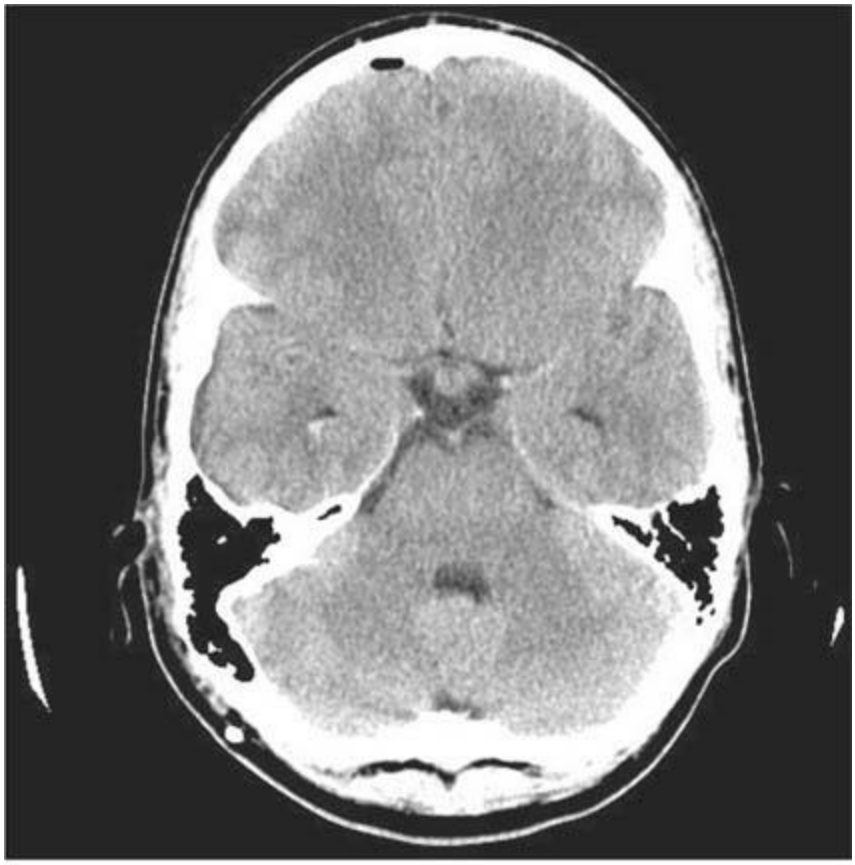

B

■**FIGURE 6-3B** Image at a more caudal level from the same unenhanced CT shows a smaller mass in the suprasellar cistern.

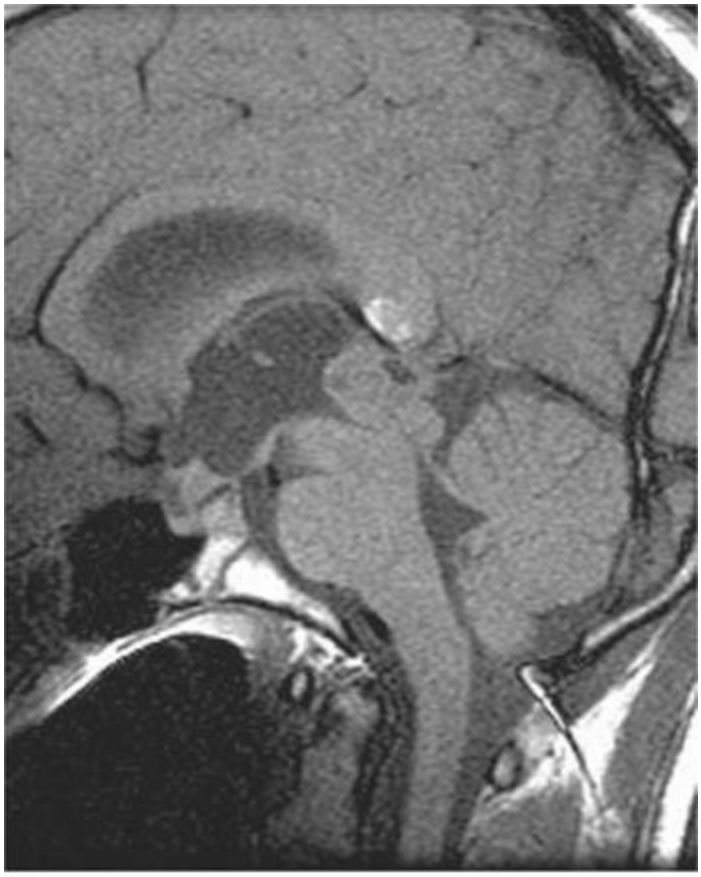

C

■**FIGURE 6-3C** Unenhanced sagittal T1-weighted image shows an inhomogeneous mass within the pineal recess with associated enlargement of the third ventricle due to obstructive hydrocephalus. Another mass is seen in the suprasellar cistern. The hyperintense signal within the splenium of the corpus callosum is due to the presence of an incidental lipoma that bears no relationship to the pineal recess mass.

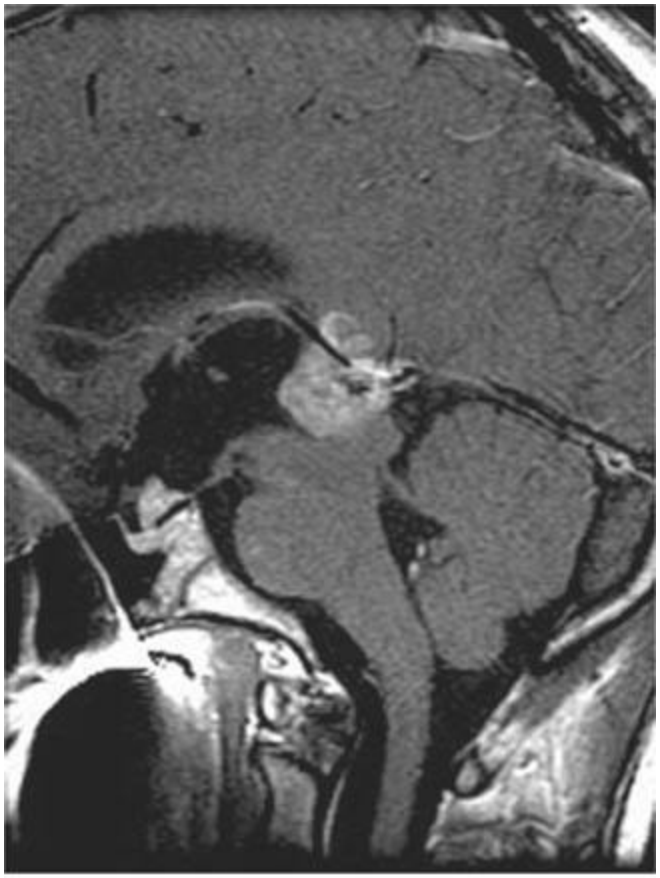

D

**FIGURE 6-3D** Contrast-enhanced sagittal T1-weighted image shows that both the pineal recess and suprasellar cistern masses contrast-enhance.

## DIFFERENTIAL DIAGNOSIS

**Primary CNS lymphoma:** Lymphoma is a consideration because this tumor can occur in an extraaxial location in adults and children. Although synchronous lymphoma lesions in the pineal and suprasellar cisterns could theoretically be seen, this event would be very rare making this diagnosis unlikely.

**Pineoblastoma:** This tumor is a consideration when a pineal region tumor is seen in a child. However, this diagnosis would not account for the suprasellar mass; this diagnosis is unlikely.

**Germinoma:** These tumors are one of the more common intracranial tumors of childhood and are located in the pineal or suprasellar region in 95% of cases. Synchronous tumors in both the pineal and suprasellar recesses are seen in about 5% of cases, which is a very rare phenomenon in other types of mass lesions. This diagnosis is correct.

**Metastases:** Intracranial metastases are uncommon in childhood. The majority of intracranial tumors are primary in origin. Furthermore, metastases are usually intraaxial

in location, unlike the extraaxial lesions shown in the case illustrated, making metastases an unlikely diagnosis.

- **Eosinophilic Granuloma:** Intracranial lesions commonly involve the pituitary stalk and are, thus, in the suprasellar region. However, this diagnosis would not account for the synchronous pineal recess mass. This diagnosis is unlikely.

## DIAGNOSIS

**Germinoma**

## KEY FACTS

### Clinical

- Germ cell tumors (GCTs) are an important category of pediatric brain tumors. The vast majority of GCTs occur in an extracranial site and do not involve the CNS.
- Intracranial GCTs typically present in the second (70%) or third decades, possibly due to increased gonadotro-pin secretion during puberty.
- Symptoms depend on tumor location: Suprasellar GCTs typically present with neuroendocrine dysfunction, visual symptoms, or headache; pineal region GCTs present with features of elevated intracranial pressure or Parinaud's syndrome (failure of upward gaze and retractory nystagmus).
- The increased thirst and urination of the patient here was due to diabetes insipidus related to the suprasel-lar lesion. When synchronous suprasellar and pineal recess lesions are present, symptoms are usually due to the suprasellar tumor.
- Two major forms of GCTs are recognized: germinomas and nongerminomatous GCTs. Germinomas are the least malignant type of GCTs. The spectrum of non-germinomatous GCTs includes embryonal carcinoma, endodermal sinus tumor, benign or malignant terato-mas, and choriocarcinoma—all are more malignant than germinomas.
- GCTs account for 1% to 3% of pediatric brain tumors in the Western hemisphere, but they are reported to be more common in Japan, where they comprise 5% to 15%.
- Ninety-five percent of intracranial GCTs are located in the midline, along an axis from the suprasellar cistern to the pineal gland. About 55% solely involve the pineal region, 35% involve the suprasellar region, and 5% to 10% involve both locations (as in the case illustrated here).
- About 70% of GCTs in the suprasellar region are germinomas. Conversely, 65% of GCTs in the pineal region are of the nongerminomatous type. Ninety percent of germinomas occur in patients younger than 20 years of age.
- Pineal region GCTs do not arise from the pineal gland itself but from rest of

embryonic germ cells.

- Suprasellar GCTs are equally frequent in males and females, but the ratio of males to females with pineal GCTs is about 10 to 1.
- Visual disturbance and neuroendocrine dysfunction are common clinical presentations of suprasellar germinomas. Pineal germinomas often present with obstructive hydrocephalus.
- Germinomas infiltrate locally and also frequently disseminate along CSF pathways; spinal imaging is an important component of evaluation of tumor progression.
- Germinomas are very radiosensitive tumors, usually rapidly shrinking within a few months of beginning radiation therapy. Nongerminomatous GCTs respond poorly to radiotherapy but are sometimes sensitive to chemotherapy.
- Overall prognosis for GCTs depends on patient age, tumor type, and tumor location. Patients <15 years at the time of diagnosis have a better 10-year survival rate (90%) than older patients (50%). The prognosis for suprasellar germinomas (90% survival at 10 years) is much better than for pineal germinomas.
- Prognosis for nongerminomatous GCTs is generally poor, with about a 50% 1-year survival rate.
- On rare occasions, germinomas may arise in sites that are not in a midline location, such as the basal ganglia, internal capsule, and thalamus.

## Radiologic

- Ideally, it would be helpful to distinguish, based on imaging studies, tumors arising from the pineal gland (e.g., pineoblastomas and pineocytomas) from those arising from nonpineal tissue (e.g., GCTs) by identification of the pineal gland as a separate structure. Unfortunately, the pineal gland is almost never seen as a structure separate from a pineal region tumor.
- The typical appearance of intracranial germinomas on unenhanced CT is that of a relatively homogeneous, mildly or moderately hyperdense mass that densely enhances after contrast administration.
- On unenhanced MRI, the solid portions of germinomas are generally isointense to gray matter on T1-weighted images and often isointense (and less commonly hyper-intense) to gray matter on T2-weighted images.
- About one-half of germinomas have cystic components, as compared to approximately 85% to 95% of nonger-minomatous GCTs.
- In reported series, germinomas have been found to homogeneously contrast-enhance in 50% to 90% of cases, whereas nongerminomatous GCTs almost always enhance in an inhomogeneous manner.

- Small suprasellar germinomas may initially be seen on imaging studies as solely thickening of the infundibulum.
- Nongerminomatous GCTs frequently have hyperintense foci on unenhanced T1-weighted images due to the presence of hemorrhage, fat, or proteinaceous fluid.
- The finding of synchronous tumors both having a hyper-dense appearance on unenhanced CT (as shown in the case above) is highly suggestive of the diagnosis of germinoma. Although only 5% of germinomas are found in both regions, no other tumor would be expected to be located at both sites and have this CT appearance.
- Brain imaging studies of patients with GCTs must be assessed for tumor extension into adjacent intracranial structures as well as dissemination throughout intracra-nial CSF spaces. Spinal imaging is usually indicated to exclude spinal metastases, seen in about 10% of cases.
- Determination of hormonal tumor markers in CSF is sometimes useful in attempting to establish the diagnosis of nongerminomatous GCTs. Alpha-fetoprotein is often secreted by endodermal sinus tumors, human chorionic gonadotropin (HCG) by choriocarcinomas, and both markers by embryonal carcinomas. However, elevated CSF HCG levels can also be seen occasionally with germinomas.

## SUGGESTED READING


Liang L, Korogi Y, Suguhara T, et al. MRI of intracranial germ-cell tumors. Neuroradiology 2004;44:382–388.

Banks KP, Brown SJ. AJR teaching file: solid masses of the pineal region. AJR Am J Roentgenol 2006;186:S233–S235.

Rao VJ, James RA, Mitra D. Imaging characteristics of common suprasellar lesions with emphasis on MRI findings. Clin Radiol 2008;63:939–947.

Kanagaki M, Miki Y, Takahashi JA, et al. MRI and CT findings of neurohypophyseal germinoma. Eur J Radiol 2004;49:204–211.

Warmuth-Metz M, Gnekow AK, Muller H, Solymosi L. Differential diagnosis of suprasellar tumors in children. Klinische Padiatrie 2004;216: 323–330.

Lee L, Saran F, Hargrave D, et al. Germinoma with synchronous lesions in the pineal and suprasellar regions. Childs Nerv Syst 2006;22: 1513–1518.

Osuka S, Tsuboi K, Takano S, et al. Long-term outcome of patients with intracranial germinoma. J Neurooncol 2007;83:71–79.


# CASE 4


### E. RALPH HEINZ AND JAMES PROVENZALE


### HISTORY

A 40-year-old man with radicular pain in the left arm and mild spasticity in the legs.

A

■**FIGURE 6-4A** Sagittal T2-weighted image shows a hyperin-tense oval mass adjacent to the cervical segment of the spinal cord.

B

■**FIGURE 6-4B** Coronal unenhanced T1-weighted image shows that the mass is hypointense on this pulse sequence. A sharp line of demarcation exists between the mass and the spinal cord; the mass is eccentric to the left.

C

■**FIGURE 6-4C** On this sagittal contrast-enhanced T1-weighted image, the mass densely and homogeneously contrast-enhances.

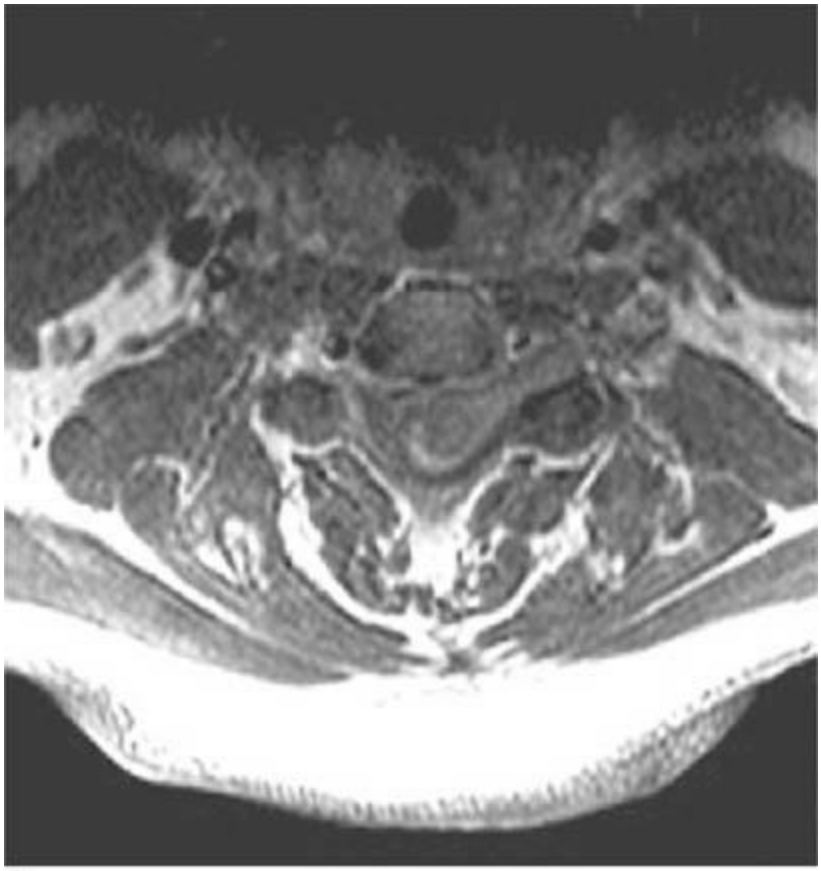

D

**FIGURE 6-4D** Axial contrast-enhanced T1-weighted image shows that the mass extends into the left neural foramen at this level.

## DIFFERENTIAL DIAGNOSIS

**Meningioma:** This is a possible consideration because the lesion shown in this case is extramedullary. Meningioma cannot be definitively excluded on the basis of the images shown. However, spinal meningiomas typically occur in patients older than the man depicted here. Furthermore, extension into the neural foramen, which is shown in Figure 6-4D, is more common in nerve sheath tumors than in meningiomas. This diagnosis is less likely than nerve sheath tumor.

**Drop metastases:** Solitary CSF metastases along the proximal nerve root can be seen occasionally but are rare. In the absence of any other likely cause, this consideration could be essentially excluded by imaging the remainder of the CNS.

**Plexiform neurofibroma:** These tumors appear as multiple, tortuous, worm-like masses arising along the axis of a major nerve—unlike the solitary, smoothly marginated mass seen in this case—making this an unlikely diagnosis.

**Nerve sheath tumor:** These lesions are typically smoothly contoured masses that are located within the spinal canal and frequently extend into the neural foramen. These

characteristics make this diagnosis the most likely consideration.

## DIAGNOSIS

**Nerve sheath tumor (schwannoma)**

## KEY FACTS

### Clinical

- Schwannoma, neurinoma, and neurilemmoma are synonymous terms used to refer to Schwann cell tumors.
- Schwannomas and neurofibromas are collectively referred to as nerve sheath tumors but are different pathologic entities.
- Nerve root schwannomas do not encase the adjacent nerve root, usually involve the dorsal (sensory) root, are typically solitary, and are not associated with neurofibromatosis. In contrast, neurofibromas encase the dorsal nerve root, are usually multiple, and are frequently associated with neurofibromatosis, even when solitary.
- Nerve sheath tumors are often associated with radicular pain or motor dysfunction related to a specific nerve root.
- Nerve sheath tumors are found most frequently in the cervical region and usually located in the extramed-ullary intradural compartment (about 60% of cases), but they are extradural in 25% of cases, and both extra- and intradural (in which case they often assume a dumbbell configuration) in 15% of cases. Rarely, these tumors can be intramedullary.
- Nerve sheath tumors can undergo malignant degeneration (seen in 5% to 10% of cases), usually after a latency period of 10 to 20 years. Thus, malignant degeneration would typically be seen in the third or fourth decade of life.

### Radiologic

- From an imaging standpoint, schwannomas and neuro-fibromas resemble one another very closely. However, distinction of the two entities on imaging studies is usually not an important issue. For these reasons, they are generally reported on imaging studies simply as nerve sheath tumors.
- One feature that can occasionally be used to distinguish schwannomas from neurofibromas is the asymmetric location of schwannomas. Because schwannomas arise from one side of the nerve root, they displace and efface the normal nerve. They appear lobulated and eccentric, whereas neurofibromas typically have a fusiform shape.
- Nerve sheath tumors generally cause widening of the neural foramina. In the setting of

neurofibromatosis, they can be associated with posterior scalloping of the vertebral bodies due to dural ectasia.

- Nerve sheath tumors can have increased signal on unenhanced T1-weighted images (probably related to mucopolysaccharide content). Furthermore, these lesions densely contrast-enhancement. Usually, markedly increased signal is seen on T2-weighted images (due to high water content). Many neurofibromas have central areas of low signal on T2-weighted images.
- Differential diagnosis of benign versus malignant: On CT and MRI, malignant nerve sheath tumors usually have irregular, infiltrative margins, whereas benign nerve sheath tumors usually have smooth margins. In addition, malignant nerve sheath tumors are typically larger than benign lesions.

## SUGGESTED READING

Conti P, Pansini G, Mouchaty H, et al. Spinal neurinomas: Retrospective analysis and long-term outcome of 179 consecutively operated cases and review of the literature. Surg Neurol 2004;61:34–43.

Liu WC, Choi G, Lee SH, et al. Radiological findings of spinal schwannomas and meningiomas: focus on discrimination of two disease entities. Eur Radiol 2009;19:2707–2715.

Parmar HA, Ibrahim M, Castillo M, Mukherji SK. Pictorial essay: diverse imaging features of spinal schwannomas. J Comput Assist Tomogr 2007;31:329–334.

# CASE 5

**JAMES PROVENZALE AND DAVID S. ENTERLINE**

### HISTORY

A 17-year-old girl with headache.

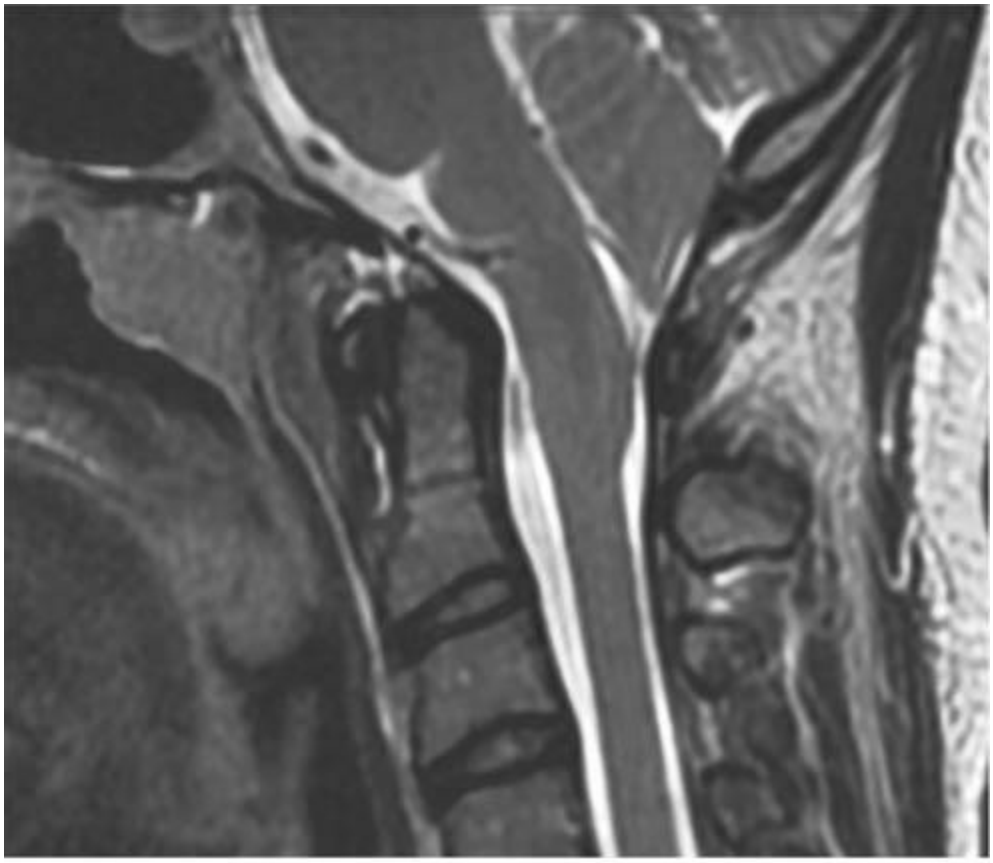

A

■**FIGURE 6-5A** Sagittal T2-weighted image shows downward displacement of the cerebellar tonsils. The tonsils were measured to be 10 mm below the level of the foramen magnum.

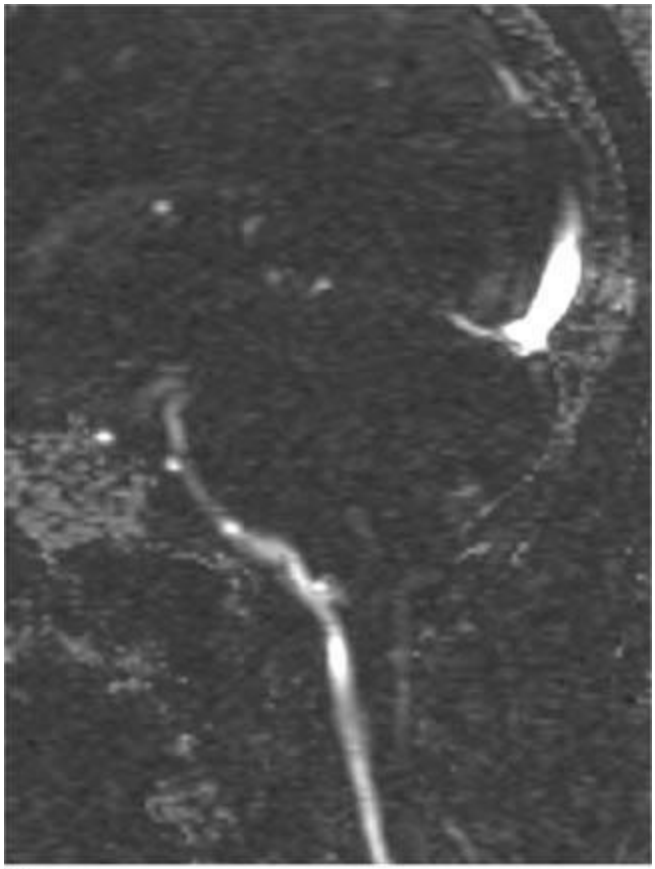

B

■**FIGURE 6-5B** Image from cine MR CSF flow study shows bright signal consistent with CSF flow anterior to the brainstem but no flow posterior to the cerebellar tonsils.

C

■**FIGURE 6-5C** Sagittal T2-weighted image in a different patient shows downward displacement of the cerebellar tonsils and a syrinx cavity in the lower cervical spinal cord.

D

**FIGURE 6-5D** Sagittal T2-weighted image in the same patient as in Figure 6-5C after surgical decompression of the posterior fossa and C1 laminectomy now shows a widened CSF space at the base of skull and near-complete resolution of the syrinx cavity.

## DIFFERENTIAL DIAGNOSIS

**Chiari I malformation:** This congenital malformation is characterized by downward displacement of the cer-ebellar tonsils through the foramen magnum, which is present in the case depicted here. The images shown here indicate an abnormality within the spinal cord that is isointense to spinal fluid on all pulse sequences, representing syringohydromyelia, which is commonly seen in patients with Chiari I malformation. These findings make Chiari I malformation the most likely diagnosis.

**Chiari II:** This entity might be considered because of the downward herniation of cerebellar tissue. However, other manifestations of Chiari II—for example, medullary kinking, tectal "beaking", a towering cerebellum, hydrocephalus, and myelomeningocele —are absent, making this diagnosis incorrect.

**Chiari III malformation:** In this malformation, hernia-tion of the hindbrain into a low occipital or high cervical encephalocele is seen, often in association with aplasia of the

posterior elements of the three highest cervical vertebral bodies. The absence of any of these features excludes this diagnosis in the case shown.

- **Other causes of cerebellar tonsillar herniation:** A posterior fossa mass can cause downward herniation of the cerebellar tonsils. Developmental disorders involving the craniovertebral junction (e.g., basilar impression or cranial settling) due to a variety of conditions (e.g., Paget's disease and rheumatoid arthritis) can also cause an abnormal relationship of the cerebellar tonsils to the foramen magnum. None of these conditions is present in the case shown.

## DIAGNOSIS

**Chiari I malformation**

## KEY FACTS

### Clinical

- Congenital hindbrain dysgenesis characterized by downward herniation of the cerebellar tonsils was described in 1891 by Hans Chiari. In Chiari I malformation, downward herniation of the cerebellar tonsils into the spinal canal is present; the fourth ventricle and cerebellar vermis remain in a relatively normal position, except in severe cases.
- This malformation is has been thought by some investigators to result from a dysplasia of bone at the cranio-cervical junction.
- In about half of cases diagnosed by MR imaging, the findings are incidental and unrelated to symptoms. In some series, the degree of tonsillar displacement in asymptomatic patients has been shown to be similar to that seen in symptomatic patients.
- Most patients with incidentally-discovered downward displacement of the cerebellar tonsils do not have a syrinx and do not develop symptoms; such patients are not treated surgically.
- Patients with Chiari I malformation typically are first diagnosed in young adulthood. Almost all symptomatic patients have at least 5 mm of cerebellar herniation. Symptoms and signs can be on the basis of either compression of the cervicomedullary junction or syringohydromyelia (which is often accompanied by widening of the spinal cord).
- The most common clinical features are hypesthesia (decreased sensation) and weakness in the extremities (about 50%) due to syringohydromyelia, headaches, cranial neuropathy, and upper motor neuron corticospinal tract findings (e.g., gait disturbance, spas-ticity, and bowel and bladder dysfunction).
- Scoliosis is common in children with Chiari malformation and syringomyelia.

- Treatment usually consists of posterior decompression of the cervicomedullary junction by suboccipital decompression of the foramen magnum and cervical laminectomy to the most caudal level of the tonsillar herniation (Figure 6-2B). Some surgeons will place a shunt tube through the foramen of Magendie into the fourth ventricle. In addition, treatment of syringohydromyelia can be performed by decompression and, on occasion, shunting.
- Following posterior fossa decompression, the diameter of the syrinx cavity typically substantially diminishes within a few months and may continue for a few years (Figure 6-2B).

## Radiologic

- The diagnosis is made by measuring the displacement of the tonsils below a line from the basion (anterior lip of foramen magnum) to the opisthion (posterior lip of the foramen magnum). The normal position of the tonsils varies with age. Tonsillar herniation is present when the tonsils are >6 mm (in children <10 years), 5 mm (age 11 to 30), or 4 mm (age 31 to 80) below this line. Most patients present in late childhood or early adulthood—hence, the usual criterion of 5 mm. The cerebellar tonsils are considered low-lying (rather than herniated) when 3 to 5 mm of inferior displacement is present in an adult 30-years old or younger.
- The peg-like configuration of the cerebellar tonsils narrows the posterior CSF space at the level of the foramen magnum, altering the CSF flow dynamics. This may be shown by cine MR flow techniques by diminished flow posterior to the cerebellar tonsils (Figure 6-5B).
- Hydrocephalus is seen in 20% to 25% of Chiari I malformation patients.
- Compression of the brainstem and upper cervical spinal cord may be an important cause of symptoms. Arachnoid adhesions may develop due to repeated trauma of the cerebellum, further compromising CSF flow.
- Syringohydromyelia has been reported in up to 60% to 70% of patients, usually in symptomatic patients. This condition is more appropriately termed hydromyelia because the CSF-filled cavity develops in the ependyma-lined central canal.
- Basilar invagination, i.e., extension of the tip of the odontoid process >5 mm above Chamberlain's line (a line drawn from the posterior margin of the hard palate to the posterior aspect of the foramen magnum), is reportedly seen in about 25% of Chiari I malformation patients.
- Skeletal anomalies are common in Chiari I malformation and include assimilation of C1 to the occiput (10%), partial nonsegmentation of C2 and C3 (15%), and Klippel-Feil deformity (5%).

## SUGGESTED READING

Novegno F, Caldarelli M, Massa A, et al. The natural history of the Chiari Type I anomaly. J Neurosurg: Pediatrics 2008;2:179–187.

Arnett BC. Tonsillar ectopia and headaches. Neurol Clin North Am 2004;22:229–236.

Hofkes SK, Iskandar BJ, Turski PA, et al. Differentiation between symptomatic Chiari I malformation and asymptomatic tonsillar ectopia by using cerebrospinal fluid flow imaging: initial estimate of imaging accuracy. Radiology 2007;245:532–540.

Wetjen NM, Heiss JD, Oldfield EH. Time course of syringomyelia resolution following decompression of Chiari malformation Type I. J Neurosurg Pediatr 2008;1:118–123.

# CASE 6

**FERNANDO M. ZALDUONDO AND JAMES M. PROVENZALE**

### HISTORY

A 31-year-old man who developed proptosis and chemosis (i.e., red eye) of the left eye and a left orbital bruit 2 days after head trauma incurred during a motor vehicle accident.


■**FIGURE 6-6A** Axial contrast-enhanced CT shows proptosis of the left eye and a fracture of the lateral wall of the left orbit. The left medial rectus and lateral rectus muscles are expanded compared to their counterparts in the right orbit.

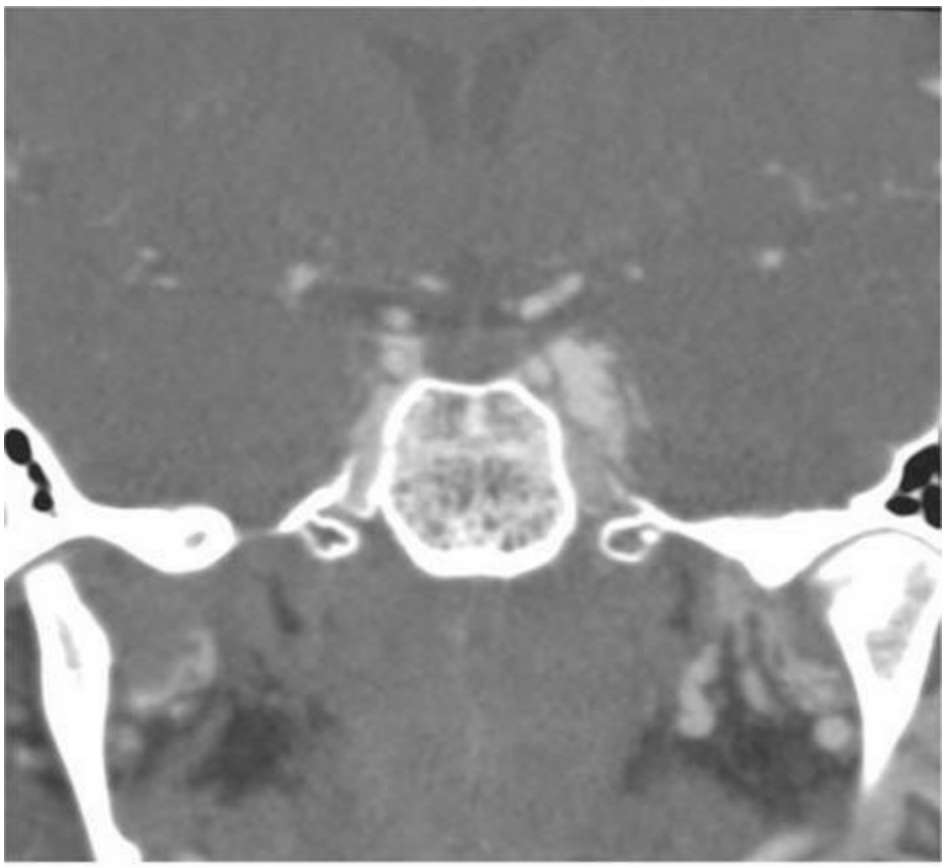

B

■**FIGURE 6-6B** Coronal reconstruction image from CT angiogram shows dilation of the left cavernous sinus.

C

■**FIGURE 6-6C** Image from CT angiogram reconstructed in the left parasagittal plane shows dilation of the superior ophthalmic vein.

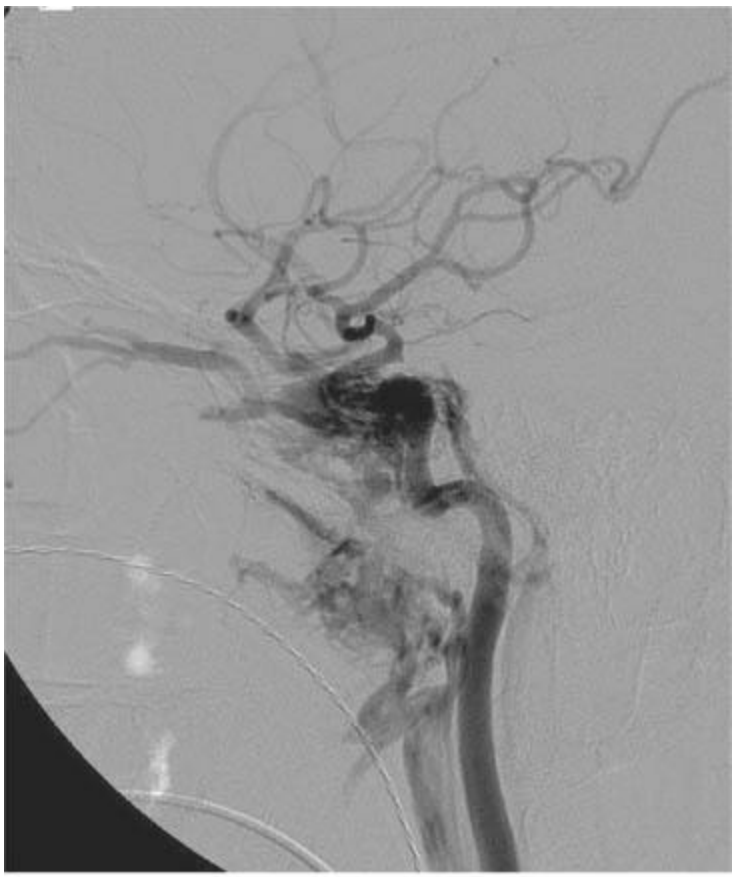

D

**FIGURE 6-6D** Lateral view from catheter angiogram, left ICA injection shows early opacification of the cavernous sinus, which is enlarged. Venous drainage from the cavernous sinus is via a dilated superior ophthalmic vein in a retrograde fashion, which is responsible for the patient's presenting symptoms of proptosis and chemosis. Venous drainage inferiorly is via the inferior petrosal sinus posteriorly and the pterygoid plexus anteriorly.

## DIFFERENTIAL DIAGNOSIS

**Orbital pseudotumor:** This diagnosis would not account for a number of features in the case shown—for example, orbital bruit, dilatation of the superior ophthalmic vein, and abnormal communication between the internal carotid artery (ICA) and superior ophthalmic vein. This diagnosis, therefore, is unlikely.

**Thyroid orbitopathy (Graves' disease):** This diagnosis might be considered because of the proptosis and extraocular muscle enlargement. However, involvement of both orbits is typical, and patients are usually much older than in the case presented. Furthermore, Graves' disease would not account for the dilated cavernous sinus and superior ophthalmic vein or the angi-ographic findings. This diagnosis is incorrect.

**Carotid-cavernous fistula (CCF):** Patients with this diagnosis typically present with

orbital pain, proptosis, and a bruit. Imaging findings can include dilation of the SOV and widening of the cavernous sinus. This is the correct diagnosis.

## DIAGNOSIS

**Carotid-cavernous fistula**

## KEY FACTS

### Clinical

- The term "carotid-cavernous fistula" (CCF) refers to an abnormal communication between the carotid artery and one or more veins in the cavernous sinus. Because arterial pressure is standardly higher than venous pressure, a CCF can produce a marked increase in the veins of the cavernous sinus, often causing dilation of the sinus and enlargement of draining veins.
- CCFs can occur following trauma or spontaneously (i.e., in the absence of trauma). The inciting traumatic event may be penetrating in nature (e.g., a missile injury) or blunt (e.g., producing basal skull fracture at or near the cavernous sinus). The cause of spontaneous direct CCFs is usually not known but in a small percentage of cases is due to rupture of an aneurysm in the cavernous segment of the ICA.
- Symptoms due to traumatic CCFs can begin within days of the injury but may be delayed by a matter of weeks. Symptoms due to spontaneous CCFs are typically slow in onset, often taking many weeks or a few months to develop.
- Clinical features of CCF depend on the predominant route of venous drainage. When the majority of the venous drainage is into the superior ophthalmic and inferior ophthalmic veins, the primary symptoms are related to the orbit, such as ocular chemosis, propto-sis (secondary to venous congestion), glaucoma, and, occasionally, unilateral visual loss. Alternatively, when the bulk of the venous drainage is into the superior, inferior, and petrosal sinuses, or when the cavernous sinus becomes greatly distended, a cavernous sinus syndrome consisting of ophthalmoplegia and facial pain can occur.
- CCFs are best classified by the nature of the arteriove-nous connection, which is either direct or indirect.
- Direct CCFs are due to a direct connection between the ICA and the veins of the cavernous sinus. Etiologies include (1) trauma, (2) rupture of an intracavern-ous ICA aneurysm, and (3) a fistulous communication due to an underlying vasculopathy (e.g., Ehlers-Danlos syndrome).
- Traumatic CCFs frequently follow skull base fracture or penetrating injuries but can

be iatrogenic (e.g., after surgery at sites near the cavernous sinus, such as sphenoidotomy or trigeminal rhizotomy). These lesions are often high flow conduits between the arterial and venous circulation.

- Indirect CCFs are typically spontaneous and caused by development of multiple fistulous communications between dural branches of the carotid circulation and the cavernous sinus. The volume of blood shunted in indirect CCFs is usually much smaller than in direct CCFs.
- CCFs sometimes involve both cavernous sinuses (and hence both orbits) because communication between the cavernous sinuses is allowed by the circular sinus, the collective term for the anterior and posterior intercav-ernous sinuses that variably connect both cavernous sinuses.
- Complications requiring emergency treatment are (1) rapid progression of proptosis or visual loss and (2) development of increased intracranial pressure (due to cortical venous hypertension, caused by diversion of blood flow into cortical veins) and intraparenchymal hemorrhage or SAH (following rupture of a large cavernous sinus varix or congested cortical vein).
- A classification system has been proposed based on the source of arterial supply to the fistulae: Type A is a direct communication between the ICA and the cavernous sinus; types B, C, and D are forms of indirect fistula. Type B is supplied solely by dural branches of the ICA, type C is supplied solely by dural branches of the external carotid artery (ECA) and type D is supplied by dural branches of both the ICA and ECA.
- Type A (i.e., direct) fistulas are standardly treated by endovascular therapy. Endovascular coiling via a trans-venous route is usually the first line treatment for a type A (direct) CCF. One preferred method is to begin coil placement at the base of the superior ophthalmic vein and then continue posteriorly past the lumen of the fistula and then into the cavernous sinus.
- Conservative treatment of patients with indirect CCFs and mild symptoms is often attempted by frequent, self-administered external compression of the carotid artery and jugular vein for many minutes at a time. However, most patients need invasive treatment.

## Radiologic

- Major findings on CT and MRI include extraocular muscle enlargement, proptosis, and dilation of the ipsilat-eral cavernous sinus and SOV.
- The diagnosis of CCF can be made noninvasively using CT angiography and MR angiography by showing enlargement of the cavernous sinus and its veins, as well as reversal of flow in the SOV (e.g., on phase-contrast MR angiography).
- CT angiography and MR angiography are unable to show the specific site of the

fistula. For this purpose, as well as for showing the exact arterial supply (needed for planning endovascular therapy), catheter angiography is necessary. In many centers, a 3D catheter angiogra-phy, which allows reconstructed images of the vascular anatomy to be rotated in space as well as endoluminal (i.e., virtual endoscopic) images to be obtained, is used.

- Catheter angiography findings include early opacification of the cavernous sinus, poor opacification of the ICA distal to the fistula, and retrograde filling of dilated venous tributaries.
- Endovascular therapy with preservation of distal ICA flow is the standard first-line therapy. Therapeutic options for direct CCFs include detachable balloons or detachable coils alone or in combination with N-butyl-2-cyanoac-rylate (n-BCA) for large-hole fistulas (e.g., direct CCFs). More recently, covered stents have been used to maintain arterial patency while occluding the fistula. Embolic agents such as isobutyl-2-cyanoacrylate or polyvinyl-alcohol particles are used for indirect CCFs. Surgery is reserved for cases that fail endovascular therapy.

## SUGGESTED READING


Coskun O, Hamon M, Catroux G, et al. Carotid-cavernous fistula: Diagnosis with spiral CT angiography. AJNR Am J Neuroradiol 2000;21:712–716.

Chen CC, Chang PCT, Shy GC, et al. CT Angiography and MR angiography in the evaluation of carotid cavernous sinus fistula prior to embolization: a comparison of techniques. AJNR Am J Neuroradiol 2005;26: 2349–2356.

Gemmete JJ, Chaudhary N, Pandey A, Ansari S. Treatment of carotid cavernous fistulas. Curr Treat Options Neurol 2010;12:43–53.

Gomez F, Escobar W, Gomez AM, et al. Treatment of carotid cavernous fistulas using covered stents: midterm results in seven patients. AJNR Am J Neuroradiol 2007;28:1762–1768.

van Rooij WJ, Sluzewski M, Beute GN. Ruptured cavernous sinus aneurysms causing carotid cavernous fistula: Incidence, clinical presentation, treatment, and outcome. AJNR Am J Neuroradiol 2006;27:185–189.

Moron FE, Klucznik RP, Mawad ME, Strother CM. Endovascular treatment of high-flow carotid cavernous fistulas by stent-assisted coil placement. AJNR Am J Neuroradiol 2005;26:1399–1404.


# CASE 7


### JOSEPH B. CORNETT AND JAMES M. PROVENZALE


### HISTORY

Images from two patients are shown. Figures 6-7A and 6-7B show a 72-year-old woman with proptosis and Figures 7-7C and 7-7D show a 58-year-old woman with proptosis.

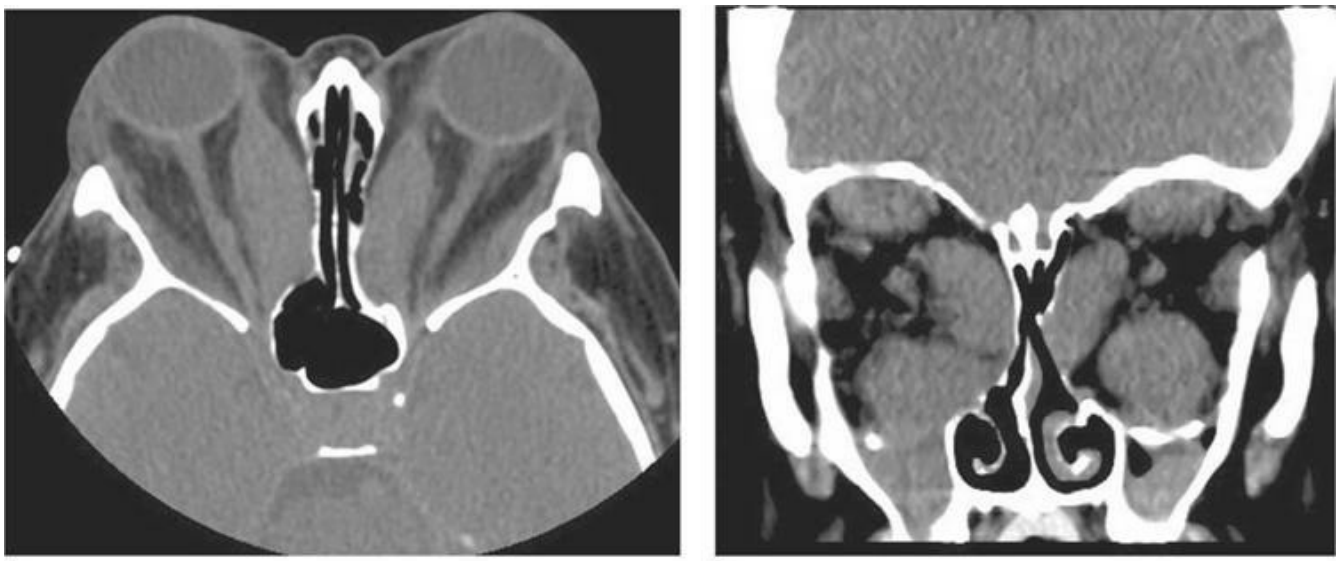


■**FIGURES 6-7A and 6-7B** Unenhanced axial CT of the orbits In a 72-year-old woman. **(A)** Axial Image shows marked enlargement of the bellies of the medial rectus muscles; the muscle tendons are of normal size. The orbital fat is normal in appearance. **(B)** Coronal image shows marked enlargement of the inferior rectus and medial rectus muscles. The superior rectus muscle is mildly enlarged. The superior ophthalmic vein is normal in diameter.

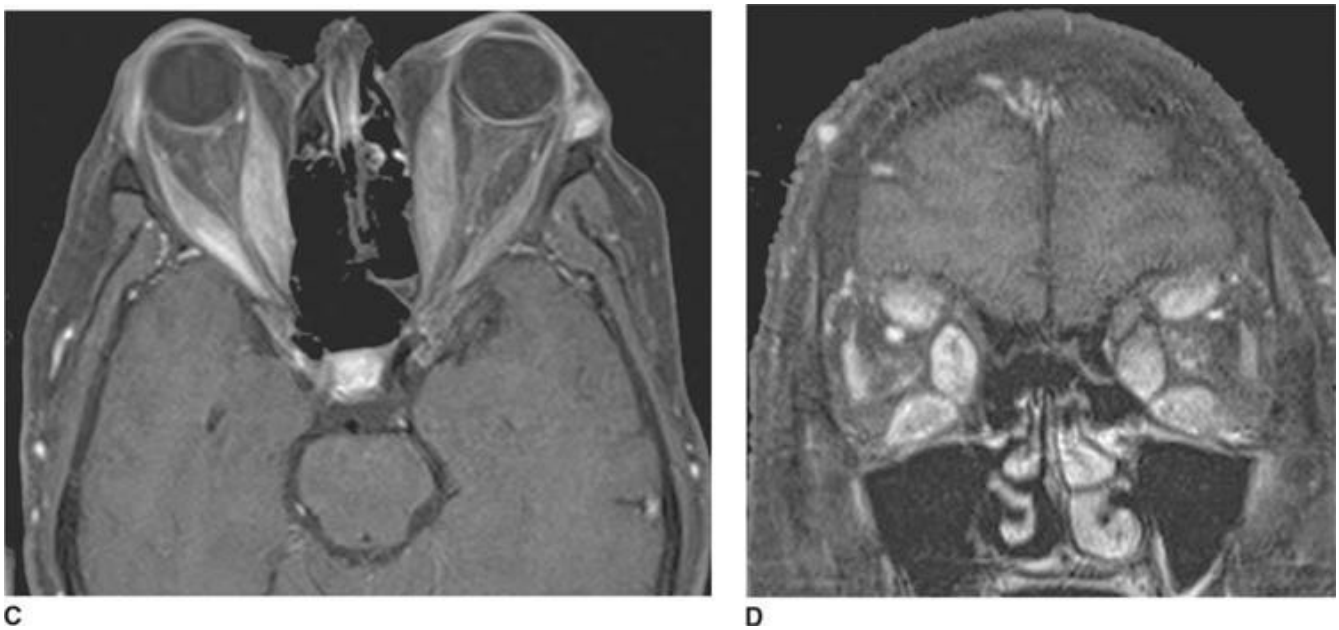


■**FIGURES 6-7C and 6-7D** Contrast-enhanced T1-weighted MR images using fat saturation technique in a 58-year-old woman with proptosis. **(C)** Axial image shows enlargement of both medial rectus muscles and the right lateral rec-tus muscle. The space around the optic nerves is narrowed bilaterally by expansion of the muscles. The

orbital fat is normal in appearance. **(D)** Coronal image shows marked expansion of the medial rectus, inferior rectus and superior rectus muscles. The orbital veins are normal in size.

## DIFFERENTIAL DIAGNOSIS

- **Orbital pseudotumor (idiopathic orbital myositis):** Myositis is one of many manifestations of orbital pseudotumor. This is an unlikely diagnosis for the case shown above because diffuse enlargement of the entire extraocular muscle is usually seen in orbital pseudotumor, whereas the tendinous portions of the muscles are not enlarged in the figures shown.
- **Neoplasm arising from muscle:** Tumors such as rhab-domyosarcoma, lymphoma, leukemia, and metastases can involve the extraocular muscles. However, bilateral, symmetric involvement makes this diagnosis unlikely.
- **Vascular congestion causing extraocular muscle enlargement:** Muscle enlargement can result from vascular congestion associated with high blood-flow states such as CCF (see Case 6). This condition is often manifested clinically by chemosis and an orbital bruit (neither of which was reported in the clinical history of these patients). On imaging, dilatation and tortuosity of the superior ophthalmic vein and distention of the cavernous sinus are typically seen; both findings are absent in the patients shown. This diagnosis is, therefore, unlikely.
- **Graves' ophthalmopathy:** This is the best diagnosis given the bilateral muscle enlargement, predominant involvement of the inferior, medial, and superior rectus muscles, and sparing of tendinous insertions of the extraocular muscles. Subsequent laboratory tests in both women showed findings indicative of hyperthyroidism.

## DIAGNOSIS

**Graves' ophthalmopathy (thyroid ophthalmopathy)**

## KEY FACTS

## Clinical

- Graves' disease is an autoimmune disease caused by circulating antibodies that are directed against the thyrotropin receptor and cause hyperthyroidism. The disease is approximately eight times more common in women and typically has onset in the fourth or fifth decade of life.
- Thyroid ophthalmopathy is a common cause of unilateral or bilateral proptosis in

adults.

- Extraocular muscle enlargement occurs due to lym-phocytic and plasmacytic infiltration of connective tissue (presumed to be autoimmune in origin) accompanied by mucopolysaccharide deposition, edema, and fibrosis.
- Enlargement of the extraocular muscles can produce proptosis, decreased range of globe motion and diplopia, and periorbital and conjunctional edema due to elevated orbital pressure.
- Visual loss is threatened in 10% of patients due to compressive optic neuropathy (caused by compression of the optic nerve at the orbital apex due to muscle enlargement) or corneal ulceration (due to corneal exposure secondary to lid retraction and exophthalmos).
- Thyroid ophthalmopathy usually occurs in patients with hyperthyroidism, but 10% of patients have no clinical or laboratory evidence of thyroid disease.
- Treatment is typically with corticosteroids. Occasionally, radiation therapy or surgical decompression of the optic nerve is performed is cases in which vision is threatened.
- In many patients, the major alternative diagnosis to be considered is orbital myositis, especially in cases of unilateral disease. Clinically, myositis usually has onset over the course of days, is painful, is often accompanied by ptosis and responds quickly to corticosteroids. Thyroid ophthalmopathy usually has an onset of many weeks, is painless, is typically accompanied by lid retraction (rather than ptosis) and has a slow and, often, incomplete response to corticosteroids. On imaging, myositis typically involves solely one muscle and involves both the muscle belly and the tendinous insertion; neither feature is present in thyroid ophthalmopathy.

## Radiologic

- Thyroid ophthalmopathy typically produces enlargement of the bellies of the extraocular muscles, with sparing of the tendinous insertions, which can be helpful in distinguishing it from other causes of extraocular muscle enlargement.
- The inferior rectus muscles and medial rectus are affected earliest and most severely. The lateral rectus muscle is usually the least involved. In 6% of cases, only one muscle is enlarged.
- Approximately 85% of cases have bilateral disease on CT or MRI. In 15% of cases, orbitopathy presents with predominantly unilateral eye findings or precedes onset of clinical hyperthyroidism, making correct diagnosis difficult.
- Imaging in the coronal or sagittal plane is better suited for determination of enlargement of the extraocular muscles, particularly the inferior rectus and superior rectus muscles (which are cut tangentially on axial images).

- Findings other than extraocular muscle enlargement that may be seen include an increase in the volume of orbital fat and enlargement or anterior displacement of the lacrimal gland. The increased orbital fat may cause bowing of the medial wall of the orbit or prolapse of fat into the superior orbital fissure.
- Indications for imaging in Graves' orbitopathy include (1) increasing certainty regarding the diagnosis and excluding other causes of clinical findings, (2) determining best treatment (e.g., immunosuppressive therapy vs. surgery), and (3) monitoring treatment response.

## SUGGESTED READING

Kirsch E, Hammer B, von Arx G. Graves' orbitopathy: current imaging procedures. Swiss Med Weekly 2009;139:618–623.

Mayer EJ, Fox DL, Herdman G, et al. Signal intensity, clinical activity and cross-sectional areas on MRI scans in thyroid eye disease. Eur J Radiol 2005;56:20–24.

Naik VMN, Naik MN, Goldberg RA, et al. Immunopathogenesis of thyroid eye disease: emerging paradigms. Ophthalmol 2010;55:215–226.

# CASE 8

**JAMES M. PROVENZALE AND CHARLES B. DONOVAN**

### HISTORY

A 9-year-old boy with diabetes insipidus.

A

■**FIGURE 6-8A** Unenhanced axial CT shows a mass with peripheral calcification located in a suprasellar location.

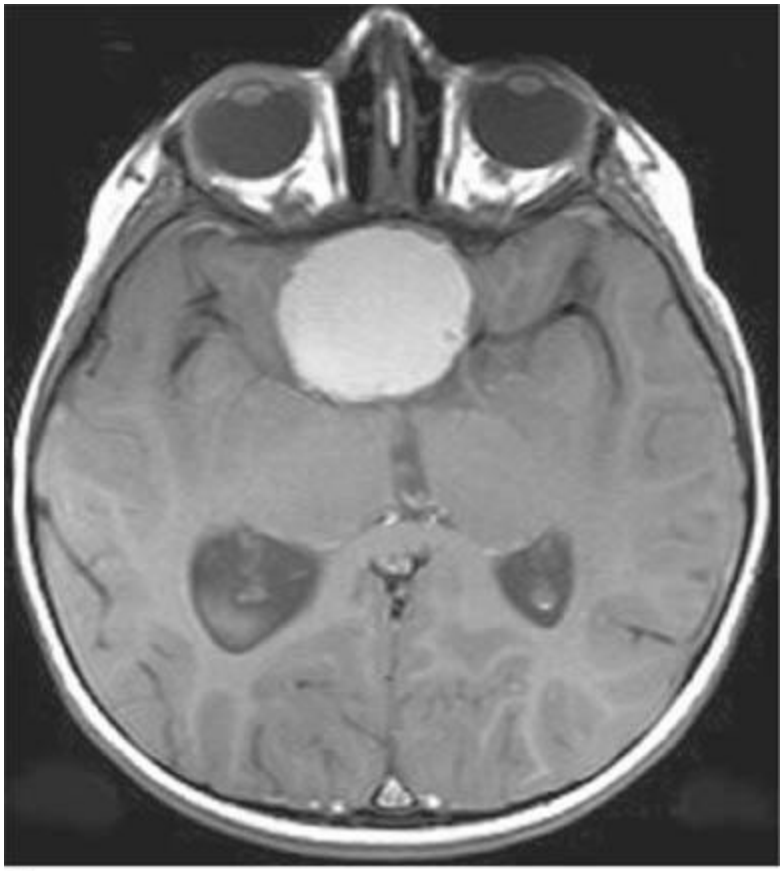

B

■**FIGURE 6-8B** Unenhanced axial T1-weighted MR image shows that the mass is hyperintense on this pulse sequence. The calcifications seen on CT are evident as very small foci along the rim of the lesion.

C

■**FIGURE 6-8C** Axial FLAIR image shows the mass is also hyperintense on this pulse sequence.

D

**FIGURE 6-8D** Sagittal contrast-enhanced T1-welghted Image shows that the lesion Is very large and extends from the sella cephalad to elevate the corpus callosum. A small enhancing region Indicative of a small soft tissue component Is seen at the caudad aspect of the mass and within the sella.

## DIFFERENTIAL DIAGNOSIS

**Optic glioma:** This diagnosis could be considered based on the fact that some of the mass shown in the case presented is located in the suprasellar space, a common location for optic glioma. However, the lesion shown in this case is not oriented along the visual pathways. Also, optic gliomas are rarely calcified or invade the sella. Although optic gliomas can have cystic regions (often indicating necrosis), unlike the case shown here, the cystic component is usually small. This diagnosis is unlikely.

**Craniopharyngioma:** This diagnosis is a common cause of a suprasellar mass in childhood, accounting for about half of suprasellar tumors. These lesions typically have both a calcified component and a cyst. This diagnosis is correct.

**Germinoma:** This diagnosis might be considered because of the suprasellar location of the lesion in the case shown here. However, germinomas are usually solid masses, unlike the cystic lesion shown here; this diagnosis is unlikely.

- **Pituitary adenoma:** Pituitary adenomas are rare in children. Furthermore, a large cystic component and calcification would be unusual. This diagnosis is incorrect.
- **Rathke's cleft cyst:** This diagnosis might be considered because of the sellar and suprasellar location of the mass in the case shown. However, Rathke's cleft cysts are typically predominantly intrasellar, usually much smaller than the lesion shown here, do not contain a soft tissue component, and are not calcified. This diagnosis is incorrect.

## DIAGNOSIS

**Craniopharyngioma**

## KEY FACTS

### Clinical

- Craniopharyngiomas are World Health Organization classification grade I tumors that are derived from squamous epithelial remnants of Rathke's cleft. Most involve both the sellar and suprasellar regions, but less commonly, they can be located solely within the sella or the third ventricle.
- These tumors represent 3% to 5% of all intracra-nial tumors, show no gender predilection, and have a bimodal age distribution. More than half occur in childhood (peak: ages 5 to10 years) and adolescence, but a second peak is seen in later years (50 to 74 years old).
- Craniopharyngiomas account for 5% to 15% of childhood intracranial tumors.
- Clinical symptoms are typically due to mass effect on adjacent structures—for example, visual field defects due to compression of the optic pathways and neuroendocrine dysfunction due to compression of the hypothalamus and pituitary gland. The most common symptoms are headache, nausea, papilledema, growth failure (in children), and hypogonadism (in adults).
- Two distinct clinicopathologic variants are recognized. The adamantinomatous type is the more common of the two variants and can be seen in both adults and children but is more common in the latter. This tumor type more frequently is calcified, exhibits necrosis, and contains cholesterol within cysts. The papillary form almost always occurs in adults but still represents only about one-third of adult craniopharyngiomas. It is more often solid, less frequently calcified, and has been reported to have a better surgical outcome than adamantinomatous tumors in the adult.
- Adamantinomatous lesions may have a surrounding region of gliosis at the interface of the lesion with brain tissue, which can cause the tumor to tightly adhere to brain tissue, often making complete resection impossible.

- Presenting symptoms and signs are usually those associated with increased intracranial pressure (headache, nausea, vomiting, and papilledema) or visual disturbance. Craniopharyngiomas are hormonally inactive but can compress the pituitary gland and hypothalamus, causing neuroendocrine dysfunction.
- There is a considerable debate regarding the best management of craniopharyngiomas —that is, whether to use surgical resection or cyst aspiration followed by radiation therapy. Surgical excision is complicated by the fact that complete resection of the tumor away from the hypothalamus and pituitary stalk is often impossible.
- Tumors with a size >5 cm have a much higher recurrence rate (80%) than that found for smaller lesions (20%).

## Radiologic

- Craniopharyngiomas are typically heterogeneous masses; the heterogeneous composition of a craniopharyngioma is often more easily discernible on MR imaging than on CT.
- The triad of suprasellar location, calcifications, and a cyst is highly suggestive of craniophrayngioma. Calcifications, readily detectable on CT, are present in about 90% of childhood lesions and 70% of adult lesions.
- Approximately 95% of lesions have a suprasellar component, including 20-40% that are solely suprasellar. Only 5% are solely intrasellar.
- About 90% of craniopharyngiomas are partially cystic. Rarely, the lesion is purely cystic. The cyst contents consist of straw-colored or oily brownish fluid with variable amounts of cholesterol crystals and triglycerides, which often produces a hyperintense appearance on unenhanced T1-weighted images.
- The unenhanced CT appearance is that of an inhomo-geneous mass that frequently has cystic components and punctate or clumpy calcifications. Occasionally, the cyst is hyperdense, reflecting very high protein concentration. Variable degrees of a soft tissue component can be seen, but administration of contrast material is frequently necessary to depict it.
- The papillary type has a more uniform CT and MR appearance with less frequent calcification and cyst formation.
- On CT and MR studies, when cyst contents are identical in appearance to CSF, the presence of calcifications and soft tissue components helps to distinguish cranio-pharyngioma from arachnoid cyst, a lesion that also commonly occurs in the suprasellar region.
- The cystic components of craniopharyngiomas are variable on T1-weighted images, varying from isointensity with CSF to hyperintensity. Fluid that is isointense to CSF is more commonly seen in small (<10 mm) lesions, while fluid that is hyperintense on T1-

weighted images (as in the case shown here) is more commonly seen in large lesions. Solid portions are frequently relatively isointense to brain on all pulse sequences.

- On occasion, various signal intensities can be seen within the cystic component of the tumor, thought due to compartments containing fluids of different protein composition.
- MRI is helpful in preoperative definition of the relationship of the tumor to the optic nerves and chiasm, internal carotid arteries and their branches, pituitary stalk, hypothalamus, and third ventricle.
- Gradient recalled echo or susceptibility-weighted images are useful for depicting the calcifications in this tumor on MR imaging.

## SUGGESTED READING


Osborn AG, Preece MT. Intracranial cysts: radiologic-pathologic correlation and imaging approach. Radiology 2006;239:650–664.

Garre ML, Cama A. Craniopharyngioma: modern concepts in pathogenesis and treatment. Curr Opin Pediatr 2007;19:471–479.

Bonneville F, Cattin F, Marsot-Dupuch K, et al. T1 signal hyperintensity in the sellar region: spectrum of findings. Radiographics 2006;26: 93–113.

Curran JG, O'Connor E. Imaging of craniopharyngioma. Child's Nerv Syst 2005;21:635–639.

Molla E, Marti'-Bonmati L, Revert A, et al. Craniopharyngiomas: identification of different semiological patterns with MRI. Eur Radiol 2002;12:1829–1836.

Karavitaki N, Cudlip S, Adams CBT, Wass JAH. Craniopharyngioma. Endo-crin Rev 2006;27:371–397.


# CASE 9


**JAMES M. PROVENZALE**


### HISTORY

A 40-year-old woman with 10 days of right hand weakness. She experienced a transient episode of painful right monocular visual loss 2 years earlier.

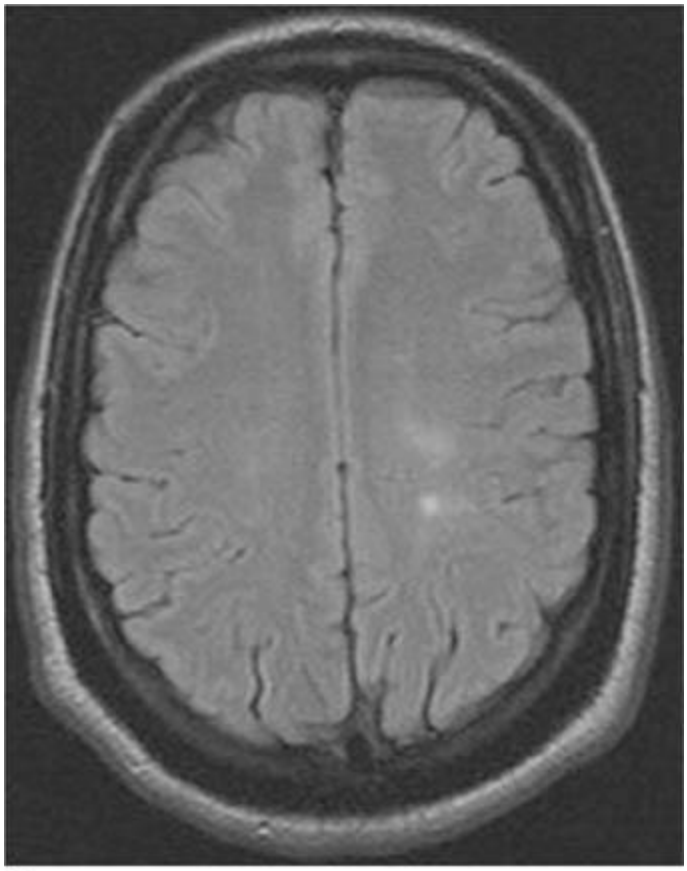

A

■**FIGURE 6-9A** Axial FLAIR image shows two hyperintense foci with ill-defined borders in the left frontal white matter.

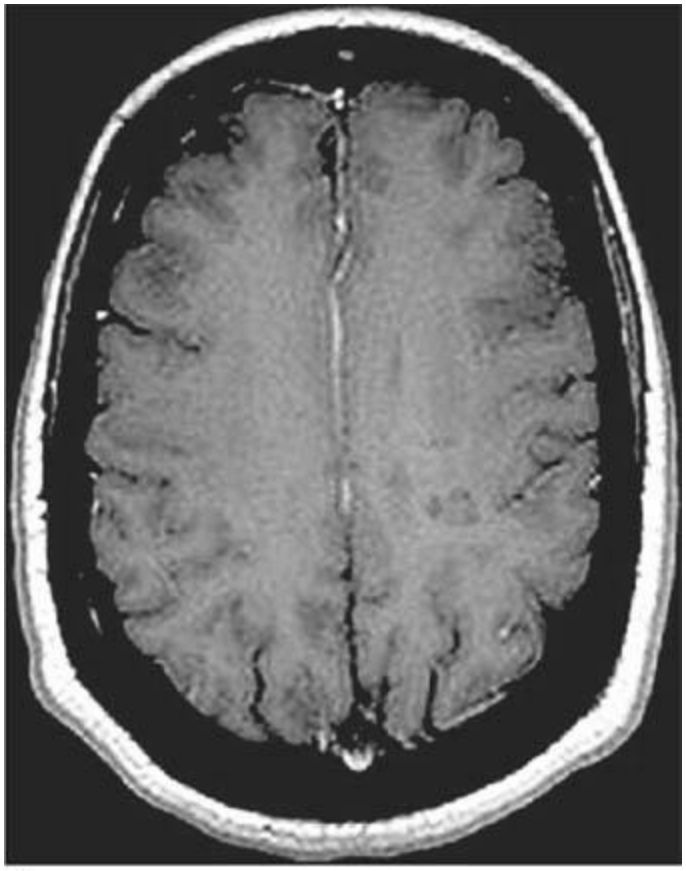

B

■**FIGURE 6-9B** Axial contrast-enhanced T1-welghted image shows that neither lesion contrast-enhances. The posterior lesion is clearly hypointense relative to white matter. The anterior lesion also has subtle decreased signal intensity.

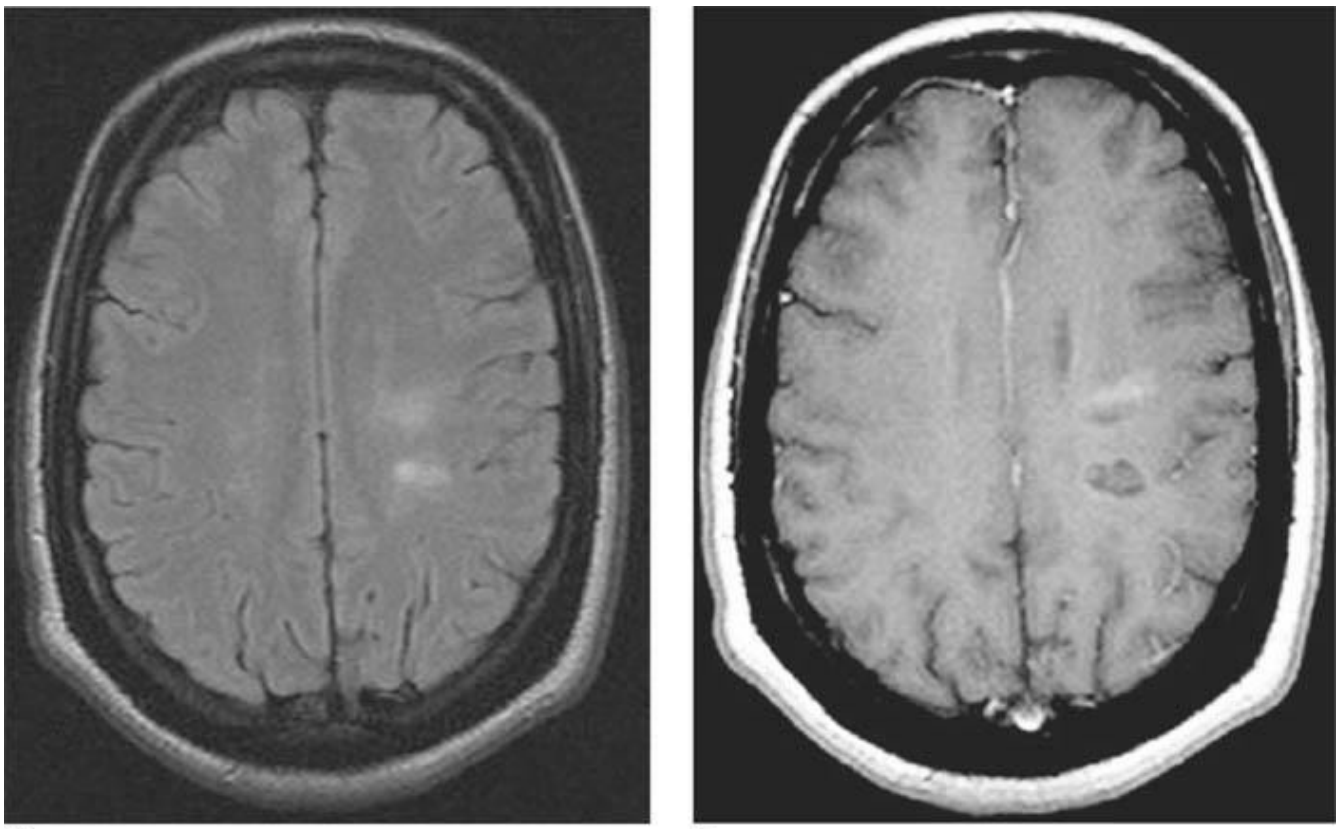


**FIGURES 6-9C and 6-9D C** Axial FLAIR image obtained 2 months after the images in 6-9A and 6-9B shows that the two hyperintense foci have increased in size. **D** Axial contrast-enhanced T1-weighted image shows that the anterior lesion is larger and now hypointense relative to white matter. The region of lesion growth anteriorly now contrast-enhances.

## DIFFERENTIAL DIAGNOSIS

**Deep "watershed" infarcts:** Such infarcts occur at border zones between major arterial territories or in deep white matter locations. They are typically seen as rounded foci or elongated foci that have their longest dimension in the anteroposterior direction. The lesions shown here are oval, with their long axis in the lateral dimension, making watershed infarct unlikely. In this particular case, it would be important to carefully look for the presence of other white matter lesions that are not in a single vascular distribution; if present, such lesions would make watershed infarction even less likely.

**Low-grade neoplasm:** This diagnosis does not account for the past medical history. The two separate lesions or the oval appearance of the abnormalities.

**Vasculitis:** The history of a previous neurologic event years before does not support this diagnosis. Furthermore, most infarcts within the white matter are rounded or linear; the oval shape of the lesions does not support this diagnosis.

- **Multiple sclerosis (MS):** The clinical history in this patient describes a bout of optic neuritis, commonly seen in MS patients. Multiple white matter lesions that are hyperintense on T2-weighted images, hypointense on T1-weighted images (so-called black holes) and aligned at right angles to the ventricular surface are common. This is the correct diagnosis.
- **Acute disseminated encephalomyelitis (ADEM):** This disease generally occurs after a systemic viral infection or a vaccination. No such history is given in this patient. Furthermore, ADEM typically has a monophasic course, unlike the history given here.

## DIAGNOSIS

**Multiple sclerosis**

## KEY FACTS

### Clinical

- MS is a demyelinating disease typified by multiple exacerbations and remissions involving different parts of the CNS. Thus, lesions are characterized by being "multiple in space and time."
- The most common sites of involvement are the white matter tracts of the centrum semiovale, corona radiata, and brain stem.
- Spinal cord involvement is seen in about 10% of cases.
- Onset of symptoms is usually in the third to fifth decades.
- Optic neuritis is common. Furthermore, a significant proportion of patients with isolated optic neuritis later are diagnosed as having MS.
- The prevalence of MS is higher at northern and temperate climates compared to regions near the equator.
- Laboratory abnormalities include the presence of oligoclonal bands in cerebrospinal and abnormal electrophysiologic studies (i.e., visual, auditory, or somatosensory evoked potentials).
- The exact etiology is unknown, but MS is generally considered an autoimmune phenomenon.

### Radiologic

- MS lesions are typically periventricular in location. Although many diseases can produce such lesions, MS plaques are often oval and have a perpendicular orientation to the lateral ventricles.

- Lesions in the corpus callosum, middle cerebellar peduncle, or spinal cord increase the likelihood of the diagnosis of MS.
- FLAIR images are most sensitive for detecting small lesions adjacent to ventricular surface.
- Contrast-enhancing lesions are relatively frequently seen and are generally considered to represent plaques in the acute ("active") stage of demyelination.
- MS plaques are generally either isointense (most commonly) or hypointense ("black holes" appearance) compared to white matter on T1-weighted images. The latter likely represent either areas of edema or severe tissues injury (e.g., axonal loss).
- Most contrast-enhancing lesions are also hypointense on unenhanced T1-weighted images.
- Solely spinal cord involvement (most commonly the cervical spinal cord) is seen in 10% to 20% of cases.
- Advanced MR imaging techniques such as diffusiontensor imaging, MR spectroscopy, and magnetization transfer imaging show that much of the white matter that appears normal on FLAIR images is, in fact, abnormal

## SUGGESTED READING


Ge Y. Multiple Sclerosis: The role of MR imaging. AJNR Am J Neuroradiol 2006;27:1165–1176.

Bourekas EC, Varakis K, Bruns D, et al. Lesions of the Corpus Callosum: MR Imaging and Differential Considerations in Adults and Children. AJR 2002;179:251–257.

Bagnato F, Jeffries N, Richert ND, et al. Evolution of T1 black holes in patients with multiple sclerosis imaged monthly for 4 years. Brain 2003;126:1782–1789.

Filippi M, Grossman RI. MRI techniques to monitor MS evolution. The present and the future. Neurology 2002;58:1147–1153.

Arnold DL, Matthews PM. MRI in the diagnosis and management of multiple sclerosis. Neurology 2002;58:S23–S31.

Guo AC, MacFall JR, Provenzale JM. Diffusion tensor imaging of multiple sclerosis: Evaluation of normal-appearing white matter. Radiology 2002;222:729–736.

Kealey SK, Kim YJ, Provenzale JM. Redefinition of multiple sclerosis plaque size using diffusion tensor MRI. AJR 2004;183:497–503.


# CASE 10


### E. RALPH HEINZ


### HISTORY

A 20-year-old man with a primary brain tumor.

A

■**FIGURE 6-10A** Unenhanced T1-weighted sagittal image of the spine. A number of nodules are seen within the thecal sac.

B

**FIGURE 6-10B** Contrast-enhanced T1-weighted sagittal image of the spine using fat saturation technique. The nodules densely contrast-enhance in a homogeneous manner.

## DIFFERENTIAL DIAGNOSIS

**Leptomeningeal ("drop") metastases:** This term refers to leptomeningeal spread of tumor arising from a primary CNS neoplasm. Small metastases disseminate through the cerebrospinal spaces and subsequently enlarge. The diffuse pattern of enhancing nodules along the entire length of the cauda equina in a patient with a known primary brain tumor makes this diagnosis the most likely consideration.

**Neurofibroma of the spinal roots:** This diagnosis is considered because neurofibromas usually contrast-enhance. However, they are usually larger and oriented along the axis of the nerve root.

**Granulomatous disease:** Granulomatous diseases—for example, sarcoidosis—can coat the spinal cord and spinal nerve roots. The appearance is usually that of contrast-enhancing nodules accompanied by adjacent enhancement of the pia and arachnoid (not present in the case shown above). Granulomatous involvement at other cranial sites (e.g., the basilar meninges) or extra-CNS sites (e.g., the lungs) might be expected, which is not reported in this patient.

- **Contrast-enhancement of spinal cord vessels:** Contrast-enhancement of veins posterior to the spinal cord is often seen on MRI, even in normal subjects. On a single axial image, contrast-enhancement within veins can be mistaken for enhancing metastases. The distinction between the two entities can be made by looking at serial axial images. Because veins are generally oriented along the craniocaudad axis, venous enhancement should be seen in the same site on serial axial images; metastases will be seen on only one or two of a series of axial images. The lesions shown above are not oriented along the spinal cord and do not represent enhancing vessels.

# DIAGNOSIS

**Drop metastases**

# KEY FACTS

## Clinical

- Between 5% and 30% of children with CNS tumors will have CSF metastasis at the time of diagnosis or at some point in the clinical course—that is, at initial diagnosis or at time of recurrence.
- Clinical status is not a good predictor of the presence of drop metastases. Unless CSF metastases are quite large, patients with drop metastases are generally asymptomatic and appear well.
- Detection of drop metastases is vital, because survival is poor if early treatment of tumor dissemination is not performed.
- Imaging studies are frequently positive for drop metastases in patients in whom cytologic examination of the CSF is negative. However, CSF cytologic findings are positive in 30% of cases in which imaging studies are negative. Therefore, CSF examination and imaging studies are complementary—either examination can be positive when the other examination is negative.
- Medulloblastoma is the most common source of drop metastasis (about 50% of all cases), followed by glio-blastoma (about 15%).
- Two age peaks of drop metastases are seen in patients with childhood brain tumors. The first peak occurs at about age 6 years, at the time of initial diagnosis. The second occurs at about age 15 years and occurs in two conditions (1) patients with an incompletely treated brain tumor who have had previous prophylactic spinal radiation but subsequently develop drop metastases, and (2) patients with previous remission of brain tumor who develop recurrence of the brain tumor with coexistent drop metastases.
- CSF cytology is still the most sensitive means for determining leptomeningeal tumor

spread, being positive on initial lumbar puncture in about half of patients with proven CSF metastases.

### Radiologic

- Drop metastases tend to be more frequent in the lower spinal canal—that is, the lumbosacral area (73%), probably due to the effects of gravity.
- Metastases within the spinal canal are usually dorsal in location, reflecting CSF flow from the head; ventral CSF flow tends to be toward the head.
- The sensitivity of contrast-enhanced MRI is greater than CT myelography or myelography alone. Rapid screening of the entire spinal axis can be performed by MRI in a noninvasive manner. CT myelography is an invasive study in which the myelogram is typically used to direct CT imaging of only a portion of the spinal canal.

## SUGGESTED READING

Heinz ER, Weiner D, Friedman H, Tien RD. Detection of cerebral spinal fluid metastasis: CT myelography or MR. AJNR 1995;16:1147–1151.

Kramer ED, Rafto S, Packer RJ, Zimmerman RA. Comparison of myelogra-phy with CT follow-up vs. gadolinium MRI for subarachnoid metastatic disease in children. Neurology 1991;41:46–50.

Yousem DM, Patrone PM, Grossman RI. Leptomeningeal metastasis: MR evaluation. J Comput Assist Tomogr 1990;14:255–261.

# CASE 11

**JAMES M. PROVENZALE**

### HISTORY

A 50-year-old woman with a sudden onset of low back pain and progressive paraparesis over 1 hour. Symptoms began suddenly after the patient sneezed.

A

■**FIGURE 6-11A** Axial image from a postmyelography CT at the T10 level shows marked compression of the spinal cord (seen anteriorly in the midline, bounded on each side by the contrast-filled thecal sac). A mass that is isodense to soft tissue is in the midline posteriorly.

B

**FIGURE 6-11B** Sagittal reconstruction derived from axial images from the postmyelography CT shows the mass is fusiform in shape and aligned along the length of the spinal canal.

## DIFFERENTIAL DIAGNOSIS

**Epidural metastasis:** Such metastases usually arise from vertebral body metastases and extend into the spinal canal, making this an unlikely diagnosis. Nonetheless, in rare instances, some metastases (e.g., lymphoma and leukemia) can infiltrate solely the soft tissues and dura. However, these diagnoses would be unlikely in light of the acute onset of symptoms and the hypointense signal of the lesion in the second patient shown above.

**Spinal epidural abscess:** Usually spinal epidural abscesses have a clinical onset lasting over a day or more and are located in the anterior epidural space and osteomyelitis or discitis is present. However, in the patients shown above, the clinical onset is very short, only the posterior epidural space is involved, and neither osteomyelitis nor discitis is present.

**Spinal epidural hematoma:** The rapid onset of neurologic deficit is consistent with this diagnosis. The absence does not exclude this diagnosis, because spinal epidural hematoma sometimes occurs after Valsalva maneuvers that accompany exertion (e.g.,

weight-lifting) or vigorous coughing or sneezing (as in this patient). Such hematomas typically occur in the posterior epidural compartment, as in the case shown here.

- **Spinal cord infarction:** This entity is a consideration based on the acute onset of neurologic findings. However, infarction would be expected to produce an intramedullary lesion, not an epidural lesion. This diagnosis is incorrect.

## DIAGNOSIS

**Spinal epidural hematoma**

## KEY FACTS

### Clinical

- The term spontaneous spinal epidural hematoma refers to a hematoma that arises without any cause known prior to development of the hematoma. Thus, spontaneous lesions occur in the absence of recognized trauma to the spine. In most cases of spontaneous spinal epidural hematoma, a cause is never identified.
- Most cases occur in the 55- to 70-year-old age range.
- A precipitating cause (e.g., spinal vascular malformation) may occasionally be found after diagnosis of the hematoma but this is seen in only about 5% of cases.
- A substantial number of patients who develop spinal epidural hematoma have been undergoing treatment with anticoagulants at the time of symptom onset.
- Spontaneous spinal epidural hematoma may occur after physiologic events that momentarily raise intraspinal pressure, for example, Valsalva maneuver or forceful coughing.
- Some spinal epidural hematomas occur after a minor invasive procedure, such as a lumbar puncture, myelo-gram, or placement of an epidural catheter or needle. Patients who have a coagulopathy or medicated with antioagulants are at increased risk for development of a hematoma.
- The typical clinical presentation is acute onset of back pain and rapid development of myelopathy inferior to the level of the hematoma. However, in some reported series, only abut 50% of patients have back pain. Early diagnosis of spinal epidural hematoma is critical because the likelihood of reversal of neurologic deficit is related to duration of symptoms.
- Lesions usually occur in the thoracic or lower cervical spine.
- In most patients, the etiology of spinal epidural hematoma is not known, even after surgery. Most spontaneous hematomas are thought to be venous in origin and related to the fact that the veins in the epidural space are valveless and, thus, more directly

influenced by changes in thoracic or abdominal pressure. Less commonly, hematomas may be due to rupture of a spinal vascular malformation or due to hemorrhage from an arterial source.

- Emergency laminectomy to evacuate the hematoma is usually performed. Preoperative radiologic demonstration of the extent of the hematoma is important for surgical planning.
- Degree of recovery of neurologic function is related to degree of preoperative deficit (which itself appears to be related to time interval between symptom onset and surgery). In patients who have incomplete sensorimotor loss prior to surgery, about 95% receive some benefit from surgery (and about 40% have complete recovery of function). However, patients with complete sensorim-otor loss have only about a 10% complete recovery and only about 45% recover some function.

## Radiologic

- Spinal epidural hematomas are typically fusiform in shape, with their longest dimension along the craniocau-dad axis. They are often best seen on sagittal MR images.
- These lesions are usually located in the posterior epi-dural space and are typically three to four vertebral bodies in length.
- MRI is the most sensitive and specific means of making the diagnosis but the diagnosis can also be, CT myelography, myelography alone and, in some instances, CT alone.
- The MR signal intensity of spinal epidural hematoma depends on the age of the hemorrhage. In the first 12 hours after symptom onset, the hematoma is relatively isointense to the spinal cord on T1-weighted images and hyperintense on T2-weighted images. After intravenous administration of contrast material, small foci of contrast-enhancement can be seen within the hematoma of T1-weighted images.
- After the first 12 hours but within the first few days after onset, the hematoma is often heterogeneous on both T1-weighted and T2-weighted images. Alternatively, the hematoma may uniformly attain the signal characteristics of intracellular methemoglobin, being hyper-intense on T1-weighted images and often hypointense on T2-weighted images. Because epidural fat is hyper-intense on T1-weighted images, use of fat-suppressed T1-weighted imaging can make the hematoma more conspicuous.
- On MR imaging, hematomas that are older than one week in onset are often hyperintense on T1-weighted and T2-weighted images. On T2-weighted images, the hyperintense appearance may render the hematoma difficult to distinguish from CSF.
- If MRI is unavailable or contraindicated, CT myelogra-phy is an acceptable means of making the diagnosis. On axial images, the lesion is seen as a (usually posterior) epidural mass that is isodense or hyperdense to spinal cord and displaces the thecal sac

or spinal cord.

- Myelographic findings are nonspecific and consist of narrowing or block of the intrathecal contrast column. The lesion can often be seen to be smoothly tapered at each end.
- The diagnosis can be difficult to make by plain CT when the epidural mass is isodense to the spinal cord.
- Spinal epidural hematoma can be difficult to distinguish from spinal subdural hematoma—a very uncommon entity. The distinction is usually not important, because surgical evacuation is usually performed in both cases. On axial CT and MRI, subdural hematoma is frequently crescentic and sometimes separated from the lamina by epidural fat. On MRI, subdural hematoma can sometimes be seen to be separated from the epidural fat by the linear hypointense signal of the dura.
- Therapy is typically emergency surgical decompression and evacuation of the hematoma. Preoperative angi-ography is generally not performed because it delays therapy and usually will not provide information that is needed in surgical decision making.

## SUGGESTED READING


Hsieh CT, Chang CF, Lin EY, et al. Spontaneous spinal epidural hematomas of cervical spine: report of 4 cases and literature review. Am J Emerg Med 2006;24:736–740.

Kreppel D, Antoniadis G, Seeling W. Spinal hematoma: a literature survey with meta-analysis of 613 patients. Neuorsurg Rev 2003;26:1–49.

Layton KF, Kallmes DF, Horlocker TT. Recommendations for anticoagulated patients undergoing image-guided spinal procedures. AJNR Am J Neuroradiol 2006;27:467–471.

Cullen DJ, Bogdanov E, Htut N. Spinal epidural hematoma occurrence in the absence of known risk factors: a case series. J Clin Anesth 2004;16:317–319.

Lonjon MM, Paquis P, Chanalet S, Grellier P. Nontraumatic spinal epidural hematoma: report of four cases and review of the literature. Neurosur-gery 1997;41:483–486.

Braun P, Kazmib K, Nogues-Melendez P, et al. MRI findings in spinal subdural and epidural hematomas. Eur J Radiol 2007;64:119–125.

Chang F-C, Lirng J-F, Chen S-S, et al. Contrast-enhancement patterns of acute spinal epidural hematomas: a report of two cases. AJNR Am J Neuroradiol 2003;24:366–369.


# CASE 12


### JAMES M. PROVENZALE AND E. RALPH HEINZ


### HISTORY

A 60-year-old man with a 2-month history of headache and confusion.

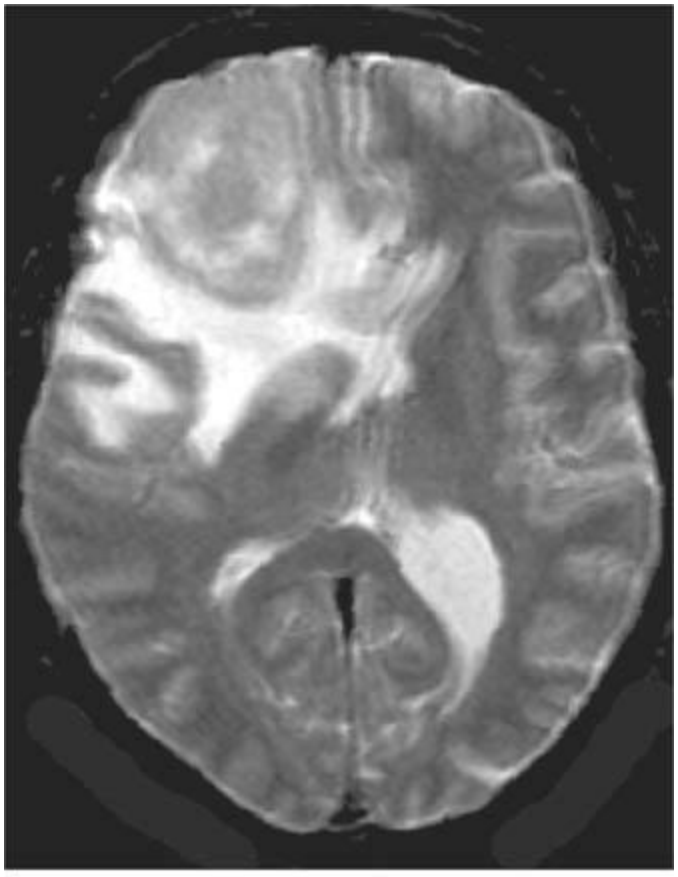

A

**FIGURE 6-12A** Axial T2-weighted image shows a large mass in the right frontal lobe surrounded by hyperintense vasogenic edema. Portions of the mass are only mildly hyperintense compared to normal gray matter.

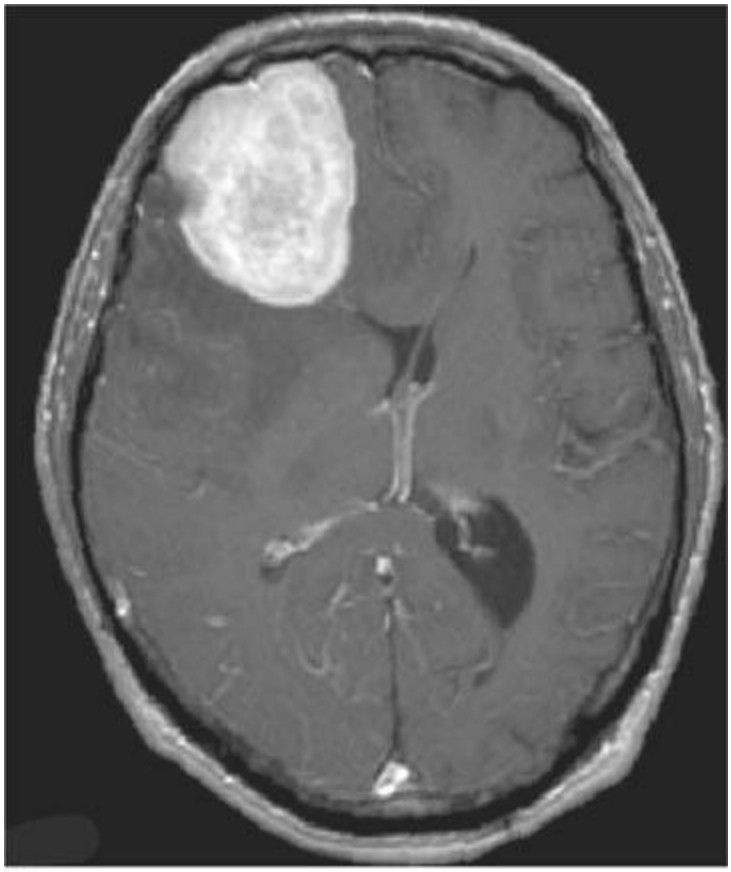

B

■**FIGURE 6-12B** Contrast-enhanced axial T1-weighted image shows marked homogeneous contrast-enhancement of the mass with adjacent hypointense edema.

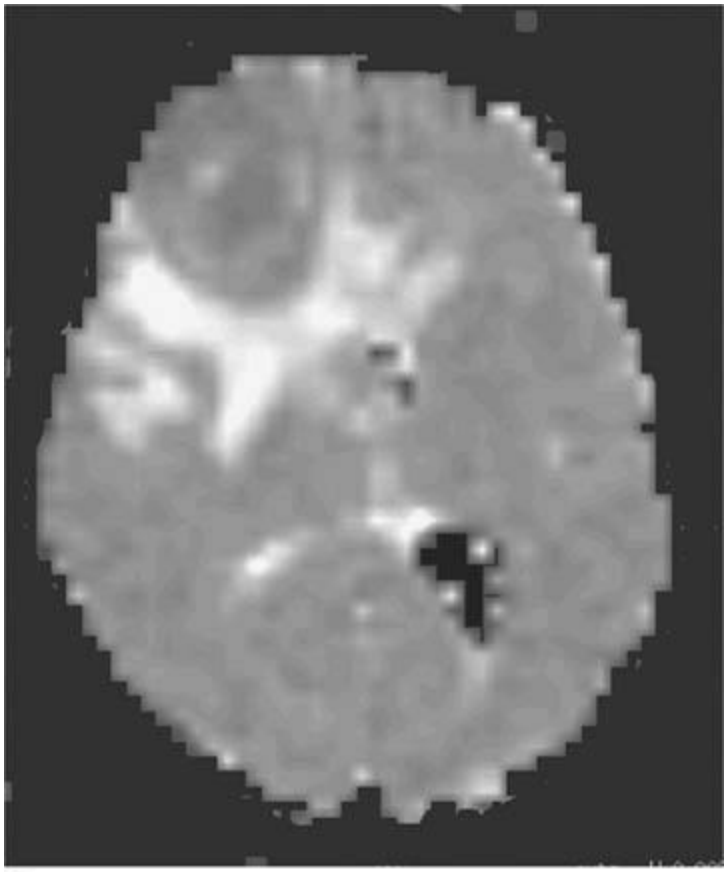

C

■**FIGURE 6-12C** Axial apparent diffusion coefficient map shows that, in general, the mass is hypointense to the remainder of the brain, indicating restricted diffusion. The vasogenic edema is seen as hyperintense signal.

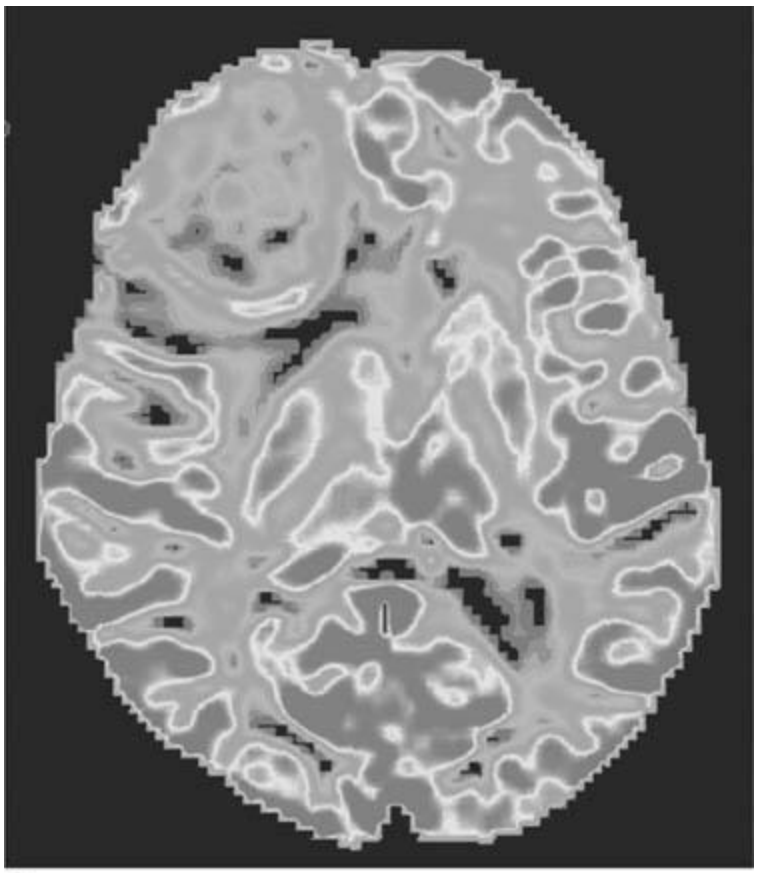

D

**FIGURE 6-12D** MR relative cerebral blood map using T2* echo planar imaging shows that the mass has low relative cerebral volume compared to normal gray matter. (See color insert)

## DIFFERENTIAL DIAGNOSIS

**Glioblastoma multiforme (GBM):** This diagnosis should be considered because the lesion is densely contrast-enhancing and has a large amount of adjacent vasogenic edema. However, the areas of restricted diffusion and low relative cerebral blood volume are atypical for GBM. This diagnosis is incorrect.

**Meningioma:** Such lesions are typically densely contrast-enhancing and have normal or restricted diffusion; they thus have some features seen in the case depicted here. However, meningiomas typically have elevated relative cerebral blood volume, making meningioma an unlikely diagnosis.

**Primary CNS lymphoma:** Lymphoma typically densely contrast-enhances, often exhibits restricted diffusion and typically does not show elevated relative cerebral blood volume. This diagnosis is correct.

## DIAGNOSIS

**Primary CNS lymphoma**

# KEY FACTS

## Clinical

- Primary CNS lymphoma accounts for about 1% of all primary brain tumors but is increasing in frequency as a complication of AIDS.
- The CNS does not have intrinsic lymphoid tissue, and the cell of origin of primary CNS lymphoma is unknown.
- Essentially, all primary CNS lymphoma is composed of the non-Hodgkin's B-call type.
- The major forms of lymphoma involving the CNS include primary CNS spread from extra-CNS lymphoma and primary CNS lymphoma (whose features differs in many ways between the immunocompetent and immu-nodeficient populations).
- Whereas primary CNS lymphoma usually is manifested by one or more parenchymal masses, CNS spread from systemic lymphoma is usually leptomeningeal. Notably, 10% to 15% of primary CNS lymphomas also have lep-tomeningeal involvement.
- Immunocompetent patients with primary CNS lymphoma usually present in later life (usually in the sixth decade) than immunodeficient patients who develop primary CNS lymphoma.
- In addition to AIDS patients, other immunocompro-mised patients (e.g., organ transplant recipients and patients with congenital immunodeficiency diseases) are at risk for primary CNS lymphoma.
- Two rare forms of primary CNS lymphoma also exist: primary leptomeningeal lymphoma and intravascular lymphoma.
- Rarely, primary CNS lymphoma can first present in a suprasellar location or a pineal recess location.
- Long-term survival is poor, being approximately 5% to 10% at five years. Age >60 years old, involvement of deep brain structures such as the basal ganglia and high protein levels in CSF are considered poor prognostic features.

## Radiologic

- Lesions due to primary CNS lymphoma are often located in the white matter of the cerebral hemispheres (about 30% of cases), corpus callosum (15%), cerebellum (15%), basal ganglia (15%), and ventricles (10%). In about half of cases, multiple lesions are present. The mean size of lesions is approximately 2 cm.

- Ependymal extension of periventricular lesions is a common finding and, when seen, should raise the diagnosis of primary CNS lymphoma.
- Calcification, necrosis, and hemorrhage are rarely seen in lesions in immunocompetent patients. Extensive per-itumoral edema can be seen in both immunocompetent and immunodeficient patients.
- Lymphoma in the immunocompetent patient is often a homogeneous mass that is hyperdense relative to white matter on unenhanced CT. However, lymphoma in immunodeficient patients is often seen as an inhomogeneous lesion with hypodense components. The two populations from the standpoint of contrast-enhancement: lymphoma in immunocom-petent patients frequently contrast-enhances in a homogeneous manner but lymphoma in immunode-ficient patients often has inhomogeneous enhancement in a ring-like manner, making distinction from toxoplasmosis difficult.
- Lymphoma, when located deep within the brain, often has large regions that are isointense or hypointense to gray matter on T2-weighted and FLAIR sequences, a finding that is also seen in other hypercellular small cell-type tumors and not commonly seen in other highgrade tumors such as high-grade gliomas. However, on occasion, the lesions can be very hyperintense on T2-weighted images.
- Parenchymal brain metastases from systemic lymphoma can be indistinguishable from primary CNS lymphoma, but parenchymal metastases are rare in the absence of leptomeningeal lesions.
- AIDS-related primary CNS lymphoma can closely simulate toxoplasmosis. However, toxoplasmosis lesions frequently have a peripheral hyperintense rim on T1-weighted MR images, which is hypointense on proton density and T2-weighted images, a finding not generally seen in lymphoma. Thallium SPECT scans have shown usefulness in distinguishing the two entities, because scans are negative in toxoplasmosis and positive in lymphoma. Similarly, most cases of primary CNS lymphoma are hypermetabolic on F18-FDG positron emission tomography at the time of diagnosis, unlike toxoplasmosis.
- In the setting of AIDS, the presence of hemorrhage argues against lymphoma; it is more frequently seen in toxoplasmosis.
- Lymphoma is relatively unique in having apparent diffusion coefficient values close to those of normal brain tissue, which reflects the high cellularity of the tumor. On the other hand, most glial neoplasms have apparent diffusion coefficient values that are 1.5 to 2.0 times normal.
- In general, primary CNS lymphoma has lower relative cerebral blood volume values on MR perfusion imaging compared to high-grade gliomas and often very similar to that of normal white matter.

## SUGGESTED READING

Buhring U, Herrlinger U, Krings T, et al. MRI features of primary central nervous system lymphomas at presentation. Neurology 2001;57: 393–396.

Erdag N, Bhorade RM, Alberico RA, et al. Primary lymphoma of the central nervous system: typical and atypical CT and MR imaging appearances. AJR Am J Roentgenol 2001;176:1319–1326.

Ferreri AJM, Blay JY, Reni M, et al. Prognostic scoring system for primary CNS lymphomas: the international extranodal lymphoma study group experience. J Clin Oncol 2003;21:266–272.

Guo AC, Cummings TJ, Dash RC, Provenzale JM. Lymphomas and high-grade gliomas comparison of water diffusibility and histologic characteristics. Radiology 2002;222:177–183.

Hakyemez B, Erdogan C, Bolca N, et al. Evaluation of different cerebral mass lesions by perfusion-weighted MR imaging. J Magn Reson Imaging 2006;24:817–824.

Mohile NA, Deangelis LM, Abrey LE. Utility of brain FDG-PET in primary CNS lymphoma. Clin Adv Hematol Oncol 2008;6:818–820.

# CASE 13

**JAMES M. PROVENZALE AND DAVID S. ENTERLINE**

## HISTORY

A 1-day-old girl with a mass in her lower back.

A

■**FIGURE 6-13A** Sagittal FLAIR Image shows that spinal cord extends to the bottom of the spinal canal. Tissue that has slightly higher signal intensity than the spinal cord extends into the base of the buttocks.

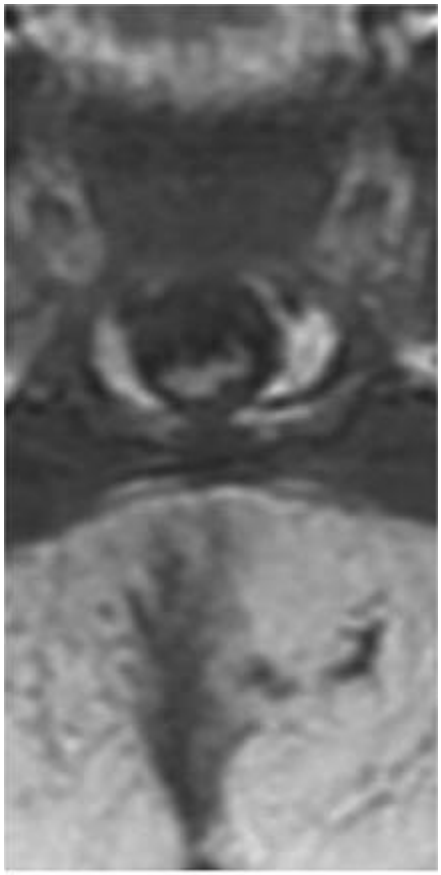

B

■**FIGURE 6-13B** Axial T1-welghted image through the level of the L5 vertebral body shows the conus medullars is located at an abnormal low position. Some of the contents of the sac are seen in the midline immediately posterior to the spinal canal.

C

■**FIGURE 6-13C** Sagittal T1-weighted image of the spine in a patient with a different diagnosis than that shown in Figure 6-13A. The conus medullaris is located at the mid-portion of the L3 vertebral body. A mass that is hyperintense is aligned along the back of the spinal canal, causing a tethered spinal cord.

D

**FIGURE 6-13D** Axial T2-weighted image in the same patient as shown in Figure 6-13C, taken at the level of the L5 vertebral body, shows the mass has the same signal intensity as fat. A curved region of bright signal is seen along the anterior surface of the mass and a curved region of dark signal is seen along the posterior aspect of the mass; these findings represent chemical shift artifact.

## DIFFERENTIAL DIAGNOSIS

There is one correct diagnosis for the patient shown in Figures 6-13A and 6-13B and another correct diagnosis for the patient shown in Figures 6-13C and 6-13D.

**Tightened fllum terminale syndrome:** In this syndrome, the conus medullaris is normal or near-normal in position, but clinical features of spastic paraparesis are present. These findings are solely due to the presence of a filum terminale that is thickened (>3 mm), stretched, and under tension. As a result, the filum terminale often has a curved course, projecting along the posterior aspect of the spinal cord ("bowstring appearance"). However, in the case shown in Figure 6-13A, other abnormalities are present: the conus medul-laris is markedly lower in position than normal, and a mass is seen projecting outside the spinal canal. This diagnosis is incorrect.

**Lipoma causing spinal cord tethering:** These lesions are composed entirely of fat,

with no sac containing neural elements; hence; this diagnosis is incorrect for the patient in Figures 6-13A and 6-13B. However, it is the correct diagnosis for the patient shown in Figures 6-13C and 6-13D.

- **Lipomyelomeningocele:** In this disorder, dysraphism of the lower lumbar and sacral posterior elements in association with a sac containing neural and fatty structures and projecting beyond the confines of the spinal canal is seen. These findings are present in Figure 6-13. This diagnosis is correct for the patient shown in Figures 6-13A and 6-13B.

## DIAGNOSIS

**Tethered spinal cord due to a lipomyelomeningocele**

## KEY FACTS

### Clinical

- The conus medullaris in normal individuals most commonly is located at the level of the middle of the L1 vertebral body. However, in 5% of normal individuals, the conus medullaris is located below the L2 vertebral body.
- There are three main congenital causes of spinal cord tethering (1) intradural lumbosacral lipoma, (2) tight filum terminale, and (3) diastematomyelia (splitting of the spinal cord with fixation due to a fibrocartilaginous or osseous septum within the spinal canal).
- Intraspinal lipomas causing spinal cord tethering can be seen in the setting of (1) a thickened filum terminale that progressively widens into a lipoma, (2) a normally formed conus medullaris adherent to an adjacent lipoma (Figures 6-13C and 6-13D), and (3) an incompletely closed conus medullaris (myeloschisis) attached to a lipoma.
- Presenting features of tethered cord can include (1) pain in the back, legs, buttocks, or perineum; (2) spastic para-paresis (i.e., abnormal gait, leg weakness and muscular atrophy, hyperreflexia, and urinary or fecal retention or incontinence); (3) sensory changes in the distribution of the lumbosacral roots; (4) tightened Achilles' tendon; (5) scoliosis; and (6) pes cavus deformity of the foot.
- Clinical features related to a tethered spinal cord typically begin in late childhood, adolescence, or early adulthood but can be seen in early childhood or middle age.
- Intraspinal lipomas are not invariably associated with neurologic findings; only about half of subjects with these lesions develop symptoms. In particular, small lipomas within the thecal sac or within the filum terminale (sometimes termed a fibrolipoma) can be incidental findings seen at autopsy (about 20% of individuals) or on cross-

sectional imaging studies.

- Tethered cord syndrome can also occur solely in the presence of a tight, slightly thickened filum terminale ("tightened filum" syndrome). When neurologic features suggestive of tethered cord syndrome are seen in the absence of other structural abnormalities on MRI, it is important to pay particular attention to the thickness and course of the filum terminale to exclude findings indicative of a tightened filum terminale please (see the section on Differential Diagnosis).
- Symptoms related to a tethered spinal cord can be precipitated (or worsened) by many factors, including increased tension on the spinal cord (e.g., during pregnancy or following acute anterior flexion of the trunk), increased crowding of intraspinal contents (e.g., disc herniation), and minor trauma.
- Standard treatment for a tethered spinal cord is surgical untethering by release of the spinal cord, spinal nerve roots, or filum terminale from the lesion causing tethering (e.g., from a spinal lipoma), or sectioning of the filum terminale (in the case of a tightened filum). Intraoperatively, only slight cephalad movement of the spinal cord would be expected to be seen after unte-thering. Therefore, little change in the position of the conus medullaris would be expected on follow-up imaging studies.

## Radiologic

- Findings on plain radiographs associated with a spinal dysraphic state are nonspecific but can include spina bifida occulta (e.g., bifid laminae and absence of the neural arches), widening of the spinal canal, and fusion of the vertebral bodies.
- MRI is the preferred method of diagnosis because it is (1) noninvasive, (2) the most sensitive method for determination of the level of the conus medullaris and detection of a tethering lesion, and (3) shows the dorsal placement of a tightened filum terminale well. T1-weighted images are the most sensitive pulse sequence for detection of a spinal lipoma.
- Myelography followed by CT is also an acceptable method of diagnosis but is generally reserved for instances in which MRI is unavailable or contraindicated.
- During myelography in patients with a suspected tethered spinal cord, care must be taken to avoid puncture of the spinal cord or filum terminale, which is often close to the posterior wall of the thecal sac. This risk can be lowered by needle puncture from an oblique angle. Myelographic evaluation can be difficult, because the lumbosacral thecal sac is frequently enlarged due to dural ectasia, which promotes pooling of the contrast material.

# SUGGESTED READING

Khanna AJ, Wasserman BA, Sponseller PD. Magnetic resonance imaging of the pediatric spine. J Am Acad Orthop Surg 2003;11:248–259.

Michelson DJ, Ashwal S. Tethered cord syndrome in childhood: diagnostic features and relationship to congenital anomalies. Neurol Res 2004;26: 745–753.

Pinto FC, Fontes RB, Leonhardt C, et al. Anatomic study of the filum terminale and its correlations with the tethered cord syndrome. Neurosurgery 2002;51:725–729.

# CASE 14

**JAMES M. PROVENZALE**

## HISTORY

A 30-year-old man with new onset of headache, decreased level of consciousness, and right third nerve paresis.

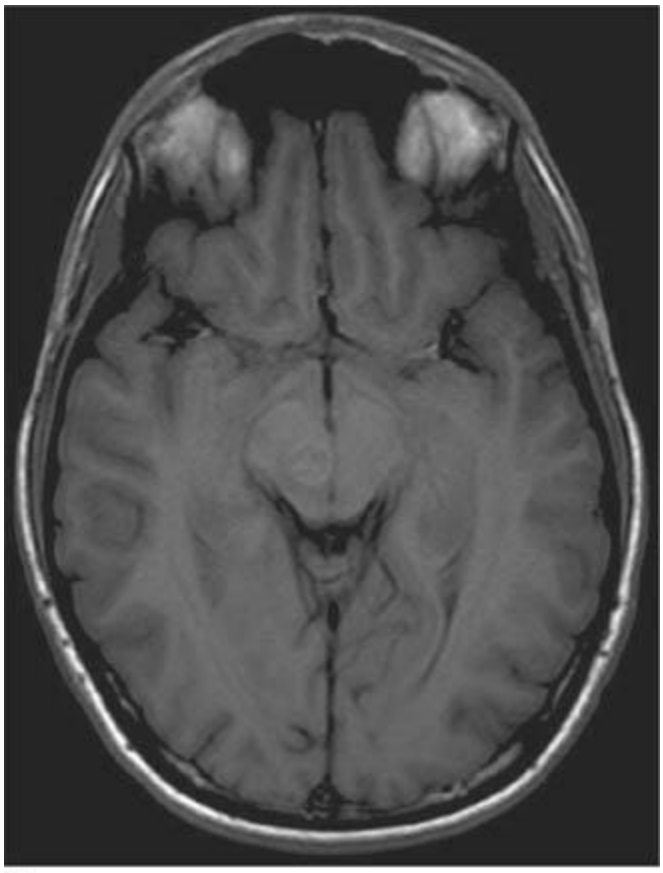

A

■**FIGURE 6-14A** Unenhanced axial T1-weighted image shows a slightly inhomogeneous round mass in the right side of the portion of the mass has hypointense signal. mesencephalon.

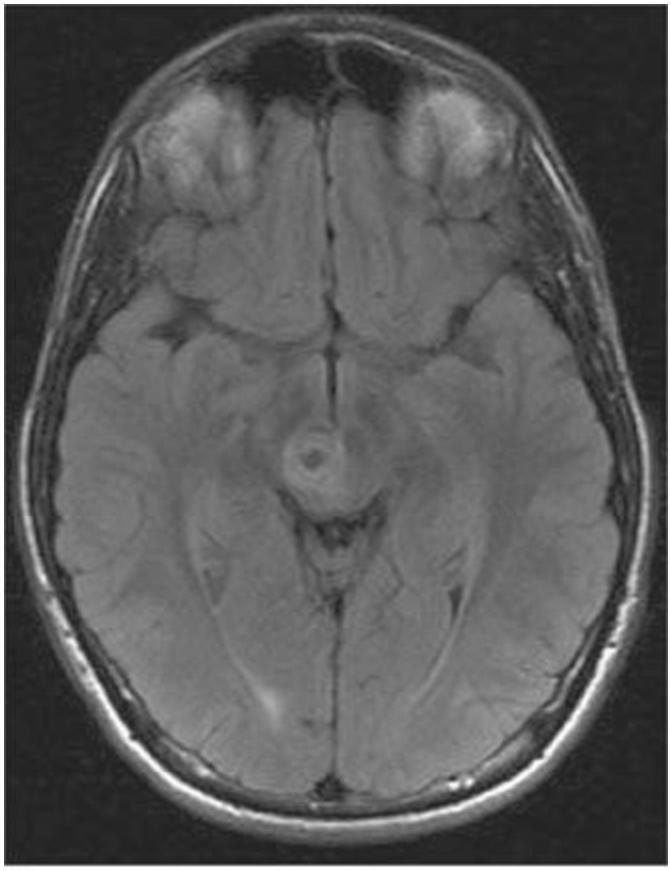

B

■**FIGURE 6-14B** Axial FLAIR image show that the central portion of the mass has hypointense signal.

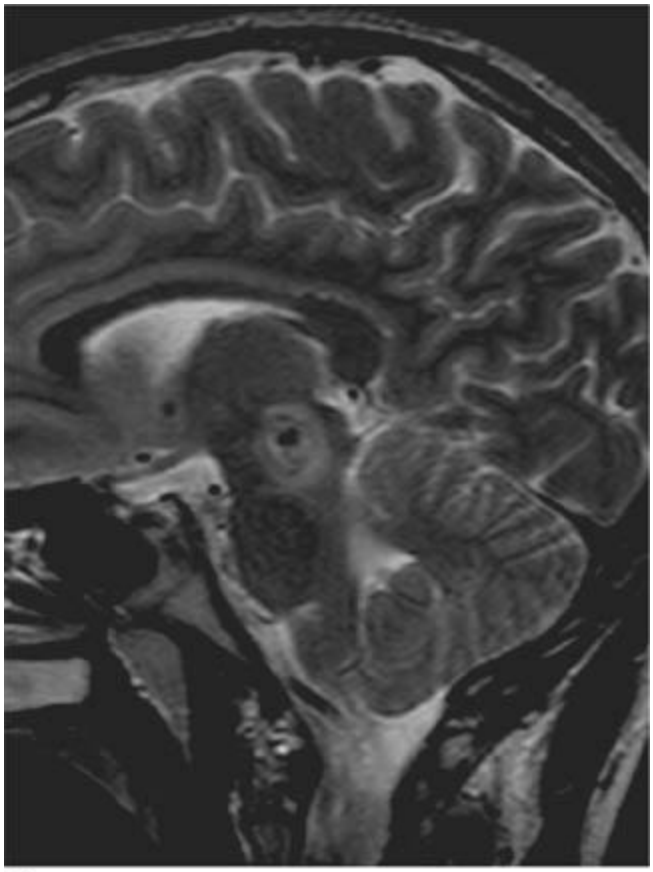

C

■**FIGURE 6-14C** Sagittal T2-weighted image again shows a central hypointense region within the mass as well as a peripheral hyperintense rim.

D

**FIGURE 6-14D** Sagittal contrast-enhanced T1-weighted image shows that the mass does nto contrast-enhance. However, a stellate array of contrast-enhancing vessels jusr posterior to the mass is seen terminating at a point in the tectum.

## DIFFERENTIAL DIAGNOSIS

**Hemorrhagic brainstem injury:** Although a hemorrhagic contusion could account for the region of hypoin-tense signal on the FLAIR and T2-weighted images, no history of head trauma is given. Furthermore, this diagnosis would not account for the unusual array of vessels seen. This diagnosis is incorrect.

**Hemorrhagic neoplasm:** This diagnosis would be more likely if the lesion contrast-enhanced. Furthermore, the prominent vessels would not be explained by a neoplasm. This diagnosis is incorrect.

**Arteriovenous malformation (AVM):** Although the central region of hypointense signal could represent hemorrhage due to the presence of an AVM, a tangle of abnormal vessels would be expected, rather than the somewhat organized array of vessels seen here. This diagnosis is unlikely.

**Cavernous angioma:** This diagnosis would explain the region of hypointense signal, which is due to hemorrhage. The array of vessels in the tectum represents a venous

angioma, with which cavernous angiomas are associated. This diagnosis is correct. The central hypointense lesion on T2-weighting imaging shown in this case is seen less commonly than the more characteristic complex appearance of alternating regions of hyperintense and hypointense signal (so-called mulberry-like appearance).

## DIAGNOSIS

**Cavernous angioma with an associated venous angioma**

## KEY FACTS

### Clinical

- Cavernous angiomas consist of a cluster of enlarged vascular channels lacking intervening brain parenchyma. Unlike AVMs, cavernous angiomas do not have a nidus of abnormal vessels with well-defined feeding arteries and draining veins.
- Cavernous angiomas can be either sporadic or familial in nature.
- Multiple angiomas are found in 10% to 15% of patients with the sporadic variety and about 75% of those with the familial form.
- Symptom onset is typically in young adulthood. The most common clinical features are seizures (40% to 70% of patients), headache, and, on occasion, sudden onset of neurologic deficit.
- Cavernous angiomas, especially those located in the posterior fossa, are often found in association with venous angiomas, which are benign venous developmental abnormalities.
- Multiple cavernous angiomas often indicate a family history of such lesions.
- Histologic examination of these lesions shows a cluster of thin-walled (often thrombosed and calcified) vascular channels that are not separated from one another by brain tissue.
- The rate of hemorrhage of cavernous angiomas has been determined to be between 0.25% and 0.70% per person year of exposure. The rates are higher for brainstem lesions and basal ganglia lesions.
- Symptomatic cavernous angiomas that are superficial are often resected if they are not located in eloquent brain tissue. Brain stem lesions may be treated by excision or by stereotactic radiosurgery. Factors reportedly associated with a poor prognosis for surgical excision include large size (i.e., >2 cm), poor initial neurologic status, and >2 prior neurologic events or hemorrhages.

### Radiologic

- Cavernous angiomas are usually <2 cm in size but occasionally can be larger, particularly when substantial hemorrhage has occurred.
- These lesions are frequently found incidentally on MRI or CT studies performed for unrelated symptoms.
- These lesions are almost always occult on angiography, although rarely a small vascular blush (without arterial feeders or early draining veins) can be seen.
- On CT, these lesions can be seen as well-circumscribed, frequently hyperdense lesions that often have one or more small foci of calcification due to previous hemorrhage. Often, however, lesions are isodense with brain, especially if they are small or have not undergone hemorrhage.
- These lesions typically do not contrast-enhance to a large degree on CT or MRI.
- Edema is typically not seen surrounding cavernous angiomas unless they have recently undergone a substantial amount of hemorrhage.
- MRI is very helpful in confirming the diagnosis when it is suspected on CT because MR can show multiple lesions (making the diagnosis more likely) and reveal the typical hemosiderin rim around lesions.
- On T2-weighted MR images, cavernous angiomas typically have alternating regions of hyperintense and hypointense signal, representative of hemorrhages of different ages. Often a hypointense rim due to the presence of hemosiderin is seen around the margins of the lesion.
- Lesions typically have a focus of hypointense signal on T2-weighted images due to the presence of chronic blood products. The conspicuity of lesions and the number of lesions is generally much greater on gradient-echo images and susceptibility-weighted images compared to T2-weighted images.
- On occasion, cavernous angiomas can be difficult to distinguish from primary or secondary brain tumors. The presence of multiple lesions is helpful in excluding a primary tumor. The presence of calcification on CT or a characteristic hemosiderin rim on MRI (both features expected with cavernous angiomas but not with metastases) is helpful in making the distinction.

## SUGGESTED READING

Gabriel RA, Kim H, Sidney S, et al. Ten-year detection rate of brain arteriovenous malformations in a large, multiethnic, defined population. Stroke 2010;41:21–26.

Lehnhardt FG, von Smekal U, Ruckriem B, et al. Value of gradient-echo magnetic resonance imaging in the diagnosis of familial cerebral cavernous malformation. Arch Neurol 2005;62:653–658.

Huang APH, Chen JS, Yang CC, et al. Brain stem cavernous malformations. J Clin Neurosci 2010;17:74–79.

Cooper AD, Campeau NG, Meissner I. Susceptibility-weighted imaging in familial cerebral cavernous malformations. Neurology 2008;71:382.

Schlamann M, Maderwald S, Becker W, et al. Cerebral cavernous heman-giomas at 7 Tesla: initial experience. Acad Radiol 2010;17:3–6.

# CASE 15

**JAMES M. PROVENZALE AND ROBERT TIEN**

## HISTORY

A 28-year-old woman with headache and ataxia.

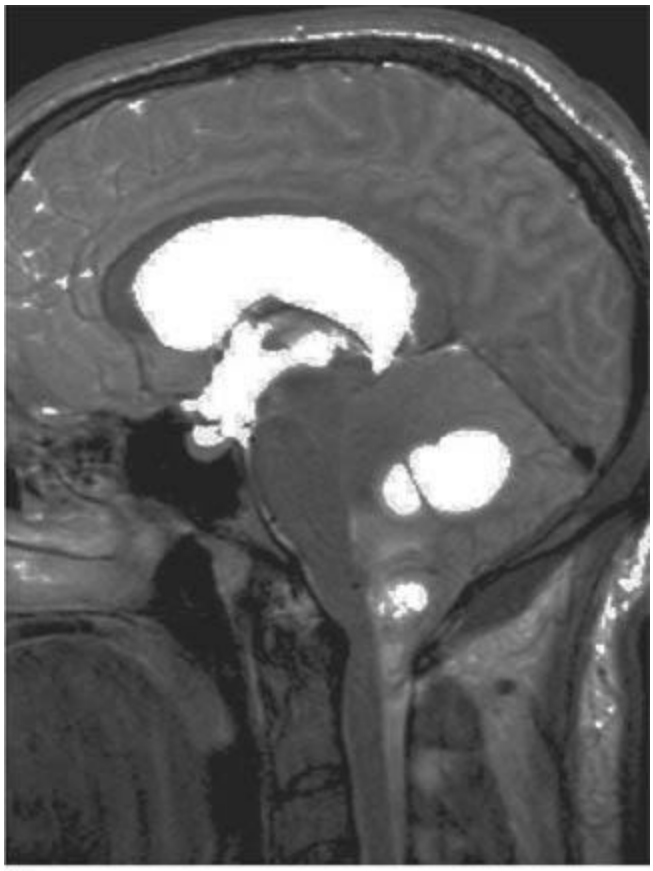

A

■**FIGURE 6-15A** Sagittal T2-weighted image shows multiple cystic masses within the cerebellum.

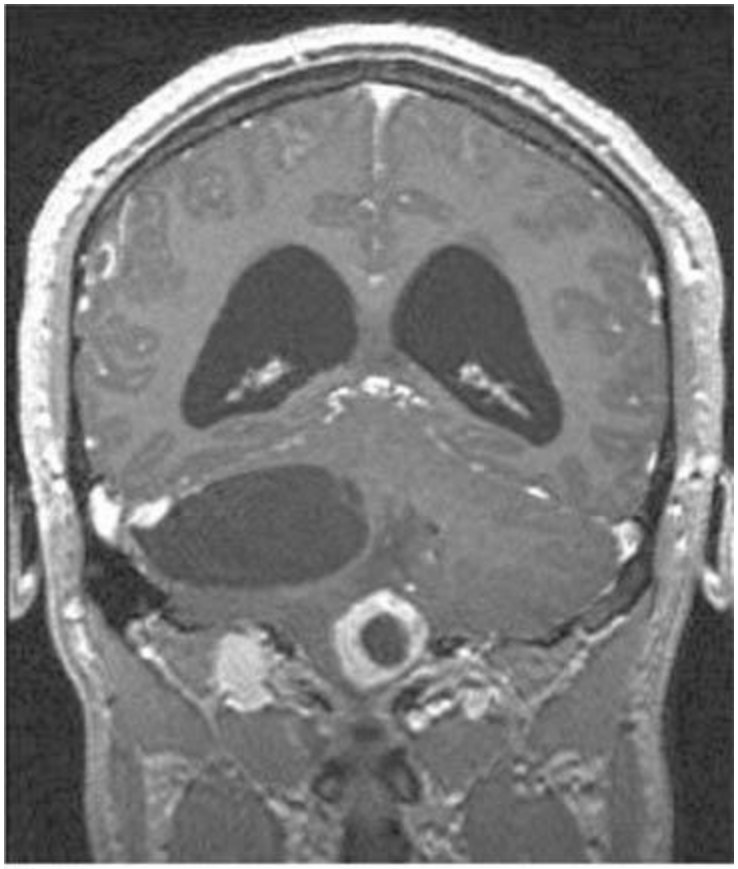

B

■**FIGURE 6-15B** Coronal contrast-enhanced T1-weighted image shows a mass in the right cerebellar hemisphere that is predominantly cystic with a small enhancing region and another mess in the inferior vermis that has a thick enhancing rim.

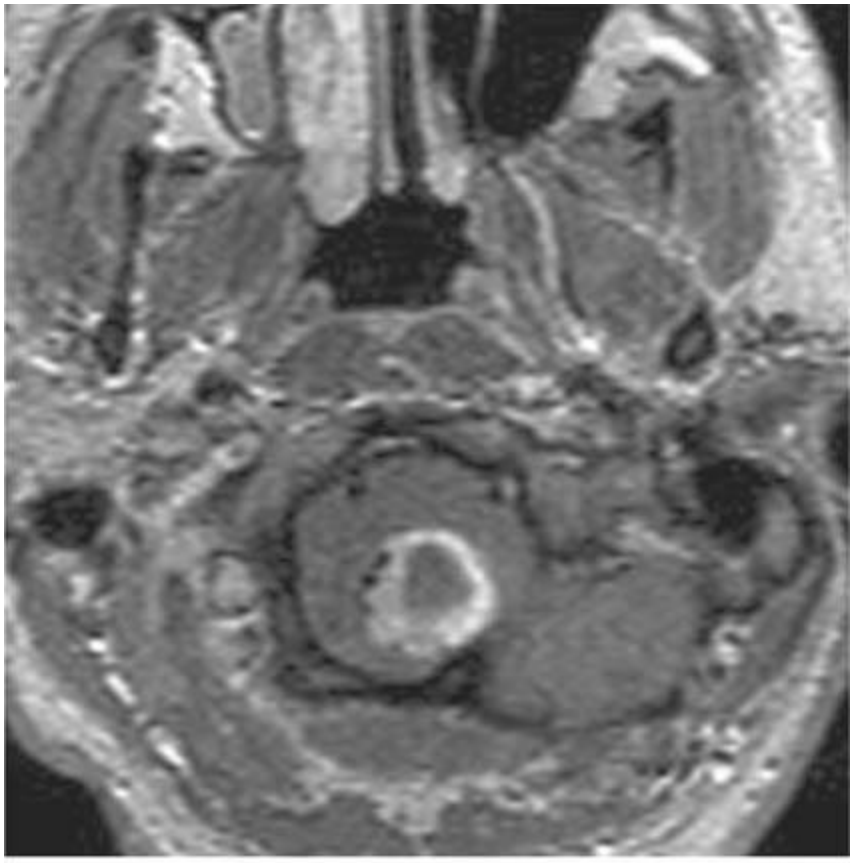

C

■**FIGURE 6-15C** Axial contrast-enhanced T1-weighted image shows that the inferior vermian mass has adjacent flow voids.

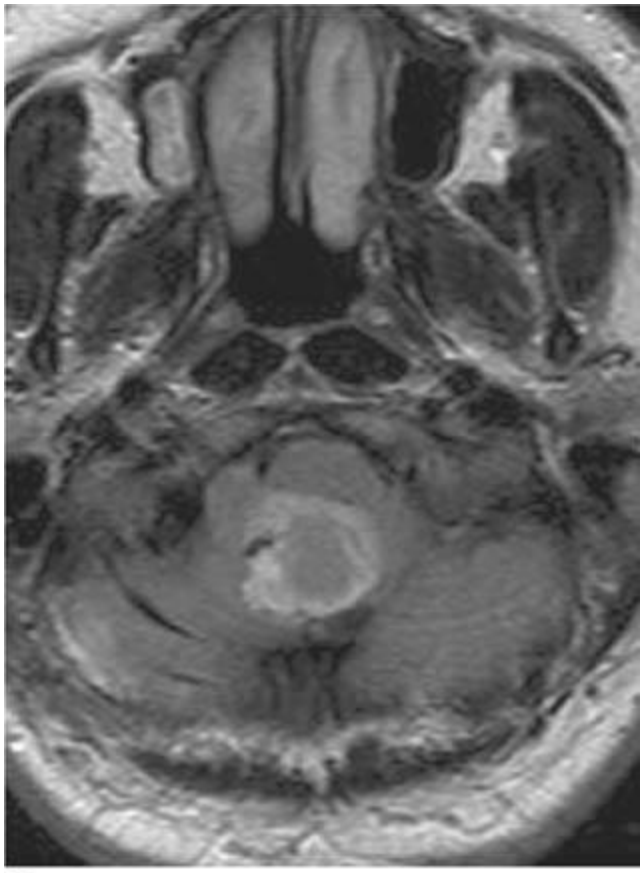

D

**FIGURE 6-15D** Axial FLAIR image again shows the flow voids adjacent to the mass. Note that on this pulse sequence the signal intensity of the cyst is not the same as that of pure water.

## DIFFERENTIAL DIAGNOSIS

**Metastasis:** This diagnosis might be considered because multiple lesions, some of which are rim enhancing, are present. Because most metastases occur in the supratentorial compartment, the appearance shown here would be very uncommon for metastases. This diagnosis is unlikely.

**Abscess:** This diagnosis might be considered because one of the lesions shown is rim-enhancing, which is common in abscesses. However, another lesion consists predominantly of a fluid-filled compartment with an adjacent small contrast-enhancing region, which would be unusual for an abscess. This diagnosis is unlikely.

**Juvenile pilocytic astrocytoma:** This tumor is a relatively common posterior fossa neoplasm in children. However, the patient illustrated here is an adult and this type of tumor is uncommon in adults. Furthermore, this tumor is almost always solitary whereas, in the case shown here, multiple lesions are present. This diagnosis is incorrect.

- **Hemangioblastoma:** Hemangioblastoma is a reasonable consideration because, when intracranial, they typically occur in the cerebellum. In addition, these tumors often have the appearance of a large cyst with an adjacent mural nodule (as seen in Figure 6-19B). Because these tumors are extremely vascular, they often can be seen to have adjacent flow voids (Figures 6-19C and 6-19D). This diagnosis is correct.

## DIAGNOSIS

**Hemangioblastoma**

## KEY FACTS

### Clinical

- Hemangioblastoma is a benign tumor of the CNS accounting for 1.0% to 2.5% of all intracranial neoplasms.
- The most common age at the time of discovery is the third through fifth decades. There is not a strong predilection for either gender.
- Many patients with hemangioblastomas have an inherited genetic disorder termed von Hippel-Lindau (VHL). Diagnostic criteria include at least one CNS heman-gioblastoma in association with one of the following features: multiple cysts or neoplasms of the visceral organs or a family history of VHL.
- Sites of VHL visceral organ system involvement include kidneys (cysts, renal cell carcinoma), pancreas (multiple cysts, microcystic adenoma or adenocarcinoma), adrenal gland (pheochromocytoma, which can also occur at other sites), epididymis (cysts), and liver (adenomas, cysts).
- Polycythemia is seen in some cases due to secretion of erythropoietin by the tumor.
- Clinical features related to CNS hemangioblastomas are usually related to peritumoral edema and mass effect from tumoral cysts (rather than from solely the solid portions of tumors).
- The most common symptoms and signs are headache (75% of symptomatic patients), and cerebellar signs such as ataxia (55%), and dysmetria (29%).

### Radiologic

- One-third of hemangioblastomas have a purely solid structure, one-third have a characteristic cyst with peripheral mural nodule (Figure 6-19B), and the remainder are cystic but with a more complex solid component than a simple mural nodule.
- In VHL, hemangioblastomas are three-times more likely to be located in the posterior

half of the cerebellum than in the anterior half and 20 times more likely to be in the posterior half of the spinal cord as compared to the anterior half.

- The distribution of hemangioblastomas in VHL is as follows: approximately 45% in the spinal cord, 45% in the cerebellum, 9% in the brainstem (almost always in the posterior medulla oblongata), and 1% in the supraten-torial brain. Almost all symptomatic spinal hemangio-blastomas are associated with syringomyelia.
- Complete evaluation of patients with VHL should include MR imaging of both the brain and spine.
- The presence of a cyst is an important factor determining whether a hemangioblastoma causes symptoms; about 75% of symptomatic lesions have cysts.
- Hemangioblastomas are often asymptomatic and many do not require treatment. Even tumors that are enlarging frequently do not require treatment if they are asymptomatic.
- In VHL, the growth rate of hemangioblastomas differs widely even within the same patient. The growth of lesions that become symptomatic is usually many times faster than lesions that remain asymptomatic; in symptomatic lesions, growth of the cyst is usually much faster than the solid component.
- On unenhanced CT and FLAIR MR imaging, the cyst contents can often be seen to differ slightly from CSF due to high protein content.
- Solid components of hemangioblastomas densely contrast-enhance on CT and MR imaging due to their high vascular-ity associated with breakdown of the blood-brain barrier.
- On MR imaging, flow voids can sometimes be seen within solid portions of hemangioblastomas due to (1) either feeding or draining vessels, or (2) large sinusoids within the tumor.
- At catheter angiography, the solid component is seen to have enlarged feeding arteries and densely stain with contrast material. Cystic portions of the tumor are seen as avascular regions next to the nodule.
- The rate of spontaneous hemorrhage is proportional to size of the solid portion of the tumor; lesions <1.5 cm have virtually no risk of hemorrhage.
- On MR perfusion imaging, hemangioblastomas have a very high relative cerebral blood volume, exceeding even that of high-grade gliomas.

## SUGGESTED READING

Jagannathan J, Lonser RR, Smith R, et al. Surgical management of cerebellar hemangioblastomas in patients with von Hippel-Lindau disease. J Neurosurg 2008;108:210–222.

Wanebo JE, Lonser RR, Glenn GM, Oldfield EH. The natural history of hemangioblastomas of the central nervous system in patients with von Hippel-Lindau disease. J Neurosurg 2003;98:82–94.

Ammerman JM, Lonser RR, Dambrosia J, et al. Long-term natural history of hemangioblastomas in patients with von Hippel-Lindau disease: implications for treatment. J Neurosurg 2006;105:248–255.

Hakyemez B, Erdogan C, Bolca N, et al. Evaluation of different cerebral mass lesions by perfusion-weighted MR imaging. J Magn Reson Imaging 2006;24:817–824.

# CASE 16

**JAMES M. PROVENZALE AND FERNANDO M. ZALDUONDO**

## HISTORY

A 57-year-old man with a 1-week history of severe headache.

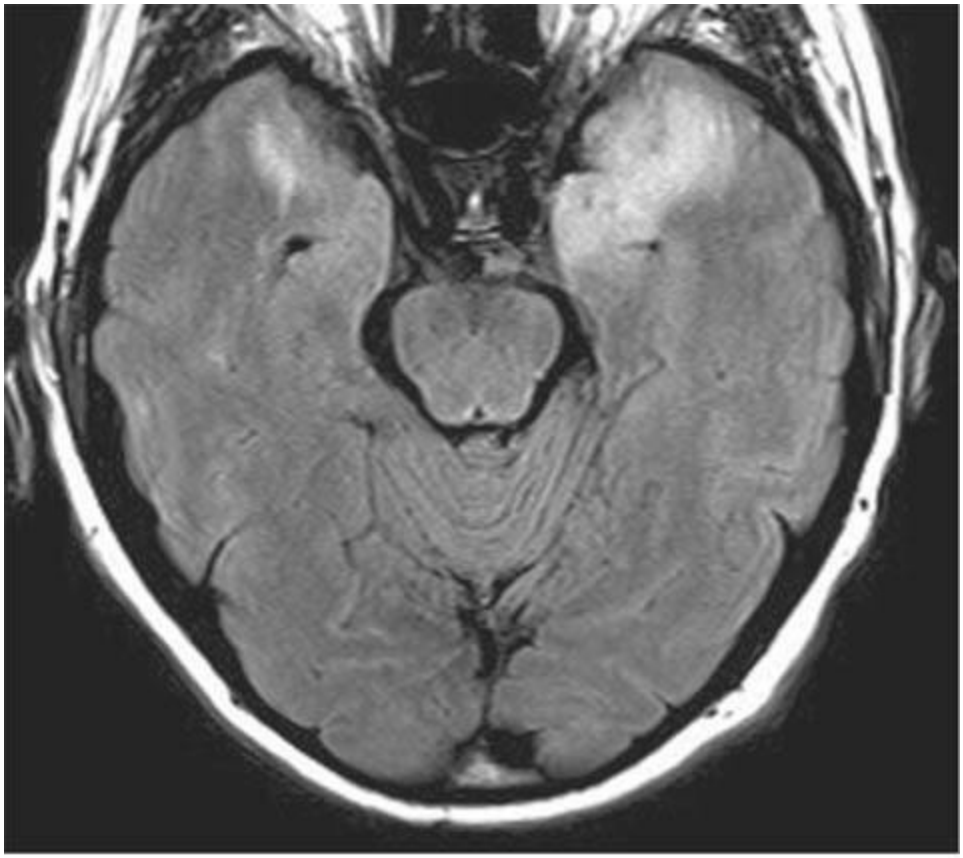

A

■**FIGURE 6-16A** Axial FLAIR image shows a large focus of increased signal intensity in the anterior aspect of the left temporal lobe. A smaller region of abnormal signal is also present in the right temporal lobe.

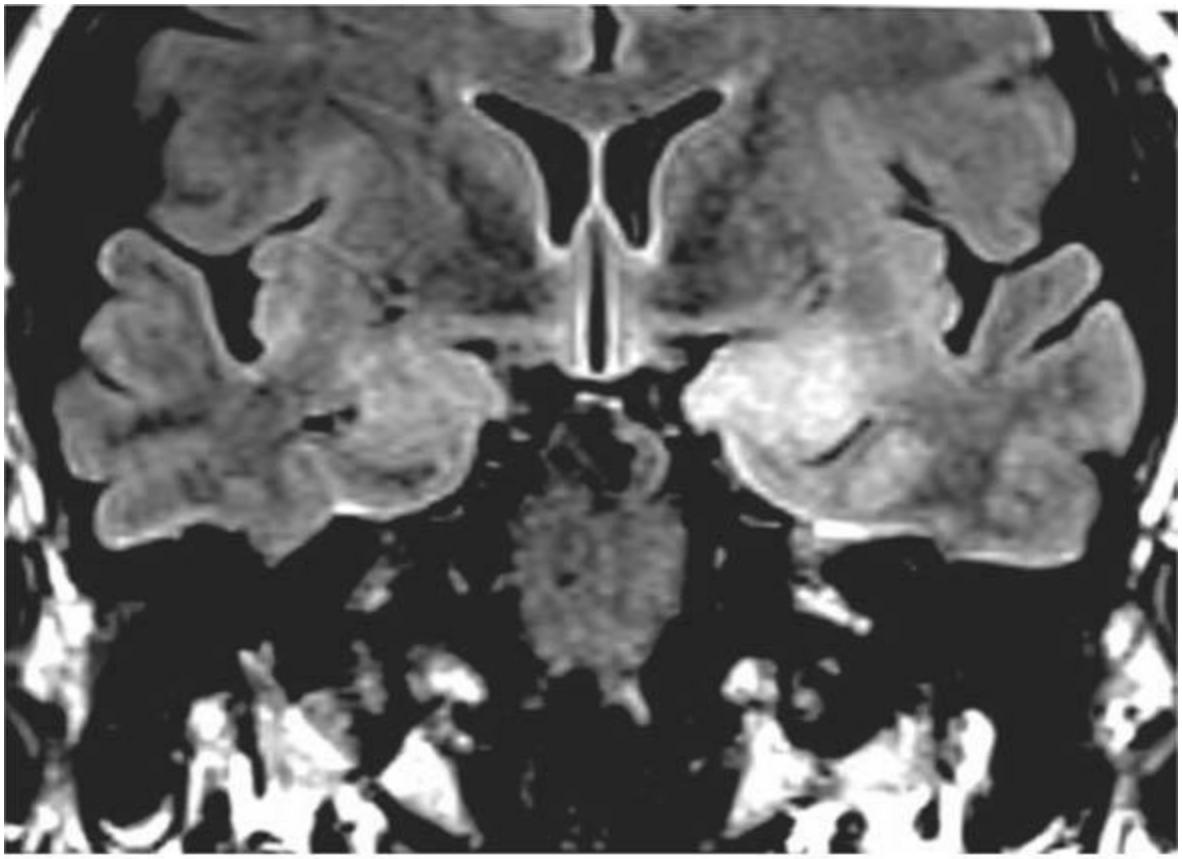

B

■**FIGURE 6-16B** Coronal FLAIR image shows that the most intense signal abnormality is present in the medial aspect of the left temporal lobe.

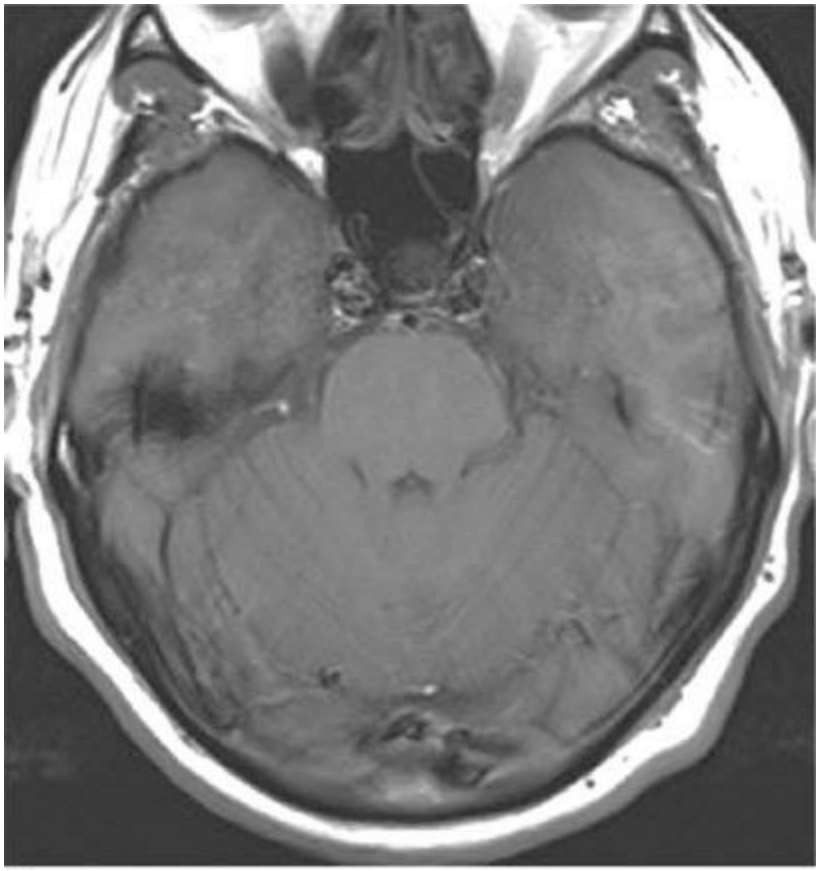

C

■**FIGURE 6-16C** Unenhanced axial T1-weighted image shows a subtle region of decreased signal intensity in the anterior aspect of the left temporal lobe.

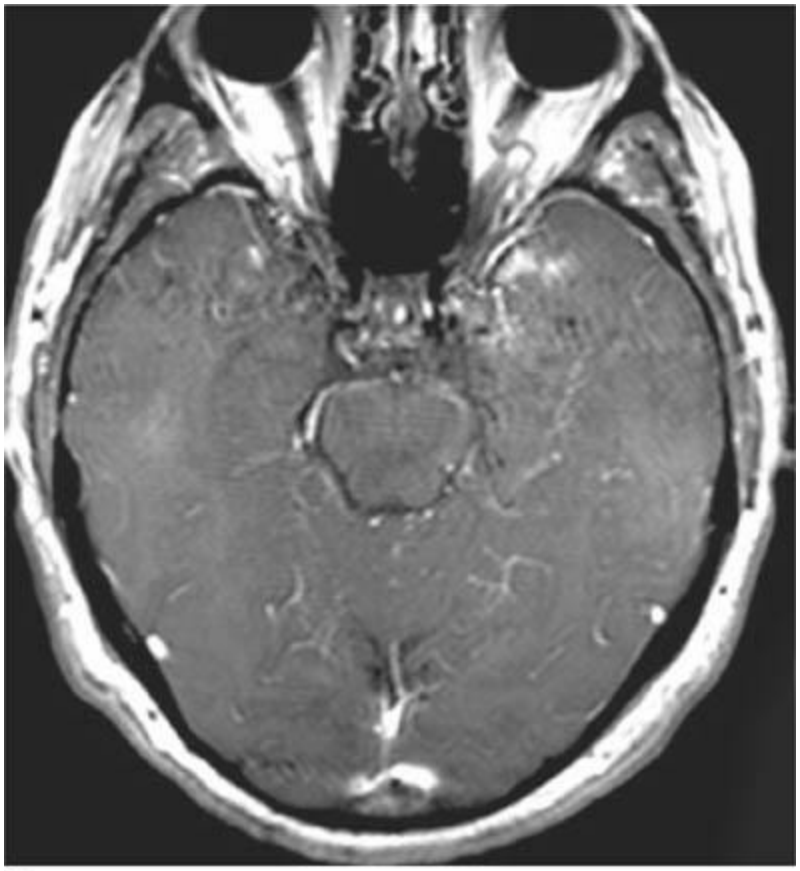

D

**FIGURE 6-16D** Contrast-enhanced axial T1-weighted image shows a region of contrast-enhancement in the medial aspect of the left temporal lobe. A very small focus of contrast-enhancement is also present in the right temporal lobe.

## DIFFERENTIAL DIAGNOSIS

**Temporal lobe contusion:** This diagnosis might be considered because the anterior aspect of the temporal lobe is a common location for temporal lobe contusions. However, no history of head trauma is presented here. Furthermore, much of the abnormal signal intensity is present in the medial portions of the temporal lobes, which would be unusual for contusion. Finally, although contrast-enhancement can occasionally be seen in contusions, it is relatively rare. This diagnosis is incorrect.

**Infarction:** Infarction confined to the anterior portion of the temporal lobe is unusual. Instead, infarction usually involves either the lateral two-thirds of the temporal lobe (middle cerebral artery territory) or the medial third of the temporal lobe and the occipital lobe (posterior cerebral artery territory). This diagnosis is unlikely.

**Tumor:** Some tumors, for example, low-grade infiltrating gliomas, can produce abnormal signal intensity in the absence of contrast-enhancement. However, the presence of abnormal signal intensity in both temporal lobes would be very unusual for

a tumor. This diagnosis is unlikely.

- **Herpes simplex virus type 1 (HSV 1) encephalitis:** Predominant involvement of the medial temporal lobe (Figure 6-17B) is typically seen in HSV 1 encephalitis. Furthermore, involvement of both temporal lobes is also characteristic of this diagnosis. This diagnosis is correct.

## DIAGNOSIS

**Herpes simplex virus type 1 encephalitis**

## KEY FACTS

### Clinical

- The term *encephalitis* refers to a diffuse parenchymal inflammatory process that may be caused by a wide variety of etiologies, but most commonly has a viral etiology.
- The most common cause of nonepidemic acute viral encephalitis in immunocompetent patients in the United States and Europe is HSV 1 (oral strand) infection. However, HSV 1 accounts for only about 10% of viral encephalitides.
- Nearly all adults have been exposed to this virus, which is responsible for "cold sores."
- HSV 1 encephalitis is thought to usually result from reactivation of latent viral infection of the trigeminal ganglion. The infection extends in a retrograde fashion along the meningeal innervation of the middle cranial fossa and inferior portion of the anterior cranial fossa.
- Clinical features include seizures, encephalopathy, headache, and low-grade fever.
- Because untreated HSV 1 encephalitis has a high mortality rate, prompt treatment with acyclovir is essential. Therapy is often started before the definitive diagnosis is established. Presently, polymerase chain reaction for identification of viral particles within CSF is considered the most appropriate diagnostic test.

### Radiologic

- The earliest CT findings, seen during the first few days after onset of overt symptoms, consist of hypodensity in one or both temporal lobes, typically in the medial portions. Over the course of the next few days, similar changes can be seen in the insula and inferior frontal lobes. Contrast-enhancement is often absent or only mild. When present, contrast-enhancement is often confined to small areas and sometimes follows a gyriform pattern.
- MRI is more sensitive than CT in establishing the early diagnosis. MR findings

include temporal lobe swelling and hyperintense lesions on T2-weighted images in the same regions as described for CT. In comparison to CT, MRI shows the lesions earlier and shows more widespread involvement. As on CT, little or no contrast-enhancement is typically seen.

- The bilateral involvement often seen in HSV 1 encephalitis is a useful feature in distinguishing this entity from a neoplasm and cerebral infarction.
- Similar to infarction, HSV 1 encephalitis lesions can appear bright on diffusion-weighted images due to restricted diffusion.
- Sparing of the basal ganglia has been described as a useful feature in helping to distinguish HSV 1 encephalitis from infarction. Furthermore, presence of bilateral lesions is helpful because bilateral temporal infarctions are uncommon.
- HSV 1 infection (as opposed to neonatal HSV 2 infection) in infants typically follows a different distribution pattern in adults. Usually, the periventricular white matter of both cerebral hemispheres is involved and the temporal lobes are spared.
- Proton MR spectroscopy findings in HSV 1 encephalitis are nonspecific and mimic those found in many other CNS disease states; these findings include decreased n-acetylaspartate and elevated levels of choline, lip-ids, and lactate. The changes may reverse following therapy.

## SUGGESTED READING

Sawlani V. Diffusion-weighted imaging and apparent diffusion coefficient evaluation of herpes simplex encephalitis and Japanese encephalitis. J Neurol Sci 2009;287:221–226.

Leonard JR, Moran CJ, Cross DT III, et al. MR imaging of herpes simplex type 1 encephalitis in infants and young children: a separate pattern of findings. AJR Am J Roentgenol 2000;174:1651–1655.

Baskin HJ, Hedlund G. Neuroimaging of herpesvirus infections in children. Pediatr Radiol 2007;37:949–963.

# CASE 17

**JAMES M. PROVENZALE**

### HISTORY

A 22-year-old woman with paraparesis and headache.

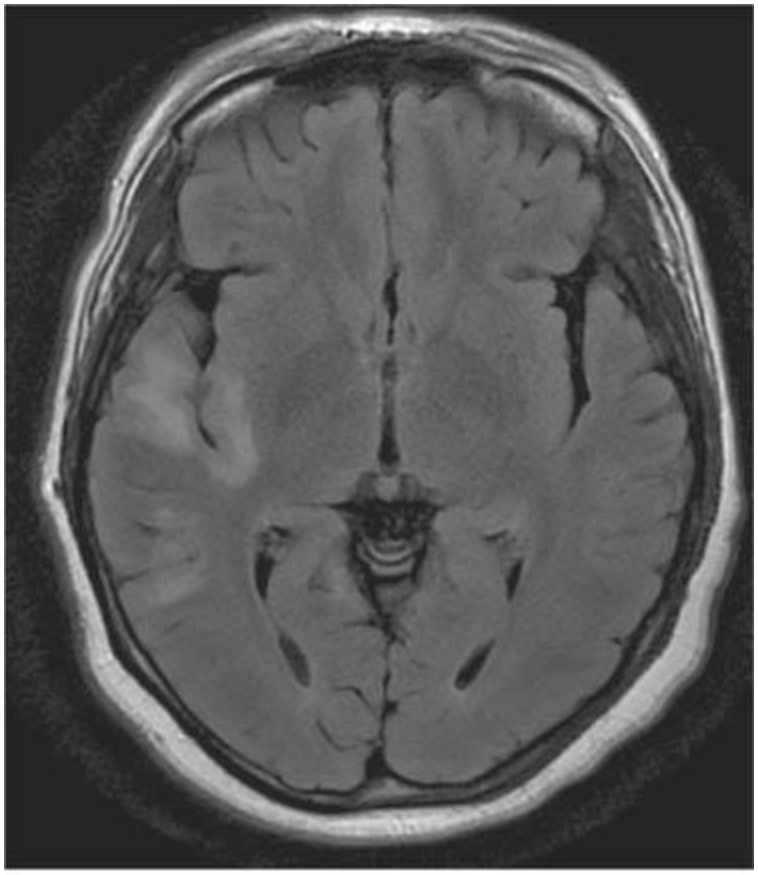

A

■**FIGURE 6-17A** Axial FLAIR image shows hyperintense signal within right temporal lobe and right insula.

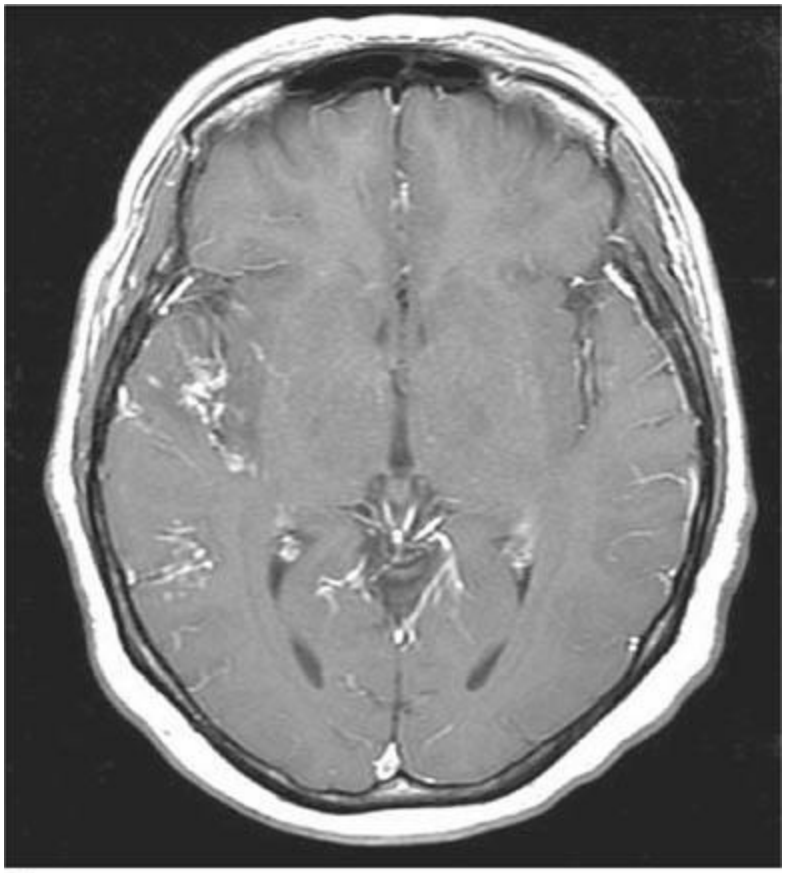

B

■**FIGURE 6-17B** Contrast-enhanced axial T1-weighted image shows prominent leptomeningeal enhancement adjacent to the regions of hyperintense signal shown in Figure 6-17A.

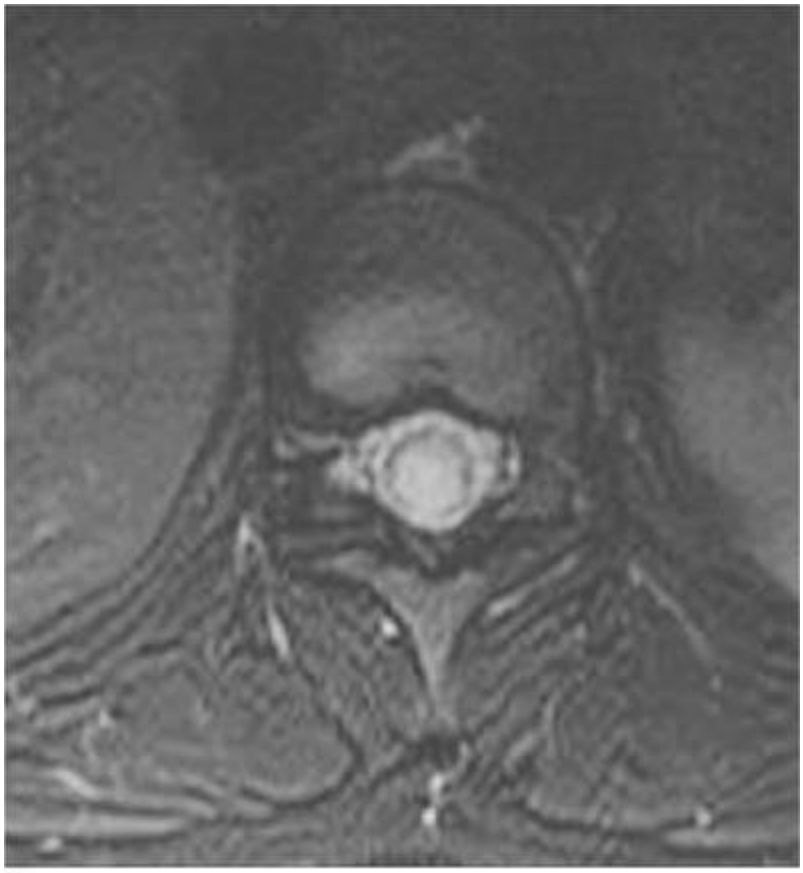

C

■**FIGURE 6-17C** Axial T2-weighted image at the level of the T9 vertebral body shows hyperlntense signal within an enlarged spinal cord.

D

**FIGURE 6-17D** Sagittai contrast-enhanced T1-weighted image show a large area of contrast-enhancement of the spinal cord in the region shown in Figure 6-17C.

## DIFFERENTIAL DIAGNOSIS

**Leptomeningeal carcinomatosis:** This diagnosis is unlikely in the absence of a prior history of a non-CNS neoplasm. Furthermore, this diagnosis would not account for the hyperintense signal present in brain parenchyma and spinal cord. This diagnosis is incorrect.

**Viral meningitis:** Leptomeningeal enhancement due to viral meningitis is typically thin, unlike the relatively thick and nodular contrast-enhancement seen in the case shown here. Furthermore, viral meningitis would not be expected to produce the spinal cord findings in the case shown here.

**Tuberculous meningitis:** This diagnosis should be strongly considered because tuberculous meningitis frequently produces thick exudates involving the lepto-meninges on the undersurface of the brain. Although, tuberculosis can produce spinal cord lesions of the type shown in this case, spinal cord lesions are much less common than involvement of the vertebral column. Nonetheless, tuberculosis cannot be definitively excluded on the basis of imaging features in the case shown above. Instead, clinical and

laboratory data (including CSF analysis) would need to be evaluated. In the case shown here, the CSF did not stain positive for acid-fast bacilli and biopsy of the leptomeninges excluded tuberculosis.

- **Neurosarcoidosis:** This disease entity has a predilection for involvement of the leptomeninges. Furthermore, spinal cord involvement is relatively common in neurosarcoidosis. In general, the diagnosis can be inferred on the basis of known extra-CNS sarcoid-osis or directly obtained by biopsy of the leptomen-inges or brain. In the case shown here, the patient had no extra-CNS symptoms or signs and the diagnosis was established by removal of the spinal cord mass, which was found to represent a noncaseating granuloma.

## DIAGNOSIS

**Neurosarcoidosis**

## KEY FACTS

### Clinical

- Sarcoidosis is an idiopathic systemic disease characterized by formation of noncaseating granulomas in multiple organ systems. The disease usually affects young adults in the third or fourth decade of life, who usually present clinically with insidious onset of malaise, weight loss, and fatigue.
- Only about 5% to 10% of patients have CNS symptoms, but 25% of patients have findings of CNS involvement at autopsy. Importantly, a substantial proportion of patients (10% to 40%) develop CNS symptoms prior to diagnosis of sarcoidosis. In 10% to 15% of all sarcoid-osis patients, clinical findings are isolated to the CNS, even years after diagnosis.
- Cranial neuropathy (especially seventh nerve paresis) is the most common neurologic manifestation, seen in more than half of patients with CNS disease.
- CNS symptoms usually begin approximately 2 years after the onset of systemic disease. The predilection of the disease to involve the midline structures at the base of the brain is reflected by the symptom distribution outlined below.
- Aseptic meningitis due to granulomatous infiltration of the leptomeninges is seen in about 20% of patients with neurosarcoidosis.
- Neuroendocrinological dysfunction due to infiltration of the hypothalamus or pituitary gland and stalk is seen in about 20% of patients with CNS involvement.
- Spinal disease manifestations are seen in about 5% of patients with neurologic disease and can have a wide variety of presentations. Myelopathy can be due to spinal cord

compression by leptomeningeal disease or granulomatous infiltration of the spinal cord (as seen in Figures 6-16C and 16D).

- The clinical diagnosis of neurosarcoidosis is based on typical neurologic features, histopathological evidence of systemic disease (e.g., from skin, bronchial washings, or lymph nodes), and CSF analysis (typically showing decreased glucose content, elevated protein, and elevated white blood cell count).
- When no systemic manifestations of sarcoidosis are present, the differential diagnosis differs according to the CNS manifestation. Solitary large granulomas can mimic primary brain tumors such as an astrocytoma or a meningioma. Alternatively, when primarily white matter lesions are present, MS and CNS vasculitis are the major diseases to be considered.
- Even when granulomatous inflammation is established on a histological basis, a number of coexistent CNS infections must be considered, including infections by bacterial (e.g., tuberculosis), fungal (e.g., cryptococco-sis) agents as well as toxoplasmosis.

## Radiologic

- Leptomeningeal contrast-enhancement is the most common finding in neurosarcoidosis. In particular, the basilar meninges are affected, a finding that can simulate tuberculous meningitis. Contrast-enhancement within the Virchow-Robin spaces due to disease extension along the subarachnoid space surrounding small penetrating vessels is a relatively common finding.
- White matter lesions that are hyperintense on T2-weighted MR images and often contrast-enhancing are the most common form of brain parenchymal involvement. These lesions are frequently periventricu-lar or subcortical in location.
- Gray matter lesions within brain cortex and in the deep gray matter structures may be difficult to detect on CT. However, these lesions often contrast-enhance on T1-weighted MRIs and are hyperintense on T2-weighted.
- Involvement of the midline basilar structures—for example, optic chiasm, hypothalamus, and pituitary stalk—is a common feature.
- On occasion, focal epidural masses can be seen. These lesions are usually isointense with brain on unen-hanced T1-weighted images and can have variable signal intensity on T2-weighted images. These lesions can simulate a wide variety of epidural masses, particularly meningiomas.
- Contrast-enhancement of the ventricular lining, representing ependymal involvement, and enhancing intraventricular lesions can sometimes be seen in association with hydrocephalus.
- Spinal disease is less common than brain involvement in neurosarcoidosis. The most

common disease patterns include intramedullary lesions and intrathecal nodular masses over the surface of the spinal cord and nerve roots.

- Patients often have little or no pulmonary disease at the time of CNS symptoms because the patient is beyond the stage of active pulmonary involvement. Therefore, a negative chest radiograph cannot be used as evidence against the diagnosis of neurosarcoidosis.

## SUGGESTED READING

Spencer TS, Campellone JV, Maldonado I, et al. Clinical and magnetic resonance imaging manifestations of neurosarcoidosis. Semin Arthritis Rheum 2004;34:649–661.

Fels C, Riegel A, Javaheripour-Otto K, Obenauer S. Neurosarcoidosis findings in MRI. J Clin Imaging 2004;28:166–169.

Shah R, Roberson GH, Cure' JK. Correlation of MR imaging findings and clinical manifestations in neurosarcoidosis. AJNR Am J Neuroradiol 2009;30:953–961.

Viñas FC, Rengachary S, Kupsky WJ. Spinal cord sarcoidosis: a diagnostic dilemma. Neurol Res 2001;23:347–352.

Nowak DA, Widenka DC. Neurosarcoidosis: a review of its intracranial manifestations. J Neurol 2001;248:363–372.

# CASE 18

**E. RALPH HEINZ AND JAMES M. PROVENZALE**

### HISTORY

A 48-year-old man with numbness in arms and legs and intermittent bowel and bladder dysfunction.

A

■**FIGURE 6-18A** Unenhanced sagittal T1-weighted MR image shows expansion of the cervical segment of the spinal cord by a mass that is isointense to normal spinal cord tissue. A crescentic hypointense region is seen posterior to the mass. The remainder of the spinal cord was normal on all pulse sequences.

B

■**FIGURE 6-18B** Sagittal T2-welghted image shows that the mass is hyperintense on this pulse sequence. The lesion has sharp margins (as seen in the thin rim of hyperintense signal) around the mass and has a less well-defined surrounding region of hyperintense signal consistent with vasogenic edema.

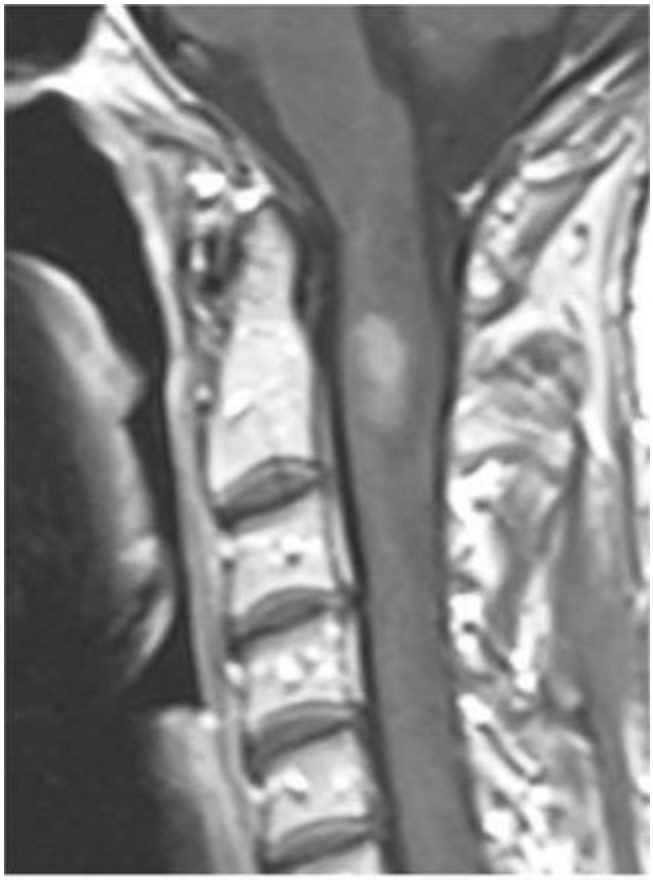

C

■**FIGURE 6-18C** On this contrast-enhanced sagittal T1-weighted MR image, dense contrast-enhancement of the mass is seen.

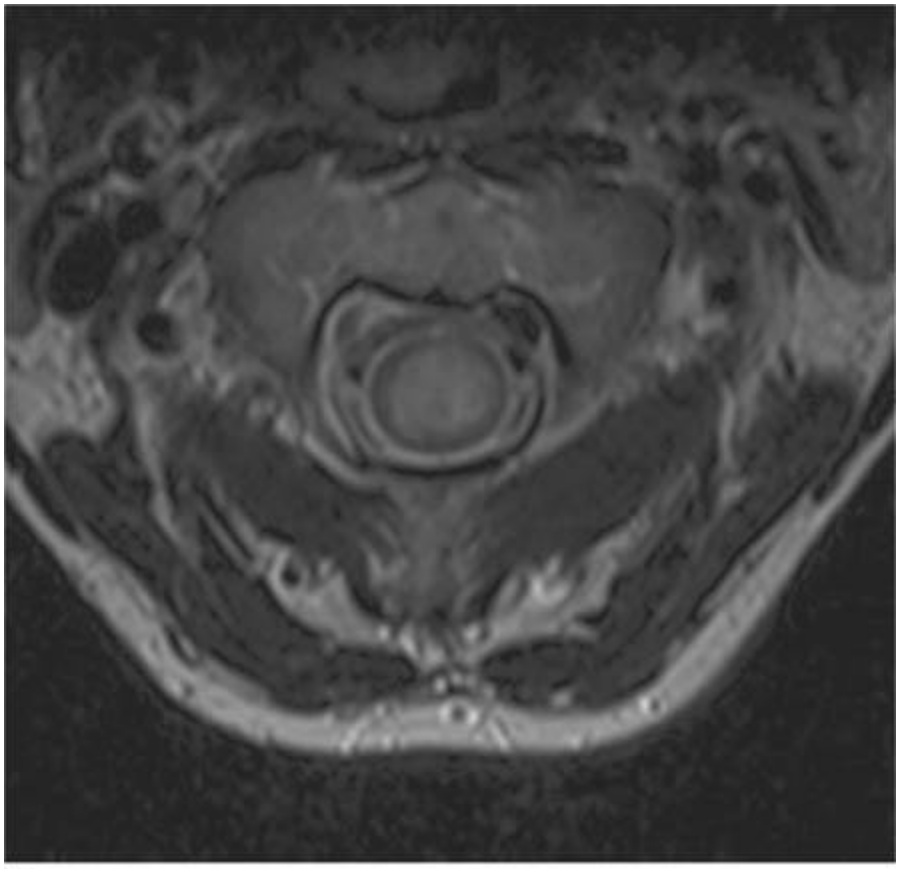

D

**FIGURE 6-18D** Contrast-enhanced axial T1-weighted MR image shows the central portion of the spinal cord contrast-enhances and the peripheral rim of tissue is unenhancing.

## DIFFERENTIAL DIAGNOSIS

**Transverse myelitis secondary to MS:** Transverse myelitis usually appears as a lesion with ill-defined margins and patchy contrast-enhancement (if contrast-enhancement is indeed present). The lesion in the case shown has very well-defined margins and densely contrast-enhances. This diagnosis is unlikely.

**Metastasis:** Intramedullary spinal cord metastases can be seen as focal regions of abnormal signal and, often, contrast-enhancement. However, a single large metastasis would be unlikely, especially in the absence of a history of a non-CNS primary neoplasm.

**Neurosarcoidosis:** This diagnosis can produce a contrast-enhancing mass in the spinal cord (see Case 17). However, a solitary spinal cord mass in the absence of any other brain or spinal cord abnormalities and in the absence of pulmonary disease would be unusual. Although neurosarcoidosis cannot be definitively excluded on the basis of the imaging findings shown here, this diagnosis is unlikely.

- **Cavernous hemangioma:** These lesions are variable in appearance, often seen as inhomogeneous regions of abnormal signal (see Case 14). They are frequently hyperintense on T1-weighted images and have hypointense regions on T2-weighted images. Contrast-enhancement is usually absent or only mild. This diagnosis is incorrect.
- **Spinal cord neoplasm:** Such tumors can be discrete masses with well-defined borders (which favors ependymoma) or infiltrative lesions with ill-defined borders (which favors glioma). Ependymomas occur most frequently in the cervical segment of the spinal cord and often densely and homogeneously contrast-enhance. Gliomas occur most commonly in the thoracic segment of the spinal cord and usually have inhomogeneous contrast-enhancement. Spinal cord ependymoma is the most likely diagnosis.

## DIAGNOSIS

**Spinal cord ependymoma**

## KEY FACTS

### Clinical

- There are three major types of intramedullary spinal cord tumors gliomas, ependymomas, and hemangio-blastomas. The first two are malignant and the third is histologically benign.
- Ependymomas arise from ependymal cells in the central spinal canal. Thus, they tend to be central in location and expand the spinal cord outward. They are soft tumors that usually have a delicate capsule that forms a plane of cleavage that allows surgical excision without damage to spinal cord tissue. They frequently form cysts.
- Spinal cord ependymomas occur with increased incidence in patients with Neurofibromatosis type 2.
- Ependymomas frequently have a sharp cleavage plane at their interface with normal spinal cord tissue, which facilitates their removal. On imaging, this cleavage plane is manifested as a sharp margin (Figure 6-18B).
- Following total removal of the ependymoma, there is only a small chance of recurrence (about 10%). If the absence of a well-defined capsule prevents total excision, tumor progression, often accompanied by metastases to the CSF or even to distant metastases, is common.
- Ependymomas arising in the filum terminale are typically of the myxopapillary type, which are mucinous and may bleed, causing SAH. They may be associated with extremely high levels of protein in the CSF. Such lesions are the most common primary

tumors of the lower spinal cord and the filum terminale. Two-thirds of intramedullary tumors at the conus medullaris are ependymomas.

- Gliomas account for about half of adult spinal cord tumors, but they comprise an even higher percentage of spinal cord tumors in children. The peak incidence is in the third and fourth decade. They are not usually encapsulated, and usually have ill-defined borders. These tumors tend to extend over the length of a few vertebral bodies but can be much longer.
- Hemangioblastoma is a much less common primary spinal cord tumor (about 3%) than glioma and ependymoma. About 30% of patients with spinal cord heman-gioblastoma have VHL syndrome. However, <5% of VHL patients are reported to have spinal hemangioblasto-mas, although the common use of MRI to screen these patients may show that the incidence is, in fact, much higher.
- Most spinal hemangioblastomas are intramedullary. About half are associated with cysts. They are usually associated with dilated veins on the surface of the spinal cord. Development of a long syrinx cavity is very common.

## Radiologic

- Ependymoma tends to arise in the center of the spinal cord and displaces the normal tissue toward the perimeter. The typical appearance is a mass in the center of the spinal cord extending both cephalad and caudad over a number of segments. The lesions generally densely and homogeneously contrast-enhance and have well-defined margins.
- Approximately 65% of spinal cord ependymomas are located either solely in the cervical segment or primarily in the cervical segment with extension into the thoracic segment.
- Approximately 25% of ependymomas have a markedly hypointense rim at one end or the other of the lesion, representing hemosiderin in small foci of chronic hemorrhage; this finding has been referred to as the “cap sign.”
- A cystic component is seen in about 15% of spinal epen-dymomas. Such cysts are reactive, rather than neoplas-tic, and need not be resected at surgery. Instead, these cysts will often decompress during tumor removal or can be simply aspirated.
- If the conus medullaris is involved, as well as the filum terminale, the diagnosis is very likely to be ependy-moma. The probability is further increased if the filum terminale is involved in isolation, in which case the myxopapillary type of ependymoma is highly likely.
- The typical appearance of a spinal cord glioma on MR imaging is an infiltrative mass that has poorly defined borders. Lesions are typically hypointense on T1-weighted images and hyperintense on T2-weighted images. The tumors essentially always contrast-enhance in an inhomogeneous manner; the contrast-enhancement is often less

avid than in ependymomas. Associated cysts are frequently seen at the cranial and caudal ends of the tumor. These cysts are typically benign and do not contrast-enhance. Malignant cystic portions of the tumor, on the other hand, typically rim enhance.

- Hemangioblastomas appear as a focal, markedly enhancing nidus, often with an adjacent cyst and marked edema. A syrinx cavity is quite common. There are frequently very small associated vascular tumor foci elsewhere in the spinal cord, particularly if the patient has VHL. Multiple associated vessels are often seen, particularly on the dorsal aspect of the spinal cord. They can sometimes be seen on myelography as focal enlargement of the spinal cord with serpiginous filling defects due to the presence of vessels on the dorsal surface of the spinal cord. These vessels can be mistaken for evidence of a dural arteriovenous fistula or a spinal cord AVM.

## SUGGESTED READING

Koeller KK, Rosenblum S, Morrison AL. Neoplasms of the spinal cord and filum terminale: radiologic-pathologic correlation. Radiographics 2000;20:1721–1749.

Lowe G. Magnetic resonance imaging of intramedullary spinal cord tumors. J Neuro-Oncol 2000;47:195–210.

Choi JY, Chang KH, Yu IK, et al. Intracranial and spinal ependymomas: review of MR images in 61 patients. Korean J Radiol 2002;3:219–228.

# CASE 19

**JAMES M. PROVENZALE AND DAVID S. ENTERLINE**

### HISTORY

A 38-year-old woman with mental retardation, glaucoma, and choroidal hemangioma in one eye.

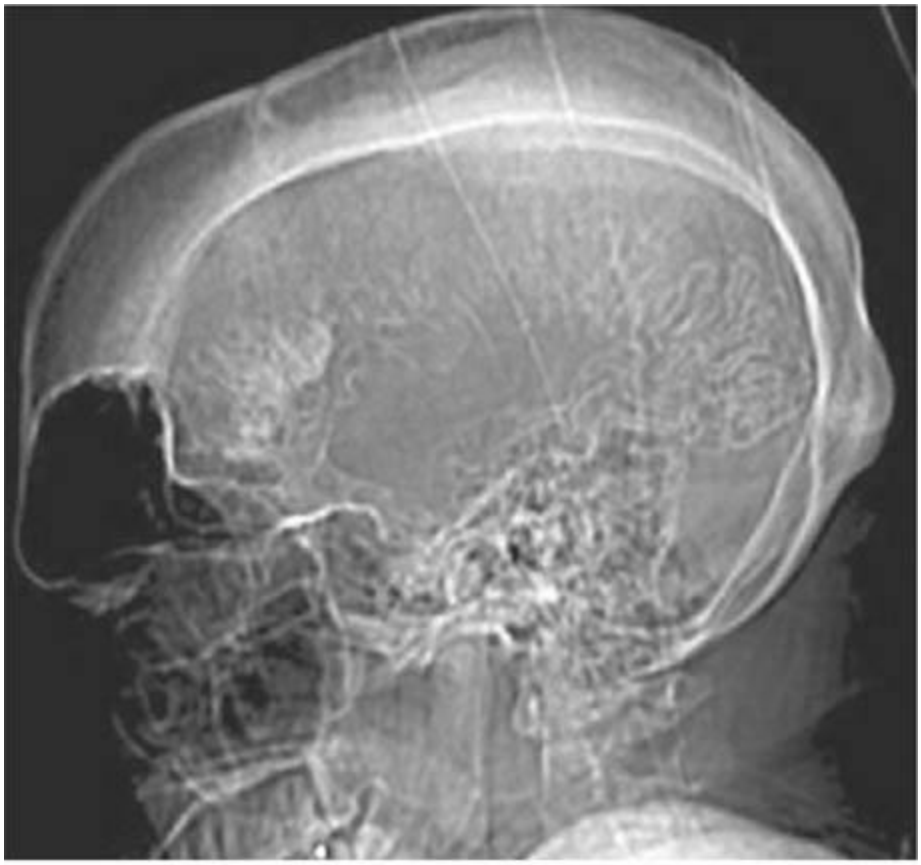

A

■**FIGURE 6-19A** Scanogram image from CT shows multiple serpiginous calcifications that could be located within skull or brain tissue. Prominent thickening of the diploic space and enlargement of the frontal sinuses is present.

B

■**FIGURE 6-19B** Unenhanced axial CT Image shows marked gyriform calcification of the brain cortex, primarily in the left cerebral hemisphere, with global cerebral atrophy.

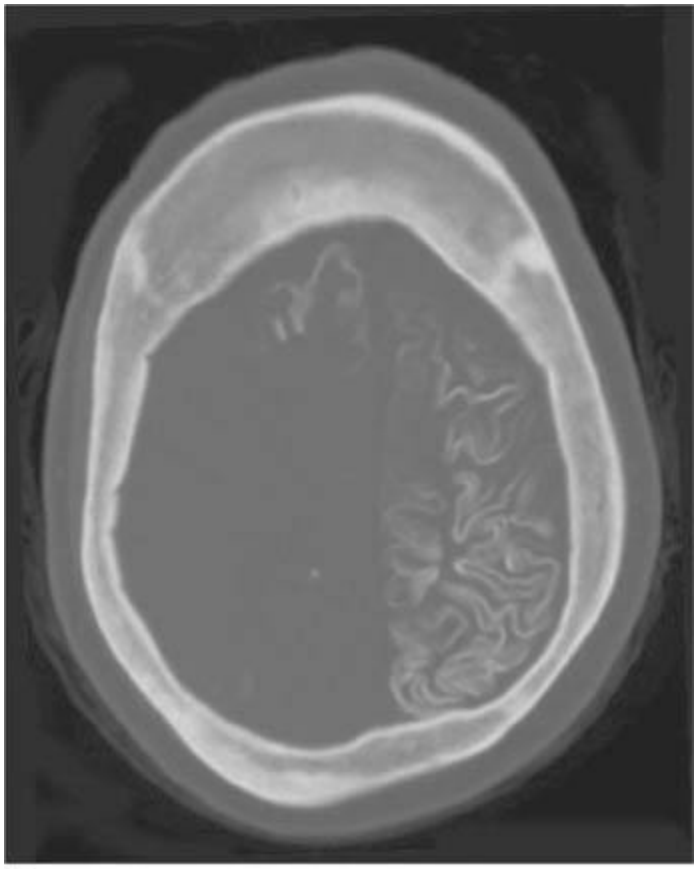

C

■**FIGURE 6-19C** Unenhanced axial CT image at same location as Figure 6-19B using bone window algorithm more clearly delineates the gyriform pattern of calcification of the brain cortex.

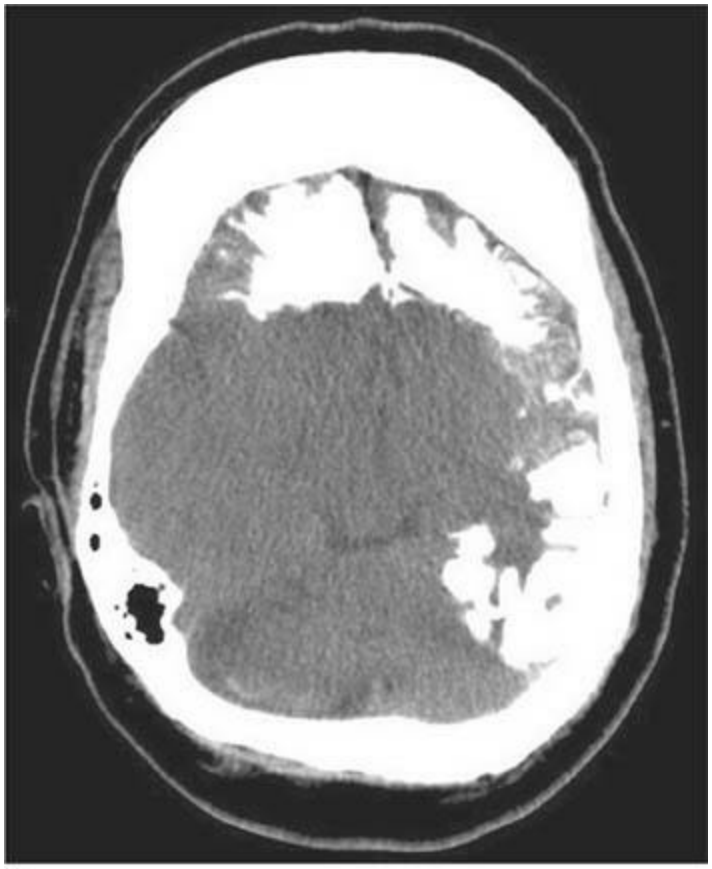

D

**FIGURE 6-19D** Unenhanced axial CT image at a more caudad level depicts more involvement of the brain cortex in the right frontal lobe than on other images.

## DIFFERENTIAL DIAGNOSIS

**Cerebral infarction:** On occasion, gyriform calcification can follow cerebral infarction after many weeks or months (usually in children). However, no findings suggestive of infarction are seen in this case; this diagnosis is unlikely.

**Meningioangiomatosis:** This entity is seen at imaging as leptomeningeal calcification in association with a calcified mass, which is not present in this case. However, in the case shown, the calcification is seen within the brain cortex. This diagnosis is unlikely.

**Sturge-Weber syndrome:** The cortical calcifications, widened diploic space, and brain atrophy in association with the choroidal hemangioma make this diagnosis likely. This patient also has enlargement of the frontal sinuses at a site adjacent to cerebral atrophy, indicating that the atrophy is long-standing.

**Herpes encephalitis:** Small cerebral calcifications can follow a wide variety of in utero or neonatal brain infections, such as toxoplasmosis, cytomegalovirus, rubella, and herpes type 2 encephalitis. In rare instances, gyriform (rather than punctuate) cortical calcification can follow herpes type 2 encephalitis. However, white matter

abnormalities are usually present in such cases; these findings are not seen in the case shown above, making this diagnosis unlikely.

## DIAGNOSIS

**Sturge-Weber syndrome**

## KEY FACTS

### Clinical

- The Sturge-Weber syndrome, also known as *encephalotri-geminal angiomatosis*, is a congenital neurocutaneous syndrome in which the main features are a facial cutaneous vascular nevus (port-wine stain), a leptomeningeal venous angiomatosis associated with cerebral cortical calcifications, and angiomatosis of the choroid of the eye.
- The major clinical manifestations are congenital glaucoma, seizures, hemiparesis, hemianopsia, and mental retardation.
- Patients with Sturge-Weber syndrome almost always have a facial nevus in the distribution of one of the sensory divisions of the trigeminal nerve. However, only 10% of patients with such facial nevi have SturgeWeber syndrome. Solely patients with a facial nevus in the upper face and eyelid (i.e., V1 distribution) are considered to be at risk for the neuro-ophthalmologic complications of Sturge-Weber syndrome.
- The intracranial lesion is an anomalous venous plexus, which is usually unilateral and located in the parietal-occipital cortex ipsilateral to the facial nevus. Progressive venous stasis produces chronic hypoxia and cortical damage, atrophy, and calcification.
- The anomalous venous plexus is associated with abnormal cortical drainage along with enlargement of trans-medullary veins and periventricular veins.
- Seizures are often the initial neurologic feature, frequently beginning in the first year of life and thereafter relentlessly progressing with advancing age. Progressive hemianopsia and hemiparesis contralateral to the leptomeningeal vascular abnormality are often seen.
- The choroid of the eye is involved by an angioma in 30% of cases, often causing buphthalmos (ocular enlargement, or “cow eye”), a form of congenital glaucoma.
- Angiomas can be seen in other organs, including the kidneys, spleen, ovaries, intestines, adrenals, thyroid, pancreas, heart, thymus, and lungs.
- Laser therapy of the facial nevus yields cosmetic improvement. Intractable seizures in Sturge-Weber patients can be surgically treated by lobectomy or hemispherectomy and corpus callosum resection, if the patient is of a sufficiently young age (i.e., <2 years of age) that the remaining hemisphere can assume motor and sensory function for both

sides of the body.

## Radiologic

- A gyriform pattern of calcification is often seen at the site of the leptomeningeal vascular malformation. This finding is due to foci of calcification within the cerebral cortex rather than vascular calcifications and is often described as a "tram-track" appearance.
- CT findings include cortical atrophy and enlargement of the choroid plexus. Cortical enhancement can be seen on contrast-enhanced CT, thought to reflect impaired superficial cortical venous outflow associated with the leptomeningeal venous angioma.
- Findings on T2-weighted MRIs include hyperintense signal abnormality in areas of gliosis, ischemia, and demyelination and hypointense gyriform signal due to cortical calcifications. As a reaction to the brain atrophy, the adjacent calvarium can thicken and the paranasal sinuses hypertrophy, changes that have been termed the *Dyke-Davidoff-Masson syndrome*.
- On contrast-enhanced T1-weighted MRIs, marked enhancement of the leptomeninges overlying the involved hemisphere, the enlarged choroid plexus ("choroidal angiomatosis"), enlarged deep medullary veins, and a retinal angioma can be seen.
- The anomalous venous drainage can be sensitively detected using susceptibility-weighted MR imaging, in which the prominent transmedullary veins, enlarged periventricular veins, gyriform signal abnormality within cortex, and hypointense signal at junction of gray matter and white matter can be seen.
- In some studies, diffusion tensor imaging has shown extensive abnormalities in white matter beyond solely the white matter subjacent to abnormal cortex.
- Catheter angiograms show abnormalities of the superficial cerebral venous drainage just deep to the area of leptomeningeal angiomatosis.

# SUGGESTED READING


Adams ME, Aylett SE, Squier W, Chong W. A spectrum of unusual neuro-imaging findings in patients with suspected Sturge-Weber syndrome. AJNR Am J Neuroradiol 2009;30:276–281.

Hu J, Yu Y, Juhasz C, et al. MR susceptibility weighted imaging (SWI) complements conventional contrast-enhanced Tl weighted MRI in characterizing brain abnormalities of Sturge-Weber Syndrome. J Magn Reson Imaging 2008;28:300–307.

Juhasz C, Haacke EM, Hu J, et al. Multimodality imaging of cortical and white matter abnormalities in Sturge-Weber syndrome. AJNR Am J Neuroradiol 2007;28:900–906.

Corey SA, O'Donovan CA. Sturge-Weber syndrome and accompanying Dyke-Davidoff-Masson syndrome. Arch Neurol 2005;62:1928–1929.

Akpinar E. The tram-track sign: cortical calcifications. Radiology 2004;231:515–516.

# CASE 20

**JAMES M. PROVENZALE**

## HISTORY

A 55-year-old man with persistent, severe cough followed by new onset of left-sided headache and Horner's syndrome.

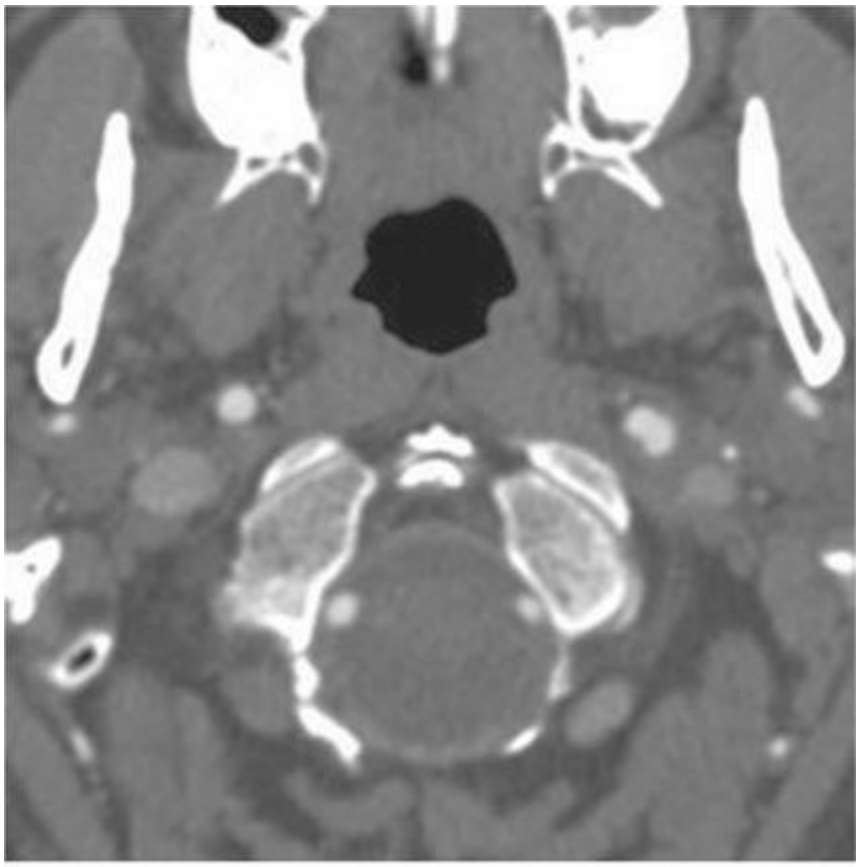

A

■**FIGURE 6-20A** Axial CT image from CT angiogram shows an unusual bilobed appearance of a dilated left internal carotid artery (ICA).

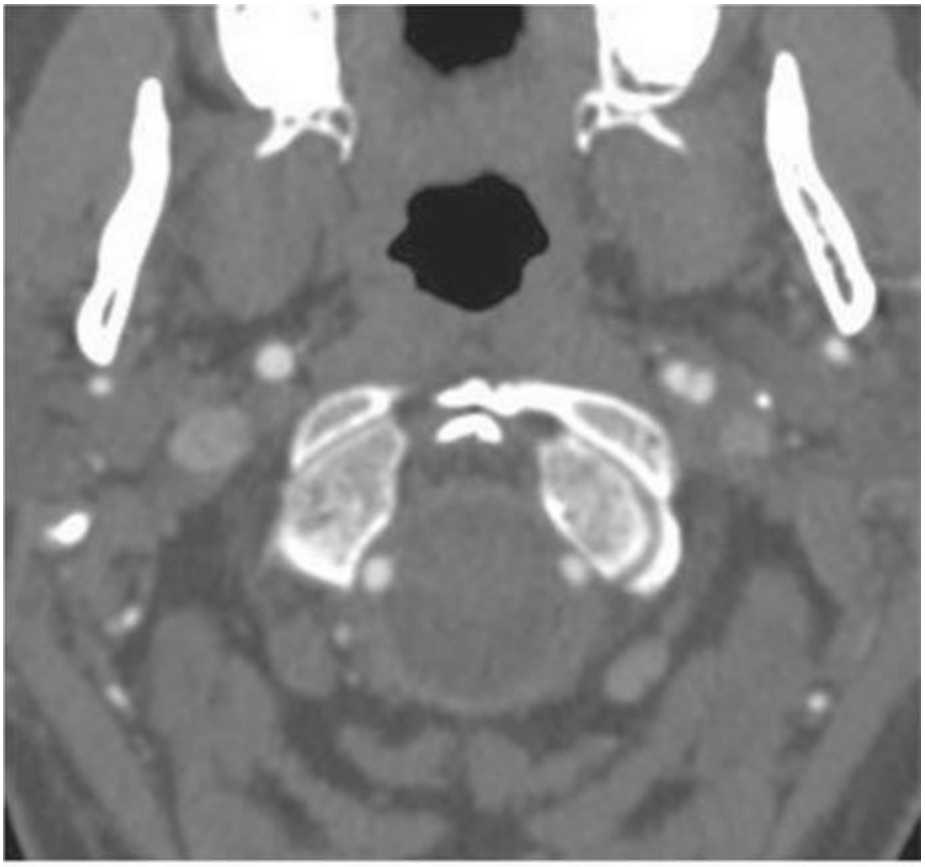

B

■**FIGURE 6-20B** Axial CT image from CT angiogram from a level adjacent to that in Figure 6-20A appears to shows that the left internal carotid has two lumens.

C

■**FIGURE 6-20C** Maximum intensity projection image from the same CT angiogram shown in Figures 6-20A and 6-20B shows an outpouching from the left ICA. In retrospect, the double lumen appearance from Figure 6-20B is now seen to be an image that was obtained at a level at which a slight degree of separation of the outpouching from the parent artery is present (i.e., at the top or bottom of the outpouching).

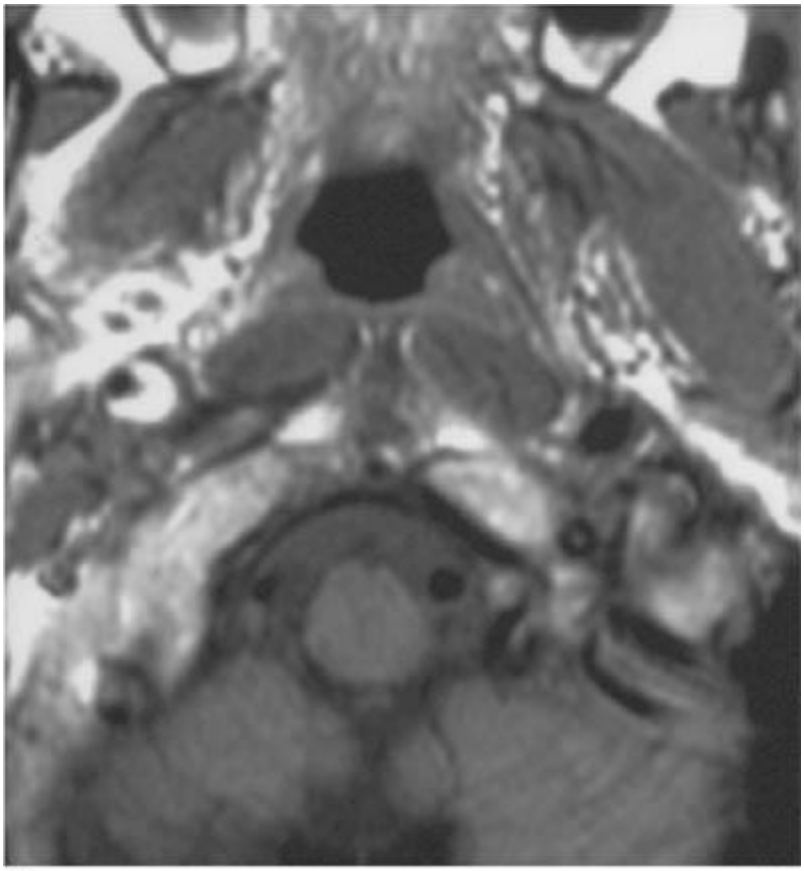

D

**FIGURE 6-20D** Axial unenhanced T1-weighted MR image from a different patient from that shown in Figures 6-20A–6-20C depicts a large crescentic region of hyperintense signal adjacent to a narrowed right ICA flow void.

## DIFFERENTIAL DIAGNOSIS

**Fibromuscular dysplasia (FMD):** This disease entity typically produces a multilobulated appearance of an artery (as opposed to the single focal outpouching of the artery shown in this case) and, in itself, would not be expected to cause pain. Figure 6-20C shows a pseudoaneurysm, indicative of arterial dissection. Although dissection can occur in patients with FMD, the diagnosis of solely FMD is not sufficient to account for all the findings in the 2 patients depicted here. This diagnosis is incorrect.

**Saccular aneurysm:** Saccular, or "berry," aneurysms, typically occur at arterial branch points, whereas the outpouching shown in this case is not at a branch point. This diagnosis is incorrect.

**Arterial dissection:** This entity often is manifested by a pseudoaneurysm (as seen in Figures 6-21A-6-21C), which represents a contained extravasation of blood. In addition, MR imaging typically shows abnormal peri-arterial signal, narrowing of the arterial flow void and increase in the external diameter of the artery due to intramural

hemorrhage (all of which are depicted in Figure 6-21D). This is the correct diagnosis.

# DIAGNOSIS

**Arterial dissection**

# KEY FACTS

## Clinical

- Dissections cause approximately 1% to 2% of all strokes in the general population but between 5% and 20% of strokes among patients <40 years old.
- Dissection can occur after trauma, on a spontaneous basis, or after movements of the head or neck that are generally considered benign ("trivial trauma").
- Dissection is often unsuspected in patients with no history of trauma. As a result, such patients often return to the emergency room multiple times before a diagnosis is established.
- The vast majority of spontaneous dissections occur in early adulthood and middle age. The average age in many published studies is approximately 40 years old.
- Headache or neckache is present in about 75% of patients. Oculosympathetic paresis (Horner's syndrome) is commonly seen in ICA dissection.
- If untreated, transient ischemic attacks and completed strokes may occur. Anterior circulation strokes usually occur in the middle cerebral artery vascular territory. In particular, Wallenberg syndrome (i.e., loss of pain and temperature sensation on the contralateral side of the body and ipsilateral side of the face as well as dys-phagia, slurred speech, ataxia, facial pain, vertigo, and nystagmus) in a young patient is suggestive of vertebral artery dissection.
- SAH can accompany intracranial dissections.
- The most common sites of spontaneous dissection are the cervical portion of the ICA (within a few centimeters of the carotid bifurcation) and the vertebral artery at the level of the C1 to C2 vertebral bodies.
- Anticoagulation or antiplatelet medications for a period of a few months is usually performed when SAH is not present and the patient is stable (i.e., no evolving ischemic symptoms).
- Patients with rapid neurologic deterioration are usually treated with endovascular treatment, for example, stenting.
- Patients with SAH related to dissection require treatment with stenting or surgery.

## Radiologic

- Whereas, in the past, most dissections were diagnosed using catheter angiography, presently most dissections are diagnosed using CT angiography or MR imaging. The diagnosis can also be made by sonography.
- On cross-sectional imaging studies, when dissection related to trauma is suspected, usually obtaining images extending over a distance from many centimeters below many centimeters above the site of trauma is sufficient to depict the abnormality. However, in order to minimize the possibility of a false negative study, many radiologists prefer to image from the level of the origin of the common carotid and vertebral arteries to the level of the circle of Willis.
- The most common findings on CT angiography are a narrowing of the arterial lumen with an adjacent pseudoa-neurysm and/or an intimal flap (Figure 6-21A-6-21C).
- The typical MR finding is a narrowed arterial flow void with an adjacent crescentic area of abnormal signal. The periarterial region of abnormal signal intensity is initially hyperintense on T1-weighted images and normal or hypointense signal on T2-weighted images (reflecting the presence of intracellular methemoglobin in the periarterial hematoma). Subsequently, the hematoma is hyperintense on both pulse sequences due to blood products in the stage of extracellular hemoglobin (Figure 6-21D).
- At MR angiography, a narrowed arterial signal column, frequently with an adjacent region of hyperintense signal aligned parallel to the artery, can often be seen (Figure 6-21D). Alternatively, a pseudoaneurysm can be seen to project from the surface of the artery.
- Diagnostic features at sonography include an echogenic intimal flap (the most specific sign, but present in only a minority of cases) and echogenic thrombus.
- The most common finding at catheter angiography is a site of smooth or irregular narrowing extending over a few centimeters in length. Other catheter angiography findings can include pseudoaneurysm formation, arterial occlusion, and, less commonly, an intimal flap. A doublelumen appearance is rare at catheter angiography.
- Resolution or marked improvement at the time of a repeat imaging study performed a few weeks later is seen in about 80% of treated cases.

# SUGGESTED READING


York G, Petrella JR, Barboriak DP, et al. Association of internal carotid artery injury with carotid fractures in head trauma patients. AJR 2005;184:1672–1678.

Goyal MS, Derdeyn CP. The diagnosis and management of supraaortic arterial dissections. Curr Opin Neurol 2009;22:80–89.

Provenzale JM. MRI and MRA for evaluation of dissection of craniocerebral arteries: lessons from the medical literature. Emerg Radiol 2009;16:185–193.

Provenzale JM, Sarikaya B. Comparison of test performance characteristics of MRI, MR Angiography, and CT

angiography in the diagnosis of carotid and vertebral artery dissection: a review of the medical literature. AJR Am J Roentgenol 2009;193:1167–1174.

# CASE 21

**JAMES M. PROVENZALE**

## HISTORY

A 74-year-old woman with headache.

A

■**FIGURE 6-21A** Unenhanced axial CT scan shows a hyperdense mass with surrounding vasogenic edema in the left inferior frontal lobe.

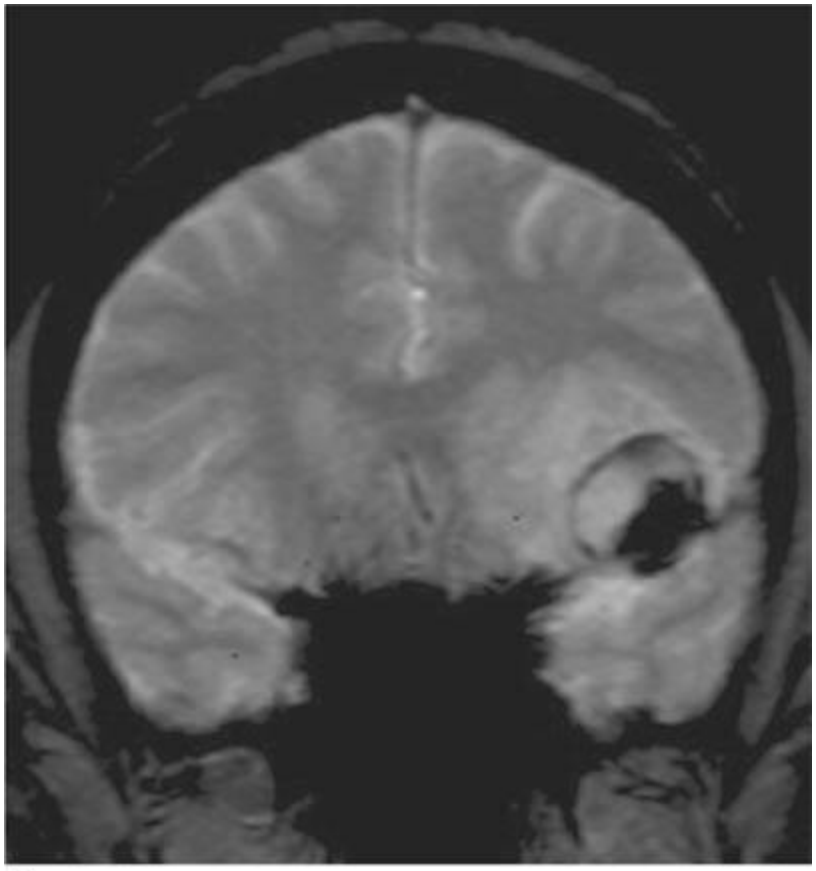

B

■**FIGURE 6-21B** Coronal T2-weighted image shows that the mass is inhomogeneous with a large region of hyperintense signal and a region of hypointense signal intensity.

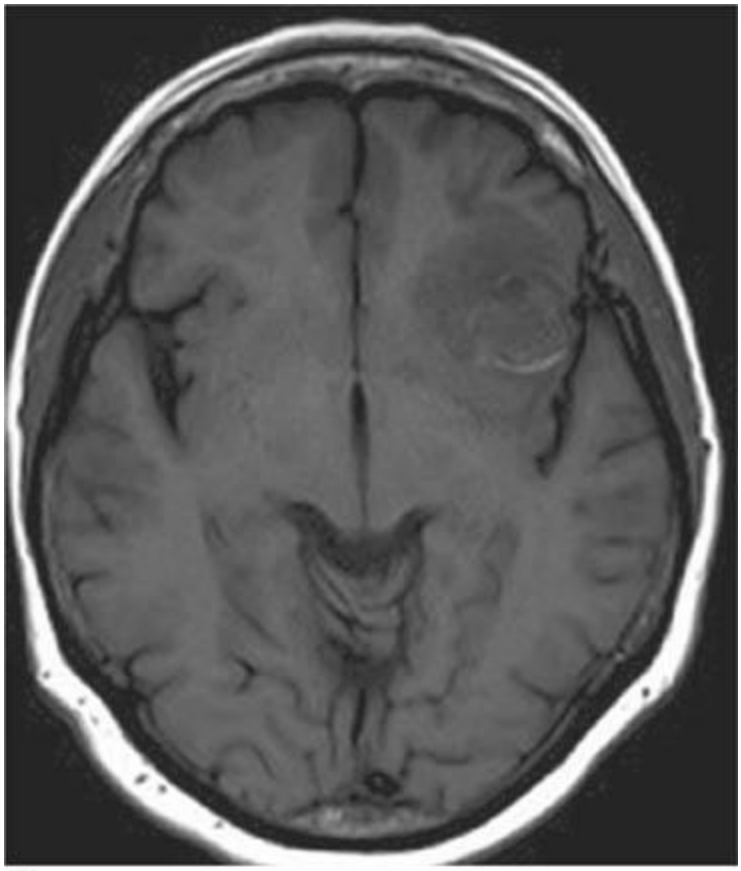

C

■**FIGURE 6-21C** Unenhanced axial T1-weighted image shows that the mass is predominantly hypointense with a crescentic region of hyperintense signal along the posterior border. No contrast material was administered in this scan.

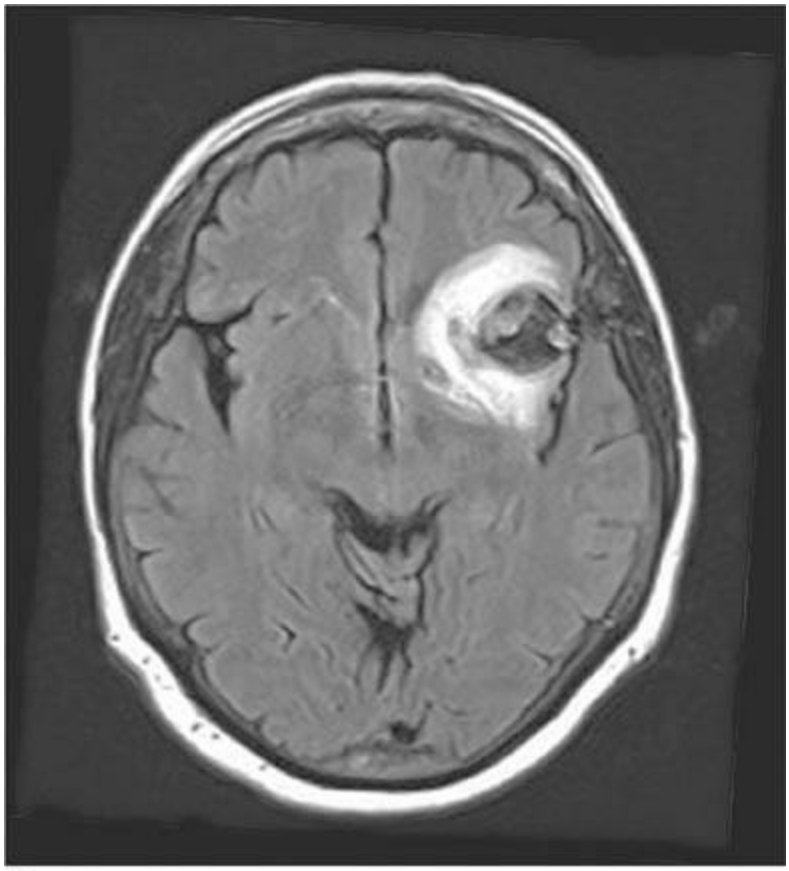

D

**FIGURE 6-21D** Axial FLAIR image again shows the mass has both a hyperintense region and a hypointense region and a large amount of surrounding edema. Note the abnormal signal intensity extending in a linear manner in the air adjacent to the lesion.

## DIFFERENTIAL DIAGNOSIS

**Meningioma:** Meningioma could reasonably be considered because the mass is hyperdense on unenhanced CT and is well circumscribed. In addition, meningiomas may be associated with substantial vasogenic edema. Such lesions typically densely contrast-enhance; because no contrast material was administered, the presence or absence of enhancement cannot be assessed.

**Dermoid cyst:** This diagnosis might be considered because of the rim of hyperintense signal along the edge of the lesion. Such a finding can reflect chemical shift artifact in the frequency-encoding direction due to the presence of fat within a lesion. However, the hyperdense appearance of the lesion on unenhanced CT makes this diagnosis unlikely.

**Aneurysm:** The findings shown here is atypical for an aneurysm because a flow void is not seen within the lesion. Nonetheless, some aneurysms fail to exhibit a flow void because of slow flow or thrombosis. The abnormal signal seen within the air on each

side of the brain at the site of the lesion is a clue to the correct diagnosis. This signal is due to pulsation artifact in the phase-encoding direction produced by flow within the mass, which is an aneurysm. The mass measured 25 mm in diameter and thus can be characterized as a "giant aneurysm."

## DIAGNOSIS

**Aneurysm**

## KEY FACTS

### Clinical

- Giant aneurysms are >25 mm in diameter and account for approximately 5% of all intracranial aneurysms.
- The most common arterial distribution for giant aneu-rysms is the carotid circulation. The tip of the basilar artery is the most common site in the vertebrobasilar circulation.
- Presentation usually is in the fourth through sixth decades. Giant aneurysms typically become symptomatic due to mass effect on adjacent intracranial structures (which may raise clinical suspicion of a neoplasm) rather than aneurysmal rupture.
- Giant intracranial aneurysms are associated with substantial neurologic morbidity or death within 5 years of diagnosis if untreated.
- Treatment options include (1) occlusion of the parent vessel (except in the case of basilar artery aneurysms) alone or in combination with surgical bypass, (2) coil occlusion of the aneurysm while employing attempts to spare the parent artery, (3) coil occlusion of the aneu-rysm combined with an assistance device such as a stent, and (4) occlusion of the aneurysm using liquid embolic agents.
- Following carotid occlusion for ICA giant aneurysms, about 75% of aneurysms will completely involute.

### Radiologic

- About half of giant aneurysms involve the ICA and its distal branches. The most common sites in the carotid circulation are near the origin of the ophthalmic artery, ICA bifurcation, and cavernous segment of the ICA. The most frequent sites in the vertebrobasilar system are at the tip of the basilar artery, junction of the basilar and superior cerebellar arteries, and the vertebrobasilar junction.
- At catheter angiography, partially thrombosed giant aneurysms often appear smaller than their actual size, which can be more accurately defined by CT and MRI.
- The CT and MRI appearance of a giant aneurysm can be mistaken for a tumor. In

particular, giant aneurysms in the parasellar region and at other sites near the skull base can be mistaken for a meningioma. It is important to consider aneurysm in the differential diagnosis of masses in these regions so that inadvertent biopsy or improper surgery can be avoided.

- On unenhanced CT, aneurysms appear as rounded or oval masses that are relatively isodense or, frequently, hyperdense relative to adjacent brain tissue. Partially thrombosed aneurysms often have a hyperintense crescentic rim. Occasionally, the rim of an aneurysm can be seen to be calcified. Following contrast material administration, nonthrombosed aneurysms densely and homogeneously contrast-enhance, while generally only the patent lumen portion of partially thrombosed aneurysms densely contrast-enhances.
- On MRI, a nonthrombosed aneurysm is seen as an oval or spherical extraaxial region of absent signal (flow void) continuous with a vessel. Partially thrombosed aneurysms typically have a laminated appearance, due to layers of thrombus of different ages. Occasionally, a thin circumferential region of abnormal perianeurysmal signal due to chronic hemorrhagic products can be seen.
- An important clue that a mass lesion seen on MRI is an aneurysm is a band of pulsation artifact extending from the aneurysm into adjacent tissues along the phase-encoding axis (Figure 6-22D). This artifact is often more pronounced after administration of contrast material.
- A number of risk factors for poor clinical outcome of giant aneurysms have recently been published; these include poor baseline disability score, aneurysm size >25 mm, and location in the posterior circulation.

## SUGGESTED READING

Darsaut TE, Darsaut NM, Chang SD, et al. Predictors of clinical and angio-graphic outcome following surgical or endovascular therapy of very large and giant intracranial aneurysms. Neurosurgery 2011;68:903–915.

van Rooij WJ, Sluzewski M. Endovascular treatment of large and giant aneurysms. AJNR Am J Neuroradiol 2009;30:12–18.

de Gast AN, Sprengers ME, van Rooij WJ, et al. Midterm clinical and magnetic resonance imaging follow-up of large and giant carotid artery aneurysms after therapeutic carotid artery occlusion. Neurosurgery 2007;60:1025–1029.

# CASE 22

**FERNANDO M. ZALDUONDO AND JAMES M. PROVENZALE**

### HISTORY

A 76-year-old man with sudden onset of bitemporal visual field deficit and headache.

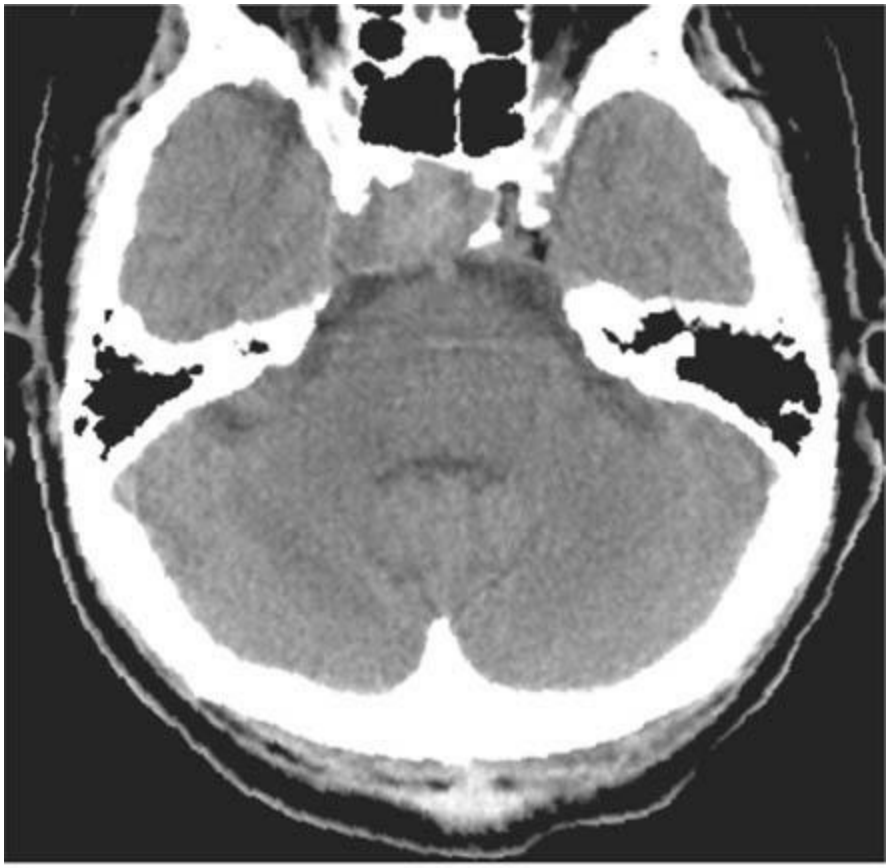

A

■**FIGURE 6-22A** Unenhanced axial CT scan shows a slightly hyperdense mass within the sella, causing mass effect on the right cavernous sinus and erosion of the right posterior clinoid process.

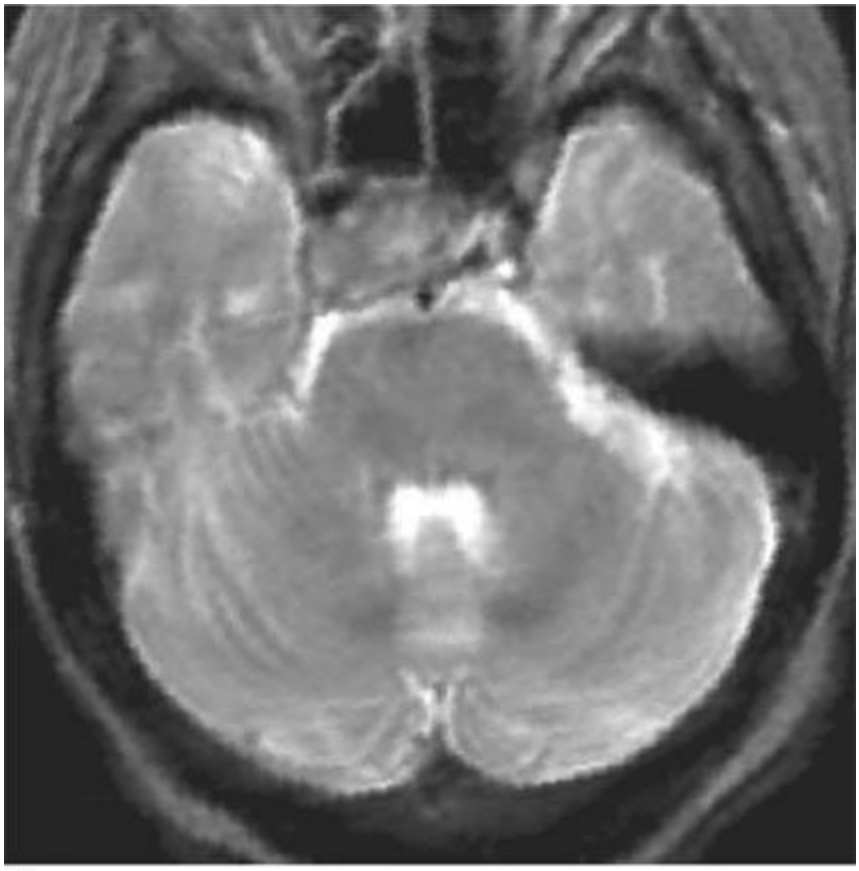

B

■**FIGURE 6-22B** Axial T2-weighted MR image shows that the mass is slightly inhomogeneous and contains a central region that is hyperintense and a peripheral region that is slightly hypointense relative to gray matter.

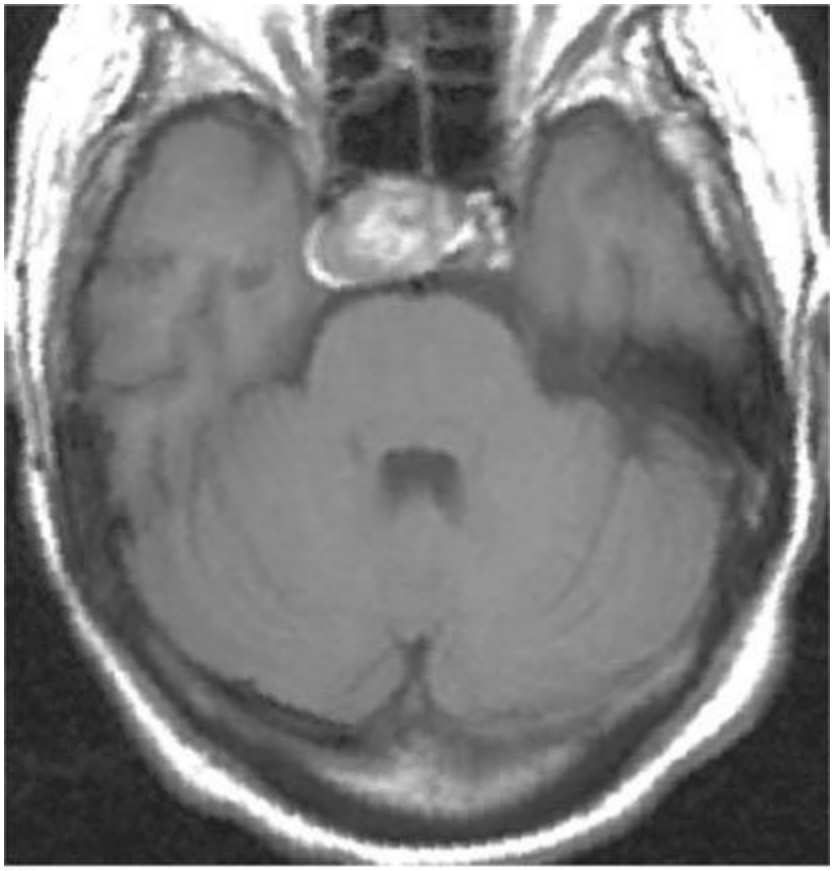

C

■**FIGURE 6-22C** Axial unenhanced T1-weighted image shows that the central portion of the mass is hyperintense and the peripheral portion relatively isointense to gray matter.

D

**FIGURE 6-22D** Coronal contrast-enhanced T1-welghted Image shows that most of the upper segment of the central portion of the mass Is hyperintense; the remainder of the mass Is unenhanclng. A small portion of the mass extends Into the suprasellar cistern. The floor of the sella is depressed by the mass.

## DIFFERENTIAL DIAGNOSIS

**Ruptured dermoid cyst:** This diagnosis might be considered because of the region of hyperintense signal on the unenhanced T1-weighted image, which could potentially represent fat within a dermoid cyst. Furthermore, this diagnosis could account for sudden onset of symptoms, although symptoms due to a ruptured dermoid usually occur at a younger age than that indicated for the patient in this case. However, no imaging findings suggestive of rupture (e.g., hyperintense foci within the CSF space) are present. An unruptured dermoid cyst would not be expected to produce sudden symptom onset. This diagnosis is incorrect.

**Craniopharyngioma:** This lesion nearly always is centered in the suprasellar cistern, although an intrasel-lar component is often present. The vast majority are calcified and cystic, features not seen in the case shown here. This diagnosis is unlikely.

**Rathke's Cleft Cyst:** These lesions frequently occupy the sella and have an ovoid

appearance but the long axis is usually in the craniocaudad direction (unlike the lesion shown here). In addition, these lesions are wholly cystic and depression of the sellar floor is very uncommon. This diagnosis is incorrect.

- **Aneurysm:** This diagnosis might be considered because the lesion shown is oval and close to the internal carotid artery. Furthermore, aneurysms can cause bone erosion due to their pulsatile nature. The absence of a flow void within the lesion is not evidence against the diagnosis of aneurysm, because aneurysms are frequently partially thrombosed (please see case 21). Pulsation artifact in the phase-encoding direction, indicative of flow, would be expected in a fully patent or partially thrombosed aneurysm. Such artifact is not present. Nonetheless, a thrombosed aneurysm cannot be fully excluded based on the images shown.
- **Meningioma:** Meningioma might be considered, based on the location of the lesion but the lack of contrast-enhancement virtually excludes this diagnosis. Furthermore, the mass shown in this case is indistinguishable from the pituitary gland. This diagnosis is incorrect.
- **Hemorrhagic pituitary macroadenoma:** This term refers to adenomas >10 mm in size. This is the correct diagnosis given the large size and intrasellar location with extension into the suprasellar cistern. Furthermore, the focus of hyperintense signal in the cephalad portion of the lesion is consistent with hemorrhage which, when present within a pituitary adenoma, is termed "pituitary apoplexy." This diagnosis is correct.

## DIAGNOSIS

**Hemorrhagic pituitary macroadenoma (i.e., pituitary apoplexy)**

## KEY FACTS

## Clinical

- Adenomas are the most common neoplasm of the pituitary gland and arise in the adenohypophysis (anterior lobe of the pituitary gland). They comprise 10% to 15% of all intracranial tumors.
- Many hormonally active pituitary adenomas become clinically apparent while still small. Three-fourths of all pituitary adenomas present with signs and symptoms related to hormonal overproduction.
- Many nonfunctioning tumors grow to large size before producing symptoms. One-fourth of all adenomas present with symptoms due to mass effect—for example, headache, visual field defects, cranial nerve palsies, and CSF rhinorrhea due to sellar erosion.

- Hormonally active adenomas may secrete prolactin, thyroid-stimulating hormone, growth hormone, adre-nocorticotropic hormone, follicle-stimulating hormone, or luteinizing hormone, alone or in various combinations. Hormonally inactive adenomas have been termed “null cell” adenomas or oncocytomas.

## Radiologic

- Unless contraindicated, MRI is generally considered the first-line imaging study for detection of pituitary adenomas.
- During the evaluation of a lesion of the sellar/juxta-sellar region, the radiologist’s role is to establish the center of the lesion and its relationship to adjacent structures. Relevant features include the relation to the optic structures, course and caliber of the cavernous segment of the internal carotid arteries, and whether the cavernous sinuses are invaded.
- Pituitary adenomas can be diagnosed on any MRI pulse sequence, but contrast-enhanced T1-weighted images in the coronal plane are the technique that is probably most widely accepted. Nonetheless, they can be detected on unenhanced T1-weighted images as a hypointense region and in 30% to 50% of cases as a hyperintense lesion on T2-weighted images. The latter finding is more common in macroadenomas.
- MRI is optimally performed within a few minutes of contrast infusion. Microadenomas contrast-enhance less rapidly than the normal pituitary tissue in that time period and appear relatively hypointense to the normal gland. Further delay in imaging can lead to false-negative studies, because over many minutes, the lesion contrast-enhances to the same degree as normal pituitary tissue.
- Macroadenomas are typically isointense to gray matter on all pulse sequences and intensely contrast-enhance, often in an inhomogeneous manner.
- Complicated adenomas can have calcification, hemorrhage, cyst formation, and necrosis and will display corresponding focal signal changes. These features are more common following medical treatment.
- If MRI is unavailable or contraindicated, adenomas can be detected on contrast-enhanced CT imaging using thin-section axial and coronal images.
- Incidental macroadenomas of moderate size can easily be missed on routine axial CT images of the brain (i.e., CT studies not specifically performed to assess the pituitary gland). Enlargement of the sella turcica on the lateral scout topogram can be the only indication that a macroadenoma is present in a routine brain CT study.
- The term clinical pituitary apoplexy refers to sudden expansion of the pituitary gland, usually due to internal hemorrhage or infarction within a pituitary adenoma, producing clinical symptoms. This entity is to be distinguished from otherwise asymptomatic pituitary masses containing hemorrhagic elements.

- The most common symptoms of pituitary apoplexy are headache (almost always present), nausea or vomiting (80% of patients), and visual symptoms (mainly impairment of visual fields or ophthalmoplegia).
- Pituitary apoplexy is difficult to diagnose on CT alone because the hemorrhage is often undetectable. One imaging clue, which is possible solely if prior CT or MR scans are available, is a marked increase in size of the pituitary gland over a short period of time. However, this finding is insensitive because hemorrhage into the gland can occur without a notable change in size of the gland. Furthermore, on routine head CT, even an enlarged pituitary gland can be difficult to detect because of volume averaging with adjacent structures.
- If CTA is performed in a patient with pituitary apoplexy to exclude aneurysm rupture as the cause of severe headache, the size of the pituitary gland can be reliably assessed on reformatted images in the coronal and sagittal planes. This technique can be used to determine the size of the gland (which can be used to assess whether a macroadenoma may be present) but will not reliably detect the presence of hemorrhage.

## SUGGESTED READING

Choi SH, Kwon BJ, Na DG, et al. Pituitary adenoma, craniopharyngioma, and Rathke cleft cyst involving both intrasellar and suprasellar regions: differentiation using MRI. Clin Radiol 2007;62:453–462.

Semple PL, Jane JA, Lopes BS, Laws ER. Pituitary apoplexy: correlation between magnetic resonance imaging and histopathological results. J Neurosurg 2008;108:909–915.

Turgut M, Ozsunar Y, Basak S, Guney E, Kir E, Meteoglu I. Pituitary apoplexy: an overview of 186 cases published during the last century. Acta Neurochir (Wien) 2010;152:749–761.

# CASE 23

**JAMES M. PROVENZALE AND DAVID S. ENTERLINE**

### HISTORY

A 12-year-old girl with seizures and hypomelanotic skin macules.

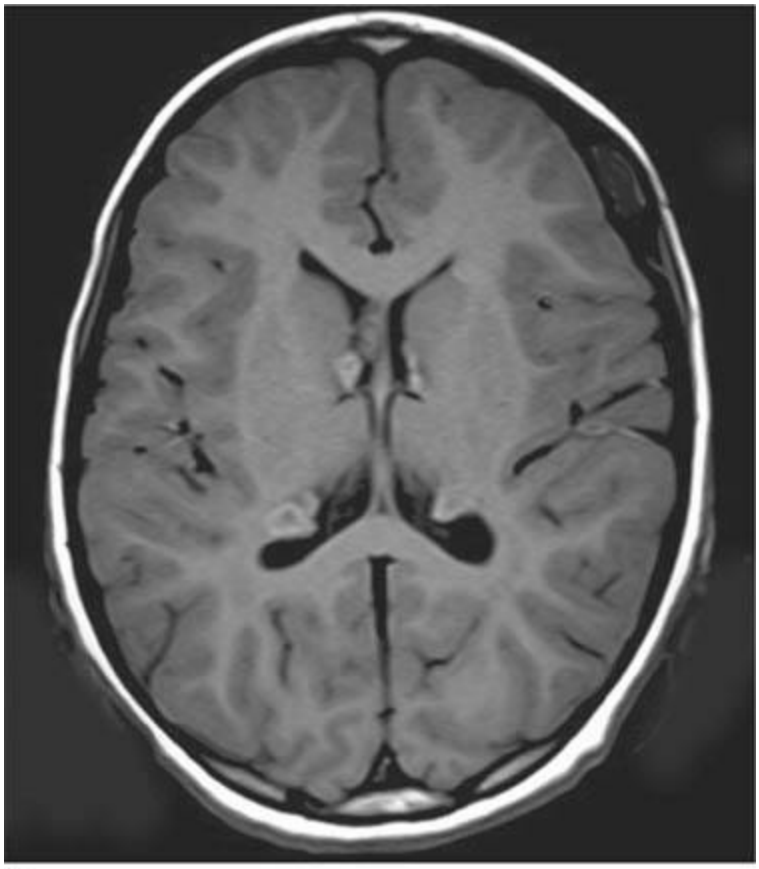

A

■**FIGURE 6-23A** Unenhanced axial MR image shows multiple oval hyperintense masses aligned along the ependymal surface of the lateral ventricles.

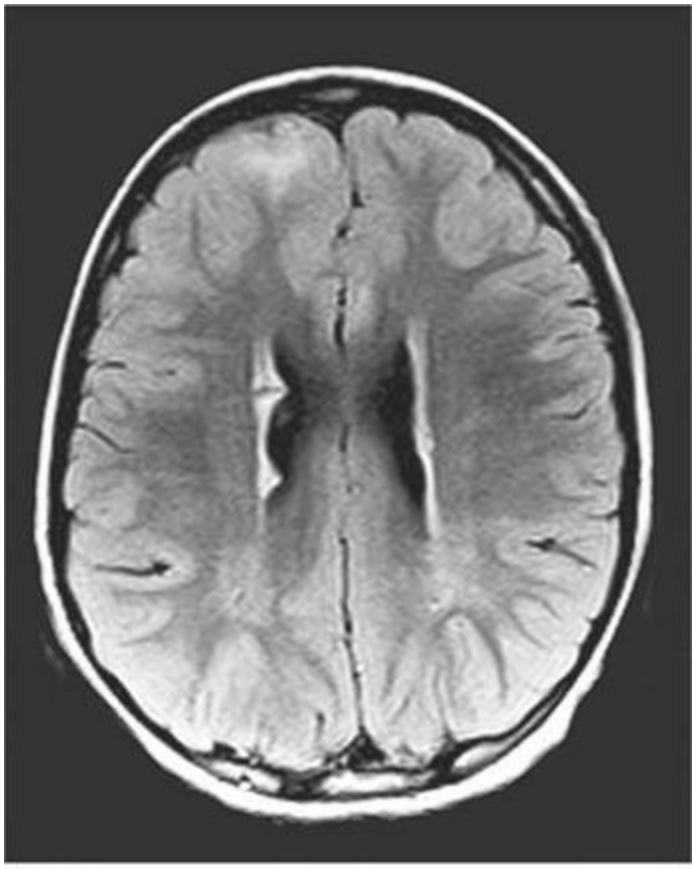

B

■**FIGURE 6-23B** Axial FLAIR Image shows the lesions along the ventricular surface are also hyperintense on this pulse sequence. An irregular hyperintense focus is also seen in the cortex of the right frontal lobe. Finally, multiple subtle, slightly hyperintense linear regions are seen extending from the ventricles to the cortex (most notable in the right frontal white matter).

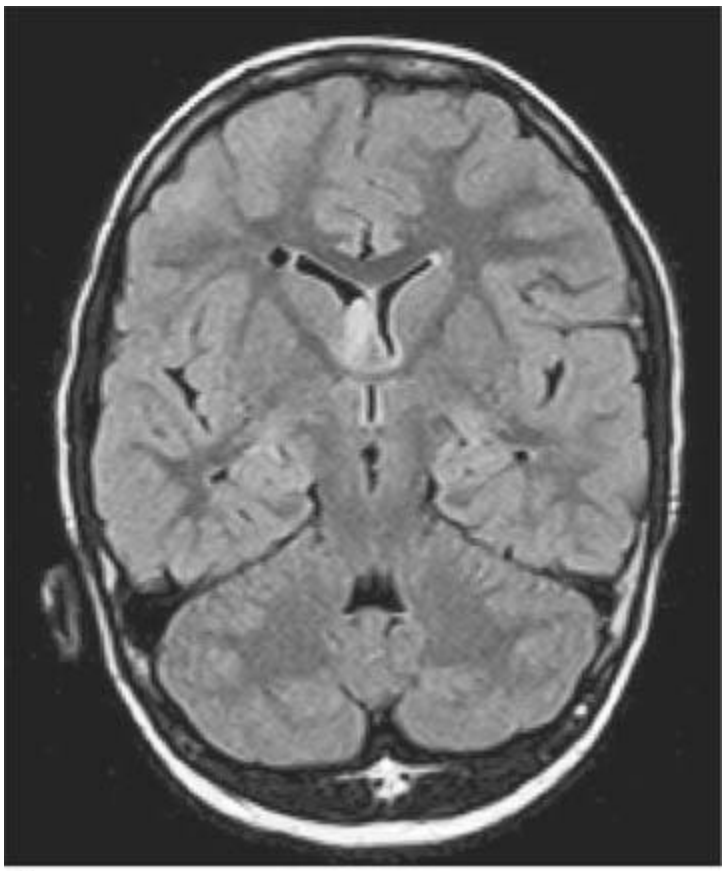

C

■**FIGURE 6-23C** Coronal FLAIR Image shows a hyperintense mass in the frontal horn of the right lateral ventricle. In addition, a curvi linear hyperintense region is seen through the subcortical white matter of the right hemisphere.

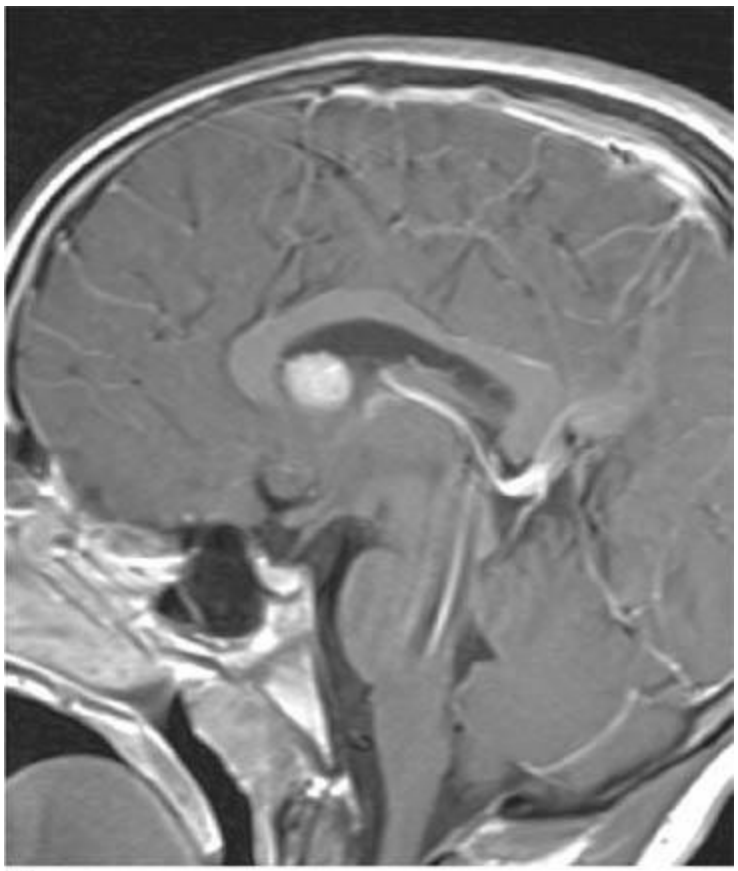

D

**FIGURE 6-23D** Sagittal contrast-enhanced T1-weighted image shows the mass in the right lateral ventricle contrast-enhances in a homogeneous manner.

## DIFFERENTIAL DIAGNOSIS

The differential diagnosis of mass lesions within the lateral ventricle includes the following:

**Choroid plexus papilloma:** This lesion might be considered, because it is an intraventricular mass that is seen more frequently in children than adults. However, because it arises from choroid plexus, it is typically found in the atrium of the lateral ventricle and not (as in the case shown here) near the foramen of Monro.

**Neurocytoma:** This lesion typically arises in the lateral ventricle and is attached to the septum pellucidum. On the images shown here, it is difficult to determine whether the mass in the frontal horn of the right lateral ventricle is attached to the septum pellucidum or merely abuts it. However, this diagnosis would not account for the presence of multiple masses (Fig. 6-24A) or the multiple regions of hyperintense signal within brain parenchyma (Figure 6-24B).

**Meningioma:** Meningiomas can arise within the ventricular system, but when they are located in the lateral ventricle, they are almost always attached to the cho-roid plexus,

unlike the lesion shown above. Furthermore, as in the case of choroid plexus papilloma and neurocytoma, the diagnosis of meningioma would not adequately account for the parenchymal signal changes and the fact that multiple intraventricular masses are present. This is an incorrect diagnosis.

- **Tuberous sclerosis (TS):** This diagnosis would account for the cortical lesion, the mass in the frontal horn of the right lateral ventricle (which represents a subep-endymal giant cell tumor) and the linear hyperintense regions in white matter (which represent cerebral white matter radial migration lines seen in TS).

## DIAGNOSIS

**Tuberous sclerosis**

## KEY FACTS

### Clinical

- TS is a phakomatosis with an autosomal dominant inheritance pattern associated with two genes termed TSC1 and TSC2. However, about two-thirds of cases are spontaneous mutations. TS occurs in about 1 in 6,000 live births; 85% of patients develop CNS manifestations.
- Clinical features have been divided into major features and minor features. Diagnosis is based on the presence of two major features or combination of one major feature and two minor features. Major features include facial angiofibromas (35%), pits in dental enamel (90%), periungal fibromas, hypomelanotic macules, shagreen patch (50%), retinal hamartomas (40% to 50%), cortical tubers, subependymal nodules, subependymal giant-cell astrocytoma, cardiac rhabdomyoma (30%), lymph-angiomyomatosis, and renal angiomyolipoma (70% to 80%). Minor features include hamartomatous rectal polyps, bone cysts, gingival fibromas, nonrenal hamar-tomas, retinal achromic patch, cerebral white matter radial migration lines, confetti-like skin lesions, and multiple renal cysts.
- Complications due to renal lesions are the most common cause of death.
- Approximately 30% of patients are mentally retarded.
- The retinal hamartomas are small, rounded masses that overlie the optic nerve head, are histologically similar to subependymal tubers, and are commonly calcify.
- Hamartomas are seen in two major locations in the brain—within the parenchyma (cortical and subcortical regions) and at subependymal sites. Histologically, these lesions consist of disorganized conglomerations of poorly differentiated neurons and are thought to result from disordered migration and differentiation of glial tissue.

- Subependymal hamartomas are typically arranged along the caudothalamic groove. In 15% of TS patients, they undergo malignant degeneration into a subepen-dymal giant cell tumors (SGCT).

## Radiologic

- Subependymal nodules are frequently calcified, allowing confident CT diagnosis of TS. When calcified, they are hypointense on T2-weighted sequences. Noncalci-fied subependymal lesions are frequently hyperintense on T2-weighted MRIs.
- In addition to TS, calcifications arranged along the ventricular surface can be seen in various congenital infections, cysticercosis, and some treated neoplasms having subependymal disease (e.g., lymphoma).
- MRI is more sensitive than CT in the detection of cortical hamartomas, which appear as regions of gyral broadening. Cortical and subcortical hamartomas in children and adults are typically hypointense on T1-weighted images and hyperintense on T2-weighted images compared to white matter. However, in the first few months of life, lesions are hyperintense on T1-weighted images and hypointense on T2-weighted images, relative to immature (as yet unmyelinated) white matter.
- Cerebral white matter radial migration lines, seen in 20% to 30% of cases, are lines that are hyperintense on T2-weighted and FLAIR images, representing neuronal or glial arrested migration. They typically extend from a central location (e.g., wall of ventricle of a subepen-dymal nodule) to brain cortex or a cortical hamartoma.
- SGCTs are grade I astrocytomas seen only in the setting of TS. They are thought to arise from subependymal nodules, are located at the foramen of Monro, and are usually detected in late childhood and adolescence.
- SGCTs can grow to large size and cause obstructive hydrocephalus. They do not invade brain parenchyma or metastasize through CSF pathways.
- Until relatively recently, it was assumed that contrast-enhancement of a subependymal nodule was an indication of early malignant degeneration to an SGCT. However, it is now generally accepted that benign sub-ependymal nodules can contrast-enhance on MRI.
- It is recommended that TS patients initially be evaluated with MRI before the age of 2 and then annually until the age of 21, if the child has clinical or imaging risk factors for SGCT.

# SUGGESTED READING

Curatolo P, Bombardieri R, Jozwiak S. Tuberous sclerosis. The Lancet 2008;372:657–668.

Rosser T, Panigrahy A, McClintock W. The diverse clinical manifestations of tuberous sclerosis complex: a review. Semin Pediatr Neurol 2006;13:27–36.

Makki MI, Chugani DC, Janisse J, Chugani HT. Characteristics of abnormal diffusivity in normal-appearing white matter investigated with diffusion tensor MR imaging in tuberous sclerosis complex. AJNR Am J Neuroradiol 2007;28:1662–1667.

# CASE 24

**JAMES M. PROVENZALE AND JOSEPH B. CORNETT**

## HISTORY

A 16-year-old boy with headache and lack of coordination.

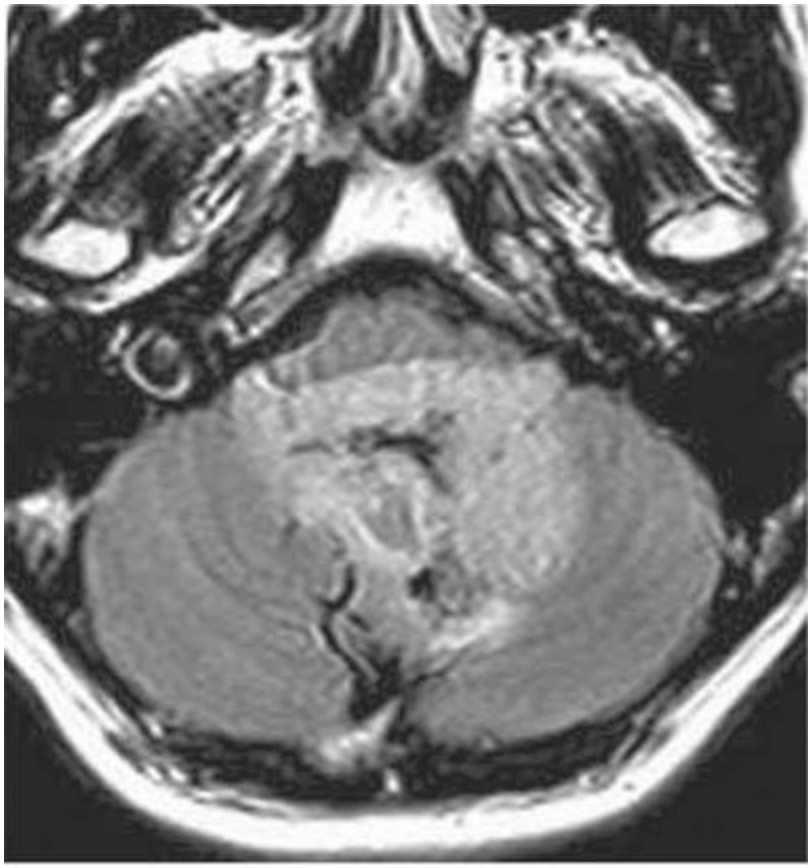

A

■**FIGURE 6-24A** Axial FLAIR Image shows an inhomoge-neous hyperintense mass within the fourth ventricle extending out both foramina of Luschka.

B

■**FIGURE 6-24B** Unenhanced sagittal T1-weighted image reveals the mass elevates the cerebellar folia and extends caudad through the foramen of Magendie.

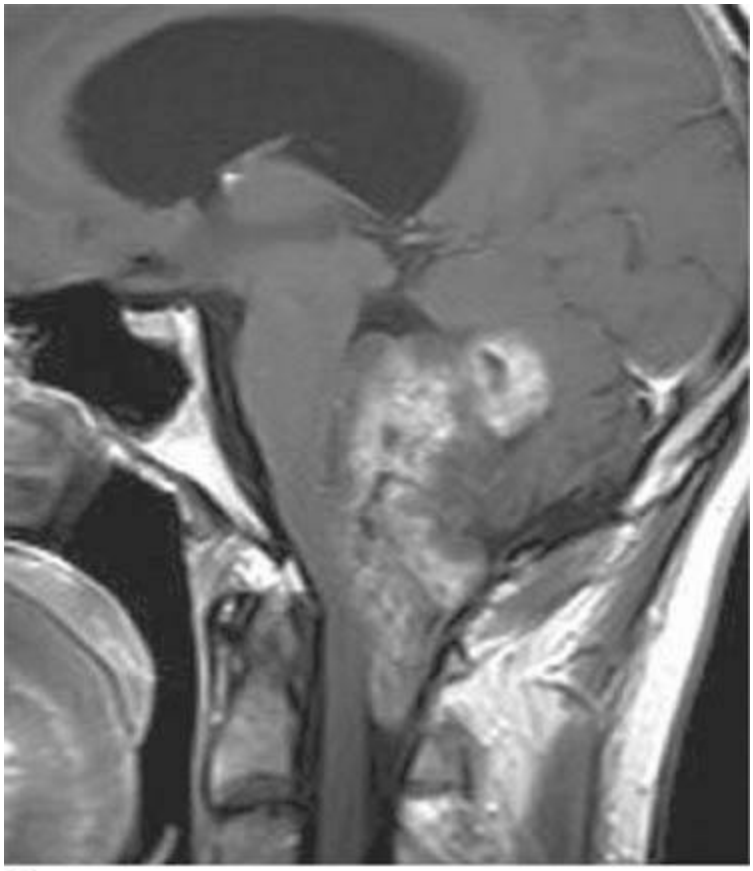

C

■**FIGURE 6-24C** Contrast-enhanced sagittal T1-weighted image shows that the mass enhances in an inhomogeneous manner.

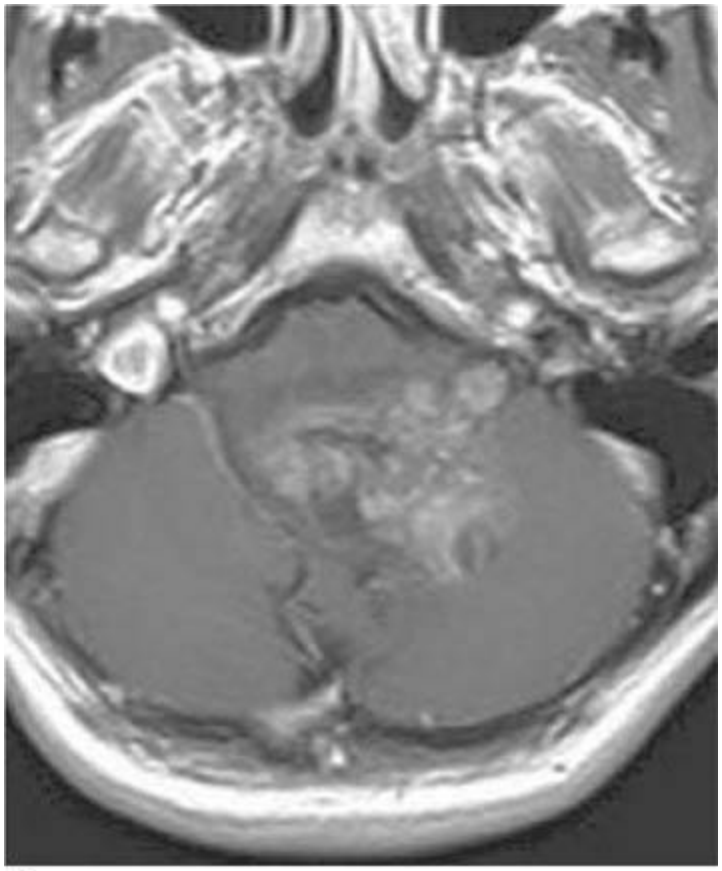

D

**FIGURE 6-24D** Contrast-enhanced sagittal T1-weighted image shows a portion of the mass extending out the left foramen of Luschka.

## DIFFERENTIAL DIAGNOSIS

**Medulloblastoma:** This tumor might be considered because it is a common posterior fossa neoplasm of childhood. This tumor usually arises from the cerebellar vermis and bulges forward from the roof of the fourth ventricle. However, medulloblastoma is usually more homogeneous than the lesion shown here. Furthermore, extension through the fourth ventricular outlet foramina is uncommon, making this diagnosis unlikely.

**Choroid plexus papilloma:** In childhood, choroid plexus papillomas usually occur in the lateral ventricle, unlike the case shown above. Occurrence in the fourth ventricle is usually seen in adults. Furthermore, unlike the lesion shown above, choroid plexus papilloma generally has a lobulated shape with multiple clefts and has internal signal voids due to a high degree of vascularity. These findings are not present in the case shown; this diagnosis is unlikely.

**Ependymoma:** Fourth ventricular ependymomas typically arise in the floor of the fourth ventricle and often extend through the foramen of Luschka and up to (and sometimes around) the anterior surface of the lower brainstem. Similarly, they often

extend through the foramen of Magendie (as in the case shown). This diagnosis is correct.

## DIAGNOSIS

**Ependymoma**

## KEY FACTS

### Clinical

- The spinal cord is the most common location for epen-dymoma, accounting for 60% of all such tumors (please see Case 18). Intracranial ependymoma is largely a tumor of children and adolescents but does occur in adults. Most cases present prior to 5 years of age.
- Among intracranial ependymomas, approximately 65% are infratentorial. The remaining 35% are supratento-rial and typically occur in either a parenchymal or peri-ventricular location.
- Infratentorial ependymoma arises from the ependymal lining of the fourth ventricle and is predominantly intra-ventricular. It is not uncommon for the tumor to invade the brain stem. Growth along adjacent brain cisterns is characteristic. The term plastic ependymoma is given to an ependymoma that has grown around the anterior surface of the brain stem or spinal cord.
- Fourth ventricular ependymoma often presents with signs and symptoms of obstructive hydrocephalus (e.g., headache, vomiting). Less often, gait or limb ataxia, nystagmus, or cranial nerve dysfunction is a presenting feature.
- CSF dissemination is uncommon (only about 10% of cases) at the time of presentation but is more common at a time of relapse.
- Treatment is generally surgical resection and radiation therapy. Prognosis is relatively poor, especially in young children with subtotal resection (adult 5-year survival: -70%; pediatric 5-year survival: -15%).
- Ependymoma can arise in the spinal cord as an intramedullary mass (see Case 18). The myxopapillary type characteristically arises from conus medullaris or filum terminale.

### Radiologic

- The correct preoperative diagnosis of infratentorial ependymoma can be made based on location and morphology of the mass. This is a solid fourth ventricular mass, often with “plastic” extension into the cerebel-lopontine angle via the foramen of Luschka or

into the foramen magnum via the foramen of Magendie.

- On unenhanced CT, posterior fossa ependymomas appear relatively isodense to gray matter but are inhomogeneous, with 50% having calcification and about 20% having cystic components. Inhomogeneous contrast-enhancement is typical.
- On MRI, ependymoma often has inhomogeneous signal intensity due to hemorrhage, necrosis, cyst formation, calcification, and hemosiderin deposition. Like most tumors, the solid component is iso- or hypointense relative to brain parenchyma on T1-weighted images and hyperintense on T2-weighted images. Contrast-enhancement is usually inhomogeneous.
- Cyst formation is much more common in supratentorial ependymomas (40% to 85% of cases) than infratentorial lesions.
- Degree of resection is the key element in patient prognosis. Symptomatic recurrences (e.g., symptoms due to hydrocephalus or spinal metastases) have a much poorer prognosis than asymptomatic recurrences solely detected on imaging.

## SUGGESTED READING

Choi J-Y, Chang KH, Yu IK, et al. Intracranial and spinal ependymomas: review of MR images in 61 patients. Korean J Radiol 2002;3:219–228.

Good CD, Wade AM, Hayward RD, et al. Surveillance neuroimaging in childhood intracranial ependymoma: How effective, how often, and for how long? J Neurosurg 2001;94:27–32.

Zacharoulis S, Ji L, Pollack IF, et al. Metastatic ependymoma: a multi-institutional retrospective analysis of prognostic factors. Pediatr Blood Cancer 2008;50:231–235.

# CASE 25

**JAMES M. PROVENZALE**

### HISTORY

A 12-year-old girl with morning headaches, nausea, and daytime somnolence.

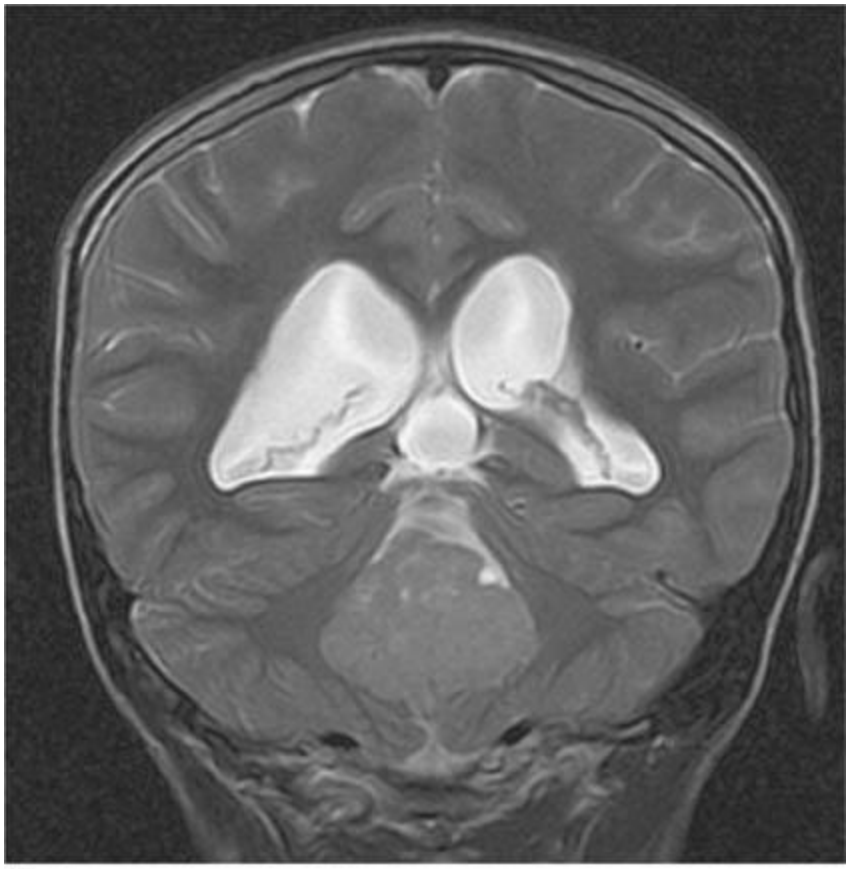

A

■**FIGURE 6-25A** Coronal T2-weighted image shows a well-marginated mass in the fourth ventricle causing hydrocephalus. Multiple small cysts are present within the mass.

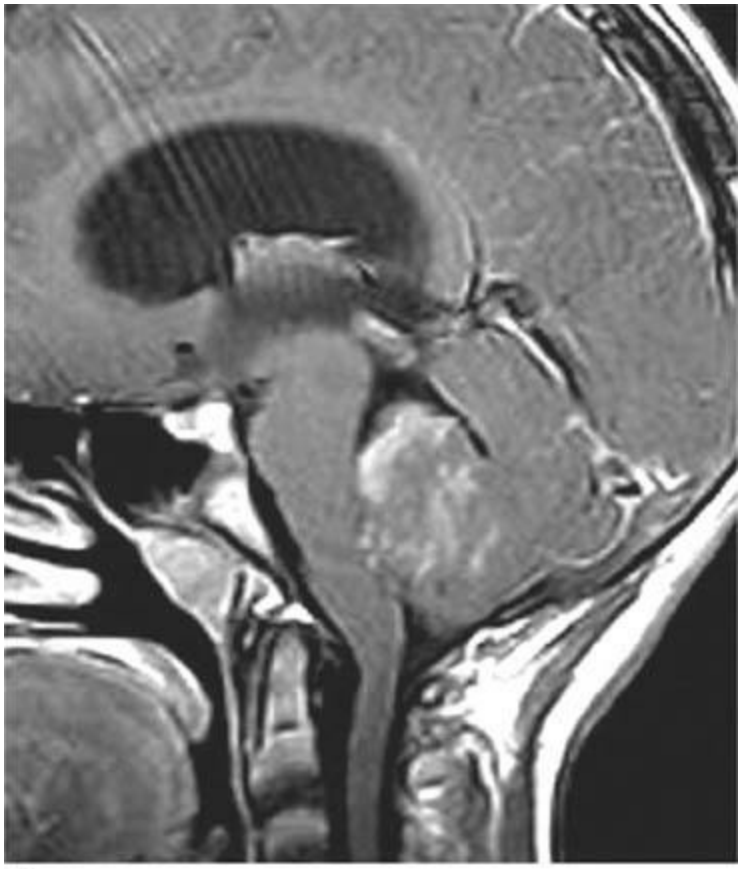

B

■**FIGURE 6-25B** Sagittal contrast-enhanced T1-weighted image shows the mass inhomogenously enhances. The fourth ventricle is displaced anteriorly and superiorly, indicating that the mass arises from the caudal aspect of the roof of the fourth ventricle.

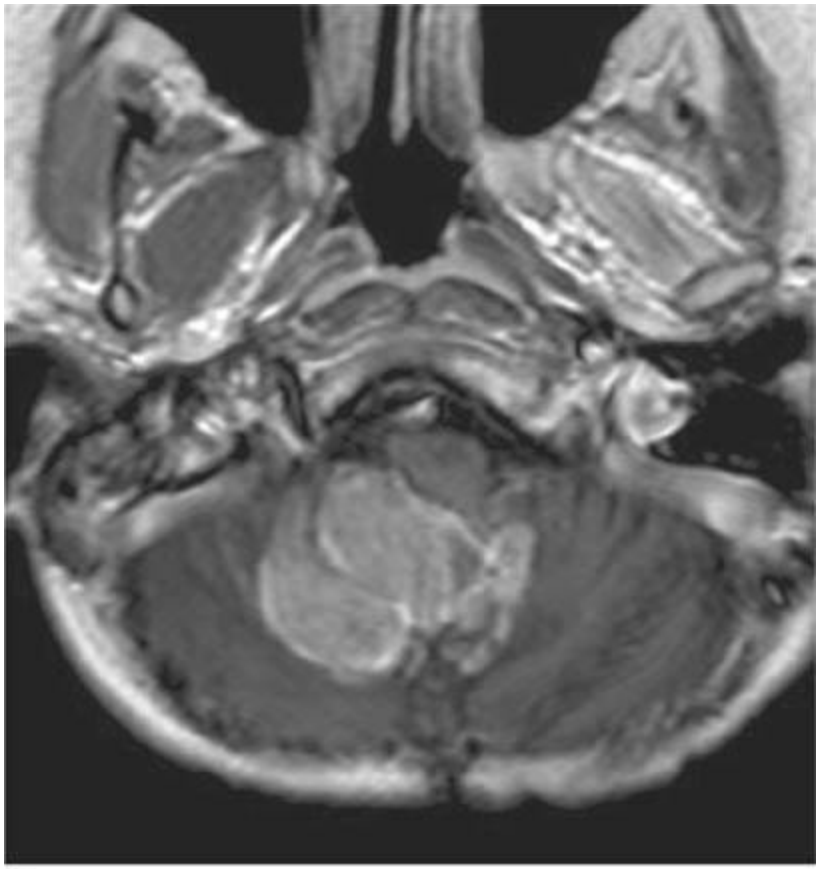

C

■**FIGURE 6-25C** Axial contrast-enhanced T1-weighted image in a different patient than shown in Figures 6-25A and 6-25B but with the same tumor type. This patient underwent suboccipital craniectomy for a tumor in the fourth ventricle 3 years before. This image shows tumor recurrence along the surgical margin.

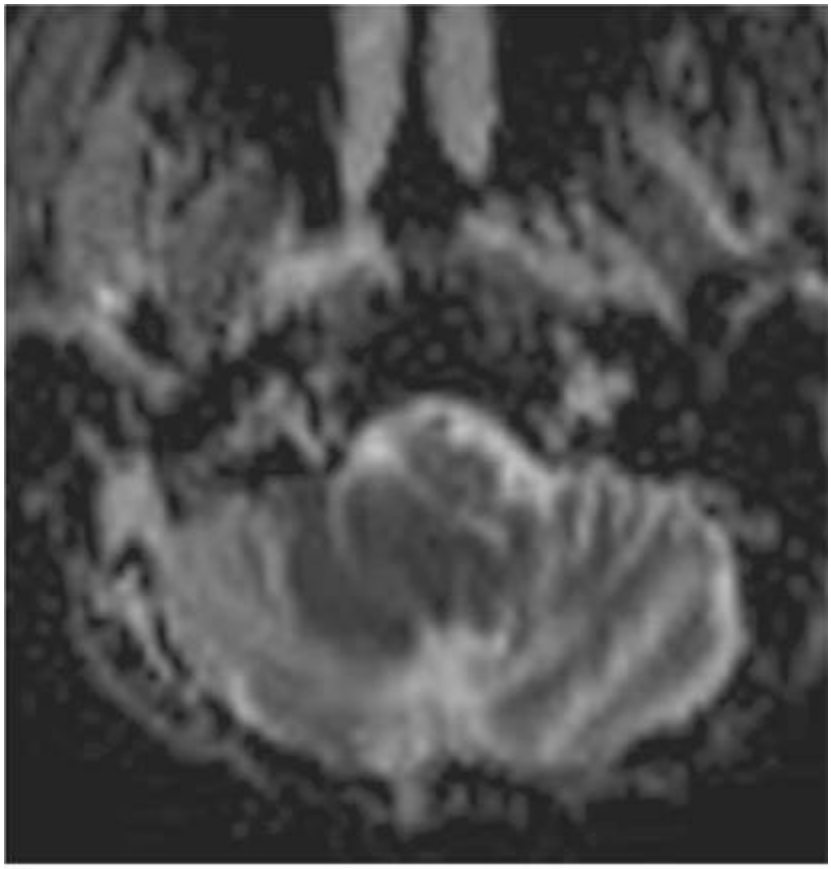

D

**FIGURE 6-25D** Axial apparent diffusion map image shows that the enhancing mass in Figure 6-27C has restricted diffusion, indicated by decreased signal intensity, compared to the remainder of the brain.

## DIFFERENTIAL DIAGNOSIS

**Ependymoma:** This tumor might be considered because it is one of the common posterior fossa tumors in the pediatric population and is usually located within the fourth ventricle. Ependymomas are frequently inho-mogeneous, and about 50% are calcified. However, they typically arise in the floor of the fourth ventricle whereas the mass shown in Figure 6-25B arise from the roof of the fourth ventricle. This answer is incorrect.

**Astrocytoma (juvenile pilocytic astrocytoma [JPA]):** This tumor is also one of the common posterior fossa tumors of the pediatric population. However, unlike the case shown in Figure 6-25, these lesions are typically cystic and located in the cerebellar hemisphere. This diagnosis is incorrect.

**Medulloblastoma:** This tumor is typically solid, often has small cysts, arises from the roof of the fourth ventricle, and frequently shows restricted diffusion on apparent diffusion coefficient maps—features that are shown in Figure 6-25. This diagnosis is

correct. The lesion shown in Figure 6-25B is slightly atypical because only a small portion of the mass contrast-enhances.

# DIAGNOSIS

**Medulloblastoma**

# KEY FACTS

## Clinical

- Medulloblastoma is a highly malignant tumor that is usually seen between the ages of 3 and 10 years. The tumor is thought to originate from precursor cells of the external granule layer of the cerebellar ventricular zone.
- Medulloblastoma is considered one type of primitive neuroectodermal tumor, along with ependymoblas-toma, pinealoblastoma, and cerebral neuroblastoma.
- A number of variants are recognized, including the classic, large cell, and desmoplastic/nodular medulloblas-toma, as well as two variants introduced in 2007 by the World Health Organization: medulloblastoma with extensive nodularity (which has a favorable prognosis) and anaplastic medulloblastoma (which has a poor prognosis).
- In childhood, the tumor typically arises in the midline, originating in the cerebellar vermis and extending into the fourth ventricle. When seen in young adults, it often occurs off the midline, in the cerebellar hemispheres. A 2:1 male predominance has been reported.
- Metastasis through the subarachnoid space of the brain and spine is common, being seen in 25% to 50% of patients at the time of diagnosis or early in the postoperative period.
- Because ventriculoperitoneal shunts are often placed in these patients for hydrocephalus, peritoneal metastasis can sometimes be seen.
- Medulloblastoma is one of the few CNS tumors that metastasizes with any notable frequency outside the CNS. Bone metastases are seen in about 5% of cases.
- The 5-year survival rate is estimated at 40% to 80%. Many survivors suffer from long-term treatment-related sequelae such as cognitive deficits from cranial radiation therapy.

## Radiologic

- On unenhanced CT, the tumor appears as a well-marginated, homogeneous, hyperdense mass that arises from the vermis and fills the fourth ventricle. The hyperdense appearance, although not invariably present, is a helpful feature in

identifying the mass as medulloblastoma. Cysts are often seen but are usually small and often multiple, as opposed to a single dominant cyst. Calcification is seen in about 20% of cases, but it is not a prominent feature when present.

- In some series, hydrocephalus is present in 95% of cases at the time of presentation.
- Medulloblastoma must be distinguished from two other common pediatric posterior fossa tumors: cerebellar JPA and ependymoma. JPA is usually hypodense on CT due to a large cystic component, and ependymoma is usually isodense or slightly hyperdense and calcified more commonly (50%) than medulloblastoma (and thus has an intrinsically inhomogeneous appearance).
- Extension through the fourth ventricular outlet foramina can be seen but is much more commonly present in ependymomas of the fourth ventricle. (See Case 24).
- Following contrast administration, medulloblastoma typically densely enhances in a homogeneous pattern except for the usually small areas of necrosis. In comparison, only the solid portions of JPAs contrast-enhance, resulting in an inhomogeneous appearance. Ependymoma also often enhances in an inhomogeneous pattern, further allowing distinction from medulloblastoma in most cases.
- Atypical appearances of medulloblastoma at the time of presentation can occasionally be seen, including a mass that is wholly cystic, a mass arising in the cerebellopon-tine angle, and multifocal tumor.
- On MR, the tumor is hypointense on T1-weighted images and iso- or hyperintense on T2-weighted images. The pattern of MR contrast-enhancement is similar to that seen on CT.
- Sagittal MRIs are often helpful in distinguishing medul-loblastoma from ependymoma. Because medullo-blastoma typically originates in the roof of the fourth ventricle, a cleavage plane can often be seen between the mass and the brain stem (Figure 6-25B). Ependy-momas are often adherent to the floor of the fourth ventricle and can grow into the brain stem. A cleavage plane, therefore, is often seen between the posterior aspect of the tumor and the vermis.
- Diffusion-weighted images of medulloblastoma often show restricted diffusion that has been attributed to the dense cellularity of this tumor.
- Imaging of the entire neuroaxis is indicated early in the clinical course to assess for drop metastases. It is important to recognize that if spinal imaging is first performed after craniotomy, postoperative extradural spinal hemorrhage can simulate drop metastases.

## SUGGESTED READING

Eran A, Ozturk A, Aygun N, Izbudak I. Medulloblastoma: atypical CT and MRI findings in children. Pediatr Radiol 2010;40:1254–1262.

Brat DJ, Parisi JE, Kleinschmidt-DeMasters BK, et al. A review of changes introduced by the WHO classification of

tumours of the central nervous system (4th ed). Arch Pathol Lab Med 2008;132:993–1007.

Jaremko JL, Jans LBO, Coleman LT, Ditchfield MR. Value and limitations of diffusion-weighted imaging in grading and diagnosis of pediatric posterior fossa tumors. AJNR Am J Neuroradiol 2010;31:1613–1616.

# CASE 26

**JAMES M. PROVENZALE**

## HISTORY

A 50-year-old woman with chronic headache and visual difficulty.

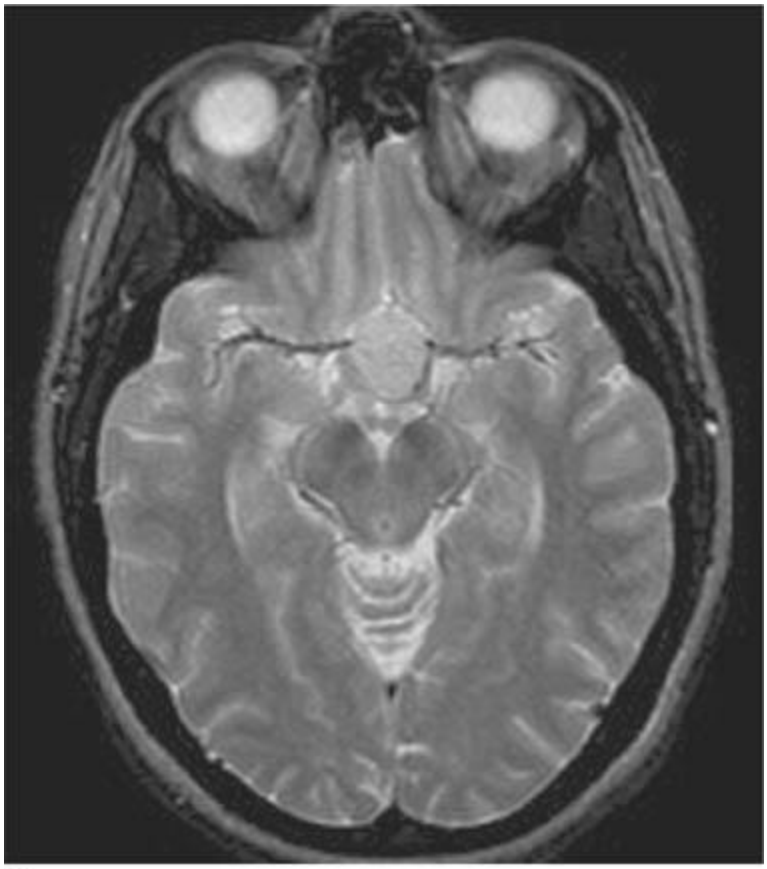

A

■**FIGURE 6-26A** Axial T2-weighted image shows a hyperintense suprasellar mass with smooth margins.

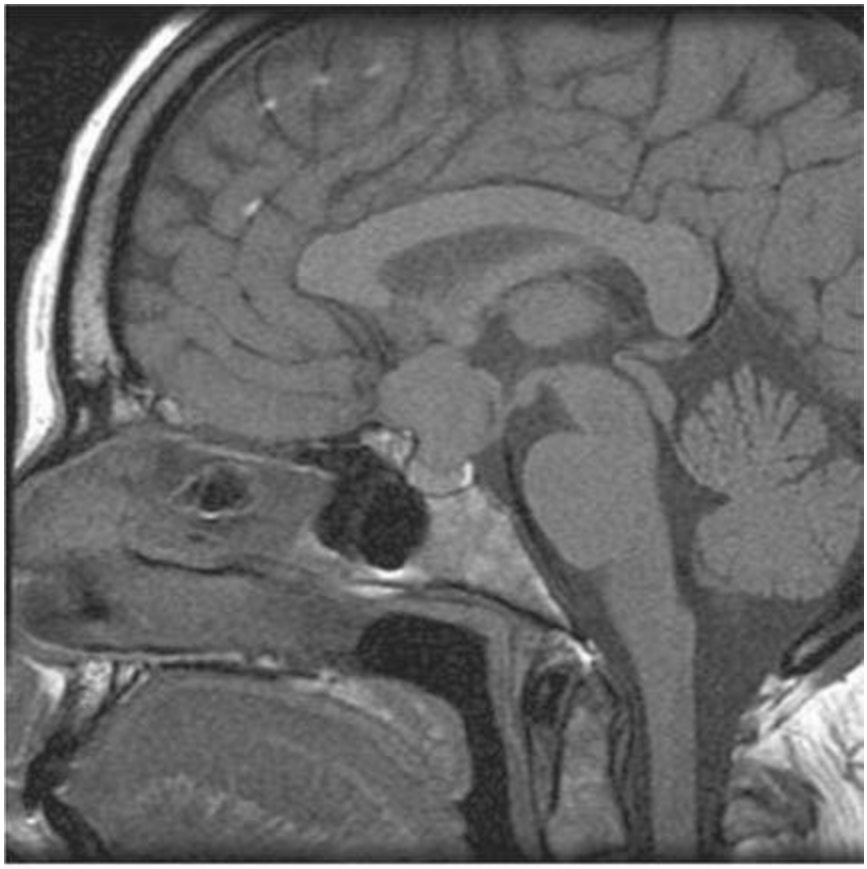

B

■**FIGURE 6-26B** Sagittal unenhanced T1-weighted image shows the mass displaces the third ventricle posteriorly. A sharp margin is seen between the mass and the pituitary gland, which is displaced inferiorly.

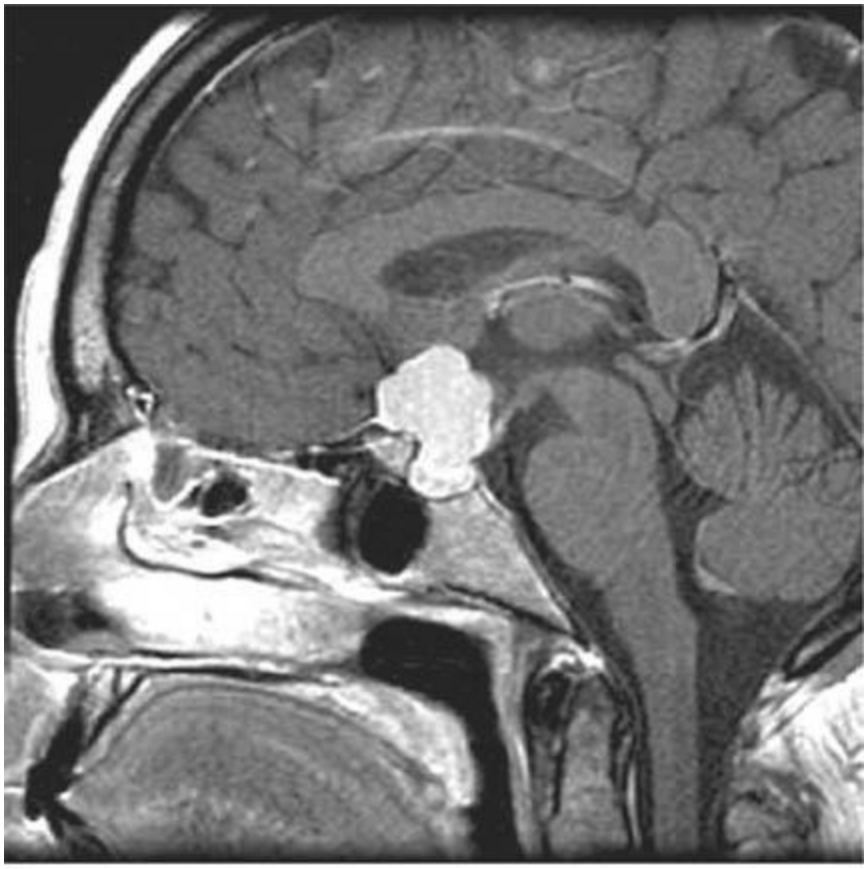

C

■**FIGURE 6-26C** On this sagittal contrast-enhanced T1-weighted image, the mass is seen to homogeneously enhance.

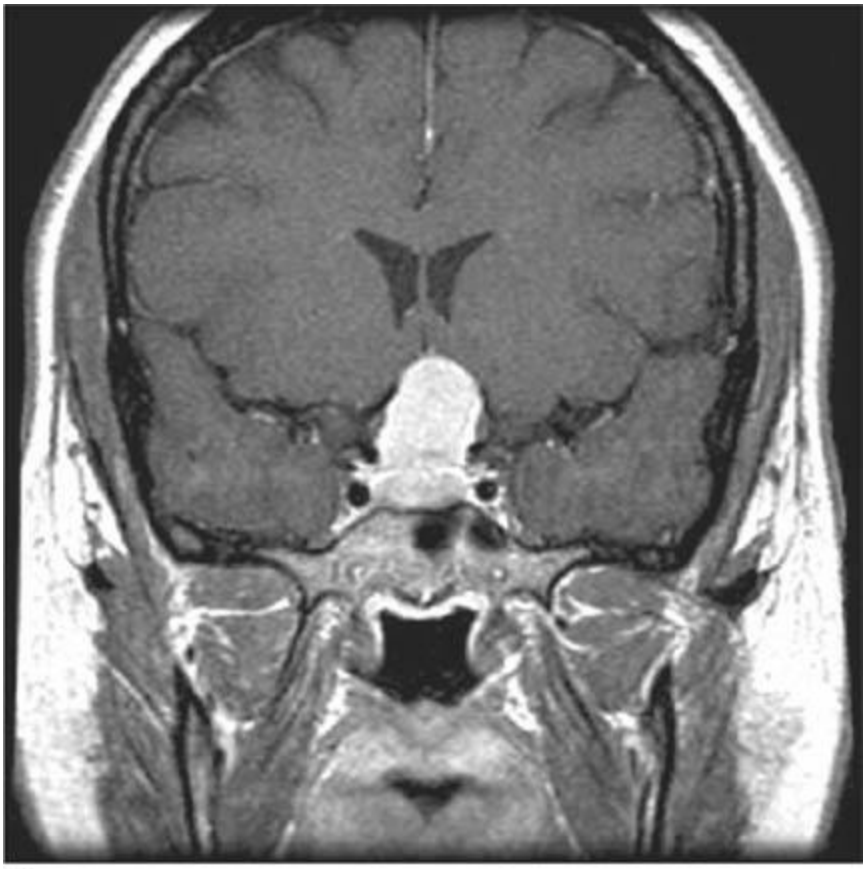

D

**FIGURE 6-26D** Coronal contrast-enhanced T1-weighted image shows the mass obliterating the suprasellar cistern and displacing both optic nerves laterally.

## DIFFERENTIAL DIAGNOSIS

**Aneurysm:** Solely based on location, an anterior communicating artery aneurysm could be considered. However, the signal intensity characteristics do not favor a patent aneurysm because no flow voids are seen in the lesion. A thrombosed aneurysm could also be considered. However, a thrombosed aneurysm typically shows a laminar appearance of blood products in various stages of evolution and also frequently produces pulsation artifact. Neither of these appearances is present. This diagnosis is very unlikely.

**Optic nerve glioma:** The rounded shape of the lesion shown here is atypical for an optic nerve glioma, which usually has an oval shape with its long axis extending from side-to-side on a coronal image. Furthermore, the optic nerves are seen to be spared in Figure 6-26D. This diagnosis is unlikely.

**Pituitary macroadenoma:** This entity commonly invades the suprasellar space and, hence, is a diagnostic consideration in the case shown here. However, the lesion in Figure 6-26 is seen to be distinct from the pituitary gland. This diagnosis is incorrect.

- **Meningioma:** The increased signal intensity on T2-weighted imaging, homogeneous enhancement and globoid shape of the lesion shown here is highly suggestive of meningioma. This diagnosis is correct.
- **Craniopharyngioma:** This tumor has two peak age distributions; the first peak is in the first decade and the second peak is in the fifth and sixth decades of life. Thus, based on the patient's age, this entity could be considered. However, these tumors are almost always cystic and calcified. The lesion shown in this case is homogeneous and lacks findings indicative of cysts or calcification. On this basis, the diagnosis is very unlikely.

## DIAGNOSIS

**Meningioma**

## KEY FACTS

### Clinical

- Meningioma is the most common nonglial intracranial neoplasm.
- The peak incidence is the fifth through seventh decades. The female-to-male ratio is 2:1.
- The vast majority of meningiomas are seen in adults. Meningiomas are rare in the pediatric population. Approximately 25% of children with a meningioma will have neurofibromatosis.
- Meningiomas arise from meningothelial cells (arachnoid "cap" cells) of the arachnoid villi and occur most often where these cells are most numerous.
- Sites of occurrence, in order of decreasing frequency, are parasagittal convexity, sphenoid wing, planum spenoidale, supra- or parasellar region, falx, posterior fossa, and spine. Less common sites include the cavernous sinus, suprasellar cistern, ventricle (especially trigone of the lateral ventricle), and orbit. These lesions may rarely occur in the diploic space and extracranial sites (e.g., nasal cavity, paranasal sinuses, nasopharynx, and infratemporal fossa).
- Four classic histologic subtypes are described: meningothelial (syncytial), fibroblastic, transitional, and angioblastic. Malignant meningiomas are rare.

### Radiologic

- Most meningiomas are well-defined, extraaxial masses. They may be broad-based, pedunculated, or flat ("en plaque").
- On CT, these lesions can be (1) isodense with brain, (2) intrinsically homogeneously

hyperdense, or (3) calcified to varying degrees. They typically strongly contrast-enhance. Calcification is seen in 15% to 20% of cases. Atypical findings (necrosis, cyst formation, hemorrhage) occur in 15% of cases.

- On MRI, meningiomas are typically isointense (60%) or hypointense (30%) relative to gray matter on unen-hanced T1-weighted images and usually densely contrast-enhance. They are isointense (50%) or hyper-intense (40%) relative to gray matter on T2-weighted images. However, densely calcified or fibrous tumors can be very hypointense on T2-weighted images (Figure 6-28C). Peritumoral hyperintense signal on T2-weighted images due to edema is seen in 75% of tumors.
- A "dural tail" is seen in approximately 60% of tumors on MRI. This finding can represent either tumor or nonneoplastic dural reaction. Although this finding is highly suggestive of meningioma, it is not specific for meningioma because it can be seen in other entities.
- Meningiomas are frequently found to produce associated hyperintense signal within adjacent white matter on T2-weighted or FLAIR images, which likely represents vasogenic edema due to secretion of tumoral proteins, such as vascular endothelial growth factor.
- On MR and CT perfusion-weighted images, meningio-mas typically are seen to have elevated relative cerebral blood volume.
- In some studies, restricted water diffusion on diffusion-weighted images has been associated with a more aggressive tumor. However, these studies are preliminary.
- The degree of adherence of meningiomas to adjacent brain, which is a factor that increases difficulty in removal, has been reported to be positively correlated with the absence of a rim of signal intensity (different from meningioma and brain tissue) between tumor and cortex as well as increasing degree of peritumoral edema.

## SUGGESTED READING

Saloner D, Uzelac A, Hetts S, et al. Modern meningioma imaging techniques. J Neurooncol 2010;99:333–340.

Takeguchi T, Miki H, Shimizu T, et al. Prediction of tumor-brain adhesion in intracranial meningiomas by MR imaging and DSA. Magn Reson Med Sci 2003;2:171–179.

Nagar VA, Ye JR, Ng WH, et al. Diffusion-weighted MRI: diagnosing atypical or malignant meningiomas and detecting tumor dedifferentiation. AJNR Am J Neuroradiol 2008;29:1147–1152.

Martin AJ, Cha S, Higashida RT, et al. Assessment of meningioma vascu-lature and the effects of embolization with intra-arterial MR perfusion imaging. AJNR Am J Neuroradiol 2007;28:196–205.

# CASE 27

**JAMES M. PROVENZALE**

**HISTORY**

A 44-year-old woman with tingling in the left hand of 2 months' duration.

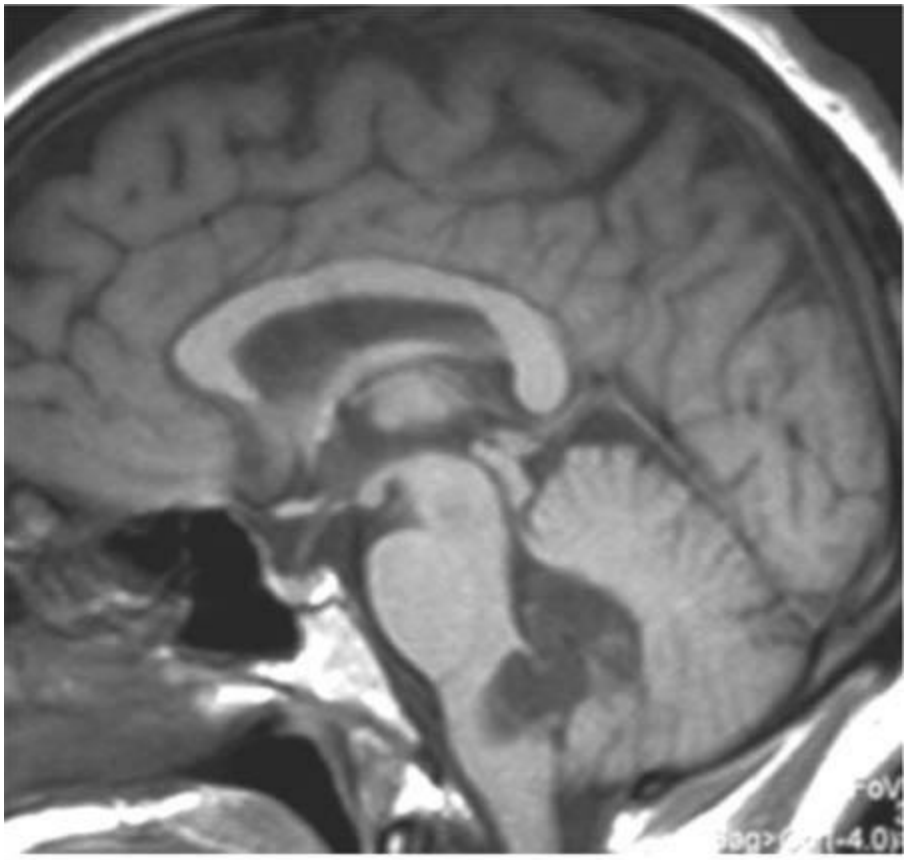

A

■**FIGURE 6-27A** Sagittal unenhanced T1-weighted image shows a mass that is relatively isointense to CSF within the fourth ventricle and extending along the lateral aspect of the brainstem. Following contrast administration (not shown), the mass did not contrast-enhance.

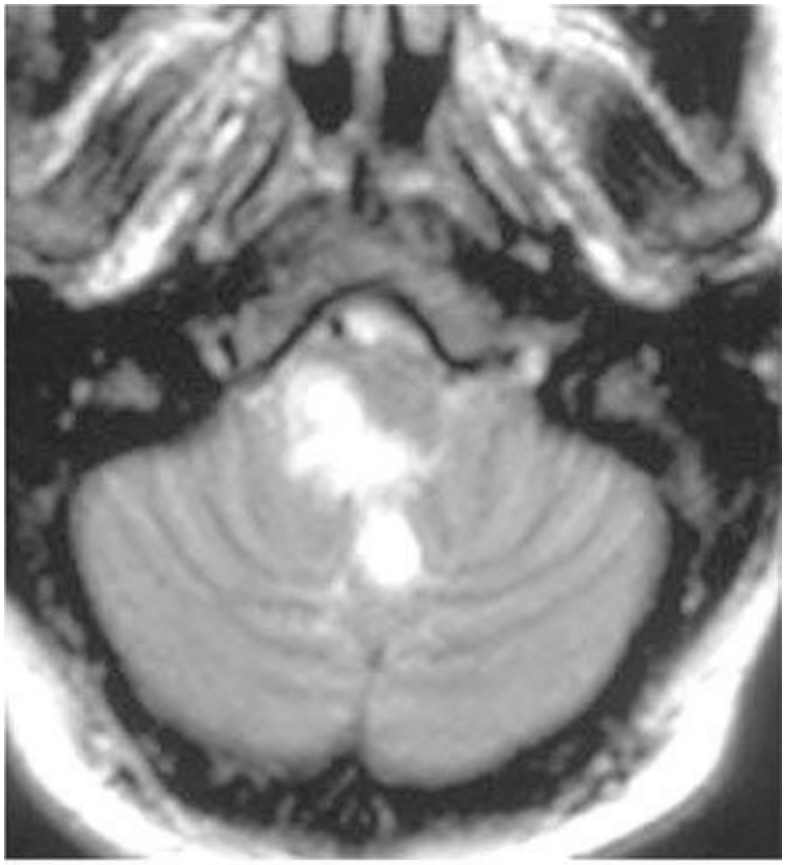

B

■**FIGURE 6-27B** Axial T2-weighted image shows the mass is relatively isointense with CSF.

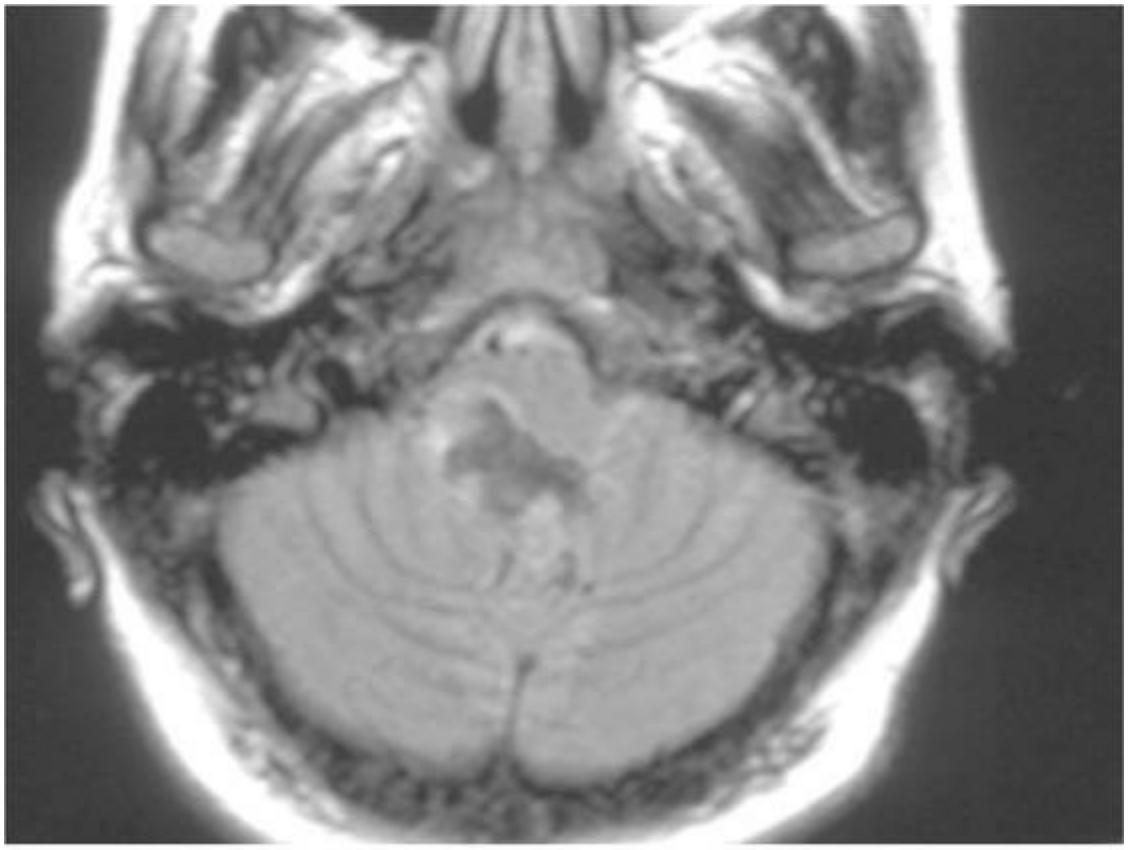

C

■**FIGURE 6-27C** Axial FLAIR image shows the mass deforming the brainstem; on this pulse sequence, the mass is seen to be inhomogeneous and brighter than CSF.

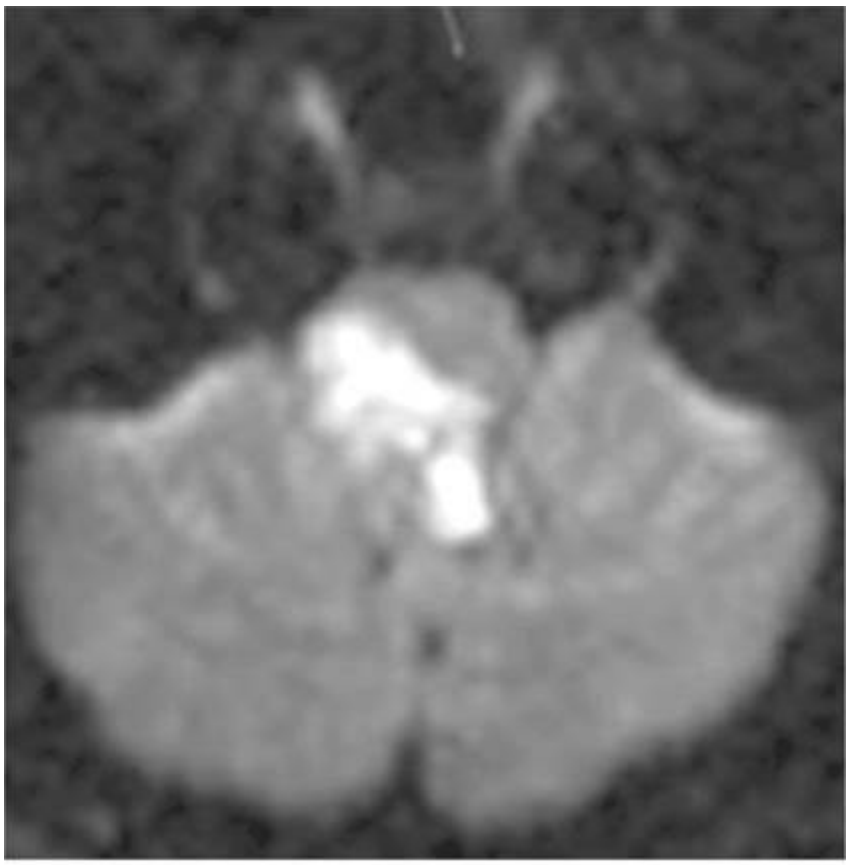

D

**FIGURE 6-27D** Axial diffusion-weighted image shows that the mass is much brighter than CSF; on an apparent diffusion coefficient map (not shown), the lesion was seen to have slightly restricted water diffusion compared to brain tissue.

## DIFFERENTIAL DIAGNOSIS

**Arachnoid cyst:** This entity, which is filled with CSF, might be considered because the lesions shown above are nearly isointense with CSF on T1- and T2-weighted images. However, the appearance on FLAIR images and diffusion-weighted images indicates that the lesion is not composed solely of CSF, making this an incorrect diagnosis.

**Cysticercosis:** Lesions within the subarachnoid space are a relatively common form of CNS cysticercosis infection. The lesions can grow to a large size and compress adjacent brain. However, they are typically isointense with CSF, unlike the lesion shown in this case; this diagnosis is unlikely.

**Epidermoid cyst:** These lesions are frequently located in the posterior fossa and deform (rather than infiltrate) adjacent brain. They are relatively isointense to CSF on T1- and T2-weighted images (Figures 6-27A and 6-27B) but are typically hyperintense to CSF on FLAIR images (Figure 6-27C) and diffusion-weighted images (Figure 6-

27D).

- **Brain abscess:** This diagnosis might be considered because of the bright signal intensity seen on the diffusion-weighted imaging sequence. However, abscesses within the subarachnoid space (as opposed to ventricu-litis) are very uncommon. This diagnosis is incorrect.

## DIAGNOSIS

**Epidermoid cyst**

## KEY FACTS

### Clinical

- Epidermoid cysts are thought to arise from inclusion of epithelial elements within the neural groove during its closure.
- Although epidermoid cysts grow with age, they are not considered neoplasms. Enlargement occurs due to progressive accumulation of breakdown products of desquamated epithelial cells, including keratin and solid cholesterol.
- Eighty percent of intracranial epidermoid cysts are intradural in location, often appearing in the infraten-torial compartment. The cerebellopontine angle is one of the more common sites. Supratentorial epidermoid cysts are usually found in the parasellar region and medial aspect of the middle cranial fossa.
- Epidermoid cysts are slow-growing lesions that conform to the surface of the brain as they enlarge, infiltrate through the subarachnoid space, and surround vessels and cranial nerves. Symptoms have often been present for many months or a few years by the time of discovery.
- Because the surfaces of intracranial epidermoid cysts have a shiny, white surface appearance, they are sometimes referred to as “pearly tumors.”
- Epidermoid cysts are similar to dermoid cysts in that both lesions have a stratified squamous epithelial lining with a fibrous connective tissue capsule, but epidermoid cysts lack sebaceous and sweat gland secretory units.
- Arachnoid cyst is the principal diagnostic consideration from which epidermoid cyst must be distinguished. Arachnoid cysts are frequently not treated due to the fact that they are asymptomatic, stable congenital lesions. Epidermoid cysts, however, are often symptomatic and continue to grow with advancing age, necessitating resection.
- Total surgical resection of an epidermoid cyst is often impossible because portions of the lesion are buried in spaces that cannot be reached without causing undue traction on important neurologic or vascular structures. Furthermore, and because the tumor is often

tightly adherent to brain and blood vessels. In those instances, partial debulking is performed, which may need to be repeated as the lesion regrows.

## Radiologic

- On unenhanced head CT, epidermoid cysts are hypodense extra-axial masses whose margins are often slightly lobulated or scalloped. Many lesions are slightly hyperdense relative to CSF and mildly inhomogeneous. However, they frequently are isodense to CSF, making distinction from arachnoid cyst difficult. Occasionally, a very small amount of calcification can be seen.
- Epidermoid cysts have a soft, pliable consistency, but they often exert a moderate degree of mass effect on adjacent brain structures. Multilocular lesions are seen in about 20% of cases.
- Lack of enhancement after contrast administration is the general rule; very mild contrast-enhancement can be seen around the rim of the lesion in about 30% of cases.
- MRI is frequently useful in distinguishing epidermoid cysts from arachnoid cysts because the lesion often appears inhomogeneous and has a signal intensity that differs from CSF on at least one pulse. The most common pulse sequences on which the signal intensity of the lesion differs from that of CSF are FLAIR, proton density-weighted and diffusion-weighted sequences.
- MRI is important in surgical planning because it is the best method for defining the limits of the mass and the spatial relationship to cranial nerves and blood vessels.
- Lesions involving the cerebellopontine angle often extend into Meckel's cave.
- When a suspected epidermoid cyst is isointense with CSF on all pulse sequences, the distinction from arachnoid cyst can be made by pulse sequences that are sensitive to water motion—for example, diffusion-weighted images and steady-state free precession images. On diffusion-weighted images, the apparent diffusion coefficient values of epidermoid cysts are typically much lower than those of CSF but often only mildly elevated or even mildly decreased compared to brain tissue.

# SUGGESTED READING

Kallmes DF, Provenzale JM, Cloft HJ, McClendon RE. Typical and atypical MR imaging features of intracranial epidermoid tumors. AJR 1997;169:883–887.

Suzuki C, Maeda M, Matsumine A, et al. Apparent diffusion coefficient of subcutaneous epidermal cysts in the head and neck comparison with intracranial epidermoid cysts. Acad Radiol 2007;14:1020–1028.

Hakyemez B, Aksoy U, Yildiz H, Ergin N. Intracranial epidermoid cysts: diffusion-weighted, FLAIR and conventional MR findings. Eur J Radiol 2005;54:214–220.

Hu XY, Hu CH, Fang XM, et al. Intraparenchymal epidermoid cysts in the brain: diagnostic value of MR diffusion-weighted imaging. Clin Radiol 2008;63:813–818.

Reddy JS, Mishra AM, Behari S, et al. The role of diffusion-weighted imaging in the differential diagnosis of

intracranial cystic mass lesions: a report of 147 lesions. Surg Neurol 2006;66:246–250.

# CASE 28

**JAMES M. PROVENZALE**

## HISTORY

A 65-year-old man with sudden onset of back pain and paraparesis occurring over the course of 20 minutes.

A

■**FIGURE 6-28A** Sagittal proton-density weighted image shows a thin linear region of increased signal intensity oriented along the long axis of the spinal cord in the anterior portion of the spinal cord. A region of hyperintense signal abnormality is also seen at the conus medullaris.

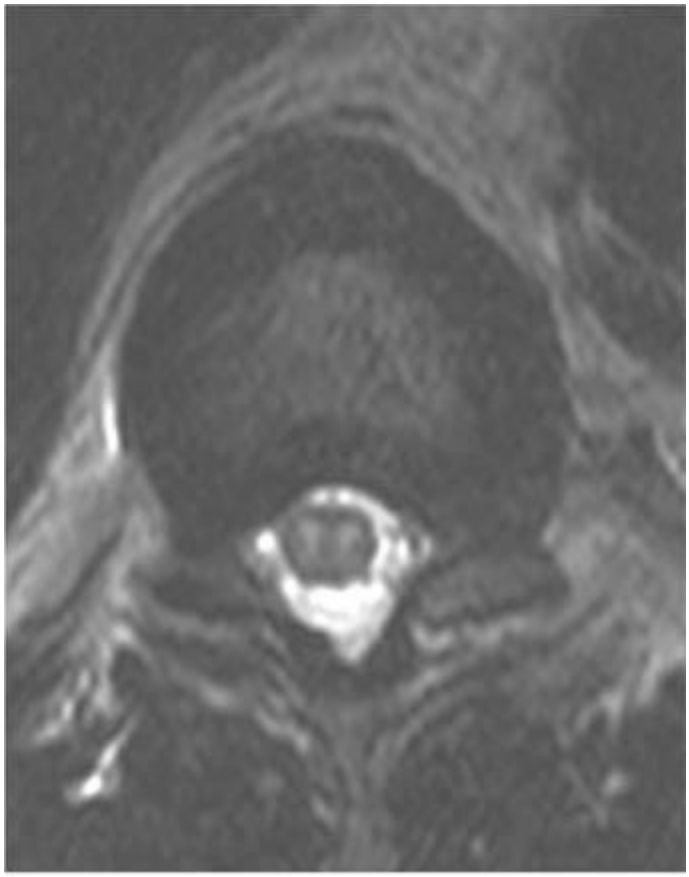

B

**FIGURE 6-28B** Axial T2-weighted image shows bilateral regions of hyperintense signal abnormality in the anterior aspect of the spinal cord.

## DIFFERENTIAL DIAGNOSIS

- **Multiple sclerosis:** MS plaques are usually seen in the periphery of the spinal cord within the spinal cord white matter. The central location of the abnormalities in this case (i.e., within gray matter) and the sudden onset are factors that make this diagnosis unlikely.
- **Transverse myelitis:** This entity usually occurs over the course of hours or days and typically involves large regions of the transverse diameter of the spinal cord, making this diagnosis an unlikely one.
- **Spinal cord infarction:** The clinical onset and bilateral small regions of hyperintense signal (so-called owl's eye appearance) seen on the axial image are characteristic of spinal cord infarction.
- **Vitamin $B_{12}$ deficiency:** This entity characteristically involves the posterior columns of the spinal cord, unlike the case shown here. Furthermore, the acute clinical onset is not consistent with vitamin B12 deficiency.
- **Spinal cord ischemia due to venous congestion caused by an acquired spinal dural**

**fistula:** This entity produces hyperintense signal abnormality but the distribution is typically diffuse and enlarged flow voids are characteristically seen posterior to the spinal cord. Furthermore, the symptom onset is usually over many weeks and, therefore, unlike that described in the case illustrated here.

## DIAGNOSIS

**Spinal cord infarction**

## KEY FACTS

### Clinical

- The vascular supply to the spinal cord is primarily composed of one anterior and two posterior spinal arteries, which extend along the length of the spinal cord in a variable manner.
- The anterior and posterior spinal arteries are connected by a pial plexus that extends around the circumference of the spinal cord.
- At many levels, the anterior and posterior spinal arteries receive vascular contributions from the radicular arteries, which course along the nerve roots and enter the spinal canal.
- Thirty-one pairs of radicular arteries exist. About 8 of these 62 arteries contribute to the spinal cord vascularity, with three major arterial regions identified: a cervicothoracic region (extending down to about T3), a midthoracic region (approximately T4 to T8, usually supplied by a radicular artery at the T7 level). and a thoracolumbar region (below T8, supplied by the artery of Adamkiewicz).
- The anterior spinal artery gives rise to central arteries at multiple levels; these arteries supply the anterior horn cells and the anterior aspect of the lateral columns on both sides of the spinal cord.
- Two major forms of spinal cord infarcts are recognized. The first involves the interruption of supply by the radicular arteries or artery of Adamkiewicz and is characterized by unilateral or bilateral infarcts of the anterior or posterior spinal arteries. The second one is caused by diffuse hypoperfusion and is manifested by central or transverse infarcts.
- Recognized causes include spinal and aortic surgery, hypotension, vertebral artery dissection, fibrocartilagi-nous embolism, vasculitis, and cocaine abuse.
- Clinically, approximately 40% of patients have a complete anterior spinal artery infarct pattern (bilateral motor deficit with spinothalamic sensory deficit), 7% have a complete posterior spinal artery pattern (bilateral motor deficit and posterior column

sensory deficit), 15% have a unilateral anterior spinal artery pattern (hemipa-resis with contralateral spinothalamic sensory deficit), 15% have a unilateral posterior spinal artery pattern (hemiparesis with ipsilateral posterior column sensory deficit), 10% have a central infarct pattern (bilateral spinothalamic tract sensory loss without motor deficit), 7% have a transverse syndrome (bilateral motor deficit and complete sensory loss), and 6% have an infarct that does not fit one of the previously mentioned patterns.

- Myelopathy onset is usually within a few minutes but, on occasion, over a few hours. In approximately half of patients, back or neck pain occurs at the level of the infarction.
- Transverse or central infarcts, typically related to hypoperfusion, can be seen after aortic dissection or surgery upon the aorta producing transient or permanent occlusion of the artery of Adamkiewicz.
- In about half of cases, infarction occurs immediately after a movement, such as back extension, an arm movement or a Valsalva maneuver, possibly causing mechanical stress on a radicular artery.
- In a minority of cases, disc herniation with subsequent compression of a vessel, such as radicular artery, appears to be the causative mechanism.

## Radiologic

- Findings are seen on spinal MR imaging in about 70% to 85% of cases. Imaging in the first few hours may be negative but then are occasionally positive in the following days or weeks. Lesions not seen on MR imaging are often clinically localized to the lower thoracic spinal cord.
- Approximately 40% of infarcts are located in the cervical spinal cord and another 40% are seen at the T10-L1 level.
- On sagittal T2-weighted images, a thin linear hyperin-tense region can be seen within the spinal cord, which is associated with spinal cord enlargement in about half of cases.
- Axial T2-weighted images typically show regions of hyperintense signal, which are usually in the anterior spinal artery territory.
- Approximately 85% to 90% of infarcts seen on axial T2-weighted images involve the central territory of the anterior spinal artery. Of these, about two-thirds are extensive and involve both central gray matter and adjacent white matter. The remaining one-third involve solely the central gray matter, giving the so-called owl's eye appearance on axial images.
- Four major patterns of signal abnormality on axial T2-weighted images have been described. From least extensive to most extensive, they are (1) involvement of solely the anterior horn cells (so-called owl eye appearance), (2) involvement of both the anterior and posterior horn cells, (3) involvement of anterior and posterior horn cells and adjacent central white matter, and (4) diffuse abnormality.

- Regions of hyperintense signal on unenhanced T1-weighted images or hypointense signal on T2-weighted images can occasionally be seen, corresponding to regions of hemorrhage.
- In some cases, rim enhancement of the infarct due to disruption of the blood-brain barrier may be seen on contrast-enhanced T1-weighted images.
- On diffusion-weighted images, acute infarcts appear bright and have lowered apparent diffusion coefficient values, similar to the findings of acute cerebral infarction. On occasion, diffusion images will show an abnormality, when the appearance on T2-weighted images is normal.

## SUGGESTED READING

Thurnher MM, Bammer R. Diffusion-weighted MR imaging (DWI) in spinal cord ischemia. Neuroradiology 2006;48:795–801.

Novy J, Carruzzo A, Maeder P, Bogousslavsky J. Spinal cord ischemia: clinical and imaging patterns, pathogenesis, and outcomes in 27 patients. Arch Neurol 2006;63:1113–1120.

Masson C, Pruvo JP, Meder JF, et al. for the Study Group on Spinal Cord Infarction of the French Neurovascular Society. Spinal cord infarction: clinical and magnetic resonance imaging findings and short term outcome. J Neurol Neurosurg Psychiatr 2004;75:1431–1435.

Weidauer S, Nichtweiss M, Lanfermann H, Zanella FE. Spinal cord infarction: MR imaging and clinical features in 16 cases. Neuroradiology 2002;44:851–867.

Mawad ME, Rivera V, Crawford S, et al. Spinal cord ischemia after resection of thoracoabdominal aortic aneurysms: MR findings in 24 patients. AJNR Am J Neuroradiol 1990;11:987–991.

# CASE 29

**JAMES M. PROVENZALE**

### HISTORY

A 5-year-old boy with developmental delay and spasticity.

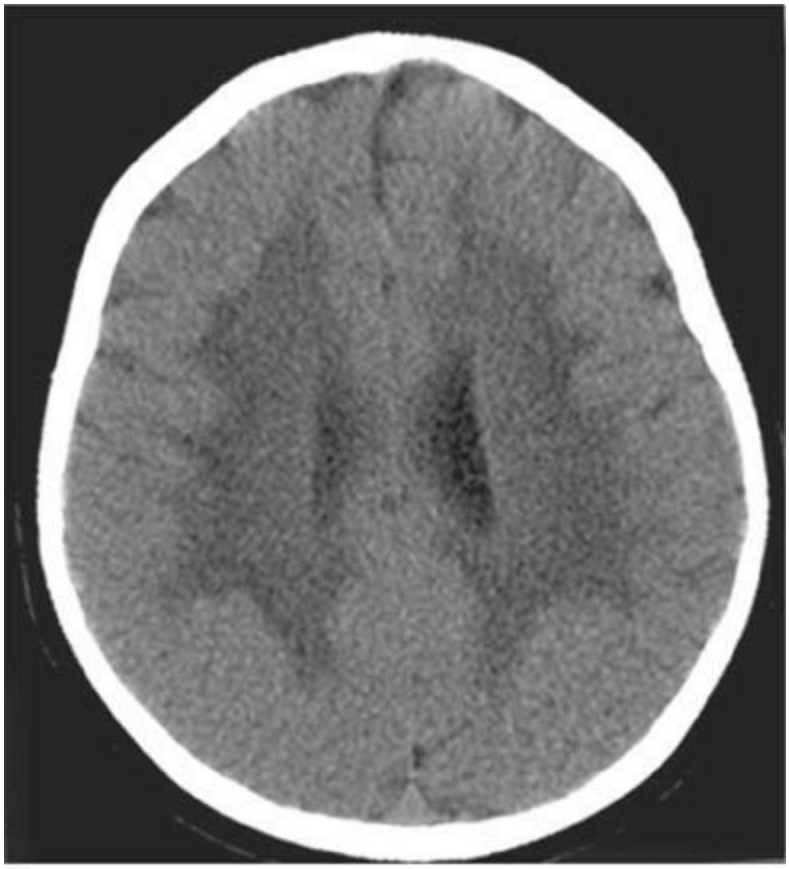

A

■**FIGURE 6-29A** Unenhanced axial CT image shows diffuse, symmetric low attenuation in the cerebral white matter.

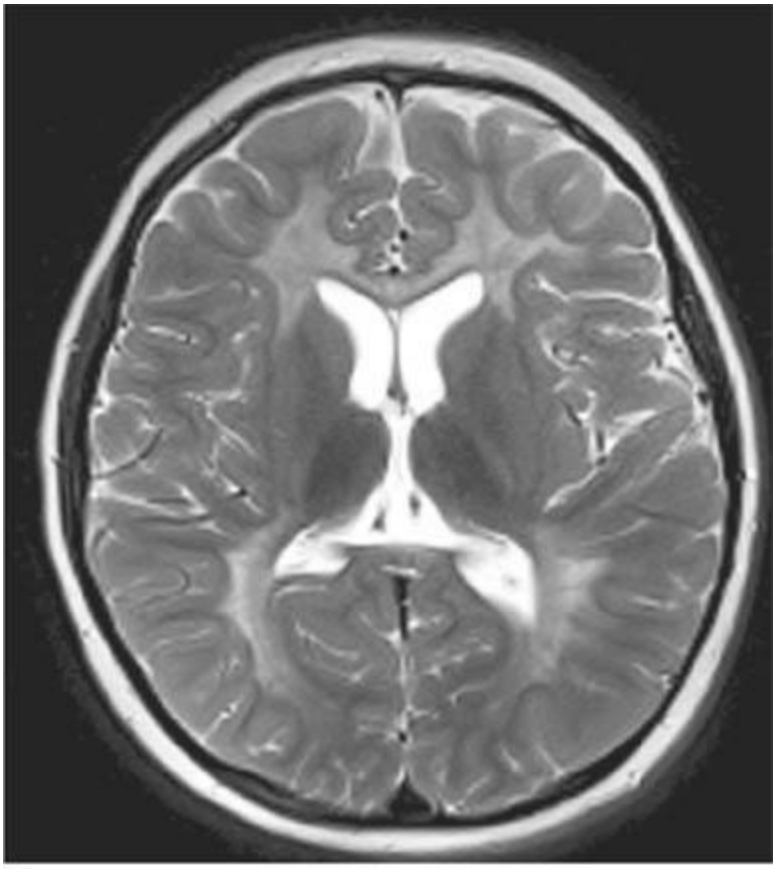

B

■**FIGURE 6-29B** T2-weighted axial image shows hyperin-tense signal in the periventricular regions and in the posterior limb of both internal capsules. The deep gray matter regions (i.e., basal ganglia and thalamus) are normal in appearance.

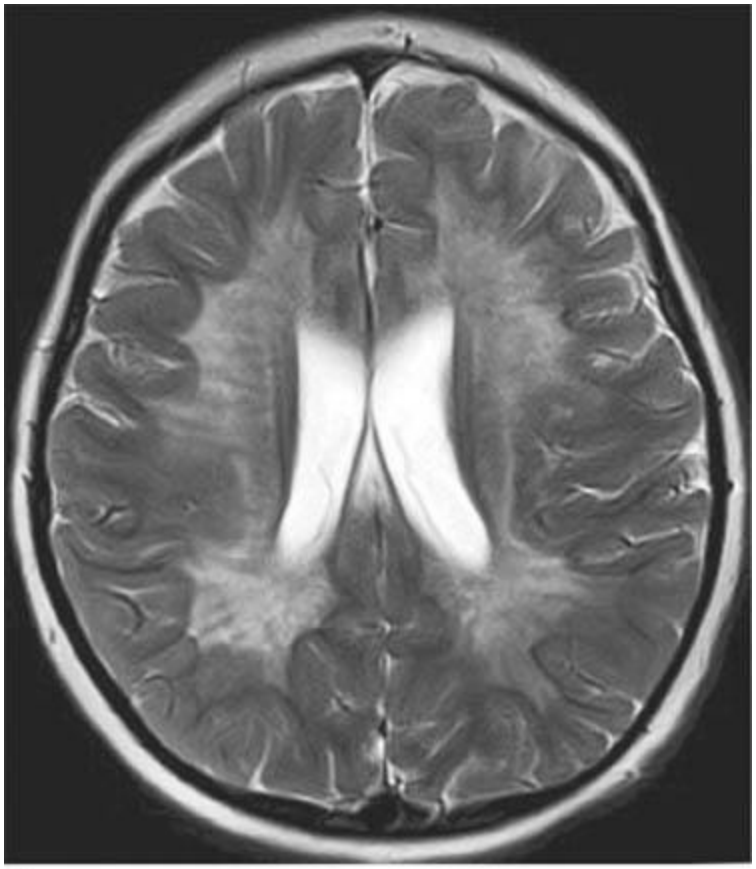

C

**FIGURE 6-29C** T2-weighted axial image shows hyperin-tense signal throughout the centrum semiovale bilaterally. Linear regions of only slightly hyperintense signal are seen oriented perpendicular to the lateral ventricles.

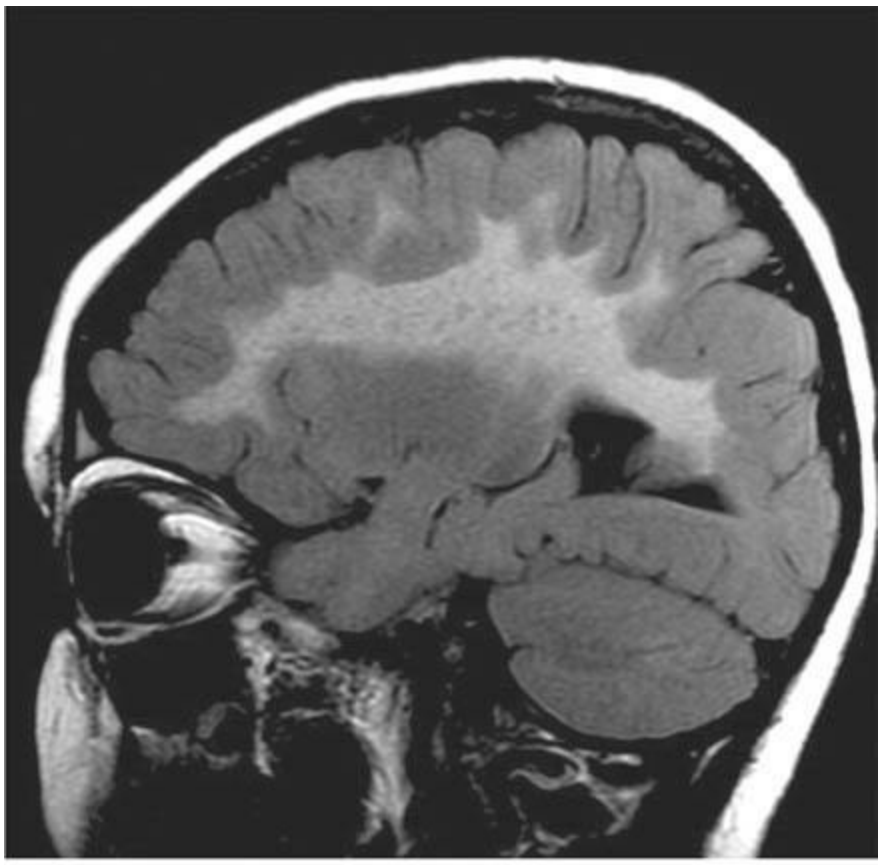

D

**FIGURE 6-29D** Para-sagittal FLAIR image shows hyperin-tense signal throughout much of the white matter, with small rounded foci of less hyperintense signal scattered throughout the whit matter. These regions represent the linear regions seen in Figure 6-29C when viewed on-end.

## DIFFERENTIAL DIAGNOSIS

**Adrenoleukodystrophy:** The imaging findings in this disease are characterized by hyperintense signal on T2-weighted or FLAIR images that, in the early stages of the disease, are predominantly in the white matter of the occipital and parietal lobes. However, the findings in the case shown here are symmetric with regard to anterior-posterior distribution. This answer is incorrect.

**Krabbe disease:** This diagnosis might be considered because it causes white matter abnormalities and neurologic decline. However, throughout much of the clinical course, the lesions are usually multiple, focal, and of various sizes rather than large, confluent and symmetric, as in the case shown here. This diagnosis is incorrect.

**Metachromatic leukodystrophy (MLD):** This entity, which begins in infancy, typically has the radiologic manifestation of symmetric, bilateral white matter abnormality (such as is seen in the case shown here). Linear regions of relatively

normal signal intensity can be seen on axial T2-weighted images, sometimes referred to as a so-called tigroid appearance (Figure 6-29C). This is the correct diagnosis.

- **Alexander's disease:** This diagnosis might be considered because of the prominent bilateral white matter abnormalities. However, the abnormalities in Alexander's disease typically predominate in the frontal white matter, unlike the case shown here. This diagnosis is incorrect.
- **Leigh's disease:** This disease is usually manifested by abnormal signal intensity in the deep gray matter regions (i.e., basal ganglia and thalamus), which are normal in the case illustrated here. This diagnosis is incorrect.

## DIAGNOSIS

**Metachromatic leukodystrophy**

## KEY FACTS

### Clinical

- MLD is an autosomal recessive disorder that is caused by deficiency of the lysosomal enzyme arylsulfatase A, which is found to be low in peripheral blood leukocytes and urine in affected patients.
- Sulfatides accumulate in the central and peripheral nervous systems and in various other organs.
- Overall, the incidence is approximately 1:40,000 but is much higher in select populations.
- Clinical features consist of mental degeneration, gait ataxia, and spastic quadriparesis.
- Three major forms are recognized: an infantile form (onset at 15 to 24 months) that results in death within 7 to 8 years, a juvenile form (onset at age 4 to 12 years), and an adulthood form.
- The juvenile form can be divided into an early juvenile form (onset at age 4 to 6 years) and a late juvenile form (onset at age 6 to 12 years).
- Laboratory test abnormalities include increased protein in CSF and delayed nerve conduction velocities.

### Radiologic

- The cross-sectional imaging findings are somewhat characteristic, with bilateral, symmetric white matter involvement that extends in a centrifugal manner to extend to the subcortical regions.

- On unenhanced CT, the lesions are seen as extensive low density within the supratentorial white matter. After intravenous infusion of contrast material, no contrast-enhancement is seen.
- Lesions are hypointense on unenhanced T1-weighted MR images and markedly hyperintense on T2-weighted and FLAIR images. Abnormalities are predominantly supratentorial but cerebellar lesions can also be seen in about 25% of patients.
- MR findings are similar among individuals with the infantile form, juvenile form, and adult form.
- Cranial nerve enhancement can be seen in a small number of cases.
- In severe cases, hyperintense signal in the internal capsule and hypointense signal in the basal ganglia and thalamus on T2-weighted images can be seen.
- A characteristic (but not pathognomonic) appearance of MLD is the so-called tigroid appearance of the white matter which, on axial images near the level of the cerebral ventricles, is seen as linear regions of relatively normal signal intensity (Figure 6-29C). These regions are conspicuous as darker regions against the backdrop of very abnormal white matter signal intensity.
- Images that are oriented perpendicular to the linear regions that produce the "tigroid appearance" are seen as small round foci, giving rise to the name "leopard skin appearance." These findings are typically seen in the cephalad aspect of the centrum semiovale and frontal and parietal subcortical regions on axial images and in the lateral brain regions on sagittal images (Figure 6-29D).
- The tigroid and leopard skin pattern can also be seen in globoid cell leukodystrophy (i.e., Krabbe disease) and Pelizaeus-Merzbacher disease.

## SUGGESTED READING

Cheon JE, Kim IO, Hwang YS, et al. Leucodystrophy in children: a pictorial review of MR imaging features. Radiographics 2002;22:461–476.

van der Voorn JP, Pouwels PJW, Kamphorst W, et al. Histopathologic correlates of radial stripes on MR Images in lysosomal storage disorders. AJNR Am J Neuroradiol 2005;26:442–446.

Eichler F, Grodd W, Grant E, et al. Metachromatic leukodystrophy: a scoring system for brain MR imaging observations. AJNR Am J Neuroradiol 2009;30:1893–1897.

# CASE 30

**JAMES M. PROVENZALE**

## HISTORY

A 29-year-old woman with headache and lethargy of 4 days' duration and mild left hemiparesis.

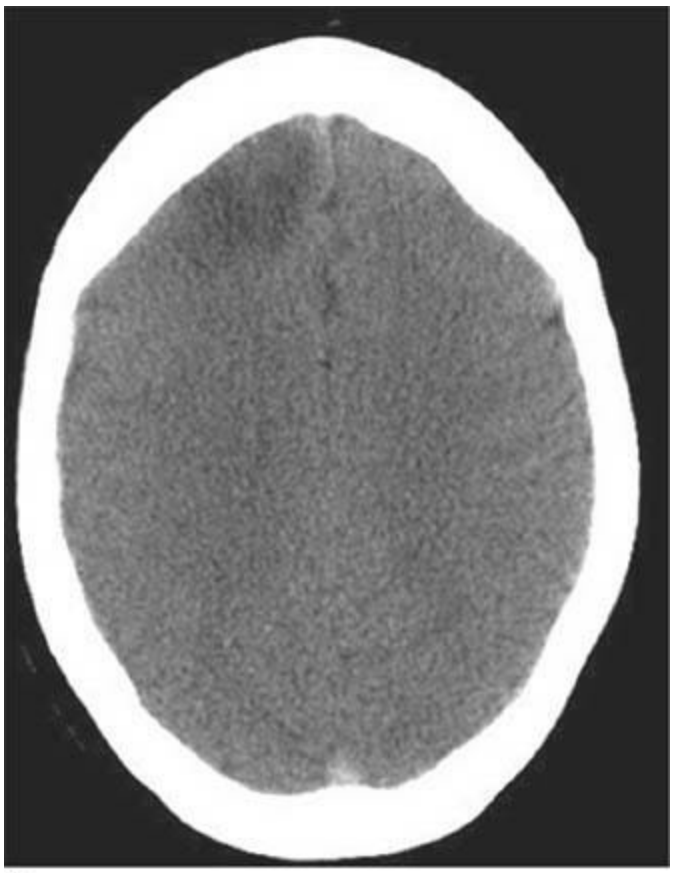

A

■**FIGURE 6-30A** Unenhanced axial CT scan shows low density region with mass effect in the right frontal lobe involving cortex and subcortical white matter.

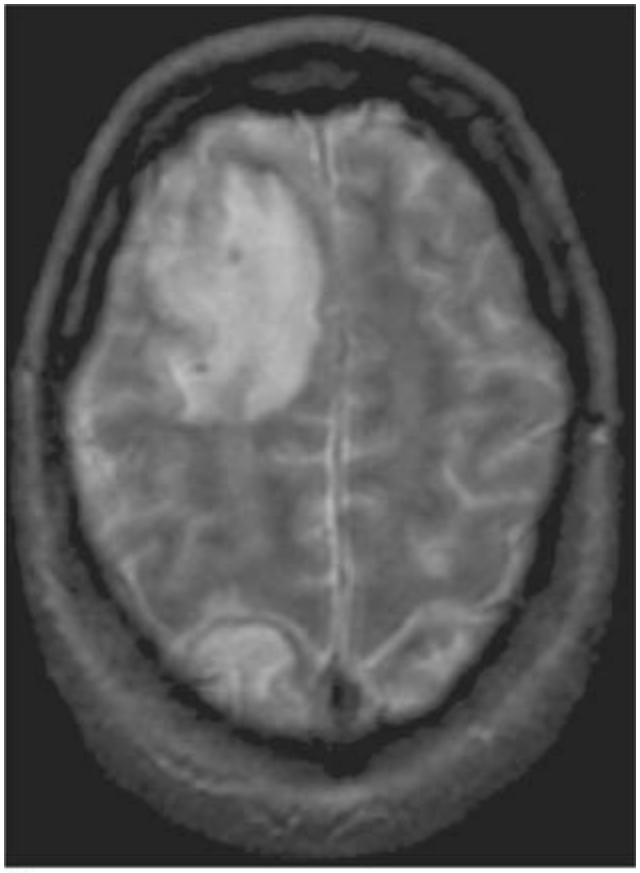

B

■**FIGURE 6-30B** Axial T2-weighted MR image shows the right frontal lobe abnormality depicted in 6-30 A as well as a right parietal lobe lesion.

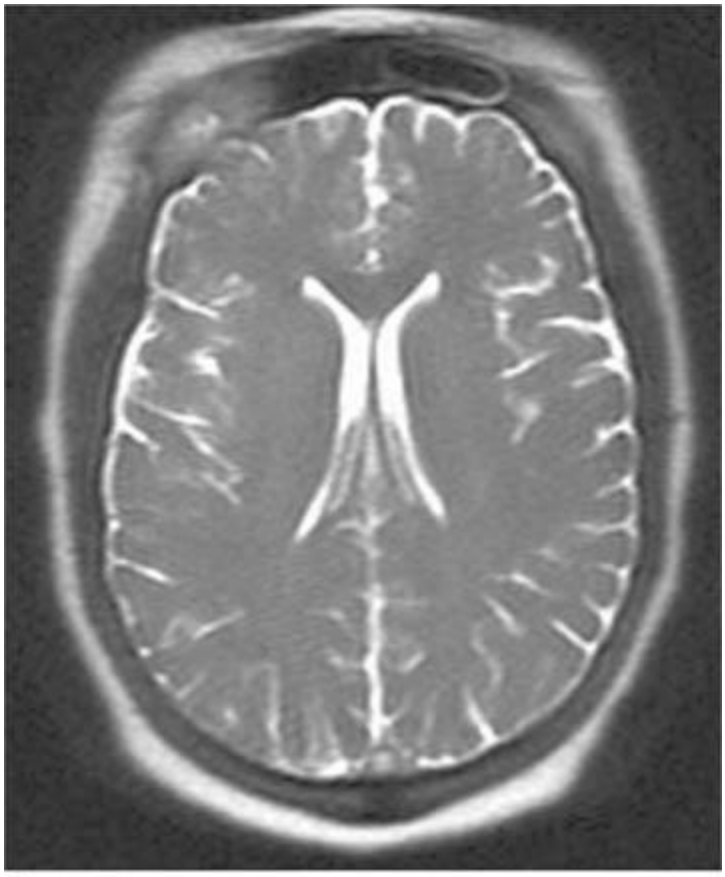

C

■**FIGURE 6-30C** Axial T2-weighted MR image at a more cephalad level than that shown in 6-30B shows no other abnormalities of the brain parenchyma.

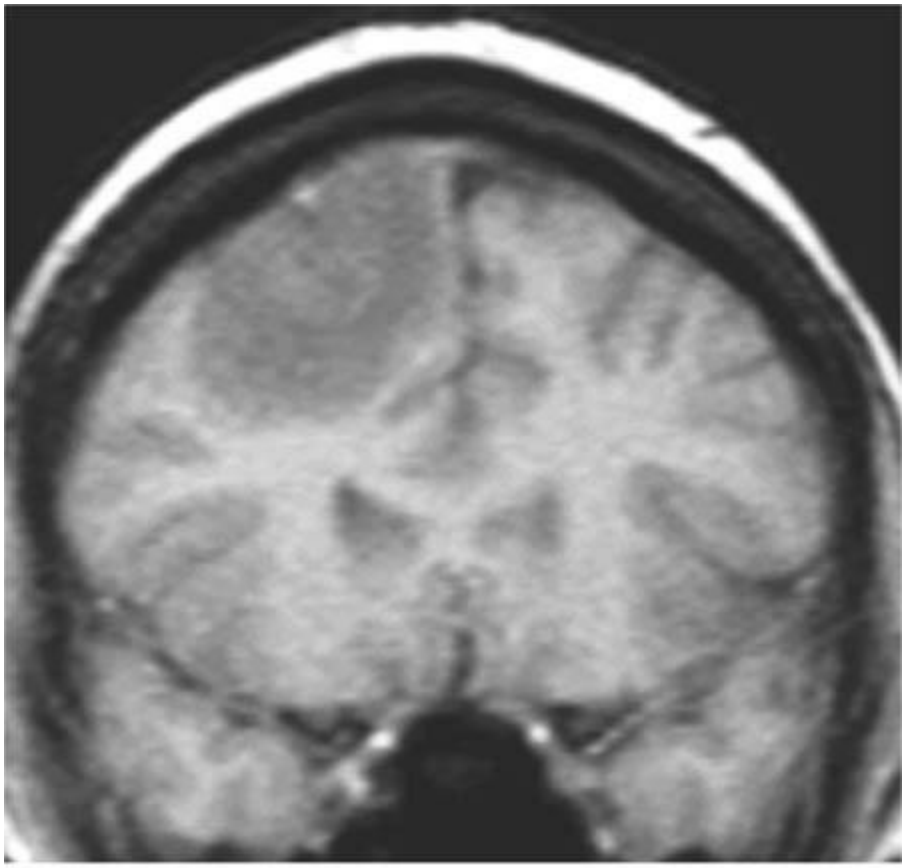

D

**FIGURE 6-30D** Coronal localizer image shows the abnormality seen in 6-30A as a large area of diminished signal intensity in the right frontal lobe. A round region of hyperintense signal is present overlying brain cortex. On follow-up imaging a year later (not shown) this hyperintense region was not seen.

## DIFFERENTIAL DIAGNOSIS

**Embolic infarction:** This diagnosis might be considered because multiple lesions, peripheral in location, are seen. However, the location of the lesion in the frontal lobe is unusual for arterial infarction because a large proportion of the lesion involves the anterior cerebral artery territory, whereas most embolic infarcts involve solely the middle cerebral artery territory. Although this diagnosis is not definitively excluded, it is an unlikely consideration.

**Metastases:** Because multiple lesions are present, metastases are a worthy consideration. In the absence of administration of contrast material, this diagnosis cannot be definitively excluded. However, the homogeneous appearance of the regions of abnormal signal intensity is somewhat unusual for metastases. Typically, metastases are seen as a focal lesion with vaso-genic edema; that finding is not present in the case shown here.

- **Progressive multifocal leukoencephalopathy:** This diagnosis might be considered based on the present of multiple lesions in a young patient. However, PML occurs exclusively in individuals who are immunosup-pressed; no such history is provided for the patient shown here. In addition, the lesions of PML typically lack mass effect or have only mild mass effect (see Case 2), whereas the lesions in the case shown have marked mass effect. This diagnosis is incorrect.
- **Infarction due to dural sinus thrombosis:** Figure 6-30A shows a hyperdense appearance of the posterior aspect of the superior sagittal sinus; this finding is reflected on Figure 6-30C, which shows absence of the flow void of the superior sinus. Figure 6-30D shows high signal intensity within a cortical vein (indicating thrombosis) adjacent to the frontal lobe lesion. This diagnosis is correct.

## DIAGNOSIS

**Dural sinus thrombosis and venous infarction**

## KEY FACTS

### Clinical

- DST can present in isolation or with accompanying venous infarction.
- A number of predisposing factors are associated with DST, including hypercoagulable states, pregnancy and puerperium, CNS infection, and dehydration. The most common hypercoagulable state to produce DST is activated protein C resistance (Factor V Leiden condition).
- DST can also occur in the setting of pregnancy and the puerperium and should be considered in the differential diagnosis of lesions causing headache or impaired consciousness in those settings.
- The most common clinical presentation is that of new onset persistent headache that is different in nature than prior headaches. Much less commonly, patients present with impaired consciousness.
- When the thrombus extends in a retrograde manner from the dural sinus into cortical veins, venous infarction can occur.
- Prior to the advent of widespread effective antibiotic therapy, CNS infection was an important cause of DST, especially for development of transverse sinus thrombosis following mastoiditis. However, presently CNS infections are a relatively uncommon cause of DST.

### Radiologic

- Imaging findings can include a hyperdense dural sinus on unenhanced CT, lack of enhancement of a dural sinus on contrast-enhanced CT and T1-weighted MR images, loss of the flow void of a dural sinus on any pulse sequence, and absence of flow-related enhancement on time-of-flight MR angiography.
- Although a hyperdense dural sinus on unenhanced CT is a finding that is strongly suspicious for DST, this sign is present in only 20% to 50% of cases; hence, it is an insensitive sign.
- Within the early stages, the thrombosed sinus may appear isointense with brain tissue on T1-weighted images and not appear particularly conspicuous. However, by the time DST is seen on most MR scans, the affected dural sinus is hyperintense compared with brain tissue on unenhanced T1-weighted images.
- In approximately 10% to 20% of cases seen on MR imaging, the thrombosed dural sinus is hypointense on T2-weighted images and can simulate a patent dural sinus. Careful attention to the presence of a corresponding flow void on other pulse sequences is important.
- Another cause of a false negative study is homogeneous enhancement of a thrombosed dural sinus after administration of contrast material, which can simulate contrast-enhancement of a patent dural sinus. Luckily, this finding is seen in only a minority of cases.
- On occasion, a hyperdense dural sinus can be seen on unenhanced CT and produce a false positive finding. A high hematocrit (e.g., in a patient with polycythemia vera) can produce this finding.
- Frequently, collateral veins become dilated around the edges of a thrombosed dural sinus. Following administration of contrast material on CT or MR imaging, these veins contrast-enhance. This finding should not be confused with a patent (i.e., contrast-filled) dural sinus.
- The most specific finding of venous infarction is a hem-orrhagic lesion within a subcortical location. Such lesions do not conform to the arterial distribution of an intracranial artery. Venous infarcts associated with thrombosis of the transverse sinus are usually located in the temporal lobe. Those associated with superior sagittal sinus thrombosis are usually located in the frontal lobes, often near the midline. Finally, those associated with thrombosis of the internal cerebral veins or straight sinus are frequently located in the thalamus.
- Slow flow within a patent dural sinus can cause replacement of the normal flow void by abnormal signal intensity; this finding can cause a false positive diagnosis on MR imaging.
- A false-positive finding can be produced on time-of-flight MR venography when the signal intensity in the blood that is flowing cephalad (e.g., in the anterior portion of the

superior sagittal sinus) is nulled by the inferior saturation pulse used to null the signal intensity of arteries.

## SUGGESTED READING

Provenzale JM, Kranz PG. Dural sinus thrombosis: sources of error in image interpretation. Am J Roentgenol 2011;196:23–31.

Provenzale JM, Barboriak DP, Ortel TL. Durai sinus thrombosis associated with activated protein C resistance: MR imaging flndings. AJR 1998; 170:499–502.

Hinman JM, Provenzale JM. Hypointense thrombus on T2-weighted MR the superior sagittal sinus) is nulled by the inferior satu- images: a potential pitfall in diagnosis of dural sinus thrombosis. Eur J Radiol 2002;41:147–152.

---

Note: Unlike most cases in this book, some findings in the images shown here are not described in the figure legends. The reader is challenged to independently discern those findings.

# CASE 31

**JAMES PROVENZALE**

## HISTORY

A 25-year-old woman with progressively worsening headaches and new onset of seizures.

A

■**FIGURE 6-31A** Axial contrast-enhanced CT shows an oval, slightly hyperdense region in the right frontal lobe, which was also present on unenhanced CT (not shown) and is consistent with fine calcification.

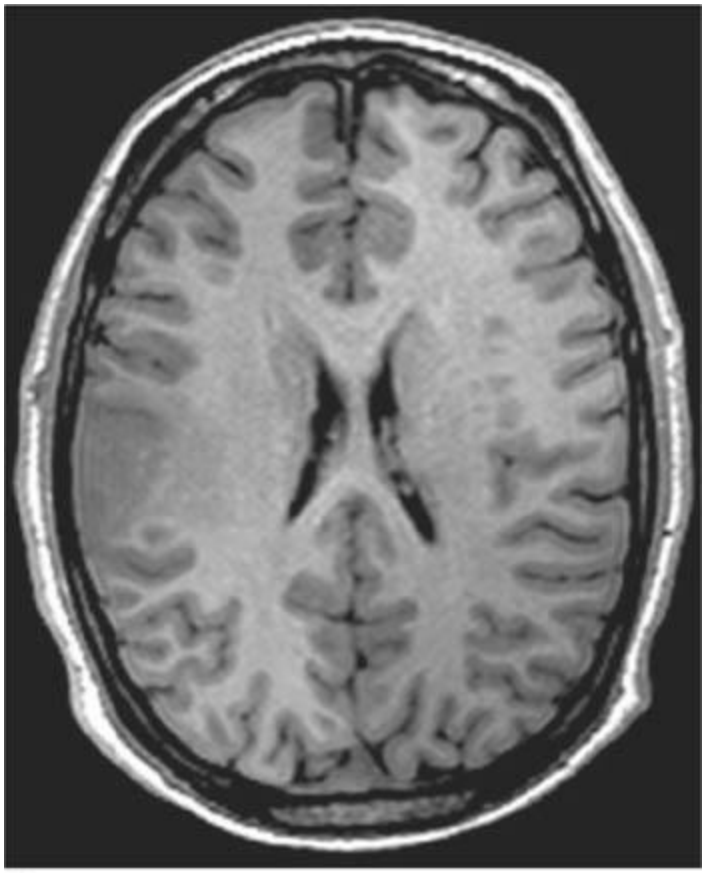

B

■**FIGURE 6-31B** Axial unenhanced T1-weighted axial image shows a relatively well-circumscribed, homogeneous mass in the right frontal lobe.

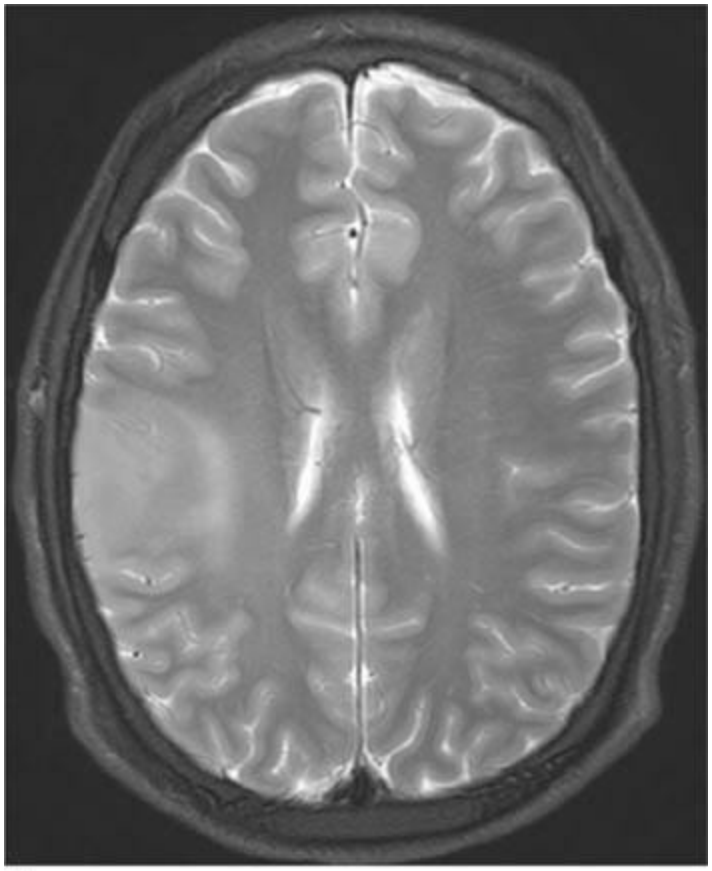

C

■**FIGURE 6-31C** Axial T2-weighted image shows a homogeneous mass involving the white matter and cortex of the right frontal lobe. Very little, if any, vasogenic edema is present.

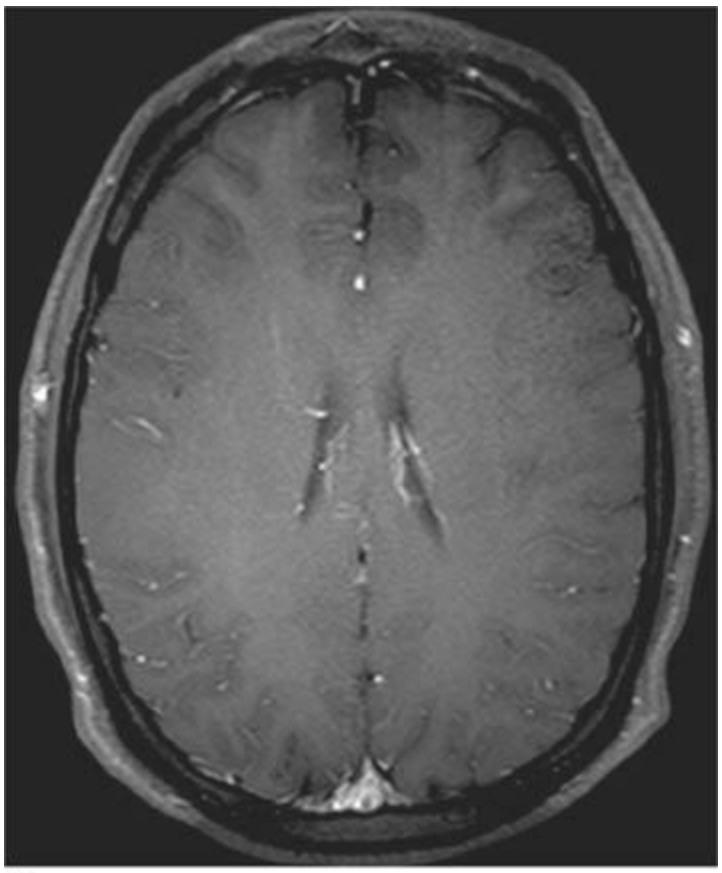

D

**FIGURE 6-31D** Axial contrast-enhanced T1-weighted image shows solely the mild mass effect associated with the lesion with no foci of contrast enhancement. (Images courtesy of Christopher G. Filippi, MD, University of Vermont College of Medicine and Fletcher Allen Radiology, Burlington, VT).

## DIFFERENTIAL DIAGNOSIS

**Meningioma:** This diagnosis might be considered because the mass is well circumscribed and has high density on CT—two features that are commonly found in meningiomas. However, meningiomas are extra-axial masses that would be expected to displace brain cortex inward—a finding that is not seen in this case. Furthermore, meningiomas almost always densely contrast enhance—a finding that is not present in the case shown. This diagnosis is incorrect.

**Glioblastoma multiforme:** Such lesions are hypoin-tense on T1-weighted images and hyperintense on T2-weighted images, so this diagnosis might be considered. However, no contrast enhancement is seen in the case provided, whereas glioblastoma multiforme almost always contrast enhances. This diagnosis is incorrect.

**Cavernous angioma:** This diagnosis might be considered because cavernous malformations frequently exhibit calcification on CT and typically do not contrast

enhance (see Case 15). However, one would expect to see hypointense signal on T2-weighted images due to the presence of susceptibility effect related to chronic blood products, which is not evident in the case shown. This diagnosis is incorrect.

- **Oligodendroglioma:** This diagnosis should be considered because the lesion is calcified, well circumscribed, does not contrast enhance, and has little, if any, vasogenic edema. This diagnosis is correct.

## DIAGNOSIS

**Oligodendroglioma**

## KEY FACTS

### Clinical

- Oligodendrogliomas are tumors that arise from oligo-dendrocytes, the cells from which central nervous system myelin forms.
- These tumors account for 5% to 20% of intracranial gliomas.
- A 2:1 male predominance is seen. The peak age is in the fourth and fifth decades.
- Slightly more than half of oligodendrogliomas occur in the frontal lobes and another 15% each in the temporal lobes and parietal lobes.
- Oligodendrogliomas are slow-growing lesions; symptoms are often present for 5 years or more. Headache and seizures are the most common presenting features.
- These tumors frequently originate in white matter and then spread to involve adjacent cortex.
- Two major forms of the tumor are recognized: a well-differentiated form and an anaplastic form. The well-differentiated form has a low level of mitosis and low degree of tumoral angiogenesis. These lesions are classified as World Health Organization (WHO) grade II tumors. The anaplastic form is characterized by higher cellularity, vascular proliferation, and necrosis and is classified as a WHO grade III tumor.
- About 50% of oligodendrogliomas (termed oligoastro-cytomas) have a mixed histology consisting of astrocy-toma and anaplastic oligodendroglioma; these lesions have a poorer prognosis than pure oligodendrogliomas.
- Tumors with 1p and 19q deletions are recognized as an important subset of tumors. They are more likely to be within the frontal lobe, be calcified, and have ill-defined margins. They are also much more likely to respond to chemotherapy. The 5-year survival rate is generally much better than for other brain tumors, in the range of 40% to 75%.

## Radiologic

- On CT, about 60% of lesions are low density. Calcification is frequently present (reported rates between 20% and 90% of cases).
- On CT and MR imaging, the tumor is usually seen as a round or oval mass with discrete margins involving brain cortex.
- The CT scan appearance is that of an inhomogeneous hypodense mass that typically has dense nodular calcification. The tumor can erode the calvarium adjacent to a site of involvement of brain cortex.
- Intratumoral cysts and hemorrhage are only occasionally seen.
- Generally, oligodendrogliomas show no or little contrast enhancement. The contrast enhancement often consists of solely small, dot-like regions of enhancement.
- Presence of contrast enhancement is not a reliable factor in distinguishing low-grade oligodendrogliomas from anaplastic oligodendrogliomas.
- No association exists between the presence of contrast enhancement and time to tumor progression.
- MRI is less sensitive than CT in detecting tumor calcification but is superior in defining tumor extent.
- MR scans show mixed hypo- and isointense areas on T1-weighted images and hyperintense foci on T2-weighted images. Regions of calcification can be seen as hyperintense foci on T1-weighted images and hypointense foci on T2-weighted images.
- Some studies have shown that the presence or absence of contrast enhancement does not reliably allow WHO grade II well-differentiated oligodendrogliomas to be distinguished from WHO grade III anaplastic oligodendrogliomas.
- Unlike most other low-grade tumors, low-grade oligo-dendrogliomas often show high rCBV on dynamic susceptibility-weighted MR images, which can cause them to be mistaken for high-grade tumors on imaging.
- MR contrast enhancement is more commonly seen in oligoastrocytomas than in oligodendrogliomas, and calcification is less common. However, these imaging features are not highly reliable for distinguishing between the two types of tumors.

# SUGGESTED READING


Cha S. Update on brain tumor imaging: From anatomy to physiology. AJNR Am J Neuroradiol 2006;27:475–487.

Collins VP. Brain tumours: Classification and genes. J Neurol Neurosurg Psychiatry 2004;75(Suppl 2):ii2–iill.

Koeller KK, Rushing EJ. From the archives of the AFIP: Oligodendroglioma and its variants: Radiologic-pathologic correlation. Radiographics 2005;25:1669–1688.

Law M, Oh S, Johnson G, et al. Perfusion magnetic resonance imaging predicts patient outcome as an adjunct to histopathology: A second reference standard in the surgical and nonsurgical treatment of low-grade gliomas. Neurosurgery 2006;58:1099–1107.

Spampinato MV, Smith JK, Kwock L, et al. Cerebral blood volume measurements and proton MR spectroscopy in grading of oligodendroglial tumors. AJR Am J Roentgenol 2007;188:204–212.

White ML, Zhang Y, Kirby P, Ryken TC. Can tumor contrast enhancement be used as a criterion for differentiating tumor grades of oligodendro-gliomas? AJNR Am J Neuroradiol 2005;26:784–790.

# Chapter SEVEN

# Vascular Radiology

**CHARLES Y. KIM** ▪ CHAPTER EDITOR

Glenn E. Newman (posthumous)

Tony P. Smith

Daniel J. Stackhouse

Paul V. Suhocki

Cynthia S. Payne

Kurt Husum

Joshua A. Bryant

Melissa A. Hayes

Bjorn Engstrom

Glen A. Toomayan

Timothy J. Amrhein

Scott Duncan

# CASE 1

**GLENN E. NEWMAN**

**AND**

**CHARLES Y. KIM**

## HISTORY

A 45-year-old woman with diabetes mellitus and exercise claudication. Both femoral artery pulses are markedly diminished and the popliteal and pedal pulses are detectable only by Doppler recording. The ankle-brachial index (ABI) at rest was 0.48 on the right and 0.47 on the left.

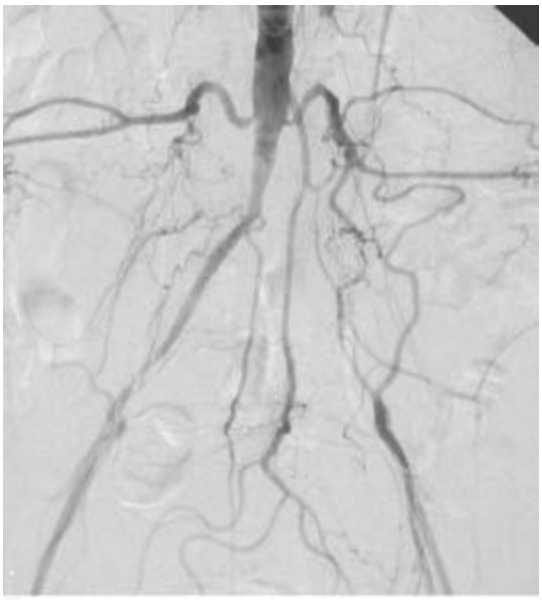

A

**FIGURE 7-1A** Pelvic arteriogram with catheter tip in the distal aorta shows that the left common iliac artery is occluded and is reconstituted by multiple collateral arteries from lumbar arteries, the middle sacral artery, and the IMA. A severe stenosis of the right external iliac artery is also present.

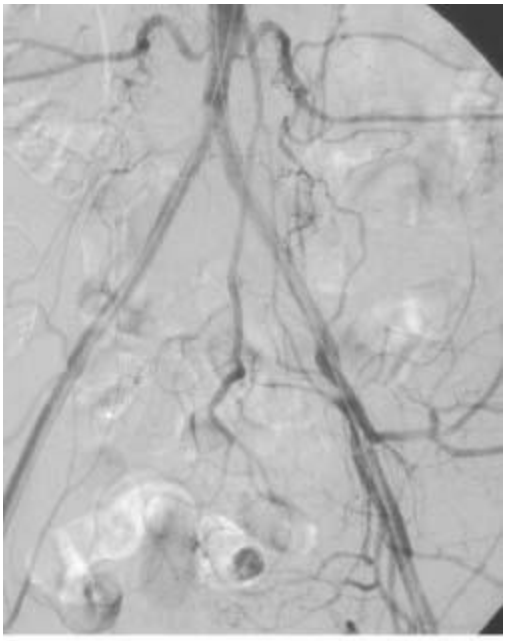

B

**FIGURE 7-1B** Repeat arteriogram after successful an-gioplasty and deployment of so-called kissing common iliac stents, extended to the bilateral external iliac arteries, shows restored patency of both common iliac and external iliac arteries.

## DIFFERENTIAL DIAGNOSIS

**Atherosclerotic peripheral vascular disease (PVD):** This diagnosis is by far the most common etiology of arterial occlusion in adults, particularly in those with risk factors such as diabetes mellitus, smoking, and hypertension. Atherosclerosis is a slow, chronic progressive disease, which allows formation of well-developed collateral arteries. Diffuse arterial involvement is typical. Given the patient's risk factors, extensive collateral circulation, and diffuse involvement, this is the most likely diagnosis.

**Vasculitis**: Vasculitis of large arteries such as Takayasu's arteritis and giant cell arteritis typically produce smooth stenoses, but occasionally occlusions can occur. These patients tend to be younger than the patient shown in this case, with an elevated erythrocyte sedimentation rate (ESR). Additionally, constitutional symptoms of fever, arthralgias, myalagias, rash, and fatigue, which are absent in this case, are often noted. The luminal irregularity of the aorta and iliac arteries, age, and comorbidities make this diagnosis unlikely.

**Embolic occlusion**: This acute process produces acute symptoms of ischemia, with an embolic source typically originating from the heart. Angiographically, due to the acuity of this process, collateral circulation would be expected to be absent or minimal (unlike the substantial collateral arteries seen in the case presented here). This diagnosis unlikely.

**Arterial dissection**: Usually, some degree of flow is preserved, although any

dissection can progress to complete occlusion. Dissection of the iliac arteries is usually seen only after recent arterial intervention (which is absent prior to the image shown in Figure 7-1A). Spontaneous dissection of the iliac arteries is very rare. Angiographically, linear margins or an actual dissection flap are typically visualized; these findings are absent in the case shown. Given the chronic appearance, diffuse arterial involvement, and lack of history of recent arterial intervention, this diagnosis is unlikely.

## DIAGNOSIS

**Atherosclerotic peripheral vascular disease**

## KEY FACTS

### Clinical

- Claudication is the development of cramping pain in the legs during exercise, related to insufficient arterial inflow to accommodate muscular demand. Physical examination findings include diminished or absent peripheral arterial pulses and trophic changes in the affected extremities such as hair loss and muscle atrophy.
- Obstructive atherosclerotic disease of the infrarenal segment of the abdominal aorta and pelvic arteries supplying the legs is relatively common, with a prevalence of approximately 40/10,000 patients.
- Obstructive PVD is more common in men than women. It generally occurs after 50 years of age unless a concomitant disease such as diabetes mellitus or a family history of atherosclerotic disease is present.
- Integration of the history, physical examination, and results of noninvasive tests allows preangiographic prediction of the disease site and severity, including the presence of inflow (i.e., suprainguinal) and outflow (i.e., infrainguinal) disease.
- The ABI, a ratio of the ankle blood pressure relative to the arm blood pressure, is used to predict the presence and severity of aortoiliac and lower extremity atherosclerotic disease. An ABI of $\geq 0.9$ is considered normal; mild insufficiency: 0.7 to 0.9; moderate insufficiency: 0.5 to 0.7; severe insufficiency (i.e., a threatened limb): $<0.5$.
- The choice of therapies is determined by the anatomic location and extent of arterial disease and comorbid features (e.g., cardiopulmonary status). Approximately 90% of patients have a clinical history of atherosclerotic disease in other locations—for example, coronary or carotid artery circulation.

### Radiologic

- Noninvasive imaging studies such as computed tomography angiography (CTA) and MR angiography (MRA) are often utilized for diagnosis and treatment-planning purposes.
- CTA and MRA have an equally high sensitivity and specificity for detecting and characterizing stenoses and occlusions of the pelvic and lower extremity arteries. However, these techniques have some limitations. Degree of stenosis may be overestimated in diseased arteries. Although underestimation of degree of stenosis can also occur, it is a less common problem. In addition, prominent vascular calcifications can limit assessment of stenoses with CTA.
- Conventional (catheter) angiography continues to be the reference standard for arterial imaging; findings are not altered by the presence of vascular calcifications.
- The major aim of radiologic assessment is to preoperatively determine the type and extent of disease, which will guide therapy. Imaging features of importance include the degree of stenosis, presence of occlusion, number of lesions, length of stenosis or occlusion, degree of calcification, luminal irregularity, and extent and location of collateral vessels. The arteries providing flow along the entire course from the aorta to the foot should be evaluated before any therapy is planned.
- Percutaneous angioplasty (PTA), alone or in combination with intravascular stenting, is the major nonsurgical means of treating atherosclerotic aortoiliac disease. Endovascular intervention is not possible when occlusive lesions cannot be crossed with a guidewire.
- Although PTA alone is frequently successful, stenting is sometimes also necessary. Indications for stenting include persistent stenosis (>30%) after PTA and flow-limiting arterial dissection at the site of angioplasty. Either a self-expanding or a balloon-mounted stent can be used.
- Factors that predict long-term patency after PTA can be divided into two categories: (1) clinical predictors and (2) anatomic predictors.
- Clinical predictors are based on the symptoms before PTA. In general, patients who present with claudication fare much better overall than those who present for limb salvage (e.g., nonhealing ulcers, rest pain, or gangrene). This finding is expected because the latter is a reflection of much more extensive vascular disease.
- Anatomic predictors are based on the location and angiographic appearance of the lesion. Patients with proximal lesions (i.e., so-called inflow disease) have a much better prognosis than those with more distal lesions. Angiographic lesion parameters include the degree of vessel narrowing, the degree of irregularity of the lesion, and its length. In general, patients with stenoses have a better result from PTA than those with occlusions. In addition, patients with short (i.e., <5 cm), concentric (smooth) lesions fare better than those with long (i.e., >5 cm), eccentric (irregular) lesions.

- The 5-year patency rate of iliac PTA alone is approximately 70% to 75%, but that of PTA with intravascular stenting is 80% to 85%.
- Simultaneous bilateral iliac angioplasty or stenting (so-called kissing iliac angioplasty and/or stenting) is indicated for stenosis or occlusion at the origin of the common iliac artery, whether unilateral or bilateral. Angioplasty and stenting are performed simultaneously, in order to prevent plaque being pushed into the contralateral common iliac artery origin.
- Aortobifemoral bypass graft surgery is preferred for patients who have extensive atherosclerotic disease and low surgical risk.

## SUGGESTED READING

Kashyap VS, Pavkov ML, Bena JF, et al. The management of severe aortoiliac occlusive disease: endovascular therapy rivals open reconstruction. J Vasc Surg 2008;48(6):1451–1457, 1457.e1–e3.

Mouanoutoua M, Maddikunta R, Allaqaband S, et al. Endovascular intervention of aortoiliac occlusive disease in high-risk patients using the kissing stents technique: long-term results. Catheter Cardiovasc Interv 2003;60(3):320–326.

Norgren L, Hiatt WR, Dormandy JA, et al. Inter-society consensus for the management of peripheral arterial disease (TASC II). Eur J Vasc Endo-vasc Surg 2007;33(Suppl 1):S1–S75.

Sharafuddin MJ, Hoballah JJ, Kresowik TF, et al. Long-term outcome following stent reconstruction of the aortic bifurcation and the role of geometric determinants. Ann Vasc Surg 2008;22(3):346–357.

Willmann JK, Wildermuth S, Pfammatter T, et al. Aortoiliac and renal arteries: prospective intraindividual comparison of contrastenhanced three-dimensional MR angiography and multi-detector row CT angiography. Radiology 2003;226(3):798–811.

# CASE 2

**TONY P.**
**SMITH**

### HISTORY

A 40-year-old woman with nephrotic syndrome and sudden onset of right-sided pleuritic chest pain.

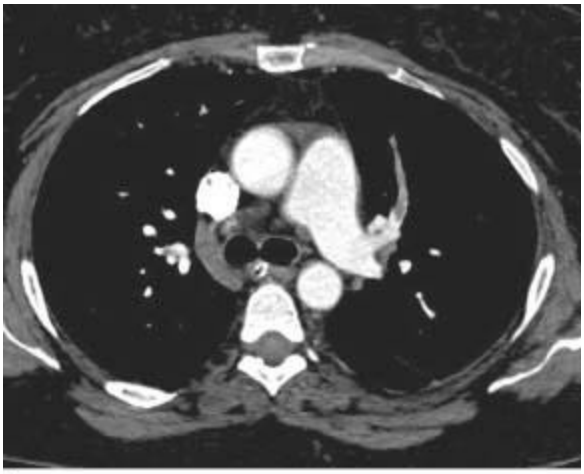

A

**FIGURE 7-2A** Axial contrast-enhanced CT image through the main pulmonary artery shows an occlusive filling defect in the left upper lobe anterior segmental pulmonary artery. This proximal margin of the filling defect has a "meniscus" appearance, which argues strongly that it is a real finding rather than an artifact.

B

**FIGURE 7-2B** Right pulmonary artery angiogram. A filling defect is seen in the interlobar artery extending into the right middle and lower lobe branches.

## DIFFERENTIAL DIAGNOSIS

**Pulmonary thromboembolus**: A filling defect within a pulmonary artery, as is seen in the case shown here, is essentially diagnostic for pulmonary embolism (PE). This diagnosis is correct.

- **Pulmonary vein thrombosis**: Occasionally a filling defect within a pulmonary vessel is due to a pulmonary vein thrombosis. Tracing the vessel to its origin reveals whether it is pulmonary artery or pulmonary vein. In the case shown, the vessel arises from the main pulmonary artery rather than the vein. Pulmonary venous thrombosis is an incorrect diagnosis.
- **Air embolus**: The density of the filling defect in an air embolus would appear the same as that of the lung. However, in the case shown, the density of the filling defect is similar to that of muscle. Therefore, this diagnosis is incorrect.
- **Artifact**: A filling defect could be due to artifact from volume averaging or motion. Inspection of adjacent contiguous images should help determine whether the finding is a true filling defect or artifact. Artifacts tend to have linear margins whereas true filling defects have a so-called meniscus appearance at their margin, which is present in this case. Therefore, artifact is an incorrect diagnosis.

## DIAGNOSIS

**Acute pulmonary thromboembolus**

## KEY FACTS

### Clinical

- PE is a common, life-threatening entity with an estimated 600,000 cases per year in the United States alone. Approximately 10% of the patients with PE do not survive the initial event.
- The clinical signs of PE are nonspecific and typically can include dyspnea, tachypnea, pleuritic pain, and hemoptysis.
- Approximately 80% of patients with PE have lower extremity deep venous thrombosis (DVT). Conversely, PE occurs in up to 50% of patients with proximal DVT.
- Risk factors include surgery, immobility, hypercoaguability, and age.
- D-dimer testing is highly sensitive for DVT and PE but nonspecific; D-dimer elevation occurs with infection, cancer, trauma, and other inflammatory states.
- Treatment usually consists of anticoagulation with heparin or low-molecular-weight heparin, followed by warfarin for at least 3 to 6 months. If an individual harbors a contraindication to anticoagulation, an inferior vena cava (IVC) filter can be inserted.
- Acute treatment of PE with intravenous thrombolytic agents has not yet definitively demonstrated advantages over long-term anticoagulation and is usually reserved for very acutely ill patients in order to decrease their clot burden.

### Radiologic

- Most patients with PE have abnormal chest radiographs, but the findings are nonspecific—for example, either or both atelectasis and pulmonary parenchymal opacities. However, in the appropriate circumstances, a normal radiograph is actually most helpful in assessment for PE. A normal chest radiograph in a patient with dyspnea and hypoxia ($PaO_2 \leq 70$ mm Hg) should strongly raise the possibility of PE, because it effectively excludes other entities that clinically mimic PE. The other main function of the chest radiograph is to aid in interpretation of the ventilation-perfusion imaging in a patient with suspected PE (see Chapter 10, Case 17).
- CTA and ventilation-perfusion scintigraphy have become the first-line imaging techniques for the evaluation for PE.
- Advantages of CTA include noninvasive nature, short imaging time, ability to identify other etiologies that may be responsible for symptoms, and detection of right-heart strain in the setting of massive PE. Disadvantages include a substantial radiation dose (of particular concern, the breasts in young females), sensitivity to motion artifact, and need for use of iodinated contrast.
- Conventional pulmonary angiography is now rarely performed for PE diagnosis, given the excellent noninvasive imaging options. Vascular access is usually from the common femoral vein, although the internal jugular and brachial vein can also be used to gain access. Selective angiography is usually performed with the pigtail-type catheter placed into the right or left pulmonary artery.
- The presence of occlusive or nearly occlusive intra-arterial filling defects on pulmonary angiography is diagnostic of acute PE. Complete arterial occlusion (so-called vessel cutoff) is also highly suggestive of the diagnosis. Linear filling defects, luminal narrowing, and occluded vessels with a smooth meniscus or tapered margin suggest chronic, rather than acute, PE.
- Catheter-directed thrombolytic therapy and mechanical fragmentation have been shown to be relatively safe and effective means of treatment of massive PE with hemodynamic compromise.

## SUGGESTED READING


Konstantinides S. Clinical practice. Acute pulmonary embolism. N Engl J Med 2008;359(26):2804–2813.

Kuo WT, Gould MK, Louie JD, et al. Catheter-directed therapy for the treatment of massive pulmonary embolism: systematic review and meta-analysis of modern techniques. J Vasc Interv Radiol 2009;20(11):1431–1440.

Remy-Jardin M, Pistolesi M, Goodman LR, et al. Management of suspected acute pulmonary embolism in the era of CT angiography: a statement from the Fleischner Society. Radiology 2007;245(2):315–329.

Tapson VF. Acute pulmonary embolism. N Engl J Med 2008;358(10):1037–1052.

Young T, Tang H, Aukes J, Hughes R. Vena caval filters for the prevention of pulmonary embolism. Cochrane Database Syst Rev 2007;(4):CD006212.

# CASE 3

**DANIEL J.
STACKHOUSE**

**AND**

**CHARLES Y.
KIM**

## HISTORY

A 51-year-old man with bright red blood per rectum.

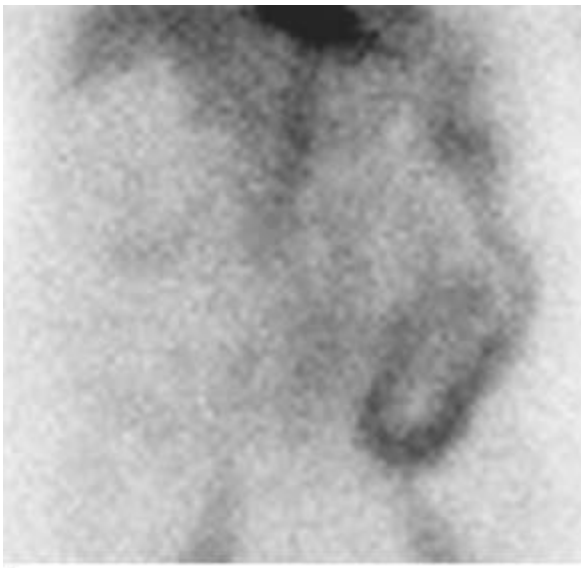

A

**FIGURE 7-3A** A Tc99-labeled red blood cell nuclear medicine study shows radiotracer uptake throughout the sigmoid colon and left colon, consistent with active lower GI bleeding.

B

**FIGURE 7-3B** Arteriogram of the IMA shows a bleeding site in the descending colon with extravasation of contrast material into the bowel. No abnormal vascularity to suggest tumor vessels or early draining veins to suggest angiodysplasia is seen.

## DIFFERENTIAL DIAGNOSIS

The following is a differential diagnosis for hemorrhage from a left colon bleeding site (as in the case shown):

**Diverticulosis**: This entity is the most common cause of colorectal bleeding. Diverticula occur more commonly in the left colon; those that occur in the right colon actually carry a higher risk of bleeding. This entity does not have a characteristic imaging feature. Given the lack of specific imaging features as described in these other differential diagnoses, this is statistically the most likely diagnosis.

**Angiodysplasia**: This acquired lesion accounts for up to 20% of cases of colorectal bleeding. The angiographic appearance is that of a small tuft of vessels with at least one early draining vein. These findings are not seen in the case illustrated and therefore this diagnosis is unlikely.

Neoplasm: Tumors account for about 10% of cases of colorectal bleeding. They typically are seen to have a focal parenchymal blush and tumor neovascularity at angiography, which are not present in this case. Therefore, this diagnosis is unlikely. Nonetheless, angiography cannot definitively exclude a neoplasm. Instead, endoscopy is typically performed.

**Colitis**: This entity accounts for 5% to 10% of cases of colorectal bleeding. At angiography, prominent opacification of involved segments of colon is typically seen

during the capillary phase, which is not present in this case. Therefore, this diagnosis is unlikely.

## DIAGNOSIS

**Active hemorrhage due to diverticulosis in the descending colon**

## KEY FACTS

### Clinical

- Prompt and adequate hemodynamic stabilization (e.g., placement of large-bore intravenous lines and vascular repletion) of the patient with gastrointestinal (GI) hemorrhage is imperative before diagnostic procedures are started.
- Eighty percent of patients with GI bleeding have spontaneous resolution of the hemorrhage without treatment.
- It is important to determine whether the source of bleeding is from the upper (i.e., above the ligament of Treitz) or lower GI tract. If gastric lavage contents are clear, the source is presumed to be distal to the pylorus. Otherwise, if positive, the source is most likely in the upper GI tract.
- Upper GI tract bleeding is five times more common than lower GI tract bleeding.
- In cases of upper GI hemorrhage, endoscopy will frequently identify the bleeding source and provide the initial means of treatment, including cautery, injection of epinephrine, or in the case of variceal bleeding, sclerotherapy or banding. Endoscopy has a lower diagnostic and therapeutic yield for lower GI hemorrhage.
- The most common source of massive bleeding from the upper GI tract is ulceration. Other causes of upper GI tract bleeding include gastritis, variceal bleeding, Dieulafoy lesion (i.e., a large tortuous arteriole within the stomach wall), tumor, Mallory-Weiss tear, and angiodyplasia.
- Sources of small bowel hemorrhage include ulceration, diverticula, enteritis, neoplasm, angiodysplasia, and aortoenteric fistula.
- Sources of colonic hemorrhage include diverticular disease, angiodysplasia, neoplasm, and colitis. The presence of bright red blood per rectum can be a false-localizing sign for colonic hemorrhage because the upper GI tract is the source of hemorrhage in up to 10% of patients with such bleeding.
- If a patient is suspected to be actively bleeding, tagged red blood cell scintigraphy, which can detect bleeding at a rate of 0.1 mL/min, can be performed to determine whether the patient is actively bleeding and to attempt to localize the site of bleeding.

### Radiologic

- Indications for urgent mesenteric angiography include massive nonvariceal GI bleeding (from either an upper GI or lower GI source) for which the bleeding site either cannot be identified or cannot be treated via endoscopic means.
- Angiography can detect active hemorrhage only if the rate of bleeding is at least 0.5 to 1.0 mL/min, a much more vigorous rate than that detectable by nuclear scintigraphy.
- Angiographic findings include active extravasation of contrast material into the bowel lumen, a pseudoaneurysm, an early draining vein in the setting of angiodysplasia, or a hypervascular mass.
- For upper GI bleeding, selective injections of the celiac, left gastric, gastroduodenal, and superior mesenteric arteries (SMAs) are performed routinely.
- For lower GI bleeding, injection of the SMA and inferior mesenteric artery (IMA) are routinely performed. If endoscopy or scintigraphy provides localizing information, selective injections are often performed.
- If a site of contrast material extravasation is identified, attempts should be made to advance a microcatheter as distal as possible toward the site of bleeding. Embolization should then be performed using coils, particles, or gelatin sponge pledgets.
- Vasopressin infusion, which was previously the mainstay of treatment of lower GI bleeding, is currently performed only when a microcatheter cannot be advanced into an appropriate distal artery.
- For upper GI bleeding, if extravasation of contrast material is not identified, empirical embolization of the gastroduodenal artery or left gastric artery is often effective when a site of suspected bleeding is seen at endoscopy.
- The risk of ischemia is relatively small given the rich collateral supply to the GI tract; the risk is higher in the lower GI tract.

## SUGGESTED READING

Burke SJ, Golzarian J, Weldon D, Sun S. Nonvariceal upper gastrointestinal bleeding. Eur Radiol 2007;17(7):1714–1726.

Edelman DA, Sugawa C. Lower gastrointestinal bleeding: a review. Surg Endosc 2007;21(4):514–520.

Hastings GS. Angiographic localization and transcatheter treatment of gastrointestinal bleeding. Radiographics 2000;20(4):1160–1168.

Millward SF. ACR Appropriateness criteria on treatment of acute nonvariceal gastrointestinal tract bleeding. J Am Coll Radiol 2008;5(4):550–554.

Walker TG. Acute gastrointestinal hemorrhage. Tech Vasc Interv Radiol 2009;12(2):80–91.

# CASE 4

**PAUL V.**

**SUHOCKI**

**AND**

**CHARLES Y.**
**KIM**

## HISTORY

A 58-year-old woman who was struck in the chest during a motor vehicle accident.

A

■**FIGURE 7-4A** Axial contrast-enhanced CT through the aortic arch shows a soft tissue density in the anterior mediastinum, which is in continuity with the aortic wall.

B

■**FIGURE 7-4B** Aortogram shows a linear lucency extending inferiorly from the left upper border of the aorta, just beyond the origin of the left subclavian artery. In this same region, there is a discontinuity ("step off") in the superior contour of the aortic lumen. These findings represent aortic injury.

## DIFFERENTIAL DIAGNOSIS

- **Mediastinal hematoma due to aortic injury**: The soft tissue density in the anterior mediastinum on the CT image is contiguous with the aortic wall, raising the possibility of hemorrhage due to an aortic tear. The abnormalities seen on the aortogram are consistent with injury to the aorta just distal to the left subclavian artery origin, and are an indication for emergent surgical repair.
- **Mediastinal hematoma due to venous bleeding**: The most common cause of mediastinal hematoma is venous hemorrhage, which can be confidently diagnosed if a distinct fat plane exists between the hematoma and the aortic wall. However, in the case shown here, the hematoma is contiguous with the aorta. Furthermore, the aortogram shows findings indicative of an arterial injury. Venous injury could certainly occur concurrently with arterial injury in the setting of blunt trauma. However, the diagnosis of venous hemorrhage becomes irrelevant when arterial injury is present, and is therefore the wrong diagnosis.
- **Residual thymus**: This diagnosis might be considered on the basis of the finding of a soft tissue density in the anterior mediastinum. However, the thymus gland reaches its peak size during puberty and gradually involutes until it is essentially replaced by fat during the fourth decade (i.e., at an age much younger than the patient in the case shown here). Furthermore, this diagnosis would not account for the angiographic findings; this diagnosis is incorrect.
- **Lymphadenopathy**: The mass in the anterior mediastinum could, in theory, represent confluent lymphadenopathy. However, additional enlarged lymph nodes would be expected; none are present in the CT scan shown here, making this diagnosis unlikely. Furthermore, lymphadenopathy would not explain the angiographic findings. This diagnosis is incorrect.

## DIAGNOSIS

**Traumatic tear at the isthmus of the thoracic aorta with associated mediastinal hematoma**

## KEY FACTS

### Clinical

- Only 10% to 20% of patients with traumatic rupture of the aorta survive long enough to be treated at a hospital. Of those, the mortality rate of untreated aortic rupture is 95% to 97%.
- The mechanism of injury is most commonly motor vehicle collisions, followed by

falls from height, pedestrian-automobile collisions, and crush injuries.

- Based on autopsy series, the majority of aortic injuries are located at the isthmus (within 2 cm of the origin of the left subclavian artery). This is the site at which the ligamentum arteriosum attaches the aorta to the left pulmonary artery. The isthmus is the site of aortic laceration in the vast majority (i.e., 90% to 95%) of patients who survive to reach the hospital.
- Approximately 10% of aortic injuries involve the ascending aorta, which is nearly always fatal.
- Less commonly involved sites are the aortic arch and the distal thoracic, diaphragmatic, and abdominal aortic segments.
- Emergency surgical repair, usually by placement of a prosthetic aortic graft, is typically indicated. Primary repair (i.e., suturing of the laceration) and patch angioplasty are other, less frequently used, procedures.

## Radiologic

- Chest radiography is neither sensitive nor specific for aortic injury, but is frequently obtained in trauma patients. A number of chest radiographic findings should strongly raise suspicion of an aortic tear in a trauma patient: (1) widened mediastinum, (2) depressed left mainstem bronchus, (3) deviation of the esophagus (deviated nasogastric tube) and trachea at the level of the T4 vertebral body, (4) obscured margins of the aortic arch, (5) left apical opacity (so-called apical cap), (6) fracture of any of the first three ribs, (7) widening of a paraspinal line, and (8) widening of the right paratracheal stripe.
- A negative chest radiograph should not preclude further radiologic evaluation, which should be prompted, based on the mechanism of trauma and clinical suspicion of aortic injury.
- CTA is currently considered the diagnostic test of choice for evaluation of aortic injury, having very high sensitivity and specificity. The advent of multidetector CT and EKG-gating have greatly improved imaging quality of the proximal ascending aorta.
- Direct CTA findings of acute aortic injury include an intimal flap, pseudoaneurysm (i.e., a contained rupture), intraluminal mural thrombus, abnormal aortic contour, and sudden change in aortic caliber. Any one of these findings is considered definitive for diagnosis and no additional imaging is necessary. Surgical consultation should be performed expeditiously.
- The presence of a mediastinal hematoma is considered an indirect finding, and its significance depends on its location. Separation of the hematoma from the aorta by an intact fat plane is an indication that the hematoma is not due to aortic injury but instead is typically due to injury of small mediastinal veins. If the hematoma is truly periaortic,

then further evaluation is warranted, since this could represent a rare occult aortic injury versus injury of small periaortic veins or the vasa vasorum.

- The rate of false negative CTA studies for aortic tear is very low. Nonetheless, the presence of a truly periaortic mediastinal hematoma is an indication for further imaging. Further evaluation could be performed with transesophageal echoaortography, intravascular ultrasound, conventional angiography, or follow-up CTA after 2 to 3 days, if the patient is stable.
- On CTA, a careful search for branch vessel injury should be performed in the presence of mediastinal hematoma.
- Conventional angiography for the diagnosis of acute aortic injury has taken on a substantially limited role in the multidetector CT era, primarily due to the time delay it imposes until treatment. However, it remains a valuable technique for problem solving in the stable patient, for planning prior to endovascular stent graft therapy, and detection of branch vessel injury. During aortography, an injection in the left anterior oblique projection should first be performed, followed by a right anterior oblique or lateral projection. The brachiocephalic vessels and region of the descending aorta above the celiac artery should be included in the field of view. An aortic laceration can be missed if only a single projection is used at aortography.
- Most patients with aortic tear develop a pseudoaneurysm at the site of laceration. Solely an intimal tear, seen as a linear lucency on the angiogram, is present in 5% to 10% of cases.
- Causes of false-positive aortograms, seen in 1% of cases, include ductus diverticulum, aortic aneurysm, atherosclerotic plaque, and artifacts due to inflow of unopacified blood (i.e., “streaming” artifacts).
- Other valuable diagnostic techniques for diagnosis of aortic tear include transesophageal echoaortography and intravascular sonography.
- Although surgical repair has been considered to be the standard of care for aortic tear, a growing body of literature supports the use of endovascular stent grafting.

## SUGGESTED READING


Alkadhi H, Wildermuth S, Desbiolles L, et al. Vascular emergencies of the thorax after blunt and iatrogenic trauma: multi-detector row CT and three-dimensional imaging. Radiographics 2004;24(5):1239–1255.

Feczko JD, Lynch L, Pless JE, et al. An autopsy case review of 142 nonpenetrating (blunt) injuries of the aorta. J Trauma 1992;33:846–849.

Malloy PC, Richard HM III. Thoracic angiography and intervention in trauma. Radiol Clin North Am 2006;44(2):239–249, viii.

Steenburg SD, Ravenel JG, Ikonomidis JS, et al. Acute traumatic aortic injury: imaging evaluation and management. Radiology 2008;248(3):748–762.

Walsh SR, Tang TY, Sadat U, et al. Endovascular stenting versus open surgery for thoracic aortic disease: systematic review and meta-analysis of perioperative results. J Vasc Surg 2008;47(5):1094–1098.

# CASE 5

**CYNTHIA S. PAYNE**

**AND**

**CHARLES Y. KIM**

## HISTORY

A 58-year-old woman with substernal pleuritic chest pain and new dyspnea on exertion. She subsequently experienced an episode of transient hemiplegia following infusion of an intravenous catheter with saline.

A

■**FIGURE 7-5A** Axial unenhanced CT image a lobulated solid-appearing lesion in the periphery of each lung. Both lesions appear to have prominent connecting vessels, which are suspicious for associated draining pulmonary veins (confirmed on adjacent images which are not shown).

B

**FIGURE 7-5B** Selective angiogram of a right lower lobe pulmonary artery shows an enlarged and tortuous pulmonary artery branch supplying a vascular nidus with a prominent early draining vein.

## DIFFERENTIAL DIAGNOSIS

**Malignancy**: Based on the CT image, malignancy should always be considered for multiple pulmonary lesions. However, the vascular nature as demonstrated on angiography is not compatible with a solid tumor.

**Hamartoma**: This diagnosis might be considered because of the presence of lobulated, well-circumscribed lesions in the periphery of the lung. However, the lesions shown in the CT image lack the characteristic "popcorn" calcifications and macroscopic fat on CT typical of hamartomas. Given the lack of these findings and the highly vascular nature of the lesions as seen on angiography, this diagnosis is unlikely.

**Granuloma**: The CT finding of multiple well-circumscribed lesions may suggest granulomatous disease related to tuberculous or fungal infection on CT. However, the large size and multilobulated configuration of the lesions on CT would be unusual for granulomatous disease. Furthermore, the angiographic findings are not consistent with this diagnosis.

**Pulmonary arteriovenous malformation (AVM)**: The lobulated appearance on CT with associated draining veins is characteristic of pulmonary AVM. This diagnosis is definitively established on the pulmonary angiogram that shows an enlarged feeding artery, a vascular nidus, and enlarged early draining veins. The multiplicity of lesions in the case shown here should strongly suggest a diagnosis of hereditary hemorrhagic

telangiectasia (HHT).

# DIAGNOSIS

**Pulmonary arteriovenous malformations in the setting of HHT**

# KEY FACTS

## Clinical

- Pulmonary arteriovenous malformations may receive arterial supply from only one arterial source (by definition termed an AV fistula) or from multiple feeding arteries (termed an AVM). Approximately 80% are AV fistulas. For the purposes of this review, the term AVM will be used to refer to both of these entities.
- Patients can present with hemoptysis, chest pain, hypoxia, and neurologic symptoms (including stroke, transient ischemic attacks, and cerebral abscess formation) from paradoxical emboli, since the AVM effectively serves as a right to left shunt.
- Clinical signs can include digital clubbing, cyanosis, polycythemia, chest bruit, and neurologic symptoms and signs due to paradoxical emboli.
- Pulmonary AVMs are rarely symptomatic if <2 cm in size. Many investigators maintain that treatment is warranted even for asymptomatic lesions <2 cm in size or those having a feeding artery with a diameter of >3 mm.
- Approximately 15% of pulmonary AVMs occur sporadically, occasionally associated with prior trauma, infection, hepatopulmonary syndrome, or surgery. Approximately 85% occur as part of HHT (also known as Osler-Weber-Rendu syndrome). HHT is an autosomal dominant condition with variable penetrance and is characteristically associated with the triad of epistaxis, telangiectasias, and family history of the syndrome. Approximately 15% to 25% of patients with HHT have pulmonary AVMs.

## Radiologic

- More than 95% of patients with pulmonary AVMs have an abnormal chest radiograph.
- Approximately two-thirds of pulmonary AVMs are solitary lesions.
- High-resolution CT has an extremely high sensitivity for detecting the presence of a pulmonary AVM, in which the enlarged draining vein is easily visualized. CTA and MRA can help confirm the vascular nature of the lesion. Arterial phase CTA images or time-resolved MRA can confirm the early arterial filling, which is diagnostic of an AVM.
- Renal and cerebral radiotracer activity during lung perfusion study is a characteristic finding that can be seen due to the right-to-left shunting resulting from pulmonary AVMs. The presence of these findings during a lung perfusion study is a clue to the diagnosis of

pulmonary AVM.

- Pulmonary angiography can confirm the diagnosis, classify the type of lesion, and provide the means for endovascular treatment.
- Treatment by permanent occlusion with coils or other embolic devices has a rate of high success with low morbidity and low mortality. The major risk to be considered during the procedure is unintentional embolization of the systemic circulation by the coil or balloon during deployment. In addition, particular care must be taken to avoid presence of air bubbles, which could enter the cerebral circulation during catheter flushing and angiography.

## SUGGESTED READING

Khurshid I, Downie GH. Pulmonary arteriovenous malformation. Postgrad Med J 2002;78(918):191–197.

Pollak JS, Saluja S, Thabet A, et al. Clinical and anatomic outcomes after embolotherapy of pulmonary arteriovenous malformations. J Vasc Interv Radiol 2006;17(1):35–44.

Remy-Jardin M, Wattinne L, Remy J. Transcatheter occlusion of pulmonary arterial circulation and collateral supply: failures, incidents, and complications. Radiology 1991;180:699–705.

# CASE 6

**DANIEL J. STACKHOUSE**

### HISTORY

A 36-year-old man with fever, hematuria, and elevated sedimentation rate. He has a history of hepatitis B infection.

A

**FIGURE 7-6A** Renal arteriogram shows multiple distal microaneurysms and distal arterial stenoses.

B

**FIGURE 7-6B** Celiac arteriogram also shows multiple microaneurysms and distal arterial stenoses.

## DIFFERENTIAL DIAGNOSIS

**Polyarteritis nodosa (PAN)**: PAN is a necrotizing vasculitis of unknown etiology, which has been associated with prior hepatitis B and C virus infection, as well as intravenous drug abuse. The typical findings consist of multiple microaneurysms and distal stenoses in the renal and other mesenteric arterial circulation. The clinical history

of fever, elevated sedimentation rate and hepatitis B infection, in the presence of the angiographic findings in the case illustrated, make this the most likely diagnosis.

- **Vasculitis of intravenous drug abuse**: This entity is also a necrotizing vasculitis, which can have an identical angiographic appearance to PAN. The absence of a history of drug abuse favors an alternative diagnosis, although it must be kept in mind that such a history is often not revealed by the patient.
- **Vasculitis associated with connective tissue disorders**: These include a number of connective tissue disorders (e.g., systemic lupus erythematosus, rheumatoid arthritis, and Sjogren's syndrome) that have an angiographic appearance similar to the findings in the case illustrated. The diagnosis is based on clinical findings (e.g., arthralgias, cutaneous manifestations) and serologic tests (e.g., antinuclear antibody levels) and is typically known by the time angiography is performed.

## DIAGNOSIS

**Polyarteritis nodosa**

## KEY FACTS

### Clinical

- PAN is an immune complex-mediated necrotizing vasculitis affecting multiple organ systems.
- PAN can be seen at any age, but the peak incidence is in the fifth to seventh decades. A 2:1 male-to-female predominance has been reported.
- The clinical symptoms reflect the multisystem involvement and include fever, weight loss, weakness, and malaise. Additional symptoms are organ system-specific and vary considerably among patients.
- Laboratory findings include elevated ESR, anemia, and elevated white blood cell count. Rheumatoid factor is present in many patients, and evidence of previous hepatitis B infection is seen in 15%. Elevated circulating immune complexes and hypocomplimentemia strongly suggest the diagnosis.
- Renal involvement, often manifested by rapidly progressive renal failure and hypertension, is present in 75% to 85% of PAN patients. Renal abnormalities can include a necrotizing glomerulonephritis with associated hematuria, vasculitis, and small renal artery aneurysms.
- Neurologic involvement is common but is usually confined to one or more peripheral or cranial nerves. Less commonly, the brain or spinal cord is involved by infarction or hemorrhage.
- GI involvement is seen in 50% of patients and may involve any organ in the GI system.

Bowel ischemia and perforation secondary to necrotizing vasculitis has been reported.

- Cardiac involvement, including congestive heart failure, myocardial infarction, and pericarditis, is seen in 80% of patients.
- Musculoskeletal involvement, including myalgias and a polyarthritis that is clinically similar to rheumatoid arthritis, is also relatively common.
- Treatment consists of high-dose corticosteroids and cyclophosphamide.

### Radiologic

- Abnormal renal angiograms are seen in 70% to 80% of PAN patients, usually involving small- and medium-sized arteries, often within intrarenal branches. The major findings (many of which are the result of necrosis and inflammation) include multiple microaneurysms (often at bifurcations), segmental narrowing or dilation (due to loss of vasomotor control), and arterial occlusions (due to a necrotizing, inflammatory process).
- Involvement of the mesenteric arteries occurs in 65% of PAN patients. The findings are generally similar to those seen in the renal arteries.
- Appropriate assessment of PAN patients by angiography includes selective renal, celiac, and superior mesenteric injections.

## SUGGESTED READING

Citron BP, Halpern M, McCarron M, et al. Necrotizing angiitis associated with drug abuse. N Engl J Med 1970;283:1003–1011.

Cupps TR, Fauci AS. Systemic necrotizing vasculitis of the polyarteritis nodosa group. In The Vasculitides. Philadelphia, PA: Saunders, 1981;26–49.

Pipitone N, Versari A, Salvarani C. Role of imaging studies in the diagnosis and follow-up of large-vessel vasculitis: an update. Rheumatology 2008;47:403–408.

Stanson AW, Friese JL, Johnson CM, et al. Polyarteritis nodosa: spectrum of angiographic findings. Radiographics 2001;21(1):151–159.

Travers RL, Allison DJ, Brettle RP, Hughes GRV. Polyarteritis nodosa: a clinical angiographic analysis of 17 cases. Semin Arthritis Rheum 1979;8:184–199.

# CASE 7

**GLENN E. NEWMAN**

**AND**

**CHARLES Y.**

**KIM**

## HISTORY

A 27-year-old woman with a painful mass in the posterior aspect of the distal left thigh. The mass was associated with a thrill and bruit.

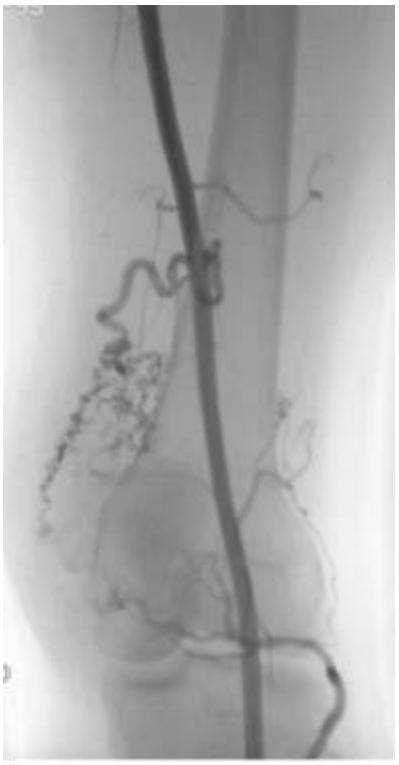

A

**FIGURE 7-7A** Early arterial phase of a right lower extremity angiogram shows a region of multiple prominent tortuous collateral arteries.

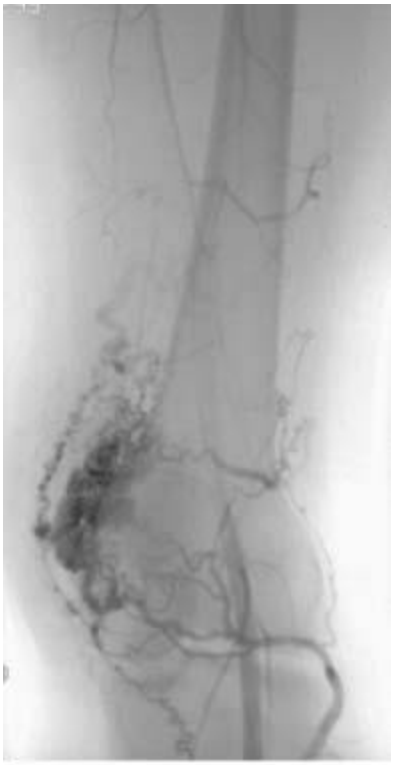

B

**FIGURE 7-7B** Slightly later in the arterial phase, dense opacification of the nidus is seen overlying the lateral condyle of the femur, with several prominent early-filling draining veins.

## DIFFERENTIAL DIAGNOSIS

**Hemangioma**: Hemangiomas are benign congenital malformations which are present at birth and typically involute during childhood. At angiography, hemangiomas typically appear as a focal parenchymal blush without large feeding arteries or draining veins. However, in the case shown here, large feeding arteries are present; this diagnosis is incorrect.

**Arteriovenous (AV) fistula**: An AV fistula is a direct communication between an artery and a vein without an interposed capillary bed, and can be posttraumatic, iatrogenic, or spontaneous (usually related to atherosclerosis or infection). Although there may be some enlargement of the feeding artery and draining vein, AV fistulas do not recruit collateral vessels. The appearance of multiple tortuous enlarged arteries and veins, as well as a large vascular nidus, is strong evidence against an AV fistula.

**Peripheral arteriovenous malformation (AVM)**: AVMs angiographically are seen to have enlarged tortuous feeding arteries, a nidus, and early filling of enlarged draining veins. All these features are seen on the images in this case, making this the correct diagnosis. Of note, some sources use the terms “AV fistula” and “AVM” interchangeably.

- **Neoplasm**: Solid tumors of bone and soft tissues can recruit arterial blood supply, resulting in multiple tortuous feeding arteries. When very large, AV shunting can occur with some degree of early venous filling. However, in the case shown here, the degree and speed of venous return is higher than would be expected in a solid tumor. Furthermore, the density of the nidus is far too prominent to represent a solid tumor during the arterial phase, making this diagnosis incorrect.

## DIAGNOSIS

**Peripheral arteriovenous malformation**

## KEY FACTS

### Clinical

- Peripheral AVMs are congenital lesions that are caused by abnormal differentiation of the vascular system during embryogenesis, resulting in aberrant vessel angiogenesis.
- The nidus of an AVM is the abnormal channel formed by the confluence of the small tortuous vessels, where AV shunting occurs without an intervening capillary bed.
- Often, AVMs are not evident until adolescence, when they are stimulated to grow and engorge in response to thrombosis, trauma, infection, or endocrine factors. The AVM usually grows in size with growth of the child.
- Some AVMs appear as part of a familial genetic disorder such as Rendu-Osler-Weber syndrome, Klippel-Trenaunay, Parkes-Weber, and other syndromes.
- AVMs can be stable lesions that require no specific therapy, e.g., solely as a cosmetic deformity. Alternatively, those within extremities can have a clinical presentation of a pulsatile mass or painful lesion. Very large AVMs can produce high-output cardiac failure due to AV shunting.
- Some AVMs aggressively expand, necessitating treatment. The primary mechanism of expansion is by enlargement of existing channels and recruitment of new collateral vessels, rather than by cellular proliferation.
- Low flow vascular malformations include venous malformations and lymphatic malformations. Neither of these have a prominent arterial component.

### Radiologic

- Imaging is important for characterizing the size, extent, flow velocity, flow direction, and relationship of AVMs to surrounding structures.
- MR imaging is excellent for assessing the size, extent, and relationship to surrounding structures. Slow-flow venous malformations have high signal intensity on T2-weighted images, whereas high-flow AVMs are typically seen to have a signal void. Time-

resolved MRA is a helpful component of MR imaging of these lesions, because it allows dynamic assessment of the flow velocity and direction.

- Sonography can be helpful for assessing superficial lesions, allowing visualization of arterial and venous flow and measurement of velocities.
- Conventional angiography remains the reference standard for diagnosing and assessing treatment options.
- When indicated, AVMs are frequently treated by trans-catheter embolization, alone or in conjunction with surgery. On occasion, AVMs are treated by surgery alone, especially when only one or a few feeding arteries are present.
- High flow AVMs can be extremely challenging to treat and often require multiple repeat therapies.
- Catheter access to the nidus can be accomplished via a direct percutaneous puncture, transarterial route, or transvenous route, depending on the anatomy and location of the lesion.
- Transcatheter embolization can be performed using a number of embolic agents. Obliteration of the nidus is considered to be critical for prevention of recurrence, and is ideally performed using a sclerosing agent such as absolute ethanol or glue. Embolization of the feeding arteries and/or draining veins using particles, coils, or other embolic agents and devices may help slow the flow to more effectively treat the nidus, especially for high-flow lesions. However, embolization of the feeding arteries or draining veins without treating the nidus is ineffective because the nidus will recruit collateral vessels, potentially resulting in an even larger lesion.

## SUGGESTED READING

Herborn CU, Goyen M, Lauenstein TC, et al. Comprehensive time-resolved MRI of peripheral vascular malformations. AJR Am J Roentgenol 2003;181(3):729–735.

Hyodoh H, Hori M, Akiba H, et al. Peripheral vascular malformations: imaging, treatment approaches, and therapeutic issues. Radiographics 2005;25(Suppl 1):S159–S171.

Lee BB. Critical issues in management of congenital vascular malformation. Ann Vasc Surg 2004;18(3):380–392.

Riles TS, Rosen RJ. Arteriovenous malformations. In DE Strandness Jr, A van Breda (eds), Vascular Diseases: Surgical and Interventional Therapy. New York, NY: Churchill Livingstone, 1994:1109–1137.

Simons ME. Peripheral vascular malformations: diagnosis and percutaneous management. Can Assoc Radiol J 2001;52(4):242–251.

# CASE 8

**TONY P.**
**SMITH**

**AND**

**CHARLES Y.**
**KIM**

## HISTORY

Two patients with hypertension: patient A, shown in Figure 7-8A, is a 67-year-old male with an abdominal bruit; patient B, shown in Figure 7-8B, is a 37-year-old female with hypertension of recent onset. In neither case did the guidewire or catheter enter the renal arteries prior to imaging.

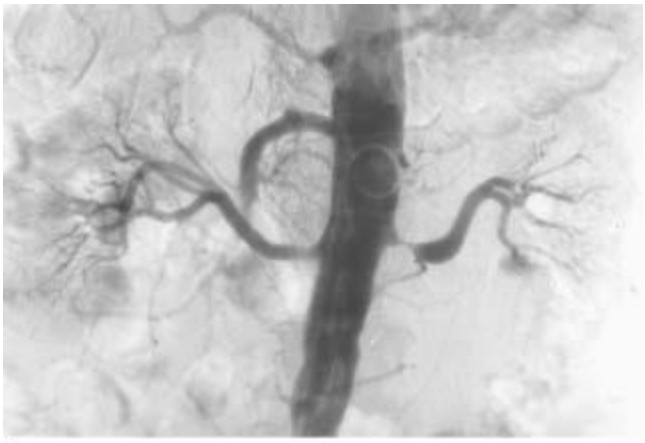

A

■**FIGURE 7-8A** Abdominal aortogram shows a smoothly contoured severe stenosis of the proximal left renal artery. Mild stenosis of the proximal right renal artery and abdominal aortic luminal irregularity are also present.

B

**FIGURE 7-8B** Abdominal aortogram shows a multilobulated ("beaded") stenosis of the mid-right renal artery. No other vascular abnormalities are present.

## DIFFERENTIAL DIAGNOSIS

**Atherosclerotic disease**: This entity is by far the most common cause of renal artery stenosis, usually occurring at, or near, the origin of the artery. The stenosis is usually irregular and can be focal. Other sites of atherosclerotic disease are typically evident. In patient A, the focal nature of the lesion and the presence of a stenosis at the origin of the artery in combination with diffuse irregularity of the abdominal aorta render atherosclerosis as the most likely diagnosis. In patient B, no other sites of luminal irregularity or narrowing are present, making atherosclerosis unlikely.

**Fibromuscular dysplasia (FMD)**: This entity characteristically causes a multilobulated, "beaded" stenosis at a site in the mid- to distal segment of the renal artery. This appearance is present in patient B but absent in patient A.

**Vasospasm**: This entity typically only occurs after manipulation of a catheter or guidewire within an artery and usually responds to intra-arterial nitroglycerin administration; the stenosis can be focal or cover a long segment of the artery and is usually smooth and tapered. The appearance of the left renal artery in patient A is compatible with focal vasospasm; however, the fact that neither a guidewire nor a catheter was placed in the renal artery prior to imaging makes this diagnosis unlikely. The irregular appearance of the right renal artery in patient B is not consistent with vasospasm.

**Vasculitis**: Vasculitides such as Takayasu's arteritis and giant cell arteritis are rare causes of renal artery stenosis. Markers of systemic inflammation are typically present. Supportive evidence in the form of arterial wall thickening and contrast-enhancement may be seen on cross-sectional imaging studies. Both vasculitides mentioned typically produce long segment stenoses, which are not present in the cases shown here. This diagnosis is incorrect.

**Neurofibromatosis**: This rare entity usually produces a multilobulated appearance of affected arteries similar to FMD; less commonly, a focal proximal stenosis can be seen. However, other clinical (e.g., cutaneous) and radiologic findings, which are not present in the cases shown, would be expected. This diagnosis is unlikely.

## DIAGNOSIS:

**Patient A: Atherosclerotic renal artery stenosis**
**Patient B: Fibromuscular dysplasia**

## KEY FACTS

### Clinical

- The clinical presentation of renal artery stenosis can be hypertension, renal failure, or both. However, many patients are asymptomatic.
- Renal artery stenosis due to any cause accounts for a small minority (i.e., <5%) of patients with systemic hypertension.
- Indications that hypertension may be due to renal artery stenosis (i.e., renovascular in nature) include (1) presence of an abdominal or flank bruit (due to renal artery stenosis), (2) increase in serum creatinine levels by at least 0.5 mg/dL following antihypertensive treatment with angiotensin-converting enzyme (ACE) inhibitor therapy, and (3) hypertension that is rapid in onset and refractory to medical therapy (i.e., so-called malignant hypertension).
- Atherosclerotic disease accounts for approximately 90% of cases of renal artery stenosis; FMD accounts for almost the entire remaining 10%.
- Atherosclerotic disease is more prevalent with increasing age and affects individuals of both genders, with men affected slightly more frequently. On the other hand, FMD tends to affect younger individuals (i.e., in the15 to 50 year old age range) and much more commonly affects women.
- A number of forms of FMD exist. The most common subtype of FMD is that affecting the media (so-called medial and perimedial fibroplasia), accounting for 80% to 90% of cases. Medial FMD produces the classic beaded appearance with alternating webs and aneurysms. FMD can cause symptoms by compromising flow, causing distal thromboembolism related to thrombus within aneurysms, and producing spontaneous dissection impairing flow. The other forms of FMD can create a smooth tapered appearance. Over half of patients have bilateral disease.
- The ideal therapy for atherosclerotic lesions in reno-vascular hypertension is a matter of active controversy.

### Radiologic

- CTA and MRA have become first-line imaging modalities for detection of renal artery stenosis. Both techniques have shown excellent sensitivity and specificity for detecting clinically significant renal artery stenoses.
- However, administration of iodinated contrast material and gadolinium-containing contrast agents is limited in patients with renal insufficiency due to concerns of contrast-induced renal nephropathy and nephrogenic systemic fibrosis, respectively. Unenhanced MRA has shown great promise for evaluation of the renal arteries. Conventional (i.e., catheter) angiography remains the reference standard for diagnosis of renal artery stenosis.

- Sonography is generally not considered reliable for detecting stenoses, although depiction of renal atrophy can suggest the diagnosis of renal artery stenosis. Nuclear scintigraphy does not directly visualize the renal arteries but can determine relative renal perfusion as well as renal function.
- Percutaneous transluminal angioplasty (i.e., PTA) is considered the first-line therapy for FMD with uncontrolled hypertension. The clinical success rate at 1 year is approximately 85%. Renal artery stenting is typically reserved for cases of arterial dissection or rupture. Endovascular therapy is less effective for atherosclerotic lesions than for FMD. The clinical success rate of angioplasty is approximately 70% at 1 year for non-ostial stenoses and even lower (i.e., ~50%) for ostial lesions. The success rate for stenting is approximately 80% for nonostial stenoses and 70% for ostial lesions. When endovascular intervention is being considered for nonostial lesions, angioplasty is typically first attempted. Stenting is performed in cases of resultant dissection or incomplete resolution of the stenosis with a persistent arterial pressure gradient. Ostial lesions are typically treated with primary stenting. Balloon-mounted stents are preferred due to their greater precision in placement compared to self-expandable stents. Comparison of endovascular techniques for renal artery stenosis against medical therapy in a recent large prospective study did not demonstrate a significant difference between the two in terms of subsequent renal function and control of blood pressure.

## SUGGESTED READING

Dworkin LD, Cooper CJ. Clinical practice. Renal-artery stenosis. N Engl J Med 2009;361(20):1972–1978.

Kaufman JA, Lee MJ. Vascular and Interventional Radiology: the requisites. Philadelphia, PA: Elsevier, 2005;327–336.

Safian RD, Textor SC. Renal-artery stenosis. N Engl J Med 2001;344(6):431–442.

Slovut DP, Olin JW. Fibromuscular dysplasia. N Engl J Med 2004;350(18):1862–1871.

Wheatley K, Ives N, Gray R, et al. Revascularization versus medical therapy for renal-artery stenosis. N Engl J Med 2009;361(20):1953–1962.

# CASE 9

**GLENN E. NEWMAN**

**AND**

**CHARLES Y. KIM**

## HISTORY

A 19-year-old male athlete with a history of progressively increasing intermittent claudication involving only the right calf. There was no history of trauma. The right femoral pulse is normal, but the right popliteal and pedal pulses were present only by Doppler examination.

A

■**FIGURE 7-9A** Angiogram showing occlusion of the right popliteal artery *(arrowheads)* at the level of the popliteal fossa.

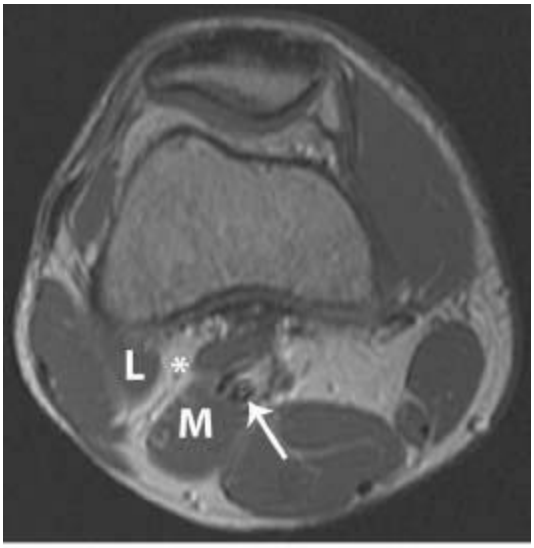


B

■**FIGURE 7-9B** Axial Tl-weighted MRI image through the right popliteal fossa shows

the lateral head (L) and the medial head (M) of the gastrocnemius muscle. The usual location of the popliteal artery is between the lateral and medial heads, denoted with an asterisk. However, in this patient, the artery *(arrow)* has an abnormal course *(arrow)* along the medial side of the medial head of the gastrocnemius head (M). At a more caudad level (not shown), the artery actually coursed through the muscle.

## DIFFERENTIAL DIAGNOSIS

- **Atherosclerotic occlusion**: An atherosclerotic popliteal occlusion is highly unlikely in this patient on the basis of age alone. Atherosclerotic occlusions typically occur in older patients and are much more common at Hunter's canal (i.e., adductor canal) than at the popliteal level. Furthermore, the other visualized arterial segments do not show evidence of atherosclerotic disease, making this diagnosis incorrect.
- **Thrombosed popliteal aneurysm**: The typical features of popliteal aneurysms are one or more of the following features: distal thromboembolism, claudication (present in the case described above), and acute thrombosis. However, an aneurysm sac would typically be easily identified on cross-sectional imaging. In the case shown here, no aneurysm is present on the MR image, making this diagnosis incorrect.
- **Popliteal artery occlusion secondary to popliteal entrapment syndrome**: The young age of the patient shown here and history of vigorous physical activity with claudication, in the setting of an anomalous popliteal artery course and presence of popliteal artery occlusion make this the most likely diagnosis.
- **Embolus**: Clinical symptoms are typically acute, as opposed to the chronic symptoms reported in the case presented here. Emboli most commonly originate from the heart in the setting of arrhythmia, are frequently multiple, tend to lodge at arterial branch points, and classically produce a meniscus-like appearance on angiography (which is not present in this case). Given the tapered appearance of the distal popliteal artery, an embolus would be unlikely.

## DIAGNOSIS

**Popliteal artery entrapment syndrome**

## KEY FACTS

### Clinical

- Popliteal artery entrapment syndrome is characteristically seen in young athletes (more common in males) with unilateral or bilateral claudication.
- The etiology is an anomalous relationship between the gastrocnemius muscle (medial or lateral head) and the popliteal artery in the popliteal fossa, resulting in extrinsic

arterial compression. Repetitive compressive trauma can result in stenosis, aneurysm, thromboembolism, and arterial thrombosis.

- Several classification systems have been proposed to describe the anomalous relationship. The most common anomalies include an aberrant accessory slip of the medial or lateral head of the gastrocnemius muscle or an excessively lateral attachment of the medial head.
- The lower extremity pulses in patients with this syndrome can be normal, diminished, or absent. Classically, plantar flexion and/or dorsiflexion of the foot will diminish or obliterate the pulses.

## Radiologic

- The angiographic findings in popliteal artery entrapment syndrome are nonspecific and include popliteal artery stenosis, occlusion, deviation, aneurysm, and/or distal embolism. If the popliteal artery is patent with the leg in the neutral position, provocative (stress) angiography during plantar flexion and/or dorsiflexion of the foot may demonstrate narrowing or occlusion of the artery.
- MRI and MRA are excellent techniques for evaluation of popliteal artery entrapment syndrome and can be diagnostic. T1- and T2-weighted images generally provide excellent visualization of the muscular structures in relation to the artery and can often define the anomalous entity for diagnostic confirmation and surgical planning. Contrast-enhanced MRA can depict arterial abnormalities such as stenosis, occlusion, and aneurysm. MRA can be performed in both neutral foot positioning and plantar flexion.
- The definitive treatment is surgery to alleviate the compressive force on the popliteal artery. Because of the progressive nature of this entity, even asymptomatic limbs should undergo surgical correction. Decompression with musculotendinous transection is typically performed. In cases of clinically significant arterial stenosis, occlusion, or aneurysm formation, arterial bypass is often performed.
- Catheter-based thrombolytic therapy prior to surgery may be helpful in cases of popliteal artery occlusion. However, angioplasty and stenting have a limited role in this disorder. If performed, surgical release of the restricting structure must always be performed first.

# SUGGESTED READING

Kim HK, Shin MJ, Kim SM, et al. Popliteal artery entrapment syndrome: Morphological classification utilizing MR imaging. Skeletal Radiol 2006;35(9):648–658.

Levien LJ. Popliteal artery entrapment syndrome. Semin Vasc Surg 2003;16(3):223–231.

Macedo TA, Johnson CM, Hallett JW Jr, Breen JF. Popliteal artery entrapment syndrome: role of imaging in the diagnosis. AJR Am J Roentgenol 2003;181(5):1259–1265.

Ohara N, Miyata T, Oshiro H, Shigematsu H. Surgical treatment for popliteal artery entrapment syndrome. Cardiovasc

Surg 2001;9(2):141–144.

Ring DH Jr, Haines GA, Miller DL. Popliteal artery entrapment syndrome: arteriographic findings and thrombolytic therapy. J Vasc Interv Radiol 1999;10(6):713–721.

# CASE 10

**DANIEL J. STACKHOUSE**

**AND**

**KURT HUSUM**

## HISTORY

A 55-year-old man ejected from a car during a motor vehicle accident.

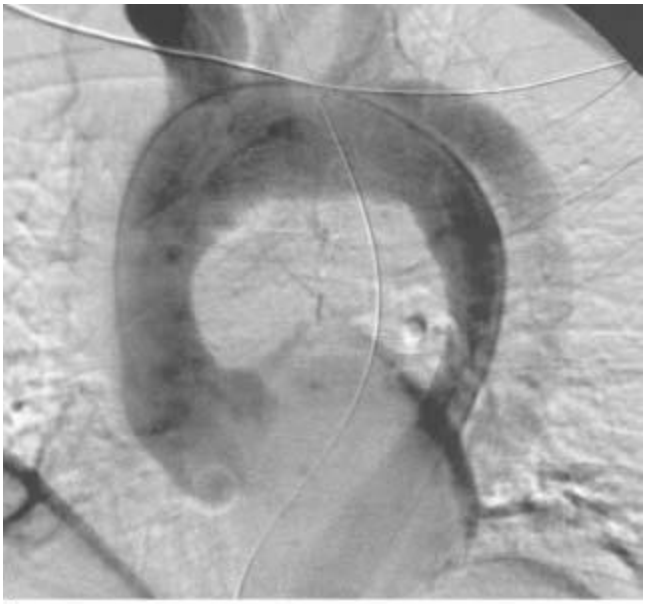

A

■**FIGURE 7-10A** Arch aortogram shows that the ascending aorta has an abnormal contour and is somewhat narrowed at its vertical segment. In the descending aorta, avid opacification is seen in only half of the lumen, with solely mild opacification of the other half. A vertically oriented filling defect (representing a dissection flap) is seen. The great vessels are patent.

B

**FIGURE 7-10B** Contrast-enhanced CT of the aortic arch shows a linear filling defect (which corresponds to the dissection flap) across the lumen of the ascending and descending aorta.

## DIFFERENTIAL DIAGNOSIS

**DeBakey type I aortic dissection**: This entity involves both the ascending aorta and descending aorta, as in the case shown here. This diagnosis is correct. Stanford type A dissections involve the ascending aorta with or without descending aorta involvement.

**DeBakey type II aortic dissection**: In this entity, the dissection is localized to the ascending aorta (and also classified as a Stanford type A dissection). In the case shown here, the descending aorta is clearly involved, making this an incorrect diagnosis.

**DeBakey type III aortic dissection**: In this entity, the dissection involves only the descending aorta (distal to the left subclavian artery origin); it is also classified as Stanford type B dissection. Given the clear involvement of the ascending aorta in the case shown here, this diagnosis is incorrect.

## DIAGNOSIS

**Thoracic aortic dissection, DeBakey type I**

## KEY FACTS

### Clinical

- The term aortic dissection refers to the physical separation of the arterial intima from the adventitia by blood tracking within the media.
- Predisposing factors include hypertension (which is the main risk factor), pregnancy,

collagen vascular disease (e.g., Marfan's syndrome), bicuspid aortic valves, aortic coarctation, mycotic aneurysm, and giant cell arteritis.

- The typical presentation is severe chest or back pain radiating into the neck, arms, abdomen, or hips. End-organ ischemia such as myocardial infarction, stroke, or limb ischemia can occur when arteries arising from the aorta (e.g., coronary, carotid or subclavian arteries) are compromised.
- Physical findings can include (1) asymmetric upper extremity pulses and/or blood pressure and (2) diminished pulses and/or blood pressure of the legs relative to the arms.
- Two schemes used for classification are the Stanford and DeBakey types. Stanford type A includes any dissection involving the ascending aorta (even if the descending aorta is involved); Stanford type B includes dissections limited to the descending aorta, which is defined as beginning just distal to the left subclavian artery. The DeBakey classification is outlined above in the Differential Diagnosis section. Rates for each type are type I: 51%; type II: 6%; and type III: 43%.
- Stanford type A dissections are treated surgically, with repair of the ascending aorta and, if necessary, the aortic valve. Stanford type B dissections are typically managed conservatively with aggressive blood pressure control. Surgical therapy for Stanford type B dissections is performed when arterial branches are compromised or if the size of the false lumen enlarges to >6 cm.
- Involvement of major branch arteries should be defined preoperatively by CTA, MRA, or catheter angiography. Surgical repair consists of placement of a mural graft at the site of the intimal tear and suturing of the false lumen, taking care to not occlude major arteries arising from the false lumen. Alternatively, several endovascular options are available, as described below.

## Radiologic

- Twenty-five percent of patients with aortic dissection have normal chest radiographs. Mediastinal widening is the most helpful radiographic finding, especially if the mediastinum appeared normal on a previous radiograph. Internal displacement of aortic calcifications from the periphery of the aorta is another finding that should raise suspicion of aortic dissection.
- Blood in the false lumen tends to remain at systolic pressures throughout the cardiac cycle. As a result, the false lumen is usually larger than the true lumen and, in fact, often compresses it. In the ascending aorta, the false lumen tends to be anterolateral, while in the descending aorta it tends to be posterolateral. Entry points and fenestrations may be identifiable as sites of communication between the true and false lumens.
- CTA is the most commonly used screening study for the evaluation of possible aortic

dissection, having been shown to be highly sensitive and specific. The presence of true and false channels separated by an intimal flap is necessary to make the diagnosis. The false lumen typically demonstrates delayed opacification and may be thrombosed. Unenhanced CT images are important for detecting intramural hematomas, which appear as a dense crescent of blood in the media. The advent of multidetector CT scanning and electrocardiogram (ECG) gating have substantially improved visualization of the ascending aorta.

- MRI is also highly sensitive and specific for the detection of aortic dissection but is better utilized for hemodynamically stable patients or for long-term surveillance of chronic dissections. Gadolinium-enhanced MRA is excellent for visualization of intimal flaps. ECG-gated imaging provides optimal imaging of the aortic root and cardiac valve leaflets. Unenhanced MR imaging is somewhat prone to artifact from motion and turbulent flow. Flowing blood has different signal characteristics (i.e., "flow void") than thrombus on both spin echo and gradient echo pulse sequences.
- Transesophageal echocardiography is also a valuable diagnostic tool and can be performed very rapidly in urgent situations. It is excellent for evaluating the aortic valve and proximal ascending aorta. Catheter angiography is rarely necessary unless an intervention is planned. Opacification of both the true and false lumen is important to determine whether aortic branches and the aortic valve are involved. Endovascular therapies include stent grafting over the entry tear to depressurize the false lumen, insertion of stents into the true lumen of aortic branches whose lumen is compromised, and fenestration (i.e., puncture) of the intimal flap to decompress the false lumen and improve distal flow.

## SUGGESTED READING


Gebker R, et al. Comparison of different MRI techniques for the assessment of thoracic aortic pathology: 3D contrast-enhanced MR angiography, turbo spin echo and balanced steady state free precession. Int J Cardiovasc Imaging 2007;23(6):747–756.

Johnson TR, et al. ECG-gated 64-MDCT angiography in the differential diagnosis of acute chest pain. AJR Am J Roentgenol 2007;188(1):76–82.

Kaufman JA, Lee MJ. Vascular and Interventional Radiology: The Requisites. Philadelphia, PA: Mosby, 2004;602–635.

Shiga T, Wajima Z, Apfel CC, et al. Diagnostic accuracy of transesophageal echocardiography, helical computed tomography, and magnetic resonance imaging for suspected thoracic aortic dissection: Systematic review and meta-analysis. Arch Intern Med 2006;166(13):1350–1356.

White C, Kuo D. Chest pain in the emergency department: role of multide-tector CT. Radiology 2007;245(3):672–681.


# CASE 11

**TONY P.**

**SMITH**

## HISTORY

A 67-year-old manual laborer with left arm cramping after exercise and gradual onset of dizziness.

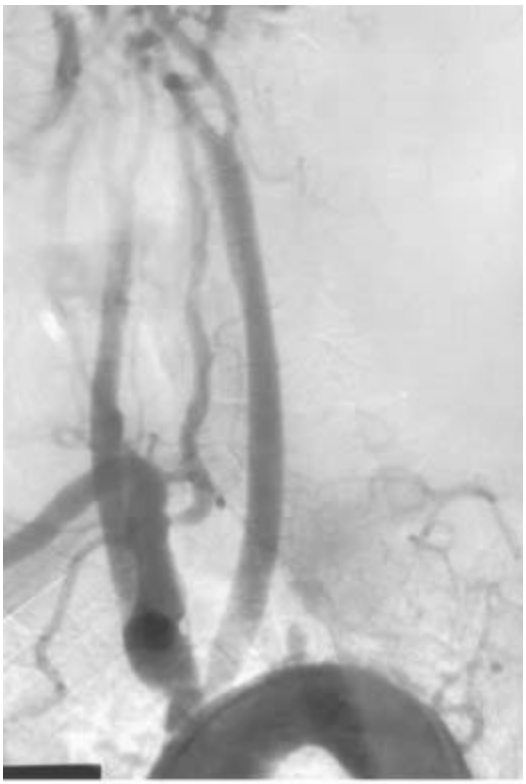

A

**FIGURE 7-11A** Early phase of an arch aortogram shows occlusion of the left subclavian artery just beyond its origin. The right brachiocephalic and left common carotid arteries are well opacified, although mild atherosclerotic narrowing of these arteries is also seen.

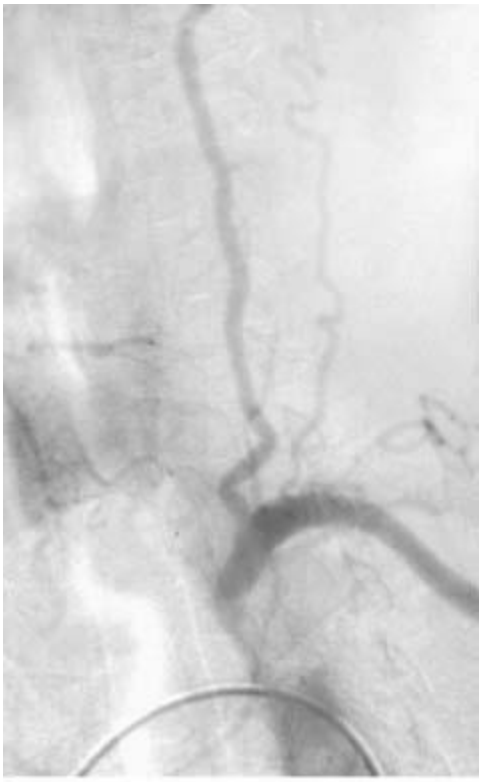

B

**FIGURE 7-11B** Late phase of an arch aortogram shows opacification of the left subclavian artery via retrograde filling from the left vertebral artery.

## DIFFERENTIAL DIAGNOSIS

**Variant aortic arch anatomy**: The appearance of the aortic arch on the arch injection is abnormal because the left subclavian artery is not opacified on the first image. This finding might lead one to suspect that an aberrant origin of the left subclavian artery is present. However, if an aberrant left subclavian artery was present, the distal subclavian artery should be opacified at the same time as the other great vessels. Instead, the left subclavian and vertebral arteries opacify only during the late phase of the arch aortogram. Therefore, this is an incorrect diagnosis.

**Severe stenosis of the proximal left subclavian artery causing delayed anterograde filling of the left subclavian artery**: This diagnosis could explain the imaging findings in Figure 7-11A; however, one would expect some degree of opacification of the left sub-clavian artery to be present in Figure 7-11A, even if delayed. In contrast, the left subclavian artery opacification is excellent, and could only be achieved via delayed *collateral* flow. Therefore, this diagnosis is incorrect.

**Occlusion of the proximal left subclavian artery with retrograde filling of the left subclavian artery by the left vertebral artery (so-called subclavian steal syndrome)**: In combination, the clinical symptoms and angiographic images in the case shown are highly suggestive of subclavian steal syndrome. Atherosclerosis is the most

common cause of subclavian artery stenosis and occlusion. Typically, there is evidence of atherosclerotic disease in other arteries, as in this case. This diagnosis is correct.

## DIAGNOSIS

**Atherosclerotic left subclavian artery occlusion with retrograde flow from the left vertebral artery supplying the left arm (subclavian steal syndrome)**

## KEY FACTS

### Clinical

- Subclavian steal syndrome is the result of severe stenosis or occlusion of the subclavian artery between its origin and the origin of the vertebral artery. Less frequently, this syndrome can occur with right brachiocephalic artery stenosis or occlusion. Collateral blood flow to the affected side occurs via retrograde flow through the ipsilateral vertebral artery via the vertebrobasilar junction.
- Most patients with retrograde flow in the vertebral artery—that is, angiographic subclavian steal—are asymptomatic. Symptoms such as arm claudication occur in only about one-third of patients with angio-graphic findings of steal phenomenon. In a minority of cases, patients may experience ischemic vertebro-basilar symptoms (e.g., dizziness, vertigo, and visual disturbance).
- The physiologic basis of neurologic symptoms due to the subclavian steal phenomenon is as follows: Upon exercise, demand for blood flow (causing vasodilation) increases in the arm supplied by the abnormal subcla-vian artery. This increased demand induces (or amplifies) retrograde flow through the ipsilateral verterbal artery, which thereby causes hypoperfusion in the territory of the vertebrobasilar circulation.
- The diagnosis is often initially suspected due to a discrepancy in blood pressures between the arms found on physical examination.

### Radiologic

- The most common initial radiologic examination for suspected subclavian steal syndrome is color Doppler sonography, in which the direction of flow in the vertebral artery can be depicted. Reversal of flow is suggestive of subclavian steal syndrome.
- When subclavian steal syndrome is highly suspected based on physical examination or by clinical symptoms and sonography, confirmation can be obtained with catheter angiography, CTA, or MRA to define the responsible lesion so that treatment can be planned. Dynamic time-resolved contrast-enhanced MRA can also be useful to depict the retrograde flow in the vertebral artery.
- The typical angiographic finding is a high-grade stenosis or occlusion of the proximal

subclavian artery proximal to the origin of the vertebral artery. Delayed images at angiography (i.e., during the late arterial phase) show retrograde flow in the vertebral artery followed by opacification of the distal segment of the subclavian artery.

- Angiographic evaluation of patients with subclavian steal should also include the carotid arteries, especially in patients in whom the symptom complex is difficult to localize to a vascular territory (i.e., whether symptoms are referable to disease in the carotid circulation or vertebrobasilar circulation).
- Angioplasty has been shown to be safe and effective in symptomatic patients with subclavian steal syndrome. In many centers, angioplasty has become the initial treatment of choice. Ischemia or infarction in the vertebrobasilar territory is a potential complication but is uncommon because the contralateral vertebral artery and carotid circulation almost always provide adequate collateral supply.
- Complete subclavian artery occlusion can be definitively treated with carotid-to-subclavian artery bypass surgery.

## SUGGESTED READING

Gosselin C, Walker PM. Subclavian steal syndrome: existence, clinical features, diagnosis and management. Semin Vasc Surg 1996;9:93–97.

Hebrang A, Maskovic J, Tomac B. Percutaneous transluminal angioplasty of the subclavian arteries: long-term results in 52 patients. AJR Am J Roentgenol 1991;156:1091–1094.

Hennerici M, Klemm C, Rautenberg W. The subclavian steal phenomenon:a common vascular disorder with rare neurological deficits. Neurology 1988;38:669–673.

Sueoka BL. Percutaneous transluminal stent placement to treat subclavian steal syndrome. J Vasc Interv Radiol 1996;7:35135–35136.

Wu C, Zhang J, Ladner CJ, et al. Subclavian steal syndrome: diagnosis with perfusion metrics from contrast-enhanced MR angiographic bolus-timing examination—initial experience. Radiology 2005;235:927–933.

# CASE 12

**PAUL V. SUHOCKI**

### HISTORY

A 46-year-old man with a history of cigarette smoking and coronary artery disease who reports a 2-year history of postprandial abdominal pain.

A

■**FIGURE 7-12A** Abdominal aortogram in an anteroposterior projection shows severe luminal irregularity of the aortic lumen as well as stenosis of the left renal artery, consistent with diffuse atherosclerotic disease.

B

■**FIGURE 7-12B** Abdominal aortogram in a lateral projection shows occlusion of the proximal segments of the celiac, SMA, and IMA.

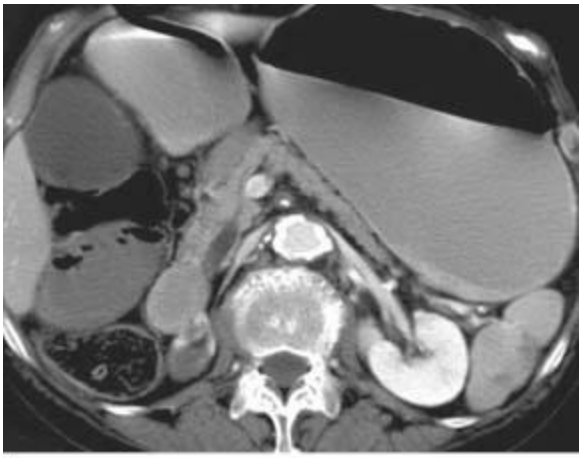

C

**FIGURE 7-12C** Contrast-enhanced CT in the late arterial phase shows occlusion of the SMA with a punctate mural calcification. Such calcifications commonly occur with atherosclerotic disease.

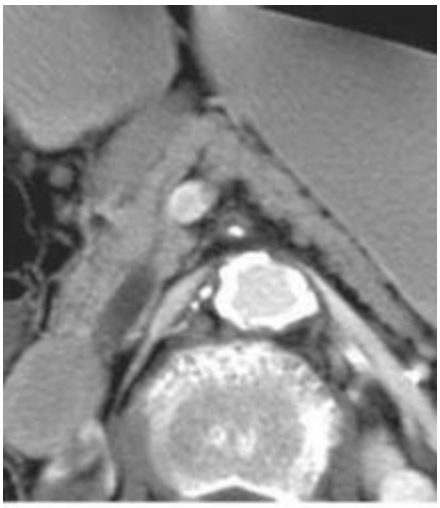

D

**FIGURE 7-12D** Enlarged image of Figure 7-12C shows the SMA occlusion as well as atherosclerotic calcification of the aorta.

## DIFFERENTIAL DIAGNOSIS

**Atherosclerotic disease**: This entity is the most common cause of proximal occlusion of the mesenteric arteries and can cause chronic mesenteric ischemia if two of the three major arteries supplying the bowel are occluded. Typically, obvious evidence of atherosclerotic disease (e.g., stenoses, luminal irregularity, and mural calcifications) will be present in the aorta and other arteries, as in this case. This is the correct diagnosis.

**Abdominal aortic aneurysm (AAA):** Mural thrombus in an AAA can compromise or occlude the origin of mesenteric arteries over time or produce an embolus that passes

into the vessels, causing acute mesenteric ischemia. Rarely, the opacified lumen of the aorta may appear to be of relatively normal caliber on a catheter angiogram and the true degree of enlargement of the aneurysm may be solely detectable on a cross-sectional imaging study; thus Figures 7-12A and 7-12B do not absolutely exclude an aneurysm. However, the CT in Figures 7-12C and 7-12D shows no evidence of AAA, making this diagnosis incorrect.

- **Aortic dissection**: The false channel of an aortic dissection can involve the mesenteric artery origins and cause acute mesenteric ischemia. However, in the presence of aortic dissection, two contrast-filled channels or a narrowed true lumen adjacent to a thrombosed false lumen would be expected. Those findings are not present in the case illustrated, making this an incorrect diagnosis.
- **Embolic occlusion**: Emboli related to cardiac arrhythmias or myocardial infarction can travel to the mesenteric arteries, resulting in *acute* mesenteric ischemia, which causes acute abdominal pain. The clinical history of chronic symptoms is not compatible with this diagnosis. Furthermore, the expected findings of intraluminal filling defects, often at branch points, are not present in the case shown above. This is not the correct diagnosis.

## DIAGNOSIS

**Chronic mesenteric ischemia due to atherosclerotic disease**

## KEY FACTS

### Clinical

- Atherosclerotic occlusion of the vessel origins occurs slowly, usually allowing formation of adequate collateral arterial supply for bowel viability.
- The pancreaticoduodenal arteries are the major source of collateral circulation between the celiac artery and SMA.
- The marginal artery of Drummond and the arc of Riolan provide collateral circulation between the SMA and the IMA.
- The IMA receives collateral supply from the middle and inferior hemorrhoidal arteries, which arise from the internal iliac arteries.
- When two or more of the major mesenteric arteries become progressively narrowed over time, the collateral blood supply is also affected, and chronic mesenteric ischemia can result.
- Symptoms of abdominal pain due to chronic mesenteric ischemia are often ill-defined and can mimic other disease states—for example, GI malignancy and peptic ulcer disease. The most common complaints are those of weight loss, diarrhea, and abdominal pain. Postprandial pain (usually within 2 hours of eating) is also common

and can cause the patient to avoid eating.

- A concern for acute mesenteric ischemia is usually raised in the setting of acute onset of severe abdominal pain with only minimal physical examination findings (until onset of necrosis and perforation). Causes include arterial emboli (most common), in situ thrombosis, hypotension, and venous thrombosis.

## Radiologic

- CTA and MRA are excellent noninvasive techniques for the evaluation of the proximal mesenteric vessels, which is where stenosis and occlusion most commonly occur.
- Catheter aortography is helpful when severe arterial calcifications limit evaluation on CTA and MRA, and provides better visualization of the more distal vessels. Lateral aortography is essential for visualizing the origins of the celiac and SMAs.
- The diagnosis of chronic mesenteric ischemia is confirmed by the angiographic finding of severe stenosis or occlusion of at least two of the three major mesenteric arteries. Well-developed collateral arteries are typically visualized.
- In the setting of acute mesenteric ischemia, well-developed collateral arteries will not likely be present except in the setting of acute occlusion superimposed upon subclinical chronic mesenteric ischemia.
- Contrast-enhanced CT is highly sensitive and specific for the diagnosis of acute mesenteric ischemia when performed in the arterial and portal venous phase. Pertinent findings include mesenteric arterial occlusion, venous thrombosis, pneumatosis, focal lack of bowel wall enhancement, portal venous gas, bowel wall thickening, and solid organ infarction.
- Peripheral branch stenoses or occlusions are rarely responsible for chronic mesenteric ischemia, although emboli to the distal circulation can cause acute mesenteric ischemia.
- Treatment of chronic mesenteric ischemia typically consists of surgical bypass in patients who are surgical candidates. Percutaneous balloon angioplasty with and without stenting has been shown to be less effective than surgery for long-term symptomatic relief.
- Acute mesenteric ischemia has a high mortality rate and is a surgical emergency. Treatment of acute mesenteric ischemia usually requires surgical resection of threatened or necrotic bowel. In the setting of arterial embolus, an embolectomy can be performed at the time of surgery.

# SUGGESTED READING

Chang JB, Stein TA. Mesenteric ischemia: acute and chronic. Ann Vasc Surg 2003;17:323–328.

Kirkpatrick ID, Kroeker MA, Greenberg HM, et al. Biphasic CT with mesenteric CT angiography in the evaluation of

acute mesenteric ischemia:initial experience. Radiology 2003;229:91–98.

Loffroy R, Steinmetz E, Guiu B, et al. Role for endovascular therapy in chronic mesenteric ischemia. Can J Gastroenterol 2009;23:365–373.

Oldenburg WA, Lau LL, Rodenberg TJ, et al. Acute mesenteric ischemia: a clinical review. Arch Intern Med 2004;164:1054–1062.

Rose SV, Quigley TM, Raker EJ. Revascularization for chronic mesenteric ischemia: comparison of operative arterial bypass grafting and percutaneous transluminal angioplasty. J Vasc Interv Radiol 6:339–349.

Scholz FJ. Ischemic bowel disease. Radiol Clin North Am 1993;31:1197–1218.

Shih MC, Angle JF, Leung DA, et al. CTA and MRA in mesenteric ischemia: part 2, normal findings and complications after surgical and endovascular treatment. AJR Am J Roentgenol 2007;188:462–471.

Shih MC, Hagspiel KD. CTA and MRA in mesenteric ischemia: part 1, role in diagnosis and differential diagnosis. AJR Am J Roentgenol 2007;188:452–461.

# CASE 13

**CYNTHIA S. PAYNE**

**AND**

**KURT HUSUM**

## HISTORY

A 61-year-old man undergoing percutaneous nephrostomy (PCN) for treatment of renal obstruction. After tract dilation, with only a guidewire (and no catheter) in place, brisk pulsatile bleeding from the PCN tract was seen.

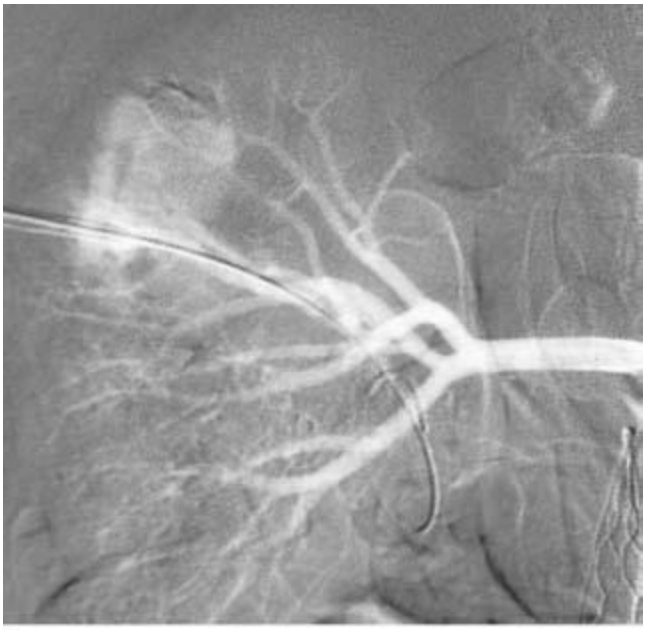

A

**FIGURE 7-13A** Renal arteriogram shows a guidewire entering the upper pole of the right kidney. An extraluminal collection of contrast material is seen adjacent to the guidewire, consistent with active contrast material extravasation due to pulsatile flow.

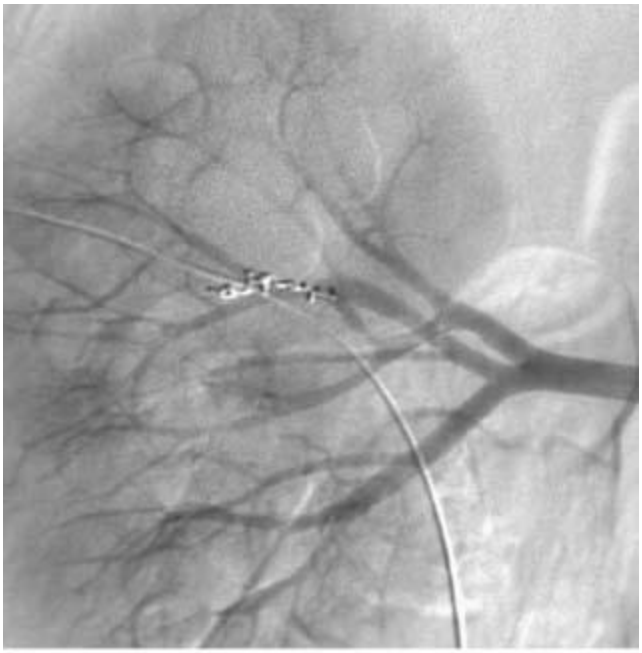

B

**FIGURE 7-13B** Renal arteriogram performed after embolization of the interlobar artery with microcoils shows cessation of the active extravasation.

## DIFFERENTIAL DIAGNOSIS

**Arterial injury**: The minimal parenchymal enhancement of the kidney in Figure 7-13A

indicates that the image is taken during the arterial phase of imaging. Frank extravasation of contrast material is present, making arterial injury highly likely. Additionally, even in the absence of these imaging findings, arterial injury should be highly suspected if the blood flow coming from the puncture site is pulsatile, brisk, and bright red.

- **Venous injury**: This type of injury is common, but pulsatile flow should not be expected. Furthermore, the fact that a moderate amount of extravasation (consistent with pulsatile flow) is present during the arterial phase of the arteriogram renders this diagnosis incorrect.
- **Parenchymal hemorrhage**: Parenchymal hemorrhage could occur secondary to a number of predisposing causes (e.g., underlying coagulopathy). Like venous injury, parenchmyal hemorrhage into the tract would not be expected to be pulsatile. Furthermore, the degree of extravasation in the arterial phase image in Figure 7-13A is markedly beyond what would be expected for parenchymal hemorrhage on arteriography, which is typically minimal or absent. Therefore, this diagnosis is incorrect.

## DIAGNOSIS

**Hemorrhage due to arterial injury**

## KEY FACTS

### Clinical

- The most common indications for PCN include (1) relief of collecting system obstruction, (2) need for collecting system access for a procedure (e.g., stone extraction or lithotripsy, or stricture dilatation), and (3) urinary diversion (e.g., during treatment of ureteral injuries, fistulas, or hemorrhagic cystitis).
- Proper preprocedure patient planning includes (1) assessment of imaging studies indicating the rationale for the procedure, (2) review of pertinent recent laboratory studies (particularly coagulation parameters), and (3) administration of broad-spectrum antibiotics for prophylaxis against gram-negative organisms.
- The rate of major complication during PCN placement is <10%. Mild hematuria frequently occurs after PCN placement and is not considered a serious complication. Serious complications of PCN placement include (1) sepsis, which is the most common complication (seen in 1% to 9% of cases); (2) hemorrhage, which can be either immediate or delayed in onset; (3) inadvertent injury of adjacent organs (usually colon or spleen); and (4) pneumothorax, when the route of entry is not subcostal.
- Brisk pulsatile hemorrhage from the PCN tract should raise the suspicion of arterial injury. Typically, renal artery branches are involved, although arteries unrelated to the

kidney (e.g., the intercostal artery) can also be injured and cause frank hemorrhage.

## Radiologic

- Either sonographic or fluoroscopic guidance can be used for needle access to the urinary collecting system. Access should be obtained via a posteriorly located calyx, ideally through the "Brodel bloodless line of incision," which is a relatively avascular plane at the posterolateral aspect of the kidney at the junction of the medial two-thirds and lateral one-third of the renal parenchyma. Entry into the renal pelvis should be avoided due to the presence of adjacent major vascular structures. An anterior calyx entry point should also be avoided because the tract traverses a greater amount of renal parenchyma, which has a higher risk of vascular injury. Furthermore, the necessary angle of entry for wires and catheters from this approach makes the procedure difficult.
- Real-time sonography usually allows good depiction of a posterior renal calyx and aids in puncture.
- If renal function is normal, the renal collecting system can be opacified using intravenous contrast administration if needed, allowing visualization at fluoroscopy. Alternatively, a "blind" approach (i.e., without infusion of contrast material) with a small bore (e.g., 22 gauge) needle may be taken solely using anatomic landmarks. The collecting system can then be delineated by injecting contrast material and a small amount of air through the needle to identify the posterior calyces. Puncture of a posterior calyx can then be performed under fluoroscopic guidance.
- Generally an 8 or 10 French, self-retaining, pigtail catheter is used, with the pigtail loop positioned within the renal pelvis.
- If the renal collecting system is already infected at the time of a PCN procedure, extreme caution must be exercised to minimize distention of the collecting system in order to minimize the risk of inducing sepsis.
- Brisk, pulsatile, or unremitting hemorrhage from the catheter, tract, or bladder should raise suspicion of arterial injury. The first step in treatment should be tamponade of the bleeding site by insertion of the catheter, which often controls the hemorrhage. Sometimes insertion of a larger catheter may be necessary.
- Severe hemorrhage during PCN is an indication for renal angiography. If the source of hemorrhage is a distal vessel (as in the case shown), embolization should be immediately performed using coils, particles, or gelatin sponge (Gelfoam) pledgets. In the case shown here, microcoils were used. Distal embolization should be performed in order to preserve the maximal amount of renal parenchyma. If the arteriogram is negative, it should be repeated with the catheter removed over a guidewire, since it may be tamponading the bleeding.
- Injuries to the proximal renal artery or vein may require surgical repair.

## SUGGESTED READING

Dyer RB, Regan JD, Kavanaugh PV, et al. Percutaneous nephrostomy with extensions of the technique: step by step. Radiographics 2002;22:503–525.

Lee WJ, et al. Emergency percutaneous nephrostomy: results and complications. J Vasc Interv Radiol 1994;5:135–139.

Lewis S, Patel U. Major complications after percutaneous nephrostomy-lessons from a department audit. Clin Radiol 2004;59:171–179.

Richstone L, Reggio E, Ost MC, et al. Hemorrhage following percutaneous renal surgery: characterization of angiographic findings. J Endourol 2008;22:1129–1135.

Uday P, Hussain F. Percutaneous nephrostomy of nondilated renal collecting systems with fluoroscopic guidance: technique and results. Radiology 2004;233:226–233.

# CASE 14

**CYNTHIA S. PAYNE**

**AND**

**CHARLES Y. KIM**

## HISTORY

A left-handed baseball pitcher with pain and numbness in the left hand and forearm when throwing.

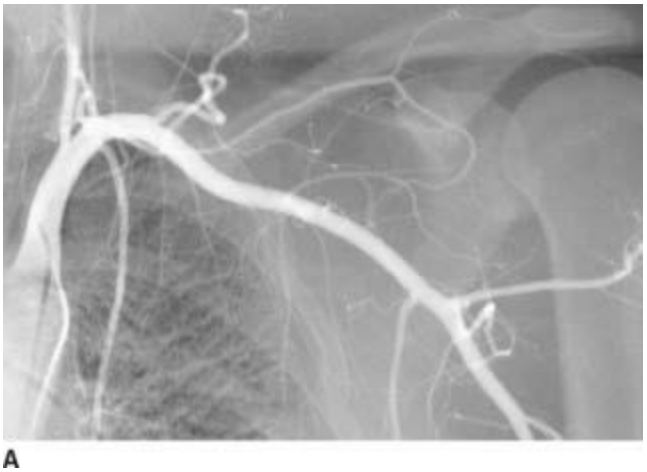

A

**FIGURE 7-14A** Selective left subclavian artery angiogram performed with the left arm in neutral position shows normal caliber of all arteries.

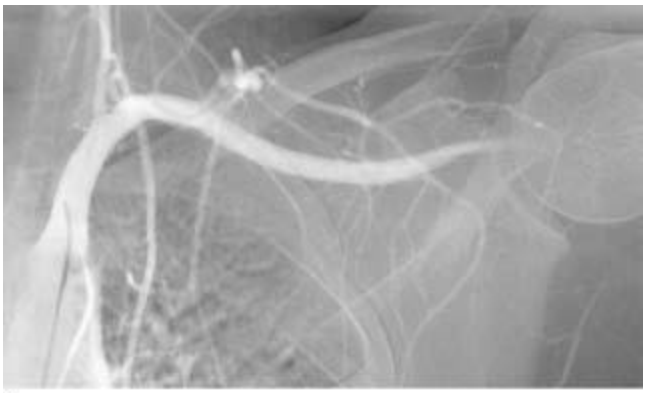

B

**FIGURE 7-14B** Repeat angiogram performed a few minutes later with the left arm in abduction shows occlusion of the distal left axillary artery.

## DIFFERENTIAL DIAGNOSIS

**Atherosclerotic disease**: The smooth tapered concentric narrowing of the axillary artery in Figure 7-14B in the absence of other involved arteries would be rare for atherosclerosis. However, atherosclerosis causes a fixed stenosis, so the key finding here that makes this diagnosis incorrect is the normal caliber and appearance on the neutral view in Figure 7-14A.

**Vasculitis**: The angiographic appearance and young age of the patient make vasculitis a reasonable consideration, if Figure 7-14B is viewed alone. Again, the normal appearance in neutral position in Figure 7-14A makes this diagnosis incorrect.

**Arterial thoracic outlet syndrome**: When the findings of both images shown are considered together, the occlusion of the subclavian artery can essentially solely be explained by arterial compression due to change in the position of the arm. Such compression would most likely be due to arterial compression by adjacent muscle or rib. This diagnosis is correct.

## DIAGNOSIS

**Arterial thoracic outlet syndrome**

## KEY FACTS

### Clinical

- Thoracic outlet syndrome produces upper extremity symptoms secondary to

compression of nerves or vessels as they exit the thoracic outlet.

- The compression is typically due to bony structures (especially cervical ribs), muscles, or tendons, which are often related to anomalous anatomy, muscle hypertrophy, fibrous bands, or posttraumatic tissue.
- The costoclavicular space is by far the most frequent site of arterial compression, followed in frequency by the interscalene triangle and retropectoralis minor space.
- Thoracic outlet syndrome can result from compression of an artery, vein, or nerve. Symptomatology depends on which structure is compressed. Neurogenic compression comprises approximately 95% of cases, with venous compression responsible for 3% to 4% and arterial compression for 1%.
- Neurogenic thoracic outlet syndrome typically presents as pain, paresthesia, and weakness in the hand, arm, and shoulder with neck pain and occipital headaches. Raynaud's phenomenon is also frequently observed.
- Arterial compression can lead to digital ischemia, claudication, pallor, coldness, paresthesias, and pain involving the hand, but seldom causes symptoms in the shoulder or neck. The repeated traumatic arterial compression can eventually produce stenosis, occlusion, or aneurysm formation, with resultant mural thrombus formation and distal emboli. Such emboli are often the cause of the hand symptoms in this syndrome.
- Venous compression classically causes arm swelling, sometimes with pain, aching, or paresthesias. Subclavian vein thrombosis in the setting of venous thoracic outlet syndrome is termed Paget-Schroeder syndrome.
- The distal location of the occlusion in the case shown suggests that compression by the pectoralis minor muscle (which can become hypertrophied secondary to the repeated arm motions involved in pitching) is the most likely etiology.

## Radiologic

- Because cervical ribs or anomalous first ribs are associated with arterial thoracic outlet syndrome, chest radiography is a reasonable first study for evaluation.
- Doppler sonography can serve as a helpful noninvasive study for detection of subclavian arterial aneurysms and stenoses.
- MRA and CTA are often useful for identifying arterial and venous abnormalities, as well as delineating the bony or soft tissue anomalies.
- Selective catheter angiography of the subclavian artery is indicated when ischemia due to arterial thoracic outlet syndrome is suspected based on clinical history and physical examination findings. Imaging should then be performed from the aortic arch to the digits.
- The classic angiographic findings in arterial thoracic outlet syndrome include

subclavian artery stenosis with a poststenotic aneurysm and evidence of distal embolization. Additional findings may include arterial occlusion, frank aneurysm formation, arterial displacement, pseudoaneurysm, and thrombosis.

- Angiography using provocative maneuvers is often performed. This procedure involves imaging with the arm in first neutral and then hyperabducted position. However, it must be kept in mind that up to half of normal patients will show normal physiologic compression of the subclavian artery with arm hyperabduction.
- Definitive therapy requires surgical decompression of the thoracic outlet prior to addressing an arterial aneurysm and/or stenosis. Surgical bypass graft placement has traditionally been the therapy of choice, although endovascular techniques can also be utilized.

## SUGGESTED READING


Chang DC, Rotellini-Coltvet LA, Mukherjee D, et al. Surgical intervention for thoracic outlet syndrome improves patient's quality of life. J Vasc Surg 2009;49:630–635.

Degeorges R, Reynaud C, Becquemin JP. Thoracic outlet syndrome surgery: Long-term functional results. Ann Vasc Surg 2004;18:558–565.

Demondion X, Herbinet P, Van Sint JS, et al. Imaging assessment of thoracic outlet syndrome. Radiographics 2006;26:1735–1750.

Fugate MW, Rotellini-Coltvet L, Freischlag JA. Current management of thoracic outlet syndrome. Curr Treat Options Cardiovasc Med 2009;11:176–183.

Huang JH, Zager EL. Thoracic outlet syndrome. Neurosurgery 2004;55:897–902; discussion 902–903.

Sanders RJ, Hammond SL, Rao NM. Diagnosis of thoracic outlet syndrome. J Vasc Surg 2007;46:601–604.


# CASE 15


**TONY P. SMITH**

**AND**

**CHARLES Y. KIM**


### HISTORY

A 55-year-old man with advanced sarcoidosis who presents acutely with a large amount of frankly bloody sputum. His PPD is negative.

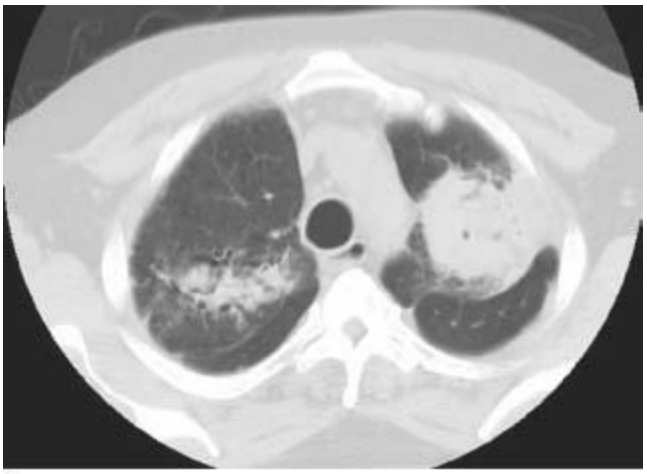

A

■**FIGURE 7-15A** Axial unenhanced CT image through the upper lobes shows bilateral confluent regions of pulmonary consolidation. A cavitary lesion in the right lung containing round soft tissue density material and local bronchiectasis is present.

B

■**FIGURE 7-15B** Angiogram of the right bronchial artery shows an enlarged and tortuous bronchial artery with associated hypervascularity in the right upper lobe.

## DIFFERENTIAL DIAGNOSIS

■**Tuberculosis (TB)/atypical mycobacterial infections**: TB is the most common cause

of massive hemoptysis in the non-Western world, and could produce the radio-logic images shown here. However, the negative PPD makes this diagnosis unlikely.

- **Aspergilloma**: This invasive fungal infection typically occurs in pulmonary bullae or cavitary lesions, such as can be seen in end-stage pulmonary sarcoidosis. This patient's CT shows soft tissue density within a cavitary lesion in the right lung, which is highly suggestive of an aspergilloma. This diagnosis is correct.
- **Lung carcinoma**: The CT findings shown in this case could potentially represent multifocal malignancy, but the findings are not typical for that diagnosis, given the associated bronchiectasis, its ill-defined margins, and semisolid appearance. Furthermore, lung carcinoma does not typically cause bronchial artery enlargement to the degree shown in this case, making this diagnosis unlikely.

## DIAGNOSIS

**Aspergilloma**

## KEY FACTS

### Clinical

- "Massive hemoptysis" is defined as >300 to 600 mL over 24 hours and can be rapidly fatal secondary to asphyxiation. Bronchial arteries are involved in 90% of cases with the remainder of the arterial supply coming from pulmonary or systemic arteries.
- When the source of hemorrhage is unilateral, selective intubation or a bifurcated double-barrel endotracheal tube can be used to protect the contralateral lung.
- When hemoptysis is caused by a lesion adjacent to the pleura and associated pleural thickening is present, arterial supply that is at least, in part, from the systemic circulation, should be suspected, which can aid in angiography planning.
- Bronchoscopy is typically useful for identifying the lung from which hemoptysis is arising and can specify the source of hemorrhage, although this can be difficult in the setting of massive hemoptysis. In some cases, the source of hemorrhage can be treated with cauterization or local injection of vasoconstrictive agents.
- The bronchial arteries usually originate from the aorta at approximately the T5-6 level. They have substantial anatomic variability, often with a right intercostobron-chial trunk bifurcating into a bronchial and intercostal artery. The typical configurations are one left and one right bronchial artery (21% of cases); two left and two right bronchial arteries (21%); or one left, two right bronchial arteries (10%).
- The bronchial arteries supply the bronchi, esophagus, visceral pleura, vasa vasorum of the aorta, and the pulmonary arteries and veins.
- When performing embolization for hemoptysis, one should always consider the

possibility of partial or complete systemic arterial supply from the internal mammary artery, thyrocervical trunk, intercostal arteries, and inferior phrenic artery, and branches of the subclavian or axillary artery.

- Surgical resection can be performed when the source of bleeding is identified as arising from within one hemitho-rax, but often these patients are poor surgical candidates.
- Medical therapies may be helpful, depending on the underlying etiology, such as antibiotic therapy for infection-related hemorrhage.

## Radiologic

- Bronchial artery embolization is a first-line therapy for massive hemoptysis.
- The most common angiographic abnormality seen at bronchial arteriography for hemoptysis evaluation is enlargement and tortuosity of the bronchial arteries. Other angiographic findings include hypervascularity, focal parenchymal blush, pseudoaneurysm, and AV shunting. All abnormal vessels should of the vascular supply coming undergo embolization. If no abnormal vessels are identified, empirical bronchial artery embolization is indicated unless there is a high level of suspicion of a pulmonary arterial source (such as recent pulmonary arterial catheter manipulation).
- Transcatheter embolization for massive hemoptysis has a 73% to 98% success rate in the short term and 50% to 90% success rate in the long term, but does not address the underlying pathology.
- Special care must be taken to identify the anterior medullary artery of Adamkiewicz, which supplies much of the arterial supply of the lower thoracic and lumbar regions of the spinal cord. This artery has a characteristic vertical “hairpin turn” appearance and typically originates from a left intercostal or lumbar artery between the T8 and L4 segments.
- The ideal embolic agent is polyvinyl alcohol (PVA) particles (350 to 500 μM). Coil embolization should be avoided, because their use would occlude the parent artery, thereby precluding access to the same artery in the event of recurrent hemoptysis. Generally, only angiography of the bronchial arteries is performed during evaluation of massive hemoptysis. Angiography of the pulmonary arteries is reserved for cases in which pulmonary arterial injury or parenchymal necrosis is suspected.
- Potential complications of angiography of the bronchial arteries include chest pain (ischemic in nature and usually transient), dysphagia (usually transient and secondary to nontarget embolization of esophageal branches), and paraplegia (very rare, secondary to non-target embolization of the anterior medullary artery of Adamkiewicz). Other, rare complications include aortic or bronchial necrosis, bronchoesophageal fistula, and pulmonary infarction.

## SUGGESTED READING

Jean-Baptiste E. Clinical assessment and management of massive hemoptysis. Crit Care Med 2000;28:1642–1647.

Kalva SP. Bronchial artery embolization. Tech Vasc Interv Radiol 2009;12:130–138.

Wang GR, Ensor JE, Gupta S, et al. Bronchial artery embolization for the management of hemoptysis in oncology patients: utility and prognostic factors. J Vasc Interv Radiol 2009;20:722–729.

Yoon W, Kim JK, Kim YH, et al. Bronchial and nonbronchial systemic artery embolization for life-threatening hemoptysis: a comprehensive review. Radiographics 2002;22:1395–1409.

# CASE 16

**PAUL V. SUHOCKI**

**AND**

**JOSHUA A. BRYANT**

### HISTORY

A 22-year-old man who sustained a gunshot wound to the left upper arm and is found to have decreased left ar pulses.

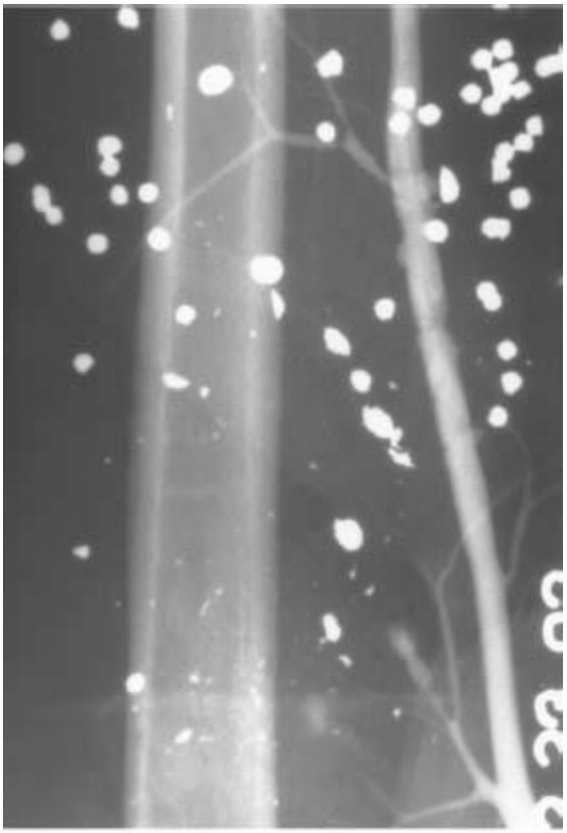

A

**FIGURE 7-16A** Left brachial arteriogram shows scattered buckshot and multiple sites of focal narrowing and outpouching of the brachial artery lumen as well as a linear defect in the distal segment of the artery. Several branches of the brachial artery terminate abruptly with associated extraluminal contrast material collections.

B

**FIGURE 7-16B** Several filling defects are seen in the princeps pollicis artery and the proper digital arteries of the first and second digits.

## DIFFERENTIAL DIAGNOSIS

**Vasospasm**: Vasospasm can occur after trauma. However, this diagnosis would not account for the findings of a linear lucency and the extraluminal contrast collections in the brachial artery, making this diagnosis by itself incorrect.

**Arterial dissection**: The linear lucency extending along the brachial artery is, in fact, due to arterial dissection. However, this diagnosis alone does not account for all the findings, such as the extraluminal contrast material collections and the findings in the digits.

**Arterial injury with distal thromboembolization**: In addition to an arterial dissection, several small foci of extravasation involving branches of the brachial artery are present. The outpouchings of the brachial artery are sites of pseudoaneurysm formation. The numerous occlusions and filling defects in the digital arteries are due to thromboembolism distal to the site of intimal injury. This diagnosis is correct.

## DIAGNOSIS

**Arterial injury with distal thromboembolism**

## KEY FACTS

### Clinical

- In a trauma patient, the clinical signs of an expanding hematoma, hypotension, or distal limb ischemia are indications of vascular injury until proven otherwise.
- Diminished or absent blood pressure or pulses are the most reliable clinical signs of arterial injury within a limb. However, in the setting of systemic hypotension, this finding can be difficult to evaluate.
- Arterial injuries can produce hematoma, arterial occlusion, pseudoaneurysm, and AV fistula formation.
- Obvious arterial injuries in an unstable, hypotensive patient are an indication for immediate surgical exploration and repair.
- Although most arterial injuries are due to penetrating trauma, injury can also result from nonpenetrating trauma, for example, stretch injury. That form of injury is typically seen following joint dislocations (e.g., posterior knee dislocations).

### Radiologic

- The role of catheter angiography in the setting of suspected arterial injury is to determine the presence or absence of injury, define the type of injury, and either temporize or definitively treat the injury via endovascular therapy.
- The two most common angiographic findings in arterial injury are luminal occlusion and extravasation of contrast material. Arterial occlusion can reflect either intimal injury with subsequent thrombus formation or transmural disruption. Other potential findings include presence of an intimal flap, vasospasm, pseudoaneurysm, AV fistula, distal embolization, and displacement of vessels by adjacent hematoma.
- CTA is a readily accessible technique to evaluate blunt and penetrating trauma of the extremities, and can be used to help stratify patients for conservative management, direct patients to conventional angiography, or provide a “road map” prior to surgery. Extravasation of contrast material, pseudoaneurysms, and arterial transection are readily identified with high sensitivity and specificity. Limitations of CTA include inadequate contrast bolus (e.g., in the setting of systemic hypotension), metallic streak artifact (particularly in the setting of gunshot wounds), and patient motion artifact. MRA may be used in more stable injuries when conservative management is anticipated. The findings are usually similar to those of CTA. However, as with CTA, the presence of metallic foreign bodies also limits visualization of adjacent structures.
- For vascular trauma of medium- and large-size arteries, stent grafts offer an option to treat bleeding due to trauma. Potentially treatable injuries include partial transections,

dissections, AV fistulas, and pseudoaneurysms. Small branch artery injury with associated extravasation can be treated with embolotherapy using coils, particles, or gel foam. These devices act in a mechanical fashion to stop flow within a vessel in an attempt to stop hemorrhage.

- In the appropriate scenarios, endovascular treatment has the advantage of decreased morbidity, decreased risk of infection, and decreased risk of injury to surrounding structures (such as the brachial plexus) when compared to surgery.

## SUGGESTED READING

Arthurs ZM, Sohn VY, Starnes BW. Vascular trauma: endovascular management and techniques. Surg Clin North Am 2007;87:1179–1192.

Connell D, Koulouris G. Contrast-enhanced MR angiography of the hand. Radiographics 2002;22:583–599.

Goldberg MC, O'Donnell TF. Acute ischemia: upper and lower extremity trauma. In DE Strandness Jr, A Van Breda (eds), Vascular Diseases. New York, NY: Churchill Livingstone, 1994;399–420.

Miller-Thomas MM, West OC, Cohen AM. Diagnosing traumatic arterial injury in the extremities with CT angiography: pearls and pitfalls. Radiographics 2005;25:S133–S142.

Soto JA, Munera F, Morales C, et al. Focal arterial injuries of the proximal extremities: helical CT arteriography as the initial method of diagnosis. Radiology 2001;218:188–194.

# CASE 17

**MELISSA A. HAYES**

**AND**

**CHARLES Y. KIM**

## HISTORY

A 33-year-old woman with acute onset of left lower extremity pain and swelling.

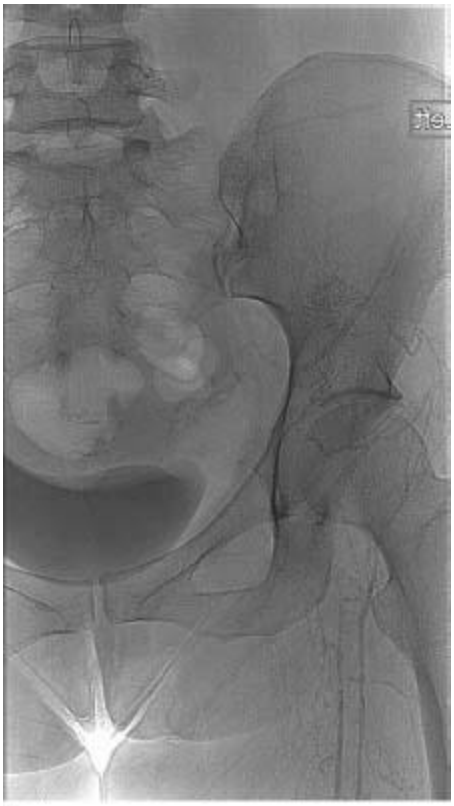

A

■**FIGURE 7-17A** Left lower extremity venogram shows filling of numerous small collateral veins without filling of the femoral or common femoral vein. This finding is compatible with acute occlusion of the left lower extremity venous system due to thrombus.

B

**FIGURE 7-17B** Repeat venogram performed after mechanical thrombectomy and overnight thrombolysis shows restored patency of the iliofemoral venous system, but with a severe focal stenosis at the origin of the left common iliac vein. Numerous collateral veins seen to the contralateral iliac system and IVC.

## DIFFERENTIAL DIAGNOSIS

**May-Thurner syndrome**: The findings in this case are acute thrombosis of the left iliofemoral venous system (Figure 7-17A) and persistent occlusion of the left common iliac vein after thrombolysis (Figure 7-17B). These findings, in combination with the patient's gender and age, are typical for May-Thurner syndrome (i.e., compression of the left common iliac vein origin by the right common iliac artery).

**Spontaneous deep venous thrombosis (DVT)**: Although DVT is indeed present in Figure 7-17A, this finding, by itself, does not explain the findings in Figure 7-17B. Risk factors for DVT are numerous and include immobility, malignancy, trauma, surgery, and a hypercoagu-lable state. When DVT is spontaneous, an underlying venous lesion (as in Figure 7-17B) is not typically present. Therefore, this diagnosis is incorrect.

**Neoplasm**: A mass may cause obstruction to venous outflow, predisposing to thrombus formation. However, a neoplasm compressing a vein would result in extrinsic mass effect on the vein, as evidenced by a tapering lumen. However, in the case shown, the stenosis is abrupt, which makes this diagnosis incorrect.

- **Inferior vena cava (IVC) occlusion**: IVC occlusion can lead to thrombosis of both iliofemoral venous systems. The presence of the IVC filter in Figure 17-17B raises the possibility that the left iliofemoral DVT in Figure 7-17A is due to IVC occlusion related to the IVC filter. However, the presence of the severe focal stenosis at the origin of the left common iliac vein makes this diagnosis unlikely.
- **Radiation therapy**: Radiation therapy can cause diffuse long segment stenosis or occlusion of the segment involved in the irradiated field. Figure 7-17A alone could be compatible with this diagnosis. However, restored luminal patency of the iliofemoral veins and the focality of this stenosis make this diagnosis incorrect.

## DIAGNOSIS

**May-Thurner syndrome (compression of the left common iliac vein origin by the right common iliac artery)**

## KEY FACTS

### Clinical

- May-Thurner syndrome is defined as left iliofemoral vein thrombosis caused by compression of the left common iliac vein by the right common iliac artery.
- The chronic compression and arterial pulsation result in intimal hyperplasia with progressive stenosis. When flow is sufficiently impeded, and especially in combination with other DVT risk factors, patients may experience thrombosis of the left-sided lower extremity veins with acute left leg pain and swelling.
- Given the chronic and progressive nature of this syndrome, patients may report a history of intermittent episodes of mild left leg swelling prior to the acute thrombotic event. Other possible presentations include pulmonary embolism, varices, and skin discoloration.
- May-Thurner syndrome is most common in women in the third to fifth decades of life.
- The goal of treatment is to alleviate symptoms, prevent additional thromboses, and importantly, to prevent the development of postthrombotic syndrome (venous valvular incompetence resulting in chronic leg swelling, pain, ulcers, and varicosities).

### Radiologic

- The initial imaging of May-Thurner syndrome often involves Duplex ultrasound imaging demonstrating acute deep vein thrombosis of the left leg extending through the left common femoral vein into the pelvis. This finding, in combination with appropriate demographic factors and otherwise lack of readily explainable cause such as trauma, prolonged bedrest, etc., should raise the suspicion of May-Thurner syndrome. If

performed, cross-sectional or venographic imaging of the pelvic veins would be expected to show thrombus extending through the external iliac vein and common iliac vein to its origin, without thrombus in the IVC.

- Conventional venography, CTA, or MRA in the nonacute setting or after thrombolysis for acute DVT classically demonstrates a stenosis at the origin of the left common iliac vein, prominent collateral veins from the left iliac venous system to the IVC and contralateral iliac veins, and sometimes sequela of prior DVT, such as nonocclusive eccentric thrombus or webs in the left venous system.
- Treatment of May-Thurner syndrome includes medical, endovascular, and surgical options. Anticoagulation alone produces a poor patency rate at 1 year because it does not address the underlying cause of thrombus formation, i.e., the venous compression and associated stenosis.
- Endovascular treatment involves dissolution of any acute thrombus via mechanical and/or pharmacologic methods. Catheter-directed infusion of tissue plasminogen activator (tPA) is a popular method. Angioplasty and stenting should be performed to treat the left common iliac vein stenosis. Stenting has been shown to provide superior patency compared to thrombolysis alone or thrombolysis with angioplasty. Therefore, thrombolysis followed by angioplasty and stenting is currently the first-line treatment.
- Surgical options include venous bypass, excision of intraluminal bands, relocation or the right common iliac artery, or surgical thrombectomy. However, the patency rates for these procedures are less than those provided by endovascular therapy while also having significantly greater morbidity.

## SUGGESTED READING

Jeon UB, Chung JW, Jae HJ, et al. May-Thurner syndrome complicated by acute iliofemoral vein thrombosis: helical CT venography for evaluation of long-term stent patency and changes in the iliac vein. AJR Am J Roentgenol 2010;195:751–757.

Kwak HS, Han YM, Lee YS, et al. Stents in common iliac vein obstruction with acute ipsilateral deep venous thrombosis: early and late results. J Vasc Interv Radiol 2005;16:815–822.

O'Sullivan GJ, Semba CP, Bittner CA, et al. Endovascular management of iliac vein compression (May-Thurner) syndrome. J Vasc Interv Radiol 2000;11:823–836.

Seidensticker D, Wilcox J, Gagne P. Treatment of May-Thurner syndrome with catheter-directed thrombolysis and stent placement, complicated by heparin-induced thrombocytopenia. Cardiovasc Surg 1998;6:607–613.

# CASE 18

**BJORN ENGSTROM**

## HISTORY

A 61-year-old man with end stage renal disease being treated with hemodialysis (HD) via a permanent arteriovenous (AV) access graft.

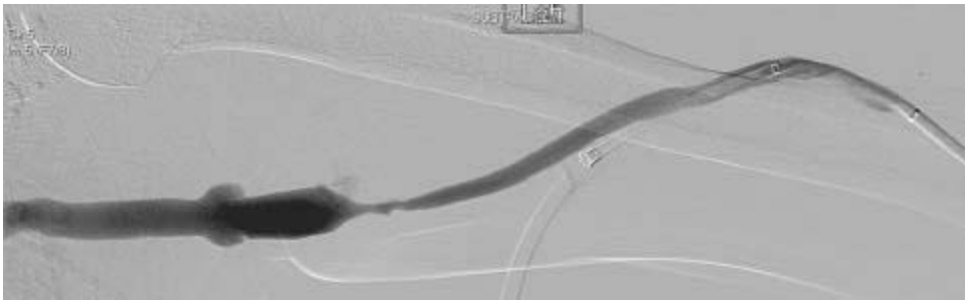

**FIGURE 7-18** Digital subtraction angiogram shows injection of contrast material into a structure having a relatively fixed-diameter in the middle of the image. The contrast material then flows across a narrowed region into a vessel having a large diameter.

## DIFFERENTIAL DIAGNOSIS

**Stenosis of native vein AV fistula**: The angiographic appearance of a native AV fistula is typically that of a large diameter (i.e., >1cm) vascular structure, which is of varying diameter throughout its length. Given the relatively small and constant diameter of the punctured structure, this is unlikely to represent a native vein AV fistula.

**Stenosis of AV graft arterial anastomosis**: The structure in the center and right side of the image is an AV access graft used for hemodialysis. This AV graft connects an artery (not seen in the image because it is located in a more peripheral location off the right side of the image) and a vein (the large caliber vessel seen on the left side of the image, which has an even larger caliber region representing a venous valve). The site of stenosis is clearly not at the anastomosis of the artery and the AV graft. This answer is incorrect.

**Stenosis of venous anastomosis of a prosthetic AV graft**: The narrowed region located between the AV graft and the vein is a characteristic appearance for a venous anastomosis of an AV graft. This location is the most common site of stenosis of an AV graft. This diagnosis is correct.

**AV graft thrombosis**: Although thrombosis is a common reason for intervention on an AV graft, filling defect(s) would be expected to be present within the graft. Near the tip of the sheath, Although poor opacification is seen near the tip of the sheath in this case, this finding is due to turbulent flow rather than stenosis. Further, when graft thrombosis occurs, the entire lumen of the graft becomes filled with thrombus, as opposed to an isolated filling defect. Therefore, this diagnosis is incorrect.

**Vasospasm**: Whenever a guidewire or catheter contacts the wall of an vein, spasm of

the vein can potentially occur. Typically, this results in a transient smooth long segment narrowing. However, given the relatively short length of the narrowing specifically at the venous anastomosis, this diagnosis is highly unlikely.

## DIAGNOSIS

**Stenosis of the venous anastomosis of an AV graft**

## KEY FACTS

### Clinical

- The number of patients on long-term HD in the United States alone is >340,000 and rising.
- AV fistula creation involves direct anastomosis of a vein with an artery. The resultant high flow rates in the vein induce luminal enlargement (termed "maturation"), which allows easier subsequent needle cannulation for HD.
- AV graft creation involves subcutaneously implanting a synthetic graft to form an anastomosis between an artery and vein. Scar tissue ingrowth into the graft is necessary prior to it being deemed adequate for puncture for HD to minimize the risk for hematoma and pseudoaneurysm formation after hemodialysis cannulation.
- AV fistulas are highly preferred over AV grafts due to their significantly higher patency rate and a significantly lower risk of infection. Drawbacks include a maturation time of up to 3 to 4 months and failure rate of up to 25%, due to nonmaturation. Furthermore, not all patients have veins that are suitable for fistula creation.
- AV graft thrombosis eventually occurs in nearly all AV grafts. The most common etiology is progressive stenosis at the venous anastomosis. When the degree of stenosis becomes severe enough, thrombosis occurs. Stenosis of the graft or outflow veins can also occur anywhere along the circuit.
- The etiology of venous anastomosis stenosis is intimal hyperplasia.
- When patients have a worsening stenosis in their AV fistula or graft, several clinical signs are present. When an outflow stenosis is present, the graft or fistula becomes more pulsatile than thrill-like and the puncture sites bleed more aggressively due to the higher outflow resistance. When an inflow stenosis is present, the thrill becomes fainter. In both situations, the flow rates during HD become detectably poorer. In cases of central venous stenosis, the ipsilateral arm may become swollen. In any of these cases, referral to interventional radiology is appropriate.
- When the AV graft or fistula is thrombosed, there is no thrill or pulse on palpation. Attempts at cannulation results in lack of any blood flow from the needle. Patients with AV graft thrombosis should be considered for a thrombolysis/thrombectomy procedure.

## Radiologic

- Although ultrasound can be performed to evaluate for stenosis or thrombosis, physical exam is fairly accurate for the detection of an abnormality, and, therefore, sonography is often an unnecessary step.
- The entire circuit, from the arterial anastomosis to the right atrium should be imaged and evaluated. Stenoses are treated with angioplasty and/or stenting.
- Postangioplasty, there should be no more than 30% residual stenosis. If this cannot be achieved, stenting should be considered.
- Bare metal stents and covered stents can be used to help salvage failing AV grafts. When treating cases of extravasation, covered stents are usually preferred. For other indications, the superiority of one over the other is still unknown.
- Recently, a prospective randomized trial demonstrated a significant decrease in the rate of restenosis for venous anastomosis stenoses when a covered stent was used, as compared with angioplasty alone.
- For the treatment of thrombosed AV grafts and fistulas, the first step is clearance of clot. This can be performed using pharmacologic means (i.e., tPA) and/or mechanical means using a variety of devices and methods. Once the thrombus is cleared, the underlying stenosis should then be identified and addressed.
- The vast majority of AV grafts and fistulas will eventually develop a stenosis somewhere within the circuit. It is important to perform interventions, often repeatedly, to maximize the life of the access because each patient has a limited number of access sites to be used.

## SUGGESTED READING

Haskal ZJ, Trerotola S, Dolmatch B, et al. Stent graft versus balloon angioplasty for failing dialysis-access grafts. N Engl J Med 2010;362:494–503.

Kaufman JK, Lee MJ. The Requisites: Vascular and Interventional Radiology (1st ed). Philadelphia, PA: Elsevier, 2004;184–191.

Kerlan RK Jr, LaBerge JM. Fistula first, stent graft second. N Engl J Med 2010;362(6):550–552.

NKF-KDOQI Clinical Practice Guidelines for Vascular Access: Update 2006. Guideline 6: Treatment of Arteriovenous Graft Complications.

# CASE 19

**GLEN A.**
**TOOMAYAN**

## HISTORY

A 61-year-old man with a 3-month history of jaundice.

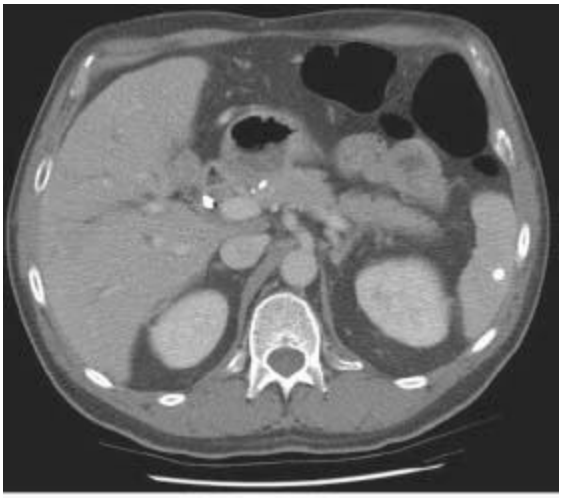

A

■**FIGURE 7-19A** Contrast-enhanced CT shows intrahepatic biliary ductal dilation (seen as multiple curvilinear regions of low density) in the portal triads without dilation of the common bile duct. No lymphadenopathy or other masses are present in the region of the porta hepatis.

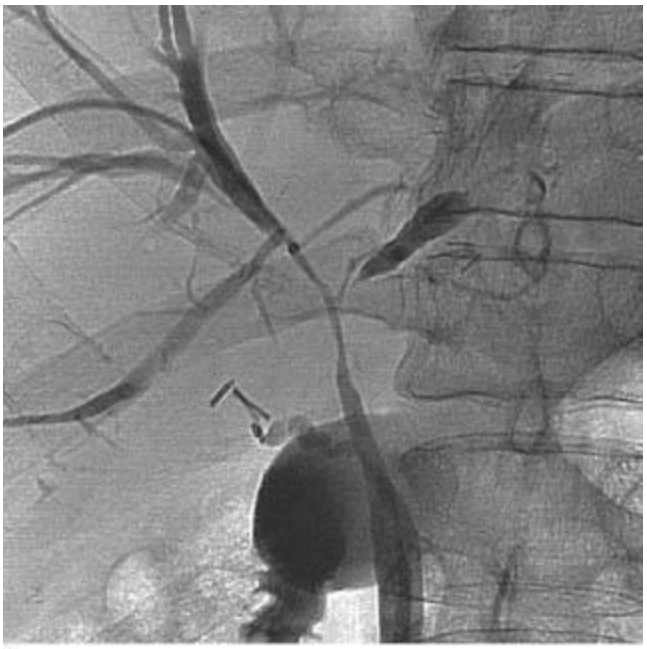

B

■**FIGURE 7-19B** A percutaneous cholangiogram shows a sheath terminating in the right hepatic duct. Bilateral intrahepatic biliary ductal dilation is seen. A long segment stricture is present, involving the origins of the right and left hepatic ducts as well as the

adjacent hepatic duct. Surgical clips from prior cholecystectomy are present.

## DIFFERENTIAL DIAGNOSIS

- **Cholangiocarcinoma (Klatskin tumor)**: A long segment stricture at the bifurcation of the common hepatic duct with irregular margins is highly suggestive of a stricture caused by a neoplasm. Cholangiocarcinoma is the most likely cause of a malignant biliary stricture at this location. A hilar cholangiocarcinoma of the type shown here is referred to as a "Klatskin tumor". This diagnosis is the most likely.
- **Porta hepatis lymphadenopathy**: Extrinsic compression from enlarged lymph nodes in the porta hepatis could cause a stricture of the extrahepatic bile ducts. CT and MRI are routinely performed to evaluate for lymphadenopathy. The absence of enlarged lymph nodes in Figure 7-19A indicates that this diagnosis is incorrect.
- **Gallbladder carcinoma**: This rare malignancy, when very advanced, can invade the extrahepatic bile ducts. However, there tends to be evidence of mass effect (not present in the case shown here). Furthermore, given the evidence of prior cholecystectomy, this diagnosis is unlikely.
- **Mirizzi's syndrome**: A large gallstone in the cystic duct can exert mass effect on the common bile duct or common hepatic duct with resultant intrahepatic biliary ductal dilatation. However, this phenomenon usually occurs more inferiorly near the level of the cystic duct insertion. Figure 7-19B shows retrograde filling of the cystic duct (which has a corkscrew appearance and terminates at the cholecystectomy clips) rather than evidence of a filling defect, indicating that this diagnosis is incorrect.
- **Sclerosing cholangitis**: This inflammatory disorder usually has the appearance of multifocal irregular strictures of the intrahepatic and extrahepatic bile ducts. Therefore, the unifocal nature of this single contiguous stricture makes this diagnosis unlikely.

## DIAGNOSIS

**Cholangiocarcinoma ("Klatskin tumor")**

## KEY FACTS

### Clinical

- Cholangiocarcinoma is an uncommon malignant tumor of the biliary tract; approximately 3,500 new cases are diagnosed annually in the United States.
- This tumor is the second most common primary malignant hepatic neoplasm (ranking behind hepatocellular carcinoma).
- Presenting signs and symptoms include jaundice, abdominal pain, weight loss, and

fever. When fever and leukocytosis are present in the setting of biliary obstruction, cholangitis is presumed to be present, and urgent decompression is warranted to avoid sepsis.

- Risk factors for development of cholangiocarcinoma include primary sclerosing cholangitis (PSC), cirrhosis, choledochal cysts, hepatic infection with such organisms as flukes or viruses (e.g., HIV and hepatitis C), hepatolithiasis in the setting of recurrent pyogenic cholangitis, and toxic exposures (e.g., Thorotrast contrast material, polyvinyl chloride, and heavy alcohol consumption).
- PSC is one of the most common risk factors for development of cholangiocarcinoma in the Western hemisphere.
- Partial hepatectomy may be attempted for resection of non-hilar cholangiocarcinoma.
- Three year survival rates of 35% to 50% have been documented following resection with negative margins.
- An obstructed biliary system requires drainage via a percutaneous biliary drainage catheter or an endoscopic stent.

## Radiologic

- Morphologically, cholangiocarcinoma may be classified as mass-forming, periductal infiltrating, or intraductal. Most hilar cholangiocarcinomas are of the periductal infiltrating type.
- Features of mass-forming cholangiocarcinoma on CT and MR imaging include the presence of an intrahepatic mass with variable enhancement, intrahepatic biliary ductal dilatation, vascular encasement, and satellite nodules.
- CT and MR imaging features of periductal infiltrating cholangiocarcinoma include biliary ductal dilation, ductal contrast-enhancement, a periductal soft tissue lesion, and regional lymphadenopathy.
- A cholangiocarcinoma involving the origins of both the right and left hepatic ducts is often termed a Klatskin tumor.
- The biliary tree can be imaged via endoscopic retrograde cholangiopancreatography (ERCP), magnetic resonance cholangiopancreatography (MRCP), or percutaneous transhepatic cholangiography (PTC).
- Features suggestive of a malignant stricture include long-segment involvement, abrupt termination, shouldering, irregular margins, and asymmetric ductal narrowing.
- Features suggestive of a benign stricture include short-segment involvement, regular margins, and symmetric ductal narrowing.
- Percutaneous access to the biliary tree can be accomplished using fluoroscopic and/or sonographic guidance using a small-gauge needle. Once needle access is attained

percutaneous cholangiography can be then performed.

- In the setting of biliary obstruction, urgent catheter drainage is indicated to avoid life-threatening cholangitis and sepsis. This can be accomplished using an external drain, with the pigtail loop peripheral to the obstruction. However, if possible, internal-external drainage should be performed, in which the drainage catheter traverses the obstruction, with the pigtail loop in the duodenum. Bile can then drain internally into the bowel, or externally into a drainage bag.
- With percutaneous access, a brush biopsy can be performed at the site of stricture. However, the sensitivity of brush biopsy for diagnosis of cholangiocarcinoma is <50%.

## SUGGESTED READING

Chamberlain RS, Blumgart RH. Hilar cholangiocarcinoma: a review and commentary. Ann Surg Oncol 2000;7:55–66.

Chung YE, Kim MJ, Park YN, et al. Varying appearances of cholangiocarcinoma: radiologic-pathologic correlation. radiographics 2009;29:683–700.

Han JK, Choi BI, Kim AY, et al. Cholangiocarcinoma: pictorial essay of CT and cholangiographic findings. radiographics 2002;22:173–187.

Park MS, Kim TK, Kim KW, et al. Differentiation of extrahepatic bile duct carcinoma from benign stricture: findings at MRCP vs. ERCP. Radiology 2004;233:234–240.

# CASE 20

**TIMOTHY J. AMRHEIN**

**AND**

**CHARLES Y. KIM**

## HISTORY

A 53-year-old man with Hepatitis C cirrhosis who underwent transjugular intrahepatic portosystemic shunt (TIPS) placement 2 years prior for recurrent esophageal variceal hemorrhage.


A

■**FIGURE 7-20A** Liver Doppler sonogram shows heterogeneous hepatic echotexture consistent with patient's history of cirrhosis. No blood flow is seen within the TIPS; flow within the portal veins is away from the shunt. A recanalized paraumbilical vein was identified on additional images (not shown). (See color insert)

B

■**FIGURE 7-20B** Portal venogram shows complete occlusion of the TIPS.

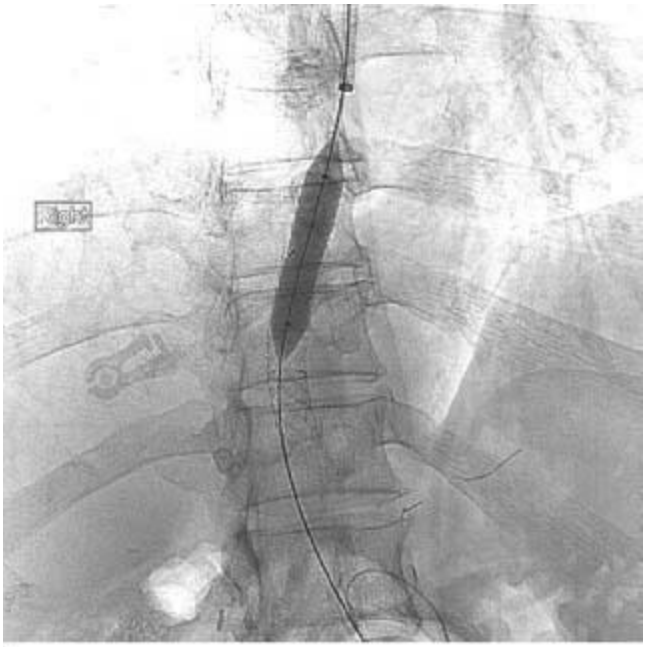

C

■**FIGURE 7-20C** Image obtained during angioplasty of the occluded TIPS stent shows deployment of an additional covered stent within the stenotic exposed hepatic vein adjacent to the TIPS stent.

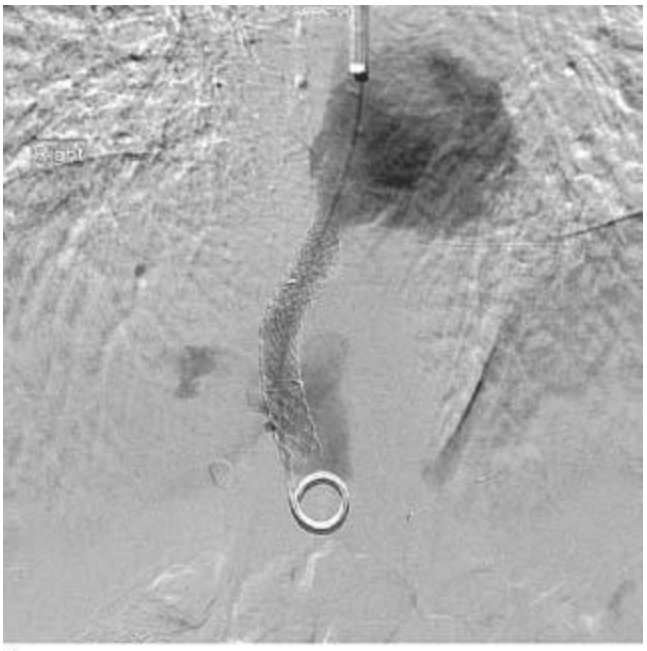

D

■**FIGURE 7-20D** Following angioplasty and placement of a new covered stent over the previously stenotic nonstented hepatic vein, good flow is seen within the now patent TIPS.

## DIFFERENTIAL DIAGNOSIS

- **TIPS occlusion**: The absence of blood flow in the TIPS on sonography is highly suggestive of thrombosis of the TIPS; this finding is confirmed on the angiographic image. This diagnosis is correct.
- **Slow flow within the TIPS**: The apparent absence of flow on the ultrasound image could be artifactual. If the pulse repetition frequency (PRF) is set too high (i.e., a wide range of color frequency shifts) the sensitivity to slow flow will be markedly reduced; slow flow could be misinterpreted as absence of flow. However, in this case the PRF was set appropriately (not shown). Additionally, the angiographic image demonstrates absence of opacification of the TIPS, making slow flow an incorrect diagnosis.
- **Biliary stent occlusion**: On sonography, the tubular structure having thin echogenic walls and without intraluminal flow could be misinterpreted as a bile duct or perhaps a biliary stent, accounting for the metallic stent demonstrated on the angiogram. However, the sheath tip in the right atrium and course of the pigtail catheter through the stent with opacification of the portal venous system virtually excludes this diagnosis.

## DIAGNOSIS

**TIPS occlusion with hepatic vein stenosis requiring angioplasty and stenting**

## KEY FACTS

### Clinical

- TIPS is an endovascular procedure performed to decompress a pressurized portal system by creation of a shunt between the portal venous system and the hepatic venous system with a covered stent (usually, between the right main portal vein and the right hepatic vein, although other combinations can be used). This results in a low-resistance channel between the portal venous system and the systemic venous system.
- The main indications for TIPS placement include vari-ceal bleeding and refractory ascites.
- Contraindications to TIPS placement include hepatic failure, severe hepatic encephalopathy, and severe right heart failure, because TIPS placement can significantly exacerbate these conditions.
- The most common complication from TIPS placement is worsening of hepatic encephalopathy (20% to 30% of cases); however, this can often be controlled medically. Rare complications include interaperitoneal hemorrhage, hemobilia secondary to bile duct or gallbladder puncture, fistula creation, intraperitoneal hemorrhage, hepatic failure, and stent malposition.
- Clinical findings suggestive of TIPS stenosis or occlusion include signs and symptoms of recurrent portal hypertension such as recurrence of variceal bleeding or

reaccumulation of ascites.

## Radiologic

- Shunt patency after TIPS placement is traditionally monitored with color duplex Doppler sonography. I maging may be performed every 3 to 6 months in patients with a prior history of variceal bleeding. Patients with a history of refractory ascites are evaluated as clinically indicated. However, given the excellent long-term patency rates of contemporary covered stents scheduled sono-graphic surveillance is controversial.
- Doppler spectral analysis is used to evaluate blood flow velocities within the portal vein as well as within the proximal, middle, and distal segments of the stent. Results are considered abnormal on the basis of identifying the following: an absolute stent velocity within any segment of <90 or >200 cm/s or a portal vein velocity <30 cm/s, although threshold criteria can vary. Alterations in the TIPS velocity on serial exams is also worrisome for a developing stenosis.
- Flow within the main portal vein should always be toward the TIPS (hepatopedal) if it is functioning normally. Flow away from the TIPS (hepatofugal) is associated with shunt stenosis or occlusion and should be referred for conventional angiography. However, direction of flow within intrahepatic portal vein branches can be variable.
- Secondary signs of shunt failure on sonographic evaluation include reappearance of varices, a recanalized paraumbilital vein or ascites.
- Shunt dysfunction is typically due to stenosis of the outflow hepatic vein or stenosis of the TIPS, which is caused by intimal hyperplasia or pseudointimal hyper-plasia. This occurs months to years after TIPS creation. When the degree of stenosis is severe, flow through the TIPS may be markedly diminished to the point that thrombosis can occur. Prior to the routine use of covered stents, leakage of thrombogenic bile through the interstices of bare metal stents resulted in a significant incidence of spontaneous thrombosis of the TIPS.
- Indications for revision include portosystemic gradients >12 mm Hg or recurrence of symptoms of portal venous hypertension.
- Treatment of TIPS stenosis includes angioplasty and/or additional stent placement. In cases of stenosis of the outflow hepatic vein, additional stenting to extend to the hepatocaval junction may be required. In cases of TIPS thrombosis, mechanical thrombolysis or infusion of thrombolytics can be performed. When revision of an existing shunt is difficult or impossible, a new parallel shunt may be placed.
- Technical success with covered stents approaches 100% in experienced hands. Primary and secondary patency rates are 76% to 84% and 98% to 100% at 1 year, respectively.

## SUGGESTED READING

Cura M, Cura A, Suri R, et al. Causes of TIPS dysfunction. AJR Am J Roentgenol 2008;191:1751–1757.

Ferral H, Banks B, Wholey M, et al. Techniques for transjugular intrahepatic portosystemic shunt revision. AJR Am J Roentgenol 1998;171:1041–1047.

Ochs A. Transjugular intrahepatic portosystemic shunt. Dig Dis 2005;23: 56–64.

Owen A, Stanley A, Vijayananthan A, Moss J. The transjugular intrahepatic portosystemic shunt (TIPS). Clin Radiol 2009;64:664–674.

# CASE 21

**SCOTT DUNCAN**

### HISTORY

A 72-year-old man with history of alcoholic cirrhosis found to have a liver mass on chest CT.

**FIGURE 7-21** Selective arteriogram of a branch of the right hepatic artery shows a large hypervascular mass in the right lobe of the liver. The arteries supplying the mass are irregular and tortuous.

## DIFFERENTIAL DIAGNOSIS

**Hepatocellular carcinoma (HCC)**: HCC is a leading consideration in any patient with cirrhosis and a liver mass. In the case shown here, the finding of tumor vas-cularity (as evidenced by increased number of small arteries supplying the mass, most of which are tortuous with a corkscrew appearance) in a cirrhotic liver is consistent with HCC. On

delayed images (not shown), a tumor blush or stain would be expected. Elevated serum alpha-fetoprotein (AFP) levels, which are found in about 90% of patients with HCC, would be added evidence of this diagnosis.

- **Hepatic metastasis**: The liver is a common location for metastases due to its rich vascular supply. The most common hypervascular metastases include renal cell, carcinoid, thyroid, choriocarcinoma, and islet cell tumors. Tumor marker levels or biopsy can help identify the origin of the tumor. Liver metastases typically present as multiple hypervascular lesions, rather than a single mass. This fact makes this diagnosis an unlikely explanation for the findings in the case shown here.
- **Cavernous hemangioma**: This entity is a relatively common benign cause of a hypervascular liver mass and is seen in approximately 20% of the normal population. This lesion usually has peripheral nodular enhancement on the arterial phase with more homogenous enhancement during delayed imaging. Although hemangiomas are hypervascular on cross-sectional imaging, they do not demonstrate arterial tumor vascularity on catheter angiography; therefore, this diagnosis is incorrect.
- **Hepatic adenoma**: This entity is a common benign hypervascular liver mass. These lesions are prone to spontaneous hemorrhage when they attain large size. However, they usually occur in young women (especially those taking oral contraceptives) rather than in older, cirrhotic men. This fact makes hepatic adenoma an unlikely diagnosis for the case shown here. Again, AFP levels and biopsy can help establish the diagnosis.

## DIAGNOSIS

**Hepatocellular carcinoma**

## KEY FACTS

### Clinical

- HCC is the most common primary malignancy of the liver, usually occurring in patients with cirrhosis. This tumor can present as a solitary lesion, multiple nodules, or a diffuse infiltrative lesion. The overall prognosis is very poor.
- Metastatic disease from HCC is uncommon, but can spread to regional lymph nodes, the lungs, bones, and adrenal glands.
- If the patient has early-stage disease, surgical resection, liver transplantation, and radiofrequency ablation (RFA) are potentially curative options.
- A large percentage of patients present with intermediate-or late-stage disease. For these patients, transarterial embolization (TAE) and chemoembolization (TACE) are palliative treatment options. TACE has been shown to improve 5-year survival to above 50%.

- Systemic chemotherapy has not yielded significant improvements in survival. However, early studies on antiangiogenesis agents (such as sorafenib) have provided promising results.

## Radiologic

- Sonography is often used for screening for HCC. However, contrast-enhanced MRI and CT are the primary imaging techniques for definitive imaging diagnosis. In fact, if the mass has the classic radiographic appearance in the setting of cirrhosis, a biopsy is generally not required for the diagnosis.
- On contrast-enhanced CT and MRI, HCC typically shows marked contrast-enhancement during the arterial phase, but appearing hypodense to normal liver parenchyma on portal venous phase and delayed imaging. It is important to note the location and extent of the mass, presence of portal or hepatic vein invasion, as well as the arterial and segmental distribution for embolization or surgical planning, respectively.
- Angiography is not a primary diagnostic imaging technique for HCC and instead is usually solely performed during endovascular therapy. The key angiographic findings for identifying the tumor include arterial tumor neovascularity (as manifested by irregular, corkscrew arteries), a tumor stain, and arterioportal shunting.
- The goal of embolization is to induce tumor necrosis by infusion of particles into hepatic artery branches feeding the tumor. This procedure takes advantage of the fact that HCC derives 90% to 95% of its blood supply from the hepatic arterial system, whereas normal hepatic parenchyma is supplied approximately only 30% by the hepatic arterial system and the remainder by the portal venous circulation. When highly concentrated local chemotherapy is concurrently infused with an embolic agent such as particles or oil, the impaired flow results in retention of chemotherapeutic agents for as long as several months, which reduces systemic side effects. Nonetheless, the degree of benefit over bland embolization is controversial.
- In order to be eligible for embolotherapy, patients must have a patent portal venous system. If embolization was performed in the setting of portal vein occlusion, acute hepatic failure could result from ischemia and necrosis of normal liver parenchyma due to loss of both arterial and portal venous blood supply.
- Approximately half of patients who undergo embolization will experience postembolization syndrome, which is characterized by abdominal pain, fever, nausea, and vomiting.
- In addition to HCC, embolic therapy has also been used to treat hypervascular hepatic metastases.
- Localized radiotherapy using embolotherapy with radioactive Yttrium-90

microspheres has also been used for palliation in both HCC and metastatic disease to the liver.

- Thermal ablation of HCC has become increasingly popular over the past few decades as a potentially curable treatment option for small tumors. Ablative techniques include RFA, cryoablation, laser, and microwave ablation. For all techniques, one or more metallic probes are inserted into the lesion using CT or sonographic guidance. The probes are then activated, inducing tissue destruction via coagulative necrosis (in the case of RFA, laser, and microwave ablation) or cellular lysis (cryoablation).
- RFA is currently the most popular thermal ablative therapy for the treatment of liver tumors. Because large blood vessels act as a heat sink, ablation of tumors adjacent to large vessels may result in incomplete ablation. Therefore, the relationship of the tumor with major blood vessels needs to be considered when choosing appropriate lesions. Evidence suggests that microwave ablation is less prone to the effect of such heat sinks.
- Chemical ablation using direct injection of ethanol can be performed on small tumors. This therapy has similar survival rates as surgery. However, compared to this technique, RFA provides more complete ablation and requires fewer treatment sessions.

## SUGGESTED READING


Baum S, Pentecost MJ. Abrams' Angiography: Interventional Radiology (2nd ed). Philadelphia, PA: Lippincott Williams & Wilkins, 2006.

El-Serag HB, Jorge A, Marrero JA, et al. Diagnosis and treatment of hepatocellular carcinoma. Gastroenterology 2008;134:1752–1763.

Kamel IR, Lawler LP, Fishman EK. Comprehensive analysis of hypervascular liver lesions using 16-MDCT and advanced image processing. AJR Am J Roentgenol 2004;183:443–452.

Liap E, Geschwind JH. Transcatheter and ablative therapeutic approaches for solid malignancies. J Clin Oncol 2007;25:978–986.

Valji K. Vascular and Interventional Radiology. Philadelphia, PA: Saunders Elsevier, 2006.

# Chapter EIGHT

# Pediatric Radiology

**DONALD P. FRUSH** ▪ CHAPTER EDITOR

Caroline L. Hollingsworth

Sara M. O'Hara

Caroline Carrico

Charles Maxfield

George S. Bisset III

Ana M. Gaca

# CASE 1

**DONALD P. FRUSH**

**HISTORY**

An 8-year-old boy with pleuritic chest pain and 39°C temperature.

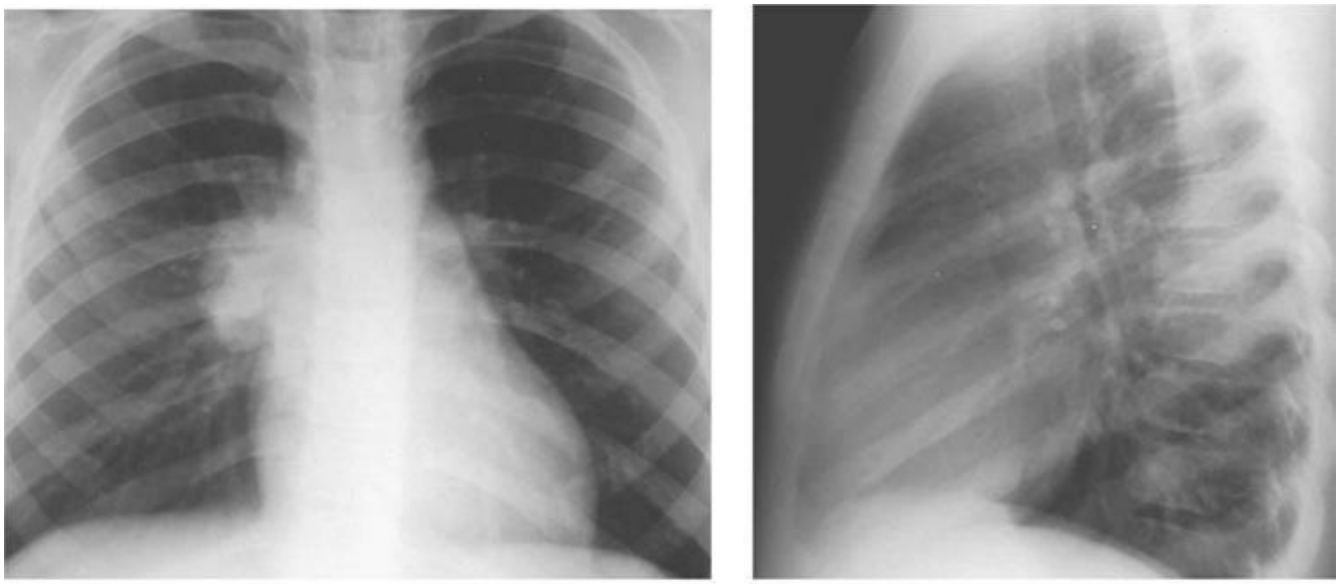


**FIGURES 8-1A and 8-1B** Frontal **(A)** and lateral **(B)** chest radiographs. A well-defined mass is present in the right lung. Notably, the right hilum is not obscured (i.e., the hilar overly sign is present) and thus the mass is not hilar in location. This mass is posterior on the lateral view, projected over the upper mid-thoracic spine and is in the superior segment of the right lower lobe.

## DIFFERENTIAL DIAGNOSIS

**Hilar adenopathy:** This diagnosis is incorrect because the right hilum is seen as separate from the "mass." Therefore, the mass must be anterior or posterior in the right hemithorax.

**Plasma cell granuloma (postinflammatory or inflammatory pseudotumor; (fibrous) histiocytoma, myo-fibroblastic tumor, xanthogranuloma):** Plasma cell granuloma can present as a mass, with calcification in up to 25% of cases. Children are usually asymptomatic or have minimal symptoms. This diagnosis is possible in the case presented and cannot be excluded on the basis of the radiographs, but it is a relatively rare entity and so would be a lesser consideration than a more common entity that is compatible with the imaging findings.

**Bronchopulmonary foregut malformation:** Such malformations—for example, parenchymal bronchogenic cyst or a pulmonary sequestration—are reasonable considerations on the basis of the findings shown. Cystic adenomatoid malformation is another malformation to be considered, but unlike in infants and young children, it rarely presents in older children or adults with air or air-fluid-filled cysts.

**Primary pulmonary malignancy:** Although sarcomas and pulmonary (or pleuropulmonary) blastomas are the most likely primary tumors to produce these findings, these lesions are exceedingly rare and the diagnosis is unlikely.

- **Metastasis:** This diagnosis is an unlikely one because there is no history of malignancy. Furthermore, a single, large metastasis would be unusual.
- **Round pneumonia:** Round pneumonia is a very common cause of a pulmonary mass in children. This entity is much more common than a bronchopulmonary fore-gut malformation. Round pneumonia would be readily distinguishable from a cystic congenital lung abnormality based on central low density. However, it would be indistinguishable by imaging features alone from a solid congenital lung abnormality. Nonetheless, on the basis of probability alone, round pneumonia is much more likely than a solid congenital lung abnormality.
- **Contusion:** This diagnosis is not a reasonable consideration because there is no history of trauma.
- **Round atelectasis:** Round atelectasis is a consideration based on the round shape of the opacity but is usually basilar in location, whereas the lesion shown in this case is in the superior segment of the right lower lobe. Furthermore, round atelectasis is very rare in children, making this diagnosis unlikely.
- **Pleural effusion caused by "pseudotumor":** This entity is unlikely because it is usually sharply defined along at least one border in at least one projection, whereas the mass in the case shown here does not have sharp margins, making this diagnosis unlikely.
- **Hamartoma:** This diagnosis is a reasonable consideration based on imaging findings alone but is usually asymptomatic and is relatively rare.

## DIAGNOSIS

**Round pneumonia in the superior segment of the right lower lobe**

## KEY FACTS

### Clinical

- Almost all pulmonary masses in children are inflammatory and primarily due to infection.
- Round pneumonia is a common cause of a pulmonary mass in children.
- The mean patient age is 5 years. Round pneumonia is rare over the age of 8.
- The male:female gender ratio is 1:1.
- *Streptococcus pneumoniae* (pneumococcus) is the most common organism responsible for round pneumonia.
- Symptoms can be mild or nonspecific early in the clinical course.

- With a clinical history typical of pneumonia and recognition of a mass on imaging studies as round pneumonia, antibiotic treatment can be started without further imaging.
- In cases in which the clinical information is unclear, a pulmonary mass can be followed with radiography after therapy (6 to 8 weeks), unless symptoms persist or worsen.

### Radiologic

- Round pneumonia is typically a well-defined, solitary (98% of cases), mass-like opacity.
- 85% are posterior; 65% of all round pneumonias are in the lower lobe.
- Two-thirds of the masses have sharply defined borders; one-third poorly defined borders. Mean age of the latter group is about 1 year older than in the former group.
- Of those cases that are followed clinically and by imaging, 95% slowly resolve and 5% develop lobar pneumonia.
- Air bronchograms are initially present in a minority of cases.
- Calcification is not a feature of this entity.
- Unlike pneumonia in adults, pneumonia is often initially confined due to immature collateral pathways, which explains the round shape.
- Adenopathy and pleural effusion are rarely seen with round pneumonia.

## SUGGESTED READING

Condon VR. Pneumonia in children. J Thorac Imaging 1991;6:31–44.

Kim Y-W, Donnelly LF. Round pneumonia. Imaging findings in a large series of children. Pediatr Radiol 2007;37:1235–1240.

Yikilmaz A, Lee EY. CT imaging of non-vascular mass-like lesions in children. Pediatr Radiol 2007;37:1253–1263.

# CASE 2

**GEORGE S. BISSET**

### HISTORY

A 14-month-old boy with a palpable abdominal mass.

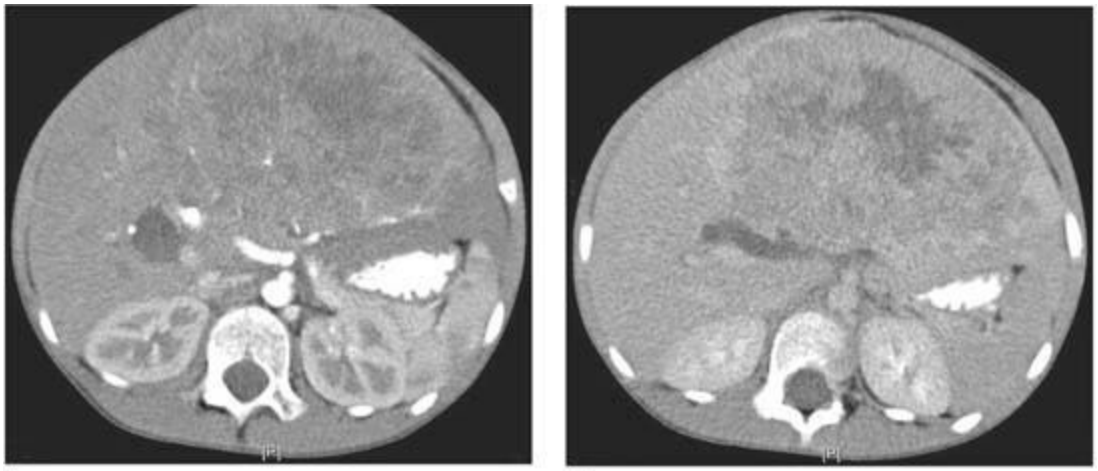



**FIGURE 8-2A, 8-2B, and 8-2C** CT of the abdomen during arterial and portal venous phases. A heterogeneously enhancing mass is seen within the left lobe of the liver. The mass displaces the pancreas and IVC posteriorly and displaces the bowel toward the left.

## DIFFERENTIAL DIAGNOSIS

**Hepatocellular carcinoma:** This diagnosis is unlikely because this neoplasm rarely occurs below the age of 2. Furthermore, frequently, there is usually a history of chronic liver disease.

**Hepatoblastoma:** This is the most common malignant primary liver tumor of

childhood, usually occurring before the age of 3. The young age of the patient and heterogeneous appearance of the mass in the present case are consistent with this diagnosis.

- **Mesenchymal hamartoma:** This diagnosis is unlikely because it is rare, cystic, and often exophytic, unlike the case illustrated. The diagnosis can be made by prenatal sonography or fetal MR imaging.
- **Hemangioendothelioma:** This entity is the most common symptomatic vascular lesion in infancy and most common mesenchymal tumor of childhood. This diagnosis is unlikely in the case illustrated because this benign tumor contains large feeding vessels, which enhance early and areas of variable enhancement. The celiac trunk and hepatic arteries may be enlarged, with tapering of the aorta below the origin of the celiac trunk when this is a high-flow lesion. An infiltrative hemangioendothelioma will demonstrate diffuse nodular enhancement of mulitple masses.
- **Hepatic adenoma:** These tumors are extremely rare in young children. Furthermore, the lesion may contains regions of fatty change or hemorrhage. This finding is not seen in the case illustrated, further making this diagnosis an unlikely one.

## DIAGNOSIS

**Hepatoblastoma**

## KEY FACTS

### Clinical

- Hepatoblastoma is probably an infantile form of hepa-tocellular carcinoma.
- This tumor primarily occurs before the age of 3 (median age: 1 year).
- A male-to-female predominance between 2:1 and 3:1 has been reported.
- The tumor is associated with Beckwith-Wiedemann syndrome (i.e., prematurity, hemihypertrophy and biliary atresia).
- Nearly all patients with this tumor have elevated serum levels of alpha-fetoprotein.
- Prognosis is usually good if there are no metastases and the tumor is limited to the liver and is completely resectable.

### Radiologic

- Hepatoblastoma usually presents as a single mass. However, multifocal involvement can sometimes occur.
- On contrast-enhanced CT examination or MR imaging, the mass usually demonstrates

heterogeneous enhancement.

- Periportal areas of low attenuation, as seen in this case, or signal abnormality are likely related to tumor invasion of periportal lymphatics. Tumoral calcification occurs in approximately 40%.
- Splaying of hepatic veins around the mass can be seen occasionally.
- The sonographic appearance is that of a hypoechoic mass with displacement of the hepatic arterial and portal venous vessels by the tumor.

## SUGGESTED READING


Boechat MI, Kangarloo H, Ortega J, et al. Primary liver tumors in children: comparison of CT and MR imaging. Radiology 1988;169:727–732.

Finegold MJ, Egler RA, et al. Liver tumors: pediatric population. Liver Transpl 2008;14:1545–1556.

Finn JP, Hall-Craggs MA, Dicks-Mireaux C, et al. Primary malignant liver tumors in childhood: assessment of resectability with high field MR and comparison with CT. Pediatr Radiol 1990;21:34–38.

Jabra AA, Fishman EK, Taylor GA. Hepatic masses in infants and children. CT evaluation. AJR Am J Roentgenol 1992;158: 143–149.

Pobiel RS, Bisset GB. Pictorial essay: imaging of liver tumors in the infant and child. Pediatr Radiol 1995;25:495–506.

Siegel MJ. Pediatric liver imaging. Semin Liv Dis 2001;21:251–269.


# CASE 3


**DONALD P. FRUSH AND SARA M. O'HARA**


### HISTORY

A toddler with urinary retention, constipation, and distended abdomen.

A

■**FIGURE 8-3A** Lateral spot film from voiding cystoure-throgram. The bladder neck is elongated, and the entire bladder is displaced upward and anteriorly out of the pelvis.

B

■**FIGURE 8-3B** Lateral spot film from barium enema examination. The rectosigmoid is compressed and displaced anteriorly. No bowel gas or stool is visible in the presacral space.

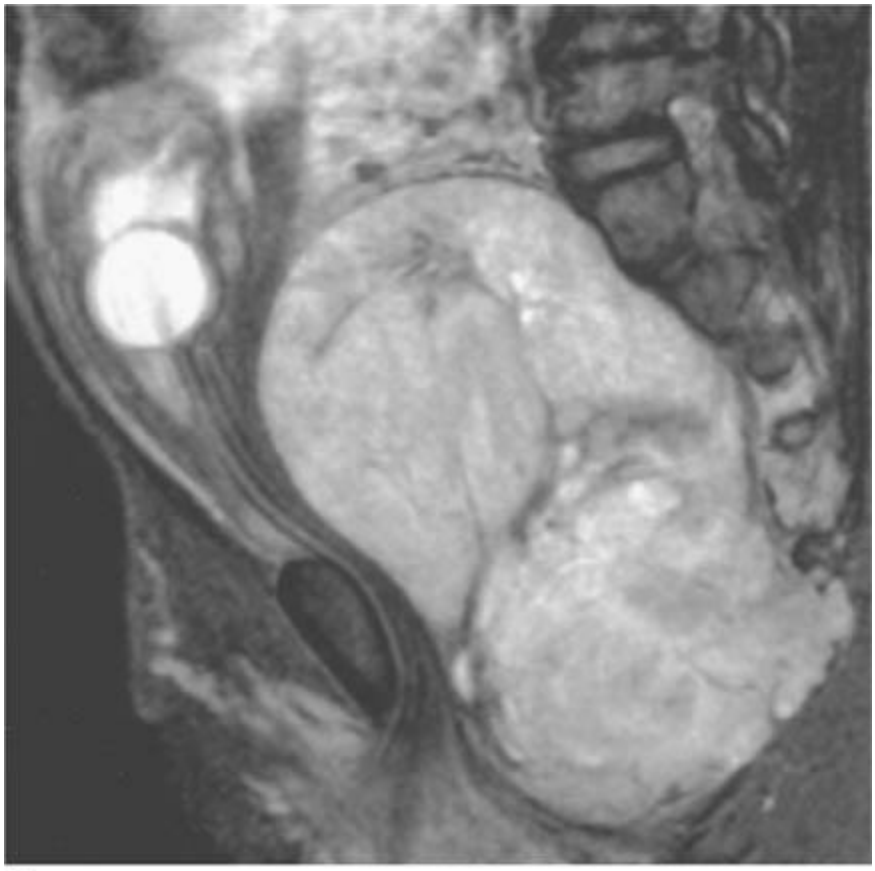

C

■**FIGURE 8-3C** Sagittal T2-weighted fast spin echo MRI with fat saturation. A mixed-signal intensity mass is present in the presacral region, extending between the sacral segments and into the posterior musculature. The Foley catheter within the bladder is displaced anteriorly and superiorly.

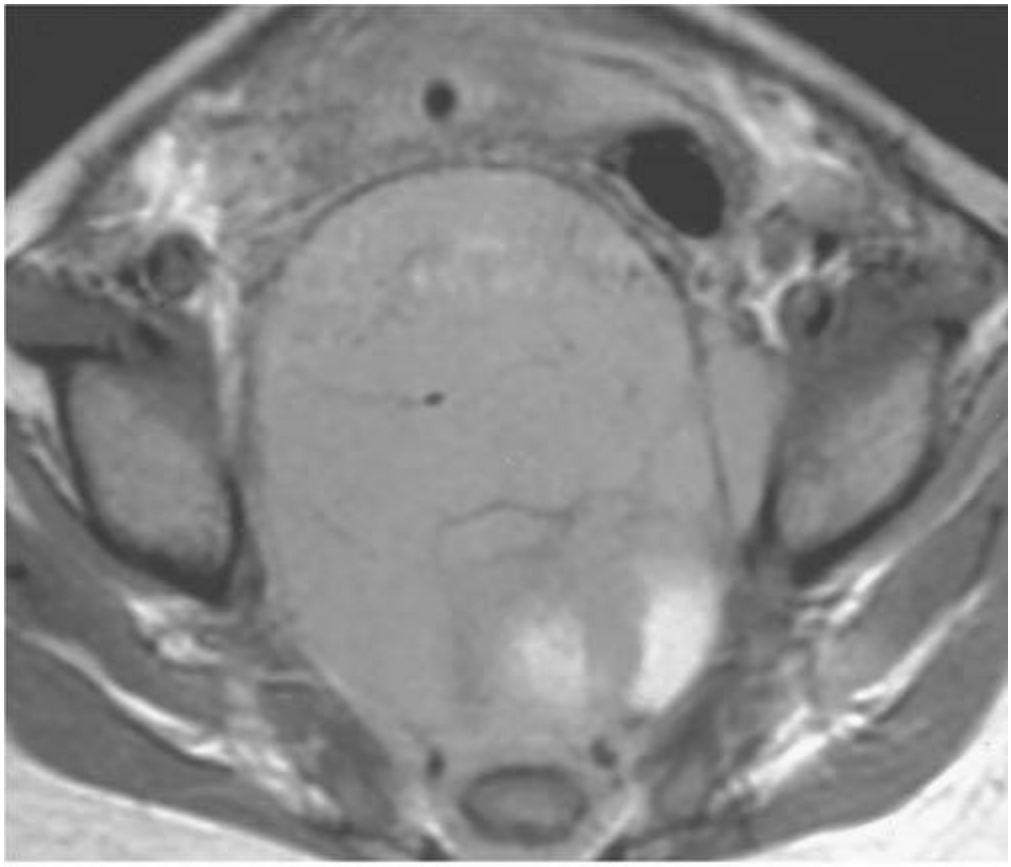

D

**FIGURE 8-3D** Axial unenhanced T1-weighted MRI. A predominantly intermediate-signal intensity soft tissue mass is seen encasing the lower sacrum and displacing the rectum anteriorly and to the left.

## DIFFERENTIAL DIAGNOSIS

**Ovarian teratoma:** Any tumorous growth from the ovary could grow to the size shown in this case. However, extension around the sacrum is not a feature seen in ovarian tumor, making this an unlikely diagnosis.

**Abscess:** This entity cannot be excluded on the basis of imaging findings alone. However, it is an unlikely diagnosis because the clinical history does not suggest the presence of infectious process.

**Neuroblastoma (or other ganglion tumor such as ganglioneuroma):** The location and appearance of the mass are consistent with this diagnosis. However, posterior encasement and direct sacral involvement are not findings that would be expected in pelvic neuroblastoma.

**Sacrococcygeal germ cell tumor (i.e., teratoma):** Ter-atoma is the best diagnosis, based on the presacral and retrorectal location and, in particular, the encasement of sacral segments.

- **Anterior meningocele:** This diagnosis is unlikely because the mass is not cystic.
- **Rhabdomyosarcoma:** Because posterior sacral extension would be unusual for rhabdomyosarcoma, this is an unlikely diagnosis.
- **Primary bone tumor:** A primary bone tumor is not a likely consideration because there is no bony destruction and sacral involvement in this case is relatively minimal. Primary sacral bone tumors are extremely rare at this age.
- **Gastrointestinal duplication:** This diagnosis is unlikely because rectal duplications are very rare and extension to sacrum would not be expected.

## DIAGNOSIS

**Malignant sacrococcygeal germ cell tumor (teratoma)**

## KEY FACTS

### Clinical

- Sacrococcygeal teratomas are relatively rare, with an estimated prevalence of 1 in 35,000 to 40,000 births.
- Sacrococcygeal teratoma is the most common solid tumor in neonates.
- Eighty percent are diagnosed before 6 months of age.
- Seventy-five percent are in females; the gender ratio for malignant lesions is equal, however.
- The category of germ cell tumors includes teratomas, choriocarcinomas, embryonal cell carcinomas, yolk sac tumors, and mixed types.
- Teratomas are the most common sacrococcygeal tumors in children.
- Teratomas are classified as mature, immature, or malignant. Malignancy is rare in mature types. Overall 60% of teratomes are benign.
- Treatment consists of chemotherapy and surgical resection.
- Early diagnosis and surgical excision is indicated because the incidence of malignant transformation increases with advancing age.
- Four types of sacral teratomas have been described, according to the internal and external components of the mass:
- Type 1: primarily external to the pelvis (50% are Type 1)
- Type 2: predominantly external to the pelvis with intra-pelvic component
- Type 3: primarily intrapelvic with only a small extra-pelvic portion
- Type 4: entirely presacral without extrapelvic extension

- In general, the greater the intrapelvic component, the greater the likelihood of malignancy.

### Radiologic

- Calcification is visible by CT in 50% to 60% of sacrococcygeal teratomas and is more frequent in benign lesions. Amorphous, chunky, punctate, and spiculated calcifications have all been described.
- Cystic and fatty components can also be seen within the mass.
- Primarily solid lesions are more likely to be malignant, and those containing fat and calcification with cystic regions are more likely benign; however, exceptions exist.
- Direct invasion of adjacent structures suggests malignant transformation.
- Elevated serum alpha-fetoprotein levels are often present and are frequently followed in conjunction with imaging findings as a measure of tumor response.

Presacral masses (usually anterior meningocele or germ cell tumor) can coexist with two other entities: anorectal malformations and sacral anomalies, a constellation that is referred to as *Currarino's triad,* or the ASP (anorectal malformation, sacral anomalies and presacral mass) triad or ASP complex (anorectal malformation, sacrococcygeal osseous defect, and presacral mass).

## SUGGESTED READING

Kocaoglu M, Frush DP. Pediatric presacral masses. Radiographics 2006;26:833–857.

Siegel MJ. Pelvic tumors in childhood. Radiol Clin North Am 1997;35: 1455–1475.

# CASE 4

**DONALD P. FRUSH**

### HISTORY

A 5-year-old boy with several months of increasing right knee pain and limping.


■**FIGURES 8-4A and 8-4B** Frontal **(A)** and lateral **(B)** radiographs of the right tibia and fibula. An ill-defined metaphy-seal lesion is present that demonstrates mixed sclerosis and lucency at the anterior aspect of the tibia.

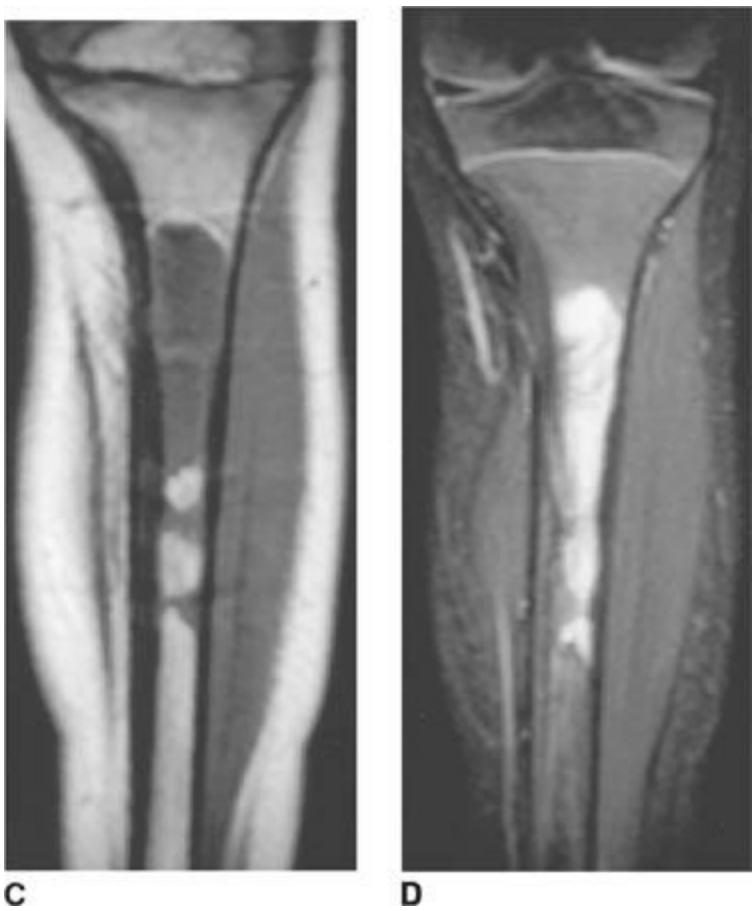


**FIGURES 8-4 C and 8-4D** Unenhanced coronal T1-weighted **(C)** and T2-weighted **(D)** images of the right tibia. Abnormal low T1, high T2 marrow signal is present in the tibial metaphysis, extending into the diaphysis, with destruction of the cortex. Extraosseous tumor and edema are demonstrated on the T2-weighted image.

## DIFFERENTIAL DIAGNOSIS

**The major considerations** in this differential are the small, round, blue cell tumors of childhood. All may present with a permeative pattern and a wide zone of transition.

**Ewing sarcoma of bone (or Ewing sarcoma family, including primitive neuroectodermal tumor or PNET, Askin's tumor, and extraosseous Ewing's sarcoma):** A likely consideration based on the history and radiographic findings.

**Metastases:** Considerations are especially those due to neuroblastoma and rhabdomyosarcoma. With rhabdo-myosarcoma, presenting symptoms are usually due to the primary mass rather than metastatic disease. The imaging findings in this case could be due to neuroblastoma metastasis.

**Leukemia or lymphoma:** This is also a reasonable consideration because the lymphoproliferative malignancies are the most common childhood cancer. Bone abnormalities in leukemia are fairly common (osteoporosis, metaphyseal lucencies,

periosteal reaction, sclerotic or lucent lesions, permeative pattern); the involvement is most often multifocal and symmetrical, however, making the appearance in this case unusual. Lymphoma may have an identical appearance. However, primary lymphoma of bone is much less likely than Ewing's sarcoma.

Considerations other than the small, round, blue cell tumors include:

- **Osteomyelitis:** It may be impossible to differentiate osteomyelitis from Ewing's sarcoma clinically and radiographically.
- **Eosinophilic granuloma:** This entity has a large variety of appearances (classically a lucent defect) that include an aggressive appearance such as this one.

## DIAGNOSIS

**Ewing sarcoma**

## KEY FACTS

### Clinical

- Although originally described as separate entities, Ewing's sarcoma, primitive neuroectodermal tumors (PNET), Askin's tumors, adult neuroblastoma, and soft tissue Ewing's sarcoma are all part of a spectrum of neoplastic diseases called the Ewing's sarcoma family of tumors (EFT).
- Classic Ewing's sarcoma occurs most commonly in the second half of the first decade of life and the first half of the second decade, a slightly younger age distribution than that of osteosarcoma.
- Ewing sarcoma affects males slightly more commonly than females (3:2), and is uncommon in Asians and African Americans.
- Pain, swelling, or both at the site of the primary tumor are the most common presenting symptoms in Ewing sarcoma. However, the presentation may be similar to that of osteomyelitis, with systemic symptoms of fever, elevated sedimentation rate and leukocytosis.
- Metastatic spread of Ewing sarcoma occurs equally to the lungs and distant bones, and is found in approximately 25% of cases at the time of diagnosis. Subclinical metastasis is thought to be present in the majority of patients because of the high rate of relapse in patients treated only with local management.
- Poor prognostic indicators include large size (> 8 cm), central location, unresectability older age, and elevated erythrocyte sedimentation rate as well as leukocyte count at the time of presentation.

### Radiologic

- Ewing sarcoma can develop in almost any bone in the body, and equally affects both long and flat bones.
- Lesions usually occur in the midshaft of a long bone, rather than the ends as with osteosarcoma.
- Plain films underestimate the extent of bone involvement. The most typical pattern is a permeative, lytic pattern with associated periosteal reaction. However, other patterns include larger, "moth-eaten" lytic foci, a mixed lytic and sclerotic pattern, bony expansion, and a predominantly sclerotic pattern.
- Ewing's sarcoma of flat bones typically has a large soft tissue component relative to the osseous component, in contrast to Ewing's sarcoma of long bones.
- MR imaging is the imaging modality of choice to determine tumor size, intra- and extraosseous extension, involvement of adjacent organs and neurovascular structures. Intravenous contrast material can be used to distinguish tumor from peritumoral edema.
- MR imaging of the entire bone at the primary site of involvement is important as skip metastases occur with Ewing's sarcoma as well as osteosarcoma.
- The assessment for metastatic disease should include a chest CT to search for pulmonary metastatic disease and a bone scan for distant bony metastases.

## SUGGESTED READING

Bielack SS, Carrle D. State-of-the-art approach in selective curable tumors: bone sarcoma. Ann Oncol 2008;19: vii155–vii160.

Grier HE. The Ewing family of tumors: Ewing's sarcoma and primitive neuroectodermal tumors. Pediatr Clin N Am 1997;44(4):991–1004.

Meyer JS, Mackenzie W. Malignant bone tumors and limb-salvage surgery in children. Pediatr Radiol 2004;34:606–613.

# CASE 5

**CHARLES MAXFIELD**

### HISTORY

A 6-year-old girl with acute stridor, high fever, and respiratory distress.

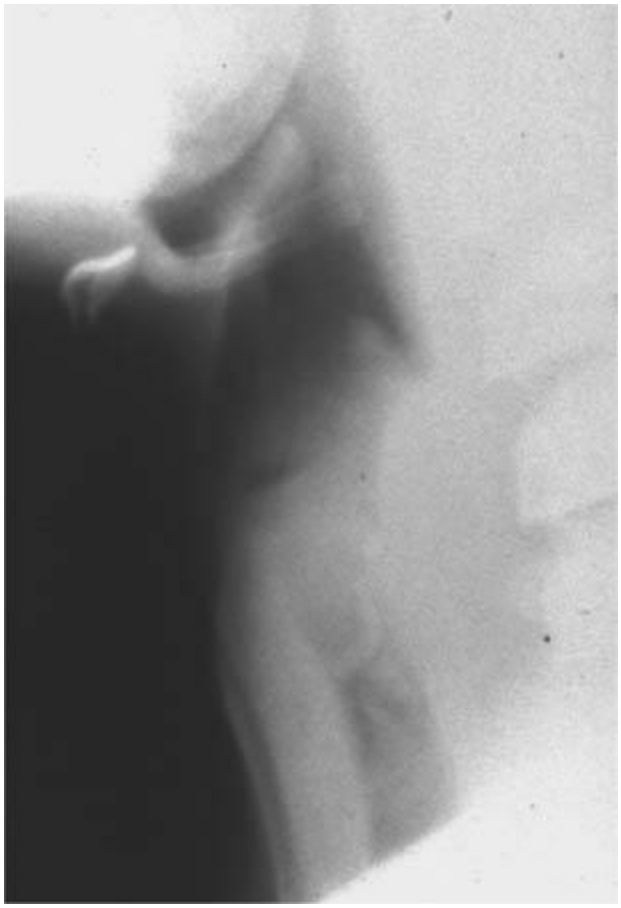

**FIGURE 8-5** A lateral airway radiograph shows subtle heterogeneous haziness (i.e., so-called clouding) in the cervical segment of the trachea, along with a curvilinear density in the subglottic trachea which represents an exudative plaque.

## DIFFERENTIAL DIAGNOSIS

- **Tracheal foreign body:** This diagnosis is a possible consideration but there is no history of aspiration of a foreign body. Furthermore, high fever would not be expected, and the age of patients with aspirated foreign bodies is usually much younger than the patient shown here. This diagnosis is unlikely.
- **Papilloma:** Papillomas usually have the clinical presentation of chronic hoarseness, rather than the acute stridor and fever found in the patient presented here. Furthermore, the opacities in the radiographs shown in this case are not mass-like, as would be expected with a papilloma. This diagnosis is an unlikely one.
- **Tracheal mucus:** Mucus within the trachea can produce intraluminal opacities on radiographs. However, the presence of tracheal mucus would not explain the toxic appearance of the patient or the tracheal narrowing and clouding in the case shown here.
- **Epiglottitis:** The history presented in this case is very suggestive of epiglottitis but the epiglottis in the radiographs is normal in appearance, making this diagnosis unlikely.

- **Laryngotracheobronchitis:** This entity, also known as croup, usually occurs in children between the ages of 6 months and 3 years, i.e., at an age that is much younger than the child presented here. Furthermore, narrowing of the subglottic trachea (the so-called steeple sign) typical of croup is not present. This diagnosis is incorrect.
- **Granuloma:** This entity is typically seen following unlikely previous tracheal intubation or other source of trauma to the trachea. No such history is given in the case shown here, making this diagnosis unlikely.
- **Bacterial tracheitis:** This entity is also known as membranous croup or membranous laryngotracheobronchi-tis. Children with this diagnosis typically have an acute, toxic presentation, such as in the case shown here. Furthermore, on radiographs, bacterial tracheitis typically is seen as subglottic tracheal narrowing in association with intraluminal plaque-like opacities, as in the images shown here. This diagnosis is correct.
- **Retropharyngeal abscess:** The retropharyngeal soft tissues are normal in the images shown here, thereby excluding the diagnosis of a retropharyngeal abscess as a cause of the stridor.

## DIAGNOSIS

**Bacterial tracheitis**

## KEY FACTS

### Clinical

- Tracheitis is a rare entity compared to other causes of respiratory difficulty in children, such as croup and ret-ropharyngeal abscess.
- Acute onset of stridor is the typical clinical presentation of bacterial tracheitis.
- The mean age at presentation is 4 years old, but bacterial tracheitis can be seen at any age.
- Prompt recognition is important because membranes can develop relatively quickly and acutely obstruct the airway.
- Infection is bacterial in origin. *Staphyloccus aureus* is the most common agent, but occasionally *Streptococcus pneumoniae* and *Haemophilus influenza* can produce the infection. However, tracheitis can also occur as a superinfection following a viral upper airway process.
- If clinical or radiographic findings suggest tracheitis, flexible endoscopy is indicated to confirm the diagnosis.

- Management primarily includes supportive care (e.g., humidification, antibiotics, and suctioning), but "elective" intubation may be necessary to protect the airway from obstruction.

## Radiologic

- Lateral airway radiographs often show an indistinct appearance (i.e., so-called clouding) of the trachea, intraluminal tracheal opacities, and tracheal wall irregularity.
- Occasionally, associated subglottic narrowing can be present.
- The epiglottis and retropharyngeal tissues are normal in tracheitis, distinguishing this entity from other infectious causes of acute stridor in children.
- Half of cases have associated pneumonia.
- A normal radiograph does not exclude the diagnosis of tracheitis.
- The major alternative diagnosis based on radiographic findings is tracheal mucus accumulation. The two entities can be indistinguishable on the lateral airway radiograph. Because early treatment of tracheitis is important, this diagnosis should be favored in equivocal cases and treatment should begin.

## SUGGESTED READING

Gallagher P, Myer CM. An approach to the diagnosis and treatment of membranous laryngotracheobronchitis in infants and children. Pediatr Emerg Care 1991;7:337–342.

Hopkins A, Lahiri T, Salerno R, Heath B. Changing epidemiology of life-threatening upper airway infections: the reemergence of bacterial tracheitis. Pediatrics 2006;118:1418–1421.

John SD, Swischuk LE. Stridor and upper airway obstruction in infants and children. Radiographics 1991;12:625–643.

Loftis L. Acute infectious upper airway obstruction in children. Semin Pediatr Infect Dis 2006;17:5–10.

Seigler R. Bacterial tracheitis: recognition and treatment. J SC Med Assoc 1993;89:83–87.

# CASE 6

**CAROLINE L. HOLLINGSWORTH AND SARA M. O'HARA**

### HISTORY

A 5-week-old girl with persistent nonbilious vomiting but with no history of diarrhea or fever.

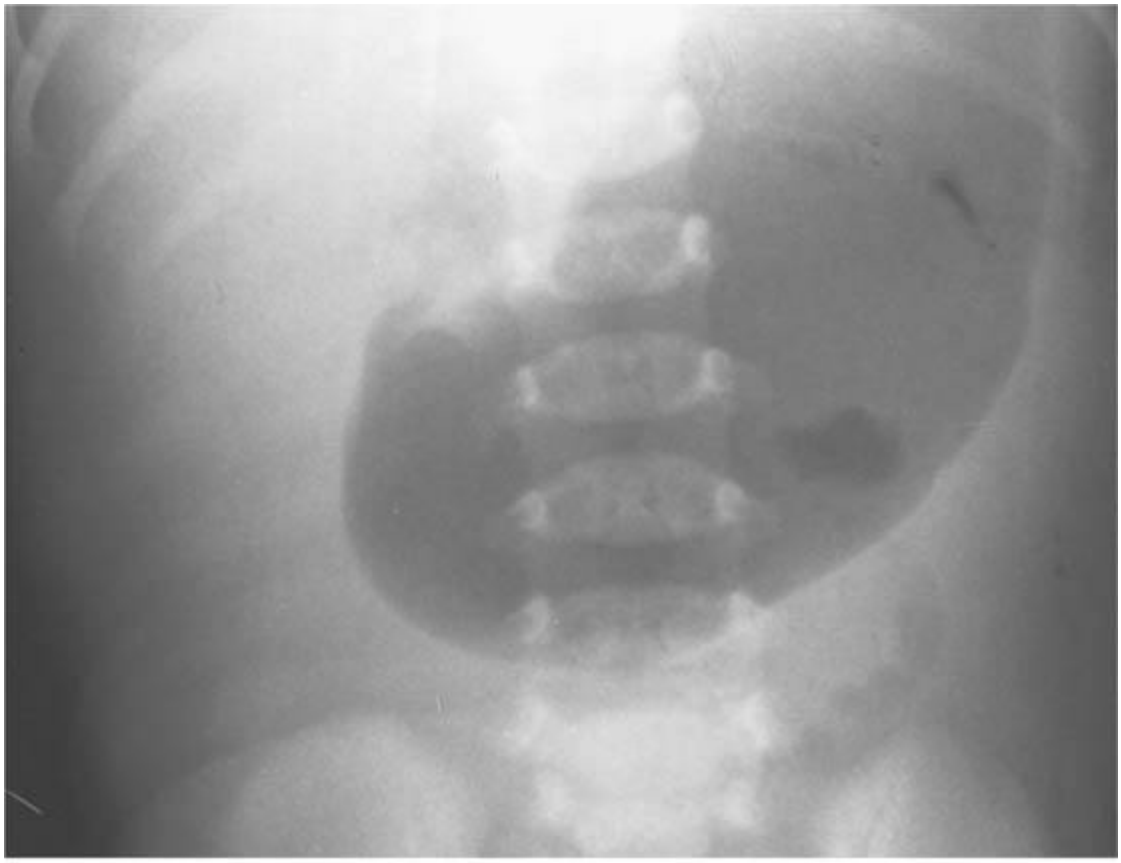

A

■**FIGURE 8-6A** Anteroposterior abdominal radiograph. The stomach is markedly distended. A large amount of gas is present in the stomach but only a minimal amount of gas is seen in the small bowel.

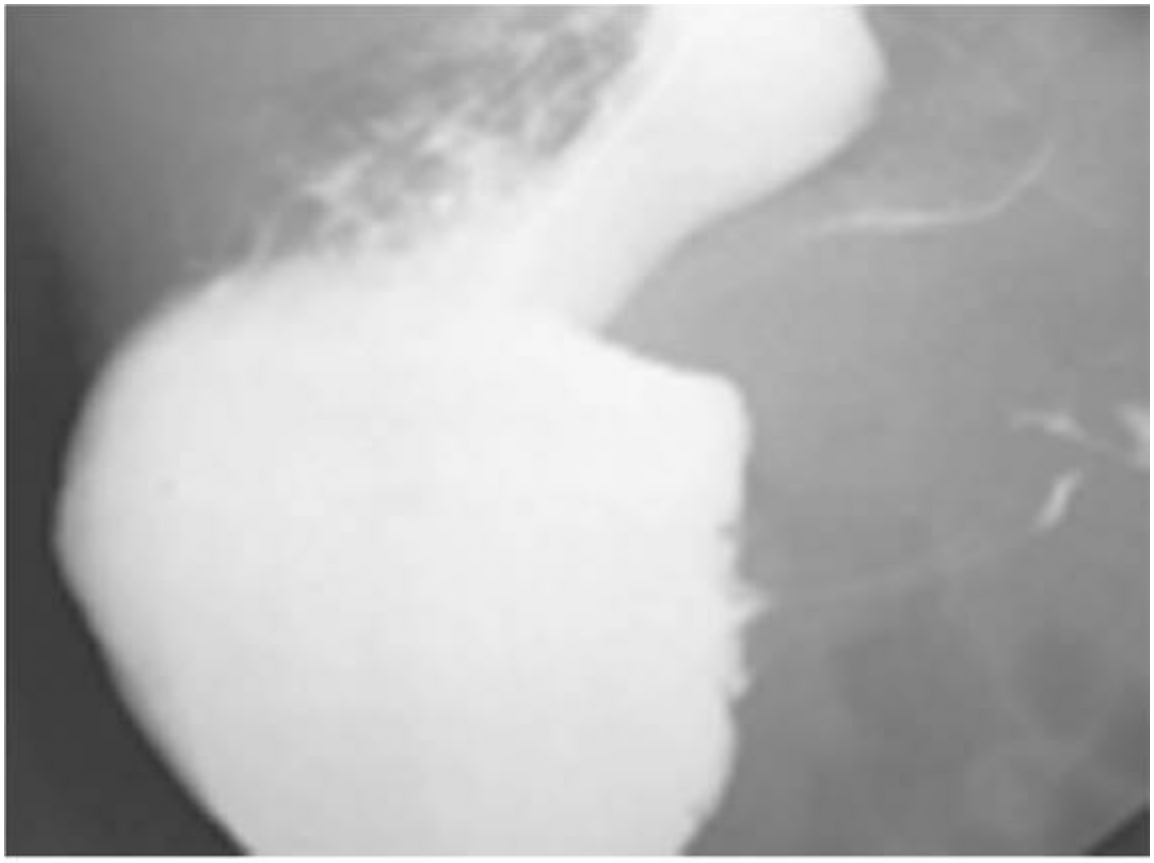

B

■**FIGURE 8-6B** Upper gastrointestinal series; lateral view of the stomach. A large pool of barium is present in the stomach. Thin lines of barium are visible in an elongated pylorus. Only a very small amount of barium is present in the duodenal bulb.

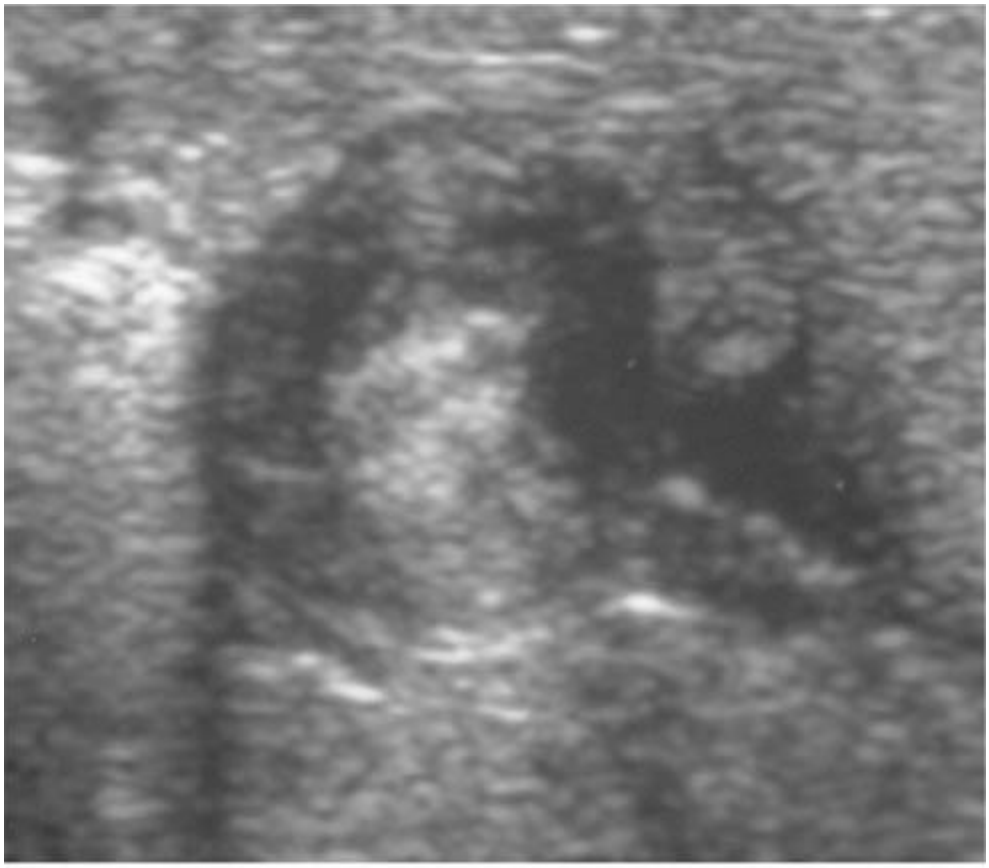

C

■**FIGURE 8-6C** Transverse sonographic view of the right upper quadrant. The hypoechoic muscularis is thickened and surrounds echogenic redundant mucosa.

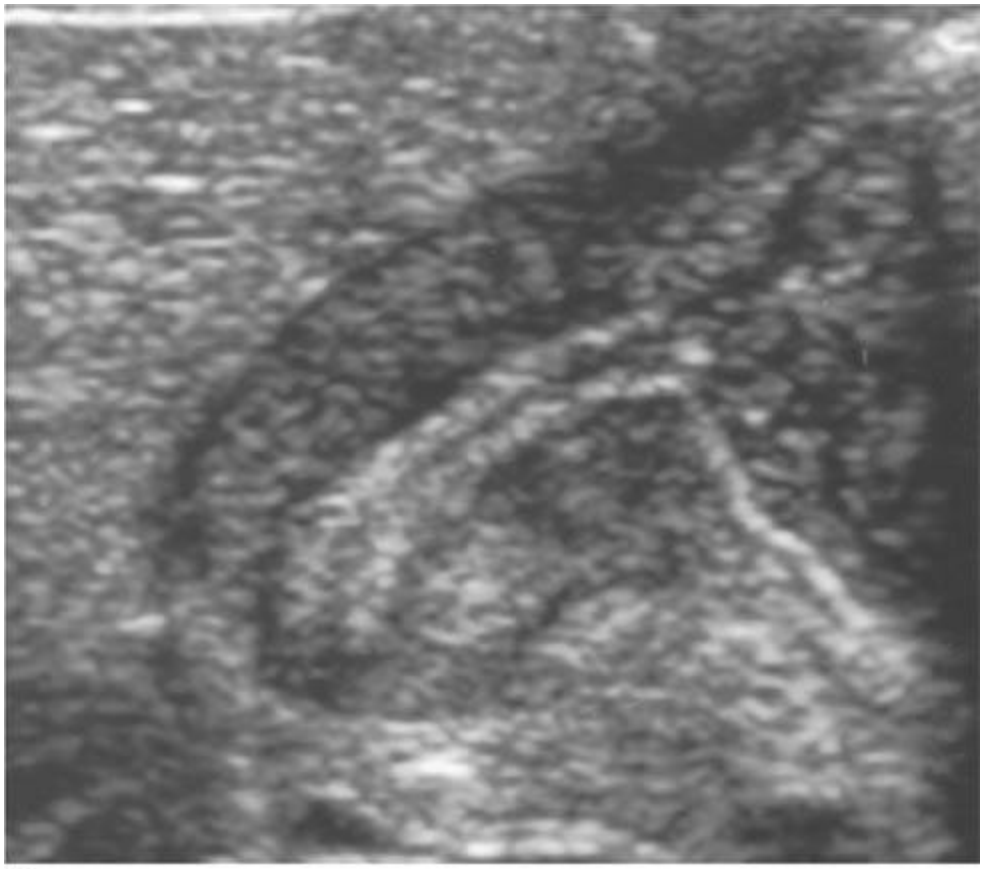

D

**FIGURE 8-6D** Longitudinal sonographic view of the right upper quadrant. The pyloric channel is elongated and has a thickened muscularis.

## DIFFERENTIAL DIAGNOSIS

**Gastroesophageal reflux:** The patient's history makes this diagnosis a possibility. However, no reflux of contrast material is seen at fluoroscopy in Figure 8-6B. Instead, a pyloric abnormality is visible on upper gastrointestinal series and sonography.

**Pylorospasm:** Pylorospasm can be seen in patients who are extremely agitated, dehydrated, or septic, unlike the patient discussed here. Furthermore, pylorospasm is unlikely to persist throughout the entire series of imaging examinations shown here but would, instead, be expected to be transitory. Thus, this diagnosis is an unlikely one based on the clinical history and imaging findings.

**Pyloric channel ulcer:** This entity could account for the delayed gastric emptying and vomiting. However, no ulcer is identified on the imaging studies shown; furthermore, this entity usually occurs at an older age.

**Antral web:** Antral web is another cause of delayed gastric emptying and vomiting. However, no evidence of an obstructing web is seen on the imaging studies, making this an incorrect diagnosis.

- **Hypertrophic pyloric stenosis (HPS):** The sonographic findings of concentric thickening of the pyloric muscu-laris and elongation of the pyloric channel, seen in the case shown here, are typical for this entity. The multiple thin tracks of barium visible in the pyloric channel on the UGI series represent folds of mucosa in a narrowed channel, further evidence of HPS. This entity is the best diagnosis based on the history and imaging findings.
- **Malrotation with obstruction:** In the first month of life the obstruction from malrotation is due to midgut volvulus. With malrotation later in infancy and childhood, peritoneal reflections (so-called Ladd bands) cross the duodenum and fix the malpositioned cecum, causing obstruction and vomiting. Thus, in malrotation the site of obstruction is the duodenum, not the pylorus (as in the case shown here). In addition, volvulus typically presents with bilious vomiting; nonbilious vomiting is rare. This diagnosis is incorrect.
- **Duodenal atresia:** Congenital bowel atresia (e.g., duodenal atresia and ileal atresia) clinically presents at a much younger age than that of the patient in the case illustrated. Duodenal atresia is evident at birth with a radiographic "double bubble" due to gas-distended stomach and proximal duodenum. Ileal atresia is also evident at birth with distension and vomiting, which is often bilious. This diagnosis is incorrect.

# DIAGNOSIS

**Hypertrophic pyloric stenosis**

# KEY FACTS

## Clinical

- The clinical presentation is that of nonbilious vomiting, which gradually progresses in severity over time from low-velocity regurgitation to projectile vomiting. Weight loss, dehydration, and hypochloremic acidosis can occur secondarily. Most patients appear healthy but hungry.
- HPS is characterized by thickening of the circular muscular layer of the pyloric canal, which results in narrowing of the pyloric channel.
- HPS is the most common condition necessitating abdominal surgery in the infant and most common cause of gastric outlet obstruction in the first few weeks of life.
- HPS typically presents in Caucasian boys between the ages of 3 weeks and 8 weeks.
- A palpable thickened pylorus (i.e., so-called olive) in the epigastrium is pathognomonic but is usually detectable only by a trained examiner. When this finding is present in the setting of suspected HPS, no preoperative imaging is necessary.

Nonetheless, in most centers a pyloric sonogram will be obtained.

- The treatment is pyloromyotomy. Although spontaneous regression of muscular hypertrophy can occur, nonoperative therapy is difficult to justify given the fact that surgery is quick, safe, and effective.

## Radiologic

- Plain film findings include (1) gastric distention, (2) mottled retained gastric contents, (3) indentations in the gastric wall by hyperperistaltic waves (i.e., so-called caterpillar stomach), and (4) diminished air beyond the pylorus.
- Barium study findings include (1) delayed gastric emptying, (2) "string sign" through the pyloric channel, (3) double- or triple-track sign in pyloric channel, (4) "shouldering" in the antrum from muscular hypertrophy, (5) a "beak" sign of oral contrast material at the pyloric entrance, and (6) indentation on the duodenal bulb by the hypertrophied muscularis.
- Sonographic findings include an elongated (i.e., $\geq$ 15 mm) pyloric channel and increased thickness (i.e., $\geq$ 3 mm) of the hypoechoic muscle, which are more sensitive findings for diagnosis of HPS than the cross-sectional diameter of the entire pylorus. A "target" or bull's eye appearance of the pyloric channel is seen on transverse sonographic images.
- Sonographic scanning at an angle tangential to the pylorus can cause a false-positive examination by producing "pseudothickening" of the muscularis. So-called pseudoelongation of the pyloric channel, another potential cause of false-positive examinations, can result from pylorospasm and use of prostaglandins.

## SUGGESTED READING

Hernanz-Schulman M, Zhu Y, Stein SM, et al. Hypertrophic pyloric stenosis in infants: US evaluation of vascularity of the pyloric canal. Radiology 2003;229:389–393.

Hernanz-Schulman M. Infantile hypertrophic pyloric stenosis. Radiology 2003;22:319–331.

Hernanz-Schulman M, Sells L, Ambrosino MM, et al. Hypertrophic pyloric stenosis in the infant without a palpable olive: accuracy of sonographic diagnosis. Radiology 1994;193:771–776.

Liao Z, Li ZS, Zhang WJ, et al. Education and imaging. Gastrointestinal: infantile hypertrophic pyloric stenosis. J Gastroenterol Hepatol 2007;22:1692.

# CASE 7

**CAROLINE CARRICO**

### HISTORY

A newborn infant with torticollis and a palpable neck mass.

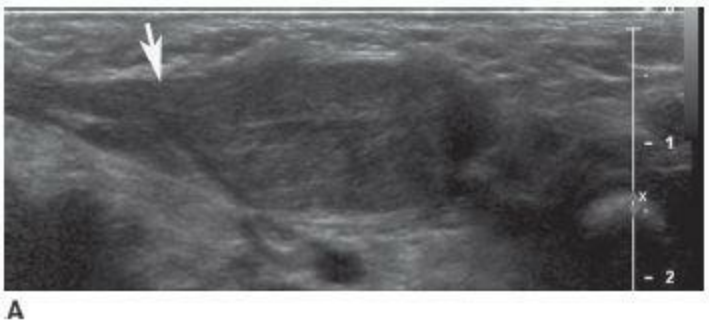


**FIGURE 8-7A** Longitudinal sonographic image of the neck shows a solitary mass that is slightly heterogeneous and nearly isoechoic with the sternocleidomastoid muscle. The muscle has a fusiform appearance *(arrow)* caused by expansion of the muscle due to the fact that the lesion is contained within it.

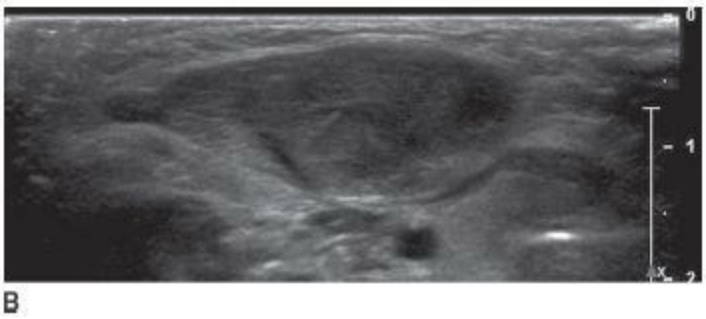


**FIGURE 8-7B** Transverse sonographic image confirms that the lesion is isoechoic with muscle and is completely contained within the sternocleidomastoid muscle.

## DIFFERENTIAL DIAGNOSIS

The differential diagnosis for an intramuscular mass in the sternocleidomastoid muscle in an infant with torticollis is very limited.

**Hemangiomas:** These are common benign tumors of infancy that are typically dermal or subcutaneous. The classic lesions proliferate in the first few months of life and progressively become uniformly solid with a few associated high-flow vessels. They usually slowly involute over ensuing months or years. The purely intramuscular location and the lack of prominent central and peripheral vessels in the case shown here makes this consideration unlikely.

**Infantile myofibromatosis:** Infantile myofibromatosis is a very rare abnormality that affects children during their first two years of life. The lesions may be solitary or multicentric and typically present as a slow growing mass of fibrous tissue. Nearly one-

third occur in the head and neck but they can also involve visceral organs (associated with a poorer prognosis). Although this diagnosis can not be absolutely excluded on the basis of the images shown in this case, the rarity of this entity makes it an unlikely diagnosis.

- **Sarcoma:** Three types of sarcoma could reasonably be considered in the case shown here.
- **Rhabdomyosarcoma:** Rhabdomyosarcoma can occur at any age and within any muscle. The margins of the lesion may be well-defined or poorly defined.
- **Infantile fibrosarcoma:** This is a childhood tumor that usually occurs in the legs, but can be found in any muscle. Both rhabdomyosarcoma and infantile fibrosarcoma could produce the imaging findings in the case shown here. However, they are both rare in the newborn period, making them unlikely diagnoses.
- **Granulocytic sarcoma (also known as myeloid sarcoma or chloroma):** Granulocytic sarcoma can occur in any location and may be solitary or multiple. This rare tumor occurs in infants and children with myeloprolif-erative disorders such as acute or chronic myelogenous leukemia (which would be expected to produce anemia and easy brusiability, absent in the case presented here).
- **Fibromatosis colli:** This entity, also known as sterno-cleidomastoid pseudotumor of infancy or congenital torticollis, is a benign mass of fibrous tissue that arises within the sternocleidomastoid muscle during the first month of life. Most newborns with torticollis have fibromatosis colli. At sonography, the mass has variable echotexture and causes well-marginated fusiform enlargement of the affected sternocleidomastoid muscle (as is present in the images in the case shown here). This diagnosis is correct.
- **Lipoblastoma or lipoblastomatosis:** As their names imply, these benign lesions contain fat as well as mysenchymal cells in a myxoid stroma. MR or CT imaging can confirm the presence of fat. Most lesions contain a large amount of fat, but some contain very little fat. The absence of fat makes this an unlikely consideration. Furthermore, lipoblastomastosis is more likely to extend to deeper tissues than in the case shown here.

## DIAGNOSIS

**Fibromatosis colli**

## KEY FACTS

### Clinical

- Fibromatosis colli is a nontender, benign mass within the sternocleidomastoid muscle

of a neonate. The mass consists of fibroblasts, myoblasts, mesenchyme-like cells, and myofibroblasts.

- Fibromatosis colli is a very common neck mass encountered in infancy; it is the most common noninflammatory mass.
- Most often the correct diagnosis is recognized clinically and no imaging is obtained.
- The exact cause of these lesions is not known. The affected infant usually has a history of difficult or traumatic birth, for example, requiring forceps for delivery. Some infants have a history of abnormal positioning of the head in utero.
- Twenty percent of affected neonates have torticollis with the head tilt and chin rotation toward the affected side. In the rare instance when lesions are bilateral, the neck appears short and the chin is tilted upward.
- Treatment is conservative. Physical therapy or no treatment may be used.
- Spontaneous resolution usually occurs by 8 months of age.
- It is uncommon for the abnormality to persist longer than a year or for facial asymmetry to develop. In these cases surgical intervention may be needed.

## Radiologic

- Sonography is often used to evaluate an infant with a nontraumatic palpable soft tissue abnormality in the neck.
- At sonography, the mass of fibrous tissue within the sternocleidomastoid muscle caused by fibromatosis colli has variable echotexture, but is relatively homogeneous, and may be well-defined. The enlarged muscle is fusiform.
- Imaging the sternocleidomastoid muscle in both the longitudinal axis and transverse axis is important to confirm that the lesion is completely intramuscular.
- Most cases are unilateral; thus, the uninvolved contralateral sternocleidomastoid muscle can be used for comparison.
- The affected portion of the sternocleidomastoid muscle may be hyperemic.
- If the diagnosis remains uncertain after sonography, MR imaging can show that the sternocleidomastoid muscle is enlarged and hyperintense or mildly hypoin-tense on T2-weighted images. However, in the case of fibromatosis colli, a focal mass may not be evident on MR imaging.
- CT imaging of fibromatosis colli typically shows an enlarged sternocleidomastoid muscle with normal CT density.
- Associated intramuscular hemorrhage or calcification has been occasionally described on CT and MR imaging.

## SUGGESTED READING

Kumar V, Prabhu BV, Chattopadhayay A, Nagendhar MY. Bilateral sternocleidomastoid tumor of infancy. Int J Pediatr Otorhinolaryngol 2003;67:673–675.

Keller MS. Musculoskeletal sonography in the neonate and infant. Pediatr Radiol 2005;35:1167–1173; quiz 1293.

Laor T. MR imaging of soft tissue tumors and tumor-like lesions. Pediatr Radiol 2004;34:24–37.

Robbin MR, Murphey MD, Temple HT, et al. Imaging of musculoskeletal fibromatosis. Radiographics 2001;21:585–600.

# CASE 8

**DONALD P. FRUSH**

## HISTORY

A neonate with persistent right upper-lobe opacity on radiography.


**FIGURE 8-8A** Contrast-enhanced axial CT image shows left upper lobe mass (S) supplied by a small systemic artery *(arrow)* arising from the left internal mammary artery.

B

**FIGURE 8-8B** Contrast-enhanced axial CT image at a more caudal level than shown in A depicts the distal course of the supplying artery *(arrowhead)*. The venous drainage *(arrow)* is via the brachiocephalic vein.

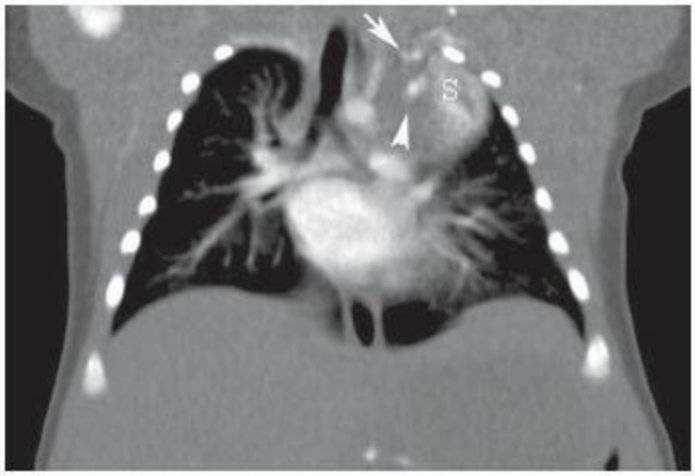


C

**FIGURE 8-8C** Coronal image reconstructed from axial CT images shows the mass (S) is vertically oriented. The arterial supply *(arrow)* and venous drainage *(arrowhead)* are also shown.

## DIFFERENTIAL DIAGNOSIS

**Atelectasis:** This diagnosis is a reasonable consideration given the presence of the lung opacity. However, the vessels on the CT examination are not typical of atelectasis. Furthermore, atelectasis would not be expected to persist unchanged on serial radiographs.

**Pulmonary sequestration:** This diagnosis is the likeliest consideration (even though a lower lobe location is more typical), given that the opacity persisted. Furthermore, the arterial supply and venous drainage are characteristic of this entity.

- **Bronchogenic cyst:** This diagnosis is unlikely because a systemic vascular supply would not be expected.
- **Arteriovenous malformation (AVM):** Pulmonary AVMs frequently have an appearance of multiple, mass-like lesions with prominent feeding arteries, which can be of systemic origin. However, in this case systemic (as opposed to pulmonary) venous drainage is present, which, by definition, is not possible with a pulmonary AVM. In addition, a mass of abnormal lung parenchyma would not be expected in an AVM, making this diagnosis unlikely.
- **Pneumonia:** The clinical history is not consistent with pneumonia. Furthermore, the prominent vascularity associated with this lesion excludes acute pneumonia.
- **Pulmonary neoplasm:** Because pulmonary neoplasms are very rare lesions in neonates and because blood supply from the aorta would not be expected in a neoplasm, this diagnosis is very unlikely.
- **Chest wall mass:** The CT in this case indicates that the mass is within the lung parenchyma as opposed to the chest wall. Furthermore, chest wall masses are rare in neonates (and much less common than pulmonary sequestration). Finally, a chest wall mass would not be expected to have the large vessel vascular pattern that is present in the case illustrated here. This diagnosis is incorrect.

## DIAGNOSIS

**Pulmonary sequestration (intralobar type)**

## KEY FACTS

## Clinical

- The term *sequestration* refers to a nonfunctioning pulmonary parenchymal abnormality that lacks normal tracheobronchial communication and has anomalous systemic (rather than pulmonary) arterial supply. Venous drainage may be via systemic or pulmonary veins.
- Seuestration can occur with other congenital lung abnormalities (e.g., bronchogenic cyst, congenital cystic adenomatoid malformation, congenital lobar emphysema [CLE]), referred to as a *hybrid* abnormality.
- Sequestration is part of a continuum of bronchopul-monary foregut malformations (which have variable contributions of anomalies of lung, airway, and vascu-lature). Traditionally, a distinction is made between an *intralobar* (i.e., no separate pleura) and an *extralobar* (i.e., having a separate pleural investment) type of sequestration.
- Modes of presentation generally differ according to the age at the time of diagnosis.

- In the prenatal period, the diagnosis is based on the finding of an echogenic chest mass at sonography or fetal MRI.
- The clinical presentation in the neonatal period can be respiratory distress. However, infants can be asymp-tomic.
- In a child (and occasionally an adult), the clinical presentation is that of recurrent pulmonary infections, with the sequestration often initially being misdiag-nosed as pneumonia. The sequestration is most often an "incidental" finding unrelated to clinical findings, suggesting lower respiratory infection.
- More than half of sequestrations present in childhood. Most extralobar sequestrations are discovered within the first year of life.
- Sequestration can occasionally present in an infant or small child as a murmur with congestive heart failure due to the arteriovenous shunting.
- The intralobar type is more common and can be congenital or acquired. Most are lower lobe in location, with two-thirds located on the left side. Drainage is usually via the pulmonary veins.
- The extralobar type also usually occurs in the lower lobe and is on the left side in 90% of cases. This type may also be subdiaphragmatic. Drainage is typically through systemic veins. Fifty percent of cases have associated anomalies e.g., heart disease, diaphragmatic hernias, gastrointestinal, and other pulmonary abnormalities.
- Treatment for pulmonary sequestrations is surgical excision, which may be deferred for a period of 6 to 12 months, if the neonate is asymptomatic.

### Radiologic

- The sequestered lung can receive air flow through collateral sources. Therefore, if recurrent infections have not occurred, the radiographic appearance can be normal.
- The diagnosis should be considered when persistent or recurrent lower lobe opacity is found.
- Catheter angiography has been replaced by other, noninvasive imaging studies to determine vascular supply. Multidetector computed tomography (MDCT) angiogra-phy is the preferred method of diagnosis but MRI can also be especially useful.
- Sonography with color Doppler can be used to document arterial supply if a good acoustic window is present to facilitate imaging; however, usually cross-sectional imaging is performed prior to complete evaluation.

## SUGGESTED READING

Frush DP, Donnelly LE. Pulmonary sequestration: a new spin with helical CT. AJR Am J Roentgenol 1997;169:679–682.

Kocaoglu M, Frush DP, Ugurel MS, Somuncu I. Bronchopulmonary fore-gut malformations presenting as mass lesions

in children: spectrum of imaging findings. Diagn Interv Radiol 2010;16:153–161.

Newman B. Congenital bronchopulmonary foregut malformations: concepts and controversies. Pediatr Radiol 2006;36:773–791.

# CASE 9

**ANA M. GACA**

## HISTORY

A three-week-old girl with a swollen left leg and foot who refuses to move her left leg. Her mother reports falling down stairs while holding the infant the day before imaging was performed.

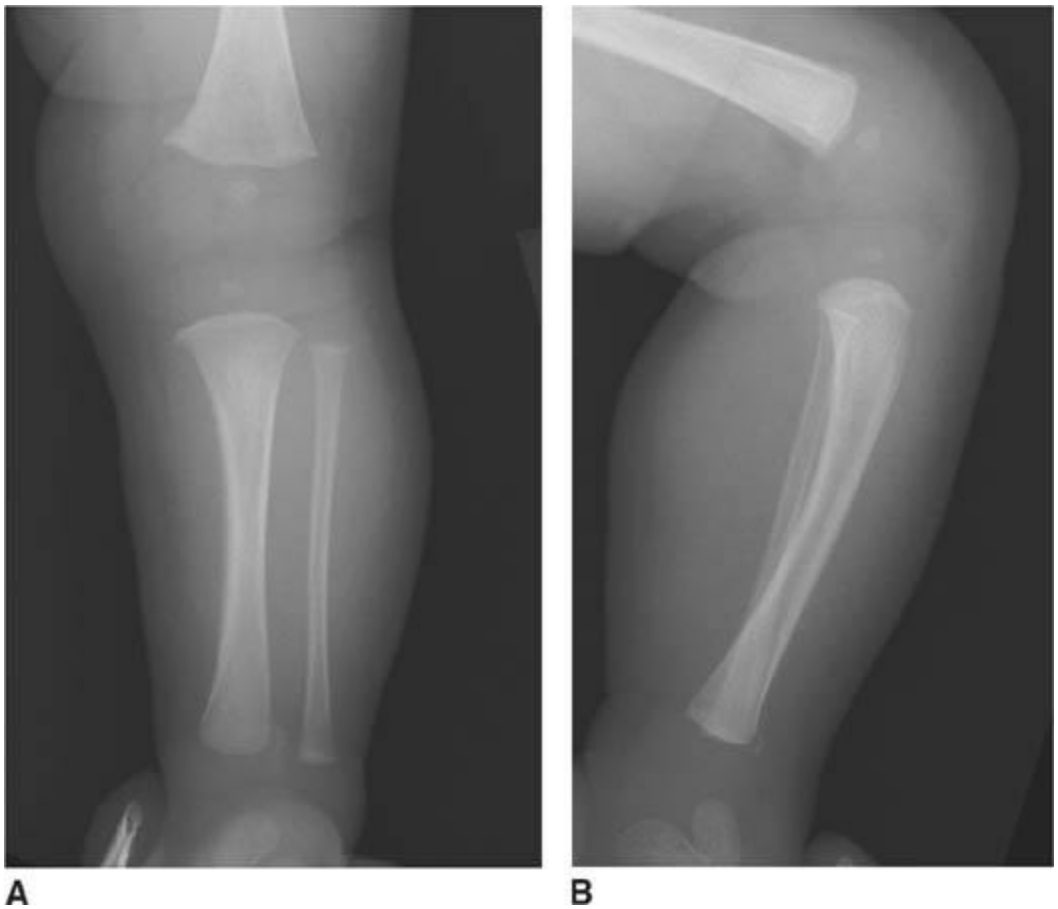


■**FIGURE 8-9A and 8-9B** Left lower extremity radiograph. A classic metaphyseal lesion (CML), also known as a corner fracture or a bucket-handle fracture (different projections of the same fracture), is present at the anterior aspect of the distal tibial metaphysis.

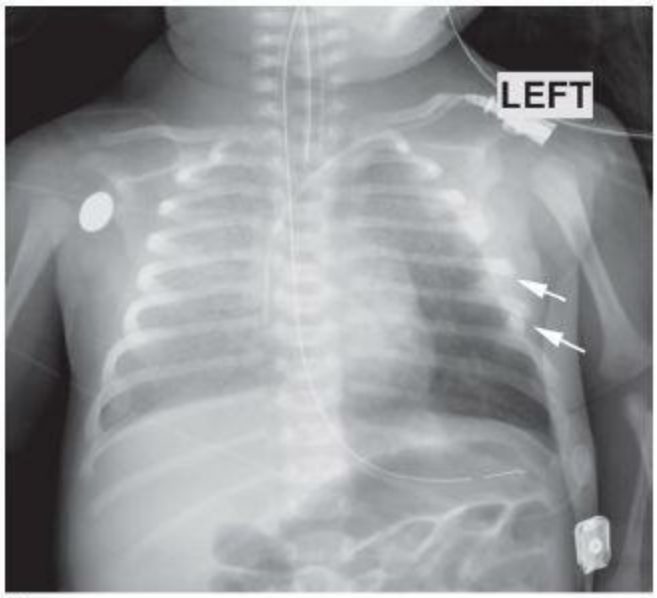


**FIGURE 8-9C** Chest radiograph on a different patient, a 1-month-old girl who presented with respiratory difficulty. Multiple acute left lateral rib fracture *(arrows)* and bilateral pulmonary opacities, worse in the right lung, are present.

## DIFFERENTIAL DIAGNOSIS

**Nonaccidental trauma (infant/child abuse):** This diagnosis is a likely consideration given the type of fracture, the classic metaphyseal lesion (CML) seen in nonaccidental trauma. In the case presented here, the pulmonary opacities are further suggestive of nonaccidental trauma because they are consistent with pulmonary contusion. In combination with the rib fractures and other fractures, nonaccidental trauma is the most likely diagnosis. As discussed below, the clinical information in any individual case is important to rule out other entities that can mimic nonaccidental trauma.

**Accidental trauma:** A CML, also known as a "corner" fracture, would not be expected to occur from accidental trauma. Fractures from accidental trauma are typically spiral or oblique fractures (often in the diaphysis) or so-called buckle fractures (commonly of the metaph-ysis or metadiaphysis). This diagnosis is incorrect.

**Osteogenesis imperfecta (OI):** The presence of multiple fractures raises this entity as a possible diagnosis. Clinical findings associated with OI include multiple fractures and bony deformity, blue sclera, hearing loss, tooth abnormalities (dentinogenesis imperfecta), and joint laxity, which are not reported to be present in this case.

**Menkes' syndrome (copper malabsorption):** The clinical history and physical examination are especially important for exclusion of this diagnosis. Patients with this very rare syndrome may have failure to thrive, delayed developmental milestones, and

kinky hair, eyebrows, and eyelashes. They later develop mental retardation and typically die in infancy. Such features are not present in the case presented, excluding the diagnosis.

- **Metaphyseal irregularity as a normal variant:** This variant is seen at the metaphyses as a beak or spur of bone that is continuous with the cortical bone. However, in the case presented here, the spur is not continuous, indicating that a fracture (i.e., a CML) is present. In questionable cases, a follow-up skeletal survey intended to identify other fractures can help distinguish a CML from a normal variant. Metaphyseal irreglarity is an incorrect diagnosis.
- **Rickets:** Congenital rickets due to maternal vitamin D deficiency can predispose a neonate or infant to insufficiency fractures. Diffuse osteopenia is often present; multiple fractures may also be encountered. The lack of oseteopenia in the case presented here makes the diagnosis of rickets unlikely.

## DIAGNOSIS

**Nonaccidental trauma (i.e., child abuse)**

## KEY FACTS

### Clinical

- In addition to the multiple types of skeletal injuries seen in the setting of abuse, central nervous system injury (e.g., subdural hematoma, diffuse edema, diffuse infarction from hypoxia, and parenchymal hemorrhage) may be present. The mechanism for these injuries is currently thought to be impact against a soft object in combination with shaking, rather than (as previously thought) shaking alone.
- Rib fractures are more common in children younger than 1 year old, whereas diaphyseal injuries are more common in those older than 1 year old. This fact reflects the manner in which the child is typically held during the trauma.
- Direct blows to the abdomen most frequently result in duodenal hematoma, pancreatitis (with its attendant complications), and hepatic and splenic injuries.
- The diagnosis of nonaccidental trauma is established using a combination of history (i.e., incompatibility of the reported history in relation to the type and extent of injuries), physical findings (e.g., burns, hand marks, sexual abuse, preretinal hemorrhages), and radiographic findings.
- A major diagnostic consideration is OI, in which a family history of fractures, deafness, blue sclerae, and poor dentition may be elicited. If necessary, the diagnosis can be confirmed with a skin biopsy demonstrating a collagen synthesis deficiency.

- Another diagnostic consideration is Menkes' syndrome, a very rare neurodegenerative disorder due to a defect in copper metabolism, leading to death within the first year of life. These patients have sparse, brittle hair, which accounts for the designation "kinky hair syndrome."
- Congenital rickets due to maternal vitamin D deficiency is a consideration in cases of suspected nonaccidental trauma, although there is still active debate over the degree of overlap in terms of clinical features between the two disease states.

## Radiologic

- Child or infant abuse can have central nervous system, abdominal, or skeletal findings evident on imaging studies. The skeletal manifestations are reviewed below.
- The CML is the most specific injury in child abuse. The CML is seen almost exclusively in children younger than 2 years old and most commonly seen in the distal femur, proximal tibia, distal tibia and proximal humerus.
- Depending on the radiographic projection, a CML may appear as a corner fracture or a so-called bucket handle fracture.
- In addition to the CML, other injuries that are highly specific for child abuse include fractures in unusual locations such as the scapulae, sternum, and posterior ribs.
- Injuries that are moderately specific for child abuse include fractures of varying ages, complex skull fractures, and fractures involving the digits or vertebral bodies.
- Spiral fractures are injuries with low specificity for child abuse. However, suspicion should be raised when such fractures are seen in children who are not old enough to have engaged in activities that would make an accidental cause likely.
- One spiral fracture that should not raise suspicion for child abuse is the "toddler's fracture," a spiral fracture of the distal tibia. This injury is seen in children who are learning to walk and is not an indication for performing a skeletal survey.
- Physiologic periostitis in the infant is a normal bony condition, which is typically seen between 1 and 6 months of age. It is characteristically manifested as a single (or occasionally multiple) thin layer of periosteal reaction on the medial aspect of the femur, tibia, humerus, and radius, and is symmetric in distribution.
- The radionuclide bone scan (and potentially whole-body MR imaging) is a complementary method to plain films for detection of injuries due to abuse. This imaging study is particularly sensitive for detection of posterior rib fractures as well as diaphyseal injuries (which may actually be bowing fractures that can be inapparent on plain films).

## SUGGESTED READING

Kleinman PK. Diagnostic Imaging in Infant Abuse. AJR Am J Roentgenol 1990;155:703–712.

Lonergan GJ, Baker MB, Morey MK, Boos SC. From the Archives of the AFIP. Child abuse: radiologic-pathologic correlation. Radiographs 2003;23:811–845.

Nimkin K, Kleinman PK. Imaging of child abuse. Radiol Clin North Am 2001;39:843–864.

Slovis TL, Chapman S. Evaluating the data concerning vitamin D insuf-flciency/deflciency and child abuse. Pediatr Radiol 2008;38:1221–1224.

# CASE 10

**CHARLES MAXFIELD**

## HISTORY

A neonate with low hematocrit following traumatic delivery.

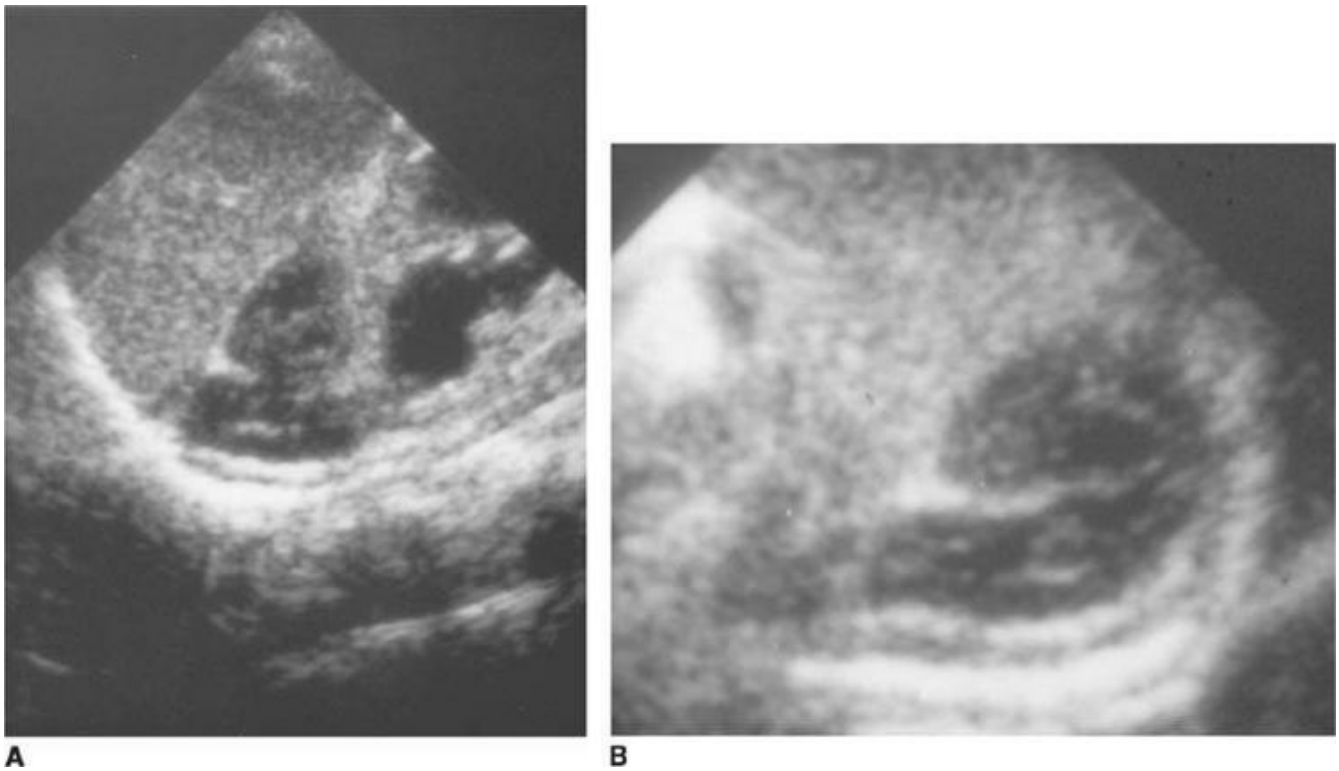


**FIGURES 8-10A and 8-10B** Longitudinal **(A)** and transverse **(B)** views from a left upper quadrant sonogram. A structure with heterogeneous echogenicity is seen just superior to the left kidney in the expected location of the left adrenal gland. The structure has the pyramidal shape expected of the adrenal gland (although the limbs are enlarged). Dilatation of the renal collecting system is seen but is an incidental finding. The right adrenal gland (not shown) had a normal appearance.

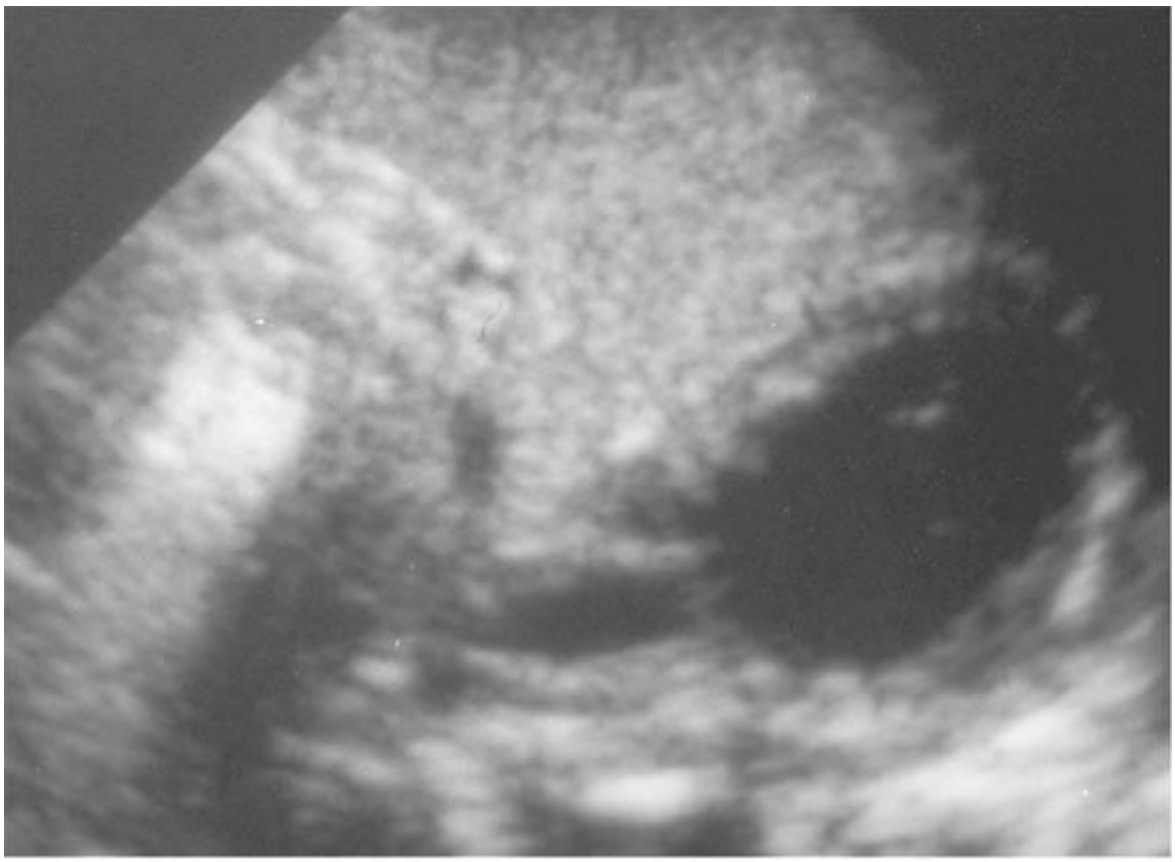

C

■**FIGURE 8-10C** Transverse sonogram 10 days after Figures 8-10A and 8-10B were obtained. During the period since the initial study, the lesion has become hypoechoic, with an anechoic central region. A slightly irregular echogenic rim is evident.

D

**FIGURE 8-10D** Transverse sonogram of adrenal gland in a different patient. An adrenal gland in a normal neonate is illustrated for comparison to the previous images. The gland has symmetric, hypoechoic limbs with a central echogenic stripe.

## DIFFERENTIAL DIAGNOSIS

**Congenital neuroblastoma:** This entity typically has the radiologic appearance of a solid (rather than cystic) mass, whereas the lesions shown in the case presented here are hypoechoic (consistent with fluid). Although neuroblastoma could become cystic following chemotherapy or a biopsy producing internal hemorrhage, no history of these events is present in the patient shown here. Finally, neuroblastoma tends to distort the shape of the adrenal gland; however, in the case presented, the shape of the adrenal gland is preserved. For these reasons, neuroblastoma is an unlikely consideration.

**Other retroperitoneal tumors (e.g., lymphangioma, teratoma):** These tumors are very rarely located in the retroperitoneum. Furthermore, such lesions are usually calcified, fluid-filled masses. This diagnosis is an unlikely one.

**Perinephric abscess:** The mixed echogenicity seen in the case presented here could be seen in a phlegmon or abscess. However, no history of infection is present; furthermore, such a process would be very unusual in a newborn. Finally, a perinephric abscess

would be expected to arise adjacent to, rather than within, the adrenal gland). However, in this case shown, the adrenal gland itself is the site of the abnormality. Perineph-ric abscess is an incorrect diagnosis.

- **Congenital adrenal hyperplasia:** This entity might be considered because of the enlargement of the adrenal glands. In congenital adrenal hyperplasia, the glands do maintain their adreniform shape. However, enlargement of both glands is present, whereas, in the case shown here, a single adrenal gland is affected. Endo-crinologic abnormalities are helpful in supporting the diagnosis of congenital adrenal hyperplasia. However, we are given no history of such abnormalities in the case presented here. Therefore, this diagnosis is unlikely.
- **Adrenal hemorrhage:** In the case shown, the echotex-ture of the mass changed relatively quickly, which would be unusual for any entity other than hemorrhage. Furthermore, the shape of the adrenal gland is maintained, which would be unusual for some of the diagnostic considerations other than hemorrhage but common for adrenal hemorrhage. This diagnosis is correct.

## DIAGNOSIS

**Neonatal adrenal hemorrhage**

## KEY FACTS

### Clinical

- Spontaneous adrenal hemorrhage occurs relatively commonly in newborn infants and is occasionally detected in utero.
- Predisposing factors include perinatal stress, traumatic birth, hypoxia, and sepsis. Hemorrhage also occurs with increased frequency in large infants and infants of diabetic mothers.
- Large hemorrhages can clinically present with systemic shock or a palpable mass; smaller hemorrhages cause mild anemia or jaundice. Biochemical abnormalities are seldom present in either the acute or convalescent phase.
- Hemorrhage is more common in the left adrenal gland and is seen bilaterally in approximately 10% of cases.
- Complications are uncommon but include renal vein thrombosis (especially when the left adrenal gland is involved) and secondary infection/abscess.

### Radiologic

- The primary diagnostic considerations for a suprarenal mass in a neonate are acute

adrenal hemorrhage and congenital neuroblastoma.

- Doppler evaluation can help distinguish adrenal hemorrhage from neuroblastoma based on vascularity; a hematoma is typically avascular while a tumor is generally well vascularized.
- At sonography, hemorrhage is typically initially echo-genic, next develops mixed echogenicity as the clot retracts, and becomes hypo- or anechoic as it liquefies.
- Serial sonographic studies documenting rapidly decreasing size of the mass are consistent with adrenal hemorrhage. Progressive enlargement of the mass suggests a diagnosis of neuroblastoma and is an indication for surgical resection.
- MR imaging has been used to establish the diagnosis but often does not definitively distinguish adrenal hemorrhage from neuroblastoma. Fortunately, small neu-roblastomas in the newborn invariably have favorable histology, which allows serial imaging with sonography without substantial risk of rapid growth.
- Dystrophic calcifications can be the first radiologic indication of previous adrenal hemorrhage. Adrenal calcification, however, can also be seen in many other entities, such as neuroblastoma, ganglioneuroblastoma, Wolman's syndrome, pheochromocytoma, tuberculosis, and adrenal carcinoma.

## SUGGESTED READING

Deeg KH, Bettendorf U, Hofmann V. Differential diagnosis of neonatal adrenal haemorrhage and congenital neuroblastoma by colour coded Doppler sonography and power Doppler sonography. Eur J Pediatr 1998;157:294–297.

Friedman GK, Castleberry RP. Changing trends of research and treatment in infant neuroblastoma. Pediatr Blood Cancer 2007;49:1060–1065.

Hendry GMA. Cystic neuroblastoma of the adrenal gland- A potential source of error in ultrasonic diagnosis. Pediatr Radiol 1982;12:204–206.

Nuchtern JG. Perinatal neuroblastoma. Semin Pediatr Surg 2006;15:10–16.

Velaphi SC, Perlman JM. Neonatal adrenal hemorrhage: clinical and abdominal sonographic findings. Clin Pediatr (Phila) 2001;40:545–548.

Westra SJ, Zaninovic AC, Hall TR, et al. Imaging of the adrenal gland in children. Radiographics 1994;14:1323–1340.

# CASE 11

**DONALD P. FRUSH**

### HISTORY

A term neonate with mild tachypnea but no cyanosis.

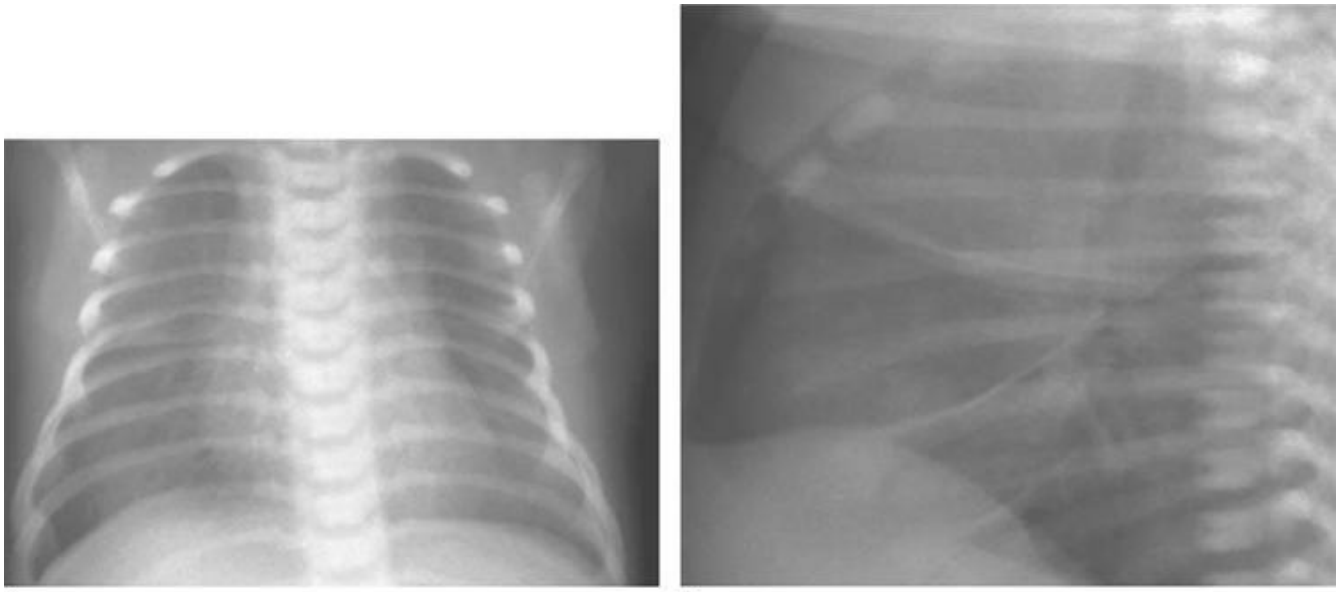


**FIGURES 8-11A and 8-11B** Frontal **(A)** and lateral **(B)** chest radiograph (2 hours postnatal). Normal lung volumes are present, with streaky hilar opacities, indistinct vascularity, and subpleural and pleural fluid. The heart size is normal.

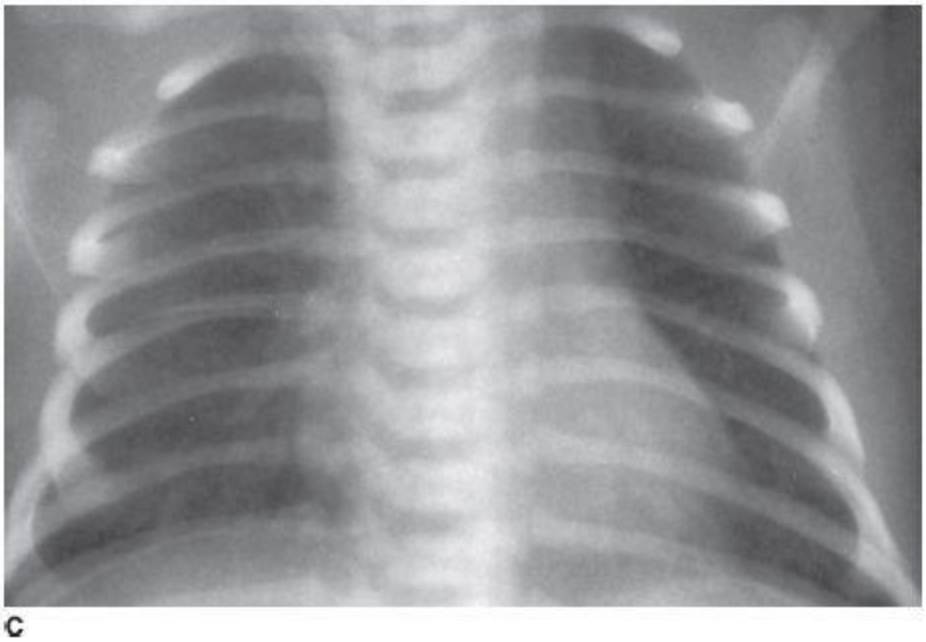


**FIGURE 8-11C** Frontal chest radiograph (48 hours postnatal). The abnormalities have almost completely resolved.

## DIFFERENTIAL DIAGNOSIS

**Transient tachypnea of the newborn (TTN):** The streaky hilar opacities and small amount of pleural fluid are consistent with TTN. The fact that the clinical and radiologic

findings quickly resolved makes TTN the most likely diagnosis.

- **Respiratory distress due to surfactant deficiency (respiratory distress syndrome, hyaline membrane disease, surfactant deficiency disease):** In respiratory distress syndrome, the lung volumes are typically reduced (except, on occasion, in infants who are intu-bated) and pleural fluid is very rarely present. The radiographic pattern is that of a diffuse, fine (so-called ground glass), granular appearance. These findings are all at variance with those depicted in the case presented here. Finally, respiratory distress syndrome is seen almost exclusively in preterm infants, whereas the patient in the case presented is a term infant. This diagnosis is unlikely.
- **Meconium aspiration:** Generally, more patchy opacities (representing atelectasis) and focal air trapping are seen in meconium aspiration, rather than the streaky opacities seen in the case illustrated. Often, infants with meconium aspiration are quite ill, have persistent fetal circulation due to pulmonary hypertension, and are intubated—features that are not present in the case depicted here. This diagnosis is unlikely.
- **Congestive heart failure:** In congestive heart failure, the heart size is typically enlarged, unlike the case shown here. This diagnosis is unlikely.
- **Neonatal pneumonia:** This entity can initially have a radiographic appearance similar to the case shown here. However, the rapid resolution is not consistent with pneumonia. Furthermore, clinical information supporting infection (e.g., prolonged rupture of membranes, maternal fever, infant leukocytosis or leukope-nia, infected amniotic fluid) is not present in the case illustrated. This diagnosis is unlikely.

## DIAGNOSIS

**Transient tachypnea of the newborn (retained fetal lung fluid, wet-lung syndrome, persistent pulmonary edema)**

## KEY FACTS

### Clinical

- The physiologic abnormality underlying TTN is delayed clearance of normal fetal lung fluid from the pulmonary interstitium.
- TTN is probably the most common cause of neonatal respiratory distress.
- This entity is slightly more common in boys.
- Risk factors for TTN include prolonged labor, delivery by cesarean section, precipitous delivery, maternal diabetes, neonatal hypoproteinemia, and maternal administration of hypotonic fluid.
- In TTN, tachypnea is present within the first few hours of life. Respiratory distress

peaks by 24 hours and is nearly always resolved by 2 to 3 days. Other clinical features include occasional grunting, sternal and intercostal retractions, and mild cyanosis.

- Treatment is conservative and usually consists of placement of the infant under an oxygen hood. Antibiotics are sometimes administered if it is unclear whether infection is the cause of symptoms.
- Neonatal pneumonia (primarily that due to infection by group B streptococcus, gram negative rods, or Listeria), hyaline membrane disease, meconium aspiration, asphyxia, congestive heart failure, and TTN can have similar clinical presentations in the first few hours of life.

### Radiologic

- The radiographic appearance is typically that of streaky, coarse reticular opacities that have hazy borders. Well-defined focal opacities are rare.
- Lung volumes are normal or increased in TTN, and the heart size is normal.
- Radiographic improvement generally parallels clinical improvement.
- Pulmonary effusions are usually small and are more common in the right hemithorax.
- Follow-up radiographs are not necessary when the clinical and radiographic presentations are typical.

## SUGGESTED READING

Bramson RT, Griscom NT, Cleveland RH. Interpretation of chest radiographs in infants with cough and fever. Radiology 2005;236:22–29.

Guglani L, Lakshminrusimha S, Ryan RM. Transient tachypnea of the newborn. Pediatr Rev 2008;29:e59–e65.

Hermansen CL, Lorah KN. Respiratory distress in the newborn. Am Fam Physician 2007;76:987–994.

Slovis TL, Bulas DI. Congenital and acquired lesions (most covering respiratory distress) of the neonatal lung and thorax. In: Slovis TL (ed), Caffey's Pediatric Diagnostic Imaging (11th ed). Philadelphia, PA: Mosby Elsevier, 2007:93–133.

Takaya A, Igarashi M, Nakajima M, et al. Risk factors for transient tachyp-nea of the newborn in infants delivered vaginally at 37 weeks or later. J Nippon Med Sch 2008;75:269–273.

# CASE 12

**GEORGE S. BISSET**

### HISTORY

A 9-year-old boy who was involved as a pedestrian in a motor vehicle accident.

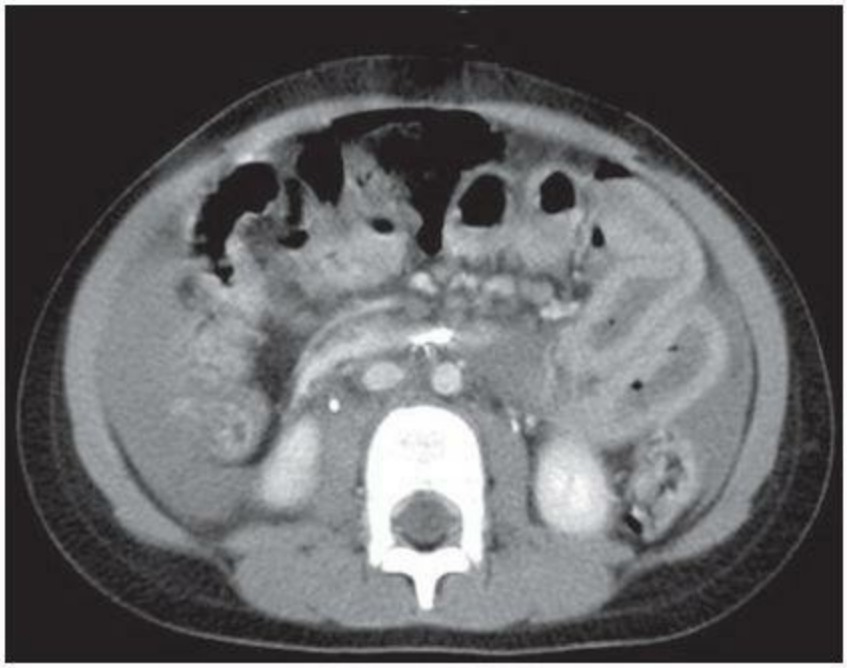

**FIGURE 8-12** Axial image from IV contrast-enhanced CT examination shows fluid-filled segments of bowel that are mildly dilated, have thickened walls and abnormally increased enhancement. Note also the presence of fluid within the peritoneal cavity. The aortic caliber is normal.

## DIFFERENTIAL DIAGNOSIS

- **Hypoperfusion complex (also known as "shock bowel"):** This entity is usually seen in the setting of posttraumatic hypovolemic shock and has the imaging findings of (1) abnormally increased contrast-enhancement of the pancreas, adrenal glands, kidneys, and bowel wall; (2) fluid-filled bowel loops with free peritoneal fluid; and (3) a small aorta and inferior vena cava (IVC) due to the reduced blood volume. In the case presented here, the IVC is relatively small but the aorta appears normal; no significant enhancement of the adrenals and pancreas is seen. This diagnosis is unlikely.
- **Uncomplicated hemoperitoneum:** The case illustrated shows free intraperitoneal fluid that could be blood (or urine and bile, because these have a similar appearance). However, bowel wall contrast-enhancement is present, which would not be expected in uncomplicated hemoperitoneum. This diagnosis is unlikely.
- **Pancreatic trauma:** Pancreatic fractures (which can be clinically undetected) may be associated with bowel dilatation secondary to local ileus. However, the resultant fluid collections would be expected to be retroperitoneal (unlike the case shown here). Furthermore, bowel wall contrast-enhancement would not be expected. This diagnosis is incorrect.

- **Bowel and mesenteric injury:** Given the free intraperitoneal fluid, bowel wall contrast-enhancement and bowel dilatation in the presence of a normal caliber aorta and IVC, this diagnosis is reasonable and is the most likely.

## DIAGNOSIS

**Bowel perforation (without evidence of pneumoperitoneum)**

## KEY FACTS

### Clinical

- Substantial bowel and mesenteric trauma are found in 3% to 5% of children with blunt abdominal trauma.
- The clinical signs of bowel injury are nonspecific, but include abdominal tenderness, guarding, rebound tenderness, and absent bowel sounds.
- Injuries of the bowel are associated with markedly increased morbidity and mortality; the decision to perform surgery is usually based on physical examination laboratory findings.

### Radiologic

- The only definitive CT signs of bowel perforation are the presence of pneumoperitoneum and extravasated oral contrast material. Pneumoperitoneum occurs in 30% to 40% of patients with documented perforation but can be subtle. Extravasation of oral contrast material is rarely seen; thus, the decision to administer (or withhold) oral contrast material should not be based on the expectation of finding extravasated contrast material.
- Typical CT findings include bowel wall thickening, contrast-enhancement, and otherwise unexplained peritoneal fluid.

## SUGGESTED READING

Bulas DI, Taylor GA, Eichelberger MR. The value of CT in detecting bowel perforation in children after blunt abdominal trauma. AJR Am J Roentgenol 1989;153:561–564.

Hanks PW, Brody JM. Blunt injury to mesentery and small bowel: CT evaluation. Radiol Clin North Am 2003;41:1171–1182.

Nghiem HV, Jeffrey RB Jr, Mindelzun RE. CT of blunt trauma to the bowel and mesentery. AJR Am J Roentgenol 1993;160:53–58.

Lubner M, Menias C, Rucker C, et al. Blood in the belly: CT findings of hemoperitoneum. Radiographics 2007;27:109–125.

# CASE 13

**CAROLINE L. HOLLINGSWORTH**

## HISTORY

A 1-year-old boy with a 3-month history of increasing abdominal girth and palpable abdominal mass.

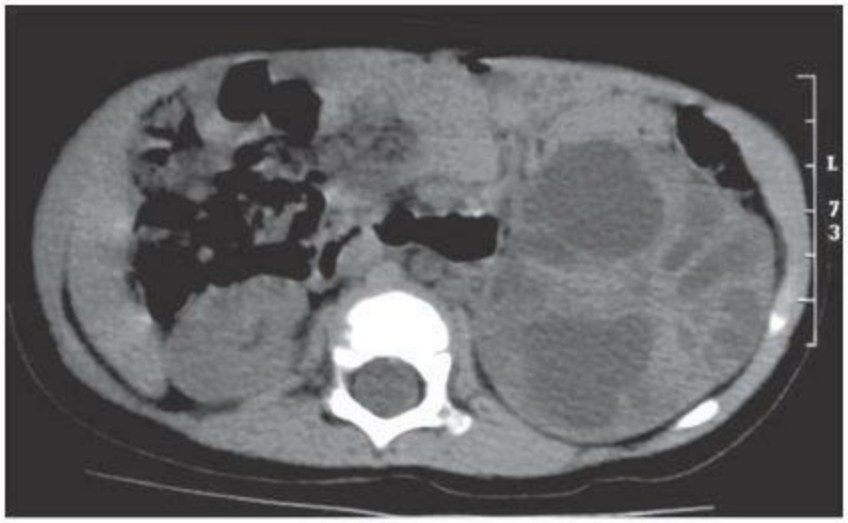


A

■**FIGURE 8-13A** Unenhanced axial CT image shows a multicystic right renal mass.


B

■**FIGURE 8-13B** Contrast-enhanced axial CT image shows enhancing septa within the

low attenuation mass.

## DIFFERENTIAL DIAGNOSIS

- **Wilms' tumor:** Wilms' tumor is the most common solid renal mass in a child. However, it is rarely cystic and would not be expected to have enhancing septa. In the rare instances of Wilms' tumor with cystic components, large areas of solid tumor are present, unlike the present case. This diagnosis is an unlikely one.
- **Multilocular cystic nephroma:** The lesion is well encapsulated and multicystic with enhancing septa. These features are typical for multilocular cystic nephroma. This diagnosis is correct.
- **Clear cell sarcoma:** This tumor is rare, making the diagnosis unlikely. Also, cystic regions in clear cell sarcoma (like Wilms' tumor) are typically due to necrosis within a predominately solid lesion. However, the low density regions in the mass shown in this case are well demarcated and are homogeneous in appearance, consistent with cysts rather than necrosis. This diagnosis is incorrect.
- **Renal abscess:** A history of fever and other systemic signs of infection would be expected in a patient with abscess. Furthermore, thicker septations than those seen in the patient presented here and perinephric inflammation would be expected. This diagnosis is unlikely.
- **Hydronephrosis:** In hydronephrosis, the fluid-filled regions would be expected to connect. Furthermore, one would not expect a hydronephrotic kidney to contain multiple cysts of variable size having enhancing septa. This diagnosis is unlikely.
- **Segmental multicystic dysplastic kidney (MCDK):** Segmental MCDK is typically very similar in appearance to multilocular cystic nephroma and cannot be absolutely distinguished from it on the images presented in this case. However, segmental MCDK is quite rare. Furthermore, the rim of enhancing normal renal parenchyma seen at the periphery of the mass in the case presented here would be very unusual for MCDK. This diagnosis is incorrect.

## DIAGNOSIS

**Multilocular cystic nephroma**

## KEY FACTS

### Clinical

- MLCN has a bimodal age distribution and tends to occur in male children (3 months to

4 years) and adult women (40 to 60 years).

- In children, this lesion typically presents as a painless enlarging abdominal mass.
- MLCN has not been described in the antenatal or neonatal periods, which can help differentiate this tumor from other congenital structural abnormalities.

### Radiologic

- MLCN is typically a solitary tumor but bilateral tumors have been described.
- Sonography is commonly the initial imaging modality used to evaluate an enlarging abdominal mass, particularly in children. At sonography, MLCN is typically seen as a multicystic renal mass with no solid or nodular components.
- At CT or MR imaging, MLCN is typically a well-circumscribed, encapsulated multicystic mass with multiple enhancing septations. There is no excretion of contrast material into the cystic spaces of the mass even when the mass extends into the renal pelvis or ureter.
- Because no clinical or radiographic feature of this tumor can predict histologic characteristics, surgery (nephrec-tomy vs. nephron-sparing procedure) is required.

## SUGGESTED READING

Lowe LH, Isuani BH, Heller RM, et al. Pediatric renal masses: Wilms tumor and beyond. Radiographics 2000;20:1585–1603.

Okada T, Yoshida H, Matsunaga T, et al. Nephron-sparing surgery for multi-locular cyst of the kidney in a child. J Pediatr Surg 2003;38:1689–1692.

Silver IM, Boag AH, Soboleski DA. Best cases from the AFIP: multilocu-lar cystic renal tumor: cystic nephroma. Radiographics 2008;28: 1221–1225.

Wootton-Gorges SL, Thomas KB, Harned RK, et al. Giant cystic abdominal masses in children. Pediatr Radiol 2005;35:1277–1288.

# CASE 14

**DONALD P. FRUSH**

### HISTORY

A 2-month-old boy with wheezing.

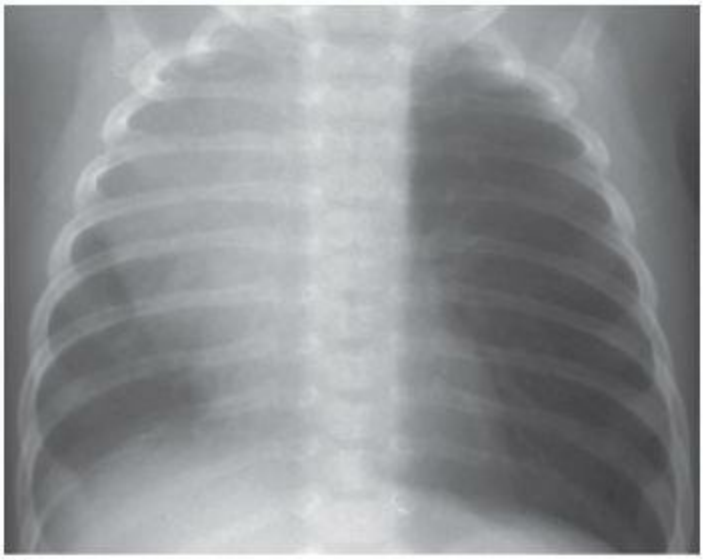

A

**FIGURE 8-14A** Frontal chest radiograph. A predominantly right-sided mediastinal mass is present along with hyperinflation of the left lung.

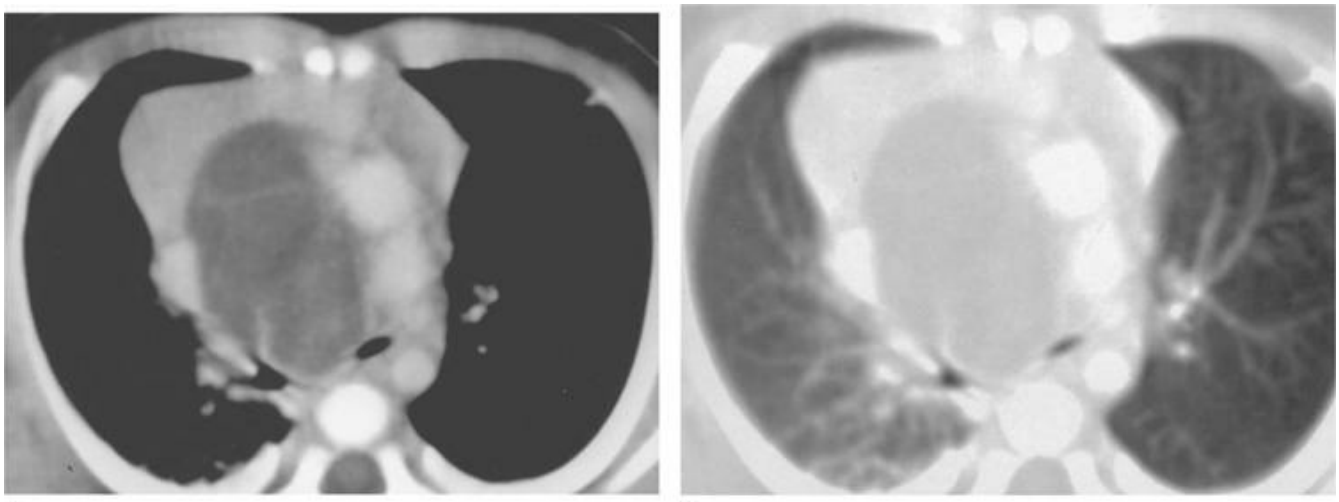

B C

**FIGURES 8-14B and 8-14C** Contrast-enhanced CT scans of the chest. **B:** CT image with soft tissue detail windows. A septated, cystic anterior mediastinal mass is present. **C:** Same CT slice as in Figure 8-14B with lung-detail windows. Air trapping is present in the left lung due to narrowing of the left main bronchus by the mass.

## DIFFERENTIAL DIAGNOSIS

**Lymphangioma/hemangioma:** The lesions shown in the figures are cystic masses with a variable amount of solid tissue. Most intrathoracic lesions extend downward from the neck. These diagnoses cannot be excluded on the basis of the images presented.

**Teratoma:** Teratomas can also be cystic mediastinal masses (with occasional

calcification and variable solid components), usually located in the anterior mediastinum. This diagnosis is a likely consideration based on the findings presented.

- **Other germ cell tumors (e.g., yolk sac tumors and embryonal cell tumors):** Such lesions are rare in infancy, making this diagnosis unlikely.
- **Bronchogenic cyst:** Bronchogenic cysts are usually not septated and, when situated in the mediastinum, are typically subcarinal in location rather than in the anterior mediastinum. This diagnosis is unlikely.
- **Esophageal duplication:** This diagnosis is unlikely because esophageal duplications are located in the middle mediatinum rather than the anterior mediastinum.
- **Lymphoma:** This diagnosis is unlikely because lymphoma is predominantly or exclusively a solid mass found in older children and adolescents.
- **Thymoma:** Thymomas are usually solid, rather than cystic, and are extremely rare at this age. This diagnosis is unlikely.
- **Normal thymus:** Normal thymic tissue can have an asymmetric anterior mediastinal location. However, normal thymus tissue does not compress the airway and is not cystic. This diagnosis is incorrect.
- **Thymic cyst:** This diagnosis is unlikely because these lesions are rare in infancy.
- **Abscess/hematoma:** These diagnoses are unlikely because there is no history of infection, instrumentation, trauma, or a bleeding disorder.
- **Aneurysm/dilated ascending aorta:** These diagnoses would be unlikely based on the young age of the patient. Furthermore, dense contrast enhancement of the lesion would be expected if the mass was vascular.

# DIAGNOSIS

**Cystic teratoma (mature type)**

# KEY FACTS

## Clinical

- Respiratory distress is a common clinical presentation of a mediastinal mass in a neonate.
- Teratomas contain tissues derived from all three embryonic cell layers, that is, mesoderm, endoderm, and ectoderm.
- The mediastinum is the third most common location for teratomas, exceeded only by the pelvis (e.g., ovarian/ sacrococcygeal location) and the central nervous system.
- Teratomas account for approximately 80% of mediasti-nal germ cell tumors.

- Most anterior mediastinal teratomas have mature his-tologic features; such lesions are almost always benign. However, teratomas with immature histologic features can be benign or malignant.
- Cystic teratomas are more likely to be benign, whereas solid teratomas are more likely malignant.
- Malignant teratomas often have some histologic components of other germ cell tumors, e.g., yolk sac tumors and embryonal cell tumors.
- Exact diagnosis of a cystic mediastinal mass using imaging methods alone can be difficult. Hence, because these lesions can produce life-threatening symptoms and signs (e.g., airway compromise), virtually all masses are removed, if possible.

## Radiologic

- A teratoma can be presumed to be malignant if it is exclusively solid, invasive, or metastatic. Absence of these features does not specifically indicate that a tera-toma is benign.
- Typical radiographic features of a mediastinal teratoma include a cyst (containing either serous or sebaceous fluid and having occasional thin septations) and presence of fat, calcification, and solid elements. CT or MR imaging is routinely performed for surgical planning and staging when malignant.
- Sonography can show the cystic structure and calcification but is usually inadequate for showing lesion extent and involvement of adjacent structures (e.g., vessels and airways), which are necessary for surgical planning.
- As with any anterior mediastinal mass, it is critically important to assess the degree of airway compression.

# SUGGESTED READING

Freud E, Ben-Ari J, Schonfeld T, et al. Mediastinal tumors in children: a single institution experience. Clin Pediatr (Phila) 2002;41:219–223.

Frush DP. Imaging of paediatric mediastinal masses. Ann Acad Med Singapore 2003;32:525–535.

Frush DP. Imaging evaluation of the thymus and thymic disorders in children. In: J Lucaya, JL Strife (eds), Pediatric Chest Imaging: Chest Imaging in Infants and Children (2nd ed). 2007;215–240.

Temes R, Allen N, Chavez T, et al. Primary mediastinal malignancies in children: report of 22 patients and comparison to 197 adults. Oncologist 2000;5:179–184.

# CASE 15

**CAROLINE CARRICO**

## HISTORY

A newborn boy with prenatal hydrouretronephrosis.


■**FIGURE 8-15A** Figures 8-15A and 8-15B are from a postnatal sonogram **A:** Longitudinal image of the left kidney shows severe pelvicaliectasis, cortical thinning and poor corticomedullary differentiation. The right kidney (not shown) had a similar appearance.


B

■**FIGURE 8-15B** Parasagittal view shows a thick-walled urinary bladder and a dilated tortuous distal right ureter. The left ureter (not shown) was also dilated and tortuous.

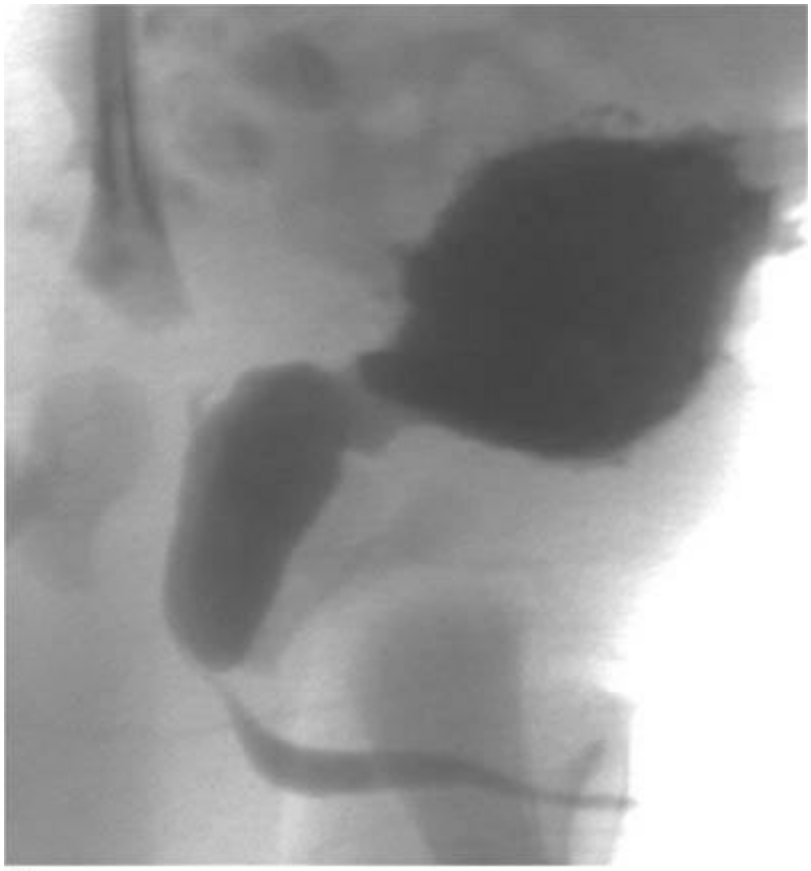

C

**FIGURE 8-15C** Voiding cystourethrogram (VCUG). Lateral oblique view of the urinary bladder and urethra during voiding after removal of the urinary catheter shows that the bladder is trabeculated and the posterior urethra is dilated. An abrupt change in caliber of the urethra is present in which the large caliber of the dilated, patent posterior urethra is juxtaposed against that of the small anterior urethra.

## DIFFERENTIAL DIAGNOSIS

**Vesicoureteric reflux:** Vesicoureteric reflux is a common cause of hydroureteronephrosis. It can be due to a patulous ureterovesicle junction or secondary to bladder outlet obstruction. If reflux occurs into a kidney with a duplicated collecting system and two completely separate ureters, the reflux occurs into the lower pole ureter. In the case shown here, hydronephrosis is identified on the sonographic images, but there is no evidence of vesicoureteric reflux on the voiding image from a voiding cystourethrogram. While there are findings consistent with bladder outlet obstruction, no reflux is seen to occur, making vesicoureteric reflux an incorrect diagnosis.

**Neurogenic bladder:** A thick-walled (trabeculated) bladder and dysfunctional voiding can occur secondary to abnormal innervation of the urinary bladder. Evaluation of the spine and spinal cord with plain films, sonography, or MR imaging may disclose an abnormality of the spinal cord or contents of the spinal canal. However, the posterior

urethra would not be expected to be dilated due to a neurogenic bladder, making this diagnosis unlikely.

- **Primary megaureter (PMU):** In PMU, a functional obstruction of the distal ureter exists at the vesicoure-teric junction. The ureter is often more dilated distally than proximally (except for the most distal 1 cm, which is not dilated). PMU often resolves spontaneously, but renal function may be compromised and surgery may be required. Reflux into a PMU can occur. However, the bladder and urethra are usually normal, unlike the case shown here, making this diagnosis unlikely.
- **Prune Belly Syndrome:** This syndrome is characterized by the triad of deficiency of the abdominal wall musculature, urinary tract anomalies including dilated ureter(s) and/or bladder, and cryptorchidism. The posterior urethra may be large due to hypoplasia of the prostate. The anterior urethra may be large due to deficiency of the penile corpora. However, the dilated urethra is usually not obstructed and thus one would not expect bladder muscular hypertrophy due to bladder outlet obstruction (as is present in the case shown), making this an incorrect diagnosis.
- **Posterior urethral valves (PUVs):** In this entity, which is also known as congential obstructive posterior ure-thral membrane, obstructing valves or membranes occur at the base of the veru montanum. The appearance of the urethra after catheter removal during voiding cystourethrography is diagnostic: the prostatic urethra is dilated and there is an abrupt caliber change with marked narrowing of the urinary stream in the anterior urethra. There may also be bladder muscle hypertrophy and/or vesicoureteric reflux secondary to the bladder outlet obstruction. This diagnosis is the most likely for the case shown here.
- **Obstructing congenital anomaly of the anterior urethra:** An obstruction of the anterior urethra can result in dilation of the posterior urethra and bladder wall thickening related to bladder outlet obstruction. However, the anterior urethra would be expected to be dilated proximal to the obstruction, which is not true in the case illustrated here; this diagnosis is incorrect.

## DIAGNOSIS

**Posterior urethral valves**

## KEY FACTS

### Clinical

- Posterior urethal valves occur only in boys. The exact embryologic abnormality is not known.

- Oliguria can result in utero and produce oligohydram-nios and pulmonary hypoplasia.
- Infants with abnormal prenatal urinary tract findings can be assessed postnatally with fluoroscopic vesico-ureterography (VCUG) and urinary tract sonography. The diagnosis of PUVs should also be considered in a newborn boy with a poor urine stream, a constantly full urinary bladder, multiple urinary tract infections, sepsis, failure to thrive, and nephropathy.
- Unilateral vesicoureteric reflux may be protective of the other kidney. Bladder rupture or calyceal fornix perforation can also occur, causing decompression of the renal collecting system.
- Treatment in utero can be performed using repeated fetal bladder decompression or vesicoamniotic stent placement but has variable results. Postnatal therapy routinely consists of valve ablation via cystoscopy.
- PUVs are responsible for up to 90% of endstage renal disease in boys less than age 4 and accounts for 70% of renal transplantation procedures needed in boys under the age of 5.

## Radiologic

- PUVs are best diagnosed on VCUG, on which the valves can balloon out and be visible as a curved filling defect, obstructing the flow of urine from the posterior urethra. The patency of the urethra is maintained posteriorly. The caliber of the anterior urethra is markedly narrowed relative to the distended posterior urethra.
- When assessing the male urethra, three important technical features must be considered to avoid a false-negative examination. First, imaging should be performed after removal of the urinary catheter. Second, the entire urethra must be imaged in a lateral/oblique projection. Third, a large amount of urine must be passing through the urethra at the time of imaging.
- A dilated posterior urethra can be diagnosed using sonography in utero or postnatally; the appearance has been likened to the shape of a “keyhole.”
- In boys with PUVs the appearance of the kidneys, ureters, and bladder is variable; some segments of the urinary tract may be normal. The bladder may have a small luminal capacity, a thick trabeculated hyper-trophied muscle wall and diverticula. One or both ureters may be dilated from obstruction and/or reflux. The kidneys may be hydronephrotic and have dysplastic parenchyma. Sonographically, dysplastic parenchyma typically lacks normal corticomedullary differentiation, has hyperechoic and thinned cortex, and may have associated cysts. Bladder perforation can produce urinary ascites and calyceal perforation can result in peri-nephric urinoma.

## SUGGESTED READING

Lacher M, Stehr M, Schiessl B, Dietz HG. Fetal urinary bladder rupture and urinary ascites secondary to posterior urethral valves. A case report. Eur J Pediatr Surg 2007;17:217–220.

Levin TL, Han B, Little BP. Congenital anomalies of the male urethra. Pediatr Radiol 2007;37:851–862; quiz 945.

# CASE 16

**GEORGE S. BISSET III**

## HISTORY

A 9-month-old girl who presented in the neonatal period with profound cyanosis.

A

■**FIGURES 8-16A and 8-16B** Frontal and lateral chest radiographs at 1 day of age. The cardiac silhouette is slightly enlarged. The aortic arch is right sided. The pulmonary vascularity is slightly decreased. The main pulmonary artery segment is diminutive. No bony abnormalities are identified.

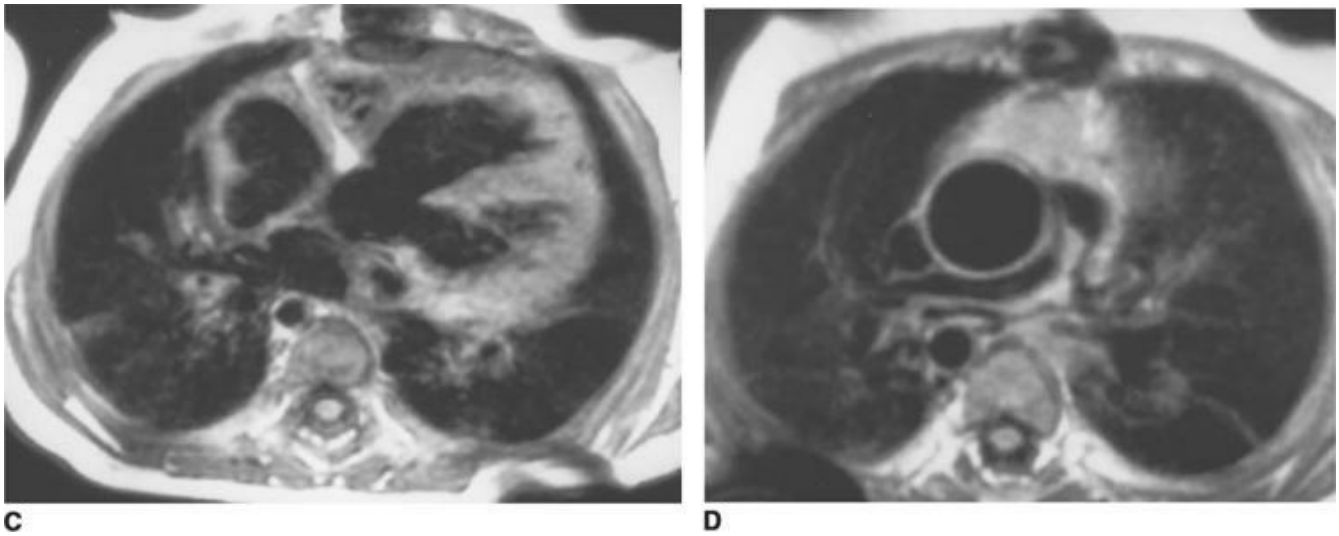


**FIGURES 8-16C and 8-16D** Axial T1-weighted MR images through the heart at 9 months of age. **C:** Axial view through the central cardiac region. A large subaortic VSD is noted. Right ventricular hypertrophy is present. The thickness of the right ventricular free wall is equal to that of the left ventricular free wall. **D:** Axial view through the pulmonary outflow tract. An artifact related to prior sternotomy for shunt placement is seen in the sternum. The ascending aorta is moderately enlarged. A right-sided aortic arch is present. The main pulmonary artery confluence is diminutive. The right and left pulmonary arteries are small and irregular.

## DIFFERENTIAL DIAGNOSIS

**Isolated pulmonic valve stenosis:** In this entity, the entirety of blood flow must pass through the lungs. Therefore, the typical finding is a dilated main pulmonary artery and occasionally dilated left pulmonary artery with normal pulmonary blood flow. A decrease in pulmonary blood flow would not be expected in the setting of isolated pulmonic valve stenosis (i.e., in the absence of an intracardiac shunt).

**Tetralogy of Fallot (TOF):** The combination of a large subaortic ventricular septal defect (VSD), right ventricular hypertrophy, and small pulmonary arteries is typical of this diagnosis. These findings are all present in the case illustrated, making this the most likely diagnosis. The majority of these patients have a left aortic arch, although 25% have a right aortic arch.

**Pulmonary valve atresia with intact ventricular septum:** The presence of cardiomegaly and diminished pulmonary blood flow on the radiographs raises this as a possible diagnosis. However, the presence of a large VSD on the MR scan excludes this diagnosis.

**Ebstein's anomaly:** Patients with Ebstein's anomaly usually present with cyanosis in the neonatal period and have marked right-sided cardiac chamber enlargement

(including both the right atrium and right ventricle) and diminished pulmonary blood flow (as a result of severe tricuspid regurgitation and right-to-left shunting across the atrial septum). This diagnosis is unlikely for two reasons: (1) cardiac size is usually (but not invariably) much larger than shown in Figure 8-16A—in particular, the right heart size is increased in Ebstein's anomaly but not in the case depicted here; and (2) the MR scan in this case shows an aorta overriding a VSD, not a feature of Ebstein's anomaly.

- **Tricuspid atresia:** These patients can present with cardiomegaly and diminished pulmonary blood flow. However, the presence of an otherwise normal, but thick-walled, right ventricular chamber on the MR examination in the case shown makes this an unlikely diagnosis.

## DIAGNOSIS

**TOF with diminutive pulmonary arteries following central shunt**

## KEY FACTS

### Clinical

- The finding of cyanosis indicates a right-to-left shunt or an admixture lesion.
- TOF can be associated with pulmonic stenosis at any of four levels: the infundibulum (most common), the pulmonic valve, the pulmonary trunk, or the pulmonary artery branches.
- If pulmonary atresia is present, the entire pulmonary blood flow is through collateral (i.e., bronchial) vessels that reach the pulmonary vasculature from the descending thoracic aorta.
- TOF is the most common malformation among cyanotic adults with congenital heart disease.

### Radiologic

- The ascending aorta and aortic knob are prominent in TOF because the aorta receives the vast majority of the blood flow from both ventricles.
- Cardiac size in TOF is usually normal because although right ventricular hypertrophy is present, little ventricular dilation is present.
- In the TOF variant, in which there is absence of the *pulmonic valve,* marked dilatation of the pulmonary trunk and its proximal branches can be seen, frequently resulting in compression of the airway.
- Occasionally, absence of a pulmonary artery branch is seen in TOF, usually involving

the side opposite the aortic arch.

- MR imaging can be a useful tool to determine the size of the pulmonary arteries, which is helpful for preoperative planning and evaluation of growth following a palliative procedure (e.g., after a systemic-arterial shunt). MR imaging also allows evaluation of important anatomic details—for example, whether the pulmonary arteries are confluent, which is a factor facilitating surgical repair.

## SUGGESTED READING

Bisset GS III. Magnetic resonance imaging of congenital heart disease. Radiol Clin North Am 1991;29:279–291.

Eichenberger AC, von-Schulthess GK. Magnetic resonance imaging of the heart and the great vessels: morphology, function, and perfusion. Curr Opin Radiol 1992;4:41–47.

Formanek AG, Witcofski RL, D'Souza VJ, et al. MR imaging of the central pulmonary arterial tree in conotruncal malformation. AJR Am J Roentgenol 1986;147:1127–1131.

Gaca AM, Jaggers JJ, Dudley LT, Bisset GS III. Repair of congenital heart disease: a primer. Radiology 2008;247:617–631.

# CASE 17

**GEORGE S. BISSET**

### HISTORY

A 12-year-old boy with a cardiac murmur.

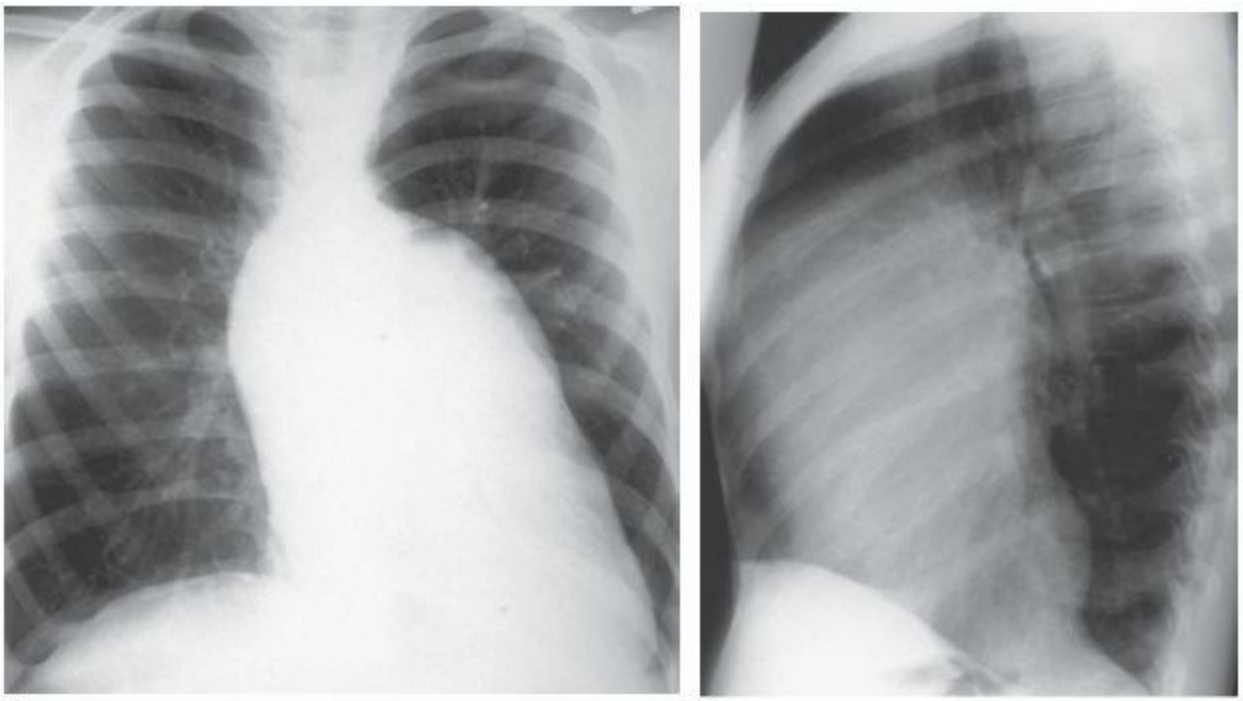


■**FIGURES 8-17A and 8-17B** Frontal and lateral chest radiographs. The left cardiac border has an unusual contour, with increased tissue in both the retrosternal clear space and posteriorly in the location of the left ventricle.

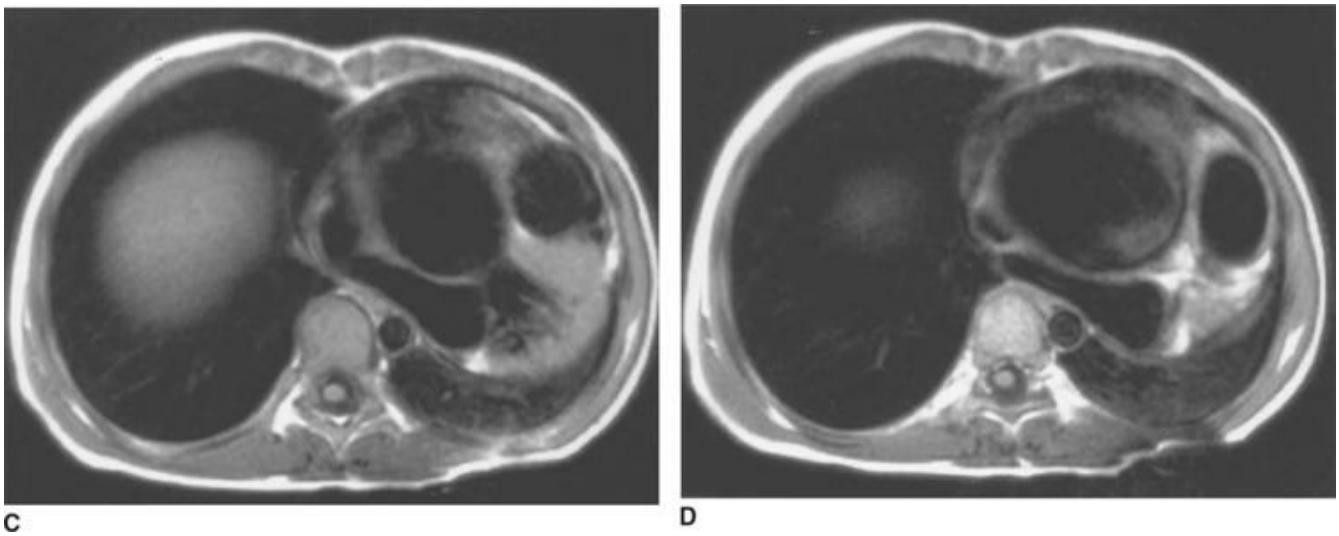


■**FIGURES 8-17C and 8-17D** Axial cardiac-gated T1-weighted MR images at the level of the aortic valve at **(C)** and just above **(D)** the sinus of Valsalva. Marked enlargement of the ascending aorta above the sinus of Valsalva is seen. The descending aorta is normal in caliber. The left atrium is compressed by the enlarged ascending aorta. On other images (not shown), the left ventricle was seen to be enlarged.

## DIFFERENTIAL DIAGNOSIS

- **Anterior mediastinal mass:** An anterior mediastinal mass might be suspected because of the frontal chest radiograph findings. However, the lateral radiograph shows that some of the abnormal density is in the posterior mediastinum (as well as the anterior mediastinum), near the location of the left ventricle. Furthermore, an anterior mediatinal mass would not account for the clinical history of a cardiac murmur. Finally, the MR study definitively shows that a structural cardiovascular lesion, rather than a mass, is present.
- **Ascending aortic aneurysm:** The MR findings explain the unusual appearance of the chest radiograph by showing that the anterior soft tissue seen on the chest radiograph is the ascending aortic aneurysm. The left ventricle enlargement is due to aortic regurgitation. This diagnosis best accounts for the imaging findings.
- **Aortic stenosis:** The enlargement of the ascending aorta in this case could potentially be due to the jet effect of aortic stenosis. However, at a point at which the aorta is enlarged to the degree shown in the illustrated case, clinical symptoms and signs (e.g., dyspnea, exertional chest pain, syncope, or an apical systolic ejection murmur) would be expected to be quite evident. This diagnosis is incorrect.

## DIAGNOSIS

**Ascending aortic aneurysm due to Marfan syndrome**

## KEY FACTS

### Clinical

- Aneurysms of the ascending aorta are rare in children but are much more common in adults (in whom the most common etiology is atherosclerotic disease).
- Ascending aortic aneurysms in children are usually due to a genetic disease such as Marfan syndrome, cutis laxa, pseudoxanthoma elasticum, osteogenesis imperfecta (OI), Ehlers-Danlos syndrome, homocystinuria, Noonan's syndrome, and Turner's syndrome.
- Marfan syndrome is a disease in which an abnormality of the elastic media is present. The term "cystic medial necrosis" has been used to describe the underlying abnormality; however, the term is a misnomer because necrosis is not present. Other major cardiac anomalies in Marfan syndrome are aortic valve and mitral valve insufficiency as well as dissection of the aneurysm.
- Ehlers-Danlos syndrome represents a group of related collagen disorders in which hyperelasticity and joint laxity are typical clinical features.
- In homocystinuria, mental retardation is typically present, unlike in the case

illustrated.

- Osteogenesis imperfecta type 1 is associated with aortic root dilatation. A clinical history of fractures or blue sclera (which are not present in the case illustrated) is typically found.
- Aortic surgery or replacement of the aortic valve or mitral valve is rarely necessary before adolescence in Marfan syndrome. On the other hand, in the adolescent or adult, repair of the ascending aorta usually is performed for an aneurysm of 6.0 cm or greater.

## Radiologic

- Plain radiographs are sometimes used as the initial imaging technique for detection of an ascending aortic aneurysm. However, they are insensitive for detection of an aneurysm and have little value in patient assessment.
- Echocardiography is a widely-used noninvasive tool for determining the dimensions of an ascending aortic aneurysm, detecting the presence of valvular regurgitation, and evaluating left ventricular function.
- MR imaging is recommended in patients in whom the acoustic window is limited (including Marfan syndrome, where pectus deformity may limit evaluation, thereby precluding effective use of sonography) and in those with known dilation of the ascending aorta and acute chest pain (in whom aortic dissection is suspected).
- MR imaging for evaluation of an ascending aortic aneu-rysm should be performed using a combination of transaxial, coronal, and sagittal cardiac-gated T1-weighted sequences. Gradient-recalled (so-called bright blood) pulse sequences may also be helpful, particularly in a cine mode.
- Catheter angiography can give much of the same information as MR imaging. However, given the increased risk of aortic injury in a patient with a known aortic aneurysm or suspected dissection, noninvasive imaging techniques are preferred.

# SUGGESTED READING


Bank ER. Magnetic resonance of congenital cardiovascular disease. Radiol Clin North Am 1993;3:553–572.

Bisset GS. Magnetic resonance imaging of congenital heart disease in the pediatric patient. Radiol Clin North Am 1991;29:279–291.

Fellows KE, Weinberg PM, Baffa JM, Hoffman EA. Evaluation of congenital heart disease with MR imaging: current incoming attractions. AJR Am J Roentgenol 1992;159:925–931.

Pierpont MEM, Moller JH. Cardiac manifestations of genetic disease. In GC Emmanouilides, HD Allen, TA Reimenschneider, HP Gutgesell (eds), Moss and Adam's Heart Disease in Infants, Children, and Adolescents Including the Fetus and Young Adult (5th ed). Baltimore, MD: Williams & Wilkins, 1995; 1486–1520.

Woodard PK, Bhalla S, Javidan-Nejad et al. Cardiac MRI in the management of congenital heart disease in children, adolescents, and young adults. Curr Treat Options Cardiovasc Med 2008;10:419–424.

# CASE 18

**ANA M. GACA**

## HISTORY

A 4-year-old Caucasian boy with left hip pain and a limp, with no clinical or laboratory findings to suggest infection.


■**FIGURE 8-18A** Anteroposterior view of the pelvis shows the left femoral head is reduced in height and subchondral lucencies are present within it.


■**FIGURE 8-18B** Frog leg lateral view of the left hip shows the deformity of the left

femoral head and the subchondral lucencies to better advantage. These findings are consistent with avascular necrosis.


**FIGURE 8-18C** Anteroposterior view of the pelvis performed on the same patient 3 months later shows further reduction in height and sclerosis of the left femoral head.


**FIGURE 8-18D** Frog leg lateral view of the left hip performed at the same time as **(C)** shows fragmentation of the left femoral head. In combination, these findings are consistent with progression of avascular necrosis.

## DIFFERENTIAL DIAGNOSIS

For this case, a differential diagnosis can be generated based on either the avascular necrosis or the epiphyseal fragmentation. The differential diagnosis for avascular necrosis of the hip in a child includes the following:

- **Sickle cell anemia:** Bony changes associated with sickle cell hemoglobinopathies can include sclerosis, “bone-within-bone” appearance in the femurs, and perios-teal reaction (from acute infarction or, less commonly, osteomyelitis). None of those changes are present in the case shown here. Furthermore, the child is Caucasian. This diagnosis is incorrect.
- **Trauma:** Trauma can produce some of the changes shown in this case. However, no history of trauma is provided, making this diagnosis unlikely.
- **Osteomyelitis:** Osteomyelitis can cause changes that mimic avascular necrosis. Clinical and laboratory features (including elevation of the sedimentation rate) consistent with infection are typically present. However, no clinical features suggestive of infection are provided in this case, making the diagnosis unlikely. In equivocal cases where infection appears to be a possibility, osteomyelitis can be distinguished from avascular necrosis by a bone scan that showed increased radiotracer activity in all phases of a three-phase scan. This test would be helpful unless mechanical factors related to infection, for example, infectious synovitis, produced decreases in the vascular supply of the femoral head.
- **Gaucher’s disease:** This entity can produce osteone-crosis but other typical features of Gaucher’s disease, for example, expanded medullary cavities with a thin cortex, osteopenia, and absence of normal metaphyseal widening, are not present in the case shown. This diagnosis is unlikely.
- **Legg-Calvé-Perthes (Legg-Perthes) disease:** This disease produces deformity of the epiphysis and subchon-dral lucencies due to avascular necrosis and typically occurs in Causcasian boys in the 4 to 8 years age range (consistent with the clinical history in the case presented). This diagnosis is the most likely.

Diagnostic considerations for causes of a fragmented epi-physis include the following:

- **Hypothyroidism:** This disease produces fragmentation in both femoral heads at the onset of ossification. However, in the case shown, the right femoral head is normal in appearance, making this diagnosis unlikely.
- **Multiple epiphyseal dysplasia:** This disease produces bilateral, symmetric epiphyseal fragmentation; the fragments often coalesce over time and mimic the coxa magna appearance seen in late Legg-Perthes disease. However, unilateral findings in the case shown here make this diagnosis unlikely.
- **Legg-Calvé-Perthes disease:** In advanced stages of this disease, fragmentation of epiphyses can occur. Unlike hypothyroidism and multiple epiphyseal dysplasia, findings of Legg-Perthes are usually unilateral, making it a realistic diagnostic possibility in the case presented here. Furthermore, it is the only entity on both differential diagnosis lists (i.e., as a cause of both fragmented epiphyses and avascular necrosis of the hip), making it the most likely diagnosis.

# DIAGNOSIS

**Legg-Calvé-Perthes (or Legg-Perthes) disease**

# KEY FACTS

## Clinical

- The age range for Legg-Perthes disease extends from 2 years of age to the early teenage years; however, most cases occur between 4 and 8 years of age. Legg-Perthes disease is most common in Caucasian boys. The male-to-female ratio is 4:1.
- Changes occur bilaterally in about 10% of cases, but usually not simultaneously. If bilateral and simultaneous, one should consider other entities such as sickle cell disease, steroid use, Gaucher's disease, or multiple epiphyseal dysplasia.
- Signs and symptoms include limp, pain, thigh and buttock atrophy, and limited internal rotation. Pain may be centered about the hip and/or groin, or referred to the knee, medial thigh, or buttock.
- Poor prognosis is associated with the onset of symptoms after 8 years of age, lateral hip subluxation and involvement of more than 50% of the femoral head.

## Radiologic

- Radiographic evaluation should include both an anterior-posterior view and a frog leg lateral view of the hips.
- Early radiographic findings may include a small and sclerotic femoral head, widening of the joint space medially and lateral displacement of the femoral head, reflective of edema of either or both the acetabular fossa tissues and a small joint effusion.
- The "cresent sign" appears following the sclerotic phase, and reflects fracture of the softened, avascular femoral head. It usually begins laterally and is more easily detected with a frog leg lateral view.
- A large area of collapse of the femoral head, extensive subchondral lucency, lateral epiphyseal extrusion, and calcification lateral to the femoral head are radiographic signs associated with poor prognosis.
- Proper scintigraphic assessment necessitates meticulous technique, using pinhole collimation.
- The scintigraphic pattern depends on whether the predominant means of repair is recanalization or neovascularization. With recanalization, radiotracer activity is first seen laterally; with neovascularlization, radiotracer activity proceeds superiorly from

the physis.

- MR imaging is particularly valuable in assessing articular cartilage. However, the loss of marrow signal in the femoral head seen in Legg-Perthes disease is nonspecific and can be seen in tumor, trauma, and edema from other causes. Nevertheless, MR imaging is currently favored over scintigraphy in evaluation of possible Legg-Perthes disease.

## SUGGESTED READING

Gough-Palmer A, McHugh K. Rational imaging: investigating hip pain in a well child. BMJ 2007;334:1216–1217.

Lee MC, Eberson CP. Growth and development of the child's hip. Orthop Clin North Am 2006;37:119–132.

Skaggs DL, Tolo VT. Legg-Calvé-Perthes disease. J Am Acad Orthop Surg 1996;4:9–16.

# CASE 19

**CAROLINE CARRICO**

### HISTORY

A 3-week-old neonate who was born after a 28-week-gestation period. The infant has feeding intolerance, abdominal distention, and guaiac-positive stools.

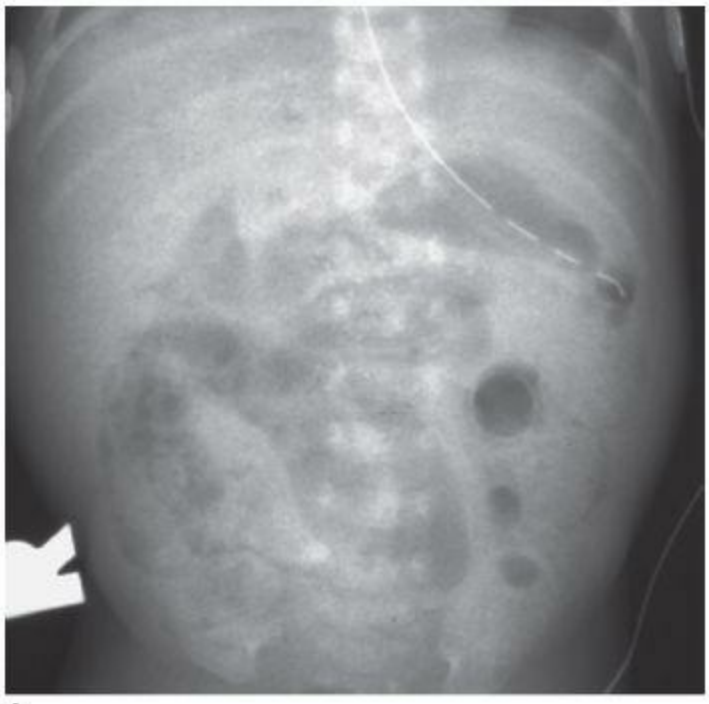

A

**FIGURE 8-19A** Supine abdominal radiograph: Gaseous distention of the stomach is present with bubbly lucencies seen in the right lower quadrant. Some separation of bowel loops can be noted in the right mid-abdomen, which could indicate bowel wall thickening.

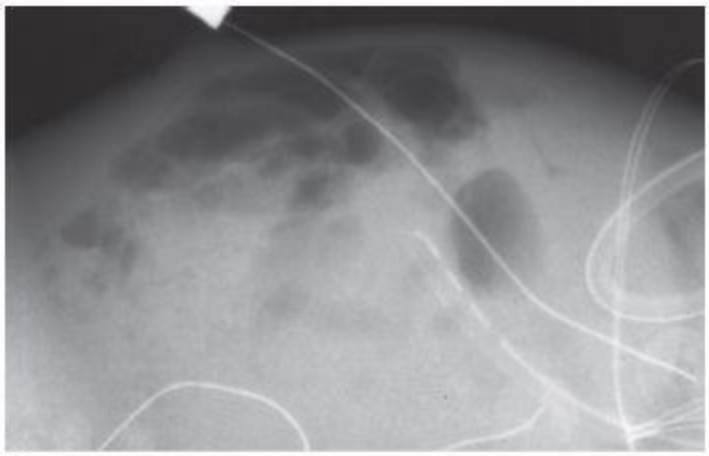

B

**FIGURE 8-19B** Cross-table lateral view of the abdomen shows free intraperitoneal air. In addition, air is present within the bowel lumen but also outside of the bowel wall (the so-called Rigler's sign). A crescentic lucency is present in the lower anterior pelvis, which is within bowel wall, likely between the muscle and serosa. Bubbly lucencies are also present, which in this setting are due to submucosal pneumatosis intestinalis.

## DIFFERENTIAL DIAGNOSIS

The differential diagnosis is focused on causes of decreased bowel motility, blood in the stool, and bubbly lucencies on abdominal radiographs in a preterm neonate.

**Necrotizing enterocolitis (NEC):** NEC usually has onset in the period between the first few days of life and the first few weeks of life. In this disease process, a combination of ischemia and infection can affect both the small bowel and large bowel. Typical radiographic findings include focally dilated loops of bowel with wall thickening and pneumatosis intestinalis. In severe cases, portal venous gas and pneumoperitoneum may develop due to bowel ischemia and perforation, respectively. Many of these findings are present in the case shown here; NEC is therefore the most likely diagnosis in this case.

**Malrotation with midgut volvulus:** Unlike the case shown here, infants with malrotation and midgut volvulus typically have normal abdominal radiographs and bilious vomiting. In addition, pneumatosis intestinalis and bowel perforation with pneumoperitoneum, which is present in the case shown, is very unusual in malrotation

with midgut volvulus. This diagnosis is incorrect.

- **Meconium ileus:** In meconium ileus, abnormalities are typically seen within the first few days of life after feeding is initiated (unlike the case shown here). This entity classically presents as distant bowl obstruction. Bubbly lucencies can be seen in the right lower quadrant on initial radiographs due to swallowed air mixing with obstructing meconium in the terminal ileum. However, in the case depicted here, air is present within the bowel wall, which would not be expected in meconium ileus. Meconium ileus is a very unlikely diagnosis in the case shown here.

## DIAGNOSIS

**Necrotizing enterocolitis**

## KEY FACTS

### Clinical

- The exact pathophysiology of NEC is not clear and likely multifactorial; however, it appears to be related to intestinal mucosal ischemic injury with subsequent bacterial invasion of the bowel wall.
- Most cases of NEC occur in preterm infants during the first few weeks of life.
- *Term* infants that develop NEC usually have an underlying abnormality of the cardiovascular system and/or immune system.
- NEC affects 1% to 5% of all neonates admitted to an intensive care nursery.
- Some clinical signs and symptoms of NEC include abdominal distention, intolerance of feeds, diarrhea, and gross blood within the stool.
- The mortality rate increases when perforation of the bowel occurs.
- Patients with NEC are at increased long-term risk of bowel strictures and adhesions.
- Severe cases may result in short-gut syndrome.
- Infants with NEC are typically treated with bowel rest (e.g., parental feeding), stomach decompression, and antibiotics.

### Radiologic

- In patients with suspected or early findings of NEC, serial anteroposterior and cross-table lateral abdominal radiographs are usually obtained at 6- to 8-hour intervals as part of a "NEC watch" to monitor response to medical treatment.
- After initial radiographic improvement, serial films are then typically performed every 12 to 24 hours. As clinical symptoms diminish, the interval between films can be

increased.

- Early in the course of the disease, mild or moderate generalized gaseous distention of the bowel is seen. Later, a focal ileus may be evident with a few dilated loops of bowel, sometimes with bowel wall thickening and separation of bowel loops.
- The term "fixed loop of bowel" refers to a loop whose appearance does not alter between imaging examinations.
- Submucosal gas has a bubbly appearance similar to that of bowel gas mixed with stool. The general appearance of the rest of the bowel gas pattern and the condition of the baby often help to differentiate NEC from a normal infant. When intramural gas enters the subse-rosal space in NEC, the serosa and muscle in the bowel wall are separated, which is typically seen as a well-defined, circumferential crescent of air.
- Pneumoperitoneum is best seen on a left-side-down decubitus view of the abdomen.
- Many of the characteristic features of NEC, for example, air within the bowel wall of within the portal vein, free or loculated fluid, bowel wall thickening and abnormalities of bowel wall perfusion, can be assessed using sonography.
- Bowel perforation can occur without radiographic or sonographic evidence of free air.
- Enteric contrast studies are not typically performed to assess infants with acute NEC.
- After infants have recovered from NEC, if they are not tolerating feeds or have clinical or radiographic findings suggestive of a partial bowel obstruction, evaluation of the small bowel and/or colon with water-soluble contrast agents is often performed to look for bowel strictures or adhesions. Such studies are also performed for preoperative planning in infants who will undergo reversal of an ostomy and bowel reanastamosis.

## SUGGESTED READING

Coursey CA, Hollingsworth CL, Gaca AM, et al. Radiologists' agreement when using a 10-point scale to report abdominal radiographic findings of necrotizing enterocolitis in neonates and infants. AJR Am J Roentgenol 2008;191:190–197.

Kim WY, Kim WS, Kim IO, et al. Sonographic evaluation of neonates with early-stage necrotizing enterocolitis. Pediatr Radiol 2005;35: 1056–1061.

Silva CT, Daneman A, Navarro OM, et al. Correlation of sonographic findings and outcome in necrotizing enterocolitis. Pediatr Radiol Mar 2007; 37:274–282.

# CASE 20

**CAROLINE CARRICO**

**HISTORY**

A newborn boy with delayed passage of meconium.

A

■**FIGURE 8-20A** Supine abdominal radiograph shows both an enteric tube with its tip in the stomach and an umbilical venous catheter. Gaseous distention of numerous loops of bowel is present, an indication that if bowel obstruction is present, the site of obstruction is very distal.

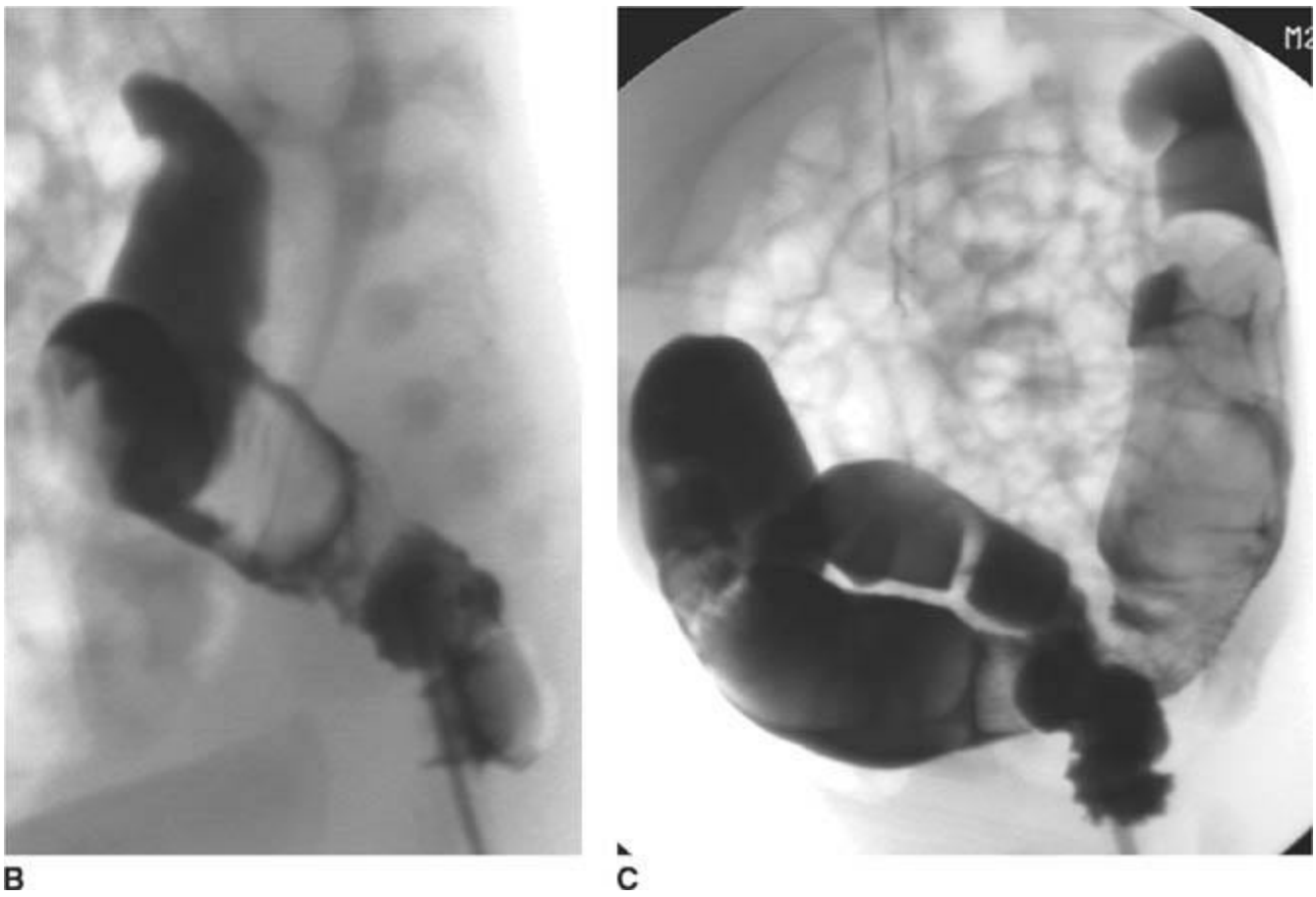


**FIGURES 8-20B and 8-20C** Images from a low-osmolality water-soluble contrast enema. **B:** A lateral early filling image and **(C)** is an AP supine image. The images show that the descending colon and sigmoid colon are markedly distended with meconium. A cone-shaped transition from normal caliber sigmoid colon to small caliber rectum is present at the rectosigmoid junction. A serrated appearance of the rectal mucosa is present, due to irregular contractions of the rectal wall smooth muscle.

## DIFFERENTIAL DIAGNOSIS

The differential diagnosis for delayed passage of meconium in a newborn typically includes Hirschsprung's disease, meconium ileus, functional immaturity of the colon, jejunal or ileal atresia, and imperforate anus/anorectal malformations. One distinguishing radiologic feature among these diseases is the appearance on a contrast enema examination, in which the rectum would be expected to be more distensible than the sigmoid colon in all entities except Hirschsprung's disease.

**Hirschsprung's disease (aganglionosis):** In Hirschsprung's disease, contrast enema studies typically show a distal bowel obstruction in a neonate, with a relatively small caliber rectal segment that is smaller than or of equal caliber to the sigmoid colon. An aganglionic segment of bowel is relatively nondistensible and the normal segment of bowel becomes distended with meconium or stool. This feature results in a "cone-

shaped" transition zone. The aganglionic bowel may have irregular spasmodic contractions that result in a saw-tooth appearance of the involved bowel segment. Although this finding is not common, when present, it supports the diagnosis of Hirschsprung's disease. These features are present in the case shown, making this diagnosis the most likely consideration.

- **Allergic colitis:** In babies with allergic colitis, the rectum is primarily affected. The contrast enema examination typically reveals irregularity of the affected rectal mucosa with luminal narrowing, which can overlap with the findings of Hirschsprung's disease. However, allergic colitis would not be expected to present in the immediate neonatal period. Furthermore, the radiographic findings standardly only develop after feeding. This diagnosis is not a likely consideration in the case presented here.

## DIAGNOSIS

**Hirschsprung's disease**

## KEY FACTS

### Clinical

- Hirschsprung's disease is the most common congential cause of distal bowel obstruction in the *term* neonate.
- The embryologic basis of Hirschsprung's disease is related to the fact that, during normal development, neural crest cell derivatives migrate from the mouth to the anus and form the myenteric and submucosal plexus of the bowel. In Hirschsprung's disease, a migra-tional arrest produces aganglionosis of the distal bowel; this segment of bowel does not function normally.
- Hirschsprung's disease is associated with Trisomy 21 and defects in neural crest migration and tumors of neural crest origin (so-called neurocristopathies).
- Symptoms begin in the newborn period and are manifested by delayed passage of meconium, chronic constipation, and emesis that may be bilious.
- Up to one-third of children with Hirschsprung's disease develop enterocolitis.

### Radiologic

- In the neonate with Hirschsprung's disease, radiographs show a large number of gas-distended loops of bowel, indicative of the presence of a distal bowel obstruction (as in the case illustrated here).
- A water-soluble contrast enema study can aid in the diagnosis. However, the following precautions must be taken: The colon should not be prepared via a cleansing

enema and a balloon catheter, which could perforate the rectum, should not be used.

- Lateral and AP views of the rectosigmoid colon during a contrast enema study are obtained to assess the rectosig-moid index. In normal children, the rectum is readily distensible and has a larger diameter than the sigmoid colon. However, in Hirschsprung's disease, the caliber of the rectum is small and the rectum does not easily distend.
- A contrast enema usually shows a cone-shaped transition zone near the junction of the nondistensible aganglionic bowel and the distended meconium/stool filled normal bowel. The transition zone may underestimate the length of aganglionic bowel in infants with *long segment* disease.
- Hirschsprungs disease is subtyped by the length of the aganglionic segment. Ultrashort-segment disease, which is rare, is limited to the internal sphincter and up to 4 cm of the distal rectum, which may appear normal on contrast enema examinations.
- Approximately 75% to 80% of cases of Hirschsprung's disease are described by the term short-segment disease. This form of the disease is typically described as affecting bowel distal to the mid-sigmoid colon; however, some define short-segment disease as extending to the junction of the sigmoid colon and the descending colon.
- Long-segment Hirschsprung's disease extends beyond the limits of short-segment disease but does not involve the entire colon.
- Total colonic Hirschsprung's disease, which can extend to involve a portion of the terminal ileum, is radio-graphically unique in a few ways. The appearance of the colon on contrast enema study may be normal, may appear "short" due to lack of redundancy, or produce the appearance of a so-called microcolon. In infants with the microcolon appearance, intraluminal calcified enteric contents may be present in the terminal ileum and a transition zone seen at the terminal ileum. Furthermore, pneumoperitoneum may occur, even in the absence of colitis.
- In some cases of Hirschsprung's disease, irregular contractions of the aganglionic bowel give the mucosa a saw-tooth appearance on contrast enema studies, which can simulate the appearance of allergic colitis (typically due to an allergy to cow milk protein).
- In some cases, Hirschsprung's disease may be present even in the setting of a normal contrast enema study. Thus, in neonates and young children with symptoms that may be referable to Hirschsprung's disease (e.g., delayed passage of meconium, chronic constipation, with or without emesis) and a normal contrast enema study, the next appropriate step in establishing the diagnosis is suction biopsy of the colonic mucosa.

## SUGGESTED READING

Bloom DA, Buonomo C, Fishman SJ, et al. Allergic colitis: a mimic of Hirschsprung disease. Pediatr Radio l 1999;29:37–41.

Cowles RA, Berdon WE, Holt PD, Buonomo C, Stolar CJ. Neonatal intestinal obstruction simulating meconium ileus in infants with long-segment intestinal aganglionosis: radiographic findings that prompt the need for rectal biopsy. Pediatr Radiol 2006;36:133–137.

Jamieson DH, Dundas SE, Belushi SA, et al. Does the transition zone reliably delineate aganglionic bowel in Hirschsprung's disease? Pediatr Radiol 2004;34:811–815.

Reid JR, Buonomo C, Moreira C, et al. The barium enema in constipation: comparison with rectal manometry and biopsy to exclude Hirschsprung's disease after the neonatal period. Pediatr Radiol 2000;30:681–684.

# CASE 21

**CAROLINE CARRICO AND DONALD FRUSH**

## HISTORY

A 5-year-old girl with chronic asthma-like symptoms and exercise intolerance.

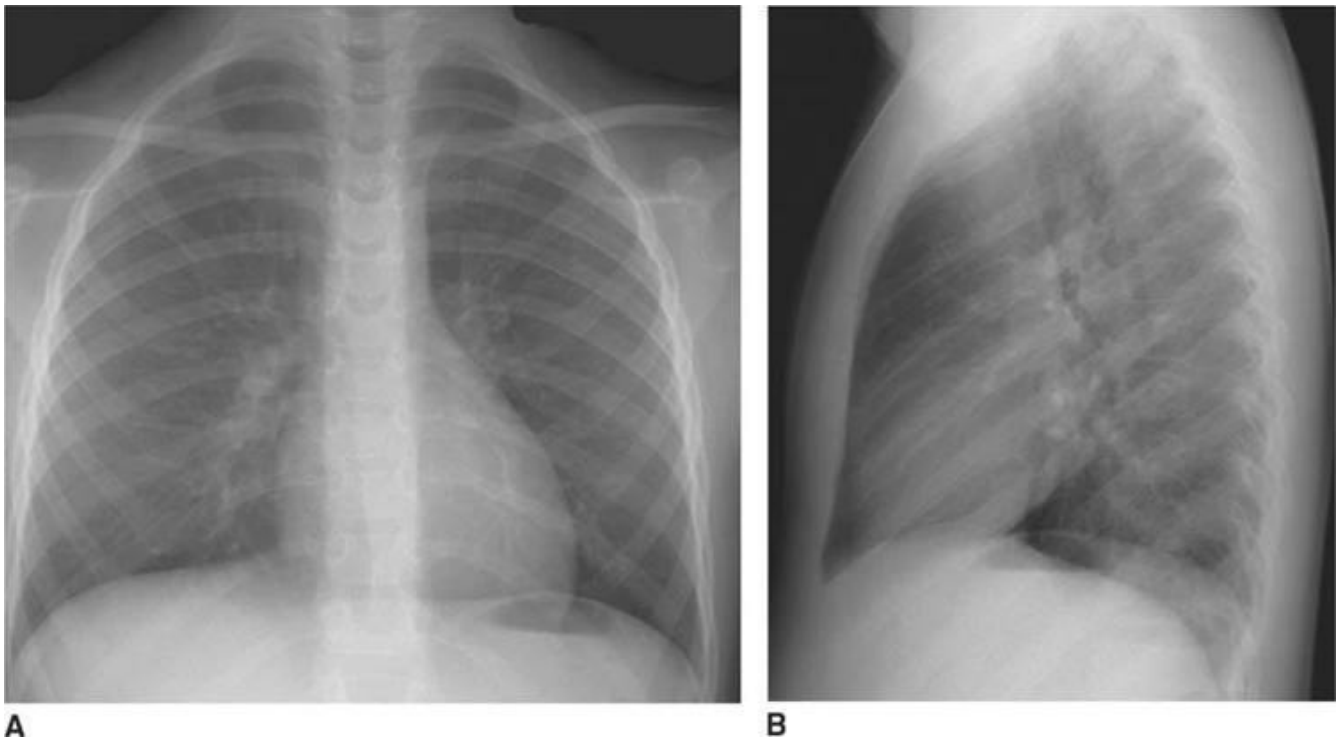


**FIGURES 8-21A and 8-21B** PA and Lateral radiographs. The only abnormality is the subtle finding of a soft tissue density between the trachea and the esophagus just above the trachea, which is seen on the lateral view only.

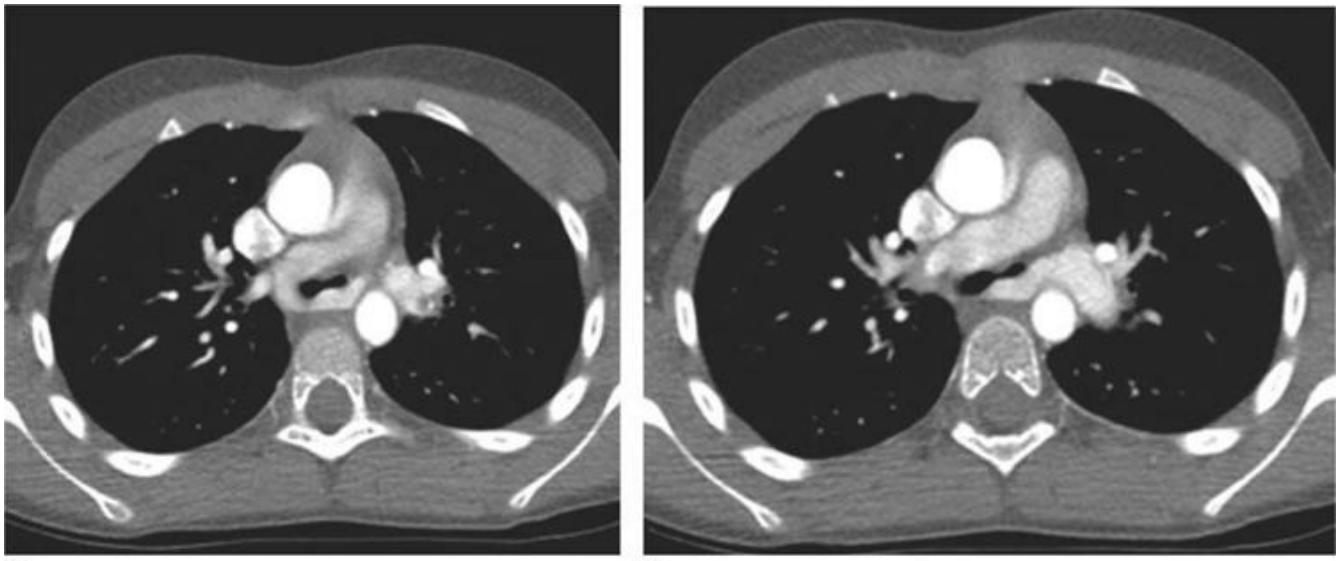


**FIGURE 8-21C and 8-21D** Two axial images from a CT arteriogram show an abnormal origin of the left pulmonary artery, which originates from the posterior wall of the right pulmonary artery. The left pulmonary artery crosses the mediastinum, passing between the trachea and esophagus, to supply the left lung. The distal trachea and carina are compressed by the pulmonary arteries.

## DIFFERENTIAL DIAGNOSIS

The differential diagnosis in the case shown here is focused on vascular causes of airway compression.

**Pulmonary sling (i.e., aberrant origin of left pulmonary artery from the right pulmonary artery):** In this entity, a pulmonary artery with an aberrant origin courses between the trachea and the esophagus. The aberrant artery may compress portions of the tracheo-broncheal tree resulting in air trapping and/or atelecta-sis. In the case shown here, an aberrant left pulmonary artery does arise from the right pulmonary artery and courses between the trachea and the esophagus to supply the left lung. This diagnosis is correct.

**Complete vascular rings causing airway compression:** Complete vascular rings encircle the trachea and esophagus and can cause severe respiratory compromise and/or dysphagia. The two major types are the double aortic arch and a right aortic arch with anomalous left subclavian artery and ligamentum arterio-sum. With a double aortic arch, the effect on the lungs is usually symmetric and two arches will be present, therefore this is not a consideration in this case. A right aortic arch with anomalous left subclavian artery and ligamentum arteriosum also forms a complete vascular ring around the trachea and esophagus. In the case shown here, the child has a left aortic arch (rather than a double aortic arch or a right aortic arch), thereby excluding both causes of a complete vascular ring.

- **Tracheal compression by the brachiocephalic artery:** This vascular anomaly can cause stridor, usually evident by 6 months of age. However, one would expect to see compression by the brachiocephalic artery rather than the pulmonary artery. This diagnosis is incorrect.
- **Other anatomic causes:** Other vascular causes of tracheal compression include enlargement or midline position of the aorta, enlargement of the left atrium, and other mediastinal mass. None of these features are present in the case shown. These diagnoses are incorrect.

## DIAGNOSIS

**Aberrant left pulmonary artery (pulmonary artery sling)**

## KEY FACTS

### Clinical

- Vascular "rings" and "slings" vary in their mass effect on the trachea and esophagus. Therefore, they can clinically present with a wide range of symptoms and at any age. These entities often produce respiratory symptoms, chiefly stridor, in infants and young children. Apnea may occur during feeding. Respiratory compromise may be life-threatening. Older children can present with nonspecific findings such as an asthma-like cough, recurrent bronchopulmonary infections, wheezing, stridor, exercise intolerance, snoring with night time wakening, or dysphagia. Many of the symptoms are similar to asthma, and children may be initially misdiagnosed if imaging studies are not performed.
- Bronchoscopy for evaluation of stridor may provide the first evidence of a vascular anomaly by showing an extrinsic, pulsatile mass compressing the trachea or a major bronchus.
- Rings and slings are often associated with tracheomalacia. In some infants, the trachea progressively spontaneously repairs with age after repair of the vascular anomaly. For other children, surgical reconstruction of the airway is necessary.
- A pulmonary sling is occasionally associated with TOF.

### Radiologic

- Vascular rings and slings may be diagnosed prenatally by echocardiography.
- In infants, barium esophogram and airway fluoroscopy will show the characteristic extrinsic compression of the esophagus and or trachea caused by a vascular ring (aortic arch/arch vessel variant) or vascular sling (aberrant pulmonary artery).

- CT and MR imaging are performed in infants or older children in whom the sonographic window for optimal echocardiography is limited due to a relatively small amount of thymic tissue or due to hyperinflated lungs.
- A pulmonary sling is a relatively rare anomaly and is associated with airway compromise. Associated tra-cheobronchial anomalies include tracheomalacia, complete cartilaginous rings, stenosis, bronchial atresia, and aberrant origins of bronchi. Aberrant bronchi may be as simple as a tracheal bronchus or more complex such as a bridging bronchus that crosses the mediastinum to supply one or more lobes on the opposite side.
- CT angiography can be performed quickly, thus obviating the need for sedation in most cases. Multiplanar reconstruction and 3D volume-rendered images are useful for preoperative planning.
- MR imaging provides excellent visualization of cardiovascular anatomy; however, relative to CT, evaluation of the pulmonary parenchyma is poor. MR imaging often requires sedation or general anesthesia for infants and young children. Sedation can be problematic in children with airway compromise.

## SUGGESTED READING

du Plessis AM, Andronikou S, Goussaard P. Bridging bronchus and sling left pulmonary artery: a rare entity demonstrated by coronal CT with 3-D rendering display and minimal-intensity projections. Pediatr Radiol 2008;38:1024–1026.

Hernanz-Schulman M. Vascular rings: a practical approach to imaging diagnosis. Pediatr Radiol 2005;35:961–979.

Yu JM, Liao CP, Ge S, et al. The prevalence and clinical impact of pulmonary artery sling on school-aged children: a large-scale screening study. Pediatr Pulmonol 2008;43:656–661.

# CASE 22

**DONALD P. FRUSH**

### HISTORY

An 18-month-old girl with fever.

A

■**FIGURE 8-22A** Frontal chest radiograph shows bilateral widening of the posterior mediastinum at the lung bases.

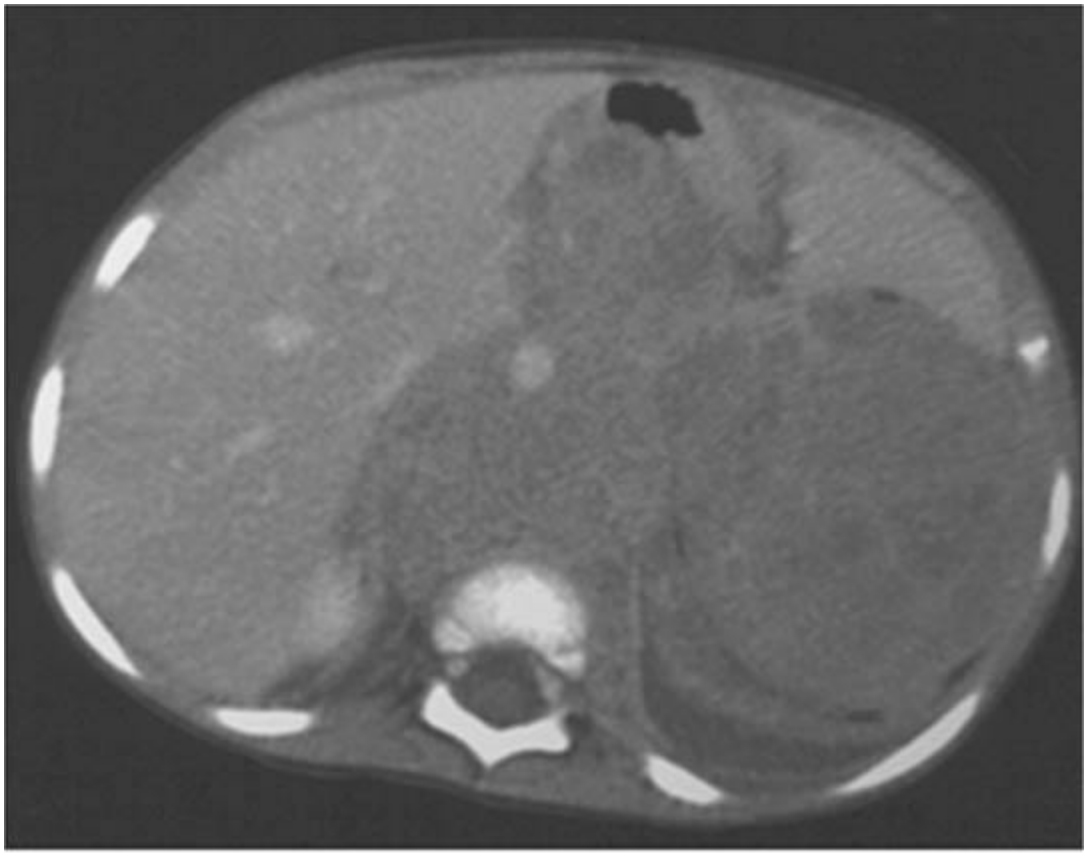

B

■**FIGURE 8-22B** Contrast-enhanced axial CT image at the level of the upper abdomen shows a large heterogeneous soft tissue mass that was subsequently determined to arise from the adrenal gland.

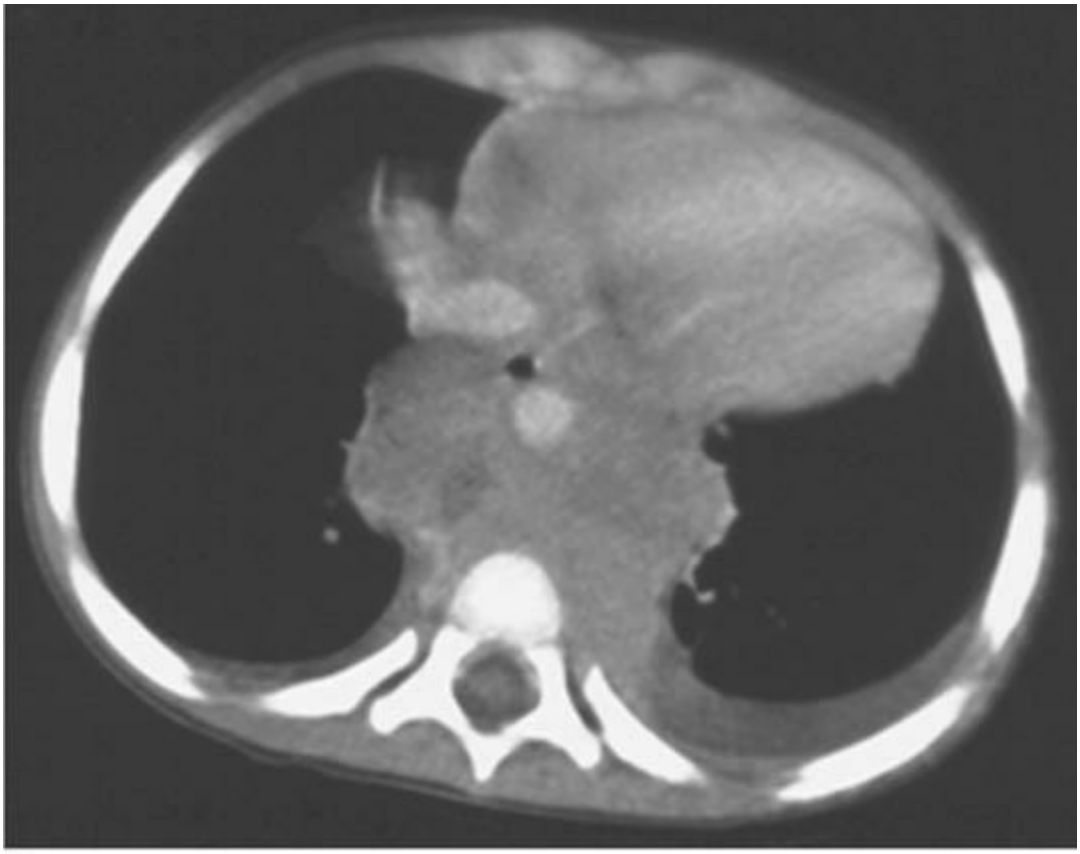

C

**FIGURE 8-22C** Axial CT image from the same CT scan as Figure 8-22B shows the mass involving both the posterior and middle mediastinal compartments, representing adenopathy from the mass shown in Figure 8-22B, and a small left pleural effusion.

## DIFFERENTIAL DIAGNOSIS

The major categories of entities to be considered in this case include abnormalities of pulmonary origin, anomalies of gastrointestinal/foregut origin, vascular abnormalities, and mediastinal adenopathy.

### Abnormalities of Pulmonary Origin

- **Bilateral lower lobe atelectasis:** This diagnosis is unlikely, given the fact that the lesion has a lobular contour, especially on the right (producing two densities behind the heart).
- **Lobulated pleural effusions:** This diagnosis is unlikely, given the double density seen on the right. In the absence of any prior medical history, effusions would likely be more dependent in nature.
- **Bilateral pulmonary sequestration:** The lesion depicted in this case is elongated, which would be unusual for sequestration. This diagnosis is extremely unlikely.

## Anomalies of Gastrointestinal/Foregut Origin

- **Bronchial pulmonary foregut malformation:** Bronchial pulmonary foregut malformations (e.g., a bron-chogenic cyst or esophageal duplication cyst) account for 15% of mediastinal masses in children. Most (50% to 80%) of foregut cysts are symptomatic. Those that are symptomatic are generally discovered before the age of 5. However, such a lesion would not be expected to be bilateral and appear as a solid mass. This diagnosis is unlikely.
- **Esophageal abnormality:** Esophageal dilation, for example, produced by achalasia, could produce an opacity on chest radiographs. However, the double density seen on the patient's right is not characteristic of an esophageal mass.

## Vascular Abnormalities

- **Descending thoracic aortic aneurysm:** An aneurysm of the descending aorta would be the most likely vascular abnormality to present as a middle mediastinal mass. However, the double contour would be unusual; furthermore, no history predisposing to the presence of an aneurysm is provided. The diagnosis of aneurysm is not compatible with the history of fever. This diagnosis is unlikely.

## Mediastinal Adenopathy

- **Middle and posterior mediastinal mass due to adenopathy:** This consideration is a reasonable one because the mass obliterates the normal paraspinal lines. Given the fact that the mass is bilateral, mediastinal adenopa-thy is the leading consideration for this case.

## DIAGNOSIS

**Middle and posterior mediastinal adenopathy secondary to metastatic neuroblastoma.**

## KEY FACTS

## Clinical

- Masses of the middle mediastinum are in general due to one of two major groups: congenital abnormalities (e.g., neurenteric cyst, esophageal duplication cyst, bronchogenic cyst) and adenopathy (i.e., infectious or neoplastic, in general). Other abnormalities such as vascular malformations, dilated aortic or aortic aneursym, and

esophageal pathology, including dilation proximal to a stricture or due to achalasia, are much less commonly encountered.

- The vast majority of middle mediastinal masses in children are due to adenopathy.
- A rule that allows one to distinguish posterior medias-tinal from middle mediastinal masses is based on the location of the mass relative to the anterior aspect of the vertebral column. A mass whose center lies at or in front of the anterior vertebral body in children is generally considered a middle mediastinal mass. A mass whose center is posterior to the anterior-most vertebral body would generally be considered a posterior medi-astinal mass. Sometimes, as in the case presented here, both compartments are involved.
- Clinical presentation can be variable. Symptoms can be constitutional (e.g., fever) if the mass is inflammatory or neoplastic in nature. Nonspecific pulmonary symptoms such as cough may also be present.
- The general distribution of masses involving the mediastinum is 40% in the anterior mediatinum, 20% in the middle mediastinum, and 40% in the posterior mediastinum.

### Radiologic

- Adenopathy can appear as a homogeneous soft tissue mass (or masses) or an inhomogenous mass (often due to cavitation). When adenopathy is due to infective causes, e.g., histoplasmosis or tuberculosis, calcifications can also be present.
- Middle mediastinal masses due to foregut abnormalities, e.g., esophageal duplications cyst and bron-chogenic cyst, are typically round, well-defined, and homogeneous in appearance, with fluid attenuation.
- Masses are often discovered on plain radiographs. Further evaluation of such masses can be performed either by CT or MR imaging. For CT, contrast-enhanced imaging is recommended. For MR, axial T1- and T2-weighted and a combination of coronal and sagittal T1- and T2-weighted images are generally sufficient. Intravenous contrast material administration is not mandatory and the decision as to whether it should be employed will depend on the level of clinical suspicion (i.e., potential infection) or preliminary review of previous CT or MR examinations.

## SUGGESTED READING

Freud E, Ben-Ari J, Schonfeld T, et al. Mediastinal tumors in children: a single institution experience. *Clin Pediatr (Phila)* 2002;41:219–223.

Frush DP. Imaging evaluation of the thymus and thymic disorders in children. In: J Lucaya, JL Strife (eds), Pediatric Chest Imaging: Chest Imaging in Infants and Children (2nd ed). 2007;215–240.

Frush DP. Imaging of paediatric mediastinal masses. Ann Acad Med Singapore 2003;32:525–535.

Jaggers J, Balsara K. Mediastinal masses in children. Semin Thorac Cardiovasc Surg 2004;16:201–208.

Kang CH, Kim YT, Jeon S-H, et al. Surgical treatment of malignant mediastinal neurogenic tumors in children. Eur J Cardiothorac Surg 2007;31:725–730.

# CASE 23

**ANA M. GACA**

## HISTORY

A 3-year-old boy with history of Down's syndrome who presents with mild tachypnea and failure to thrive. He is not cyanotic.

A

■**FIGURE 8-23A** Frontal view of the chest shows enlargement of the right atrium (seen as increased convexity of the right heart border) and the right ventricle (manifested by uplifting of the cardiac apex). Pulmonary hyperinflation and increased pulmonary vascularity without pulmonary edema is present. Only 11 rib pairs are present.

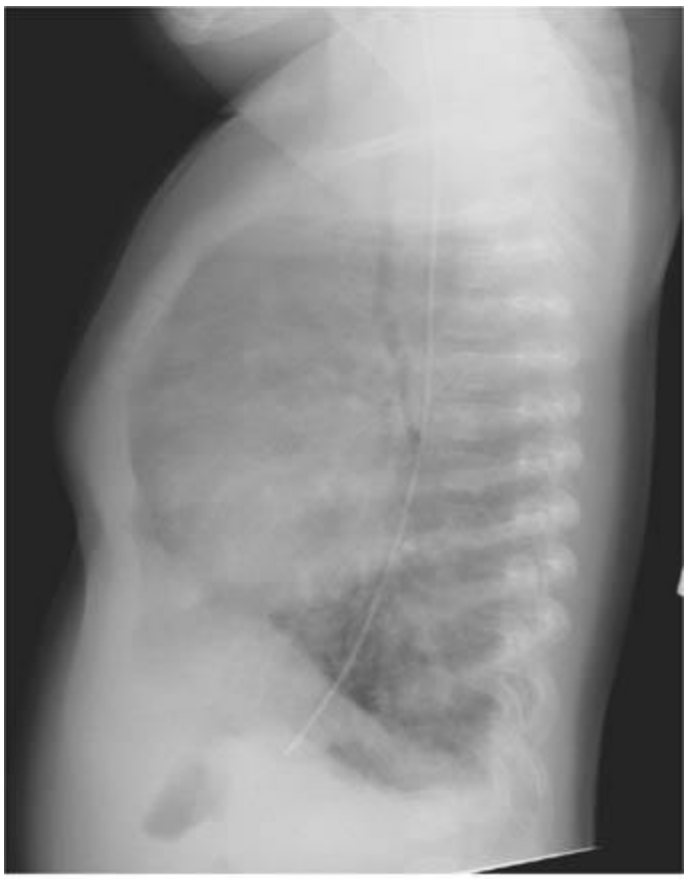

B

**FIGURE 8-23B** Lateral view of the chest shows enlargement of both the right ventricle (evidenced by filling of the retrosternal clear space) and the left ventricle (demonstrated by the fact that the left ventricular contour is seen posterior to the IVC). Left atrial enlargement is suggested by mild posterior displacement of the esophageal tube.

## DIFFERENTIAL DIAGNOSIS

The major considerations in this differential diagnosis in a noncyanotic patient includes left-to-right shunts.

**Atrial septal defect (ASD):** Radiographic findings of an ASD include enlargement of the right atrium, right ventricle, and the main pulmonary artery, with increased pulmonary vascularity. In the presence of an ASD, left atrial size is normal because its excess volume is decompressed into the right atrium and left ventricle. However, in the case shown here, mild enlargement of the left atrium, manifested by slight posterior displacement of the nasogastric tube on the lateral view, is present. Therefore, an ASD is unlikely.

**Ventricular septal defect (VSD):** In patients with a VSD, volume overload occurs at the level of the right ventricle (RV). Thus, moderate or large shunts with low pulmonary vascular resistance will be associated with enlargement of the RV, the main PA, the left

atrium, and the left ventricle, with increased pulmonary vascularity. The right atrium and the aorta remain normal in size. However, in the case shown here, enlargement of the right atrium is present, as seen by increased convexity of the right heart border on the frontal view. Therefore, a VSD is unlikely.

- **Patent ductus arteriosus (PDA):** In patients with a PDA, volume overload occurs from the aorta to the main PA. The result is enlargement of the PA with increased pulmonary vascularity, and enlargement of the left atrium, left ventricle, and the aorta. An enlarged aortic arch helps distinguish a PDA from an ASD and VSD. However, in the case shown, the patient has a normal aortic arch, making PDA an unlikely diagnosis.
- **Atrioventricular septal defect (AVSD):** In patients with an atrioventricular defect, imaging findings vary because volume overload can occur at various levels depending on the size and particular type of the defect. However, typical imaging findings include enlargement of the right atrium and both ventricles and increased pulmonary vascularity. The left atrium may be normal or enlarged. The aorta is typically normal. In the case shown here, the patient indeed does have enlargement of all four cardiac chambers, increased pulmonary vas-cularity and a normal aorta. An AVSD is the most likely diagnosis.

## DIAGNOSIS

**Atrioventricular septal defect**

## KEY FACTS

### Clinical

- The inferior atrial septum, the superior ventricular septum, septal leaflet of the tricuspid valve, and the anterior leaflet of the mitral valve develop from the endocardial cushion tissue.
- An AVSD, also known as an atrioventricular canal defect or endocardial cushion defect, occurs when these structures abnormally or inadequately fuse.
- In the absence of right ventricular outflow tract obstruction, an AVSD is typically associated with a left-to-right shunt.
- Clinical symptoms depend on either the degree of shunting, degree of atrioventricular insufficiency, or both.
- The degree of left-to-right shunting is related both to the size of the defect and to the relative compliance of the atria and ventricles, which, in turn, is affected by pulmonary vascular resistance. In a newborn with relatively high pulmonary vascular resistance, less left-to-right shunting occurs. However, as pulmonary vascular resistance decreases

with age, left-to-right shunting increases, with progressively severe right ventricular enlargement and increased pulmonary vascularity.

- Over a long period of time, increased pulmonary blood flow results in increased pulmonary vascular resistance and pulmonary hypertension.
- Approximately 40% to 50% of patients with Trisomy 21 have a congenital heart defect, with an AVSD being the most common defect.

### Radiologic

- Radiography is not sufficiently sensitive or specific for the diagnosis of congenital heart disease. Any patient with a cardiac type of shunt may have a normal chest radiograph if the shunt is sufficiently small (e.g., less than about 2 to 2.5:1).
- Many radiologists and cardiologists consider echocar-diography to be the best imaging technique for diagnosis of congenital heart disease, including AVSD.
- Radiographic findings of a left-to-right shunt include increased pulmonary vascularity (when pulmonary resistance is normal) and cardiac chamber enlargement.
- Large left-to-right shunts can cause pulmonary hyperinflation, possibly due to edema or the effect of enlarged pulmonary arterioles adjacent to airways.

## SUGGESTED READING

Gaca AM, Jaggers JJ, Dudley LT, Bisset GS 3rd. Repair of congenital heart disease: a primer - Part 2. Radiology 2008;248:44–60.

Laya BF, Goske MJ, Morrison S, et al. The accuracy or chest radiographs in the detection of congenital heart disease and in the diagnosis of specific congenital cardiac lesions. Pediatr Radiol 2006;36:677–681.

# CASE 24

**ANA M. GACA**

### HISTORY

A newborn boy with a cystic mass in the chest on prenatal sonography, which raised the possibility of a congenital diaphragmatic hernia (CDH). A CT angiogram of the chest was performed to further characterize the pulmonary abnormality and its relationship to vessels and the airway.

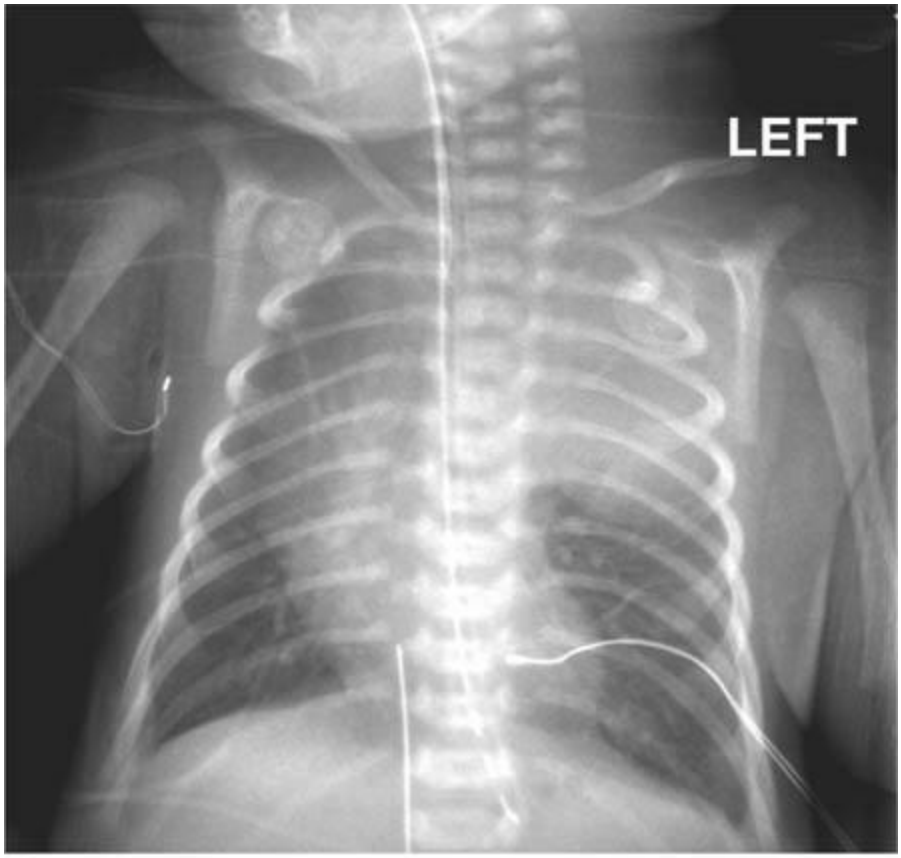


A

■**FIGURE 8-24A** Anteroposterior view of the chest shows a homogeneous opacity overlying the left upper hemithorax that causes mild mass effect and rightward shift of the cardiothymic contour.

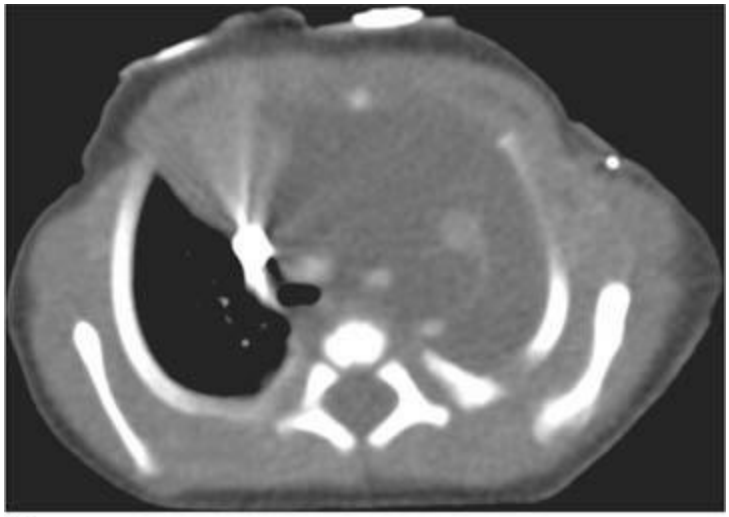

B

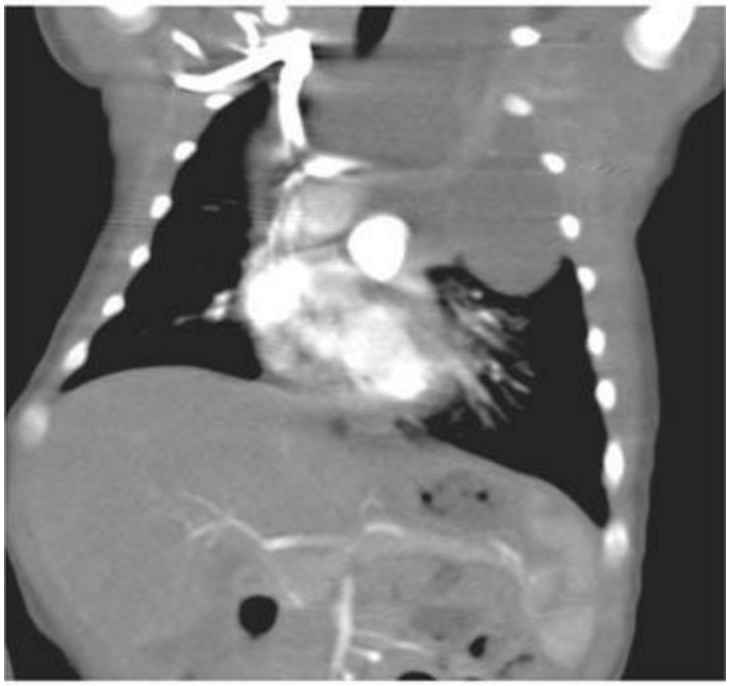

C

■**FIGURES 8-24B and 8-24C** Axial image **(B)** and coronal reconstruction **(C)** images from a chest CT angiogram shows a low attenuation mass in the left anterior and superior mediastinum. The lesion encases the great vessels and causes mass effect on the mediastinum.

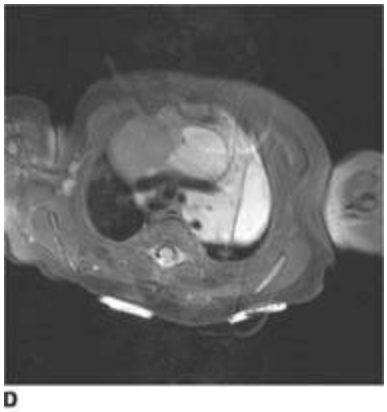

D

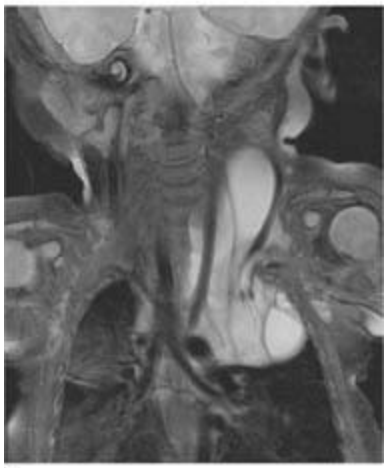

E

**FIGURES 8-24D and 8-24E** Axial **(D)** and coronal **(E)** T2-weighted images from a neck and chest MRI shows the same cystic mass that was seen in Figures 8-24B and 8-24C. The lesion is now seen to have multiple septations. The mass extends into the left side of the neck, adjacent to the trachea, and surrounds the left common carotid and subclavian arteries.

## DIFFERENTIAL DIAGNOSIS

**Congenital diaphragmatic hernia (CDH):** A chest radiograph in a patient with CDH would typically show air-filled loops of bowel in the chest, which are not present in the case shown. Furthermore, aerated lung is seen between the mass and the abdomen; in CDH, the mass would be expected to be seen adjacent to the abdomen. This diagnosis is incorrect.

**Congenital lobar emphysema (CLE):** CLE is a reasonable diagnostic consideration, given the presence of a soft tissue mass in the upper lobe on the chest radiograph. CLE is typically located in the upper lobes or the right middle lobe. In the first few days of life, a CLE may be fluid-filled but eventually becomes hyperlucent. CT imaging features of CLE typically include a mass involving an entire lobe of the lung, hyperaeration, and attenuated vessels. Mass effect can be present due to air trapping. None of these features are present on the CT angiogram in the case shown. Additionally, the CT and MR scans

show extension of the lesion into the mediastinum and neck, which is not a feature seen in CLE. This diagnosis is unlikely.

- **Pulmonary sequestration:** A pulmonary sequestration is a congenital mass of aberrant pulmonary tissue without connection to the pulmonary arteries or the tracheobronchial tree. This diagnosis is a reasonable possibility in the case shown based on the presence of a pulmonary mass lesion. However, pulmonary sequestrations are most often located in the lower lobes and have systemic arterial supply (typically arising from the aorta) and venous drainage. Thus, in the case shown, the location would be unusual for a pulmonary sequestration. Furthermore, the CT angiogram does not show a systemic arterial supply or venous drainage, making pulmonary sequestration an unlikely diagnosis.
- **Congenital pulmonary adenomatoid malformation (CPAM):** This entity consists of a hamartomatous proliferation of the terminal bronchioles, which usually communicates with the tracheobroncheal tree. CT usually shows both solid and cystic components as well as aerated portions shortly after birth. However, in the CT in the case shown, aerated components are lacking. Furthermore, the mass involves the mediastinum and neck, which would not be expected in a CPAM. This diagnosis is an unlikely one.
- **Vascular malformation:** Vascular malformations and hemangiomas have a nonspecific appearance on chest radiography, appearing as a soft tissue mass. In the case shown, CT and MR imaging for this patient indicate this lesion is fluid-filled with numerous septations, and extends into the neck. No soft tissue component, as would be seen with a hemangioma, or large vessels are present to suggest an arterial or venous malformation. Furthermore, with a venous malformation, the fluid within the cystic spaces would be expected to contrast-enhance. None of those features are present in the case shown, making this diagnosis unlikely.
- **Lymphatic malformation:** A lymphatic malformation has a nonspecific appearance on chest radiographs, appearing as a soft tissue mass. However, characteristic findings are seen on CT and MR imaging and include well-defined cystic spaces and septations, which cross tissue boundaries. These findings are present in the case shown, making this diagnosis the correct one. Contrast-enhanced MR imaging, if it had been provided in the patient under discussion, would be expected to show lack of enhancement of the fluid-filled spaces but enhancement of the septae.

## DIAGNOSIS

**Lymphatic malformation**

## KEY FACTS

## Clinical

- Lymphatic malformations, often referred to as cystic hygromas, consist of chyle-filled cysts lined with epithelium.
- The most common locations for a lymphatic malformation are the head and neck (75%) and the axilla (25%), with lesions in the mediastinum, mesentery, retroperitoneum, pelvis, and groin less common.
- Approximately 65% of lymphatic malformations are present at birth; 90% are present by the age of 2 years.
- Therapeutic considerations are primarily surgical (if the intent is complete resection) and alcohol ablation.
- Vascular malformations and hemangiomas are both endothelial malformations.
- Hemangiomas are benign neoplasms of endothelial cells, which may be absent or small at birth. They typically proliferate shortly after birth, and then involute (70% have involuted by the age of 7 years). On imaging, hemangiomas look like a mass.
- Vascular malformations are made up of dysplastic vessels that do not proliferate and never involute. They are present at birth and progressively grow.
- Vascular malformations are characterized as high-flow, slow-flow, or mixed lesions and by the predominant anomalous vessel—arteriovenous, venous, or lymphatic.

## Radiologic

- At sonography, lymphatic malformations appear as a multilocular cystic mass with absent flow except in the septations. Fluid-fluid levels may be seen, representing internal hemorrhage (which is often accompanied by a history of sudden enlargement of the mass).
- On CT imaging, lymphatic malformations have the appearance of a mass with fluid density; the walls of the mass are often seen to contrast-enhance.
- On MR imaging, these lesions are seen as a septated mass having signal intensity that is decreased on T1-weighted images and increased on T2-weighted sequences, similar to the signal intensity of cerebrospinal fluid. However, the signal intensity can be altered by the presence of protein or hemorrhage in the lesion.
- The goals of imaging hemangiomas and vascular malformations include characterizing the lesion, defining its extent, and evaluating mass effect on adjacent structures (e.g., vessels and the airway).
- Imaging can be performed with sonography, CT, or MR imaging for axial lesions. For extremity lesions, MR imaging is preferred. The preferred MR sequences include T1-weighted sequences, T2-weighted sequences with fat saturatation, and flow sensitive sequences (e.g., gradient-echo).

## SUGGESTED READING

Donnelly LF, Adams DM, Bissett GS 3rd. Vascular malformations and hemangiomas: a practical approach in a multidisciplinary clinic. AJR Am J Roentgenol 2000;174:597–608.

Dubois J, Garel L. Imaging and therapeutic approach of hemangiomas and vascular malformations in the pediatric age group. Pediatr Radiol l999;29:879–893.

Mulliken JB, Glowacki J. Hemangiomas and vascular malformations in infants and children: a classification based on endothelial characteristics. Plast Reconstr Surg l982;69:412–422.

# CASE 25

**CHARLES MAXFIELD**

## HISTORY

A 5-year-old boy with a monoarticular arthropathy who is being treated with methotrexate for presumed juvenile rheumatoid arthritis. He has developed fever and shortness of breath.

A

■**FIGURE 8-25A** A posteroanterior chest radiograph shows a diffuse pattern of tiny nodules consistent with a miliary pattern. No focal alveloar opacities, lymphadenopathy or pleural effusions are present.

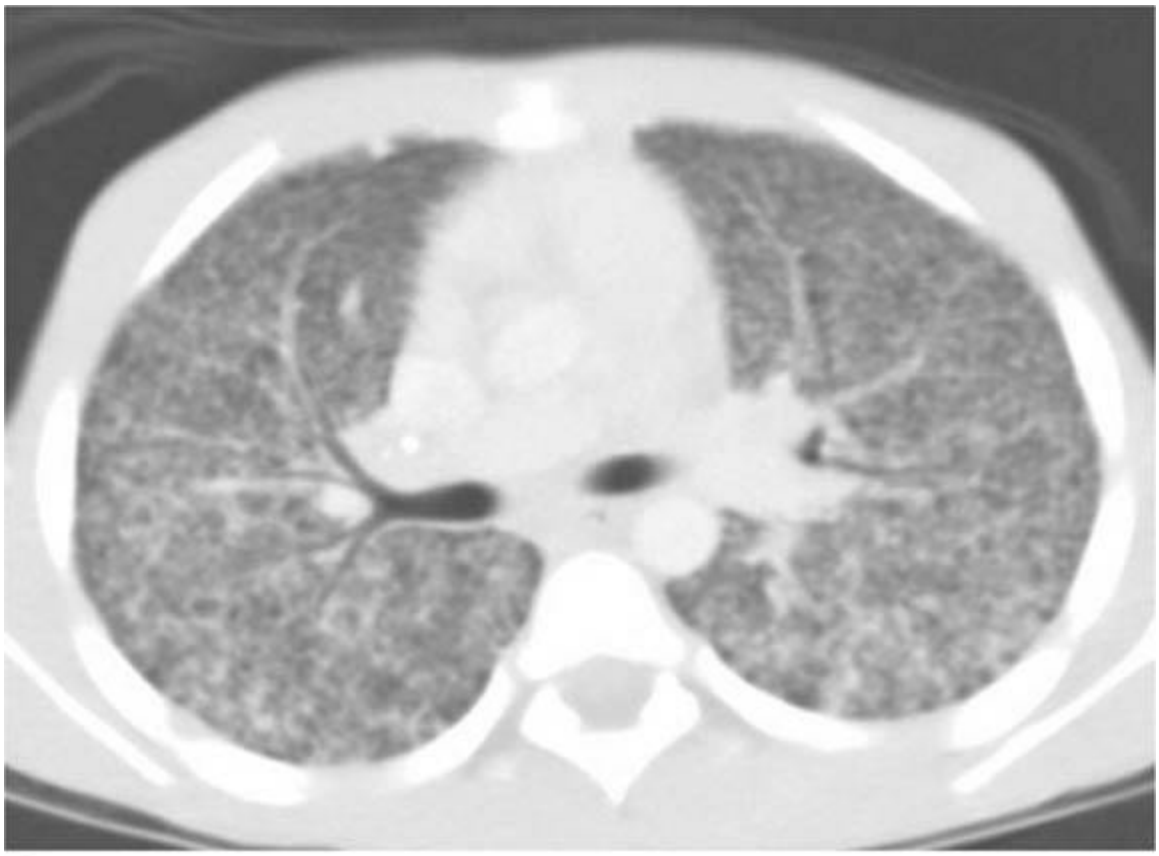

B

■**FIGURE 8-25B** High-resolution axial chest CT image depicts innumerable, almost confluent tiny nodules.

C

**FIGURE 8-25C** A sagittal T2-weighted image of the left knee shows anterior subluxation of the femur upon the tibia. Marked signal abnormalities involving the epiphyses and a large joint effusion are present.

## DIFFERENTIAL DIAGNOSIS

For a miliary pattern on chest radiography:

- **Langerhans cell histiocytosis (LCH):** When the pulmonary nodules of LCH are tiny, a miliary pattern can be on chest radiographs. However, fever and arthropathy would not be expected to be seen in LCH. Furthermore, LCH is typically associated with diffuse cystic changes in the lungs, which are not seen in the case presented here. This diagnosis is an unlikely one.
- **Metastatic disease:** A miliary pattern of metastatic disease can be seen in adults, usually caused by thyroid cancer or melanoma; however, these tumors are rare in children. This pattern would not be expected in a child, particularly in a child with no known primary maling-nancy. Furthermore, the presence of fever favors an infective, rather than a neoplastic, etiology. This diagnosis is unlikely.
- **Sarcoidosis:** The presence of fever and the patient's young age essentially exclude this uncommon cause of a miliary pattern. The fever in this case is helpful in narrowing the

differential diagnosis by essentially excluding rare noninfective causes of a miliary pattern. Bacterial infections do not produce a miliary pattern. However, fungal, viral, and tuberculous infections can also produce this pattern.

- **Tuberculosis (TB):** Mycobacterium TB is the most common cause of a miliary pattern. Miliary TB is often accompanied by fever, as in this case. Furthermore, the patient described here could have been susceptible to TB due to immunosuppression conferred by metho-trexate, given for the presumed JRA. The accompanying knee MR findings, as a monoarticular process, also suggest tuberculous infection. This diagnosis is correct.
- **Fungal infection:** Fungal infections (e.g., histoplasmosis, coccidiomycosis, blastomycosis) can rarely produce a miliary pattern, but much more commonly produce larger pulmonary nodules, often ill-defined early in the disease course and subsequently organizing into more well-defined nodules.
- **Viral infections:** Varicella pneumonia is more common in children than adults. However, the characteristic skin lesions of chicken pox are not described in this case, making this an unlikely diagnosis.

## DIAGNOSIS

**Miliary tuberculosis**

## KEY FACTS

### Clinical

- Miliary TB is most frequently a complication of primary tuberculous infection and generally occurs within 6 months of initial infection. Less commonly, it can complicate post-primary TB.
- A miliary pattern implies hematogenous dissemination of TB and is most often seen in the immunocompro-mised patient, typically the elderly.
- The military pattern develops when tubercle bacilli are discharged from a focal infection into the lymphatics or blood and then disseminate to the capillary beds of multiple organs, where they lodge and proliferate.

### Radiologic

- A true miliary pattern on chest radiographs can be difficult to detect because the nodules are very small (i.e., 1 to 2 mm).
- In a true miliary pattern, the nodules are 1 to 2 mm. However, most diseases that can produce a miliary pattern can also cause nodules up to 3 to 4 mm. Thus, the presence of nodules slightly larger than 1 to 2 mm does not exclude these disease entities.

- The tiny nodules are typically best seen at the lung bases, probably due to summation of shadows rather than any preference in distribution.
- CT imaging is very helpful in distinguishing a miliary pattern from other patterns that can simulate a miliary pattern on chest radiographs alone. Thus, high-resolution CT imaging should be considered if an interstitial pulmonary process is suspected.

## SUGGESTED READING

Fonseca-Santos J. Tuberculosis in children. Eur J Radiol 2005;55:202–208.

Gurjan F, Bosnak M, Dikici B, et al Miliary tuberculosis in children: a clinical review. Scand J Infect Dis 1998;30:359–362.

Kim WS, Moon WK, Kim IO et al. Pulmonary tuberculosis in children: evaluation with CT. AJR Am J Roentgenol 1997;168:1005–1009.

Leung AN, Muller NL, Pineda PR, Fitzgerald JM. Primary tuberculosis in childhood: radiographic manifestations. Radiology 1992;182:87–91.

# CASE 26

### CHARLES MAXFIELD

### HISTORY

A 15-year-old girl with two weeks of right upper quadrant pain, vomiting, and general malaise.


A

■**FIGURE 8-26A** Contrast-enhanced axial CT shows a large, predominantly low-attenuation mass in the posterior segment of the right hepatic lobe and another lesion in the anterior segment of the left hepatic lobe.


B

■**FIGURE 8-26B** CT image from the same imaging study as shown in Figure 8-26A depicts an abnormal air-containing space in the right lower quadrant with an air-debris level. A calcification is present, which likely represents an appendicolith.

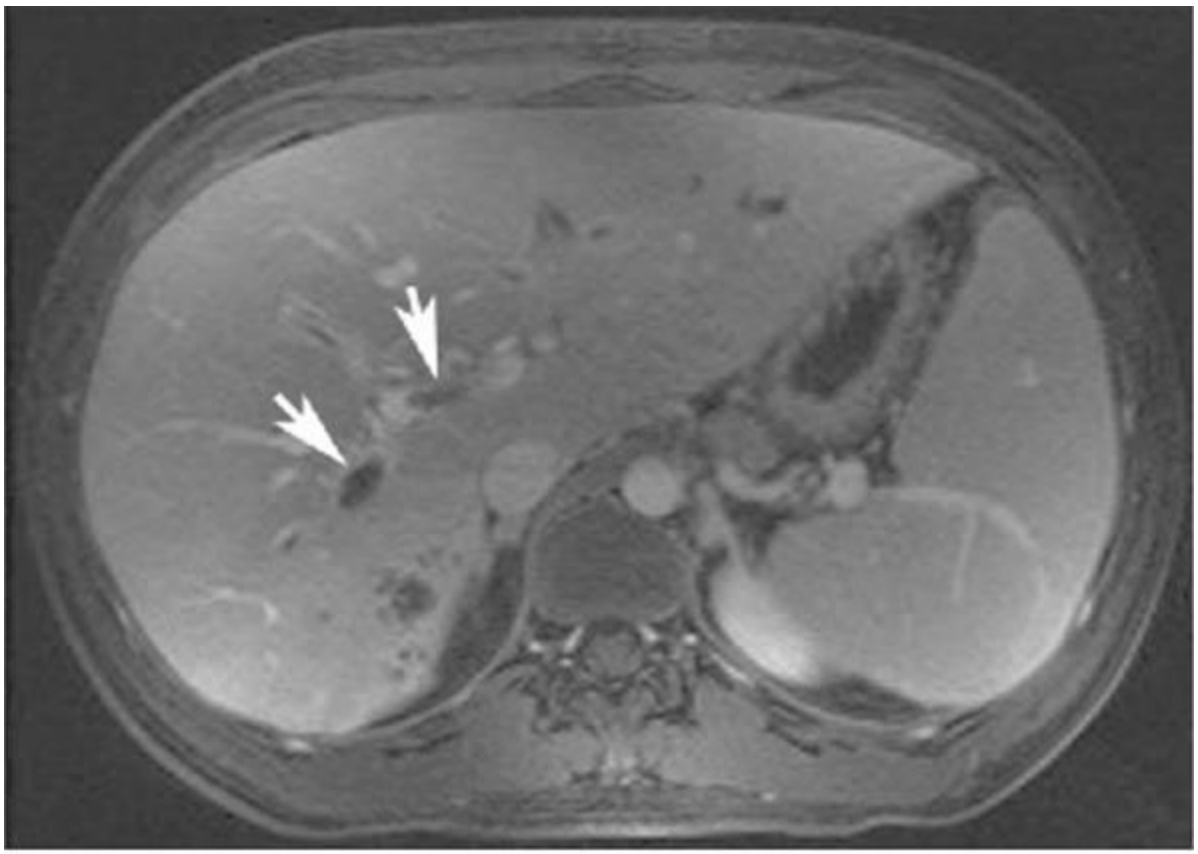

C

**FIGURE 8-26C** Contrast-enhanced T1-weighted axial MR image with fat saturation technique through the level of the portal vein shows defects in enhancement in the left and right branches of the portal vein *(arrows),* consistent with portal vein thrombosis. The hepatic parenchymal lesions are incompletely seen on this image.

## DIFFERENTIAL DIAGNOSIS

- Hepatocellular carcinoma: This diagnosis should be considered based on the fact that it can have the appearance of a multifocal lesion within the liver. Although hepatocellular carcinoma can also invade into the portal vein and cause thrombus, it would not be expected to extend into the mesenteric vein, making this diagnosis unlikely. In addition, risk factors for hepatocellular carcinoma, e.g., chronic liver disease, and serologic markers of this tumor, e.g., an elevated alpha-fetoprotein level, are absent. Finally, this diagnosis would not account for the lesion in the right lower quadrant. This diagnosis is incorrect.
- Other, benign liver tumors: Hemangiomas, focal nodular hyperplasia, and hepatic adenomas are all benign, focal hepatic masses. All three entities densely enhance following contrast administration (unlike the lesions shown here), making them unlikely. Portal and mesen-teric vein thrombosis would not be expected features of any of these benign liver lesions. Furthermore, focal nodular hyperplasia is a unifocal mass, unlike

the masses shown here. In addition, hepatic adenomas are very uncommon outside the setting of rare hepatic storage diseases. These diagnoses are incorrect.

- Hepatic metastases: The presence of multiple low attenuation lesions in the liver should raise the diagnostic possibility of metastases. However, no history of a known primary malignancy is given. Furthermore, venous thrombosis would not be expected. This diagnosis is incorrect.
- Hepatic abscesses: These lesions are commonly mul-tifocal, often in clusters, and can be associated with thrombus in the portal vein and mesenteric veins, as in the case shown here. Hence, this diagnosis is a reasonable one to consider. Consideration of hepatic abscesses should elicit a search for an inflammatory process elsewhere in the abdomen or pelvis. In the case shown here, an inflammatory process is indeed present in the form of an appendicular abscess (i.e., the structure having an air-debris level and an associated appendicolith) in Figure 8-26B. This diagnosis is correct.

## DIAGNOSIS

**Mesenteric and portal vein thrombosis and liver abscesses secondary to perforated appendicitis**

## KEY FACTS

### Clinical

- Hepatic abscesses are often secondary to infection at an adjacent abdominal site, with subsequent spread to the liver via the portal vein. Common etiologies include acute appendicitis, infectious enteritis, and Crohn's disease.
- In young children, hepatic abscess are often due to instrumentation (e.g., during surgery) or occur in the presence of immunosuppression.
- In the United States, pyogenic abscesses are more common than amebic and hydatid abscesses.
- Most hepatic abscesses respond to a combination of antibiotics and percutaneous catheter drainage.
- In young children, portal vein thrombosis is usually secondary to sepsis and dehydration, but in older children and adults, the common precipitating factors are cirrhosis, hepatoma, and mesenteric inflammation.

### Radiologic

- The most characteristic CT appearance of a hepatic abscess is that of a well-circumscribed, low-attenuation mass with rim-enhancement. Less common appearances

include multiple lesions, or a focal cluster of small lesions. The most specific (although uncommon) imaging sign of hepatic abscess is intracavitary gas.

- Radiologic signs of mesenteroportal vein thrombosis include increased size of the veins, and low-density, unenhancing intraluminal thrombus.

## SUGGESTED READING

Balthazar EJ, Gollapundi P. Septic thrombophlebitis of the mesenteric and portal veins: CT imaging. J Comput Assist Tomogr 2000;24:755–760.

Chang TN, Tang L, Keller K, et al. Pylephlebitis, portal-mesenteric thrombosis, and multiple liver abscesses owing to perforated appendicitis. J Pediatr Surg 2001;36:E19.

Percutaneous aspiration versus open drainage of liver abscess in children. Pediatr Surg Int 2007;23:69–74.

Syed MA, Kim TK, Jang HJ. Portal and hepatic vein thrombosis in liver abscess: CT findings. Eur J Radiol 2007;61:513–519.

# CASE 27

### CHARLES MAXFIELD

### HISTORY

A severely cyanotic newborn infant.


**FIGURE 8-27** A frontal chest radiograph shows massive cardlomegaly, nearly filling the chest. A focal right heart bulge suggests right atrial enlargement. Pulmonary vascularity is decreased.

## DIFFERENTIAL DIAGNOSIS

- **Ebstein's anomaly:** Ebstein's anomaly (i.e., downward displacement of 2 leaflets of the tricuspid valve and elongation and tethering of the third leaflet) presenting in the newborn period is typically severe, with marked cardiomegaly (due to dilation of the right atrium and an atrialized portion of the right ventricle) and decreased pulmonary vascularity. The findings in the case presented here are consistent with that diagnosis and Ebstein's anomaly cannot be excluded on the basis of the image shown.
- **Pulmonary atresia with intact septum:** This entity also presents with severe cardiomegaly with right heart enlargement indistinguishable from Ebstein's anomaly. Thus, pulmonary atresia with intact septum is a diagnosis consistent with the clinical and imaging findings in the case presented here.
- **Peripheral arteriovenous malformation (AVM):** Large AVMs (e.g., within the liver or associated with the vein of Galen) can cause massive cardiomegaly due to markedly increased cardiac output. However, patients are not cyanotic as a result. Furthermore,

the pulmonary vasculature would be expected to be increased rather than decreased. This diagnosis is incorrect.

- **Cardiac tumor:** Pediatric cardiac tumors are extremely rare, especially in newborns, and would not be accompanied by cyanosis or decreased pulmonary blood flow. This diagnosis is incorrect.

## DIAGNOSIS

**Pulmonary atresia with intact septum**

## KEY FACTS

### Clinical

- In pulmonary atresia with an intact ventricular septum, blood cannot flow from the right heart to the lungs. There is gross tricuspid insufficiency and the right atrium and the atrialized portion of the right ventricle massively dilate.
- Because the pulmonary valve is atretic, the amount of pulmonary blood flow depends on patency of the ductus arterosus. Newborn cyanosis worsens considerably when the ductus arteriosus closes. Prostoglandin is often administered to maintain ductal patency until surgery can be performed.
- Definitive repair is surgical. The exact surgical approach depends on the size and morphology of the tricuspid valve and right ventricle, as well as the coronary artery anatomy.

### Radiologic

- The right atrium can expand quite dramatically and often contributes to the most striking cases of cardio-megaly in newborns. When massive cardiomegaly is associated with decreased pulmonary vasculature, the two most likely diagnoses are Ebstein's anaomly and tricuspid atresia with an intact septum. The two cannot be reliably distinguished on radiographs but can be distinguished by echocardiography.
- The degree of cardiomegaly in pulmonary atresia with intact ventricular septum is related to the competency of the tricuspid valve. When tricuspid regurgitation is present, blood flows "back and forth" from the right ventricle to the right atrium and both the right atrium and right ventricle can become massively enlarged.

## SUGGESTED READING

Benya EC, Rigsby CK. Right heart lesions. In: Slovis, TL (ed), Caffey's Pediatric Diagnostic Imaging. Philadelphia, PA: Mosby;2008:1532–1549.

Bichell DP. Evaluation and management of pulmonary atresia with intact ventricular septum. Curr Opin Cardiol 1999;14:60–66.

Chen JTT. Essentials of Cardiac Roentgenology (1st ed). Boston, MA: Little, Brown and Company, 1987.

Donnelly LF, Gelfand KJ, Schwartz DC, Strife JL. The wall to wall heart: differential diagnosis for massively large cardiothymic silhouette in newborns. Appl Radiol 1997;26:23–28.

Pawade A, Karl T. Management strategy in neonates presenting with pulmonary atresia with intact ventricular septum. Curr Opin Pediatr 1994;6:600–605.

# CASE 28

**CAROLINE L. HOLLINGSWORTH**

## HISTORY

A 2-day-old girl with a deep sacral dimple. A radiograph of the lumbosacral spine (not shown) is normal.

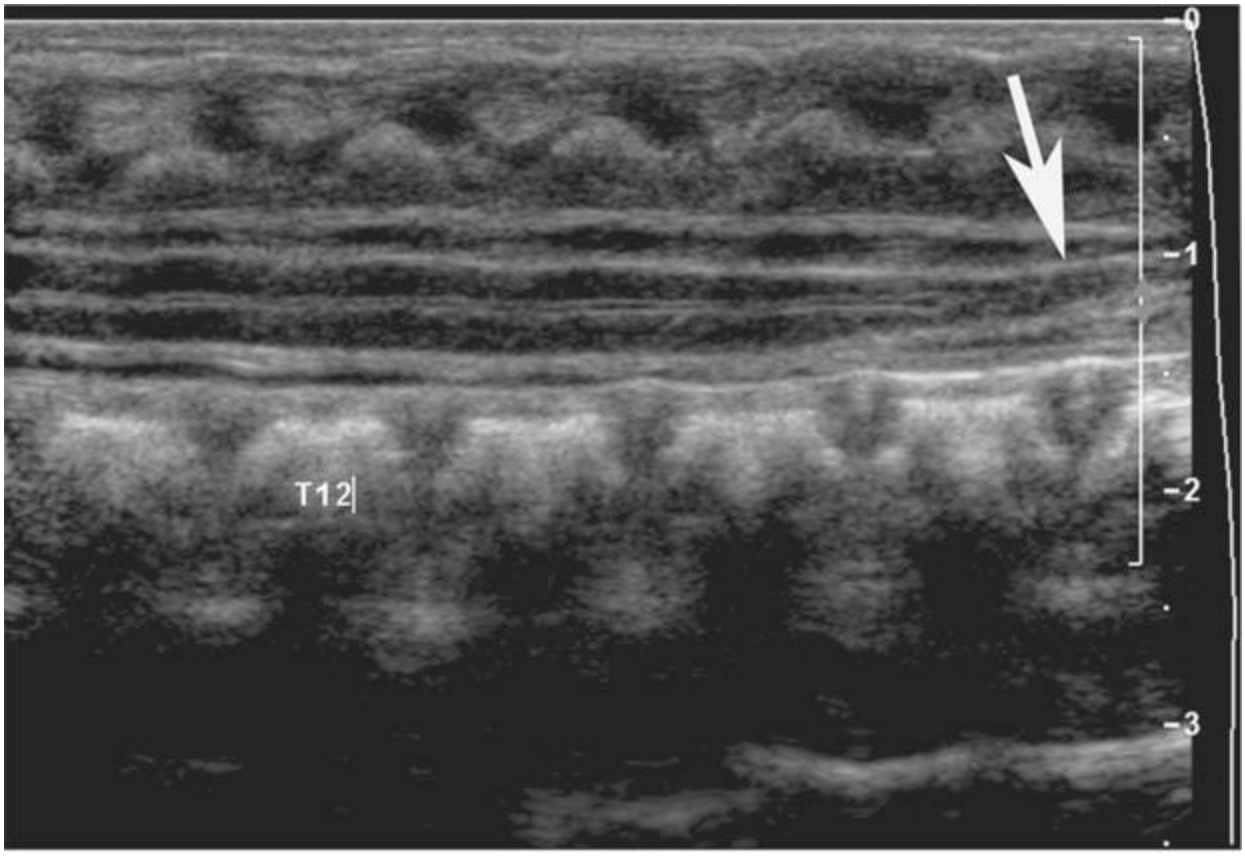


A

■**FIGURE 8-28A** Sagittal sonographic image from a lumbar spine ultrasound

examination shows that the conus medullaris *(arrow)* terminates well below the L-3 vertebral body, consistent with a low-lying, tethered spinal cord.

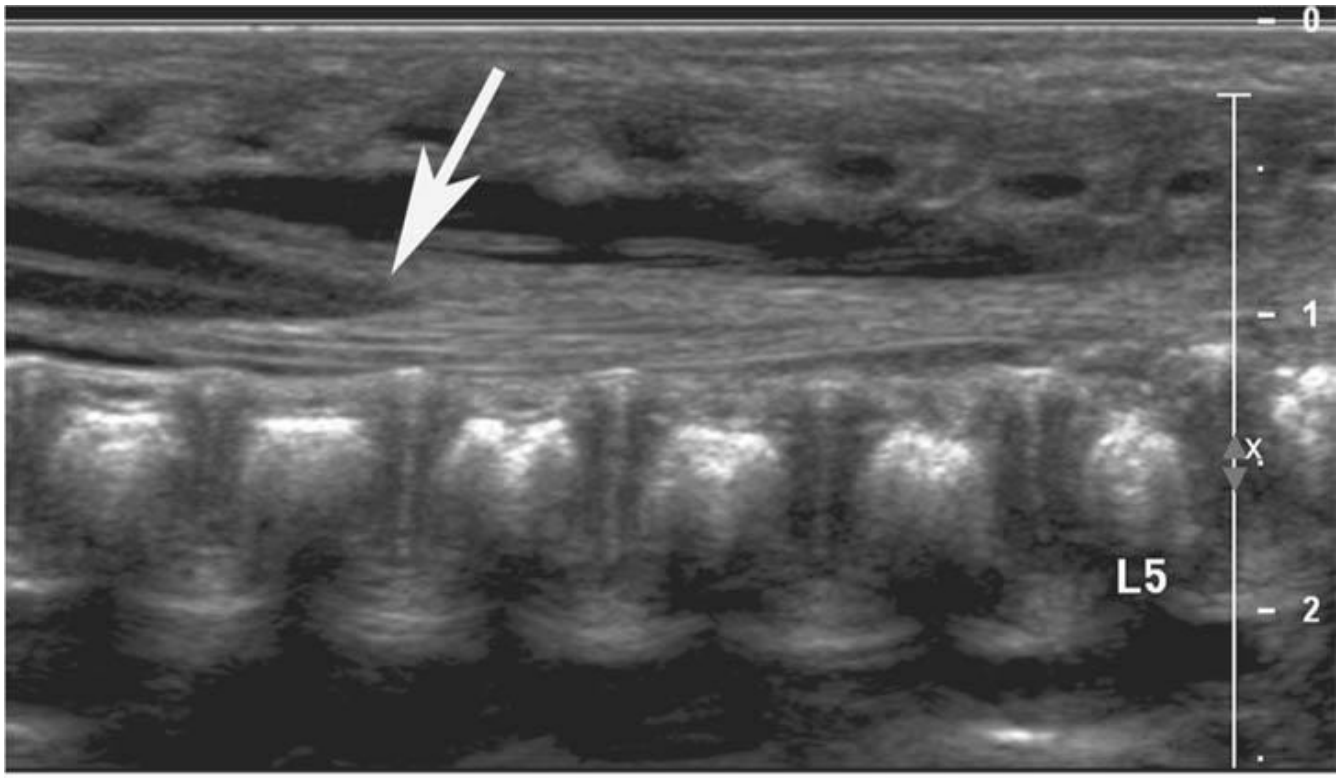


B

**FIGURE 8-28B** Sagittal image from the lumbar spine ultrasound examination of a comparison normal infant shows a normal lumbar spinal cord. The conus medullaris *(arrow)* terminates at the caudal end of the L1 vertebral body and, thus, above the L2-L3 disc space.

## DIFFERENTIAL DIAGNOSIS

**Spina bifida occulta with lipomyelomeningocele:** Spina bifida occulta is an osseous defect in the posterior elements with protrusion of various neural elements. In the case shown here, the radiograph is reported to show a normal spine. On the sonogram, no neural elements protrude outside the spinal canal on sonography. This diagnosis is incorrect.

**Spinal lipoma:** Spinal lipomas can be intradural, extra-dural, or both. In the case shown, no mass is found in the lumbosacral spine region on the sonogram. This diagnosis is incorrect.

**Tethered cord:** The conus medullaris is seen to be located caudal to the L3 vertebral body; this diagnosis is correct.

- **Caudal regression syndrome:** A maternal history of diabetes is almost always elicited in infants with this diagnosis; however, no such history is present in the case shown here. Furthermore, no stigmata of regression of the coccyx, sacrum, or lumbar spine are present on the sonogram. This diagnosis is incorrect.

## DIAGNOSIS

**Tethered spinal cord**

## KEY FACTS

### Clinical

- Disruption of basic embryologic processes accounts for most congenital spinal anomalies. These include premature separation of ectoderm from the neural tube, failed neurulation, and abnormalities in formation of the filum terminale.
- A tethered spinal cord results from failed involution of the terminal cord, which leads to abnormal anchoring of the filum terminale and nerve roots. Symptoms (see below) occur due to abnormal traction on the spinal cord and nerve roots.
- A tethered spinal cord may present clinically at any age. Signs and symptoms can include difficulty with ambulating or delayed ambulation, weakness, abnormal reflexes or tone, and bladder or bowel dysfunction.
- Treatment of the condition centers on release of the tethered spinal cord to preserve nerve root function. Following surgical release, symptoms can recur if retethering of the spinal cord occurs due to adhesion by scar tissue.

### Radiologic

- Sonography is a useful screening tool in neonates in whom tethered cord or other spinal dysraphic abnormalities are being considered. Infants can be diagnosed on the basis of a low-lying conus medullaris (i.e., below the L2-L3 disc space) and absence of normal nerve root motion during real-time sonography.
- Associated sonographic findings include a thick filum terminale (> 2mm), fatty infiltration of the filum (depicted by an echogenic filum), spinal dysraphism, syringomyelia, scoliosis, and a spinal or subcutaneous mass or cyst.
- MRI of the spine is typically performed to further evaluate abnormalities detected by sonography (please see Neuroradiology Case 6-13).
- Associated congenital anomalies include those seen in the so-called VATER anomaly spectrum, which includes tracheoesophageal fistula, congenital heart disease, and renal abnormalities.

## SUGGESTED READING

Bao N, Chen ZH, Gu S, et al. Tight filum terminale syndrome in children: analysis based on positioning of the conus and absence or presence of lumbosacral lipoma. Childs Nerv Syst 2007;23:1129–1134.

Lowe LH, Johanek AJ, Moore CW. Sonography of the neonatal spine: part 1, normal anatomy, imaging pitfalls and variations that may simulate disorders. AJR Am J Roentgenol 2007;188:733–738.

Lowe LH, Johanek AJ, Moore CW. Sonography of the neonatal spine: part 2, spinal disorders. AJR Am J Roentgenol 2007;188:739–744.

Khanna AJ, Wasserman BA, Sponseller PD. Magnetic resonance imaging of the pediatric spine. J Am Acad Orthop Surg 2003;11:248–259.

# CASE 29

### CAROLINE L. HOLLINGSWORTH

### HISTORY

A 12-year-old boy with a 4-hour history of right scrotal pain.

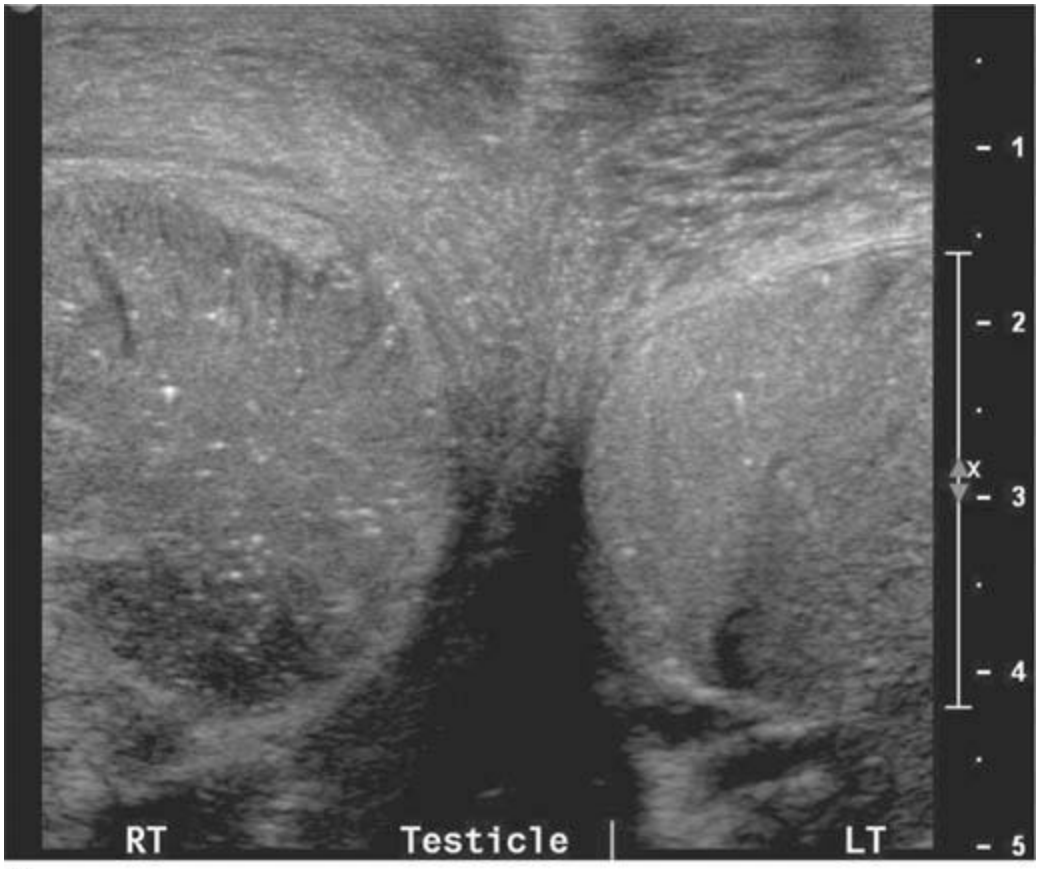


A

■**FIGURE 8-29A** Transverse sonogram through the scrotum shows the right testicle is heterogeneous and enlarged compared to the left testicle.

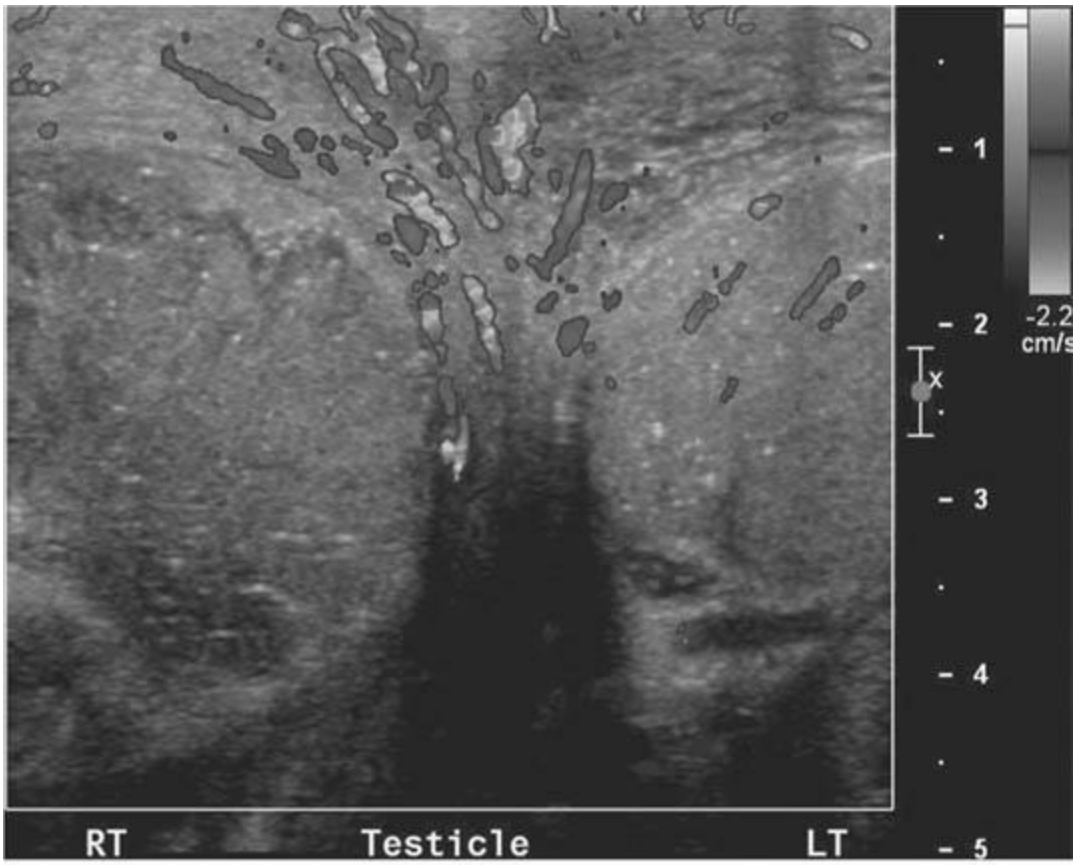


B

■**FIGURE 8-29B** Transverse image with color Doppler Imaging shows absence of color flow in the right testicle. (See color insert)

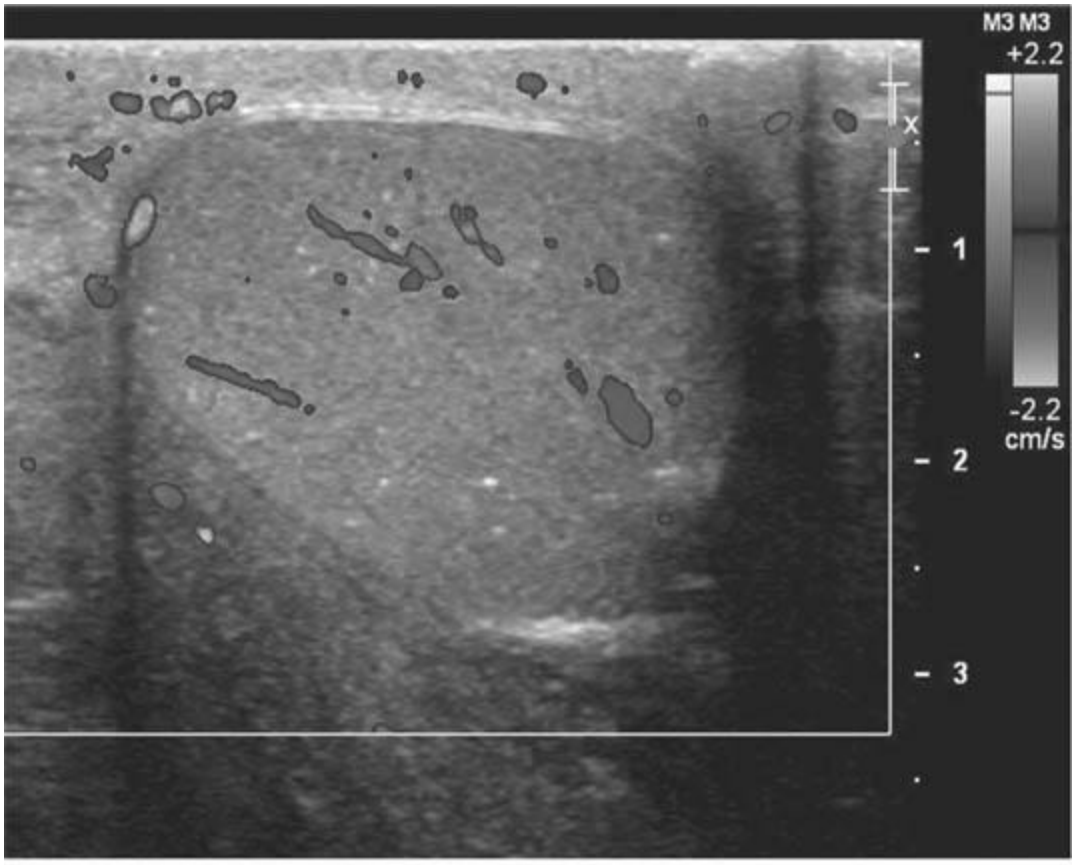


C

■**FIGURE 8-29C** Sagittal color Doppler image of the left testicle shows normal echotexture and normal blood flow. (See color insert)

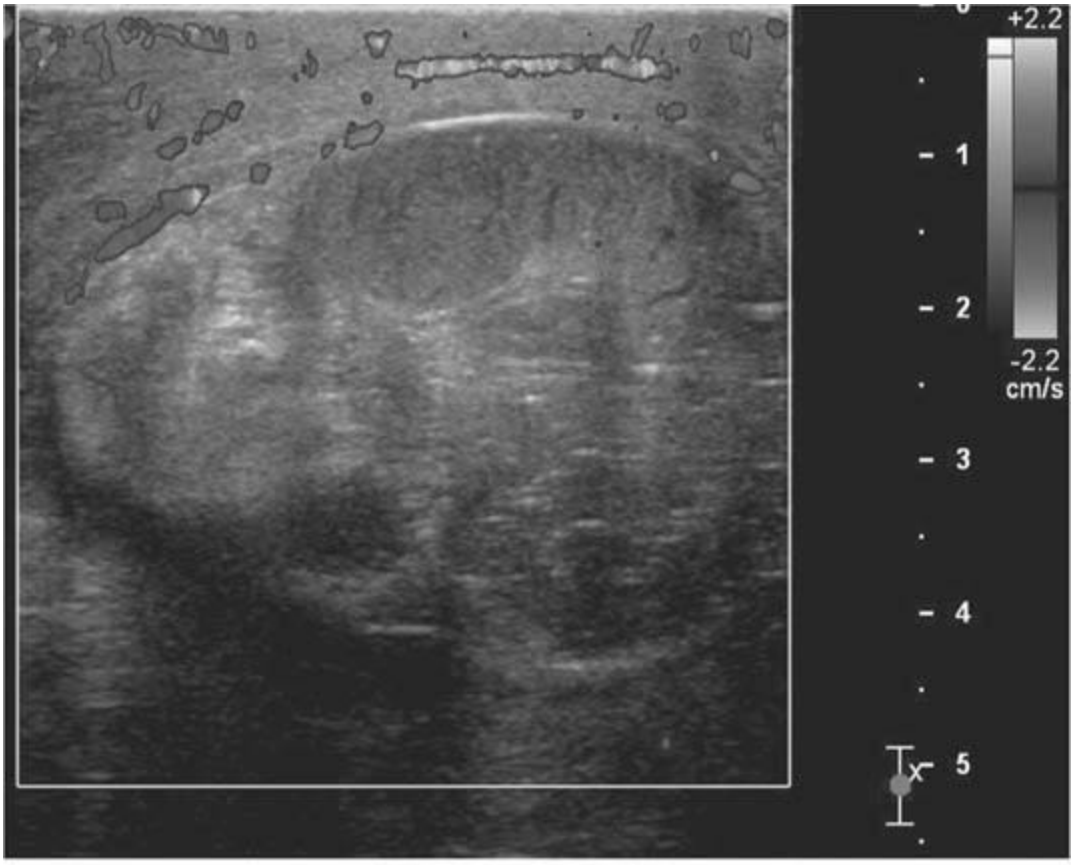


D

**FIGURE 8-29D** Sagittal color Doppler image of the right testicle depicts abnormal, inhomogeneous echotexture and absent color Doppler flow. (See color insert)

## DIFFERENTIAL DIAGNOSIS

**Epidydymo-orchitis:** This entity can cause the affected testicle to appear enlarged and heterogeneous (as in the case shown). However, characteristically the findings are those of increased blood flow as seen on Doppler sonography, unlike the findings in the case presented here. This diagnosis is unlikely.

**Hematoma:** On the basis of imaging findings alone, this diagnosis is a reasonable one for the case shown because posttraumatic scrotal hematomas have absent blood flow by Doppler sonography. However, because a clinical history of trauma is not provided, this diagnosis is unlikely.

**Seminoma (or other primary testicular neoplasm):** Seminomas are the most common primary testicular neoplasm. However, this diagnosis is unlikely because no intratesticular mass is seen by sonography in the case presented here.

**Leukemia/Lymphoma:** Both leukemia and lymphoma can present as diffuse bilateral testicular enlargement or with multiple hypoechoic masses. Acute lymphoblas-tic leukemia is the most common secondary malignant testicular neoplasm in children.

However, both lymphoma and leukemia are unlikely because both usually present as bilateral testicular enlargement whereas the patient in the case presented here has unilateral involvement.

- **Varicocele:** Varicoeles have the appearance of a vascular serpiginous structure, which is not evident on the imaging studies shown here. This diagnosis is incorrect.
- **Testicular Torsion:** Testicular torsion can produce many abnormal, but nonspecific, sonographic findings, such as an enlarged heterogenous testicle (as seen in the case presented here), a hydrocele, and scrotal edema. Lack of color flow by Doppler sonography (as in the imaging studies presented here) is considered diagnostic. Testicular torsion is the correct diagnosis.

# DIAGNOSIS

**Testicular torsion**

# KEY FACTS

## Clinical

- Testicular torsion can occur at any age but is most common in adolescence.
- With torsion, obstruction of venous flow first occurs followed by obstruction of arterial flow and, ultimately, ischemia and infarction.
- Testicular torsion is a surgical emergency. Testicular salvage rate depends on both the degree of torsion (which can vary between 180 degrees and 720 degrees) and the duration of symptoms (close to 100% rate of salvage in the first 6 hours).
- The so-called bell-clapper deformity is a congenital abnormality that places an individual at increased risk of testicular torsion. This abnormality, which is usually bilateral, occurs when the tunica vaginalis completely envelops the distal spermatic cord, epididymis and gubernaculums, and testis rather than anchoring to the posterolateral testes, leaving the testes free to torse within the capacious tunica vaginalis.
- Acute testicular torsion presents with sudden pain in the scrotum, which may be accompanied by nausea and vomiting.
- The clinical presentation of torsion overlaps greatly with that of epididymo-orchitis. Evaluation with Dop-pler, or power Doppler, sonography plays an important role in distinguishing the two entities.

## Radiologic

- Sonographic findings in torsion vary with duration of symptoms and degree of rotation of the spermatic cord.
- Sonography with gray-scale, color, and Doppler is well established as the initial step in imaging evaluation of the acute scrotum.
- Gray-scale image findings of an enlarged heterogeneous testical are nonspecific and can be seen in other pathologic conditions such as epididymo-orchitis. For this reason, Doppler or power Doppler sonography to determine lack of blood flow is essential when evaluating acute scrotal pain.
- During the first few hours after onset of clinical symptoms of testicular torsion, gray-scale sonographic imaging findings can be normal.
- The absence of blood flow within the testicle during color Doppler and power Doppler imaging is considered diagnostic for testicular torsion.

## SUGGESTED READING

Aso C, Enri'quez G, Fite M, et al. Gray-scale and color Doppler sonog-raphy of scrotal disorders in children: an update. Radiographics 2005;25:1197–1214.

Dogra VS, Gottlieb RH, Oka M, Rubens DJ. Sonography of the scrotum. Radiology 2003;227:18–36.

Dogra VS, Rubens DJ, Gottlieb RH, Bhatt S. Torsion and beyond: new twists in spectral Doppler evaluation of the scrotum. J Ultrasound Med 2004;23:1077–1085.

Hormann M, Balassy C, Philipp MO, Pumberger W. Imaging of the scrotum in children. Eur Radiol 2004;14:974–983.

# CASE 30

**CAROLINE L HOLLINGSWORTH**

### HISTORY

A 11-year-old girl with a 2-week history of crampy abdominal pain. The patient's imaging findings are depicted in Figure 8-30A and compared with a companion case of a patient with a different diagnosis shown in Figure 8-30B.

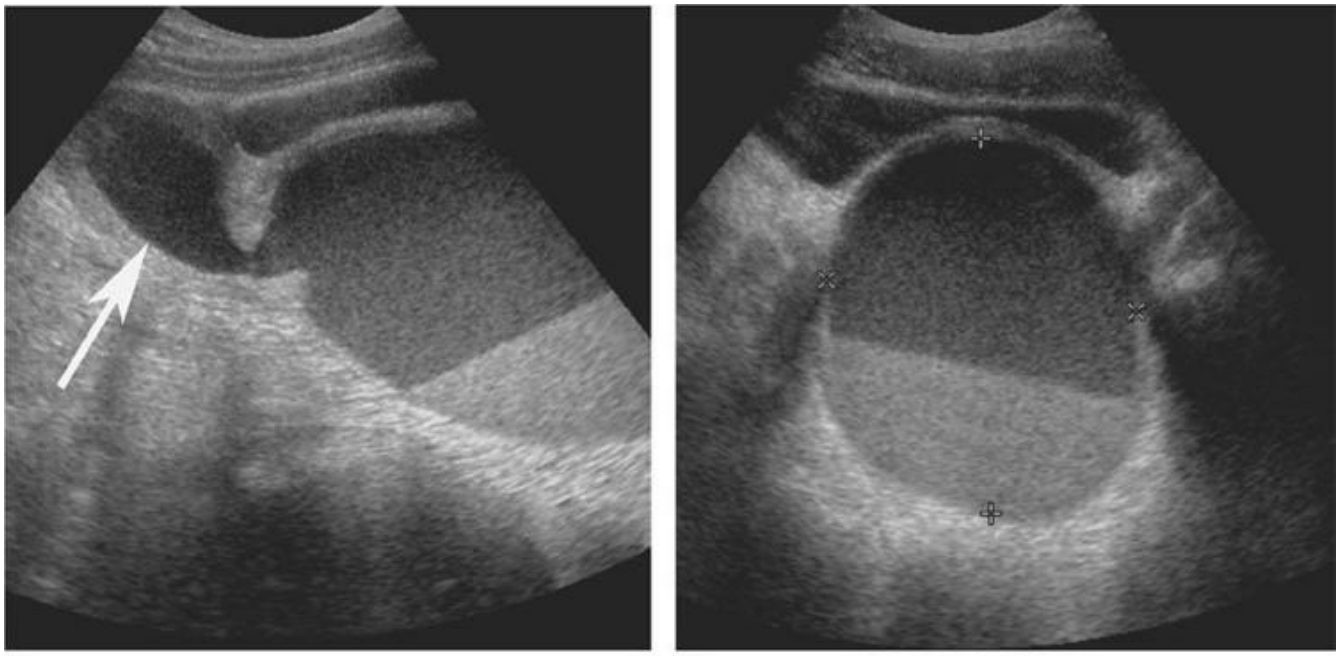

A B

■**FIGURES 8-30A and 8-30B** Sagittal and transverse images from a transabdominal sonogram of the pelvis show a cystic midline pelvic mass with a fluid-debris level. This mass communicates with the endometrial cavity *(arrow)*. Figure 8-30B. Transverse image shows to better advantage the fluid-debris level within the mass.


C

**FIGURE 8-30C** Companion case to Figure 1 showing sagittal image from a transabdominal ultrasound of the pelvis in a different patient. The image also shows a cystic midline pelvic mass but (unlike the patient shown in Figure 1), the endome-trial cavity is not dilated.

## DIFFERENTIAL DIAGNOSIS

**Hydrocolpos:** The fluid-debris level in Figures 8-30A and 8-30B is in the vagina and the fluid extends into the endometrium. However, hydrocolpos refers to dis-tention of solely the vagina (as opposed to distention of the vagina and endometrial cavity) by serous fluid, blood, or urine (e.g., in the presence of a urogenital sinus). Therefore, hydrocolpos is the incorrect diagnosis for Figures 8-30A and 8-30B. However, the findings in Figure 8-30C are consistent with hydrocolpos.

**Hydrometrocolpos:** In this entity, the vagina *and* endo-metrial canal are distended by serous fluid, blood, or urine. Typically, the vagina (which is more compliant than the endometrial canal) will be distended by fluid and debris to a greater extent than the endometrial canal. This diagnosis is the correct one for the patient shown in Figure 8-30A and 8-30B.

**Cystic ovarian tumor:** Cystic ovarian tumors can occur in children. However, the fluid shown in Figure 8-30A and 8-30B is not within the ovary but instead is in the endometrial canal, excluding this diagnosis.

**Anterior meningocele:** Anterior meningoceles can present as a cystic pelvic mass. However, they would be expected to be seen as a mass extrinsic to, rather than within, the endometrial canal and vagina. Therefore, this diagnosis is incorrect.

**Pelvic abscess:** A fluid-debris level can be present in an abscess. However, this diagnosis is excluded because the fluid collection is within the vagina and endometrial cavity rather than within the pelvic cavity.

**Gastrointestinal duplication:** Duplication of the rectum could potentially cause a pelvic mass with the appearance shown in Figure 8-30A and 8-30B. However, this diagnosis is unlikely because rectal duplications are very rare.

## DIAGNOSIS

**Hydrometrocolpos**

## KEY FACTS

### Clinical

- Both hydrocolpos and hydrometrocolpos occur secondary to cervical or vaginal stenosis, hypoplasia, or agenesis. In adolescent girls, an imperforate hymen may be the cause. The term hydrocolpos refers to solely distention of the vagina while the term hydrometrocolpos refers to distention of both the vagina and endometrial cavity.
- Meyer-Rokitansky-Kuster-Houser syndrome is a syndrome in which hydrometrocolpos can be present. In this syndrome, varying degrees of vaginal or cervical stenosis or atresia are associated with other congenital anomalies such as uterine anomalies and renal anomalies.
- McKusick-Kaufman syndrome is a rare, recessively inherited syndrome characterized by vaginal atresia, hydrometrocolpos, postaxial polydactyly, and congenital heart defect.

## Radiologic

- Hydrocolpos and hydrometrocolpos are distention of the vagina or vagina and endometrial cavity, respectively. Sonography typically shows a midline fluid- and debris-filled structure inferior and posterior to the bladder. The vagina is more distended, to various degrees, than the endometrial cavity.
- Occasionally, the obstruction will be at the level of the cervix and only the endometrial cavity will dilate forming a hydrometra.
- Associated congenital anomalies are frequent. The most commonly associated anomaly in infants is imperforate anus. However, abnormalities of the uterus and urinary tract are also common.

# SUGGESTED READING

Capito C, Echaieb A, Lortat-Jacob S, et al. Pitfalls in the diagnosis and management of obstructive uterovaginal duplication: a series of 32 cases. Pediatrics 2008;122:e891–e897.

Dhombres F, Jouannic JM, Brodaty G, et al. Contribution of prenatal imaging to the anatomical assessment of fetal hydrocolpos. Ultrasound Obstet Gynecol 2007;30:101–104.

Lang IM, Babyn P, Oliver GD. MR imaging of paediatric uterovaginal anomalies. Pediatr Radiol 1999;29:163–170.

Nalaboff KM, Pellerito JS, Ben-Levi E. Imaging the endometrium: disease and normal variants. Radiographics 2001;21:1409–1424.

Nazir Z, Rizvi RM, Qureshi RN, et al. Congenital vaginal obstructions: varied presentation and outcome. Pediatr Surg Int 2006;22:749–753.

# Chapter NINE

# Ultrasound

**CLARE HAYSTEAD** ▪ CHAPTER EDITOR

Clare M. Haystead

James D. Bowie

Mark A. Kliewer

Barbara S. Hertzberg

Tamra M. Knutson

Barbara A. Carroll

# CASE 1

**CLARE M.
HAYSTEAD**

## HISTORY

A 28-year-old female presents with vaginal bleeding and a beta-human chorionic gonadotropin (0-HCG) of 100,000 units.

A

**FIGURE 9-1A** Sagittal transvaginal gray-scale US scan of the uterus shows a large echogenic mass with multiple hypoechoic foci distending the endometrial cavity.

B

**FIGURE 9-1B** Corresponding color Doppler ultrasound image demonstrates absence of flow within the cystic spaces. (See color insert)

## DIFFERENTIAL DIAGNOSIS

**Gestational trophoblastic disease or complete molar pregnancy:** The uterus is enlarged and the endometrial canal is filled with echogenic material. Anechoic areas

within the endometrium do not fill with color consistent with cystic spaces. This would be the most likely diagnosis given the sonographic findings and P-HCG.

- **Partial molar pregnancy:** The imaging characteristics of a partial mole can be very similar to a complete molar pregnancy or abortion; however, in a partial molar pregnancy, a gestational sac or fetal tissue is present. The gestational sac and yolk sac are frequently abnormal and fetal anomalies are present. No evidence of an IUP was present in this case.
- **Hydropic degeneration of the placenta:** This can occur in a first trimester abortion but the β-HCG will be lower than in a molar pregnancy and will trend downwards.
- **Ectopic pregnancy:** A decidual reaction in the setting of an ectopic pregnancy can result in a thickened, echogenic endometrium. Careful evaluation of the adnexa should be performed in any patient with a positive β-HCG.

## DIAGNOSIS

**Gestational trophoblastic disease (molar pregnancy)**

## KEY FACTS

### Clinical

- Vaginal bleeding is the most common presentation. Other symptoms include hyperemesis gravidarum, hyperthyroidism, and toxemia. On physical exam, the uterus is larger than expected for dates.
- Risk factors include advancing maternal age, prior history of a molar pregnancy, and Asian ancestry.
- Management is suction and curettage. Pathologic evaluation of the placenta demonstrates hydropic villi and trophoblastic proliferation.
- There is a 20% incidence of associated malignancy and surveillance is performed with serial P-HCG. Contraception for at least a year is recommended.
- Twin pregnancies have been reported with a coexisting normal fetus and placenta.

### Radiologic

- Distinguishing a complete mole, partial mole, and hydropic degeneration of the placenta can be difficult sonographically. The clinical presentation and serum β-HCG are important in making the correct diagnosis.
- The endometrial canal is distended with multiple tiny, hypoechoic spaces. Early in pregnancy, the only finding may be echogenic material within the endometrial canal. Cystic spaces develop as the placental villi degenerate.

- There is incomplete or inadequate vascularization and evaluation with color Doppler demonstrates decreased flow.
- Theca lutein cysts are present in up to 50% of molar pregnancies. They occur later in gestation and are thought to be secondary to the elevated β-HCG levels.

## SUGGESTED READING


Dighe M, Cuevas C, Moshiri M, et al. Sonography in first trimester bleeding. J Clin Ultrasound 2008;36:352–366.

Fraser-Hill MA, Wilson SR. Gestational trophoblastic neoplasia. In CM Rumack, SR Wilson, JW Charbonneau (eds). Diagnostic Ultrasound (3rd ed) (Vol 1). 2004; 589–601.

Green CL, Angtuaco TL, Shah HR, Parmley TH. Gestational trophoblastic disease: A spectrum of radiologic diagnosis. Radiographics 1996;16:1371–1384.

Lazarus E, Hulka C, Seiwert B, Levine D. Sonographic appearance of early complete molar pregnancies. J Ultrasound Med 1999;18:589–594.

Nalaboff KM, Pellerito S, Ben-Levi E. Imaging the endometrium: Disease and normal variants. Radiographics 2001;21:1409–1424.


# CASE 2

**JAMES D.**
**BOWIE**

### HISTORY

A 32-year-old pregnant woman who by examination is “large for dates.”

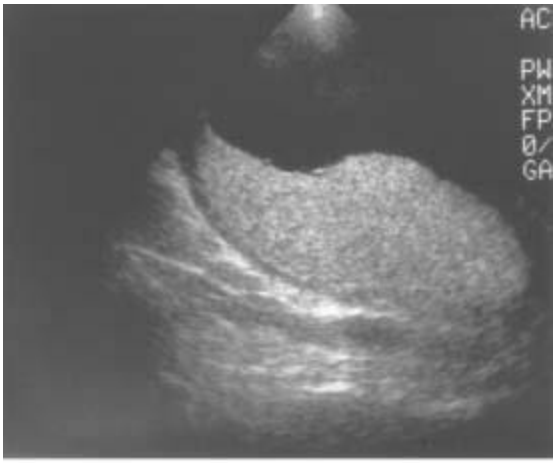


A

**FIGURE 9-2A** Longitudinal sonogram of the placenta. There is slight thickening of the placenta, with a large pocket of amniotic fluid.

B

■**FIGURE 9-2B** Transverse sonogram of the fetal head. There is marked thickening of the skin over the fetal head.


C

■**FIGURE 9-2C** Transverse sonogram of the fetal body. There is fetal ascites outlining the liver and spleen. There is also skin edema.

## DIFFERENTIAL DIAGNOSIS

■**Placental enlargement:** This is one manifestation of hydrops. It is also seen with intrauterine infections and certain chromosomal abnormalities (triploidy most commonly) and in some patients with diabetes.

■**Polyhydramnios:** This is another manifestation of hydrops. It is also seen in a large

number of conditions, including twins, diabetic mothers, and various fetal abnormalities including high gastrointestinal obstructions, central nervous system abnormalities, cardiac abnormalities (both structural and arrhythmias), and in a host of miscellaneous conditions including certain types of limb-shortening syndromes. Many cases of polyhydramnios have no known cause.

- **Skin edema:** This is a common feature of hydrops. A similar appearance is seen in lymphangiectasia, which is often present in association with cystic hygromas. Infants of diabetic mothers with severe macrosomia are often mistaken for babies with skin edema.
- **Fluid collections:** Collections of fluid within the fetus are frequently seen as an indicator of hydrops. Isolated fluid collections can be seen as a result of local inflammation, obstruction, or unknown mechanisms in conditions other than hydrops. For example, obstruction of the thoracic duct can lead to pleural fluid, and meconium peritonitis can lead to peritoneal fluid, as can rupture of an obstructed bladder or ureter.

# DIAGNOSIS

**Hydrops fetalis of undetermined etiology**

# KEY FACTS

## Clinical

- Hydrops fetalis is a condition in the fetus characterized by accumulation of fluid, or edema, in at least two fetal compartments.
- Most hydrops is still a result of an immune reaction between the fetus and the mother. Rh incompatibility is no longer the most common cause of these in Western nations.
- Rhogam is given routinely to Rh-negative mothers in situations of potential Rh exposure.
- Alpha-thalassemia is an important cause of hydrops in Asia.
- Nonimmune fetal hydrops (NIFH) has a 50% to 95% mortality.
- Clinical workup for hydrops fetalis includes blood type and Rh, antibody screen, VDRL, Kleihauer-Betke test for fetal cells, acute and convalescent TORCH titers, and, in some cases, maternal hemoglobin electrophoresis.
- Careful sonographic examination of the fetus, cord, and placenta is essential.

## Radiologic

- The diagnosis of hydrops is made when some combination of the following findings are observed: placental thickening, polyhydramnios, dilatation of the umbilical vein, pericardial fluid, pleural fluid, ascites, and subcutaneous edema. It is not clear what the

earliest indicator of hydrops is or how many or which signs are the most specific. In general, if any one sign is present, early hydrops should be in the differential diagnosis unless there is another well-documented explanation for the abnormality. When three or more of the findings are present, it is highly likely that hydrops is the appropriate diagnosis.

- The task of the sonologist in hydrops is to either guide for percutaneous umbilical blood sampling (PUBS) or to investigate the intrauterine contents carefully for an identifiable cause of NIFH. NIFH has too many causes to list in detail, and hence careful examination of the entire intrauterine contents is necessary. A rough grouping of these conditions is as follows:
    - Structural cardiac defects. Also consider trisomy 13 and 18 if these are seen.
    - Fetal arrhythmia. Either very fast or very slow. Look for arteriovenous block and consider an autoimmune process in the mother.
    - Fetal infections. These are usually detected by serum titers, but focal fluid collections and abdominal calcifications might suggest this as a possibility.
    - Peripheral shunts. (1) Placental tumors such as chorioangiomas, if near the cord insertion or large, may cause fetal hydrops. (2) Vein of Galen aneurysm, when large, may be associated with hydrops. (3) Acardiac twin. In this rare condition, one fetus supplies blood to a partial twin via placental vessels.
    - Masses restricting blood return to the heart. (1) Cystic adenomatoid malformation of the fetal lung. (2) Mediastinal teratoma.

## SUGGESTED READING

Bellini C, Hennekam RC, Fulcheri E, et al. Etiology of nonimmune hydrops fetalis: A systematic review. Am J Med Genet A 2009;149A;844–851.

Fleischer AC, Killam AP, Boehm FH, et al. Hydrops fetalis: Sonographic evaluation and clinical implications. Radiology 1981;141:163–168.

Hoddick WK, Mahony BS, Callen PW, Filly RA. Placental thickness. J Ultrasound Med 1985;4:479–482.

Marino T. Ultrasound abnormalities of the amniotic fluid, membranes, umbilical cord, and placenta. Obstet Gynecol Clin North Am 2004;31:177–200.

# CASE 3

**JAMES D.**
**BOWIE**

### HISTORY

A 29-year-old pregnant woman who by examination is small for gestational age.

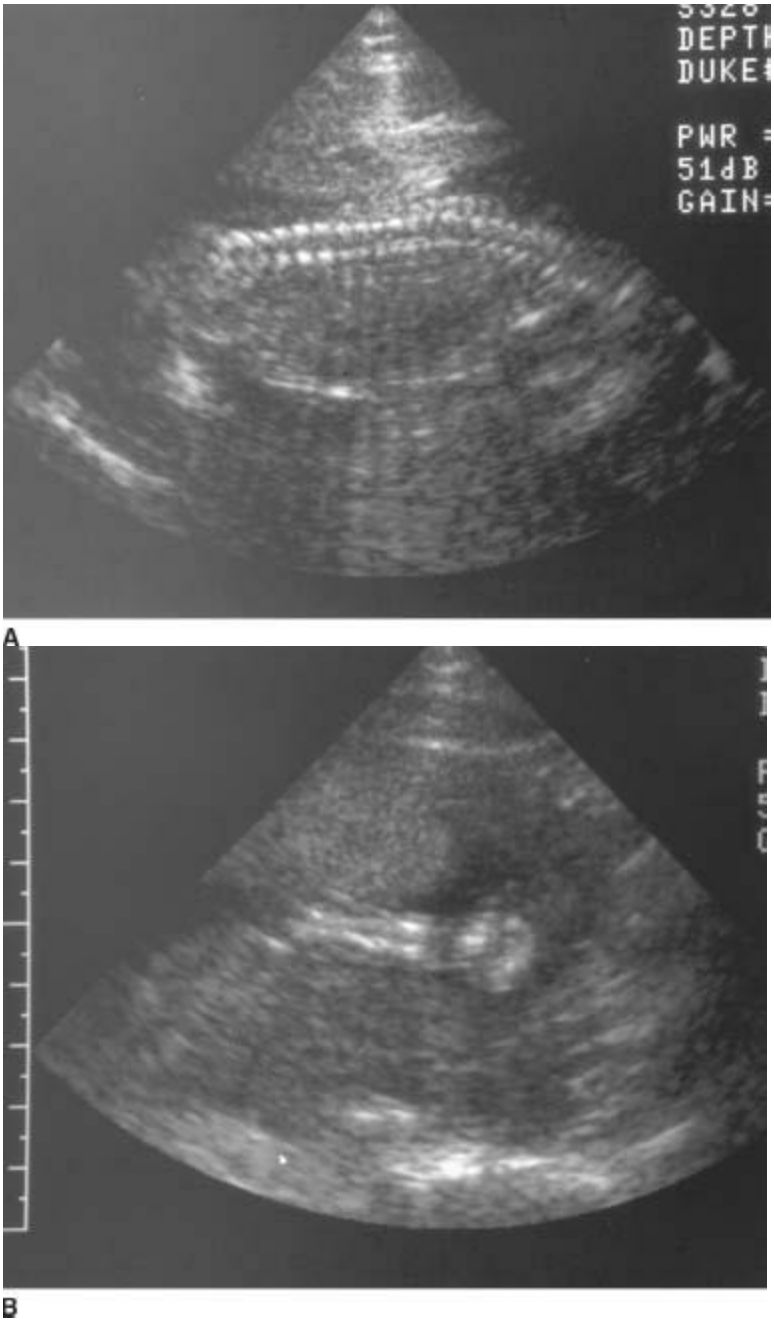


■**FIGURES 9-3A and 9-3B A**: Longitudinal sonogram of the fetal spine. **B:** Longitudinal sonogram of the fetal limb. In both figures, there is marked absence of amniotic fluid, with crowding of fetal parts, increased contact of fetal structuinition of the fetus.

## DIFFERENTIAL DIAGNOSIS

■**Oligohydramnios:** The appearance is characteristic for oligohydramnios with little else to consider. The real issue is the cause of the oligohydramnios.

- **Abdominal pregnancy:** One feature of a rare abdominal pregnancy is the lack of amniotic fluid. This is variable and can be simply a manifestation of the unusual distribution of amniotic fluid. More typically, the fetus is in an extended position and the fetal limbs are spread rather than crowded. The diagnosis in this condition is made by tracing the myometrium from the cervix.

## DIAGNOSIS

**Oligohydramnios from premature rupture of membranes, not clinically suspected**

## KEY FACTS

### Clinical

- Fetal renal function becomes the primary determinant of amniotic fluid volume at about the 18th week of pregnancy.
- Normal amniotic fluid volume increases steadily until about 32 to 34 weeks of pregnancy, then decreases slightly until 42 weeks, then decreases more rapidly.
- The normal variability of amniotic fluid volume at any gestational age is high.
- Amniotic fluid volume is approximately 125 to 300 mL at 16 weeks and 400 to 2,000 mL at 32 weeks.
- Clinically, oligohydramnios is suspected if the fundal height is >4 cm less than expected or fails to grow appropriately by serial examination.
- Clinically, oligohydramnios is defined as <300 mL of fluid at term.
- Oligohydramnios in the second trimester has a poor prognosis and is associated with fetal pulmonary hypoplasia.
- Causes for oligohydramnios include the following:
    - Ruptured membranes: Perhaps the most common, but usually clinically apparent.
    - Fetal distress: Including IUGR, but oligohydramnios may appear before IUGR is detected and also as an independent indicator of fetal distress.
    - Fetal death: Cardiac motion should be looked for in every case.
    - Postmaturity: Oligohydramnios does not diagnose this state but is confirmatory and indicates a possible poor outcome.
    - Fetal renal abnormalities: These require that renal excretion into the amniotic fluid be reduced in volume or electrolyte content. The most common are complete bladder outlet obstruction, renal agenesis, obstruction of one kidney (usually a ureteropelvic junction obstruction [UPJ]), or multicystic dysplasia (MCDK) with an abnormal contralateral kidney (UPJ, MCDK, or agenesis).

### Radiologic

- Diagnosis of oligohydramnios can be made by inspection. This subjective impression has been shown to be as good as objective measurements. The appearance of poor fetal definition, increased contact of the fetus with the uterine wall, crowding of fetal parts, and lack of fluid are consistent with this diagnosis.
- Some observers have looked for the largest single pocket of fluid and have measured either the volume or the greatest vertical diameter. When the latter is <2 cm, oligohydramnios is present.
- The amniotic fluid index is commonly used. This index measures the largest vertical diameter of the pockets of fluid in each of the four quadrants of the uterus and takes their sum. The number is looked up in a gestational age-adjusted table. Generally, any number P5 cm is consistent with oligohydramnios.
- The use of color Doppler in oligohydramnios before attempting to withdraw fluid will reveal that what appears to be a small pocket of fluid in many cases is actually the umbilical cord.
- A phenomenon called first-trimester oligohydramnios has been described. This is a misnomer. The term refers to a gestational sac that is small for the occupying embryo and suggests a poor prognosis.

## SUGGESTED READING


Bromley B, Harlow BL, Laboda LA, et al. Small sac size in the first trimester: A predictor of poor fetal outcome. Radiology 1991;178:375–377.

Goldstein RB, Filly RA. Sonographic estimation of amniotic fluid volume: Subjective assessment versus pocket measurements. J Ultrasound Med 1988;7:363–369.

Marino, T. Ultrasound abnormalities of the amniotic fluid, membranes, umbilical cord, and placenta. Obstet Gynecol Clin North Am 2004;31:177–200.

Moore TR, Cayle JE. The amniotic fluid index in normal human pregnancy. Am J Obstet Gynecol 1990;162:1168–1173.

Queenan JT, Thompson W, Whitfield CR, et al. Amniotic fluid volumes in normal pregnancies. Am J Obstet Gynecol 1972;114:34–38.

Seeds, AE. Current concepts of amniotic fluid dynamics. Am J Obstet Gynecol 1980;138:575–586.

Schrimmer, DB Moore, TR Sonographic evaluation of amniotic fluid volume. Clin Obstet Gynecol 2002;45:1026–1038.


# CASE 4


**JAMES D.**
**BOWIE**


## HISTORY

A 29-year-old pregnant woman is referred for a routine fetal ultrasound.

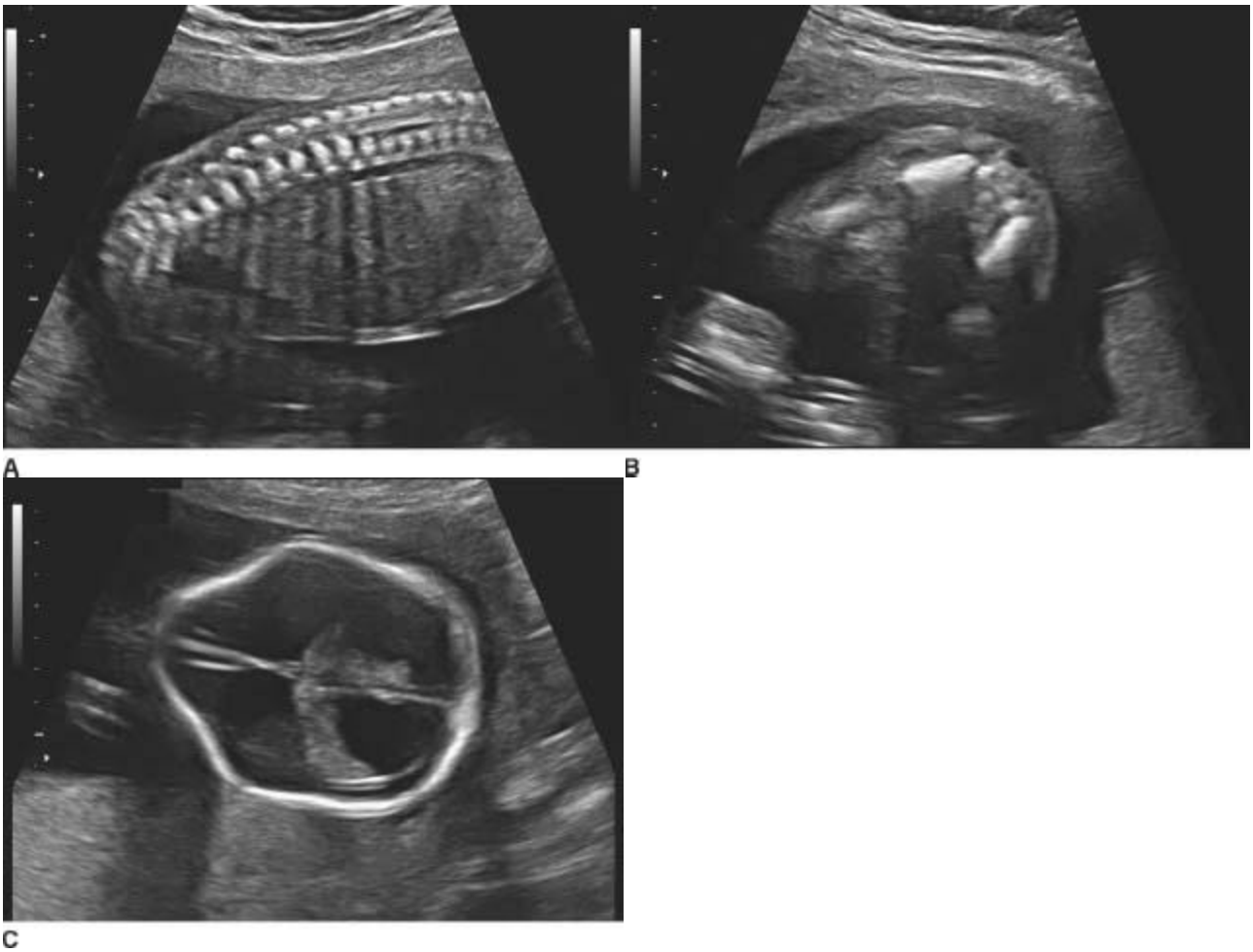


**FIGURE 9-4A, 9-4B, and 9-4C** Sagittal (**A**) and transverse (**B**) gray-scale sonographic images of the fetal lumbosacral region show a small lumbar meningomyelocele. **C** : Transverse gray-scale US image of the fetal head shows scalloping of the frontal bones (the so-called, lemon sign) and ventriculomegaly. Note the dangling choroid plexus protruding into the dilated ventricles.

## DIFFERENTIAL DIAGNOSIS

- **Chiari II malformation:** This is the most likely diagnosis given the findings. A small sacral myelomeningocele is present, which should prompt for evaluation of the presence of Chiari II and associated ventriculomegaly. The frontal bones have a "lemon"configuration; however, this can be seen in normal pregnancies.
- **Meningocele:** This is the likely reason for the small echogenic focus at the distal spine, but a skin lesion such as a hemangioma could have a similar appearance.

- **Sacrococcygeal teratomas:** These may occur in the distal spine, but they are not directly posterior since they originate anterior to the spine. Furthermore, they tend to be much larger.

## DIAGNOSIS

**Chiari II malformation with a small sacral meningocele**

## KEY FACTS

### Clinical

- Chiari II malformation is characterized by a small posterior fossa with downward displacement of the brain-stem, resulting in protrusion of the tonsils and vermis below the cisterna magna.
- Secondary features seen prenatally include a meningocele or encephalocele in about 90% of cases and partial or complete absence of the corpus callosum in about 40% of cases.
- Hydrocephalus is commonly seen by sonography as the first indication of Chiari II, but it is not always present early. The presence of ventriculomegaly is much more common after 24 weeks of gestation.
- Many of the computed tomography (CT) or magnetic resonance imaging (MRI) features of this condition, such as a large massa intermedia, polymicrogyria, beaking of the tectal plate, hydromelia, and syringomelia, have not been described as prenatal sonographic features of Chiari II.
- Periconceptional intake of 0.4 mg of folic acid significantly reduces the risk of neural tube defects.
- The overall prognosis for a myelomeningocele diagnosed in utero depends on the presence and type of other abnormalities. Approximately 50% to 80% of fetuses have other abnormalities.
- Most deaths in patients with an isolated myelomeningocele are the result of the hindbrain dysfunction associated with Chiari II malformation. About 15% of patients die by the age of 10.
- About 30% of survivors have IQs >100. About 30% have IQs <80. About one-third have hindbrain dysfunction.
- Ninety percent of neonatal survivors require ventriculoperitoneal shunts. About half of these shunts must be revised by age 6. About a third require two shunt revisions and a fifth three or more.
- Almost 100% of survivors have some loss of motor function. Urinary incontinence is common.

### Radiologic

- The lemon sign has been said to be a specific finding of Chiari II malformations, but it is also seen in normals. This is especially true for milder degrees of frontal bone contour abnormalities.
- Infratentorial findings of Chiari II include the “banana”cerebellum and effacement of the cisterna magna. The degree of severity of the posterior fossa deformity correlates with the degree of hydrocephaly.
- Both the degree and prevalence of hydrocephaly increases with gestational age.
- The absence of ventriculomegaly prior to 24 weeks does not exclude either a meningocele or Chiari II.
- Other sonographic findings have been described more recently in Chiari II including the ventricular “point,”abnormal tectal morphology, and the presence of an interhemispheric cyst.

## SUGGESTED READING

Babcock CJ, Goldstein RB, Barth RA, et al. Prevalence of ventriculomegaly in association with myelomeningocele and severity of posterior fossa deformity. Radiology 1994;190:703–707.

Callen AL, Filly RA. Supratentorial abnormalities in the Chiari II malformation, I: The ventricular point. J Ultrasound Med 2008;27:33–38.

Callen AL, Stengel JW, Filly RA. Supratentorial abnormalities in the Chiari II malformation, II: Tectal morphologic changes. J Ultrasound Med 2009;28:29–35.

Filly RA. The “lemon”sign: A clinical perspective. Radiology 1998;167:573–575.

Wong SK, Barkovich AJ, Callen AL, Filly RA. Supratentorial abnormalities in the Chiari II malformation, III: The interhemispheric cyst. J Ultrasound Med 2009;28:999–1006.

# CASE 5

**CLARE M.**
**HAYSTEAD**

### HISTORY

A 54-year-old who underwent CT evaluation for vague abdominal pain. An ultrasound was recommended for further evaluation of the gallbladder.

A

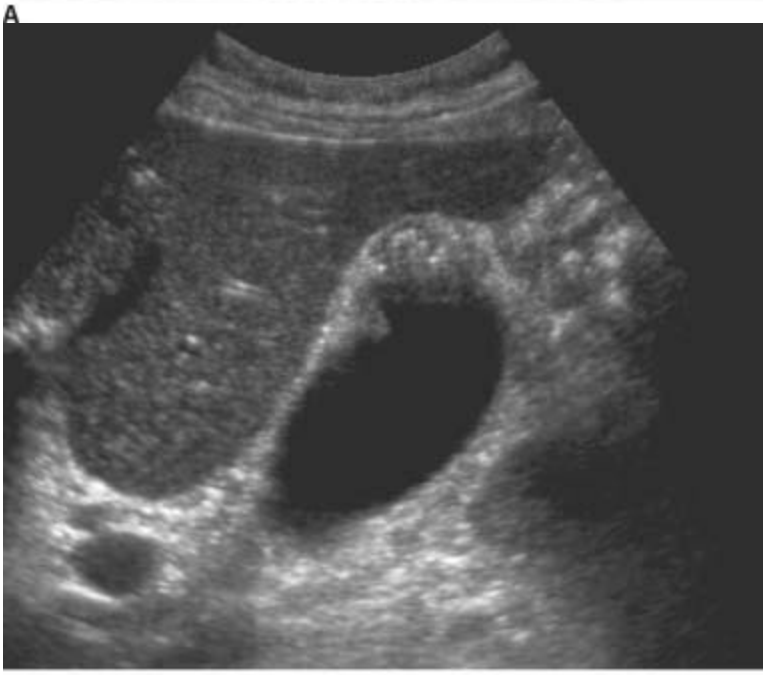

B

**FIGURES 9-5A and 9-5B** Longitudinal gray-scale US images obtained with a 5.0-MHz curvilinear-array transducer demonstrate focal thickening of the gallbladder fundus with echogenic intramural foci and associated "comet tail"reverberation artifacts.

## DIFFERENTIAL DIAGNOSIS

**Primary gallbladder malignancy:** Adenocarcinoma can present as irregular wall thickening, both focal and diffuse. The most common presentation is a mass replacing the gallbladder in the gallbladder fossa. Associated findings include wall calcification,

biliary ductal dilatation, gallstones, and the presence of metastatic disease, especially liver involvement.

- **Adenomyomatosis:** The classic appearance is focal wall thickening in the gallbladder fundus. The presence of cystic spaces and echogenic foci with "comet tail"reverberation artifact is diagnostic of adenomyomatosis.
- **Emphysematous cholecystitis:** Air within the gallbladder wall can cause echogenic foci with ring down artifacts. The gallbladder lumen is difficult to identify in diffuse emphysematous cholecystitis and patients are usually acutely symptomatic.
- **Acute cholecystitis:** Gallbladder wall thickening is one of the findings described in acute cholecystitis; however, the "comet tail"reverberation artifact in this case is diagnostic of adenomyomatosis.

# DIAGNOSIS

**Adenomyomatosis**

# KEY FACTS

## Clinical

- Adenomyomatosis is characterized by benign hyper-plasia of the gallbladder mucosa that creates invaginations through the thickened muscular layer known as Rokitansky-Aschoff sinuses.
- It is thought to be acquired and somewhat similar to colonic diverticulosis. Most patients are asymptomatic. Those that are symptomatic typically undergo a non-emergent cholecystectomy.
- Ninety percent have associated gallstones; however, the association is unclear.
- It is considered one of the hyperplastic cholecystosis, the other being cholesterolosis. As the name implies, it is a benign process.

## Radiologic

- Adenomyomatosis can cause focal, segmental, or diffuse wall thickening. Focal adenomyomatosis tends to be fundal in location as in this case. An "hourglass"shaped gallbladder can be seen in the segmental subtype resulting in thickening and narrowing of the midportion of the gallbladder wall.
- Multiple cystic spaces are present representing enlarged Rokitansky-Aschoff sinuses that are filled with bile.
- Echogenic foci within the sinuses are thought to represent cholesterol deposits or small stones.

- This condition can appear as focal gallbladder wall thickening on CT and differentiating it from gallbladder cancer can be difficult. The presence of intramural diverticuli increases diagnostic confidence.
- The “pearl necklace”sign has been described on MRCP corresponding to curvilinear foci of high T2 signal within the gallbladder wall. Stones can form within the diverticuli causing signal voids on MRI.

## SUGGESTED READING

Boscak AR, Al-hawary M, Ramsburgh SR. Best cases from the AFIP: Adenomyomatosis of the gallbladder. Radiographics 2006;26:941–946.

Ching BH, Yeh BM, Westphalen AC, et al. CT differentiation of adenomyomatosis and gallbladder cancer. AJR Am J Roentgenol 2007;182:62–66.

Ghersin E, Soudack M, Gaitini D. Twinkling artifact in gallbladder adenomyomatosis. J Ultrasound Med 2003;22:229–231.

Secil M, Karasu S, Sagol O, Coker A. Combined segmental and focal adenomyomatosis involving the body of the gallbladder. J Clin Ultrasound 2005;33:248–250.

Yoon, JH, Cha SS, Han SS, et al. Gallbladder adenomyomatosis: Imaging findings. Abdom Imaging 2006;31:555–563.

# CASE 6

**MARK A.**
**KLIEWER**

### HISTORY

A 35-year-old woman presents with vague right upper quadrant pain.

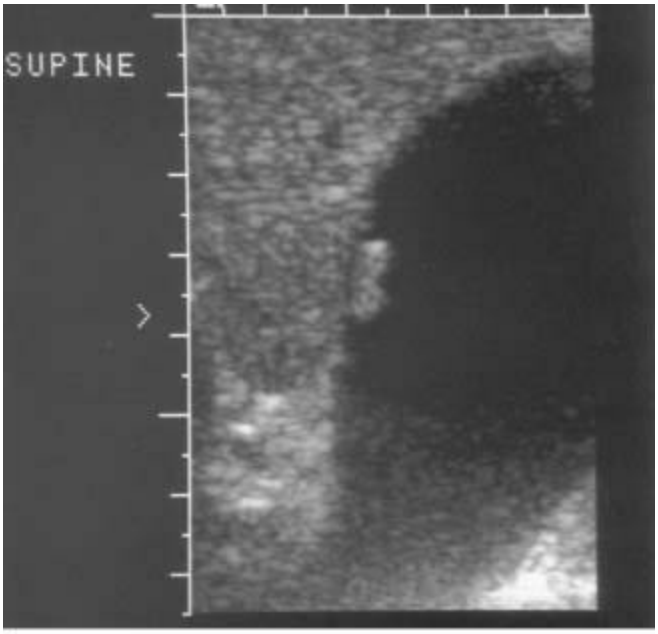

A

■**FIGURE 9-6A** Longitudinal sonogram of the gallbladder fossa. Attached to the gallbladder wall is a small echogenic mass. This mass does not cause significant ring down or shadowing artifacts.

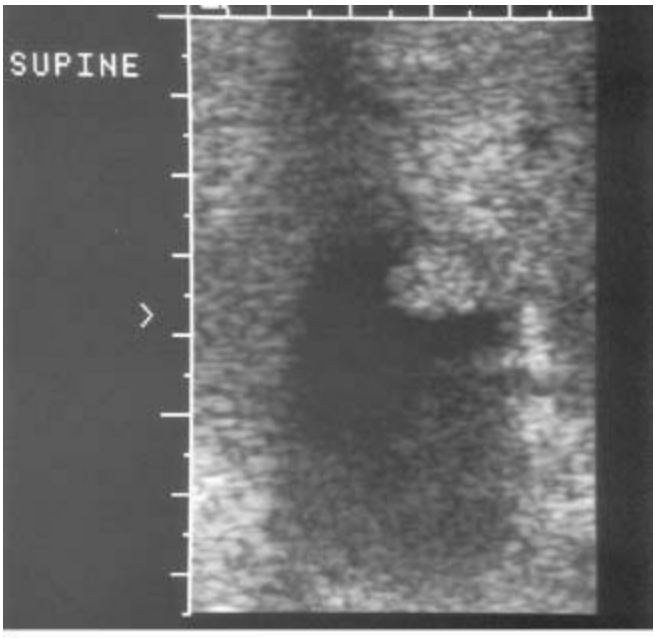

B

■**FIGURE 9-6B** High-resolution sonogram of this same location. High-resolution image reveals the lobular contour of the gallbladder wall mass.

## DIFFERENTIAL DIAGNOSIS

■**Gallstone:** A gallstone is unlikely because the abnormality is adherent to the wall and

nonmobile, and because of the absence of posterior acoustic shadowing.

- **Cholesterol polyp:** These polyps are common intraluminal masses that are most often multiple. The polyps tend to be small, usually <5 mm in size, and almost always <1 cm in size. They are not associated with acoustic shadowing.
- **Adenoma or papilloma:** These lesions are almost always singular and are much less common than cholesterol polyps. These masses can be sessile and broad based (adenomas) or pedunculated and lobulated (papillary adenomas). Masses are usually <1 cm.
- **Primary gallbladder carcinoma:** Carcinomas are most often seen as a large, solid mass replacing the gallbladder in the gallbladder fossa. Occasionally, in earlier stages focal intraluminal masses are seen, but these are usually >1 cm in size. Associated findings include wall calcification, biliary duct dilatation, gallstones (80%), and evidence for metastatic spread, particularly to the liver.
- **Tumefactive sludge:** This echogenic bile is not usually adherent to the wall but rather shifts location as the patient is repositioned.

## DIAGNOSIS

**Cholesterol polyp**

## KEY FACTS

### Clinical

- Cholesterolosis results from the accumulation of cholesterol within the wall of the gallbladder. This accumulation can either be diffuse or polypoid.
- Cholesterol nodules can stud the mucosal surface, producing the so-called strawberry gallbladder seen pathologically.
- Cholesterolosis is equally common in men and women. The etiology is uncertain.

### Radiologic

- Intraluminal masses are commonly seen during gallbladder ultrasound. Fortunately, the majority of these are cholesterol polyps that are benign.
- Sonographically, cholesterol polyps are most commonly multiple and small. Most of these benign polypoid masses in the gallbladder are <1 cm. It is common clinical practice to follow polyps between 5 mm and 1 cm for a 2-year period to document any change or growth of the lesion. Lesions that are significantly >1 cm may require surgery.
- Cholesterol polyps are nonmobile intraluminal masses that are firmly adherent to the wall. They do not cause acoustic shadowing. Such polyps can be hypo-or hyperechoic,

though most, in our experience, are hyperechoic.

## SUGGESTED READING

Collett JA, Allan RB, Chisholm RJ, et al. Gallbladder polyps: Prospective study. J Ultrasound Med 1998;17:207–211.

Jutras JA. Hyperplastic cholecystoses. AJR Am J Roentgenol 1960;83:795–827.

Levy AD, Murakata LA, Abbott RM, Rohrmann CA Jr. From the archives of the AFIP. Benign tumors and tumorlike lesions of the gallbladder and extrahepatic bile ducts: Radiologic-pathologic correlation. Armed Forces Institute of Pathology. Radiographics 2002;22:387–413.

Middleton WD. Gallbladder. In BB Goldberg (ed), Textbook of Abdominal Ultrasound. Baltimore: Williams & Wilkins, 1993;116–145.

Price RJ, Stewart ET, Foley WD, Dodds WJ. Sonography of polypoid cholesterolosis. AJR Am J Roentgenol 1982;139:1197–1198.

Ruhe AH, Zachman JP, Mulder BD, Rime AE. Cholesterol polyps of the gallbladder: Ultrasound demonstration. J Clin Ultrasound 1979;7:386–388.

# CASE 7

**MARK A. KLIEWER**

## HISTORY

A 53-year-old man presents with acute abdominal pain and vomiting.

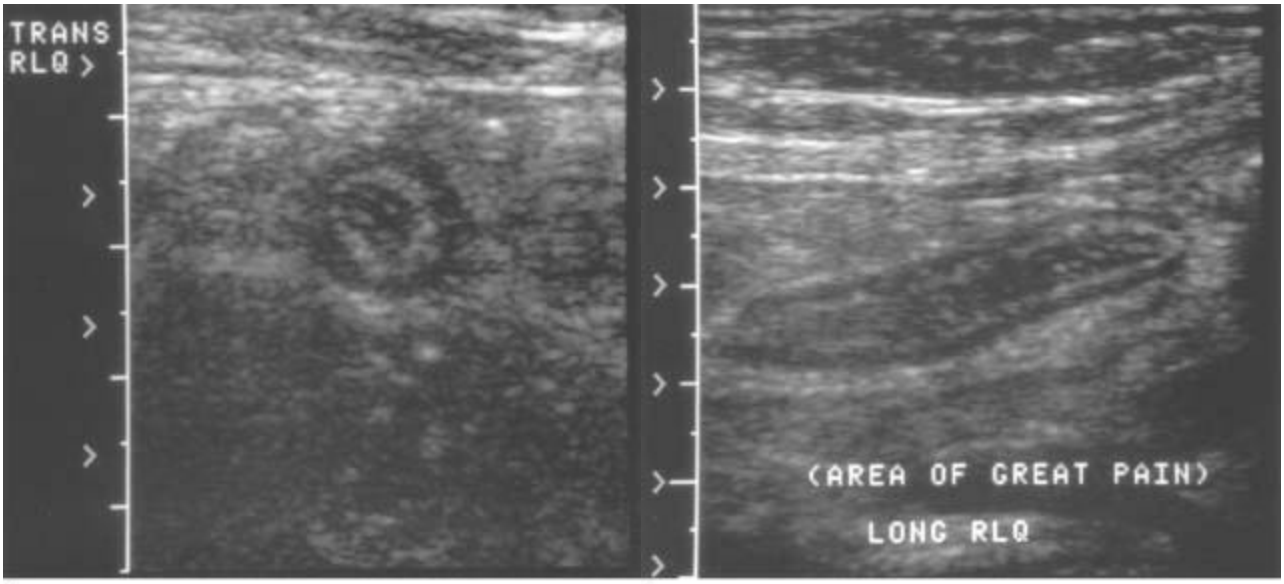


■**FIGURES 9-7A and 9-7B A**: Transverse sonogram of the right lower quadrant. **B:**

Longitudinal sonogram of the same area in the right lower quadrant. The transducer was placed over the area of greatest tenderness. Longitudinal and transverse images demonstrate a noncompressible, tubular structure measuring 11 mm in diameter. The rounded end of the structure is clearly identifiable. The structure demonstrates a hyperechoic inner layer and a surrounding, peripheral hypoechoic layer.

## DIFFERENTIAL DIAGNOSIS

- **Normal appendix:** The normal appendix should have a diameter of <6 mm and should be compressible. In addition, there should be no evidence of inflammatory changes in the periappendiceal fat.
- **Crohn's disease:** Hypoechoic, uniform thickening of the bowel wall in the terminal ileum would surround compressed echogenic mucosa centrally. Furthermore, the terminal ileum would not have a blind end.
- **Appendicitis:** This is the best diagnosis for a rigid tubular structure located in the right lower quadrant at the site of maximal tenderness. The diameter measurement from the outer wall to the outer wall of the structure exceeds 6 mm. The structure is noncompressible and blind ended. On the longitudinal view, a region of increased echogenicity surrounding the appendix suggests inflammation in the periappendiceal fat.
- **Mesenteric adenitis:** With this disease process, enlarged lymph nodes and mural thickening of the terminal ileum will be evident. Peristalsis should also be present in the terminal ileum. Inflamed lymph nodes would be unlikely to have such a smooth tubular contour, or the layering of hyperechoic and hypoechoic strata that constitute the gut signature.
- **Pelvic inflammatory disease (PID):** Though PID is a possible pitfall, findings should be located more in the pelvis than the right lower quadrant. A hydrosalpinx would not have the same echo pattern as the bowel.

## DIAGNOSIS

**Appendicitis**

## KEY FACTS

### Clinical

- Though the clinical suspicion of appendicitis is correct in 70% of patients with this disease, the clinical picture can be confusing. As a result, surgeons have long accepted a removal rate of normal appendices between 15% and 33%. This percentage has diminished, however, with the widespread use of multidetector CT.

- Young women can be particularly difficult to diagnose because of the similarity of symptoms between appendicitis, PID, and ovarian torsion.

## Radiologic

- The technique of examination requires using high-frequency, linear transducers (5 or 7 MHz). The sonologist applies graded compression with the transducer and moves from the right upper quadrant to the right lower quadrant following the right colon inferiorly. Alternatively, the iliac vessels can be identified in the groin and followed superiorly.
- The patient can often direct attention to pathology by localizing pain. Be alert to areas of maximal tenderness.
- The goal is to compress the inflamed appendix against the posterior abdominal wall or the psoas muscles.
- An inflamed appendix is noncompressible and has a diameter of >6 mm.
- A fecalith may be seen within the appendix and may be associated with acoustic shadowing.
- Look also for periappendiceal fluid, abscess, or an inflammatory mass. The circumferential echogenic mucosal layer of the appendix may be disrupted when perforation occurs. The periappendiceal fat may be echogenic, indicating inflammatory involvement.
- Increased Doppler signal (blood flow) can be found both within and surrounding the inflamed appendix.

## SUGGESTED READING

Noguchi N, Yoshimitsu K, Yoshida M. Periappendiceal hyperechoic structure on sonography: A sign of severe appendicitis. J Ultrasound Med 2005;24:323–327.

Puylaert JB. Ultrasonography of the acute abdomen: Gastrointestinal conditions. Radiol Clin North Am 2003;41:1227–1242.

Rettenbacher T, Hollerweger A, Macheiner P, et al. Outer diameter of the vermiform appendix as a sign of acute appendicitis: Evaluation at US. Radiology 2001;218:757–762.

Worrell JA, Droishagen LF, Kelly TC, et al. Graded compression ultrasound in the diagnosis of appendicitis. J Ultrasound Med 1990;9:145–150.

# CASE 8

**MARK A.**
**KLIEWER**

## HISTORY

A 26-year-old woman presents for a routine obstetric ultrasound.


A

■**FIGURE 9-8A** Longitudinal sonogram of the fetal body, cephalic presentation. The fetal thorax is on the right of the image and the fetal abdomen on the left. The hypoechoic arc of the diaphragm is apparently disrupted. Superior to the diaphragm and posterior to the heart, there is a rounded, fluid-filled structure that most likely represents the stomach.


B

■**FIGURE 9-8B** Transverse sonogram through the fetal chest at the level of the heart demonstrates the fluid-filled structure adjacent to the heart. In this cephalic presentation, the heart is on the right side of the fetal body, indicating displacement from its normal position.

## DIFFERENTIAL DIAGNOSIS

- **Cystic adenomatoid malformation:** This entity is typically seen as multiple large cysts or an echogenic mass. Occasionally, it can occur with a diaphragmatic hernia.
- **Congenital diaphragmatic hernia (CDH):** A hernia of this type is a likely possibility given the displacement of the stomach into the chest and the apparent discontinuity of the hypoechoic diaphragm.
- **Bronchogenic and esophageal duplication cyst:** It is possible that the fluid-filled structure in the left chest could be a foregut abnormality; however, the stomach is not present in its expected location.
- **Cystic teratoma:** These are typically complex masses with cystic and solid components arising in the mediastinum.
- **Eventration of the diaphragm:** It is difficult to exclude eventration with certainty, considering how difficult it is to demonstrate the full contour of the diaphragm in the normal fetus.

## DIAGNOSIS

**Congenital diaphragmatic hernia**

## KEY FACTS

### Clinical

- Herniation of bowel or solid organs can occur through defects in the diaphragm that form from incomplete closure during embryologic development. Most are Bochdalek defects, which occur posteriorly, usually on the left side.
- Bowel herniating through the left-sided defect will cause displacement of thoracic structures, particularly the heart, to the right.
- When hernias occur on the right side, the liver may be involved.
- Patients sometimes present because their fundal size is greater than their dates. This results when there is associated polyhydramnios, which most often develops in the third trimester.
- More than half of babies with CDH will have an associated anomaly. These anomalies can involve the heart, genitourinary system, the central nervous system, and the gastrointestinal tract. The diaphragmatic hernia can be part of a larger syndrome, such as the trisomy syndromes.
- There is a high mortality rate for infants born with diaphragmatic hernias resulting primarily from pulmonary hypoplasia.

## Radiologic

- Sonographic diagnosis depends on the demonstration of bowel in the fetal thorax. On a true transverse image, the heart should never be at the same level as the stomach. Occasionally, hepatic, portal, and mesenteric blood vessels will be displaced toward the defect. The stomach will not be located in its expected left upper quadrant position, and the abdomen can appear scaphoid due to the relocation of bowel from the abdomen to the thorax.
- Intrathoracic structures are usually displaced to the right with left-sided lesions. The heart, in particular, will be found on the right side. Occasionally, the diaphragm can be inspected directly and a defect identified. The motion of the two hemidiaphragms can be compared during fetal breathing for evidence of dissynchronous motion.
- Polyhydramnios frequently complicates the pregnancy.
- The sonologist should always look for other evidence of fetal abnormality, including other structural anomalies and intrauterine growth retardation.
- MRI is used increasingly in the evaluation of CDH.

## SUGGESTED READING

Chinn DH, Filly RA, Callen PW, et al. Congenital diaphragmatic hernia diagnosed prenatally by ultrasound. Radiology 1983;148:119–123.

Comstock CH. The antenatal diagnosis of diaphragmatic anomalies. J Ultrasound Med 1986;5:391–396.

Leung JW. Prenatal MR imaging of congenital diaphragmatic hernia. AJR Am J Roentgenol 2000;174:1607–1612.

May DA, Barth RA, Yeager S, et al. Perinatal and postnatal chest sonography. Radiol Clin North Am 1993;31:499–516.

Morin L, Crombleholme TM, D'Alton ME. Prenatal diagnosis and management of fetal thoracic lesions. Semin Perinatol 1994;18:228–253.

Vettraino IM, Lee W, Comstock CH. The evolving appearance of a congenital diaphragmatic hernia. J Ultrasound Med 2002;21:85–89.

# CASE 9

**BARBARA S. HERTZBERG**

### HISTORY

A 28-year-old woman has vaginal bleeding and a positive β-HCG level.


A

■**FIGURE 9-9A** Sagittal endovaginal sonogram of the uterus. There is no evidence of an intrauterine pregnancy. The endometrial stripe is normal.


B

■**FIGURE 9-9B** Coronal endovaginal sonogram of the left adnexa. An echogenic ring surrounds a rounded fluid collection in the left adnexa, consistent with an "adnexal ring sign."


C

■**FIGURE 9-9C** Sagittal endovaginal sonogram of the pelvic cul-de-sac. Echogenic free

fluid surrounds loops of bowel in the cul-de-sac, due to hemoperitoneum.

## DIFFERENTIAL DIAGNOSIS

- The differential diagnosis includes conditions found in patients with a positive serum β-HCG but no ultrasound evidence of an intrauterine pregnancy:
- **Early intrauterine pregnancy:** This is unlikely because there are abnormal findings in both the adnexa and the cul-de-sac.
- **Spontaneous abortion:** This condition is also unlikely because of the abnormalities in the adnexa and the cul-de-sac.
- **Gestational trophoblastic disease:** This disease is unlikely because the endometrial stripe is normal. There is no evidence of an echogenic intrauterine mass with multiple internal cysts, the finding usually seen in patients with gestational trophoblastic disease.
- **Ectopic pregnancy:** This is the best diagnosis because demonstration of an "adnexal ring sign"in conjunction with sonographically demonstrable hemoperitoneum is highly suggestive of ectopic pregnancy in a patient with a positive β-HCG and no intrauterine pregnancy.

## DIAGNOSIS

**Left ectopic pregnancy**

## KEY FACTS

### Clinical

- The spectrum of clinical symptoms ranges from pelvic pain and vaginal bleeding (often clinically indistinguishable from spontaneous abortion) to catastrophic intra-abdominal hemorrhage.
- A β-HCG is necessary to interpret the ultrasound findings: a negative serum β-HCG effectively excludes an ectopic pregnancy.
- The "classic clinical triad"suggesting ectopic pregnancy is amenorrhea, pain, and palpable adnexal mass. This triad, however, is often not present.
- All women with positive β-HCG should be considered at risk for ectopic pregnancy. The following groups are at especially high risk: history of PID, intrauterine contraceptive device, prior ectopic pregnancy, tubal reconstructive surgery, prior tubal ligation, or invitro fertilization.
- A minority of patients with ectopic pregnancy are critically ill and hemodynamically unstable due to massive intra-abdominal hemorrhage. They require rapid fluid resuscitation and immediate laparotomy, and there may be no time for ultrasound

imaging in this group.

## Radiologic

- Ultrasound is the imaging procedure of choice in the patient with a suspected ectopic pregnancy.
- One of the main goals of ultrasound is to assess whether there is an intrauterine pregnancy. An intrauterine pregnancy and a coexistent ectopic pregnancy is a rare entity, so if an intrauterine pregnancy is documented, it is generally considered safe to assume there is no ectopic pregnancy.
- An intrauterine pregnancy can be diagnosed based on the demonstration of at least one of the following ultrasound findings: (1) intrauterine embryo with cardiac activity, (2) intrauterine yolk sac, and (3) intrauterine gestational sac. An intrauterine gestational sac must be distinguished from a pseudogestational sac of an ectopic pregnancy because ectopic pregnancies can frequently be associated with fluid collections within the uterus. Demonstration of either a “double decidual sac sign”or an “intradecidual sign,”in which the uterine cavity is shown to be separate from the developing gestational sac, indicates the presence of an intrauterine gestational sac.
- The only ultrasound finding 100% diagnostic of ectopic pregnancy is identification of an extrauterine embryo with cardiac activity.
- The adnexal ring sign, produced when echogenic trophoblastic tissue grows on the inner surface of the fallopian tube around the developing gestational sac, is the next most reliable sign of ectopic pregnancy. Other adnexal findings include pelvic and tubal hematomas. These can assume a wide variety of ultrasound appearances depending on the stage of the hematoma.
- In the appropriate setting, fluid in the cul-de-sac should also raise the level of concern for ectopic pregnancy, particularly if it contains low-level echoes suggesting the presence of blood.
- A negative pelvic ultrasound (empty uterus, normal-appearing ovaries, no adnexal masses, and no free fluid in the cul-de-sac) does not exclude an ectopic pregnancy.

# SUGGESTED READING


Bhatt S, Ghazale H, Dogra VS. Sonographic evaluation of ectopic pregnancy. Radiol Clin North Am 2007;45:549–560.

Filly RA. Ectopic pregnancy: The role of sonography. Radiology 1987;162:661–668.

Hertzberg BS. Ultrasound evaluation for ectopic pregnancy. Radiologist 1994;1:11–18.

Lin EP, Bhatt S, Dogra VS. Diagnostic clues to ectopic pregnancy. Radiographics 2008;28:1661–1671.

Nyberg DA, Hughes MP, Mack LA, Wang KY. Extrauterine findings of ectopic pregnancy at transvaginal US: Importance of echogenic fluid. Radiology 1991;178:823–826.

Parvey RH, Maklad N. Pitfalls in the transvaginal sonographic diagnosis of ectopic pregnancy. J Ultrasound Med

1993;3:139–144.

# CASE 10

**BARBARA S.
HERTZBERG**

## HISTORY

A 38-year-old pregnant woman presents with third-trimester bleeding.

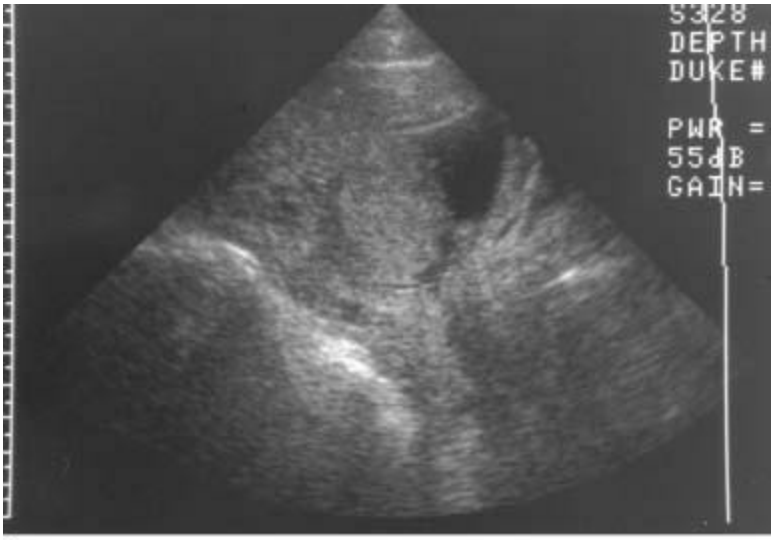


A

V**FIGURE 9-10A** Midline sagittal transabdominal sonogram of the lower uterus and cervix. There is a posterior placenta. The lower edge of the placenta overlies the endocervical canal.

B

**FIGURE 9-10B** Transperineal sonogram of the lower uterus and cervix. The transperineal image confirms the presence of placental tissue covering the endocervical canal. (The endocervical canal is delineated by electronic measurement calipers.)

## DIFFERENTIAL DIAGNOSIS

Placenta previa should be considered whenever placental tissue overlies the region of the cervix at ultrasonography. False-positive diagnoses of placenta previa are common and must be considered prior to making a definitive diagnosis.

- **False-positive due to distended urinary bladder:** This is unlikely, because the bladder does not appear distended on the ultrasound images.
- **False-positive due to uterine contraction:** A contraction is unlikely because there is no evidence of a lower uterine contraction on either of the images. A uterine contraction might be associated with an elongated cervix that is distorted in its overall appearance. The cervix in this patient is normal in length and configuration.
- **Subchorionic hematoma overlying the cervix:** This condition would be possible if the hematoma were imaged in an acute stage, because the sonographic pattern of an acute hematoma can be remarkably similar to that of placental tissue. It may be possible to appreciate a subtle difference in the echo pattern of the hema-toma versus the echo pattern of placental tissue. At times, the distinction is only made at the time of follow-up sonography because a subchorionic hematoma will show evolution in its appearance.
- **Fibroid overlying cervix:** Such a fibroid is unlikely because the tissue overlying the cervix is continuous with placental tissue and does not have a sonographic pattern typical for a leiomyoma.
- **Complete placenta previa:** This is the best diagnosis because placental tissue completely overlies the internal os.

# DIAGNOSIS

**Complete placenta previa**

# KEY FACTS

## Clinical

- Painless vaginal bleeding is the clinical hallmark of placenta previa. Bleeding most commonly occurs in the third trimester but can also occur during the second trimester.
- Vaginal delivery can result in disastrous complications, including either or both maternal and fetal death due to massive bleeding.
- A cesarean section is required in patients with complete placenta previa. Some patients with milder degrees of placenta previa can deliver vaginally.
- There is a high association between placenta previa and abnormalities of placental attachment, such as placenta accreta, increta, and percreta. Cesarean hysterectomy may be necessary in some patients with these disorders.

## Radiologic

- Ultrasound is the imaging method of choice for placental localization.
- It is necessary to see both the lower edge of the placenta and the cervix to assess placenta previa accurately. Visualization of just the lower edge of the placenta excludes a placenta previa due to the main mass of the placenta but does not exclude an accessory lobe of the placenta overlying the cervix.
- Ultrasound for placenta previa should be done with an empty urinary bladder. If the bladder is full and ultrasound suggests placenta previa, scanning should be repeated after voiding.
- If the cervix cannot be seen using a transabdominal approach, alternate methods such as transperineal or endovaginal scanning can be attempted. In most cases, endovaginal scanning can be avoided by using transperineal scanning. If endovaginal scanning is done, it should be performed with caution, because bleeding is a well-recognized complication of manual examination of the cervix in patients with placenta previa. Nevertheless, a substantial risk from endovaginal imaging has not been documented in patients with placenta previa.
- Grading systems for placenta previa vary from institution-to-institution, so it is important that the radiologist and clinician be aware of the meaning of the terminology used.
- In general, complete placenta previa refers to the situation in which placental tissue is implanted on both sides of the internal cervical os, completely covering the os. Complete placenta previa can be subdivided into *central complete previa,* in which the

placenta is centered over the cervix, and *asymmetric complete placenta previa,* in which the placenta is not centered over the cervix but a margin of placental tissue is implanted on both sides of the os.

- *Partial placenta previa* refers to the situation when placental tissue covers a portion of the internal cervical os, but not the entire os. *Marginal placenta previa* covers part of the cervix without involving the os. It is frequently difficult to distinguish between marginal and partial placenta previa.

## SUGGESTED READING


Artis AA, Bowie JD, Rosenberg ER, Rauch RF. The fallacy of placental migration: Effect of sonographic techniques. AJR Am J Roentgenol 1985;144:79–81.

Elsayes KM, Trout AT, Friedkin AM, et al. Imaging of the placenta: A multi-modality pictorial review. Radiographics 2009;29:1371–1391.

Hertzberg BS, Bowie JD, Carroll BA, Kliewer MA. Diagnosis of placenta previa during the third trimester: Role of transperineal sonography.

AJR Am J Roentgenol 1992;159:83–87.

Leerentveld RA, Gilberts EC, Arnold MJ, Wladimiroff JW. Accuracy and safety of transvaginal sonographic placental localization. Obstet Gynecol 1990;76:759–762.

Predanic M, Perni SC, Baergen RN, et al. A sonographic assessment of different patterns of placenta previa "migration"in the third trimester of pregnancy. J Ultrasound Med 2005;24:773–780.


# CASE 11


**BARBARA S. HERTZBERG**


## HISTORY

A 38-year-old woman is referred for obstetric ultrasound at 27 menstrual weeks.


A

■**FIGURE 9-11A** Axial sonogram through the fetal abdomen. There are two rounded, fluid-filled structures in the midabdomen. The more laterally located structure corresponds to the fetal stomach. The second cystic structure, located just to the right of midline, is abnormal. The combination of findings is consistent with the "double bubble"sign.


B

■**FIGURE 9-11B** Oblique sonogram through the fetal abdomen. The two "bubbles"demonstrated in Figure 9-12A are now seen to connect, assuming a configuration typical for the stomach emptying into a dilated duodenal bulb.

## DIFFERENTIAL DIAGNOSIS

The "double bubble"sign implies duodenal obstruction, but it must be distinguished

from other sources of extra cysts in the fetal abdomen.

- **Normal stomach, imaged twice due to oblique scan plane:** This is not simply a normal stomach because Figure 9-12B demonstrates a configuration consistent with the gastric antrum and pylorus emptying into a dilated duodenal bulb.
- **Splenic cyst:** This would be unlikely because the extra cyst is located in the right, not the left upper quadrant.
- **Bowel duplication cyst:** This is a possibility except that the extra cyst is in an ideal location for a dilated duodenal bulb.
- **Choledochal cyst:** This entity would be consistent with the appearance in Figure 9-12A, as the location of the second cyst is appropriate for a choledochal cyst. However, it is not consistent with Figure 9-12B because of the connection between the stomach and the second cyst. A choledochal cyst would not connect to the fetal stomach.
- **Renal cyst:** Because of the location of the extra cyst, a renal cyst would be unlikely.
- **Dilated duodenal bulb owing to duodenal atresia:** This is the likely diagnosis based on the appearance and location of the two abdominal cysts, in conjunction with sonographic demonstration of fetal stomach emptying into dilated duodenal bulb. At real-time evaluation, peristalsis was observed, further confirming a bowel etiology.

## DIAGNOSIS

**Duodenal atresia**

## KEY FACTS

### Clinical

- Duodenal atresia is the most common type of congenital small bowel obstruction.
- The likely etiology is failure to recanalize the duodenal lumen during the 10th to 11th week of gestation.
- There is a high incidence of associated anomalies in fetuses with duodenal atresia. These include esopha-geal atresia, congenital heart disease, imperforate anus, other small bowel atresias, biliary atresia, renal anomalies, and vertebral anomalies.
- Because 20% to 30% of fetuses with duodenal atresia also have trisomy 21, chromosomal analysis should be offered when duodenal atresia is suspected.

### Radiologic

- The fluid-filled double bubble sign seen in utero is analogous to the gas-filled double bubble sign seen on post-partum radiographs of infants with duodenal atresia.
- The bubbles comprising the double bubble sign consist of an overdistended stomach in

the left upper quadrant and a dilated duodenal bulb in the right upper quadrant.

- Polyhydramnios is common.
- The double bubble sign is not specific for duodenal atresia but can occur secondary to any obstructive process at the level of the duodenum. Among the other possible causes are annular pancreas, duodenal web, duodenal stenosis, and obstruction due to an intestinal duplication.
- Many fetuses with duodenal atresia have a completely normal ultrasound, without polyhydramnios or the double bubble sign, until the late second or early third trimester.

## SUGGESTED READING


Berrocal T, Torres I, Gutierrez J, et al. Congenital anomalies of the upper gastrointestinal tract. Radiographics 1999;19;855–872.

Gross BH, Filly RA. Potential for a normal fetal stomach to simulate the sonographic “double bubble”sign. Can Assoc Radiol J 1982;33:39–40.

Hertzberg BS. Sonography of the fetal gastrointestinal tract: Anatomic variants, diagnostic pitfalls, and abnormalities. AJR Am J Roentgenol 1994;162:1175–1182.

Hung JH, Shen SH, Chin TW, Hung CY. Prenatal diagnosis of double duodenal atresia by ultrasound and magnetic resonance imaging. Prenat Diagn 2007;27:381–383.

Nelson LH, Clark CE, Fishburne JI, et al. Value of serial sonography in the in utero detection of duodenal atresia. Obstet Gynecol 1982;59:657–660.


# CASE 12


**BARBARA S. HERTZBERG**


## HISTORY

A 55-year-old woman presents with a palpable pulsatile abdominal mass.


A

■**FIGURE 9-12A** Sagittal sonogram of the upper abdomen. The upper and midabdominal aorta appears normal without evidence of an aneurysm. The celiac axis and superior mesenteric artery are seen arising from the aorta.


B

■**FIGURE 9-12B** Sagittal sonogram of the lower abdomen. The lower abdominal aorta also appears normal without evidence of an aneurysm. There is a soft tissue mass immediately anterior to the inferior portion of the aorta.


C

**FIGURE 9-12C** Transverse sonogram of the lower abdomen. The soft tissue mass seen anterior to the aorta crosses the midline and extends laterally.

## DIFFERENTIAL DIAGNOSIS

- **Adenopathy/lymphoma:** Patients with lymphoma and retroperitoneal or mesenteric adenopathy could present with the soft tissue mass seen in Figure 9-13B, but it would not be expected to have the configuration seen laterally on Figure 9-13C.
- **Other primary retroperitoneal neoplasm:** Again, this could explain the configuration in Figure 9-13B, but not the configuration in Figure 9-13C.
- **Retroperitoneal fibrosis:** This is likely to be more circumferential than the soft tissue mass shown in Figure 9-13B. It does not explain the configuration in Figure 9-13C.
- **Horseshoe kidney:** This is the best diagnosis. The soft tissue mass seen anterior to the aorta corresponds to the parenchymal isthmus of a horseshoe kidney. The explanation for the palpable pulsatile abdominal mass at physical examination is pulsations transmitted from the aorta to the isthmus of the horseshoe kidney.

## DIAGNOSIS

**Horseshoe kidney**

## KEY FACTS

### Clinical

- The horseshoe kidney is a congenital renal fusion anomaly, in which the lower poles of both kidneys are joined by a fibrous or parenchymal band.
- Horseshoe kidneys are a common entity, occurring in between 1 in 400 to 500 births.
- Horseshoe kidneys are more susceptible to trauma compared to normally located kidneys.
- Due to urinary stasis from draping of the ureters over the kidneys, there is an increased incidence of stones and infection.
- Multiple renal arteries and ectopic renal arteries are common.
- Patients with a horseshoe kidney are not uncommonly referred to ultrasound for evaluation of a pulsatile abdominal mass, as in this case.
- There is an association with Turner's syndrome.

### Radiologic

- Abnormal renal orientation is common in patients with a horseshoe kidney. The renal

pelvis is frequently directed more anteriorly than usual.

- The horseshoe kidney is typically found in a relatively low position, either in the lower abdomen or the upper pelvis. A possible explanation for the low position of the horseshoe kidney is that normal ascent of the kidney is prevented by the inferior mesenteric artery.
- The fused lower renal poles are commonly found at the level of the L4 and L5 vertebrae.
- At sonography, a soft tissue mass may be seen anterior to the abdominal aorta. The lower poles of the kidneys can sometimes be followed into the mass by scanning in an oblique plane. The upper portions of the kidneys are not usually in their typical locations in the flanks but are relatively low in position.
- In many cases, the isthmus, which connects the two sides of the horseshoe kidney and which can be either parenchymal (most common) or fibrous, cannot be seen by ultrasound, due to overlying bowel gas. When this occurs, sonography may miss the diagnosis.

## SUGGESTED READING

Cho JY, Lee YH, Toi A, Macdonald B. Prenatal diagnosis of horseshoe kidney by measurement of the renal pelvic angle. Ultrasound Obstet Gynecol 2005;25:554–558.

Mindell HJ, Kupic EA. Horseshoe kidney: Ultrasonic demonstration. AJR Am J Roentgenol 1977;129:526–527.

Strauss S, Dushnitsky T, Peer A, et al. Sonographic features of horseshoe kidney: Review of 34 patients. J Ultrasound Med 2000;19:27–31.

Trackler RT, Resnick ML, Leopold GR. Pelvic horseshoe kidney: Ultrasound findings and case report. J Clin Ultrasound 1978;6:51–52.

Weizer AZ, Silverstein AD, Auge BK, et al. Determining the incidence of horseshoe kidney from radiographic data at a single institution. J Urol 2003;170:1722–1726.

# CASE 13

**TAMRA M. KNUTSON**

### HISTORY

A 40-year-old African American male with a history of groin trauma and a palpable right testicular mass on physical exam.

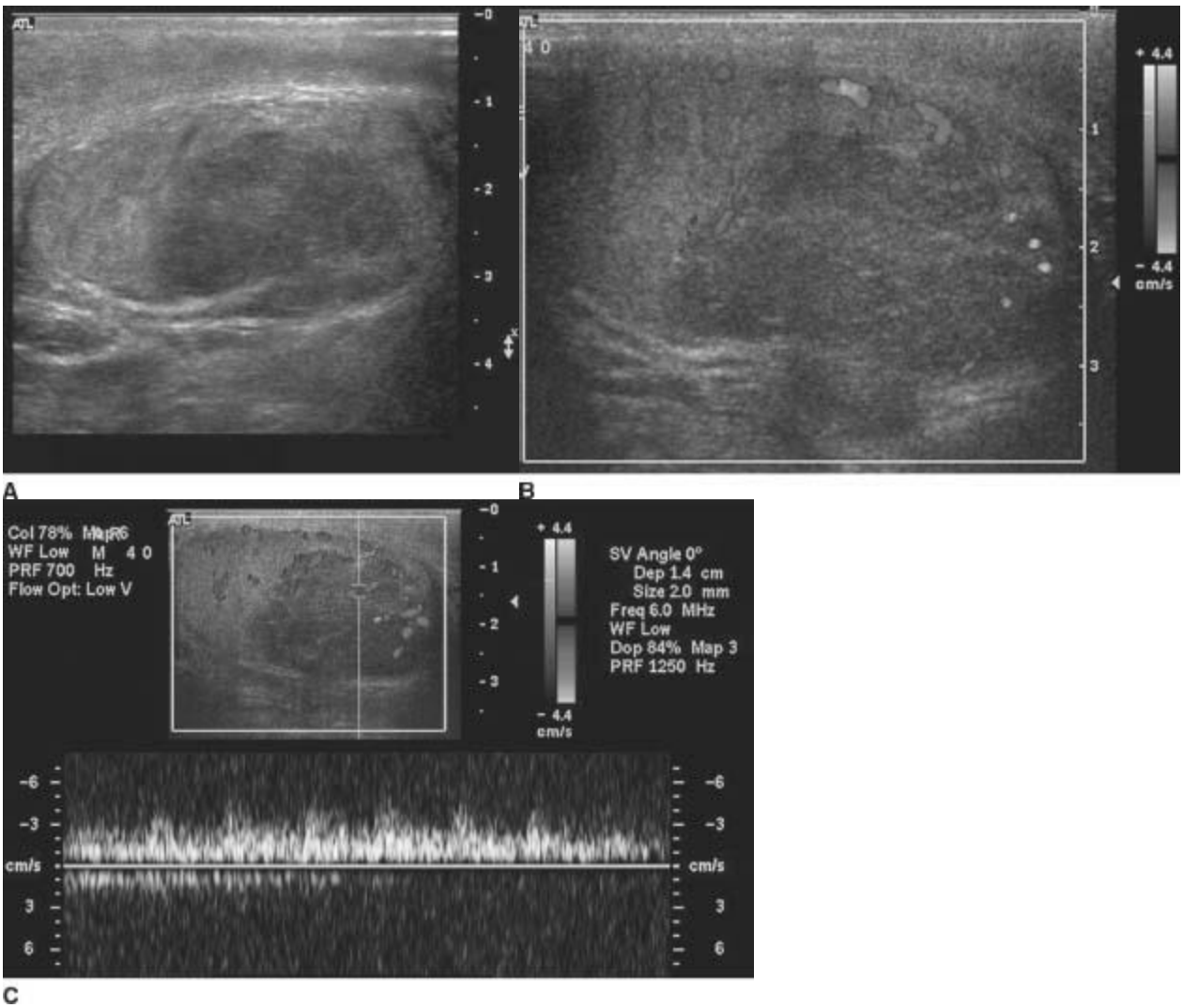


**FIGURES 9-13A, 9-13B, and 9-13C A**: Longitudinal gray-scale sonographic image obtained with a 10-MHz linear-array transducer demonstrates a large, relatively homogenous, hypoechoic mass in the posterior part of the right testis. Corresponding color **(B)** and spectral Doppler **(C)** sonographic images demonstrate increased vascularity within the lesion. (See color insert)

## DIFFERENTIAL DIAGNOSIS

- **Hematoma:** Intratesticular hematomas are generally heterogeneous lesions that lack internal vascularity.
- **Primary testicular neoplasm:** This is the best diagnosis based on imaging and physical exam findings.
- **Sarcoidosis:** Given the fact that testicular cancer is relatively rare in African Americans, sarcoidosis is a consideration. However, sarcoidosis more commonly involves the epididymis and tends to present as multiple, small, bilateral masses rather than a single lesion.

- **Infarct:** While testicular infarction can present as a focal hypoechoic lesion or as a diffusely hypoechoic testicle, internal vascularity would not be expected in the involved region.
- **Metastatic disease:** Metastatic disease is less common than primary testicular neoplasms and tends to affect patients over the age of 60. The most common primary neoplasms are prostate, lung, colon, kidney, and melanoma.
- **Lymphoma:** Testicular lymphoma can present as a homogenous, hypoechoic mass as seen here, but like metastatic disease it generally affects older men. Nearly all of testicular lymphomas are non-Hodgkin B-cell lymphomas.

## DIAGNOSIS

**Testicular seminoma**

## KEY FACTS

### Clinical

- The majority of testicular neoplasms are germ cell tumors (95%) with seminomas accounting for approximately 50%. Mixed germ cell tumors are the second most common subtype.
- Seminomas have the best prognosis of all germ cell tumors due to the tumors sensitivity to radiation therapy.
- The majority of testicular tumors metastasize via the lymphatics; choriocarcinoma is an exception and has a propensity for early hematogenous spread.
- Risk factors for testicular cancer include prior testicular neoplasm, positive family history, cryptorchidism, infertility, and intersex syndromes.
- The risk of cancer in the setting of cryptorchidism increases with the degree of ectopy and is not reduced by orchiopexy.
- Serum markers for testicular cancer include human chorionic gonadotropin (elevated in seminomas and choriocarcinomas) and alpha fetal protein (elevated in yolk sac tumors and mixed germ cell tumors with yolk sac elements).

### Radiologic

- Essentially all solid, hypoechoic intratesticular masses should be considered neoplasms while the majority of extratesticular lesions and cystic intratesticular lesions are nonneoplastic.
- Seminomas are characteristically homogeneous, hypoechoic, round lesions. The entire testicle is commonly replaced by tumor.

- Seminomas can be lobulated which may mimic multifocal disease; however, true multifocal lesions are rare.
- Although large seminomas can be heterogeneous, the presence of calcifications and cystic elements is highly suggestive of a mixed germ cell tumor rather than a seminoma.
- Color Doppler ultrasound cannot distinguish neoplasms from inflammatory lesions; however, it may be helpful to depict subtle lesions. Furthermore, the absence of power and color Doppler flow in a large lesion suggests infarction or hematoma.
- Testicular cancer mimics include hematomas, abscesses, focal orchitis, granulomatous orchitis, focal atrophy, infarcts, and adrenal rests.

## SUGGESTED READING

Dogra VS, Gottlieb RH, Oka M, et al. Sonography of the scrotum. Radiology 2003;227:18–36.

Howlett DC, Marchban NDP, Sallomi DF. Ultrasound of the testis: Pictorial review. Clin Radiol 2000;55(8):595–601.

Woodward PJ, Sohaey R, O'Donoghue MJ, et al. From the archives of the AFIP: Tumors and tumor-like lesions of the testis: Radiologic-pathologic correlation. Radiographics 2002;22:189–216.

Woojin K, Rosen MA, Langer FE. US-MR imaging correlation in pathologic conditions of the scrotum. Radiographics 2007;27:1239–1253.

# CASE 14

**BARBARA A. CARROLL**

### HISTORY

A 62-year-old man presents with a pulsatile mass and bruit in the right groin 2 days after coronary angioplasty via the right femoral artery.

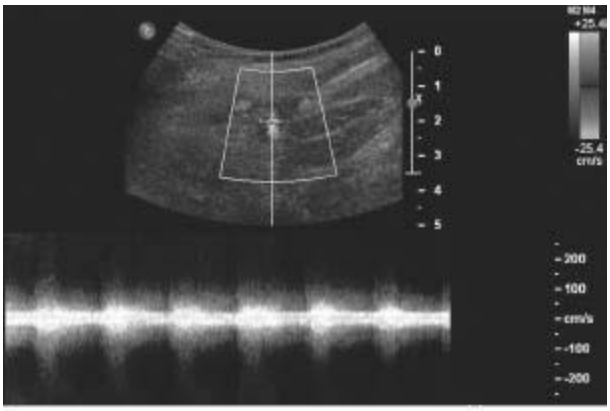


A

■**FIGURE 9-14A** A duplex sonogram of the right common femoral artery at the puncture site. There is a disturbed arterial flow pattern with increased end-diastolic flow (a low-resistance arterial waveform) and marked spectral broadening ("turbulence"). (See color insert)

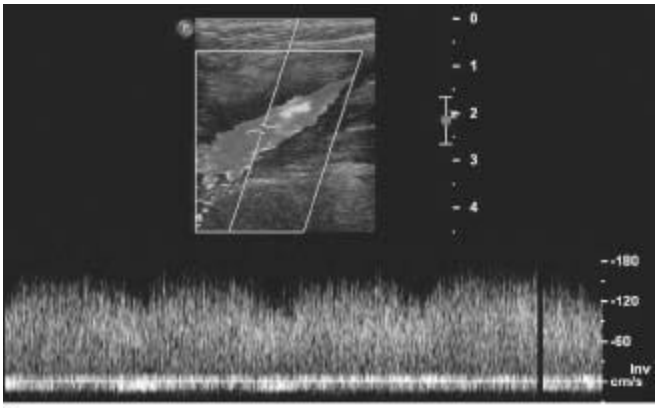


B

■**FIGURE 9-14B** A duplex sonogram of the right common femoral vein at the puncture site: there is pulsatile, high-velocity venous flow. (See color insert)

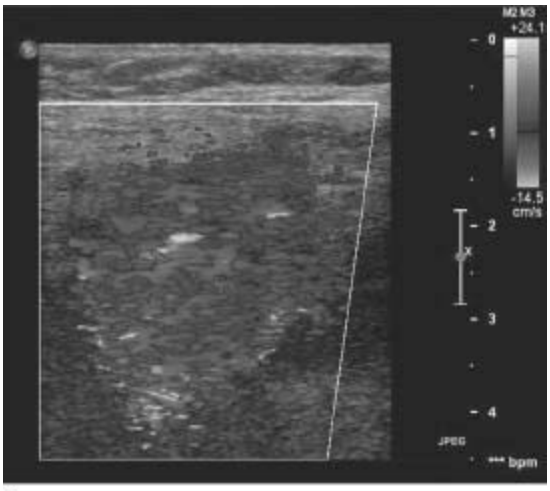


C

■**FIGURE 9-14C** A color Doppler sonogram in the region of the puncture site. A color Doppler "bruit"is manifested as scattered color Doppler pixels in the soft tissues surrounding the femoral artery and vein. (See color insert)

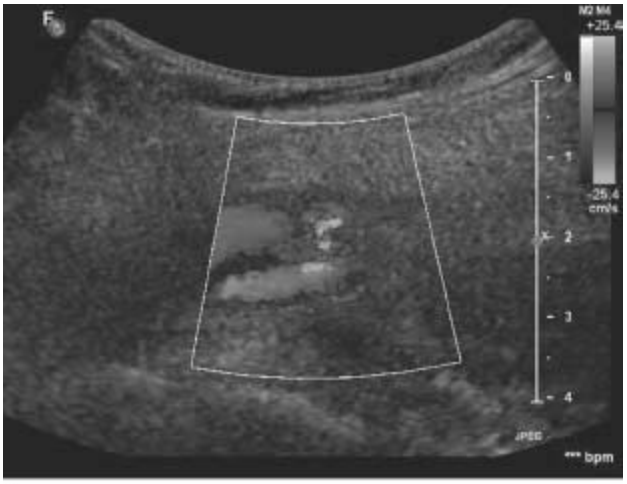

D

**FIGURE 9-14D** A color Doppler sonogram demonstrates a fistulous connection between the artery and vein. (See color insert)

## DIFFERENTIAL DIAGNOSIS

- **Arterial stenosis:** A stenosis of the femoral artery could cause increased diastolic flow, loss of a resistance arterial waveform, and color Doppler bruit, but it should not alter the venous waveforms.
- **Arterial dissection:** A dissection or flap may have features similar to atherosclerotic narrowing, but no venous waveform changes should occur.
- **Venous stenosis:** A narrowed and stenotic vein may cause high-velocity venous flow, but no arterial changes.
- **Arteriovenous fistula (AVF):** This is the best diagnosis because it explains both the arterial and venous waveform changes.

## DIAGNOSIS

**Femoral arteriovenous fistula**

## KEY FACTS

### Clinical

- An AVF resulting from arterial puncture and catheterization is a less common complication than a pseudoa-neurysm.
- An AVF is an abnormal communication between the arterial and venous systems that creates a shunt from the high-resistance arterial system into the low-resistance venous system.
- An AVF is caused by simultaneous puncture of the adjacent artery and vein and by

simultaneous arterial and venous catheterization.

- An AVF is manifest clinically by a continuous bruit or thrill in the region of trauma.
- An AVF may be asymptomatic or can produce localized symptoms, including pain, claudication distal to the AVF secondary to decreased arterial flow, and venous stasis due to increased venous pressure. Systemic symptoms such as high-output congestive heart failure and angina may also result.
- An asymptomatic AVF does not require treatment and may resolve spontaneously.
- Surgical treatment or stent placement may be necessary.
- An AVF may coexist with a postcatheterization pseudoaneurysm.

### Radiologic

- The classic arterial pattern is high diastolic flow (a low resistance waveform) with spectral broadening just proximal to the fistula.
- The classic venous pattern is increased flow velocity with pulsatile disturbed waveforms near the fistula.
- Color Doppler signal in the soft tissues surrounding the AVF is caused by the transmitted thrill from disturbed flow.
- A visible tract of flow connecting the artery and vein may be seen, especially with color Doppler.
- There is often decreased arterial flow distal to the fistula.
- Some AVFs may not demonstrate all of these features.

## SUGGESTED READING

Gonzalez SB, Busquets JC, Figueiras RG, et al. Imaging arteriovenous fistulas. AJR Am J Roentgenol 2009;193:1425–1433.

Helvie MA, Rubin J. Evaluation of traumatic groin arteriovenous fistulas with duplex Doppler sonography. J Ultrasound Med 1989;8:21–24.

Igidbashian VN, Mitchell DG, Middleton WD, et al. Iatrogenic femoral arteriovenous fistula: Diagnosis with color Doppler imaging. Radiology 1989;170:749–752.

Robidoux MA, Hertzberg BS, Carroll BA, Hedgepeth CA. Color flow and image-directed Doppler ultrasound evaluation of iatrogenic arteriovenous fistulas in the groin. J Clin Ultrasound 1990;18:463–469.

Thalhammer C, Kirchherr AS, Uhlich F, et al. Postcatheterization pseudoaneurysms and arteriovenous fistulas: Repair with percutaneous implantation of endovascular covered stents. Radiology 2000;214:127–131.

# CASE 15

**BARBARA A.**
**CARROLL**

**HISTORY**

A 62-year-old man presents with a pulsatile right groin mass 24 hours after coronary angioplasty via the right femoral artery.

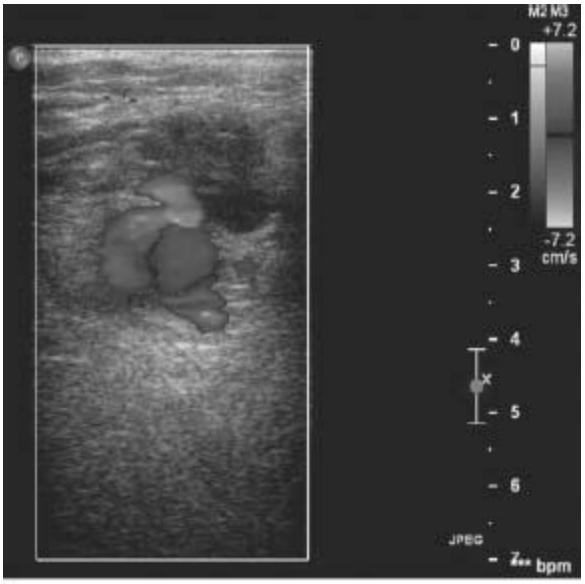


A

■**FIGURE 9-15A** A transverse color Doppler sonogram of the right groin in the region of the visible catheterization puncture site demonstrates a "yin-yang"appearance of swirling bidirectional color flow within a hypoechoic mass. (See color insert)

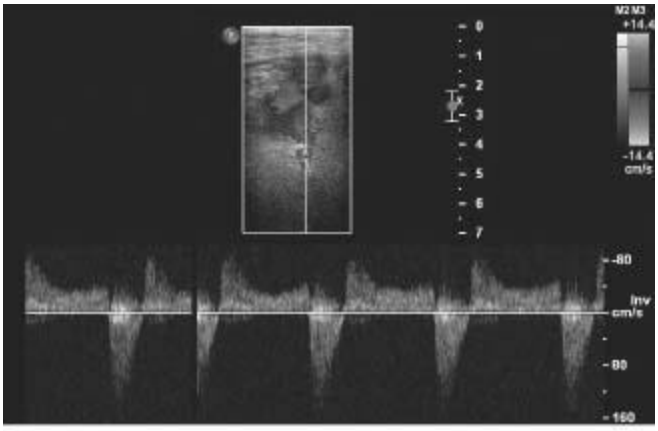


B

■**FIGURE 9-15B** Pulsed Doppler spectral waveform in the region of the "neck"shows a "to-and-fro"waveform. (See Color insert)

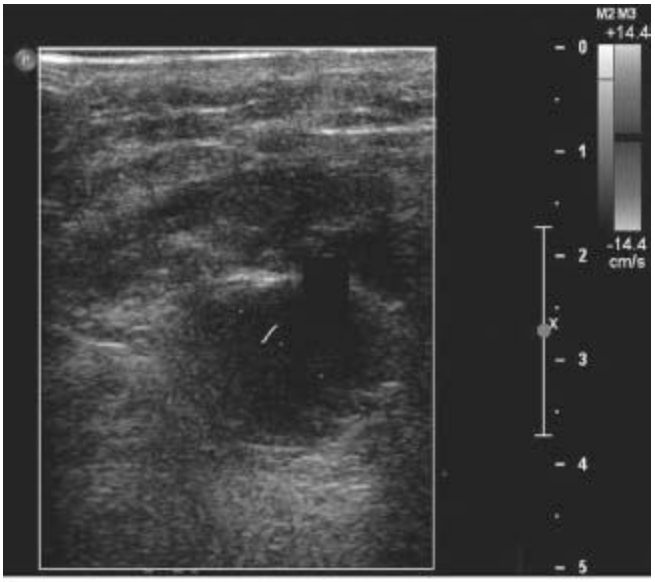


C

**FIGURE 9-15C** A longitudinal color Doppler sonogram of the right groin following ultrasound-guided thrombin injection shows no flow within the mass. (See color insert)

## DIFFERENTIAL DIAGNOSIS

**Postcatheterization hematoma:** Hematomas in the region of a puncture site can produce an anechoic or hypoechoic mass. This mass may contain flecks of color due to transmitted pulsations from the adjacent femoral artery. However, pulsed Doppler evaluation will not reveal a "to-and-fro"arterial waveform.

**Arteriovenous fistula (AVF):** The localized intense soft tissue bruit associated with an AVF may sometimes mimic this color Doppler flow pattern. However, the pulsed Doppler waveforms within the adjacent artery and vein should demonstrate characteristics consistent with an AVF.

**Hyperplastic lymph nodes:** The increased flow in hyperplastic lymph nodes can produce a very vascular mass on color Doppler ultrasound. However, no neck connecting the hyperplastic lymph node to the femoral artery will be observed, and the flow within the node will not have a "yin-yang"appearance.

**Inguinal hernia:** Particulate material within ascites in an inguinal hernia sac may produce a similar swirling color flow pattern. Pulsed Doppler evaluation will show that these swirling color changes are associated with transmitted motion from respiration and abdominal peristaltic activity rather than vascular pulsations.

**Arterial pseudoaneurysm:** This is the best diagnosis considering the pulsatile swirling blood flow in the mass and the waveform in the "neck"connecting the artery to the pseudoaneurysm.

# DIAGNOSIS

**Femoral artery pseudoaneurysm**

# KEY FACTS

## Clinical

- A femoral artery pseudoaneurysm is an increasingly common complication of therapeutic catheterization procedures, including percutaneous transluminal coronary angioplasty and stenting.
- Occurrence rates as high as 8% have been reported. Pseudoaneurysms can produce complications including hemorrhage, pain, neuropathy, infection, local skin ischemia, peripheral embolization, and even frank rupture leading to exsanguination.
- Factors that lead to pseudoaneurysm development include large catheters and sheaths, use of anticoagulant or thrombolytic agents during and following the procedure, simultaneous arterial and venous catheterizations, the length of the procedure, and suboptimal postprocedural compression.
- Pseudoaneurysms are not true aneurysms. They develop a fibrous capsule but do not have a complete arterial wall surrounding them.
- Pseudoaneurysms present as pulsatile masses near the arterial puncture site. Audible systolic bruits are frequently heard but are not always present.
- Pseudoaneurysms must be distinguished from overlying hematomas with transmitted pulsations.
- Pseudoaneurysms may coexist with AVFs.
- Although the natural history of pseudoaneurysms is variable, spontaneous thrombosis is common. Unfortunately, there is no way of discerning which pseudoaneurysms will thrombose based on their ultrasound appearance.
- Ultrasound-guided compression has been used successfully to treat small, superficial pseudoaneurysms. More recently, ultrasound-guided thrombin injection has replaced compression at many institutions. It has a greater success rate, shorter procedural time and higher patient tolerance.
- Under direct ultrasound visualization, a 22-gauge needle is placed into the pseudoaneurysm with care taken to avoid the neck. Once the needle tip is visualized, color Doppler is turned on and the thrombin is injected slowly. Absence of flow on color Doppler is indicative of successful thrombosis.
- The most serious complication of thrombin injection is distal ischemia; however, this complication is rare. Distal pulses should be assessed pre- and postprocedure.

## Radiologic

- Pseudoaneurysms demonstrate a characteristic appearance on both color Doppler and pulsed Doppler ultrasound. Color Doppler demonstrates the neck of the pseudoaneurysm, which connects the pseudoaneurysm with the underlying femoral artery. During early systole, a color Doppler jet of blood flow into the pseudoaneurysm is seen. During the remainder of the cardiac cycle, eddy currents of color Doppler flow swirl around within the pseudoaneurysm and flow exits the pseudoaneurysm through the neck. The internal appearance of a pseudoaneurysm is frequently likened to the yin-yang sign, with equal parts of the pseudoaneurysm cavity filled with antegrade and retrograde swirling blood flow.
- To-and-fro pulsed Doppler waveforms are localized to the region of the pseudoaneurysm neck.
- Pseudoaneurysms may be multiple and create a "string-of-beads"appearance.

## SUGGESTED READING


Abu-Yousef MM, Wiese JA, Shamma AR. The "to-and-fro"sign: Duplex Doppler evidence of femoral artery pseudoaneurysm. AJR Am J Roentgenol 1988;150:632–634.

Ahmad F, Turner SA, Torrie P, Gibson M. Iatrogenic femoral artery pseudoaneurysms: A review of current methods of diagnosis and treatment. Clin Radiol 2008;63:1310–1316.

Mitchell DG, Needleman L, Bezzi M, et al. Femoral artery pseudoaneurysm: Diagnosis with conventional duplex and color Doppler US. Radiology 1987;165:687–690.

Morrison SL, Obrand DA, Steinmetz OK, Montreuil B. Treatment of femoral artery pseudoaneurysms with percutaneous thrombin injection. Ann Vasc Surg 2000;14:634–639.

Ward E, Buckley O, Collins A, et al. The use of thrombin in the radiology department. Eur Radiol 2009;19:670–678.


# CASE 16


**BARBARA A.**
**CARROLL**


### HISTORY

A 67-year-old woman presents with a history of intermittent left upper extremity weakness and numbness. On physical examination, there is a right carotid bruit.

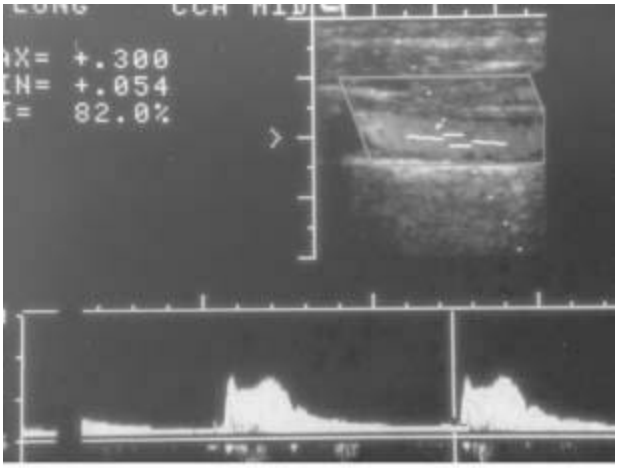


A

■**FIGURE 9-16A** A duplex sonogram of the right CCA demonstrates very low peak systolic and end-diastolic velocities, 30 and 5 cm/s, respectively.

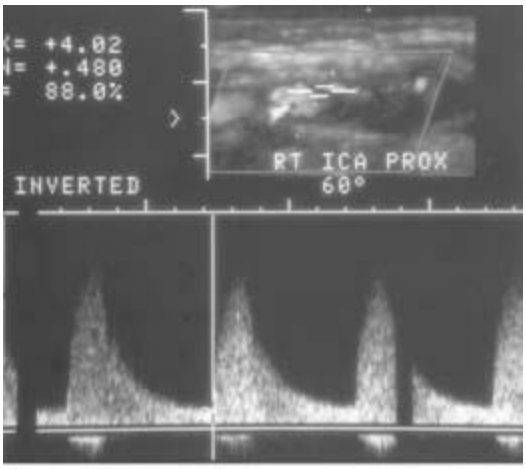


B

■**FIGURE 9-16B** A duplex sonogram of the right ICA in the region of a visible hypoechoic plaque demonstrates a markedly elevated peak systolic velocity and an elevated end-diastolic velocity, measuring 402 and 48 cm/s, respectively.

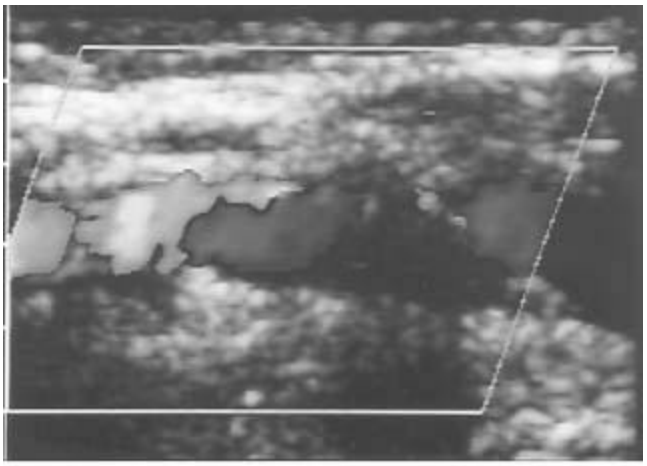

C

**FIGURE 9-16C** A color Doppler sonogram of the right ICA demonstrates an extremely high-grade stenosis with flow disturbance and a relatively hypoechoic plaque. Tiny areas of slow reversed flow are seen within the hypoechoic plaque, a finding that can be suggestive of plaque ulceration.

D

**FIGURE 9-16D** A right common carotid arteriogram demonstrates a markedly narrowed long segment stenosis involving the proximal ICA as well as the external carotid artery. Plaque ulceration is also present.

## DIFFERENTIAL DIAGNOSIS

**Carotid dissection:** Dissections are less common than atherosclerotic plaque in the seventh decade. However, dissections should be considered as a cause of carotid stenosis or occlusion in younger patients, particularly those with a history of trauma, in those with no atherosclerotic risk factors and when there is relative paucity of visible plaque.

**Carotid stenosis:** This is the best diagnosis considering the age of the patient, the intraluminal lesions and the focal velocity elevation.

**Spurious velocity elevations due to contralateral stenosis:** Collateral shunting of blood to the circle of Willis on the side opposite a high-grade carotid stenosis can result in spuriously elevated velocities disproportionate to the amount of visible vessel narrowing. In this case, there was no evidence for a contralateral lesion, and the color Doppler sonogram clearly shows a large intraluminal filling defect associated with the

areas of high velocity in the internal carotid artery (ICA).

- **Suboptimal Doppler angle:** If the angle theta used to obtain velocity values exceeds 70°, spurious results may be obtained that are not representative of true flow velocity. In this case, the Doppler angle theta is 60°, which is an acceptable Doppler angle. Ideally, the Doppler angle should not exceed 60°.

## DIAGNOSIS

**Less than ninety percent diameter stenosis of the proximal ICA with plaque ulceration**

## KEY FACTS

### Clinical

- Stroke caused by atherosclerotic disease is the third leading cause of death in the United States.
- Approximately 50% of these strokes are caused by atherosclerotic disease located within 2 cm of the carotid bifurcation.
- Carotid sonography using duplex ultrasound has become a valuable, noninvasive screening technique to determine which patients have potentially “operable”lesions.
- Carotid endarterectomy is now thought to be highly beneficial for symptomatic patients who have a 70% to 99% diameter stenosis involving the ICA.
- The benefits for asymptomatic patients is less well established.
- Ultrasound screening allows selection of appropriate patients for angiography (including CT or MR angiography) before surgery. There are some instances in which surgery can be performed without angiography.

### Radiologic

- Pulsed Doppler spectral analysis and color Doppler ultrasound are approximately of equal accuracy for diagnosing >50% diameter stenoses (>90% accuracy).
- The hallmark of a high-grade stenosis is a progressive increase in peak systolic and end-diastolic velocities beginning at approximately 50% diameter stenosis and continuing until one reaches a preocclusive stenosis (>95% diameter), at which time the peak systolic and end-diastolic velocities decrease precipitously.
- Visible plaque and peak systolic velocities of 125 to 230 cm/s are associated with a 50% to 69% stenosis and velocities >230 cm/s are associated with a >70% stenosis. The ICA/CCA peak systolic velocity ratio has also been used to evaluate the degree of stenosis with a ratio of 2.0 to 4.0 and >4.0 associated with 50% to 69% stenosis and >70% stenosis, respectively. The ICA/CCA ratio is useful when there is a discrepency

between the gray scale findings and peak systolic velocities.

- Color Doppler ultrasound allows one to display blood flow information in real-time over a selected area. Stationary soft tissue structures that lack phase or frequency shifts associated with flowing blood receive an amplitude gray scale value, while the flowing blood in the vessels receives a color assignment dependent on the direction of blood flow relative to the Doppler transducer, as well as the Doppler angle and the velocity of the flowing blood.
- Color Doppler ultrasound is helpful as an initial screen during the carotid examination to pinpoint areas of vascular narrowing and abnormal flow for subsequent pulsed Doppler interrogation.
- Carotid plaque characterization is a controversial topic; however, plaque such as the one seen in this case, which is heterogeneous and hypoechoic and contains areas of low velocity disturbed flow within the plaque, is frequently associated with ulceration.
- With an extremely high-grade stenosis or occlusion of the ICA, flow in the proximal common carotid artery (CCA) may become damped with relatively low peak systolic and end-diastolic velocity readings.

## SUGGESTED READING


Fayad P. Endarterectomy and stenting for asymptomatic carotid stenosis: A race at breakneck speed. Stroke 2007;38:707–714.

Gardner DJ, Gosink BB, Kallman CE. Internal carotid artery dissections: Duplex ultrasound imaging. J Ultrasound Med 1991;10:607–614.

Grant EG, Benson CB, Moneta GL et al. Carotid artery stenosis: Gray-scale and Doppler US diagnosis-Society of Radiologists in Ultrasound Consensus Conference. Radiology 2003;229:340–346.

Mitchell DG. Color Doppler imaging: Principles, limitations, and artifacts. Radiology 1990;177:1–10.

North American Symptomatic Carotid Endarterectomy Trial Collaborators. Beneficial effect of carotid endarterectomy in symptomatic patients with high-grade stenosis. N Engl J Med 1991;325:445–453.


# CASE 17

**JAMES D.**
**BOWIE**

### HISTORY

A 26-year-old woman is referred for fetal ultrasound because of uncertainty about her dates.


A

■**FIGURE 9-17A** Sagittal sonogram of the lower uterus. There is a fluid-like structure that extends from the amniotic cavity through the cervix into the upper vagina.


B

■**FIGURE 9-17B** Transverse sonogram of the upper uterus. This view shows a normal amount of amniotic fluid in the upper uterus.

## DIFFERENTIAL DIAGNOSIS

■**Hourglass membranes:** This term refers to the presence of fluid in the upper vagina as a result of herniation of the amniotic membranes through the cervix. The sonographic finding is characteristic, and few conditions mimic this appearance. The important thing to recognize is the location of the uterine cervix.

- **Nabothian cyst:** A very large nabothian cyst can have a similar appearance. In this case, the cervix is normal.

## DIAGNOSIS

**Incompetent cervix with herniation of the amnion into the upper vagina, often referred to as "hourglass membranes"**

## KEY FACTS

### Clinical

- Preterm labor continues to be a major cause of perinatal death and morbidity.
- The patients are often without symptoms and do not have a history of premature delivery.
- There is no universally accepted treatment for this condition once it has progressed to this point. Various regimens have been suggested including: (1) doing nothing, (2) bed rest in the Trendelenburg position with tocolytic agents, and (3) cerclage for some patients.

### Radiologic

- Routine images should be obtained of the cervix from 15 to 30 weeks of gestation. Ideally, these are done with an empty bladder. Often the transabdominal approach is adequate, but transperineal and endovaginal imaging may be needed in some cases. It is wise to examine the patient with a transabdominal scan before any endovaginal imaging to exclude the possibility of hourglass membranes.
- The normal cervix is about as high as it is wide. Measurements are taken of the length of the endocervical canal from the internal to the external os. This length should exceed 3 cm up to about 30 weeks.
- The normal endocervical canal can be hypoechoic or echogenic. A hypoechoic endocervical canal should not be mistaken for cervical incompetence.
- Myometrial contractions can give the appearance of an elongated endocervical canal. Measurements of the length of the endocervical canal should not be taken when a contraction distorts this area.
- The cervix can change in length during the course of an examination. Generally, the shortest measurement is most representative of the true clinical state. Also, "funneling"of the cervix is sometimes intermittent. The clinical consequences of intermittent funneling are the same in a cervix that consistently remains funneled—that is, there is a significant increase in risk for preterm labor and delivery of a premature infant.

## SUGGESTED READING

Andersen HF. Transvaginal and transabdominal ultrasonography of the uterine cervix during pregnancy. J Clin Ultrasound 1991;19:77–83.

Bowie JD, Andreotti RF, Rosenberg ER. Sonographic appearance of the uterine cervix in pregnancy: The vertical cervix. AJR Am J Roentgenol 1983;140:737–740.

Hertzberg BH, Bowie JD, Weber TM, et al. Sonography of the cervix during the third trimester of pregnancy: Value of the transperineal approach. AJR Am J Roentgenol 1991;157:73–76.

Macdonald R, Smith P, Vyas S. Cervical incompetence: The use of transvaginal sonography to provide an objective diagnosis. Ultrasound Obstet Gynecol 2001;18:211–216.

Mahony BS, Nyberg DA, Luthy DA, et al. Translabial ultrasound of the third-trimester uterine cervix: Correlation with digital examination. J Ultrasound Med 1990;9:717–723.

McGahan JP, Phillips HE, Bowen MS. Prolapse of the amniotic sac ("hourglass membranes"). Radiology 1981;140:463–466.

Owen J, Iams, JD, Hauth JC. Vaginal sonography and cervical incompetence. Am J Obstet Gynecol 2003;188:586–596.

Parulekar SG, Kiwi R. Dynamic incompetent cervix uteri: Sonographic observations. J Ultrasound Med 1988;7:481–485.

Sarti DA, Sample WF, Hobel CJ, Staisch KJ. Ultrasonic visualization of a dilated cervix during pregnancy. Radiology 1979;130:417–420.

# CASE 18

**BARBARA S. HERTZBERG**

## HISTORY

A 47-year-old man presents with intermittent episodes of right flank discomfort.

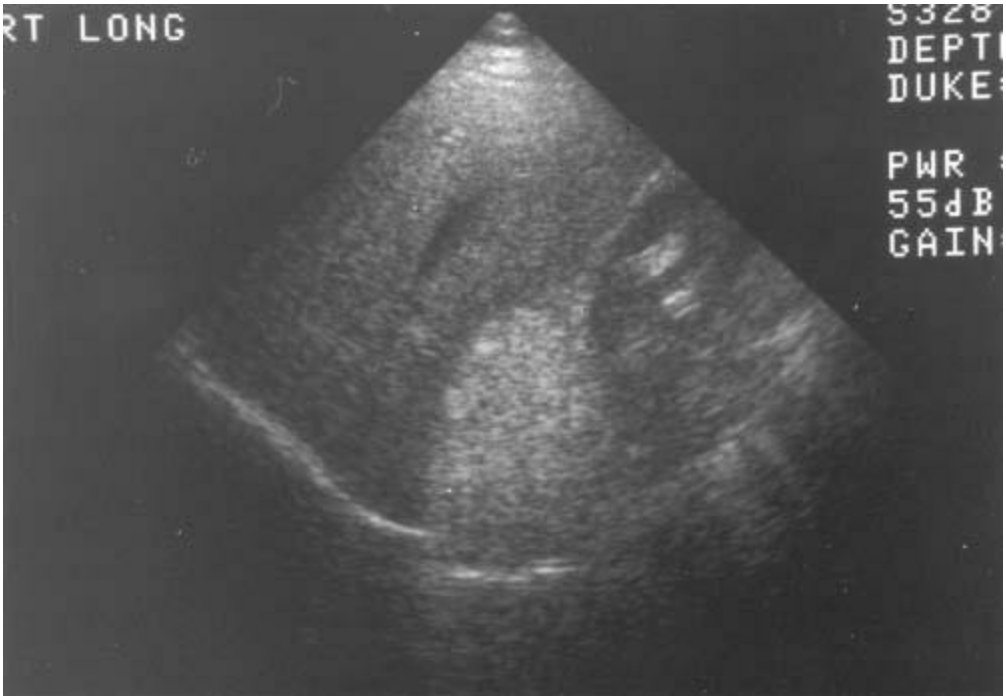


**FIGURE 9-18** Longitudinal sonogram of the right upper quadrant. An echogenic mass is seen, posteroinferior to the liver and immediately superior to the kidney. Behind the mass, the diaphragm appears to be interrupted and displaced posteriorly.

## DIFFERENTIAL DIAGNOSIS

- **Adrenal hemorrhage:** Acute hemorrhage could cause a mass of markedly increased echogenicity, but it would not result in the apparent discontinuity and posterior displacement of the diaphragm behind the mass.
- **Renal angiomyolipoma:** This hamartomatous mass is possible, although it appears more suprarenal rather than originating from the kidney.
- **Retroperitoneal fat-containing mass such as a liposarcoma:** It would be unlikely for anatomic fat to be as well-defined as this mass or be localized solely to the suprarenal area.
- **Adrenal myelolipoma:** This is the most likely diagnosis because the apparent discontinuity and posterior displacement of the diaphragm is due to a "speed propagation artifact."This occurs because the speed of ultrasound is slower in fatty masses than in many other soft tissues, resulting in misregistration of the location and apparent posterior displacement of the diaphragm immediately behind the fatty mass.
- **Adrenal carcinoma with acute hemorrhage:** This could result in an echogenic mass in a suprarenal location, but it would be unlikely to cause discontinuity and posterior displacement of the diaphragm behind the mass.

# DIAGNOSIS

**Adrenal myelolipoma**

# KEY FACTS

## Clinical

- An adrenal myelolipoma is an uncommon, benign, non-functioning hamartomatous adrenal mass that contains both fatty and bone marrow elements.
- Many patients with adrenal myelolipomas are asymptomatic, but some present with pain or discomfort. Discomfort can be secondary to hemorrhage, necrosis, or pressure on surrounding structures.
- They are most common in the fourth to sixth decades of life, and they occur with approximately equal frequency in men and women.
- These lesions span a variety of sizes, ranging from microscopic to 30 cm or more in diameter.

## Radiologic

- The ultrasound appearance depends on the relative quantities of the various tissue components.
- Many myelolipomas are markedly echogenic on ultrasound. This is considered the most characteristic appearance and is more likely to be seen when there is a high fat content.
- If the fat content is relatively low, a hypoechoic or heterogeneous mass may result.
- In some cases, the “speed propagation artifact”is subtle, seen only in certain scan planes, or not seen at all. Inability to demonstrate this particular artifact does not exclude an adrenal myelolipoma.
- Even in the presence of a “speed propagation artifact,”the diagnosis should be confirmed with a CT or MRI. The CT or MRI can confirm the presence of both fatty components as well as the adrenal origin of the mass.
- Adjacent retroperitoneal fat may mask a small adrenal myelolipoma.

# SUGGESTED READING


Cyran KM, Kenney PJ, Memel, DS, Yacoub, I. Adrenal myelolipoma. AJR Am J Roentgenol 1996;166:395–400.

Mayo-Smith WW, Boland GW, Noto RB, Lee MJ. State-of-the-art adrenal imaging. Radiographics 2001;21:995–1012.

Musante F, Derchi LE, Zappasodi F, et al. Myelolipoma of the adrenal gland: Sonographic and CT features. AJR Am J Roentgenol 1988;151:961–964.

Vick CW, Zeman RK, Mannes E, et al. Adrenal myelolipoma: CT and ultrasound findings. Urol Radiol 1984;6:7–13.

# CASE 19

**BARBARA S.
HERTZBERG**

## HISTORY

A 32-year-old pregnant woman has an elevated serum alpha-fetoprotein.

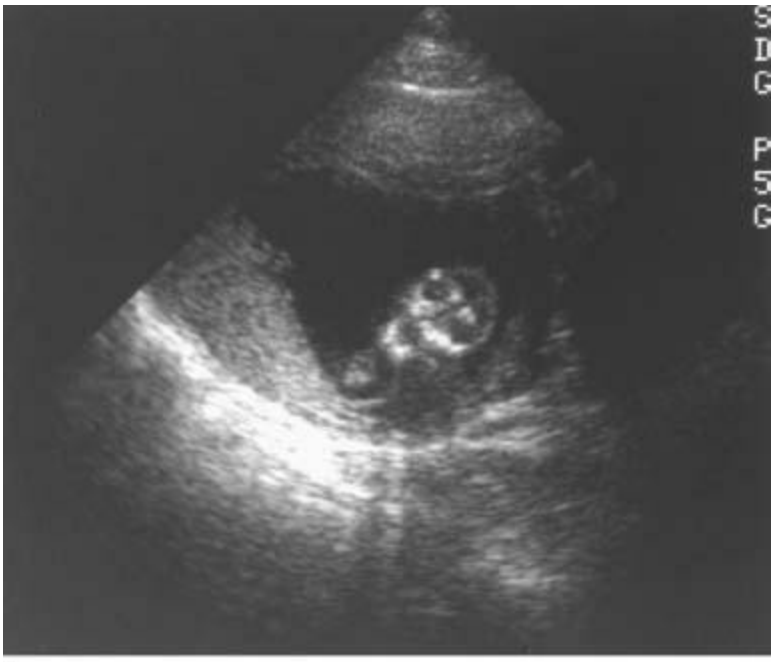

A

**FIGURE 9-19A** Transabdominal coronal sonogram of the fetal head. The brain and calvarium are not seen above the level of the orbits. Only a small amount of disordered soft tissue is identified.

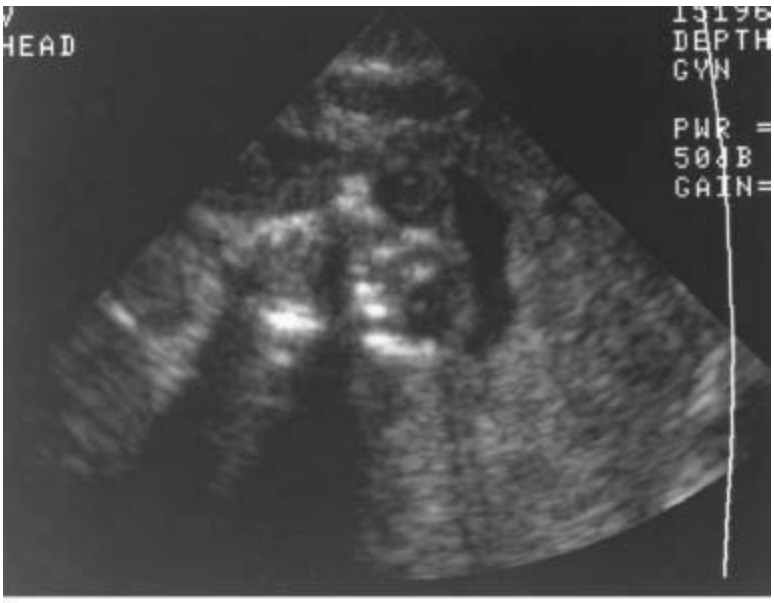

B

**FIGURE 9-19B** Endovaginal sonogram of the fetal head. Endovaginal sonogram confirms the absence of calvarium and brain above the level of the orbits.

## DIFFERENTIAL DIAGNOSIS

The differential diagnosis includes congenital malformations characterized by absence or decreased prominence of the calvarium:

- **Amniotic band syndrome:** This diagnosis is possible but unlikely because there is no evidence of intrauterine membranes. Additionally, the loss of the cranial vault is complete and symmetric, as opposed to amniotic band syndrome in which it is typically incomplete and asymmetric. Finally, additional lesions characteristic of amniotic band syndrome such as amputated limbs and atypical abdominal wall defects are not seen.
- **Severe microcephaly:** It could resemble this case if the calvarium is not recognized because of its diminutive size. Microcephaly is unlikely, however, because the images demonstrate complete absence of the calvarium, rather than a small calvarium.
- **Exencephaly:** Absence of the calvarium is consistent with exencephaly, but a larger amount of abnormally developed brain tissue would be seen in exencephaly.
- **Osteogenesis imperfecta:** This is a consideration because it is associated with marked undermineralization of the cranium. It is unlikely, however, because the underlying brain tissue would be normal in quantity and have a normal sonographic pattern.
- **Anencephaly:** This is the best diagnosis because of the combination of complete symmetric absence of the calvarium in conjunction with absence of normal brain tissue above the level of the orbits.

# DIAGNOSIS
**Anencephaly**

# KEY FACTS
## Clinical
- Anencephaly is a neural tube defect characterized by absence of the fetal cranium and cerebral hemispheres.
- Despite the implications of literal translation of the term *anencephaly,* there is not a complete absence of brain and head. Functioning neural tissue and calvarial structures are almost always present at the base of the skull.
- The disorder is uniformly fatal. Most affected infants die in utero or within a few days of birth.
- Anencephaly is often associated with additional defects, including spine anomalies, facial clefts, cardiovascular anomalies, and urinary tract malformations.
- After birth of one fetus with a neural tube defect, the risk of recurrence in a subsequent pregnancy is approximately 3% to 5%.

## Radiologic
- Ultrasound changes in anencephaly are dramatic, so the detection rate approaches 100% by the early second trimester.
- If the fetal head is low in the pelvis, directly abutting the uterine wall or cervix, the diagnosis may not be immediately obvious by transabdominal sonography. In such a case, the abnormality should still be perceived when the examiner is unable to obtain a biparietal diameter in the conventional scan plane. Endovaginal or transperineal sonography can then be used to confirm the diagnosis.
- The combination of lack of cranial vault and of normal brain tissue above the level of the orbits results in a fetal head pattern that has been termed “frog-like.”
- Identification of disorganized soft tissue above the level of the orbits does not exclude anencephaly. Such soft tissue is frequently seen due to the presence of angiomatous stroma. It tends to be most prominent when anencephaly is detected early in the pregnancy.
- Though additional anomalies occur in up to 50% of affected fetuses, detection of these lesions is not usually considered a critical component of the ultrasound study, since anencephaly is uniformly fatal.
- Polyhydramnios is identified in many but not all cases.
- Exencephaly is considered an embryologic precursor to anencephaly. It is

characterized by complete or partial absence of the calvarium, in association with a large amount of abnormally developed brain tissue. Absence of the calvarium in exencephaly is postulated to expose the brain to repeated trauma and amniotic fluid, leading to eventual brain destruction and anencephaly.

## SUGGESTED READING

Goldstein RB, Filly RA. Prenatal diagnosis of anencephaly: Spectrum of sonographic appearances and distinction from the amniotic band syndrome. AJR Am J Roentgenol 1988;151:1547–1550.

Goldstein RB, Filly RA, Callen PW. Sonography of anencephaly: Pitfalls in early diagnosis. J Clin Ultrasound 1989;17:397–402.

Hendricks SK, Cyr DR, Nyberg DA. Exencephaly—Clinical and ultrasonic correlation to anencephaly. Obstet Gynecol 1988;72:898–901.

Stumpf DA, Cranford RE, Elias S, et al. The infant with anencephaly. N Engl J Med 1990;322:669–674.

Wilkins-Haug L, Freedman W. Progression of exencephaly to anencephaly in the human fetus—An ultrasound perspective. Prenat Diag 1991;11:227–233.

# CASE 20

**CLARE M.**
**HAYSTEAD**

### HISTORY

A 37-year-old man who is 2 days status postrenal transplant is noted to have a rising serum creatinine.

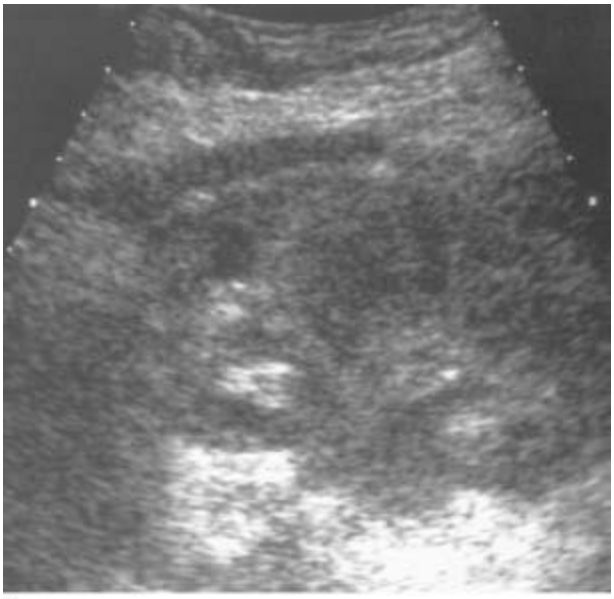

A

■**FIGURE 9-20A** Longitudinal sonogram of the right iliac fossa renal allograft demonstrates heterogenous internal architecture without evidence of renal obstruction. There is a small perinephric fluid collection anteriorly.

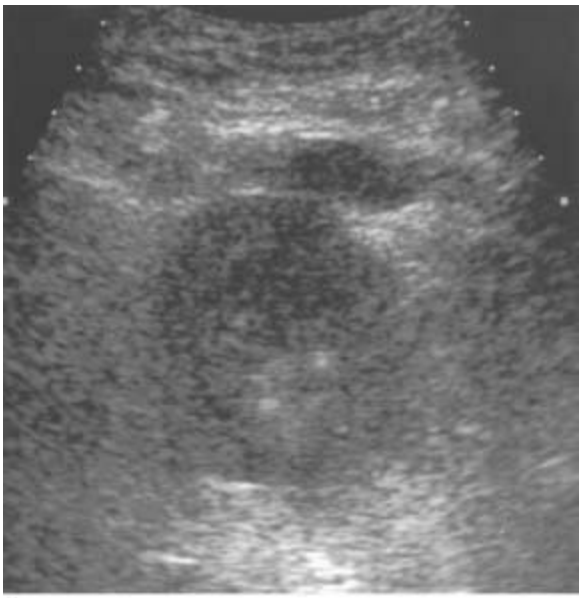

B

■**FIGURE 9-20B** "Transverse sonogram through the interpolar region of the right renal allograft demonstrates no evidence of postrenal obstruction. The small anterior fluid collection is again noted."

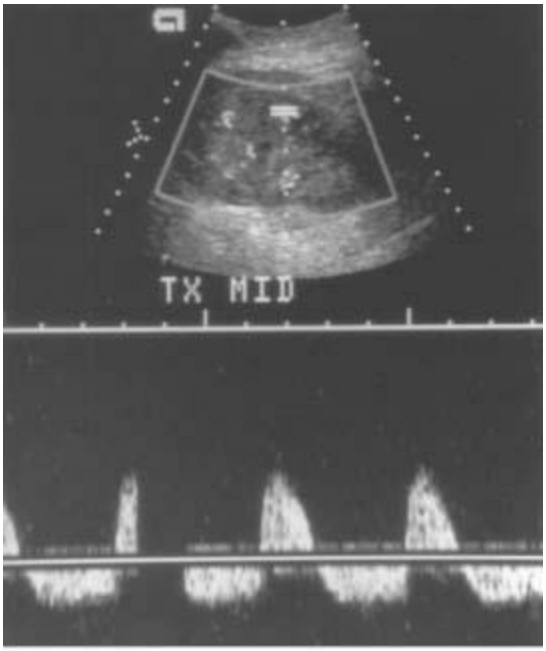


C

**FIGURE 9-20C** Duplex sonogram of an interlobar artery in the interpolar region of the right renal allograft demonstrates reversal of flow during end-diastole.

## DIFFERENTIAL DIAGNOSIS

- **Acute transplant rejection:** Acute transplant rejection can present with elevated resistive indices, reversal of diastolic flow, or absent diastolic flow.
- **Severe acute tubular necrosis (ATN):** ATN and acute graft rejection have a similar appearance sonographically and both occur frequently in the first few days to 1 week posttransplant. ATN tends to present slightly earlier in the posttransplant period making this the more likely diagnosis.
- **Subcapsular hematoma:** Subcapsular hemorrhage can produce a Page kidney effect; however, there is no evidence of a large subcapsular hematoma.
- **Renal vein thrombosis:** In renal vein thrombosis, the arterial waveform demonstrates a reversal of diastolic flow. Doppler evaluation of the renal vein would demonstrate no flow.

## DIAGNOSIS

**Acute tubular necrosis**

## KEY FACTS

### Clinical

- Causes of renal allograft dysfunction are myriad, including acute rejection, ATN, drug

toxicity, obstruction, infection, subcapsular hematoma, and vascular complications. ATN and acute rejection can be difficult to distinguish sonographically and percutaneous biopsy is often required to obtain a histologic diagnosis.

- The normal renal allograft is similar to the normal native kidney in that it has a low resistance vascular system requiring perfusion throughout the cardiac cycle (i.e., both systolic and diastolic flow). Renal blood flow changes reflect the relative severity of disease by increased resistance to allograft perfusion. The more severe the renal disease, the greater the increase in resistance to arterial flow.
- ATN is thought to be related to the ischemic time of the donor kidney and is more commonly seen in cadaveric transplants compared with living related donors. Dialysis can be required in the immediate posttransplant period until the ATN resolves.
- Vascular complications are frequent events following renal transplantation. Renal artery stenosis, arterial or venous thrombosis, AVFs, and pseudoaneurysms may all occur. Duplex and color Doppler ultrasound have proven useful for detecting the presence of flow as well as vascular abnormalities. Whereas renal artery stenosis/occlusion in renal transplants occurs in anywhere from 1.6% to 16% of allografts, renal vein thrombosis as a cause of acute renal failure is uncommon.
- The main role of diagnostic imaging in the immediate posttransplant period is to exclude renal obstruction, evaluate the presence of arterial and venous flow, assess the presence or absence of peritransplant fluid collections, and guide renal biopsies and fluid drainages.

## Radiologic

- The image findings in this renal allograft are nonspecific. On the first day posttransplant, a normal arterial waveform and normal resistive indices are present within the allograft. On day 2, there is an absent diastolic flow throughout the allograft. Subsequent biopsy confirmed ATN.
- Increased resistance to allograft perfusion is reflected by a disproportionate decrease in diastolic flow. This results in an elevation of the arterial resistance:

$$\mathrm{RI}\left(\text{Resistive index} = \frac{A - B}{A}\right)$$

and

$$\mathrm{PI}\left(\text{Pulsatility index} = \frac{A - B}{\text{time averaged mean velocity}}\right)$$

where $A$ = peak systolic velocity and $B$ = end-diastolic velocity.

- Reversed end-diastolic flow or absent diastolic flow indicates markedly increased resistance to renal allograft perfusion. This nonspecific finding does not allow one to distinguish between ATN and acute rejection. Elevated resistive indices and no detectable flow in the renal vein are highly suggestive of renal vein thrombosis.
- Occasionally, very slow venous flow may mimic renal vein thrombosis. In the absence

of color Doppler flow, the use of power or amplitude Doppler to direct subsequent pulsed Doppler spectral analyses may alleviate these diagnostic problems.

- While ultrasound can document the presence of arterial and venous flow and assess for obstruction and peritransplant fluid collections, the Doppler arterial waveforms are not sufficient for distinguishing between different causes of transplant dysfunction, many of which produce an increased RI.
- Ultrasound provides a valuable service in guiding renal transplant biopsies, particularly for avoiding extrarenal vessels.

## SUGGESTED READING

Gao J, Ng A, Shih G, et al. Intrarenal color duplex ultrasonography: A window to vascular complications of renal transplants. J Ultrasound Med 2007;10:1403–1418.

Kirkpantur A, Yilmaz R, Baydar DE, et al. Utility of the Doppler ultrasound parameter, resistive index, in renal transplant histopathology. Transplant Proc 2008;40:104–106.

Park S, Kin J, Cho K. Complications of renal transplantation: Ultrasonographic evaluation. J Ultrasound Med 2007;26:615–633.

Tublin M, Bude R, Platt J. The resistive index in renal Doppler sonography: Where do we stand? AJR Am J Roentgenol 2003;180:885–892.

# CASE 21

**MARK A. KLIEWER**

## HISTORY

A 27-year-old pregnant woman is referred for an elevated maternal serum alpha-fetoprotein level at 16 menstrual weeks.

A

■**FIGURE 9-21A** Transverse sonogram at the level of the fetal abdomen. A lobulated and echogenic mass is seen contiguous with the fetal abdomen. This mass is not obviously contained within a membrane.

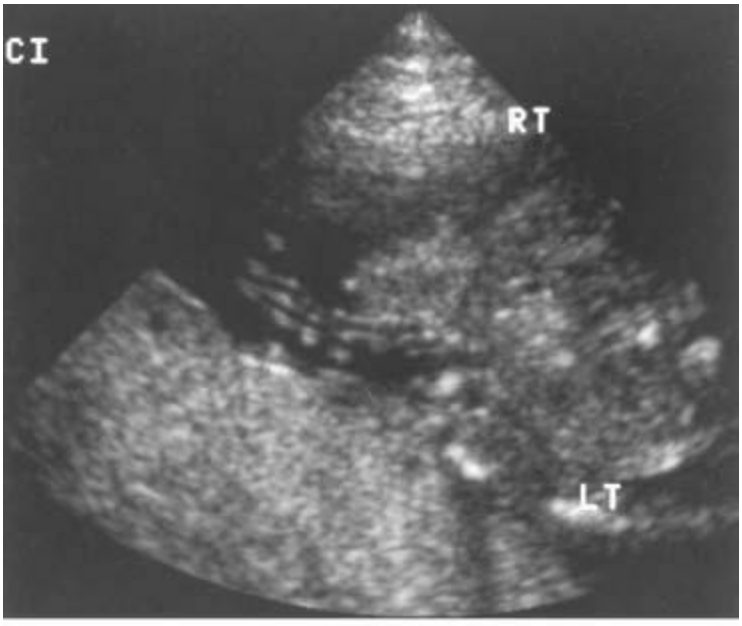


B

■**FIGURE 9-21B** Transverse sonogram at the level of the umbilical cord insertion into the fetal abdomen. The umbilical cord insertion is seen separate from and medial to the mass. No bowel dilatation is seen within the abdomen.

## DIFFERENTIAL DIAGNOSIS

■**Omphalocele:** This is a possibility, but to be the correct diagnosis the mass should be

surrounded by a membrane and the cord insertion should be into the mass, not to one side of it. The abdominal wall defect tends to be large in omphalocele, and the mass may contain liver. Ascites can be found in the fetal abdomen.

- **Gastroschisis:** This is the most likely possibility because of the eccentric location of the mass, the insertion of the cord adjacent to the mass, the absence of a limiting membrane, and the echogenicity and lobulation of the mass resulting from the conglomeration of bowel loops that are possibly thick walled.
- **Limb-body wall complex:** This is characterized by severe and widespread abnormalities, which can include eviscerated liver, cranial and extremity defects, and scoliosis. Eviscerated organs are often entangled with membranes.
- **Pentalogy of Cantrell:** This is an unlikely diagnosis given that the pentalogy is defined by the presence of an omphalocele, ectopic cordis, diaphragmatic hernia, cardiac malformation, and sternal cleft.
- **Cloacal extrophy:** This is less likely as it is diagnosed on the basis of the failure to identify a normal urinary bladder and splaying of the pubic rami. There are often additional genitourinary abnormalities.
- **Amniotic band syndrome:** This diagnosis is suggested by an unusual collection of abnormalities that could include abdominal wall defects, limb reduction abnormalities or amputations, eccentric cephaloceles, and a cleft lip. The absence of associated membranes also argues against this diagnosis.

## DIAGNOSIS

**Gastroschisis**

## KEY FACTS

### Clinical

- The etiology of gastroschisis has been attributed to abnormal involution of the right umbilical vein and to omphalomesenteric artery disruption.
- Though this defect was once thought to mandate a cesarean section, many obstetricians now perform vaginal delivery, at least for subsets of these fetuses.
- Most cases occur sporadically, although there are reports of familial recurrence.
- Most cases come to attention because of an abnormally elevated maternal serum alpha-fetoprotein level.
- Gastroschisis is not usually associated with chromosomal abnormality or other malformations.

### Radiologic

- The diagnosis is based on the presence of an abdominal wall defect from which a mass protrudes that is not covered by a membrane. The defect is usually to the right of the umbilical cord, and ascites is not typically present in the fetal abdominal cavity.
- Though a systematic search for other abnormalities should be performed, fetuses with gastroschisis usually do not have additional structural abnormalities.
- In most cases, bowel alone is eviscerated, though portions of the genitourinary system can also be involved in the defect. Some reports have suggested that liver can rarely be involved, though these reports have been contested.
- Usually the task of the sonographer is to distinguish gastroschisis from omphalocele. The two most telling features of gastroschisis are its paramedian location (lateral to the umbilical insertion) and the absence of a limiting membrane. In contrast, an omphalocele is encased by a membrane and occurs at the umbilical cord insertion such that the cord inserts directly into the mass.
- The extruded bowel can become thick walled and matted. Furthermore, the mass can become encased by fibrous bands.
- Fetuses may develop evidence of bowel wall thickening, bowel obstruction, and perforation. Meconium peritonitis is suspected when there are abdominal calcifications or pseudocysts. Ischemic injury to the bowel can occur.
- Intrauterine growth retardation is a frequent complication.

## SUGGESTED READING


Bair JH, Russ PD, Pretorius DH, et al. Fetal omphalocele and gastroschisis: A review of 24 cases. AJR Am J Roentgenol 1986;147:1047–1051.

DeVries PA. The pathogenesis of gastroschisis and omphalocele. J Pediatr Surg 1980;15:245–251.

Durfee SM, Downard CD, Benson CB, Wilson JM. Postnatal outcome of fetuses with the prenatal diagnosis of gastroschisis. J Ultrasound Med 2002;21:269–274.

Kirk EP, Wah R. Obstetric management of the fetus with omphalocele or gastroschisis: A review and report of 112 cases. Am J Obstet Gynecol 1983;146:512–518.

Lindfors KK, McGahan JP, Walter JP. Fetal omphalocele and gastroschisis: Pitfalls in sonographic diagnosis. AJR Am J Roentgenol 1986;147:797–800.

Nelson PA, Bowie JD, Filston HC, et al. Sonographic diagnosis of omphalocele in utero. AJR Am J Roentgenol 1981;138:1178–1180.

Stringer MD, Brereton RJ, Wright VM. Controversies in the management of gastroschisis: A study of 40 patients. Arch Dis Child 1991;66:34–36.


# CASE 22


**CLARE M.**
**HAYSTEAD**

**HISTORY**

A 22-year-old male who had a “close encounter”with a lacrosse ball.

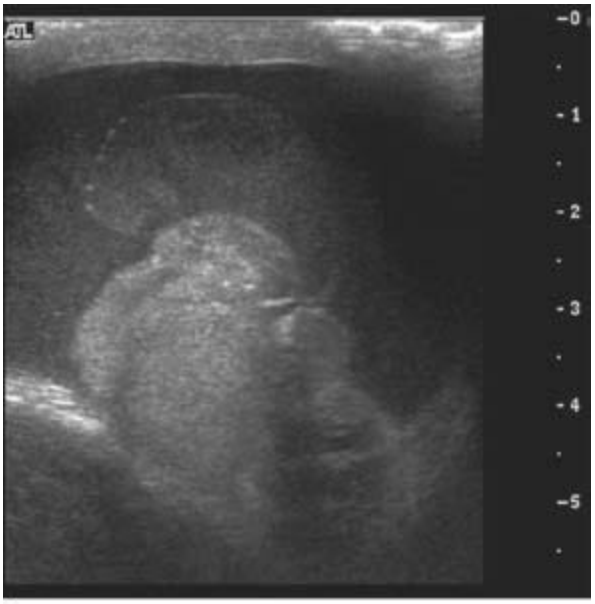


A

■**FIGURE 9-22A** Transverse gray-scale sonographic image obtained with a 10-MHz linear-array transducer demonstrates the superior pole of the testis surrounded by complex fluid and a large, irregular echogenic mass.

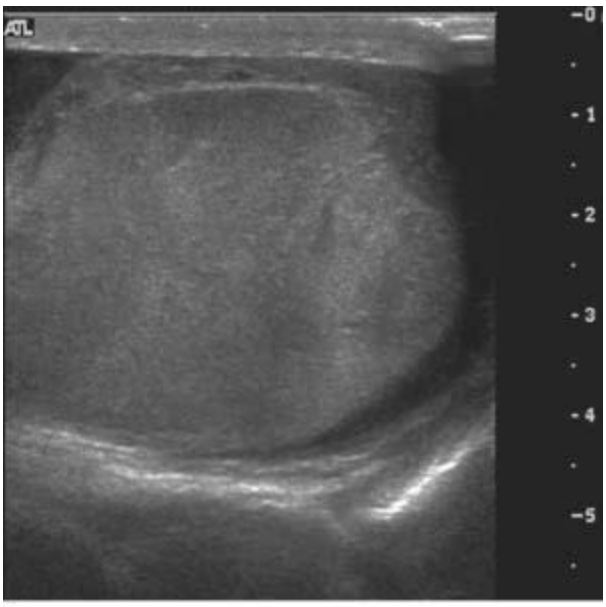


B

■**FIGURE 9-22B** Longitudinal sonographic image demonstrates marked heterogeneity

of the testis with disruption of the tunica albuginea.

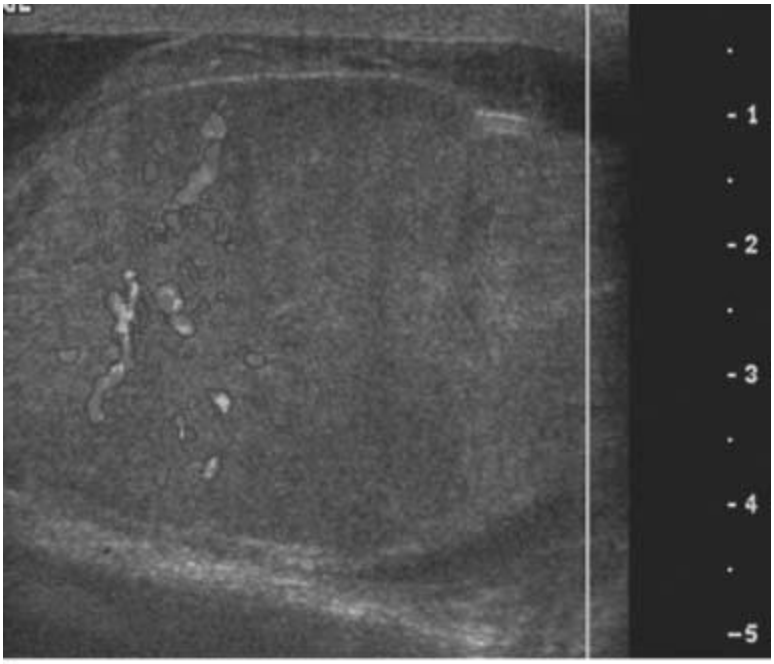


C

**FIGURE 9-22C** Decreased intratesticular blood flow is identified with color Doppler ultrasound. (See color insert)

## DIFFERENTIAL DIAGNOSIS

- **Testicular rupture:** This case demonstrates interruption of the tunica albuginia resulting in an abnormal testicular shape, appearance, and blood flow consistent with testicular rupture. There is a large fluid collection with internal echoes consistent with a hematocele.
- **Testicular fracture:** Testicular fracture is similar in appearance to testicular rupture. There is a break in the normal testicular architecture but the testicular shape and integrity of the tunica albuginia are maintained.
- **Testicular contusion:** This is a consideration given the clinical history; however, the ultrasound appearance is not consistent. Contusions tend to be hypoechoic relative to the testes and a normal testicular shape is maintained.
- **Testicular neoplasm:** Testicular neoplasms can be discovered in the setting of trauma but increased flow would be expected on color Doppler ultrasound.

## DIAGNOSIS

**Testicular rupture**

## KEY FACTS

### Clinical

- Testicular rupture is a common sports-related injury resulting from a direct blow to the groin.
- It is considered a urologic emergency and early surgical intervention is required. Surgical success rate is high with >80% of testicles saved if surgery is performed within 72 hours. Delayed intervention can result in infertility, atrophy, and secondary infection.
- Management requires drainage of the hematocele, surgical debridement, and primary repair of the tunical albuginea.
- Orchiectomy is occasionally performed in cases of complete infarction or extensive injury resulting in a shattered testicle.

### Radiologic

- Disruption of the tunica albuginea is identified as discontinuity of the normal echogenic rim surrounding the testicle and the testicular contour is irregular. However, a discrete fracture plane is frequently not identified.
- A scrotal hematocele is the most common sonographic finding and, in the appropriate clinical setting, should prompt surgical exploration. Both extruded testicular contents and a hematoma can appear as an echogenic mass adjacent to the testicle. Testicular rupture is frequently mistaken as a hematocele.
- Disruption of the normal capsular blood flow on color Doppler imaging is suggestive of testicular rupture. Decreased testicular blood flow can also be detected but is nonspecific and can be seen with both contusion and infarction.

## SUGGESTED READING

Bhandary P, Abbitt P, Watson, L. Ultrasound diagnosis of traumatic testicular rupture. J Clin Ultrasound 1992;20:346–348.

Dogra VS, Gottlieb RH, Oka M, Rubins DJ. Sonography of the scrotum. Radiology 2003;227:18–36.

Herbener T. Ultrasound in the assessment of the acute scrotum. J Clin Ultrasound 1996;24:405–421.

Jeffrey RB, Laing FC, Hricak H, McAninch JW. Sonography of testicular trauma. AJR Am J Roentgenol 1983;141:993–995.

Kim SH, Park S, Choi SH, et al. Significant predictors for determination of testicular rupture on sonography: A prospective study. J Ultrasound Med 2007;26:1649–1655.

# CASE 23

**CLARE M.**

**HAYSTEAD**

## HISTORY

A 24-year-old male presents with an underlying metabolic disorder.

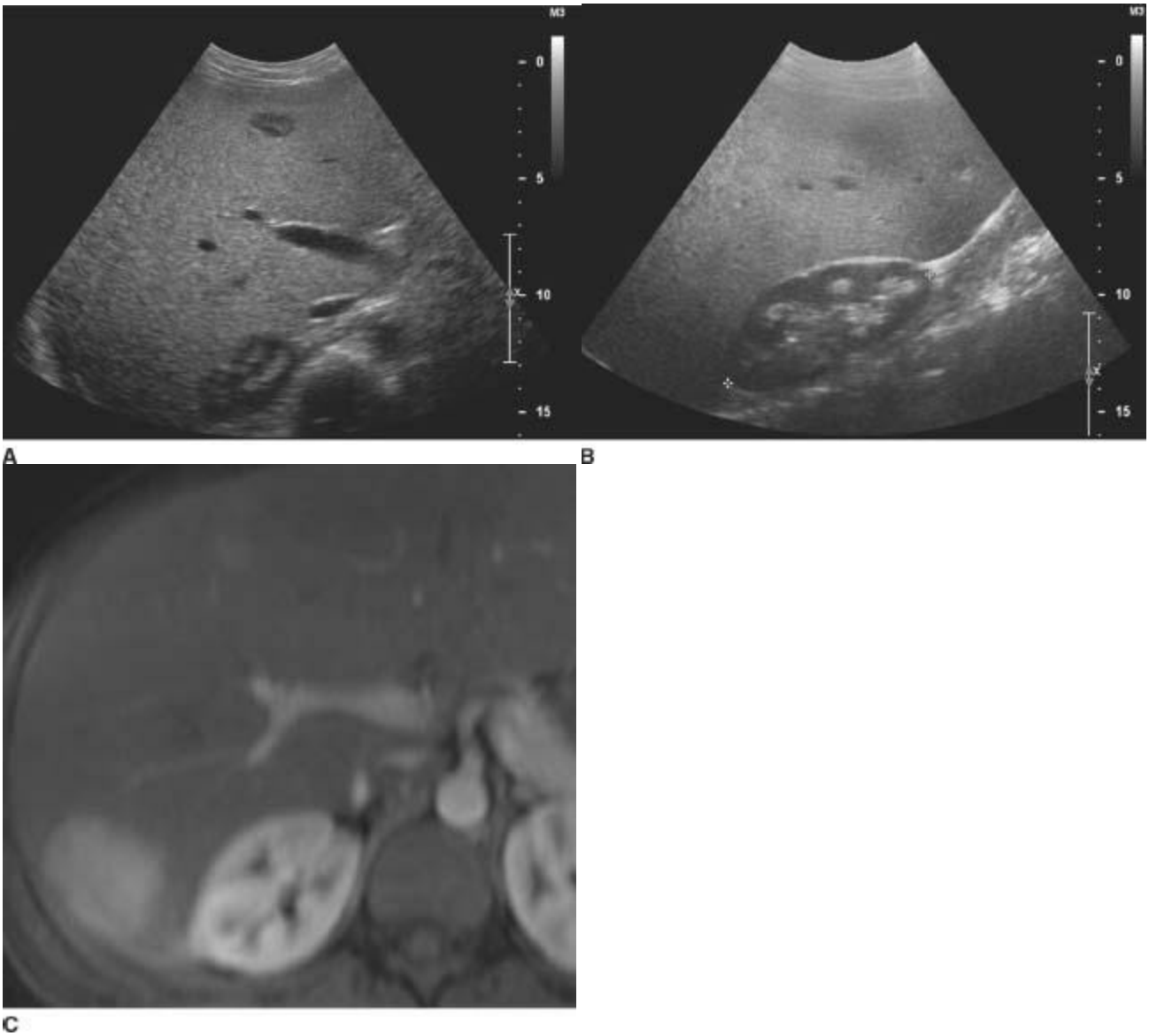


■**FIGURES 9-23A-C** Longitudinal **(A)** and transverse **(B)** gray-scale ultrasound images of the upper abdomen obtained with a 5-MHz curvilinear-array transducer demonstrates two well-circumscribed, predominantly hypoechoic masses in the periphery of the liver. The lesions demonstrate internal echogenicity possibly related to hemorrhage or fat. Note diffusely increased echogenicity of the liver parenchyma compared to the right kidney indicative of diffuse hepatic steatosis. **C:** On contrast-enhanced MR imaging during the late hepatic arterial phase, both lesions show marked, homogenous

enhancement compared to the surrounding liver.

## DIFFERENTIAL DIAGNOSIS

- **Metastatic disease:** Given the multiplicity of lesions, metastatic disease is a strong consideration and on imaging findings alone, it would remain at the top of the differential, however, the patient is young and has no known history of malignancy.
- **Hepatic adenomas:** Given the history and imaging findings, this is the best diagnosis. Adenomas are usually well circumscribed but can vary in echogenicity. The lesions in this case have echogenic areas centrally suggestive of necrosis, hemorrhage, or calcification and the liver is diffusely echogenic consistent with hepatic steatosis.
- **Focal nodular hyperplasia** (FNH): FNH is much more common in females but can be multiple in up to 20% of cases. It can be difficult to distinguish adenomas from FNH on gray scale sonographic imaging.
- **Hemangiomas:** Multiple hemangiomas is a consideration for multiple liver lesions however, the appearance of these lesions would be atypical. Hemangiomas are the most common solid hepatic neoplasm and are multiple in 10% of cases. They are usually well circumscribed, homogenous, and echogenic. The posterior acoustic enhancement described in about 60% of hemangiomas is also absent in this case.
- **Hepatocellular carcinoma (HCC):** Multifocal HCC arising in a noncirrhotic liver makes this diagnosis unlikely.

## DIAGNOSIS

**Multiple hepatic adenomas in the setting of glycogen storage disease (GSD)**

## KEY FACTS

### Clinical

- Hepatic adenomas are associated with oral contraceptive use, anabolic steroids, liver adenomatosis, and glycogen storage disease type 1 (GSD I) (von Gierke's disease). GSD I is the most common GSD resulting from a deficiency in glucose-6-phosphatase.
- The clinical presentation in patients with an adenoma is acute abdominal pain related to spontaneous hemorrhage. Patients can also present with right upper quadrant pain from mass effect. Most adenomas are detected incidentally on imaging studies.
- Adenomas can be multiple in 20% of cases.
- Malignant transformation to HCC is rare but has been reported.
- Large adenomas are resected because of the risk of hemorrhage.
- Adenomas consist of hepatocytes but bile duct epithelium is absent—one of the factors

distinguishing adenomas from FNH. Fat is present in up to 10% of adenomas.

### Radiologic

- On ultrasound, adenomas are well-circumscribed and hypoechoic. The lesions become more heterogeneous if there is associated fat, hemorrhage, or necrosis. Internal calcification is present in up to 10% of adenomas. Flow on color Doppler is usually peripheral as opposed to the central flow detected in FNH.
- Multiphasic CT or contrast-enhanced MRI is considered the next step in lesion evaluation and characterization.
- On unenhanced imaging, adenomas can be high in attenuation because of hemorrhage; however, many adenomas are inconspicuous. Small adenomas demonstrate rapid enhancement during the arterial phase relative to the hepatic parenchyma and become isoattenuating to the liver on portal venous and equilibrium phase imaging.
- The appearance on MRI can be variable. Adenomas can be isointense or hyperintense on T1-weighted imaging. On T2-weighted imaging, adenomas tend to be slightly higher in signal intensity than the hepatic parenchyma. The enhancement pattern is similar to CT with lesions demonstrating hyperenhancement during the late arterial phase and becoming isointense to the hepatic parenchyma on portal venous and equilibrium phase imaging. Delayed imaging with hepatobiliary MR contrast agents demonstrates no excretion due to the lack of bile ducts.

## SUGGESTED READING

Brancatelli G, Federle MP, Vullierme M, et al. CT and MR imaging evaluation of hepatic adenoma. J Comput Assist Tomogr 2006;30:745–750.

Faria S, Iyer R, Rashid A, Whitman G. Hepatic adenoma. AJR Am J Roentgenol 2004;182:1520.

Grazioli L, Federle MP, Brancatelli G, et al. Hepatic adenomas: Imaging and pathologic findings. Radiographics 2001;21:877–894.

Harvey C, Albrecht T. Ultrasound of focal liver lesions. Eur Radiol 2001;11:1578–1593.

Paulson E, Mcclellan J, Washington K, et al. Hepatic Adenoma: MR characteristics and correlation with pathologic findings. AJR Am J Roentgenol 1994;163:113–116.

# CASE 24

**CLARE M.**
**HAYSTEAD**

### HISTORY

A 32-year-old female presents with an enlarged right thyroid lobe on physical exam.

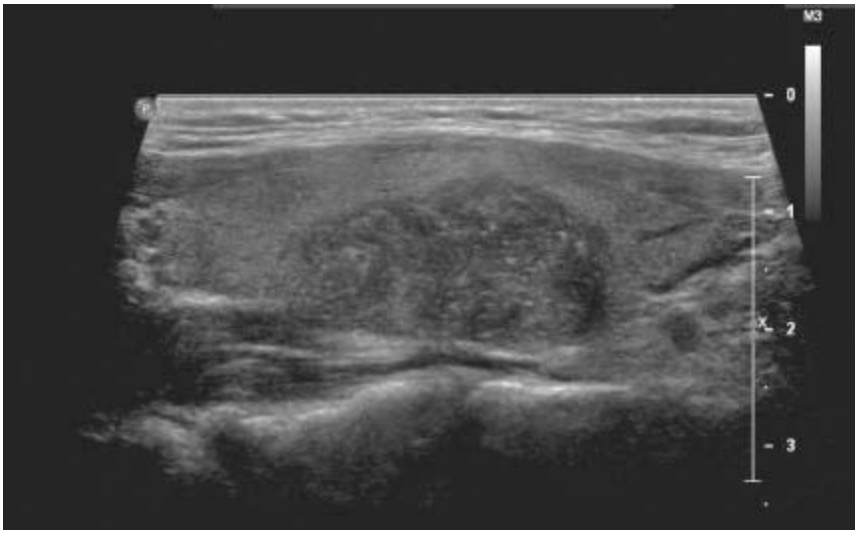


**FIGURE 9-24** Longitudinal sonogram of the right thyroid lobe shows an irregular, hypoechoic nodule with microcalcifications.

## DIFFERENTIAL DIAGNOSIS

**Papillary thyroid cancer:** There is an irregular, hypoechoic nodule with punctate echogenic foci consistent with calcifications in an otherwise normal appearing right thyroid lobe. The appearance is concerning for thyroid malignancy with papillary cancer being the most likely diagnosis and a biopsy should be recommended.

**Colloid cyst:** Colloid can cause echogenic foci similar to calcifications, but to confidently call a lesion a colloid cyst, there must be associated reverberation artifact. Colloids cysts can also have a spongiform appearance; however, the nodule in this case is solid.

**Thyroid adenoma:** The differential diagnosis for a solid thyroid nodule includes benign and malignant etiologies and it can be difficult to distinguish these entities on imaging features alone. In this case, the presence of punctate calcifications raises the concern for malignancy.

**Metastatic disease:** The finding of an incidental thyroid nodule in a patient with metastatic disease prompts a biopsy in most patients. Metastatic disease to the thyroid is much less common than a primary thyroid cancer.

**Anaplastic thyroid carcinoma:** This malignancy is more aggressive, tends to be larger at the time of presentation and locally invasive.

## DIAGNOSIS

**Papillary thyroid cancer**

# KEY FACTS

## Clinical

- Primary thyroid carcinomas include papillary, follicular, medullary, and anaplastic, with papillary being the most common. Papillary and follicular are well-differentiated carcinomas. Medullary and anaplastic are less well-differentiated and more aggressive.
- Up to 50% of the population have thyroid nodules with <10% of nodules being malignant. Most thyroid nodules are detected on physical exam; however, increasingly nodules are detected incidentally on imaging studies. With aggressive tumors, extracapsular extension can cause hoarseness, dysphagia, and pain. Some patients present with lymphadenopathy.
- Thyroid cancer is more common in females with a 3:1 predominance. Risk factors include a family history of thyroid cancer and prior radiation.
- Papillary thyroid cancer is an indolent disease that has a very low mortality. The rates for locally recurrent disease have been reported in the range of 15% to 30% so close surveillance is performed. Distant metastatic disease involves the lungs and skeleton.
- Treatment involves surgery and radioiodine therapy. Surveillance after treatment includes focused neck ultrasound and serum thyroglobulin.

## Radiologic

- Ultrasound is the most common modality used for the evaluation of thyroid nodules. It can be a challenge to distinguish benign from malignant thyroid nodules but certain characteristics have been described in malignancy. These include microcalcifications, a markedly hypoechoic nodule with irregular margins, absence of a hypoechoic halo around the nodule and increased vascularity relative to the thyroid parenchyma.
- Microcalcifications appear as punctate echogenic foci and are highly suggestive of papillary carcinoma. Inspissated colloid can have a similar appearance and it is important not to mistake calcifications for colloid. If it is unclear, the nodule should be biopsied. Coarse calcifications also have an association with thyroid malignancies, most commonly medullary thyroid carcinoma.
- Current recommendations for fine needle aspiration include the following:
    Solid nodule with microcalcifications, which is 1.0 cm or more in largest diameter
    1.5 cm solid nodule or 1.5 cm nodule with coarse calcifications
    A partially cystic nodule >2 cm
    Significant growth (>15%) since the prior exam
- The history and clinical presentation should also be considered in the decision to

perform an FNA.

- Evaluation of the cervical nodes should be performed if the patient has a suspicious thyroid nodule. Features concerning for nodal involvement include cystic or calcified nodes, rounded shape, loss of the fatty hilum, and a short axis >7 mm.

## SUGGESTED READING

**Frates MC, Benson CB, Charboneau JW, et al. Management of thyroid nodules detected at US: Society of Radiologists in Ultrasound Consensus Conference statement. Ultrasound Q 2006;22:231–238; discussion 239–240.**

Hoang JK, Lee WK, Lee M, et al. US Features of thyroid malignancy: Pearls and pitfalls. Radiographics 2007;27:847–860.

Johnson NA, Tublin ME. Postoperative surveillance of differentiated thyroid carcinoma: Rationale, techniques, and controversies. Radiology 2008;249:429–444.

Moon WJ, Jung SL, Lee JH, et al. Thyroid Study Group, Korean Society of Neuro- and Head and Neck Radiology. Benign and malignant thyroid nodules: US differentiation—Multicenter retrospective study. Radiology 2008;247:762–770.

O'Malley ME, Weir MM, Hahn PF, et al. US-guided fine-needle aspiration biopsy of thyroid nodules: Adequacy of cytologic material and procedure time with and without immediate cytologic analysis. Radiology 2002;222:383–387.

# CASE 25

**CLARE M.**
**HAYSTEAD**

## HISTORY

A 26-year-old woman presents with right lower quadrant pain. Her β-HCG is negative.


A

■**FIGURE 9-25A** Transabdominal sonogram of the right ovary. The right ovary is enlarged with multiple peripheral follicles.

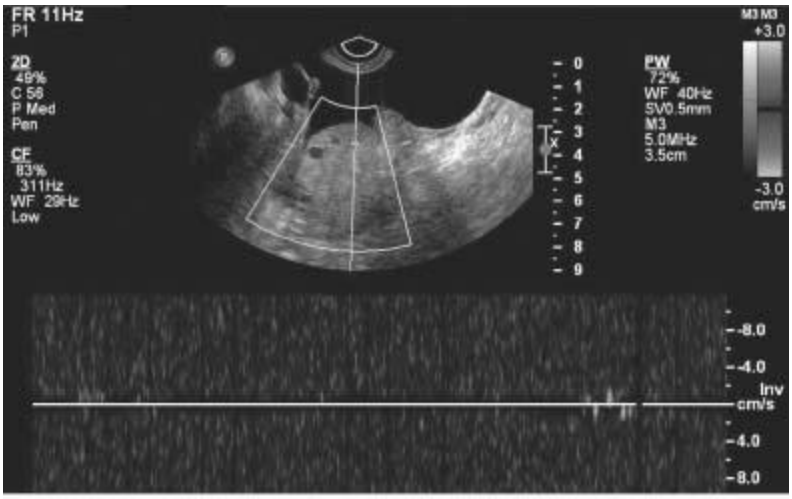


B

■**FIGURE 9-25B** Transvaginal sonogram of the right ovary. The right ovary is enlarged, free fluid is present and no flow is detected on color or spectral Doppler. (See color insert)

## DIFFERENTIAL DIAGNOSIS

■**Ovarian torsion:** The ovary is enlarged and no blood flow is detected making this the most likely diagnosis.

■**Ovarian neoplasm:** No discrete mass is identified; however, many cases of torsion are associated with an ipsilateral ovarian mass and a careful evaluation of the ovary should be performed.

■**Ectopic pregnancy:** If the β-HCG was positive, this would be a consideration, but the

imaging findings and history exclude this diagnosis.

- **Hemorrhagic cyst:** A hemorrhagic cyst can have a varying appearance depending on the age of the hemorrhage. Initially, a discrete lesion with multiple internal echoes similar to an endometrioma is present. With development and evolution of the clot, a reticular pattern with low-level echoes and internal septations develops followed by clot retraction. Fluid-fluid levels can also be present. No discrete mass is identified in this case.
- **Endometrioma:** Endometriomas are discrete lesions, usually unilocular with diffuse, low-level internal echoes. Fluid-fluid levels are also associated with endometriomas.

## DIAGNOSIS

**Ovarian torsion**

## KEY FACTS

### Clinical

- Ovarian torsion can be a challenging diagnosis both clinically and radiographically. Common presenting symptoms include pain, nausea, and vomiting. The differential diagnosis includes appendicitis, ectopic pregnancy, and other causes of acute abdominal pain. In up to half the cases, a palpable mass has been described. Most patients present with acute pain but there are reports of chronic pain related to torsion.
- Adnexal torsion results from a twisting of the vascular pedicle supplying the ovary, fallopian tube, or both leading to vascular compromise and ultimately ischemia and necrosis. Torsion usually involves both the ovary and the fallopian tube.
- Many patients have an ipsilateral ovarian lesion such as a cyst, dermoid, or fibroma. Torsion of a normal ovary occurs in children and younger patients because the adnexa are more mobile. There is also a reported right-side predominance.
- Torsion is considered a surgical emergency because of the risk of ischemia and loss of the ovary. If diagnosed promptly, the vascular pedicle can be untwisted and ovary salvaged. Any underlying cyst or mass is resected to prevent future torsion.

### Radiologic

- The classic sonographic description of torsion is an enlarged ovary with multiple peripheral follicles and no detectable blood flow. Arterial flow has been described in surgically proven cases of torsion and the presence of flow does not exclude the diagnosis. One theory is that the dual blood supply to the ovary from both the ovarian artery and the ovarian branch of the uterine artery leads to persistent arterial flow to the adnexa. Another theory is that venous thrombosis occurs first and leads to symptoms

before arterial compromise occurs. Comparison of flow to the contralateral ovary can be helpful. Free fluid is often present.

- A twisted vascular pedicle has been described in torsion. The pedicle consists of the ovarian arteries and veins, fallopian tube, and broad ligament. On ultrasound, twisting of the vascular pedicle appears as an echogenic mass with multiple concentric hypoechoic stripes (target appearance) or a tubular mass. Evaluation of flow within the pedicle has been described with absence of flow associated with hemorrhagic infarction and necrosis of the ovary and fallopian tube. The presence of flow within the pedicle suggests a greater likelihood of viable ovarian tissue.
- CT and MR findings include an enlarged ovary or displaced adnexal mass, deviation of the uterus to the affected side, thickening of the fallopian tube and ascites.

## SUGGESTED READING


Chiou SY, Lev-Toaff AS, Masuda E, et al. Adnexal torsion: New clinical and imaging observations by sonography, computed tomography, and magnetic resonance imaging. J Ultrasound Med 2002;26:1289–1301.

Graif M, Shalev J, Strauss S, et al. Torsion of the ovary: Sonographic features. AJR Am J Roentgenol 1984;143:1331–1334.

Lee EJ, Kwon HC, Joo HJ, et al. Diagnosis of ovarian torsion with color Doppler sonography: Depiction of twisted vascular pedicle. J Ultrasound Med 1998;17:83–89.

Rha SE, Byun JY, Jung SE, et al. CT and MR imaging features of adnexal torsion. Radiographics 2002;22:283–294.

Rosado WM Jr, Trambert MA, Gosink BB, Pretorius DH. Adnexal torsion: Diagnosis by using Doppler sonography. AJR Am J Roentgenol 1992;159:1251–1253.

# Chapter TEN

# Nuclear Medicine

**R. EDWARD COLEMAN** ▪ CHAPTER EDITOR

R. Edward Coleman

Salvadore Borges-Neto

Robert H. Wilkinson, Jr.

Sara M. O'Hara

Michael W. Hanson

Robert R. Reiman, Jr.

Rosalie J. Hagge

Bennett B. Chin

# CASE 1

**R. EDWARD COLEMAN**

**HISTORY**

A 54-year-old woman with left knee pain.

A

■**FIGURE 10-1A** Anteroposterior view of the left knee obtained at the time of presentation. There is no evidence of a fracture on this radiograph.

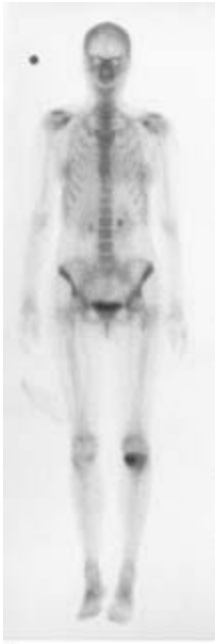

B

■**FIGURE 10-1B** Anterior whole body image of a bone scan obtained 2 hours after the intravenous administration of Tc-99m methylene diphosphate. A focal area of abnormal accumulation is present in the proximal left tibia.

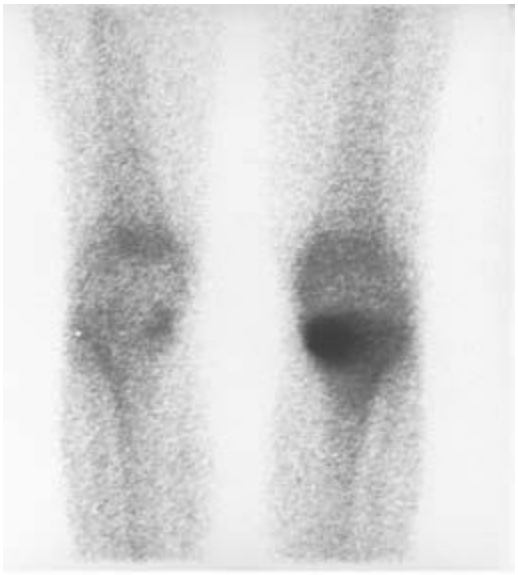

C

**FIGURE 10-1C** Anterior image of the knees. A region of increased radiotracer activity is present in the left tibial plateau, with greater accumulation medially than laterally.


D

**FIGURE 10-1D** Anteroposterior view of the left knee obtained 1 month after the initial radiograph and bone scan. A linear region of sclerosis has developed in the medial left tibial metaphysis.

## DIFFERENTIAL DIAGNOSIS

**Metastatic disease:** This is an unlikely diagnosis because of the absence of a primary malignancy and because only a single abnormality is present. Multiple abnormalities

would be expected with metastatic disease.

- **Osteosarcoma:** This diagnosis is unlikely because the tumor usually occurs in the 10- to 25-year age range and is apparent radiographically at the time of presentation.
- **Insufficiency fracture:** This is the best diagnosis because initial radiographs commonly are normal in the face of an abnormal bone scan, with development of sclerosis at the fracture site demonstrable on radiographs a few weeks later.
- **Osteomyelitis:** This diagnosis is unlikely because the patient is older than most patients with osteomyelitis and because of the absence of a predisposing factor. Furthermore, at least some radiographic abnormality would be expected in osteomyelitis.
- **Degenerative joint disease:** This diagnosis is unlikely because the bone scan abnormality is not in the joint space but in the tibial metaphysis. Furthermore, the radiograph does not demonstrate changes of degenerative joint disease.

# DIAGNOSIS

## Insufficiency fracture

## KEY FACTS

### Clinical

- Musculoskeletal injury accounts for 15% to 20% of patient visits to emergency departments and 30% of routine orthopedic visits.
- Physical examination and plain film radiography of the site of injury are typically performed at the time of presentation.
- Insufficiency fractures occur when bones that are weakened by osteoporosis or other metabolic bone diseases are placed under normal stress.
- Stress fractures occur when normal bones are exposed to abnormal stress of a repetitive type.
- Pathologic fractures occur when bones that are weakened by tumor involvement are exposed to normal stress.

### Radiologic

- Radiographic studies are often initially normal at the time of development of an insufficiency fracture or a stress fracture. In fact, abnormalities may not be present until 1 to 2 weeks later.
- If pain is considered to be of osseous origin and the plain radiographs are normal, a

radionuclide bone scan is the next imaging modality that is generally used to evaluate for a possible fracture. The bone scan will typically be abnormal at that time.

- On a three-phase bone scan, acute fractures demonstrate increased perfusion on the dynamic phase, poorly defined abnormal radiotracer accumulation on the blood pool images, and focal abnormal accumulation on delayed images.
- Magnetic resonance imaging (MRI) can demonstrate cortical and marrow changes associated with the fracture.
- Insufficiency fractures in elderly patients with osteoporosis can mimic metastatic disease on plain films.

## SUGGESTED READING

de Castro SM, Joosse P, Unlii C, Steller EP. Images in emergency medicine. Pain in the leg after jogging. Emerg Med J 2009;26:806.

Holder LE. Clinical radionuclide bone imaging. Radiology 1990;176:607–614.

Holder LE. Bone scintigraphy in skeletal trauma. Radiol Clin North Am 1993;31:739–781.

Krestan C, Hojreh A. Imaging of insufficiency fractures. Eur J Radiol 2009;71:398–405.

Martin P. Basic principles of nuclear medicine techniques for detection and evaluation of trauma and sports medicine injuries. Semin Nucl Med 1988;18:90–112.

# CASE 2

**SALVADORE BORGES-NETO**

### HISTORY

A 76-year-old woman with a history of coronary artery disease, hypertension, elevated serum lipids, and atrial fibrillation presents with increasing shortness of breath.

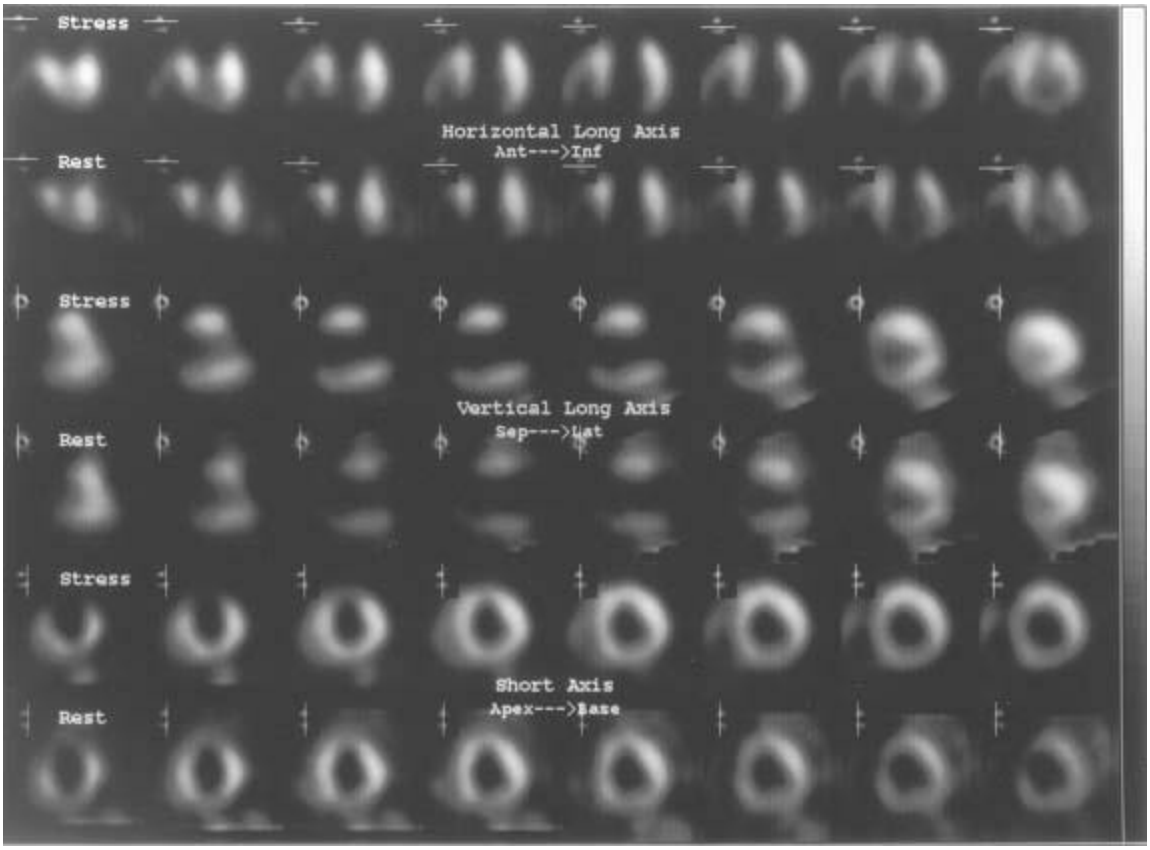


**FIGURE 10-2** Stress (Tc-99m sestamibi) and rest (Tl-201) SPECT myocardial perfusion images displayed in the horizontal long axis **(top 2 rows),** vertical long axis **(middle 2 rows),** and short axis views **(bottom 2 rows).** The stress perfusion images show an area of markedly decreased perfusion involving the low anterior, anteroapical, anteroseptal, and inferoapical regions. The rest perfusion images also show decreased activity in the same areas. The extent and severity of the perfusion defects are essentially the same on the stress and rest perfusion images.

## DIFFERENTIAL DIAGNOSIS

- **Myocardial infarction without stress-induced ischemia:** This is the best diagnosis based on the presence of a fixed perfusion defect with essentially no change in the extent and severity of the perfusion abnormalities between the rest and stress studies.
- **Myocardial ischemia without infarction:** This diagnosis is made when a perfusion defect induced by stress is not present on the rest study. This is not the situation in the case illustrated.
- **Myocardial infarction and stress-induced ischemia:** This diagnosis is made when a stress-induced perfusion abnormality incompletely or only partially normalizes on the rest images.
- **Nonischemic cardiomyopathy:** Large perfusion defects while at rest, during stress, or

during both rest and stress are typically absent in nonischemic cardiomy-opathy. The large defects that are present in this study make this diagnosis unlikely. Furthermore, left ventricular dilatation is a prominent feature of nonischemic cardiomyopathy, a finding that is not present in this patient.

## DIAGNOSIS

## Myocardial infarction without stress-induced ischemia

## KEY FACTS

### Clinical

- Several risk factors are known to predispose to coronary artery disease, including age, family history, hypertension, smoking, and diabetes.
- Patients with coronary artery disease may present with symptoms of either angina, shortness of breath, or both. However, silent ischemia is a well-recognized entity, particularly in diabetic patients. Such patients can have arterial occlusion and infarction in the absence of symptoms.
- Myocardial infarction with coexistent low left-ventricular ejection fraction (LVEF) is associated with a poor prognosis.

### Radiologic

- Myocardial perfusion studies are performed to determine the severity and extent of myocardial ischemia and infarction and to assess prognosis.
- Tl-201 and Tc-99m sestamibi are myocardial perfusion radiotracers that distribute in proportion to blood flow. There is good correlation between the myocardial per-fusion defect size and the actual infarct size.
- Tc-99m pyrophosphate and In-111 antimyosin are myocardial infarct imaging radiotracers. These radiotracers are infarct-avid, localizing in infarcted myocardium. However, these radiotracers are used infrequently because the information provided by these agents can be obtained from other tests.
- On perfusion imaging, myocardial infarction is typically seen as one or more persistent defects on both rest and exercise studies. However, areas of persistent defects at 4 hours on the redistribution Tl-201 study can decrease or resolve (indicating myocardial viability) after rein-jection or on 24-hour redistribution images.
- Large perfusion defects are associated with poor left ventricular function and a poor prognosis.

- The term *hibernating myocardium* refers to regions of wall motion abnormality or ventricular dysfunction that improve on perfusion images at 24-hour redistribution or reinjection Tl-201 studies. Foci of hibernating myocardium are thought to result from chronic reduction in coronary artery blood flow and represent areas of impaired function with reversible myocardial damage.
- The gold standard study for myocardial viability is positron emission tomography (PET) imaging with F-18 fluorodeoxyglucose (FDG) and N-13 ammonia. Approximately 25% of areas with fixed perfusion defects on Tl-201 studies are found to be viable on FDG studies.

## SUGGESTED READING

Bonow RO, Dilsizian V. Thallium-201 for assessment of myocardial viability. Semin Nucl Med 1991;21:230–241.

Druz RS. Current advances in vasodilator pharmacological stress perfusion imaging. Semin Nucl Med 2009;39:204–209.

Palmer EL, Scott JA, Strauss HW. Practical Nuclear Medicine. Philadelphia, PA: Saunders, 1992;71–120.

Verani MS. Tl-201 myocardial perfusion imaging. Curr Opin Radiol 1991;3:797–809.

# CASE 3

### SALVADORE BORGES-NETO

### HISTORY

This is a 49-year-old woman who underwent complete thyroidectomy for papillary carcinoma of the thyroid. A metastasis to a left superior jugular node was found at surgery but not resected. An I-131 whole body scan was performed to evaluate for residual thyroid tissue and metastases after the patient developed hypothyroidism.

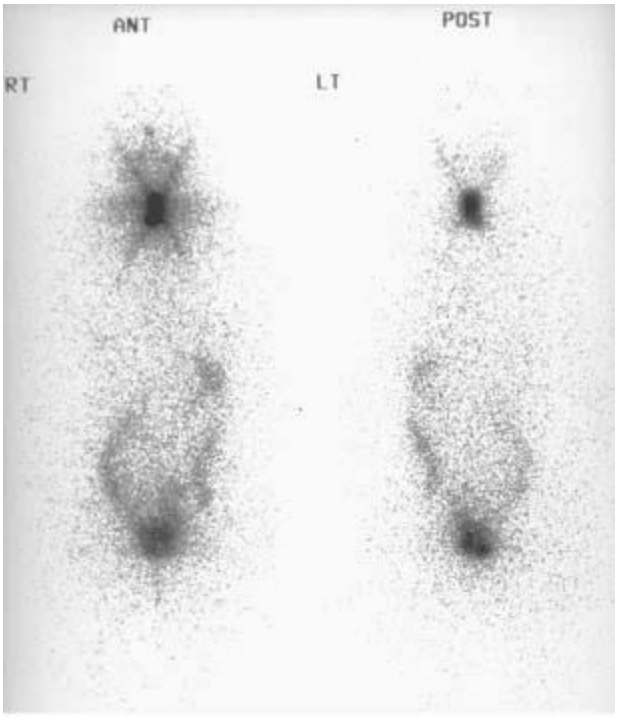


A

■**FIGURE 10-3A** I-131 total body scans in the anterior **(left image)** and posterior **(right image)** projections obtained at 48 hours after the oral administration of 5 mCi of I-131 sodium iodide. A prominent region of radiotracer accumulation is seen within the neck. The star pattern that is seen in the neck region is caused by septal penetration of the collimator by the high-energy photons (364 keV). Normal activity is present in the salivary glands, stomach, bladder, and bowel.

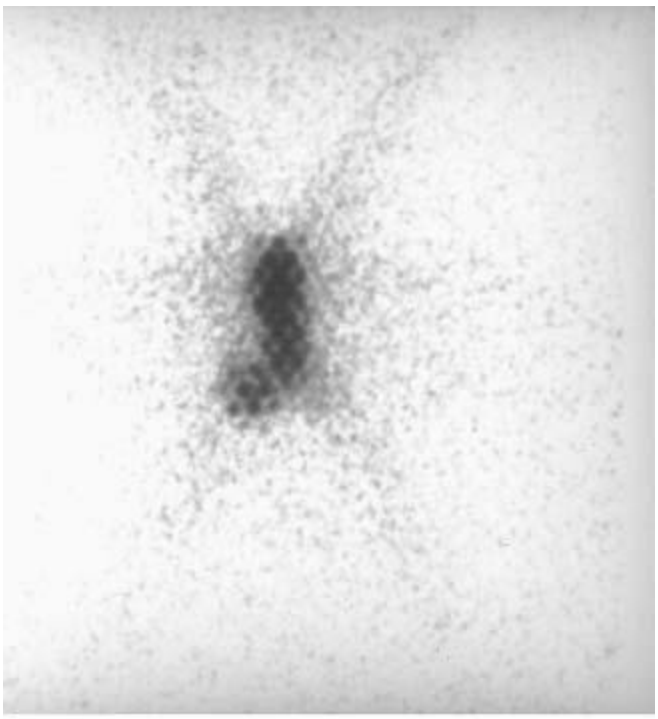

B

**FIGURE 10-3B** Anterior magnification view of the neck. The region of radiotracer accumulation in the neck is actually seen to consist of two foci. The larger focus is in the midline. Another smaller focus is present along the right lower border of the larger focus. The very small photopenic regions within each focus of radiotracer accumulation are due to attenuation of activity by the lead collimator. The star pattern mentioned in Figure 10-4A is seen again.

## DFFERENTIAL DIAGNOSIS

- **Solely residual thyroid tissue:** The presence of residual thyroid tissue alone could produce the larger, mid-line focus of radiotracer accumulation but would not account for the smaller focus to the right of midline. Furthermore, it is known that residual metastatic disease was left at the time of surgery. Therefore, this diagnosis is incorrect.
- **Functioning thyroid metastatic disease alone:** This diagnosis is incorrect because it would not account for the large midline focus, which is at the expected site of the thyroid gland. In addition, it is quite unusual to have no residual thyroid tissue remaining after attempted total thyroidectomy.
- **Residual thyroid tissue and functioning metastasis:** This diagnosis would account for both foci of radio-tracer accumulation and is the most likely consideration.
- **Swallowed radioiodine:** Radioiodine that is swallowed can often be seen in the esophagus. This artifact is prevented by having the patient ingest small amounts of food and fluids. However, the radiotracer activity would be expected to be seen only in the midline. This diagnosis is incorrect because it would not account for the small focus of radiotracer accumulation to the right of midline.
- **Residual thyroid tissue in the neck with metastatic spread to the abdomen and pelvis:** The radiotracer activity in the abdomen and pelvis in the case illustrated is that which is normally seen on I-131 total body scans, due to excretion into the stomach, colon, and bladder. This radiotracer activity does not represent metastatic disease.

## DIAGNOSIS

### Residual functioning thyroid tissue and functioning metastasis

## KEY FACTS

### Clinical

- Thyroid cancers are rarely of a single cell type and are designated by the predominant histologic type.

- Three types of carcinoma: (1) well-differentiated papillary carcinoma, (2) follicular carcinoma, and (3) mixed papillary-follicular carcinoma, comprise about 75% of all primary thyroid malignancies.
- Anaplastic and poorly differentiated thyroid carcinomas comprise 20% of all thyroid malignancies and occur primarily in elderly patients.
- Medullary thyroid carcinoma constitutes approximately 5% of all primary thyroid cancers and can be associated with other endocrine lesions such as pheochromocy-toma as part of a multiple endocrine neoplasia (MEN) syndrome.
- In well-differentiated thyroid cancers, the overall prognosis is good, with a 5-year survival rate of >95% in properly treated patients.
- Well-differentiated papillary carcinoma tends to metas-tasize to local lymph nodes in the neck, whereas fol-licular carcinoma tends to spread hematogenously, producing metastases to the lungs and bones.
- When evaluating patients with well-differentiated thyroid cancer using I-131 sodium iodide, it is important to stop thyroid replacement therapy and allow thyroid-stimulating hormone (TSH) levels to elevate before administration of radiotracer for a total body scan. The resultant high TSH levels stimulate any remaining thyroid tissue or functioning metastases and increase detection of these sites on imaging studies.
- Elevation of endogenous TSH takes approximately 4 to 6 weeks to occur after a total thyroidectomy or after cessation of exogenous thyroxin.

## Radiologic

- Normal radiotracer accumulation of I-131 occurs within the salivary glands, stomach, bladder, and bowel.
- To optimize the tumor-to-background ratio, imaging should be performed 48 or 72 hours after administration of I-131.
- The usual dose of I-131 administered for whole body imaging for the detection of metastatic differentiated thyroid cancer is 5 to 10 mCi.
- Tl-201 can be used to differentiate functioning metas-tases from well-differentiated thyroid carcinoma. An advantage of Tl-201 over I-131 is that the patients do not need to be in a hypothyroid state for the Tl-201 to detect metastatic foci.
- Medullary and anaplastic thyroid cancers rarely, if ever, concentrate I-131.
- Significant residual thyroid tissue can produce a star pattern that is caused by septal penetration of the col-limator by the high-energy photons. The star pattern is less likely to result from accumulation in thyroid cancer because the accumulation in functioning thyroid cancer is usually less than in normal thyroid gland.

## SUGGESTED READING

Hurley JR, Becker DV. Treatment of thyroid carcinoma with radioiodine. In A Gottschalk, PB Hoffer, EJ Potchen (eds), Diagnostic Nuclear Medicine. Baltimore, MD: Williams & Wilkins, 1988;792–814.

KüÇük NO, Külak HA, Aras G. Clinical importance of technetium-99m-methoxyisobutylisonitrile (MIBI) scintigraphy in differentiated thyroid carcinoma patients with elevated thyroglobulin levels and negative I-131 scanning results. Ann Nucl Med 2006;20:393–397.

Lind P, Kohlfurst S. Respective roles of thyroglobulin, radioiodine imaging, and positron emission tomography in the assessment of thyroid cancer. Semin Nucl Med 2006;36:194–205.

Mettler FA, Guiberteau MJ. Essentials of Nuclear Medicine Imaging. Philadelphia, PA: Saunders, 1991;87–93.

# CASE 4

### ROBERT H.

### WILKINSON, JR.

### HISTORY

A 77-year-old Englishman with progressive swelling and deformity of his legs and right arm has noted an increasing frequency of headaches and an increase in hat size over the past several years. Laboratory studies include an elevated alkaline phosphatase level and normal acid phosphatase and prostate-specific antigen (PSA) values.

A

■**FIGURE 10-4A** Anterior **(left)** and posterior **(right)** images of a whole body bone scan obtained after the intravenous administration of Tc-99m MDP. Markedly abnormal regions of increased radiotracer bone uptake are noted within the axial and appendicular skeleton.

B

■**FIGURE 10-4B** Anteroposterior radiograph of the pelvis revealing bony expansion, sclerosis, and cortical thickening.

## DIFFERENTIAL DIAGNOSIS

- **Paget's disease of bone:** The pattern seen on the radionuclide bone scan is that of regions of markedly increased bone tracer accumulation with an expanded appearance to the entire bone. These features are typical of Paget's disease, the most likely diagnosis.
- **Metastases:** Metastases can simulate lesions of Paget's bone disease. The advanced degree of tracer accumulation and expanded bone appearance seen in this case, however, are atypical even for advanced prostate, breast, or lung carcinoma. This diagnosis is an unlikely consideration.
- **Fractures:** The expanded bone and diffuse tracer accumulation make fractures unlikely considerations.
- **Osteomyelitis:** Regions of intense tracer accumulation can be seen in osteomyelitis, but the clinical setting, the diffuse nature of the abnormalities, and the expansile changes seen on the radiograph make this diagnosis highly unlikely.
- **Fibrous dysplasia:** Polyostotic fibrous dysplasia can produce increased tracer accumulation in multiple bones, as is seen in this case. However, the history of progressive bony expansion late in life and the radio-graphic findings make this diagnosis unlikely.

## DIAGNOSIS

## Paget's disease of bone

## KEY FACTS

## Clinical

- Paget's disease is most commonly encountered in Eastern and Western Europe (with the exception of Scandinavia), with a prevalence of 3.5% to 4.5% and with a 3 to 2 male-to-female predominance.
- The etiology of Paget's disease is not known definitively. Slow virus inoculation early in life is one hypothesis that has been strongly considered.
- Progression of Paget's disease can be classified into three stages: (1) bone resorption, (2) mixed bone resorp-tion and deformation, and (3) decline in resorption accompanied by a decrease in irregularity and fibrosis.
- The prevalence of fractures in Paget's disease is reported to be 8% to 18%, based on retrospective series.
- Sarcomatous degeneration of pagetoid bone can occur and can be solitary or multicentric.

- Elevated cardiac output is seen in some patients with Paget's disease due to the increased vascularity of acute pagetoid bone.

## Radiologic

- On radiographs, vertebrae appear enlarged and deformed; the scapulae and pelvic bones appear expanded and thickened; the skull enlarges with basi-lar flattening and cortical thickening; and the long bones bow and develop cortical thickening.
- The degree of radiotracer accumulation in pagetoid bone is variable.
- The radionuclide study is reported to be more sensitive than radiographs: 5% to 20% of patients have abnormal bone scans and normal radiographs, compared to 1% with abnormal radiographs and normal radionuclide bone scan.
- Bone scan findings do not correlate well with the severity of bone pain in Paget's disease.
- Reduced accumulation of In-111-labeled leukocytes and of Tc-99m sulfur colloid has been reported to occur in Paget's disease.
- Photopenic regions can be seen in pagetoid bone in instances of sarcomatous degeneration, most likely due to proliferation of nonosteoblastic tissue.
- A photopenic area in a bone scan that occurs in a radio-graphically evident region of Paget's disease can represent either early disease or sarcomatous degeneration.
- Ga-67 may be useful for sarcoma detection. In one small study, slightly more than half of Paget's disease patients with sarcomas and a focal photopenic area on bone scan were found to have increased Ga-67 accumulation at the site of the sarcoma. Another small series found the Ga-67 scan to be less sensitive.

## SUGGESTED READING

Altman RD. Paget's disease of bone. In FL Coe, MJ Favus (eds), Disorders of Bone and Mineral Metabolism. New York, NY: Raven, 1992;1027–1061.

Boudreau RJ, Lisbona R, Hadjipavtou A. Observations on serial radionuclide blood flow studies in Paget's disease. J Nucl Med 1983;24:880–885.

Hain SF, Fogelman I. Nuclear medicine studies in metabolic bone disease. Semin Musculoskelet Radiol 2002;6:323–329.

Ryan PJ. Orthopaedic manifestations of systemic disease. Semin Nucl Med 1998;28:124–131.

Smith J, Bitet JF, Yeh SJ. Bone sarcomas in Paget's disease: a study of 85 patients. Radiology 1984;152:583–590.

# CASE 5

**ROBERT H.**

**WILKINSON, Jr.**

## HISTORY

The bone scans of three patients are presented. Patient A is a 67-year-old man with an elevated prostate-specific antigen (PSA) value of 86 ng/mL and biopsy-proven prostate carcinoma. Patient B is a 69-year-old man with a history of prostate carcinoma and a borderline normal PSA value of 6 ng/mL. Patient C is a 71-year-old woman with a history of stage IV breast carcinoma. A different diagnosis is possible in each of the cases.


A

■**FIGURE 10-5A** Patient A: Posterior image from a total body bone imaging study. Multiple foci of abnormally increased bone radiotracer accumulation are seen in the axial and proximal appen-dicular skeleton.

B

**FIGURE 10-5B** Patient B: Right posterior oblique view of the chest shows foci of increased radiotracer accumulation in adjacent ribs in a "string-of-pearls" pattern.

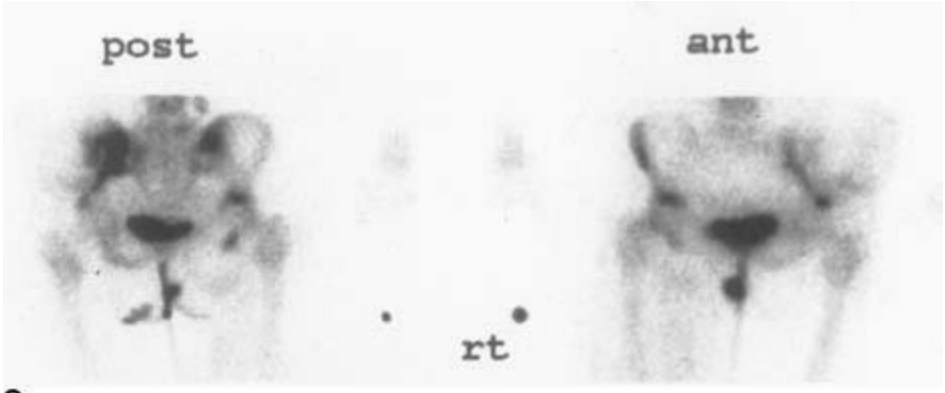


C

**FIGURE 10-5C** Patient C: Anterior and posterior pelvic images. A mixed pattern of abnormal foci of abnormally increased and decreased radiotracer accumulation is seen in the left ilium.

## DIFFERENTIAL DIAGNOSIS

**Metastases:** Bone metastases can appear on bone scans as any or all of the following: multiple foci of increased radiotracer accumulation (Figure 10-7A), increased or decreased radiotracer accumulation (Figure 10-7C), and normal bone radiotracer accumulation. The pattern and location of the abnormalities in Figures 10-7A and 10-7C make bone metastases the most likely consideration.

**Pathologic fractures:** Pathologic fractures can be solitary or multiple and usually occur in metastatic bone lesions that are subject to stress or trauma. Bone metastases in weight-bearing regions are particularly susceptible to fracture.

- **Multiple benign fractures:** The pattern, location, and clinical history are important in distinguishing benign fractures from metastatic disease. Some patterns of fractures (e.g., the string-of-pearls appearance in Figure 10-7B) are typical of benign fractures. This is the diagnosis in patient B.
- **Degenerative joint disease/arthritides:** These processes occur at joints and can be difficult to distinguish from metastases. Concomitant benign arthropathic disease can occur in patients with metastatic disease, but the pattern of nonarticular bone abnormalities in all three patients shown above makes benign arthropathic disease alone unlikely.

## DIAGNOSIS

## Patients A and C: multiple bone metastases; Patient B: benign rib fractures

## KEY FACTS

### Clinical

- The likelihood of bone metastases depends on the primary tumor (e.g., most primary bone tumors rarely metastasize) and the stage of disease.
- The lifetime risk of developing breast cancer in American women is reported to be approximately 11%, and over one-half of breast cancers occur in women after the age of 65 years. In autopsy series of women with metastatic breast carcinoma, the frequency of bone metastases has been reported to be between 44% and 71%.
- The digital rectal examination and serum PSA test are currently the recommended screening procedures for prostate carcinoma. Approximately one-third of men over the age of 50 years harbor foci of prostatic carcinoma without clinical evidence of disease.
- Approximately 80% of patients with detectable prostate carcinoma and distant metastases are found to have bone metastases.

### Radiologic

- The majority of metastatic bone tumors appear as focal regions of increased radiotracer accumulation on radionuclide bone scan. However, photopenic foci can be seen in malignancies such as breast, lung, renal, and anaplastic carcinomas; neuroblastoma; and multiple myeloma.
- Soft tissue neoplasms can invade bone and produce increased radiotracer uptake or a photopenic focus, which usually has a rim of increased radiotracer accumulation.

- Benign bone conditions that can appear photopenic include bone infarction, bone resection, very early osteomyelitis, radiation-induced bone changes, and histiocytosis X.
- Skeletal involvement from multiple myeloma, plasma-cytoma, neuroblastoma, and eosinophilic granuloma can produce normal, increased, or decreased radio-tracer accumulation.
- Particular care must be taken in evaluating the radio-nuclide bone imaging study of a patient with bone metastases during the first 4 to 6 months after starting chemotherapy, because a disparity between the clini-cal/radiologic status and findings on radionuclide bone scan can be seen. These patients can improve clinically and have a decrease in the number and size of bone lesions on radiographs but no change or apparent worsening of lesions (the so-called flare phenomenon) on the radionuclide bone imaging study. This pattern change presumably reflects healing of lesions and is most commonly reported in bone metastases from a primary breast or prostate tumor. Following further healing of bone lesions after this initial period, the radionuclide bone study reflects the clinical and radiologic status more accurately.
- Patients with a PSA value of <10 ng/mL during their initial evaluation for prostate carcinoma have a very low likelihood of having a positive radionuclide bone imaging study for metastases.
- The likelihood of a solitary bone scan lesion being a metastasis is reported to range from 10% (in adults) to 60% (in children).
- In the presence of a known primary malignancy, approximately 10% to 20% of solitary rib lesions on bone scans are metastases. On the other hand, focal rib lesions having a string-of-pearls pattern are highly likely to be benign rib fractures.
- Correlation with radiographs or other imaging studies is often useful to confirm the presence of bone metas-tases in patients with bone scan abnormalities. In the presence of an abnormal radionuclide bone scan, a normal radiograph actually makes a bone metastasis a likely consideration by excluding other possible causes.

## SUGGESTED READING


Beheshti M, Langsteger W, Fogelman I. Prostate cancer: Role of SPECT and PET in imaging bone metastases. Semin Nucl Med 2009;39:396–407.

Ben-Haim S, Israel O. Breast cancer: Role of SPECT and PET in imaging bone metastases. Semin Nucl Med 2009;39:408–415.

Chua S, Gnanasegaran G, Cook GJ. Miscellaneous cancers (lung, thyroid, renal cancer, myeloma, and neuroendocrine tumors): role of SPECT and PET in imaging bone metastases. Semin Nucl Med 2009;39:416–430.

Hanks GE, Myers CE, Scardino PT. Cancer of the prostate. In VT DeVita Jr, S Hellman, SA Rosenberg (eds), Cancer—Principles and Practice of Oncology (4th ed). Philadelphia, PA: Lippincott, 1993;1073–1113.

Janicek MJ, Hayes DF, Kaplan WD. Healing flare in skeletal metastases from breast cancer. Radiology 1994;192:201–204.

O'Connor MK, Brown ML, Hung JC, Hayostek RJ. The art of bone scintigra-phy—technical aspects. J Nucl Med 1991;32:2332–2341.

# CASE 6

**R. EDWARD**

**COLEMAN**

## HISTORY

A 75-year-old man being treated for hypercalcemia.

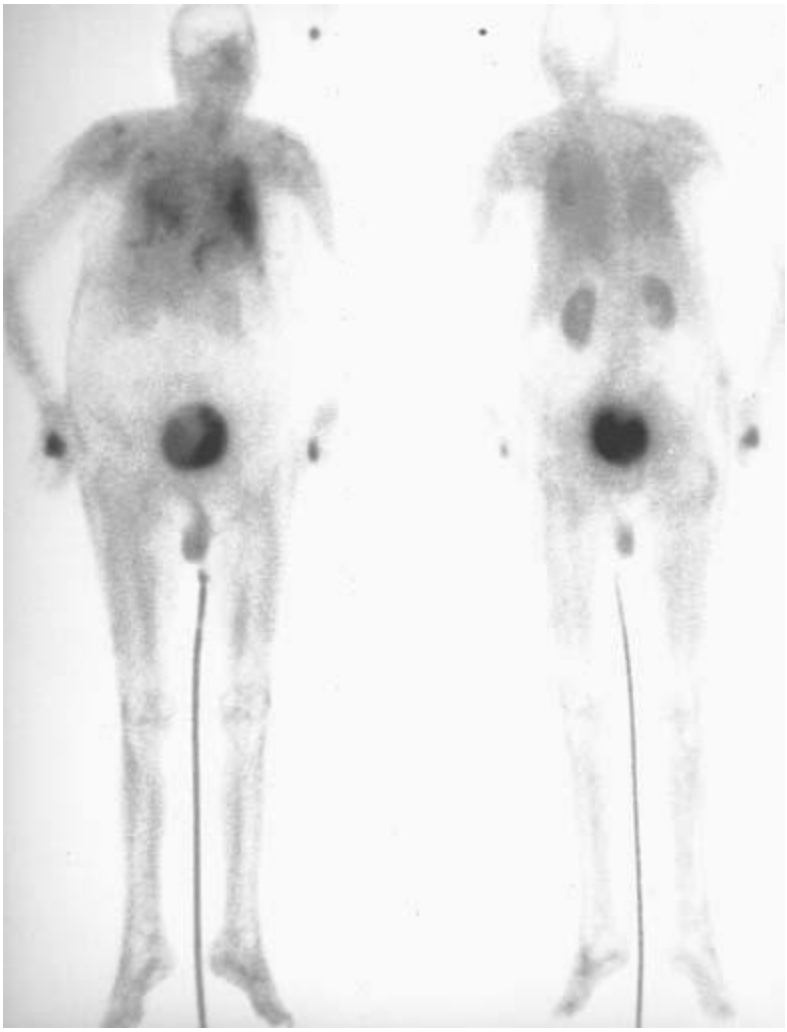

■**FIGURE 10-6** Anterior **(left)** and posterior **(right)** images from a radionuclide bone scan obtained 2 hours after the IV administration of 20 mCi of Tc-99m MDP. Abnormal

accumulation of radiotracer is present in the lungs and in the stomach as a result of the hypercalcemia. However, no radiotracer accumulation is seen in the bones. Normal renal and bladder radiotracer accumulation are seen, as well as a small focus of activity at the injection site in the right hand.

## DIFFERENTIAL DIAGNOSIS

- **Administration of incorrect radiopharmaceutical:** This diagnosis is unlikely because no radiopharmaceu-tical has the pattern of distribution seen in this patient.
- **Presence of excess aluminum ion:** Contamination of Tc-99m methylene diphosphonate (MDP) with aluminum ion from the eluate or the presence of high plasma aluminum levels in patients taking aluminum hydroxide antacids can alter biodistribution of the radiophar-maceutical agent. However, these conditions cause increased uptake in the liver and kidneys and not the lung accumulation, seen in the case illustrated.
- **Effect of therapy for hypercalcemia:** The patient shown above was receiving intravenously administered etidronate for treatment of hypercalcemia. Etidronate (hydroxyethylidene diphosphonic acid [HEDP]) inhibits the formation, growth, and dissolution of hydroxyap-atite crystals. This agent can cause the lack of radio-pharmaceutical accumulation within bones, as shown above.
- **Premature imaging:** Images obtained immediately after administration of Tc-99m MDP will typically show blood pool activity, prominent soft tissue activity, and some bone accumulation. However, accumulation in the lungs would not be expected, making this diagnosis unlikely.
- **Iron overload:** This diagnosis might be considered because in iron overload, such as in hemochromatosis or following multiple blood transfusions, the accumulation of Tc-99m MDP into bone is diminished and renal excretion is increased. However, pulmonary deposition of the radiotracer would not be expected.

## DIAGNOSIS

## Hypercalcemia with etidronate therapy

## KEY FACTS

## Clinical

- Hypercalcemia can occur secondary to a number of entities, including hyperparathyroidism, metastatic skeletal disease, hyperthyroidism, and sarcoidosis.

- Biphosphonates such as etidronate and pamidronate are used to treat the hypercalcemia of malignancy because of their effect on bone turnover. The biphosphonates interact with the hydroxyapatite crystal, inhibiting bone resorption, and may impair osteoclast function. These agents are also used to treat Paget's disease and heterotopic ossification and may have a role in treating osteoporosis.
- Radionuclide bone scans in patients with hypercalcemia and elevated calcium phosphorus products frequently show abnormal localization of the radiopharmaceutical in the lungs, stomach, and kidneys, reflecting the acid-base changes that occur in these tissues. Furthermore, these are the sites of metastatic calcification that can occur in these patients.
- The effect of biphosphonates on Tc-99m MDP bone scans is variable. The biphosphonate used and the method of administration (oral or intravenous) may make a difference in the effect on the bone scan. Some studies report difficulty in interpretation of radionu-clide bone scans in patients undergoing biphosphonate therapy, whereas other studies have shown no effect on the sensitivity of the bone scan.

## Radiologic

- A Tc-99m MDP bone scan that shows poor bone uptake and prominent soft tissue accumulation usually results from a radiopharmaceutical preparation problem, with excess Tc-99m pertechnetate in the preparation. The excess pertechnetate is manifested by radiotracer accumulation in the thyroid and stomach.
- The clue to the diagnosis in the patient shown above is accumulation of the Tc-99m MDP in the lungs, which occurs with hypercalcemia. In a patient with accumulation of Tc-99m MDP in the lungs, associated bone scan findings should be considered as possibly related to hypercalcemia or its treatment.
- Radionuclide bone scans usually provide diagnostic information in patients receiving biphosphonates, but as noted above, this agent can affect the scan. The effect of this therapy needs to be taken into account when interpreting the images.

# SUGGESTED READING

Chong WK, Cunningham DA. Case report: intravenous etidronate as a cause of poor uptake on bone scanning, with a review of the literature. Clin Radiol 1991;44:268–270.

Lam MG, de Klerk JM, van Rijk PP, Zonnenberg BA. Bone seeking radio-pharmaceuticals for palliation of pain in cancer patients with osseous metastases. Anticancer Agents Med Chem 2007;7:381–397.

Paes FM, Serafini AN. Systemic metabolic radiopharmaceutical therapy in the treatment of metastatic bone pain. Semin Nucl Med 2010;40:89–104.

Pecherstorfer M, Schilling T, Janisch S, et al. Effect of clodronate treatment on bone scintigraphy in metastatic breast cancer. J Nucl Med 1993;34:1039–1044.

Sahni M, Guenther HL, Fleisch H, et al. Biphosphonates act on rate of bone resorption through mediation of

osteoblasts. J Clin Invest 1993;91:2004–2011.

# CASE 7

**SARA M. O'HARA**

## HISTORY

A 6-week-old girl presents with jaundice. Her total bilirubin is 19.8 mg/dL, and conjugated bilirubin is 7.8 mg/dL.

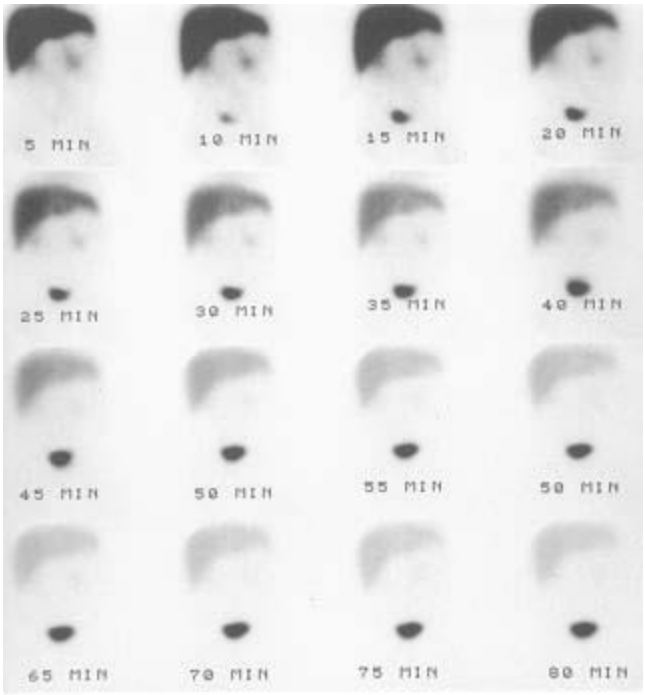


A

■**FIGURE 10-7A** Anterior images of a diisopropyliminodiace-tic acid scan obtained immediately after injection. Good extraction of the radiopharmaceutical by the hepatocytes is seen, with prompt clearance of the blood pool. Homogenous radiotracer activity is present throughout the liver. Tracer activity is identified in both kidneys and the bladder. However, the central bile ducts, GI tract, and gallbladder have not accumulated the radiotracer. This pattern persisted on 24-hour delayed films (not shown).

B

**FIGURE 10-7B** Follow-up study 1 month later. In the interim since the previous study, the patient has undergone a Kasai procedure (portoenterostomy). This is an anterior image obtained 3.5 hours after injection. Radiopharmaceutical is again distributed homogeneously throughout the liver parenchyma. GI activity is now identified in the midabdomen, partially superimposed over the lower pole of the right kidney.

## DIFFERENTIAL DIAGNOSIS

**Idiopathic neonatal hepatitis:** Jaundice and bile stasis are features of idiopathic neonatal hepatitis, but the biliary system is patent (unlike the case illustrated). Hepatic uptake and blood pool clearance of radiotracer can be delayed in neonatal hepatitis, and the degree of delay reflects the severity of hepatocyte damage.

**Choledochal cyst:** The absence of visualization of the proximal ducts or an actual cyst makes this diagnosis unlikely.

**Biliary atresia:** This is the best diagnosis because good hepatocyte extraction of radiopharmaceutical is seen in the absence of visible intrahepatic bile ducts or gastrointestinal (GI) activity, even on 24-hour images.

**Bile plug syndrome:** This rare condition results in conjugated hyperbilirubinemia due to obstruction of the common bile duct (CBD) by inspissated bile/secretions. Sepsis, hemolytic disorders, dehydration, total par-enteral nutrition, and cystic fibrosis are predisposing conditions. Careful ultrasound examination to exclude echogenic, nonshadowing bile plugs within the dilated biliary tree is necessary to distinguish this condition from biliary atresia.

- **Arteriohepatic dysplasia (Alagille syndrome):** This syndrome is characterized by typical dysmorphic facies, pulmonary artery stenosis, and hepatic ductular hypoplasia. Distinction from true biliary atresia can be difficult if the other components of the syndrome are not recognized.

## DIAGNOSIS

## Biliary atresia

## KEY FACTS

## Clinical

- Hyperbilirubinemia is a common problem in neo-nates and infants. Unconjugated hyperbilirubinemia, in which <15% of the total bilirubin is conjugated (or "direct," which is the nomenclature used on laboratory reports), is most often due to physiologic jaundice of the newborn, breast milk jaundice, or erythroblasto-sis fetalis. In conjugated hyperbilirubinemia, where at least 30% of the bilirubin is conjugated, a search for causes of obstructive jaundice is necessary. The most common causes of obstructive jaundice are included in the differential diagnosis listed above.
- Biliary atresia is the most common cause of extrahe-patic cholestasis in infants. The incidence ranges from 1 in 8,000 to 1 in 10,000 live births.
- Distinction between idiopathic neonatal hepatitis, a nonsurgical disease, and biliary atresia, a surgical disease, is important within the first 3 months of life. The Kasai procedure (or portoenterostomy) is performed using a Roux-en-Y loop of intestine to bypass the hypo-plastic or absent biliary duct segments. The surgical success rate varies according to the patient age at the time of surgery. The procedure is 90% effective in patients <2 months of age, but only 17% effective in patients <3 months of age.

## Radiologic

- Diisopropyliminodiacetic acid (DISIDA, disofenin) and mebrofenin (trimethyl-bromo-IDA) have the highest extraction rate by hepatocytes and shortest transit time of the IDA derivatives. Between 5% and 15% of the disofenin is excreted via the kidneys in normal subjects. Dynamic image acquisition immediately after radiopharmaceutical injection is helpful to determine hepatocyte extraction and hepatocyte function. Static images performed over the next 1 to 2 hours with delayed images taken up to 24 hours are generally required.
- Pretreatment with oral phenobarbital (5 mg/kg/day for 5 days) is recommended to improve bile flow. With phe-nobarbital pretreatment, biliary scintigraphy is

approximately 95% accurate in determining biliary patency in infants <3 months of age.

- Progressive hepatocyte damage and hepatic cirrhosis occur in the setting of untreated biliary atresia and in persistent neonatal hepatitis. The two diseases can be indistinguishable in patients >3months of age.

## SUGGESTED READING

Esmaili J, Izadyar S, Karegar I, Gholamrezanezhad A. Biliary atresia in infants with prolonged cholestatic jaundice: diagnostic accuracy of hepatobiliary scintigraphy. Abdom Imaging 2007;32:243–247.

Kasai M, Suzuke H, Ohashi E, et al. Technique and results of operative management of biliary atresia. World J Surg 1978;2:571–580.

Paltiel HJ. Imaging of neonatal cholestasis. Semin Ultrasound CT MR 1994;15:290-305.

Sevilla A, Howman-Giles R, Saleh H, et al. Hepatobiliary scintigraphy with SPECT in infancy. Clin Nucl Med 2007;32:16-23.

Treves ST, Jones AG, Markisz J. Liver and spleen. In ST Treves (ed), Pedia-tric Nuclear Medicine. New York, NY: Springer, 1995;466-495.

Wells RG, Sty JR. Radionuclide imaging of the liver, biliary system, and spleen. In JH Miller, MJ Gelfand (eds), Pediatric Nuclear Imaging. Philadelphia, PA: Saunders, 1994;103-156.

# CASE 8

### MICHAEL W.

### HANSON

## HISTORY

A 68-year-old man with a history of Crohn's disease of the terminal ileum and colon presents with a 3-day history of nausea and right upper quadrant pain radiating posteriorly to the back. The pain is worsened by eating.

A

■**FIGURE 10-8A** Ultrasound shows small calculi in the gallbladder with mild thickening of the gallbladder wall. There is no pericholecystic fluid. The CBD (not shown) was normal in caliber.

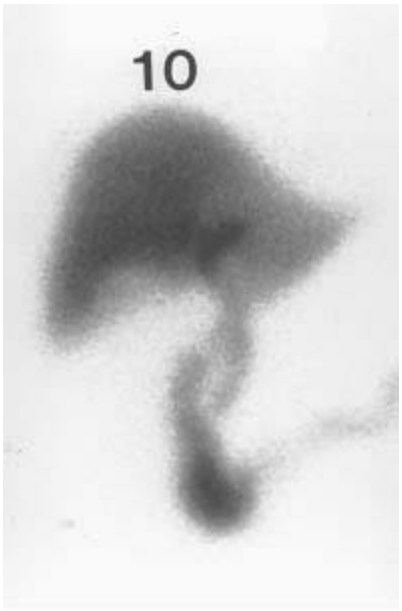


B

■**FIGURE 10-8B** Hepatobiliary imaging study at 10 minutes. There is good hepatic extraction of Tc-99m disofenin with good visualization of the hepatic parenchyma. Radiotracer in the CBD and the duodenum indicates patency of the CBD.

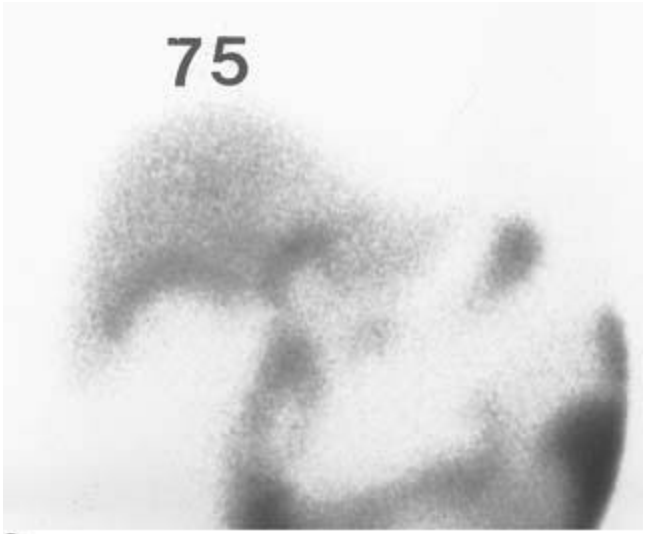


C

**FIGURE 10-8C** Hepatobiliary imaging study at 75 minutes. Persistent radiotracer is seen in the CBD and within the small bowel. No radiotracer is present in the gallbladder, but a region of relatively increased radiotracer is seen within the liver parenchyma along the gallbladder fossa.

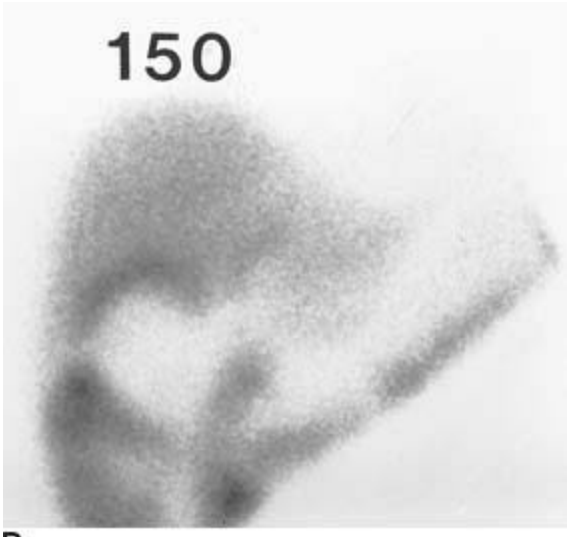


D

**FIGURE 10-8D** Hepatobiliary imaging study at 150 minutes. The gallbladder is not visualized. A persistent region of prominent radiotracer accumulation exists in the liver parenchyma, consistent with pericholecystic hepatic uptake of Tc-99m disofenin.

## DIFFERENTIAL DIAGNOSIS

**Acute pancreatitis:** This process presents with abdominal pain and can be seen in patients with Crohn's disease. An elevated serum amylase and/or lipase is usually present. Hepatobiliary imaging studies are normal unless pancreatitis is due to underlying hepatobili-ary disease. This diagnosis is therefore unlikely.

- **Acalculous cholecystitis:** Acute inflammation of the gallbladder can occur in the absence of cholelithiasis, most often as a complication of severe underlying illnesses (e.g., burns, trauma, sepsis, and following major surgery) associated with bile stasis. The benign clinical features and sonographic finding of gallstones make this diagnosis unlikely.
- **Common bile duct obstruction:** Approximately 10% to 15% of patients with cholelithiasis will pass a gallstone into the CBD, where it can: (1) pass into the duodenum, (2) remain in the CBD without producing symptoms, or (3) obstruct the CBD. The presence of radiotracer in the CBD and the duodenum by 10 minutes essentially excludes CBD obstruction.
- **Chronic cholecystitis:** Patients with chronic cholecystitis frequently have gallstones and gallbladder wall thickening, and can have repeated bouts of biliary colic without cystic duct obstruction. The most frequent abnormal finding on scintigraphy is delayed visualization of the gallbladder beyond 1 hour, but imaging is often normal. Scintigraphy is generally an ineffective study in the evaluation of chronic cholecystitis, except to exclude a superimposed acute cystic duct obstruction. The majority of patients with chronic cholecystitis alone would be expected to have visualization of the gallbladder by 180 minutes, making this diagnosis unlikely in the case illustrated.
- **Acute cholecystitis:** This entity typically has the presentation of right upper quadrant pain and tenderness with fever and leukocytosis. It often begins as an attack of biliary colic that progressively worsens and is associated with anorexia, nausea, and, commonly, emesis. With cystic duct obstruction, bile does not flow into or out of the gallbladder (as in the case presented above). The imaging findings in this case make this the most likely diagnosis.

## DIAGNOSIS

## Cholelithiasis with acute cholecystitis

## KEY FACTS

## Clinical

- Patients with Crohn's disease have an increased risk for developing cholelithiasis (due to altered bile salt absorption) as well as acute cholecystitis.
- Acute cholecystitis is most commonly caused by acute occlusion of the cystic duct by a gallstone.
- Seventy-five percent of patients with acute cholecystitis respond to medical therapy, of whom 25% have recurrent acute cholecystitis within 1 year. Another 25% of patients

treated conservatively develop a major complication, such as empyema, hydrops, gangrene, emphy-sematous cholecystitis, perforation of the gallbladder, or gallstone ileus. Therefore, early surgical therapy is the preferred treatment.

- As expected, patients with suspected empyema, emphy-sematous cholecystitis, or perforated gallbladder require more urgent surgical intervention than those with uncomplicated acute cholecystitis. It is important to search for evidence of these complications at the time of imaging.
- Perforation of the gallbladder has an estimated 30% mortality rate. These patients can have sudden transient relief of right upper quadrant pain as the distended gallbladder decompresses but then develop generalized signs of peritonitis.

## Radiologic

- The diagnosis of acute cholecystitis can be confidently excluded on the basis of a normal hepatobiliary imaging study (negative predictive value of 98%).
- False-positive hepatobiliary scans can be seen in the following settings: (1) alcoholism, (2) total parenteral nutrition or prolonged fasting, (3) within 2 hours of eating, and (4) in severe intercurrent illnesses.
- Radiotracer in the duodenum or pericholecystic hepatic uptake of radiotracer (the "rim sign") can be mistaken for gallbladder uptake, resulting in a false-negative interpretation. The finding of pericholecystic hepatic uptake of radiotracer is important to recognize. It is present in 57% of patients with gangrenous cholecystitis and 31% of patients with perforated gallbladder.
- Potential mechanisms by which pericholecystic hepatic uptake occurs include hyperemia with increased delivery and extraction of radiotracer along the gallbladder fossa, focal hepatic cellular injury with impaired excretion of radiotracer, and mechanical obstruction with focally delayed clearance of radiotracer.
- If the gallbladder is not seen by 30 to 45 minutes but there is radiotracer in the small bowel, the study can be shortened from 4 to 2 hours by giving intravenous morphine sulfate (0.04 mg/kg; maximum 4 mg). Morphine sulfate contracts the sphincter of Oddi and redirects bile flow into the gallbladder if the cystic duct is patent. The study can be stopped when the gallbladder is filled or at 2 hours (whichever occurs first).

# SUGGESTED READING

Alobaidi M, Gupta R, Jafri SZ, Fink-Bennet DM. Current trends in imaging evaluation of acute cholecystitis. Emerg Radiol 2004;10:256–258.

Grossman SJ, Joyce JM. Hepatobiliary imaging. Emerg Med Clin North Am 1991;9:853–874.

Krishnamurthy GT, Turner FE. Pharmacokinetics and clinical application of technetium-99m-labeled hepatobiliary agents. Semin Nucl Med 1990;2:130–149.

Watson A, Kalff V. Hepatobiliary imaging. Curr Opin Radiol 1991;3:851–858.

Ziessman HA. Acute cholecystitis, biliary obstruction, and biliary leakage. Semin Nucl Med 2003;33:279–296.

# CASE 9

**MICHAEL W.**

**HANSON**

## HISTORY

A 59-year-old man with a history of melena presents with brisk, bright red rectal bleeding. Upper and lower GI endoscopy failed to show a bleeding source.

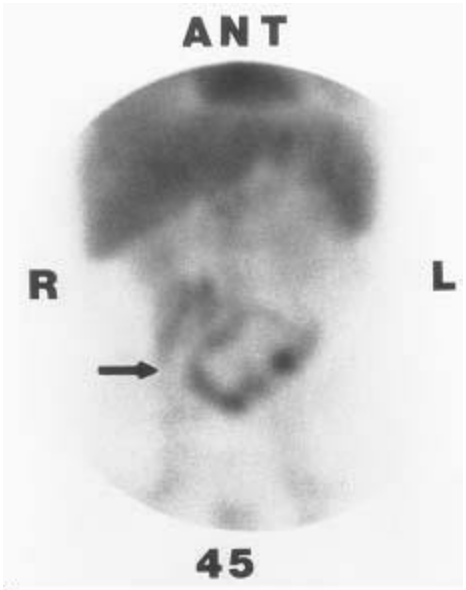


A

■**FIGURE 10-9A** Anterior abdominal blood pool images at 45 minutes. Expected radiotracer is seen in the cardiac blood pool, liver, and spleen. Major abdominal vasculature and both kidneys are seen faintly. Moderately intense abnormal radiotracer accumulation is seen in the mid abdomen, the pattern of which conforms to the midportion of the small bowel, most likely the jejunum *(arrow)*.

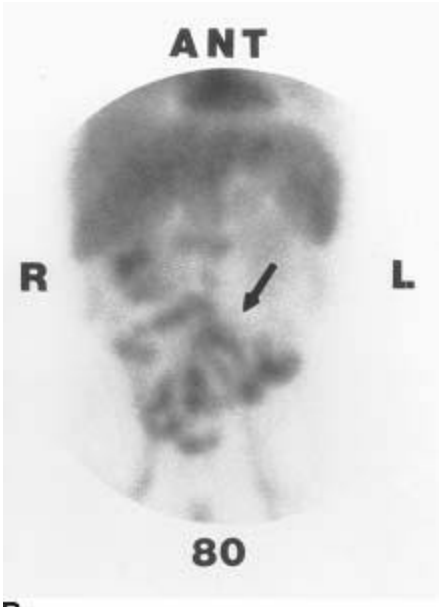


B

■**FIGURE 10-9B** Anterior abdominal blood pool images at 80 minutes. The pattern of abnormal radiotracer accumulation now conforms to multiple bowel loops in the mid and distal segments of the small bowel (arrow).

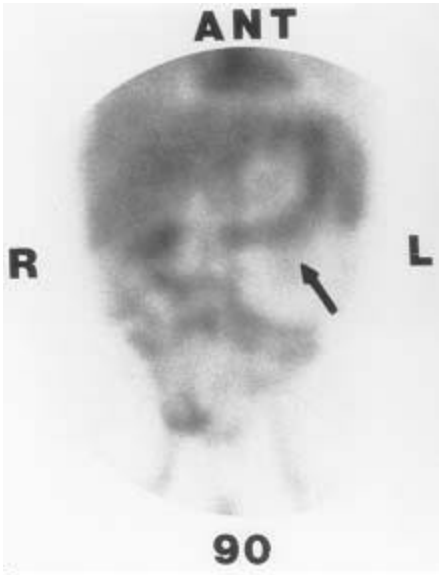


C

■**FIGURE 10-9C** Anterior abdominal blood pool images at 90 minutes show further abnormal radiotracer accumulation in small bowel loops. Abnormal radiotracer is now seen in the transverse colon and the splenic flexure (arrow).

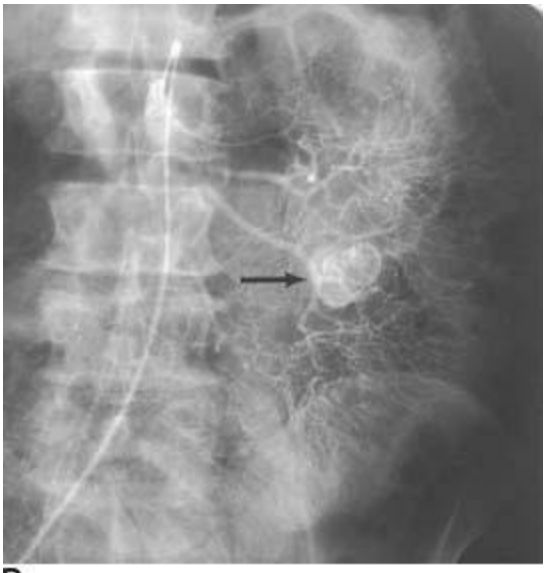

D

**FIGURE 10-9D** Selective arteriogram of the superior mesenteric artery. A brisk bleeding site is seen during the late arterial phase of the arteriogram in the left upper quadrant (arrow), proximal to the midjejunum.

## DIFFERENTIAL DIAGNOSIS

**Abdominal aortic aneurysm:** An abdominal aortic aneurysm can have focally increased radiotracer on blood pool imaging. This is an unlikely diagnosis because it is generally seen early and does not change in shape or location during the study.

**Free Tc-99m pertechnetate in the bowel:** Free Tc-99m sodium pertechnetate can be present on reinjection of tagged red blood cells. Pertechnetate is normally secreted by gastric mucosa. The stomach will be visualized, and during the latter part of the study, some of the normally secreted pertechnetate can occasionally enter small bowel. However, the intensity of radiotracer activity within bowel is usually faint and moves only minimally, making free pertechnetate an unlikely diagnosis in this case.

**Inflammatory bowel disease:** Inflammatory bowel disease can produce a positive GI bleeding scan by two mechanisms: (1) active bleeding, and (2) blood pool accumulation of radiotracer at sites of inflammation, even in the absence of active bleeding (in which case the sites remain static during the study). The latter possibility is unlikely in the case shown because the abnormal radiotracer accumulation in the case presented above is seen to progress through the small bowel:

**Active bleeding originating in the colon:** Unless retrograde movement of radiotracer from the cecum into the terminal ileum occurs, radiotracer activity in the small bowel is generally not seen after hemorrhage from a colonic bleeding source. The findings in the patient shown are therefore unlikely to be due to an active bleeding site originating in the colon.

- **Active small bowel bleeding:** Active small bowel hemorrhage can usually be distinguished from that arising in large bowel and further localized to the proximal, mid-, or distal small bowel. The findings of this case make the diagnosis of a mid-small bowel (jejunal) bleeding site the most likely diagnosis.

## DIAGNOSIS

## Acute midjejunal gastrointestinal hemorrhage

## KEY FACTS

### Clinical

- The presence of melena usually denotes bleeding from the esophagus, stomach, or duodenum, but lesions in the jejunum, ileum, and the ascending colon can cause melena, depending on the transit time of blood within the GI tract.
- Hematochezia generally signifies a bleeding site from a source distal to the ligament of Treitz, but rapid hemorrhage from the esophagus, stomach, or duodenum with rapid peristalsis can also produce bright red rectal bleeding.
- Initial attempts to localize a GI bleeding site should include nasogastric tube insertion, esophagogastroduo-denoscopy, sigmoidoscopy, and colonoscopy (which is impaired when the lumen of the colon is obscured by large amounts of brisk bleeding).
- Peptic ulceration, erosive gastritis, variceal bleeding, and Mallory-Weiss syndrome account for 90% of all cases of upper GI hemorrhage in which a definite cause is found.

### Radiologic

- The primary purpose of the scintigraphic GI bleeding study is to localize an active bleeding site to serve as a guide before selective abdominal angiography.
- In general, the rate of bleeding required for scin-tigraphic detection of GI bleeding is less than that required for detection by angiography. Therefore, if the scintigraphic GI bleeding study is negative, angiogra-phy is not indicated.
- Evaluation for GI bleeding by scintigraphy can be performed using sulfur colloid. The major disadvantage of this technique is rapid removal of the sulfur colloid by the liver, spleen, and bone marrow. Active bleeding must occur within minutes of radiotracer injection if the bleeding site is to be shown.
- Because GI bleeding is often intermittent, the labeled red blood cell technique is the preferred method for scintigraphic evaluation. Imaging is performed for a minimum of 2 hours, allowing a reasonable time for bleeding to occur.

■ GI bleeding study findings are evaluated best by reviewing the images in a dynamic cine display (obtained at a rate of 1 frame per minute), which increases conspicu-ity of radiotracer movement and makes subtle findings more apparent. Dynamic display should be a routine part of the imaging protocol.

## SUGGESTED READING


Alavi A, McLean G. Radioisotopic detection and localization of gastrointestinal bleeding: A combined endoscopic, angiographic and scintigraphic approach. In LM Freeman, HS Weissmann (eds), Nuclear Medicine Annual 1980. New York, NY: Raven, 1980.

Bunker SR, Lull RJ, Tanasescu DE, et al. Scintigraphy of gastrointestinal hemorrhage. Superiority of Tc-99m red blood cells over Tc-99m sulfur colloid. AJR Am J Roentgenol 1984;143:543–548.

Warrington JC, Charron M. Pediatric gastrointestinal nuclear medicine. Semin Nucl Med 2007;37:269–285.

Winzelberg GG. The versatility of Tc-99m red blood cell pool imaging in demonstrating bleeding sites. In LM Freeman, HS Weissmann (eds), Nuclear Medicine Annual 1985. New York, NY: Raven, 1985.

Zink SI, Ohki SK, Stein B, et al. Noninvasive evaluation of active lower gastrointestinal bleeding: comparison between contrast-enhanced MDCT and 99mTc-labeled RBC scintigraphy. AJR Am J Roentgenol 2008;191:1107–1114.


# CASE 10


**R. EDWARD COLEMAN**


### HISTORY

A 43-year-old woman presents with a history of multiple hepatic masses.

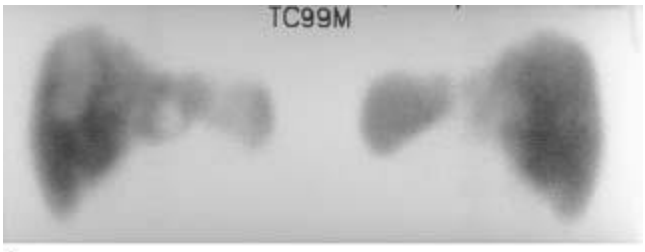


A

■**FIGURE 10-10A** Anterior **(left)** and posterior **(right)** images of the liver and spleen obtained after the intravenous administration of 4 mCi of Tc-99m sulfur colloid. Multiple large focal areas of decreased activity are seen in the right and left lobes of the liver.

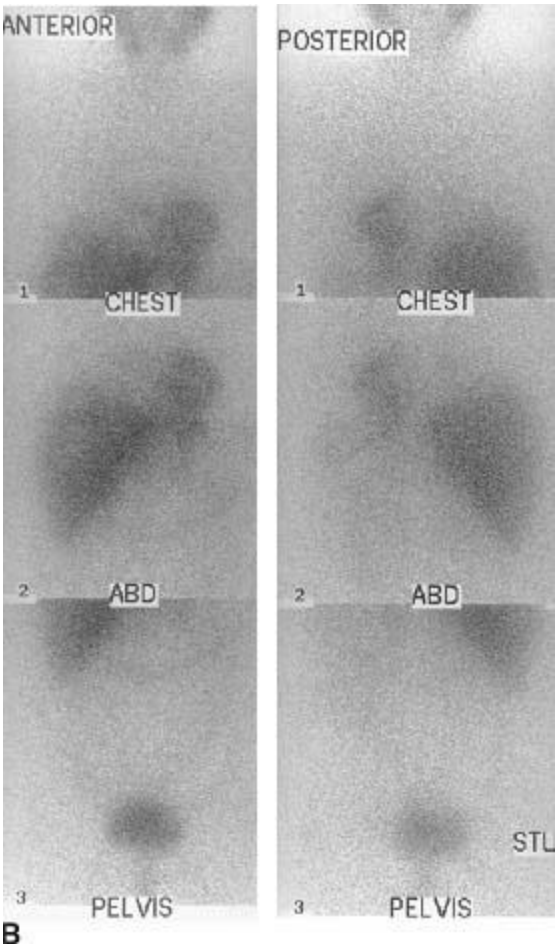


■**FIGURE 10-10B** Anterior **(left)** and posterior **(right)** images obtained 24 hours after the intravenous administration of 2 mCi of I-131 MIBG. Focal areas of decreased activity are present in the right and left lobes of the liver. Normal accumulation of radiotracer is noted in the left ventricular myocardium.

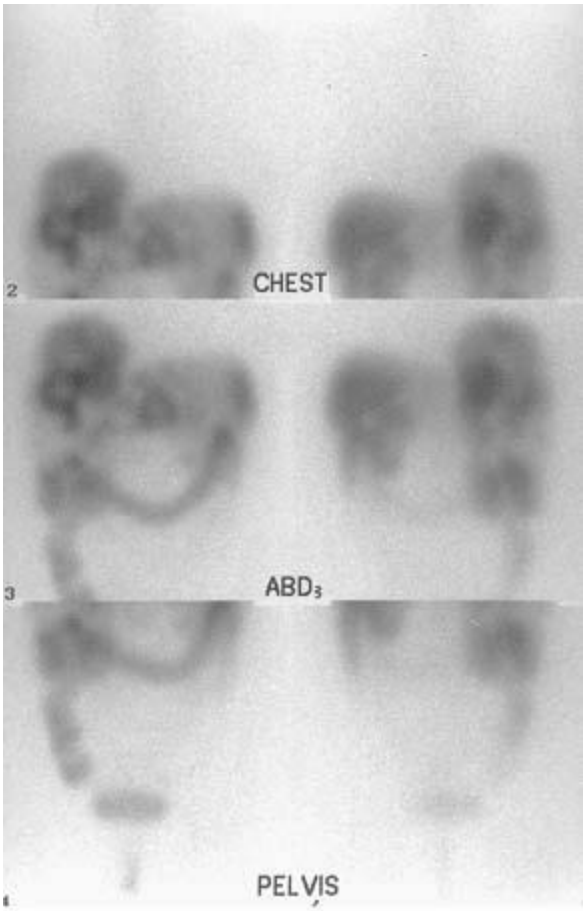


C

**FIGURE 10-10C** Anterior **(left)** and posterior **(right)** images obtained 24 hours after the intravenous administration of 6.2 mCi of In-111 octreotide. Multiple areas of increased accumulation of the radiotracer in the liver are seen with central areas of decreased activity compatible with necrosis. Normal excretion of radiotracer is seen in the bowel and bladder.

## DIFFERENTIAL DIAGNOSIS

- **Neuroendocrine tumor metastatic to the liver:** This is the likely diagnosis because of the increased accumulation of In-111 octreotide in the focal masses in the liver.
- **Metastatic colon cancer:** This diagnosis is unlikely because In-111 octreotide does not accumulate in met-astatic colon cancer.
- **Pheochromocytoma:** This is an unlikely consideration because neither the meta-iodobenzylguanidine (MIBG) scan nor the In-111 octreotide scan showed abnormal accumulation in the region of the adrenal glands.
- **Neuroendocrine tumor metastatic to the left chest:** This diagnosis is unlikely because the accumulation in the left chest on the MIBG scan is a normal finding related to cardiac innervation.

- **Multicentric hepatocellular carcinoma:** This diagnosis is unlikely because hepatocellular carcinomas do not accumulate In-111 octreotide.

## DIAGNOSIS

## Liver metastases from neuroendocrine tumor

## KEY FACTS

### Clinical

- Neuroendocrine tumors are derived from the amine precursor uptake and decarboxylation (APUD) system and contain secretory granules.
- Somatostatin, a peptide hormone consisting of 14 amino acids, has a short plasma half-life (2 to 4 minutes).
- Octreotide, a peptide that has eight amino acids, is an analog of somatostatin that is used therapeutically to block secretions from neuroendocrine tumors that contain somatostatin receptors.
- Somatostatin receptors have been demonstrated in a wide variety of tumors, including pituitary tumors, gas-trinomas, insulinomas, glucagonomas, paragangliomas, medullary thyroid carcinomas, pheochromocytomas, carcinoid tumors, small cell lung cancer, neuroblasto-mas, meningiomas, breast cancers, lymphomas, granu-lomatous diseases, and the thyroid glands of patients with Graves' disease.

### Radiologic

- Indium-111 octreotide localizes in most neuroendocrine tumors because they have somatostatin receptors.
- Indium-111 octreotide imaging can be used to select patients who are likely to respond to octreotide treatment.
- MIBG labeled with either I-131 or I-123 localizes in most neuroendocrine tumors because of the presence of a neuronal pump mechanism for norepinephrine.
- MIBG and In-111 octreotide demonstrate different metabolic functions, and the images in a patient may be abnormal with one radiotracer but not with the other.
- Iodine-131 MIBG has been used therapeutically in patients who have neuroendocrine tumors that accumulate radiotracer on diagnostic imaging.
- At present, there is no therapeutic analog of In-111 octreotide.

## SUGGESTED READING

Hanson MW, Feldman JM, Leight GS, Coleman RE. Iodine 131-labeled meta-iodobenzylguanidine scintigraphy and biochemical analyses of pheochromocytomas. Arch Intern Med 1991;151:1397–1402.

Kvols LK. Somatostatin-receptor imaging of human malignancies: a new era in the localization, staging, and treatment of tumors. Gastroenterol-ogy 1993;105:1909–1911.

Oyen WJ, Bodei L, Giammarile F, et al. Targeted therapy in nuclear medicine-current status and future prospects. Ann Oncol 2007;18: 1782–1792.

Sutcliffe R, Maguire D, Ramage J, et al. Management of neuroendocrine liver metastases. Am J Surg 2004;187:39–46.

Tenenbaum F, Lumbroso J, Schlumberger M, et al. Comparison of radiola-beled octreotide and meta-iodobenzylguanidine (MIBG) scintigraphy in malignant pheochromocytoma. J Nucl Med 1995;36:1–6.

# CASE 11

**ROBERT H.**

**WILKINSON, Jr.**

## HISTORY

A 28-year-old woman presents with a nontender, firm, palpable thyroid nodule.

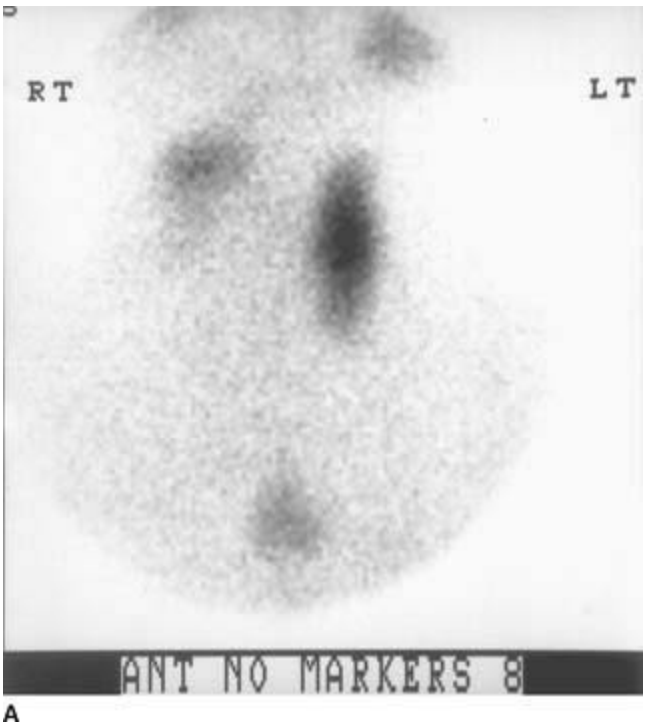


A

■**FIGURE 10-11A** Anterior pinhole images of the thyroid obtained following the intravenous administration of 6 mCi of Tc-99m sodium pertechnetate. There is a solitary focal region of markedly decreased accumulation of radiopharmaceutical involving

most of the right lobe of the thyroid.

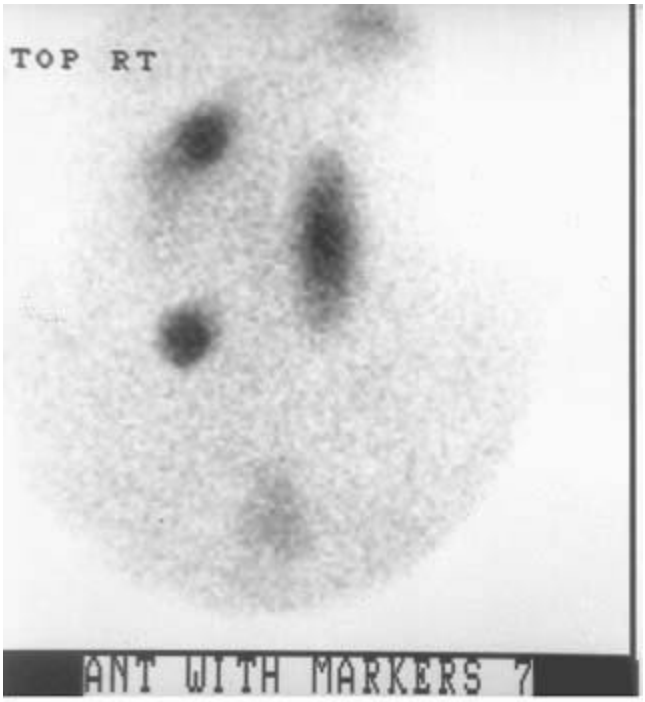


B

**FIGURE 10-11B** An image with markers on the superior and inferior margins of the palpable nodule. The focal region of decreased accumulation between the markers corresponds to the palpable nodule.

## DIFFERENTIAL DIAGNOSIS

**Thyroid carcinoma:** Carcinoma constitutes 10% to 20% of solitary nonfunctioning thyroid nodules. The nodules are usually very firm or hard on palpation. This is the most likely diagnosis.

**Functioning thyroid adenoma:** These lesions are usually firm but not hard in texture. This is an unlikely diagnosis because a functioning adenoma would be expected to accumulate Tc-99m sodium pertechnetate.

**Colloid cyst:** This entity is usually soft on palpation and therefore unlikely to be the etiology in this case. These lesions are usually well-defined by sonography, but biopsy is definitive.

**Chronic thyroiditis (Hashimoto's disease):** This is an unlikely diagnosis because chronic thyroiditis is usually multinodular on palpation and has a more heterogeneous appearance on radionuclide imaging than the finding in the patient illustrated.

**Hemorrhage:** Hemorrhage into an adenoma or cyst can present as a solitary nodule but is usually tender, making it an unlikely diagnosis in this patient.

# DIAGNOSIS

## Thyroid carcinoma

## KEY FACTS

### Clinical

- Papillary carcinomas are the most common thyroid neoplasm in North America (>70%), are four times more frequent in women, and have a peak incidence between ages 20 and 40 years. They metastasize primarily via the lymphatic system. Patients with papillary carcinomas have about a 90% 10-year survival rate.
- Follicular carcinomas comprise about 15% of thyroid carcinomas and usually occur after the age of 40 years. They metastasize via hematogenous spread. Patients with follicular carcinomas have a 70% 10-year survival rate.
- Hurthle cell carcinomas are considered variants of fol-licular cell carcinoma, are relatively rare, and have a variable prognosis.
- Medullary carcinomas comprise 5% to 10% of thyroid carcinomas. About one-fifth of these patients inherit this disease as part of one of the following three syndromes: MEN groups 1 and 2 and a non-MEN syndrome. The familial non-MEN group has the best prognosis, followed by the familial MEN 2A, and then the nonfamilial (sporadic) form. Familial MEN 2B syndrome has the worst prognosis. The 10-year survival rate for all patients with medullary carcinoma of the thyroid is about 60%.
- Anaplastic carcinomas comprise about 10% of thyroid carcinomas, usually occur late in life (after the sixth decade), and have a 5-year survival rate of <5%.
- The risk of metastasis increases with age at the time of diagnosis, particularly for follicular thyroid carcinoma. In addition, recurrence and mortality rates are significantly higher after 45 years of age.
- External beam radiation therapy to the neck region before late adolescence increases the risk of developing either or both benign and malignant thyroid nodules.
- Based on autopsy series, incidental small foci of occult malignant thyroid cells are found in about 10% of patients with no prior clinical evidence of thyroid malignancy.
- Between 10% and 20% of solitary nonfunctioning nodules seen on radioiodine thyroid imaging studies in adults are malignant.
- Only 5% of thyroid nodules are hyperfunctioning and cause suppression of normal thyroid tissue. These nodules may result in a toxic nodular goiter. A very small percentage (2% to 4%) of hyperfunctioning thyroid nodules have been reported to have regions of malignant neoplasia. Clinicians who treat toxic nodular goiter with

radioiodine usually presume the hyperfunc-tioning nodule to be of benign histology.

- Because of fine-needle aspiration biopsy, large-needle aspiration biopsy, and large-needle cutting ("core") biopsy as definitive means of evaluating thyroid nodules, radionuclide imaging studies for this purpose are performed infrequently. Nonetheless, these studies can be useful in defining an autonomous functioning or hyperfunctioning thyroid nodule, which usually precludes the need for biopsy.
- A solitary thyroid nodule in a prepubescent child has a higher likelihood of being malignant than that in an adult.
- Initial reports suggested that the presence of a diffuse toxic goiter offered protection from developing a thyroid malignancy. However, it has subsequently been shown that the likelihood of a solitary nonfunctioning thyroid nodule being malignant does not differ in patients with diffuse toxic goiter and patients who are euthyroid.

## Radiologic

- The radiopharmaceutical tracer of choice for thyroid imaging is I-123 sodium iodide. Tc-99m sodium pertech-netate, which is less expensive and readily available, is an acceptable alternative. I-131 sodium iodide can be used when I-123 sodium iodide is not available or in patients who are suspected of having a substernal thyroid.
- Thyroid gland palpation at the time of imaging is mandatory and allows the examiner to outline the thyroid nodule or superimpose a radionuclide point source marker in the region of the nodule.
- The hypertrapping nodule on Tc-99m sodium pertech-netate images is usually hyperfunctioning on radio-iodine images. However, there is an approximately 10% frequency of hypertrapping nodules on a Tc-99m sodium pertechnetate study that are hypo- to non-functioning on radioiodine thyroid images (so-called discordant nodules). Even less frequent are instances in which a nontrapping thyroid nodule on a Tc-99m sodium pertechnetate study is seen to be a functioning nodule on radioiodine imaging.
- An acronym for the differential diagnosis of solitary nonfunctioning thyroid nodules is CATCH PALLM: *Carcinoma, Adenoma, Thyroiditis, Colloid cyst, Hemorrhage, Parathyroid adenoma, Abscess, Lymph node, Lymphoma, and Metastasis*.

# SUGGESTED READING


Ashcraft MW, Van Herle AJ. Management of thyroid nodules. Parts I and II. Head Neck Surg 1981;3:216-230, 297–322.

Livadas D, Psarras A, Koutras DA. Malignant cold nodules in hyperthyroidism. Br J Surg 1976;63:726–728.

Ridgeway EC. Clinical evaluation of solitary thyroid nodules. In LE Braver-man, RD Utiger (eds), Werner and Ingbar's The Thyroid (6th ed). Philadelphia, PA: Lippincott, 1991;1197–1203.

Smith JR, Oates E. Radionuclide imaging of the thyroid gland: patterns, pearls, and pitfalls. Clin Nucl Med 2004;29:181–193.

Middendorp M, Grunwald F. Update on recent developments in the therapy of differentiated thyroid cancer. Semin Nucl Med 2010;40:145–152.

# CASE 12

**MICHAEL W.**

**HANSON**

## HISTORY

A 26-year-old woman has partial complex seizures that are refractory to anticonvulsants. The seizures are preceded by an aura of a feeling of fear, followed by staring and oral automatic movements. An interictal F-18 FDG PET brain scan is performed for seizure focus localization before temporal lobectomy.

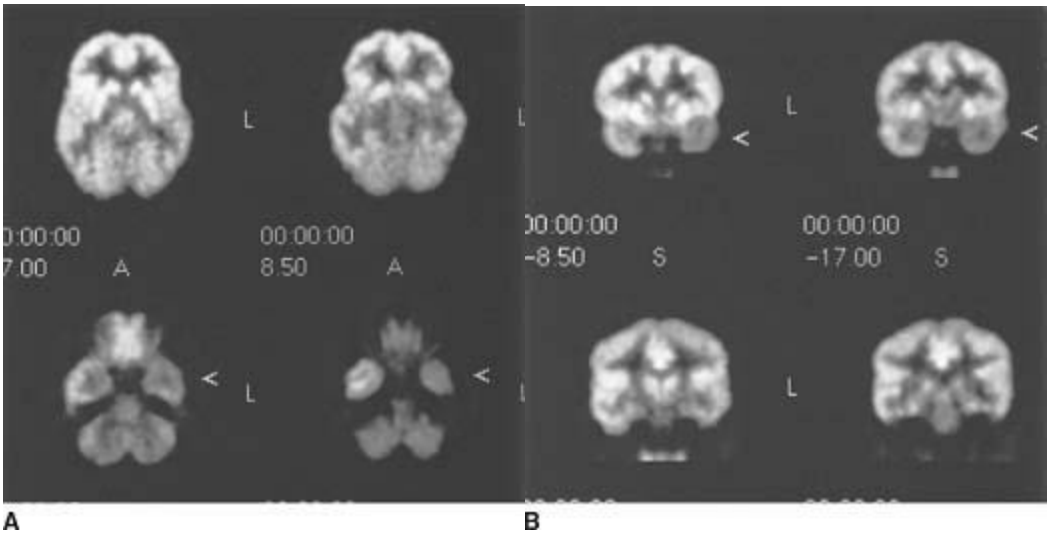


■**FIGURES 10-12A and 10-12B** Transverse **(A)** and coronal **(B)** F-18 FDG PET images through the temporal lobes. Marked F-18 FDG hypometabolism is seen in the left temporal lobe *(arrows)*.


C

**FIGURE 10-12C** Coronal T2-weighted MRI through the temporal lobes. The left hippocampus is decreased in size and has slightly increased signal intensity.

## DIFFERENTIAL DIAGNOSIS

- **Low-grade tumor:** A low-grade tumor with associated edema can have diminished F-18 FDG uptake. The loss of hippocampal volume, rather than a mass lesion, on the magnetic resonance (MR) image makes this diagnosis unlikely.
- **Radiation necrosis:** Tissue necrosis following radiation therapy can have diminished F-18 FDG uptake, but the absence of a brain tumor or prior radiation therapy excludes this diagnosis.
- **Ictal seizure focus:** After F-18 FDG injection at the time of a seizure, increased radiotracer uptake would be expected rather than the decreased uptake seen in the case presented, making this diagnosis incorrect.
- **Interictal seizure focus:** When F-18 FDG is injected at a point when the patient is between seizures (i.e., interictally), the uptake of radiotracer in the dormant seizure focus is diminished. This choice, therefore, is the most likely diagnosis.
- **Infarction:** Infarcted brain tissue can have diminished F-18 FDG uptake. The clinical history and the fact that the abnormality is confined to the hippocampus on the MR image make this diagnosis unlikely.

# DIAGNOSIS

## Interictal seizure focus

## KEY FACTS

### Clinical

- Complex partial seizures (psychomotor or temporal lobe seizures) are frequently preceded by an aura manifested by hallucinations, illusions, affective changes, or aberrations of cognition, and often are accompanied by complex movements. These auras are characteristic of a seizure focus in certain regions of the temporal lobe or limbic system.
- Most complex partial seizures are due to epileptiform activity in the temporal lobes (especially the hippocampus or amygdala), but they can also originate from mesial parasagittal or orbital frontal regions.
- The surface electroencephalogram (EEG) can be normal in patients with complex partial seizures. Depth electrode placement may be required to define the seizure focus by EEG criteria more accurately.
- Complex partial seizures can progress to generalized major motor (grand mal) seizures, manifested by loss of consciousness and tonic/clonic movements.

### Radiologic

- F-18 FDG is a positron-emitting radiopharmaceutical with a half-life of 110 minutes that functions as an analog of glucose. It accumulates in viable cells in proportion to the individual cellular consumption of glucose.
- F-18 FDG imaging of the central nervous system is optimally performed at approximately 30 minutes following the injection of radiotracer. During the 30-minute delay, the patient should be unstimulated—that is, kept in a quiet, dimly lit environment with only background noise.
- In the evaluation of patients for a seizure focus, an EEG should be acquired during the 30-minute uptake phase of F-18 FDG to document the presence or absence of seizure activity that may not be apparent clinically during this interval.
- Metabolic imaging with F-18 FDG of patients with seizures can show functional abnormalities even when MRI studies and histologic specimens obtained from the temporal lobe fail to show an abnormality.
- F-18 FDG imaging is more useful for localization of a seizure focus in patients with suspected temporal lobe seizures than in those with a suspected extratemporal lobe

origin of seizure activity.

- Single-photon emission computed tomography (SPECT) brain perfusion imaging performed in the ictal and interictal states has an accuracy similar to F-18 FDG PET in localizing the seizure focus.
- High-resolution MRI of the hippocampus also has an accuracy similar to F-18 FDG PET in localization of the seizure site.

## SUGGESTED READING

Engel J Jr, Henry TR, Risinger MW, et al. Presurgical evaluation for partial epilepsy: relative contributions of chronic depth-electrode recordings versus FDG-PET and scalp-sphenoidal ictal EEG. Neurology 1990;40:1670–1677.

la Fougère C, RÖminger A, Forster S, et al. PET and SPECT in epilepsy:a critical review. Epilepsy Behav 2009;15:50–55.

Goffin K, Dedeurwaerdere S, Van Laere K, Van Paesschen W. Neuronuclear assessment of patients with epilepsy. Semin Nucl Med 2008;38:227–239.

Radtke RA, Hanson MW, Hoffman JM, et al. Temporal lobe hypometabolism on PET: Predictor of seizure control after temporal lobectomy. Neurology 1993;43:1088–1092.

Radtke RA, Hanson MW, Hoffman JM, et al. Positron emission tomography: Comparison of clinical utility in temporal lobe and extra-temporal epilepsy. J Epilepsy 1994;7:27–33.

# CASE 13

**MICHAEL W.**

**HANSON**

### HISTORY

A 59-year-old man with diabetes, hypertension, and hyperlipidemia presents with dyspnea on exertion and peripheral edema. The patient has no history of prior myocardial infarction. Cardiac catheterization (not shown) reveals normal coronary arteries but diminished left ventricular ejection fraction (LVEF). He is referred for a multiple gated acquisition (MUGA) study.

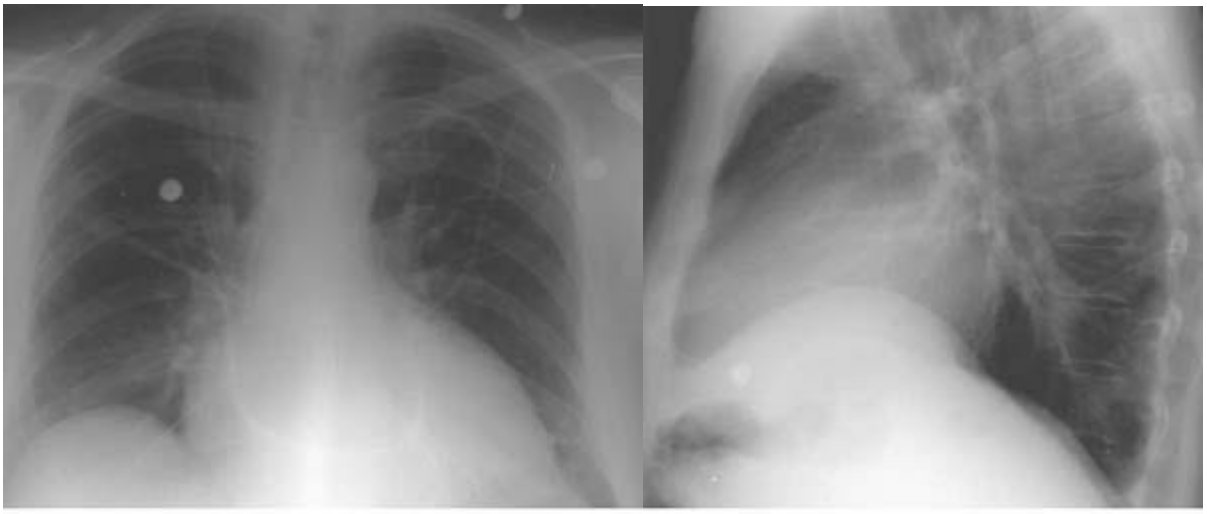

A B

**FIGURES 10-13A and 10-13B** Posteroanterior **(A)** and lateral **(B)** chest radiographs. Marked cardiomegaly is present without findings of pulmonary edema.

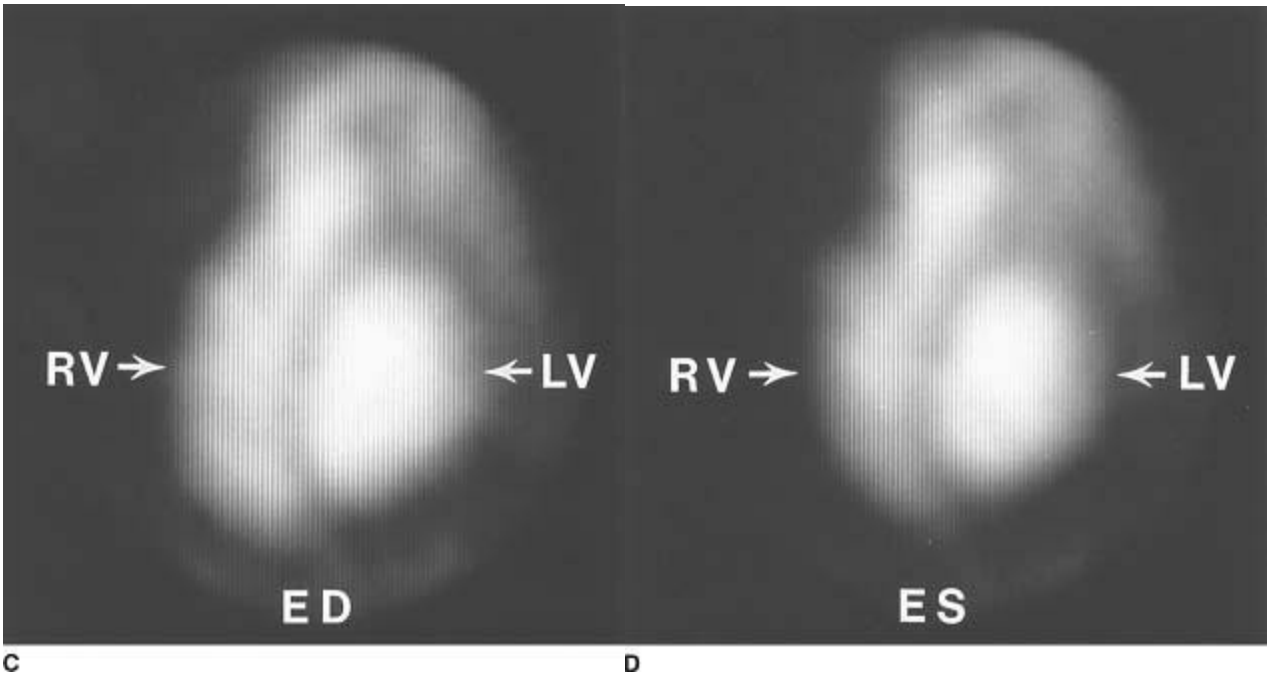


C D

**FIGURES 10-13C and 10-13D** A 45° left anterior oblique MUGA at end diastole **(C)** and end systole **(D).** Markedly dilated ventricles are noted, with increased volumes in diastole and systole. Global hypokinesis of the left ventricle is seen. The LVEF was measured at 15%. The RVEF was measured at 20%.

## DIFFERENTIAL DIAGNOSIS

- **Left ventricular aneurysm:** The ventricular abnormalities in the case illustrated are diffuse, rather than focal, as would be expected with an aneurysm.

- **Restrictive cardiomyopathy:** Typical findings of restrictive cardiomyopathy are mild cardiac enlargement and a left ventricle that has preserved systolic function but is resistant to diastolic filling. In the case illustrated, however, a dilated left ventricle with poor systolic function is seen, making this an incorrect diagnosis.
- **Myocardial infarction:** A focal abnormality, typically involving the left ventricle, would be expected with infarction, rather than the diffuse dysfunction involving both ventricles in the case illustrated.
- **Dilated (congestive) cardiomyopathy:** Dilated car-diomyopathy produces varying degrees of cardiac enlargement (as seen in Figures 10-16A and 10-16B), left ventricular dilatation, increased left ventricular volume, global patterns of abnormal contractility, and a diminished LVEF (as seen in Figures 10-16C and 10-16D). This is the most likely diagnosis for the case illustrated.
- **Hypertrophic cardiomyopathy:** Hypertrophic car-diomyopathy can produce mild to moderate cardiac enlargement, but it is usually associated with vigorous left ventricular contractility and septal thickness that is increased out of proportion to the thickness of the left ventricular free wall. The absence of these findings in the case shown above makes this diagnosis unlikely.

## DIAGNOSIS

## Dilated (congestive) cardiomyopathy

## KEY FACTS

## Clinical

- Dilated cardiomyopathy is most commonly seen in middle-aged men but can occur at any age.
- Infectious, metabolic, and toxic causes are the most common etiologies of dilated cardiomyopathy. Known specific causes include alcohol, adriamycin, cyclo-phosphamide, neuromuscular disease (muscular dystrophies), and pregnancy. However, a definite etiology cannot be discerned in many cases.
- Histologic examination of the myocardium in dilated cardiomyopathy reveals extensive regions of perivascu-lar and interstitial fibrosis accompanied by mild necrosis and cellular infiltration.
- Patients with dilated cardiomyopathy present with symptoms of left- or right-sided congestive heart failure—for example, fatigue, peripheral edema, dyspnea on exertion, orthopnea, paroxysmal nocturnal dyspnea, and palpations. Vague chest discomfort can occur, but typical angina pectoris is uncommon and, when present, implies the presence

of concomitant coronary artery disease.

- Most patients with dilated cardiomyopathy have progressive clinical deterioration. The disease is often fatal within 2 years of the onset of symptoms, especially for older (>55years old) patients. Progressive congestive heart failure and ventricular arrhythmias are the most common causes of death.

## Radiologic

- The gated blood pool study is widely accepted as an accurate imaging technique for evaluation of left ventricular function and is often used for assessment of congestive heart failure, effects of cardiotoxic drugs, left ventricular function following cardiac surgery, and effects of exercise on left ventricular function in patients with suspected coronary artery disease.
- A gated blood pool study can be performed using either Tc-99m sodium pertechnetate-labeled autologous red blood cells (the preferred technique) or Tc-99m-labeled human serum albumin.
- The best septal view is one that allows separation of the ventricles, facilitating determination of both the LVEF and the right ventricular ejection fraction (RVEF). This view is typically a 45° left anterior oblique projection (Figures 10-16C and 10-16D above).
- Correct determination of background activity (usually 30% to 60% of left ventricular end diastolic counts) is critical in calculating an accurate LVEF. Overestima-tion of background activity falsely elevates the LVEF, while underestimation of background activity falsely decreases the LVEF.
- Calculation of the RVEF on a gated blood pool study is less accurate than LVEF calculation. This fact is primarily due to the contribution of activity from the right atrium into the right ventricular region of interest and the uncertainty of the location of the pulmonic valve. Because of the larger volume of the right ventricle, the accepted normal RVEF is generally 5% to 10% less than the normal LVEF.

# SUGGESTED READING


Borges-Neto S, Coleman RE. Radionuclide ventricular function analysis. Radiol Clin North Am 1993;31:817–830.

Friesinger GC. Accuracy of radionuclide ventriculography for estimation of left ventricular volume changes and end-systolic pressure-volume relationships. J Am Coll Cardiol 1985;6:1064–1072.

Kronenberg MW, Parrish MD, Jenkins DW, et al. Cardiac blood pool imaging. II: Applications in noncoronary heart disease. J Nucl Med 1990;31:10–22.

Marwick TH, Schwaiger M. The future of cardiovascular imaging in the diagnosis and management of heart failure, part 1: Tasks and tools. Circ Cardiovasc Imaging 2008;1:58–69.

Marwick TH, Schwaiger M. The future of cardiovascular imaging in the diagnosis and management of heart failure, part 2: Clinical applications. Circ Cardiovasc Imaging 2008;1:162–170.

# CASE 14

**ROBERT R. REIMAN, Jr.**

**AND**

**R. EDWARD COLEMAN**

## HISTORY

A 27-year-old woman being treated for gestational trophoblastic disease presents with a 36-hour history of severe, intermittent, left pleuritic chest pain.

A

■**FIGURE 10-14A** Posteroanterior chest radiograph shows no parenchymal abnormalities, normal pulmonary arteries, and a small left pleural effusion.

B

**FIGURE 10-14B** Tc-99m macroaggregated albumin perfusion study performed in the anterior projection shows multiple segmen-tal defects involving both lungs, with the largest involving most of the lower left lung zone. A Xe-133 ventilation study (not shown) was normal.

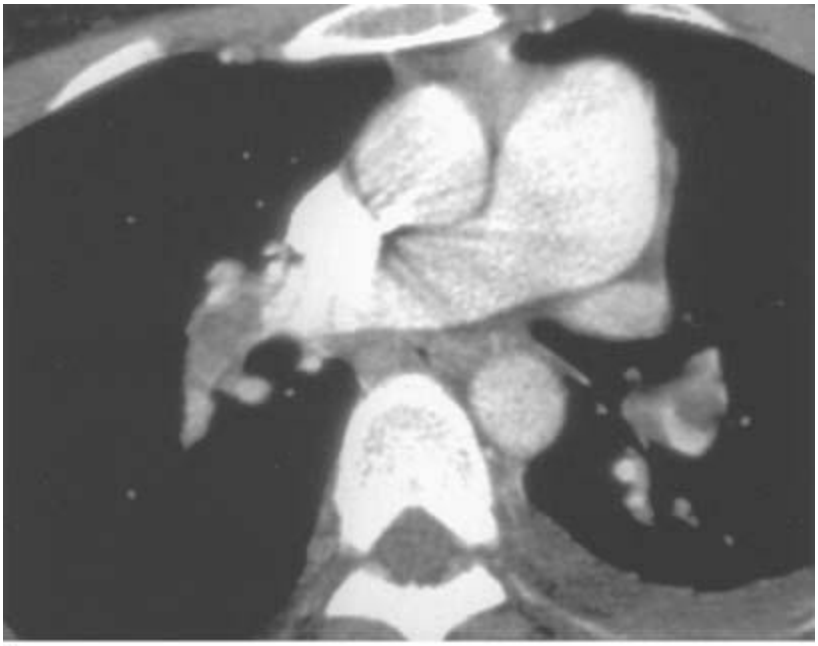

C

**FIGURE 10-14C** CT angiogram of the thorax shows filling defects in the left lower lobe and right interlobar pulmonary arteries.

## DIFFERENTIAL DIAGNOSIS

**Pulmonary artery obstruction by an extrinsic mass:** A focal area of ventilation-

perfusion V/Q mismatch can result from compression by a hilar or mediastinal mass. The presence of multiple bilateral mismatched V/Q abnormalities makes this diagnosis unlikely. Furthermore, no extrinsic mass is seen compressing the pulmonary arteries on the CT scan.

- **Radiation therapy port:** The presence of multiple per-fusion defects that correspond to vascular segments makes this diagnosis incorrect.
- **Vasculitis:** The multiple segmental V/Q mismatches and the presence of emboli on the CT scan make this diagnosis unlikely.
- **Pulmonary embolism (PE):** The multiple segmental perfusion defects in areas that are normal on the ventilation study and the relatively normal chest radiograph make this diagnosis the most likely one. The diagnosis is confirmed by the contrast-enhanced CT scan, which reveals the presence of thromboemboli in the pulmonary arteries.
- **Multiple peripheral pulmonary arterial stenoses:** The presence of thromboemboli in the central pulmonary arteries on the CT scan makes this an incorrect diagnosis.

# DIAGNOSIS

## Pulmonary embolism

## KEY FACTS

### Clinical

- Risk factors for PE include advanced age, immobilization, history of previous PE, concurrent malignancy (usually adenocarcinoma), and hereditary causes of a hypercoagulable state—for example, factor S deficiency.
- The presence of abnormal blood gas findings, the typical history of pleuritic chest pain, shortness of breath, and characteristic electrocardiogram changes can be helpful in raising a strong suspicion of the diagnosis. However, because some of these features are often not present, imaging studies, in particular CT angiography (CTA) and V/Q scans, are important in helping to establish the diagnosis firmly.

### Radiologic

- The chest radiograph is frequently normal in patients with PE. Atelectasis, a small pleural effusion, and elevated hemidiaphragm are nonspecific radiographic findings that are seen in many patients with PE.
- The high probability pattern—that is, two or more perfusion abnormalities without matching ventilatory abnormalities—is most often caused by PE. Some entities—for

example, vasculitis—can produce a pattern of V/Q mismatch simulating the high probability pattern, but these entities often result in a more heterogeneous pattern than seen in the case illustrated above.

- The low-probability pattern includes: (1) defects surrounded by normal lung (stripe sign), (2) corresponding defects and large pleural effusion, (3) nonsegmental perfusion defects, (4) corresponding defects and opacity in the upper or middle lung zones, (5) a perfusion defect with a substantially larger radiographic abnormality, (6) matched ventilation and perfusion abnormalities with a normal radiograph, and (7) more than three small perfusion defects.
- The intermediate probability pattern includes: (1) one moderate to two large perfusion defects without corresponding ventilation or radiographic abnormalities, (2) corresponding ventilation, perfusion, and parenchymal abnormalities in the lower lung zones, and (3) corresponding defects and small pleural effusion.
- The very low probability category consists of three or fewer small defects. The normal category consists of no perfusion abnormalities.
- The gold standard examination for the diagnosis of PE is pulmonary CTA.

## SUGGESTED READING


Freeman LM, Stein EG, Sprayregen S, et al. The current and continuing important role of ventilation-perfusion scintigraphy in evaluating patients with suspected pulmonary embolism. Semin Nucl Med 2008;38:432–440.

Gottschalk A, Sostman HD, Coleman RE, et al. Ventilation-perfusion scin-tigraphy in the PIOPED study. Part II. Evaluation of the scintigraphic criteria and interpretations. J Nucl Med 1993;34:1119–1126.

Grist TM, Sostman HD, MacFall JR, et al. Pulmonary angiography using MRI: Initial clinical experience. Radiology 1993;189:528–530.

Gutte H, Mortensen J, Jensen CV, et al. Detection of pulmonary embolism with combined ventilation-perfusion SPECT and low-dose CT: head-to-head comparison with multidetector CT angiography. J Nucl Med 2009;50:1987–1992.

Worsley DF, Alavi A. Comprehensive analysis of the results of the PIOPED study. J Nucl Med 1995;36:2380–2387.


# CASE 15

### ROSALIE J.

### HAGGE

### HISTORY

A 67-year-old man complains of pain and swelling in both knees 3 years after left upper lobe resection and radiation therapy for adenocarcinoma of the lung.

A

■**FIGURE 10-15A** Frontal radiograph of the right knee. A thin layer of smooth periosteal new bone formation is seen along the distal femur, involving both the metaphysis and distal diaphysis.

B

■**FIGURE 10-15B** Lateral radiograph of the left knee. The periosteal reaction is seen best along the anterior femoral cortex. There is mild soft tissue fullness in the suprapatellar area, consistent with a joint effusion.

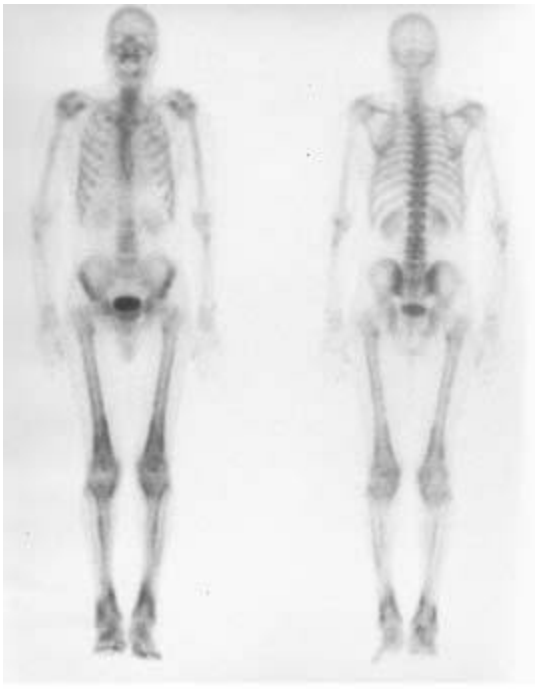

C

**FIGURE 10-15C** Whole body bone scintigraphy, anterior **(left)** and posterior **(right)** views. Symmetrically increased radiotracer uptake is seen in a cortical distribution ("tram track" pattern) within the long bones of both lower extremities. The uptake is most increased in the metaphyseal regions at the knees and ankles but also involves the diaphyses.

## DIFFERENTIAL DIAGNOSIS

**Primary hypertrophic osteoarthropathy (pachydermoperiostosis):** This is a rare, familial, autosomal dominant disorder that occurs predominantly in men. However, the periostitis appears shaggy, irregular, and commonly involves epiphyses, unlike the findings in this case (metaphyseal and diaphyseal), making it an unlikely diagnosis.

**Vascular insufficiency:** The distribution of periostitis in vascular insufficiency is similar to that seen in the case under discussion, but the appearance is typically thicker and undulating.

**Thyroid acropachy:** The typical periostitis of thyroid acropachy appears solid and spiculated, not smooth (as in the case illustrated), and primarily involves the diaphyses of metacarpals and phalanges (and not the long bones).

**Fluorosis:** Solid, undulating periosteal thickening (periostitis deformans) in the appendicular skeleton, somewhat similar to that in the present case, can occur in fluorosis. However, osteosclerosis of the axial skeleton, the most striking feature in fluorosis, is absent in the case illustrated.

- **Secondary hypertrophic osteoarthropathy (HOA):** HOA is the best diagnosis because of the metaphyseal and diaphyseal involvement, soft tissue swelling, joint pain, and a history of lung cancer.

## DIAGNOSIS

## Hypertrophic osteoarthropathy (secondary to a previously undiagnosed recurrence of lung adenocarcinoma)

## KEY FACTS

### Clinical

- HOA can be secondary to a wide variety of conditions, including pulmonary (bronchogenic carcinoma, lymphoma, abscess, bronchiectasis, cystic fibrosis, metastasis, emphysema), pleural (mesothelioma, fibroma), cardiovascular (cyanotic congenital heart disease, infected vascular grafts), and GI (inflammatory disorders, biliary cirrhosis, biliary atresia, polyposis, neoplasms) etiologies.
- The pathogenesis is unknown, but neurogenic mechanisms, increased blood flow, and chemical mediators have been implicated.
- Articular findings occur in about 40% of patients with HOA. Joint pain and swelling can be the presenting complaint. Joint effusions are common.
- Digital clubbing is a frequent, but nonspecific, finding.
- Treatment of the underlying lesion (e.g., thoracotomy, chemotherapy, or radiotherapy for lung carcinoma) is often followed by rapid clinical improvement of symptoms related to HOA.
- There is anecdotal evidence that regrowth of a previously treated neoplasm causing HOA is associated with worsening HOA. In the case illustrated, appearance of HOA was the first indication of a recurrence of lung carcinoma.

### Radiologic

- Bone scintigraphy is a highly sensitive method for detecting HOA. The scintigraphic findings appear before radiographic abnormalities, correspond to clinical signs and symptoms, and regress with therapy.
- The “tram track” or “parallel stripe” sign is due to diffuse cortical radiotracer uptake in the metaphyses and diaphyses of tubular bones that results from periosteal new bone formation.
- HOA findings are typically bilateral and symmetric and primarily involve the

appendicular skeleton. Less common sites include the clavicles, scapulae, pelvis, digits, and facial bones.

- Increased periarticular radiotracer uptake in HOA often indicates associated synovitis.
- Plain film appearance of periostitis in HOA is variable. Findings include: (1) simple periosteal elevation, (2) smooth laminated ("onion-skin") periostitis, (3) irregular, wavy, or solid periostitis, and (4) cortical thickening.
- The periostitis of HOA begins in the diaphyses then later involves the metaphyses and sometimes tendinous insertions.
- Digital clubbing can manifest as soft tissue swelling, with or without focal tuftal resorption or hypertrophy.
- The soft tissue swelling, periarticular osteoporosis, and joint effusions of HOA can mimic rheumatoid arthritis. However, the joint space narrowing and erosions seen in rheumatoid arthritis are not present in HOA.

## SUGGESTED READING

Pineda CJ, Sartoris DJ, Clopton P, Resnick D. Periostitis in hypertrophic osteoarthropathy: Relationship to disease duration. AJR Am J Roentgenol 1987;148:773–778.

Resnick D. Bone and Joint Imaging. Philadelphia, PA: Saunders, 1989;1237–1246.

Shih WJ. Pulmonary hypertrophic osteoarthropathy and its resolution. Semin Nucl Med 2004;34:159–163.

# CASE 16

**ROBERT**

**WILKINSON, Jr.**

### HISTORY

A 24-year-old woman severely injured her left forearm. Several months following reparative surgery, she developed increasing pain and a burning sensation in her left distal forearm, hand, and wrist.

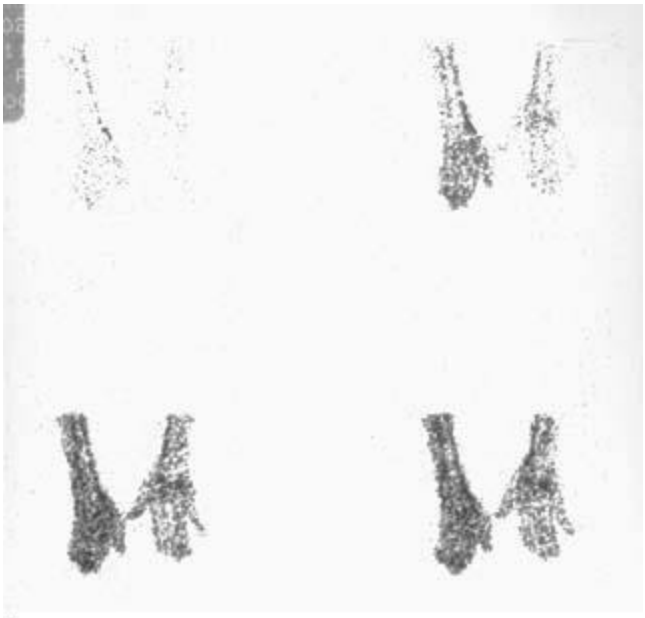

A

■**FIGURE 10-16A** Dynamic perfusion images of the distal forearms, wrists and hands reveal earlier perfusion and subsequently greater perfusion on the left compared to the same region on the right (the patient's left upper extremity is on the reader's left).

B

■**FIGURE 10-16B** Immediate "blood pool" image of the upper extremities distally reveals generalized greater soft tissue as well as early and poorly defined periarticular and osseous radiotracer accumulation on the left compared to the right (a focal right image marker is present distal to the right hand).

C

**FIGURE 10-16C** Delayed image of the upper extremity distally reveals very pronounced periarticular radiotracer accumulation as well as greater soft tissue and osseous radiotracer accumulation on the left compared to the right. There is involuntary flexion at the left distal interphalyngeal joints.

## DIFFERENTIAL DIAGNOSIS

- **Complex regional pain syndrome type I:** This diagnosis is the most likely diagnosis because of: (1) the history of trauma to the affected limb, (2) the clinical findings of pain and dysesthesias, and (3) the abnormal three-phase bone scan pattern.
- **Acute arthritis:** This entity can produce the three-phase bone scan findings seen in the case illustrated, but the periarticular radiotracer uptake pattern is usually less uniform.
- **Extremity immobilization:** This entity can produce the bone scan findings shown above but is not associated with the dysesthesias present in this patient.
- **Fracture:** A recent fracture of the wrist or hand can produce increased radiotracer activity on all three phases of the bone scan, but a focal abnormality, rather than the diffuse pattern seen in the case illustrated, would be expected at the site of the fracture.
- **Osteomyelitis:** The same argument against a diagnosis of fracture applies to osteomyelitis—although all three phases of the bone scan can be abnormal, a focal lesion, rather than a diffuse pattern, would be expected.

## DIAGNOSIS

### Complex regional pain syndrome, type I

## KEY FACTS

### Clinical

- "Complex regional pain syndrome, type I" (CRPS I) was formerly identified as "reflex sympathetic dystrophy syndrome," "Sudeck's atrophy," "Sudeck's dystrophy," and "algodystrophy."
- Clinically, CRPS I may present with the following findings: (1) involvement of an upper or lower extremity, (2) history of trauma to the affected limb, (3) persistent pain disproportionate to the inciting event, (4) hyper-esthesia, (5) edema, (6) atypical sweating, (7) skin temperature and/or color alteration from normal, (8) altered mobility, (9) trophic changes to skin, hair or nail, (10) hyperalgesia or (11) allodynia.
- The CRPS I complex includes a spectrum of clinical abnormalities, which include such variations as cau-salgia (with or without evidence of peripheral nerve injury), shoulder-hand syndrome, and Sudeck's atrophy of bone. Not all of the clinical manifestations can be explained on the basis of a single unifying pathophysio-logic process. There is sympathetic neural involvement in this phenomenon.
- CRPS I is clinically divided into three stages—acute, dystrophic, and atrophic.
- Diagnosis of CRPS I is based primarily on clinical criteria. One was established in 1993 by the International Association for the Study of Pain. Another was created in 1999 by Bruehl. The three-phase radionuclide bone scan, radiographs, thermography, and MR have been proposed to lessen clinical diagnosis subjectivity. However, recent work indicates that these procedures take weeks to months before demonstrating significant findings.

### Radiologic

- Kozin et al. and Holder and Mackinnon (H & MacK) have published criteria for the three-phase bone scan diagnosis of CRPS I. Comparison between the two studies is difficult because Kozin et al. has less strict criteria but a longer duration of symptoms. The sensitivity and specificity for Kozin et al. was 60% and 92%, respectively, compared to H & MacK at 96% and 98%, respectively. A meta-analysis of 19 articles found an upper extremity sensitivity for CRPS I of 50%. The duration of symptoms may be an important factor, since cases with a prolonged duration tend to revert to a normal pattern.
- The H&MacK criteria for "definite" CRPS I include hyperperfusion on the first phase, the "blood pool" phase and delayed phases, and increased tracer accumulation in a periarticular distribution of the carpal, metacarpal, and phalangeal joints of the affected upper extremity.
- MR imaging is inconclusive in the early period following onset of symptoms. In one

small series using clinical criteria as the "gold standard," from 8 to 16 weeks following the onset of symptoms, sensitivity dropped from 43% to 14%. In this same period, specificity rose from 78% to 98%.

- In children with CRPS I undergoing a three-phase radionuclide bone scan, there may well be the reverse pattern reported in adults. That is, the affected limb will demonstrate *decreased* perfusion during the "blood pool" phase and "delayed" tracer accumulation. Reportedly, the incidence is as high as 70%. This favors a vasoconstriction phenomenon. There are case reports showing this pattern in adults as well.
- Another apparent difference in the disease pattern is that children tend to have more lower extremity involvement while adults have more upper extremity involvement.

## SUGGESTED READING


Bruehl S, Harden RN, Galer RS, et al. External validation of IASP diagnostic criteria for complex regional pain syndrome and proposed research diagnostic criteria. International association for the study of pain. Pain 1999;81:147–154.

Fournier RS, Holder LE. Reflex sympathetic dystrophy: diagnostic controversies. Semin Nucl Med 1998;28:116–123.

Holder LE, MacKinnon SE. Reflex sympathetic dystrophy in the hands. Clinical and scintigraphic criteria. Radiology 1984;152:517–521.

Intenzo CM, Kim SM, Capuzzi DM. The role of nuclear medicine in the evaluation of complex regional pain syndrome type 1. Clin Nucl Med 2005;30:400–407.

Oud CF, Legein J, Everaert H, et al. Bone scintigraphy in children with persistent pain in an extremity, suggesting algoneurodystrophy. Acta Orthop Belg 1999;65:364–366.

Schurmann M, Zaspel J, Lohr P, et al. Imaging in early posttraumatic complex regional pain syndrome. A comparison of diagnostic methods. Clin J Pain 2007;23:449–457.

Turpin S, Taillefer R, Lambert R, Leveille J. "Cold" reflex sympathetic dystrophy in an adult. Clin Nucl Med 1996;21:94–97.


# CASE 17


**R. EDWARD COLEMAN**


### HISTORY

A 69-year-old man with recurrent hypercalcemia after previous parathyroidectomy is being evaluated for hyperparathyroidism. Physical examination is normal.

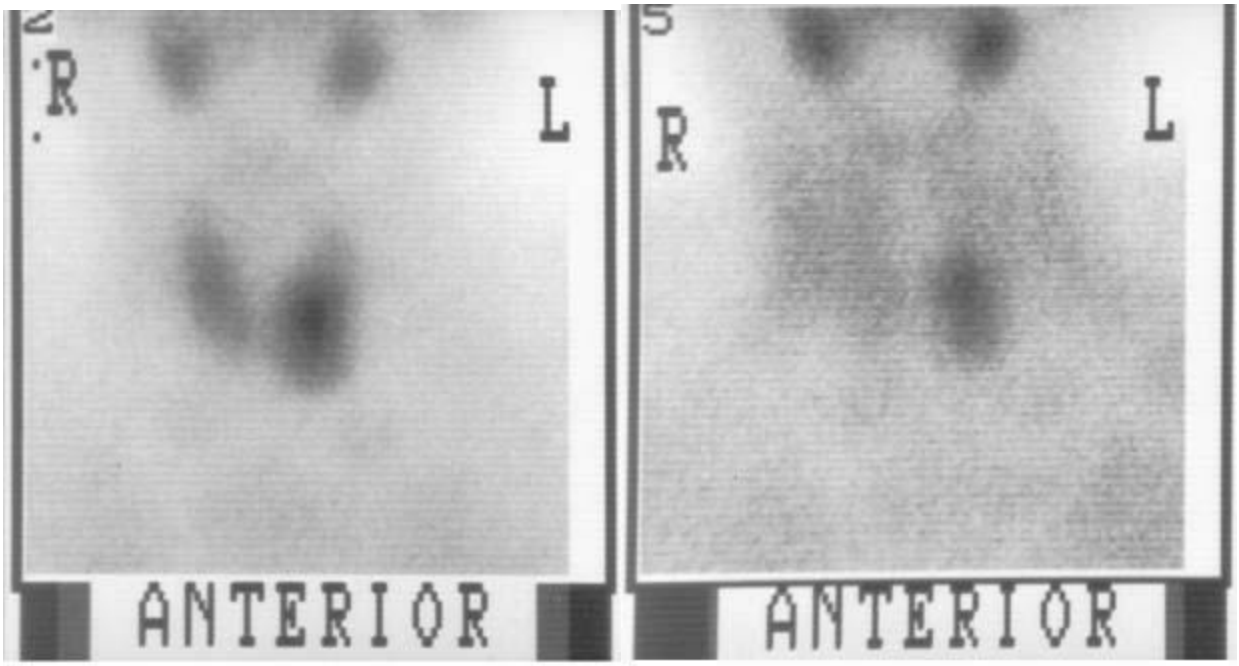

A B

■**FIGURES 10-17A and 10-17B** Anterior image of the neck obtained: **(A)** 10 minutes, and **(B)** 2 hours after the intravenous administration of 20 mCi of Tc-99m sestamibi. In **(A)** there is normal accumulation of the tracer in the thyroid and salivary glands. In **(B)** the radioactivity has cleared from the right thyroid gland, but radioactivity persists in the region of the inferior pole of the left thyroid gland.

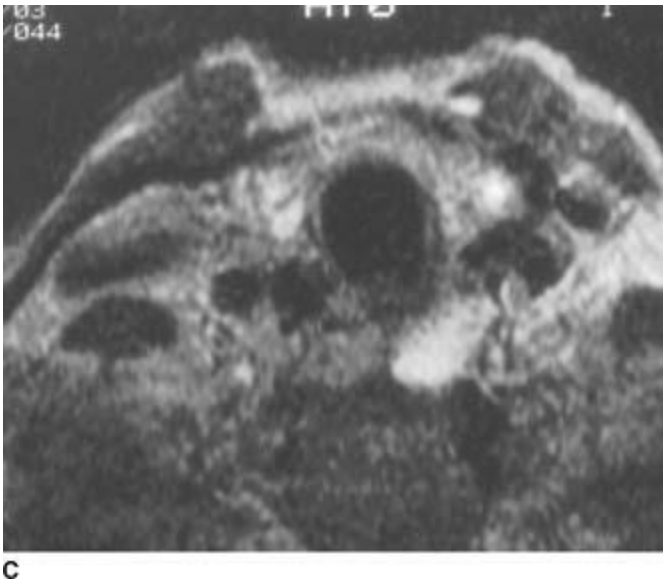
C

■**FIGURE 10-17C** T2-weighted MRI of the neck. A 1.5 x 1.0 cm area of increased signal is seen posterior to the left lobe of the thyroid gland.

## DIFFERENTIAL DIAGNOSIS

- **Parathyroid hyperplasia:** This is an unlikely diagnosis because only a single abnormality is present. Multiple foci of tracer activity would be expected with parathyroid hyperplasia.
- **Thyroid cancer:** The absence of a palpable mass on physical examination, an elevated serum calcium level, and normal images obtained 10 minutes after radio-pharmaceutical administration make this diagnosis unlikely.
- **Thyroid adenoma:** The history of hypercalcemia makes this diagnosis less likely. Furthermore, the abnormality on the MR image is located posterior to the thyroid gland.
- **Metastatic disease to a supraclavicular node:** The lack of a history of a primary malignancy and absence of other abnormalities on the MRI study make this diagnosis unlikely, although it is not excluded.
- **Parathyroid adenoma:** The presence of a single, focal abnormality on the Tc-99m sestamibi image in a patient with hypercalcemia makes parathyroid adenoma the most likely diagnosis.

## DIAGNOSIS

## Parathyroid adenoma

## KEY FACTS

### Clinical

- Hyperparathyroidism is the result of increased para-thormone production. Two types of hyperparathyroid-ism are recognized—primary and secondary.
- Primary hyperparathyroidism is due to endogenous hypersecretion of parathormone, which is caused by an adenoma (usually a solitary lesion) in 80% of cases, hyperplasia (usually of all four glands) in 10% to 15% of cases, and parathyroid carcinoma in about 5% of cases.
- Secondary hyperparathyroidism results from hypocal-cemia causing stimulation of the parathyroid glands and increased parathormone production. It is usually secondary to renal failure but can be seen in malab-sorption and renal tubular disorders.
- Tertiary hyperparathyroidism occurs when one or more glands hypertrophy due to secondary hyperpara-thyroidism and then function(s) autonomously.
- Symptomatic patients with hyperparathyroidism and a radiologic or metabolic abnormality should be treated by surgery.
- Persistent hypercalcemia after surgery for hyperpara-thyroidism occurs in 3% to 10% of cases and results from failure to remove all hyperfunctioning glands.

- The combination of radionuclide imaging and new parathormone assays that can be performed very quickly (<15 minutes) and, hence, intraoperatively, permit decreased operative time and help in identifying all hyperfunctioning tissue, thereby facilitating total resection of all hyperfunctioning glands.

## Radiologic

- The double-phase Tc-99m sestamibi study consists of early (10 to 20 minutes after radiopharmaceutical administration) and delayed (2 to 3 hours) imaging. It is very accurate for the localization of hyperfunctioning parathyroid tissue.
- The double-phase technique is based on the more rapid tracer clearance from normal thyroid than from abnormal parathyroid tissue.
- Tc-99m sestamibi is more accurate in localizing abnormal parathyroid tissue than other radionuclide techniques, such as sonography, CT, and MRI, which are also used for this purpose.
- The detection rate of abnormal parathyroid tissue depends on the gland size. Adenomas are generally larger than hyperplastic glands (frequently <500mg) and, thus, more accurately detected.
- Tc-99m sestamibi is very accurate in detecting ectopic parathyroid glands that cause hyperparathyroidism, but the abnormality must be within the field of view. Parallel-hole, high-resolution collimation is used to ensure that the neck and upper chest are included in the field of view.
- Thyroid adenomas, thyroid carcinomas, and lymph nodes involved with sarcoidosis have been reported to cause false-positive results on Tc-99m sestamibi imaging studies for parathyroid adenoma evaluation.

## SUGGESTED READING

Coakley AJ. Parathyroid imaging. Nucl Med Comm 1995;16:522–533.

Irvin GL, Prudhomme DL, Deriso GT, et al. A new approach to parathyroidectomy. Ann Surg 1994;219:574–581.

Kettle AG, O'Doherty MJ. Parathyroid imaging: how good is it and how should it be done? Semin Nucl Med 2006;36:206–211.

Lavely WC, Goetze S, Friedman KP, et al. Comparison of SPECT/CT, SPECT, and planar imaging with single- and dual-phase (99m)Tc-sestamibi parathyroid scintigraphy. J Nucl Med 2007;48:1084–1089.

Lee VS, Wilkinson RH, Leight GS, et al. Hyperparathyroidism in high-risk surgical patients: evaluation with double-phase technetium-99m sesta-mibi imaging. Radiology 1995;197:627–633.

Rubello D, Gross MD, Mariani G, AL-Nahhas A. Scintigraphic techniques in primary hyperparathyroidism: from pre-operative localisation to intra-operative imaging. Eur J Nucl Med Mol Imaging 2007;34:926–933.

# CASE 18

**SALVADOR BORGES-NETO**

## HISTORY

A 61-year-old woman has a history of coronary artery disease, congestive heart failure, severe peripheral vascular disease, hypertension, and a creatinine level of 2.8 mg/dl.

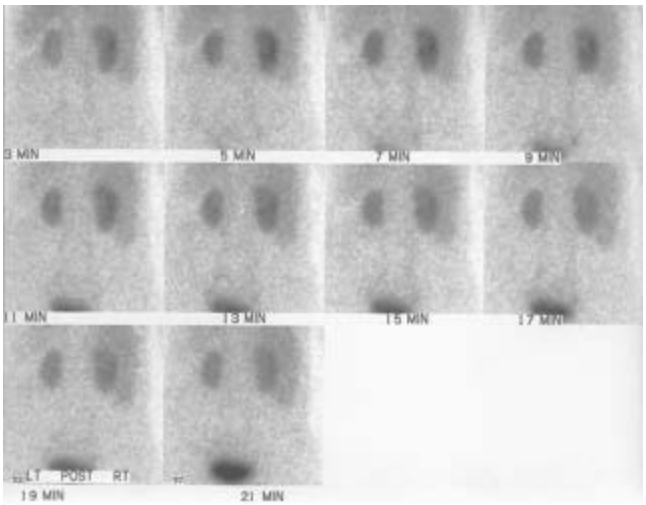


A

■**FIGURE 10-18A** Baseline posterior images of the abdomen obtained after the administration of 1 mCi of Tc-99m MAG3. Asymmetric parenchymal radiotracer uptake is seen on the immediate image with less uptake in the left kidney than in the right kidney. The left kidney is also smaller than the right. There is no evidence for obstruction to drainage in either kidney. The image obtained at 21 minutes shows less cortical activity bilaterally than the image obtained at 5 minutes.

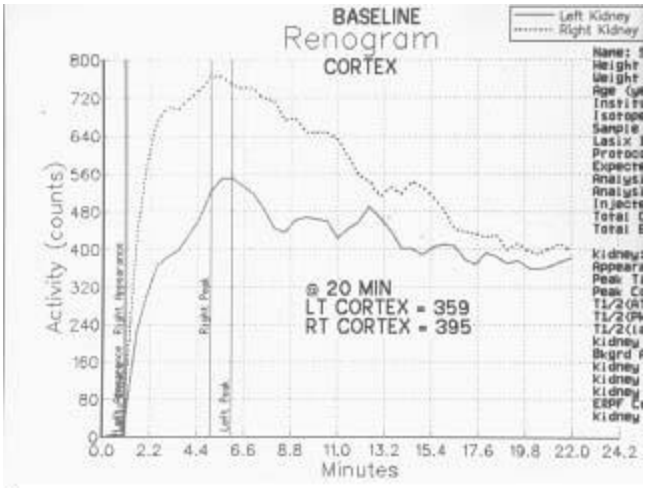


B

■**FIGURE 10-18B** Baseline time activity curves from the right and left renal cortex. A slight delay in peak cortical activity is seen, more pronounced for the left kidney. The residual cortical activity is 48% for the right kidney and 65% for the left.

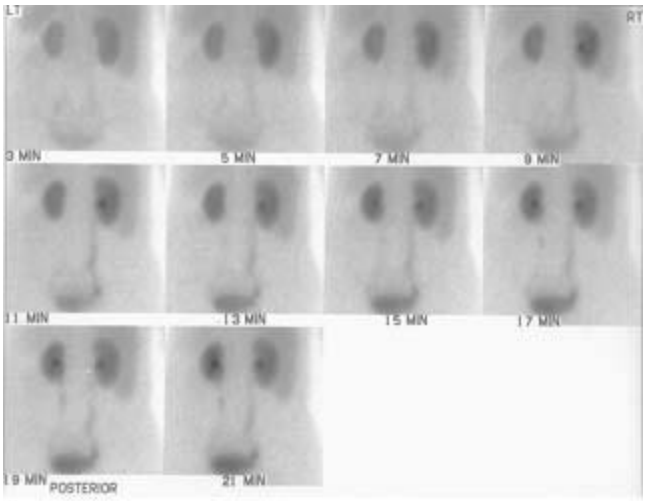


C

■**FIGURE 10-18C** Posterior images of the abdomen obtained after intravenous administration of 2.5 mg of enalaprilat, followed by 9 mCi of Tc-99m MAG3. Asymmetry of the kidneys is again noted. Progressive radiotracer accumulation is seen within the left renal cortex. There is also significant residual activity within the right renal cortex.

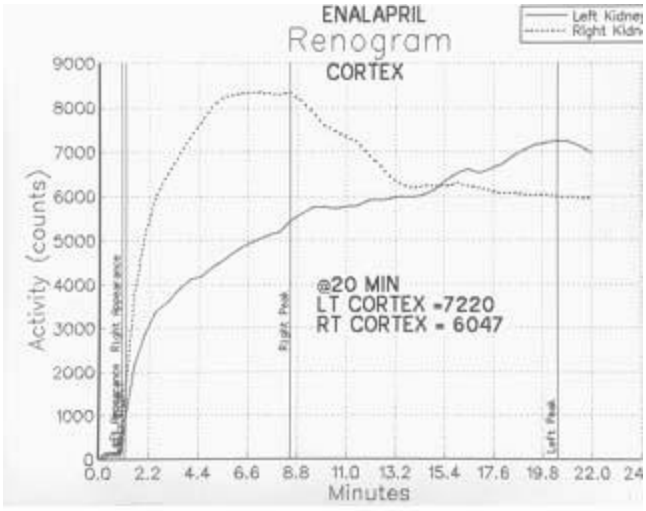


D

■**FIGURE 10-18D** Time activity curves from the right and left renal cortex after the administration of enalaprilat. The right cortical renogram has significant residual radiotracer activity at the end of 21 minutes, with 61% retention from the peak and a 13% increase from the baseline study. The left cortical renogram shows an ascending pattern with a 35% increase from baseline.

## DIFFERENTIAL DIAGNOSIS

- **High-grade urinary obstruction:** This diagnosis is unlikely because the baseline study does not show a rising baseline renogram, as would be expected with high-grade obstruction.
- **Acute tubular necrosis:** This diagnosis is very unlikely because there is no history of an appropriate precipitating event (e.g., an episode of hypotension) and because acute tubular necrosis would be expected to affect both kidneys in a symmetric fashion.
- **Unilateral renal artery stenosis:** This is not the appropriate diagnosis because the function of both kidneys (rather than one kidney) worsened after administration of an angiotension-converting enzyme inhibitor.
- **Bilateral renal artery stenoses:** This is the best diagnosis because the function of both kidneys decreased following enalaprilat administration. The findings in the left kidney are characteristic for severe renal artery stenosis—there is a change from an ascending/ descending pattern on the baseline cortical renogram to an ascending pattern after enalaprilat administration. The pattern in the right kidney, however, is also abnormal, with a prolonged cortical phase, significant residual tubular radiotracer activity relative to peak, and a 13% increase from the baseline study (which exceeds 10% from baseline, thereby meeting criteria for renal artery stenosis).
- **Chronic renal disease not causing hypertension:** This diagnosis is unlikely because of the abnormal response to the angiotension converting enzyme inhibitor.

## DIAGNOSIS

## Bilateral renal artery stenoses (75% right kidney and 99% left kidney)

## KEY FACTS

## Clinical

- Renal artery stenosis is a common cause of secondary hypertension and is present in 1% to 4% of hypertensive patients. It predominantly occurs in whites.
- Renovascular hypertension is produced by excessive renin release, which itself results from a decrease in renal perfusion.
- In 70% of cases, renovascular hypertension results from atherosclerotic stenosis.
- Fibromuscular hyperplasia is the etiology in 30% of patients who have renovascular hypertension (being more common in women) and is the predominant cause of

renovascular hypertension in adults <40 years of age.

- The following clinical features increase the likelihood that hypertension is secondary to renal artery stenosis:
    - Onset at age <20 and >50 years
    - Abdominal bruit
    - Atherosclerotic disease at other sites
    - Abrupt deterioration of renal function after the administration of angiotensin-converting enzyme inhibitors
- Some patients may be managed medically if renal function does not deteriorate.
- The use of angiotensin-converting enzyme inhibitors has improved the success rate of medical therapy.
- However, patients with bilateral renal artery stenosis may develop marked hypotension and deterioration of renal function after administration of these agents.
- Surgical treatment is generally successful, but percutaneous transluminal angioplasty is now the preferred approach for fibromuscular hyperplasia and discrete atherosclerotic lesions.

## Radiologic

- Angiography is the gold standard diagnostic procedure for determining renal artery stenosis but has a number of drawbacks: (1) it is an invasive procedure, and (2) it provides an anatomic definition of the arterial luminal diameter but not the physiologic significance of a stenosis—that is, that hypertension is on a renovascular basis. Renal vein renin determination is also an invasive procedure and has not proved to be accurate in the diagnosis.
- CT angiography (CTA) and MR angiography (MRA) is primarily used to evaluate for renal artery stenosis. These techniques have the advantage of: (1) being noninvasive, (2) having the ability to depict not only the lumen of the artery but also the wall and the surrounding soft tissue, and (3) having the ability to evaluate other abdominal organs such as the adrenal glands. Disadvantages of CTA and MRA include: (1) the requirement for intravenous contrast agents that may be con-traindicated if the patients have renal insufficiency, especially when the glomerular filtration rate (GFR) is <30 mL/min, (2) the fact that MRA cannot visualize calcifications, and (3) the fact that CTA uses ionizing radiation. A limited MRA can be performed without intravenous contrast material using a white blood technique but the efficacy is lower.
- Urography and conventional radionuclide scintigraphy have an unacceptably high rate of false-negative and false-positive results in the diagnosis of renovascular hypertension. Doppler ultrasonography also has variable sensitivity and specificity in

the diagnosis of reno-vascular hypertension, particularly in larger patients.

- Response of hypertension to renal artery angioplasty cannot be predicted from the degree of arterial stenosis alone but must be combined with provocative tests such as scintigraphy following the administration of angio-tensin-converting enzyme. Some patients with mild stenosis but positive angiotensin-converting enzyme inhibitor scintigraphy have substantial reduction in hypertensin following angioplasty, whereas patients with severe stenoses but negative scintigraphic studies do not generally respond to revascularization.

## SUGGESTED READING


Blaufox MD. Procedures of choice in renal nuclear medicine. J Nucl Med 1991;32:1301–1309.

Dunnick NR, Sfakianakis GN. Screening for renovascular hypertension. Radiol Clin North Am 1991;29:497–510.

Durand E, Blaufox MD, Britton KE, et al., International Scientific Committee of Radionuclides in Nephrourology (ISCORN). International Scientific Committee of Radionuclides in Nephrourology (ISCORN) consensus on renal transit time measurements. Semin Nucl Med 2008;38:82–102.

Fine EJ. Diuretic renography and angiotensin converting enzyme inhibitor renography. Radiol Clin North Am 2001;39:979–95.

Glockner JF, Vrtiska TJ. Renal MR and CT angiography: current concepts. Abdom Imaging 2007;32:407–420.

Sfakianakis GN, Bourgoignie JJ, Georgiou M, Guerra JJ Jr. Diagnosis of renovascular hypertension with ACE inhibition scintigraphy. Radiol Clin North Am 1993;4:831–848.


# CASE 19


**MICHAEL W. HANSON**


### HISTORY

A 76-year-old man presents with a history of a transient episode of chest pain on returning to bed after voiding during the night and an episode of unexplained syncope. He is referred for exercise stress testing and myocardial perfusion imaging.

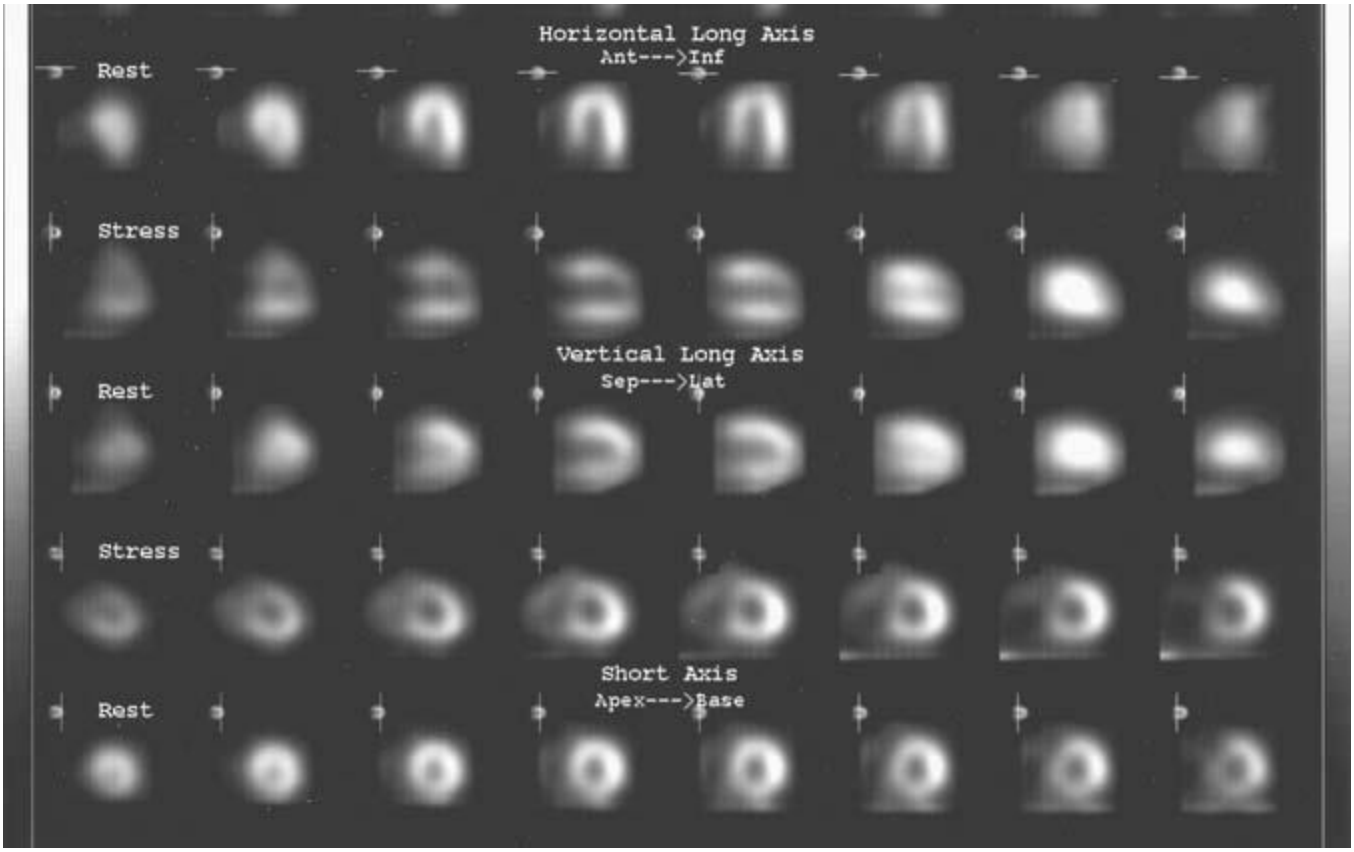


**FIGURE 10-19** Stress Tc-99m sestamibi (rows 1, 3, and 5) and rest Tl-201 (rows 2, 4, and 6) myocardial perfusion images. The axes are noted on the images. The rest Tl-201 myocardial perfusion images (rows 2, 4, and 6) show normal homogeneous radiotracer uptake throughout the myocardium. No perfusion defects are seen on the rest images. The stress Tc-99m sestamibi myocardial perfusion images (rows 1, 3, and 5) show a segmental region of diminished perfusion involving the low anterior, anteroapical, and interventricular septal areas.

## DIFFERENTIAL DIAGNOSIS

**Myocardial infarction:** Myocardial infarction would not be expected to have normal homogeneous radiotracer uptake on the resting Tl-201 study, making this diagnosis incorrect.

**Myocardial ischemia:** The development of a stress-induced perfusion defect that is not present on the resting perfusion image is the typical finding in myocardial ischemia. The findings in this case are most consistent with this diagnosis.

**Attenuation artifact:** Most often a problem in obese women, this artifact should be seen on both the rest and stress images. It usually involves the lower anterior wall and the anteroapex regions. The defect seen in the case presented is larger than that typically seen due to attenuation artifact. Furthermore, attenuation artifact would not be expected to involve the septum, as in the present case.

- **Artifact from a left bundle branch block:** This elec-trocardiographic abnormality can create a reversible perfusion defect, but it most often involves primarily the interventricular septum and is not as extensive as the defect presented in this case.
- **Artifact from patient motion on the stress image:** Motion artifact can create apparent perfusion defects that usually, though not exclusively, occur in the apex. This diagnosis is incorrect because the defect seen in the case presented is much more extensive than that expected from patient motion. In general, review of the raw data in a cine mode can often identify patient motion of a degree sufficient to create apparent perfu-sion defects.

## DIAGNOSIS

## Stress-induced myocardial ischemia in the vascular territory of the left anterior descending coronary artery

## KEY FACTS

### Clinical

- The symptoms, pain location, and radiation patterns, as well as the precipitating factors of angina pectoris due to myocardial ischemia can be variable. If the clinical index of suspicion is sufficiently high—that is, a >10% probability that the patient has significant coronary artery disease—further evaluation is indicated.
- The episode of unexplained syncope in this patient is worrisome because it may have been related to transient myocardial ischemia and a potentially fatal arrhythmia.
- Based on this patient's presentation and perfusion images, the diagnosis is significant coronary artery disease, which was documented at cardiac catheteriza-tion.
- Prevention of myocardial infarction and left ventricular damage is a primary objective in the treatment of this patient.

### Radiologic

- The scintigraphic findings in the case presented are the typical pattern seen with stress-induced myo-cardial ischemia. A perfusion defect following stress testing that is not seen on the resting image indicates segmental myocardial ischemia. The perfusion defect is secondary to altered blood flow during coronary artery dilatation that occurs in response to physical (e.g., exercise) or pharmacologic (e.g., dipyridamole or dobutamine) stress testing.
- A fixed defect at rest and stress can be caused by either myocardial infarction or

artifact due to attenuation of photons by surrounding soft tissue or noncardiac structures.

- Myocardial perfusion imaging can be performed with Tl-201 alone, Tc-99m sestamibi alone, or as above, with a combination of the two agents. The dual isotope technique combines the advantage of Tl-201 (the preferred single-photon radiopharmaceutical for identifying viable myocardium) and the advantage of Tc-99m sestamibi (superior image quality following stress). The dual isotope technique also decreases overall imaging time.

## SUGGESTED READING


Berman DS, Kiat HS, Van Train KF, et al. Myocardial perfusion imaging with technetium-99m sestamibi: comparative analysis of available imaging protocols. J Nucl Med 1994;35:681–688.

Kiat H, Germano G, Friedman J, et al. Comparative feasibility of separate or simultaneous rest thallium-201/stress technetium-99m sestamibi dualisotope myocardial perfusion SPECT. J Nucl Med 1994;35:542–548.

Maddahi J, Rodrigues E, Berman DS, et al. State-of-the-art myocardial perfusion imaging. Cardiol Clin 1994;12:199–222.

Vesely MR, Dilsizian V. Nuclear cardiac stress testing in the era of molecular medicine. J Nucl Med 2008;49:399–413.

Vincenti G, Nkoulou R, Steiner C, et al. Noninvasive stress testing of myo-cardial perfusion defects: head-to-head comparison of thallium-201 SPECT to MRI perfusion. J Nucl Cardiol 2009;16:549–561.

Wackers FJT. Artifacts in planar and SPECT myocardial perfusion imaging. Am J Card Imaging 1992;6:42–58.

Wackers FJT. The maze of myocardial perfusion imaging protocols in 1994. J Nucl Cardiol 1994;1:180–188.


# CASE 20


### MICHAEL W. HANSON


### HISTORY

A 15-year-old boy presents with a 2-week history of severe lower back pain (worse on the right) that had its onset while he was playing tennis. Mild point tenderness is present at L4 and L5, primarily on the right side.

A

■**FIGURE 10-20A** Lumbosacral spine radiograph (right posterior oblique view). No abnormalities are seen on the plain radiograph.

B

■**FIGURE 10-20B** Posterior planar bone scan image. Radiotracer uptake is slightly more prominent at L4 than in the other lumbar vertebrae. The abnormality is bilateral

but more marked on the right.

C

**FIGURE 10-20C** Coronal single-photon emission CT bone scan images. Prominent abnormal radiotracer uptake is clearly defined, bilaterally, at L4 in the posterior elements (right greater than left).

D

**FIGURE 10-20D** Transverse single-photon emission CT bone at the L4 level. Bilateral foci of abnormal radiotracer uptake are seen (right greater than left). The transverse projection further localizes the abnormal radiotracer to the region of the pars interarticularis.

## DIFFERENTIAL DIAGNOSIS

**Mechanical low back pain:** This entity occurs secondary to mechanical strain on paraspinal and spinal ligaments, muscles, and facet joints. Clinical findings can mimic skeletal trauma. Imaging studies are typically normal. The abnormal bone scan in the case illustrated, therefore, excludes this diagnosis as the sole explanation of symptoms. Instead, it indicates the presence of skeletal pathology.

**Herniated lumbar disk:** Symptoms and signs can make distinction of this diagnosis from other causes of low back pain difficult. CT/myelography or MRI would be needed to confirm this diagnosis. However, the bone scan would be expected to be negative, unlike the study in the case illustrated. Furthermore, the location of abnormality in the posterior elements on the bone scan makes this diagnosis unlikely.

**Stress fracture of the lamina:** This entity has typically been reported in runners with low back pain. The plain radiographs can be entirely normal. However, an abnormal accumulation of radiotracer would be expected to be seen in the lamina, rather than in the pars interarticularis (as shown in Figure 10-24D), making lamina fracture unlikely.

- **Pars interarticularis stress fracture (spondylolysis):** This entity is commonly seen in athletes with low back pain. Radiographs are commonly normal but a bone scan, which is more sensitive, typically shows abnormal radiotracer uptake in the region of the one or both pars interarticularis. The localization of abnormal radio-tracer uptake on the SPECT bone scan in the case illustrated makes this the most likely diagnosis.
- **Tumor or infection:** The bone scan findings are nonspecific. However, tumor or infection in the case illustrated would be unlikely to cause the small, focal, bilateral abnormalities shown.

## DIAGNOSIS

## Bilateral stress fractures of the pars interarticularis

## KEY FACTS

### Clinical

- Spondylolysis refers to a break in bone continuity that results from a defect in the junction between the superior and inferior processus articularis.
- Spondylolysis is present in approximately 7% of individuals and in up to 50% of athletes who have low back pain.
- Spondylolysis is more commonly seen in gymnasts, football linemen, and weight lifters, and it is likely due to repeated hyperflexion and hyperextension of the lumbar spine.
- Spondylolysis is usually treated by conservative means (e.g., bracing and restricted activity).
- Spondylolysis is one of three principal causes of spon-dylolisthesis, a condition characterized by the forward (or occasionally, backward) displacement of a vertebra relative to the next lowest vertebra.

### Radiologic

- Bone scintigraphy is a more sensitive indicator of acute stress injury than plain radiography; radiographic changes may not be seen acutely even when the bone scan is abnormal.
- Radionuclide bone scanning can help to determine the chronicity of fractures seen on plain radiographs. Acute fractures have increased radiotracer activity, and chronic fractures have decreased radiotracer activity.
- SPECT bone imaging offers an advantage over planar scintigraphic imaging by

avoiding the superimposition of bony structures that is present on planar imaging. Image contrast is improved by SPECT imaging, often allowing abnormalities to be more confidently localized by SPECT than by planar imaging.

## SUGGESTED READING

Campbell RS, Grainger AJ, Hide IG, et al. Juvenile spondylolysis: a comparative analysis of CT, SPECT and MRI. Skeletal Radiol 2005;34:63–73.

Collier BD, Johnson RP, Carrera GF, et al. Painful spondylolysis or spon-dylolisthesis studied by radiology and single-photon emission computed tomography. Radiology 1985;54:207–211.

Holder LE. Bone scintigraphy in skeletal trauma. Radiol Clin North Am 1993;31:739–781.

Pecina MM, Bojanic I. Overuse injuries of the musculoskeletal system. Boca Raton, FL: CRC, 1993;89–120.

Pennell RG, Maurer AH, Bonakdarpour A. Stress injuries of the pars inter-articularis: radiologic classification and indications for scintigraphy.AJR Am J Roentgenol 1985;145:763–766.

Rogers LF. Radiology of Skeletal Trauma (2nd ed). New York, NY: Churchill Livingstone, 1992;565–572.

Zukotynski K, Curtis C, Grant FD, et al. The value of SPECT in the detection of stress injury to the pars interarticularis in patients with low back pain. J Orthop Surg Res 2010;5:13.

# CASE 21

**MICHAEL W. HANSON**

### HISTORY

A 37-year-old man with severe three-vessel coronary artery disease, prior myocardial infarction, and percutaneous transluminal coronary angioplasty presents with chest pain and cardiac enzyme elevation compatible with recurrent myocardial infarction. A multigated cardiac blood pool study showed a dilated left ventricle, multiple segmental wall motion abnormalities, and an left ventricular ejection fraction (LVEF) of 14%. He is referred for a Tl-201 myocardial perfusion study for assessment of myocardial viability.

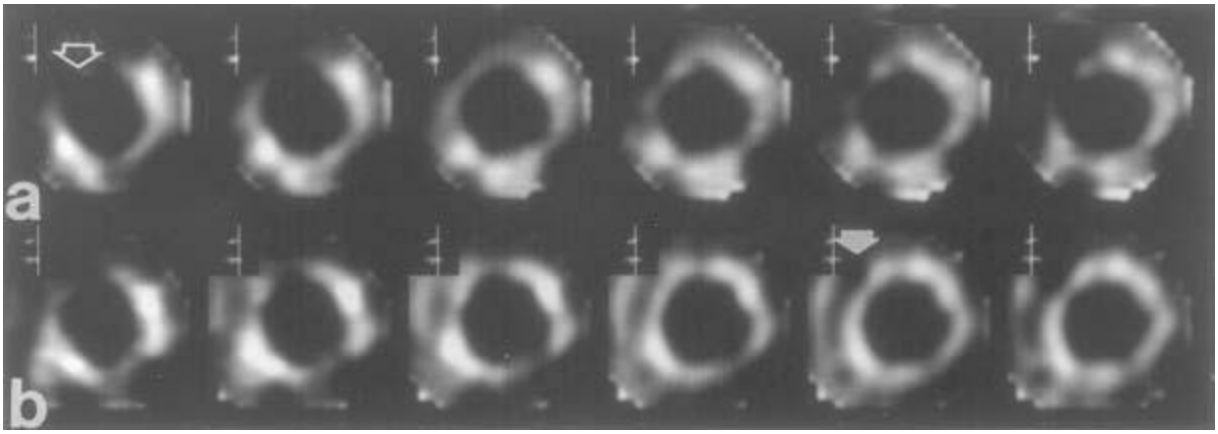


**FIGURE 10-21** Short axis images from a Tl-201 study performed at rest **(top row, a)** and after 4-hour redistribution **(bottom row, b).** The left ventricle is dilated. Markedly diminished radiotracer uptake is seen in the low anterior wall, low an-teroseptum and anterior and inferior apex on the rest study which does not change at 4 or 24 hours (open arrow), consistent with infarcted, nonviable myocardium. The mid and basilar anteroseptum has diminished radiotracer at rest that improves at 4 hours (closed arrow), consistent with ischemic, viable myocardium. The anterolateral and posterolateral walls also contain viable myocardium.

## DIFFERENTIAL DIAGNOSIS

**Normal myocardium:** This diagnosis is unlikely because of the segmental changes over time in a pattern consistent with either infarcted, nonviable myocardium, or ischemic, viable myocardium.

**Hypertrophic cardiomyopathy:** The marked dilatation of the left ventricle with segmentally heterogeneous distribution of radiotracer makes this diagnosis unlikely.

**Ischemic cardiomyopathy:** The distribution of Tl-201 is heterogeneous, with segmental areas of diminished Tl-201 uptake on the immediate image that improves over time (indicating viable myocardium) and areas of markedly diminished Tl-201 uptake that do not change over time (indicating nonviable myocardium). These findings, in conjunction with the prior cardiac catheterization findings, make this the most likely diagnosis.

**Idiopathic dilated cardiomyopathy:** The left ventricle in this case is dilated, which can be seen in idiopathic dilated cardiomyopathy. However, the myocardial per-fusion is more heterogeneous in this study than is typically seen in idiopathic cardiomyopathy, making this diagnosis unlikely.

## DIAGNOSIS

# Ischemic cardiomyopathy with areas of ischemic and viable myocardium

## KEY FACTS

### Clinical

- The term *stunned myocardium* is used to refer to transiently dysfunctional myocardium (i.e., myocardium having impaired contractility) that is reversible after restoration of coronary artery blood flow. Stunned myocardium is seen in several settings, including: (1) after an acute episode of myocardial ischemia (e.g., an episode of angina pectoris) and (2) after acute coronary artery occlusion reversed by thrombolytic therapy.
- The term *hibernating myocardium* is used to refer to longstanding (but potentially reversible) dysfunctional myocardium in the resting basal state. Hibernating myocardium is seen with chronic myocardial ischemia from prolonged periods of reduction in coronary artery blood flow (i.e., in the setting of chronic coronary artery disease). This impaired myocardial contractility is reversible after restoration of coronary artery perfusion.
- An accurate, noninvasive determination of viable (i.e., stunned or hibernating) myocardium is important for identification of myocardial segments that will benefit most from revascularization procedures.
- In patients with unexplained congestive heart failure, severely depressed LVEF and no history of angina pectoris or myocardial infarction, it is important to distinguish ischemic from idiopathic left ventricular dysfunction so that appropriate therapy can be started.
- Myocardial viability studies in patients with known severe multivessel coronary artery disease and left ventricular dysfunction can help to decide which revas-cularization procedure (i.e., complete revascularization with bypass surgery or limited revascularization with coronary angioplasty) should be performed.

### Radiologic

- Myocardium can be confidently assumed to be viable if there is normal contractility on imaging studies that are used to assess wall motion (e.g., MUGA, first-pass radionuclide angiography, contrast ventriculography, or echocardiography). However, if there is a resting wall motion abnormality, the status of myocardial viability (i.e., whether the myocardium is stunned, hibernating, or nonviable) cannot be reliably determined based on the wall motion abnormality alone. Segmental myocar-dial viability can, however, be assessed reliably using Tl-201 myocardial perfusion imaging

by either a rest-redistribution method or a stress-reinjection method.

- An alternative imaging technique for assessment of myocardial viability is PET using F-18 FDG, viewed by some investigators as the preferred imaging technique. Viable myocardium takes up this radiotracer, while nonviable myocardium does not take it up. Limitations include availability, cost, the need to regulate plasma glucose levels to optimize F-18 FDG uptake, and regional heterogeneity of F-18 FDG uptake that can occur even in normal subjects.
- Same-day rest/stress myocardial perfusion imaging with Tc-99m sestamibi is another technique for assessment of myocardial viability in patients with chronic coronary artery disease and left ventricular dysfunction. However, in comparison to Tl-201 redistribution or reinjection and F-18 FDG PET, it underestimates the extent of viable myocardium.

## SUGGESTED READING

Candell-Riera J, Romero-Farina G, Aguade-Bruix S, et al. Prognostic value of myocardial perfusion-gated SPECT in patients with ischemic cardio-myopathy. J Nucl Cardiol 2009;16:212–221.

Dilsizian V, Arrighi JA, Diodati JG, et al. Myocardial viability in patients with chronic coronary artery disease. Comparison of Tc-99m sestamibi with thallium reinjection and F-18 fluorodeoxyglucose. Circulation 1994;89:578–587.

Dilsizian V, Bonow RO. Current diagnostic techniques of assessing myo-cardial viability in patients with hibernating and stunned myocardium. Circulation 1993;87:1–20.

Schelbert HR. Metabolic imaging to assess myocardial viability. J Nucl Med 1994;35(Suppl):8S–14S.

Tio RA, Dabeshlim A, Siebelink HM, et al. Comparison between the prognostic value of left ventricular function and myocardial perfusion reserve in patients with ischemic heart disease. J Nucl Med 2009;50:214–219.

# CASE 22

**BENNETT B. CHIN**

### HISTORY

A 50-year-old female presents with newly diagnosed breast cancer and an axillary mass.

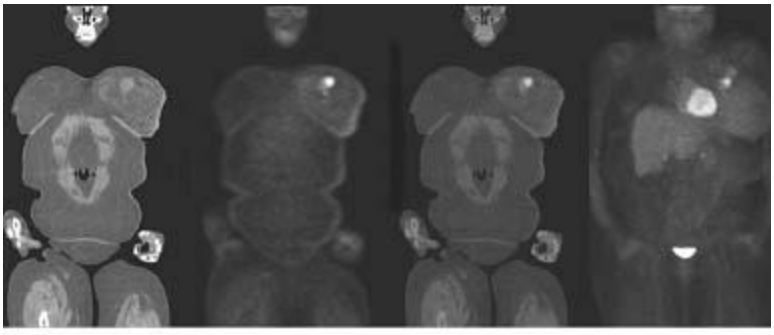

A

■**FIGURE 10-22A** PET CT scan following the intravenous administration of F-18. Coronal CT **(left),** FDG PET **(second from left),** FDG PET CT fusion **(second from right),** and maximum intensity reprojection (MIP; **right)** images. There is a focus of increased FDG activity in the medial aspect of the left breast. (See color insert).

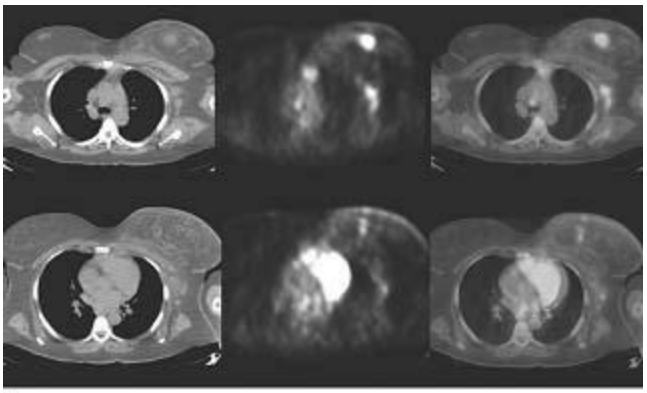

B

■**FIGURE 10-22B** Axial CT **(left),** FDG PET **(middle),** and FDG PET CT fusion **(right)** images. **(Top row)** Intense focal FDG uptake in the large breast lesion, and multiple lymph nodes regions (axillary, anterior mediastinal, and precarinal). Mild increased FDG uptake is also present in adjacent skin thickening and subcutaneous tissues. **(Bottom row)** Second focus in the left breast, skin thickening, and additional left axillary lymph nodes also show increased FDG uptake. (See color insert)

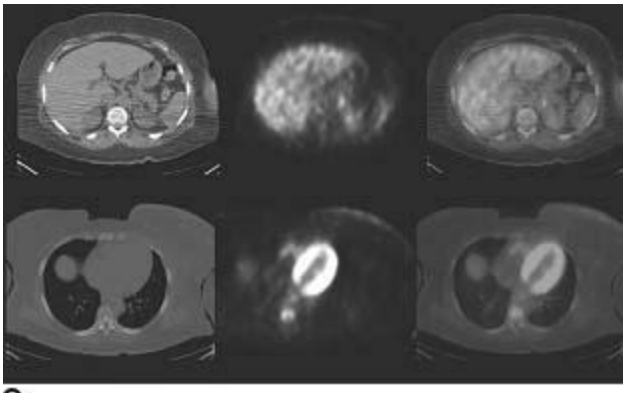

C

■**FIGURE 10-22C** Axial CT **(left),** FDG PET **(middle),** and FDG PET CT fusion

**(right)** images. **(Top row)** Left adrenal shows moderate focal FDG uptake. **(Bottom row).** Thoracic vertebral marrow shows intense focal FDG uptake without CT abnormality. (See color insert)

## DIFFERENTIAL DIAGNOSIS

- **Breast cancer and artifacts from postoperative inflammation, radiotherapy, and brown fat.** Although FDG accumulation may occur in postsurgical sites due to inflammation, several lymph node sites are asymmetrically enlarged and intensely FDG avid, corresponding to pathologically enlarged lymph nodes draining the primary breast tumor. There is no evidence of prior surgical intervention. The skin thickening is relatively focal and correlates to increased FDG activity in both the skin and subcutaneous tissues. Although concurrent radiotherapy can cause FDG uptake, inflammatory uptake due to radiation are typically more diffuse and less FDG avid. Brown fat can occur in multiple sites, including intra-abdominal sites; however, CT findings should co-localize to adipose density tissue. Intra-abdominal "brown fat" is also more commonly seen when there is involvement of the more common sites such as the supraclavicular regions.
- **Breast cancer and metastatic melanoma.** Melanoma can have a metastatic distribution that may mimic other primary malignancies such as breast cancer, lymphoma, and other highly glycolytic tumors with widespread metastases. Metastases can disseminate to virtually any site; however, the largest and most extensive abnormalities in this case are located in a single breast. In the absence of more diffuse widespread whole body involvement, the predominant involvement within a single breast makes metastatic melanoma less likely.
- **Breast cancer and lung cancer.** Although synchronous tumors can occur, the absence of a primary lung lesion, and the absence of secondary signs of obstructive airways disease make this less likely.
- **Inflammatory breast cancer and distant metastases.** Intense, focal accumulation within the breast mass makes breast cancer the primary consideration. Additional satellite lesions in the breast are highly suggestive of multifocal breast cancer. Moderate uptake in the thickened skin and adjacent subcutaneous soft tissues are typical of inflammatory breast cancer. Lymph node metastases to the axillary, internal mammary, and distant mediastinal lymph nodes may be seen in advanced metastatic breast cancer. Bone metastases may be evident by FDG PET without evidence of involvement by CT. Also, early adrenal metastases may be seen by FDG PET.

## DIAGNOSIS

## Inflammatory Breast Carcinoma with distant metastases

## KEY FACTS

### Clinical

- Breast cancer, the most common malignancy in women, frequently has intraductal histology (-80% incidence); this is typically FDG avid.
- Lobular breast carcinoma is relatively uncommon (˜5% to 10% incidence) but may have low FDG uptake and thus is a potential *false negative.*
- Metastatic breast cancer first spreads to the draining axillary lymph nodes. Because breast cancer is most commonly detected at an early stage, sentinel lymph node (SLN) biopsy is the most accurate first staging procedure. Small, early microscopic metastatic disease cannot be accurately detected by whole body FDG PET.
- In clinically late stage disease, FDG PET is highly sensitive and accurate in detecting distant metastases.
- Additional sites of metastases commonly include lung, liver, adrenal glands, soft tissues and bone.
- FDG PET CT is used primarily for staging of advanced stage breast cancer, and for detection of recurrent disease.
- FDG PET CT can also be used to accurately predict response to neoadjuvant chemotherapy in locally advanced breast cancer.
- Multifocal breast cancer is difficult to identify by conventional modalities such as mammography in which sensitivities as low as 10% have been reported. FDG PET can identify multifocal breast cancer with a sensitivity of approximately 50% to 60%.
- Incidentally discovered intense focal uptake in the breast is uncommon, but an early report suggests that this may represent malignancy with a relatively high incidence (<50%).
- Osseous metastatic lesions seen by CT may be either lytic or sclerotic. Sclerotic lesions are associated with a better long-term prognosis compared to lytic metas-tases. Sclerotic lesions have been reported to have a lower FDG uptake, and thus, are potentially *false negative* by FDG PET.

### Radiologic

- Mild, diffuse uptake is a normal finding in fibroglandu-lar breast tissue.
- Higher density fibroglandular breast tissue has higher normal uptake compared to primarily fatty or entirely fatty breast tissue.
- Overall, the meta-analysis of literature for FDG PET shows high overall accuracy in

the detection of recurrent disease (~90%).

- Potential *false positives* include inflammation or infection, and fibroadenomas (rarely). Focal "brown fat" may occur in the supraclavicular area, and, thus, careful correlation with CT is necessary to improve specificity.
- Recent surgery may result in inflammatory FDG uptake in draining lymph node basins; however, this is relatively uncommon.
- Concurrent or recent radiotherapy may also result in diffuse, and mild to moderate in intensity inflammatory FDG uptake; however, this is also relatively uncommon.
- A potential *false negative* is breast cancer of lobular histology. It occurs with a relatively low incidence (˜5% to 10%), but may show low FDG uptake.
- Early metastatic disease to axillary lymph nodes is more accurately identified by SLN biopsy. FDG PET CT is most useful in late stage disease and detection of recurrence.
- Sclerotic bone metastases from breast cancer have been reported to show low FDG uptake.
- FDG PET can accurately assess response to neoadju-vant chemotherapy in locally advanced breast cancer with a positive predictive value of >90%.

## SUGGESTED READING


Avril N, Rose CA, Schelling M, et al. Breast imaging with positron emission tomography and fluorine-18 fluorodeoxyglucose: use and limitations. J Clin Oncol 2000;18:3495–3502.

Cook GJ, Houston S, Rubens R, et al. Detection of bone metastases in breast cancer by (18)FDG PET: differing metabolic activity in osteoblastic and osteolytic lesions. J Clin Oncol 1998;16:3375–3379.

Isasi CR, Moadel RM, Blaufox MD. A meta-analysis of FDG-PET for the evaluation of breast cancer recurrence and metastases. Breast Cancer Res Treat 2005;90:105–112.

Schelling M, Avril N, Nahrig J, et al. Positron emission tomography using [F-18]fluorodeoxyglucose for monitoring primary chemotherapy in breast cancer. J Clin Oncol 2000;18:1689–1695.

Wahl RL, Siegel BA, Coleman RE, Gatsonis CG. Prospective multicenter study of axillary nodal staging by positron emission tomography in breast cancer: a report of the staging breast cancer with PET study group. J Clin Oncol 2004;22:277–285.


# CASE 23


**BENNETT B. CHIN**


### HISTORY

A 67-year-old female with colon carcinoma, and who is 6 months status post partial colectomy and right hepatectomy presents with fatigue and ascites. Repeat FDG PET CT for restaging. Previous initial staging FDG PET CT study showed only metastases to

the right hepatic lobe.

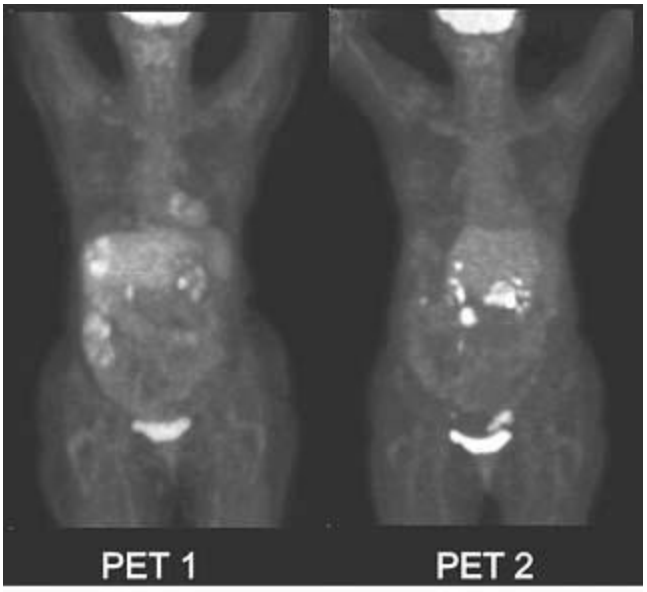


A

■**FIGURE 10-23A** Initial staging maximum intensity reprojection (MIP) images prior to resection **(left)** show only focal activity of liver metastases in the right hepatic lobe. MIP images 6 months after adjuvant chemotherapy and surgical right hepatectomy **(right)** shows several new foci of FDG accumulation within the abdomen and pelvis.

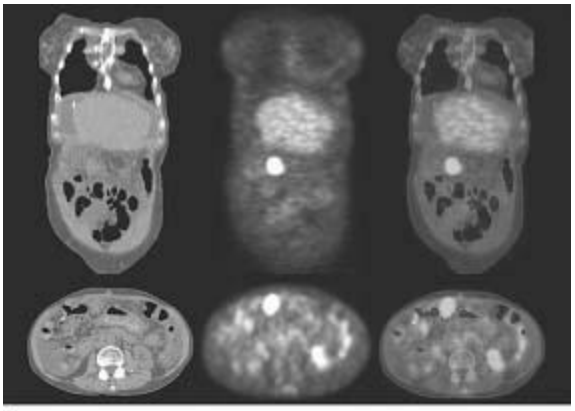

B

■**FIGURE 10-23B** Coronal and axial images from CT **(left),** PET **(middle)** and PET CT fusion **(right).** There is intense focal activity in a soft tissue mass in the greater omentum. (See color insert)

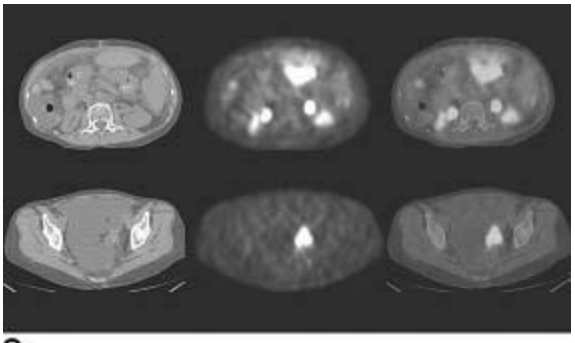

C

**FIGURE 10-23C** Axial images of CT **(left),** PET **(middle)** and PET CT fusion **(right).** There is intense focal activity within peritoneal and pelvic soft tissue masses. CT shows ascites with only mild FDG uptake. (See color insert)

## DIFFERENTIAL DIAGNOSIS

**Normal variant of focal bowel activity.** Focal activity within the bowel may occasionally occur as a normal variant; however, the intensity is typically mild to moderate, and the distribution is most commonly diffuse. Intense focal activity within the bowel, especially when associated with a soft tissue density or mass, is associated with a high incidence of malignancy even when detected incidentally. In the context of prior colon cancer, recurrent or metastatic disease is the primary considerations.

**Postoperative inflammation.** Although FDG accumulation may occur in postsurgical inflammatory sites such as surgical incisions, the presence of intra-abdominal inflammatory masses is uncommon. Inflammatory FDG uptake in postoperative sites typically occurs in subcutaneous or superficial soft tissues, and is commonly seen in association with inflammatory changes by CT such as soft tissue stranding. The clinical history may reveal signs or symptoms of complications including fever, abdominal pain, or postoperative wound infection.

**Liver and peritoneal abscesses.** As above, both clinical history and CT findings help distinguishing postoperative inflammatory changes from residual or recurrent tumor. In this case, FDG PET alone may be difficult to interpret due to prior partial hepatectomy in the right upper quadrant. CT co-localization clearly shows intense focal extrahepatic FDG accumulation, as well as focal FDG accumulation in soft tissue masses.

**Peritoneal and mesenteric metastases.** Intense, focal accumulation within soft tissue masses in the omen-tum and mesentery are highly predictive of metastases. FDG PET CT has the highest sensitivity for detection of recurrence. The addition of CT improves the accuracy compared to FDG PET alone, primarily by improving the specificity and certainty of localization.

## DIAGNOSIS

# Colorectal carcinoma recurrence with mesenteric and peritoneal metastases

## KEY FACTS

### Clinical

- The histology of colorectal carcinoma is most commonly adenocarcinoma (>90%), and this histology is typically very FDG avid.
- A variant of adenocarcinoma, the mucinous subtype, may have low FDG uptake, and thus, is a potential false negative. In the context of suspected metastases from mucinous adenocarinoma, such as enlarging lung nodules by CT, recurrence should remain a primary consideration.
- FDG PET CT is utilized for staging and detection of recurrent disease. The primary diagnosis is made via endoscopy.
- Colorectal carcinomas typically first metastasize via lymphatics, but hematogenous spread to liver and lungs is also common. Peritoneal and mesenteric metastases may also occur. Distant metastases to bone and soft tissues more typically occur at later stages.

### Radiologic

- Combined FDG PET CT has the highest overall accuracy in staging and detection of recurrent colorectal carcinoma; sensitivity is over 90%.
- Incidentally discovered focal uptake in the GI tract, especially when associated with a soft tissue mass, is commonly (>50%) associated with either a precancerous or cancerous GI malignancy. Thus, focal, intense FDG uptake in the GI tract discovered incidentally is generally considered concerning for malignancy.
- Potential *false positives* include inflammation/infection, normal physiologic uptake (typically bowel), and adenomas (rarely).
- Intra-abdominal focal “brown fat” has been reported, but is rare.
- Recent abdominal surgeries (typically within <1 month), including staging and debulking surgeries, may result in inflammatory FDG uptake in adjacent lymph node basins.
- Concurrent or recent radiotherapy may cause focal inflammatory uptake at the site of the primary; however, this is typically modest and decreases over several months.
- In residual masses (e.g., a presarcal mass postradio-therapy), intense, focal FDG uptake commonly represents residual tumor if radiotherapy or surgery are remote (typically >3 months).

- Asymmetric, decreased bone marrow activity may be present in a geometric configuration corresponding to the radiation port.
- Potential *false negatives* include mucinous adenocar-cinomas and neuroendocrine GI tumors, which may show relatively low FDG uptake.
- Carcinoid, the most common neuroendocrine tumor, may have low FDG avidity.
- Concurrent chemotherapy may lower FDG uptake in tumors.
- Small, early peritoneal metastases may be very difficult to identify by either CT or FDG PET alone; combined FDG PET CT has the highest overall diagnostic accuracy.
- Another GI tumor that may commonly show *low* FDG uptake is primary hepatocellular carcinoma. Some gastric carcinomas and GIST may show low or modest FDG uptake and thus are potentially false negatives by FDG PET alone. Size assessment by CT may be helpful in these cases.
- Other GI tumors typically showing *high* FDG uptake include cholangiocarcinoma, small bowel adenocarci-noma, and pancreatic adenocarcinoma.

## SUGGESTED READING

Chin BB, Chang PPL. Gastrointestinal malignancies evaluated with F-18-fluoro-2-deoxyglucose positron emission tomography. Best Pract Res Clin Gastroenterol 2006;20:3–21.

Cohade C, Osman M, Leal J, et al. Direct comparison of 18F-FDG PET and PET/CT in patients with colorectal carcinoma. J Nucl Med 2003;44:1797–1803.

Huebner RH, Park KC, Shepherd JE, et al. A meta-analysis of the literature for whole-body FDG PET detection of recurrent colorectal cancer. J Nucl Med 2000;41:1177–1189.

Kalff V, Hicks RJ, Ware RE, et al. The clinical impact of 18F-FDG PET in patients with suspected or confirmed recurrence of colorectal cancer: A prospective study. J Nucl Med 2002;43:492–499.

Kamel EM, Thumshirn M, Truninger K, et al. Significance of incidental 18F-FDG accumulations in the gastrointestinal tract in PET/CT: Correlation with endoscopic and histopathologic results. J Nucl Med 2004;45:1804–1810.

# Chapter ELEVEN

# Cardiac Imaging

**LAURA E. HEYNEMAN** ▪ CHAPTER EDITOR

Glen A. Toomayan

Nicole Proscia

Phil B. Hoang

Joshua A. Bryant

Christopher J. Roth

Melissa Hayes

Danielle L. Wellman

## CASE 1

**LAURA E.
HEYNEMAN**

### HISTORY

An 18-year-old woman with exertional dyspnea and chest pain.

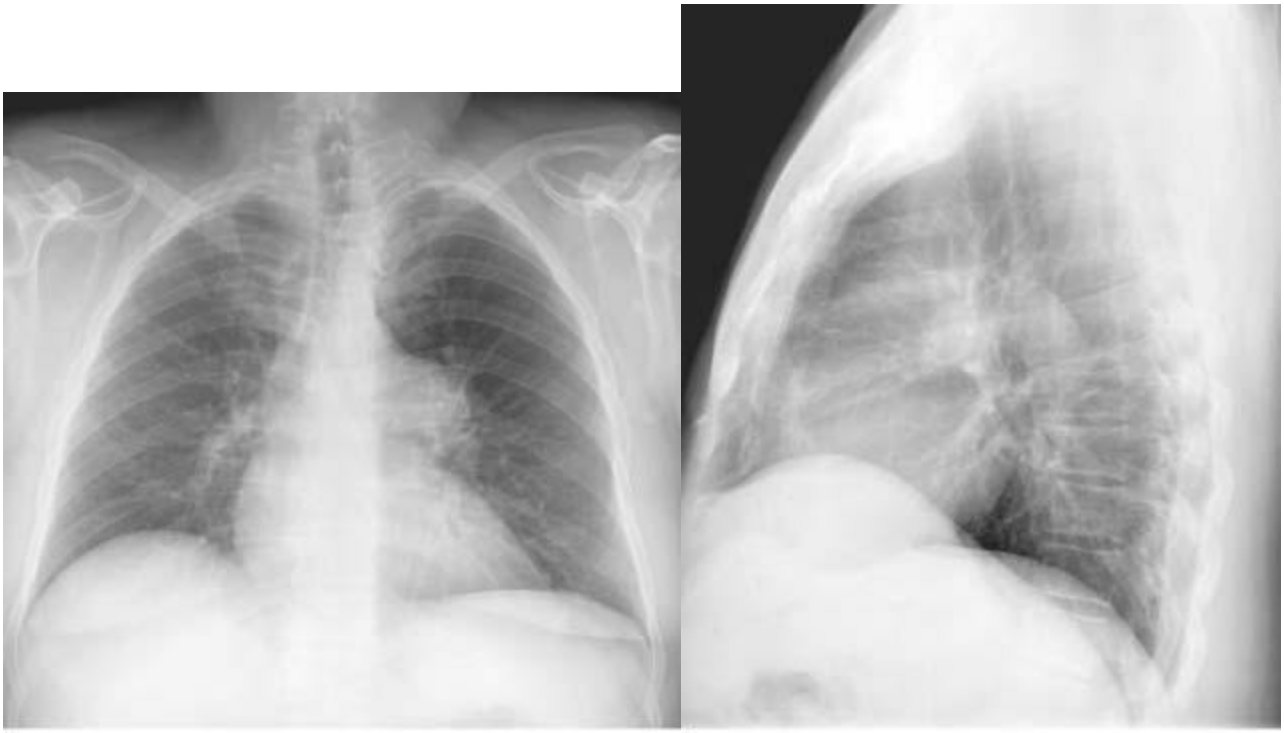


■**FIGURES 11-1A and 11-1B** Frontal and lateral chest radiographs. There is enlargement of the main pulmonary artery and left pulmonary artery. On the lateral radiograph, there is mild right ventricular prominence and enlargement of the left pulmonary artery.


■**FIGURES 11-1C and 11-1D** Axial **(C)** and volume-rendered **(D)** images from contrast-enhanced chest CT. There is enlargement of the main and left pulmonary artery, with a smaller right pulmonary artery. (See color insert)

## DIFFERENTIAL DIAGNOSIS

- **Valvular pulmonary stenosis:** Enlargement of the main pulmonary artery (PA) and left hilum (with resultant asymmetric pulmonary blood flow to the left) and mild enlargement (with hypertrophy) of the right ventricle are the hallmarks of this entity and make it the most likely diagnosis.
- **Pulmonary artery hypertension (PAH):** This entity might be a consideration, because the main and left pulmonary arteries are enlarged. However, the blood flow pattern in PAH would be one of symmetric hilar enlargement with pruning of peripheral vessels. The asymmetric blood flow seen in the case shown above is not characteristic of PAH.
- **Atrial septal defect (ASD):** Right ventricular enlargement and increased pulmonary blood flow is a feature of an ASD. In an ASD, all of the pulmonary vessels should be enlarged rather than the asymmetric enlargement as in this case.
- **Right pulmonary artery hypoplasia:** This entity might be considered because of the discrepancy in size of the two pulmonary arteries. However, in the setting of PA hypoplasia, the right lung is almost always hypoplastic and there is resultant mediastinal shift to the right. In the case provided, the right lung is normal in size and there is no mediastinal shift; therefore, PA hypoplasia is unlikely.
- **Pulmonary embolism:** This entity can produce asymmetric pulmonary blood flow if there is a large central blood clot. However, no emboli are evident on the CT.

## DIAGNOSIS

**Valvular pulmonary stenosis**

## KEY FACTS

### Clinical

- Valvular pulmonary stenosis is a relatively common congenital heart disorder. Dypsnea and fatigue are the most common symptoms.
- A loud ejection systolic murmur heard at the upper left sternal border is typical. Electrocardiogram (ECG) findings indicate right ventricular hypertrophy and right axis deviation. Cardiac MR and catheterization show valvular pulmonary stenosis with a systolic pressure gradient across the pulmonic valve.

### Radiologic

- The characteristic radiographic findings of valvular pulmonary stenosis can be explained on the basis of the abnormal hemodynamics.
    - During systole, the high pressure within the right ventricle is converted into high-velocity flow, creating a forceful jet in the direction of the main and left

pulmonary arteries. Dilatation of the main and left pulmonary artery results.

- A low-pressure zone can be created immediately lateral to the central axis of the jet stream. Such reduced pressure has a suction effect, facilitating the leftward flow at the expense of right pulmonary flow. The resultant abnormal flow pattern can be shown by chest radiographs, CTs, pulmonary angiograms, or perfusion lung scan.

- The high pressure felt by the right ventricle proximal to the stenosis results in right ventricular hypertrophy. On the lateral chest radiograph, the effects on the right ventricle are evident by mild enlargement of the right ventricular shadow. On cross-sectional imaging, enlargement of the right ventricular chamber and thickening of the right ventricular wall are evident.
- Cardiac MR may not only demonstrate the effects on the right ventricle but also the turbulent flow across the pulmonic valve, and phase contrast cardiac MR imaging can calculate the pressure gradient across the valve.
- The above-mentioned left lateralized pulmonary blood flow pattern of valvular pulmonary stenosis is distinctly different from the bilaterally symmetric increase in pulmonary vascularity seen in an ASD or the symmetric central enlargement with peripheral pruning seen in PAH.

## SUGGESTED READING

Castaner E, Gallardo X, Rimola J, et al. Congenital and acquired pulmonary artery anomalies in the adults: radiologic overview. Radiographics 2006;26:349–371.

Chen JJ, Manning MA, Frazier AA, et al. CT angiography of the cardiac valves: normal, diseased, and postoperative appearances. Radiographics 2009;29:1393-1412.

# CASE 2

**LAURA E. HEYNEMAN**

### HISTORY

A 15-year-old boy with a 5-year history of exertional dyspnea, cyanosis, and intermittent chest pain.

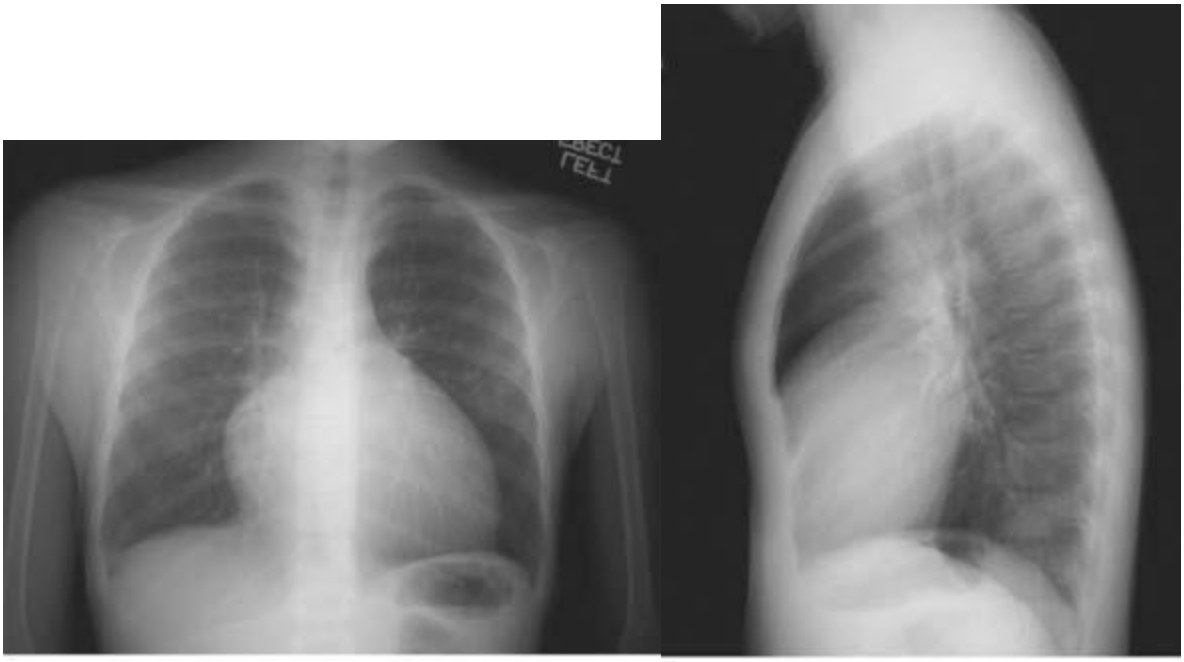

A B

**FIGURES 11-2A and 11-2B** Frontal **(A)** and lateral **(B)** chest radiographs. There is decreased pulmonary blood flow as evidenced by a small main pulmonary artery, small hila, and small peripheral vessels. Marked right-sided cardiomegaly is seen without evidence of left-sided involvement.

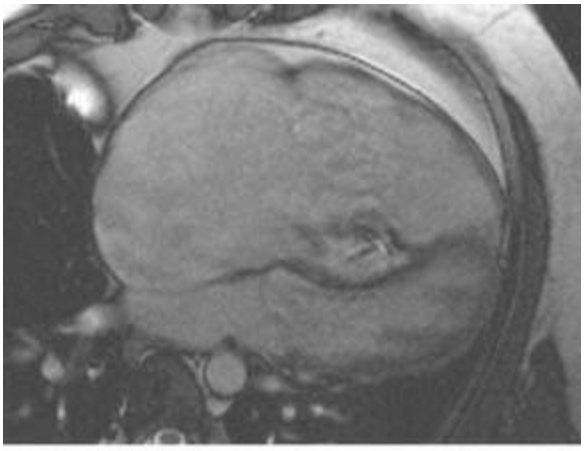

C

**FIGURE 11-2C** Long axis SSFP MR image confirms massive right heart enlargement. The septal leaflet of the tricuspid valve is apically displaced and plastered to the septal wall, and the anterior leaflet of the tricuspid valve is tethered to the anterior wall of the right ventricle. The interventricular septum is bowed toward the left; on cine imaging (not shown), this bowing is more prominent in diastole, indicative of right ventricular volume overload. There is a regurgitant jet of systolic dephasing deep within the right ventricular cavity, indicating the abnormally positioned and regurgitant tricuspid valve. On cine views (not shown), there is virtually no contraction of the base and midportion of the RV, with only a small portion of the RV apex contracting normally. Additionally,

there is an ASD.

## DIFFERENTIAL DIAGNOSIS

- **Ebstein's anomaly:** This is the best diagnosis based on the decreased pulmonary blood flow, markedly enlarged right heart, and abnormality of the tricuspid valve as demonstrated on the MR.
- **Pulmonary atresia (without a ventricular septal defect [VSD] and with an incompetent tricuspid valve):** The markedly enlarged right heart raises this entity as a possible diagnosis. However, without benefit of surgery, patients with this entity usually die in infancy.
- **Tetralogy of Fallot (TOF):** Despite the similarity of pulmonary oligemia and clinical cyanosis in both entities, the heart in patients with TOF would not attain the size shown above for two reasons. First, the right ventricle in TOF is subjected to increased pressure in the setting of infundibular stenosis; therefore, the right ventricular wall hypertrophies but the cavity does not dilate excessively. Additionally, in patients with TOF, there is a large VSD, which serves as a pathway for blood flow when the pulmonary outflow tract is obstructed. This prevents the right ventricle from markedly dilating. Furthermore, there is no reason for the right atrium to be dilated in TOF. Additionally, in TOF, the tricuspid valve would be normal.
- **Tricuspid regurgitation (TR):** Acquired tricuspid insufficiency is a strong consideration as TR will result in enlargement of the right atrium and right ventricle (RV), as well as decreased blood flow once the RV fails. The clinical history is helpful in distinguishing the two entities. In an infant, a congenital etiology would be favored. In an older child or young adult, acquired TR is usually caused by acute endocarditis (often in the setting of intravenous drug abuse or an infected central venous catheter), whereas Ebstein's would result in a more chronic history of symptoms.
- **Cardiomyopathy:** Marked cardiomegaly on the radiograph can be seen with a dilated cardiomyopathy, but it would be very unusual for the cardiomegaly to be purely right sided. Additionally, the pulmonary blood flow is rarely decreased in the setting of a dilated cardiomy-opathy. Usually, patients with dilated cardiomyopathy demonstrate pulmonary edema from left ventricular (LV) failure rather than diminished blood flow.
- **Pericardial effusion:** This entity can produce marked enlargement of the cardiac silhouette. Large effusions are usually chronic. Normal pulmonary blood flow is maintained in the setting of a pericardial effusion unless there is tamponade; when tamponade impairs the function of the right heart, pulmonary blood flow will be decreased. Additionally, if there is a pericar-dial effusion, the pericardial fluid collection (and not a markedly enlarged right heart) would be seen on the MR images.

# DIAGNOSIS
**Ebstein's anomaly**

# KEY FACTS
## Clinical
- Ebstein's anomaly can present in the newborn period (with cyanosis and marked cardiomegaly) or later in childhood, usually with cyanosis, dyspnea, chest pain, or arrhythmias.
- The primary abnormality in Ebstein's anomaly involves the tricuspid valve. The posterior and septal leaflets of the tricuspid valve are delaminated and apically displaced into the right ventricle. The anterior leaflet is often adherent to the anterior wall of the right ventricle. The septal leaflet may be absent. The overall result is severe tricuspid insufficiency.
- The portion of the RV into which the tricuspid leaflets are displaced and the anterior leaflet is tethered do not contract normally. This portion of the RV wall is somewhat redundant and boggy, and the affected portion of the RV acts essentially as a collecting chamber. This is referred to as the "atrialized" portion of the RV.
- A right-to-left shunt across an ASD or patent foramen ovale is often present.
- Standard surgical repair involves replacement of the tricuspid valve, plication of the atrialized right ventricle, and closure of an ASD.

## Radiologic
- The radiographic findings in Ebstein's anomaly are highly suggestive of the diagnosis, which can often be established definitively by echocardiography or cardiac MR.
- Gross enlargement of the right ventricle and the right atrium is typical for Ebstein's anomaly because severe tricuspid insufficiency causes considerable right-sided volume overload without a runoff at the ventricular level.
- Pulmonary oligemia is caused by (1) a marked decrease in forward pulmonary blood flow, (2) severe tricuspid insufficiency, and (3) right-to-left shunting across the atrial septum in those patients in whom there is an ASD.
- On MRI, the abnormalities of the tricuspid valve are apparent, with gross enlargement of the right heart. The interventricular septum may be convex toward the left during diastole, indicating right ventricular volume overload.
- When evaluating a patient with Ebstein's anomaly, a search for an associated ASD should be conducted.

## SUGGESTED READING

Ferguson EC, Krishnamurthy R, Oldham SAA. Classic imaging signs of congenital cardiovascular abnormalities. Radiographics 2007;27:1323–1334.

Leschka S, Oechslin E, Husmann L, et al. Pre- and postoperative evaluation of congenital heart disease in children and adults with 64-section CT. Radiographics 2007;27:829–846.

Cook, AL, Hurwitz LM, Valente AM, Herlong JR. Right heart dilatation in adults: congenital causes. Am J Roentgenol 2007;189:592–601.

# CASE 3

**LAURA E. HEYNEMAN**

### HISTORY

A 2-year-old asymptomatic girl with a cardiac murmur since birth.


■**FIGURES 11-3A and 11-3B** Frontal and lateral chest radiographs show increased pulmonary blood flow as evidenced by dilation of all pulmonary vessels including the main pulmonary artery. There is moderate cardiomegaly with predominantly left-sided enlargement. The aortic arch is prominent.

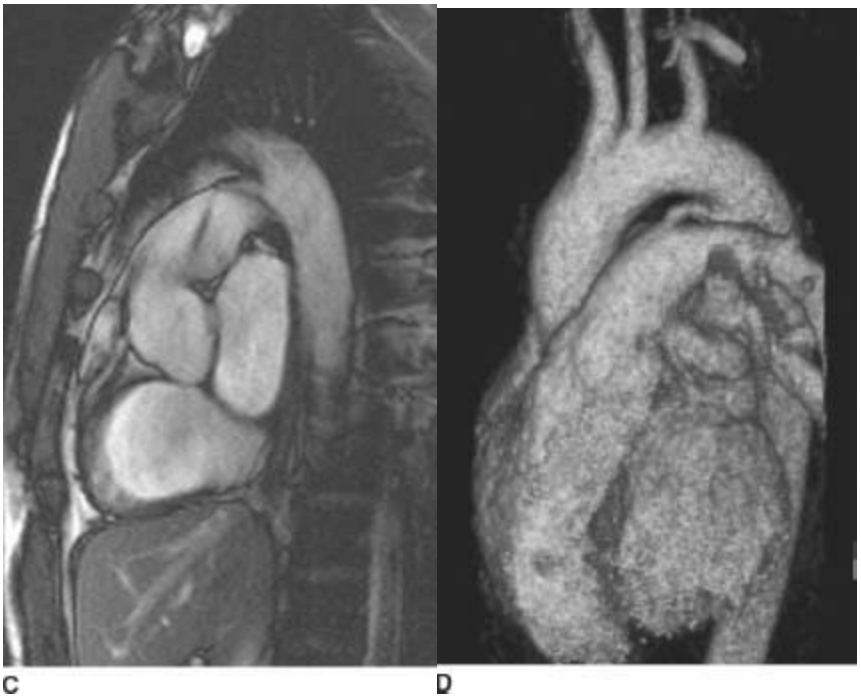


**FIGURES 11-3C and 11-3D** Oblique sagittal SSFP MR image **(C)** performed in a different patient with the same diagnosis demonstrates a flow jet within the main pulmonary artery. This flow jet appears to originate from a connection between the proximal descending aorta and the main pulmonary artery. Volume-rendered image from an MR angiogram **(D)** in this second patient reveals a connection between the proximal descending aorta and the main pulmonary artery. (See color insert)

## DIFFERENTIAL DIAGNOSIS

**Patent ductus arteriosus (PDA):** This lesion is the correct diagnosis because on the radiograph it results in increased pulmonary blood flow and pure left-sided cardiac enlargement. The transverse aorta may be enlarged. Additionally, the MR images demonstrate the connection between the aorta and the pulmonary artery with the resultant jet of turbulent flow within the pulmonary artery.

**Ventricular septal defect (VSD):** VSDs show increased pulmonary blood flow on a radiograph, but the right ventricle should be enlarged due to the fact that the RV has to accommodate the increased volume of blood coursing across the ventricular septum. Additionally, a VSD would not explain a connection between the aorta and PA as seen on the MR images.

**Atrial septal defect (ASD):** ASDs demonstrate increased pulmonary blood flow on a radiograph, but enlargement should be purely right-sided. The aortic arch may be small. Furthermore, an ASD would not explain the connection between the aorta and the PA as evidenced by the MR images.

## DIAGNOSIS

**Patent ductus arteriosus**

## KEY FACTS

### Clinical

- Patients with a large PDA are usually symptomatic in infancy because of congestive heart failure. Older children and adults with a small PDA may be asymptomatic until they develop Eisenmenger's physiology.
- Because there is a left-to-right shunt with no admixture of oxygenated and deoxygenated blood, PDA patients are not cyanotic.
- A continuous, "machinery-like" murmur is usually heard over the left upper sternal border.

### Radiologic

- There is increased pulmonary blood flow with dilation of all pulmonary vessels due to the substantial left-to-right shunt.
- In the absence of congestive heart failure or Eisen-menger's physiology, there is usually pure left-sided cardiomegaly with dilatation of both great arteries. The left atrium and left ventricle dilate to accommodate increased circulating blood volumes. The right heart is spared until the development of Eisenmenger's physiology, at which point right ventricular hypertrophy may be evident.
- On cross-sectional imaging, a direct communication between the proximal descending thoracic aorta (distal to the origin of the left subclavian artery) and the main pulmonary artery may be visualized. On cine bright blood MR imaging, a continuous jet of turbulent flow may be identified within the main pulmonary artery.

## SUGGESTED READING

Frank L, Dillman JR, Parish V, et al. Cardiovascular MR imaging of conotruncal anomalies. Radiographics 2010;30:1069–1094.

Martinez-Jimenez S, Heyneman LE, McAdams HP, et al. Nonsurgi-cal extracardiac vascular shunts in the thorax: clinical and imaging characteristics. Radiographics 2010;30:e41.

# CASE 4

**LAURA E. HEYNEMAN**

## HISTORY

A 2-day-old child with tachypnea, cyanosis, bilateral crackling rales, and a heart murmur.

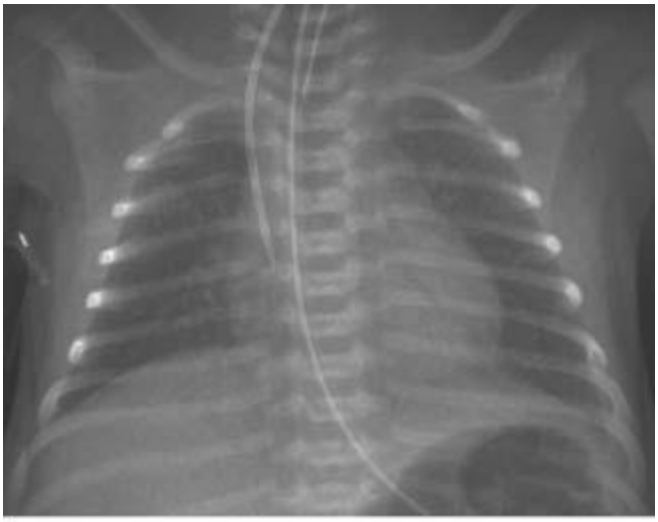

A

**FIGURE 11-4A** Frontal chest radiograph demonstrates an endotracheal tube, an enteric tube, a right internal jugular central venous catheter, diffuse pulmonary edema, and a normal cardiac size.

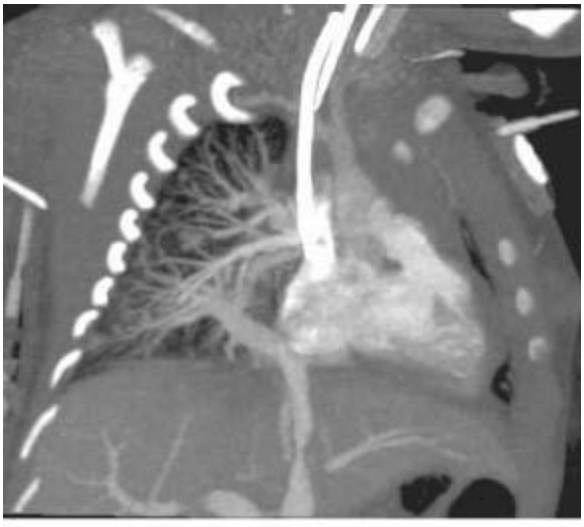

B

**FIGURE 11-4B** Oblique coronal MIP image from the venous phase of a pulmonary arteriogram shows that the pulmonary veins converge into a common collecting vessel; this common collecting vessel traverses the diaphragm and empties into the portal vein. Additional images (not shown) confirm that all of the pulmonary veins from both lungs drain into the common collecting vessel.

## DIFFERENTIAL DIAGNOSIS

- **Total anomalous pulmonary venous return, obstructed variety:** In this entity, patients are cyanotic, have pulmonary edema, and have a normal heart size. These features, along with the pulmonary angiogram findings, make this the correct diagnosis.
- **Hypoplastic left heart syndrome:** This entity is a cause of neonatal cyanotic heart disease and severe pulmonary edema. There are severe left-sided obstructive lesions with a right-to-left shunt at the ductal level and a left-to-right shunt at the atrial level. However, two facts make this diagnosis unlikely in this patient: (1) the cardiac size is usually markedly enlarged, and (2) the pulmonary veins drain normally into the left atrium. Neither of these features is present in the case shown.
- **Left-sided obstructive lesions:** These lesions—for example, aortic stenosis (AS) and coarctation of the aorta—may present in the neonatal period with severe congestive heart failure. However, two facts make this diagnosis unlikely: (1) patients with these lesions are not cyanotic, and (2) the heart is usually enlarged from left-sided failure, unless the obstruction is very proximal on the left (e.g., cor triatriatum).
- **Systemic arteriovenous (AV) fistulae:** These lesions—for example, vein of Galen malformation or hepatic hemangioendothelioma—can cause frank congestive heart failure early in life. However, this diagnosis is unlikely for two reasons: (1) patients with these lesions are not cyanotic, and (2) the heart is markedly enlarged due to high output failure.

## DIAGNOSIS

**Total anomalous pulmonary venous return, obstructed variety**

## KEY FACTS

### Clinical

- In the infradiaphragmatic, obstructed version of total anomalous pulmonary venous return, the common collecting pulmonary vein usually empties into the hepatic portal circulation. As a result, all pulmonary blood flow must course through the relatively high-resistance hepatic sinusoids before reconstituting within the inferior vena cava. Additionally, there is often a focal stenosis of the collecting vein at the level of the diaphragm; this results in further obstruction.
- Neonates with severe congestive heart failure due to this disorder present with cyanosis, tachypnea, and crackling rales. Frequently, the rales are loud enough to obscure the cardiac murmur. Because the heart size is normal, newborn respiratory distress syndrome can be mistakenly diagnosed.

- Helpful clues to the correct diagnosis include (1) normal heart size, (2) severe pulmonary edema, and (3) deepening cyanosis with feeding.
- Emergency surgical repair is indicated and consists of anastomosis of the pulmonary venous confluence to the left atrium. Thereafter, the ASD is repaired.

### Radiologic

- There is severe pulmonary edema from the obstruction of pulmonary venous outflow.
- All patients with total anomalous pulmonary venous return have a shunt that allows admixture of oxygenated and deoxygenated blood. This shunt is usually in the form of an ASD.
- In this entity, the heart is normal in size because of the severe obstruction to pulmonary venous outflow; as a result of the obstruction, not enough blood returns to the right heart to cause dilation.

## SUGGESTED READING

Ferguson EC, Krishnamurthy R, Oldham SAA. Classic imaging signs of congenital cardiovascular abnormalities. Radiographics 2007;27:1323–1334.

Leschka S, Oechslin E, Husmann L, et al. Pre- and postoperative evaluation of congenital heart disease in children and adults with 64-section CT. Radiographics 2007;27:829–846.

# CASE 5

**LAURA E. HEYNEMAN**

### HISTORY

A newborn boy noted to be extremely cyanotic, tachypneic, and tachycardic.

A

■**FIGURE 11-5A** Frontal chest radiograph. The pulmonary blood flow is increased. Moderate cardiomegaly with an egg-shaped cardiac contour is seen. The superior mediastinum is narrow.

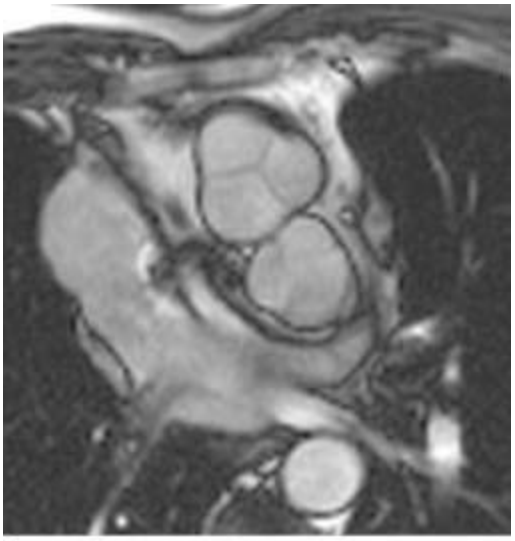

B

■**FIGURE 11-5B** Axial SSFP MR image in a different patient with the same disorder. The aortic valve with the sinuses of Valsalva is anterior and to the right of the pulmonic valve.

C

**FIGURE 11-5C** Oblique sagittal SSFP MR image shows that the aorta arises off of the anterior, heavily trabeculated right ventricle and the pulmonary artery arises off of the posterior, smooth-walled left ventricle. Note that there is right ventricular hypertrophy as a result of the right ventricle having to pump against systemic pressures.

## DIFFERENTIAL DIAGNOSIS

- **D-loop transposition of the great arteries (D-TGA):** This diagnosis is the best choice, given the history, the radiographic findings of increased blood flow, and the "egg on a string" appearance of the cardiomediastinal silhouette. The characteristic findings are present on the MR, confirming the diagnosis.
- **Large ventricular septal defect (VSD):** Patients with a VSD should not be cyanotic. Additionally, newborns with a VSD usually do not have increased pulmonary blood flow due to physiologic high pulmonary vascular resistance. Shunting in patients with a VSD is most often insignificant until pulmonary resistance falls at 6 weeks of life; it is at that point that their chest radiographs reflect increased pulmonary blood flow from left-to-right shunting. Furthermore, patients with a VSD do not have a narrow mediastinum because their great vessels are normally related.
- **Hypoplastic left heart syndrome:** Patients with this syndrome are also cyanotic neonates, but they are almost always in profound heart failure with pulmonary edema (and do not have increased pulmonary flow, as in the case presented). Furthermore, their hearts tend to be larger than those seen in the cases shown. These factors make this diagnosis unlikely.

- **Total anomalous pulmonary venous return with obstruction:** These patients are also cyanotic neonates, but their radiographs usually demonstrate severe pulmonary edema with a normal cardiac size.

# DIAGNOSIS

**D-loop transposition of great arteries (D-TGA)**

# KEY FACTS

## Clinical

- D-TGA accounts for 4% of congenital cardiac defects in children.
- D-TGA is the most common lesion to present with severe cyanosis immediately after birth.
- The basic pathologic anatomy of D-TGA is as follows: The aorta arises from the right ventricle and the pulmonary artery arises from the left ventricle. This results in two "closed loop" circulations that are incompatible with life without the presence of a shunt that allows admixture of oxygenated and deoxygenated blood. The shunt may be in the form of a patent foramen ovale, an ASD, or a PDA. However, these shunts may only temporize the situation, and emergent balloon septostomy may need to be performed to allow adequate mixing of pulmonary and systemic circulations.
- Current definitive repair is the Jatene procedure, in which the aorta and pulmonary vessels are switched. Previously, Mustard and Senning atrial baffle procedures were performed. In the Mustard or Senning procedures, the right venticle remained connected to the aorta. As a result, these patients would demonstrate marked right ventricular hypertrophy and eventually would develop right ventricular failure.

## Radiologic

- On the radiograph, there is increased pulmonary blood flow with moderate (right greater than left) cardiomegaly.
- The "egg on the string" appearance of the cardiomediastinal contour is due to several factors. The "egg" is due to cardiomegaly; the right heart is pumping against the high systemic vascular resistance and is enlarged to a greater degree than the left heart. Hence, a globular cardiac contour results. The "string" is due to a narrow mediastinum. The mediastinum is narrowed due to the fact that the aorta and main pulmonary artery have an abnormal relationship and have a more overlapping configuration than normal. Additionally, the mediastinum is narrowed due to involution of the thymus from stress.
- On cross-sectional imaging, the diagnosis of D-TGA may be made when the aortic valve is identified anterior and to the right of the pulmonic valve. The aorta is

connected to the anterior, trabeculated right ventricle and the pulmonary artery arises from the more posterior, smooth-walled left ventricle.

## SUGGESTED READING

Ferguson E, Krishnamurthy R, Oldham SAA. Classic imaging signs of congenital cardiovascular abnormalities. Radiographics 2007;27: 1323–1334.

Warnes, CA. Transposition of the great arteries. Circulation 2006;114:2699–2709.

# CASE 6

**GLEN A.**
**TOOMAYAN**

### HISTORY

A 14-year-old male presenting with a syncopal episode requiring cardiopulmonary resuscitation.

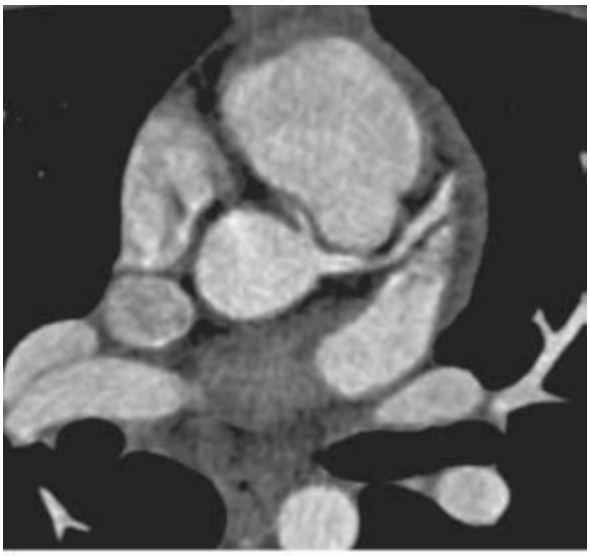

A

■**FIGURE 11-6A** Axial image from an EKG-gated contrast-enhanced cardiac CT reveals an anomalous origin of the RCA off of the left coronary sinus. The visualized portion of the RCA courses between the aorta and the right ventricular outflow tract.

B

**FIGURE 11-6B** Oblique axial CTA image along the axis of the main pulmonary artery demonstrates the anomalous origin of the right coronary artery from the left coronary sinus and its anomalous interarterial course as it heads toward its normal location within the right atrioventricular groove.

## DIFFERENTIAL DIAGNOSIS

**Anomalous origin of the right coronary artery (RCA) from the left coronary sinus with interarterial course:** There is no differential diagnosis. Coronary CT arteriography demonstrates both the right and left coronary arteries to arise from the left coronary sinus. The RCA passes between the ascending aorta and the main pulmonary artery.

## DIAGNOSIS

**Anomalous origin of the right coronary artery from the left coronary sinus with interarterial course**

## KEY FACTS

### Clinical

- Coronary artery anomalies have been identified in 0.3% to 1% of healthy individuals and are an important cause of myocardial ischemia, syncope, and sudden death in young adults. This particular anomaly is very rare, occurring in 0.019% to 0.17% of adults.
- Coronary artery anomalies may be classified as anomalies of coronary artery origin, course, or termination.
- They may also be classified as hemodynamically significant or insignificant.

- Hemodynamically significant anomalies result in abnormal myocardial perfusion and are associated with an increased risk of myocardial ischemia and sudden death.
- Hemodynamically significant anomalies include anomalous origin of a coronary artery from the pulmonary artery, anomalies of coronary artery origin with an interarterial course (between the aorta and pulmonary artery), and occasionally myocardial bridges.
- Treatment options for an anomalous coronary artery with an interarterial course include coronary artery bypass grafting or unroofing or reimplantation of the coronary artery.

## Radiologic

- Coronary artery anomalies were traditionally diagnosed with conventional angiography. However, only 53% of coronary anomalies detected by CT angiogram (CTA) are correctly identified with conventional angiography. The RCA normally arises from the anterior right coronary sinus and passes posterior and to the right of the main pulmonary artery before descending within the right atrioventricular groove.
- The left coronary artery (LCA) normally arises from the posterior left coronary sinus and passes posterior and to the left of the main pulmonary artery. The LCA normally bifurcates into the left circumflex (LCx) and left anterior descending (LAD) coronary arteries.
- The LAD normally passes to the left of the main pulmonary artery before descending within the anterior interventricular groove. The LCx normally descends in the left atrioventricular groove.
- Anomalies of coronary artery origin include (1) RCA arising from the left coronary sinus, (2) LCA, LCx, or LAD arising from the right coronary sinus, (3) either a coronary artery or a coronary artery branch arising from the noncoronary sinus, or (4) a coronary artery (usually the left) arising from the main pulmonary artery.
- The anomalous artery may then take one of four courses—(1) interarterial (between the aorta and pulmonary artery), (2) retroaortic, (3) prepulmonic, or (4) subpulmonic. The interarterial course is associated with myocardial ischemia, syncope, and sudden cardiac death and requires surgical treatment.
- Potential mechanisms for sudden death with an interarterial course of an anomalous coronary artery include cyclical compression between the aorta and pulmonary artery, stretching of the intramural segment, or kinking of its origin due to an abnormal acute angulation of the takeoff from the aorta. Furthermore, when the coronary artery arises anomalously off of the aorta, the orifice is often slit-like and more easily compressed by the muscular wall of the aorta.

## SUGGESTED READING

Dodd JD, Ferencik M, Liberthson RR, et al. Congenital anomalies of coronary artery origin in adults: 34-MDCT appearance. Am J Roentgenol 2007;188:W138–W146.

Kini S, Kostaki GB, Weaver L. Normal and variant coronary arterial and venous anatomy on high-resolution CT angiography. Am J Roentgenol 2007;188:1665–1674.

# CASE 7

**GLEN A.**
**TOOMAYAN**

## HISTORY

A 66-year-old asymptomatic obese male with a recent positive exercise treadmill stress test performed as part of a comprehensive physical examination. Subsequent stress-rest myocardial perfusion scintigraphy demonstrated inferior wall ischemia. Coronary CTA was performed for further evaluation, as the referring cardiologist believed the scintigraphic findings may represent a false-positive result.

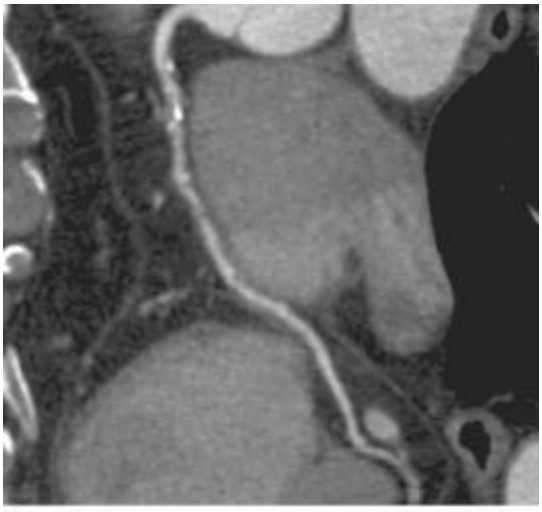

A

■**FIGURE 11-7A** Curved multiplanar reformatted (MPR) image of the RCA from a coronary CT angiogram (CTA) demonstrates several calcified and noncalcified plaques in the proximal RCA, which cause mild (<25%) narrowing of luminal diameter. In the mid-RCA, there is an eccentric noncalcified plaque causing significant (>50%) narrowing of the vessel diameter.

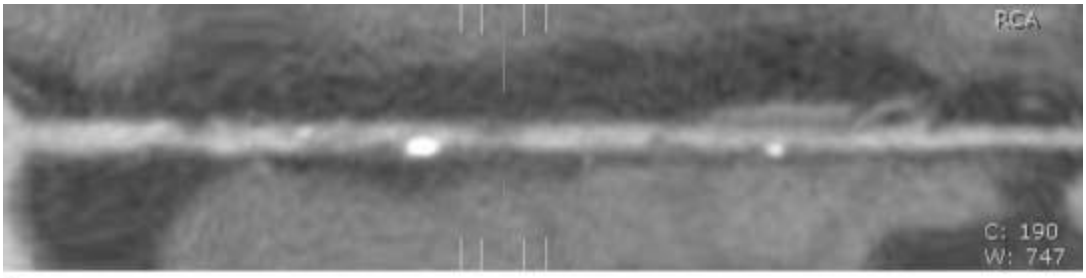

B

**FIGURE 11-7B** Straight MPR image of the RCA from the same examination demonstrates this complex soft plaque in the mid-RCA just distal to a coarse calcified plaque (left is proximal, right is distal). There is significant (>50%) focal narrowing of the luminal diameter at the site of this noncalcified plaque (between long lines) when compared to the normal caliber RCA distally. Several <25% stenoses are seen proximally and distally.

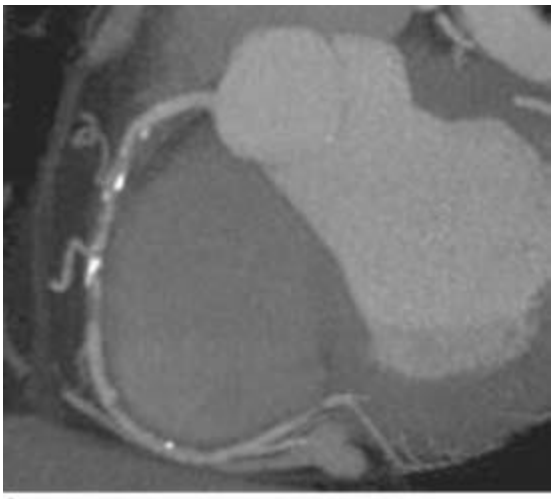
C

**FIGURE 11-7C** Maximum intensity projection (MIP) image of the right coronary artery from the same examination demonstrates the same eccentric non-calcified plaque (just distal to the coarse calcification), which causes a focal >50% stenosis.

## DIFFERENTIAL DIAGNOSIS

**Atherosclerotic stenosis of the right coronary artery (RCA):** Coronary CTA demonstrated multiple eccentric calcified and noncalcified plaques within the RCA. A noncalcified plaque in the mid-RCA caused a >50% narrowing of the luminal diameter. The patient was therefore referred to coronary artery angiography, which revealed a stenosis of 90% in the mid-RCA. This lesion was treated with balloon angioplasty and stenting.

## DIAGNOSIS

**Hemodynamically significant atherosclerotic stenosis of the right coronary artery**

# KEY FACTS

## Clinical

- Coronary artery disease (CAD) is the leading cause of morbidity and mortality in the United States.
- The prevalence of CAD in the United States is 16 million.
- 1.2 million new cases of CAD are diagnosed annually in the United States.
- Annually, 450,000 deaths are attributed to CAD in the United States.
- Symptomatic CAD manifests as angina, heart failure, or acute coronary syndrome. Due to the potential need for intervention, patients with high suspicion for atherosclerotic CAD are directed to coronary angiography.
- Roles for noninvasive imaging of the coronary arteries are currently being defined.
- Coronary CTA has a high negative predictive value (95% to100%). Therefore, one of its greatest strengths is in excluding coronary artery stenosis in low-to-intermediate risk patients.
- In comparison with conventional coronary angiography, 16- and 64-slice CTA has a sensitivity of 83% to 99% and a specificity of 93% to 98% for the detection of hemodynamically significant coronary artery stenosis (>50% luminal narrowing) in arteries with a diameter >1.5 to 2.0 mm.
- When clinical distinction must be made between atherosclerotic and nonatherosclerotic CAD, coronary CTA can demonstrate causes of nonatherosclerotic CAD including coronary artery anomalies, myocardial bridges, and coronary artery aneurysms.
- Coronary CTA may be useful in assessing a patient's CAD risk by quantification of calcified and soft plaque.
- Coronary CTA may one day be used to monitor response of CAD to pharmacological treatment by monitoring changes in plaque burden.

## Radiologic

- Recent technological advances have made noninvasive imaging of the coronary arteries possible.
- The introduction of 16- and more recently 64-slice CT scanners and dual source CT scanners has led to improved temporal and spatial resolution, fewer motion artifacts, and decreased reliance on patient cooperation.
- Imaging the heart during diastole minimizes cardiac motion. With 64-slice CT, lower

heart rates are preferable to lengthen the optimal imaging window during diastole. Beta-blockers may be administered to lower the heart rate.

- Imaging may be acquired with either prospective ECG triggering or retrospective ECG gating.
- *Prospective triggering* monitors the ECG and triggers image acquisition only during a predefined portion of the cardiac cycle (diastole). Images are not acquired during systole, resulting in a lower radiation dose to the patient compared with retrospective gating.
- *Retrospective gating* acquires continuous images of the heart and records the patient's ECG simultaneously. Images during diastole are then reconstructed retrospectively by analyzing the ECG. Patient dose is higher with retrospective gating due to continuous image acquisition throughout the cardiac cycle.
- Patient radiation dose from coronary CTA can be as high as 8 to 22 mSv with retrospective EKG gating and is lower with prospective EKG gating, usually in the order of 2 to 4 mSV. Radiation dose from conventional coronary catheter angiography ranges from 2 to 10 mSV.
- Accurate evaluation of coronary arteries for significant (50%) luminal narrowing requires software capable of generating multiplanar, straight, and curved reformations.
- Coronary CTA may be used to divide patients into three different groups: those with no evidence of coronary atherosclerotic disease, those with atherosclerotic plaque that results in luminal narrowing of >50%, and those with plaque that causes a luminal stenosis of >50%.
- Patients with coronary stenosis >50% on coronary CTA may be further evaluated with functional stress testing or conventional catheter angiography.
- Limitations of coronary CTA include difficulty imaging patients with rapid heart rates and cardiac arrhythmias, streak artifact from extensive calcified plaque or coronary artery stents, and inability to intervene at the time of diagnosis.

## SUGGESTED READING


Cody DD, Mahesh M. AAPM/RSNA physics tutorial for residents: Technologic advances in multidetector CT with a focus on cardiac imaging. Radiographics 2007;27:1829–1837.

Achenbach S. Computed tomography coronary angiography. J Am Coll Cardiol 2006;48:1919–1928.

Gaspar T, Halon D, Rubinshtein R, et al. Clinical applications and future trends in cardiac CTA. Eur Radiol 2005;15(Suppl 4):D10-D14.

Schoenhagen P, Halliburton SS, Stillman AE, et al. Noninvasive imaging of coronary arteries: current and future role of multi-detector row CT. Radiology 2004;232:7-17.

Schoepf UJ, Zwerner PL, Savino G, et al. How I do it: Coronary CT angiography. Radiology 2007:244:48-63.

# CASE 8

**NICOLE PROSCIA**

## HISTORY

A 63-year-old female with hypertension and hyperlipidemia presents with chest pain.

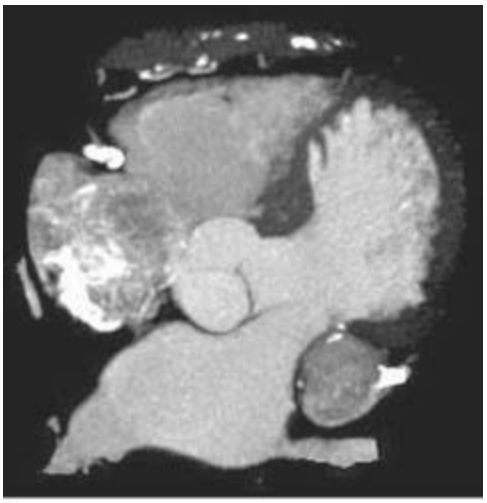

A

**FIGURE 11-8A** MIP axial image from a coronary CT angiogram (CTA) demonstrates a heterogeneously enhancing round mass with peripheral calcification in the left atrioventricular (AV) groove. Note marked calcification of the right coronary artery in the right AV groove.

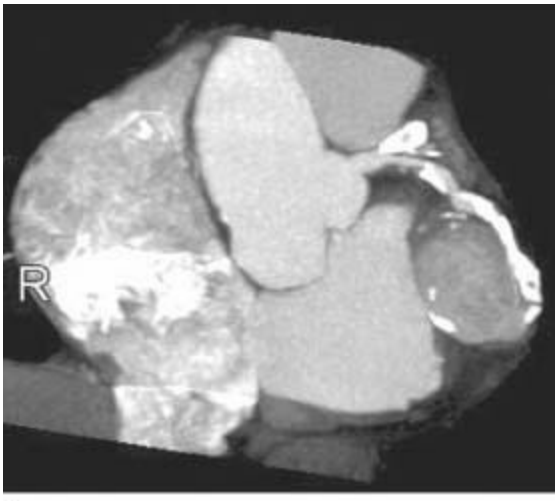


B

**FIGURE 11-8B** Curved planar reformat image from a coronary CTA demonstrates a

heavily calcified left circumflex artery intimately associated with the peripherally calcified mass in the left AV groove.

C

**FIGURE 11-8C** MIP image from a coronary CTA shows large amount of calcification throughout the right and left coronary systems, consistent with marked atherosclerotic disease.

## DIFFERENTIAL DIAGNOSIS

**Coronary artery aneurysm/pseudoaneurysm:** This diagnosis is the most likely given the fact that the mass has a broad base against the coronary artery, demonstrates a small amount of peripheral calcification, and enhances heterogeneously. Additionally, the presence of severe atherosclerotic disease throughout the remainder of the patient's coronary arterial system provides evidence that the patient is at risk for aneurysm formation. The mass's location in the left atrioventricular groove indicates that it arises from the left circumflex (LCx) artery. Distinction between an aneurysm and a pseudoaneurysm is difficult and may sometimes only be made based on history (a history of trauma favors pseudoaneurysm) or upon resection.

**Pericardial metastasis:** This diagnosis might be considered, especially in a patient with a primary malignancy known to involve the pericardium, such as lung, breast, melanoma, lymphoma, or renal cell cancer. However, the fact that the mass is intimately associated with a coronary artery and the fact that the patient has no known history of malignancy would make this diagnosis much less likely.

**Ventricular or atrial pseudoaneurysm:** This diagnosis could be considered if the mass is perceived as a sac-cular outpouching from the heart itself. However, the broad

attachment to the coronary artery and the location in the left AV groove makes this diagnosis unlikely; ventricular pseudoaneurysms usually arise from the inferior posterior wall of the left ventricle and should displace rather than disrupt the coronary artery. Atrial pseudoaneurysms are very rare and are usually caused by disruption of a suture line from cardiac surgery.

- **Left atrial or ventricular diverticulum:** This is an extremely rare condition and would enhance homogeneously and to the same degree as the cardiac chambers.

## DIAGNOSIS

**Coronary artery aneurysm**

## KEY FACTS

### Clinical

- In the Western world, atherosclerosis is the most common cause of coronary artery aneurysm. Worldwide, the most common cause is Kawasaki's disease. Other etiologies include iatrogenic, infectious (e.g., mycotic aneurysm), connective-tissue disorder (e.g., Marfan's syndrome), vasculitis (e.g., polyarteritis nodosa), and congenital anomalies.
- Complications include thrombus, embolization, ischemia/ infarct, and rupture of the aneurysm.
- Patients may be asymptomatic or symptomatic. Symptomatic patients may present with congestive heart failure, myocardial infarction, or angina.
- Medical management for asymptomatic patients consists of antiplatelet and anticoagulation therapy.
- Surgical treatment includes coronary artery bypass graft or stent placement and is reserved for symptomatic patients, large aneurysms, and those patients with associated CAD.

### Radiologic

- Coronary artery aneurysm is defined as a dilatation ≥1.5 times the diameter of the adjacent normal caliber coronary artery.
- May be saccular (as in this patient), fusiform, or involve the coronary artery diffusely, in which case it is termed *coronary ectasia.*
- Most common sites for coronary artery aneurysms to occur (in descending order) are the RCA, LAD artery, and LCx artery. The left main stem artery is a rare site, comprising only 0.1% of coronary artery aneurysms.
- Coronary angiography is considered the gold standard in diagnosing coronary artery aneurysms. However, since coronary angiography only evaluates intraluminal flow

within the aneurysm, it may underestimate the overall size of the aneurysm if substantial intraluminal thrombus is present.

- Coronary CTA provides a noninvasive approach to evaluate coronary artery aneurysms. Advantages of coronary CTA include evaluation of aneurysm size and location, as well as extent of intraluminal thrombus and calcification.

## SUGGESTED READING

Murthy PA, Mohammed TL, Read K, et al. MDCT of coronary artery aneurysms. Am J Roentgenol 2005;184:S19–S20.

Konen E, Feinberg MS, Morag B. Giant right coronary aneurysm: CT angiographic and echocardiographic findings. Am J Roentgenol 2001;177:689–691.

Tan KT, Challenor V, McGann G. CT diagnosis of coronary artery aneurysms. Int J Cardiol 2007;118:273-274.

Aggarwala G, Iyengar N, Burke SJ, et al. Kawasaki disease: Role of coronary CT angiography. Int J Cardiovasc Imaging 2006;22:803-805.

# CASE 9

**LAURA E.**
**HEYNEMAN**

### HISTORY

A 45-year-old female with progressive dyspnea.

A

■**FIGURE 11-9A** Frontal view of the chest reveals marked enlargement of the main and hilar pulmonary arteries, with rapid tapering of the peripheral pulmonary arteries. The lungs are otherwise normal, with no evidence of chronic lung disease. The cardiac silhouette is mildly enlarged.

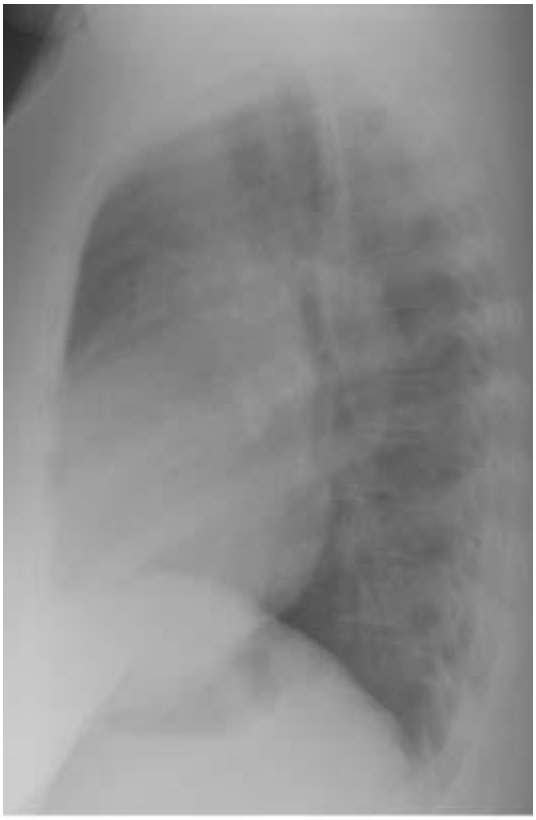

B

■**FIGURE 11-9B** Lateral view of the chest demonstrates hilar enlargement as well as enlargement of the right ventricle.

C

**FIGURE 11-9C** Short-axis SSFP MR image in the same patient reveals enlargement and hypertrophy of the right ventricle, as well as straightening of the interventricular septum which, on cine imaging (not shown), is most marked in systole.

## DIFFERENTIAL DIAGNOSIS

- **Pulmonary artery hypertension (PAH):** This is the most likely diagnosis given the radiographic finding of prominent central pulmonary vasculature (main pulmonary artery and hilar vessels) but normal- to small-sized peripheral vessels as well as the MR findings of enlargement and hypertrophy of the right ventricle and straightening of the interventricular septum.
- **Hilar lymphadenopathy:** Hilar lymphadenopathy may cause hilar enlargement, but the hila are usually lobulated rather than smooth (as in this case). Additionally, hilar lymphadenopathy should not cause enlargement or hypertrophy of the right ventricle.
- **Left-to-right shunt:** Shunt vascularity will enlarge the central pulmonary vessels (as seen in this case), but the peripheral vessels should be enlarged as well. Furthermore, on MR, the right ventricle may be enlarged in the setting of an ASD, but should not be hypertrophied, as seen in this case.
- **Pulmonary valve stenosis:** While this can cause enlargement of the main and left pulmonary artery as well as hypertrophy of the right ventricle, the right pulmonary artery should be small, as opposed to the bilateral hilar enlargement seen in this patient.

## DIAGNOSIS

**Pulmonary artery hypertension (idiopathic)**

## KEY FACTS

### Clinical

- PAH is defined as a mean pulmonary artery pressure >25 mm Hg during rest.
- PAH is divided into precapillary, capillary, and postcapillary causes.
- The three main *precapillary* causes of PAH are primary (idiopathic), chronic thromboembolic disease, and chronic left-to-right shunt leading to Eisenmenger's physiology.
- *Capillary* causes of PAH include different forms of chronic lung disease and diseases that lead to chronic hypoxemia from alveolar hypoventilation, such as emphysema, interstitial or pleural fibrosis, cystic fibrosis, restrictive chest wall deformities, and sleep apnea.
- *Postcapillary* causes of PAH include causes of increased pulmonary venous pressures

such as chronic LV failure and mitral stenosis. The chronic increase in left-sided cardiac pressures is transmitted into the pulmonary vasculature and eventually results in PAH.

- Patients typically present with dyspnea, fatigue, nonproductive cough, and peripheral edema.
- Treatment of PAH includes continuous vasodilator infusion, treatment of underlying cause (e.g., bilevel positive airway pressure, or BiPAP, for sleep apnea), and heart-lung transplantation.

## Radiologic

- PAH is manifest on a chest radiograph by enlarged central pulmonary arteries that rapidly taper as they course to the periphery of the lungs.
- The radiograph should be examined for capillary or postcapillary causes of PAH, including evidence of chronic lung disease such as fibrosis, emphysema, or cystic fibrosis, and evidence of chronic LV failure or mitral valve disease.
- The presence of mural calcification within central pulmonary arteries is indicative of long-standing, supra-systemic PA pressures and is most commonly seen in the setting of a chronic left-to-right shunt and Eisenmenger's physiology.
- On cross-sectional imaging, findings of PAH include enlargement of the pulmonary arteries (main PA > 3 cm), right ventricular hypertrophy from increased afterload, mild right ventricular dilation, and straightening of the interventricular septum. The straightening of the septum is particularly prominent during ventricular systole.
- High resolution chest CT often demonstrates mosaic perfusion within the lungs; geographic ground glass is present in regions where there are large blood vessels, and decreased lung attenuation is present in regions where the vessels are small. Mosaic perfusion is most pronounced in patients with PAH secondary to chronic thromboembolic disease.
- Delayed-enhancement MR sequences may show a small focus of enhancement at the junction of the right ventricle and interventricular septum; this is a pattern often seen in the setting of right ventricular pressure overload.
- Pulmonary valve insufficiency may be present on cine imaging due to the increased pulmonary artery pressures.

# SUGGESTED READING

Chin KM, Rubin LJ. Pulmonary arterial hypertension. J Am Coll Cardiol 2008;51:1527–1538.

Tektonidou M. Pulmonary hypertension. N Engl J Med 2005;352:418–419.

Frasier AA, Galvin JR, Franks TJ, Rosado-de-Christenson ML. Pulmonary vasculature: hypertension and infarction. Radiographics 2000;20:491–524.

# CASE 10

**PHIL B.**
**HOANG**

## HISTORY

A 50-year-old woman complains of a 6-week history of progressively worsening shortness of breath, exacerbated with changes in position. A cardiac mass was noted on a chest CT that was performed to rule out pulmonary embolism. Cardiac MRI was subsequently performed for further evaluation.

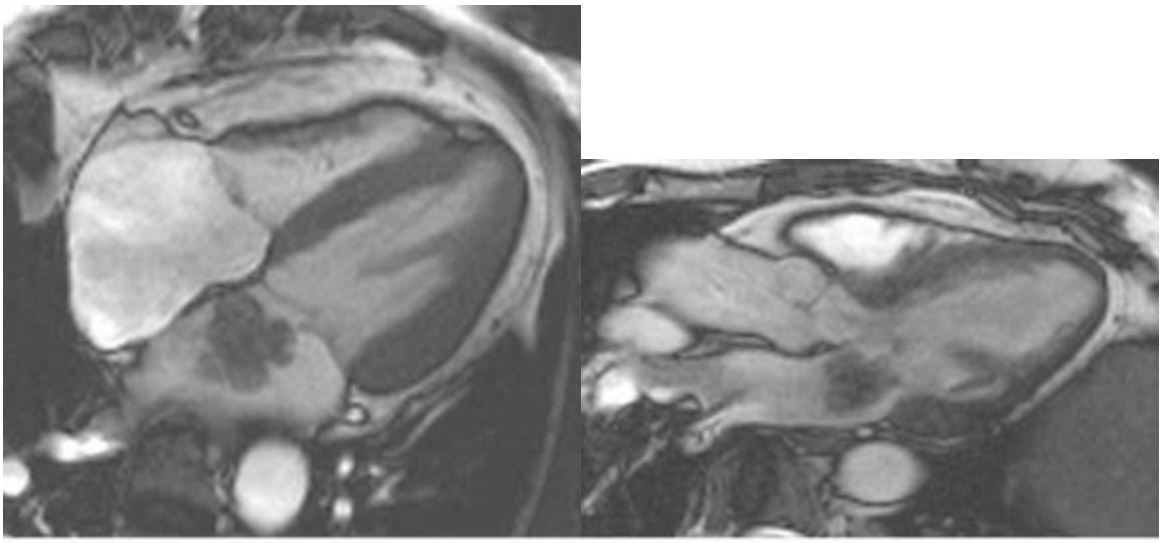


■**FIGURES 11-10A and 11-10B** SSFP MR four-chamber **(A)** and three-chamber **(B)** views of the heart demonstrate a polypoid left atrial mass, which is mildly hyperintense to the ventricular myocardium, with small foci of hypointense signal centrally. The mass appears connected to the interatrial septum on the four-chamber view **(A)**.

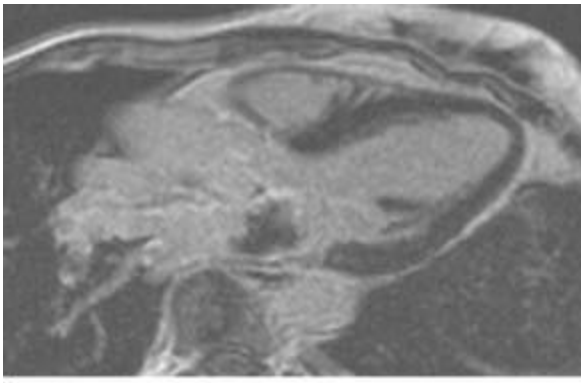

C

**FIGURE 11-10C** Delayed-enhancement postcontrast three-chamber MR image demonstrates predominantly low signal intensity with minimal enhancement anteriorly.

## DIFFERENTIAL DIAGNOSIS

- **Myxoma:** This is the most likely diagnosis given the left atrial location of the mass, the apparent attachment to the interatrial septum, and the presence of minimal postcontrast enhancement.
- **Thrombus:** While thrombus is the most common intra-cardiac mass and may be pedunculated, the presence of enhancement precludes this diagnosis.
- **Metastatic disease:** Malignant cardiac tumors are 20 times more likely to be due to metastatic disease than primary cardiac malignancies. Lymphoma, melanoma, and breast and lung cancers are the most frequently associated primary malignancies to involve the heart and may be intracavitary or intramyocardial. Metastases to the heart tend to enhance vividly after contrast administration. While most metastases tend to have nonspecific signal characteristics—hyperintense to myocardium on T2-weighted sequences and with vivid enhancement after contrast administration—the signal intensity of melanoma metastases may be more specific, with high signal on precontrast T1-weighted sequences.
- **Cardiac sarcoma:** Sarcomas are the most common primary cardiac malignancy, with angiosarcoma the most frequent subtype (35% to 40%). Most often presents as an ill-defined, infiltrative mass arising from the free wall of the atrium (right greater than left) with invasion of the pericardium and sparing of the atrial septum.
- **Other cardiac masses:** Lipomas, fibromas, hemangiomas, and paragangliomas are other infrequent cardiac masses.

## DIAGNOSIS

**Atrial myxoma**

## KEY FACTS

### Clinical

- Most common benign cardiac tumor.
- Up to 90% of myxomas present in the age range of 30 to 60 years and more frequently affect women.
- Patients complain of chest pain, shortness of breath, and constitutional symptoms (fever, weight loss).
- Mobility of these masses can cause symptoms related to changes in body position.
- Prolapse into the atrioventricular valve can cause outflow obstruction, arrhythmia, and/or syncope. Chronic atrioventricular valvular obstruction can mimic valvular stenosis, both clinically and radiographically.
- Given the friability of these masses, nearly 40% may clinically present with symptoms caused by tumor thromboembolism (CNS stroke, coronary artery ischemia, renal/splenic infarction, pulmonary embolism).

### Radiologic

- Usual presentation is a lobulated, pedunculated intracavitary mass arising within one of the atria (80% within the left atrium) and connected to the interatrial septum near the fossa ovalis by a thin stalk.
- MRI: Signal characteristics are as follows: isointense-to-hypointense to myocardium on T1-weighted images; hyperintense on T2-weighted images due to poly-saccharide-rich matrix in nonfibrotic areas; variable amount of enhancement after contrast administration, with contrast enhancement often scant. Varying degrees of tumoral hemorrhage, necrosis, calcification, and fibrosis determine signal heterogeneity.
- CT: Well-defined, intraluminal filling defect on contrast-enhanced images. Myxomas are typically lower in attenuation than thrombus due to gelatinous matrix. Calcification may be apparent.
- Radiographs: Left atrial myxomas causing obstruction of the mitral valve will mimic sequela of mitral valve stenosis (pulmonary venous hypertension, left atrial enlargement). However, the left atrial appendage is usually not enlarged, which can help distinguish myx-oma from mitral valve stenosis. Calcified myxomas may be directly visible on a radiograph.
- Right atrial myxomas can mimic tricuspid valvular stenosis (right atrial enlargement, decreased pulmonary blood flow, and distended superior/inferior vena cavae). Multifocal, bilateral pulmonary opacities may reflect septic emboli from friable tumor.

## SUGGESTED READING

Anavekar NS, Bonnichsen CR, Foley TA, et al. Computed tomography of cardiac pseudotumors and neoplasms. Radiol Clin North Am 2010;48:799–816.

Syed IS, Feng D, Harris SR, et al. MR imaging of cardiac masses. Magn Reson Imaging Clin N Am 2008;16:185–199.

# CASE 11

**JOSHUA A.**
**BRYANT**

## HISTORY

A 40-year-old male with a history of lupus erythematosus presents with signs of biventricular heart failure. Cardiac catheterization revealed normal coronary arteries and pressure tracings suggestive of decreased ventricular compliance.

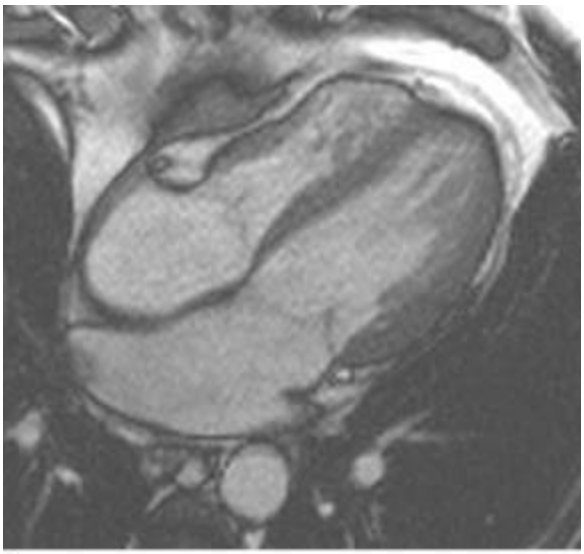

A

■**FIGURE 11-11A** Four-chamber SSFP MR image reveals focal pericardial thickening over the free wall of the right ventricle. The right ventricle is conical in shape. Both ventricles demonstrate normal myocardial thickness and myocardial signal. Additionally, there is mild biatrial (left greater than right) enlargement.

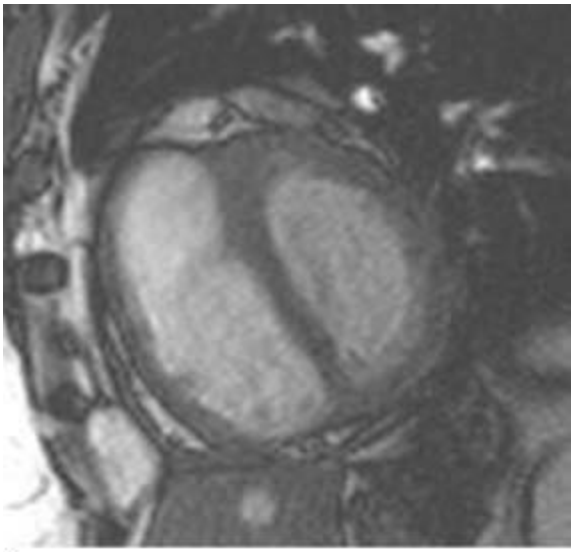

B

**FIGURE 11-11B** Short-axis SSFP MR image demonstrates pericardial thickening and straightening of the interventricular septum.

## DIFFERENTIAL DIAGNOSIS

**Constrictive pericarditis:** The conical appearance of the ventricles, the normal appearance of the myocardium, the presence of pericardial thickening, and the clinical evidence of decreased ventricular function make this the leading differential consideration.

**Restrictive cardiomyopathy:** This is the other major differential consideration in a patient with biventricular failure and decreased ventricular compliance. In restrictive cardiomyopathy, the pericardium will be normal but there will be abnormal ventricular wall thickness and/or abnormal myocardial enhancement.

**Calcific or thickened pericarditis without constriction:** Calcific/fibrotic pericarditis after a pericardial insult (surgery, radiation, infection, collagen vascular disease) without constriction has to be included in the differential diagnosis, but does not explain the conical appearance of the ventricles, the straightening of the interventricular septum, or the patient's symptoms.

**Acute pericarditis:** This is almost always accompanied by a pericardial effusion and may demonstrate pericardial enhancement. Additionally, a diagnosis of uncomplicated acute pericarditis would not explain the ventricular configuration or the straightening of the interventricular septum seen in this case.

**Pericardial metastasis:** Focal pericardial masses are most commonly due to loculated hemopericardium or a loculated exudative pericardial effusion. However, pericardial neoplasms do exist. Metastatic disease to the pericardium is more common than primary pericardial malignancies. However, the images in this example demonstrate a long

segment of pericardial thickening rather than a discrete mass.

# DIAGNOSIS

**Constrictive pericarditis**

# KEY FACTS

## Clinical

- Patients often present with biventricular heart failure characterized by dyspnea, orthopnea, fatigue, hepatomegaly, and ascites. Onset is typically gradual, although acute to subacute cases have been reported.
- The most common causes of constrictive pericarditis are idiopathic, prior surgery, and radiation therapy. Other causes include infection, connective-tissue disease, uremia, and malignancy.
- An insult to the pericardium results in fibrosis and possibly calcification, with progressive rigidity of the pericardium. There is resultant abnormal ventricular diastolic filling and increased filling pressures. Once the heart can no longer tolerate the increased filling pressures, the patient presents with diastolic cardiac failure.
- Differentiating constrictive pericarditis from restrictive cardiomyopathy is clinically important, as constrictive pericarditis is potentially curable with a pericardiectomy, while restrictive cardiomyopathy treatment is often palliative and has a poor prognosis.

## Radiologic

- CT findings (not shown): Pericardial calcification is easily identified on CT and can be a diagnostic clue. Occasionally pericardial thickening (>4 mm) can be visualized on CT. These findings are nonspecific and should be correlated with the patient's symptoms and functional assessment by cardiac MR.
- Anatomic MR findings:
  - Pericardial thickening: >4 mm. Ninety-three percent sensitivity for differentiating constrictive pericarditis from restrictive cardiomyopathy.
  - Tubular or conical ventricle: Flattening of the lateral wall of the ventricle narrows the ventricle and results in a tubular or exaggerated conical appearance. This finding is fairly specific for constrictive pericarditis. However, the absence of this finding does not help distinguish constrictive pericarditis from restrictive cardiomyopathy.
  - Atrial enlargement: Biatrial enlargement may also be seen with constrictive pericarditis, and is a result of the atria trying to pump blood into ventricles that are encased by thickened pericardium. Biatrial enlargement may also be seen in

restrictive cardiomyopathy.

- Functional MR findings:
  - Pericardial restriction of the ventricles can result in interventricular dependence. Essentially, the position of one ventricle is dependent on the other, since a relative constant volume is maintained by the fibrotic pericardium. This often results in inter-ventricular septal straightening, particularly during early diastolic filling.
  - On cine images, an abnormal septal "bounce" or sigmoid motion of the septum is often seen.
  - Regurgitation of the atrioventricular valves is common.

## SUGGESTED READING

Grizzard JD. Magnetic resonance imaging of pericardial disease and intracardiac thrombus. Heart Fail Clin 2009;5(3):401–419.

Misselt AJ, Harris SR, Glockner J, et al. MR imaging of the pericardium. Magn Reson Imaging Clin N Am 2008;16:185–199.

O'Leary SM, Williams PL, Williams MP, et al. Imaging the pericardium:appearances on ECG-gated 64-detector row cardiac computed tomography. Br J Radiol 2010;83(987):194–205.

# CASE 12

**LAURA E. HEYNEMAN**

### HISTORY

A 65-year-old male with known coronary artery disease presents with dyspnea on exertion and orthopnea.

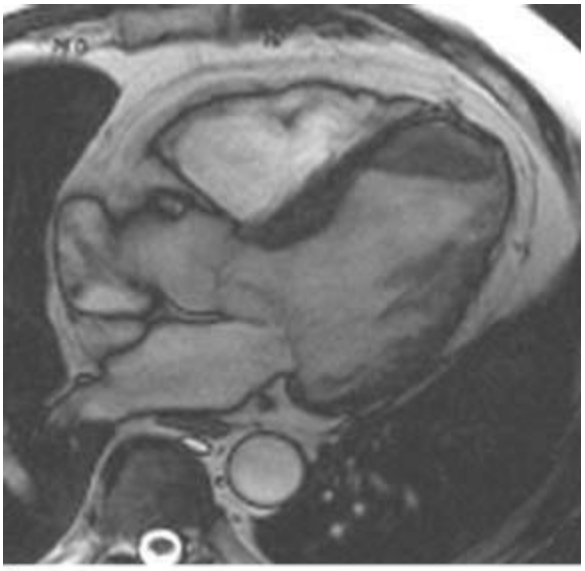

A

■**FIGURE 11-12A** Three-chamber SSFP MR image reveals LV apical thinning. Additionally, there is a focus of intermediate signal within the LV cavity at the apex.

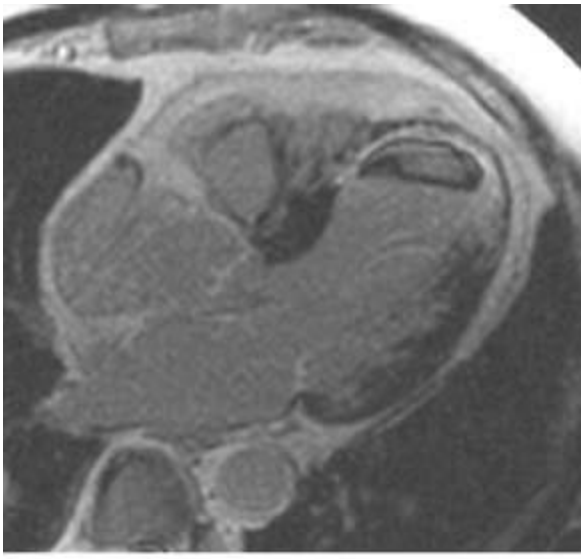

B

■**FIGURE 11-12B** Three-chamber contrast-enhanced inversion recovery MR image (viability sequence). The thinned LV apex demonstrates transmural enhancement, whereas the remainder of the LV myocardium is normal. The low signal intracavitary mass lies adjacent to the enhanced myocardium.

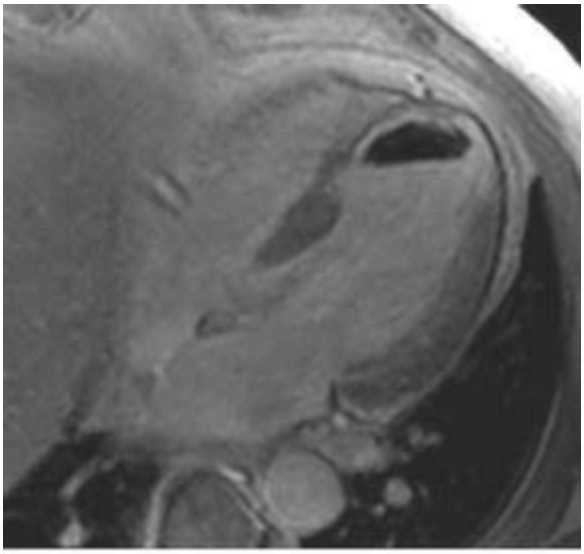

C

**FIGURE 11-12C** Four-chamber contrast-enhanced inversion recovery MR image reveals no enhancement of the intracavitary mass.

## DIFFERENTIAL DIAGNOSIS

- **Intracavitary thrombus within left ventricular (LV) aneurysm:** The presence of a nonenhancing cavitary mass at the cardiac apex, in conjunction with thinning and enhancement of the adjacent ventricular myocardium, is most suggestive of this diagnosis.
- **Ventricular malignancy:** Metastatic disease or a primary cardiac malignancy such as an angiosarcoma can result in an intracavitary mass. However, these generally enhance vividly. Additionally, an intracavitary malignancy would not explain the delayed enhancement and thinning of the LV apical myocardium.
- **Ventricular myxoma:** While myxomas are the most common benign cardiac neoplasm, they are found almost exclusively in the atria. Additionally, the findings of the adjacent LV apical myocardium would not be explained.
- **Infiltrative cardiomyopathy:** An inflammatory process such as myocarditis or sarcoid can result in myocar-dial enhancement. However, the enhancement in these diseases is often confined to the midmyocardium or epicardium. Furthermore, focal myocardial thinning would be very unusual, and the intracavitary mass would not be explained.

## DIAGNOSIS

**Intracavitary thrombus within a left ventricular aneurysm**

## KEY FACTS

## Clinical

- LV apical thinning is most often a result of a prior transmural myocardial infarction involving the LAD artery. A true aneurysm is lined by fibrotic myocardium, and results in a focal wall motion abnormality.
- Scarring as evidenced by delayed enhancement on cardiac MR has prognostic importance. In patients with dilated ischemic cardiomyopathy, regions of myocardium with scarring involving >50% of the wall thickness are unlikely to regain function after revascularization.
- Thrombus is the most common intracavitary cardiac mass. Thrombus tends to form in regions of slow blood flow and stasis. Therefore, it may deposit within the atria in patients with atrial fibrillation or within the ventricles in patients with systolic dysfunction.
- Patients with cardiac thrombus are usually placed on anticoagulation therapy due to risk of pulmonary or systemic thromboembolism.

## Radiologic

- Myocardial viability is assessed on contrast-enhanced inversion recovery sequences performed approximately 5 to 15 minutes after IV gadolinium administration. The sequences are performed with an inversion time set to null normal myocardium. Therefore, a normal study will show uniformly black myocardium.
- Delayed myocardial enhancement on the viability sequence signifies the presence of scarring or inflammation. The pattern of enhancement may be helpful in establishing a diagnosis. Scarring from myocardial infarction always involves the subendocardium, with variable extension from the subendocardium into the midmyocardium and epicardium. If enhancement is confined to the midmyocardium or epicardium, the pattern is suggestive of a nonischemic or inflammatory cardiomyopathy.
- Delayed enhancement may be seen in the setting of either acute or chronic myocardial infarction. In patients with acute myocardial infarction, the involved wall is either normal or slightly increased in thickness due to edema. In patients with chronic myocardial infarction, the involved wall is thinned due to replacement by fibrotic scar.
- Cine bright blood imaging in patients with ischemic cardiomyopathy shows regional hypokinesis (decreased contraction and decreased myocardial thickening in systole). An aneurysm is diagnosed when there is regional dyskinesis (akinesis and myocardial thinning during systole).
- Intracavitary thrombus is avascular and does not enhance. Thrombus will appear as a nonenhancing defect surrounded by bright signal blood pool (cine bright blood imaging) or contrast-enhanced myocardium (delayed-enhancement inversion recovery sequence).

## SUGGESTED READING

Grizzard JD. Magnetic resonance imaging of pericardial disease and intracardiac thrombus. Heart Fail Clin 2009;5:401–419.

Krombach GA, Niendorf T, Gunther RW, et al. Characterization of myocardial viability using MR and CT imaging. Eur Radiol 2007;17:1433–1444.

Lim RP, Srichai MB, Lee VS. Non-ischemic causes of delayed myocardial hyperenhancement on MRI. Am J Roentgenol 2007;188:1675–1681.

# CASE 13

**LAURA E. HEYNEMAN**

### HISTORY

A 70-year-old with history of coronary artery disease presenting with chest pain.

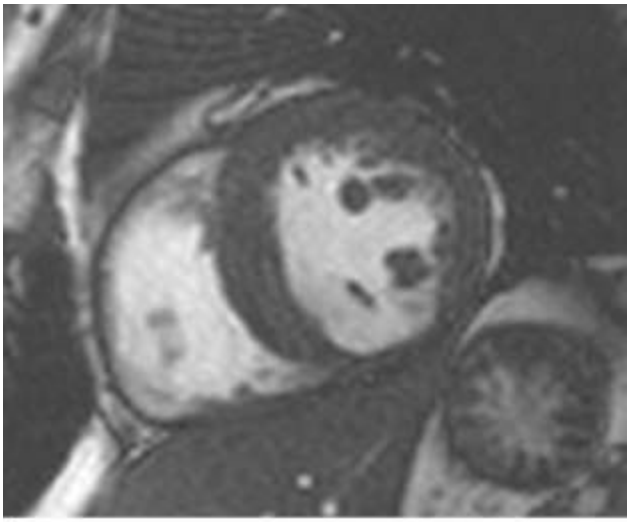

A

**FIGURE 11-13A** Short-axis SSFP MR image reveals a thin inferior left ventricular wall.

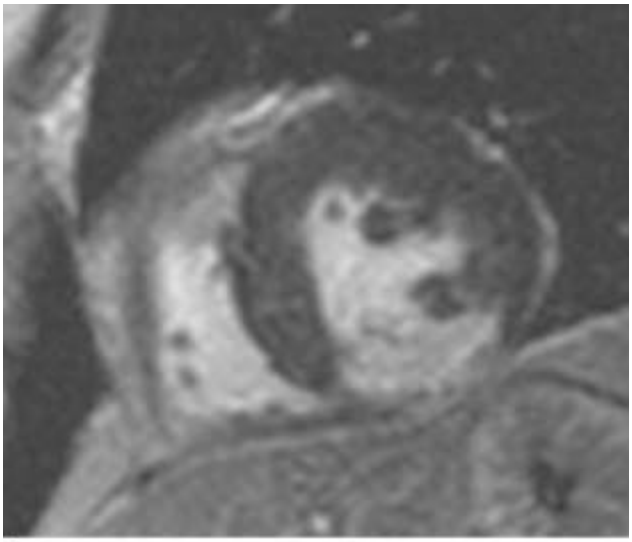

B

**FIGURE 11-13B** Short-axis delayed-enhancement MR image demonstrates transmural enhancement of the inferior wall. The remaining myocardium shows no enhancement.

## DIFFERENTIAL DIAGNOSIS

- **Chronic myocardial infarction:** This is the most likely diagnosis given the focal thinning of the LV inferior wall with associated transmural enhancement. The abnormality is in the distribution of the RCA.
- **Infectious myocarditis:** This is less likely given that focal wall thinning is very unusual in the setting of an infectious (viral) myocarditis. Furthermore, myocarditis usually results in either no myocardial enhancement or extensive enhancement of the epicardial wall; a solitary focus of transmural enhancement would be rare.
- **Cardiac amyloid:** This infiltrative process usually results in extensive myocardial thickening rather than focal thinning. On delayed-enhancement sequences, amyloid may cause diffuse, circumferential subendo-cardial enhancement that progresses with the course of the disease to diffuse transmural enhancement. A solitary region of enhancement would be highly unusual.
- **Cardiac sarcoid:** While sarcoidosis can cause focal wall thinning, there are usually multiple sites of deposition of the sarcoid granulomata; this frequently results in multifocal enhancement on delayed-enhancement imaging. Furthermore, at least one site of the enhancement usually demonstrates a nonischemic pattern of enhancement: either midmyocardial or epicardial. The presence of a single focus of transmural enhancement as evidenced in this case would be unusual for sarcoid.

## DIAGNOSIS

**Chronic myocardial infarction**

## KEY FACTS

### Clinical

- Pathophysiology: In the setting of acute myocardial infarction, there is a sudden loss of integrity of myocyte cell membranes. The ventricular wall remains normal in size, or occasionally is slightly thickened by edema. In chronic myocardial infarction, myocytes are replaced by fibrous tissue. This myocyte replacement by fibrosis often results in thinning of the ventricular wall.
- Myocyte injury from myocardial infarction always begins at the subendocardium and then extends to a variable degree through the myocardium and epicardium of the adjacent wall. Therefore, a small infarction that was reperfused quickly may only cause death within the subendocardial layer of myocardium. A large infarct may be transmural.
- Treatment: Patients with either acute or chronic myo-cardial infarction in which scar involves >50% of the wall thickness (see delayed-enhancement MR imaging, below) are unlikely to show improvement in wall function after revascularization. In such patients, emphasis is placed on medical therapy.

### Radiologic

- The LV wall is mapped to different coronary artery territories. In general, the LAD artery serves the anterior wall and anteroseptal walls; the LCx artery serves the lateral wall, and the RCA serves the inferolateral, inferior, and inferoseptal walls.
- Cine MR:
  - Wall function provides indirect evidence of the status of the supplying coronary artery since normal wall function requires normal myocardial perfusion. Therefore, patients who have had a myocar-dial infarction may show a wall motion abnormality that involves the portion of the left ventricle that was supplied by the affected artery. However, very small infarcts involving only a tiny amount of the subendocardium usually do not result in a wall function abnormality.
  - Wall thickness can provide clues to the chronicity of the process. The wall thickness may be normal in the setting of both acute and chronic infarctions, but wall thinning is usually indicative of chronic infarction.
- Delayed-enhancement MR findings:
  - Delayed-enhancement imaging is performed approximately 5 to15 minutes after intravenous gadolinium administration. Images are obtained so as to null normal myocardial signal. Therefore, in this sequence, normal myocardium is uniformly

black in signal. Fibrosis and scar enhance.

- Both acute and chronic infarcts result in delayed enhancement on delayed-enhancement (also known as "viability") sequences. Acute infarcts enhance due to the loss of integrity of the cell membranes which, in turn, allow gadolinium to accumulate within the intracellular space. Chronic infarcts enhance due to the large amount of extracellular space within fibrotic tissue.
- All myocardial infarctions result in subendocardial enhancement. As the infarction progresses, more of the thickness of the wall is affected, resulting in a greater amount of transmural enhancement on delayed-enhancement imaging.
- Ventricular enhancement that spares the subendo-cardium (i.e., enhancement confined to the midmyo-cardium or epicardium) is indicative of a nonischemic process. Infectious myocarditis and cardiac sarcoid are examples of inflammatory processes that demonstrate a nonischemic pattern of enhancement on delayed-enhancement MR. Cardiac amyloidosis tends to cause diffuse, circumferential subendocar-dial enhancement; the global involvement indicates that the pathology is not a result of CAD.

## SUGGESTED READING

Vogel-Claussen J, Rochitte CE, Wu KC, et al. Delayed-enhancement MR imaging: utility in myocardial assessment. Radiographics 2006;26:795–810.

Lim RP, Srichai MB, Lee VS. Non-ischemic causes of delayed myocardial hyperenhancement on MRI. Am J Roentgenol 2007;188:1675-1681.

White JA, Patel MR. The role of cardiovascular MRI in heart failure and the cardiomyopathies. Cardiol Clin 2007;25:71–95.

# CASE 14

**CHRISTOPHER J. ROTH**

### HISTORY

A 17-year-old male with no significant past medical history collapsed during a basketball game and required cardiac life support measures for resuscitation.

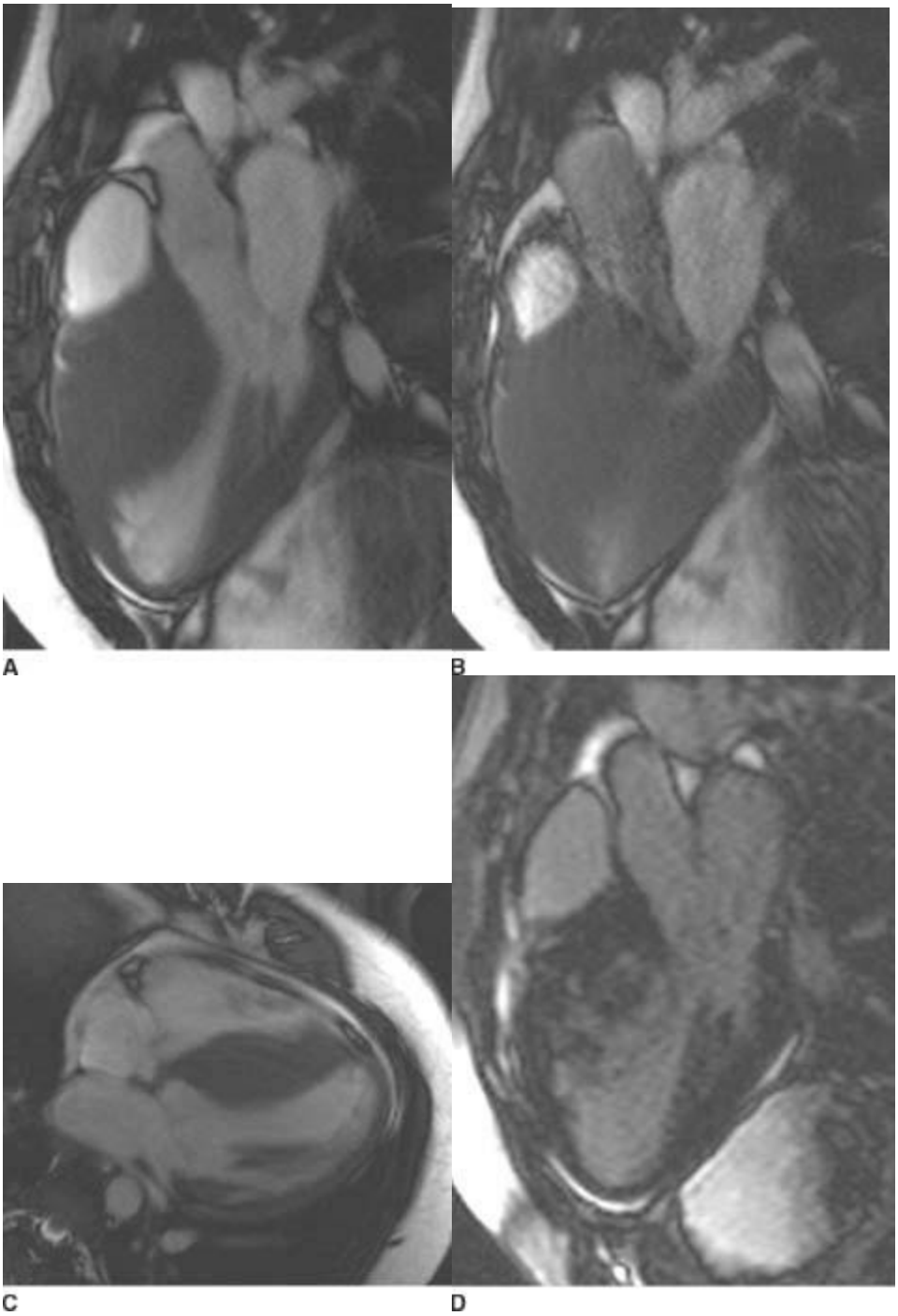


■**FIGURES 11-14A-11-14D** SSFP three-chamber view in diastole **(A)** and peak systole **(B),** and four-chamber view **(C)** demonstrate marked LV wall hypertrophy with outflow tract obstruction. A jet of turbulent flow is identified in the LV outflow tract on the peak systolic image **(B).** Hypertrophy preferentially involves the basal septum on the four-chamber view **(C).** Contrast-enhanced inversion recovery three chamber MR image demonstrates patchy, midwall enhancement in the region of septal hypertrophy **(D)**.

## DIFFERENTIAL DIAGNOSIS

- **Hypertrophic obstructive cardiomyopathy (HOCM):** The presence of asymmetric septal wall thickening, a turbulent jet of blood in the subvalvular LV outflow tract, and patchy midmyocardial septal enhancement on the delayed-enhancement image make this the most likely cause of the patient's cardiac arrest.
- **Aortic stenosis (AS):** The presence of asymmetric septal hypertrophy would be unusual in the setting of AS, which most often would result in concentric hypertrophy. Additionally, the jet of turbulent flow during systole would originate from the level of the aortic valve rather than the subvalvular level, as seen in this case.
- **Amyloidosis:** Cardiac amyloidosis generally results in global hypertrophy and extensive subendocardial enhancement rather than the asymmetric hypertrophy and midmyocardial focal enhancement as seen in this case.
- **Sarcoidosis:** Cardiac sarcoidosis does not usually result in the severe myocardial hypertrophy as seen in this case. While delayed enhancement in sarcoidosis may be midmyocardial in location, it may also be epicardial or transmural.
- **Fabry's disease:** Fabry's disease is a rare X-linked metabolic storage disorder with cardiac manifestations that include concentric LV wall thickening and midmyocardial enhancement involving the basal inferolateral wall.

## DIAGNOSIS

**Hypertrophic obstructive cardiomyopathy (HOCM)**

## KEY FACTS

### Clinical

- Histologically, hypertrophic cardiomyopathy (HCM) is characterized by disarrayed ventricular myocyte organization, manifesting in ventricular hypertrophy.
- HCM may demonstrate concentric or asymmetric ventricular hypertrophy. In the Western hemisphere, in patients with asymmetric hypertrophy, the ventricular septum is preferentially involved; less commonly, asymmetric hypertrophy involves the LV apex or right ventricle.
- HCM can be subdivided into *obstructive* and *nonobstructive* physiologies. The obstruction is at the level of the LV outflow tract. Patients with asymmetric HCM involving the septum are at increased risk for obstructive physiology.
- In the *obstructive* subtype of hypertrophic cardiomyopathy (HOCM)—previously referred to as idiopathic hypertrophic aortic stenosis (IHSS)—there is systolic LV outflow tract stenosis as a result of the asymmetric ventricular hypertrophy superimposed on an abnormal motion of the mitral valve in which the anterior leaflet shifts anteriorly and toward the septum during systole (SAM, systolic anterior motion of

the mitral valve).

- Patients with either the obstructive or nonobstructive variety of HCM are at risk of sudden death due to arrhythmogenic foci within the regions of ventricular hypertrophy.
- Patients with the obstructive subtype (HOCM) are additionally at risk for sudden death due to acute obstruction of the LV outflow tract, particularly during periods of exercise. Other patient complaints can include dyspnea, angina, fatigue, or syncope.
- All forms of HCM are genetically transmitted in 50% of cases, with autosomal dominant inheritance and variable penetrance. Therefore, asymptomatic relatives of patients diagnosed with this disorder are often screened for the disease.
- Treatment options for HCM include medical therapy such as beta-blockade. However, a dual-chamber pacemaker or automated internal cardiac defibrillator is often placed due to risk of fatal arrhythmia. For patients with the obstructive subtype (HOCM), myocardectomy may also be considered. Cardiac t ransplantation may be an option of last resort.

## Radiologic

- Most affected patients have a normal chest radiograph.
- When present, chest radiographic manifestations tend to be vague and nonspecific, including mild cardiomegaly and pulmonary venous hypertension. In late stage disease, LV dilation can develop prior to the onset of LV failure.
- MR imaging can differentiate between obstructive and nonobstructive HCM, evaluate ejection fraction, and quantify mitral regurgitation, a common finding in HOCM.
- Several diagnostic criteria exist, including a ratio of end-diastolic septal thickness to the high posterolateral LV free wall thickness >1.3, and concentric end-diastolic wall thickness >1.2 cm.
- On cine MR images, in patients with the obstructive subtype, a jet of turbulent flow is seen in the subvalvular LV outflow tract. Additionally, the systolic anterior motion of the anterior leaflet of the mitral valve (SAM) may also be directly visualized in these patients.
- On delayed-enhancement MRI, patchy, midwall myo-cardial gadolinium enhancement is a common finding, particularly within the regions of LV hypertrophy. Midmyocardial enhancement at the junction of the interventricular septal junction and the anterior ventricular free wall is also common. The foci of enhancement represent regions of fibrosis and scar tissue that, in turn, are thought to act as arrhythmogenic foci.

# SUGGESTED READING

Hansen M, Merchant N. MRI of hypertrophic cardiomyopathy: part 1, MRI appearances. Am J Roentgenol 2007;189:1335–1343.

Hansen M, Merchant N. MRI of hypertrophic cardiomyopathy: part 2, differential diagnosis, risk stratification, and posttreatment MRI appearances. Am J Roentgenol 2007;189:1344–1352.

Chun EJ, Choi SII, Kim KN, et al. Hypertrophic cardiomyopathy: assessment with MR imaging and multidetector CT. Radiographics 2010;30:1309–1328.

# CASE 15

**LAURA E.**
**HEYNEMAN**

## HISTORY

A 35-year-old female with angina and cardiac murmur.

A

■**FIGURE 11-15A** Frontal chest radiograph with normal pulmonary blood flow. The cardiac silhouette is upper normal in size. There is enlargement of the ascending aorta for the patient's age.

B

■**FIGURE 11-15B** SSFP MR aortic outflow view reveals a jet of turbulent blood extending from the aortic valve into the tubular ascending aorta.

C

■**FIGURE 11-15C** SSFP three-chamber MR image reveals thickening of the aortic valve as well as a turbulent jet extending from the aortic valve into the ascending aorta.

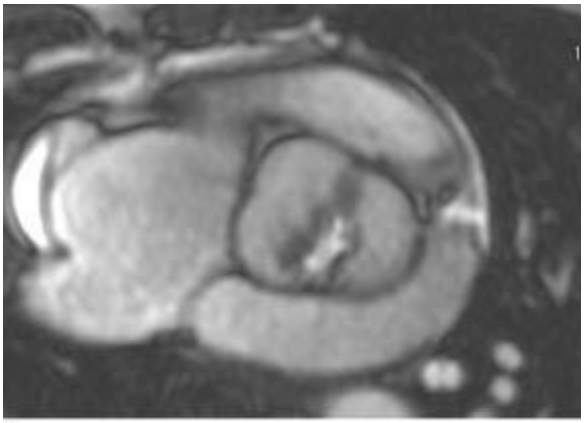

D

**FIGURE 11-15D** SSFP MR image of the aortic valve demonstrates a thickened, bicuspid valve with a very small aperture.

## DIFFERENTIAL DIAGNOSIS

**Aortic stenosis (AS):** Enlargement of the tubular portion of the ascending aorta, thickening of the aortic valve, turbulent flow extending through the valve into the ascending aorta during systole, and narrowed aperture of a bicuspid aortic valve are most suggestive of this diagnosis.

**Aortic regurgitation:** Aortic regurgitation can be seen in conjunction with AS. However, on steady-state free precession (SSFP) MR, the turbulent flow jet would extend from the aortic valve into the left ventricle during diastole, a finding that is not seen in this case. Furthermore, a tangential view of the aortic valve in patients with aortic regurgitation would demonstrate lack of coaptation of the aortic valve leaflets during diastole.

**Cystic medial necrosis:** This can result in dilation of the ascending aorta, but generally results in dilation of the aortic root and sinuses of Valsalva as well as the tubular portion of the ascending aorta. The result is a "tulip bulb" shape of the ascending aorta. Cystic medial necrosis is often associated with aortic insufficiency as well as aortic dissection.

**Atherosclerotic ascending aortic aneurysm:** One of the most common causes of ascending aortic enlargement. This would spare the sinuses of Valsalva and involve only the tubular portion of the aorta. However, this would not explain the thickening of the aortic valve, the flow jet through the aortic valve, or the fused valvular commissures.

## DIAGNOSIS

**Aortic stenosis (AS)**

## KEY FACTS

### Clinical

- AS may be due to congenital fusion of the commissures of the aortic valve, resulting in either an anatomic or functionally bicuspid aortic valve.
- Acquired AS may be caused by rheumatic heart disease or senile degeneration of the valve.
- Regardless of cause, AS may be classified according to its severity: mild (valve area >1.2 $cm^2$ and <2.0 $cm^2$); moderate (valve area 0.8 to 1.2 $cm^2$) and severe (valve area <0.8 $cm^2$).
- Patients with mild AS are usually asymptomatic. As the severity of the AS increases, the cardiac output and ventricular contractility begin to decrease, and can result in congestive heart failure. Furthermore, diastolic flow into the coronary arteries begins to decrease, causing angina pectoris.
- Surgical repair of AS is indicated in symptomatic patients. Some surgeons also intervene in patients with severe AS prior to the advent of symptoms.
- Tubular ascending aortic aneurysms may occur in patients with a bicuspid valve, even when the valve is not functionally stenotic. This is referred to as “bicuspid aortic valve syndrome” or “bicuspid aortopathy”. These aneurysm may enlarge more rapidly than atherosclerotic aneurysms and may be prone to dissection.

### Radiologic

- Chest radiograph:
  - Radiographic findings of AS include enlargement of the ascending aorta secondary to poststenotic dilation, a cardiac silhouette that is upper normal in size (due to LV hypertrophy), and normal pulmonary blood flow (until LV failure develops, at which point pulmonary edema develops).
  - Visualization of valve calcification on a radiograph is indicative of valvular stenosis. The calcification is generally seen earlier in patients with AS from a congenitally bicuspid valve than in patients who have AS from an acquired cause such as rheumatic heart disease or senile degeneration of the valve. Calcification of a stenotic bicuspid valve is typically seen in patients who are >35 years of age.
- Anatomic MR:
  - The aortic valve is thickened and may be black in signal due to calcifications.
  - The area of the valve aperture can be directly measured on images obtained at the level of the valve.
  - The number of valve leaflets can be directly visualized. Valves may be bicuspid or tricuspid. Even if there are three valves, fusion of commissures may result in

a functionally bicuspid valve.

- Functional MR:
  - On cine MR, a jet of turbulent flow extends from the valve into the tubular portion of the ascending aorta, resulting in postobstructive dilation.
  - Phase contrast MR imaging can be used to calculate the transvalvular gradient, which, in turn, can help classify severity of stenosis. A transvalvular gradient of <25 mm Hg corresponds to mild AS, a gradient of 25 to 50 corresponds to moderate AS, and a gradient of >50 corresponds to severe AS.

## SUGGESTED READING

Chen JJ, Manning MA, Frazier AA, et al. CT angiography of the cardiac valves: normal, diseased, and postoperative appearances. Radiographics 2009;29:1393–1412.

Vogel-Claussen J, Pannu H, Spevak PJ, et al. Cardiac valve assessment with MR imaging and 64-section multidetector row CT. Radiographics 2006;26:1769–1784.

# CASE 16

**MELISSA HAYES**

### HISTORY

A 67-year-old woman who presents with dyspnea.

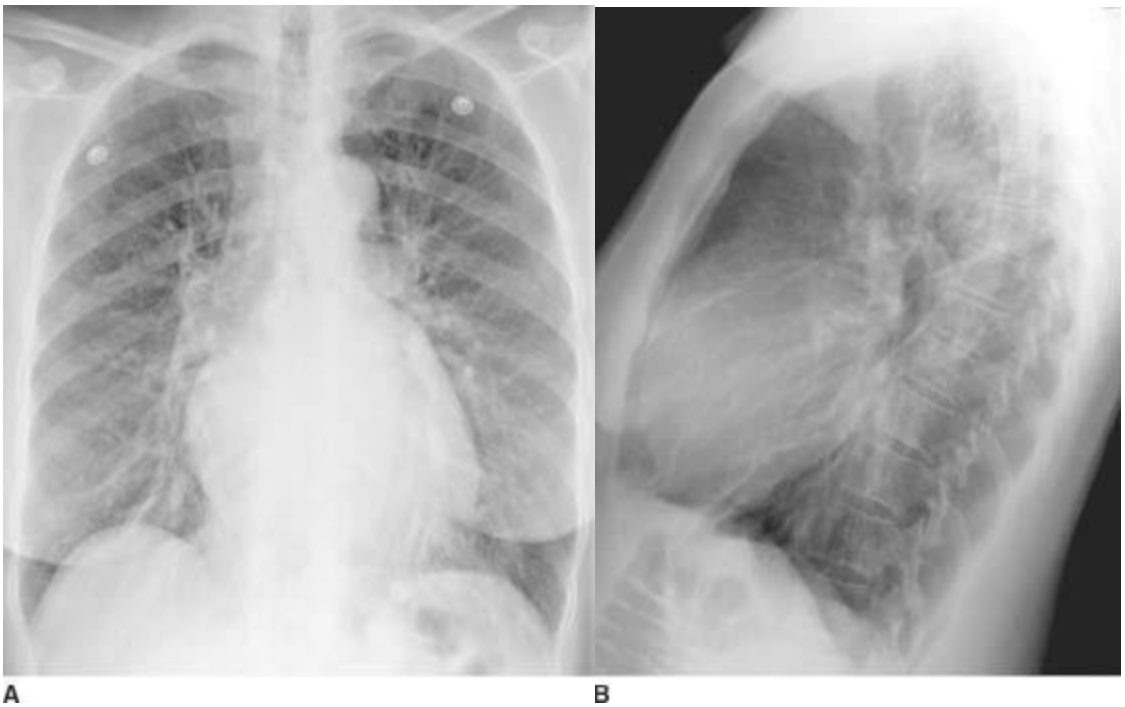

A B

■**FIGURES 11-16A and 11-16B** Frontal and lateral chest radiographs demonstrate left atrial enlargement, right ventricular enlargement and redistribution of pulmonary blood flow, indicative of pulmonary venous hypertension.

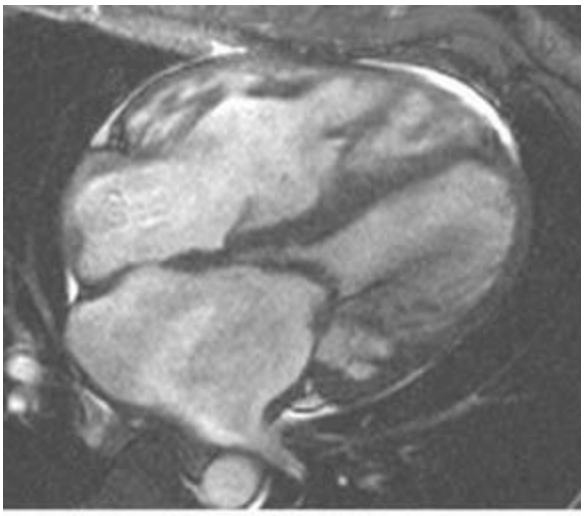

C

■**FIGURE 11-16C** Four-chamber SSFP MR image demonstrates thickening of the mitral valve and left atrial enlargement. There is a jet of turbulent flow seen extending from the mitral valve into the left ventricle during ventricular diastole. Additionally, there is mild right ventricular hypertrophy and enlargement.

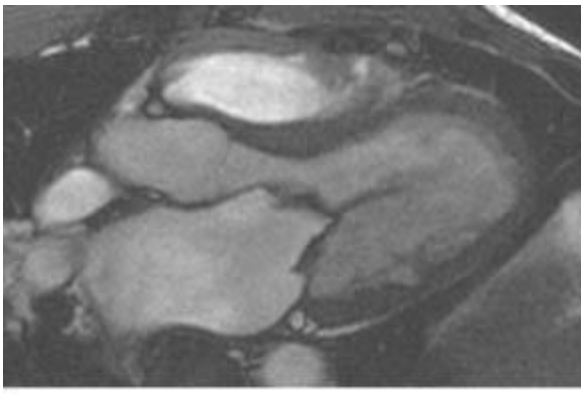

D

■**FIGURE 11-16D** Three-chamber SSFP MR image confirms the thickening of the mitral valve and the jet of turbulent flow that extends from the valve into the left ventricle. The tips of the mitral valve leaflets are adherent to one another during diastole, indicating severe stenosis.

## DIFFERENTIAL DIAGNOSIS

■**Mitral stenosis:** This is the most likely diagnosis considering the presence of left atrial enlargement, right ventricular enlargement, normal LV size, and pulmonary venous

hypertension. On the MR images, the presence of mitral valve thickening and a flow jet extending into the left ventricle from the mitral valve confirm this as the most likely diagnosis.

- **Mitral regurgitation:** This is also a consideration because of the presence of left atrial enlargement and mitral valve thickening on MR images. However, patients with mitral regurgitation should have LV enlargement. In addition, on MR imaging a mitral regurgitation flow jet would extend from the mitral valve into the left atrium rather than into the left ventricle (as in this case).
- **Mitral endocarditis:** This may cause focal thickening of the mitral valve; the presence of diffuse thickening would be uncommon in the setting of endocarditis. Additionally, endocarditis is more commonly associated with mitral regurgitation than with mitral stenosis. As previously noted, this would result in a turbulent flow jet extending from the valve into the left atrium rather than into the left ventricle.

# DIAGNOSIS

**Mitral stenosis**

# KEY FACTS

## Clinical

- Mitral stenosis is a condition that can be acquired or congenital in etiology. Up to 60% of cases of mitral stenosis are caused by rheumatic heart disease.
- Narrowing of the mitral valve results in a pressure gradient across the valve. This means that the left atrial pressure has to increase to maintain blood flow into the left ventricle. The increase in left atrial pressure results in increased pulmonary venous pressure and eventually interstitial or alveolar edema.
- The normal mitral valve orifice is 4 to 6 $cm^2$. When the mitral valve area drops below 2 $cm^2$, there is impedance to blood flow into the left ventricle.
- Mild mitral stenosis occurs when the valve area is between 1.5 and 2 $cm^2$. Moderate mitral stenosis indicates a valve area of between 1 and 1.5 $cm^2$. Mitral stenosis is considered severe when the valve area decreases below 1 $cm^2$.
- Mild mitral valve disease can be asymptomatic. In moderate stenosis, dyspnea and fatigue develop as left atrial pressure increases. Orthopnea, paroxysmal nocturnal dyspnea, and right heart failure develop with severe cases of mitral stenosis.
- Hemoptysis may develop secondary to the rupture of bronchial submucosal varices that form as a result of long standing pulmonary venous hypertension. These are caused by the development of anastomoses between pulmonary veins and bronchial veins secondary to the high-pressure state.

- Fifty percent to 80 percent of patients with mitral stenosis develop atrial fibrillation that may be refractory to treatment.

### Radiologic

- Radiographic features include left atrial enlargement, vascular redistribution, interstitial edema, or alveolar edema. Splaying of the carina, a "double density" over the right heart border and prominence of the left atrial appendage are all radiographic findings suggestive of left atrial enlargement.
- Enlargement of the left atrial appendage is most often associated with mitral stenosis from rheumatic heart disease.
- Calcification of the mitral valve is present in approximately 60% of patients with severe mitral stenosis. Visualization of mitral valve calcification on the radiograph is indicative of valvular stenosis.
- Rare pulmonary manifestations of mitral stenosis include diffuse alveolar hemorrhage, pulmonary hemosiderosis, and pulmonary ossification.
- Echocardiography is initially used in the evaluation of mitral stenosis because it is inexpensive, fast, and portable. In addition, it provides information on the mitral valve area and gradient and pulmonary artery pressures.
- MR imaging can demonstrate valve thickening and/or calcification, chamber enlargement, and a jet of turbulent flow extending from the valve into the left ventricle. Additionally, MR imaging is helpful in quantifying the severity of mitral stenosis. Velocities across the mitral valve may be measured using phase contrast imaging. Once the velocity across the valve is known, the pressure differential across the valve may be calculated using the modified Bernoulli equation: $\Delta P = 4 \times v2$.

## SUGGESTED READING

Chen JJ, Manning MA, Frazier AA, et al. CT angiography of the cardiac valves: normal, diseased, and postoperative appearances. Radiographics 2009;29:1393–1412.

Aguilar F, Nesser HF, Faletra F, et al. Imaging modalities in valvular heart disease. Curr Cardiol Rep 2008;10:98–103.

# CASE 17

**PHIL B.**
**HOANG**

### HISTORY

A 17-year-old boy with hypertension on routine physical examination.

A

■**FIGURE 11-17A** Frontal chest radiograph demonstrates a widened mediastinum, with a smooth, convex soft tissue opacity in the left mediastinum just superior to the descending aorta. Note the focal indentation located between the convexity and descending aorta. Bilateral rib notching is present, and the ascending aorta is enlarged for the patient's age. Pulmonary blood flow is normal.

B

■**FIGURE 11-17B** Sagittal SSFP MR image demonstrates narrowing of the proximal descending aorta immediately distal to a dilated left subclavian artery, with a small,

low signal intensity jet extending through the narrowing into the descending aorta. Multiple enlarged intercostal arteries are present; note the low signal intensity jet extending from a huge intercostal collateral vessel *into* the descending aorta.

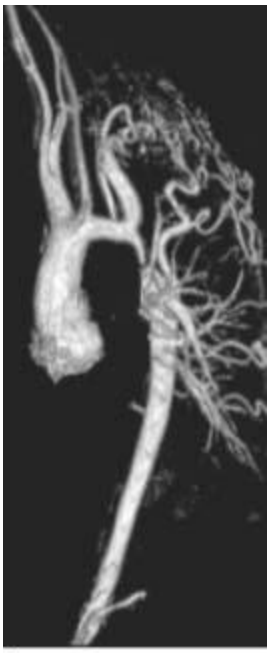

C

**FIGURE 11-17C** Maximum intensity projection image from a 3D-MRA demonstrates focal aortic narrowing of the distal aortic arch as well as numerous enlarged intercostal collaterals.

## DIFFERENTIAL DIAGNOSIS

**Coarctation of the aorta:** This is the most likely diagnosis given the contour abnormality of the left mediastinum and the presence of rib notching. The diagnosis is confirmed on MR, which demonstrates focal stenosis of the aorta at the level of the ligamentum arteriosum, prestenotic and poststenotic aortic dilatation, and presence of enlarged collateral vessels.

**Pseudocoarctation of the aorta:** Pseudocoarctation results from congenital elongation and redundancy of the aortic arch, which tends to buckle in the region of the ligamentum arteriosum. While a mediastinal contour abnormality similar to that seen in true coarctation is seen, there is no rib notching or collateral vessels in pseudocoarctation because no functionally significant stenosis is present.

**Takayasu's arteritis:** This rare but important differential consideration results in stenosis and occlusion of the arch vessels, most commonly the subclavian arteries (producing the classic "pulseless" clinical presentation). Poststenotic dilatation and aneurysm formation may also occur; collateral vessels can develop and may be

extensive. A longer stenotic segment, as well as symmetric, mural wall thickening, are more characteristic findings of Takayasu's arteritis, making this a less likely diagnosis.

- **Mediastinal mass:** Saccular aneurysm/pseudoaneurysm, lymphadenopathy, thoracic goiter, and other non-vascular mass lesions are considerations based on the radiograph. However, the presence of rib notching and the findings on MRI do not support this diagnosis.
- **Postradiation vasculitis:** Unlikely given no history of thoracic malignancy or radiation therapy. Additionally, geographic fibrosis in the adjacent lung would also be expected.

# DIAGNOSIS

**Coarctation of the aorta**

# KEY FACTS

## Clinical

- Coarctation of the aorta accounts for 5% to 10% of all congenital cardiovascular defects, and is divided into two general types: *preductal* and *juxtaductal*.
- *Juxtaductal coarctation*, also known as localized coarctation (and previously referred to as "adult-type"), is the most common type (90% to 95%). It is characterized by medial hypertrophy and intimal proliferation, resulting in posterior infolding of the aorta and focal stenosis. The coarctation most frequently occurs at the aortic isthmus at the level of the ligamentum arteriosum, just distal to the orifice of the left subclavian artery; however, any portion of the ascending aorta, aortic arch, and great vessels may be affected and can change the clinical and radiographic findings.
- *Preductal coarctation*, the less common subtype (and previously referred to as "juvenile-type"), manifests as a long segment of tubular hypoplasia involving the aortic arch. Focal stenosis at the level of the ligamentum arteriosum is also usually present. Preductal coarctation is a common cause of congestive heart failure in the newborn and is associated with other congenital cardiac anomalies, particularly transposition of the great arteries and hypoplastic left heart syndrome.
- In both forms of coarctation, there is a functionally significant stenosis within the aorta that results in obstruction to flow and a pressure gradient across the stenosis.
- Upper extremity systolic blood pressures exceeding that of the lower extremities by at least 20 mm Hg is characteristic. Enlargement of the internal thoracic and intercostal arteries occurs to provide adequate collateral blood flow below the obstruction.
- Associated intracardiac defects include bicuspid aortic valve (up to 85%), VSD, and PDA. Intracranial berry aneurysms occur with increased frequency (up to 5%) and are an important extracardiac finding. Bicuspid aortic valve is also commonly present in the

setting of pseudocoarctation.

- Juxtaductal coarctation is the most frequent cardiac lesion in Turner's syndrome (33%).
- Untreated coarctation results in progressively higher mortality rates (25% by the second decade, 90% by the fifth decade) due to congestive heart failure, aortic dissection, intracerebral aneurysm rupture, or infective aortitis at the site of coarctation. Early coarctation repair results in 20-year survival rates approaching 90%.

## Radiologic

- The "Figure 3" sign is the classic chest radiographic description. The superior convexity of the three represents either the dilated arch or left subclavian artery proximal to the stenosis; the indentation reflects the coarctation; the lower convexity is formed by poststenotic dilatation of the aorta.
- The "Reverse 3" sign is described on LAO views in barium esophagograms and represents changes in the esophageal contour due to mass effect from the adjacent coarctation.
- Rib erosions typically involve the 3rd-8th ribs and present as posteroinferior scalloping with sclerotic margins, typically not evident radiographically until the ages of 5 to 10 years. The 1st and 2nd ribs are unaffected as their intercostal arteries arise from the costocervical trunk instead of the descending thoracic aorta.
- The ascending aorta may be aneurysmal, often due to both the fact that it is subjected to higher pressures proximal to the coarctation and to the presence of a bicuspid aortic valve.
- The cardiac silhouette is upper normal in size due to LV hypertrophy from increased afterload. Pulmonary blood flow is normal until the left ventricle begins to fail from the increased afterload, eventually leading to ventricular dilatation.
- MRI is effective in the diagnosis of coarctation and characterization of any associated intracardiac defects. The aortic isthmus, degree of AS, and associated collateral vessels are readily evaluated with the use of contrast-enhanced 3D MRA. Cine MRA demonstrates flow turbulence across the stenosis, while phase contrast sequences provide an accurate estimate of the pressure gradient.
- MRI is also useful in evaluating the aortic valve for associated bicuspid configuration and resultant stenosis.
- Postrepair MRI evaluation of coarctation is obtained to characterize complications, such as dissection, recoarctation, and aneurysm at the repair site.

## SUGGESTED READING

Ferguson, EC, Krishnamurthy, R, Oldham, SA. Classic imaging signs of congenital cardiovascular abnormalities.

Radiographics 2007;27:1323–1334.

Russo V, Renzulli M, La Palombara C, Fattori R. Congenital diseases of the thoracic aorta. Role of MRI and MRA. Eur Radiol 2006;16:676–684.

# CASE 18

**DANIELLE L. WELLMAN**

## HISTORY

A 26-year-old female presents with history of progressive dyspnea on exertion. Past medical history significant for history of heart murmur as a child without further workup.


■**FIGURES 11-18A and 11-18B** Frontal and lateral chest radiographs demonstrate increased pulmonary blood flow and right-sided cardiac enlargement.

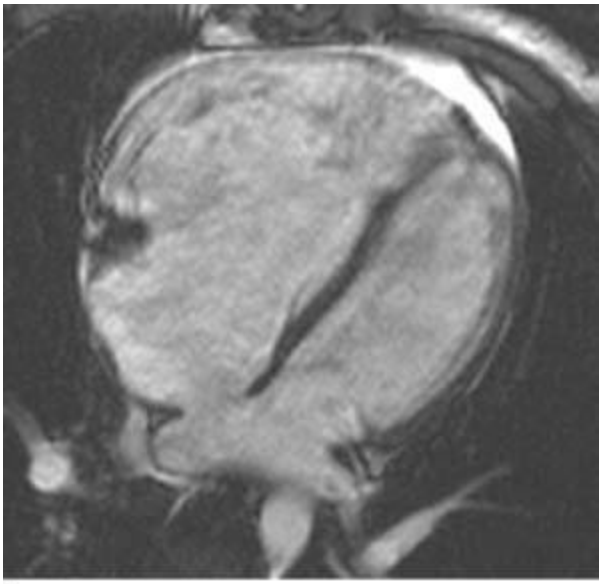

C

**FIGURE 11-18C** Four-chamber SSFP MR image demonstrates right atrial and right ventricular enlargement with large atrial septal defect.

B

**FIGURE 11-18D** Short-axis cardiac SSFP MR image demonstrates right ventricular enlargement without evidence of right ventricular hypertrophy or straightening of the ventricular septum, findings that would be seen with PAH.

## DIFFERENTIAL DIAGNOSIS

**Atrial septal defect (ASD):** The presence of shunt vascularity and right-sided cardiac

enlargement along with reported cardiac murmur on exam are most suggestive of this diagnosis.

- **Ventricular septal defect (VSD):** With this diagnosis you would see shunt vascularity and right heart enlargement, but would also expect left-sided cardiac enlargement. In addition, VSDs almost always present at a younger age.
- **Partial anomalous pulmonary venous connection (PAPVR):** This may also result in shunt vascularity and right-sided cardiac enlargement. Occasionally, there is radiographic evidence of an anomalous vein draining the right upper lobe into the SVC or the left upper lobe into a vertical vein.
- **Primary pulmonary hypertension:** Can cause progressive shortness of breath in a young female with resulting pulmonary artery and right-sided cardiac enlargement if severe. However, would expect enlargement of the central pulmonary arteries with more distal tapering.

## DIAGNOSIS

**Atrial septal defect—ostium secundum/fossa ovalis type**

## KEY FACTS

### Clinical

- ASD is a common congenital heart disease. It represents approximately 30% of congenital heart disease in adults.
- Possible complications arising in individuals with ASDs include right ventricular volume overload, pulmonary hypertension, atrial fibrillation, rarely paradoxical embolism, and even progression to Eisenmenger's syndrome if left untreated.
- The development of the interatrial septum is a multistep coordinated process. The three most common lesions that result from failure of normal septal development are
    - Ostium primum defect—occurs in the region of the fossa primum, at the caudal aspect of the septum primum and secundum, most often caused by or concomitant with nonfusion of the medial AV cushions.
    - Ostium secundum/fossa ovalis defect—most common defect. Occurs due to resorption of the septum primum or incomplete formation of the septum secundum.
    - Sinus venosus ASD—defect in the region of the normal fossa secundum due to lack of formation or reabsorption of the adjacent septum secundum. This defect occurs near the superior vena cava entrance to the right atrium and is associated with partial anomalous pulmonary venous return.
- Treatment of an ASD depends on the size, location, and degree of symptoms. If the

defect is small, closure can be attempted via transcatheter occlusion device. Larger and more complicated defects may require open surgical correction.

### Radiologic

- Radiographic findings of ASD include shunt vascularity, right atrial enlargement, and right ventricular enlargement.
- MR evaluation includes T1-weighted and cine gradient-echo sequences often performed in short-axis and four-chamber views as well as orthogonal to the septal defect. MR angiography is also commonly performed.
- On MR and CT, the thin fossa ovalis may be mistaken for an ASD. On MR, the ASD must be seen on two contiguous slices and be confirmed by a flow jet on cine MR images.
- Velocity-encoding MR may be used to estimate the pulmonary to systemic flow gradient (Qp/Qs) which, if >1, can indicate the hemodynamic significance of the defect.
- CTA may be useful in evaluation if cardiac gating is utilized and fine cuts (slice thickness of 1.25 mm or below) are obtained, although the functional significance of the defect is better assessed with MR.
- Evaluation with MR can be useful in evaluating the coronary and cardiac anatomy, the present of Eisen-menger's physiology, and myocardial viability in a patient under consideration for correction of ASD.

## SUGGESTED READING

Babar JL, Jones RG, Hudsmith L, et al. Application of MR imaging in assessment and follow-up of congenital heart disease in adults. Radiographics 2010;e40:1145

Leschka S, Oechslin E, Husmann L, et al. Pre- and postoperative evaluation of congenital heart disease in children and adults with 64-section CT. Radiographics 2007;27: 829-846.

# CASE 19

**LAURA E.**
**HEYNEMAN**

### HISTORY

A 40-year-old asymptomatic female.

A

**FIGURE 11-19A** Frontal chest radiograph reveals normal pulmonary blood flow, normal cardiac silhouette, and a contour abnormality of the right mediastinum. There is slight tracheal deviation to the left at the level of the contour abnormality as well as absence of normal impression on the left aspect of the trachea by a left aortic arch. The descending aorta is on the right.

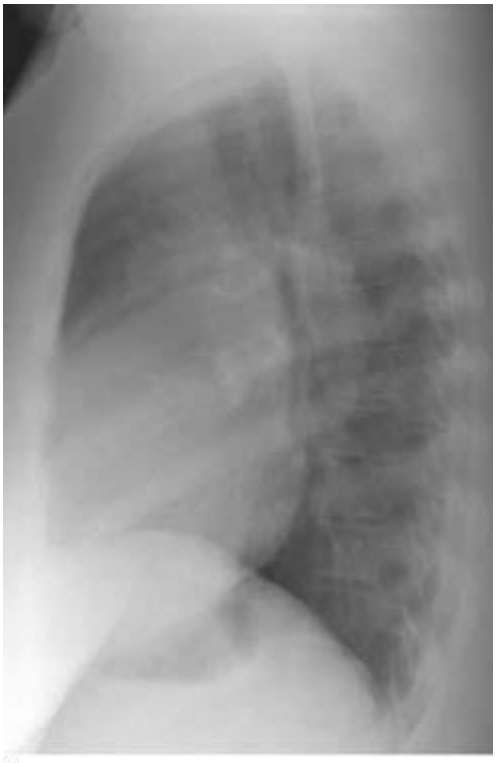

B

**FIGURE 11-19B** Lateral chest radiograph reveals normal cardiac silhouette and mild anterior deviation of the tracheal air column. Slightly increased opacity is present in the

retrotracheal region, just posterior to the region of anterior tracheal deviation.

## DIFFERENTIAL DIAGNOSIS

- **Right aortic arch with aberrant left subclavian artery (ALSA):** This is the primary differential consideration given the slight tracheal deviation to the left on the frontal film and slight tracheal deviation anteriorly on the lateral film. On the frontal film, there is no tracheal deviation to the right in the expected region of a left aortic arch. Additionally, the descending aorta is on the right.
- **Double aortic arch:** This would explain the tracheal deviation to the left, but double arches usually also have tracheal deviation to the right from the left arch component. Additionally, double aortic arches usually descend on the left.
- **Ascending aortic aneurysm:** An ascending aortic aneurysm can cause a right mediastinal contour abnormality. However, the lack of a left transverse aorta and the fact that the descending aorta is on the right lead to the diagnosis of a right aortic arch.
- **Achalasia:** The tubular appearance of the mediastinal contour abnormality raises the possibility of a dilated, fluid filled esophagus. However, the tracheal deviation to the left on the frontal film would be unexpected in achalasia, and there is no tracheal deviation to the right to suggest the presence of a left aortic arch. Furthermore, there is no air/fluid level within the mediastinal abnormality (as often seen in achalasia).

## DIAGNOSIS

**Right aortic arch with aberrant left subclavian artery**

## KEY FACTS

### Clinical

- There are two common forms of right aortic arches: right arch with mirror image branching and right aortic arch with an aberrant left subclavian artery.
- Right aortic arch with mirror image branching (first branch is left innominate artery; second branch is right common carotid artery; third branch is right subclavian artery) is strongly associated (95% to 98%) with congenital heart disease. Tetrology of Fallot (TOF) is the most common association, and truncus arteriosus is the second most common.
- Right aortic arch with ALSA (first branch is left common carotid artery; second branch is right common carotid artery; third branch is right subclavian artery; fourth branch is aberrant left subclavian artery) is only associated with congenital heart disease in approximately 5% patients. In those patients who do have congenital heart disease in association with an aberrant left subclavian type of right arch, TOF is the

most common associated entity.

- The aberrant left subclavian artery usually arises off of a diverticulum (the diverticulum of Kommerell). The aberrant subclavian artery then courses posterior to both the trachea and the esophagus to reach the left arm.
- Right aortic arches are a form of complete vascular ring, with a left ligamentum arteriosum completing the vascular ring.
- Patients with a mirror image type of right aortic arch usually present as a result of their associated congenital heart disease. Rarely, patients have respiratory symptoms as a result of tracheal compression from the vascular ring.
- Older patients with a right aortic arch and ALSA may develop an aneurysm of the left subclavian artery, resulting in esophageal compression and dysphagia lusoria.

## Radiological

- Presence of a right aortic arch is most accurately determined by tracheal deviation to the left on the frontal radiograph. There will be no tracheal deviation to the right, as would be expected if there was a left-sided transverse aorta.
- The diverticulum of Kommerell results in anterior deviation of the tracheal air column (and the esophagus) on the lateral view. Frequently, there will be a prominent soft tissue density in the retrotracheal region, just posterior to the area of tracheal deviation.
- On the frontal film, the diverticulum of Kommerell may cause a slight left mediastinal contour abnormality, but will not impress on the left tracheal wall.
- Right aortic arches usually descend on the right. However, this is variable, particularly in older patients in whom the descending aorta may be tortuous.
- The radiograph should be inspected for signs of associated congenital heart disease, particularly TOF: decreased pulmonary blood flow, “boot” shaped heart, and right ventricular hypertrophy.
- On cross-sectional imaging, the aberrant left subclavian artery can be seen coursing behind the trachea and the esophagus.

## SUGGESTED READING

Onbas O, Kantarci M, Koplay M, et al. Congenital anomalies of the aorta and vena cava: 16-detector-row CT imaging findings. Diagn Interv Radiol 2008;14:163–171.

Kanne JP, Godwin JD. Right aortic arch and its variants. J Cardiovasc Compu Tomogr 2010;4:293–300.

# INDEX

## A

- Acute pericarditis
- Acute pulmonary thromboembolus
- Acute tubular necrosis
- Adenocarcinoma
  - gastric
  - pancreatic
  - of stomach, diffusely infiltrating (scirrhous)
- Adenoid cystic carcinoma
- Adenoma
  - adrenal
  - adrenocortical, nonhyperfunctioning
  - gallbladder
  - hemorrhagic pituitary
  - hepatic
    - in child
  - hepatocellular
  - parathyroid
  - pituitary
  - thyroid
- Adenomatoid malformation, cystic, in fetus
- Adenomyomatosis, of gallbladder
- Adenopathy
  - hilar
  - mediastinal
  - retroperitoneal or mesenteric
- Adrenal adenoma
- Adrenal carcinoma
  - with acute hemorrhage
  - with inferior vena cava invasion
- Adrenal hemorrhage
  - neonatal
- Adrenal hyperplasia, congenital, in neonate
- Adrenal metastasis
- Adrenal myelolipoma

Astrocytoma, pilocytic
Asymmetric breast parenchyma
Asymmetric breast tissue
Asymmetric glandular parenchyma
Asymmetric soft tissues
Atelectasis
  bilateral lower lobe
  in child
  lobar
  round
Atherosclerotic ascending aortic aneurysm
Atherosclerotic disease
  causing chronic mesenteric ischemia
Atherosclerotic left subclavian artery occlusion, with subclavian steal syndrome
Atherosclerotic occlusion
Atherosclerotic peripheral vascular disease
Atherosclerotic popliteal occlusion
Atherosclerotic renal artery stenosis
Atherosclerotic renovascular disease
Atherosclerotic stenosis, of right coronary artery
Atresia
  biliary, in neonate
  bowel, in neonate
  congenital, in infant
  duodenal, with dilated duodenal bulb, in fetus
  pulmonary valve, with intact ventricular septum, in infant
  tricuspid, in infant
Atrial diverticulum, left
Atrial myxoma
Atrial pseudoaneurysm
Atrial septal defect
  and ostium secundum/fossa ovalis type
Atrioventricular septal defect
Attenuation artifact

# B

# C

- renal medullary
- scirrhous, of antrum
- thyroid
- transitional cell, of bladder
- urothelial

Cardiac amyloid
Cardiac sarcoid
Cardiac sarcoma
Cardiac tumor, in infant
Cardiomyopathy
- dilated (congestive)
  - low-grade
- hypertrophic
  - obstructive
- idiopathic dilated
- ischemic
- nonischemic
- restrictive

Carney's triad
Carotid dissection
Carotid stenosis
Carotid-cavernous fistula (CCF)
Caudal regression syndrome
Caustic ingestion
Cavernous angioma
Cavernous hemangioma
Cavernous transformation, PVT with
Celiac disease
Centrilobular emphysema
Cerebellar tonsillar herniation
Cerebral infarction
Cerebrospinal fluid metastases
Cervical radiculopathy
Cervix, incompetent

Chagas disease
Chance fracture
Chemical ablation
Chest wall mass, in child
Chiari malformation
  on ultrasound
Child abuse
Chloroma
Cholangiocarcinoma
  hilar
Cholangitis
  primary sclerosing
  secondary sclerosing
Cholecystitis
  acalculous
  acute, of gallbladder
  acute, with cholelithiasis
  chronic, with cholelithiasis
  emphysematous
Choledochal cyst
  in fetus
  in neonate
Cholelithiasis, with acute cholecystitis
Cholesterol polyp
Chondroblastoma
  of medial talus
Choroid plexus papilloma
Choroidal angiomatosis
Chronic hypersensitivity pneumonitis (CHP)
Chronic myocardial infarction
Chronic pulmonary embolism (CPE)
Chronic renal disease
Chronic thromboembolic pulmonary hypertension (CTEPH)
Chronic thyroiditis

# D

Dysplasia
  arteriohepatic, in neonate
  fibromuscular
  fibrous, with cystic degeneration
  monostotic fibrous
  multiple epiphyseal, in child
  polyostotic fibrous
Dyspnea, progressive

# E

Ebstein's anomaly
  in infant
Ectopic pancreatic rest
Ectopic pregnancy
Edema
  of breast
  noncardiogenic
  pulmonary
Ehlers-Danlos syndrome
Embolic infarction
Embolic occlusion
Embolism
  pulmonary
    chronic
    septic
Embolus
Emphysema
  centrilobular
  panlobular secondary to alpha-1-antit-rypsin disease (A1AD)
Emphysematous cholecystitis
Emphysematous cystitis
Empyema
  complicated, by bronchopleural fistula
  loculated

Encephalitis
  herpes simplex virus type 1
  herpes type 2
Encephalotrigeminal angiomatosis
Enchondromatosis
Endobronchial metastasis
Endometrioma
Endometriosis
Enlarged celiac axis lymph node
Enteric duplication cyst
Enterovesicle fistula
Eosinophilic gastritis
Eosinophilic granuloma
Eosinophilic pneumonia
Ependymoma
  plastic
  of spinal cord
Epidermoid cyst
Epidural metastasis
Epidydymo-orchitis
Epiglottitis, in child
Epiphyseal dysplasia, multiple
Epiphyses, fragmented, in child
Epiploic appendagitis, acute
Erosive gastritis
Esophageal abnormality
Esophageal carcinoma
Esophageal diverticula
Esophageal duplication, in infant
Esophageal intramural pseudodiverticula
Esophagitis
  cytomegalovirus
  infectious
  medication-induced

## F

# G

# H

# I

spinal cord
testicular
venous
Infection, opportunistic
Infectious esophagitis
Infectious gastritis
Infectious myocarditis
Inferior vena cava occlusion
Infiltrating ductal carcinoma of breast
Infiltrative cardiomyopathy
Infiltrative lung disease
Inflammatory arthritides
Inflammatory bowel disease
Inflammatory breast carcinoma
and distant metastases
Inguinal hernia
Insufficiency fracture
Interhemispheric cyst
Interictal seizure focus
Interstitial pneumonia, usual
Interstitial pulmonary edema
Intracavitary thrombus, within left ventricular aneurysm
Intraductal papillary mucinous neoplasm, pancreatic duct
Intraductal papilloma
Intralobar sequestration (ILS)
Intramammary lymph nodes
Intramural hemorrhage
Intramural pseudodiverticulosis
Intra-osseous ganglion
Intraperitoneal bladder rupture
Intussusception, small-bowel
Invasive ductal carcinoma
of breast
Invasive metaplastic carcinoma

## J



## K



## L

- maligant
- non-Hodgkin
- pancreatic
- primary central nervous system (CNS)
- primary, of lung
- pulmonary
- renal
- of small bowel
- splenic
- thoracic

# M

Macroadenoma, pituitary
Malaise
Malrotation
- duodenal, with obstruction
- with midgut volvulus, in neonate

Marfan's syndrome, with ascending aortic aneurysm in child
Massive hemoptysis
Mastitis
- with abscess and reactive lymph node
- plasma cell

Mastocytosis, systemic
May-Thurner syndrome
Mechanical low back pain
Meckel diverticulitis
Meconium aspiration
Meconium ileus, in neonate
Medial collateral ligament bursitis
Mediastinal hematoma
- due to aortic injury
- due to venous bleeding

Mediastinal mass
Mediastinal radiation strictures

- in child
- colon cancer
- drop
- epidural
- hepatic
  - in child
- Hodgkin's lymphoma
- hypervascular
- intracranial
- intramedullary spinal cord
- leptomeningeal
- lung
  - in child
- mesenteric and peritoneal
- omentum
- pancreatic
- pancreatic hypervascular
- pericardial
- renal
- spinoglenoid notch
- of spleen
- supraclavicular node
- testicular

Microadenoma, pituitary
Microcephaly, severe
Miliary tuberculosis
Milk of calcium calcifications
Mirizzi's syndrome
Mitral endocarditis
Mitral regurgitation
Mitral stenosis
Molar pregnancy
Monostotic fibrous dysplasia
Mosaic perfusion pattern secondary to chronic thromboembolic disease

Mosaic perfusion pattern secondary to small airways disease
Mucinous cystic neoplasm
Mucinous pancreatic cystadenoma
Mucoepidermoid cancer
Mucoepidermoid carcinoma
Multicentric breast cancer
Multicentric hepatoma
Multicystic dysplastic kidney
  in toddler
Multifocal breast cancer
Multifocal bronchioalveolar carcinoma (BAC)
Multifocal invasive ductal carcinoma
Multilocular cystic nephroma, in toddler
Multiloculated cystic nephroma
Multiple hamartoma syndrome
Multiple peripheral pulmonary arterial stenoses
Multiple sclerosis
Mycobacterial infections, atypical
*Mycobacterium tuberculosis*
Myelofibrosis
Myeloid sarcoma
Myeloma
  of bone
  multiple
Myocardial infarction
  stress-induced ischemia
  without stress-induced ischemia
Myocardial ischemia
  stress-induced, in vascular territory of left anterior descending coronary artery
  without infarction
Myocardium
  hibernating
  normal
  stunned

# N

# O

Omental infarction
Omphalocele, fetal
Oncocalyx
Oncocytoma, renal
  fat-containing
Opportunistic infection
Optic glioma
Optic nerve glioma
Orbital myositis, idiopathic
Orbital pseudotumor
Organizing pneumonia
Ormond's disease
Osler-Weber-Rendu syndrome
Osteitis deformans
Osteoarthritis
Osteoarthropathy, hypertrophic secondary
Osteochondral fragments, loose
Osteochondral injury
  of lateral femoral condyle
Osteochondroma
Osteochondromatosis
Osteodystrophy, renal, with secondary hyperparathyroidism
Osteogenesis imperfecta
  in child
  in fetus
Osteoid osteoma
Osteomyelitis
  in child
Osteopetrosis
Osteosarcoma
  conventional
  parosteal
  telangiectatic
Ovarian neoplasm

Ovarian teratoma, in toddler
Ovarian torsion

# P

Paget's disease of bone
Pancreatic adenocarcinoma
Pancreatic carcinoma
Pancreatic cystadenoma
  mucinous
  serous
Pancreatic hypervascular metastasis
Pancreatic islet cell tumor
  functioning
  nonfunctioning
Pancreatic lymphoma
Pancreatic metastases
Pancreatic neoplasm, cystic
Pancreatic pseudocyst
Pancreatic rest, ectopic
Pancreatic trauma, in child
Pancreatitis
  acute
  chronic
  chronic calcific
Panlobar emphysema
Panlobular (PL) emphysema secondary to alpha-1-antitrypsin disease (A1AD)
Papillary carcinoma in situ, of breast
Papillary thyroid cancer
Papilloma
  in airway
  breast
    intraductal
  choroid plexus
  gallbladder

Postsurgical scar, of breast
Preductal coarctation
Pregnancy
  abdominal
  early intrauterine
  ectopic
  molar
Primary achalasia
Primary central nervous system lymphoma
Primary ciliary dyskinesia
Primary megaureter
Primary sclerosing cholangitis
Primary synovial chondromatosis with ossification
Primitive neuroectodermal tumor, in child
Progressive dyspnea
Progressive multifocal leukoencephalopathy (PML)
Proteinosis, pulmonary alveolar
Prune belly syndrome
Pseudoaneurysm
  coronary artery
  femoral artery
Pseudoangiomatous stromal hyperplasia (PASH), nodular
Pseudocoarctation, of aorta
Pseudocyst, pancreatic
Pseudodiverticulosis
  intramural
  ureteral
Pseudomembranous colitis
*Pseudomonas*
Pseudotumor, postinflammatory, in child
Pseudoureterocele
  secondary to transitional cell carcinoma of bladder
Psoriasis
Psoriatic arthritis

Pulmonary alveolar proteinosis
Pulmonary amyloid
Pulmonary arteriovenous malformations
Pulmonary artery hypertension
Pulmonary artery hypoplasia, right
Pulmonary artery sling, in infant
Pulmonary atresia
  with intact septum, in infant
  without ventricular septal defect
Pulmonary edema
  interstitial
  noncardiogenic
Pulmonary embolism
  chronic
  septic
Pulmonary fibrosis, idiopathic
Pulmonary hemorrhage
Pulmonary histiocytosis X (PHX)
Pulmonary hypertension, primary
Pulmonary infarct
Pulmonary lymphoma
Pulmonary malignancy
  primary, in child
Pulmonary neoplasm, in child
Pulmonary sequestration, in child
Pulmonary stenosis, valvular
Pulmonary thromboembolus
Pulmonary trauma
Pulmonary valve atresia, with intact ventricular septum, in infant
Pulmonary valve stenosis
Pulmonary vein thrombosis
Pulmonic valve stenosis, isolated, in infant
Pyelonephritis
  acute

# R

- cystic
- hemorrhagic
- multifocal
- multilocular cystic
- multiple, with von Hippel-Lindau disease

Renal contusion
Renal cysts
- complicated, of left upper pole
- in fetus
- hemorrhagic

Renal duplication with agenesis of contralateral kidney
Renal ectopia, crossed
Renal failure, changes in breast due to
Renal fracture
Renal laceration, with perinephric hematoma/urinoma
Renal lymphoma
Renal medullary carcinoma
Renal metastases
Renal obstruction
Renal oncocytoma
Renal osteodystrophy with secondary hyperparathyroidism
Renal vein thrombosis
Renovascular disease, atherosclerotic
Renovascular injury
Replacement lipomatosis of kidney
Residual thymus
Respiratory distress in neonate, due to surfactant deficiency disease
Restrictive cardiomyopathy
Retroperitoneal fibrosis
- idiopathic (nonmaligant)
- maligant

Retroperitoneal mass, causing displacement of kidney
Retroperitoneal neoplasm
Retroperitoneal tumor, in neonate

## S

Stress-induced myocardial ischemia, vascular territory of left anterior descending coronary artery
Strictures
  traumatic biliary
Sturge-Weber syndrome
Subcapsular hematoma
Subchorionic hematoma overlying cervix
Subclavian artery occlusion, atherosclerotic left, with subclavian steal syndrome
Subclavian steal syndrome
Superior peroneal retinaculum injury with peroneal tendon dislocation
Superior vena cava obstruction changes in breast due to
Suprascapular neuropathy, caused by spinoglenoid notch paralabral cyst
Swallowed radioiodine
Swyer-James syndrome
Synovial chondromatosis
  primary, with ossification
  secondary
Synovial cyst
Synovial hemangioma
Synovitis, pigmented villonodular
Systemic lupus erythematosus
Systemic mastocytosis
Systemic sclerosis

# T

Tachypnea, transient, of newborn
Takayasu's arteritis
Tc-99m pertechnetate in bowel
Telangiectasia, hereditary haemorragic
Telangiectatic osteosarcoma
Temporal lobe contusion
Tendinosis
Teratoma
  cystic

in fetus
in infant
ovarian
sacrococcygeal
on ultrasound
Testicular contusion
Testicular fracture
Testicular infarction
Testicular neoplasm
Testicular rupture
Testicular seminoma
Testicular torsion
Tethered spinal cord, due to lipomyelomeningocele
Tetralogy of Fallot
in infant
Thoracic aorta, traumatic tear of, at isthmus
Thoracic aortic aneurysm, descending
Thoracic aortic dissection
Thoracic outlet syndrome
Thromboangiitis obliterans
Thromboembolism, distal, with arterial injury
Thrombosed popliteal aneurysm
Thrombosis, arteriovenous graft
Thymic cyst, in infant
Thymoma
Thymus
normal, in infant
residual
Thyroid acropachy
Thyroid adenoma
Thyroid cancer
Thyroid carcinoma
Thyroid metastatic disease, functioning alone
Thyroid ophthalmopathy

## U

# V

# W



# X

# Y

***Yersinia* ileitis**

# Z

Zollinger-Ellison syndrome